FuelSolutions™ W74 Canister Storage
Final Safety Analysis Report

Revision 4
April 2005

Document No. WSNF-223
Docket No. 72-1026

Prepared by:

BNFL Fuel Solutions Corporation
Campbell, California

©2005 BNFL Fuel Solutions Corporation
All Rights Reserved

This page intentionally left blank.

TABLE OF CONTENTS

Section **Title** **Page**

1. GENERAL DESCRIPTION 1-1
1.1 Introduction 1.1-1
1.2 General Descriptions 1.2-1
1.2.1 FuelSolutions™ Storage System Characteristics 1.2-1
1.2.1.1 FuelSolutions™ Storage Cask 1.2-1
1.2.1.2 FuelSolutions™ Transfer Cask 1.2-1
1.2.1.3 FuelSolutions™ W74 Canister 1.2-2
1.2.1.4 FuelSolutions™ Support Equipment 1.2-7
1.2.2 Operational Features 1.2-11
1.2.2.1 Canister Loading 1.2-12
1.2.2.2 Canister Closure/Opening 1.2-13
1.2.2.3 Canister Horizontal Transfer 1.2-15
1.2.2.4 Canister Vertical Transfer 1.2-15
1.2.2.5 Storage 1.2-15
1.2.2.6 Transportation Cask Loading 1.2-15
1.2.3 FuelSolutions™ W74 Canister Contents 1.2-15
1.3 Identification of Agents and Contractors 1.3-1
1.4 On-Site Storage Array Configurations 1.4-1
1.5 Supplemental Data 1.5-1
1.5.1 Drawings 1.5-1
1.5.2 Product Literature 1.5-3
1.5.2.1 Borated Stainless Steel Literature 1.5-3
1.5.2.2 Electroless Nickel Plating Literature 1.5-5

2. PRINCIPAL DESIGN CRITERIA 2-1
2.1 Structures, Systems, and Components Important to Safety 2.1-1
2.1.1 Identification of Items Important to Safety 2.1-1
2.1.2 Design Bases and Criteria 2.1-1
2.2 Spent Fuel to be Stored 2.2-1

TABLE OF CONTENTS (continued)

Section	Title	Page
2.2.1	Mixed-Oxide (MOX) Fuel Assemblies	2.2-2
2.2.2	Partial Fuel Assemblies	2.2-2
2.2.3	Damaged Fuel Assemblies	2.2-3
2.3	Design Loadings	2.3-1
2.3.1	Normal Conditions	2.3-3
2.3.1.1	Normal Ambient Conditions	2.3-3
2.3.1.2	Internal Pressure	2.3-3
2.3.1.3	Dead Load	2.3-3
2.3.1.4	Handling Load	2.3-3
2.3.1.5	Leakage of the Confinement Boundary Under Normal Conditions	2.3-4
2.3.2	Off-Normal Conditions	2.3-4
2.3.2.1	Extreme Ambient Conditions	2.3-4
2.3.2.2	Internal Pressure	2.3-4
2.3.2.3	Misaligned Casks During Horizontal Canister Transfer	2.3-4
2.3.2.4	Reflood Pressure	2.3-5
2.3.2.5	Hydraulic Ram Failure During Horizontal Transfer	2.3-5
2.3.2.6	Leakage of the Confinement Boundary Under Off-Normal Conditions	2.3-5
2.3.3	Postulated Accident Conditions	2.3-5
2.3.3.1	Accident Thermal Conditions	2.3-5
2.3.3.2	Cask Drop and Tip-over	2.3-6
2.3.3.3	Fire	2.3-6
2.3.3.4	Internal Pressure	2.3-6
2.3.3.5	Leakage of the Confinement Boundary Under Accident Conditions	2.3-6
2.3.3.6	Explosive Overpressure	2.3-6
2.3.4	Natural Phenomena	2.3-7
2.3.4.1	Flooding	2.3-7
2.3.4.2	Tornado	2.3-7

TABLE OF CONTENTS (continued)

Section **Title** **Page**

2.3.4.3 Earthquake 2.3-7
2.3.4.4 Wind 2.3-7
2.3.4.5 Burial Under Debris 2.3-7
2.3.4.6 Lightning 2.3-8
2.3.4.7 Snow and Ice 2.3-8
2.3.4.8 Site-Specific Conditions 2.3-8
2.3.5 Load Combination Criteria 2.3-8
2.4 Safety Protection Systems 2.4-1
2.5 Supplemental Information 2.5-1
2.5.1 ASME Code Compliance 2.5-1
2.5.2 FuelSolutions™ Canister Top End Closure Weld Design Basis and Nondestructive Examination Justification 2.5-12
2.5.2.1 Introduction 2.5-12
2.5.2.2 NUREG-1536 Criteria 2.5-12
2.5.2.3 Background 2.5-15
2.5.2.4 FuelSolutions™ Closure Design Description 2.5-23
2.5.2.5 Comparison of FuelSolutions™ versus VSC-24 Canister Design Features 2.5-25
2.5.2.6 Additional NDE and Testing Requirements 2.5-27
2.5.2.7 Summary 2.5-33

3. STRUCTURAL EVALUATION 3-1
3.1 Structural Design 3.1-1
3.1.1 Discussion 3.1-1
3.1.1.1 Shell Assembly 3.1-1
3.1.1.2 Basket Assembly 3.1-2
3.1.1.3 Damaged Fuel Can 3.1-6
3.1.2 Design Criteria 3.1-7
3.1.2.1 Basic Design Criteria 3.1-7
3.1.2.2 Applicable Codes and Standards 3.1-7

TABLE OF CONTENTS (continued)

Section	Title	Page
	3.1.2.3 Supplemental Structural Criteria	3.1-8
3.2	Weights and Centers of Gravity	3.2-1
3.3	Mechanical Properties of Materials	3.3-1
3.4	General Standards for Casks	3.4-1
	3.4.1 Chemical and Galvanic Reactions	3.4-1
	3.4.2 Positive Closure	3.4-2
	3.4.3 Lifting Devices	3.4-2
	3.4.4 Canister Service Life	3.4-6
3.5	Evaluation of Normal Conditions	3.5-1
	3.5.1 Normal Temperature and Insolation Loadings	3.5-2
	3.5.1.1 Summary of Pressures and Temperatures	3.5-2
	3.5.1.2 Differential Thermal Expansion	3.5-3
	3.5.1.3 Thermal Stress Calculations	3.5-7
	3.5.1.4 Fatigue Evaluation	3.5-12
	3.5.2 Internal Pressure	3.5-15
	3.5.2.1 Canister Draining Internal Pressure	3.5-15
	3.5.2.2 Normal Transfer and Storage Internal Pressure	3.5-16
	3.5.3 Dead Weight Load	3.5-17
	3.5.3.1 Canister Shell Assembly	3.5-17
	3.5.3.2 General and LTP Spacer Plates	3.5-19
	3.5.3.3 Engagement Spacer Plate	3.5-21
	3.5.3.4 Support Tubes	3.5-22
	3.5.3.5 Support Sleeves	3.5-23
	3.5.3.6 Guide Tubes	3.5-23
	3.5.4 Normal Handling	3.5-27
	3.5.4.1 Vertical Canister Transfer	3.5-28
	3.5.4.2 Horizontal Canister Transfer	3.5-29
	3.5.4.3 On-Site Transport	3.5-30
	3.5.5 Load Combinations and Comparison with Allowable Stresses	3.5-34

TABLE OF CONTENTS (continued)

Section **Title** **Page**

3.5.5.1 Shell Assembly 3.5-34
3.5.5.2 Basket Assembly 3.5-35
3.5.5.3 Damaged Fuel Can 3.5-35
3.5.6 Cold 3.5-35
3.6 Evaluation of Off-Normal Conditions 3.6-1
3.6.1 Off-Normal Temperature and Insolation Loadings 3.6-1
3.6.1.1 Summary of Pressures and Temperatures 3.6-2
3.6.1.2 Differential Thermal Expansion 3.6-2
3.6.1.3 Thermal Stress Calculations 3.6-3
3.6.2 Off-Normal Internal Pressure 3.6-4
3.6.3 Cask Misalignment 3.6-4
3.6.4 Canister Opening/Reflood 3.6-5
3.6.5 Off-Normal Load Combinations 3.6-6
3.6.5.1 Canister Shell Assembly 3.6-7
3.6.5.2 Canister Basket Assembly 3.6-7
3.6.5.3 Damaged Fuel Can 3.6-7
3.7 Evaluation of Accident Conditions 3.7-1
3.7.1 Fully Blocked Storage Cask Inlet and Outlet Vents 3.7-2
3.7.2 Loss of Transfer Cask Neutron Shield 3.7-2
3.7.3 Storage Cask Drop 3.7-4
3.7.3.1 Canister Shell 3.7-5
3.7.3.2 Basket Assembly 3.7-7
3.7.4 Storage Cask Tip-Over 3.7-14
3.7.4.1 Canister Shell Assembly Tip-Over Analysis 3.7-15
3.7.4.2 Canister Basket Assembly Tip-Over Analysis 3.7-15
3.7.5 Transfer Cask Drop 3.7-22
3.7.5.1 Canister Shell Assembly Side Drop Analysis 3.7-23
3.7.5.2 Canister Basket Assembly Side Drop Analysis 3.7-24
3.7.6 Fire 3.7-38

TABLE OF CONTENTS (continued)

Section **Title** **Page**

3.7.7 Flood 3.7-38
3.7.8 Earthquake 3.7-39
3.7.8.1 Canister Shell Assembly 3.7-40
3.7.8.2 Canister Basket Assembly 3.7-40
3.7.9 Accident Internal Pressure 3.7-41
3.7.10 Accident Condition Load Combinations 3.7-42
3.7.10.1 Canister Shell Assembly 3.7-42
3.7.10.2 Canister Basket Assembly 3.7-43
3.7.10.3 Damaged Fuel Can 3.7-43
3.8 Fuel Rods 3.8-1
3.9 Supplemental Data 3.9-1
3.9.1 Spacer Plate In-Plane Tributary Weights 3.9-1
3.9.2 Finite Element Model Descriptions 3.9-1
3.9.2.1 Canister Shell Axisymmetric Finite Element Model 3.9-1
3.9.2.2 Canister Shell Half-Symmetry Finite Element Model 3.9-3
3.9.2.3 Top Shield Plug Model 3.9-5
3.9.2.4 General and LTP Spacer Plate Models 3.9-5
3.9.2.5 Engagement Spacer Plate Models 3.9-11
3.9.2.6 Guide Tube Models 3.9-14
3.9.3 Stress Evaluation Criteria 3.9-16
3.9.3.1 Canister Shell Stress Evaluation Locations 3.9-16
3.9.3.2 Canister Shell Stress Classifications 3.9-17
3.9.3.3 General and LTP Spacer Plate Stress Evaluation Points 3.9-17
3.9.4 Canister Closure Weld Critical Flaw Size Determination 3.9-18

4. THERMAL EVALUATION 4-1
4.1 Discussion 4.1-1
4.1.1 Design Features 4.1-1
4.1.1.1 W74 Canister 4.1-1
4.1.1.2 Storage Cask 4.1-3

TABLE OF CONTENTS (continued)

Section **Title** **Page**

4.1.1.3 Transfer Cask 4.1-3
4.1.2 Design Basis Ambient Conditions 4.1-4
4.1.3 Bounding Axial Heat Flux Profile 4.1-5
4.1.3.1 Development of Bounding Axial Heat Flux Profiles 4.1-5
4.1.3.2 Application of Axial Heat Profiles for Canister Analysis 4.1-6
4.1.4 Thermal Operating Modes 4.1-7
4.1.4.1 W74 Canister within Storage Cask 4.1-7
4.1.4.2 W74 Canister within Transfer Cask 4.1-8
4.1.5 Thermal Rating Summary 4.1-9
4.1.6 Canister Internal Pressure Summary 4.1-10
4.2 Summary of Thermal Properties of Materials 4.2-1
4.2.1 W74 Canister 4.2-1
4.2.2 Big Rock Point Fuel 4.2-1
4.3 Specifications for Components 4.3-1
4.3.1 W74 Canister 4.3-1
4.3.2 Fuel Cladding Allowable Temperatures 4.3-1
4.3.2.1 Cladding Temperature Decay 4.3-3
4.3.2.2 Fuel Rod Pressure and Hoop Stress 4.3-3
4.3.2.3 Long-Term Allowable Cladding Temperatures 4.3-4
4.3.2.4 Short-Term Allowable Cladding Temperature 4.3-5
4.4 Thermal Evaluation for Normal Conditions of Storage 4.4-1
4.4.1 W74 Canister within Storage Cask 4.4-1
4.4.1.1 W74 Thermal Model In Storage Cask 4.4-1
4.4.1.2 Canister Thermal Rating 4.4-7
4.4.1.3 Maximum Temperatures 4.4-8
4.4.1.4 Minimum Temperatures 4.4-9
4.4.1.5 Internal Pressures 4.4-9
4.4.1.6 Fuel Rod Fill Gas 4.4-10
4.4.1.7 Fuel Rod Fission Gas Generation 4.4-10

TABLE OF CONTENTS (continued)

Section **Title** **Page**

4.4.1.8 Normal Canister Pressure 4.4-11
4.4.1.9 Maximum Thermal Stresses 4.4-12
4.4.1.10 Evaluation of Canister Performance for Normal Conditions 4.4-13
4.4.2 W74 Canister within Transfer Cask 4.4-31
4.4.2.1 W74 Thermal Model in Transfer Cask 4.4-31
4.4.2.2 Conditions During Canister Loading 4.4-32
4.4.2.3 Conditions During Canister Reflooding 4.4-34
4.4.2.4 Maximum Temperatures 4.4-38
4.4.2.5 Minimum Temperatures 4.4-39
4.4.2.6 Internal Pressures 4.4-39
4.4.2.7 Maximum Thermal Stresses 4.4-39
4.4.2.8 Evaluation of Canister Performance for Normal Conditions 4.4-40
4.5 Thermal Evaluation for Off-Normal Conditions of Storage 4.5-1
4.5.1 W74 Canister within Storage Cask 4.5-1
4.5.1.1 Thermal Model 4.5-1
4.5.1.2 Maximum Temperatures 4.5-1
4.5.1.3 Minimum Temperatures 4.5-3
4.5.1.4 Internal Pressures 4.5-3
4.5.1.5 Maximum Thermal Stresses 4.5-3
4.5.1.6 Evaluation of Canister Performance for Off-Normal Conditions 4.5-4
4.5.2 W74 Canister within Transfer Cask 4.5-8
4.5.2.1 Thermal Model 4.5-8
4.5.2.2 Maximum Temperatures 4.5-8
4.5.2.3 Minimum Temperatures 4.5-9
4.5.2.4 Internal Pressures 4.5-9
4.5.2.5 Maximum Thermal Stresses 4.5-9
4.5.2.6 Evaluation of Canister Performance for Off-Normal Conditions 4.5-9
4.6 Thermal Evaluation for Accident Conditions of Storage 4.6-1

TABLE OF CONTENTS (continued)

Section **Title** **Page**

4.6.1 W74 Canister within Storage Cask 4.6-1
4.6.1.1 Thermal Model 4.6-1
4.6.1.2 Maximum Temperatures 4.6-3
4.6.1.3 Minimum Temperatures 4.6-4
4.6.1.4 Internal Pressures 4.6-4
4.6.1.5 Maximum Thermal Stresses 4.6-5
4.6.1.6 Evaluation of Canister Performance for Accident Conditions 4.6-5
4.6.2 W74 Canister within Transfer Cask 4.6-11
4.6.2.1 Thermal Model 4.6-11
4.6.2.2 Maximum Temperatures 4.6-11
4.6.2.3 Minimum Temperatures 4.6-12
4.6.2.4 Maximum Internal Pressures 4.6-12
4.6.2.5 Maximum Thermal Stresses 4.6-12
4.6.2.6 Evaluation of Canister Performance for Accident Conditions ... 4.6-12
4.7 Supplemental Data 4.7-1
4.7.1 Canister Internal Convection 4.7-1
4.7.2 Other Modes of Heat Transfer 4.7-6
4.7.3 Computer Code Descriptions 4.7-7
4.7.3.1 SINDA/FLUINT Computer Code 4.7-7
4.7.3.2 RadCAD Computer Code 4.7-8
4.7.4 Big Rock Point Mixed-Oxide (MOX) Fuel 4.7-8
4.7.4.1 Heat Generation of BRP MOX Fuel 4.7-8
4.7.4.2 Axial Heat Flux Profile of BRP MOX Fuel 4.7-9
4.7.4.3 Effective Thermal Conductivity of BRP MOX Fuel 4.7-9
4.7.4.4 Allowable Cladding Temperature for BRP MOX Fuel 4.7-9
4.7.4.5 Canister Internal Pressure for BRP MOX Fuel 4.7-10
4.7.4.6 Thermal Summary for BRP MOX Fuel 4.7-10
4.7.5 Big Rock Point Partial Fuel Assemblies 4.7-11
4.7.5.1 Required Cooling Time for BRP Partial Fuel Assemblies 4.7-11

TABLE OF CONTENTS (continued)

Section **Title** **Page**

4.7.5.2 Effective Thermal Conductivity of BRP Partial Fuel Assemblies 4.7-11
4.7.5.3 Thermal Summary for BRP Partial Fuel Assemblies 4.7-12
4.7.6 Big Rock Point Damaged Fuel 4.7-12
4.7.6.1 Heat Generation of BRP Damaged Fuel 4.7-12
4.7.6.2 Axial Heat Flux Profile of BRP Damaged Fuel 4.7-12
4.7.6.3 Effective Thermal Conductivity of BRP Damaged Fuel 4.7-13
4.7.6.4 Allowable Cladding Temperature for BRP Damaged Fuel 4.7-14
4.7.6.5 Estimated Cladding Temperature for BRP Damaged Fuel 4.7-15
4.7.6.6 Estimated Cladding Temperature for BRP Fuel Rubble 4.7-16
4.7.6.7 Canister Internal Pressure for BRP Damaged Fuel 4.7-17
4.7.6.8 Thermal Summary for BRP Damaged Fuel Assemblies 4.7-17

5. SHIELDING EVALUATION 5-1
5.1 Discussion and Results 5.1-1
5.1.1 FuelSolutions™ W74 Canister Shielding Design Features 5.1-1
5.1.2 FuelSolutions™ W74 Canister Fuel Cooling Tables 5.1-1
5.1.3 FuelSolutions™ W74 Canister Adjoint Shielding Models 5.1-1
5.2 Source Specification 5.2-1
5.2.1 Fuel Cooling Tables 5.2-1
5.2.2 Design Bases for the Fuel Cooling Tables 5.2-1
5.2.3 Special Considerations for the W74 Fuel Cooling Tables 5.2-2
5.2.4 Use of the Fuel Cooling Tables 5.2-3
5.3 Model Specification 5.3-1
5.3.1 Description of the Shielding Configuration 5.3-1
5.3.2 Shield Regional Densities 5.3-2
5.4 Shielding Evaluation 5.4-1
5.4.1 W74 Canister Adjoint Calculation Methodology 5.4-1
5.4.2 W74 Canister Adjoint Calculation Results 5.4-1
5.5 Supplemental Data 5.5-1

TABLE OF CONTENTS (continued)

Section **Title** **Page**

5.5.1 Fuel Cooling Table Domains 5.5-1
5.5.2 BRP Mixed-Oxide (MOX) Fuel Assembly Qualification 5.5-1
5.5.3 BRP Partial Fuel Assembly Qualification 5.5-5
5.5.4 BRP Damaged Fuel Assembly Qualification 5.5-5

6. CRITICALITY EVALUATION 6-1
6.1 Discussion and Results 6.1-1
6.2 Spent Fuel Loading 6.2-1
6.3 Model Specification 6.3-1
6.3.1 Configuration 6.3-2
6.3.1.1 Hypothetical Accident Conditions 6.3-7
6.3.1.2 Normal Operating Condition 6.3-9
6.3.2 Material Properties 6.3-11
6.4 Criticality Evaluation 6.4-1
6.4.1 Computer Programs 6.4-1
6.4.2 Multiplication Factor 6.4-1
6.4.2.1 Package Array 6.4-1
6.4.2.2 Single Package 6.4-8
6.5 Criticality Benchmark Experiments 6.5-1
6.6 Big Rock Point MOX, Partial, and Damaged Fuel Assemblies 6.6-1
6.6.1 Big Rock Point Mixed-Oxide Fuel Assembly Criticality Evaluation 6.6-1
6.6.1.1 MOX Fuel Criticality Analyses 6.6-1
6.6.1.2 MOX Fuel Criticality Benchmarks 6.6-6
6.6.2 Big Rock Point Partial Fuel Assembly Criticality Evaluation 6.6-10
6.6.2.1 Partial Assemblies with Missing Corner Rods 6.6-10
6.6.2.2 Partial Assemblies with Missing Array-Interior or Array-Edge Rods 6.6-12
6.6.3 Big Rock Point Damaged Fuel Assembly Criticality Evaluation 6.6-16
6.6.3.1 W74 Canister Model for the Damaged Assembly Analyses 6.6-16
6.6.3.2 Damaged Fuel Can Contents Model Description 6.6-17

TABLE OF CONTENTS (continued)

Section **Title** **Page**

6.6.3.3 Damaged Assembly Criticality Analysis Results 6.6-18
6.6.3.4 Damaged Fuel Can Preferential Flooding Analysis 6.6-20
6.6.3.5 Damaged BRP MOX Assembly Analyses 6.6-21
6.6.3.6 Other Allowable Damaged Fuel Can Contents 6.6-22

7. CONFINEMENT 7-1

7.1 Confinement Boundary 7.1-1
7.1.1 Confinement Vessel 7.1-2
7.1.2 Confinement Penetrations 7.1-3
7.1.3 Seals and Welds 7.1-3
7.1.4 Closure 7.1-4
7.2 Requirements for Normal and Off-Normal Conditions of Storage 7.2-1
7.2.1 Release of Radioactive Material for Normal and Off-Normal Conditions 7.2-1
7.2.1.1 Confinement Integrity During Dry Storage 7.2-1
7.2.1.2 Control of Radioactive Material During Fuel Loading Operations 7.2-2
7.2.1.3 External Contamination Control 7.2-2
7.2.2 Pressurization of Confinement Vessel for Normal and Off-Normal Conditions 7.2-3
7.2.3 Normal and Off-Normal Doses 7.2-3
7.3 Confinement Requirements for Hypothetical Accident Conditions 7.3-1
7.3.1 Fission Products 7.3-1
7.3.1.1 Fuel Fission Gases, Volatiles, and Particulates 7.3-1
7.3.1.2 CRUD Radionuclides 7.3-2
7.3.2 Release of Contents 7.3-2
7.3.2.1 Fraction Available for Release 7.3-2
7.3.2.2 Fraction of Fuel Rods Breached 7.3-2
7.3.2.3 Atmospheric Dispersion 7.3-2
7.3.2.4 Dose Conversion Factors 7.3-2

TABLE OF CONTENTS (continued)

Section **Title** **Page**

7.3.2.5 Event Duration and Occupancy Factor 7.3-2
7.3.2.6 Canister Release Fraction 7.3-3
7.3.3 Postulated Accident Doses 7.3-3
7.3.4 Site Boundary 7.3-3
7.4 Supplemental Data 7.4-1
7.4.1 Calculation of Bounding Fuel Assembly Surface Area for Co-60 CRUD Contribution Evaluation 7.4-1
7.4.2 MOX, Partial, and Damaged BRP Fuel 7.4-1
7.4.2.1 MOX BRP Fuel 7.4-1
7.4.2.2 Partial BRP Fuel 7.4-2
7.4.2.3 Damaged BRP Fuel 7.4-2

8. OPERATING PROCEDURES 8-1
8.1 Procedures for Loading the Cask in the Spent Fuel Pool 8.1-1
8.1.1 Stage Canister and Transfer Cask 8.1-1
8.1.1.1 Prepare a FuelSolutions™ W74 Canister for Fuel Loading 8.1-1
8.1.1.2 Stage a Transfer Cask 8.1-1
8.1.2 Insert Canister into Transfer Cask 8.1-1
8.1.3 Place Canister and Transfer Cask into Fuel Pool 8.1-1
8.1.4 Load Fuel into Canister 8.1-1
8.1.4.1 Load Damaged Fuel into Damaged Fuel Can 8.1-1
8.1.5 Remove Loaded Cask/Canister from Fuel Pool 8.1-2
8.1.6 Decontaminate Cask Exterior 8.1-2
8.1.7 Install Canister Inner Closure Plate 8.1-2
8.1.8 Drain and Backfill Canister with Helium 8.1-3
8.1.9 Install Canister Outer Closure Plate 8.1-3
8.1.10 Transfer Canister from Transfer Cask to Storage Cask (Horizontally) 8.1-3
8.1.11 Transfer Canister from Transfer Cask to Storage Cask (Vertically) 8.1-3
8.2 Procedures for Unloading the Cask in the Spent Fuel Pool 8.2-1
8.2.1 Retrieve Canister Using Horizontal Canister Transfer 8.2-1

TABLE OF CONTENTS (continued)

Section **Title** **Page**

8.2.2 Retrieve Canister Using Vertical Canister Transfer 8.2-1
8.2.3 Open Canister and Unload Fuel 8.2-1
8.2.4 Horizontal Canister Transfer from a Storage Cask to a Transportation Cask 8.2-1
8.2.5 Horizontal Canister Transfer from a Transfer Cask to a Transportation Cask 8.2-1
8.2.6 Vertical Canister Transfer from a Transfer Cask to a Transportation Cask 8.2-2
8.3 Procedures for Loading the Canister Outside of the Spent Fuel Pool 8.3-1
8.3.1 Stage Canister and Transfer Cask 8.3-1
8.3.1.1 Prepare a FuelSolutions™ W74 Canister for Fuel Loading 8.3-1
8.3.1.2 Stage a Transfer Cask 8.3-1
8.3.2 Prepare Canister and Transfer Cask for Fuel Loading 8.3-1
8.3.3 Load Fuel into the Lower Basket 8.3-2
8.3.4 Load Fuel into the Upper Basket 8.3-3
8.3.5 Decontaminate Cask Exterior 8.3-4
8.3.6 Install Canister Inner Closure Plate 8.3-5
8.3.7 Drain and Backfill Canister with Helium 8.3-5
8.3.8 Install Canister Outer Closure Plate 8.3-5
8.3.9 Transfer Canister from Transfer Cask to Storage Cask (Horizontal Transfer) 8.3-5
8.4 Procedures for Unloading the Cask Outside of the Spent Fuel Pool 8.4-1
8.4.1 Retrieve Canister Using Horizontal Transfer 8.4-1
8.4.2 Retrieve Canister Using Vertical Transfer 8.4-1
8.4.3 Unload Fuel 8.4-1
8.4.3.1 Move Loaded Canister to Cask Loading Area 8.4-1
8.4.3.2 Prepare Canister for Vent and Fill 8.4-1
8.4.3.3 Vent and Fill Canister with Water 8.4-1
8.4.3.4 Remove the Canister Inner and Outer Closure Plates 8.4-1
8.4.3.5 Prepare Canister and Transfer Cask for Fuel Unloading 8.4-2

TABLE OF CONTENTS (continued)

Section **Title** **Page**

8.4.3.6 Remove Fuel from the Upper Basket 8.4-2
8.4.3.7 Remove Fuel from the Lower Basket 8.4-2
8.4.4 Horizontal Canister Transfer from a Storage Cask to a Transportation Cask 8.4-3
8.4.5 Horizontal Canister Transfer from a Transfer Cask to a Transportation Cask 8.4-3
8.4.6 Vertical Canister Transfer from a Transfer Cask to a Transportation Cask 8.4-3
8.5 Preparation of the Cask 8.5-1
8.5.1 Prepare Transfer Cask for Canister Loading 8.5-1
8.5.2 Prepare Storage Cask for Canister Loading 8.5-1

9. ACCEPTANCE CRITERIA AND MAINTENANCE PROGRAM 9-1
9.1 Acceptance Criteria 9.1-1
9.1.1 FuelSolutions™ W74 Canister 9.1-1
9.1.2 Damaged Fuel Can 9.1-1
9.1.3 Visual Inspection and Nondestructive Examination 9.1-8
9.1.3.1 FuelSolutions™ W74 Canister 9.1-8
9.1.3.2 Damaged Fuel Can 9.1-9
9.1.4 Structural 9.1-10
9.1.5 Leak Tests 9.1-11
9.1.6 Criticality Safety 9.1-11
9.1.7 Shielding Integrity 9.1-12
9.1.8 Thermal Acceptance 9.1-12
9.1.9 Components 9.1-13
9.1.9.1 Functional Performance Tests 9.1-13
9.1.9.2 Identification Inspections 9.1-13
9.2 Maintenance Program 9.2-1
9.3 First Cask In Use Requirements 9.3-1

10. RADIATION PROTECTION 10-1

TABLE OF CONTENTS (continued)

Section **Title** **Page**

10.1 Ensuring that Occupational Radiation Exposures Are As Low As Is Reasonably Achievable (ALARA) 10.1-1
10.2 Radiation Protection Design Features 10.2-1
10.3 Estimated On-Site Collective Dose Assessment 10.3-1
10.3.1 FuelSolutions™ W74 Canister-Unique Considerations 10.3-1
10.3.1.1 Canister Design Differences that Affect Occupational Exposures 10.3-1
10.3.1.2 Canister Operations Differences that Affect Occupational Exposures 10.3-1
10.3.2 On-Site Exposure Estimate 10.3-2
10.4 Estimated Off-Site Collective Dose Assessment 10.4-1
10.4.1 Off-Site Dose for Normal Operations 10.4-1
10.4.2 Off-Site Dose for Off-Normal Conditions 10.4-1
10.4.3 Off-Site Dose for Accident Conditions 10.4-1

11. ACCIDENT ANALYSES 11-1
11.1 Off-Normal Operations 11.1-1
11.1.1 Off-Normal Temperature and Insolation Loadings 11.1-1
11.1.1.1 Postulated Cause of the Event 11.1-2
11.1.1.2 Detection of the Event 11.1-2
11.1.1.3 Summary of Event Consequences and Regulatory Compliance 11.1-2
11.1.1.4 Corrective Actions 11.1-2
11.1.2 Off-Normal Internal Pressure 11.1-3
11.1.2.1 Postulated Cause of the Event 11.1-3
11.1.2.2 Detection of the Event 11.1-3
11.1.2.3 Summary of Event Consequences and Regulatory Compliance 11.1-3
11.1.2.4 Corrective Actions 11.1-4
11.1.3 Cask Misalignment During Horizontal Canister Transfer 11.1-4
11.1.3.1 Postulated Cause of the Event 11.1-4

TABLE OF CONTENTS (continued)

Section **Title** **Page**

11.1.3.2 Detection of the Event 11.1-4
11.1.3.3 Summary of Event Consequences and Regulatory Compliance 11.1-5
11.1.3.4 Corrective Actions 11.1-5
11.1.4 Hydraulic Ram Failure During Horizontal Transfer 11.1-5
11.1.4.1 Postulated Cause of the Event 11.1-5
11.1.4.2 Detection of the Event 11.1-6
11.1.4.3 Summary of Event Consequences and Regulatory Compliance 11.1-6
11.1.4.4 Corrective Action 11.1-6
11.1.5 Canister Reopening/Reflood 11.1-6
11.1.5.1 Postulated Cause of the Event 11.1-7
11.1.5.2 Detection of the Event 11.1-7
11.1.5.3 Analysis of Effects and Consequences 11.1-7
11.1.5.4 Corrective Action 11.1-8
11.1.6 Off-Normal Load Combinations 11.1-8
11.2 Accidents 11.2-1
11.2.1 Fully Blocked Storage Cask Inlet and Outlet Vents 11.2-1
11.2.1.1 Postulated Cause of the Event 11.2-2
11.2.1.2 Detection of the Event 11.2-2
11.2.1.3 Summary of Event Consequences and Regulatory Compliance 11.2-2
11.2.1.4 Corrective Action 11.2-3
11.2.2 Storage Cask Drop 11.2-3
11.2.2.1 Postulated Cause of the Event 11.2-3
11.2.2.2 Detection of the Event 11.2-3
11.2.2.3 Summary of Event Consequences and Regulatory Compliance 11.2-3
11.2.2.4 Corrective Action 11.2-4
11.2.3 Storage Cask Tip Over on J-Skid 11.2-4

TABLE OF CONTENTS (continued)

Section **Title** **Page**

11.2.3.1 Postulated Cause of the Event 11.2-4
11.2.3.2 Detection of the Event 11.2-4
11.2.3.3 Summary of Event Consequences and Regulatory Compliance 11.2-4
11.2.3.4 Corrective Action 11.2-5
11.2.4 Transfer Cask Drop 11.2-6
11.2.4.1 Postulated Cause of the Event 11.2-6
11.2.4.2 Detection of the Event 11.2-6
11.2.4.3 Summary of Event Consequences and Regulatory Compliance 11.2-6
11.2.4.4 Corrective Action 11.2-7
11.2.5 Fire 11.2-7
11.2.5.1 Postulated Cause of the Event 11.2-7
11.2.5.2 Detection of the Event 11.2-7
11.2.5.3 Summary of Event Consequences and Regulatory Compliance 11.2-7
11.2.5.4 Corrective Action 11.2-8
11.2.6 Flood 11.2-8
11.2.6.1 Postulated Cause of the Event 11.2-8
11.2.6.2 Detection of the Event 11.2-8
11.2.6.3 Summary of Event Consequences and Regulatory Compliance 11.2-8
11.2.6.4 Corrective Action 11.2-9
11.2.7 Earthquake 11.2-9
11.2.7.1 Postulated Cause of the Event 11.2-9
11.2.7.2 Detection of the Event 11.2-9
11.2.7.3 Summary of Event Consequences and Regulatory Compliance 11.2-10
11.2.7.4 Corrective Action 11.2-10
11.2.8 Accident Internal Pressure 11.2-10
11.2.8.1 Postulated Cause of the Event 11.2-11

TABLE OF CONTENTS (continued)

Section **Title** **Page**

11.2.8.2 Detection of the Event 11.2-11
11.2.8.3 Summary of Event Consequences and Regulatory Compliance 11.2-11
11.2.8.4 Corrective Actions 11.2-11
11.2.9 Accident Condition Load Combinations 11.2-12

12. OPERATING CONTROLS AND LIMITS 12-1
12.1 Proposed Operating Controls and Limits 12.1-1
12.2 Development of Operating Controls and Limits 12.2-1
12.3 Supplemental Data 12.3-1
12.3.1 Technical Specifications and Bases for the FuelSolutions™ W74 Canister 12.3-1

13. QUALITY ASSURANCE 13-1

14. DECOMMISSIONING 14-1

This page intentionally left blank.

LIST OF TABLES

Tables **Title** **Page**

Table 1.0-1 - FuelSolutions™ Storage System FSAR Regulatory Compliance Cross-Reference Matrix (16 pages) 1-9
Table 1.2-1 - Principal Characteristics of the FuelSolutions™ W74 Canister 1.2-17
Table 1.2-2 - Matrix of FuelSolutions™ W74 Canister Configurations 1.2-18
Table 1.2-3 - FuelSolutions™ W74 Canister Fuel Assembly Accommodation 1.2-19
Table 2.0-1 - W74 Canister Design Criteria Summary (7 Pages) 2-2
Table 2.2-1 - Fuel Assemblies Acceptable for Storage in the FuelSolutions™ W74 Canister 2.2-4
Table 2.3-1 - W74 Canister Load Combinations[1, 2] 2.3-9
Table 2.5-1 - ASME Code Requirements Compliance Summary (10 Pages) 2.5-2
Table 3.1-1 - Summary of FuelSolutions™ W74 Canister Component Functions and Design Codes 3.1-11
Table 3.1-2 - W74 Canister Shell Assembly Structural Evaluation Summary (3 Pages) 3.1-12
Table 3.1-3 - W74 Canister Basket Assembly Structural Evaluation Summary (3 Pages) 3.1-15
Table 3.1-4 - Canister Confinement and Subcriticality Component Allowable Stresses 3.1-18
Table 3.1-5 - Canister Shell Assembly Non-Confinement Component Allowable Stresses 3.1-19
Table 3.2-1 - W74 Canister Weights and Centers of Gravity 3.2-2
Table 3.3-1 - FuelSolutions™ W74M Canister Materials Summary 3.3-3
Table 3.3-2 - FuelSolutions™ W74T Canister Material Summary 3.3-4
Table 3.3-3 - Type 316 and Type 304 Stainless Steel Material Properties 3.3-5
Table 3.3-4 - Type 316 Stainless Steel Plastic Material Properties 3.3-6
Table 3.3-5 - Type XM-19 Stainless Steel Material Properties 3.3-6
Table 3.3-6 - SA-36 or A36 Carbon Steel Material Properties 3.3-7
Table 3.3-7 - SA-517, Grades P and F, and A514, Grades P and F Carbon Steel Material Properties 3.3-8
Table 3.3-8 - Neutron Absorber Material Properties 3.3-9
Table 3.3-9 - SA-516, Grades 55 and 60 Carbon Steel Material Properties 3.3-10
Table 3.5-1 - W74 Canister Temperatures for Normal Thermal Conditions 3.5-37
Table 3.5-2 - Comparison of W74 Canister Shell Temperatures for Normal Thermal Conditions 3.5-38
Table 3.5-3 - W74 Engagement Spacer Plate Normal Thermal Temperatures 3.5-39
Table 3.5-4 - W74 Canister Shell Assembly Normal Condition Stress Summary 3.5-40
Table 3.5-5 - W74 Canister Basket Assembly Normal Condition Stress Summary (2 Pages) 3.5-42
Table 3.5-6 - W74 Canister Shell Assembly Normal Load Combination Results 3.5-44
Table 3.5-7 - W74 Canister Basket Assembly Normal Load Combination Results 3.5-46
Table 3.6-1 - W74 Canister Shell Assembly Off-Normal Condition Stress Summary 3.6-8
Table 3.6-2 - W74 Canister Shell Assembly Off-Normal Load Combination Results (2 Pages) 3.6-9
Table 3.7-1 - W74 Canister Shell Assembly Accident Condition Stress Summary 3.7-45
Table 3.7-2 - W74 Canister Basket Assembly Accident Condition Stress Summary 3.7-46
Table 3.7-3 - W74 General Spacer Plate Allowable Buckling Stresses 3.7-47
Table 3.7-4 - W74 LTP Spacer Plate Allowable Buckling Stresses 3.7-48
Table 3.7-5 - W74 General Spacer Plate Tip-Over Stresses and Buckling Interaction Ratios 3.7-49
Table 3.7-6 - W74 Spacer Plate 60*g* Side Drop Elastic Stress Analysis Results 3.7-50
Table 3.7-7 - W74 General Spacer Plate 60*g* Side Drop (No Thermal) Stresses and Buckling Interaction Ratios 3.7-51

LIST OF TABLES (continued)

Table **Title** **Page**

Table 3.7-8 - W74 General Spacer Plate 60*g* Side Drop + Thermal Stresses and Buckling Interaction Ratios 3.7-52
Table 3.7-9 - W74 LTP Spacer Plate 60*g* Side Drop (No Thermal) Stresses and Buckling Interaction Ratios 3.7-53
Table 3.7-10 - W74 LTP Spacer Plate 60*g* Side Drop + Thermal Stresses and Buckling Interaction Ratios 3.7-54
Table 3.7-11 - W74 Canister Shell Assembly Accident Load Combination D1 Results 3.7-55
Table 3.7-12 - W74 Canister Shell Assembly Accident Load Combination D2 Results 3.7-56
Table 3.7-13 - W74 Canister Shell Assembly Accident Load Combination D3 Results 3.7-57
Table 3.7-14 - W74 Canister Shell Assembly Accident Load Combination D4 Results 3.7-58
Table 3.7-15 - W74 Canister Shell Assembly Accident Load Combination D5 Results 3.7-59
Table 3.7-16 - W74 Canister Basket Assembly Accident Load Combination Results 3.7-60
Table 3.9-1 - W74M Lower Basket Assembly Spacer Plate In-Plane Tributary Weights 3.9-21
Table 3.9-2 - W74M Upper Basket Assembly Spacer Plate In-Plane Tributary Weights 3.9-22
Table 3.9-3 - Canister Shell Top Outer Closure Plate Bending Stresses with No Edge Moment Restraint 3.9-23
Table 4.1-1 - Bounding W74 Canister Axial Heat Profile 4.1-11
Table 4.1-2 - Design Basis Thermal Cases for W74 Canister within Storage Cask 4.1-12
Table 4.1-3 - Design Basis Thermal Cases for W74 Canister within Transfer Cask 4.1-13
Table 4.1-4 - W74 Canister Thermal Rating for Storage(1) 4.1-14
Table 4.1-5 - FuelSolutions™ W74 Canister Design Internal Pressures 4.1-14
Table 4.2-1 - W74 Canister Homogenous Material Properties (3 Pages) 4.2-3
Table 4.2-2 - W74 Canister Surface Emissivities 4.2-6
Table 4.2-3 - W74 Canister Material Properties, Fluids 4.2-7
Table 4.3-1 - W74 Canister Component Allowable Temperatures 4.3-7
Table 4.4-1 - W74 Canister Thermal Rating in Storage Cask 4.4-14
Table 4.4-2 - W74 Canister System Temperature at Q_{max} in Storage Cask 4.4-14
Table 4.4-3 - Maximum W74 Canister System Temperature at Q_{max} for Storage(1) 4.4-15
Table 4.4-4 - W74 Canister Normal Conditions Pressure Summary 4.4-16
Table 4.4-5 - Big Rock Point Fuel Normal Pressure Nominal Parameters 4.4-16
Table 4.4-6 - W74 System Temperatures for Normal Transfer(1) 4.4-41
Table 4.4-7 - W74 Canister System Temperatures During Handling(1) 4.4-42
Table 4.4-8 - W74 Canister Pressures for Normal Transfer(1) 4.4-43
Table 4.5-1 - Maximum W74 Canister System Temperature at Q_{max} for Storage(1) 4.5-5
Table 4.5-2 - W74 Canister Off-Normal Pressures 4.5-6
Table 4.5-3 - W74 System Temperatures for Off-Normal Transfer(1) 4.5-10
Table 4.5-4 - W74 Canister Pressures for Off-Normal Transfer at Q_{max}(1) 4.5-11
Table 4.6-1 - W74 Canister System Temperature for All Vents Blocked(1) 4.6-7
Table 4.6-2 - W74 Canister Accident Pressures 4.6-8
Table 4.6-3 - W74 System Temperatures for Postulated Transfer Cask Loss of Neutron Shield Accident(1) 4.6-14
Table 4.6-4 - W74 Canister Peak Temperatures During Transfer Cask Fire Accident(1) 4.6-15
Table 4.7-1 - W74 Damaged Fuel Effective Conductivity 4.7-18
Table 5.1-1 - FuelSolutions™ W74 Canister Shielding Design Features Summary 5.1-3
Table 5.2-1 - Fuel Cooling Table W74-1-A 5.2-4
Table 5.2-2 - Fuel Cooling Table W74-1-B 5.2-5

LIST OF TABLES (continued)

Table **Title** **Page**

Table 5.2-3 - Heat Load Criteria for Constructing the W74 Fuel Cooling Tables 5.2-6
Table 5.2-4 - Burnup-Specific Heat Load Factors 5.2-7
Table 5.2-5 - Burnup-Specific Gamma Factors 5.2-8
Table 5.2-6 - Burnup-Specific Neutron Factors 5.2-9
Table 5.3-1 - FuelSolutions™ W74 Canister Adjoint Model Parameters 5.3-3
Table 5.3-2 - FuelSolutions™ W74 Canister-Specific Regional Densities 5.3-3
Table 5.4-1 - Key W74 Canister Adjoint Model Parameters 5.4-2
Table 5.4-2 - W74 Canister Primary Gamma Adjoint Importance Functions 5.4-3
Table 5.4-3 - W74 Canister Secondary Gamma Adjoint Importance Functions 5.4-4
Table 5.4-4 - W74 Canister Neutron Adjoint Importance Functions 5.4-5
Table 5.5-1 - ORIGEN 2.1 Data for BRP MOX Fuel Assemblies 5.5-8
Table 5.5-2 - BRP MOX Fuel Gamma Source Strengths 5.5-9
Table 5.5-3 - BRP MOX Assembly Total Neutron Source Strengths 5.5-9
Table 5.5-4 - Fuel Cooling Table W74-1-A Domains 5.5-10
Table 5.5-5 - Fuel Cooling Table W74-1-B Domains 5.5-11
Table 6.1-1 - W74 Canister Fuel Specification for Big Rock Point 6.1-3
Table 6.2-1 - Specific Fuel Assembly Parameters 6.2-3
Table 6.3-1 - W74 Basket Model Differences Between Intact, Partial, MOX, and Damaged BRP Assembly Criticality Analyses 6.3-12
Table 6.3-2 - Worst Case Material and Fabrication Tolerances for the FuelSolutions™ W74 Canister 6.3-12
Table 6.3-3 - UO_2 Number Densities as a Function of Enrichment 6.3-13
Table 6.3-4 - Water Number Densities as a Function of Density 6.3-14
Table 6.3-5 - Zircaloy-4 Number Densities 6.3-15
Table 6.3-6 - 304 Stainless Steel Number Densities 6.3-15
Table 6.3-7 - Borated Stainless Steel Number Densities (1.0 w/o natural boron)(1) 6.3-16
Table 6.3-8 - 316 Stainless Steel Number Densities 6.3-16
Table 6.3-9 - 517 P Carbon Steel Number Densities 6.3-17
Table 6.3-10 - XM-19 Stainless Steel Number Densities 6.3-17
Table 6.3-11 - Depleted Uranium Number Densities 6.3-18
Table 6.3-12 - Solid Neutron Shield Number Densities 6.3-18
Table 6.3-13 - Borated Stainless Steel Number Densities (1.25 w/o natural boron)(1) 6.3-19
Table 6.4-1 - MCNP Results for the Canister Design Case Studies 6.4-9
Table 6.4-2 - Material and Fabrication Tolerance Results for the FuelSolutions™ W74 Canister 6.4-10
Table 6.4-3 - Optimum Interspersed Moderator Case Results for the FuelSolutions™ W74 Canister 6.4-11
Table 6.4-4 - Optimum Interior Moderator Case Results for the FuelSolutions™ W74 Canister 6.4-12
Table 6.4-5 - MCNP Results for the Single Package Transportation Cask and the Single Package Transfer Cask 6.4-12
Table 6.4-6 - MCNP Results for the FuelSolutions™ W74 Canister and Big Rock Point Fuel Assemblies with Multiple Fuel Rod Enrichments 6.4-13
Table 6.4-7 - MCNP Results for the FuelSolutions™ W74 Canister and Big Rock Point Fuel Assemblies with Multiple Fuel Rod Enrichments 6.4-14

LIST OF TABLES (continued)

Table **Title** **Page**

Table 6.4-8 - Multiple Package Array, Hypothetical Accident Condition Results to Determine the Bounding Fuel Assembly Configuration....6.4-15
Table 6.4-9 - Big Rock Point Fuel Assembly USL Value Ranges....6.4-15
Table 6.4-10 - Multiple Package Array, Normal Operating Condition Results....6.4-16
Table 6.4-11 - MCNP Results for the Single Package Models....6.4-16
Table 6.5-1 - Benchmark Critical Experiments (2 Pages)....6.5-3
Table 6.6-1 - Uranium Isotope Atom Densities for UO_2 Fuel Rods in BRP MOX Assemblies....6.6-25
Table 6.6-2 - BRP Assembly MOX Fuel Pin Isotope Densities (atom/barn-cm)....6.6-26
Table 6.6-3 - MCNP Calculated Keff Values for W74 Baskets Fully Loaded with BRP MOX Fuel (Full Water Density)....6.6-27
Table 6.6-4 - MCNP Calculated K_{eff} for MOX Fuel vs. W74 Interior Water Density (G-Pu Fuel Assemblies)....6.6-28
Table 6.6-5 - MOX Fuel Benchmark Critical Experiments....6.6-29
Table 6.6-6 - Upper Sub-Critical Limit Formulas for the MOX Only, UO_2 Only, and MOX + UO_2 Sets of Critical Experiments....6.6-30
Table 6.6-7 - Parameter Ranges Covered by Critical Experiments....6.6-31
Table 6.6-8 - Calculated K_{eff} Values for BRP Assemblies with Missing Array Corner Rods....6.6-32
Table 6.6-9 - Calculated K_{eff} vs. Fuel Rod Pitch for 4.1% Enriched GE 9x9 BRP Assembly Fuel Rods (Single Assembly with Full Water Reflection)....6.6-32
Table 6.6-10 - Calculated K_{eff} vs. Fuel Rod Pitch for 4.1% Enriched Siemens 11x11 BRP Assembly Fuel Rods (Single Assembly with Full Water Reflection)....6.6-33
Table 6.6-11 - Calculated K_{eff} for BRP Partial Assemblies at Maximum Allowable Enrichment (Optimum Pitch Fuel Rod Arrays Inside the W74 Canister)....6.6-33
Table 6.6-12 - Physical Parameters and USL Values for the Optimum BRP Fuel Rod Arrays....6.6-34
Table 6.6-13 - Calculated K_{eff} Values for a W74 Canister w/ 8 Damaged Fuel Cans Containing a Square Array of 0.471" Diameter Fuel Cylinders (Guide Tubes Contain Partial 9x9 BRP Assembly Configurations)....6.6-34
Table 6.6-14 - Calculated K_{eff} Values for a W74 Canister w/ 8 Damaged Fuel Cans Containing a Square Array of 0.3715" Diameter Fuel Cylinders (Guide Tubes Contain Partial 9x9 BRP Assembly Configurations)....6.6-35
Table 6.6-15 - Calculated K_{eff} Values for a W74 Canister w/ 8 Damaged Fuel Cans Containing a Hexagonal Array of 0.471" Diameter Fuel Cylinders (Guide Tubes Contain Partial 9x9 BRP Assembly Configurations)....6.6-35
Table 6.6-16 - Calculated K_{eff} Values for a W74 Canister w/ 8 Damaged Fuel Cans Containing a Hexagonal Array of 0.3715" Diameter Fuel Cylinders (Guide Tubes Contain Partial 9x9 BRP Assembly Configurations)....6.6-36
Table 6.6-17 - Calculated K_{eff} Values for a W74 Canister w/ 8 Damaged Fuel Cans Containing a Hexagonal Array of 0.9 cm Diameter Fuel Spheres (Guide Tubes Contain Partial 9x9 BRP Assembly Configurations)....6.6-36
Table 6.6-18 - Calculated K_{eff} Values for a W74 Canister w/ 8 Damaged Fuel Cans Containing a Square Array of 0.3715" Diameter Fuel Cylinders (Guide Tubes Contain Intact 11x11 BRP Assembly Configurations)....6.6-37
Table 6.6-19 - W74 Damaged Assembly 10CFR72 Criticality Margin Calculation (0.655" Pitch Square Array of 0.3715" Diameter Fuel Cylinders in All Damaged Fuel Cans)....6.6-37
Table 6.6-20 - MOX Fuel Isotope Densities (atom/barn-cm)....6.6-38

LIST OF TABLES (continued)

Table **Title** **Page**

Table 6.6-21 - Calculated K_{eff} Values for a W74 Canister w/ 8 Damaged Fuel Cans Containing a Square Array of 0.3715" Diameter MOX Fuel Cylinders (Guide Tubes Contain Partial 9x9 BRP Assembly Configurations) 6.6-38
Table 7.2-1 - Normal Condition Atmospheric Release Doses for FuelSolutions™ W74 Canister(1) 7.2-4
Table 7.2-2 - Off-Normal Condition Atmospheric Release Doses for FuelSolutions™ W74 Canister(1) 7.2-5
Table 7.3-1 - Accident Condition Atmospheric Release Doses for FuelSolutions™ W74 Canister(1) 7.3-4
Table 7.4-1 - Fuel Assembly Surface Area Summary 7.4-4
Table 7.4-2 - Comparison of BRP MOX and Design Basis UO_2 Isotope Activity Levels (Ci/assembly) 7.4-5
Table 8.1-1 - Helium Backfill Gas Quantities for the FuelSolutions™ W74 Canister 8.1-4
Table 9.1-1 - FuelSolutions™ W74 Canister Inspection and Test Acceptance Criteria (3 Pages) 9.1-3
Table 9.1-2 - FuelSolutions™ W74 Canister Damaged Fuel Can Inspection and Test Acceptance Criteria (2 Pages) 9.1-6
Table 10.3-1 - Estimated Cumulative Occupational Exposure for Placing Fuel into Dry Storage 10.3-3
Table 10.3-2 - Estimated Cumulative Occupational Exposure for Retrieval of Fuel from Dry Storage 10.3-4
Table 12.1-1 - Summary of FuelSolutions™ W74 Canister Operating Controls and Limits 12.1-2

This page intentionally left blank.

LIST OF FIGURES

Figures **Title** **Page**

Figure 1.0-1 - FuelSolutions™ Spent Fuel Management System Elements 1-7
Figure 1.0-2 - FuelSolutions™ Storage System Certification Application Approach 1-8
Figure 1.2-1 - FuelSolutions™ Spent Fuel Management System 1.2-20
Figure 1.2-2 - FuelSolutions™ W74 Canister 1.2-21
Figure 1.2-3 - FuelSolutions™ W74 Canister Top and Bottom Closure 1.2-22
Figure 1.2-4 - Canister Fuel Loading Using Fuel Assembly Shuttle Cask and Shielded Loading Collar 1.2-23
Figure 1.2-5 - Shielded Loading Collar 1.2-24
Figure 1.2-6 - Fuel Loading of Lower Basket 1.2-25
Figure 2.5-1 - Original Closure Configuration 2.5-17
Figure 2.5-2 - Original Shield Plug-to-Canister Shell Weld Configuration 2.5-18
Figure 2.5-3 - Modified Canister Closure and Weld Configuration 2.5-20
Figure 2.5-4 - Modified Canister Shell Chamfer 2.5-20
Figure 2.5-5 - Localized Reduction of Top Shield Plug Outside Diameter 2.5-21
Figure 2.5-6 - Modified Top Shield Plug Design 2.5-21
Figure 2.5-7 - Enhanced Canister Closure Design Configuration 2.5-22
Figure 2.5-8 - Reduction of Shell "Draw-in" 2.5-23
Figure 2.5-9 - FuelSolutions™ Canister Closure Design 2.5-24
Figure 2.5-10 - VSC-24 Top Closure Configuration 2.5-26
Figure 2.5-11 - Outside Shell Chamfer and J-Bevel Weld Prep Nose Challenges to Angle Beam UT Examination 2.5-30
Figure 2.5-12 - Outer Closure Plate-to-Canister Shell Offset Challenge to Angle Beam UT Examination 2.5-30
Figure 2.5-13 - Weld Crown (Reinforcement) Challenge to Straight Beam UT Examination 2.5-31
Figure 2.5-14 - Outer Closure Plate Lower Chamfer and J-Bevel Weld Prep Nose Challenges to Straight Beam UT Examination 2.5-31
Figure 2.5-15 - Outer Closure Plate-to-Canister Shell Offset Challenge to Straight Beam UT Examination 2.5-32
Figure 2.5-16 - Canister Shell Chamfer and J-Bevel Weld Prep Nose Challenges to Angle Beam UT Examination 2.5-32
Figure 2.5-17 - Canister Shell Chamfer and J-Bevel Weld Prep Nose Challenges to Straight Beam UT Examination 2.5-33
Figure 3.1-1 - Expanded View of FuelSolutions™ W74M Canister 3.1-20
Figure 3.1-2 - Expanded View of FuelSolutions™ W74T Canister 3.1-21
Figure 3.1-3 - FuelSolutions™ W74 Canister Support Tube Assembly Detail 3.1-22
Figure 3.1-4 - FuelSolutions™ W74 Damaged Fuel Can 3.1-23
Figure 3.2-1 - FuelSolutions™ W74 Canister Center of Gravity Diagram 3.2-3
Figure 3.3-1 - Type 316 Stainless Steel Plastic Stress-Strain Curve at 715°F 3.3-11
Figure 3.4-1 - W74 Damaged Fuel Can Top Lid Assembly Base Plate ¼-Symmetry Finite Element Model 3.4-9
Figure 3.4-2 - Free Body Diagram of Attachment Dog for Vertical Lift 3.4-10
Figure 3.4-3 - W74 Damaged Fuel Can Top Lid Base Plate Vertical Lift Stress Intensity Contour Plot 3.4-11
Figure 3.5-1 - Canister Shell Axial Temperature Distribution for the Bounding Normal Thermal Condition 3.5-48

LIST OF FIGURES (continued)

Figure **Title** **Page**

Figure 3.5-2 - W74 Canister Support Tube and End Spacer Plate Curvature due to Lateral Thermal Gradient 3.5-49
Figure 3.7-1 - Guide Tube End Drop Buckling Boundary Conditions 3.7-62
Figure 3.7-2 - W74 Spacer Plate Design Thermal Gradient 3.7-63
Figure 3.7-3 - W74 General Spacer Plate Longitudinal Displacement For Tip-Over (45*g*) plus Thermal Plastic Instability Analysis 3.7-64
Figure 3.7-4 - W74 General Spacer Plate and LTP Spacer Plate Side Drop Impact Orientations 3.7-65
Figure 3.7-5 - W74 General and LTP Spacer Plate Side Drop Loading Diagram 3.7-66
Figure 3.7-6 - W74 General Spacer Plate Longitudinal Displacement For 45° Side Drop (90*g*) plus Thermal Plastic Instability Analysis 3.7-67
Figure 3.7-7 - W74 Engagement Spacer Plate Side Drop Impact Orientations 3.7-68
Figure 3.7-8 - W74 Canister Support Tube On-Site Transport Loading Diagram 3.7-69
Figure 3.7-9 - W74 Guide Tube 60*g* Side Drop Loads for Concentrated Fuel Grid Spacer Loading Evaluation 3.7-70
Figure 3.7-10 - W74 Guide Tube 60*g* Side Drop Plastic Strain for Concentrated Load at Fuel Assembly Grid Spacer 3.7-71
Figure 3.7-11 - W74 Guide Tube 60*g* Side Drop Permanent Deformation for Concentrated Load at Fuel Assembly Grid Spacer 3.7-72
Figure 3.9-1 - Bounding Canister Shell Assembly Axisymmetric Finite Element Model 3.9-24
Figure 3.9-2 - Canister Shell Half-Symmetry Finite Element Model 3.9-25
Figure 3.9-3 - Canister Shell Assembly Half-Symmetry Finite Element Model, Shell Assembly Mesh 3.9-26
Figure 3.9-4 - Canister Shell Assembly Half-Symmetry Finite Element Model - Spacer Plate Mesh and Loading 3.9-27
Figure 3.9-5 - W74 Top Shield Plug Assembly Quarter-Symmetry Vertical Deadweight Finite Element Model 3.9-28
Figure 3.9-6 - W74 Top Shield Plug Quarter-Symmetry Model Adjusted Density Regions 3.9-29
Figure 3.9-7 - W74 Canister General and LTP Spacer Plate Plane Stress Finite Element Model 3.9-30
Figure 3.9-8 - W74 Canister General and LTP Spacer Plate Shell Model for Thermal Bending Stress Analysis 3.9-31
Figure 3.9-9 - W74 Canister General Spacer Plate Half-Symmetry Multi-Span Shell Model for Tip-Over and 0° Side Drop Plastic Instability Analyses 3.9-32
Figure 3.9-10 - W74 General Spacer Plate Half-Symmetry Multi-Span Shell Finite Element Model Boundary Conditions 3.9-33
Figure 3.9-11 - W74 General Spacer Plate Half-Symmetry Multi-Span Shell Finite Element Model Applied Loads 3.9-34
Figure 3.9-12 - W74 General Spacer Plate Full Multi-Span Shell Finite Element Model for 45° Side Drop Plastic Instability Analysis 3.9-35
Figure 3.9-13 - W74 General Spacer Plate Full Multi-Span Shell Finite Element Model Applied Loads for 45° Side Drop 3.9-36
Figure 3.9-14 - W74 Engagement Spacer Plate Bottom End Drop Quarter-Symmetry Finite Element Model 3.9-37
Figure 3.9-15 - W74 Engagement Spacer Plate End Drop Loading Regions 3.9-38
Figure 3.9-16 - W74 Engagement Spacer Plate Half-Symmetry Plane Stress Finite Element Model 3.9-39

LIST OF FIGURES (continued)

Figure **Title** **Page**

Figure 3.9-17 - W74 Engagement Spacer Plate Full Plane Stress Finite Element Model 3.9-40
Figure 3.9-18 - W74 Guide Tube Half-Symmetry Single Span Finite Element Model 3.9-41
Figure 3.9-19 - W74 Guide Tube Half-Symmetry Multi-Span Finite Element Model 3.9-42
Figure 3.9-20 - W74 General and LTP Spacer Plate Stress Evaluation Sections 3.9-43
Figure 3.9-21 - Canister Shell Stress Evaluation Locations, Top and Bottom End Region 3.9-44
Figure 3.9-22 - Canister Shell Stress Evaluation Locations, Cavity Region 3.9-45
Figure 4.1-1 - Design Basis Axial Heat Profiles for W74 and Generic BWR Canister Analysis 4.1-15
Figure 4.3-1 - W74 Canister Heat Load (Q_{max}) vs. Temperature 4.3-8
Figure 4.3-2 - Big Rock Point BWR Fuel Decay Heat Curve 4.3-9
Figure 4.3-3 - Big Rock Point Temperature Decay Curves 4.3-10
Figure 4.4-1 - FuelSolutions™ W74M Canister Thermal Submodel Layout 4.4-17
Figure 4.4-2 - Node Layout for W74 Canister Bottom End 4.4-18
Figure 4.4-3 - Typical Node Layout Between W74 Spacer Plates 4.4-19
Figure 4.4-4 - Node Layout for W74 Canister Fuel Load Configuration 4.4-19
Figure 4.4-5 - Typical Node Layout for W74 Spacer Plate 4.4-20
Figure 4.4-6 - Isometric View of Node Layout Between Typical Set of W74 Spacer Plates 4.4-21
Figure 4.4-7 - Node Layout for W74 Canister Mid-Body Section 4.4-22
Figure 4.4-8 - Node Layout for W74 Top End 4.4-23
Figure 4.4-9 - Gas Node Layout for Vertical W74 Canister 4.4-24
Figure 4.4-10 - Modeled Flow Pattern within Vertical W74 Canister 4.4-25
Figure 4.4-11 - Thermal Submodel Alignment for Storage Cask and W74 Canister 4.4-26
Figure 4.4-12 - W74 Canister Axial Temperature Distribution for Normal Hot Condition in Storage Cask at Q_{max} 4.4-27
Figure 4.4-13 - W74 Canister Axial Temperature Distribution for Normal Cold Condition in Storage Cask at Q_{max} 4.4-28
Figure 4.4-14 - W74 Spacer Plate Temperature Distribution for Normal Hot Condition in Storage Cask at Q_{max} 4.4-29
Figure 4.4-15 - W74 Spacer Plate Temperature Distribution for Normal Cold Condition in Storage Cask at Q_{max} 4.4-29
Figure 4.4-16 - W74 Canister Heat Balance for Normal Hot Storage Conditions at Q_{max} 4.4-30
Figure 4.4-17 - Assumed Flow Pattern within Horizontal Canister 4.4-44
Figure 4.4-18 - Typical Spacer Plate Axial Temperature Distribution Prior to Reflood (with 4 hours of cooling) 4.4-45
Figure 4.4-19 - Clad Thermal Stress During Core Reflooding 4.4-45
Figure 4.4-20 - Canister Pressure During Limiting Spacer Plate Quenching 4.4-46
Figure 4.4-21 - W74 Canister Axial Temperature Distribution for Normal Hot Transfer Condition at Q_{max} 4.4-47
Figure 4.4-22 - W74 Canister Axial Temperature Distribution for Normal Cold Transfer Condition at Q_{max} 4.4-47
Figure 4.4-23 - W74 Spacer Plate Temperature Distribution for Normal Hot Transfer Condition at Q_{max} 4.4-48
Figure 4.4-24 - W74 Spacer Plate Temperature Distribution for Normal Cold Transfer Condition at Q_{max} 4.4-49
Figure 4.4-25 - Transfer Cask Handling (Case 10) Transient at Q_{max} 4.4-50
Figure 4.4-26 - W74 Canister Heat Balance within the Transfer Cask for Normal Hot Transfer Conditions at Q_{max} 4.4-51

LIST OF FIGURES (continued)

Figure **Title** **Page**

Figure 4.5-1 - W74 Canister/Storage Cask Temperatures During Horizontal Unload Transient (26.4 kW) 4.5-7
Figure 4.5-2 - Generic Canister Loading Cycle Temperature Histogram For Vertical Transfer 4.5-12
Figure 4.6-1 - Storage Cask all Vents Blocked Transient with W74 Canister 4.6-9
Figure 4.6-2 - Storage Cask and Canister Response To 5 Minute Engulfing Fire 4.6-10
Figure 4.6-3 - Storage Cask and Canister Response To 5 Minute Inlet Vent Fire 4.6-10
Figure 4.6-4 - Canister and Transfer Cask Fire Accident Temperature Response (0-10 minutes) 4.6-16
Figure 4.6-5 - Canister and Transfer Cask Fire Accident Temperature Response (0-2 hours) 4.6-16
Figure 4.7-1 - Gas Node and Flow Pattern in Horizontal Canister 4.7-19
Figure 4.7-2 - Circulation Pattern within NUHOMS® 24 Unit DSC 4.7-20
Figure 4.7-3 - Temperature Distribution in NUHOMS® 24 Unit Basket 4.7-21
Figure 4.7-4 - Double Open-ended Cavity with Two Heated Walls 4.7-21
Figure 4.7-5 - Average Cavity Nusselt Number as a Function of Rayleigh Number and Aspect Ratio 4.7-22
Figure 4.7-6 - Gas Node Layout for Vertical Canister 4.7-23
Figure 4.7-7 - Flow Pattern for Vertical Canister 4.7-24
Figure 4.7-8 - Effect of Reconfigured Damaged Fuel On W74 Canister Temperatures, Storage Conditions 4.7-25
Figure 4.7-9 - Effect of Reconfigured Damaged Fuel On W74 Canister Temperatures, Transfer Conditions 4.7-26
Figure 5.3-1 - FuelSolutions™ W74 Canister Adjoint Model 5.3-4
Figure 6.3-1 - FuelSolutions™ W74 Basket Model for Intact Assembly Analyses (Nominal Dimensions) 6.3-20
Figure 6.3-2 - FuelSolutions™ W74 Basket Model for MOX and Damaged Assembly Analyses (Nominal Dimensions) 6.3-21
Figure 6.3-3 - FuelSolutionsTM W74 Basket Model for Partial Assembly Analyses (Nominal Dimensions) 6.3-22
Figure 6.3-4 - W74 Damaged Fuel Can Configuration 6.3-23
Figure 6.3-5 - FuelSolutions™ W74 Type A Guide Tube Assembly (Nominal Dimensions) 6.3-24
Figure 6.3-6 - FuelSolutions™ W74 Type B Guide Tube Assembly (Nominal Dimensions) 6.3-25
Figure 6.3-7 - FuelSolutions™ W74 Shell Assembly and Transport Cask 6.3-26
Figure 6.3-8 - Horizontal Cross-Section of MCNP Model 6.3-27
Figure 6.3-9 - Side View of Lower Portion of FuelSolutions™ W74 Hypothetical Accident Conditions Model (cut-away) 6.3-28
Figure 6.3-10 - Side View of Middle Portion of the FuelSolutions™ W74 Hypothetical Accident Conditions Model (cut-away) 6.3-29
Figure 6.3-11 - Side View of Upper Portion of the FuelSolutions™ W74 Hypothetical Accident Conditions Model (cut-away) 6.3-30
Figure 6.3-12 - FuelSolutions™ W74 Fuel Pattern No. 1 Basket Configuration 6.3-31
Figure 6.3-13 - FuelSolutions™ W74 Pattern No. 2 Basket Configuration 6.3-32
Figure 6.3-14 - FuelSolutions™ W74 Pattern No. 3 Basket Configuration 6.3-33
Figure 6.3-15 - Side View of Lower Portion of FuelSolutions™ W74 Normal Conditions Model (cut-away) 6.3-34
Figure 6.3-16 - Side View of Middle Portion of FuelSolutions™ W74 Normal Conditions Model (cut-away) 6.3-35

LIST OF FIGURES (continued)

Figure **Title** **Page**

Figure 6.3-17 - Side View of Upper Portion of the FuelSolutions™ W74 Normal Conditions Model (cut-away) 6.3-36
Figure 6.4-1 - Multiple Pin Enrichment Pattern 1 for the Big Rock Point GE 9x9 Fuel 6.4-17
Figure 6.4-2 - Multiple Pin Enrichment Pattern 2 for the Big Rock Point GE 9x9 Fuel Assembly. 6.4-18
Figure 6.4-3 - Multiple Pin Enrichment Pattern 3 for the Big Rock Point GE 9x9 Fuel Assembly 6.4-19
Figure 6.4-4 - Multiple Pin Enrichment Pattern 4 for the Big Rock Point Siemens 9x9 Fuel Assembly 6.4-20
Figure 6.4-5 - Multiple Pin Enrichment Pattern 1 for the Big Rock Point Siemens 11x11 Fuel Assembly 6.4-21
Figure 6.4-6 - Multiple Pin Enrichment Pattern 2 for the Big Rock Point Siemens 11x11 Fuel Assembly 6.4-22
Figure 6.4-7 - Multiple Pin Enrichment Pattern 3 for the Big Rock Point Siemens 11x11 Fuel Assembly 6.4-23
Figure 6.4-8 - Multiple Pin Enrichment Pattern 4 for the Big Rock Point Siemens 11x11 Fuel Assembly 6.4-24
Figure 6.6-1 - J2 (9x9) BRP MOX Assembly Array 6.6-39
Figure 6.6-2 - DA (11x11) BRP MOX Assembly Array 6.6-40
Figure 6.6-3 - G-Pu (11x11) BRP MOX Assembly Array 6.6-41
Figure 6.6-4 - UO_2 9x9 BRP Assembly with Two Inserted MOX Rods 6.6-42
Figure 6.6-5 - D72 Partial Assembly Array - J2 Assembly Type 6.6-43
Figure 6.6-6 - D73 Partial Assembly Array - J2 Assembly Type 6.6-44
Figure 6.6-7 - G01 Partial Assembly Array - G-Pu Assembly Type 6.6-45
Figure 6.6-8 - G02 Partial Assembly Array - G-Pu Assembly Type 6.6-46
Figure 6.6-9 - K_{eff} vs. H-to-^{235}U Ratio for GE 9x9 BRP Fuel Rod Arrays (Single Assembly Sized Fuel Rod Array with Full Water Reflection) 6.6-47
Figure 6.6-10 - K_{eff} vs. H-to-^{235}U Ratio for Siemens 11x11 BRP Fuel Rod Arrays (Single Assembly Sized Fuel Rod Array with Full Water Reflection) 6.6-48
Figure 6.6-11 - K_{eff} vs. H / ^{235}U Ratio for a Square Array of 0.471" Diameter Fuel Cylinders 6.6-49
Figure 6.6-12 - K_{eff} vs. H / ^{235}U Ratio for a Square Array of 0.3715" Diameter Fuel Cylinders 6.6-50
Figure 6.6-13 - K_{eff} vs. H / ^{235}U Ratio for a Hexagonal Array of 0.471" Diameter Fuel Cylinders 6.6-51
Figure 6.6-14 - K_{eff} vs. H / ^{235}U Ratio for a Hexagonal Array of 0.3715" Diameter Fuel Cylinders 6.6-52
Figure 6.6-15 - K_{eff} vs. H / ^{235}U Ratio for a Hexagonal Array of 0.9 cm Diameter Fuel Spheres 6.6-53
Figure 6.6-16 - W74 Canister k_{eff} vs. Damaged Fuel Can Interior and Canister Interior Moderator Densities 6.6-54
Figure 7.1-1 - FuelSolutions™ Canister Confinement Boundaries 7.1-5
Figure 7.2-1 - Normal Condition Atmospheric Release Dose vs. Distance for FuelSolutions™ W74 Canister 7.2-6
Figure 7.2-2 - Off-Normal Condition Atmospheric Release Dose vs. Distance for FuelSolutions™ W74 Canister 7.2-7
Figure 7.3-1 - Accident Condition Atmospheric Release Dose vs. Distance for FuelSolutions™ W74 Canister 7.3-5

LIST OF FIGURES (continued)

Figure **Title** **Page**

Figure 8.0-1 - Operations Flow Diagram to Place Fuel into Dry Storage in a FuelSolutions™ W74 Canister at Sites with Limited Cask Handling Crane Capacities 8-2
Figure 8.0-2 - Operations Flow Diagram to Retrieve Fuel from Dry Storage and Remove from a FuelSolutions™ W74 Canister at Sites with Limited Cask Handling Crane Capacities 8-3
Figure 8.0-3 - Operations Flow Diagram to Place a Loaded FuelSolutions™ W74 Canister in a Transportation Cask at Sites with Limited Cask Handling Crane Capacities 8-4
Figure 8.3-1 - Sequence for Loading a FuelSolutions™ W74 Canister Outside of the Spent Fuel Pool 8.3-6
Figure 8.4-1 - Sequence for Unloading Fuel Outside of the Spent Fuel Pool 8.4-4

ACRONYMS AND ABBREVIATIONS

ACI	American Concrete Institute
ACTL	Activation Library
AISC	American Institute of Steel Construction
ALARA	As Low As Reasonably Achievable
ANS	American Nuclear Society
ANSI	America National Standards Institute
ASCE	American Society of Civil Engineers
ASME	American Society of Mechanical Engineers
ASME Code	ASME B&PV Code
ASTM	American Society of Testing and Materials
AWS	American Welding Society
AW/OS	Automated Welding/Opening System
B&PV Code or BPVC	Boiler and Pressure Vessel Code
BRL	Ballistic Research Laboratory
BRP	Big Rock Point
BU	Burnup
BWR	Boiling Water Reactor
C of C	Certificate of Compliance
CE	Combustion Engineering
CFR	Code of Federal Regulation
CG	Center of Gravity
CGA	Compressed Gas Association
CISF	Centralized Interim Storage Facility
CMAA	Crane Manufacturers Association of America
CMTR	Certified Material Test Report
CNFD	Commercial Nuclear Fuel Division
CRUD	Chalk River Unidentified Deposits (debris/residues)
CRWMS	Civilian Radioactive Waste Management System
CS	Carbon Steel
DAR	Design Analysis Report
DBE	Design Basis Earthquake

ACRONYMS AND ABBREVIATIONS

DBT	Design Basis Tornado
DBW	Design Basis Wind
DCCG	Diffusion Controlled Cavity Growth
DFD	Design for Disassembly
DLF	Dynamic Load Factor
DM	Design Margins
DOE	U.S. Department of Energy
DU	Depleted Uranium
ENDF	Evaluated Nuclear Data File
ENDL	Evaluated Nuclear Data Library
EPFM	Elastic-Plastic Fracture Mechanics
EPRI	Electric Power Research Institute
ESBU	Westinghouse Energy Systems Business Unit
FSAR	Final Safety Analysis Report
FuelSolutions™ System	BNFL Fuel Solutions Spent Fuel Management System (formerly referred to as the Wesflex™ System)
GE	General Electric
GTCC	Greater than Class C
GTSD	Government Technical Services Division
HAC	Hypothetical Accident Condition
HCN	United States Historical Climatology Network
HEPA	High Efficiency Particulate Air
HVAC	Heating, Ventilating, and Air Conditioning
ISFSI	Independent Spent Fuel Storage Installation
ISI	Inservice Inspection
ITS	Important to Safety
LLNL	Lawrence Livermore National Laboratory
LOCA	Loss-of-Coolant Accident
LSA	Low Specific Activity
LTP	Long-Term Performance
LWR	Light Water Reactor

ACRONYMS AND ABBREVIATIONS

MGDS	Mined Geological Disposal Site
MOX	Mixed Oxide
MPC	Multi-Purpose Canister
MRC	Material Review Committee
MRS	Monitored Retrievable Storage
MT	Magnetic Particle Examination
M&TE	Measuring and Testing Equipment/Instrumentation
NA or N/A	Not Applicable
NCT	Normal Conditions of Transport
NDE or NDT	Non-Destructive Examination or Testing
NDRC	National Defense Research Council
NFC	Non-fuel Components
NFPA	National Fire Protection Association
NIAC	Nuclear Industry Assessment Committee
NITS	Not Important to Safety
NLTP	Non-Long-Term Performance
NOAA	National Oceanographic and Atmospheric Agency
NP	Non-Proprietary
NPT	National Pipe Thread
NRC	U.S. Nuclear Regulatory Commission
OCRWM	Office of Civilian Radioactive Waste Management
PC	Personal Computer
PT	Liquid Penetrant Examination
PWR	Pressurized Water Reactor
QA	Quality Assurance
QMS	Quality Management System
RC	Reinforced Concrete
RG	Regulatory Guide
RT	Radiographic Examination
SAE	Society of Automotive Engineers
SAR	Safety Analysis Report

ACRONYMS AND ABBREVIATIONS

SER	Safety Evaluation Report
SFMS	Spent Fuel Management System
SNF	Spent Nuclear Fuel
SRP	Standard Review Plan
SRSS	Square Root Sum of the Squares
SS	Stainless Steel
SSC	Structures, Systems, and Components
TEDE	Total Effective Dose Equivalent
TSC	Transportable Storage Canister
U.S.	United States
UT	Ultrasonic Examination
VDS	Vacuum Drying System
VT	Visual Inspection
WELCO	Westinghouse Electric Company
Wesflex™ System	Former name of the FuelSolutions™ System (any reference to Wesflex™ shall be taken to mean FuelSolutions™)
ZPA	Zero Period Acceleration

1. GENERAL DESCRIPTION

Overview

This Final Safety Analysis Report (FSAR) provides the technical basis for the design, fabrication, and operation of the FuelSolutions™ W74 canister, which is an integral component of the FuelSolutions™ Spent Fuel Management System (SFMS). In conjunction with the FuelSolutions™ Storage System FSAR, this FuelSolutions™ W74 Canister Storage FSAR serves to demonstrate compliance with the applicable requirements of 10CFR72.[1] The FuelSolutions™ W74 canister has a capacity of up to 64 Big Rock Point (BRP) Boiling Water Reactor (BWR) spent fuel assemblies. There are an additional 10 cell locations in the FuelSolutions™ W74 canister that are mechanically blocked to prevent fuel assembly loading and are not used. The FuelSolutions™ W74 canister, as described and analyzed in the subsequent chapters of this FSAR, is used to safely dry store spent nuclear fuel (SNF) on-site in an Independent Spent Fuel Storage Installation (ISFSI), in accordance with the requirements of 10CFR72, and subsequently be transported off-site, in accordance with 10CFR71.[2]

The FuelSolutions™ SFMS is a fully integrated, canister-based system that provides for the storage and transport of a broad range of SNF assembly classes. The elements of the FuelSolutions™ SFMS are shown in Figure 1.0-1. The "Storage System" components of the FuelSolutions™ SFMS include the FuelSolutions™ W74 canister described in this FuelSolutions™ Canister Storage FSAR, the FuelSolutions™ storage cask and transfer cask, described in the FuelSolutions™ Storage System FSAR,[3] and various other FuelSolutions™ canisters described in their respective FuelSolutions™ Canister Storage FSARs. Taken together, these FSARs are intended to demonstrate compliance with the applicable portions of 10CFR72, Subpart L, for generic certification of the FuelSolutions™ Storage System. The organization of the FuelSolutions™ storage FSARs is shown schematically in Figure 1.0-2.

This FSAR also identifies the FuelSolutions™ SFMS support equipment that interfaces with and is unique to the FuelSolutions™ W74 canister for use at the BRP plant. The balance of the FuelSolutions™ SFMS support equipment is described further in the FuelSolutions™ Storage System FSAR.

The FuelSolutions™ W74 canister is classified as "important to safety" in accordance with 10CFR72, Subpart G. The safety classification of other FuelSolutions™ Storage System components and equipment is discussed in the FuelSolutions™ Storage System FSAR. Safety analyses for on-site dry storage conditions are provided only for the FuelSolutions™ W74 canister in this FSAR. Safety analyses for other FuelSolutions™ canisters are provided in their respective FuelSolutions™ Canister Storage FSARs. Safety analysis for the FuelSolutions™ storage cask and transfer cask are provided in the FuelSolutions™ Storage System FSAR.

---

[1] Title 10, U.S. Code of Federal Regulations, Part 72 (10CFR72), *Licensing Requirements for the Independent Storage of Spent Nuclear Fuel and High-Level Radioactive Waste*, 1995.

[2] Title 10, U.S. Code of Federal Regulations, Part 71 (10CFR71), *Packaging and Transportation of Radioactive Materials*, 1996.

[3] WSNF-220, *FuelSolutions™ Storage System Final Safety Analysis Report*, NRC Docket No. 72-1026, BNFL Fuel Solutions Corporation.

By this FSAR and its companion FuelSolutions™ Storage System FSAR, generic certification of the FuelSolutions™ Storage System is sought by BNFL Fuel Solutions Corporation (BFS) in accordance with 10CFR72, Subpart L. Upon review and acceptance by the U.S. Nuclear Regulatory Commission (NRC), the resulting Safety Evaluation Report (SER) and Certificate of Compliance (C of C) would include the FuelSolutions™ W74 canister, in conjunction with the reviewed and approved FuelSolutions™ storage cask and transfer cask for on-site dry storage of SNF at an ISFSI. The then certified FuelSolutions™ Storage System may be implemented by the licensee in accordance with the general license provisions of 10CFR72, Subpart K. The NRC-approved FuelSolutions™ storage FSARs may also be used as a reference in site-specific license applications, in accordance with 10CFR72, Subpart B.

The generic design basis and the corresponding safety analysis of the FuelSolutions™ Storage System contained in this FuelSolutions™ W74 Canister Storage FSAR and the FuelSolutions™ Storage System FSAR are intended to bound the SNF characteristics, design conditions, and interfaces that exist at the vast majority of domestic power reactor sites and potential away-from-reactor storage sites in the contiguous United States. In addition, the FuelSolutions™W74 canister is designed for the plant-specific conditions and interfaces that exist at the BRP Plant.

These FuelSolutions™ storage FSARs also provide the basis for component fabrication and acceptance, and the requirements for safe operation and maintenance of the FuelSolutions™ Storage System components, consistent with the design basis and safety analysis documented herein. In accordance with 10CFR72, Subpart K, site-specific implementation of the generically certified FuelSolutions™ Storage System requires that the licensee perform a site-specific safety evaluation, as defined in 10CFR72.212. The FuelSolutions™ Storage System FSAR identifies a limited number of conditions that are necessarily site-specific and are to be addressed in the licensee's 10CFR72.212 evaluation. These include:

- Siting of the ISFSI and design of the storage pad and security system. Site-specific demonstration of compliance with regulatory dose limits. Implementation of a site-specific ALARA program.
- An evaluation of site-specific hazards and design conditions that may exist at the ISFSI site or the transfer route between the plant's cask receiving bay and the ISFSI. These include but are not limited to explosion and fire hazards, flooding conditions, volcanism, land slides, and lightning protection.
- Determination that the physical and nucleonic characteristics and the condition of the SNF assemblies to be dry stored meet the fuel acceptance requirements of *technical specifications* contained in the C of C.
- An evaluation of interface and design conditions that exist within the plant's fuel building in which canister fuel loading, canister closure, and canister transfer operations are to be conducted in accordance with the applicable 10CFR50[4] requirements and *technical specifications* for the plant.

[4] Title 10, U.S. Code of Federal Regulations, Part 50 (10CFR50), *Domestic Licensing of Production and Utilization Facilities*, 1995.

- Detailed site-specific operating, maintenance, and inspection procedures prepared in accordance with the generic procedures provided in the FuelSolutions™ storage FSARs and the *technical specifications* contained in the C of C.
- Performance of pre-operational testing.
- Implementation of a safeguards and accountability program in accordance with 10CFR73.[5] Preparation of a physical security plan in accordance with 10CFR73.55.
- Review of the reactor emergency plan, quality assurance program, training program, and radiation protection program.

The generic safety analyses contained in the FuelSolutions™ storage FSARs may be used as input and for guidance by the licensee in performing a 10CFR72.212 evaluation.

Licensing Approach

BFS has elected to use a modular approach to organization of the FuelSolutions™ storage FSARs, as illustrated in Figure 1.0-2, which separates the system elements that are common to all canisters from those that are canister-specific. In addition, the generic system descriptions, design criteria, and analysis methodologies applicable to the safety evaluations performed for all system components are included in the FuelSolutions™ Storage System FSAR, to the maximum extent possible. Similarly, the generic operating procedures, maintenance requirements, *technical specifications*, and quality assurance requirements applicable to all system components are included in the FuelSolutions™ Storage System FSAR. Chapters 1 through 14 of this FuelSolutions™ W74 Canister Storage FSAR contain the following information:

1. A description of the FuelSolutions™ W74 canister, including the canister contents.
2. The design criteria specific to the FuelSolutions™ W74 canister and its contents.
3. The structural design and analysis of the FuelSolutions™ W74 canister for all loading conditions.
4. The thermal design and analysis of the FuelSolutions™ W74 canister and its contents for all design conditions.
5. Tabulation of the acceptable cooling times for each enrichment and burnup combination for the SNF assemblies qualified to be loaded into the FuelSolutions™ W74 canister. The shielding design and analysis for any FuelSolutions™ W74 canister-unique conditions and the resulting component dose rates.
6. The criticality safety analysis for the FuelSolutions™ W74 canister and tabulation of the maximum acceptable initial enrichment for each SNF assembly class qualified to be loaded into the canister.
7. Reference to the methodology used for analysis of a postulated radiological release from a FuelSolutions™ canister for various conditions, including the radionuclide release fractions contained in the FuelSolutions™ Storage System FSAR. The confinement features and the resulting postulated accident dose rates for the FuelSolutions™ W74 canister.

[5] Title 10, U.S. Code of Federal Regulations, Part 73 (10CFR73), *Physical Protection of Plants and Materials*, 1995.

8. Operating procedures that are unique to the FuelSolutions™ W74 canister design.
9. The acceptance criteria and maintenance requirements applicable to the FuelSolutions™ W74 canister.
10. Reference to the radiation protection features of the canister, representative occupational exposure estimates, and sample ISFSI dose estimates contained in the FuelSolutions™ Storage System FSAR. Descriptions of the radiation protection features that are unique to the FuelSolutions™ W74 canister design and the associated occupational exposure estimates.
11. The accident analyses for the FuelSolutions™ W74 canister.
12. The *technical specifications* that are unique to the FuelSolutions™ W74 canister, including the SNF assembly acceptance specification.
13. Reference to the quality assurance requirements contained in the FuelSolutions™ Storage System FSAR.
14. Reference to the decommissioning assessment for the FuelSolutions™ Storage System components contained in the FuelSolutions™ Storage System FSAR.

Chapters 1 through 14 of the FuelSolutions™ Storage System FSAR contain the following information:

1. Identification of all FuelSolutions™ Storage System components and support equipment. Descriptions of the FuelSolutions™ W150 Storage Cask and W100 Transfer Cask. Summary descriptions of all support equipment that is not unique to a particular canister design, if any.
2. The design criteria applicable to all FuelSolutions™ Storage System components including canister interface requirements, but excluding those specifically related to canister contents or the canister itself. The safety protection systems for the FuelSolutions™ Storage System, excluding those that are unique to a particular canister design, if any.
3. The structural design and analysis of the FuelSolutions™ W150 Storage Cask and W100 Transfer Cask for all loading conditions, including the design basis canister interface loadings.
4. The thermal design and analysis of the FuelSolutions™ W150 Storage Cask and W100 Transfer Cask for all design conditions, including the design basis canister interface thermal conditions.
5. Descriptions of the FuelSolutions™ Storage System component shielding design features, excluding those that are unique to a particular canister design, if any. The generic methodology used for fuel qualification, including that used for determination of the acceptable cooling times for combinations of initial enrichments and burnups. The shielding analysis of the FuelSolutions™ W150 Storage Cask and W100 Transfer Cask and representative component dose rates for all design conditions including the design basis canister radiological conditions, excluding those that are unique to a particular canister design, if any.
6. A summary of the criticality analysis approach. Reference to the criticality safety analysis contained in each FuelSolutions™ Canister Storage FSAR.

7. A description of the methodology used for analysis of a postulated radiological release event including the radionuclide release fractions, excluding the canister-specific radionuclide inventory and the resulting event dose rates.
8. The generic operating procedures for the FuelSolutions™ Storage System, excluding those that are unique to a particular canister design, if any.
9. The acceptance criteria and maintenance requirements applicable to the FuelSolutions™ Storage System, excluding those that are specific to the canister.
10. Descriptions of the FuelSolutions™ Storage System component radiation protection features and operational "as low as reasonably achievable" (ALARA) measures, excluding those that are unique to a particular canister design, if any. Representative occupational exposure estimates that are not unique to a particular canister design. Site dose calculations for a sample ISFSI.
11. The accident analyses of the FuelSolutions™ W150 Storage Cask and W100 Transfer Cask for all design conditions, including the design basis canister interface conditions.
12. The *technical specifications* applicable to the FuelSolutions™ Storage System, including those generically applicable to all FuelSolutions™ canisters, excluding those that are unique to a particular FuelSolutions™ canister design.
13. The quality assurance requirements applicable to the FuelSolutions™ Storage System.
14. The decommissioning assessment for the FuelSolutions™ Storage System components, including the storage cask, transfer cask, and canister.

The purpose of this approach is that once reviewed and generically certified by the NRC, the C of C can more easily be amended to include additional or alternate FuelSolutions™ canister designs or payloads without having to re-review the information contained in the FuelSolutions™ Storage System FSAR, which is applicable to all FuelSolutions™ canisters.

To facilitate this approach, canister interface parameters with the storage cask and transfer cask such as canister size, weight, heat generation, and dose rates are established. Values for these canister interface parameters are defined in the FuelSolutions™ Storage System FSAR within which all acceptance criteria for the system are met. Using this approach, all FuelSolutions™ canisters and their contents that remain within the acceptance values established for these interface parameters, as demonstrated in the respective FuelSolutions™ Canister Storage FSAR, and that meet all the applicable acceptance criteria for the canister itself are qualified for use in the FuelSolutions™ Storage System. This will be accomplished by submittal of additional or revised FuelSolutions™ Canister Storage FSARs for review and approval by the NRC, which will rely on the FuelSolutions™ Storage System FSAR as approved by the NRC.

Safety Analysis Report Preparation

The format and content of this FSAR, and the associated FuelSolutions™ Storage System FSAR, is based on Regulatory Guide 3.61[6] and NUREG-1536.[7] The guidance provided by the

[6] Regulatory Guide 3.61, *Standard Format and Content for a Topical Safety Analysis Report for a Spent Fuel Dry Storage Cask*, U.S. Nuclear Regulatory Commission, February 1989.

NUREG-1536 review criteria on meeting the regulatory requirements is addressed by more than one FuelSolutions™ storage FSAR. Table 1.0-1 provides a matrix of the topics in NUREG-1536 and Regulatory Guide 3.61, the corresponding 10CFR72 requirements, and a reference to the applicable FuelSolutions™ storage FSAR section that addresses each topic. The formatting guidelines provided in Regulatory Guide 3.61 were closely followed when possible; however, in order to address the review criteria delineated by NUREG-1536, amended or additional subsections were added to this FSAR. In addition, this FSAR revision incorporates the changes resulting from the NRC Requests for Additional Information (RAIs) received prior to the issue date of this revision.

In complying with the guidance provided by NUREG-1536 and Regulatory Guide 3.61, efforts have been made to report the same information only once in the most relevant location in a particular FSAR to avoid the potential for conflicts, contradictions and ambiguities, and to facilitate the maintenance and future updates to these FSARs required by 10CFR72. Appropriate cross-references are provided to aid the reader in locating information provided elsewhere in the FSARs, when necessary to support the discussions of a particular FSAR section, rather than to repeat the same information in that section.

Off-site transport of the FuelSolutions™ W74 canister, in accordance with the requirements of 10CFR71, is addressed independently by a separate transportation license application.

This chapter provides a general description of the FuelSolutions™ W74 canister, drawings of the FuelSolutions™ W74 canister and related structures, systems, and components (SSCs) that are classified as important to safety, specifications for the SNF to be stored in the FuelSolutions™ W74 canister, and the technical qualifications of the applicant.

[7] NUREG-1536, *Standard Review Plan for Dry Cask Storage Systems*, U.S. Nuclear Regulatory Commission, January 1997.

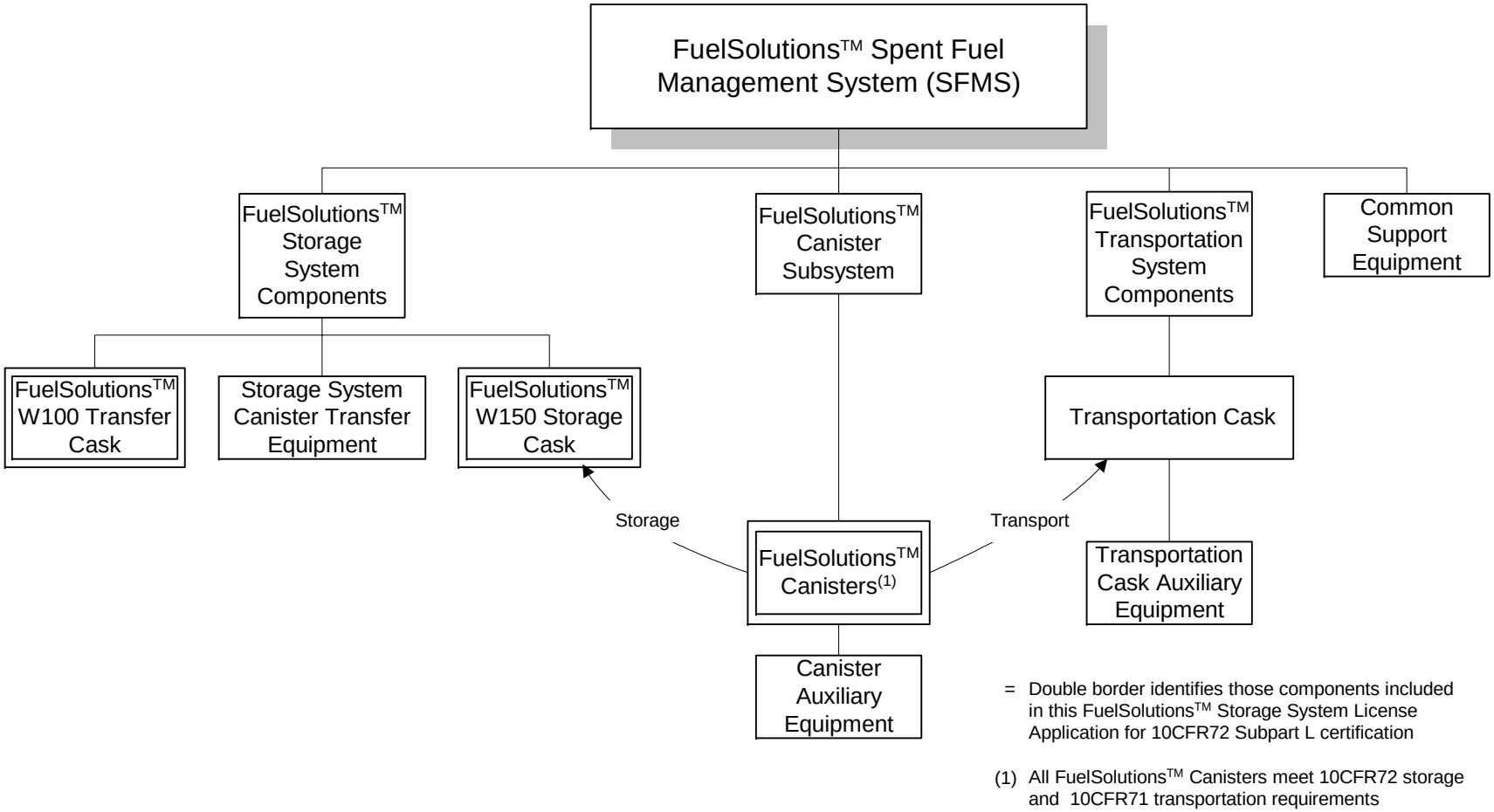

Figure 1.0-1 - FuelSolutions™ Spent Fuel Management System Elements

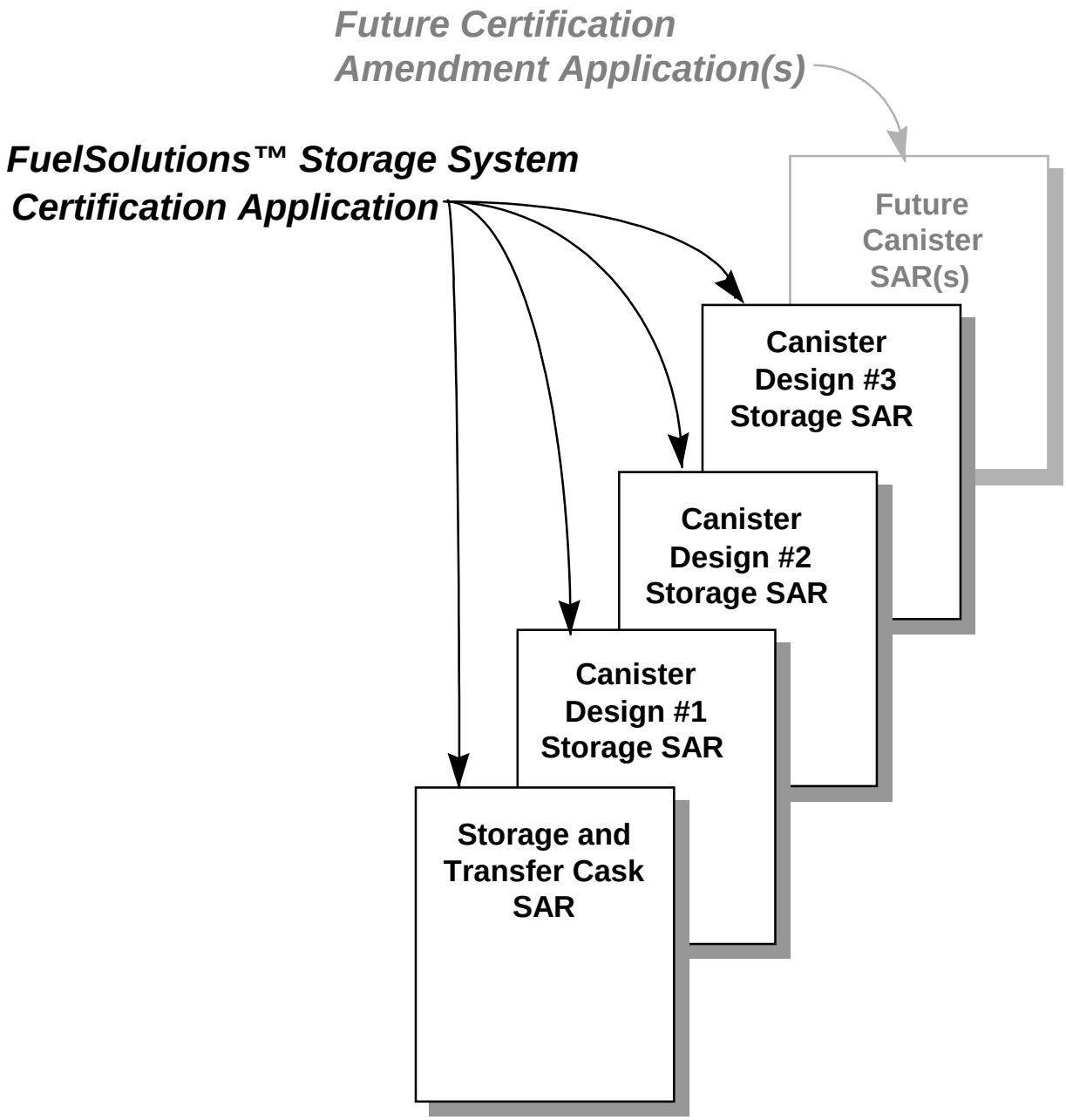

Figure 1.0-2 - FuelSolutions™ Storage System Certification Application Approach

Table 1.0-1 - FuelSolutions™ Storage System FSAR Regulatory Compliance Cross-Reference Matrix (16 pages)

Regulatory Guide 3.61 Section and Content	Associated NUREG-1536 Review Criteria	Applicable 10CFR72 or 10CFR20 Requirement	FuelSolutions™ Storage System FSAR	FuelSolutions™ Canister Storage FSAR
1. General Description				
1.1 Introduction	1.III.1 General Description & Operational Features	10CFR72.24 (b)	1.1	1.1
1.2 General Description	1.III.1 General Description & Operational Features	10CFR72.24 (b)	1.2	1.2
1.2.1 Cask Characteristics	1.III.1 General Description & Operational Features	10CFR72.24 (b)	1.2.1	1.2.1
1.2.2 Operational Features	1.III.1 General Description & Operational Features	10CFR72.24 (b)	1.2.2	1.2.2
1.2.3 Cask Contents	1.III.3 DCSS Contents	10CFR72.2 (a) (1) 10CFR72.236 (a)	--	1.2.3
1.3 Identification of Agents & Contractors	1.III.4 Qualification of the Applicant	10CFR72.24 (j) 10CFR72.28 (a)	1.3	1.3
1.4 Generic Cask Arrays	1.III.1 General Description & Operational Features	10CFR72.24 (c) (3)	1.4	--
1.5 Supplemental Data	1.III.2 Drawings	10CFR72.24 (c) (3)	1.5	1.5
NA	1.III.6 Consideration of Transport Requirements	10CFR72.230 (b) 10CFR72.236 (m)	(1)	(1)
2. Principal Design Criteria				
2.1 Spent Fuel To Be Stored	2.III.2.a Spent Fuel Specifications	10CFR72.2 (a) (1) 10CFR72.236 (a)	--	2.2

Table 1.0-1 - FuelSolutions™ Storage System FSAR Regulatory Compliance Cross-Reference Matrix (16 pages)

Regulatory Guide 3.61 Section and Content	Associated NUREG-1536 Review Criteria	Applicable 10CFR72 or 10CFR20 Requirement	FuelSolutions™ Storage System FSAR	FuelSolutions™ Canister Storage FSAR
2.2 Design Criteria for Environmental Conditions and Natural Phenomena	2.III.2.b External Conditions	10CFR72.122 (b)	2.3.4.7	--
	2.III.3.b Structural 2.III.3.c Thermal	10CFR72.122 (c)	2.3.3.4, 2.3.3.8	2.3.3.6, 2.3.4.1
		10CFR72.122 (b) (1)	2.3.1	
		10CFR72.122 (h) (1)	--	2.1.2
2.2.1 Tornado and Wind Loading	2.III.2.b External Conditions	10CFR72.122 (b)	2.3.4.2 2.3.4.3 2.3.4.5	--
2.2.2 Water Level (Flood)	2.III.2.b External Conditions 2.III.3.b Structural	10CFR72.122 (b) (2)	2.3.4.1	2.3.4.1
2.2.3 Seismic	2.III.3.b Structural	10CFR72.102 (f) 10CFR72.122 (b) (2)	2.3.4.4	2.3.4.3
2.2.4 Snow and Ice	2.III.2.b External Conditions 2.III.3.b Structural	10CFR72.122 (b)	2.3.4.8	--
2.2.5 Combined Load	2.III.3.b Structural	10CFR72.24 (d) 10CFR72.122 (b)(2)(ii)	2.3.5	2.3.5
NA	2.III.1 Structures, Systems, and Components Important to Safety	10CFR72.122 (a)	2.1.1	2.1.1
	2.III.3 Design Criteria for Safety Protection Systems	10CFR72.236 (g) 10CFR72.24 (c) (1) 10CFR72.24 (c) (2) 10CFR72.24 (c) (4) 10CFR72.120 (a) 10CFR72.236 (b)	2.1.2	2.1.2
	2.III.3.c Thermal	10CFR72.128 (a) (4)	2.1.2	2.1.2

Table 1.0-1 - FuelSolutions™ Storage System FSAR Regulatory Compliance Cross-Reference Matrix (16 pages)

Regulatory Guide 3.61 Section and Content	Associated NUREG-1536 Review Criteria	Applicable 10CFR72 or 10CFR20 Requirement	FuelSolutions™ Storage System FSAR	FuelSolutions™ Canister Storage FSAR
	2.III.3.f Operating Procedures	10CFR72.24 (f) 10CFR72.128 (a) (5)	10.1	--
		10CFR72.236 (h)	8.0	8.0
		10CFR72.24 (l) (2)	2.1.2	2.1.2
		10CFR72.236 (i)	1.2.1, 1.2.1.4.1	--
		10CFR72.24 (e) 10CFR72.104 (b)	1.2.1, 8.0, 10.1, 10.2	1.2.1, 8.0
		10CFR72.122 (l)	--	1.2.2.2
	2.III.3.g Acceptance Tests & Maintenance	10CFR72.236 (g) 10CFR72.122 (f) 10CFR72.128 (a) (1)	9.0	9.0
2.3 Safety Protection Systems	--	--	2.4	--
2.3.1 General	--	--	2.4.1	--
2.3.2 Protection by Multiple Confinement Barriers and Systems	2.III.3.b Structural	10CFR72.236 (l)	2.4.2	--
	2.III.3.c Thermal	10CFR72.236 (f)	2.4.2.2	--
	2.III.3.d Shielding/ Confinement/ Radiation Protection	10CFR72.126 (a) 10CFR72.128 (a) (2)	2.4.5	--
		10CFR72.128 (a) (3)	2.4.2.1	--
		10CFR72.236 (d)	2.4.5, 2.4.2.1	--
		10CFR72.236 (e)	2.4.2.1	--
2.3.3 Protection by Equipment & Instrument Selection	2.III.3.d Shielding/ Confinement/ Radiation Protection	10CFR72.122 (h) (4) 10CFR72.122 (i) 10CFR72.128 (a) (1)	2.4.3	7.1
2.3.4 Nuclear Criticality Safety	2.III.3.e Criticality	10CFR72.124 (a) 10CFR72.236 (c)	2.4.4, 6.0	6.0
		10CFR72.124 (b)	6.6	--

Table 1.0-1 - FuelSolutions™ Storage System FSAR Regulatory Compliance Cross-Reference Matrix (16 pages)

Regulatory Guide 3.61 Section and Content	Associated NUREG-1536 Review Criteria	Applicable 10CFR72 or 10CFR20 Requirement	FuelSolutions™ Storage System FSAR	FuelSolutions™ Canister Storage FSAR
2.3.5 Radiological Protection	2.III.3.d Shielding/ Confinement/ Radiation Protection	10CFR72.24 (d) 10CFR72.104 (a) 10CFR72.236 (d)	10.4.1	--
		10CFR72.24 (d) 10CFR72.106 (b) 10CFR72.236 (d)	10.4.2	--
		10CFR72.24 (m)	2.4.2.1	7.3
2.3.6 Fire and Explosion Protection	2.III.3.b Structural	10CFR72.122 (c)	2.3.3.4, 2.3.3.8	--
2.4 Decommissioning Considerations	2.III.1.h Decommissioning	10CFR72.130 10CFR72.236 (i)	14	--
	14.III.1 Design	10CFR72.130	14	--
	14.III.2 Cask Decontamination	10CFR72.236 (i)	14	--
	14.III.3 Financial Assurance & Record Keeping	10CFR72.30	(2)	(2)
	14.III.4 License Termination	10CFR72.54	(2)	(2)
3. Structural Evaluation				
3.1 Structural Design	3.III.1 SSC Important to Safety	10CFR72.24 (c) (3) 10CFR72.24 (c) (4)	3.1	3.1
	3.III.6 Concrete Structures	10CFR72.182 (b) 10CFR72.182 (c)	(2)	(2)
3.2 Weights and Centers of Gravity	3.V.1.b.2 Structural Design Features	--	3.2	3.2
3.3 Mechanical Properties of Materials	3.V.1.c Structural Materials	10CFR72.24 (c) (3)	3.3	3.3
	3.V.2.c Structural Materials			

Table 1.0-1 - FuelSolutions™ Storage System FSAR Regulatory Compliance Cross-Reference Matrix (16 pages)

Regulatory Guide 3.61 Section and Content	Associated NUREG-1536 Review Criteria	Applicable 10CFR72 or 10CFR20 Requirement	FuelSolutions™ Storage System FSAR	FuelSolutions™ Canister Storage FSAR
3.4 General Standards for Casks	--	--	3.4	3.4
3.4.1 Chemical and Galvanic Reactions	3.V.1.b.2 Structural Design Features	--	3.4.1	3.4.1
3.4.2 Positive Closure	--	--	3.4.2	3.4.2
3.4.3 Lifting Devices	3.V.1.ii(4)(a) Trunnions	--	3.4.3	3.4.3
3.4.4 Heat	3.V.1.d Structural Analysis	10CFR72.24 (d) 10CFR72.122 (b) 10CFR72.236 (g)	3.5	3.5
3.4.5 Cold	3.V.1.d Structural Analysis	10CFR72.24 (d) 10CFR72.122 (b) 10CFR72.236 (g)	3.5	3.5
NA	3.V.1.d Structural Analysis	10CFR72.24 (d) 10CFR72.122 (b)	3.6	3.6
	3.V.1.d Structural Analysis	10CFR72.24 (d) 10CFR72.102 (f) 10CFR72.122 (b) 10CFR72.122 (c)	3.7	3.7
3.5 Fuel Rods	--	10CFR72.122 (h) (1)	--	3.8, 4.3.2
3.6 Supplemental Data	4.V.6 Supplemental Info.	--	--	3.6
4. Thermal Evaluation				
4.1 Discussion	4.III Regulatory Requirements	10CFR72.24 (c) (3) 10CFR72.128 (a) (4) 10CFR72.236 (f)	4.1	4.1
		10CFR72.122 (l)	--	1.2.2.2
		10CFR72.236 (h)	8.0	8.0

Table 1.0-1 - FuelSolutions™ Storage System FSAR Regulatory Compliance Cross-Reference Matrix (16 pages)

Regulatory Guide 3.61 Section and Content	Associated NUREG-1536 Review Criteria	Applicable 10CFR72 or 10CFR20 Requirement	FuelSolutions™ Storage System FSAR	FuelSolutions™ Canister Storage FSAR
4.2 Summary of Thermal Properties of Materials	4.V.4.b Material Properties	--	4.2	4.2
4.3 Specifications for Components	4.IV Acceptance Criteria	--	4.3	4.3
		10CFR72.122 (h) (1)	--	4.3.2
4.4 Thermal Evaluation for Normal Conditions of Storage	4.IV Acceptance Criteria	10CFR72.24 (d) 10CFR72.236 (g)	4.4	4.4
NA	4.IV Acceptance Criteria	10CFR72.24 (d)	4.5	4.5
	4.IV Acceptance Criteria	10CFR72.24 (d) 10CFR72.122 (c)	4.6	4.6
4.5 Supplemental Data	4.V.6 Supplemental Info.	--	4.7	4.7
5. Shielding Evaluation				
5.1 Discussion and Results	--	--	5.1	5.1
5.2 Source Specification	5.V.2 Radiation Source Definition	--	5.2	5.2
5.2.1 Gamma Source	5.V.2.a Gamma Source	--	5.2.2	5.2
5.2.2 Neutron Source	5.V.2.b Neutron Source	--	5.2.2	5.2
5.3 Model Specification	5.V.3 Shielding Model Specification	--	5.3	5.3
5.3.1 Description of the Radial and Axial Shielding Configurations	5.V.3.a Configuration of the Shielding and Source	--	5.3.2, 5.3.3	5.3.1
5.3.2 Shield Regional Densities	5.V.3.b Material Properties	10CFR72.24 (c) (3)	5.3.4	5.3.2

Table 1.0-1 - FuelSolutions™ Storage System FSAR Regulatory Compliance Cross-Reference Matrix (16 pages)

Regulatory Guide 3.61 Section and Content	Associated NUREG-1536 Review Criteria	Applicable 10CFR72 or 10CFR20 Requirement	FuelSolutions™ Storage System FSAR	FuelSolutions™ Canister Storage FSAR
5.4 Shielding Evaluation	5.V.4 Shielding Analysis	10CFR72.24 (d) 10CFR72.104 (a) 10CFR72.106 (b) 10CFR72.128 (a) (2) 10CFR72.236 (d)	5.4	5.4
5.5 Supplemental Data	5.V.5 Supplemental Info.		5.5	--
6. Criticality Evaluation				
6.1 Discussion and Results	--	--	6.1	6.1
6.2 Spent Fuel Loading	6.V.2 Fuel Specification	--	6.2	6.2
6.3 Model Specifications	6.V.3 Model Specification	--	6.3	6.3
6.3.1 Description of Calculational Model	6.V.3.a Configuration	--	--	6.3.1
6.3.2 Cask Regional Densities	6.V.3.b Material Properties	10CFR72.24 (c) (3)	--	6.3.2
6.4 Criticality Calculation	6.V.4.a Computer Programs	--	6.4	6.4
6.4.1 Calculational or Experimental Method	--	--	--	6.4.1
6.4.2 Fuel Loading or Other Contents Loading Optimization	--	--	--	6.4.2
6.4.3 Criticality Results	6.IV Acceptance Criteria	10CFR72.24 (d) 10CFR72.124 10CFR72.236 (c)	--	6.4.2
6.5 Critical Benchmark Experiments	6.V.4.b Benchmark Comparisons	--	6.5	6.5

Table 1.0-1 - FuelSolutions™ Storage System FSAR Regulatory Compliance Cross-Reference Matrix (16 pages)

Regulatory Guide 3.61 Section and Content	Associated NUREG-1536 Review Criteria	Applicable 10CFR72 or 10CFR20 Requirement	FuelSolutions™ Storage System FSAR	FuelSolutions™ Canister Storage FSAR
6.6 Supplemental Data	6.V.5 Supplemental Info.	10CFR72.236 (g)	6.6	--
7. Confinement				
7.1 Confinement Boundary	7.V.1.b Design Features	10CFR72.24 (c) (3)	--	7.1
7.1.1 Confinement Vessel	7.III.2 Protection of Spent Fuel Cladding	10CFR72.122 (h) (l)	--	7.1.1
7.1.2 Confinement Penetrations	--	--	--	7.1.2
7.1.3 Seals and Welds	--	--	--	7.1.3
7.1.4 Closure	7.III.3 Redundant Sealing	10CFR72.236 (e)	--	7.1.4
7.2 Requirements for Normal Conditions of Storage	7.III.7 Evaluation of Confinement System	10CFR72.24 (d) 10CFR72.236 (l)	--	7.2
7.2.1 Release of Radioactive Material	7.III.6 Release of Radionuclides to the Environment	10CFR72.24 (1) (1)	--	7.2.1
	7.III.4 Monitoring of Confinement	10CFR72.122 (h) (4) 10CFR72.128 (a) (1)	--	7.2.1
	7.III.5 Instrumentation	10CFR72.24 (1) 10CFR72.122 (i)	--	7.2.1
	7.III.8 Annual Dose	10CFR72.104 (a)	--	7.2.1
7.2.2 Pressurization of Confinement Vessel	--	--	--	7.2.2

Table 1.0-1 - FuelSolutions™ Storage System FSAR Regulatory Compliance Cross-Reference Matrix (16 pages)

Regulatory Guide 3.61 Section and Content	Associated NUREG-1536 Review Criteria	Applicable 10CFR72 or 10CFR20 Requirement	FuelSolutions™ Storage System FSAR	FuelSolutions™ Canister Storage FSAR
7.3 Confinement Requirements for Hypothetical Accident Conditions	7.III.7 Evaluation of Confinement System	10CFR72.24 (d) 10CFR72.122 (b) 10CFR72.236 (l)	--	7.3
7.3.1 Fission Gas Products	--	--	--	7.3.1
7.3.2 Release of Contents	--	--	7.3.2	--
NA	--	10CFR72.106(b)	--	7.3.3, 7.3.4
7.4 Supplemental Data	7.V Supplemental Info.	--	--	7.4
8. Operating Procedures				
8.1 Procedures for Loading the Cask	8.III.1 Develop Operating Procedures	10CFR72.40 (a) (5)	8.1	8.1
	8.III.2 Operational Restrictions for ALARA	10CFR72.24 (e) 10CFR72.104 (b)		
	8.III.3 Radioactive Effluent Control	10CFR72.24 (1) (2)		
	8.III.4 Written Procedures	10CFR72.212 (b) (9)		
	8.III.5 Establish Written Procedures & Tests	10CFR72.234 (f)		
	8.III.6 Wet or Dry Loading and Unloading Compatibility	10CFR72.236 (h)		
	8.III.7 Cask Design Facilitate Decon	10CFR72.236 (i)	1.2.1, 1.2.1.4.1	--

Table 1.0-1 - FuelSolutions™ Storage System FSAR Regulatory Compliance Cross-Reference Matrix (16 pages)

Regulatory Guide 3.61 Section and Content	Associated NUREG-1536 Review Criteria	Applicable 10CFR72 or 10CFR20 Requirement	FuelSolutions™ Storage System FSAR	FuelSolutions™ Canister Storage FSAR
8.2 Procedures for Unloading the Cask	8.III.1 Develop Operating Procedures	10CFR72.40 (a) (5)	8.2	8.2
	8.III.2 Operational Restrictions for ALARA	10CFR72.24 (e) 10CFR72.104 (b)		
	8.III.3 Radioactive Effluent Control	10CFR72.24 (1) (2)		
	8.III.4 Written Procedures	10CFR72.212 (b) (9)		
	8.III.5 Establish Written Procedures and Tests	10CFR72.234 (f)		
	8.III.6 Wet or Dry Loading and Unloading Compatibility	10CFR72.236 (h)		
	8.III.8 Ready Retrieval	10CFR72.122 (1)		
8.3 Preparation of the Cask	--	--	8.3	8.3
8.4 Supplemental Data	--	--	--	--
NA	8.III.9 Design Minimize Radwaste	10CFR72.24 (f) 10CFR72.128 (a) (5)	10.1	--
	8.III.10 SSCs Permit Inspection, Maintenance, Testing	10CFR72.122 (f)	9.0	9.0
9. Acceptance Criteria and Maintenance Program				
9.1 Acceptance Criteria	9.III.1.a Preoperational Testing & Initial Operations	10CFR72.24 (p)	9.1	9.1
	9.III.1.c SSC Tested & Maintained to Appropriate Quality Standards	10CFR72.24 (c) 10CFR72.122 (a)		
	9.III.1.d Test Program	10CFR72.162		

Table 1.0-1 - FuelSolutions™ Storage System FSAR Regulatory Compliance Cross-Reference Matrix (16 pages)

Regulatory Guide 3.61 Section and Content	Associated NUREG-1536 Review Criteria	Applicable 10CFR72 or 10CFR20 Requirement	FuelSolutions™ Storage System FSAR	FuelSolutions™ Canister Storage FSAR
	9.III.1.e Appropriate Tests	10CFR72.236 (l)		
	9.III.1.f Inspection for cracks, pinholes, voids, defects	10CFR72.236 (j)		
	9.III.1.g Provisions that permit Commission Tests	10CFR72.232 (b)		
9.2 Maintenance Program	9.III.1.b Maintenance	10CFR72.236 (g)	9.2	9.2
	9.III.1.c SSC Tested & Maintained to Appropriate Quality Standards	10CFR72.122 (f) 10CFR72.128 (a) (1)		
	9.III.1.h Records of Maintenance	10CFR72.212. (b) (8)		
NA	9.III.2 Resolution of Issues Concerning Adequacy of Reliability	10CFR72.24 (i)	(3)	(3)
	9.III.1.d Submit Pre-op Test Results to NRC	10CFR72.82 (e)	(2)	(2)
	9.III.1.i Casks conspicuously and durably marked	10CFR72.236 (k)	9.1.2.7.1, 9.1.3.7.1	9.1.7.2
	9.III.3 Cask Identification			
10. Radiation Protection				
10.1 Ensuring that Occupational Radiation Exposures Are As Low As Is Reasonably Achievable (ALARA)	10.III.4 ALARA	10CFR20.1101 10CFR72.24 (e) 10CFR72.104 (b) 10CFR72.126 (a)	10.1	--
10.2 Radiation Protection Design Features	10.V.1.b Design Features	10CFR72.126 (a) (6)	10.2	--

Table 1.0-1 - FuelSolutions™ Storage System FSAR Regulatory Compliance Cross-Reference Matrix (16 pages)

Regulatory Guide 3.61 Section and Content	Associated NUREG-1536 Review Criteria	Applicable 10CFR72 or 10CFR20 Requirement	FuelSolutions™ Storage System FSAR	FuelSolutions™ Canister Storage FSAR
10.3 Estimated Onsite Collective Dose Assessment	10.III.2 Occupational Exposures	10CFR.20.1201 10CFR20.1207 10CFR20.1208 10CFR20.1301	10.3	--
NA	10.III.3 Public Exposure	10CFR72.104 10CFR72.106	10.4	--
	10.III.1 Effluents & Direct Radiation	10CFR72.104		
11. Accident Analyses				
11.1 Off-Normal Operations	11.III.2 Meet Dose Limits for Anticipated Events	10CFR72.24 (d) 10CFR72.104 (a) 10CFR72.236 (d)	11.1	11.1
	11.III.4 Maintain Subcritical Condition	10CFR72.124 (a) 10CFR72.236 (c)		
	11.III.7 Instrumentation & Control for Off-Normal Condition	10CFR72.122 (i)		
11.2 Accidents	11.III.1 SSC Important to Safety Designed for Accidents	10CFR72.24 (d) (2) 10CFR72.122 (b) (2) 10CFR72.122 (b) (3) 10CFR72.122 (d) 10CFR72.122 (g)	11.2	11.2
	11.III.5 Maintain Confinement for Accident	10CFR72.236 (l)		
	11.III.4 Maintain Subcritical Condition	10CFR72.124 (a) 10CFR72.236 (c)	11.2	11.2, 6.0

Table 1.0-1 - FuelSolutions™ Storage System FSAR Regulatory Compliance Cross-Reference Matrix (16 pages)

Regulatory Guide 3.61 Section and Content	Associated NUREG-1536 Review Criteria	Applicable 10CFR72 or 10CFR20 Requirement	FuelSolutions™ Storage System FSAR	FuelSolutions™ Canister Storage FSAR
	11.III.3 Meet Dose Limits for Accidents	10CFR72.24 (d) (2) 10CFR72.24 (m) 10CFR72.106 (b)	11.2	11.2, 7.3
	11.III.6 Retrieval	10CFR72.122 (l)	8.2	--
	11.III.7 Instrumentation & Control for Accident Cond.	10CFR72.122 (i)	(4)	--
NA	11.III.8 Confinement Monitoring	10CFR72.122 (h) (4)	--	7.2.1
12. Operating Controls and Limits				
12.1 Proposed Operating Controls and Limits	--	10CFR72.44 (c)	12.3	12.3
	12.III.1.e Administrative Controls	10CFR72.44 (c) (5)		
12.2 Development of Operating Controls and Limits	12.III.1 General Requirement for Technical Specifications	10CFR72.24 (g) 10CFR72.26 10CFR72.44 (c) 10CFR72 Subpart E 10CFR72 Subpart F	12.3	12.3
12.2.1 Functional and Operating Limits, Monitoring Instruments, and Limiting Control Settings	12.III.1.a Functional/ Operating Units, Monitoring Instruments and Limiting Controls	10CFR72.44 (c) (1)	12.3	--

Table 1.0-1 - FuelSolutions™ Storage System FSAR Regulatory Compliance Cross-Reference Matrix (16 pages)

Regulatory Guide 3.61 Section and Content	Associated NUREG-1536 Review Criteria	Applicable 10CFR72 or 10CFR20 Requirement	FuelSolutions™ Storage System FSAR	FuelSolutions™ Canister Storage FSAR
12.2.2 Limiting Conditions for Operation	12.III.1.b Limiting Controls	10CFR72.44 (c) (2)	12.3	12.3
	12.III.2.a Type of Spent Fuel	10CFR72.236 (a)	--	12.3
	12.III.2.b Enrichment			
	12.III.2.c Burnup			
	12.III.2.d Minimum Acceptable Cooling Time			
	12.III.2.f Maximum Spent Fuel Loading Limit			
	12.III.2.g Weights and Dimension			
	12.III.2.h Condition of Spent Fuel			
	12.III.2.e Maximum Heat Dissipation	10CFR72.236 (a)	12.3	12.3
	12.III.2.i Inerting Atmosphere Requirements	10CFR72.236 (a)	--	12.3
12.2.3 Surveillance Specifications	12.III.1.c Surveillance Requirements	10CFR72.44 (c) (3)	12.3	12.3
12.2.4 Design Features	12.III.1.d Design Features	10CFR72.44 (c) (4)	12.3	12.3
12.2.5 Suggested Format for Operating Controls and Limits	--	--	12.3	12.3

Table 1.0-1 - FuelSolutions™ Storage System FSAR Regulatory Compliance Cross-Reference Matrix (16 pages)

Regulatory Guide 3.61 Section and Content	Associated NUREG-1536 Review Criteria	Applicable 10CFR72 or 10CFR20 Requirement	FuelSolutions™ Storage System FSAR	FuelSolutions™ Canister Storage FSAR
NA	12.III.2 SSC Design Bases & Criteria	10CFR72.236 (b)	2.1.2	2.1.2
	12.III.2 Criticality Control	10CFR72.236 (c)	2.4.4, 6.0	6.4.2
	12.III.2 Shielding and Confinement	10CFR20 10CFR72.236 (d)	5.4, 10.4	5.4, 7.2, 7.3
	12.III.2 Redundant Sealing	10CFR72.236 (e)	2.4.2.1	7.1.4
	12.III.2 Passive Heat Removal	10CFR72.236 (f)	2.4.2.2, 4.1, 4.4.1.1.1	4.1, 4.4.1
	12.III.2 20 Year Storage and Maintenance	10CFR72.236 (g)	2.1.2, 3.5, 4.4, 9.2	2.1.2, 3.5, 4.4, 9.2
	12.III.2 Decontamination	10CFR72.236 (i)	1.2.1, 1.2.1.4.1	--
	12.III.2 Wet or Dry Loading	10CFR72.236 (h)	8.0	8.0
	12.III.2 Confinement Effectiveness	10CFR72.236 (j)	9.1	9.1
	12.III.2 Evaluation for Confinement	10CFR72.236 (l)	2.4.2, 9.1	7.2, 7.3, 9.1
13. Quality Assurance				
13. Quality Assurance	1.III.5 Quality Assurance	10CFR72.24 (n) 10CFR72 Subpart G	13.0	--
	13.III Regulatory Requirements	10CFR72.24 10CFR72 Subpart G		

Table 1.0-1 Notes:

"--" There is no corresponding NUREG-1536 criteria, no applicable 10CFR72 or 10CFR20 regulatory requirement, or the item is not addressed in the particular FSAR.

"NA" There is no Regulatory Guide 3.61 section that corresponds to the NUREG-1536, 10CFR72, or 10CFR20 requirement being addressed.

(1) Transportation performance of the FuelSolutions™ canisters is evaluated in a separate transportation license application.

(2) The stated requirement is the responsibility of the licensee (i.e., utility) as part of the ISFSI and is therefore not addressed in this application.

(3) The stated requirement is not applicable to the FuelSolutions™ Storage System. The functional adequacy of all important to safety components is demonstrated by analysis and/or previously licensed designs.

(4) The stated requirement is not applicable to the FuelSolutions™ Storage System. No monitoring is required for accident conditions.

1.1 Introduction

The FuelSolutions™ SFMS is a fully integrated, canister-based system that provides for the storage and transport of a broad range of SNF assembly classes. The FuelSolutions™ SFMS is designed to be suitable for the vast majority of commercial reactor sites in the contiguous United States. The FuelSolutions™ SFMS is also designed to be suitable for the U.S. Department of Energy's (DOE) Centralized Interim Storage Facility (CISF) and the Mined Geologic Disposal Site (MGDS). In addition it is suitable for use at private CISFs.

The FuelSolutions™ SFMS is comprised of four basic system components. These components can be used in a variety of ways to satisfy a particular licensee's requirements throughout the life of the plant and ISFSI. Together with site-specific support equipment, loaded FuelSolutions™ W74 canisters may be transferred vertically or horizontally. A synopsis for each of the four basic components of the FuelSolutions™ SFMS is as follows:

1. A *FuelSolutions™ Canister* is designed for dry storage of SNF in accordance with 10CFR72 and for transportation of SNF in accordance with 10CFR71. The canister is placed in an overpack cask for fuel loading, closure, transfer, on-site storage, and off-site transport. It provides confinement for storage, criticality control and passive heat removal for storage and transport, and biological shielding for closure and handling operations for the enclosed SNF. The canister interfaces are standardized to be compatible with each of the system cask components identified below. The FuelSolutions™ W74 canister is addressed within this FSAR for storage. Transportation of the FuelSolutions™ W74 canister is addressed in a separate transportation license application.

2. A *FuelSolutions™ W150 Storage Cask* provides passive vertical dry storage of a loaded canister in an on-site ISFSI or at an off-site CISF, in accordance with 10CFR72. The storage cask is capable of accommodating both vertical or horizontal canister transfer to the transfer cask or transportation cask. It provides biological shielding, structural protection, and passive convective heat removal for the enclosed canister and SNF. The FuelSolutions™ W150 Storage Cask is addressed in the FuelSolutions™ Storage System FSAR.

3. A *FuelSolutions™ W100 Transfer Cask* provides canister loading, closure, and handling capability, in accordance with 10CFR50 and 10CFR72. The transfer cask has the capability to be used in the following operational modes:

   a. Loading or unloading of a canister with SNF in a spent fuel pool, in a cask receiving area using a fuel assembly transfer cask and shielded loading collar, or in a shielded hot cell.

   b. Vertical transfer of a sealed canister to or from a FuelSolutions™ W150 Storage Cask inside the plant's fuel building or a licensed cask handling facility.

   c. Horizontal transfer of a sealed canister to or from a FuelSolutions™ W150 Storage Cask within an ISFSI or the licensee's owner-controlled area.

   d. Vertical transfer of a sealed canister to or from a transportation cask inside the plant's fuel building or a licensed cask handling facility.

   e. Horizontal transfer of a sealed canister to or from a transportation cask within an ISFSI or the licensee's owner-controlled area.

4. The FuelSolutions™ W100 Transfer Cask provides biological shielding, structural protection, and passive heat removal for the enclosed canister and SNF. The transfer cask is addressed in the FuelSolutions™ Storage System FSAR.
5. A suitable transportation cask with impact limiters, designed and licensed in accordance with 10CFR71, are used for off-site shipment of a FuelSolutions™ canister. The transportation cask can be used to load or unload a canister with SNF in a spent fuel pool or a shielded hot cell. The transportation cask can also be used to transfer a sealed canister to and from either the storage cask or the transfer cask. It provides containment, structural protection, biological shielding, and passive heat removal for the enclosed canister and SNF. The transportation cask and impact limiters are addressed in a separate transportation license application.

FuelSolutions™ W74 Canister Description. Key features of the FuelSolutions™ W74 canister design are as follows:

- The shell assembly confinement boundary for dry storage is designed, analyzed, and fabricated in accordance with the applicable provisions of the American Society of Mechanical Engineers (ASME) Code, Section III, Subsection NB.[8]
- The internal basket assemblies are designed, analyzed, and fabricated in accordance with the applicable provisions of ASME Section III, Subsection NG.[9] Upper and lower basket assemblies are used to maximize the SNF payload capacity.
- A thick shield plate is provided at the canister top end and a shield plug at the bottom end to maintain occupational exposures ALARA. Individual top shield plugs are provided, which nest with the shield plate, at each fuel assembly location to allow loading the canister outside the spent fuel pool.
- Fixed borated neutron absorbers for criticality control are integral with the basket assemblies.
- Double closure plates and seal welds are used on both ends of the canister.
- Vent, drain, instrument, and leak test ports are provided at the top end of the canister.

The design of the FuelSolutions™ W74 canister is described further in Section 1.2.1.3.

FuelSolutions™ W74 Canister Operations Overview. The principal FuelSolutions™ W74 canister storage operations performed under the plant's 10CFR50 license or a stand-alone storage facility's 10CFR72 license, in accordance with the FuelSolutions™ Storage System C of C, include the following:

- A FuelSolutions™ W74 canister is loaded with SNF in a spent fuel pool using conventional methods, while within a FuelSolutions™ W100 Transfer Cask. The canister lower basket is loaded first, and then the empty upper basket is installed within the canister above the lower basket and loaded.

[8] American Society of Mechanical Engineers (ASME) Boiler and Pressure Vessel Code, Section III, Division 1, Subsection NB, *Class 1 Components*, 1995 Edition.

[9] American Society of Mechanical Engineers (ASME) Boiler and Pressure Vessel Code, Section III, Division 1, Subsection NG, *Core Support Structures*, 1995 Edition.

- Alternatively, a FuelSolutions™ W74 canister may be loaded with SNF using a fuel assembly shuttle cask, a shielded loading collar, and the basket loading sequence described above, while within a FuelSolutions™ W100 Transfer Cask. This loading occurs outside the spent fuel pool, while inside the plant's fuel building.
- Following fuel loading, the FuelSolutions™ W74 canister is vacuum dried and helium backfilled using conventional methods. Canister seal welding uses remote automated welding equipment.
- A sealed FuelSolutions™ W74 canister is transferred vertically to or from a FuelSolutions™ W150 Storage Cask or a transportation cask, using a FuelSolutions™ W100 Transfer Cask inside the plant's (or CISF's) cask receiving bay or a licensed cask handling facility.
- Alternatively, a sealed FuelSolutions™ W74 canister can be transferred horizontally to or from a FuelSolutions™ W150 Storage Cask, using a FuelSolutions™ W100 Transfer Cask or a transportation cask within an ISFSI or CISF, or the licensee's owner-controlled area.
- A sealed FuelSolutions™ W74 canister can also be transferred horizontally to or from a transportation cask, using a FuelSolutions™ W100 Transfer Cask within an ISFSI or CISF, or the licensee's owner-controlled area.
- The FuelSolutions™ W74 canister is stored vertically in a passively cooled FuelSolutions™ W150 Storage Cask at an ISFSI or CISF.

The operation of a FuelSolutions™ W74 canister for on-site storage is described further in Section 1.2.2.

Spent Fuel to be Stored. The FuelSolutions™ W74 canister is designed to accommodate BRP BWR fuel, including mixed oxide (MOX), partial, and damaged fuel assemblies. Additional information regarding the SNF to be stored in the FuelSolutions™ W74 canister is provided in Section 1.2.3 of this FSAR.

This page intentionally left blank.

1.2 General Descriptions

The FuelSolutions™ Storage System consists of the components and equipment that provide the on-site handling, transfer, and dry storage of SNF in canisters. The primary storage components of the FuelSolutions™ Storage System are as follows:

- Canister: The FuelSolutions™ W74 canister is addressed in this FSAR.
- Storage Cask: The FuelSolutions™ W150 Storage Cask is addressed in the FuelSolutions™ Storage System FSAR.
- Transfer Cask: The FuelSolutions™ W100 Transfer Cask is addressed in the FuelSolutions™ Storage System FSAR.
- Support Equipment: The support equipment that is unique to the FuelSolutions™ W74 canister is addressed in this FSAR. The balance of the support equipment is addressed in the FuelSolutions™ Storage System FSAR.

A schematic of the entire FuelSolutions™ SFMS, including the FuelSolutions™ Storage System components and equipment, is shown in Figure 1.2-1. This section provides a general description of the FuelSolutions™ Storage System components, with a more detailed description of the FuelSolutions™ W74 canister. A description of the associated canister-specific support equipment is also provided.

1.2.1 FuelSolutions™ Storage System Characteristics

1.2.1.1 FuelSolutions™ Storage Cask

The FuelSolutions™ storage cask is a modular reinforced concrete component that provides structural support and biological shielding for the canister and SNF. The storage cask design uses passive heat removal, with inlet and outlet air vents provided to allow ambient air to circulate within the cask to cool the canister and SNF assemblies. This passive ventilation also maintains the concrete temperatures within allowable values. The SNF assemblies are stored within a sealed FuelSolutions™ canister in a vertical orientation, providing optimum heat dissipation from a canister by the vertical annular air flow. The design of the storage cask incorporates a top cover to facilitate horizontal or vertical transfer of a canister to and from a transfer cask or transportation cask. The choices of materials used in the construction of the storage cask provide long life, require no replacement parts, minimize periodic maintenance, and easily disassemble after use. The FuelSolutions™ W150 Storage Cask is described further in the FuelSolutions™ Storage System FSAR.

1.2.1.2 FuelSolutions™ Transfer Cask

The FuelSolutions™ transfer cask is a right circular cylindrical shielded vessel, has covers on both ends, and provides structural support and biological shielding for the canister and SNF. It provides complete versatility for FuelSolutions™ canister transfer operations. The transfer cask is used to handle FuelSolutions™ canisters during fuel loading, canister closure, and on-site transfer operations. It also provides the capability for transferring loaded canisters to or from a

storage cask or transportation cask in a horizontal or vertical orientation. The general methods for canister transfer are described as follows:

- Using the horizontal canister transfer method, the bottom end of a transfer cask is docked horizontally with the top end of a storage cask or transportation cask. The canister is then transferred using a hydraulic ram.
- Using the vertical canister transfer method, the bottom end of a transfer cask is docked with the top end of a storage cask or transportation cask and the loaded canister is transferred using a vertical lift fixture.

The FuelSolutions™ W100 Transfer Cask is described further in the FuelSolutions™ Storage System FSAR.

1.2.1.3 FuelSolutions™ W74 Canister

This section provides a description of the FuelSolutions™ W74 canister design characteristics. The specific design characteristics of other FuelSolutions™ canisters are addressed in their respective FuelSolutions™ Canister Storage FSARs.

The FuelSolutions™ W74 canister shown in Figure 1.2-2 is designed to meet the performance requirements of 10CFR71 and 10CFR72. The FuelSolutions™ W74 canister has 74 cell locations with a capacity for up to 64 BRP BWR spent fuel assemblies, as discussed in Section 1.2.3. The additional 10 cell locations at the center of the basket are mechanically blocked to prevent fuel assemblies from being loaded in these locations.

A conservative design is used that does not require either burnup credit or moderator exclusion for criticality control. Upper and lower basket assemblies, each containing 32 SNF assemblies, stack on top of each other. The FuelSolutions™ W74 canister is shielded at both ends to facilitate and allow a full range of operational alternatives and to provide flexibility. The top end shield plate contains 37 independent shield plugs. The principal characteristics of the W74 canister are summarized in Table 1.2-1. General arrangement drawings of the FuelSolutions™ W74 canister are provided in Section 1.5.1.

Design Characteristics

The FuelSolutions™ W74 canister subsystem includes two different classes of FuelSolutions™ canister assemblies. The two classes are:

- The FuelSolutions™ W74M class Multi-Purpose Canister (MPC) for storage, transportation, and disposal.
- The FuelSolutions™ W74T class Transportable Storage Canister (TSC) for storage and transportation.

Unlike other FuelSolutions™ canister types, the FuelSolutions™ W74 canister design includes only one canister length and cavity size. Only carbon steel shield plugs are used with the top end shield plug assembly comprised of a shield plate with individual shield plugs. No fuel assembly spacers are used. The configurations of the two FuelSolutions™ W74 canister classes are described in Table 1.2-2.

The FuelSolutions™ W74 canister is comprised of a shell assembly and an internal basket assembly, as shown in Figure 1.2-2. The FuelSolutions™ W74 canister shell assembly is

designed and fabricated as an ASME Section III, Class 1 pressure vessel, in accordance with the applicable requirements of Subsection NB, as discussed in Section 2.1.2 of this FSAR. The basket assembly is designed and fabricated as an ASME Section III core support structure, in accordance with the applicable requirements of Subsection NG, as discussed in Section 2.1.2 of this FSAR. All canister shell assembly confinement boundary material and basket assembly structural materials are ASME Code-approved stainless steel or carbon steel materials.

The canister shell assembly consists of a right circular cylindrical shell with a top end inner closure plate, a top end outer closure plate, a bottom closure plate, and a bottom end plate. In addition, vent, drain, instrumentation, and leak test ports are provided. Each FuelSolutions™ W74 canister shell assembly, including both the W74M class and the W74T class canisters, contains a top and bottom end carbon steel shield plug. The bottom end shield plug is encased by the canister closure plate, the shell extension, and the bottom end plate. The top end shield plug is an assembly comprised of a thick shield plate with 37 independent shield plugs aligned with each upper basket storage location.

The FuelSolutions™ W74 upper and lower canister basket assemblies consist of a series of circular spacer plates with machined openings, held in position axially by four welded support tubes that run through support sleeves placed between the spacer plates. The bottom end of the upper basket assembly is equipped with a thick stainless steel engagement plate that rests on top of the lower basket support tubes. The engagement plate provides support for the fuel assemblies in the upper basket with the canister in the vertical orientation. Two engagement sleeves on the bottom of the engagement plate rest with the top ends of two of the lower basket support tubes at diagonally opposing support tube locations. The basket openings are fitted with guide tube assemblies that consist of built-up layers of an inner structural tube and borated neutron absorber sheets (borated stainless). Additional product literature for borated stainless material is provided in Section 1.5.2. No borated materials are formed/bent, welded, or used as structural members.

The basket spacer plates and support tubes are fabricated from high-strength carbon steel or stainless steel to provide maximum strength, optimize thermal performance, and minimize weight. The carbon steel basket components are coated with electroless nickel for corrosion protection following canister fabrication and during the brief period when the canister is filled with water for fuel loading. The use of electroless nickel is discussed further in Section 3.4.1. Additional product literature for electroless nickel for this application is provided in Section 1.5.2. All FuelSolutions™ W74 basket assemblies are designed for storage and transport conditions.

The FuelSolutions™ W74M basket spacer plates are fabricated from high-strength stainless steel and electroless nickel-coated, high-strength carbon steel. The FuelSolutions™ W74T basket spacer plates, except for the bottom spacer plate, are fabricated from high-strength carbon steel material and coated with electroless nickel. The bottom spacer plate is constructed from high-strength stainless steel to facilitate a welded attachment of the guide tube retainer clip. The support tubes for both the FuelSolutions™ W74T and the W74M basket are constructed of high-strength stainless steel. All basket support sleeves are constructed of stainless steel. The extended legs of the support sleeves provide additional longitudinal support for the spacer plates. The basket openings are fitted with guide tube assemblies that consist of built-up layers of an inner structural tube and borated neutron absorber sheets. The inner structural tube is constructed of austenitic stainless steel for both the FuelSolutions™ W74T and W74M class basket

assemblies. The borated stainless steel neutron absorbers are attached to the inner tubes with welded stainless steel retainers. The specific material designations for the FuelSolutions™ W74T class basket assemblies are shown on the drawings in Section 1.5.

The FuelSolutions™ W74 canister top end closure, shown in Figure 1.2-3, consists of a thick shield plug assembly, an inner closure plate with an instrument port cover, a vent port cover, a drain port cover, and an outer closure plate with leak test port cover. The shield plug assembly provides biological shielding for loading of the SNF assemblies in the upper basket and for canister closure operations. The inner and outer closure plates and port covers provide redundant welded closures to assure that the canister maintains confinement function. This assures that the inert helium atmosphere, the integrity of the canister basket assemblies, and the contained SNF assemblies are maintained during storage and transportation. All FuelSolutions™ W74 canister top end closure welds are accomplished using a remote automated welding and opening system (AW/OS).

The field closure welds are designed to provide structural integrity, while minimizing heat input and distortion of the canister shell. Shop fit-up of the inner closure plate with the canister shell is carefully controlled to minimize weld shrinkage during field welding. The outer closure plate is toleranced to allow for weld shrinkage and can be installed with minimal field fit-up or grinding. All canister top end closure welds are liquid dye penetrant examined; the inner closure weld at the root and final weld passes, and the outer closure weld at the root, intermediate, and final weld passes. In addition, the top end inner closure welds (with the exception of the vent, drain, and leak test port covers) are helium pressure tested and leak tested. Additional discussion of the FuelSolutions™ canister closure is provided in Section 2.5.2 of this FSAR.

Separate drain and vent ports are provided at the top end of the FuelSolutions™ W74 canister assembly. The ports are integral with the top end shield plug assembly and are offset from the shell to facilitate automated welding. Adjacent to the drain port, a sealed instrument port is provided for canister reflooding and opening, to facilitate removal of the fuel assemblies. The port penetrations are staggered to minimize radiation streaming paths. A typical drain port is shown in Figure 1.2-3.

The drain port is connected to a tube that extends to the bottom of the canister cavity, which facilitates the removal of water from the canister during blowdown and reintroduction of water during canister reflood. Unlike some FuelSolutions™ canister designs, the drain tube for the FuelSolutions™ W74 canister is connected to the bottom of the shield plate instead of the canister shell assembly. Guide sleeves are installed through the upper and lower basket to enable smooth installation of the drain tube with the shield plug assembly.

The vent port is similar in design to the drain port shown in Figure 1.2-3, but does not include the drilled hole for connection of the drain tube. The side hole is open to the canister cavity. In addition, the vent port includes a small through-hole to allow the insertion of a thermocouple used to monitor canister water temperature. Both ports are used for vacuum drying and for backfilling of the cavity with helium to provide an inert atmosphere. Unlike some FuelSolutions™ canister designs, the vent port for the FuelSolutions™ W74 canister is installed in the shield plug assembly instead of the canister shell assembly. The drain and vent port include quick connect fittings to facilitate the connections to the vacuum drying system and to provide temporary closure of the ports, until the port covers are welded into place. Each port is

labeled to preclude accidental connection of the draining, vacuum drying, and inerting equipment connections to the wrong port.

The instrument ports for the inner closure plate and the leak test port for the outer closure plate are sealed closed during canister fabrication by covers that are welded to the respective closure plate. The cover is removed prior to reflooding the canister, if canister opening and unloading is required. The instrument port allows the canister internal pressure to be accurately monitored without compensation for the flow losses due to venting. The leak test port in the outer closure plate is similar to the instrument port in configuration. This auxiliary port can be used to perform gas sampling, helium pressure testing, and leak testing of the canister top end closure welds following canister fuel loading, if it becomes necessary.

The canister shell and bottom end plate welding, examination, pressure testing, and leak testing are performed during canister fabrication. All longitudinal and circumferential seam welds in the canister shell are 100% radiographically examined, full penetration butt welds. The canister bottom end plate includes a weld neck to facilitate a full penetration weld to the canister shell. The canister bottom end weld to the canister shell is 100% radiographically examined. In addition, the bottom end plate weld and canister shell seam welds are helium pressure tested and leak tested. The canister shell extension and bottom end plate attachment welds are non-pressure retaining welds and are liquid dye penetrant examined.

Physical Dimensions

The breakdown of weights for both FuelSolutions™ W74 canister classes with the associated SNF assembly classes and configurations are provided in Chapter 3 of this FSAR. The maximum loaded dry weight of a sealed FuelSolutions™ W74 canister is approximately 76,300 lbs. This is within the design criteria for use within the transfer and storage casks, as discussed in Section 2.2 of the FuelSolutions™ Storage System FSAR.

The overall dimensions of each type of FuelSolutions™ W74 canister are summarized in Table 1.2-2, and are shown on the drawings contained in Section 1.5.1 of this FSAR. These canister dimensions conform to the standardized physical interface with the FuelSolutions™ storage cask and transfer cask, as discussed in the FuelSolutions™ Storage System FSAR.

Structural Capabilities

The FuelSolutions™ W74 canisters are designed for all design basis normal, off-normal, and postulated accident condition loadings, as defined in Section 2.3 of this FSAR. These include dead weight, handling loads, internal pressure, thermal expansion, cask drop loads, cask tip-over loads, and a range of loads resulting from natural phenomena. The internal basket assembly maintains the geometric spacing of the SNF assemblies, which assures criticality safety and retrievability of the SNF assemblies for all design basis loadings. Similarly, the canister shell assembly provides for confinement of radioactive materials for all design basis loadings. The structural analysis of the FuelSolutions™ W74 canister for normal, off-normal, and postulated accident conditions loads is provided in Chapter 3 of this FSAR. Load combinations, comparisons to allowable stresses, and the resulting design margins are also provided in Chapter 3.

Heat Removal Capabilities

The SNF assemblies stored within the FuelSolutions™ W74 canister generate decay heat, which is transferred to the canister and the storage cask or transfer cask. Removal of decay heat from the SNF assemblies to the ambient is accomplished by a combination of conduction, convection, and radiation heat transfer within and through these components. The increased conductivity of an internal helium atmosphere compared with that of air also facilitates heat removal. A FuelSolutions™ W74 canister maintains the SNF assembly cladding temperatures and the temperatures of canister structural materials within conservative allowable temperatures during dry storage, when subjected to bounding decay heat generation rates. Further discussion of the FuelSolutions™ W74 canister thermal characteristics is provided in Chapter 4 of this FSAR. The heat dissipation and removal capabilities of the storage cask and transfer cask are discussed in the FuelSolutions™ Storage System FSAR.

Shielding and Radiation Protection

The FuelSolutions™ W74 canister contains both neutron and gamma radiation sources. The canister shell provides minimal biological shielding in the radial direction for these sources, and relies on the transfer cask and storage cask to provide sufficient biological shielding for the attenuation of neutron and gamma radiation, to maintain occupational exposures ALARA, and to satisfy regulatory requirements. Both ends of the FuelSolutions™ W74 canister provide axial gamma shielding in the form of steel closure plates and steel shield plugs. The shielded top end of the canister provides radiological protection during upper basket fuel loading, canister closure operations, and canister transfer operations. Shielding for fuel loading of the lower basket is provided by the water-filled canister. Similarly, the shielded bottom end of the canister provides radiological protection during canister transfer operations.

The canister end shielding provides sufficient axial attenuation of gamma radiation to maintain occupational exposure ALARA for all canister closure and handling operations. Temporary or portable shielding can be used as required to further attenuate radiation and scatter that may occur in the annular area between the storage cask or transfer cask and the canister during canister handling operations. The shielding analysis of the FuelSolutions™ W74 canister is discussed further in Chapter 5 of this FSAR. An occupational dose assessment for the FuelSolutions™ W74 canister is provided in Chapter 10 of this FSAR.

Criticality Control

The FuelSolutions™ W74 canister design provides criticality control under all design basis normal, off-normal, and postulated accident conditions. The FuelSolutions™ W74 basket assembly uses a conservative design to maintain criticality control. The effective neutron multiplication factor, k_{eff}, meets the regulatory acceptance limits for storage and transportation conditions with optimum fresh water moderation and close reflection considering all biases and uncertainties. As discussed in Section 6.1 of the FuelSolutions™ Storage System FSAR, the design basis for criticality control is the limiting 10CFR71 transportation conditions that bound 10CFR72 storage conditions. The FuelSolutions™ W74 basket is designed to accommodate enriched fuel without the need for burnup credit, as discussed in Section 2.1.2 of this FSAR.

Criticality control is provided in the FuelSolutions™ W74 basket assembly by the geometric spacing of the guide tube assemblies and by borated stainless steel neutron absorbing material incorporated into the guide tube assemblies. The geometric spacing is maintained by the spacer

plates that support the guide tubes and the fuel assemblies. The borated neutron absorber panels are secured to the guide tubes by welded stainless steel retainers. The borated neutron absorber materials in the basket are non-structural members, and no structural credit is taken for borated materials. The criticality safety design features and analysis are discussed further in Chapter 6 of this FSAR.

Confinement

The FuelSolutions™ W74 provides for confinement of all radioactive materials during dry storage. The confinement boundary for the FuelSolutions™ W74 canister is provided by the canister shell assembly, including the cylindrical shell, the redundant top end closure plates and closure welds, and the bottom end plate and weld to the canister shell.

The canister shell seam welds and bottom end plate weld are full penetration 100% radiographed welds that are helium pressure and leak tested. The top end inner closure plate to canister shell weld is a multi-pass weld. The root and final passes of this weld are dye-penetrant examined and subjected to a helium pressure test and leak test. The top end outer closure plate to canister shell weld is also a multi-pass weld, and the root pass, intermediate pass, and final pass of this weld are dye-penetrant examined. The internal helium atmosphere provides corrosion protection and facilitates heat removal, to assure that the integrity of the SNF assembly cladding during dry storage is maintained. The confinement design features and analysis for the FuelSolutions™ W74 canister are discussed further in Chapter 7 of this FSAR.

1.2.1.4 FuelSolutions™ Support Equipment

The FuelSolutions™ SFMS support equipment used to facilitate FuelSolutions™ W74 canister loading, closure, and transfer operations is shown schematically in Figure 1.2-1 and identified in the paragraphs that follow. Generally, this equipment is commercial grade equipment designed for high reliability in a heavy industrial environment. The safety classification for the FuelSolutions™ support equipment is provided in the sections that follow. Although this equipment is generally classified as not important to safety or safety related, calibration and preoperational testing of some equipment is performed to assure proper interface with system components and equipment that are classified as important to safety or safety related.

Descriptions of the FuelSolutions™ support equipment are provided in Section 1.2.1.4 of the FuelSolutions™ Storage System FSAR to facilitate a complete understanding of FuelSolutions™ Storage System operations and the basic design features of this equipment. The support equipment that is unique to the FuelSolutions™ W74 canister is described in the sections that follow. The support equipment identified herein, or alternate equivalent equipment, may be used consistent with the design basis for the FuelSolutions™ W74 canister and other FuelSolutions™ Storage System components and equipment that are classified as important to safety or safety related. The safety classification of the FuelSolutions™ support equipment is discussed further in Section 2.1.1 of the FuelSolutions™ Storage System FSAR.

1.2.1.4.1 Canister Closure/Opening Equipment

The support equipment used for FuelSolutions™ W74 canister closure and opening operations is described in Section 1.2.1.4.1 of the FuelSolutions™ Storage System FSAR. This equipment is classified as not important to safety and includes the following:

- Annulus Seal
- Shield Plug Retainers
- Vacuum Drying System
- Inner Closure Plate Strongback
- Automated Welding/Opening System
- Helium Leak Detection System

In addition, specialty equipment is used for FuelSolutions™ W74 canister fuel loading outside the spent fuel pool, within the plant's fuel building. With the exception of the fuel assembly shuttle cask, which is classified as safety related, this equipment is also classified as not important to safety and includes the following:

- Fuel Assembly Shuttle Cask
- Shielded Loading Collar
- Lower Basket Loading Funnel
- Shield Plug Installation Fixture
- Transfer Cask Support Skid

1.2.1.4.2 Equipment for Horizontal Canister Transfer

The support equipment used for horizontal transfer of the FuelSolutions™ W74 canister is described in Section 1.2.1.4.2 of the FuelSolutions™ Storage System FSAR. With the exception of the storage cask impact limiter, which is classified as important to safety, this equipment is classified as not important to safety and includes the following:

- Horizontal Transfer Trailer
- Horizontal Transfer Skid
- Hydraulic Ram System
- Upender/Downender
- Storage Cask Impact Limiter
- Horizontal Lid Handling Fixture

1.2.1.4.3 Equipment for Vertical Canister Transfer

The support equipment used for vertical transfer of the FuelSolutions™ W74 canister is described in Section 1.2.1.4.3 of the FuelSolutions™ Storage System FSAR. With the exception of the vertical canister lift fixture, which is classified as safety related, this equipment is classified as not important to safety. Equipment for vertical canister transfer includes the following:

- Vertical Transporter
- Vertical Transport Trailer

- Air Pallet System
- Vertical Canister Lift Fixture

1.2.1.4.4 Common Equipment for Horizontal or Vertical Canister Transfer

The support equipment common to both horizontal or vertical transfer of the FuelSolutions™ W74 canister is described in Section 1.2.1.4.4 of the FuelSolutions™ Storage System FSAR. With the exception of the cask lifting yoke and the empty canister lift fixture, which are classified as safety related, this equipment is classified as not important to safety. Equipment common to both horizontal or vertical canister transfer includes the following:

- Cask Lifting Yoke
- Docking Collar
- Cask Restraints
- Empty Canister Lift Fixture
- Standard Lifting Slings

1.2.1.4.5 Specialty Equipment for the FuelSolutions™ W74 Canister

In addition to the standard FuelSolutions™ Storage System support equipment listed above and described in the FuelSolutions™ Storage System FSAR, additional canister specific support equipment is needed for FuelSolutions™ W74 canister fuel loading outside the spent fuel pool within the BRP reactor building. This equipment is not shown on Figure 1.2-1. This additional equipment is described in this FSAR to allow evaluation of the operational interfaces with the FuelSolutions™ W74 canister. The FuelSolutions™ W74 canister-specific support equipment is described in the following paragraphs.

Fuel Assembly Shuttle Cask

The fuel assembly shuttle cask is used to load SNF assemblies into a FuelSolutions™ W74 canister outside the spent fuel pool. It is used to bring a single SNF assembly from the spent fuel pool to the FuelSolutions™ W100 Transfer Cask and canister positioned in the plant's cask receiving area. The shuttle cask is an existing device that is used at BRP for loading and transferring fuel assemblies within the spent fuel pool to and from the reactor. The shuttle cask interfaces with the FuelSolutions™ shielded loading collar for loading each fuel assembly into the upper and lower baskets of the FuelSolutions™ W74 canister. The shuttle cask is equipped with a grapple, cabling system (for raising and lowering SNF assemblies), biological shielding (axial and radially), and a lower closure door. The fuel assembly shuttle cask is handled by the 75 ton reactor building crane.

Shielded Loading Collar

The shielded loading collar, shown in Figure 1.2-4, mates with the top of the FuelSolutions™ W100 Transfer Cask to allow loading of the FuelSolutions™ W74 canister outside of the spent fuel pool using the existing BRP fuel assembly shuttle cask (described above). The shielded loading collar is a welded, machined, carbon steel assembly that provides additional gamma shielding during canister loading. Lead shielding is used in the areas where the collar thickness is reduced. Canister guide tube alignment for fuel loading is performed by rotating the loading

collar assembly on an externally geared bearing driven by a manually rotated pinion gear (providing circumferential alignment) and moving the alignment tray in and out using the hand wheel/drive screw assembly (providing radial alignment), as shown in Figure 1.2-5. The shielded loading collar system includes miscellaneous components, including alignment fixtures and the fuel assembly loading funnel. These components are used to facilitate alignment of the loading collar over the basket guide tube and to facilitate fuel assembly placement in the FuelSolutions™ W74 canister upper and lower baskets.

Once alignment with the guide tube is complete, the transfer collar is locked in position to prevent further movement. During fuel assembly transfer from the shuttle cask (described above) the water level in the canister and transfer cask rises. The water overflow due to fuel assembly water displacement is controlled through a shielded loading collar water management system, as shown in Figure 1.2-6. The water management system collects the overflow water in a reservoir. A pump is used to direct the reservoir water back to the spent fuel pool.

Lower Basket Loading Funnel

The lower basket loading funnel interfaces with the shielded loading collar to provide alignment of SNF assemblies when loading the FuelSolutions™ W74 canister lower basket, as shown in Figure 1.2-6. The funnel is aligned with the shielded loading collar and guide tube to be loaded, to maintain the fuel assembly position during placement in the basket.

Shield Plug Installation Fixture

In order to provide additional shielding for loading the FuelSolutions™ W74 upper basket, the shield plug assembly is installed in the canister before fuel loading. As described above, the shield plug assembly in the upper basket of the FuelSolutions™ W74 canister contains 37 individual shield plugs that are inserted into a thick machined shield plate. In order to allow loading of the upper basket, each individual shield plug is removed (prior to loading in an empty guide tube), using the shield plug installation fixture. The shield plug installation fixture consists of a shield bell with a hand-winch hoist system that is used to secure and lift a shield plug individually. The fixture interfaces to the shielded loading collar. The loading collar is used to align the shield plug installation fixture over the basket guide tube for removal and installation of the shield plug.

Transfer Cask Support Skid

In order to allow vertical loading of the FuelSolutions™ W74 canister inside the FuelSolutions™ transfer cask, the horizontal transfer skid (described in Section 1.2.1.4.2 of the FuelSolutions™ Storage System FSAR) is used to maintain the transfer cask in a stable, vertical position. The horizontal transfer skid is augmented with outriggers, jacks, and a support arm in order to provide vertical and lateral stability for the transfer cask during canister loading operations outside the spent fuel pool. The outriggers are designed for shimming or attachment of the skid to the building floor, if required. The transfer cask support skid is designed for ease of installation and removal of the transfer cask to and from the reactor building so that occupational exposures are ALARA.

The design of the canister specific support equipment used for the FuelSolutions™ W74 canister is very similar to that used for the Three Mile Island Unit 2 defueling using the NUPAC-125B

cask system. It is also much the same operation as is currently performed at BRP for reactor refueling.

1.2.2 Operational Features

A description of the FuelSolutions™ Storage System operational design features and a system operations overview is provided in Section 1.2.2 of the FuelSolutions™ Storage System FSAR. This section provides a description of the operational design features for the FuelSolutions™ W74 canister and an overview of the FuelSolutions™ Storage System operations using the FuelSolutions™ W74 canister. Operating procedures that are specific to the FuelSolutions™ W74 canister are provided in Chapter 8 of this FSAR.

FuelSolutions™ W74 Canister

The FuelSolutions™ W74 canister incorporates several design features to facilitate canister fuel loading, closure, and transfer operations. These features include the following:

- Top and bottom end shield plugs, which allow vertical or horizontal canister transfer.
- A top shield plate with individual shield plugs to facilitate canister fuel loading outside the spent fuel pool.
- Ports and a drain tube for canister draining, drying, inerting and leak testing, which are integral with the top shield plate.
- An inner closure plate instrument port to monitor canister internal pressure during reflood operations.
- An auxiliary outer closure plate leak test port for canister closure weld leak testing following canister fuel loading, if it becomes necessary.
- Threaded counterbores on the top end outer closure plate for vertical lifting fixture attachment and installation of the horizontal transfer pintle.
- Threaded counterbores on the bottom end plate for installation of the horizontal transfer pintle plate.
- Upper and lower basket assemblies for a capacity of up to 64 fuel assemblies. The 10 center cell locations are mechanically blocked to prevent fuel assemblies from being loaded in these locations.

FuelSolutions™ W150 Storage Cask

The FuelSolutions™ W150 Storage Cask design incorporates several design features that facilitate transfer of a FuelSolutions™ canister between a storage cask and a transfer or transportation cask. Key operational features of the storage cask are discussed further in Section 1.2.2 of the FuelSolutions™ Storage System FSAR.

FuelSolutions™ W100 Transfer Cask

The FuelSolutions™ W100 Transfer Cask is designed to facilitate FuelSolutions™ canister loading, closure, and transfer to and from a storage cask or transportation cask. Key operational

features of the transfer cask are discussed further in Section 1.2.2 of the FuelSolutions™ Storage System FSAR.

1.2.2.1 Canister Loading

Loading Outside the Spent Fuel Pool

The FuelSolutions™ W74 canister is designed to be loaded outside a spent fuel pool using the BRP fuel assembly shuttle cask, a shielded loading collar, and a transfer cask. Procedures for these operations are provided in Section 8.3 of this FSAR. The basic operations for canister fuel loading using this approach are as follows:

- Place the transfer cask in the plant's cask receiving area. Upend the transfer cask to a vertical orientation and support the transfer cask in the vertical position on the horizontal transfer skid.
- Fill the transfer cask liquid neutron shield.
- Remove the transfer cask top cover and insert an empty FuelSolutions™ W74 canister, containing only a lower basket assembly, into the transfer cask. Fill the cask/canister annulus with clean demineralized water and install the inflatable seal. Fill the FuelSolutions™ W74 cavity with fuel pool water.
- Install the shielded loading collar onto the top of the transfer cask. Install the water management system.
- Align the shielded loading collar over the basket guide tube that is to be loaded.
- Load the lower basket using the BRP fuel assembly shuttle cask.
- Remove the shielded loading collar, insert the empty upper basket assembly into the canister. (The water management system is used to handle the water from the canister that overflows due to basket insertion and fuel loading.)
- Re-install the top shield plug assembly and the shielded loading collar.
- Load the upper basket by removing the individual shield plugs with the shield plug installation fixture and inserting the fuel assemblies using the shuttle cask and shielded loading collar. Reinsert the individual shield plugs after each guide tube is loaded.

Loading In the Spent Fuel Pool

A FuelSolutions™ W74 canister may also be loaded in a spent fuel pool using either a transfer cask or a transportation cask consistent with the plant's crane capacity. The procedures for these operations are discussed in Section 8.1 of this FSAR. Using a transfer cask as an example, the basic operations are as follows:

- Remove the transfer cask top cover and insert the empty canister containing only the lower basket assembly, without the top end shield plug assembly or closure plates, into the transfer cask cavity.
- Fill the annulus between the transfer cask and canister with clean demineralized water and install the inflatable seal. Fill the canister cavity with fuel pool water.

- Lower the transfer cask with the empty canister into the spent fuel pool using the cask lifting yoke. Load the SNF assemblies into the lower basket guide tubes using standard plant fuel handling procedures.
- Insert the upper basket assembly into the canister. Load the SNF assemblies into the upper basket guide tubes using standard plant fuel handling procedures.
- Insert the canister shield plug assembly, remove the transfer cask from the spent fuel pool using the cask lifting yoke, engage the shield plug retainers, and place the cask in the decontamination area.
- If not already full, fill the cask neutron shield with demineralized water and decontaminate the cask exterior and canister shell weld prep exposed surfaces.

1.2.2.2 Canister Closure/Opening

Canister Closure

After canister fuel loading operations, the loaded transfer cask is typically staged in the cask decontamination area for canister draining, drying, inerting, and sealing operations. These operations are discussed in Section 8.1 of this FSAR. The basic operations for the closure of the FuelSolutions™ W74 canisters are as follows:

- Mount the automated welder to the inner closure plate and install the inner closure plate above the shield plug.
- Adjust the canister water level for welding, remove the annulus seal, and install a protective barrier over the annulus to prevent weld debris from entering the annulus.
- Check for combustible gases (e.g., hydrogen) and purge the canister with a non-combustible inert gas (e.g., argon), if required. Monitor the canister water temperature using the thermocouple inserted through the vent port.
- Weld the inner closure plate to the canister shell and the vent/drain port adapters.
- Perform a dye penetrant inspection (final surface) of the inner closure plate seal welds to the canister shell and vent/drain port adapters.
- Install the inner closure plate strongback and fully drain the canister cavity by pressurizing the canister with dry inert gas (e.g., helium).
- Dry the canister using the vacuum drying system.
- Backfill the canister with helium and perform a final pneumatic pressure test and a helium leak test.
- Vent and re-inert the canister by backfilling it with helium. Weld the vent and drain port covers to the vent and drain port bodies.
- Perform a dye-penetrant inspection (final surface) of the vent and drain port cover welds.
- Mount the automated welder to the outer closure plate and install the outer closure plate on top of the inner closure plate.

- Weld the outer closure plate to the canister shell.
- Perform a dye-penetrant inspection (root, intermediate, and final surface) of the outer closure plate weld to the canister shell.
- Evacuate and backfill the space between the inner and outer closure plates with helium and perform a final pneumatic pressure test and a helium leak test.
- Weld the leak test port cover to the outer closure plate.
- Perform a dye-penetrant inspection (root and final surface) of the leak test port cover weld.

Canister Opening

In the unlikely event that canister opening is required, the canister is retrieved from the storage cask into a transfer cask and staged in the cask decontamination area. These operations are provided in Section 8.2 of this FSAR. The canister opening sequence involves reflooding the cavity with fuel pool water, removing the outer and inner closure plates, lowering the transfer cask into the fuel pool, removing the shield plug, and unloading SNF assemblies from the canister basket into the fuel pool storage racks. The basic operations are as follows:

- Slowly fill the annulus between the transfer cask and canister with clean demineralized water by using the transfer cask annulus ports.
- Install the inflatable annulus seal. Initiate recirculation of cooling water through the cask/canister annulus, as necessary, to supplement canister heat removal through the canister shell.
- Cut an access hole through the outer closure plate at the vent, drain, and instrument port scribed circles and remove the port covers.
- Vent the canister through the vent port fitting and collect a gas sample to check for indication of damaged fuel and combustible gas (licensee option).
- Remove the vent port fitting to increase the vent area and vent the canister to the fuel pool.
- Monitor the canister cavity temperature, via a thermocouple inserted into the canister through the vent port, to verify that canister temperatures are decreasing or remaining constant.
- Connect a pressure gauge to the instrument port.
- Slowly introduce fuel pool water into the drain line and fill the canister cavity. Closely monitor canister pressure at the instrument port pressure gauge.
- If necessary, reinitiate cask/canister annulus cooling until the canister cavity temperature is within an acceptable range to complete the filling operation without exceeding allowable canister pressures.
- Remove the outer and inner closure plates using the AW/OS.
- Place the transfer cask and canister in the spent fuel pool.
- Remove the shield plug and unload the SNF assemblies.

Fuel assembly removal operations are essentially the reverse of fuel loading operations, as described in Section 1.2.2.1.

1.2.2.3 Canister Horizontal Transfer

The FuelSolutions™ W74 canister is designed for horizontal canister transfer between a transfer cask and a storage cask or transportation cask, and between a storage cask and a transportation cask. Equipment descriptions and the basic operations for horizontal canister transfer are discussed further in Sections 1.2.1.4.2 and 1.2.2.3, respectively, of the FuelSolutions™ Storage System FSAR.

1.2.2.4 Canister Vertical Transfer

The FuelSolutions™ W74 canister is designed for vertical canister transfer between a transfer cask and a storage cask, and between a transfer cask and a transportation cask. Equipment descriptions and the basic operations for vertical canister transfer are discussed further in Sections 1.2.1.4.3 and 1.2.2.4, respectively, of the FuelSolutions™ Storage System FSAR.

1.2.2.5 Storage

On-site FuelSolutions™ W74 canister storage with the FuelSolutions™ Storage System is accomplished by arranging freestanding vertical FuelSolutions™ W150 Storage Casks in arrays on an ISFSI pad. The basic operations for storage are discussed further in Section 1.2.2.5 of the FuelSolutions™ Storage System FSAR.

1.2.2.6 Transportation Cask Loading

The transportation cask can be used to directly load FuelSolutions™ W74 canisters in a plant's spent fuel pool and to ship the FuelSolutions™ W74 canisters off-site. The components and operational features related to the transport cask are discussed in a separate transportation license application. Horizontal and vertical canister transfers between a storage cask, a transportation cask, and a transfer cask are discussed further in Section 1.2.2.6 of the FuelSolutions™ Storage System FSAR.

1.2.3 FuelSolutions™ W74 Canister Contents

A FuelSolutions™ W74 canister is designed to accommodate up to 64 BRP zircaloy-clad BWR fuel assemblies (the ten center cell locations are not used). The design criteria for FuelSolutions™ W74 canister contents are provided in Section 2.2 of this FSAR.

As designed, a FuelSolutions™ W74 canister also accommodates BRP MOX, partial, and damaged fuel assemblies. The safety analysis and payload specifications for these fuel assemblies are provided in this FSAR.

Qualification of BRP SNF fuel assemblies for dry storage in the FuelSolutions™ W74 canister is dependent on the characteristics of the unburned fuel assembly, the characteristics of the fuel assembly at the time of reactor discharge, and the time since discharge (cooling time). The *technical specification* in Section 12.3 of this FSAR defines an acceptable range of enrichments, burnups, and cooling times for use by the licensee in qualifying SNF assemblies for dry storage. Table 2.0-1 includes the fuel assembly parameter values that form the basis for the safety evaluation documented herein.

A FuelSolutions™ W74 canister internal cavity is backfilled with helium following fuel loading and canister drying during canister closure operations. The SNF payload remains in an inert

environment throughout dry storage. The design basis normal, off-normal, and postulated accident condition canister internal pressures are included in Table 2.0-1 of this FSAR.

As discussed in Section 2.2, any FuelSolutions™ W74 canister and SNF payload that does not exceed the storage cask or transfer cask maximum thermal rating may be safely stored and handled by these casks. Similarly, any FuelSolutions™ W74 canister and SNF payload that does not exceed the storage cask design basis allowable dose rates discussed in Section 2.2 may be safely stored and handled by these casks.

Table 1.2-1 - Principal Characteristics of the FuelSolutions™ W74 Canister

Characteristic	W74M	W74T
Gross Weight (empty) - nominal	44,350 lbs.	42,200 lbs.
Materials of Construction[(1)]	Stainless Steel	
Materials Used As Neutron Absorbers and Moderators	Borated Stainless Steel	
External Dimensions: Diameter	66 inches	
Length (max.)	182.3 inches	
Cavity Size: Diameter	64.8 inches	
Length (min.)	173.0 inches	
Internal Structures	Coated Carbon and Stainless Steel Spacer Plates and Stainless Steel Support Tube Basket Assembly	
External Structures	None	
Receptacles	N/A	
Valves	Vent & Drain Fittings	
Sampling Ports	Instrument Port Available during Canister Reflooding, Outer Closure Plate Test Port	
Means of Passive Heat Dissipation	Conduction, Convection, and Radiation	
Volume of Coolant	N/A	
Type of Coolant	N/A	
Outer Protrusions	None	
Inner Protrusions	Vent & Drain Port Bodies and Drain Tube	
Lifting Devices	Separate Lifting Fixture	
Impact Limiters	N/A	
Amount of Shielding: Radial	5/8-inch thick Stainless Steel	
Bottom End	5.75-inch Carbon Steel / 2.75-inch Stainless Steel	
Top End	7.25-inch Carbon Steel / 3.00-inch Stainless Steel	
Pressure Relief Systems	None	
Closures	Welded Inner and Outer Top and Inner Bottom Closure Plates	
Means of Confinement	All Welded Construction with No Penetrations or Mechanical Seals	
Model Number-Cavity Designator	W74M	W74T
Description of How Individual Casks Will Be Identified	Individually Stamped (see Section 9.1.7.2)	

Note:

(1) Structural confinement materials only.

Table 1.2-2 - Matrix of FuelSolutions™ W74 Canister Configurations

	W74M[1]	W74T[1]
Canister Configuration	**LS[2]**	**LS[2]**
Overall Length, inch (max.)	192.3	192.3
Outside Diameter, inch	66.0	66.0
Shell Thickness, inch	0.63	0.63
Upper Basket		
Basket Length (including engagement sleeve), inch	88.3	88.3
Number of Spacer/Engagement Plates	15	14
CS Spacer Plate Thickness, inch	0.75	0.75
SS Spacer Plate Thickness, inch	2.00	NA
SS Engagement Spacer Plate Thickness, inch	2.00	2.00
Borated Neutron Absorber Panel Thickness, inch	0.075	0.075
Lower Basket		
Basket Length, inch	85.3	85.3
Number of Spacer Plates	14	13
CS Spacer Plate Thickness, inch	0.75	0.75
SS Spacer Plate Thickness, inch	2.00	NA
Borated Neutron Absorber Panel Thickness, inch	0.075	0.075
Basket Support and Guide Tubes		
Number of Support Tubes, each basket	4	4
SS Support Tube Inside Dimension (square), inch	7.40	7.40
SS Support Tube Thickness, inch	0.75	0.75
Number of Guide Tubes, each basket	28	28
SS Guide Tube Inside Dimension (square), inch	6.90	6.90
SS Guide Tube Thickness, inch	0.09	0.09
Top Closure		
Shield Plug Thickness, inch	7.25	7.25
Shield Plug Material	CS	CS
Inner Closure Plate Thickness, inch	1.00	1.00
Outer Closure Plate Thickness, inch	2.00	2.00
Bottom Closure		
End Plate Thickness, inch	1.75	1.75
Shield Plug Thickness, inch	5.75	5.75
Shield Plug Material	CS	CS
Closure Plate Thickness, inch	1.00	1.00
Cavity Length, inch (min.)	173.0	173.0
Available Basket Thermal Gap, inch (min. cavity)	0.50	0.50

Notes:

(1) All dimensions are nominal, unless noted otherwise.

(2) LS - Long, Steel, CS - Carbon Steel, SS - Stainless Steel

Table 1.2-3 - FuelSolutions™ W74 Canister Fuel Assembly Accommodation

Fuel Assembly Class	Irradiated Length (in)	Width (in)	Weight (lb)	Canister Type[1]
BWR Fuel Class				
	Fuel without Channels			
Big Rock Point 9x9	84.8	6.52	485	LS
Big Rock Point 11x11	84.8	6.52	485	LS

Note:
(1) Canister type definitions are provided in Table 1.2-2.

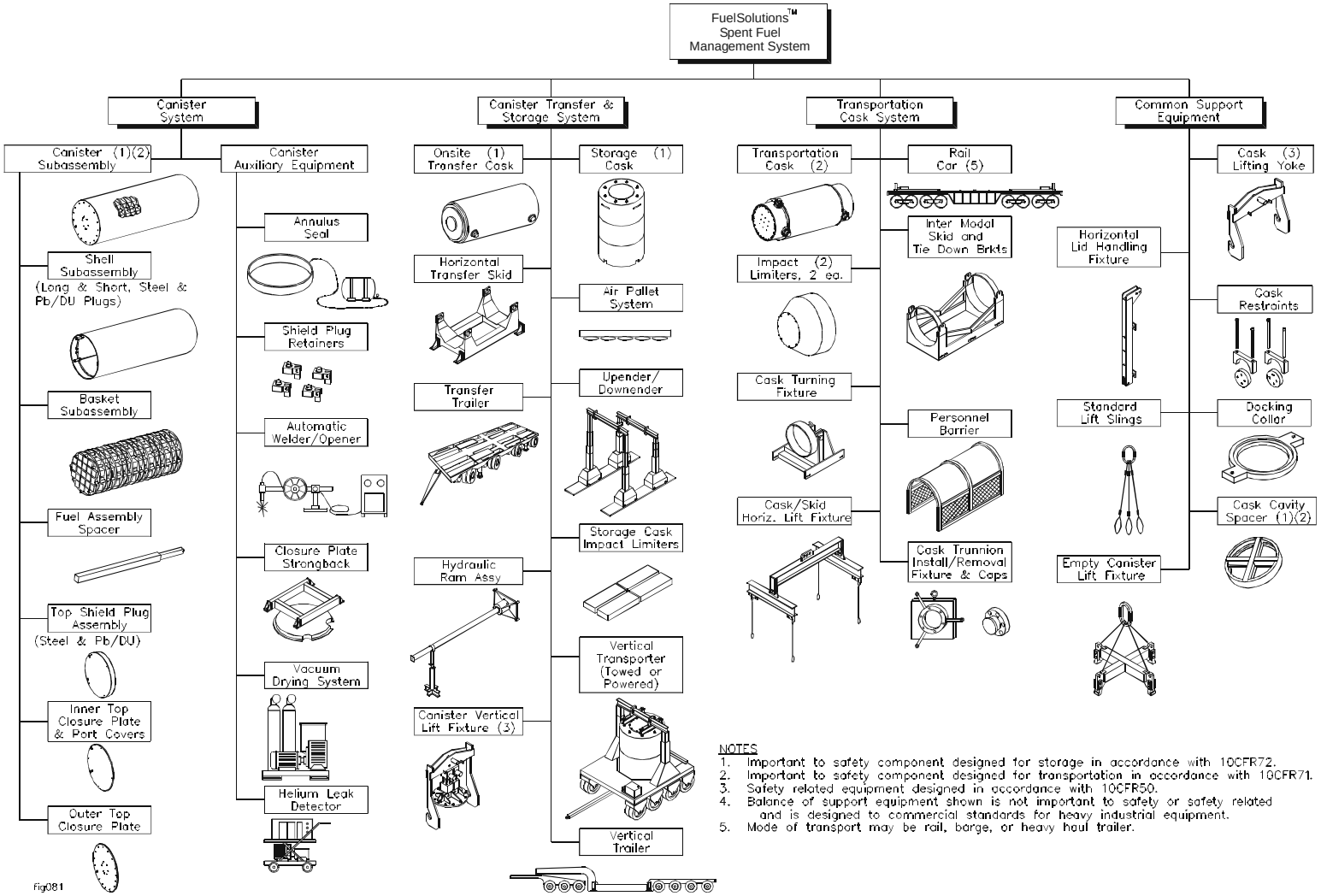

Figure 1.2-1 - FuelSolutions™ Spent Fuel Management System

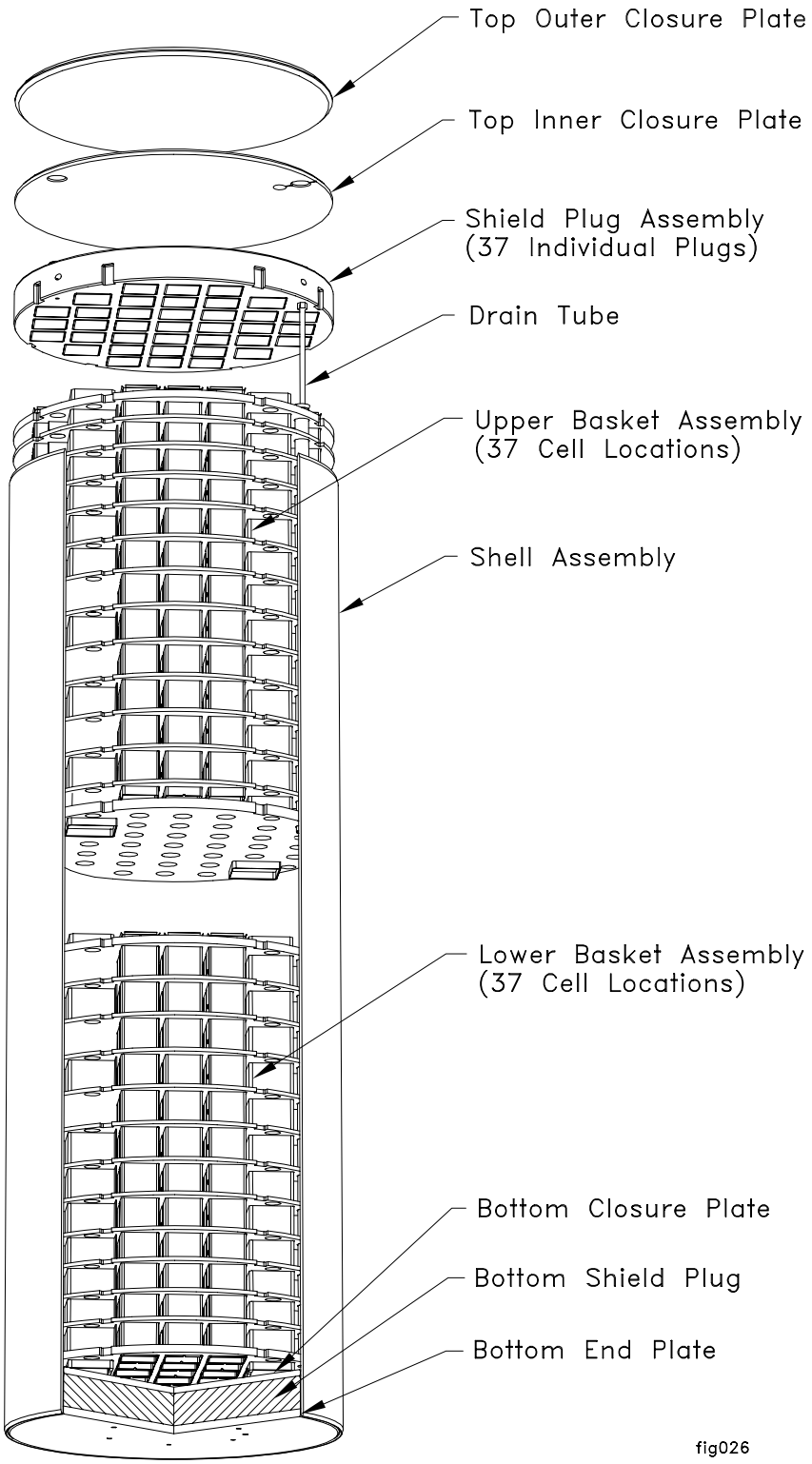

Figure 1.2-2 - FuelSolutions™ W74 Canister

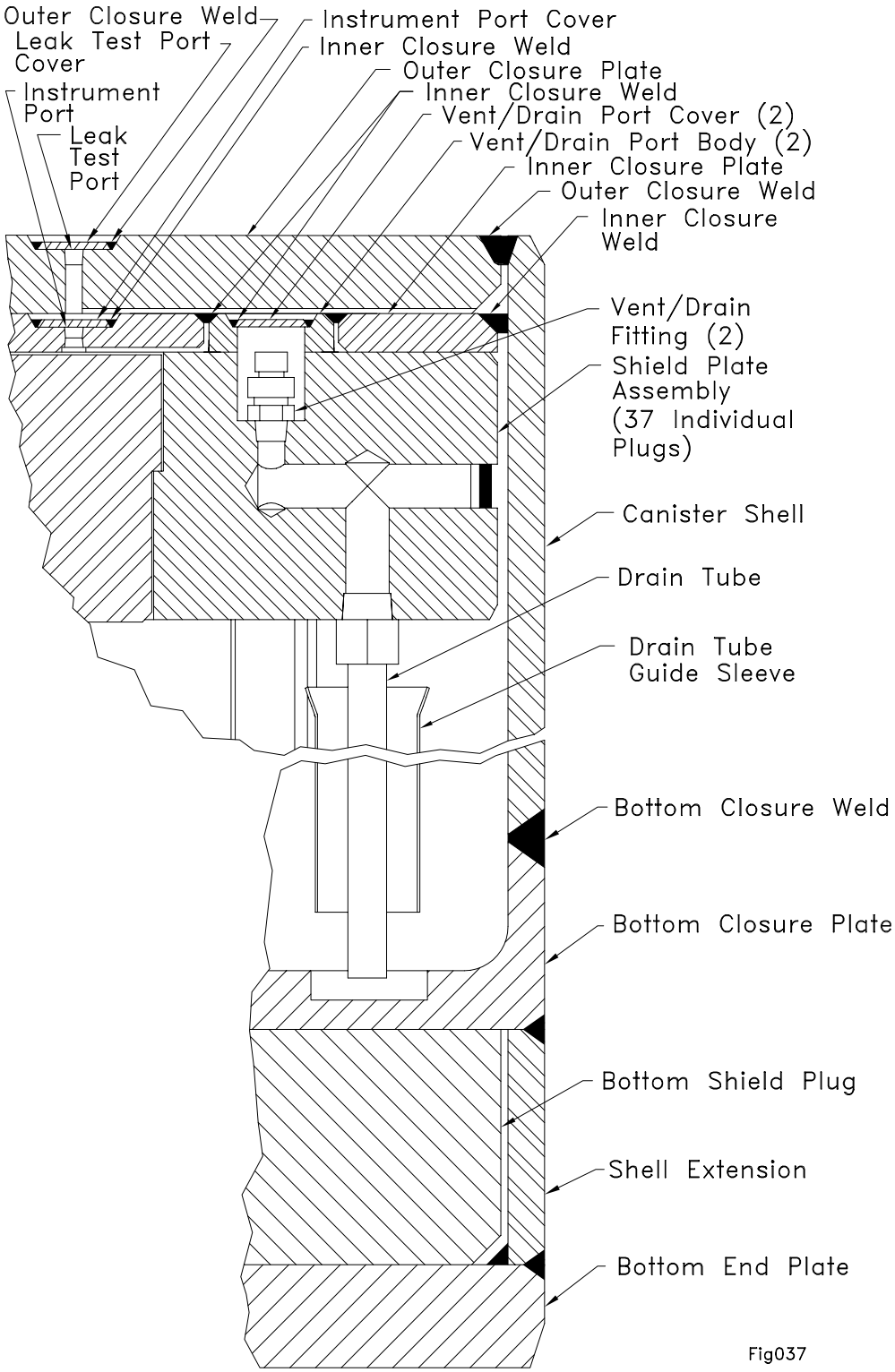

Figure 1.2-3 - FuelSolutions™ W74 Canister Top and Bottom Closure

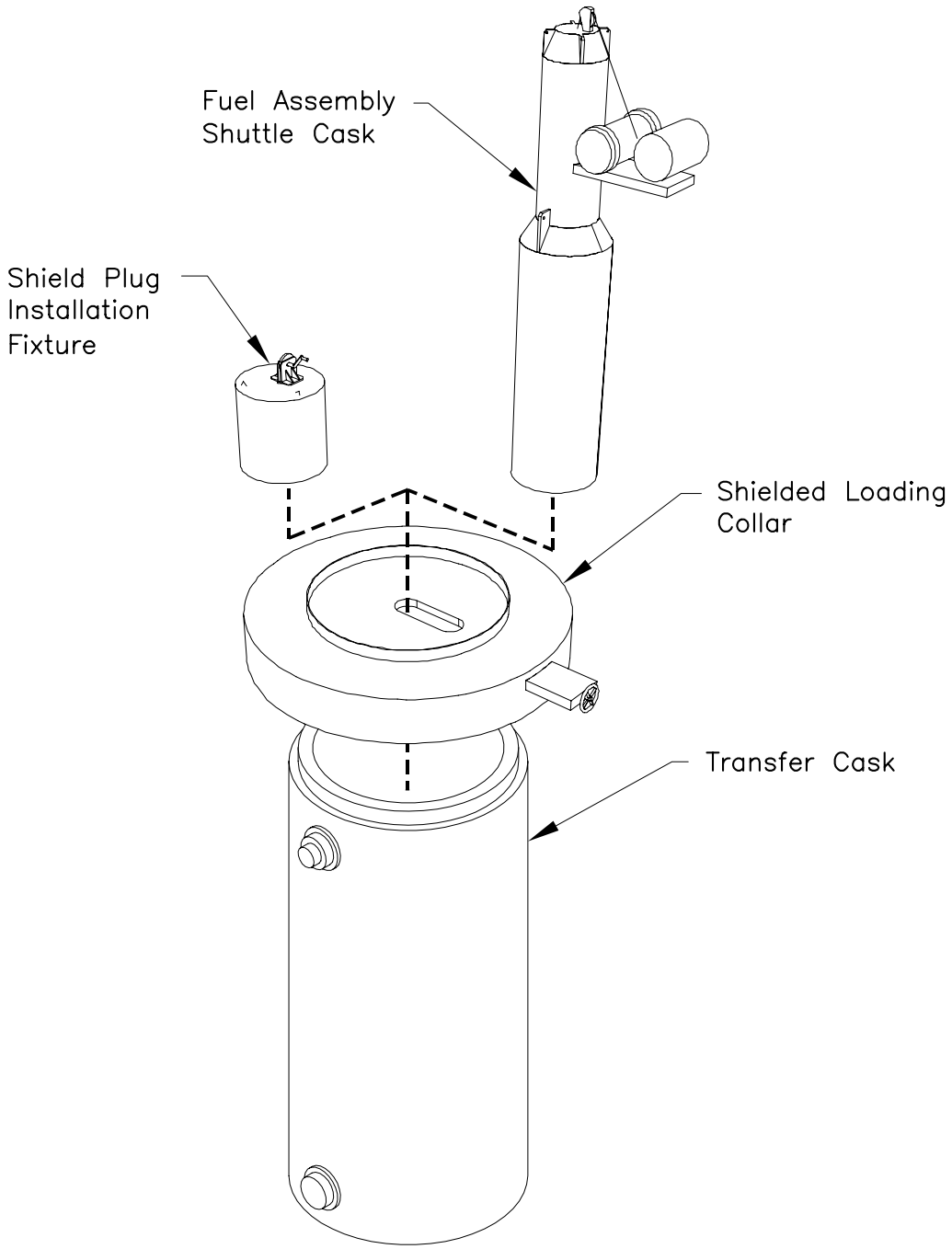

Figure 1.2-4 - Canister Fuel Loading Using Fuel Assembly Shuttle Cask and Shielded Loading Collar

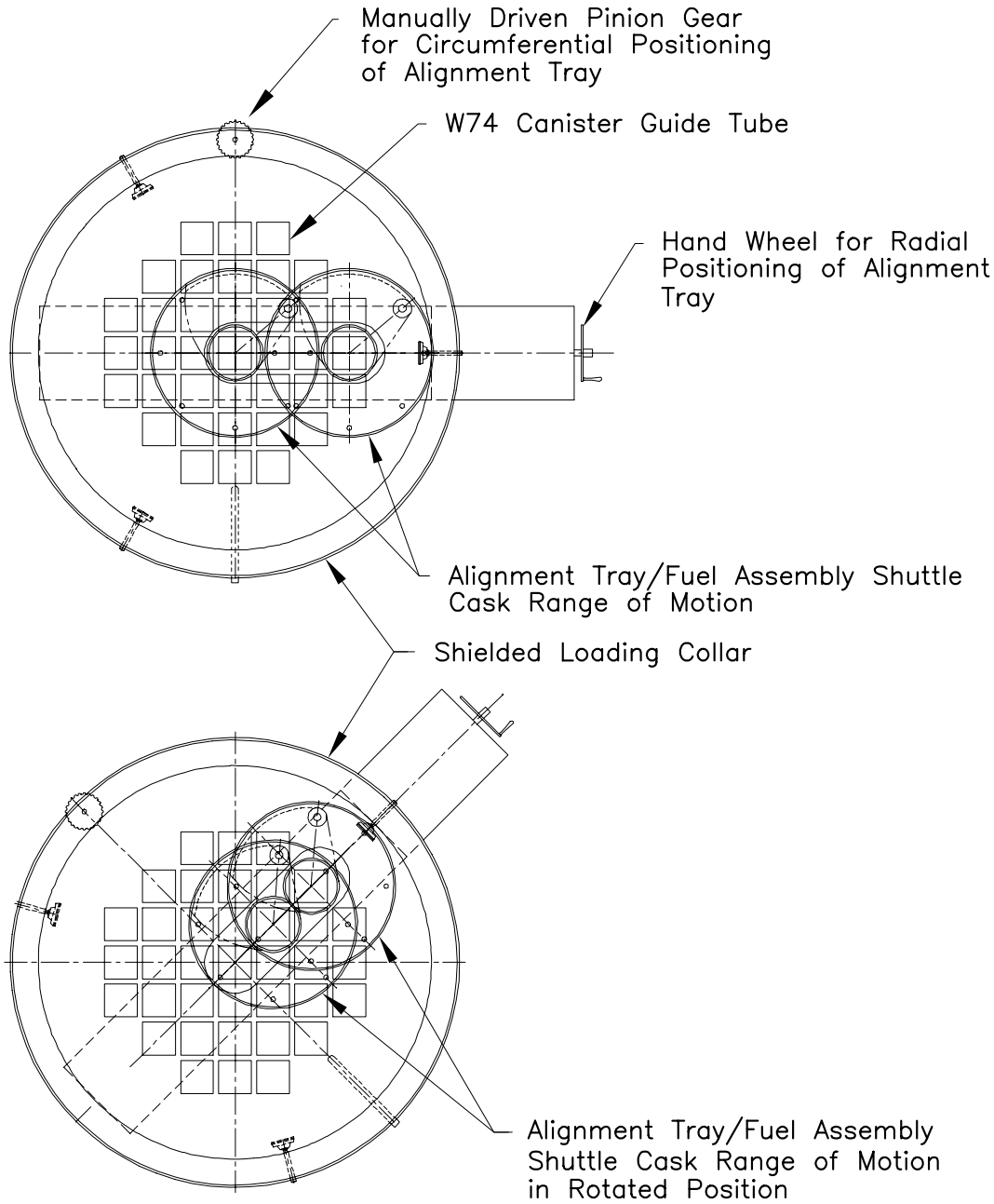

Figure 1.2-5 - Shielded Loading Collar

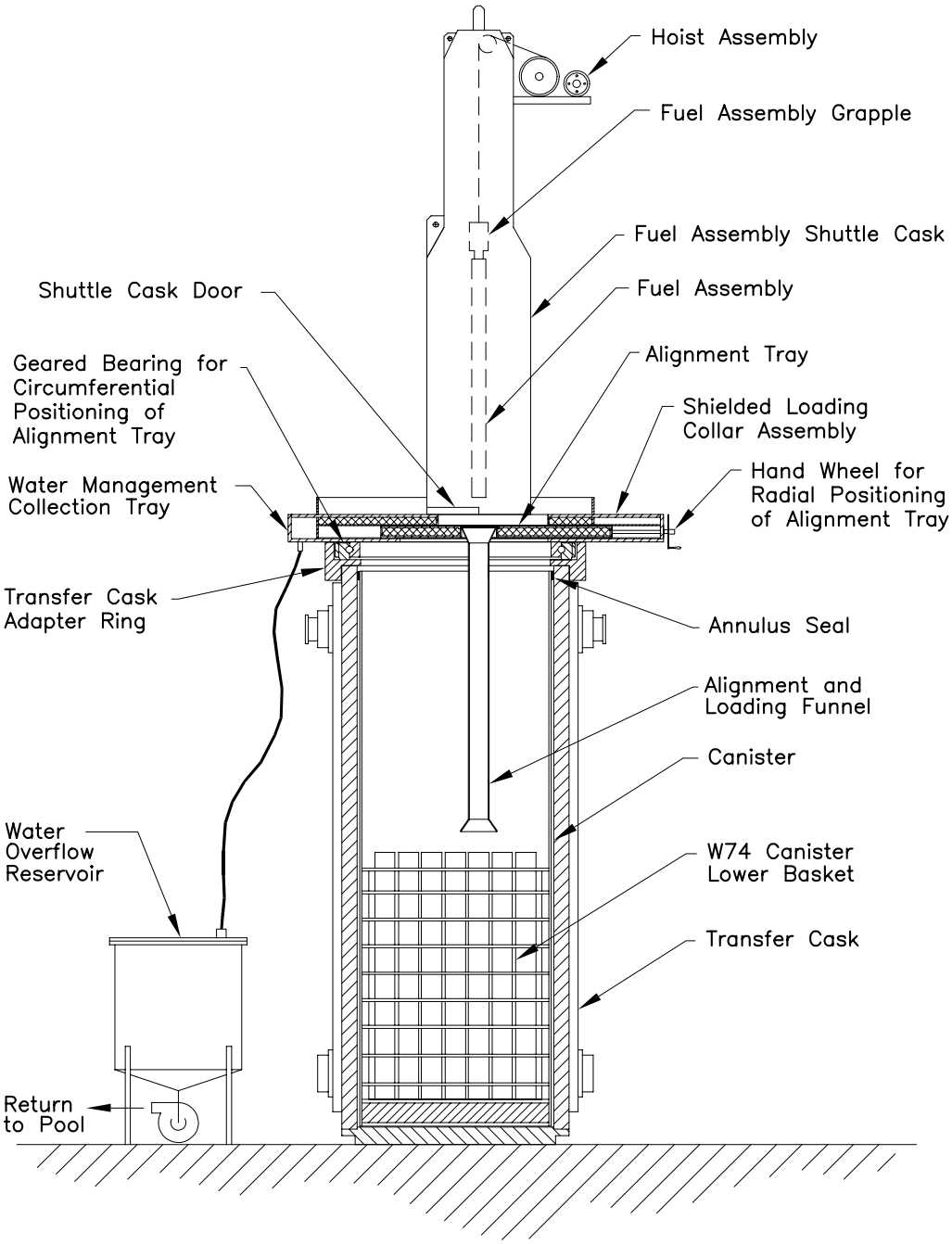

Figure 1.2-6 - Fuel Loading of Lower Basket

This page intentionally left blank.

1.3 Identification of Agents and Contractors

BNFL Fuel Solutions (BFS) is the prime contractor for design, fabrication, construction, assembly, testing, and operations of the FuelSolutions™ Storage System components. BFS is technically qualified and suitably experienced to conduct these activities and to be the 10CFR72, Subpart L, certificate holder for the FuelSolutions™ SFMS. A description of BFS' related capabilities and experience is provided in Section 1.3 of the FuelSolutions™ Storage System FSAR.

This page intentionally left blank.

1.4 On-Site Storage Array Configurations

Typical FuelSolutions™ Storage System ISFSI pad layouts are presented in Section 1.4 of the FuelSolutions™ Storage System FSAR.

This page intentionally left blank.

1.5 Supplemental Data

1.5.1 Drawings

General arrangement drawings of the FuelSolutions™ W74 canister are provided in this section. The drawings for the FuelSolutions™ W74 Canister include the following:

Title	Number	Revision
FuelSolutions™ W74 Canister Assembly	W74-110	5
FuelSolutions™ W74 Canister Basket Assembly	W74-120	5
FuelSolutions™ W74 Canister Spacer Plates	W74-121	7
FuelSolutions™ W74 Canister Basket Guide Tube Assembly	W74-122	6
FuelSolutions™ W74 Canister Shell Assembly	W74-130	6
FuelSolutions™ Canister Shield Plug Assembly	W74-140	5
FuelSolutions™ Canister Closure Plates, Vent/Drain Port Cover	W74-150	5
FuelSolutions™ W74 Assembly and Detail Damaged Fuel Can	3319	5

This page intentionally left blank.

ML051250077 2

8	7	6	5	4	3	W74-110	7	5	1

NOTES:

FIGURE WITHHELD UNDER 2.390

CANISTER ASSEMBLY

D	W74-110	5

SCALE NTS | FILE NO. CMPC.1205.110 | SHEET 1 OF 1

2 | 1

99/966

FIGURE WITHHELD UNDER 2.390

A

BNFL Fuel Solutions

D

W74-110

5

2 OF 2

2

1

100/966

8 7 6 5 4 3

FIGURE WITHHELD UNDER 2.390

TITLE	FuelSolutions™ W74 CANISTER BASKET ASSEMBLY
SIZE D	DWG NO W74-120 REV 5
SCALE NTS	FILE NO. CMPC.1205.120 SHEET 1 OF 8

2 1

101/966

8	7	6	5	4	3	1

FIGURE WITHHELD UNDER 2.390

BNFL Fuel Solutions	D		W74-120	5
2			1	

102

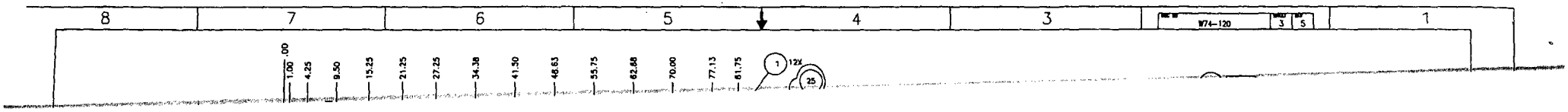

FIGURE WITHHELD UNDER 2.390

Fuel Solutions | SCALE NTS | FILE NO. CMPC.1205.120 | SHEET 3 OF 4

2 | 1

103

[redacted]

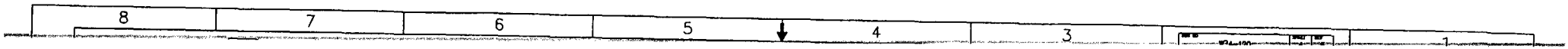

FIGURE WITHHELD UNDER 2.390

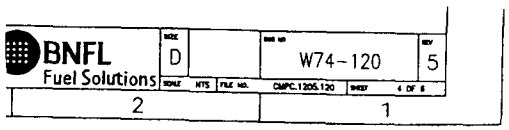

104

8 7 6 5 4 3 1

FIGURE WITHHELD UNDER 2.390

BNFL Fuel Solutions

SIZE D		DWG NO W74-120	REV 5
SCALE NTS	FILE NO.	CMPC-1200-120	SHEET 5 OF 6

2 1

105

8 7 6 5 4 3

FIGURE WITHHELD UNDER 2.390

BNFL Fuel Solutions

SIZE		DWG NO	REV
D		W74-120	5
SCALE	NTS	FILE NO. CMPC.1205.120	SHEET 6 OF 6

2 1

106

FIGURE WITHHELD UNDER 2.390

Fuel Solutions

FuelSolutions™ W74 CANISTER SPACER PLATES

D | W74-121 | 7

SCALE NTS | FILE NO. CMPC.1205.121 | SHEET 1 OF 1

2 | 1

107

FIGURE WITHHELD UNDER 2.390

Fuel Solutions

TITLE: FuelSolutions™ W74 CANISTER BASKET GUIDE TUBE ASSEMBLY

SIZE	DWG NO	REV
D	W74-122	6

SCALE	NTS	FILE NO.	CMPC.1205.122	SHEET	1 OF 1

108

FIGURE WITHHELD UNDER 2.390

-W74T SHELL ASSEMBLY

DESCRIPTION	SPECIFICATION	DUNS CAT
LIST OF MATERIAL		

BNFL Fuel Solutions

A

TITLE: FuelSolutions™ W74 CANISTER SHELL ASSEMBLY

SIZE	DWG NO	REV
D	W74-130	6

SCALE: NTS | FILE NO. CMPC.1205.130 | SHEET 1 OF 2

2 1

FIGURE WITHHELD UNDER 2.390

BNFL Fuel Solutions	D		W74-130	6
	SCALE NTS	FILE NO.	CMPC.1205.130	SHEET 2 OF 2

2 1

110

FIGURE WITHHELD UNDER 2.390

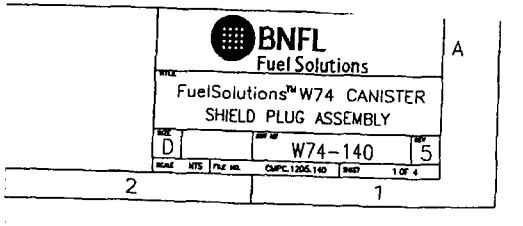

8 7 6 5 4 3

FIGURE WITHHELD UNDER 2.390

BNFL Fuel Solutions

SIZE D		DWG NO W74-140	REV 5
SCALE NTS	FILE NO. CMPC.1205.140	SHEET 2 OF 4	

2 1

112

8 | 7 | 6 | 5 | 4 | 3 | 1

FIGURE WITHHELD UNDER 2.390

BNFL Fuel Solutions | SIZE D | W74-140 | REV 5

SCALE NTS | FILE NO. CMPC.1205.140 | SHEET 3 OF 4

2 | 1

113

FIGURE WITHHELD UNDER 2.390

BNFL Fuel Solutions | SIZE D | W74-140 | REV 5

2 | 1

114

FIGURE WITHHELD UNDER 2.390

BNFL
Fuel Solutions

A

TITLE
FuelSolutions™ W74 CANISTER
TOP CLOSURE PLATES
AND PORT COVERS

SIZE D | DWG NO. W74-150 | REV 5

SCALE NTS | FILE NO. CMPC.1205.150 | SHEET 1 OF 2

2 | 1

115

FIGURE WITHHELD UNDER 2.390

BNFL
Fuel Solutions

TITLE
FuelSolutions™ W74 CANISTER
TOP CLOSURE PLATES
AND PORT COVERS

SIZE D | DWG NO W74-150 | REV 5

SCALE NTS | FILE NO. | CMPC.1205.150 | SHEET 2 OF 2

A

2 1

116

FIGURE WITHHELD UNDER 2.390

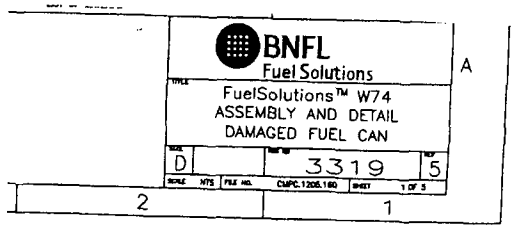

117

8 7 6 5 4 3

FIGURE WITHHELD UNDER 2.390

BNFL Fuel Solutions

SIZE		DWG NO	REV
D		3319	5

SCALE NTS FILE NO. CMPC.1205.180 SHEET 2 OF 5

2 1

118

8 | 7 | 6 | 5 | 4 | 3 | 1

FIGURE WITHHELD UNDER 2.390

BNFL Fuel Solutions | D | 3319 | 5

2 | 1

119

8 | 7 | 6 | 5 | 4 | 3 | 2 | 1

FIGURE WITHHELD UNDER 2.390

BNFL Fuel Solutions

SIZE		DWG NO	REV
D		3319	5
SCALE	NTS	FILE NO.	CMPC.1205.160	SHEET 4 OF 5

2 | 1

120/966

8 | 7 | 6 | 5 | 4 | 3 | 1

FIGURE WITHHELD UNDER 2.390

BNFL Fuel Solutions

SIZE		DWG NO	REV
D		3319	5
SCALE NTS	FILE NO.	CMPC.1205.160	SHEET 5 of 5

2 | 1

(2)/966

This page intentionally left blank

1.5.2 Product Literature

Literature describing special materials used for the FuelSolutions™ W74 canister are provided in this section.

1.5.2.1 Borated Stainless Steel Literature

Literature describing typical borated stainless steel neutron absorbing materials used for the FuelSolutions™ W74 canister basket assembly is provided in this section (pages 1 - 18). Note that this information is considered to be typical and the accompanying nomogram does not imply that product forms are limited to the range shown.

This page intentionally left blank.

BOHLER SPECIAL PLATES -
DO THE JOB ALL OVER THE WORLD

BÖHLER
BLECHE

BÖHLER NEUTRONIT A976

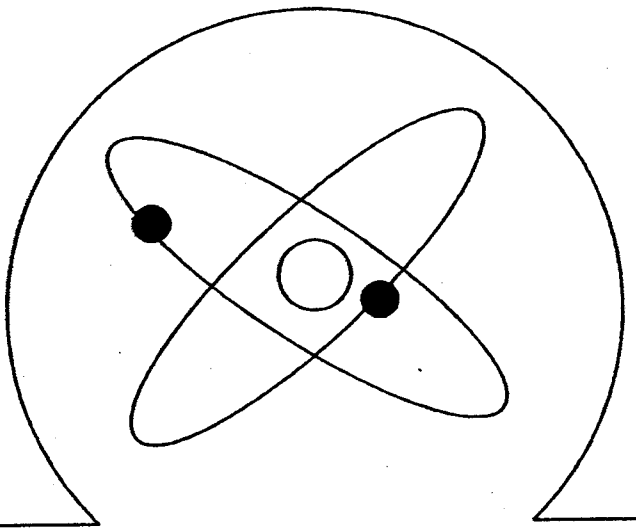

SHEET AND PLATE FOR NUCLEAR ENGINEERING

Dr. A. KÜGLER

BBG/T/Dr.K/September 1997

Copyright Böhler Bleche GmbH

APPLICATIONS

In nuclear engineering borated stainless steels are predominantly used as a shielding material for radwaste disposal equipment, such as

⇒ components for compact storage racks (intermediate storage)

⇒ transportation baskets

The main demands made on sheet and plate used for these applications are:

⇒ largest possible thermal neutron absorption cross section which is uniform over the whole surface area

⇒ toughness

⇒ resistance to general types of corrosion

⇒ intergranular corrosion resistance

⇒ weldability

Based on persistant research and development work BÖHLER BLECHE GMBH are able to offer stainless steel grades with different boron contents which fully meet these requirements.

Copyright Böhler Bleche GmbH

NEUTRON ABSORPTION

The neutron absorption properties of boron alloyed stainless steel depend on the content of B10 isotope. The boron isotope B10 has an absorption cross section for thermal neutrons of more than 3800 barns. B10 is exceeded only by Gadolinium and Samarium.

σ_{abs} of	Cd 113	20.000 barn
	Sm 149	41.000 barn
	Gd 155	61.000 barn
	Gd 157	247.000 barn

Among all elements having large absorption cross sections for thermal neutrons, up to now only boron is of importance for steelmaking. The reason is that production of shielding material is not only a physical but an economical problem and metallurgical problem as well.

Natural boron is commonly used as starting material for the production of Ferrobor. Natural boron consists of more than 19.6 at.-% B10. This level may also be expected in boron stainless steel products, because it is influenced neither by the melting process nor by forming operations.

The cross sections of the alloying elements chromium, molybdenum and nickel are considerably smaller and may be disregarded for the evaluation of neutron absorption capacity.

Copyright Böhler Bleche GmbH

METALLURGICAL BACKGROUND

The solubility of boron in steel is very low, at room temperature negligible small. 100 % of the boron content in steel is precipitated in the form of borides, predominantly with the tetragonal structure Fe_2B. With increasing boron content in steel both the size of the precipitates and the number of particles increase. But even for 2 % boron the particles are of microscopical size.

The transition elements Cr, Ni, Mn and Mo form boride structures very similar to Fe. Furthermore Carbon, which is always present in steel can replace Boron on some lattice places. The boride in stainless steel can therefore be described for the annealed equilibrium condition as:

$$(\mathbf{Fe}, Cr, Ni, Mn, Mo)_2\,(\mathbf{B}, C).$$

The boride is very hard, e.g. comparable with the hardness of a carbide. Furthermore, the boride is very resistant to oxidation and chemical attack e.g. the boride is completely resistant against corrosion attack under the environmental conditions of a nuclear power station.

The carbon of the stainless steel is completely bound to the precipitated boride particles. A boron alloyed stainless steel therefore reacts like a stabilized stainless steel type which is very important for the application of welded components.

There is a practical upper limit for alloying boron into steel. This limit is about 1.9 % because of the tendency of boron to produce the low melting point eutectic together with iron and some accompanying elements. Such eutectic makes it impossible to roll the material to a sheet. During hot rolling, the melting eutectic creates surface cracks. These surface cracks may lead to a fracture of the material. The risk of such a fracture can be minimized by taking certain steps e.g. preforging. In view of this, the fabrication of a boron alloyed stainless steel sheet with more than 1.9 % boron has always an unsatisfying result.

BOHLER SPECIAL PLATES -
DO THE JOB ALL OVER THE WORLD

BÖHLER
BLECHE

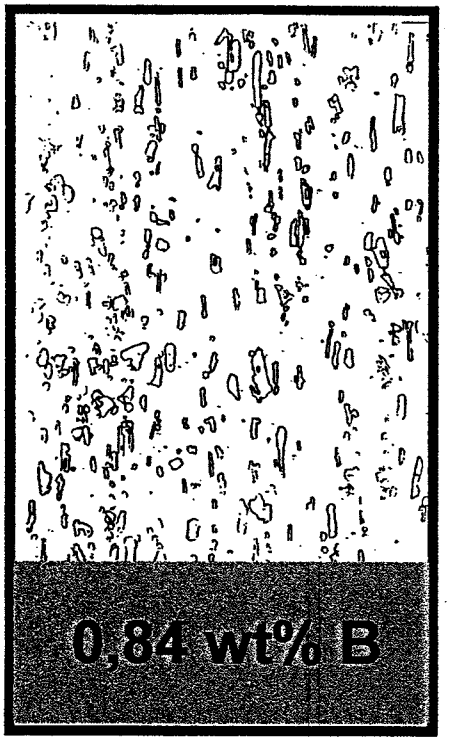

MICROSTRUCTURE BÖHLER NEUTRONIT A976

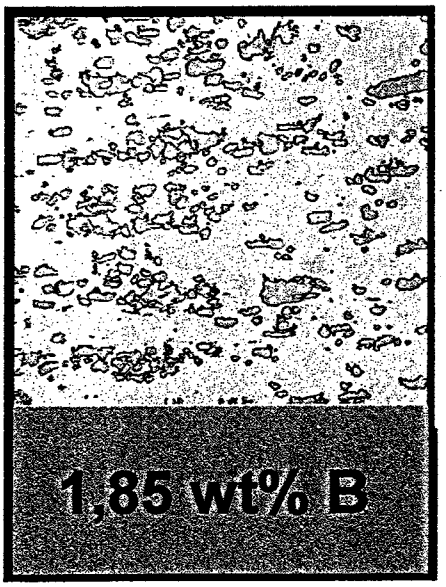

magnification 500x
etched

BBG/T/Dr.K/September 1997

Copyright Böhler Bleche GmbH

VERIFICATION OF BORON CONTENT

Boron alloyed stainless steel has a heterogen structure. But nevertheless, the boron distribution is macroscopically uniform. Only when investigated by microscope, there is a discontinuity in distribution which has no practical effect.

The boron content is certificated both for heat analysis and product analysis. Determination is effected by the wet chemical or spectroscopic method with an error of less than 0.03 % B (95% confidential level).

BÖHLER BLECHE GMBH has the unique possibility to subject each sheet of a batch to nondestructive neutron control using portable test equipment JEN3 developed by the **Office des Rayonnements Ionisants**, Section d'Application des Radioéléments, Saclay, France.

This test equipment consists of a neutron source (Cf 252) and a scintillation counter and is used for determining the absorption of a neutron flux passing twice through the plate. This equipment allows a 100 % material identification test and provides proof of the homogeneous distribution of boron.

By comparative measurements using sheets made from steel with different boron contents including standard stainless grades the test equipment can be calibrated to indicate the content of B10-isotope. If only natural boron is used for steel melting, the counting rate of JEN3 indicates the content of boron. The result can be compared with the result of the standard chemical analysis.

This test is the only method to check whether enriched boron is used for alloying by comparing the result of the chemical analysis with the counting rate of JEN3.

Copyright Böhler Bleche GmbH

BÖHLER
BLECHE

JEN3 TRANSPORTABLE TEST EQUIPMENT

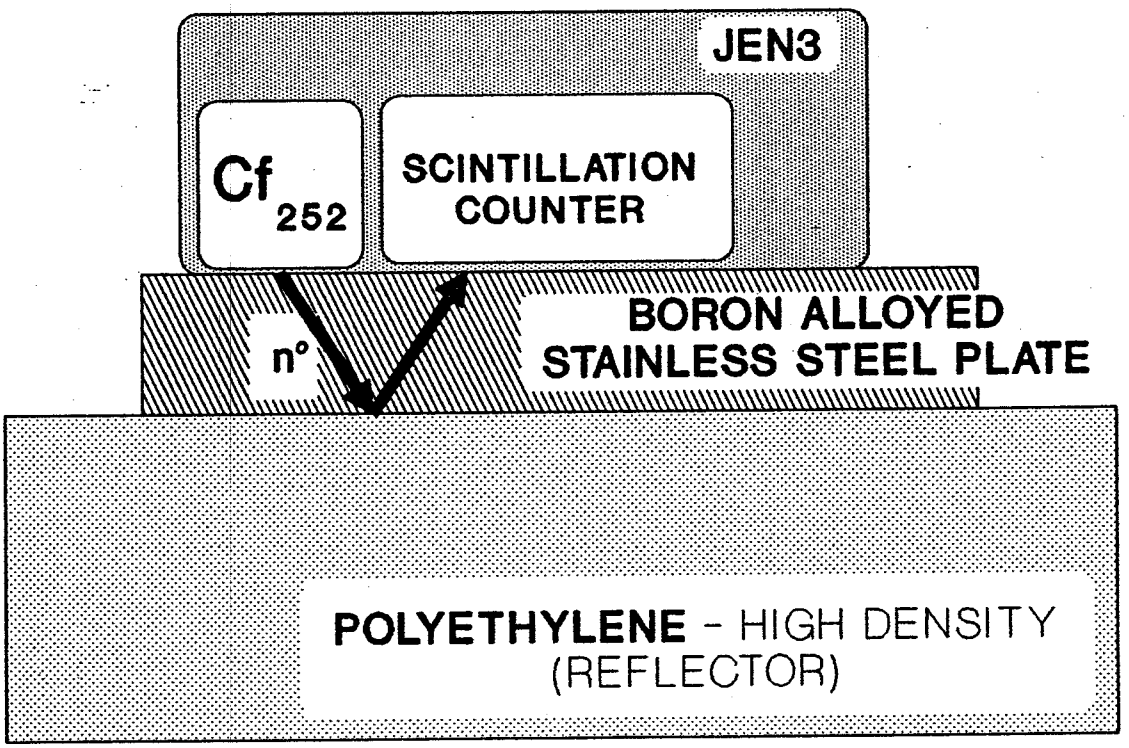

JEN3 is the only method to check in the state of delivery whether the stainless plate is boron alloyed or not.

Copyright Böhler Bleche GmbH

BÖHLER
BLECHE

CORRELATION BETWEEN B10-CONTENT AND JEN3-COUNT RATE

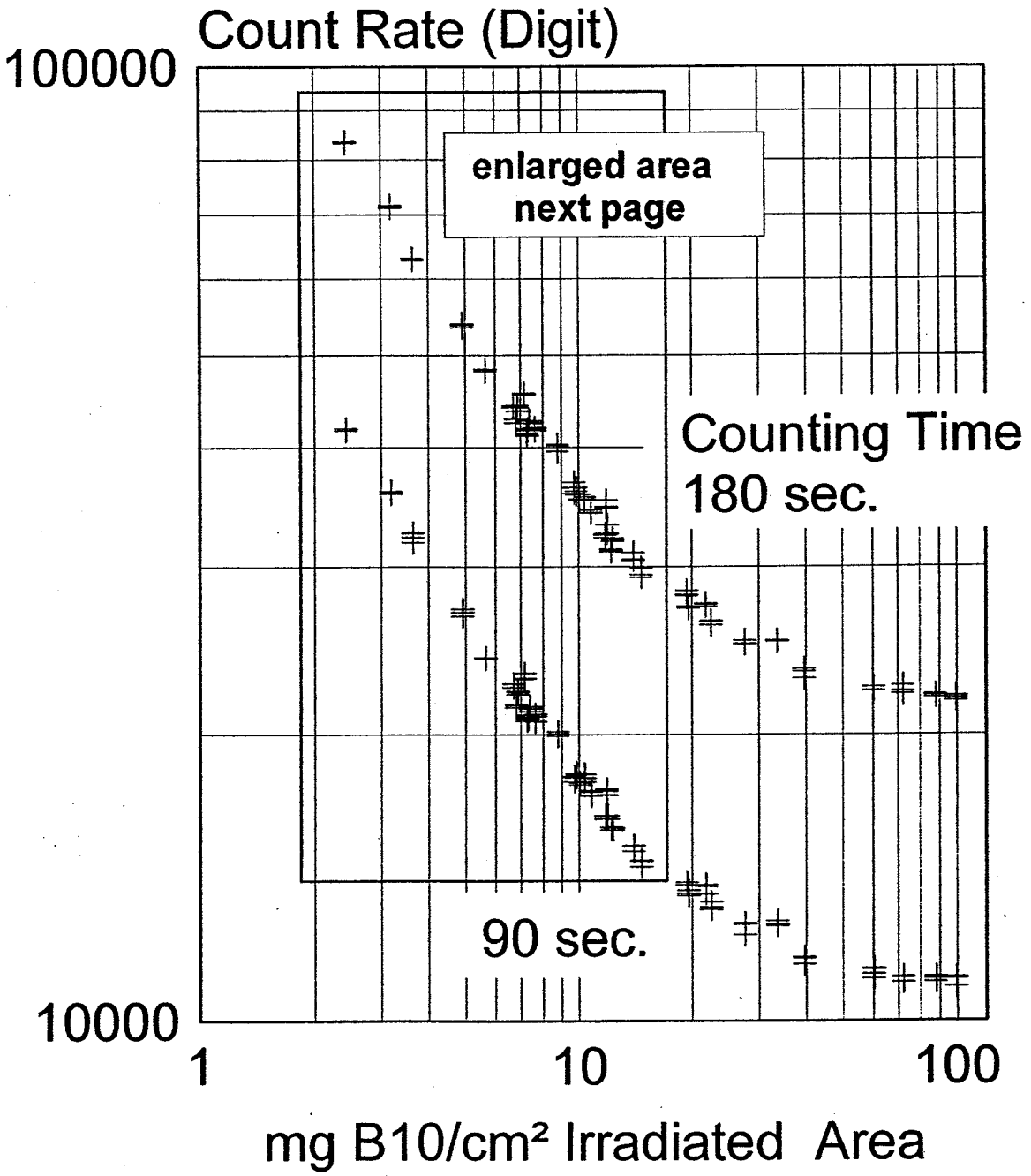

Notice : Absolute value of count rate depends on the actual activity of the neutron source Cf 252

Copyright Böhler Bleche GmbH

BÖHLER
BLECHE

CORRELATION BETWEEN B10-CONTENT AND JEN3-COUNT RATE

In-linear between 2 - 17 mg B10/cm²

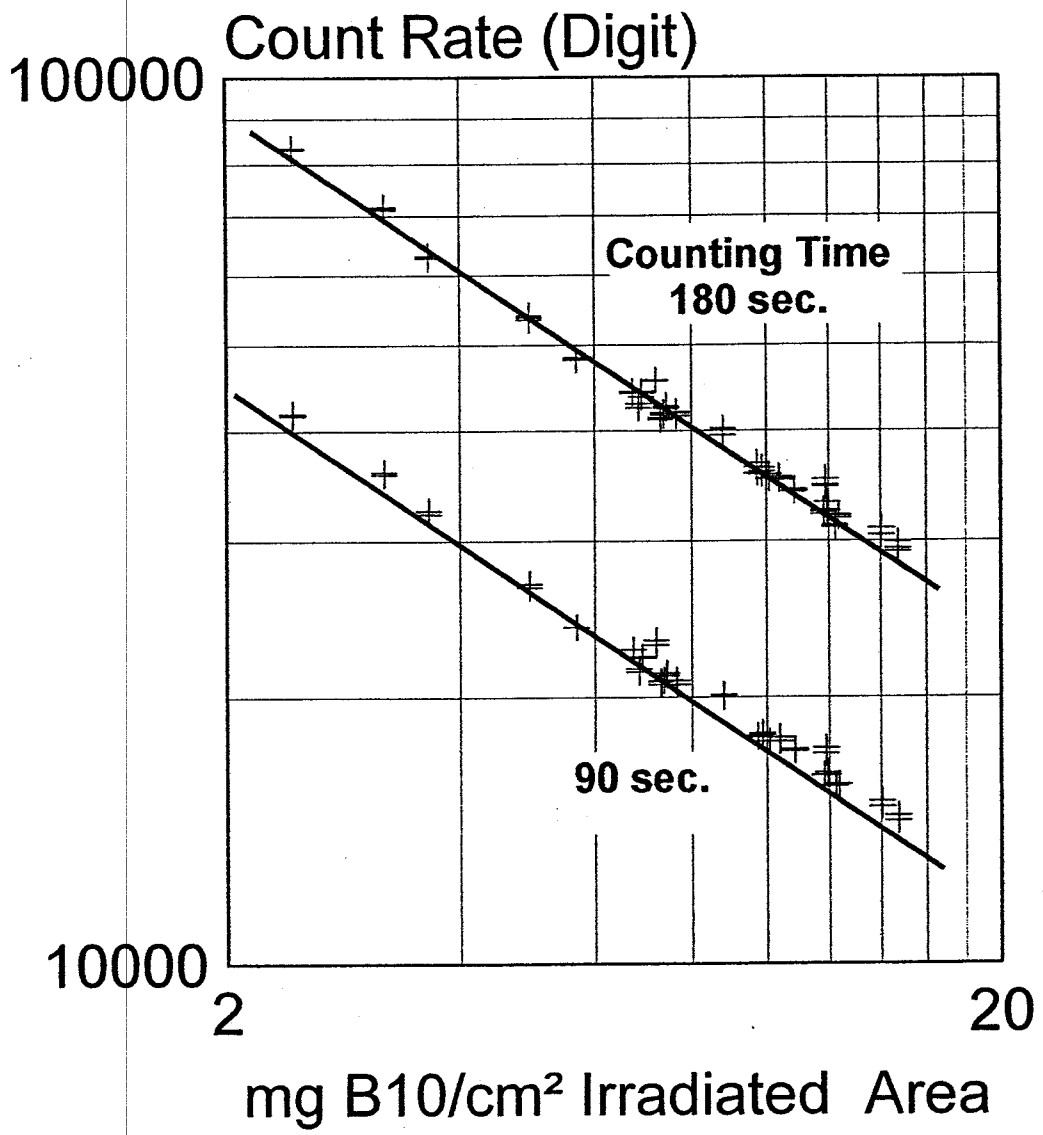

Notice : Absolute value of count rate depends on the actual activity of the neutron source Cf 252

Copyright Böhler Bleche GmbH

BÖHLER
BLECHE

PROPERTIES OF BORON ALLOYED STEEL

The properties of the steel are closely correlated with the heterogenity of the structure. Because of this and a comparable hardness between borides and carbides boron alloyed stainless steel behaves similar to high alloyed tool steel types in the annealed condition.

It is evident that for mechanical properties and corrosion resistance only the total boron content is of importance and not the B10-content.

Copyright Böhler Bleche GmbH

CHEMICAL COMPOSITION

The special boron alloyed **BÖHLER NEUTRONIT** steel grades are based on the AISI type 304.

AVERAGE VALUES					
BÖHLER NEUTRONIT	C	Cr	Ni	Co	B
A 976	0,04 max.	18,5	13	0,20 max.	acc. spec.

The **Nickel** content is increased to 13 % as compared with AISI type 304 to obtain a stable austenitic structure with better forming properties.

The **Boron** content is according to the customer specification. Most common are Boron values similar to ASTM A887, tpye B3, B4 and B6.

In addition to ASTM A887 a **Molybdenum** alloyed type **BÖHLER NEUTRONIT A978** can be supplied on special request too. This steel type is capable of meeting the most stringent requirements for corrosion resistance, but not necessary for standard application conditions.
On special request, the **Chromium** content can be increased to 22 % for the same reason.
Both changes in chemical analysis need a surcharge in price because of higher alloying costs.

After producing more than 2000 tons of boron alloyed stainless steel BÖHLER BLECHE GMBH is in the position to guarantee a uniform distribution of boron within all sheets of one heat.

Copyright Böhler Bleche GmbH

BÖHLER
BLECHE

NOMOGRAM for the calculation of the plate thickness of borated stainless steel Böhler NEUTRONIT A976

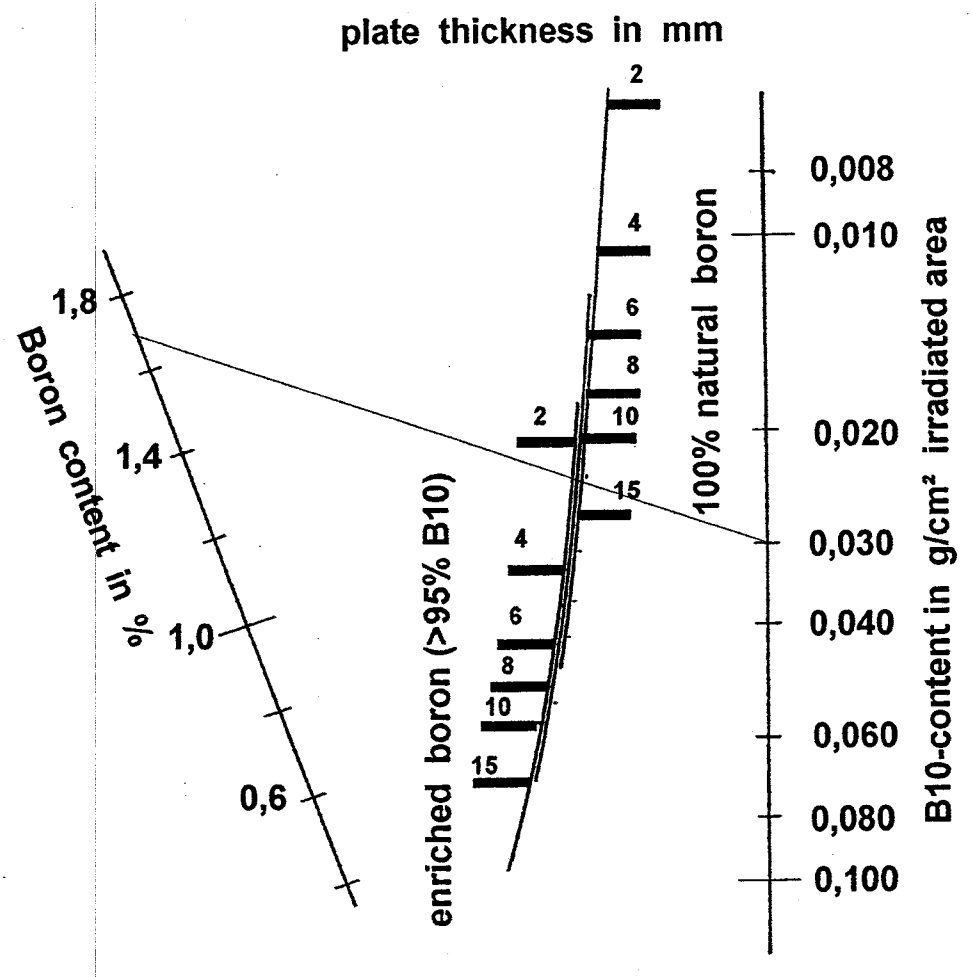

EXAMPLE

Required :	B10-content	0,030	g/cm²	
	boron content	1,70	%	
Wanted :	plate thickness	12,0	mm	with natural boron
		2,35	mm	with enriched boron

NUC08.PRS

Copyright Böhler Bleche GmbH

MECHANICAL PROPERTIES

Tensile strength and hardness rise with increasing boron content while toughness is reduced.

Boron content %	Yield strength MPa min.	Tensile strength MPa min.	Elongation in $L_o=5t_o$ %, min.
0,8	250	550	19
0,9 - 1,2			16
1,4 - 1,6			13
> 1,7			6

The loss of toughness is due to the bi-phase structure. Impact strength decreases with increasing proportions of hard borides in the structure, but fracture is not yet 100 % brittle, even in case of boron content of about 1,9 %. After fracture the specimen show a marked reduction of area which is due to the fine distribution of borides and to the increased nickel content of the matrix.

Toughness properties are retained both at low and elevated temperatures.

The mechanical properties of **BÖHLER NEUTRONIT A976** are conform to the requirements specified in ASTM A887, Grade B.

Copyright Böhler Bleche GmbH

BÖHLER
BLECHE

Toughness of BÖHLER NEUTRONIT A976

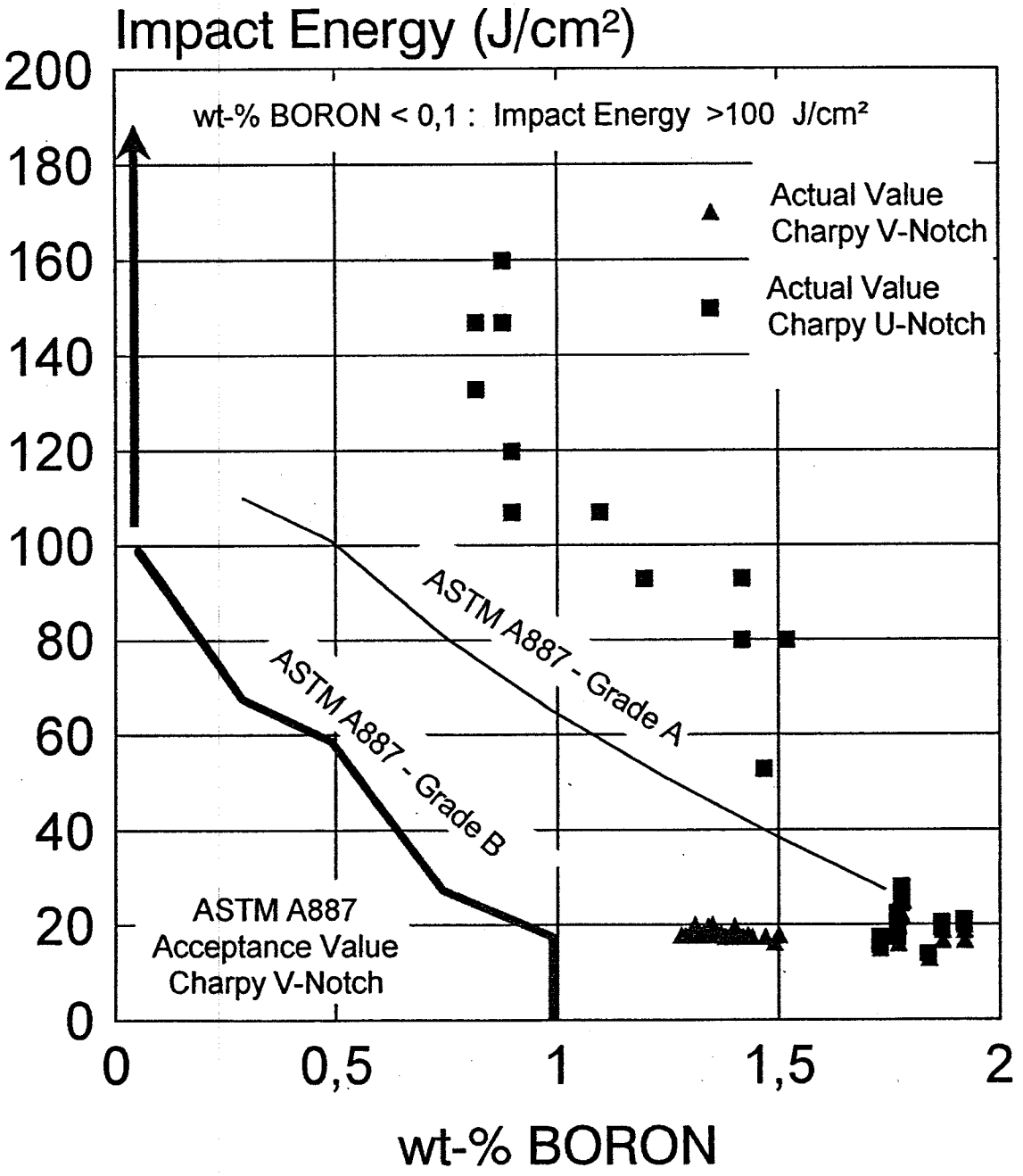

NOTE :
ASTM A887 requires standard size of thickness(=10 mm)
Usual sheet thickness 2,5 - 4,5 mm,e.g. actual tests only with subsized specimen possible.

Copyright Böhler Bleche GmbH

CORROSION RESISTANCE

Corrosion resistance has proven satisfactory under the conditions encountered in practice.

Because of the chromium content of the borides, the precipitates extract chromium from the matrix. Therefore, corrosion resistance is less than it could be expected from the heat analysis but nevertheless similar to a AISI 321 type.

The chromium value in the matrix is depending on the boron content. For **BÖHLER NEUTRONIT A976** with about 1.2 % boron no corrosion attack under reactor conditions is known to us. Higher boron contents might be a problem. An analogous increase of the chromium content to about 21.5 % could solve the problem, if there is any.

Due to the fact that the carbon is dissolved with the borides, no sensitivity takes place even after welding plate material or after specific heat treatment cycles for simulation of a cast process. Intergranular corrosion is not a problem for boron alloyed stainless steel types.
An additional limitation of the carbon content to 0.03% - compaired with the ASTM-requirement of max. 0.08 % - is a further step to minimize the risk of intergranular corrosion attack in the heat affected zone.

Copyright Böhler Bleche GmbH

BÖHLER
BLECHE

INSPECTION AND QUALITY ASSURANCE

Unless otherwise specified in the order, material tests are conducted on the basis of DIN or ASTM, quality specifications for stainless steels. All tests and inspections are performed by our shop independent Quality Control Department. We are able to comply with all national standards and special customer requirements for production inspection, testing and final inspection.

We have been granted a **Quality Assurance Certificate** according to **ISO 9000 / 9002**. Our Quality Assurance System is well implemented and meets the requirements of all important national standards and the specific requirements of manufacturers of nuclear components.

To make sure our products are safe - Quality, for us, is a matter of course.

Copyright Böhler Bleche GmbH

BÖHLER
BLECHE

FORMS AVAILABLE

According to thickness and tolerances required, our sheets and plates in **BÖHLER NEUTRONIT** can be supplied

⇒ hot rolled, heat treated, pickled (**No.1 Finish** ASTM A480.8)

⇒ cold rolled, heat treated, pickled (**No.2D Finish** ASTM A480.8)

For sheet / plate which are used in compact storage racks a surface grinding before final pickling / passivation is standard.

Brushing with nylon brushers after pickling is a standard fabrication step for this special grade too. A final treatment with hot air prevents mineral spots in the state of delivery.

These procedures guarantee a clean and shiny surface, free of defects. Cleaning operations can be easily carried out during life time.

Sheets and plates from our steel grade **BÖHLER NEUTRONIT** are available in essentially the same sizes and thicknesses as those made from standard stainless steels. The most widely used thicknesses, however, are within the range of 1.5 mm to 10.0 mm.

A plate length of up to 5 m, necessary for shielding in compact storage racks, is within the standard production program of Böhler Bleche.

For cutting to the ordered sizes and for cuttings as per drawing we have the facilities for LASER-cutting. As an alternative we can offer guillotine shearing, under water plasma cutting or cold sawing.

Copyright Böhler Bleche GmbH

BÖHLER
BLECHE

LASER-cut EDGES

LASER-cut sheets and strips offer very low size tolerances, which are comparable with machined products-

but at a lower cost level.

BÖHLER BLECHE offers
size tolerances of **+0,5/-0,0 mm** (+0,02/-0,0 in.) for any size available.

LASER-cutting is a thermal cutting process. Because of the very low energy input during cutting the time on high temperature level is very short - too short for any change in analysis or structure.

BÖHLER NEUTRONIT A976
with **1,45 wt% boron**

At the edge the borides are transformed to oxids during cutting.

Pickling after cutting removes the oxid layer. The remaining micro-pits are less than 0,05 mm (0,002 in.)

etched, magnification 200x

Copyright Böhler Bleche GmbH

1.5.2.2 Electroless Nickel Plating Literature

Reference information describing the electroless nickel plating used for coating the carbon steel piece parts of the FuelSolutions™ W74 canister basket assembly is included in this section (pages 443 - 445).

This page intentionally left blank.

Nonelectrolytic Nickel Plating

*By the ASM Committee on Nickel Plating**

THREE METHODS may be employed for depositing nickel coatings without the use of electric current:

1 Immersion plating
2 Chemical reduction of nickelous oxide at 1600 to 2000 F
3 Autocatalytic chemical reduction of nickel salts by hypophosphite anions in an aqueous bath at 190 to 205 F ("electroless" nickel plating).

All three methods are, under certain limited conditions, useful substitutes for nickel electroplating; they are particularly useful in applications in which electroplating is impracticable or impossible because of cost or technical difficulties. Of the three methods, electroless nickel plating is in widest use, and is the method to which the most attention is devoted in this article.

Immersion Plating

The composition and operating conditions of an aqueous immersion plating bath are as follows:

Nickel chloride ($NiCl_2 \cdot 6H_2O$)	80 oz per gal
Boric acid (H_3BO_3)	4 oz per gal
pH	3.5 to 4.5
Temperature	160 F

When using this bath, it is desirable, but not mandatory, to move the work at a rate of about 16 ft per min.

This solution is capable of depositing a very thin (about 0.025 mil) and uniform coating of nickel on steel in periods of up to 30 min. The coating is porous and possesses only moderate adhesion, but these conditions can be improved by heating the coated part at 1200 F for 45 min in a nonoxidizing atmosphere. (Higher temperatures will promote diffusion of the coating.)

High-Temperature Chemical-Reduction Coating

By the reduction of a mixture of nickelous oxide and dibasic ammonium phosphate in hydrogen or other reducing atmosphere at 1600 to 2000 F, a nickel coating can be deposited without the use of electric current. This method (U. S. Patent 2,633,631) consists of applying a slurry of the two chemicals to all or selected surfaces of the workpiece, drying the slurry in air, and performing the chemical reduction at elevated temperature. No special tanks or other plating facilities are required. Some diffusion of nickel and phosphorus into the basis metal occurs at elevated temperature; when the coating is applied to steel, it will consist of nickel, iron, and about 3% phosphorus. The slurry may be used for brazing.

Electroless Nickel Plating

The electroless nickel plating process employs a chemical reducing agent (sodium hypophosphite) to reduce a nickel salt (such as nickel chloride) in hot aqueous solution and to deposit nickel on a catalytic surface. The deposit obtained from an electroless nickel solution is an alloy containing from 4 to 12% phosphorus and is quite hard. (As indicated later in this article, the hardness of the as-plated deposit can be increased by heat treatment.) Because the deposit is not dependent on current distribution, it is uniform in thickness, regardless of the shape or size of the plated surface.

Electroless nickel deposits may be applied to provide the basis metal with resistance to corrosion or wear, or for the buildup of worn areas. Typical applications of electroless nickel for these purposes are given in Table 1, which also indicates plate thicknesses and postplating heat treatments.

Surface Cleaning. In general, the methods employed for cleaning and preparing metal surfaces for electroless nickel plating are the same as those used for conventional electroplating. Heavy oxides are removed mechanically, and oils and grease are removed by vapor degreasing. A typical precleaning cycle might consist of alkaline cleaning (either agitated soak or anodic) and acid pickling, both followed by water rinsing.

Prior to electroless plating, the surfaces of all stainless steel parts must be chemically activated in order to obtain satisfactory adhesion of the plate. One activating treatment consists of immersing the work for about 3 min in a hot (200 F) solution containing equal volumes of water and concentrated sulfuric acid. Another treatment consists of immersing the work for 2 to 3 min in the following solution at 160 F:

Sulfuric acid (66° Bé)	25% by volume
Hydrochloric acid (18° Bé)	5% by volume
Ferric chloride hexahydrate	0.53 oz per gal

Pretreatments that are unique to electroless nickel plating include:

1 A strike copper plate must be applied to parts made of or containing lead, tin, cadmium or zinc, to insure adequate coverage and to prevent contamination of the electroless solution.
2 Massive parts are preheated to bath temperature to avoid delay in the deposition of nickel from the hot electroless bath.

Bath Characteristics. A simplified equation that describes the formation of electroless nickel deposits is:

$$NiSO_4 + NaH_2PO_2 + H_2O \xrightarrow[\text{catalyst}]{\text{heat}} Ni + NaH_2PO_3 + H_2SO_4$$

The essential requirements for any electroless nickel solution are:

1 A salt to supply the nickel
2 A hypophosphite salt to provide chemical reduction
3 Water
4 A complexing agent
5 A buffer to control pH
6 Heat
7 A catalytic surface to be plated.

Detailed discussions of the chemical characteristics of electroless baths, and of the critical concentration limits of the various reactants, can be found in several of the references listed at the end of this article.

Both alkaline (pH, 7.5 to 10) and acid (pH, 4.5 to 6) electroless nickel baths are used in industrial production. Although the acid baths are easier to maintain and are more widely used, the alkaline baths are reported to have greater compatibility with sensitive substrates (such as magnesium, silicon and aluminum).

Catalysis. Nickel and hypophosphite ions can exist together in a dilute solution without interaction, but will react on a catalytic surface to form a deposit. Furthermore, the surface of the deposit is also catalytic to the reaction, so that the catalytic process continues until any reasonable plate thickness is applied. This autocatalytic effect is the principle upon which all electroless nickel solutions are based.

Metals that catalyze the plating reaction are members of group VIII in the periodic table, which group includes nickel, cobalt and palladium. A deposit will begin to form on surfaces of these metals by simple contact with the solution. Other metals, such as aluminum or low-alloy steel, first form an

* See page 432 for committee list.

Table 1. Typical Applications of Electroless Nickel Plating

Part and basis metal	Typical plate thickness, mils	Postplating heat treatment(a)
Plate Applied for Corrosion Resistance		
Valve body, cast iron	5.0	None
Printing rolls, cast iron	1.0	None
Electronic chassis, 1010 steel	1.0	None
Railroad tank cars, 1020 steel	3.5	1 hr at 1150 F
Reactor vessels, 1020 steel	4.0	1 hr at 1150 F
Pressure vessel, 4130 steel	1.5	3 hr at 350 F
Tubular shaft, 4340 steel	1.5	3 hr at 375 F
Plate Applied for Wear Resistance		
Centrifugal pump, steel	1.0	2 hr at 400 F
Plastic extrusion dies, steel	2.0	2 hr at 375 F
Printing-press bed, steel	1.0	None
Valve inserts, steel	0.5	2 hr at 1150 F
Hydraulic pistons, 4340 steel	1.0	1 hr at 750 F
Screws, 410 stainless	0.2	None
Stator and rotor blades, 410 stainless	0.8 to 1.0	1 hr at 750 F
Spray nozzles, brass	0.5	None
Plate Applied for Buildup of Worn Areas		
Carburized gear (bearing journal)	0.8 to 1.0	5 hr at 275 F
Splined shaft (ID spline), 16-25-6 stainless	0.5	1 hr at 750 F
Connecting arm (dowel-pin holes), type 410	5.0	1 hr at 750 F

(a) Heat treatments above 450 F should be carried out in an inert or reducing atmosphere.

immersion deposit of nickel on their surfaces, which then catalyzes the reaction; still others, such as copper, require a galvanic nickel deposit in order to be plated. Such a galvanic nickel deposit can be formed by the plating solution itself, if the copper is in contact with steel or aluminum.

Plastics, glass, ceramics and other nonmetallics also can be plated, if their surfaces can be made catalytic. This usually is done by the application of traces of a strongly catalytic metal to the nonmetallic surface by chemical or mechanical means.

There is, however, a group of metals that not only do not display any catalytic action, but also interfere with all plating activity. The salts of these metals, if dissolved in a solution even in comparatively small amounts, are poisons and stop the plating reaction on all metals, thus necessitating the discarding of the solution and the formulation of a new one. Examples of these anticatalysts are Pb, Sn, Zn, Cd, Sb, As and Mo.

Paradoxically, the deliberate introduction of extremely minute traces of poisons has been practiced by a number of users of electroless nickel, with the intent of stabilizing the solution. Being an inherently metastable mixture, electroless nickel solutions are likely to decompose spontaneously, with the nickel and hypophosphite reacting on trace amounts of solid impurities present in any plating bath. In order to minimize this problem, a poisoning element is added in trace concentrations of parts per million (or per trillion) to the original make-up of the solution. The poison is adsorbed on the solid impurities in quantities large enough to destroy their catalytic nature. This selective adsorption on catalytic centers decreases the concentration of the catalytic poison to a level below the critical threshold, so that normal deposition of nickel is not impeded, although the rate of deposition is somewhat reduced. The deliberate introduction of catalytic poisons for the purpose of stabilization is covered by several patents, including U. S. Patents 2,762,723 and 2,847,327.

Table 2. Alkaline Electroless Nickel Baths

Constituent or condition	Bath 1	Bath 2	Bath 3
Composition, Grams per Liter			
Nickel chloride	30	45	30
Sodium hypophosphite	10	11	10
Ammonium chloride	50	50	50
Sodium citrate	..	100	..
Ammonium citrate	..	..	65
Ammonium hydroxide	to pH	to pH	to pH
Operating Conditions			
pH	8 to 10	8.5 to 10	8 to 10
Temperature, F	195 to 205	195 to 205	195 to 205
Plating rate (approx), mil per hr	0.3	0.4	0.3

Alkaline Baths. Most alkaline baths in commercial use today are based on the original formulations developed by Brenner and Riddell. They contain a nickel salt, sodium hypophosphite, ammonium hydroxide, and an ammonium salt; they may also contain sodium citrate or ammonium citrate. The ammonium salt serves to complex the nickel and buffer the solution. Ammonium hydroxide is used to maintain the pH between 7.5 and 10. Table 2 gives the compositions and operating conditions of three alkaline electroless baths.

At the operating temperatures of these baths (about 200 F), ammonia losses are considerable. Thorough ventilation and frequent adjustment of pH are required. The alkaline solutions are inherently unstable and are particularly sensitive to the poisoning effects of anticatalysts such as lead, tin, zinc, cadmium, antimony, arsenic and molybdenum — even when these elements are present in only trace quantities. However, when depletion occurs, these solutions undergo a definite color change from blue to green, indicating the need for addition of ammonium hydroxide.

Acid baths are more widely used in commercial installations than alkaline baths. Essentially, acid baths contain a nickel salt, a hypophosphite salt, and a buffer; some solutions also contain a chelating agent. Frequently, wetting agents and stabilizers also are added.

These baths are more stable than alkaline solutions, are easier to control, and usually provide a higher plating rate. Except for the evaporation of water, there is no loss of chemicals when acid baths are heated to their operating range. Table 3 gives the compositions and operating conditions of several acid electroless baths.

Solution Control. In order to assure optimum results and consistent plating rates, the composition of the plating solution should be kept relatively constant; this requires periodic analyses for the determination of pH, nickel content, and phosphite and hypophosphite concentrations. The rate at which these analyses should be made depends on the quantity of work being plated and the volume and type of solution being used. The following methods have been employed:

pH — Standard electrometric method

Nickel — Any one of the colorimetric, gravimetric or volumetric methods is satisfactory; the cyanide method is probably the most popular.

Phosphite — A 10-ml sample of the plating solution is combined with 20 ml of a 5% solution of sodium bicarbonate and cooled in an ice bath. Next, 50 ml of 0.1*N* iodine solution is added and the flask containing this mixture is stoppered and permitted to stand for 2 hr at room temperature. Then the flask is cooled for 15 min in ice water, after which it is unstoppered, the mixture is acidified with acetic acid, and the excess iodine is titrated with 0.1*N* sodium thiosulfate, with starch as an indicator. Determination is then made as follows:

$$NaH_2PO_2 \text{ per liter} = \frac{\text{net ml of } 0.1N \text{ iodine} \times 6.3}{\text{ml of plating solution}}$$

Hypophosphite (U. S. Patent 2,697,651) — A 25-ml sample of the plating solution is diluted to 1 liter. A 5-ml aliquot of the

Table 3. Acid Electroless Nickel Plating Baths(a)

Constituent or condition	Bath 4	Bath 5	Bath 6	Bath 7	Bath 8	Bath 9
Composition, Grams per Liter						
Nickel chloride	30	..	..	30	..	30
Nickel sulfate	..	21	20	..	15	..
Sodium hypophosphite	10	24	27	10	14	12
Sodium acetate	..	..	..	..	13	..
Sodium hydroxyacetate	50	..	..	10	..	..
Sodium succinate	..	..	16	..	..	..
Lactic acid (80%)	..	34 ml	..	..	..	..
Propionic acid (100%)	..	2.2 ml	..	..	..	10
Operating Conditions						
pH	4 to 6	4.3 to 4.6	4.5 to 5.5	4 to 6	5 to 6	4.5 to 5.5
Temperature, F	190 to 210	203	200 to 210	190 to 210	190 to 210	190 to 210
Plating rate (approx), mil per hr	0.5	1.0	1.0	0.4	0.7	0.6

(a) Baths 4 and 7 are covered by U. S. Patent 2,532,283 (a public patent assigned to the National Bureau of Standards); bath 5, by U. S. Patents 2,822,293 and 2,822,294, and bath 6 by U. S. Patents 2,658,841 and 2,658,842.

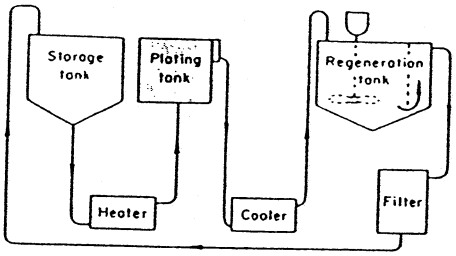

Fig. 1. Schematic of continuous-type system for electroless nickel plating. See text.

dilution is combined with 10 ml of a 10% solution of ammonium molybdate and 10 ml of fresh 6% sulfurous acid. The sample is covered and heated to boiling, and a deep blue color develops. The sample is cooled and diluted to 100 ml, and transmittance at a wave length of 440 microns is determined. The calibration curve on semilog paper is linear.

Hypophosphite (alternative method) — A 5-ml sample of the plating solution is mixed in a beaker with 5 ml of methyl orange solution made up of 1 gram of methyl orange in 1 liter of water. In another beaker is placed 15 ml of an acid solution made up by (*a*) dissolving 40 grams of sodium metabisulfate in 200 ml of water, (*b*) slowly adding the sodium metabisulfate solution to a cold solution of 82 ml of sulfuric acid in 650 ml of water, and then (*c*) diluting this mixture with water to 1 liter. When the acid solution and the solution containing the sample and methyl orange reach a temperature of 77 F in a thermostat, the two solutions are mixed. The time between mixing and the disappearance of the red color is recorded. The hypophosphite concentration is a function of this time and is read from a concentration-time curve made from known standards.

Equipment Requirements. The precleaning and post-treating equipment for an electroless nickel line is comparable to that employed in conventional electrodeposition. The plating tank itself, however, is unique.

The preferred plating tank for batch operations is constructed of stainless steel or aluminum and is lined with a coating of an inert material, such as tetrafluoroethylene or a phenolic-base organic. The size and shape of the tank are usually dictated by the parts to be plated, but the surface area of the plating solution should not be so large that excessive heat loss occurs as a result of evaporation.

A large heat-transfer area and a low temperature gradient are necessary between the heating medium and the plating solution. This combination provides for a reasonable heat-up time without local hot spots that could decompose the solution. It is accepted practice to surround the plating tank with a hot-water jacket or to immerse it in a tank containing hot water. Heating jackets using low-pressure steam also have been used successfully. The use of immersed steam coils is not favored, however, because it entails the sacrifice of a large amount of working area in the tank.

Accessory equipment required or recommended for the tank includes:

1 An accurate temperature controller
2 A filter to remove any suspended solids
3 A pH meter
4 An agitator to prevent gas streaking
5 On small tanks, a cover, to minimize heat loss and exclude foreign particles.
6 On large tanks, a separate small tank to dissolve and filter additives before they are put into the plating tank.

Considerably more equipment is required for a continuous-type system, such as that shown in Fig. 1. The bath is prepared and stored in a separate tank and flows through a heater (which raises its temperature to 205 F) into the plating tank. From the plating tank, the solution is pumped through a cooler, which decreases its temperature to 175 F or below, and then to an agitated regeneration tank, where reagents are added in controlled amounts to restore the solution to its original composition. The solution is then directed past a vertical underflow baffle and out of the regeneration tank to a filter, and then returned to storage.

In externally heated continuous-type systems such as the one shown in Fig. 1, the plating tank and other components of the system that come in contact with the plating solution are constructed of type 304 stainless steel and are not lined or coated; these components are periodically deactivated by chemical treatment. Details of this type of system are covered by several patents, including U. S. Patents 2,941,902; 2,658,839 and 2,874,073.

Properties of the Deposit. Electroless nickel is a hard, lamellar, brittle, uniform deposit. As plated, the hardness

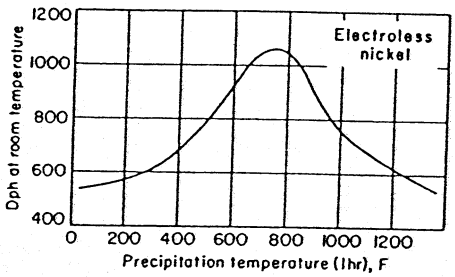

Effect of temperature of 1-hr precipitation heat treatment on room-temperature hardness of a typical electroless nickel deposit (Eberbach tester, 100-gram load). Above 450 F, heat treatment was in an inert atmosphere.

Fig. 2. Heat treatment of coating

varies over a considerable range (425 to 575 dph), depending primarily on phosphorus content, which ranges from 4 to 12%. This hardness can be increased by a precipitation heat treatment. As indicated in Fig. 2, which shows temperature-hardness relationships for a typical deposit, by heating at 750 F for ½ to 1 hr, hardness can be increased to about 1000 dph.

The corrosion resistance of electroless nickel deposits is superior to that of electrodeposited nickel of comparable thickness, but this superiority varies with exposure conditions. Outdoor exposure and salt spray corrosion data indicate that about 25% more resistance is given a steel panel by electroless nickel than by electrolytic.

Table 4. Physical Properties of Electroless Nickel Deposits

Property	Value
Specific gravity	7.8 to 8.5
Melting point	1635 to 1850 F
Electrical resistivity	60 microhm-cm
Thermal expansion	13×10^{-6} per °C
Thermal conductivity	0.0105 to 0.0135 cal/cm sec/°C

Table 5. Costs for Electroless Nickel Plating (Example 2) (a)

Cost factor	Cost per year (b)
Original investment	$18,000
Fixed costs:	
Depreciation (10 years)	$ 1,800
Insurance	450
Floor space (200 sq ft)	192
Repairs and maintenance	450
Variable costs:	
Raw material	6,100
Utilities	740
Labor costs:	
Direct	10,400
Indirect	2,630
Total	$22,762
Total cost per hr	$9.48
Total cost per sq ft coated to 1 mil	$1.00

(a) Exclusive of costs for: overhead and administration; racking, cleaning and unracking; and preplating and postplating processes. (b) Based on deposition of 1 mil on 0.1-sq-ft parts at rate of 0.8 mil per hr (capacity: 117 pieces, or 9.4 sq-ft/mil, per hr), on a schedule of 10 hr per day, 20 days per month, 2400 hr per year.

Some of the physical properties of electroless nickel are listed in Table 4.

Advantages and Limitations. Some advantages of electroless nickel are:

1 Good resistance to corrosion and wear
2 Excellent uniformity
3 Solderability and brazability
4 Good oxidation resistance.

Limitations of electroless nickel are:

1 High cost
2 Brittleness
3 Poor welding characteristics
4 Lead, tin, cadmium and zinc must be copper strike plated before electroless nickel can be applied
5 Slower plating rate (in general), as compared to electrolytic methods
6 Full brightness in deposit cannot be obtained without extreme brittleness.

Cost. Electroless nickel is considerably more expensive than electrodeposited nickel. Actual costs for electroless nickel plating, as reported by two users, are given in the following examples.

Example 1. Based on the experience of one manufacturing plant, it costs $1.20 to deposit an electroless nickel coating 1 mil thick on a square foot of surface area: 37¢ for chemicals, 59¢ for labor, and 24¢ for equipment and maintenance.

Example 2. Another manufacturing plant reports that it costs $1 per sq ft to plate a 1-mil thickness of electroless nickel on specific parts with a surface area of 0.1 sq ft, on the basis of data obtained over a one-year period (2400 working hours). An analysis of their costs is given in Table 5.

Selected References

A. Brenner, Electroless Plating Comes of Age, *Metal Finishing*, November 1954, p 68-76; December 1954, p 61-68

A. Brenner and G. Riddell, Nickel Plating on Steel by Chemical Reduction, *J Res Nat Bur Stds*, July 1946, p 31-34, and *Proc Am Electroplaters' Soc*, 1946, p 23-29; Deposition of Nickel and Cobalt by Chemical Reduction, *J Res Nat Bur Stds*, Nov 1947, p 385-395, and *Proc Am Electroplaters' Soc*, 1948, p 156-169

G. Gutzeit, Industrial Nickel Coating by Chemical Catalytic Reduction, *Trans Inst Metal Finishing*, 33, 383-423 (1955-1956), and *Corrosion Technol*, 3, 208 (1956)

G. Gutzeit, An Outline of the Chemistry Involved in the Process of Catalytic Nickel Deposition from Aqueous Solution, *Plating*, Oct 1959, p 1158-1164; Nov 1959, p 1275-1278; Dec 1959, p 1377-1378; Jan 1960, p 63-70

C. H. de Minjer and A. Brenner, Studies on Electroless Nickel Plating, *Plating*, December 1957, p 1297-1305

Symposium on Electroless Nickel Plating (Catalytic Deposition of Nickel-Phosphorus Alloys by Chemical Reduction in Aqueous Solution), ASTM STP No. 265 (1959)

This page intentionally left blank

2. PRINCIPAL DESIGN CRITERIA

As documented in the FuelSolutions™ Canister Storage FSARs, the FuelSolutions™ Storage System component designs (including the storage cask and transfer cask) are based on the bounding FuelSolutions™ canister dimensions and weights, and the thermal and radiological source terms. This chapter defines the design criteria that are specific to the FuelSolutions™ W74 canister design and demonstrates that the FuelSolutions™ W74 canister and its contents are within the design basis parameters used for the FuelSolutions™ W150 Storage Cask and W100 Transfer Cask. The FuelSolutions™ W74 canister design criteria are summarized in Table 2.0-1 and described in the sections that follow.

Table 2.0-1 - W74 Canister Design Criteria Summary (7 Pages)

Type	Criteria	Basis	FSAR Reference
Design Life:			
Design	100 yrs	-	Section 2.1.2
Regulatory	20 yrs.	10CFR72.42(a) & 10CFR72.236(g)	-
Structural:			
Design & Fabrication Codes:			
Shell Assembly	ASME Code Section III, Subsection NB	10CFR72.24(c)(4)	Sections 1.2.1.3 & 2.1.2
Basket Assembly	ASME Code Section III, Subsection NG	10CFR72.24(c)(4)	Sections 1.2.1.3 & 2.1.2
Outer Closure Plate Vertical Lifting Points	ANSI N14.6/NUREG-0612	10CFR72.24(c)(4)	Section 2.1.2
Design Dead Weights:			
Max. Loaded Canister (Dry)	76,259 lb.	ANSI/ANS 57.9	Table 3.2-1
Max. Empty Canister (Dry)	44,899 lb.	ANSI/ANS 57.9	Table 3.2-1
Design Cavity Pressures:			
Normal:			
Dry Storage	10 psig	ANSI/ANS 57.9	Section 2.3.1.2
Blowdown	30 psig	ANSI/ANS 57.9	Section 2.3.1.2
Off-normal:			
Dry Storage	16 psig	ANSI/ANS 57.9	Section 2.3.2.2
Reflood	100 psig	ANSI/ANS 57.9	Section 2.3.2.4
Postulated Accident	69 psig	ANSI/ANS 57.9	Section 2.3.3.4
Response and Degradation Limits	Spent fuel assemblies confined in dry, inert environment	10CFR72.122(h)(1)	Section 1.2.1.3

Table 2.0-1 - W74 Canister Design Criteria Summary (7 Pages)

Type	Criteria	Basis	FSAR Reference
Thermal:			
Maximum Design Temperatures:			
Structural Materials (Carbon steel)	700°F	ASME Code Section II, Part D	Section 4.3.1
Structural Materials (Stainless steel)	800°F	ASME Code Section II, Part D	Section 4.3.1
Structural Materials (No drop loads)	1000°F	ASME Code Section II, Part D	Section 4.3.1
Shielding Materials	1000°F	-	Section 4.3.1
Fuel Cladding:			
> 0 ≤ 40 GWd/MTU	385.5°C	-	Section 4.3.2
Canister Backfill Gas	Helium	-	Section 12.3
Canister Backfill Density	0.0376 g-moles/liter nominal	-	Section 4.4
Short-term Allowable Fuel Cladding Temperature		-	
Normal & Off-normal	400°C	-	Section 2.1.2
Accident	570°C	-	Section 2.1.2
Insolation	Protected by Cask	10CFR71.71	-
Confinement:		10CFR72.128(a)(3) & 10CFR72.236(d) & (e)	
Closure Welds:			
Shell Seams & Bottom Closure Plate	Full Penetration	-	Sections 1.2.1.3 & 7.1.1
Inner Closure Plate	Multi-pass Partial Penetration	10CFR72.236(e)	Sections 1.2.1.3 & 7.1.1
Outer Closure Plate	Multi-pass Partial Penetration		
Port Covers	Multi-pass Partial Penetration		

Table 2.0-1 - W74 Canister Design Criteria Summary (7 Pages)

Type	Criteria	Basis	FSAR Reference
NDE:			
Shell Seams & Bottom Closure Plate	100% RT	-	Sections 1.2.1.3 & 7.1
Inner Closure Plate	Root Pass and Final Surface 100% PT	-	Sections 1.2.1.3 & 7.1
Outer Closure Plate	Root, Intermediate, and Final Surface 100% PT	-	Sections 1.2.1.3 & 7.1
Port Covers	Final Surface 100% PT	-	Sections 1.2.1.3 & 7.1
Leak Testing:			
Welds Tested	Shell Seams & Bottom Closure Plates-to-Shell, Inner Closure Plate-to-Shell, Inner Closure Plate-to-Vent & Drain Port Adapters	-	Sections 1.2.1.3 & 7.1
Medium	Helium	-	Sections 1.2.1.3 & 7.1
Max. Leak Rate	8.52×10^{-6} ref-cc/sec	-	Section 12.3 of WSNF-200
Test Pressure	12.5 psig	-	Section 12.3 of WSNF-200
Monitoring System	Concrete Liner Thermocouple and Daily Surveillance	10CFR72.128(a)(1)	Section 12.3 of WSNF-200
Retrievability:			
Normal and Off-normal	No Encroachment on Fuel Assemblies	10CFR122(f), (h)(1), & (l)	Section 3.1.2.1
Post (design basis) Accident			
Criticality:		10CFR72.124 & 10CFR.236(c)	
Method of Control	Fixed Borated Neutron Absorber	-	Sections 1.2.1.3 & 2.1.2
Min. Boron Loading	1.25% by wgt. B_n	-	Section 6.3.1
Max. k_{eff}	0.95	-	Section 6.1
Min. Burnup	0.0 GWd/MTU (fresh fuel)	-	Section 2.1.2 & 6.3.7

Table 2.0-1 - W74 Canister Design Criteria Summary (7 Pages)

Type	Criteria	Basis	FSAR Reference
Radiation Protection/Shielding:		10CFR72.126, & 10CFR72.128(a)(2)	
Confinement Cask: (normal/off-normal/accident)			
Canister Closure	ALARA	10CFR20	Sections 10.1, 10.2 & 10.3
Canister Transfer	ALARA	10CFR20	Sections 10.1, 10.2 & 10.3
Exterior of Shielding (Normal/Off-normal/Accident)			
Transfer Mode Position	ALARA	10CFR20	Section 5.4.2 of WSNF-200
Storage Mode Position	See FuelSolutions™ Storage System FSAR	10CFR20	Section 5.4.1 of WSNF-200
ISFSI Controlled Area Boundary	See FuelSolutions™ Storage System FSAR	10CFR72.104 & 10CFR72.106	Section 10.4
Design Bases:		10CFR72.236(a)	
Spent Fuel Specification:			
Assemblies/Canister	Up to 64	-	Section 2.2 & Section 12.3
Type of Cladding	Zircaloy	-	Section 2.2 & Section 12.3
Fuel Condition	Intact/Partial(1)/Damaged(2)	-	Section 2.2 & Section 12.3
Class/Type/Configuration	Big Rock Point (BWR)	-	Section 2.2 & Table 2.2-1
Max. Burnup (all fuels)	40,000 MWd/MTU	-	Section 12.3
Max. Enrichment:			
Intact:			
UO_2	4.1 w/o ^{235}U	-	Section 6.1
MOX	See Figures 6.6-1 through 6.6-3	-	Section 6.6.1

Table 2.0-1 - W74 Canister Design Criteria Summary (7 Pages)

Type	Criteria	Basis	FSAR Reference
Partial (UO_2):[1]			
Missing Corner Rods[3]	4.1 w/o ^{235}U	-	Section 6.6.2
Missing Array Interior or Edge (GE 9x9)[3]	3.55 w/o ^{235}U	-	Section 6.6.2
Missing Array Interior or Edge (Siemens 11x11)	3.6 w/o ^{235}U	-	Section 6.6.2
Partial (MOX)[1]	See Figures 6.6-5 through 6.6-8	-	Section 6.6.1
Damaged [2, 4]	4.61%[5]	-	Section 6.6.3
Max. Decay Heat/Canister:			
> 0 ≤ 40 GWd/MTU	26.4 kW (0.230 kW/in)	-	Section 4.1.5
Max. Fuel Assembly Weight:			
w/o Channels	485 lb.	-	Table 1.2-3
Max. Fuel Assembly Irradiated Length:	84.8 in.	-	Table 1.2-3
Max. Fuel Assembly Irradiated Width (w/o Channels):	6.52 in.	-	Table 1.2-3
Fuel Rod Fill Gas:			
Pressure (max.)	30 psig	-	Section 4.4.1.6
Volume (max.)	602 cu. in.	-	Section 4.4.1.6
Normal Design Event Conditions:		10CFR72.122(b)(1)	
Ambient Outside Temperatures	See FuelSolutions™ Storage System FSAR	ANSI/ANS 57.9	Section 2.3.1.1
Handling Loads:			
Vertical	15% of dead wt.	CMAA #70	Section 2.3.1.4
Horizontal	45,000 lb. push or pull, either end	-	Section 2.3.1.4
Wet/Dry Loading	Wet	-	Section 1.2.2
Transfer Orientation	Vertical or Horizontal	-	Section 1.2.2
Storage Orientation	Vertical	-	Section 1.2.2

Table 2.0-1 - W74 Canister Design Criteria Summary (7 Pages)

Type	Criteria	Basis	FSAR Reference
Fuel Rod Rupture Releases:			
Fuel Rod Failures	1%	-	Section 2.3.1.2 & 4.4.1.5
Fill Gases	100%	-	Section 2.3.1.2& 4.4.1.5
Fission Gases	30%	-	Section 2.3.1.2& 4.4.1.5
Confinement Boundary Leakage	2×10^{-5} atm-cm^3/sec	-	Section 2.3.1.5 & 7.2
Off-Normal Design Event Conditions:		10CFR72.122(b)(1)	
Ambient Temperature	See FuelSolutions™ Storage System FSAR	ANSI/ANS 57.9	Section 2.3.2.1
Misaligned Cask Horizontal Transfer Load	70,000 lb. push/50,000 lb. pull, either end	-	Section 2.3.2.3
Fuel Rod Rupture Releases:			
Fuel Rod Failures	10%	-	Section 2.3.2.2
Fill Gases	100%	-	Section 2.3.2.2
Fission Gases	30%	-	Section 2.3.2.2
Confinement Boundary Leakage	2×10^{-5} atm-cm^3/sec	-	Section 2.3.2.6 & 7.2
Design-Basis (Postulated) Accident Design Events and Conditions:		10CFR72.24(d)(2) & 10CFR72.94	
Drop/Tip-Over Cases	See FuelSolutions™ Storage System FSAR	-	Section 2.3.3.2
Fire	See FuelSolutions™ Storage System FSAR	10CFR72.122(c)	Section 2.3.3.3
Fuel Rod Rupture Releases:			
Fuel Rod Failures	100%	-	Section 2.3.3.4 & 4.4.1.5
Fill Gases	100%	-	Section 2.3.3.4 & 4.4.1.5
Fission Gases	30%	-	Section 2.3.3.4 &4.4.1.5
Particulates & Volatiles	See Table 7.4-1 of FuelSolutions™ Storage System FSAR	-	Sections 2.3.3.5 & 7.3.1
Confinement Boundary Leakage	2×10^{-5} atm-cm^3/sec	-	Section 2.3.3.5 & 7.3

Table 2.0-1 - W74 Canister Design Criteria Summary (7 Pages)

Type	Criteria	Basis	FSAR Reference
Explosive Overpressure	See FuelSolutions™ Storage System FSAR	10CFR72.122(c)	Section 2.3.3.6
Air Flow Blockage:			
Vent Blockage	See FuelSolutions™ Storage System FSAR	10CFR72.128(a)(4)	Section 2.3.3.1.1
Ambient Temperature	See FuelSolutions™ Storage System FSAR	10CFR72.128(a)(4)	Section 2.3.3.1.1
Design-Basis Natural Phenomenon Design Events and Conditions:		10CFR72.92 & 10CFR72.122(b)(2)	
Flood Water Depth	50 ft.	ANSI/ANS 57.9	Section 2.3.4.1
Seismic	See FuelSolutions™ Storage System FSAR	10CFR72.102(f) & RG 1.60	Section 2.3.4.3
Wind	Protected by Casks	ASCE 7	Section 2.3.4.4
Tornado & Missiles	Protected by Casks	RG 1.76 & NUREG-0800	Section 2.3.4.2
Burial Under Debris	Bounded by Air Flow Blockage Criteria	-	Section 2.3.4.5
Lightning	See FuelSolutions™ Storage System FSAR	NFPA 78	Section 2.3.4.6
Snow and Ice	Protected by Casks	ASCE 7	Section 2.3.4.7

Notes:

(1) Partial includes fuel assemblies with missing corner rods, with up to one rod missing from each of the four FA corners; and assemblies with missing array interior or array edge rods.

(2) Damaged includes fuel rod damage in excess of hairline cracks or pinhole leaks. Fuel assemblies with damaged grid spacers (defined as damaged to a degree where fuel rod structural integrity cannot be assured, or where grid spacers have shifted vertically from their design position) will also be stored in damaged fuel cans.

(3) Assembly average.

(4) Peak pellet.

(5) The damaged fuel enrichment limit is in w/o ^{235}U for UO_2 fuel assemblies. It is based on the equation $E_{U-235} + 0.7 \times P_{Pu}$ for MOX fuel assemblies, where E_{U-235} is the ^{235}U enrichment of the uranium in the fuel, and P_{Pu} is the overall weight percentage of plutonium metal.

2.1 Structures, Systems, and Components Important to Safety

2.1.1 Identification of Items Important to Safety

As identified in Chapter 1 of this FSAR, the FuelSolutions™ W74 canister is a structure, system, and component (SSC) that is classified as important to safety in accordance with 10CFR72. Table 2.1-1 of the FuelSolutions™ Storage System FSAR[1] provides a summary of the FuelSolutions™ Storage System components and support equipment (including the FuelSolutions™ canisters and related equipment) and defines their safety classification.

2.1.2 Design Bases and Criteria

General

Consistent with the findings of the NRC's Waste Confidence Decision Review,[2] the FuelSolutions™ W74 canister is designed for 100 years of service, while satisfying the requirements of 10CFR72. The design considerations that assure canister performance throughout the service life include addressing the following:

- Corrosion
- Structural fatigue effects
- Maintenance of helium atmosphere
- Allowable fuel cladding temperatures
- Neutron absorber boron depletion.

The adequacy of the canister design for the intended service life is discussed in Section 3.4.4 of this FSAR.

Structural

The FuelSolutions™ W74 canister structural components include the internal basket assembly and the shell assembly. As discussed in Section 2.5.1, the internal basket assembly is designed and fabricated as a core support structure in accordance with the applicable requirements of Section III, Subsection NG[3] of the ASME Code, to the maximum extent practicable. The shell assembly is designed and fabricated as a Class 1 component pressure vessel in accordance with Section III, Subsection NB[4] of the ASME Code, to the maximum extent practicable. The

[1] WSNF-220, *FuelSolutions™ Storage System Final Safety Analysis Report*, NRC Docket No. 72-1026, BNFL Fuel Solutions Corporation.

[2] *Nuclear Regulatory Commission 10 CFR Part 51 Waste Confidence Decision Review*, U.S. Nuclear Regulatory Commission, September 11, 1990.

[3] American Society of Mechanical Engineers (ASME) Boiler and Pressure Vessel Code, Section III, Division 1, Subsection NG, *Core Support Structures*, 1995 Edition.

[4] American Society of Mechanical Engineers (ASME) Boiler and Pressure Vessel Code, Section III, Division 1, Subsection NB, *Class 1 Components*, 1995 Edition.

principal exception is the top end inner and outer closure plate welds to the canister shell, as discussed in Section 2.5.2. The top end closure design complies with guidance provided in NRC Interim Staff Guidance #4 (ISG-4).[5] In addition, the top end outer closure plate is designed in accordance with the requirements of ANSI N14.6[6] for critical lifts to facilitate vertical canister transfer.

The canister top end closure plate welds are partial penetration welds that are structurally qualified by analysis, as presented in Chapter 3 of this FSAR. The inner closure plate welds are inspected by performing a liquid penetrant examination of the root pass and final weld surface The integrity of the top end inner closure plate welds is verified by performing a pneumatic pressure test, and a helium leak test in accordance with the *technical specification* requirements contained in Section 12.3 of the FuelSolutions™ Storage System FSAR. The outer closure plate weld is inspected by performing a liquid penetrant examination of the root pass, intermediate pass, and final weld surface. This weld NDE is in compliance with ISG-4. The associated critical flaw size evaluation to support the NDE acceptance basis is provided in Section 3.9.4 of this FSAR. This critical flaw size evaluation also supports the optional use of UT inspection of the outer closure plate to shell weld.

The structural analysis of the FuelSolutions™ W74 canister, in conjunction with the redundant closures and non-destructive examination, pneumatic pressure testing, and helium leak testing performed during canister fabrication and canister closure, provides assurance of canister closure integrity in lieu of the specific weld joint requirements of Section III, Subsection NB.

Further discussion and justification for the FuelSolutions™ canister closure design and fabrication requirements are provided in Section 2.5.2. Compliance with the ASME Code as it is applied to the design and fabrication of the FuelSolutions™ W74 canister and the associated justification are discussed in Section 2.5.1.

The FuelSolutions™ W74 canister is designed for all normal, off-normal, and postulated accident condition loadings, as defined in Section 2.3. These design loadings include the postulated drop accidents while in the cavity of the FuelSolutions™ W150 Storage Cask or the FuelSolutions™ W100 Transfer Cask, as defined in the FuelSolutions™ Storage System FSAR. The load combinations for which the canister is designed are defined in Section 2.3.5 of this FSAR.

The structural components of the FuelSolutions™ W74 canister damaged fuel can are designed and fabricated in accordance with the applicable requirements of Section III, Subsection NG of the ASME Code. The damaged fuel can is designed for all normal, off-normal, and postulated accident condition loadings and load combinations, as defined in Section 2.3.

As analyzed in Chapter 3 of this FSAR, the damaged fuel can, with its enclosed fuel assembly, is designed to fit within the support tubes of the FuelSolutions™ W74 canister basket.

---

[5] ISG-4, *Cask Closure Weld Inspections*, Spent Fuel Project Office Interim Staff Guidance-4, United States Nuclear Regulatory Commission, Revision 1, May 21, 1999.

[6] ANSI N14.6, *Special Lifting Devices for Shipping Containers Weighing 10,000 Pounds (4,500 kg) or More*, American National Standards Institute, 1993.

Thermal

As discussed in Section 4.3.2 of this FSAR, the FuelSolutions™ W74 canister allowable fuel cladding temperatures imposed to prevent cladding degradation during long-term dry storage conditions are based on a cladding creep methodology, with strains due to creep not exceeding 1% and remaining below the tertiary creep regime. In addition, allowable fuel cladding temperatures are developed using the Diffusion Controlled Cavity Growth (DCCG) methodology provided in UCID-21181.[7] The DCCG methodology is not limited by fuel assembly burnup levels and is, therefore, applicable to the full range of burnups for which SNF assemblies are qualified for dry storage by this FSAR.

The allowable cladding temperatures, which correspond to moderate and high burnups for the SNF assembly classes (including partial and damaged fuel assemblies) to be stored in the FuelSolutions™ W74 canister, are provided in Section 4.3.2 of this FSAR. The allowable cladding temperatures for MOX fuel are discussed in Section 4.7.4.4 of this FSAR.

The short-term cladding temperature that is applicable to normal and off-normal conditions, as well as the fuel loading, canister closure, and canister transfer operations in the storage cask and transfer cask, is limited to 400ºC to avoid accelerated cladding creep and/or cladding annealing effects. For accident conditions, the allowable cladding temperature is 570ºC based on PNL-4835.[8] Further, the FuelSolutions™ W74 canister is backfilled with helium during canister sealing operations to promote heat transfer and prevent cladding degradation in accordance with the *technical specification* contained in Section 12.3 of this FSAR.

The allowable temperatures for the structural steel components of the FuelSolutions™ W74 canister are based on the temperature limits provided in ASME Section II, Part D[9] tables referenced in ASME Section III, Subsection NB and NG, for those load conditions under which material properties are relied on for a structural load combination. For off-normal and accident conditions in which there are no concurrent significant structural loads (e.g., a postulated accidental cask drop), a short-term allowable temperature is established based on ASME Code Case N-47-33.[10] The specific allowable temperatures for the components of the canister are provided in Section 4.3.1 of this FSAR.

The FuelSolutions™ W74 canister is designed for a bounding thermal source term, as described in Section 4.1.5 of this FSAR. The MOX, partial, and damaged fuel are bounded by this thermal source term, as described in Sections, 4.7.4, 4.7.5, and 4.7.6, respectively. The maximum allowable storage cask temperatures are limited when containing the FuelSolutions™ W74 canister, in accordance with the *technical specification* contained in Section 12.3 of this FSAR.

---

[7] UCID-2118, *Spent Fuel Cladding Integrity During Dry Storage*, M.W. Schwartz and M.C. Witte, Lawrence Livermore National Laboratory, September 1987.

[8] PNL-4835, *Technical Basis for Storage of Zircaloy-Clad Spent Fuel in Inert Gases*, A.B. Johnson and E.R. Gilbert, Pacific National Laboratories, September 1983.

[9] American Society of Mechanical Engineers (ASME), Boiler and Pressure Vessel Code, Section II, "Materials," Part D, "Properties," 1995 Edition.

[10] Case N-47-33, *Class 1 Components in Elevated Temperature Service*, American Society of Mechanical Engineers (ASME), Boiler and Pressure Vessel Code, 1995 Code Cases, Nuclear Components, 1995 Edition.

Shielding

The allowable doses for an ISFSI or CISF using the FuelSolutions™ Storage System with the FuelSolutions™ W74 canister are delineated in 10CFR72.104 and 72.106.[11] Compliance with these criteria is necessarily site-specific and is to be demonstrated by the licensee, as discussed in Section 2.1.2 of the FuelSolutions™ Storage System FSAR.

The FuelSolutions™ W74 canister provides axial shielding at the top and bottom ends to maintain occupational exposures ALARA during canister closure and canister transfer operations. The maximum allowable axial dose rates for the FuelSolutions™ W74 canister are controlled in accordance with plant-specific procedures and ALARA requirements (discussed in Section 10.1.3 of the FuelSolutions™ Storage System FSAR).

The FuelSolutions™ W74 canister is designed for the radiological source term specification, as described in Section 5.2 of this FSAR. The radiological source term for the FuelSolutions™ W74 canister is limited based on the Functional and Operating Limits in the *technical specification* contained in Section 12.3 of this FSAR. Section 5.5.2 of this FSAR describes how BRP MOX fuel satisfies the radiological criteria for the FuelSolutions™ W74 canister.

Representative calculated dose rates for the FuelSolutions™ W74 canister are provided in Section 5.4.2 of the FuelSolutions™ Storage System FSAR. These dose rates are used to perform an occupational exposure evaluation in accordance with 10CFR20,[12] as discussed in Sections 10.1 and 10.3 of the FuelSolutions™ Storage System FSAR.

The minimum cooling times determined in Section 5.2 of this FSAR are based on intact BRP assemblies with maximum fuel loading. Partial BRP assemblies have lower overall fuel loadings, and therefore lower radiation source strengths for a given burnup, enrichment, and cooling time. The qualification of BRP partial fuel assemblies is discussed in Section 5.5.3 of this FSAR. Damaged fuel assemblies have the same radiation source strengths as intact fuel. The qualification of damaged BRP fuel assemblies is discussed in Section 5.5.4.

Criticality

The FuelSolutions™ W74 canister provides criticality control for all design basis normal, off-normal, and postulated accident conditions, as discussed in Section 6.3.1 of this FSAR. The effective neutron multiplication factor for storage and transportation is limited to $k_{eff} < 0.95$ for fresh unirradiated intact fuel with optimum fresh water moderation and close reflection, including all biases and uncertainties. In addition, k_{eff} is shown to be less than the upper subcritical limit (USL) established using the methodology presented in NUREG/CR-5661.[13]

Criticality control is maintained by the geometric spacing of the fuel assemblies and fixed borated neutron absorbing materials incorporated into the canister basket assembly. The

[11] Title 10, U.S. Code of Federal Regulations, Part 72 (10CFR72), *Licensing Requirements for the Independent Storage of Spent Nuclear Fuel and High-Level Radioactive Waste*, 1995.

[12] Title 10, U.S. Code of Federal Regulations, Part 20 (10CFR20), *Standards for Protection Against Radiation*, 1986.

[13] Dyer, H. R., and Parks, C. V., *Recommendations for Preparing the Criticality Safety Evaluation of Transportation Packages*, NUREG/CR-5661, Oak Ridge National Laboratories, April 1997.

minimum specified boron concentration verified during material manufacture is further reduced by 25% for criticality analysis. No credit is taken for soluble boron or burnup. Permanent deformations of the canister basket assembly for postulated accident conditions are considered in the criticality analysis. The maximum allowable initial enrichment for fuel assemblies to be stored in the FuelSolutions™ W21 canister are limited in accordance with the *technical specification* contained in Section 12.3 of this FSAR.

Different allowable enrichments apply for MOX, partial, and damaged BRP fuel assemblies. Qualifications of BRP MOX, partial, and damaged fuel assemblies are described in Sections 6.6.1, 6.6.2, and 6.6.3, respectively.

Confinement

The FuelSolutions™ W74 canister provides for confinement of all radioactive materials in UO_2 spent fuel for all design basis normal, off-normal, and postulated accident conditions, as discussed in Sections 1.2.1.3 and 7.1 of this FSAR. The radionuclide inventory for BRP MOX fuel differs from that for UO_2 fuel, as addressed in Chapter 7.

An evaluation of the release of available fission products in accordance with specified release fractions based on the canister design leak rate is discussed in Section 7.3. The confinement function of the FuelSolutions™ W74 canister is verified through pneumatic pressure testing and helium leak testing performed in accordance with the *technical specifications* contained in Sections 12.3 of the FuelSolutions™ Storage System FSAR.

Operations

There are no radioactive effluents that result from storage or transfer operations. Effluents generated during canister loading are handled by the plant's radwaste system and procedures.

Generic operating procedures for the FuelSolutions™ Storage System using the FuelSolutions™ W74 canister are provided in Chapter 8 of the FuelSolutions™ Storage System FSAR. Canister-specific parameters are provided in Chapter 8 of this FSAR. The operations associated with the use of the damaged fuel can are also summarized in Chapter 8.

The licensee will develop site-specific detailed operating procedures based on requirements that comply with the 10CFR50[14] *technical specifications* for the plant and the 10CFR72 *technical specifications* contained in Section 12.3 of this FSAR and the FuelSolutions™ Storage System FSAR.

Acceptance Tests & Maintenance

The fabrication acceptance basis and maintenance program to be applied to the FuelSolutions™ W74 canister are described in Chapter 9 of this FSAR. The acceptance tests and maintenance requirements associated with use of the damaged fuel can are also summarized in Chapter 9.

The operational controls and limits to be applied to the FuelSolutions™ W74 canister are contained in Chapter 12 of this FSAR and the FuelSolutions™ Storage System FSAR. Application of these requirements will assure that the FuelSolutions™ W74 canister is

[14] Title 10, U.S. Code of Federal Regulations, Part 50 (10CFR50), *Domestic Licensing of Production and Utilization Facilities*, 1995.

fabricated, operated, and maintained in a manner that satisfies the design criteria defined in this chapter.

Decommissioning

The FuelSolutions™ W74 canister is designed to be transportable in a transportation cask and is not required to be unloaded prior to shipment off-site. Decommissioning of the FuelSolutions™ Storage System using the FuelSolutions™ W74 canister is addressed in Chapter 14 of the FuelSolutions™ Storage System FSAR.

2.2 Spent Fuel to be Stored

The FuelSolutions™ W74 canister is designed to accommodate up to 64 SNF assemblies (up to 32 each in the upper and lower baskets). The FuelSolutions™ W74 canister accommodates Big Rock Point (BRP) BWR SNF assemblies without the need for fuel assembly spacers. BRP SNF assemblies are stored without flow channels. Table 2.2-1 lists the specific fuel assembly types and associated characteristics acceptable for storage in the FuelSolutions™ W74 canister.

In addition to dimensional acceptance (specified in Table 1.2-3), the SNF assemblies to be stored in the FuelSolutions™ W74 canister must be zircaloy-clad fuel. It is the responsibility of the licensee to assure that the fuel assemblies to be placed in the FuelSolutions™ W74 canister meet these criteria. Missing fuel rods may be replaced with dummy rods that displace an equal amount of water as the original rods to permit storage in the FuelSolutions™ W74 canister.

The structural analysis of the FuelSolutions™ W74 canister for the bounding BRP fuel assembly (maximum total weight and maximum weight per unit length) and demonstration of compliance with the applicable acceptance criteria, as documented in Chapter 3 of this FSAR, qualifies the BRP fuel assemblies (see Table 1.2-3) for storage in either FuelSolutions™ W74 canister class (see Tables 1.2-1 and 1.2-2). In addition, the maximum total loaded weight of the FuelSolutions™ W74 canister is shown to be bounded by or equivalent to the design basis canister weight used in the structural analysis of the FuelSolutions™ W150 Storage Cask and W100 Transfer Cask, as documented in Section 2.2 of the FuelSolutions™ Storage System FSAR.

Thermal qualification of the BRP SNF assembly classes listed in Table 1.2-3 for storage in the FuelSolutions™ W74 canister is dependent on the characteristics of the unburned fuel assembly, the characteristics of the fuel assembly at the time of reactor discharge, and the time since discharge (cooling time). A range of combinations of initial enrichment and burnup are included in the development of thermal and radiological source terms, as documented in Section 5.2 of this FSAR. The required minimum cooling time as a function of initial enrichment and burnup is determined such that all thermal acceptance criteria for the FuelSolutions™ Storage System are satisfied as the basis for thermal fuel qualification, as described in Section 5.2 of this FSAR and the FuelSolutions™ Storage System FSAR.

For the purpose of evaluating the thermal performance of the FuelSolutions™ W74 canister, bounding design basis thermal source terms (decay heat power axial peaking profile) are used in the thermal analysis of the canister, as documented in Section 4.1.3 of this FSAR. In addition, the maximum total heat load and the axial heat load distribution for the FuelSolutions™ W74 canister are shown to be bounded by or equivalent to those used in the design basis thermal analysis of the FuelSolutions™ W150 Storage Cask and W100 Transfer Cask, as documented in Section 4.1.3 of the FuelSolutions™ Storage System FSAR.

Radiological qualification of the SNF assembly classes listed in Table 1.2-3 to be stored in the FuelSolutions™ W74 canister is also dependent on the characteristics of the unburned fuel assembly, the characteristics of the fuel assembly at the time of reactor discharge, and the time since discharge (cooling time). A range of combinations of initial enrichment and burnup are included in the development of thermal and radiological source terms, as documented in Section 5.2 of this FSAR. As described in Section 5.2 of this FSAR and the FuelSolutions™

Storage System FSAR, the required minimum cooling time as a function of initial enrichment and burnup is determined such that the design basis allowable dose rates for the FuelSolutions™ Storage System are satisfied as the basis for radiological fuel qualification. For the purpose of evaluating the radiological performance of the FuelSolutions™ W74 canister, representative radiological source terms (neutron and gamma) are used in the shielding analysis of the canister, as documented in Section 5.2.2 of this FSAR and the FuelSolutions™ Storage System FSAR. In addition, representative dose rates for the FuelSolutions™ W150 Storage Cask and W100 Transfer Cask are provided, as documented in Section 5.4 of the FuelSolutions™ Storage System FSAR.

As documented in Section 6.3 of this FSAR, the criticality analysis for the most reactive BRP fuel assembly and the demonstration of compliance with the applicable acceptance criteria, qualifies BRP fuel assemblies listed in Table 1.2-3 and the specific fuel assembly types listed in Table 2.2-1 for storage in either FuelSolutions™ W74 canister class (see Tables 1.2-1 and 1.2-2). The maximum acceptable initial enrichments, regardless of burnup or cooling time for the fuel assembly, are provided in Section 6.1 of this FSAR and summarized in Table 2.2-1.

The *technical specification* requirements that must be satisfied to qualify SNF assemblies for storage in the FuelSolutions™ W74 canister are contained in Section 12.3 of this FSAR.

The FuelSolutions™ W74 canister, as designed, will also accommodate BRP MOX, partial, and damaged SNF assemblies. These fuels are discussed below.

2.2.1 Mixed-Oxide (MOX) Fuel Assemblies

The BRP MOX fuel assemblies have the same envelope dimensions and weight as the UO_2 assemblies. Thus, the structural parameters evaluated for the FuelSolutions™ W74 canister and basket are unaffected by MOX fuel.

BRP MOX fuel has significantly longer cooling times than those required for UO_2 fuel. The BRP MOX fuel is shown to have thermal source terms that are bounded by the design basis UO_2 assembly thermal source, as discussed in Section 4.7.4 of this FSAR.

Similarly, the longer cooling times result in the BRP MOX fuel dose rates being bounded by the design basis UO_2 fuel dose rates.

There are different BRP MOX fuel assembly designs. The criticality qualification for BRP MOX fuel is performed explicitly for each BRP MOX fuel design, as discussed in Section 6.6.2.

2.2.2 Partial Fuel Assemblies

The weight of the BRP partial fuel assembly is bounded by that of the intact assembly. Thus, the structural parameters evaluated for the W74 canister and basket are bounding for partial fuel.

The thermal and radiological sources for partial fuel are likewise bounded by intact fuel, thus the thermal and radiological evaluations of the W74 canister for intact fuel are bounding for partial fuel.

Partial fuel assemblies have different enrichment limits than intact assemblies, due to the potential for a more reactive assembly. The enrichment limits for partial BRP fuel are provided in Section 6.6.2 of this FSAR.

2.2.3 Damaged Fuel Assemblies

BRP damaged fuel assemblies are those with fuel rod cladding damage in excess of pinhole leaks or hairline cracks. Fuel assemblies with damaged grid spacers (defined as damaged to a degree where fuel rod structural integrity cannot be assured, or where grid spacers have shifted vertically from their design position) will also be stored in damaged fuel cans.

Fuel assemblies are placed in a damaged fuel can when loaded into the FuelSolutions™ W74 canister. The combined weight of the fuel assembly and the damaged fuel can is considered in the structural analysis of the FuelSolutions™ W74 canister, as discussed in Chapter 3 of this FSAR.

The thermal and radiological sources for partial fuel are bounded by intact fuel. However, the damaged fuel can provides an additional item through which the decay heat of the fuel assembly is to be removed. This is addressed in Section 4.7.6 of this FSAR. The damaged fuel can provides additional radiological shielding, thus the radiological evaluations of the W74 canister for intact fuel are bounding for damaged fuel as discussed in Section 5.5.4.

Damaged fuel assemblies have different enrichment limits than intact assemblies, due to the potential for a more reactive assembly configuration. The enrichment limits for damaged BRP fuel are provided in Section 6.6.3 of this FSAR.

Table 2.2-1 - Fuel Assemblies Acceptable for Storage in the FuelSolutions™ W74 Canister

Assembly Class(1),(2)	Assembly Type	Maximum Uranium Loading (kg)	Linear Uranium Loading (kg/in)	W74-1(3) Initial Enrichment (w/o ^{235}U)	Applicable Cooling Table(4) (5)	Criticality Class(5)
Big Rock Point	9x9 GE	143	2.04	≤4.1	74-1-A	GE 9x9
	9x9 ANF	143	2.04	≤4.1	74-1-A	Siemens 9x9
	11x11 ANF	143	2.04	≤4.1	74-1-A	Siemens 11x11
	Other(7)					

Notes:

(1) Assembly Class is defined per EIA Spent Fuel Discharge Report.[15]

(2) Fuel cladding shall be zircaloy. Maximum assembly burnup is limited to 40,000 MWd/MTU. Fuel assembly dimensions and weights for each fuel assembly class are provided in Table 1.2-3.

(3) The fuel loading specification W74-1 is defined in accordance with the *technical specifications* contained in Section 12.3.

(4) Cooling tables in Section 5.2 include information on heat load and provide the required cooling time as a function of burnup and initial enrichment, which meets the thermal and radiological acceptance criteria defined in Chapters 4 and 5, respectively.

(5) For any versions of these assembly types that contain more than 2.9 grams cobalt in the non-fuel hardware in the core zone, the Applicable Cooling Table is 74-1-B. Assemblies with over 15 grams cobalt in the non-fuel hardware in the core zone are not qualified for storage in the W74 canister.

(6) Criticality Class definitions are per Table 6.1-1, and include definitions of cladding type and other fuel assembly characteristics relevant to criticality safety.

(7) Other fuel assemblies that meet the defined parameters are qualified for storage.

[15] Energy Information Administration, *Spent Nuclear Fuel Discharges from U.S. Reactors 1993*, U.S. Department of Energy, 1995.

2.3 Design Loadings

The FuelSolutions™ W74 canister is designed to provide safe dry storage of SNF (including MOX, partial, and damaged fuel assemblies) in an ISFSI or CISF for 100 years at any location in the contiguous United States. The storage cask and transfer cask serve to provide biological shielding, physical protection, and structural support for the canister during storage and transfer under all design basis normal, off-normal, and postulated accident conditions, as addressed in the FuelSolutions™ Storage System FSAR. The FuelSolutions™ W74 canister is also designed for off-site transportation.

In accordance with 10CFR72, a range of long- and short-term natural ambient conditions are considered in the thermal evaluation of the W74 canister in the storage cask and transfer cask. These ambient conditions are assumed to occur concurrently with the design basis normal, off-normal, postulated accident (e.g., blocked vents, loss of neutron shield, etc.) and natural phenomena events and form the basis for the design of the W74 canister within the storage cask and transfer cask.

The design basis off-normal, postulated accident, and natural phenomena conditions are defined in Sections 2.3.1.5, 2.3.2.6, and 2.3.4, respectively. Consistent with the definitions in ANSI/ANS-57.9,[16] off-normal events are anticipated to occur with moderate frequency or on the order of once per calendar year. Postulated accident events are defined as those that might occur only once during the use of the canister within the storage cask or transfer cask.

The design basis conditions considered for the FuelSolutions™ W74 canister are as follows:

<u>Normal Conditions</u>

- Normal Ambient Conditions
- Internal Pressure
- Dead Load
- Handling Load
- Leakage of the Confinement Boundary

<u>Off-Normal Conditions</u>

- Extreme Ambient Conditions
- Internal Pressure
- Misaligned Cask During Horizontal Transfer
- Reflood Pressure
- Hydraulic Ram Failure During Horizontal Transfer
- Leakage of the Confinement Boundary

[16] ANSI/ANS 57.9, *Design Criteria for an Independent Spent Fuel Storage Installation (Dry Storage Type)*, American National Standards Institute, 1992.

Accident Conditions

- Accident Thermal Conditions
  - Storage Cask Vent Blockage
  - Transfer Cask Loss of Neutron Shield
- Cask Drop
- Storage Cask Tip-over on J-skid
- Fire
- Internal Pressure
- Leakage of the Confinement Boundary
- Explosive Overpressure

Natural Phenomena

- Flooding
- Tornado
- Earthquake
- Wind
- Burial Under Debris
- Lightning
- Snow and Ice

The canister is designed for the most severe environmental conditions and the natural phenomena postulated to occur during storage over the entire service life of the canister, including canister fuel loading, closure, and transfer using the FuelSolutions™ W100 Transfer Cask, and canister dry storage in the FuelSolutions™ W150 Storage Cask. The normal environmental conditions include the annual variation of ambient temperature, solar radiation (insolation), wind, snow, and ice conditions. The off-normal environmental conditions include extreme ambient temperatures and insolation. The accident environmental conditions and natural phenomena include wind resulting from a tornado, impact of a missile generated by tornado, flood, earthquake, fire, and explosion. Totally blocked inlet and/or outlet vents on the storage cask and loss of the neutron shield on the transfer cask are also included in the accident conditions.

The effects of the normal, off-normal, and accident condition loadings defined in this section on the FuelSolutions™ W150 Storage Cask and W100 Transfer Cask are evaluated in the FuelSolutions™ Storage System FSAR.

2.3.1 Normal Conditions

2.3.1.1 Normal Ambient Conditions

The ambient conditions used for the design basis analysis of the FuelSolutions™ W74 canister for normal conditions are provided in Section 2.3.1.1 of the FuelSolutions™ Storage System FSAR. The corresponding structural and thermal analyses of the FuelSolutions™ W74 canister for normal ambient conditions during canister fuel loading, closure, transfer, and dry storage are documented in Sections 3.5 and 4.4 of this FSAR.

2.3.1.2 Internal Pressure

The normal condition internal pressure for the FuelSolutions™ W74 canister during dry storage is based on the initial canister helium backfill pressure, the normal condition canister temperatures, and an assumed failure of 1% of the fuel rods with complete release of their associated fill gases and 30% of their fission gases to the canister cavity. The design basis internal pressure for this condition is 10 psig. The structural effects of normal condition internal pressure on the canister are evaluated in Section 3.5 of this FSAR.

Normal condition internal pressure during draining of the canister cavity after the inner closure plate is welded to the canister shell is also evaluated. This load is defined as a 30 psig internal pressure, which is monitored in accordance with the operating procedures contained in Section 8.1.8 of the FuelSolutions™ Storage System FSAR. The structural effects of this load are also evaluated in Section 3.5 of this FSAR.

2.3.1.3 Dead Load

This load includes the dead weight of the materials of construction and the contents for the FuelSolutions™ W74 canister, acting either horizontally or vertically.

2.3.1.4 Handling Load

For normal conditions, this load includes normal handling loads associated with vertical or horizontal transfer of the FuelSolutions™ W74 canister from or to a FuelSolutions™ W100 Transfer Cask, and to or from the FuelSolutions™ W150 Storage Cask or a transportation cask.

For vertical canister transfer, the handling load is defined as 15%[17] of the maximum loaded canister weight, which acts on the top end outer closure plate of the canister. For horizontal canister transfer between a storage cask, transfer cask, or transportation cask, the handling load is defined as a pushing or pulling axial force of 45,000 pounds acting on the outer closure plate of either end of the canister due to friction forces that developed between the canister shell and cask rails. The vibration loading normally incident to on-site transfer is conservatively defined in accordance with NUREG/CR-0128[18] as ±0.6 *g* acting in the vertical direction, ±0.3 *g* acting in the longitudinal direction, and ±0.2 *g* acting in the lateral direction, simultaneously.

---

[17] CMAA #70, *Specifications for Electric Overhead Traveling Cranes*, Crane Manufacturers Association of America (CMAA), 1988.

[18] NUREG/CR-0128, *Shock and Vibration Environment for a Large Shipping Container During Truck Transport*, U.S. Nuclear Regulatory Commission, May 1978.

The structural effects of normal condition handling loads on the canister are evaluated in Section 3.5 of this FSAR. The effects of these loads on the FuelSolutions™ W100 Transfer Cask and W150 Storage Cask are addressed in the FuelSolutions™ Storage System FSAR.

2.3.1.5 Leakage of the Confinement Boundary Under Normal Conditions

The FuelSolutions™ W74 canister is evaluated for the release of internal gases and aerosol contents to the atmosphere based on the design leak rate of the canister as defined in the *technical specification* in Section 12.3 of the FuelSolutions™ Storage System FSAR. It is assumed for this evaluation that 1% of all fuel rods fail. The corresponding nuclide release fractions are used to determine the quantity of radioactive material available for release. The radiological evaluation for this postulated event, including the assumptions used in the analysis, is documented in Section 7.2 of this FSAR.

2.3.2 Off-Normal Conditions

2.3.2.1 Extreme Ambient Conditions

The extreme ambient conditions used for the design basis analysis of the FuelSolutions™ W74 canister for off-normal conditions are provided in Section 2.3.2.1 of the FuelSolutions™ Storage System FSAR. The temperature distribution in the canister for off-normal conditions and comparisons to allowable values is provided in Section 4.5 of this FSAR. The structural effects of off-normal condition temperatures on the canister are evaluated in Section 3.6 of this FSAR.

2.3.2.2 Internal Pressure

The off-normal condition internal pressure for the FuelSolutions™ W74 canister during dry storage is based on the initial canister helium backfill pressure, the off-normal condition canister temperatures, and an assumed failure of 10% of the fuel rods with complete release of their associated fill gases and 30% of their fission gases to the canister cavity. The design basis internal pressure for this condition is 16 psig. The structural effects of off-normal condition internal pressure on the canister are evaluated in Section 3.6 of this FSAR.

The off-normal condition internal pressure is conservatively used as the initial condition for the evaluation of the FuelSolutions™ W74 canister for a postulated blockage of the storage cask vents discussed in Section 2.3.3.1.

2.3.2.3 Misaligned Casks During Horizontal Canister Transfer

This off-normal loading condition is postulated to occur as a result of a misalignment of a transfer cask with a storage cask or transportation cask during horizontal transfer of the FuelSolutions™ W74 canister. This load is defined as a pushing axial force of 70,000 pounds or pulling axial force of 50,000 pounds acting on the outer closure plate at either end of the canister, which is reacted by the storage cask, transfer cask, or transportation cask, as described in Section 2.3.2.4 of the FuelSolutions™ Storage System FSAR. The structural effects of off-normal condition misalignment loads on the canister are evaluated in Section 3.6 of this FSAR. The effects of this load on the transportation cask are addressed in a separate transportation license application.

2.3.2.4 Reflood Pressure

In the unlikely event of canister reopening, the canister cavity is reflooded with water. Depending on the temperatures inside the canister, the water may flash to steam resulting in internal pressures in the canister during reflood. This load is defined as a 100 psig internal pressure.

2.3.2.5 Hydraulic Ram Failure During Horizontal Transfer

During horizontal transfer of the canister between the storage cask and transfer cask, the transfer cask and transportation cask, or the storage cask and transportation cask, a hydraulic ram is used to slide the canister between casks by pushing or pulling the canister. Under normal conditions, the hydraulic ram operates normally and canister horizontal transfer operations are completed. However, it is postulated that a mechanical failure of the hydraulic ram may occur during the canister transfer operation with the canister transfer only partially completed. The effects of this postulated off-normal event are evaluated in Section 11.1 of this FSAR.

2.3.2.6 Leakage of the Confinement Boundary Under Off-Normal Conditions

As demonstrated in Chapter 3 of this FSAR, the confinement boundary of the FuelSolutions™ W74 canister (which consists of the canister shell, the bottom closure plate, the top end inner and outer closure plates, and the closure welds) is not compromised by any design basis normal, off-normal, or postulated accident condition loadings. The evaluation of the release of internal gases and aerosol contents to the atmosphere is based on the design leak rate of the canister, as defined in the *technical specification* in Section 12.3 of the FuelSolutions™ Storage System FSAR. It is assumed for this postulated event that 10% of all fuel rods fail. The corresponding nuclide release fractions are used to determine the quantity of radioactive material available for release. The radiological evaluation for this postulated event, including the assumptions used in the analysis, is documented in Section 7.2 of this FSAR.

2.3.3 Postulated Accident Conditions

2.3.3.1 Accident Thermal Conditions

2.3.3.1.1 Storage Cask Vent Blockage

The extreme ambient conditions used for the design basis analysis of the FuelSolutions™ W74 canister for postulated accident conditions are provided in Section 2.3.3.1 of the FuelSolutions™ Storage System FSAR. The temperature distribution in the canister for accident conditions, including the effects of a complete blockage of the storage cask inlet and outlet vents and comparisons to allowable values are provided in Section 4.6 of this FSAR. The corresponding structural effects of accident condition temperatures on the canister are evaluated in Section 3.7 of this FSAR.

2.3.3.1.2 Transfer Cask Loss of Neutron Shield

The extreme ambient conditions used for the design basis analysis of the FuelSolutions™ W74 canister for postulated accident conditions are provided in Section 2.3.3.1 of the FuelSolutions™ Storage System FSAR. The temperature distribution in the canister for accident conditions,

including the effects of a loss of the transfer cask neutron shield and comparisons to allowable values are provided in Section 4.6 of this FSAR. The corresponding structural effects of accident condition temperatures on the canister are evaluated in Section 3.7 of this FSAR.

2.3.3.2 Cask Drop and Tip-over

The postulated drop accident conditions for a loaded storage cask or transfer cask are defined in Section 2.3.3.2 of the FuelSolutions™ Storage System FSAR. The postulated storage cask tip-over on the J-skid accident condition is defined in Section 2.3.3.3 of the FuelSolutions™ Storage System FSAR. The determination of the resulting impact loads is documented in Section 3.7 of the FuelSolutions™ Storage System FSAR. The structural evaluation of the FuelSolutions™ W74 canister for these postulated cask drop and tip-over accident conditions is documented in Section 3.7 of this FSAR.

2.3.3.3 Fire

The postulated design basis fire is defined in Section 2.3.3.4 of the FuelSolutions™ Storage System FSAR. The resulting thermal effects on the storage cask and transfer cask are documented in Section 4.6 of the FuelSolutions™ Storage System FSAR. The evaluation of the thermal effects for the design basis fire on the FuelSolutions™ W74 canister is provided in Section 4.6 of this FSAR.

2.3.3.4 Internal Pressure

The postulated accident condition internal pressure for the FuelSolutions™ W74 canister is based on the initial canister helium backfill pressure, the off-normal condition canister temperatures, and the assumed failure of 100% of the fuel rods with complete release of their associated fill gases and 30% of their fission gases. The design basis internal pressure for this condition is 69 psig. The structural effects of accident condition internal pressure on the canister are evaluated in Section 3.7 of this FSAR.

2.3.3.5 Leakage of the Confinement Boundary Under Accident Conditions

As demonstrated in Chapter 3 of this FSAR, the confinement boundary of the FuelSolutions™ W74 canister (which consists of the canister shell, the bottom closure plate, the top end inner and outer closure plates, and the closure welds) is not compromised by any design basis normal, off-normal, or postulated accident condition loadings. The evaluation of the release of internal gases and aerosol contents to the atmosphere is based on the design leak rate of the canister, as defined in the *technical specification* in Section 12.3 of the FuelSolutions™ Storage System FSAR. It is assumed for this postulated event that 100% of all fuel rods fail. The corresponding nuclide release fractions are used to determine the quantity of radioactive material available for release. The radiological evaluation for this postulated event, including the assumptions used in the analysis, is documented in Section 7.3 of this FSAR.

2.3.3.6 Explosive Overpressure

The FuelSolutions™ W74 canister is protected against explosive overpressure, as the canister is completely enclosed in the storage cask or transfer cask. Therefore, the canister is not subjected to direct explosive overpressure-related loadings. For the purpose of providing a design basis

external pressure criteria for comparison to site-specific hazards, the explosive overpressure acting on the canister is taken to be the same as the external pressure due to flooding, as described in Section 2.3.4.1.

2.3.4 Natural Phenomena

2.3.4.1 Flooding

The FuelSolutions™ W74 canister is designed for an enveloping design basis flood, postulated to result from natural phenomena such as a tsunami and seiches. For the purpose of this bounding generic evaluation, the 50-foot flood height presented in Section 2.3.4.1 of the FuelSolutions™ Storage System FSAR is used.

The canister is conservatively evaluated for a 50-foot hydraulic head of water, which corresponds to an external pressure of:

$$p = 50\ ft \times 62.4\ pcf = 3{,}120\ psf = 21.7\ psi$$

The structural evaluation of the FuelSolutions™ W74 canister for the effects of external pressure due to flooding is documented in Section 3.7 of this FSAR. Since the FuelSolutions™ W74 canister uses fixed borated neutron absorbers and is designed for fresh water optimum moderation, criticality safety during flooding is assured.

2.3.4.2 Tornado

Since the canister is completely enclosed in the storage cask or transfer cask, the canister is protected against design basis tornado (DBT) missile impact for all types of missiles and tornado winds. Therefore, the canister is not subjected to any tornado-related loadings.

2.3.4.3 Earthquake

The design basis earthquake (DBE) load is determined in Section 2.3.4.4 of the FuelSolutions™ Storage System FSAR. The FuelSolutions™ W74 canister is evaluated for the effects of seismic accelerations with the canister in the storage cask or the transfer cask. The resulting structural analysis is documented in Section 3.7 of this FSAR.

2.3.4.4 Wind

Since the canister is completely enclosed in the storage cask or transfer cask, the FuelSolutions™ W74 canister is protected against design basis wind (DBW). Therefore, the canister is not subjected to any wind-related loading.

2.3.4.5 Burial Under Debris

Debris may be deposited around the storage cask due to a number of phenomena, such as wind storms, floods, or land slides. The consequence of such events is anticipated to be partial or complete blockage of the storage cask inlet vents. This condition is bounded by the fully blocked vent case described in Section 2.3.3.1.

2.3.4.6 Lightning

The effects of lightning are addressed in Section 2.3.4.7 of the FuelSolutions™ Storage System FSAR.

2.3.4.7 Snow and Ice

Since the canister is completely enclosed within the transfer cask or storage cask, the FuelSolutions™ W74 canister is protected from snow and ice loadings. Therefore, the canister is not subjected to any snow- and ice-related loadings.

2.3.4.8 Site-Specific Conditions

Other site-specific conditions will be addressed on a site-specific basis, as applicable. Each licensee is required to perform a 10CFR72.212 evaluation to assure that no site-specific environmental phenomena or design conditions exist that are not bounded by or equivalent to those defined in this chapter and the C of C.

2.3.5 Load Combination Criteria

The FuelSolutions™ W74 canister is subjected to normal, off-normal, postulated accident, and natural phenomena condition loadings as defined in this chapter. These loads are summarized as follows:

- Normal Loads – Normal ambient conditions, internal pressure, dead weight, handling.
- Off-Normal Loads – Extreme ambient conditions, off-normal internal pressure, misalignment during canister horizontal transfer, reflood.
- Postulated Accident and Natural Phenomena Loads – Complete blockage of storage cask air inlet and outlet vents, transfer cask loss of neutron shield, cask drop, cask tip-over, fire, accident internal pressure, flood, earthquake.

The FuelSolutions™ W74 canister internal basket and shell assembly components are designed for the load combinations shown in Table 2.3-1. These combinations are categorized based on the ASME service level criteria for evaluation against the associated allowable values. The allowable values are provided in Chapter 3 of this FSAR.

Load combination results and comparisons to allowable values for the FuelSolutions™ W74 canister for normal, off-normal, and accident conditions are provided in Sections 3.5, 3.6, and 3.7 of this FSAR, respectively.

Table 2.3-1 - W74 Canister Load Combinations[1, 2]

Comb. No.	Dead-weight	Handling	Internal Pressure	Thermal	Earth-quake	Drop or Tip-over	Flood
Normal Operating Conditions (Service Level A)							
A1	D_{V1}		P_b				
A2	D_v		P	T			
A3	D_h		P	T			
A4	D_v	L_{hv}	P	T			
A5	D_h	L_{hh1} or L_{hh2}	P	T			
Off-Normal Conditions (Service Level B)							
B1	D_v		P_o	T_o			
B2	D_v	L_{hv}	P_o	T_o			
B3	D_h	L_{hh1} or L_{hh2}	P_o	T_o			
B4	D_h	L_m	P	T			
Off-Normal Conditions (Service Level C)							
C1	D_v		P_r	T_r			
Postulated Accident Conditions (Service Level D)							
D1	D_v	L_{hv}	P_a	T_o			
D2	D_h	L_{hh1} or L_{hh2}	P_a	T_o			
D3			P_o	T		A_S	
D4			P_o	T		A_t	
D5			P_o	T		A_{S1}	
D6	D_v or D_h		P_o	T	E		
D7	D_v or D_h		P_o	T_a			
D8	D_v		P	T			F

Table 2.3-1 Notes:

(1) Allowable canister shell stresses are in accordance with ASME Section III, Subsection NB. Allowable canister basket stresses are in accordance with ASME Section III, Subsection NG.

(2) Load definitions are as follows:

D_v = Loading due to deadweight - vertical canister

D_{V1} = Loading due to deadweight - vertical canister with weight of auxiliary shield plate and automatic welder, excluding weight of outer closure plate

(continued on next page)

Table 2.3-1 Notes (cont'd):

D_h	=	Loading due to deadweight - horizontal canister
L_{hv}	=	Loading due to normal handling - vertical canister transfer
L_{hh1}	=	Loading due to normal handling - horizontal canister transfer
L_{hh2}	=	Loading due to normal handling - on-site transport
L_m	=	Loading due to misalignment
P_b	=	Loading due to draining pressure
P	=	Loading due to normal internal pressure including 1% cladding failure
P_o	=	Loading due to off-normal internal pressure including 10% cladding failure
P_a	=	Loading due to accident internal pressure including 100% cladding failure
P_r	=	Loading due to reflood internal pressure
T	=	Loading due to normal thermal
T_o	=	Loading due to off-normal thermal, including canister vacuum drying
T_a	=	Loading due to accident thermal (fully blocked storage cask vents, transfer cask loss of neutron shield, or fire)
T_r	=	Loading due to reflood thermal
E	=	Loading due to earthquake
A_S	=	Loading due to postulated storage cask drop
A_t	=	Loading due to postulated transfer cask drop
A_{S1}	=	Loading due to postulated storage cask tip-over
F	=	Loading due to postulated flood

2.4 Safety Protection Systems

The safety protection systems associated with the FuelSolutions™ Storage System are described in the FuelSolutions™ Storage System FSAR.

This page intentionally left blank.

2.5 Supplemental Information

2.5.1 ASME Code Compliance

As discussed in Section 2.1.2, the FuelSolutions™ W74 canister is designed and fabricated with Section III of the ASME Code to the maximum extent practicable, consistent with other canister-based dry storage systems previously approved by the NRC. The clarifications made to the applicable portions of the ASME Code and the basis for these clarifications is provided in Table 2.5-1.

Table 2.5-1 - ASME Code Requirements Compliance Summary (10 Pages)

Item	ASME Code Requirement	Issue	Alternative Compliance Basis
Section III, Subsection NCA (applicable to both Canister and Basket):			
1	**General for Subsection NCA**	1. The terms "Certificate Holder" and "Owner" used throughout this subsection are not applicable for a 10CFR72 system. 2. The Division 2 (concrete) requirement provided throughout this subsection are not applicable for a 10CFR72 system.	1. BNFL Fuel Solutions (BFS) bears the responsibilities associated with a "Certificate Holder" or "Owner" relative to the FuelSolutions™ SFMS. 2. This compliance summary table only addresses FuelSolutions™ canisters, which do not contain any concrete.
2	**NCA-1140, "Use of Code Editions, Addenda, and Cases:"** "(a)(1) Under the rules of this Section, the Owner or his designees shall establish the Code Edition and Addenda to be included in the Design Specifications . . ."	The FuelSolutions™ SFMS documentation does not include an ASME Code Design Specification.	The requirements and criteria typically contained in an ASME Code Design Specification are contained in this FSAR.

Table 2.5-1 - ASME Code Requirements Compliance Summary (10 Pages)

Item	ASME Code Requirement	Issue	Alternative Compliance Basis
3	**NCA-1210, "Components:"** "Each component of a nuclear power plant shall require a Design Specification (NCA-3250), Design Report (NCA-3350, NCA-3550), and other design documents specified in NCA-3800. Data Reports and stamping shall be as required in NCA-8000."	The FuelSolutions™ SFMS documentation does not contain the following ASME Code documents: 1. Design Specification, 2. Design Report, 3. Owner's Certificate of Authorization, 4. Authorized Inspection Agency written agreement, 5. Owner's Data Report, 6. Overpressure Protection Report.	1. See Item 2. 2. The information typically reported in an ASME Code Design Report is contained in this FSAR. 3. An Owner's Certificate of Authorization, a written agreement with an Authorized Inspection Agency, an Owner's Data Report, and an Overpressure Protection Report are not typically provided for components licensed under 10CFR72.
4	**NCA-1220, "Materials"**	Not all non-pressure retaining materials specified in this FuelSolutions™ Canister Storage FSAR are listed as ASME Section III materials.	FuelSolutions™ canisters are purchased, identified, controlled, and manufactured using a graded quality approach in accordance with the NRC-approved BFS Quality Assurance Program based on NQA-1, NRC Regulatory Guide 7.10, and NUREG/CR-6407 criteria.
5	**NCA-1281, "Activities and Requirements:"** "… Data Reports and stamping shall be as required in NCA-8000."	See Item 19.	See Item 19.
6	**NCA-2000, "Classification of Components"**	The classification of components is usually provided in a Design Specification.	See Item 2.

Table 2.5-1 - ASME Code Requirements Compliance Summary (10 Pages)

Item	ASME Code Requirement	Issue	Alternative Compliance Basis
7	**NCA-2142, "Establishment of Design, Service, and Test Loadings and Limits:"** "In the Design Specification, the Owner or his designee shall identify the loadings and combinations of loadings and establish the appropriate Design, Service, and Test Limits for each component or support . . ."	See Item 2.	See Item 2.
8	**NCA-3100, "General"**	ASME Code accreditation does not apply.	See Item 1.
9	**NCA-3200, "Owner's Responsibilities"**	An Owner's responsibilities under the ASME Code do not apply.	An Owner's Certificate of Authorization, a Design Specification, a Design Report, an Overpressure Protection Report, and an Owner's Data Report are not typically provided for components licensed under 10CFR72.
10	**NCA-3300, "Responsibilities of a Designer - Division 2"**	See Item 1.	See Item 1.
11	**NCA-3400, "Responsibilities of an N Certificate Holder - Division 2"**	See Item 1.	See Item 1.
12	**NCA-3500, "Responsibilities of an N Certificate Holder - Division 1"**	See Item 1.	See Item 1. Design and fabrication requirements are provided in this FSAR and related procurement/fabrication drawings and specifications.
13	**NCA-3600, "Responsibilities of an NPT Certificate Holder"**	See Item 1.	See Item 12.
14	**NCA-3700, "Responsibilities of an NA Certificate Holder"**	See Item 1.	See Item 12.

Table 2.5-1 - ASME Code Requirements Compliance Summary (10 Pages)

Item	ASME Code Requirement	Issue	Alternative Compliance Basis
15	**NCA-3800, "Metallic Material Organization's Quality System Program"**	Materials for a FuelSolutions™ canister may be purchased from suppliers that are not certified per the requirements of NCA-3800.	Material suppliers are qualified per NCA-3800 or the NRC-approved BFS Quality Assurance Program based on the requirements of NQA-1, NRC Regulatory Guide 7.10, and NUREG/CR-6407 criteria.
16	**NCA-3900, "Nonmetallic Material Manufacturer's and Constituent Suppliers Quality System Programs"**	See Item 1.	See Item 1.
17	**NCA-4000, "Quality Assurance"**	These quality assurance requirements do not apply.	See Item 4.
18	**NCA-5000, "Authorized Inspection"**	The manufacturing or operation of the FuelSolutions™ SFMS does not use an Authorized Inspection Agency.	An Authorized Inspection Agency is not typically used in the manufacturing or operation of components licensed under 10CFR72.
19	**NCA-8000, "Certificates of Authorization, Nameplates, Code Symbol Stamping, and Data Reports"**	The FuelSolutions™ SFMS does not use an ASME Code Certificate of Authorization, Code Symbol Stamping, or a Data Report.	An ASME Code Certificate of Authorization, Code Symbol Stamping, or a Data Report are not typically required for components licensed under 10CFR72. Nameplate information is provided on each FuelSolutions™ canister.
Section III, Subsection NB (applicable to Canister):			
20	**NB-1130, "Boundary of Components:"** "The Design Specification shall define the boundary of a component to which piping or another component is attached."	See Item 6.	See Item 6.

Table 2.5-1 - ASME Code Requirements Compliance Summary (10 Pages)

Item	ASME Code Requirement	Issue	Alternative Compliance Basis
21	**NB-1132.2, "Jurisdictional Boundary:"** "The jurisdictional boundary between a pressure-retaining component and an attachment defined in the Design Specification shall not be any closer to the pressure-retaining portion of the component than as defined in (a) through (g) below . . ."	See Item 6.	See Item 6.
22	**NB-2160, "Deterioration of Material In Service:"** "It is the responsibility of the Owner to select material suitable for the conditions stated in the Design Specifications (NCA-3250), with specific attention being given to the effects of service conditions upon the properties of the material. . . . Any special requirement shall be specified in the Design Specifications (NCA-3252 and NB-3124) . . ."	See Item 2.	See Item 2.
23	**NB-2610, "Documentation and Maintenance of Quality System Programs:"** "(a) Except as provided in (b) below, Material Manufacturers and Material Suppliers shall have a Quality System Program or an Identification and Verification Program, as applicable, which meets the requirements of NCA-3800 . . ."	See Item 15.	See Item 15.

Table 2.5-1 - ASME Code Requirements Compliance Summary (10 Pages)

Item	ASME Code Requirement	Issue	Alternative Compliance Basis
24	**NB-3113, "Service Conditions:"** "Each service condition to which the components may be subjected shall be classified in accordance with NCA-2142 and Service Limits (NCA-2142.4(b)) designated in the Design Specifications in such detail as will provide a complete basis for design, construction, and inspection in accordance with this Article . . ."	See Item 2.	See Item 2.
25	**NB-3134, "Leak Tightness:"** "Where a system leak tightness greater than that required or demonstrated by a hydrostatic test is required, the leak tightness requirements for each component shall be set forth in the Design Specifications."	See Item 2.	See Item 2.
26	**NB-3220, "Stress Limits for Other Than Bolts"**	This section makes a number of references to an ASME Code Design Specification. See Item 2.	See Item 2.
27	**NB-4121, "Means of Certification:"** "The Certificate Holder for an item shall certify, by application of the appropriate Code Symbol and completion of the appropriate Data Report in accordance with NCA-8000, that materials used comply with the requirements of NB-2000 and that the fabrication or installation complies with the requirements of this Article."	The FuelSolutions™ SFMS does not use an ASME Code Symbol Stamp or a Data Report.	An ASME Code Symbol Stamp or Data Report are not typically required for components licensed under 10CFR72. Also see Item 15.

Table 2.5-1 - ASME Code Requirements Compliance Summary (10 Pages)

Item	ASME Code Requirement	Issue	Alternative Compliance Basis
28	**NB-4243, "Category C Weld Joints in Vessels and Similar Weld Joints in Other Components:"** "Category C weld joints in vessels and similar weld joints in other components shall be full penetration joints . . . Either a butt welded joint or a full penetration corner joint as shown in Fig. NB-4243-1 shall be used."	The FuelSolutions™ canister top end closure employs the following cover-to-shell weld types: 1. Top inner cover - a single-sided partial penetration weld. 2. Top outer cover - a single-sided partial penetration weld.	The FuelSolutions™ canister top end closure employs multi-pass, redundant welds. The inner closure weld is subjected to multi-level liquid penetrant examinations and a combined pneumatic pressure and helium leak rate test at a hydrostatic test pressure to assure structural integrity and leak tightness. The outer closure weld is subjected to multi-level liquid penetrant examinations only. The design of the inner closure weld incorporates a stress-reduction factor of 0.9 to account for use of multi-pass PT examination and helium leak testing. The design of the outer closure weld complies with ISG-4. The examination of the inner and outer closure plate welds complies with guidance provided in ISG-4.
29	**NB-5231, "General Requirements:"** "(a) Category C full penetration butt welded joints in vessels and similar welded joints in other components shall be examined by the radiographic and either liquid penetrant or magnetic particle method."	The FuelSolutions™ canister top end closures are not radiographically examined.	See Item 28.

Table 2.5-1 - ASME Code Requirements Compliance Summary (10 Pages)

Item	ASME Code Requirement	Issue	Alternative Compliance Basis
30	**NB-6112, "Pneumatic Testing:"** "A pneumatic test in accordance with NB-6300 may be substituted for the hydrostatic test when permitted by NB-6112.1(a)." **NB-6112.1, "Pneumatic Test Limitations:"** "(a) A pneumatic test may be used in lieu of a hydrostatic test only when any of the following conditions exists: (1) when components, appurtenances, or systems are so designed or supported that they cannot safely be filled with liquid; (2) when components, appurtenances, or systems which are not readily dried are to be used in services where traces of the testing medium cannot be tolerated. (b) A pneumatic test at a pressure not to exceed 25% of the Design Pressure may be applied, prior to either a hydrostatic or a pneumatic test, as a means of locating leaks."	The FuelSolutions™ canisters employ a combined pneumatic pressure and helium leak rate test at a hydrostatic test pressure to assure structural integrity and leak tightness.	Because a dry SNF assembly storage canister is a 10CFR72 licensed component requiring a helium leak rate test, the combination of this leak rate test with a pneumatic pressure test at a hydrostatic test pressure is operationally efficient and consistent with ALARA principles, while still being very conservative due to the molecular size of the testing medium and the use of helium leak rate vs. visual examination acceptance criteria.
31	**NB-6200, "Hydrostatic Tests"**	See Item 30.	See Item 30.
32	**NB-7000, "Overpressure Protection"**	A FuelSolutions™ canister is not designed to include an overpressure protection device.	By their very nature, canisters and casks designed to dry store SNF assemblies are licensed without any type of overpressure protection device or vent path of any kind.

Table 2.5-1 - ASME Code Requirements Compliance Summary (10 Pages)

Item	ASME Code Requirement	Issue	Alternative Compliance Basis
33	**NB-8000, "Nameplates, Stamping, and Reports"**	The FuelSolutions™ SFMS does not use an ASME Code Symbol Stamp or a Data Report.	An ASME Code Symbol Stamp or a Data Report are not typically required for components licensed under 10CFR72. Nameplate information is provided on each FuelSolutions™ canister.
Section III, Subsection NG (applicable to Basket):			
34	**NG-2160, "Deterioration of Material In Service:"** "It is the responsibility of the Owner to select material suitable for the conditions stated in the Design Specifications (NCA-3250), with specific attention being given to the effects of service conditions upon the properties of the material."	See Item 2.	See Item 2.
35	**NG-2330, "Test Requirements and Acceptance Standards"**	FuelSolutions™ canister basket material is not impact tested to the requirements of NG-2330.	Canister basket is licensed for storage and transportation, and therefore materials are impact tested in accordance with NRC criteria provided in Regulatory Guide 7.11 and NUREG/CR-6407 for Category II materials.
36	**NG-2610, "Documentation and Maintenance of Quality System Programs:"** "(a) Except as provided in (b) below, Material Manufacturers and Material Suppliers shall have a Quality System Program or an Identification and Verification Program, as applicable, which meets the requirements of NCA-3800 . . ."	See Item 15.	See Item 15.

Table 2.5-1 - ASME Code Requirements Compliance Summary (10 Pages)

Item	ASME Code Requirement	Issue	Alternative Compliance Basis
37	**NG-3113, "Service Loadings:"** "Each loading to which the structure may be subjected shall be classified in accordance with NCA-2142 and Service Limits (NCA-2142.4(b)) designated in the Design Specifications in such detail as will provide a complete basis for design, construction, and inspection in accordance with this Article . . ."	See Item 2.	See Item 2.
38	**NG-3220, "Stress Limits for Other Than Threaded Structural Fasteners"**	This section makes a number of references to an ASME Code Design Specification. See Item 2.	See Item 2.
39	**NG-4121, "Means of Certification:"** "The Certificate Holder for an item shall certify, by application of the appropriate Code Symbol and completion of the appropriate Data Report in accordance with NCA-8000, that materials used comply with the requirements of NG-2000 and that the fabrication or installation complies with the requirements of this Article."	The FuelSolutions™ SFMS does not use an ASME Code Symbol Stamp or a Data Report.	An ASME Code Symbol Stamp or Data Report are not typically required for components licensed under 10CFR72. Also see Item 15.
40	**NG-8000, "Nameplates, Stamping, and Reports"**	The FuelSolutions™ SFMS does not use an ASME Code Symbol Stamp or a Data Report.	An ASME Code Symbol Stamp or a Data Report are not typically required for components licensed under 10CFR72. Nameplate information is provided on each FuelSolutions™ canister.

2.5.2 FuelSolutions™ Canister Top End Closure Weld Design Basis and Nondestructive Examination Justification

This FSAR section discusses the FuelSolutions™ canister top end closure design basis, including the justification for performing PT examination of the canister closure welds. The canister top end closure design and examination are in compliance with guidance provided in NRC Interim Staff Guidance #4 (ISG-4).

2.5.2.1 Introduction

The NRC has recently raised concerns relative to top closure weld details and nondestructive examination (NDE) practices used in canisters for the storage of dry SNF assemblies. As required by 10CFR72 for independent SNF assembly and high-level radioactive waste storage systems, a "cask" must be designed to provide redundant sealing of confinement systems (10CFR72.236(c)) and be inspected to ascertain that there are no "cracks, pinholes, uncontrolled voids, or other defects" that could significantly reduce confinement effectiveness (10CFR72.236(j)). The current NRC concerns are based on recurring defects in Ventilated Storage Cask (VSC)-24 canister closure welds since 1995, as discussed in a recent NRC inspection report.[19]

The following presents a justification for the closure weld details and the associated NDE for the FuelSolutions™ canisters to be used to dry store SNF assemblies. The weld details and examination and testing practices described herein meet or exceed those for existing NRC-certified systems. They are based on related operating experience gained since the late 1980s and the resulting steady evolution in canister weld geometry and welding processes. This section also addresses technical issues raised by the VSC-24 closure weld details as they relate to a FuelSolutions™ canister.

2.5.2.2 NUREG-1536 Criteria

NUREG-1536[20] provides guidelines for use by the NRC staff in the preparation of safety reviews for dry cask storage systems. NUREG-1536 provides the following statements concerning canister closure details and inspection practices:

Section 3.0, "Structural Evaluation," paragraph V.1.b.ii, "Structural Design Features:"

> *"Review confinement boundary weld designs for compliance with the design code used for the confinement boundary. Acceptable requirements appear in ASME* (American Society of Mechanical Engineers) *Code* (Boiler and Pressure Vessel Code - BPVC) *Section III, Subsections NB-3352 and NC-3352, "Permissible Types of Welded Joints," and NB-4240 and NC-4240, "Requirements for Weld Joints in Components."*

[19] Inspection Report 72-1007/97-212, U.S. Nuclear Regulatory Commission, August 29, 1997.

[20] NUREG-1536, *Standard Review Plan for Dry Cask Storage Systems*, U.S. Nuclear Regulatory Commission, January 1997.

The NRC has previously accepted alternative confinement boundary weld designs (such as NB-5200 or NC-5200, typically for Category C welded joints). These acceptable alternatives achieve equivalent structural integrity, but do not meet all the provisions of NB-3352 or NC-3352 for full penetration welds, or do not meet the NDE requirements for full volumetric nondestructive examination. The NRC has also accepted alternative designs for the welds of the head or flat end plate to the cylindrical portion of the confinement vessel. However, the NRC has required the alternative designs to include redundant welds to provide redundant sealing of the confinement systems."

Section 7.0, "Confinement Evaluation," paragraph III.3, "Redundant Sealing:"

"The cask design must provide redundant sealing of the confinement boundary. (10 CFR 72.236(e))."

Section 7.0, paragraph V.2, "Confinement Monitoring Capabilities:"

"For redundant seal welded closures, ensure that the applicant has provided adequate justification that the seal welds have been sufficiently tested and inspected to ensure that the weld will behave similarly to the adjacent parent material of the cask. Any inert gas should not leak or diffuse through the weld and cask material in excess of the design leak rate."

Section 8.0, "Operating Procedures," paragraph V.1, "Welding and Sealing:"

"For seal-welded confinement cask closures, and to ensure ALARA, verify that the SAR specifies the use of a remotely operated welder to make seal welds of the confinement closures. Also verify that the procedures provide for acceptable non-destructive examination of these welds. In addition to leak testing discussed above, the NRC accepts dye penetrant tests on both the root and cover pass of the seal welds on the confinement cask closures (including inner closure; any closure over vent accesses for draining, evacuating, purging, and backfilling the cask interior; and the outer closure).

Verify that the SAR includes acceptable provisions for correction of weld defects and any additional drying and purging that may be necessary. Weld tests should be specified, and be in compliance with descriptions for those tests in the American Society of Mechanical Engineers (ASME) Boiler and Pressure Vessel Code (B&PV)."

Section 9.0, "Acceptance Tests and Maintenance Program," paragraph IV, "Acceptance Criteria:"

"In general, the acceptance tests and maintenance programs outlined in the SAR should cite appropriate authoritative codes and standards. The staff has previously accepted the following as the regulatory basis for the design, fabrication, inspection, and testing of DCSS components: . . ."

SYSTEM/COMPONENT	*ACCEPTABLE REGULATORY BASIS**
Confinement System	*American Society of Mechanical Engineers (ASME), "Boiler and Pressure Vessel (B&PV) Code," Section III, Subsection NB or NC.* *"American National Standard for Radioactive Materials— Leakage Tests on Packages for Shipment" (ANSI N14.5-1987).*
---	---
* *The SAR should clearly identify any exceptions to the listed codes and standards.*	

Section 9.0, paragraph V.1.a, "Visual and Nondestructive Inspections:"

"Confinement boundary welds and welds for components associated with redundant sealing, must meet the requirements of ASME Code, Section III, Article NB/NC-5200, "Required Examination of Welds." This section generally requires RT for volumetric examination and either PT or MT for surface examination. The ASME-approved specifications for RT, PT, and MT are detailed in ASME Code, Section V, Articles 2, 6, and 7, respectively.

For confinement welds that cannot be volumetrically examined using RT, the licensee may use 100-percent UT. The ASME-approved UT specifications are detailed in ASME Code, Section V, Article 5. Acceptance criteria should be defined in accordance with NB/NC-5330, "Ultrasonic Acceptance Standards." Cracks, lack of fusion, or incomplete penetration are unacceptable, regardless of length.

The NRC has accepted multiple surface examinations of welds, combined with helium leak tests for inspecting the final redundant seal welded closures."

Section 9.0, paragraph V.1.b, "Structural/Pressure Tests:"

"The confinement boundary (including that of the redundant seal) should be hydrostatically tested to 125 percent of the design pressure, in accordance with ASME Code, Section III, Article NB-6000. (Article NCA-2142.1, defines the design pressure as it applies to Level A Service Limits. As such, in determining the design pressure, the licensee should consider fission gas release from 1 percent of the fuel rods.) The test pressure should be maintained for a minimum of 10 minutes, after which a visual inspection should be performed to detect any leakage. All accessible welds should be inspected using PT. Any evidence of cracking or permanent deformation should constitute cause for rejection. SAR Section 9 should clearly specify the hydrostatic test pressure."

Section 9.0, paragraph V.1.c, "Leak Tests:"

> *"The licensee should perform leak tests on all boundaries relevant to confinement. These include the primary confinement boundary, the boundary of the redundant seal, and (if applicable) any additional boundaries used in the pressure monitoring system. For all-welded cask confinements, the NRC staff has, with adequate justification, considered it acceptable for licensees to omit leak testing of the second cask closure weld and the seal welds for the closure plates of the purge and vent valves. For such cases, leak testing must show that the inner closure weld meets the leakage limits."*

In addition to these requirements, NRC has issued ISG-4 regarding cask closure weld inspections. This guidance states that the "closure weld for the outer cover plate for austenitic stainless steel designs may be inspected using either volumetric or multiple pass dye penetrant techniques", subject to certain conditions.

As demonstrated in this section, the FuelSolutions™ canister closure weld design, NDE, and leak testing requirements are in complete compliance with NUREG-1536 and ISG-4. Any exceptions to the ASME Code requirements that are taken are consistent with NUREG-1536 and ISG-4.

2.5.2.3 Background

The FuelSolutions™ canister closure weld design, NDE, and leak testing requirements are based on operating experience gained since the late 1980s and the resulting steady evolution in canister weld geometry and welding process improvements. An Electric Power Research Institute (EPRI) report, NP-6941,[21] documents closure welding issues observed and solutions implemented during the Carolina Power & Light (CP&L)/DOE Cooperative Dry Storage Demonstration Project in the late 1980s. The purpose of this project was to performance test the handling/loading practices and heat transfer and shielding characteristics of the NUHOMS®-07P[22] SNF dry storage system. The system used an IF-300 transportation cask to transfer loaded Dry Shielded Canisters (DSCs) from the plant's fuel building to Horizontal Storage Modules (HSMs) within an ISFSI at the H. B. Robinson Nuclear Power Plant.

Figure 2.5-1 presents the general configuration of the original NUHOMS® DSC closure details. This original DSC design has an overall length to accommodate PWR fuel and a relatively thin cylindrical shell with thick lead shield plugs at its ends. The closure plate and canister shell are made from stainless steel, as are the top shield plug plates that encase a lead core. The absence of shielding along the cylindrical shell requires the canister to be placed inside a transfer or transportation cask during all fuel loading and handling outside the spent fuel pool.

Consequently, with the canister inside a cask, the location that can best accommodate a closure plate-to-shell weld and still permit the placement of the top shield plug following SNF assembly

[21] NP-6941, *NUHOMS® Modular Spent-Fuel Storage System: Performance Testing*, Electric Power Research Institute, September 1990.

[22] NUH-001, *Topical Report for the NUTECH Horizontal Modular Storage System for Irradiated Nuclear Fuel*, NUTECH Engineers, Inc., Revision 2A.

loading is a corner joint in-board of the canister shell flush with the end of the canister. This location poses inherent difficulties in using weld details that can be volumetrically examined reliably. Repositioning of the closure weld along the canister shell side-wall would result in substantially higher radiation exposure to the operators of this system and is not considered to be a desirable alternative. Thus, the original canister weld closure design incorporates the following features and requirements dating back to 1986[23] to meet the intent of an ASME Code, Class 1 pressure vessel:

- Volumetric examination of all full penetration canister shell seam welds.
- A "double closure" to assure confinement through the ends of the canister by requiring the welding of both the top shield plug and closure plates to the canister shell.
- Multi-level liquid penetrant (PT) examinations. These examinations include the final surface of the top shield plug-to-canister shell weld and the root pass and final surface of the closure plate-to-canister shell weld.
- Helium leak testing of the top shield plug-to-canister shell weld.
- No penetrations in the canister's outer confinement boundary that could lead to a leak path.

Until recently, this approach was judged to provide a "closure system" with safety margins equivalent to a single full penetration, volumetrically examined weld as discussed NUREG-1536 for SNF storage systems and the NRC safety evaluation report (SER)[24] for the NUHOMS® system. The NRC NUHOMS® system SER states the following:

> "*The double seal welds at the top and bottom of the DSC do not comply with all the requirements for the ASME B&PV Code, Section III, Subsection NB. The inspection procedures outlined in the SAR do not comply with the Code; however, the NRC staff has determined that an exception to Code requirements for volumetric weld inspection is permissible due to the following:*
>
> 1. *The closure to the confinement boundary is a double-weld design, i.e., two weld joints provide confinement.*
> 2. *The gauge pressure (for normal operation) inside the DSC is on the order of 1 psig. Therefore, pressure stresses are very low.*
> 3. *The test method of ensuring a gas tight seal for the inner top seal weld is helium leak detection which is very sensitive. Also dye penetrant testing will be performed at two levels including the weld root pass and cover pass on the outer seal weld to ensure no weld surface imperfections. The test method of ensuring a gas tight seal for the bottom welds consists of a helium leak test by the fabricator for the inner seal weld in accordance with ASTM E499, in addition to two levels*

[23] *Safety Analysis Report for NUTECH Horizontal Modular System for Irradiated Fuel Topical Report*, U.S. Nuclear Regulatory Commission, March 28, 1986.

[24] *Safety Evaluation Report of VECTRA Technologies, Inc. (a.k.a. Pacific Nuclear Fuel Services, Inc.) Safety Analysis Report for the standardized NUHOMS® Horizontal Modular Storage System for Irradiated Nuclear Fuel*, U.S. Nuclear Regulatory Commission, December 1994.

of dye penetrant testing for this weld. For the outer seal weld, a multi-level dye penetrant test is specified."

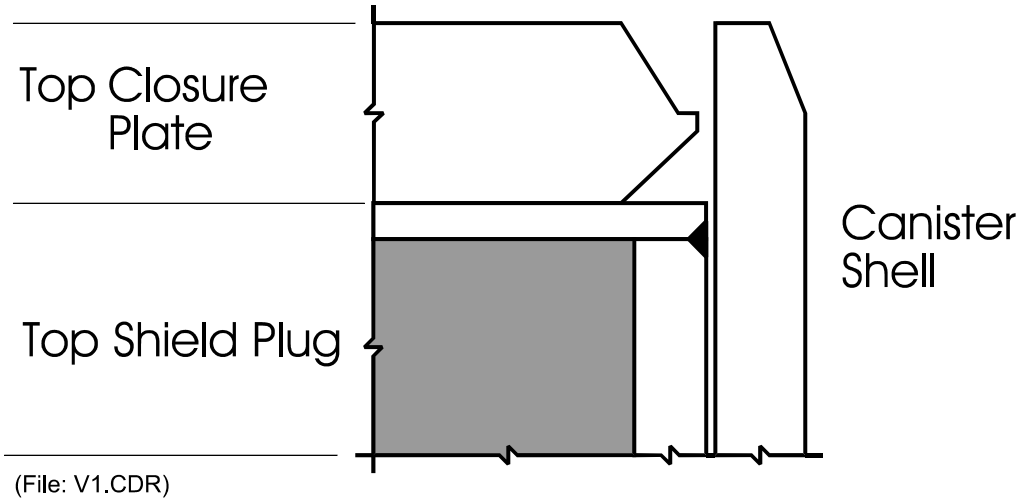

Figure 2.5-1 - Original Closure Configuration

(prior to closure welding)

After SNF assembly loading, placement of the top shield plug, and transfer of the canister within the cask from the spent fuel pool to the decontamination area, the shield plug-to-canister shell weld is placed (see Figure 2.5-2). The final surface of this weld is inspected using the PT examination technique and ASME Code, Class 1 pressure vessel original construction acceptance criteria. The DSC is then drained of water, vacuum dried, and inerted with helium gas. The shield plug-to-shell weld is then helium leak rate tested using techniques in accordance with American Society for Testing and Materials (ASTM) Standard E 499.[25] The closure plate is then installed and the root pass of the closure plate-to-canister shell weld is placed. Before the balance of this weld is completed, the root pass is inspected using the PT examination technique and ASME Code acceptance criteria. This same examination technique and acceptance criteria is then used to inspect the final surface of this weld.

[25] ASTM E 499, *Standard Test Methods for Leaks Using the Mass Spectrometer Leak Detector in the Detector Probe Mode*, American Society of Testing and Materials.

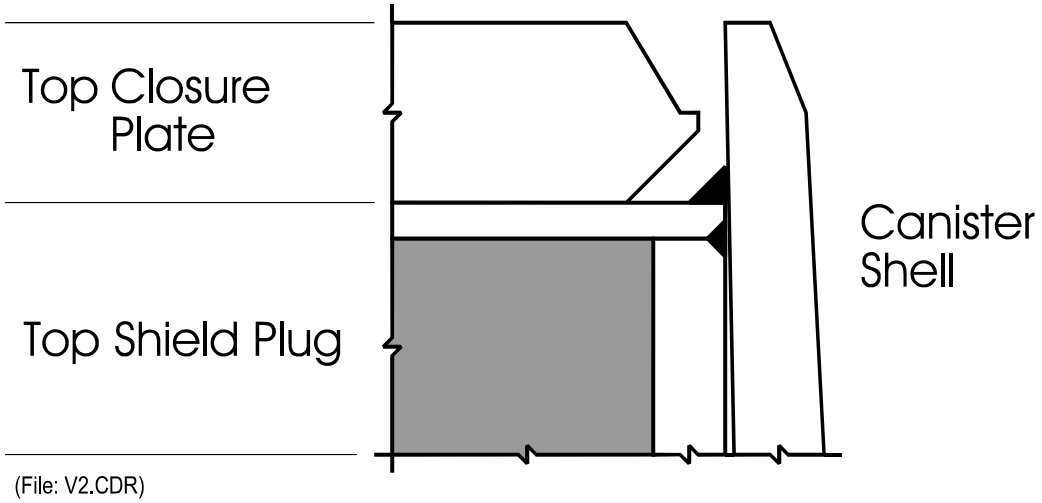

Figure 2.5-2 - Original Shield Plug-to-Canister Shell Weld Configuration

The canister closure weld described above was first implemented on a prototypical canister weld mock-up at the H. B. Robinson Nuclear Power Plant. EPRI Report No. NP-6941 provides the following discussion of welding issues observed during the CP&L/DOE demonstration project:

"Weld Mockups and Weld Improvement Program

Another license requirement was the performance of a weld mockup test on a "dummy" canister as well as the removal of the cover plate and lead plug to demonstrate the ability to retrieve fuel assemblies. The original design called for the lead plug to be fillet welded to the DSC and for a full penetration weld to be performed in welding the top cover plate to the DSC shell (see Figure 2.5-1). *Welding of the dummy canister began by welding the lead plug to the DSC shell. Although the welding process was successful, the DSC shell was drawn in during the welding, resulting in a tight fit for the cover plate to seat itself past the drawn-in portion of the DSC. Once past that point, the drawn-in shell* (actually the top cover weld preparation modified to clear the drawn-in shell inside diameter corner) *resulted in a larger-than-anticipated gap on the land area where the top cover plate would be welded to the DSC* (see Figure 2.5-2). *The welding procedure called for first tacking the cover plate in place before beginning the full penetration weld. The first tack was manually welded. When the second tack was made, the weld cracked. Two additional manual welds were attempted and both of them cracked as well. An automatic welder was brought in to try to control the heat during the tacking process, but these welds also cracked. At that point, the test was discontinued and the weld design and parameters were re-evaluated.*

Root causes of the cracked weld were thought to be:

1. *Too much shrinkage occurred during the welding of the lead plug; the top of the DSC had drawn in during welding. Consequently, when the top cover plate was being welded, the weakest place was the weld itself. When residual stresses in the weld needed relief, the tack weld was the location at which the stress was relieved.*
2. *The heat input was too high, resulting in excessive shrinkage.*
3. *The gap between the top cover plate and the DSC shell was too great.*

To resolve these concerns, a welding development program was begun that instituted welding of six additional mockup DSCs. Principal improvements made during this program were as follows:

1. *A change was made from a fillet weld to a bevel weld, which required chamfering of the lead plug, but resulted in much less weld metal being added to the DSC; thus, less shrinkage occurred* (see Figure 2.5-3).
2. *Using a high ferrite content weld metal, again resulted in less shrinkage.*
3. *Sequencing the welding pattern allowed more control over the heat input into the weld.*
4. *Reducing the gap between the cover plate and DSC shell resulted in reducing the amount of weld metal."*

The changing of the shield plug-to-shell weld from a fillet to a partial penetration detail permitted a reduction in the weld volume (i.e., shrinkage) a minimum of 30% (fillet vs. partial penetration weld throat widths), while maintaining the same weld strength.

The lessons learned during the CP&L/DOE demonstration project were incorporated into the NUHOMS®-24P[26] DSC design for the Oconee Nuclear Station, while maintaining the same inspection and testing requirements. This design continued to evolve with the incorporation of a chamfer at the inside diameter top corner of the shell (see Figure 2.5-4). This chamfer eliminated the need for any field reworking of the closure plate weld preparation to clear any draw-in of the canister shell caused by the top shield plug-to-canister shell weld.

[26] NUH-002, *Topical Report Amendment 2 for the NUTECH Horizontal Modular Storage System for Irradiated Nuclear Fuel - NUHOMS®-24P*, NUTECH Engineers, Inc., Revision 2A.

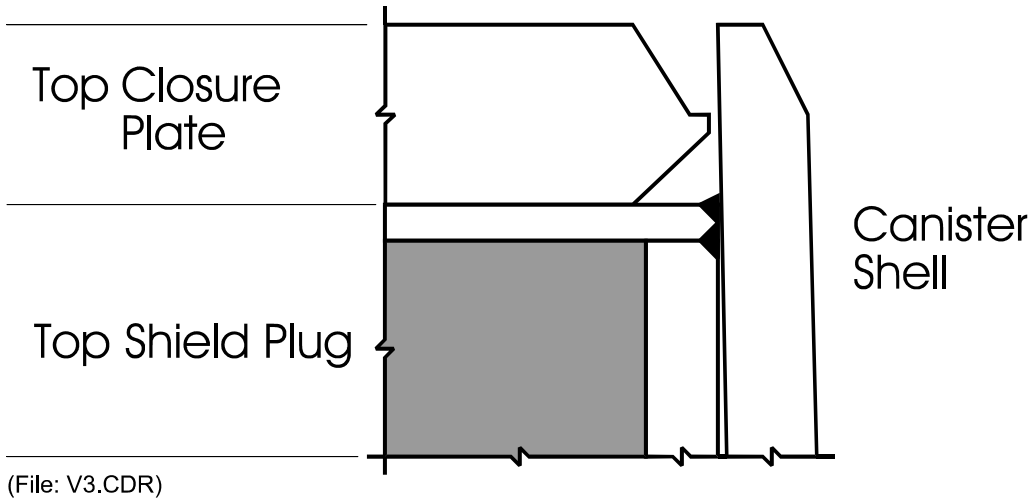

Figure 2.5-3 - Modified Canister Closure and Weld Configuration

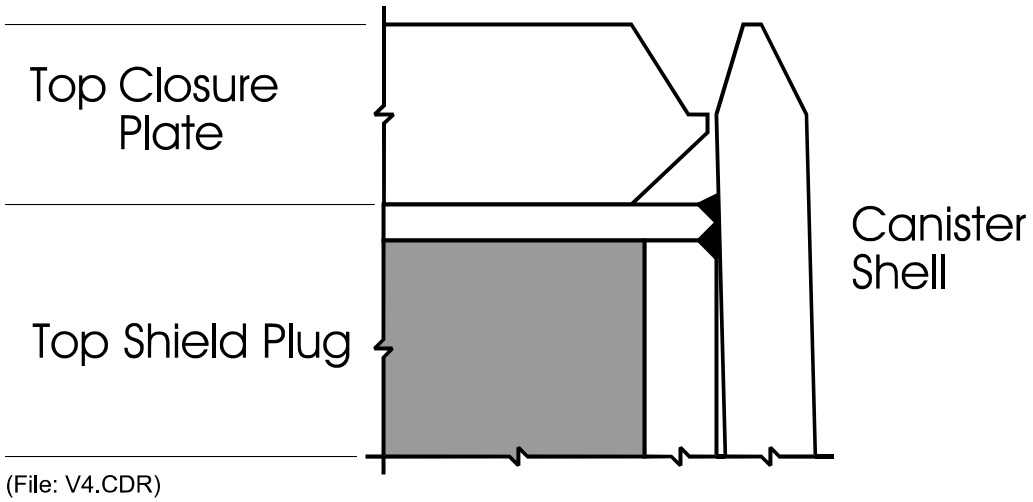

Figure 2.5-4 - Modified Canister Shell Chamfer

However, as the outside diameter of the top shield plugs were locally reduced to provide the required shield plug-to-canister shell gap during shop fabrication activities, the partial penetration weld joining the top and cylinder plates of the shield plug was also reduced (see Figure 2.5-5). In a few instances, this reduction in weld root size was large enough that trace amounts of the lead contained inside the shield plug appear to have remelted and caused

"wicking" of the lead into the shield plug-to-canister shell weld during canister closure welding operations. This lead contamination resulted in weld cracks that were discovered during PT examinations or helium leak rate testing and subsequently repaired. To prevent recurrence of this problem, the shield plug top plate-to-cylinder plate weld was relocated, as shown in Figure 2.5-6, for subsequent canisters successfully loaded at the Oconee and Calvert Cliffs plants over the past three to four years.

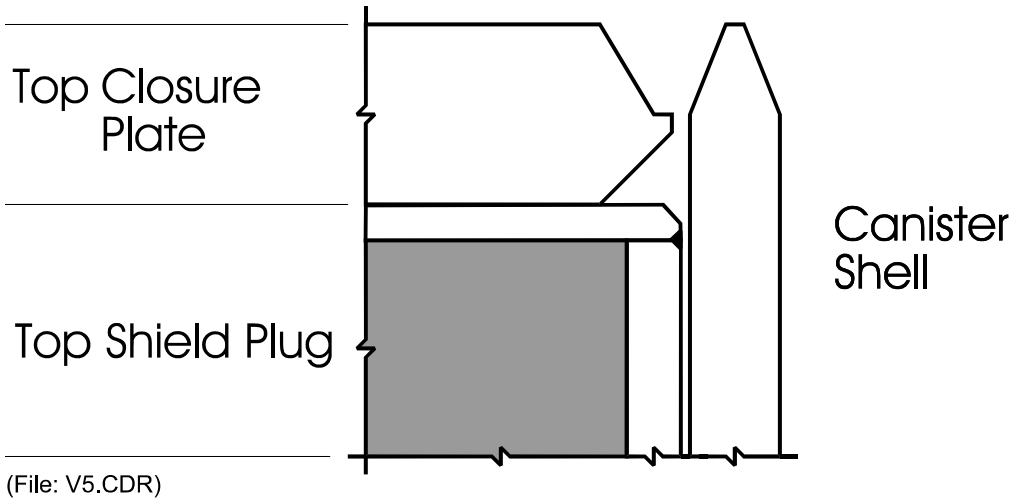

Figure 2.5-5 - Localized Reduction of Top Shield Plug Outside Diameter

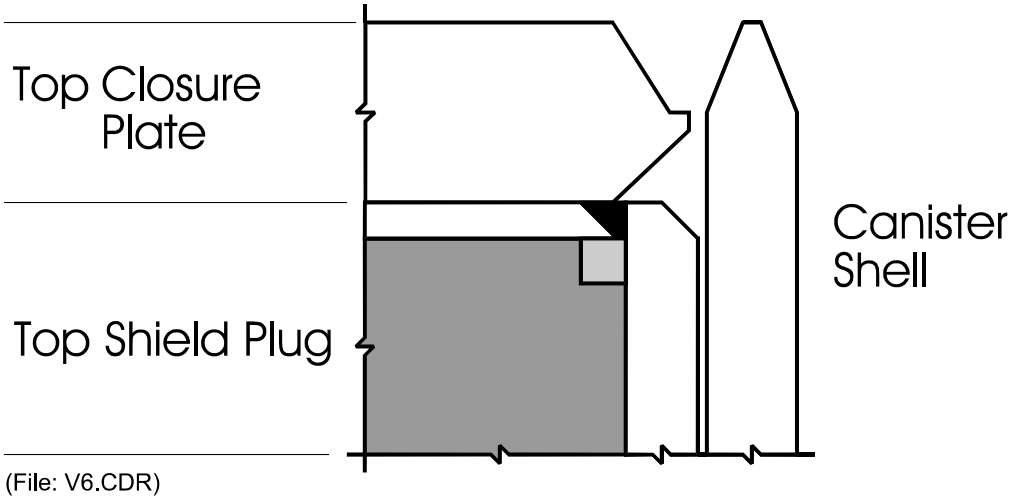

Figure 2.5-6 - Modified Top Shield Plug Design

Figure 2.5-7 presents the final enhancement in the current NUHOMS® DSC closure design,[27] while maintaining the same inspection and testing requirements as the original design. This design simplifies the fabrication process for the DSC closure by introducing an inner closure plate that is separate from the shield plug. This design permits the introduction of a shield plug-to-canister shell gap that is controlled by shielding and operating considerations and is independent of any weld gap requirements. Consequently, the new inner closure plate is fabricated to provide an optimum inner closure plate-to-canister shell weld gap that reduces welding shrinkage stresses and any draw-in of the canister shell (see Figure 2.5-8). This design was used to successfully load canisters at the Davis-Besse plant in late 1995/early 1996 and more recently at the Oconee Nuclear Station.

The closure design for these canisters has undergone a substantial evolution based on lessons learned and continuous improvement, with the goal of achieving optimum weld joint integrity and reliability. Unlike the VSC-24 design, no difficulties have been encountered in the placement or inspection of the current generation of canister closures. Consideration of any alternative or revised weld closure designs that have not undergone such an evolution, although they may be more amenable to volumetric examination, would not have the benefit of this operating experience and may be prone to unforeseen problems.

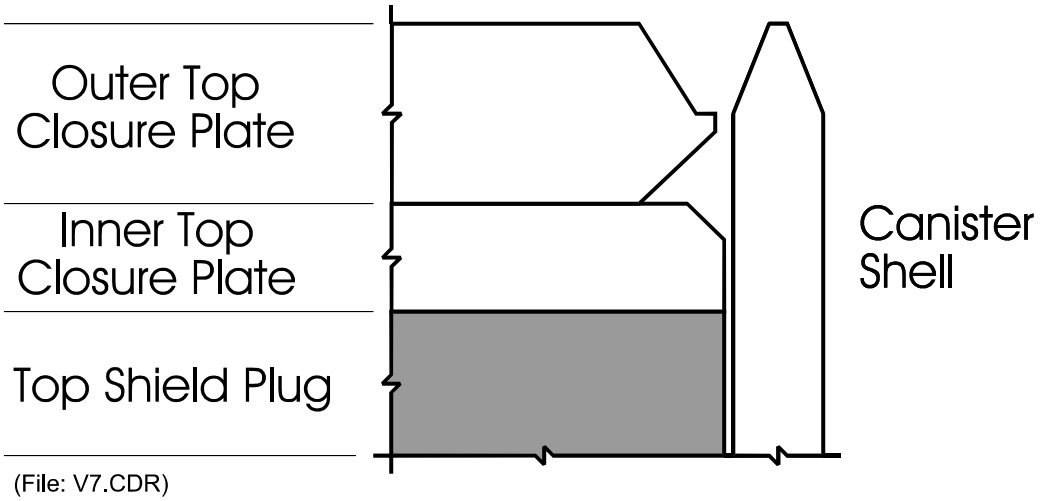

Figure 2.5-7 - Enhanced Canister Closure Design Configuration

[27] NUH-003, *Safety Analysis Report for the Standardized NUHOMS® Horizontal Modular Storage System for Irradiated Nuclear Fuel*, VECTRA Technologies, Inc.

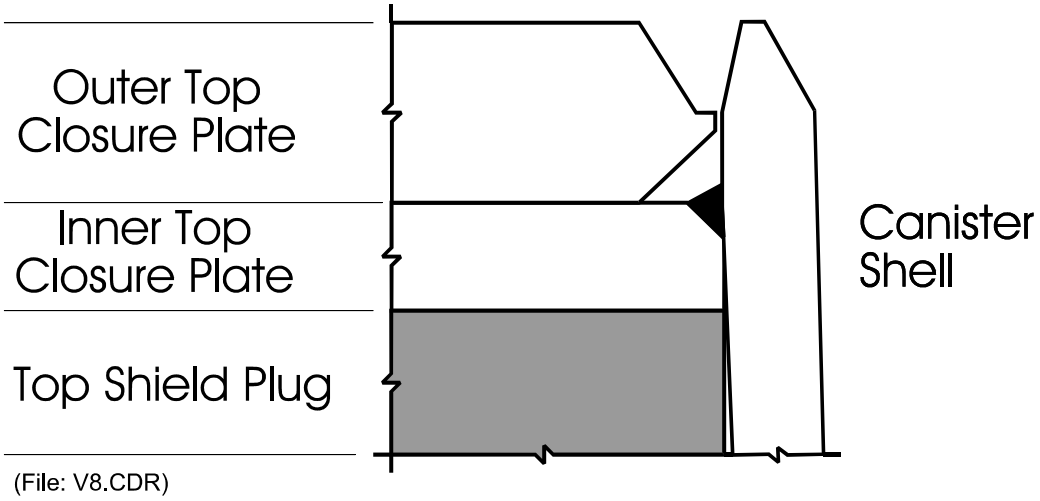

Figure 2.5-8 - Reduction of Shell "Draw-in"

2.5.2.4 FuelSolutions™ Closure Design Description

The closure design for the FuelSolutions™ canister builds on the experience gained on similar canister closure designs. As shown in Figure 2.5-9, the closure design for the FuelSolutions™ canister described in Section 1.2.1.3 of this FSAR is very similar to that shown in Figure 2.5-7. In addition, enhancements to the weld examination and leak testing requirements for this closure design have been incorporated, as discussed in Section 2.5.2.6.

The following design features have been incorporated into the FuelSolutions™ canister closure details based on the lessons learned and discussed above:

1. The shield plug is separate from the inner closure plate. This permits the fabrication of the shield plug to provide a gap based on operating and shielding considerations, as opposed to any weld gap requirements. This gap is larger than the inner top closure plate-to-shell weld gap, optimizing placement of the shield plug in the spent fuel pool after SNF assembly loading and assuring that the shield plug provides no inner top closure plate-to-shell welding shrinkage constraint.
2. Because the inner closure plate and shield plug are separate pieces, the fabrication of the inner closure plate provides an inner closure plate-to-shell weld gap that is optimized to provide the design partial penetration root depth and avoid welding shrinkage restraint, while minimizing the potential weld shrinkage volume.

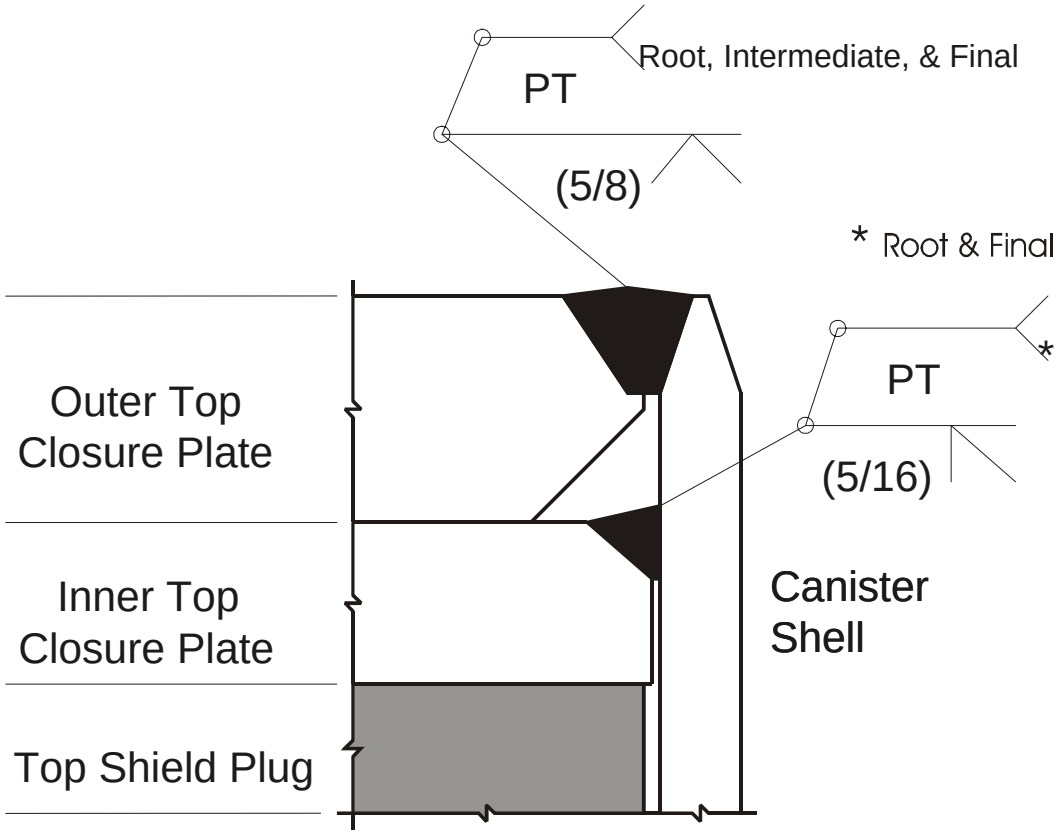

(File: V10r1.CDR)

Figure 2.5-9 - FuelSolutions™ Canister Closure Design

3. The canister shell inside diameter top corner is chamfered to assure that the outer closure plate weld preparation will not need to be modified during canister SNF assembly loading operations. This assures that excessive outer closure plate-to-canister shell gaps are not created to provide clearance past any shell draw-in caused by shrinkage in the inner closure plate-to-canister shell weld. By preventing these excessive gaps, tack and root pass welds will not crack due to excessive weld shrinkage. In addition, it facilitates welding torch access and orientation, and remote camera viewing by the AW/OS.

In addition to these top closure configuration details, all plate materials used in the fabrication of the FuelSolutions™ canister shell and inner and outer top and bottom closure plates are austenitic stainless steel, procured in accordance with the vessel requirements of ASME Code, Section III, Subsection NB. Paragraph NB-2530 requires the ultrasonic examination of 100% of at least one major surface of all plates for vessels using the straight beam technique. This inherent requirement of Subsection NB assures that there are no significant subsurface defects in the inner and outer top closure plates and the canister shell that could lead to weld and base metal defects or base material delaminations in a material that is inherently free of these types of defects.

In addition to the closure configuration details designed to minimize welding shrinkage stresses, all filler materials used in field closure welding of the FuelSolutions™ canisters shall be stainless steel with a minimum ferrite content of 10 FN. As noted in the EPRI NP-6941 report, the use of "high" ferrite content weld metal results in less welding shrinkage and, therefore, shrinkage stress.

The long-term integrity of stainless steel materials in the design of a canister used for the dry storage of SNF assemblies is addressed in EPRI TR-102462.[28] This document addresses the following "specific aging phenomena:"

- Radiation effects,
- Thermal aging,
- Elevated temperature creep, and
- Low cycle fatigue.

EPRI TR-102462 concludes that there is little to no risk from the items listed above to the long-term integrity of SNF assembly dry-storage canisters fabricated from austenitic stainless steel.

The FuelSolutions™ canister design requires the following:

- PT examination of the root pass and final surface of the inner closure plate-to-shell weld and inner closure plate to vent and drain port welds.
- PT examination of the root, intermediate, and final surface of the outer closure plate weld.
- Helium leak rate testing of these completed inner closure plate welds at an ASME Code pneumatic pressure test internal pressure using ASTM E 499 techniques.

Multi-level PT has historically been an acceptable substitute for volumetric examinations in difficult weld/component configurations and/or conditions and was successfully used to identify defects during the CP&L/DOE demonstration project and at Oconee and Calvert Cliffs. In addition, a helium leak rate test at a hydrostatic test pressure greatly exceeds the requirements of an ASME Code, Article NB-6000, pressure test based on the relative molecular size of the leakage medium. A similar combination of techniques and requirements satisfactorily verified that there were no significant defects in the top closure welds implemented during the loading of stainless steel canisters at the Robinson, Oconee, Calvert Cliffs, and Davis-Besse plants. The same methods can assure the long-term integrity of the FuelSolutions™ canisters in the future.

2.5.2.5 Comparison of FuelSolutions™ versus VSC-24 Canister Design Features

The FuelSolutions™ and VSC-24 canister closure design details differ in the following significant ways:

1. As shown in Figure 2.5-10, the VSC-24 permits a large gap between the top shield plug and the canister shell for ease in operations. This gap is so large that the insertion of shim plates

[28] TR-102462, *Shipment of Spent Fuel in Storage Canisters*, Electric Power Research Institute, June 1993.

is required prior to welding. These shims not only provide high welding shrinkage constraint, but significantly increase the weld volume. These two factors combine to set up a test of strengths between the top shield plug-to-canister shell weld and the canister shell through-wall tearing resistance potentially leading to defects in either or both materials.

This welding shrinkage constraint and magnitude of weld shrinkage volume do not exist in the FuelSolutions™ canister closure design. As discussed in Section 2.5.2.4, the separation of the shield plug and inner closure plate permits optimization of the gaps between these components and the canister shell to minimize/prevent any welding shrinkage constraint and minimize weld shrinkage volume. In addition, the FuelSolutions™ canister uses a 5/8-inch canister shell thickness as opposed to a 1-inch shell thickness used by the VSC-24 design. This difference in shell thicknesses/stiffnesses provides additional welding shrinkage stress in the VSC-24 design not present in the FuelSolutions™ canister. Further, the ductile stainless steel material used for the FuelSolutions™ canister containment boundary is not susceptible to the laminar tearing or hydrogen-induced cracking experienced in the carbon steel VSC-24 canister.

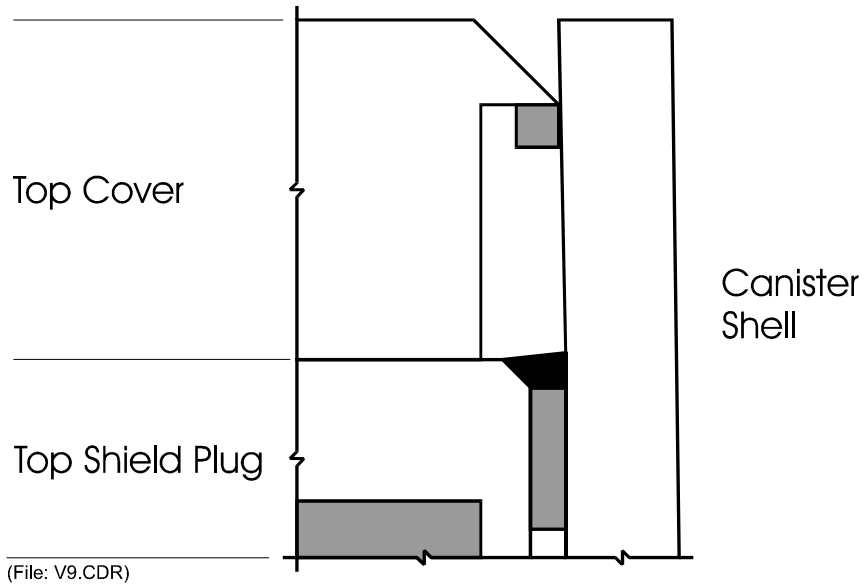

Figure 2.5-10 - VSC-24 Top Closure Configuration[29]

2. As discussed in the VSC SAR,[29] the VSC-24 canister shell is made from SA-516,[30] Grade 70 carbon steel and is constructed in accordance with ASME Code, Section III,

[29] PSN-91-001, *Safety Analysis Report for the Ventilated Storage Cask System*, Pacific Sierra Nuclear Associates and Sierra Nuclear Corporation.

[30] ASME/ASTM SA-516/SA-516M, *Specification for Pressure Vessel Plates, Carbon Steel, for Moderate- and Lower-Temperature Service*.

Subsection NC.[31] Unlike Subsection NB, Paragraph NC-2530 only requires that the plate be examined in accordance with its material specification. In the case of SA-516 materials, ultrasonic examination is a "supplementary requirement" that must be specified in a purchase order for this material. This examination requirement was not specified for the VSC-24 shell materials that exhibited the defects noted in the NRC inspection report 72-1007/97-212.

The FuelSolutions™ canister top closure design greatly eliminates any concern about potential canister shell delaminations. Stainless steel plate materials are inherently more ductile than carbon steel materials because they have been shown historically to be much less susceptible to subsurface delaminations and other defects than carbon steel materials. Consequently, stainless steel plate materials are more resistant ("tougher") to the propagation of defects than in carbon steel plate materials. In addition, stainless steel is predicted to have better long-term integrity than carbon steel due to the potential lowering of fracture toughness caused by thermally induced strain aging and general corrosion in carbon and low-alloy steels over the design life of a canister.

In addition to these welding detail and material differences, the PT examination of carbon versus stainless steel canisters has resulted in very different observed defects. The PT examinations noted in NRC inspection report 72-1007/97-212 revealed indications that sometimes grew significantly in length and depth as they were excavated for repair in their carbon steel materials. This was not the experience for the defects observed during the CP&L/DOE demonstration project or at Oconee or Calvert Cliffs. In these cases, the defects were highly localized, as evidenced by relatively small repair excavations in the stainless steel materials employed in these projects.

2.5.2.6 Additional NDE and Testing Requirements

As the result of recurring defects in the VSC-24 canister top closure welds, additional NDE and leak testing requirements have been proposed by the NRC for the closure welds of the TranStor™ canisters. These proposed additional NDE and leak testing requirements include the following:

1. PT examination of successive deposited weld layers, each having a maximum thickness of 1/8-inch,[32] and/or
2. Ultrasonic (UT) examination of the outer top closure weld volume and weld-to-cover fusion zone using an angle beam technique and the weld-to-shell fusion zone using a straight beam technique.[33]

[31] American Society of Mechanical Engineers (ASME) Boiler and Pressure Vessel Code, Section III, Division 1, Subsection NC, *Class 2 Components*, 1986 Edition with 1988 Addenda.

[32] Letter from the U.S. Nuclear Regulatory Commission to Sierra Nuclear, ACN 9705010064, Docket 7109268, Item 1-3, May 24, 1997.

[33] Letter from the U.S. Nuclear Regulatory Commission to Sierra Nuclear, ACN 9705010064, Docket 7109268, Item 7-1, May 24, 1997.

These proposed new NDE requirements have not been proven necessary for the closure design employed by the FuelSolutions™ canister discussed in Sections 2.5.2.3 and 2.5.2.4, especially in light of ALARA impacts associated with these requirements.

The PT examination specified for the FuelSolutions™ inner closure plate-to-canister shell root pass and final surface and combined pneumatic pressure/helium leak rate testing of the weld assures that there are no significant defects that could undermine the structural integrity of this weld or any through-wall defects that could undermine the confinement integrity of this weld. The PT examination of the FuelSolutions™ outer closure plate-to-canister shell weld root, intermediate, and final surface assures that there are no significant defects that could undermine the structural integrity of this redundant weld.

UT examination is specified as an alternate inspection method for the FuelSolutions™ canister top end outer closure plate-to-shell weld. Assuming various geometric detail and material transmissibility difficulties associated with UT examination of stainless steel in general and the outer closure weld in particular can be overcome, manual UT methods probably do not add sufficient assurance of structural integrity to offset added examination personnel radiation exposure. Remotely operated UT examination methods could provide added assurance of structural integrity for the outer closure plate weld, while reducing examination personnel radiation exposure compared to manual UT methods. However, the geometry of the outer closure plate-to-canister shell weld still presents the following challenges in obtaining an acceptable UT examination:

1. As shown in Figure 2.5-11, the geometry of any weld with a throat depth less than the thickness of the outer closure plate will introduce indications/reflectors that will be very difficult, if not impossible, to evaluate during UT examinations. The nose of the outer closure plate J-bevel weld prep will make it difficult to detect and interpret angle beam UT indications at the root of the weld and the chamfered outer top corner of the canister shell will do the same relative to the canister shell weld fusion zone.
2. As shown in Figure 2.5-12, adding to the outside top chamfer and J-bevel nose geometry challenges for angle beam UT examination are additional geometric reflectors associated with a permissible 1/8-inch maximum offset of the outer closure plate with the canister shell.
3. As shown in Figure 2.5-13, the crown (reinforcement) of the outer closure plate-to-canister shell weld may require its surface to be ground or machined flush to assure coupling between the UT transducer and the closure plate/weld surface during straight beam UT examinations. As shown in Figure 2.5-14, this coupling problem can be eliminated by “flat topping” the weld at an ALARA cost to operating personnel. In addition, the outer closure plate’s chamfered lower corner (surface “a-b”) and the nose of the weld’s J-bevel will still confuse the detection and interpretation aspects of the UT examination process. These latter challenges will only be increased by the introduction of the permissible offset of the outer closure plate with the canister shell, as shown in Figure 2.5-15.
4. As shown in Figure 2.5-16 and Figure 2.5-17, it may be possible to insert angle and straight beam UT transducers between the outer surface of the canister and the inside surface of the cask top flange during “nominal” (1.25-inch gap) conditions (0.75- to 1.75-inch gap range).

However, the canister shell's outside chamfer, in combination with the weld prep J-bevel nose, will make UT detection and interpretation very difficult.

In addition to these geometry detail challenges, the ability to identify and size indications along the canister shell weld fusion zone from the top of the outer closure plate (see Figure 2.5-11 and Figure 2.5-12) or the outer closure plate weld fusion zone from the outside vertical face of the canister shell (see Figure 2.5-16 and Figure 2.5-17) will be difficult due to the inherent difficulty in the UT examination of stainless steel, which will be further complicated by differences in the base and weld metal grain structures. As demonstrated in various studies of the effectiveness of the UT examination technique on IGSCC in stainless steel reactor piping system weldments, it is very difficult to identify and size indications through weld metal.

Therefore, remotely operated UT examination methods might be shown to be able to examine a predetermined ("design") throat depth of the outer top closure weld while ignoring any indications/reflectors below this design depth. This approach has been used in the application of weld overlay repairs on IGSCC-susceptible reactor piping system weldments as part of an ASME Code, Section XI[34] inservice repair, but has not previously been acceptable for an ASME Code, Section III (new) construction.

These issues will need to be addressed in developing a UT weld examination approach and acceptance criteria in order to implement this alternative inspection technique. The acceptance criteria will need to be based upon and compatible with the critical flaw size as determined in Section 3.9.4 of this FSAR.

[34] American Society of Mechanical Engineers (ASME) Boiler and Pressure Vessel Code, Section XI, *Rules for Inservice Inspection of Nuclear Power Plant Components*, 1995 Edition.

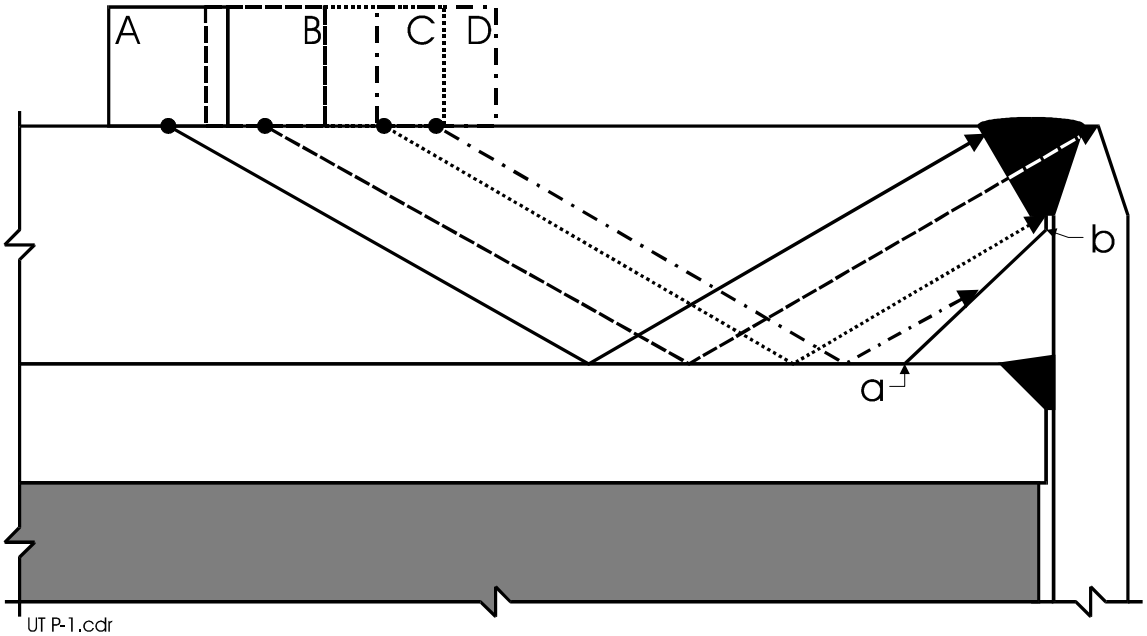

Figure 2.5-11 - Outside Shell Chamfer and J-Bevel Weld Prep Nose Challenges to Angle Beam UT Examination

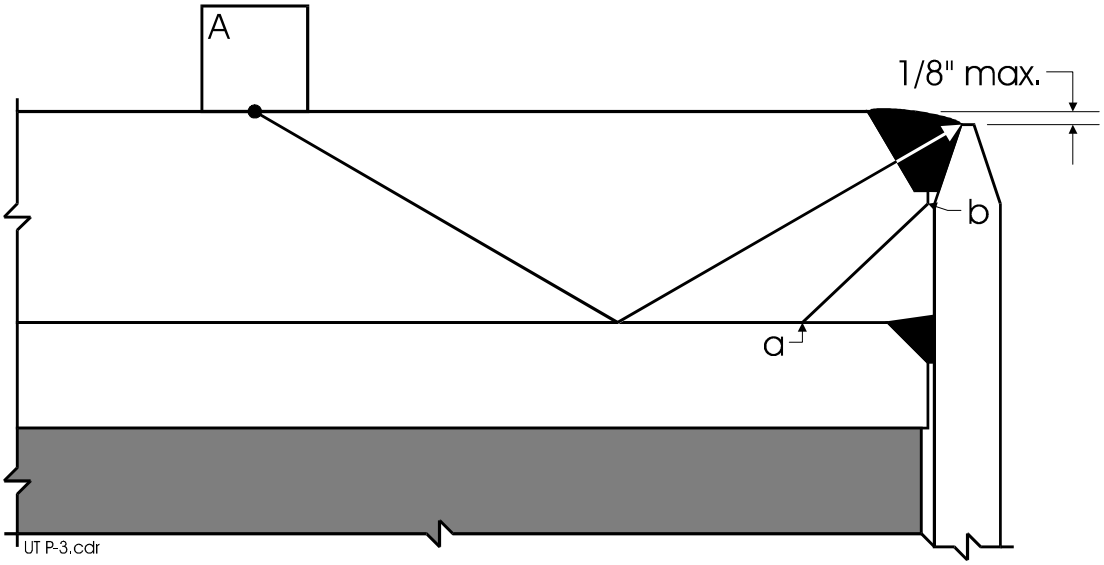

Figure 2.5-12 - Outer Closure Plate-to-Canister Shell Offset Challenge to Angle Beam UT Examination

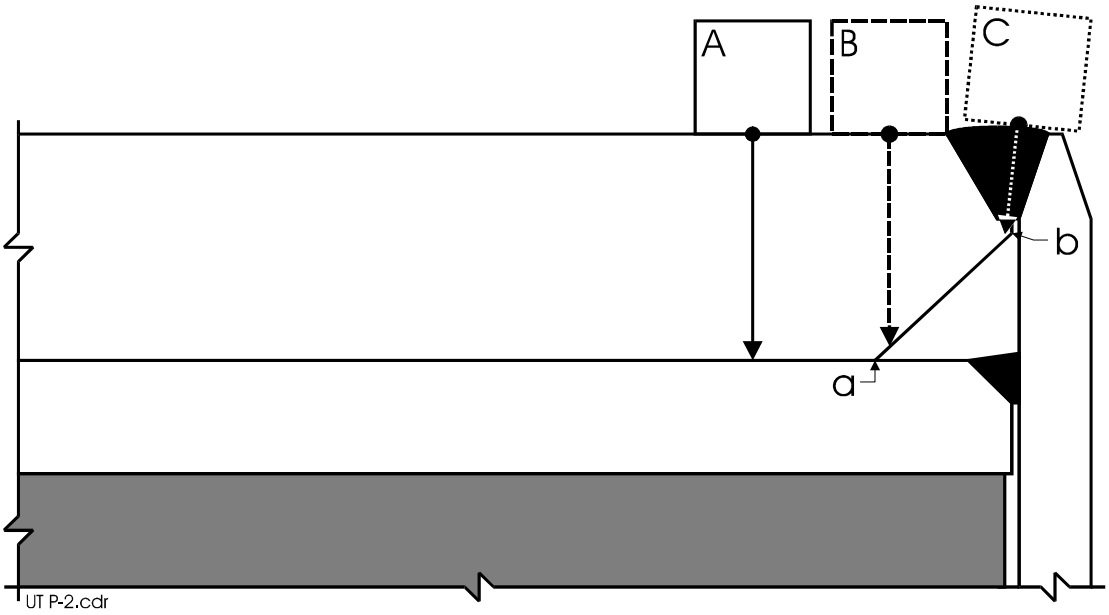

Figure 2.5-13 - Weld Crown (Reinforcement) Challenge to Straight Beam UT Examination

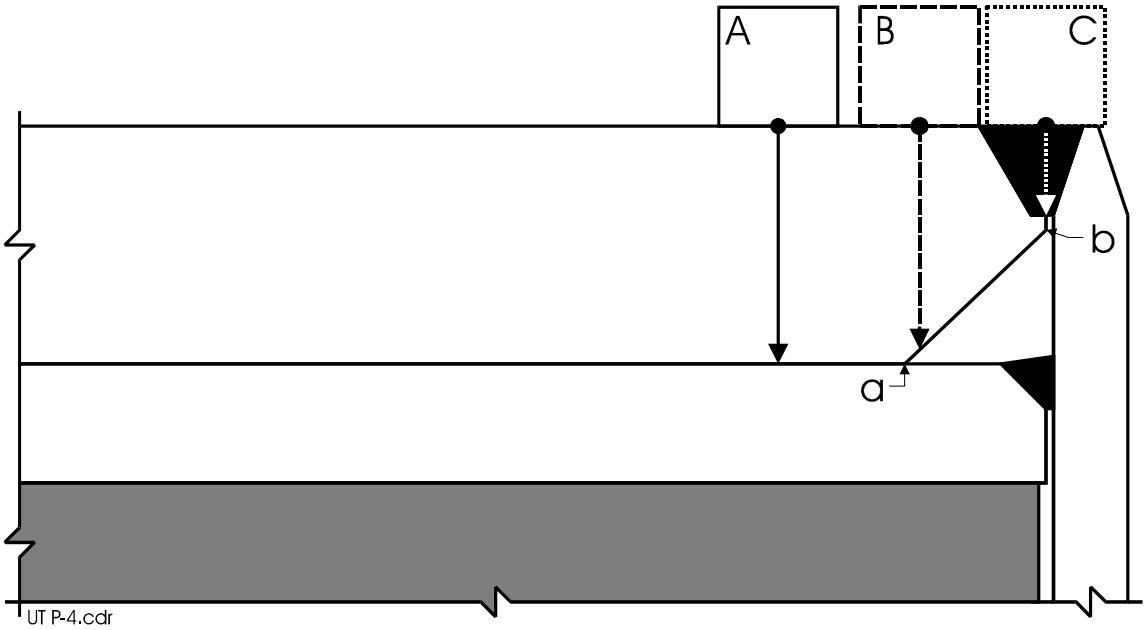

Figure 2.5-14 - Outer Closure Plate Lower Chamfer and J-Bevel Weld Prep Nose Challenges to Straight Beam UT Examination

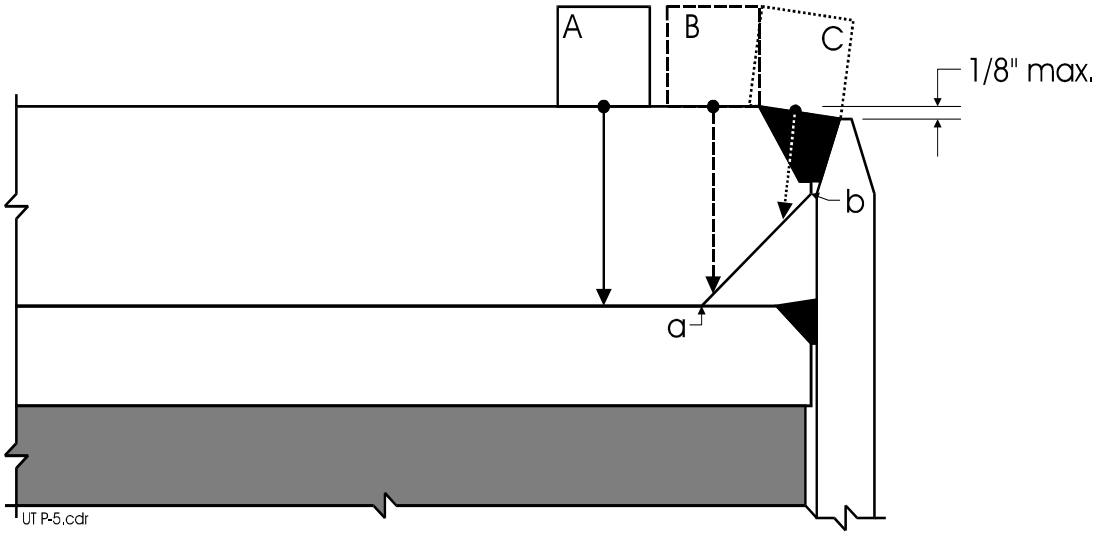

Figure 2.5-15 - Outer Closure Plate-to-Canister Shell Offset Challenge to Straight Beam UT Examination

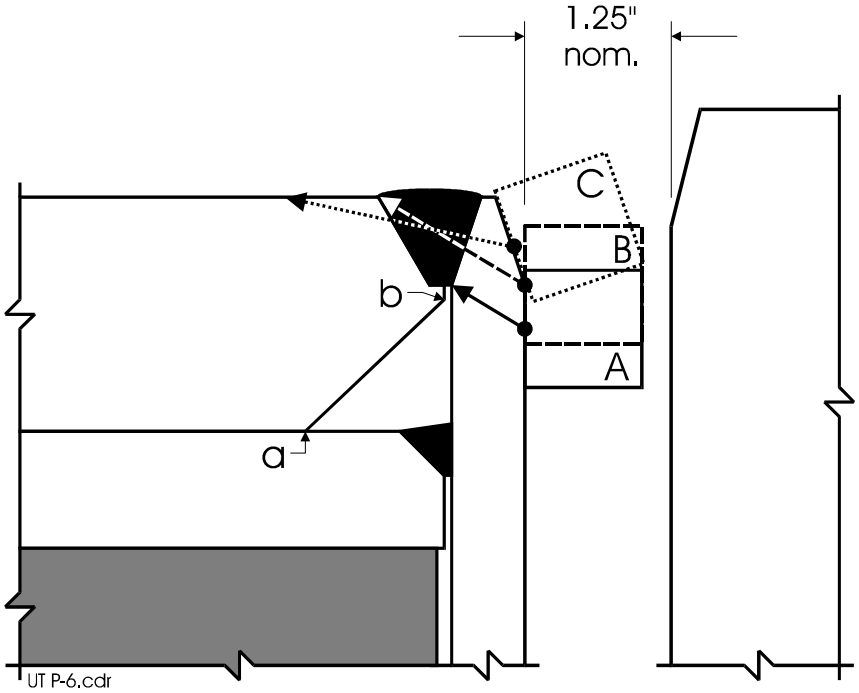

Figure 2.5-16 - Canister Shell Chamfer and J-Bevel Weld Prep Nose Challenges to Angle Beam UT Examination

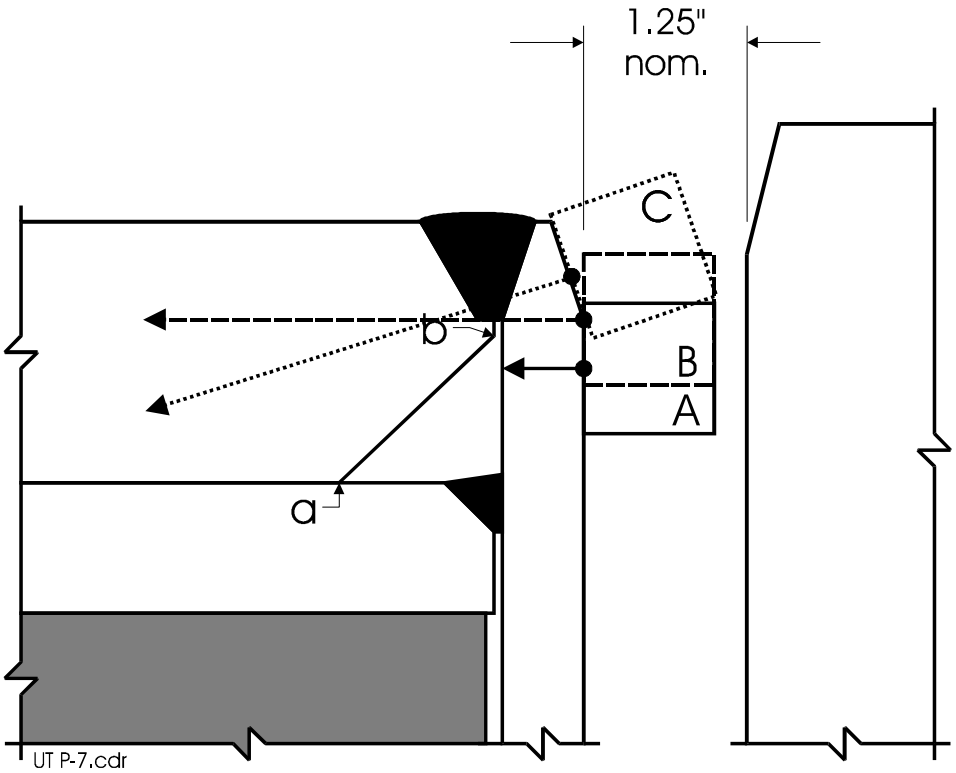

Figure 2.5-17 - Canister Shell Chamfer and J-Bevel Weld Prep Nose Challenges to Straight Beam UT Examination

2.5.2.7 Summary

The FuelSolutions™ canister closure weld design, NDE, and leak testing requirements comply with current licensing requirements in the following ways:

1. The closure detail involves a flat end plate-to-cylindrical shell alternate confinement boundary weld design found acceptable by NUREG-1536, Section 3.0, and the NRC SER, when used as part of a redundant weld sealing system.
2. The redundant confinement boundary weld sealing system also complies with the requirements of 10CFR72.236(e).
3. Helium leak rate testing of the completed inner closure plate weld to assure that this inert gas does not leak or diffuse through the weld or “cask” material in excess of the design leak rate complies with NUREG-1536, Section 7.0, confinement monitoring capabilities criteria.
4. Dye penetrant testing of the root and cover passes of the confinement closure welds meeting the requirements of ASME Code, Subsection NB, complies with NUREG-1536, Section 8.0, welding and sealing criteria.
5. The presentation of the FuelSolutions™ canister closure weld details and NDE requirements provided in this FSAR complies with the acceptance criteria reporting criteria of NUREG-1536, Section 9.0.

6. The use of multiple surface examinations of closure welds in combination with helium leak testing, complies with NUREG-1536, Section 9.0, visual and NDE inspection criteria.
7. A combined helium leak rate test and ASME Code NB-6000 pressure test, using helium as the pressure test medium at a hydrostatic test pressure, meets the intent of the NUREG-1536, Section 9.0, structural/pressure test criteria.
8. The inability to leak test the outer top closure and vent/drain port cover welds is acknowledged as acceptable for an "all-welded cask" confinement in the NUREG-1536, Section 9.0, leak test criteria.
9. The use of multi-pass PT for examination of the outer closure of austenitic stainless steel canister designs has been found to be acceptable per NRC ISG-4.

Recent concerns raised during carbon steel canister top closure weld inspections do not offset the successful implementation of stainless steel top closure welds over the past ten years based on the following original NRC licensing commitments/requirements:

1. A "double closure" concept to assure confinement through the ends of the canister by requiring the welding of both the top shield plug and closure plate to the canister shell.
2. PT examinations including the final surface of the top shield plug-to-canister shell weld and the root pass and final surface of the closure plate-to-canister shell weld.
3. Helium leak testing of the top shield plug-to-canister shell weld.

The successful implementation of stainless steel closure welds has also been based on the following design details:

1. A separate inner closure plate and top shield plug that permits:
   a. The optimization of the top shield plug-to-canister shell gap relative to operating and shielding considerations, as opposed to weld fit-up gap considerations.
   b. The optimization of the inner closure plate-to-canister shell gap to provide the design partial penetration root depth, while avoiding excessive shrinkage restraint and minimizing weld shrinkage volume.
2. Chamfering of the canister shell inside diameter top corner to assure that the outer closure plate weld preparation will not need to be modified during canister SNF assembly loading operations. This will assure that excessive outer closure plate-to-canister shell gaps will not be created to avoid tack and root pass weld cracking due to excessive weld shrinkage.
3. The use of inherently tough stainless steel plate materials purchased to the requirements of ASME Code, Subsection NB vessel requirements.
4. The use of stainless steel filler materials with a minimum ferrite content of 10 FN in field closure welding of the FuelSolutions™ canisters to minimize welding shrinkage and, therefore, shrinkage stress.

All of the above licensing requirements and fundamental design details have resulted in a minimum of observed defects in stainless steel top closure welds and an ease in the repair of these defects due to their highly localized nature. The small quantity and size of these observed defects provides assurance that there are no significant defects in the top closure welds

implemented during the loading of stainless steel canisters at the Robinson, Oconee, Calvert Cliffs, and Davis-Besse plants in the past, and assure the long-term integrity of these and new stainless steel canisters in the future.

This page intentionally left blank.

3. STRUCTURAL EVALUATION

This chapter presents the structural evaluation of the FuelSolutions™ W74 canister for normal and off-normal operating conditions and postulated accident conditions. Structural evaluations are performed for two classes of FuelSolutions™ W74 canisters including the multi-purpose canister (referred to as a W74M class canister) and the transportable storage canister (referred to as a W74T class canister). Each of these FuelSolutions™ W74 canister classes is shown in general arrangement drawings provided in Section 1.5.1 and described in Section 1.2.1.3 of this SAR.

The structural evaluation of the FuelSolutions™ W74 canister is performed for the design basis normal, off-normal, and accident condition loadings defined in Section 2.3 of this SAR using a combination of classical closed form solutions (hand calculations) and finite element analyses. The finite element analyses are performed using the ANSYS[1] general purpose finite element code. ANSYS is a widely used finite element code in the nuclear industry and has been well benchmarked. In general, the elements and features of ANSYS used in the structural analysis are limited to those well tested and proven to provide accurate results when properly used.

As discussed in Section 1.2.1.3, there are two different W74 canister configurations, both of which are similar in design. The structural analysis of the W74 canisters is performed using nominal canister sub-assembly and piece part dimensions. In order to limit the number of structural analyses, bounding structural evaluations are conservatively used to demonstrate the structural adequacy of the components of the different FuelSolutions™ W74 canister configurations. The bounding structural evaluations are performed for the most heavily loaded components and/or the lowest strength structural materials. The results of the bounding structural calculations are conservatively applied to the components shown to be bounded. Further discussion of the bounding structural analyses are provided in Sections 3.1.1.1 and 3.1.1.2.

The results of the structural analyses demonstrate that the W74 canisters maintain geometry for criticality control, confinement, and the ability to retrieve the SNF under all design basis loadings as defined in Section 2.3 of this SAR and in accordance with the requirements of 10CFR72.[2]

[1] ANSYS Inc., *ANSYS Finite Element Program*, Versions 5.3, 5.4, and 5.5, Houston, PA.

[2] Title 10, Code of Federal Regulations Part 72 (10CFR72), *Licensing Requirements for the Independent Storage of Spent Nuclear Fuel and High Level Radioactive Waste*, U.S. Nuclear Regulatory Commission, 1995.

This page intentionally left blank.

3.1 Structural Design

3.1.1 Discussion

The FuelSolutions™ Storage System consists of three principal structural components: 1) the storage cask, 2) the transfer cask, and 3) the canister. A description of these component designs, including the FuelSolutions™ W74 canister, is provided in Section 1.2.1 of this SAR. The FuelSolutions™ storage cask and transfer cask designs are described further in Section 1.2.1 of the FuelSolutions™ Storage System SAR.[3] The principal structural members of the FuelSolutions™ W74 canister are identified in the following sections.

The FuelSolutions™ W74M and FuelSolutions™ W74T canisters, which are designed for on-site storage in the FuelSolutions™ W150 Storage Cask and transport in a transportation cask, are comprised of a shell assembly and a basket assembly. The FuelSolutions™ W74M and W74T canisters are shown in Figure 3.1-1 and Figure 3.1-2, respectively. The shell assembly is designed as the confinement boundary for on-site storage conditions, but it is not relied on for confinement during transportation. The basket assembly, which is sealed inside the canister shell assembly cavity, maintains the positions of the spent fuel assemblies and neutron absorbing materials, thus providing criticality control. The function and design code for each of the W74 canister assembly structural components are presented in Table 3.1-1.

As discussed in Section 2.2 of this SAR, intact BRP MOX and partial fuel assemblies are stored in the FuelSolutions™ W74 canister in the same manner as intact UO_2 fuel assemblies. Damaged MOX and UO_2 fuel may also be stored in the FuelSolutions™ W74 canister inside of specially designed FuelSolutions™ W74 damaged fuel can assemblies. Section 3.1.1.3 describes the principal structural members of the FuelSolutions™ W74 damaged fuel can which is used to accommodate BRP damaged fuel within the W74 canisters.

3.1.1.1 Shell Assembly

The shell assembly consists of a right circular shell with redundant welded closure plates and a shield plug assembly at the top end; and a bottom closure plate, bottom shield plug, and bottom end plate at the bottom of the canister. The shell assembly confinement components (including the shell; top inner closure plate; top outer closure plate; bottom closure plate; vent and drain port bodies and covers; and top outer closure plate leak test port cover, as shown in Figure 7.1-1) are fabricated from Type 316 stainless steel for the W74M class canisters and Type 304 stainless steel for the W74T class canisters. The licensee may also elect to use Type 304 stainless steel with a reduced carbon content for the W74T class canister on a site-specific basis. The shell assembly stainless steel material provides excellent corrosion protection and has minimum susceptibility to weld sensitization.

Each shell assembly contains a carbon steel bottom shield plug and a carbon steel shield plug assembly at the top end. The bottom shield plug is encased by the bottom closure plate, cylindrical shell extension, and bottom end plate. The top shield plug assembly consists of a partitioned shield plate and individual shield caps (plugs) for each basket fuel cell. The caps are

[3] WSNF-220, *FuelSolutions™ Storage System Final Safety Analysis Report*, NRC Docket Number 72-1026, BNFL Fuel Solutions Corporation.

captured inside the sealed canister between the shield plate and top inner closure plate. The top shield plate includes integral vent and drain ports. All exposed surfaces of the top shield plug assembly are coated to provide corrosion protection.

The structural evaluation of the W74 canister shell assemblies are performed using a combination of finite element analyses and classical closed form solutions. The evaluations performed for the W74 canister shell assemblies for all normal, off-normal, and accident conditions and load combinations are summarized in Table 3.1-2 along with the analytical methods employed.

The structural evaluation of all W74 canister shell components, with the exception of the top shield plug assembly and support bars, is based on a bounding canister shell configuration. The bounding canister shell configuration, which is described in Section 3.9.2.1, is based on the geometry of the W21 canister shell assemblies with lead top and bottom shield plugs. The only differences between the bounding canister shell configuration and the W74M and W74T canister shell configurations are the bottom shield plug weight and material, and the top shield plug assembly weight, material, and support conditions.

Since the bounding canister shell configuration includes top and bottom shield plugs that are heavier and weaker than those in the W74M and W74T canister shell assemblies, the stresses calculated for the bounding canister shell assembly configuration bound those for the W74 canister shell assemblies. Furthermore, as shown in Table 3.2-1, the weights of the W74M and W74T internals (i.e., upper and lower basket assemblies and fuel in upper and lower basket assemblies) are 51.6 kips and 49.4 kips, respectively. A bounding weight of 57 kips is conservatively used for the structural evaluation of the bounding canister shell configuration. Since all of the materials used in the construction of the W74T canister shell assembly are either of the same strength or weaker than those of the W74M canister shell assembly, the allowable stresses for the W74T canister shell govern. Therefore, the allowable stresses used for the canister shell structural evaluation are conservatively based on the weaker canister shell material.

3.1.1.2 Basket Assembly

Each FuelSolutions™ W74 canister includes an upper and lower basket assembly. The upper and lower basket assemblies, shown in Figure 3.1-1 and Figure 3.1-2, are similar in construction. Each assembly consists of a series of spacer plates, support tube assemblies, and guide tube assemblies. In addition, the upper basket assembly includes an engagement spacer plate which supports the SNF assemblies in the upper basket assembly for normal vertical transfer and storage. The guide tube assemblies provide lateral support for the SNF assemblies and maintain the position of the neutron absorbing material. The spacer plates maintain the relative spacing between guide tubes and provide structural support for the basket assembly and SNF assemblies in the lateral direction. The spacer plates are positioned and supported longitudinally by four support tube assemblies. The W74M and W74T basket assembly designs are shown on the general arrangement drawings included in Section 1.5.1 of this SAR.

The W74M upper and lower basket assemblies include 14 spacer plates each. The top and bottom end spacer plates of each W74M basket assembly, referred to as long-term performance (LTP) spacer plates, are fabricated from 2-inch thick SA-240, Type XM-19 stainless steel. All interior spacer plates, referred to as general spacer plates, are fabricated from 0.75-inch thick SA-517 or A514, Grade P or Grade F carbon steel.

The W74T upper and lower basket assemblies each contain 13 general spacer plates fabricated from 0.75-inch thick SA-517 or A514, Grade P or Grade F carbon steel. The dimensions of all spacer plate cutouts are identical. Each spacer plate includes thirty-three 7.25-inch by 7.40-inch guide tube openings and four 9.05 inches square support tube openings. The rows and columns of guide tube openings are aligned relative to their centerlines with the orientations of adjacent guide tube openings rotated 90° relative to one another. The support tube openings are located in the diagonal positions furthest from the center of the plate.

Each basket assembly includes four support tube assemblies that maintain the longitudinal spacing of the spacer plates and provide longitudinal support of the basket assembly. The support tube assemblies consist of a full length support tube and support sleeves. The support sleeves are positioned over the support tube and between spacer plates, as shown in Figure 3.1-3. For the W74M basket assemblies, the top and bottom end LTP spacer plates are welded to the support tubes to maintain the longitudinal positions of the spacer plates, as shown in Figure 3.1-3. The W74T upper and lower basket assembly top and bottom end spacer plates are captured using stainless steel sleeves which are inserted over and welded to the support tubes, as shown in Figure 3.1-3. The W74M and W74T support tubes and support sleeves are fabricated from SA-240 Type, XM-19 stainless steel and SA-240, Type 304 stainless steel, respectively.

The W74M and W74T guide tube assembly design dimensions and materials are identical. Each guide tube assembly consists of a 13 gage (0.090-inch thick) inner guide tube and either one or two 14 gage (0.075-inch thick) neutron absorber sheets, depending on the location within the basket assembly. Each neutron absorber sheet is attached to the guide tube using seven 20 gage (0.036-inch thick) stainless steel neutron absorber sheet retainers. Each retainer fits within a small hole in the neutron absorber sheet and is welded to the guide tube to capture and support the neutron absorber sheet prior to insertion into the basket assembly. Once installed in the basket assembly, the retainers are relied upon only to prevent the neutron absorber sheets from sliding in the longitudinal direction relative to the guide tube.

Each W74M guide tube assembly is secured to the bottom end LTP spacer plate within each basket assembly with two attachment brackets to maintain their positions during normal operations and prevent removal of the guide tube during fuel unloading operations. A nominal 1/8-inch clearance is provided between the bottom end of the guide tubes and the bottom end of the support tubes to assure that the basket assembly does not rest on the guide tubes when oriented vertically. The guide tube attachment brackets are not designed to withstand the postulated cask end drop condition.

Each W74T guide tube assembly is secured within the basket assembly by a stainless steel retainer clip. A single retainer clip is welded to the side of each guide tube just below the top spacer plate. The retainer clips are designed to secure the guide tube assemblies to the basket assembly in order to maintain criticality control in the unlikely event that it becomes necessary to apply an increased pull force to remove a jammed fuel assembly during fuel retrieval. However, the W74T guide tube retainer clips are designed with sufficient longitudinal clearance between the adjacent spacer plates to allow the guide tube assemblies to move in the longitudinal direction within a sealed canister without imposing out-of-plane loading on the basket assembly spacer plates.

The W74M and W74T guide tubes are fabricated from SA-240, Type 316 stainless steel. For both the W74M and W74T guide tube assemblies, the neutron absorber sheet retainers are

fabricated from SA-240, Type 304 stainless steel and the neutron absorber sheets are fabricated from A887, Type 304 B5 borated stainless steel. The borated neutron absorber materials used in the basket assemblies are not relied upon for structural support of other structural components, but are considered to only support their own self weight.

The mechanical properties of the canister basket assembly materials of construction are discussed in Section 3.3.

The W74 canister basket assemblies are evaluated using a combination of finite element analyses and classical closed form solutions. The evaluations performed for the basket assembly components for all normal, off-normal, and accident conditions and load combinations are summarized in Table 3.1-3, along with the analytical methods employed. The load conditions in which the basket component stresses are scaled from the stress results of other load conditions are identified and the scale factors are provided.

Where possible, the FuelSolutions™ W74 basket assembly structural evaluation is performed for the most limiting basket assembly components. The bounding W74 basket assembly components for each normal load condition are identified in each of the following sections.

Bounding General and LTP Spacer Plate Evaluations

As discussed above, two types of spacer plates are used in the W74M and W74T canister basket assemblies: 0.75-inch thick carbon steel general spacer plates and 2-inch thick stainless steel LTP spacer plates. Bounding structural evaluations are performed only for the most heavily loaded W74 general spacer plate and LTP spacer plate for each normal, off-normal, and accident load condition and load combinations. The most highly loaded W74 spacer plates are identified based on the total in-plane tributary weight that each spacer plate supports.

For the conditions in which the spacer plates are loaded by the weight of the SNF assemblies, two bounding fuel loading assumptions are considered: 1) uniform fuel load, i.e., fuel weight evenly distributed over its entire length, and 2) concentrated fuel loading at the fuel assembly grid spacers. Under relatively low magnitude loads, such as horizontal dead weight and on-site transport vibration, the SNF assembly loads are applied to the spacer plates as concentrated loads at the grid spacers. The fuel grid spacers are conservatively assumed to be located at the longitudinal positions which result in the highest spacer plate loading (i.e., directly above the spacer plates having the largest tributary lengths). For the postulated storage cask tip-over and transfer cask side drop conditions, elastic stress and buckling evaluations are performed using the uniform fuel loading assumption. In addition, plastic stress and plastic instability evaluation are performed for these conditions using the concentrated fuel loading assumption.

For longitudinal loading, such as vertical dead weight, vertical handling, seismic, and postulated storage cask or transfer cask end drop conditions, each general spacer plate supports only its own weight. Therefore, a single representative general spacer plate is evaluated for these conditions and the results are applied to all similar spacer plates. The bottom end LTP spacer plates in the W74M upper and lower basket assemblies support their own weight plus the weight of the guide tube assemblies, whereas the top end LTP spacer plates support only their own weight. Therefore the bounding LTP spacer plate structural evaluations are performed for both the top and bottom end LTP spacer plates.

The spacer plate thermal stress evaluation is performed for the general and LTP spacer plates subjected to the highest radial thermal gradients. The thermal stresses in these spacer plates

bound those in all other spacer plates subjected to lower radial thermal gradients. The bounding radial thermal gradients used for the spacer plate thermal stress evaluation are calculated in Chapter 4 for the design basis heat loads and axial heat profiles. The W74 canister LTP and general spacer plate thermal stress evaluation is presented in Section 3.5.1.3.2.

Bounding Support Tube Assembly Evaluations

As discussed previously, each W74 canister basket assembly includes four support tube assemblies, all having similar construction, identical materials of construction, and identical cross section dimensions.

For longitudinal loading, such as vertical dead weight, vertical handling, seismic, and postulated storage cask or transfer cask bottom end drop conditions, the controlling support tubes are those in the W74M lower basket assembly, since they support the greatest weight and have the same allowable stresses as the W74T support tubes.

For lateral loads (e.g., normal to the basket longitudinal axis) resulting from horizontal dead weight, on-site transfer, seismic, and postulated storage cask and transfer cask side drop conditions, the support tube assemblies are loaded by their own weight and the weight of the contained SNF assembly and damaged fuel canister. They are supported by the basket assembly spacer plates. The structural evaluations of the W74 support tube assemblies for these conditions are conservatively performed for the largest free span distance between the spacer plates.

Thermal stresses in the W74 support tube assemblies resulting from differential thermal expansion between the support tube, support sleeve, and spacer plate materials are evaluated for both the W74M and W74T support tube assemblies. Bounding thermal stress evaluations are performed for the longest support tube free spans in both the W74M and W74T canisters, since the differential thermal expansion is proportional to length. In addition, the support tube stresses due to longitudinal differential thermal expansion are evaluated only for the thermal condition resulting in the highest support tube temperatures. This is bounding since the support tube assembly longitudinal differential expansion is greater at elevated temperatures while the gradients are essentially the same.

Bounding Guide Tube Evaluations

As discussed above, the dimensions and top and bottom end details of all W74 canister guide tube assemblies are identical. In addition, all W74 guide tubes are fabricated from the same material. However, there are two different guide tube configurations which differ in the number of neutron absorber sheets which are attached to the guide tube. All of the W74 guide tubes in the interior of the basket assemblies include two neutron absorber sheet on opposing faces, whereas the guide tubes on the perimeter of the basket assembly include only one neutron absorber sheet. Since no structural credit is taken for the support that the neutron absorber sheets provide to the guide tube and their mass is assumed to load the guide tube, bounding structural evaluation of the W74 guide tube is performed for the interior guide tubes which include two neutron absorber sheets.

For lateral loads (e.g., normal to the basket longitudinal axis) resulting from horizontal dead weight, on-site transfer, seismic, and postulated storage cask and transfer cask side drop, the guide tubes are loaded by their own weight plus the weight of the SNF assembly, and supported by the basket assembly spacer plates. The structural evaluations of the W74 guide tubes for these conditions are performed only for the largest unsupported span between adjacent spacer plates.

Both uniform fuel loading with the weight of the fuel assembly spread evenly along the length of the guide tube, and concentrated fuel loading at the locations of the fuel grid spacers on the fuel assemblies are evaluated. Limiting loads for the uniform load case are determined using the maximum guide tube free span length and maximum line load for each basket design.

For longitudinal loading due to vertical dead weight, vertical handling, seismic, and postulated storage cask and transfer cask end drop conditions, the W74 guide tubes are loaded only by their own weight. Therefore, for the same vertical loading the bounding guide tubes are those in the interior region of the basket assembly since they include two neutron absorber sheets rather than one and, consequently, are the heaviest.

3.1.1.3 Damaged Fuel Can

The FuelSolutions™ W74 canister is designed to accommodate up to eight damaged fuel assemblies. Each damaged fuel assembly is placed inside a FuelSolutions™ W74 damaged fuel can within the upper or lower basket assembly support tubes. The FuelSolutions™ W74 damaged fuel can is designed to contain damaged or undamaged BRP fuel assemblies during all normal, off-normal, and accident conditions for on-site storage and transfer operations. The FuelSolutions™ W74 damaged fuel can, containing a damaged BRP fuel assembly, is designed to be handled vertically.

The FuelSolutions™ W74 damaged fuel can, shown in Figure 3.1-4, consists of a damaged fuel can and a removable top lid assembly. The structural design of the damaged fuel can is similar to that of the FuelSolutions™ W74 guide tube assembly. The damaged fuel can consists of a 13 gage (0.090-inch thick) tube and a 12 gage (0.105-inch thick) bottom end plate. The bottom end of the damaged fuel can includes screened holes to allow for water drainage. The damaged fuel can includes borated stainless steel neutron absorber sheets on all four faces of the tube. The damaged fuel can neutron absorber sheet attachment detail is similar to that of the guide tubes, as discussed in Section 3.1.1.2 of the FuelSolutions™ W74 Canister Storage SAR.

The principal structural members of the damaged fuel can top lid assembly include the handle, base plate, and attachment hardware. As shown in Figure 3.1-4, the top lid assembly handle has four legs that are each 0.25-inch thick by 2-inch wide. Each leg of the handle is attached to the base plate using full penetration groove welds. The top lid assembly base plate consists of a 6.7-inch square by 3/8-inch thick plate with a 5.5-inch long by 1.25-inch wide rectangular cutout in the center to accommodate the fuel assembly bail handle. The base plate also includes eight slotted holes to accommodate the attachment hardware.

The top lid assembly attachment hardware consists of four attachment bars or “dogs.” The top lid attachment dogs are used to secure and lock the top lid assembly to the damaged fuel can after insertion of the damaged fuel assembly. Each attachment dog is secured to the top lid base plate using two cap screws. Slotted holes in the base plate allow the attachment dogs to be retracted for insertion into the damaged fuel can. Once inserted, the attachment dogs are extended to engage the slotted holes in the corners of the damaged fuel can and secured with the cap screws. In the extended position, the heads of the cap screws are positioned in recessed holes to prevent the attachment dogs from inadvertently retracting.

3.1.2 Design Criteria

The principal design criteria for the FuelSolutions™ W74 canister is presented in Section 2.1.2 of this SAR. This section discusses the general structural criteria used for the design of the canister shell, basket assemblies, and damaged fuel cans. In addition, the design criteria used for other structural failure modes such as brittle fracture, fatigue, and buckling are discussed. The function and design code for each of the W74 canister assembly structural components are presented in Table 3.1-1.

3.1.2.1 Basic Design Criteria

The FuelSolutions™ W74 canister is designed such that no significant deformation results from normal or off-normal operation. High margins of safety are provided during these conditions. The structural design of the canister is also required to withstand all postulated accident conditions and natural phenomena events without impairing its ability to maintain confinement, radiation shielding, criticality control, and the ability to retrieve the stored fuel. Under accident conditions, permanent deformation of the canister is permitted, provided the capability to perform the principal safety functions is not compromised.

3.1.2.2 Applicable Codes and Standards

The FuelSolutions™ W74 canister shell subassembly provides primary confinement for storage conditions. As such, the FuelSolutions™ W74 canister shell assembly confinement components are designed in accordance with the applicable requirements of Subsection NB of the ASME Code[4] and guidance provided in ISG-4,[5] as discussed in Section 2.1.2 of this SAR.

The FuelSolutions™ W74 canister cylindrical shell seam welds are full penetration groove welds that are designed and RT inspected per Subsection NB. The FuelSolutions™ W74 shell assembly includes redundant confinement welds at the joints between the cylindrical shell and the top end inner and outer closure plates. The weld details between the top inner and outer closure plates, and the cylindrical shell are partial penetration groove welds. All canister top end closure welds are liquid penetrant examined with the inner closure weld examined at the root and final weld passes, and the outer closure weld at the root, intermediate, and final weld passes. The full penetration weld between the bottom closure plate and the canister shell is examined by both liquid penetrant and radiographic examination. The canister shell extension and bottom end plate attachment welds are non-pressure retaining welds and are liquid penetrant examined.

The analytical stress acceptance criteria of Subsection NB of the ASME Code and ISG-4 are applied to the FuelSolutions™ W74 closure welds with additional conservative measures to assure that the design margins inherent in the NB rules are maintained. These measures include:

- Redundant closure welds at the top end of the FuelSolutions™ W74 shell assembly.
- Full penetration welds at the bottom closure plate and canister seam welds with 100% radiographic examination.

---

[4] American Society of Mechanical Engineers (ASME) Boiler and Pressure Vessel Code, Section III, *Rules for Construction of Nuclear Power Plant Components*, 1995 Edition.

[5] ISG-4, *Cask Closure Weld Inspections*, Spent Fuel Project Office Interim Staff Guidance-4, United States Nuclear Regulatory Commission, Revision 1, May 21, 1999.

- PT weld inspection of all closure welds.
- Helium leak rate test of the top inner closure welds.
- Pneumatic pressure test of the top inner closure welds in accordance with NB-6000.

These measures provide additional assurance of the FuelSolutions™ W74 canister closure integrity, and the weld redundancy ensures that potential failure of any single confinement closure weld does not result in release of radioactive material to the environment. The allowable stresses for the canister shell assembly confinement components are summarized in Table 3.1-4.

In accordance with guidance provided by ISG-4, a weld efficiency factor of 0.8 is applied to the allowable stress for the canister shell top outer closure weld. Based on stress reduction factors provided in ASME Section III, a weld efficiency factor of 0.9 is applied to the allowable stress for the canister shell top inner closure weld.

The canister shell assembly components which do not provide confinement, including the shield plug assemblies, top shield plug support bars (referred to as alignment bars in the drawings in Section 1.5.1), bottom end shell extension, bottom end plate, and all associated welds, are designed in accordance with Section III, Subsection NF, of the ASME Code. The allowable stresses for the canister shell assembly non-confinement components are summarized in Table 3.1-5.

The criticality control components, consisting of the FuelSolutions™ W74 basket assembly components that maintain the relative positions of the fissile and neutron absorbing materials (including the general and LTP spacer plates, engagement spacer plate, support tubes, support sleeves, and guide tube assemblies), and the W74 damaged fuel can, are designed in accordance with the applicable requirements of Section III, Subsection NG[6] of the ASME Code as discussed in Section 2.1.2 of this SAR. Use of these criteria also assures retrievability of the SNF assemblies for all postulated accident conditions in accordance with 10CFR72. The allowable stresses for the canister criticality control components are summarized in Table 3.1-4.

3.1.2.3 Supplemental Structural Criteria

Brittle Fracture

The FuelSolutions™ W74M and W74T canister shell and basket assemblies are designed using materials which provide degrees of safety against failure due to brittle fracture which are appropriate for the intended uses. The fracture toughness requirements used for the W74 canisters are based on a Lowest Service Temperature (LST) for all on-site storage and transfer conditions which produce significant dynamic tensile stress levels in the canister components. The results of the W74 canister structural evaluation show that the only conditions which produce significant dynamic stresses in the canister shell and basket assembly structural components are the cask drop and tip-over conditions which are postulated to occur during canister transfer and handling operations. A *technical specification* has been established in Section 12.3 of FuelSolutions™ Storage System SAR which limits the minimum temperature of the transfer cask structural shell to 40°F during normal transfer operations when the ambient air

[6] American Society of Mechanical Engineers (ASME) Boiler and Pressure Vessel Code, Section III, Division 1, Subsection NG, *Core Support Structures*, 1995 Edition.

temperature is below 32°F. This requirement also assures that the temperature of the canister will be at least 40°F during normal transfer operations. However, a conservative LST of 0°F is used to establish the fracture toughness requirements for the W74 canister assemblies.

The FuelSolutions™ W74 canister shell assembly confinement components are designed in accordance with the fracture toughness requirements of ASME NB-2300. The FuelSolutions™ W74 canister shell assembly confinement components are fabricated entirely from SA-240, Type 304 and Type 316 austenitic stainless steels. These materials do not undergo a ductile-to-brittle transition in the temperature range of interest (i.e., down to 0°F), and thus are not susceptible to brittle fracture. Accordingly, impact testing is not required for austenitic stainless steels in accordance with NB-2311(a)(6).

The W74 carbon steel shield plugs are designed in accordance with the fracture toughness requirements of ASME NF-2300. Per NF-2311(b)(7) impact testing is not required for materials for which the maximum stress does not exceed 6,000 psi tension or is compressive since brittle fracture failure under these conditions is not credible. As shown in the W74 canister shell structural evaluation, the maximum stress in the bottom carbon steel shield plug is less than 6,000 psi for the storage cask bottom end drop, which is the controlling on-site storage and transfer load condition. Therefore, brittle fracture failure of the W74 canister carbon steel bottom shield plugs is not a credible failure mode and impact testing of these materials is not required. For the W74 top shield plugs, impact testing will be performed in accordance with NF-2300 to assure adequate fracture toughness of the material.

The FuelSolutions™ W74 canister basket assembly and the W74 damaged fuel can are designed in accordance with the fracture toughness requirements of NG-2300, except that the impact testing requirements of NUREG/CR-1815[7] are used in lieu of NG-2330. Since the basket assembly components do not provide containment, the fracture toughness testing requirements from NUREG/CR-1815 for Category II steel are used. These requirements assure that the fracture toughness of the material is sufficient to prevent fracture initiation of pre-existing cracks under dynamic loading. The basket assembly structural components are fabricated from SA-240, Type 316, Type 304, and Type XM-19 austenitic stainless steels and SA-517 or A514, Grade P or Grade F, carbon steels. Austenitic stainless steel materials do not undergo a ductile-to-brittle transition in the temperature range of interest (i.e., down to 0ºF), and thus are not susceptible to brittle fracture. Accordingly, impact testing of austenitic stainless steels is not required by ASME NG-2311(a)(5).

The W74 general spacer plate material (i.e., 0.75-inch thick SA-517, Grades F or P, or A514, Grades F or P carbon steel plate) experiences a ductile-to-brittle transition at a temperature lower than the NUREG/CR-1815 prescribed maximum NDT temperature. Drop weight testing of the general spacer plate material in accordance with ASTM E-208 will be performed to demonstrate that the NDT temperature is at or below the TNDT test temperature. The TNDT test temperature for the general spacer plate material is established based upon the material thickness and the Lowest Service Temperature (LST) using Figure 7 of NUREG/CR-1815 as follows:

$$T_{NDT} = LST - A = -10°F$$

[7] NUREG/CR-1815, *Recommendations for Protection Against Failure by Brittle Fracture in Ferritic Steel Shipping Containers Up to Four Inches Thick*, U.S. Nuclear Regulatory Commission, June 15, 1981.

where:

LST = 0°F, LST for all on-site storage and transfer conditions for which the cask drop and tip-over accidents are postulated to occur.

A = 10°F, Offset temperature established using Figure 7 (curve KID/(yd) of NUREG/CR-1815.

The effects of irradiation on material toughness properties is considered in accordance with the requirements of ASME NG-2332(d). The evaluation is based on an exposure of 100 years, conservatively assuming no decay of the neutron source. The total neutron fluence (8.81E+14 n/cm^2 for E>1.0 MeV and 3.97E+15 n/cm^2 for E>0.1 MeV) results in 1.88E-06 dpa Iron atom displacements. According to Figure 3-1 of NUREG-1509,[8] the entire neutron energy spectrum of 1.88E-06 dpa will not change the fracture toughness properties of SA-517 or A514 carbon steels.

Fatigue

The principal mechanism for fatigue damage to the FuelSolutions™ W74 canister is low amplitude high cycle fatigue due to normal ambient temperature and internal pressure cycling over the 100 year service life.[9] As discussed in Sections 3.5.1.4.1 and 3.5.1.4.2, the analyses of the FuelSolutions™ W74 canister shell assembly and basket assembly demonstrate that normal operating cycles do not present a fatigue concern for the W74 canister components over the 100-year service life.

Buckling

The stability of the FuelSolutions™ W74 canister shell is evaluated in accordance with ASME Code Case N-284.[10] The evaluation includes factors to account for geometric and loading eccentricities in the shell. The buckling evaluation of the canister shell for the storage cask end drop is presented in Section 3.7.3.1. The buckling evaluation due to external pressure is presented in Section 3.7.7.

The buckling criteria of NUREG/CR-6322 and Article F-1331.5(a)(1) of the ASME Code are used for the basket assembly structural components. For the basket assembly buckling evaluations performed in accordance with NUREG/CR-6322, the basket components are considered linear type members subjected to axial compression and bending. The basket assembly component stresses are evaluated using interactions 26, 27, and 28 of NUREG/CR-6322. The only exception to this is for the guide tube buckling evaluation for the storage cask end drop, in which the guide tube stress is limited to 2/3 of the theoretical buckling stress calculated based on classical plate buckling theory in accordance with Section 5.3 of NUREG/CR-6322. For the W74 basket assembly spacer plate plastic instability analyses performed in accordance with Article F-1341.4(a) of the ASME Code, the maximum applied load in each basket criticality control component is limited to 0.7PI, where PI is the plastic instability load determined in accordance with Article NB-3213.24 of the ASME Code.

---

[8] NUREG-1509, *Radiation Effects on Reactor Vessel Supports*, U.S. Nuclear Regulatory Commission.

[9] Title 10, U.S. Code of Federal Regulations, Part 51 (10CFR51), *Waste Confidence Decision Review*, U.S. Nuclear Regulatory Commission, September 11, 1990.

[10] Case N-284, *Metal Containment Shell Buckling Design Methods*, American Society of Mechanical Engineers (ASME) Boiler and Pressure Vessel Code, Code Cases, Nuclear Components, August 25, 1980.

Table 3.1-1 - Summary of FuelSolutions™ W74 Canister Component Functions and Design Codes

Assembly	Component[1]	Function	Codes & Standards
Shell Assembly	Cylindrical Shell	Confinement	NB
	Bottom End Plate	Structural	NF
	Bottom End Shell Extension	Structural	NF
	Bottom Shield Plug	Shielding	NF
	Bottom Closure Plate	Confinement	NB
	Top Outer Closure Plate	Confinement	NB
	Top Inner Closure Plate	Confinement	NB
	Top Shield Plug	Shielding	NF
	Top Shield Plug Support Bars	Structural	NF
Basket Assembly	General Spacer Plates	Criticality Safety	NG
	LTP Spacer Plate (W74M)	Criticality Safety	NG
	Support Tube	Criticality Safety	NG
	Support Sleeve	Criticality Safety	NG
	Guide Tube	Criticality Safety	NG
	Neutron Absorber Panel	Criticality Safety	NG
	Neutron Absorber Panel Button	Criticality Safety	NG
	Guide Tube Attachment Bracket (W74M)	Criticality Safety	NG
	Damaged Fuel Can	Criticality Control	NG

Note:
(1) Components are included in both the W74M and W74T canisters, unless otherwise specified.

Table 3.1-2 - W74 Canister Shell Assembly Structural Evaluation Summary (3 Pages)

Load Condition or Load Combination	Canister Shell Assembly Type or Component	Reference Section	Evaluation	Method of Analysis
Normal Thermal (T)	Typical Shell Assy.	3.5.1.2.1	Differential Thermal Expansion	Bounding evaluation presented in WSNF-200
	Bounding Shell Assy.(1)	3.5.1.3.1	Thermal Stress	Linear Elastic Finite Element Analysis
Fatigue	Typical Canister Shell	3.5.1.4.1	Various	Hand Calculations
Canister Draining Internal Pressure (P_b)	Bounding Shell Assy.(1)	3.5.2.1	Stress	Linear Elastic Finite Element Analysis
Normal Internal Pressure (P)	Bounding Shell Assy.(1)	3.5.2.2	Stress	Linear Elastic Finite Element Analysis and Hand Calculations(2)
Vertical Dead Weight (D_v)	Bounding Shell Assy.(1)	3.5.3.1.1	Stress	Linear Elastic Finite Element Analysis and Hand Calculations(2)
	Top Shield Plug & Support Bar Welds	3.5.3.1.1	Stress	Scaled from A_s (x 1*g*/50*g*)
Horizontal Dead Weight (D_h)	W21M-LS(3)	3.5.3.1.2	Stress	Linear Elastic Finite Element Analysis
Vertical Handling (L_{hv})	Bounding Shell Assy.(1)	3.5.4.1	Stress	Linear Elastic Finite Element Analysis and Hand Calculations(2)
	Top Shield Plug & Support Bar Welds	3.5.4.1	Stress	Scaled from A_s (x 1.15*g*/50*g*)
Horizontal Handling (L_{hh1} and L_{hh2})	Bounding Shell Assy.(1)	3.5.4.2 & 3.5.4.3.1	Stress	Linear Elastic Finite Element Analysis and Hand Calculations(2)
Normal Load Combinations	Bounding Shell Assy.(1) and W21M-LS(3)	3.5.5.1	Stress	Linear Elastic Finite Element Analysis and Hand Calculations(2). Stresses from axisymmetric and three-dimensional models combined using hand calculations.
Off-Normal Temperature (T_o)	Bounding(1)	3.5.1.2.1	Differential Thermal Expansion	Evaluated in WSNF-200
	Bounding(1)	3.6.1.3	Thermal Stress	Linear Elastic Finite Element Analysis

Table 3.1-2 - W74 Canister Shell Assembly Structural Evaluation Summary (3 Pages)

Load Condition or Load Combination	Canister Shell Assembly Type or Component	Reference Section	Evaluation	Method of Analysis
Off-Normal Internal Pressure (P_o)	Bounding[1]	3.6.2	Stress	Linear Elastic Finite Element Analysis and Hand Calculations[2]
Reflood Internal Pressure (P_r)	Typical W74 canister shell	3.6.4	Stress	Linear Elastic Finite Element Analysis and Hand Calculations[2]
Cask Misalignment (L_m)	Bounding[1]	3.6.3	Stress	Linear Elastic Finite Element Analysis and Hand Calculations[2]
Off-Normal Load Combinations	Bounding[1]	3.6.5.1	Stress	Linear Elastic Finite Element Analysis. Stresses from axisymmetric and three-dimensional models combined using hand calculations.
Storage Cask End Drop (A_s)	Bounding[1]	3.7.3.1	Stress	Linear Elastic Finite Element Analysis and Hand Calculations[2]
	Top End Inner Closure Plate and Weld	3.7.3.1	Stress	Hand Calculations
	Top Shield Plug	3.7.3.1	Stress	Hand Calculations
	Canister Shell	3.7.3.1	Buckling	Hand Calculation per Code Case N-284
Storage Cask Tip-Over (A_{s1})	W21M-LS[3]	3.7.4.1	Stress	Linear Elastic Finite Element Analysis
Transfer Cask Side Drop (A_t)	W21M-LS[3]	3.7.5.1	Stress	Linear Elastic Finite Element Analysis
Flood (F)	All	3.7.7	Bounded by accident internal pressure	N/A
Earthquake (E)	All	3.7.8.1	Bounded by accident drops	N/A
Accident Internal Pressure (P_a)	Bounding[1]	3.7.9	Stress	Linear Elastic Finite Element Analysis and Hand Calculations[2]
Accident Load Combinations	Bounding[1]	3.7.10.1	Stress	Linear Elastic Finite Element Analysis. Stresses from axisymmetric and three-dimensional models combined using hand calculations.

Notes for Table 3.1-2:

(1) Analyses performed for the "bounding" canister shell configuration, which bounds all W74M and W74T canister shell designs.

(2) Hand calculations are performed for the top outer closure plate in Section 3.9.3.2 for simply supported edge conditions to demonstrate that the bending stresses in the top outer closure weld can be classified as secondary. The maximum bending stress in the top outer closure plate for the simply supported condition are used for the stress evaluation since they bound those from the finite element analysis in which the top outer closure plate bending restraint is included.

(3) The W21M-LS canister assembly is the bounding design for these load conditions since it has the heaviest top shield plug and the heaviest basket assembly and fuel.

Table 3.1-3 - W74 Canister Basket Assembly Structural Evaluation Summary (3 Pages)

Load Condition or Load Combination	Basket Assembly Component	Reference Section	Evaluation	Method of Analysis
Normal Thermal (T)	General and LTP Spacer Plates	3.5.1.2.2	Differential Thermal Expansion	Hand Calculations.
		3.5.1.3.2	Thermal Stress(1)	Linear Elastic FEA
	Engagement Spacer Plate	3.5.1.2.2	Differential Thermal Expansion	Hand Calculations.
		3.5.1.3.3	Thermal Stress(1)	Linear Elastic FEA
	Support Tubes and Sleeves	3.5.1.2.2	Differential Thermal Expansion	Hand Calculations
		3.5.1.3.4	Thermal Stress(2)	Hand Calculations
	Guide Tube	3.5.1.2.2	Differential Thermal Expansion	Hand Calculations
		3.5.1.3.5	N/A	Free Thermal Expansion
Fatigue	Entire Assembly	3.5.1.4.2	Various	Hand Calculations
Vertical Dead Weight (D_v)	General and LTP Spacer Plates	3.5.3.2.1	Stress	Linear Elastic FEA
	Engagement Spacer Plate	3.5.3.3.1	Stress	Scaled from A_s (x 1*g*/50*g*)
	Support Tubes	3.5.3.4.1	Stress	Scaled from A_s (x 1*g*/14*g*)
	Support Sleeve	3.5.3.5.1	Stress	Scaled from A_s (x 1*g*/50*g*)
	Guide Tube	3.5.3.6.1	Stress(3)	Hand Calculations
Horizontal Dead Weight (D_h)	General and LTP Spacer Plates	3.5.3.2.2	Stress(4)	Linear Elastic FEA
	Engagement Spacer Plate	3.5.3.3.2	Stress	Scaled from L_{hh2} (x 1*g*/2*g*)
	Support Tubes	3.5.3.4.2	Stress	Scaled from A_t (x 1*g*/60*g*)
	Guide Tubes	3.5.3.6.2	Stress(5)	Linear Elastic FEA
Vertical Handling (L_{hv})	All Basket Assembly Components	3.5.4.1.2	Stress	Scaled from D_v (x 1.15)
Horizontal Handling (L_{hh})	Spacer Plates	3.5.4.3.2	Stress	Scaled from D_v (x 0.3) and D_h (x 2.0)
	Support Tubes and Sleeves	3.5.4.3.4 / 3.5.4.3.5	Stress	Scaled from D_v (x 0.3) and D_h (x 1.61)
	Guide Tubes	3.5.4.3.6	Stress	Scaled from D_v (x 0.3) and D_h (x 1.65)

Table 3.1-3 - W74 Canister Basket Assembly Structural Evaluation Summary (3 Pages)

Load Condition or Load Combination	Basket Assembly Component	Reference Section	Evaluation	Method of Analysis
Normal Load Combinations (A4 & A5)	Spacer Plates	3.5.5.2	Stress	Absolute sum of maximum stresses
	Support Tubes	3.5.5.2	Stress	Absolute sum of maximum stresses
			Buckling	In accordance with NUREG/CR-6322
	Guide Tubes	3.5.5.2	Stress	Absolute sum of maximum stresses
Off-Normal Thermal (T_o)	All Structural Components	3.6.1.3.2	Thermal Stress	Hand Calculations
Accident Thermal (T_a)	Spacer Plates	3.7.1 / 3.7.2	N/A(6)	N/A(6)
	Support Tubes and Sleeves	3.7.2	Buckling	In accordance with NUREG/CR-6322
	Guide Tube	3.7.1 / 3.7.2	N/A(6)	N/A(6)
Storage Cask End Drop (A_s)	Spacer Plates	3.7.3.2.1 / 3.7.3.2.2	CS & SS Spacer Plate Stresses	Scaled from D_v (x 50)Linear Elastic FEA
	Support Tubes and Sleeves	3.7.3.2.3 / 3.7.3.2.4	Support Tube & Sleeve Stresses	Hand Calculation - Elastic Analysis
			Support Tube & Sleeve Buckling	In accordance with NUREG/CR-6322
	Guide Tube	3.7.3.2.5	Stress	Scaled from D_v (x 50)
			Buckling	In accordance with NUREG/CR-6322
Storage Cask Tip-Over (A_{s1})	Spacer Plates	3.7.4.2.1	Stresses(7)	Linear Elastic FEA
			Permanent Deformation(3)	Plastic FEA
			Elastic Buckling(7, 8)	In accordance with NUREG/CR-6322
			Plastic Instability(9)	Plastic Large-Deflection FEA
	Support Tubes and Sleeves	3.7.4.2.3	N/A	Bounded by A_t
	Guide Tubes	3.7.4.2.4	N/A	Bounded by A_t
Transfer Cask Side Drop (A_t)	Spacer Plates	3.7.5.2.1 / 3.7.5.2.2	Stresses(7)	Linear Elastic FEA
			Permanent Deformation(3)	Plastic FEA
			Elastic Buckling(7, 8)	In accordance with NUREG/CR-6322
			Plastic Instability(9)	Plastic Large-Deflection FEA
	Support Tubes and Sleeves	3.7.5.2.3 / 3.7.5.2.4	Stress	Hand Calculations

Table 3.1-3 - W74 Canister Basket Assembly Structural Evaluation Summary (3 Pages)

Load Condition or Load Combination	Basket Assembly Component	Reference Section	Evaluation	Method of Analysis
Transfer Cask Side Drop (A_t)	Guide Tubes	3.7.5.2.5	Stresses[7]	Linear Elastic FEA
			Permanent Deformation[10]	Plastic Large-Deflection FEA
			Buckling	In accordance with NUREG/CR-6322
Earthquake	Spacer Plates		Stress	Scaled from D_v (x 1.1) and D_h (x 1.3)
	Support Tubes and Sleeves		Stress	Scaled from D_v (x 1.1) and D_h (x 1.3)
	Guide Tubes		Stress	Scaled from D_v (x 1.1) and D_h (x 1.3)
Accident Load Combinations	Spacer Plates	3.7.5.2.1 / 3.7.5.2.2	Stress	Absolute Sum of Maximum Stresses[11]
			Elastic Buckling[7, 8]	In accordance with NUREG/CR-6322
			Plastic Instability[9]	Plastic Large-Deflection FEA
	Support Tubes and Sleeves	3.7.5.2.3 / 3.7.5.2.4	Stress	Absolute Sum of Maximum Stresses
	Guide Tubes	3.7.5.2.5	Stress	Absolute Sum of Maximum Stresses

Notes for Table 3.1-3:

(1) Separate analyses performed for hottest general and LTP spacer plates for controlling normal thermal conditions.
(2) Support tube and sleeve stresses calculated for longest span in both W74M and W74T canisters.
(3) Bounding stresses calculated for guide tube and guide tube attachments for heaviest W74 guide tube assembly.
(4) Analyses performed for most highly loaded W74 general and LTP spacer plates assuming concentrated loads at SNF assembly grid spacers.
(5) Stresses evaluated in the guide tube base material and longitudinal seam weld for both uniform SNF loading assumption and concentrated fuel load at SNF grid spacers.
(6) Thermal stresses are classified as secondary and do not require evaluation for accident conditions.
(7) Evaluated using elastic system analysis with uniform fuel load assumption.
(8) Evaluated for impact loads with and without controlling normal thermal loading superimposed.
(9) Analyses performed for most highly loaded general spacer plate only.
(10) Permanent deformation evaluated in the guide tube for both uniform SNF loading assumption and concentrated fuel load at SNF grid spacers.
(11) Thermal stresses are classified as secondary and as such are not evaluated for accident conditions. However, thermal loads are considered in combination with other accident loads only for buckling evaluation.

Table 3.1-4 - Canister Confinement and Subcriticality Component Allowable Stresses

Component Type	Stress Category	Service Conditions			
		Normal Conditions (Service Level A)	Off-Normal Conditions (Service Level B)	Off-Normal Conditions (Service Level C)	Accident Conditions (Service Level D)
Shell Assembly Confinement Components[1] (Subsection NB)	P_m	S_m	$1.1S_m$	Greater of $1.2S_m$ or S_y	Lesser of $2.4S_m$ or $0.7S_u$
	$P_m + P_b$	$1.5S_m$	$1.65S_m$	Greater of $1.8S_m$ or $1.5S_y$	150% of P_m Allowable
	$P_m + P_b + Q$	$3.0S_m$	$3.3S_m$	N/A	N/A
	Avg. Bearing Stress	S_y	S_y	S_y	$2.1S_u$[2]
	Pure Shear Stress	$0.6S_m$	$0.6S_m$	$0.6S_m$	$0.42S_u$
Basket Assembly and Damaged Fuel Can Subcriticality Components (Subsection NG)	P_m	S_m	$1.1S_m$	$1.5S_m$	Lesser of $2.4S_m$ or $0.7S_u$ (Elastic) $0.7S_u$ (Plastic)
	$P_m + P_b$	$1.5S_m$	$1.65S_m$	$2.25S_m$	150% of P_m Allowable (Elastic) $0.9S_u$ (Plastic)
	$P_m + P_b + Q$	$3.0S_m$	$3.3S_m$	N/A	N/A
	Avg. Bearing Stress	S_y	S_y	$1.5S_y$	Lesser of $2S_y$[3] or $2.1S_u$[2]
	Avg. Shear Stress	$0.6S_m$	$0.6S_m$	$0.9S_m$	Lessor of $1.2S_m$[3] or $0.42S_u$

Notes:

(1) For the canister shell assembly inner and outer closure welds, efficiency factors of 0.9 for the inner closure weld and 0.8 for the outer closure weld are applied to the base metal allowable stresses in accordance with Section 3.1.2.2 of this SAR and ISG-4, respectively.

(2) Applicable only for pinned or bolted joints for Service Level D.

(3) In accordance with NG-3225, special stress limits for Service Level D conditions are limited to twice the allowable stress for Service Level A and B conditions.

Table 3.1-5 - Canister Shell Assembly Non-Confinement Component Allowable Stresses

Component Type	Stress Category	Service Condition			
		Normal Conditions (Service Level A)	Off-Normal Conditions (Service Level B)	Off-Normal Conditions (Service Level C)	Accident Conditions (Service Level D)
Shell Assembly Non-Confinement Components (Subsection NF)	P_m	S_m	**$1.33S_m$**	$1.5S_m$	Greater of $1.2S_y$ and $1.5S_m$, not to exceed $0.7S_u$
	$P_m + P_b$	$1.5S_m$	**$2.0S_m$**	$2.25S_m$	150% of P_m Allowable
	Avg. Bearing Stress	S_y	**S_y**	S_y	$2.1S_u$ (1)
	Pure Shear Stress	$0.6S_m$	**$0.6S_m$**	$0.6S_m$	$0.42S_u$

Note:
(1) Applicable only for pinned or bolted joints for Service Level D.

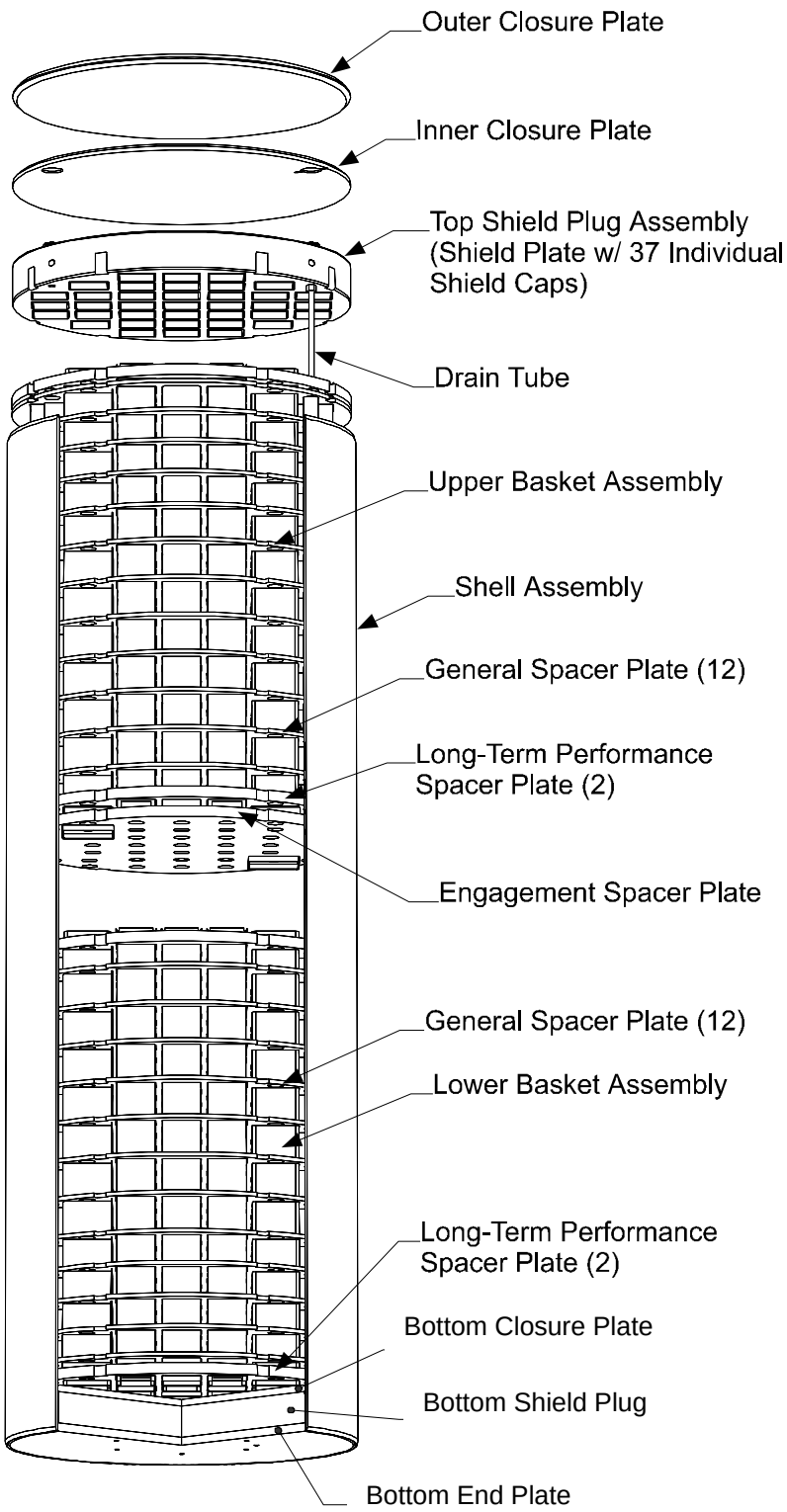

Figure 3.1-1 - Expanded View of FuelSolutions™ W74M Canister

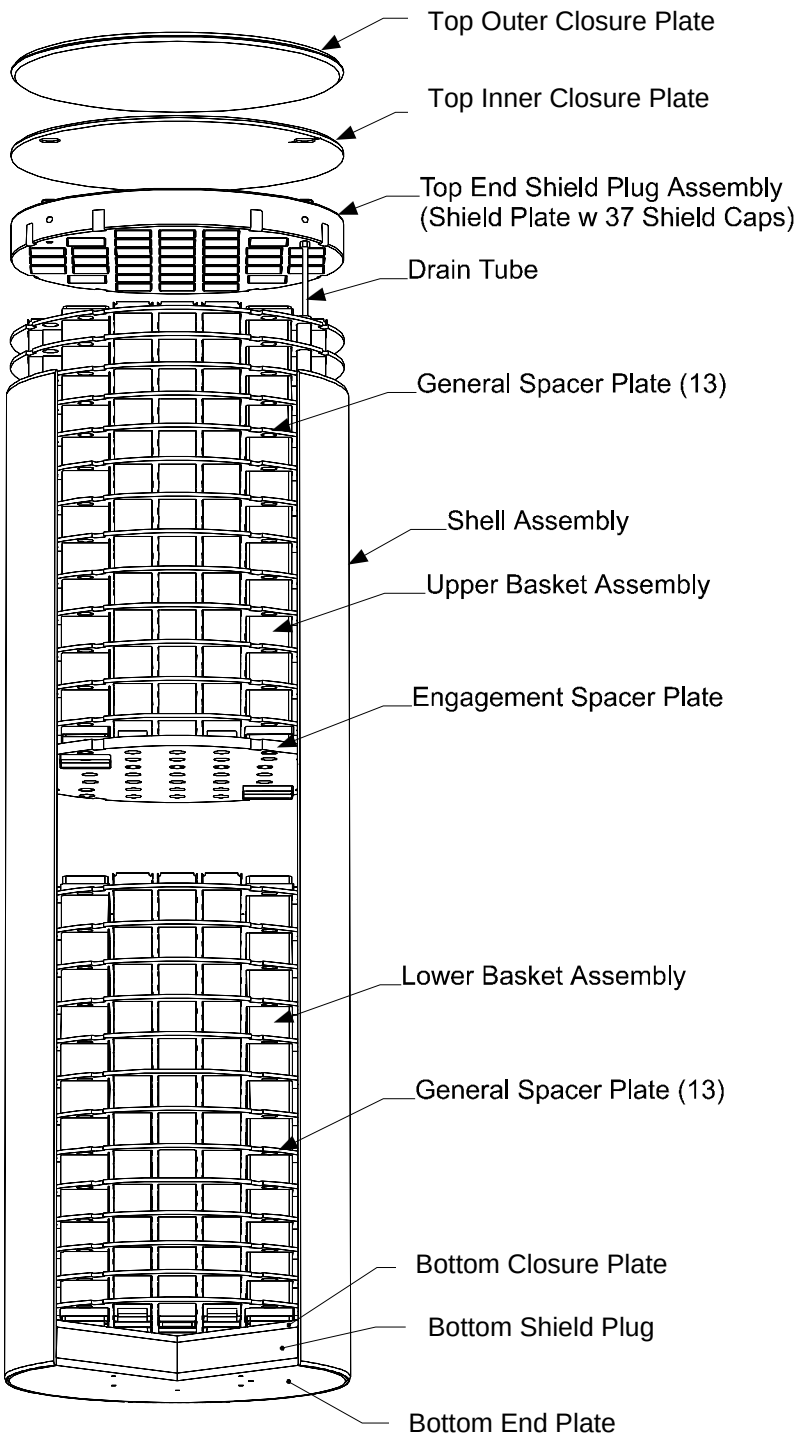

Figure 3.1-2 - Expanded View of FuelSolutions™ W74T Canister

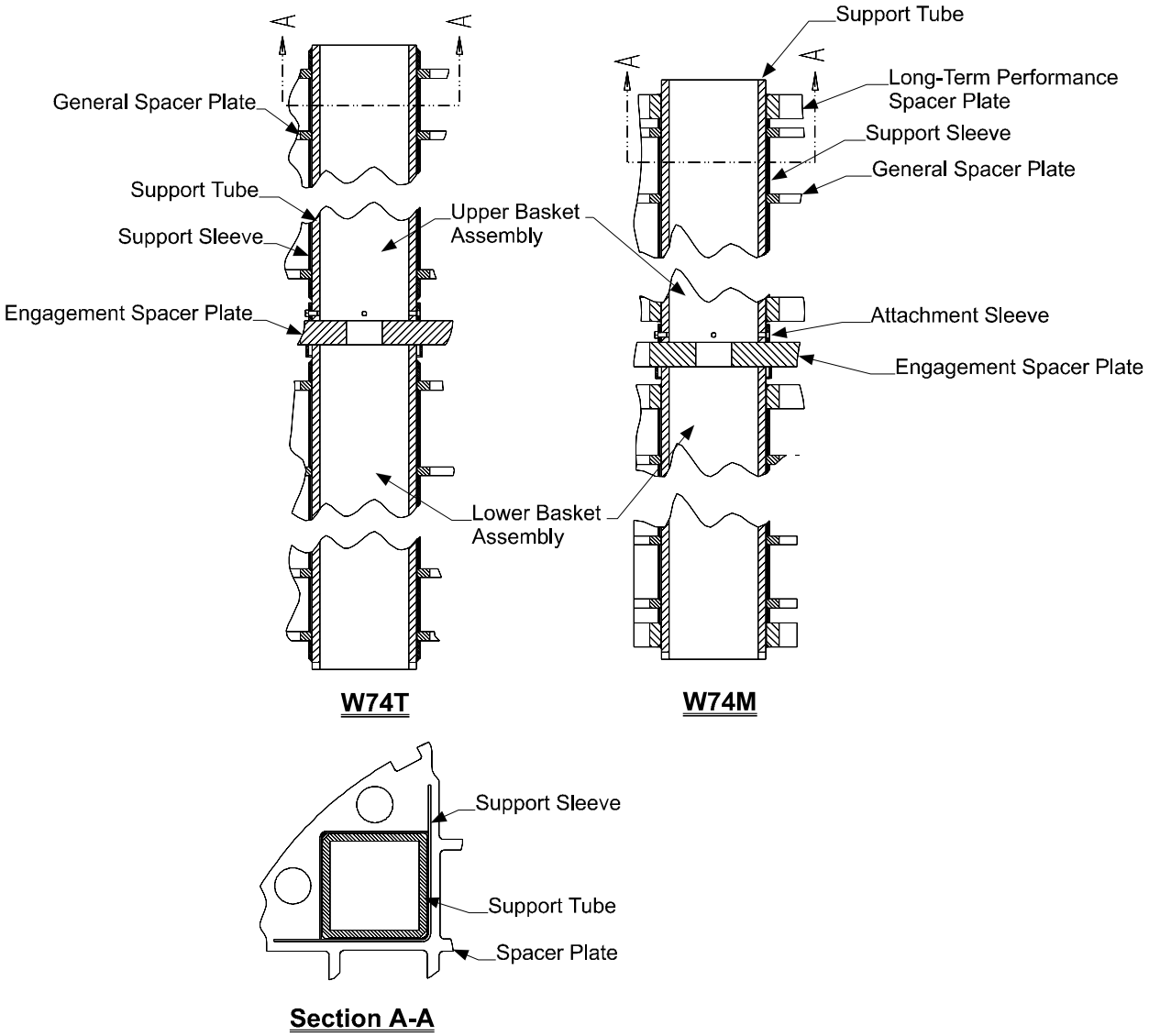

Figure 3.1-3 - FuelSolutions™ W74 Canister Support Tube Assembly Detail

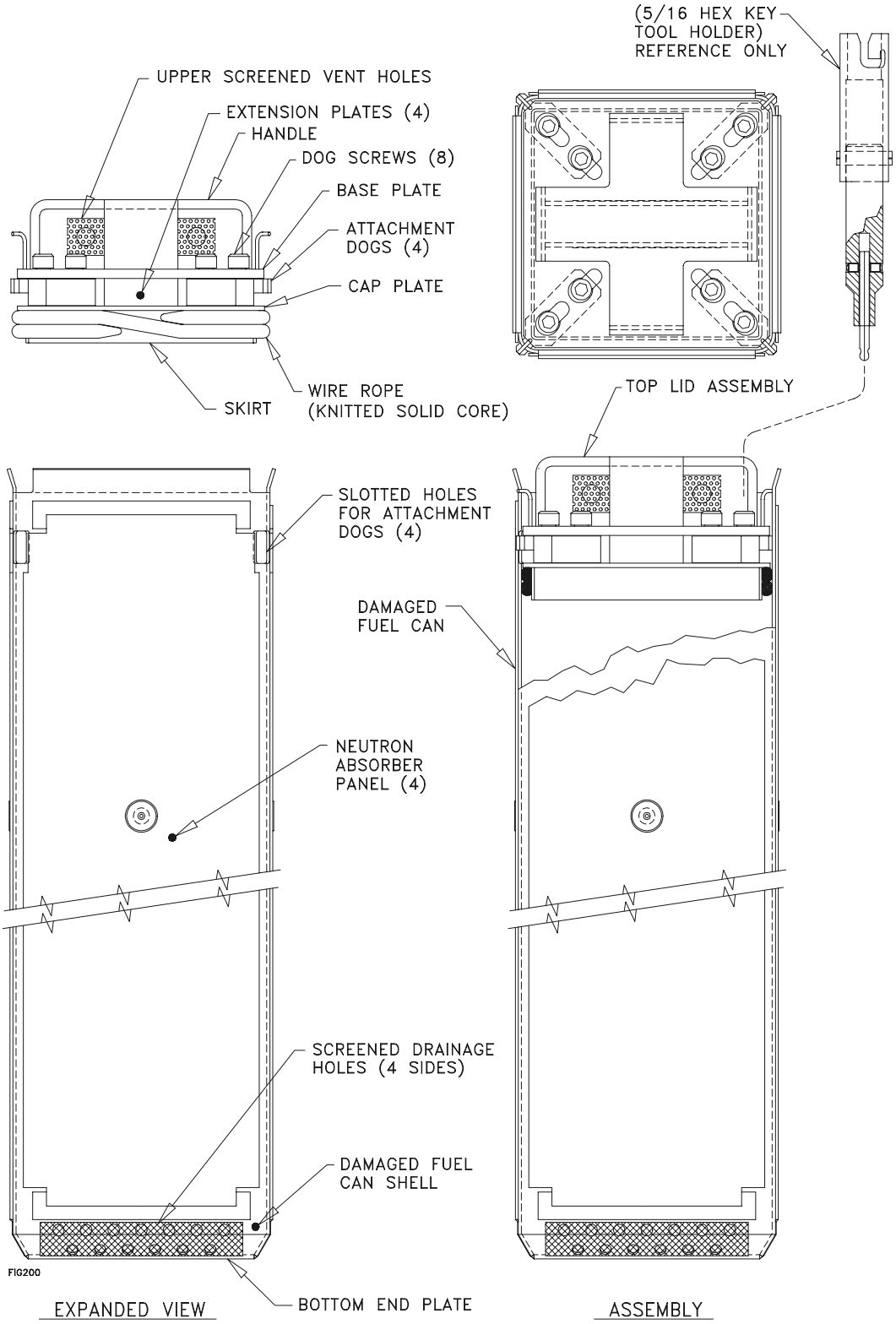

Figure 3.1-4 - FuelSolutions™ W74 Damaged Fuel Can

This page intentionally left blank.

3.2 Weights and Centers of Gravity

The weights of the major FuelSolutions™ W74 canister components and payload (SNF assemblies) are summarized in Table 3.2-1. The total weight and center of gravity of each canister configuration, with maximum payload weights, are shown for the dry storage configuration (i.e., dry sealed canister containing payload). The BRP fuel assembly weights reported in Table 3.2-1 include a bounding weight of 200 pounds for four damaged fuel cans in both the upper and lower baskets. The calculated weight of each damaged fuel can is 121 pounds.

As discussed in Sections 2.2.1 and 2.2.2 of this SAR, the weights of BRP MOX and partial fuel assemblies are bounded by those of intact BRP fuel assemblies. Thus, the W74M and W74T canister weights provided in Table 3.2-1 are bounding.

Table 3.2-1 - W74 Canister Weights and Centers of Gravity

Component	W74M		W74T	
	Weight (pounds)	Center of Gravity[1] (in.)	Weight (pounds)	Center of Gravity[1] (in.)
Canister Field Assembly	24,681	101.6	24,681	101.6
Shell Assembly	15,143	48.1	15,143	48.1
Top Shield Plug	6,673	184.9	6,673	184.9
Inner Closure Plate	955	189.5	955	189.5
Outer Closure Plate	1,910	191.0	1,910	191.0
Lower Basket Assembly	9,255	50.2	8,171	50.4
Upper Basket Assembly	10,963	132.5	9,883	131.7
Fuel in Lower Basket[2]	15,680	50.9	15,680	50.9
Fuel in Upper Basket[2]	15,680	138.2	15,680	138.2
Sealed Canister[2]	**76,259**	**96.9**	**74,095**	**97.0**
Heaviest Sealed Canister[3]	**77,539**	**---**	**75,375**	**---**

Notes:

(1) Centers of gravity are relative to bottom end of canister, as shown in Figure 3.2-1.

(2) Payload weight includes 32 SNF assemblies plus four damaged fuel canisters per basket at the support tube locations. Weights are based on nominal SNF assembly weight of 465 pounds and bounding damaged fuel canister weight of 200 pounds.

(3) Payload weight includes 32 SNF assemblies plus four damaged fuel canisters per basket at the support tube locations. Weights are based on nominal SNF assembly weight of 485 pounds and bounding damaged fuel canister weight of 200 pounds.

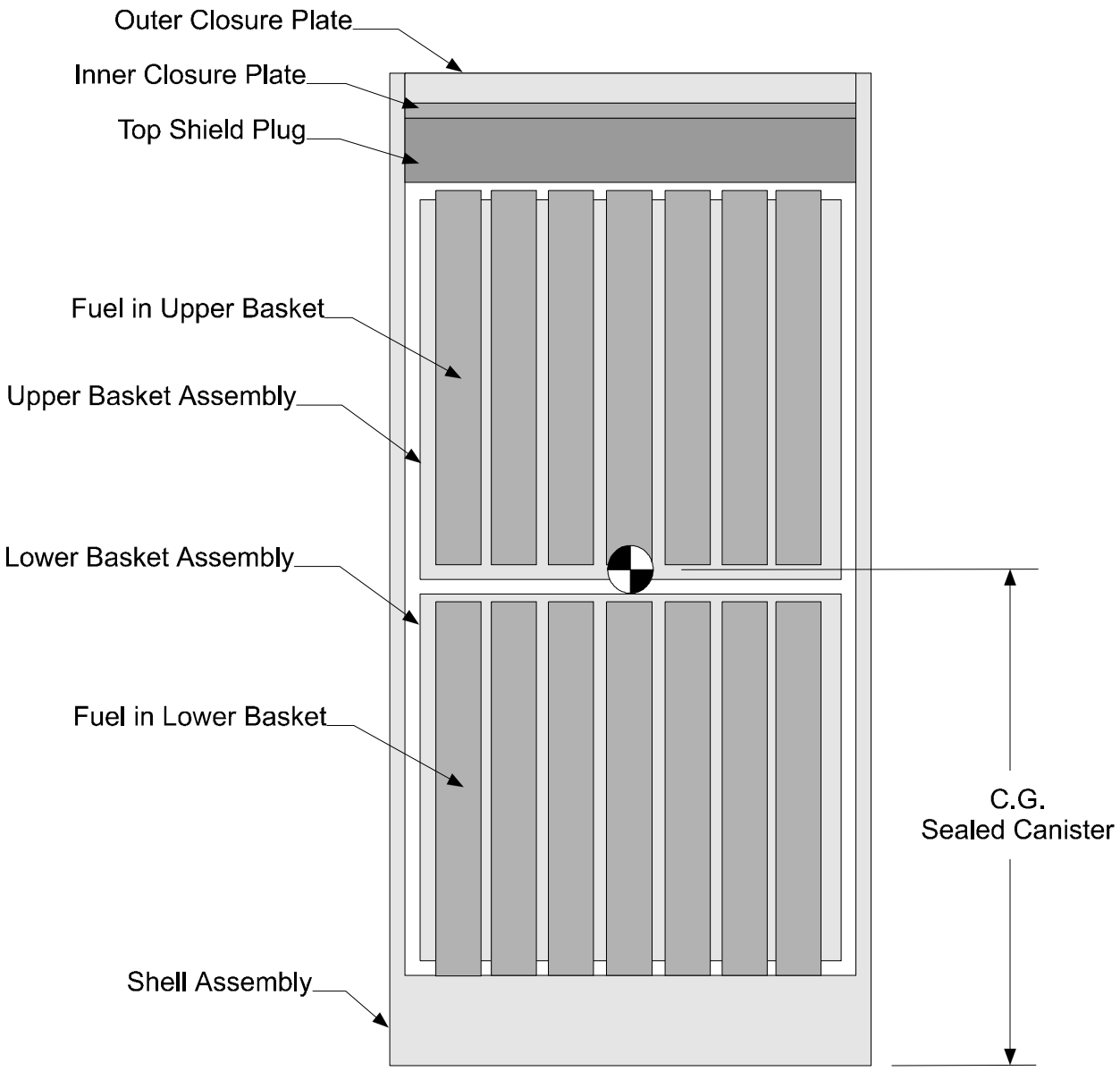

Figure 3.2-1 - FuelSolutions™ W74 Canister Center of Gravity Diagram

This page intentionally left blank.

3.3 Mechanical Properties of Materials

The FuelSolutions™ W74M and W74T canister structural components are fabricated entirely from austenitic stainless steel and carbon steel. Table 3.3-1 and Table 3.3-2 identify components, material specifications, and the corresponding material data tables for the W74M and W74T canisters, respectively.

In all cases the weight density and Poisson's ratio for stainless steel is taken to be 0.290 lb/in^3 and 0.29, respectively, and the weight density and Poisson's ratio for carbon steel is taken to be 0.283 lb/in^3 and 0.3, respectively. Detailed descriptions of the W74M and W74T canister materials of construction are included in the following paragraphs.

Both the FuelSolutions™ W74M and W74T canister shell assembly designs are of identical construction and vary only in the type of stainless steel used for the shell and closure plates. The canister shell assembly structural components for the W74M, with the exception of the top and bottom shield plugs, are all fabricated from SA-240, Type 316 austenitic stainless steel. The canister shell assembly structural components for the W74T canister are all fabricated from SA-240, Type 304 austenitic stainless steel. The licensee may also elect to use Type 304 stainless steel with a reduced carbon content for the W74T canister shell assembly on a site-specific basis. The bottom shield plug is fabricated from ASTM A36 carbon steel. The bottom shield plug is encased between the bottom closure plate and the bottom end plate within the cylindrical shell extension. The top shield plug assembly consists of a shield plate and 37 shield caps. The shield plate is fabricated from ASTM A516, Grade 55 or 60 carbon steel and the shield caps are fabricated from ASTM A36 carbon steel. The shield plate and shield caps are coated to provide corrosion protection.

The W74M and W74T basket assembly designs are of similar construction and vary only in the materials used for the top and bottom end spacer plates of each basket. The general spacer plates used in the W74T and W74M basket assembly are all fabricated from electroless nickel coated SA-517 or A514, Grade P or Grade F carbon steel. The W74M upper and lower basket assemblies each include a top and bottom end LTP spacer plate fabricated from SA-240, Type XM-19 austenitic stainless steel.

The guide tube materials are identical for the W74M and W74T basket assembly designs. Each W74M and W74T guide tube assembly consists of a guide tube and two neutron absorber panels. The guide tubes are fabricated from SA-240, Type 316 stainless steel. For accident drop conditions, the guide tubes are evaluated using plastic analysis to determine the maximum permanent deformation for use in the criticality evaluation. The elastic-plastic material properties for this analysis are based on information from NUREG/CR-0481[11] and Part II, Section A of the ASME Code. Since the guide tube evaluations are conservatively performed at a bounding temperature of 715°F and the stress-strain values from the report are at a maximum temperature of 600°F, a "normalization" factor is used to determine the equivalent plastic material properties at 715°F. This factor is computed based on the ASME Code value for yield stress of Type 316 stainless steel at 715°F divided by the report value at 0.2% strain for a temperature of 600°F.

[11] NUREG/CR-0481, SAND77-1872, *An Assessment of Stress-Strain Data Suitable for Finite-Element Elastic-Plastic Analysis of Shipping Containers*, Rack, H.J., Knorovsky, G.A., R-7, September 1978.

This factor is then applied to the report stress values at 600°F, to arrive at the stress vs. strain values at 715°F. These values, as presented in Table 3.3-4 and plotted in Figure 3.3-1, are used in the plastic analysis of the guide tube.

All structural materials used for the W74 canisters are permitted for use in Section III construction per Section II, Part D and Code Case N-71-16[12] of the ASME Code. The SA-517 and A514, Grade P and Grade F carbon steel materials used for the spacer plates and support tubes are permitted for supports only. Use of these materials for the basket assembly spacer plates and support tubes is acceptable since there are no significant effects on the material properties for the intended service conditions. As discussed in Section 3.1.2.3, the cumulative effect of irradiation from the SNF does not significantly affect the fracture toughness of the SA-517 and A514, Grade P and Grade F carbon steel materials over the 100 year design life of the canister.

The maximum allowable temperatures of the canister materials for all normal design conditions are limited to those tabulated in ASME, Section II, Part D. Short-term elevated temperatures in excess of these allowable values may occur during loading operations, off-normal transfer, or storage accident events. The maximum temperatures in the basket assembly components remain below 1,000°F for all short-term thermal conditions. As shown in ASME Code Case N-47-33,[13] the strength properties of austenitic stainless steels do not change due to exposure to 1,000°F for up to 10,000 hours. Therefore, short-term exposure to the temperatures of this magnitude does not have any significant effect on mechanical properties of the basket assembly materials.

The principal structural members of the FuelSolutions™ W74 damaged fuel can are fabricated from SA-240, Type 316 stainless steel. The welding process and weld filler material used for the damaged fuel can are the same as those identified for the guide tube in Table 3.3-1 and Table 3.3-2.

The mechanical properties of SA-240, Type 316 stainless steel are provided in Table 3.3-3. The weight density and Poisson's ratio for stainless steel are taken to be 0.29 lb/in^3 and 0.3, respectively.

The damaged fuel can neutron absorber panels are fabricated from A887, Type 304B5 borated stainless steel. The neutron absorber panels are not relied on for structural support of the damaged fuel can. The weight density of borated stainless steel is taken to be 0.28 lb/in^3.

[12] Case N-71-16, *Additional Materials for Subsection NF, Class 1, 2, 3, and MC Component Supports Fabricated by Welding*, American Society of Mechanical Engineers (ASME) Boiler and Pressure Vessel Code, Nuclear Components, 1995 Edition.

[13] Case N-47-33, *Class 1 Components in Elevated Temperature Service*, American Society of Mechanical Engineers (ASME) Boiler and Pressure Vessel Code, Nuclear Components, 1995 Edition.

Table 3.3-1 - FuelSolutions™ W74M Canister Materials Summary

Assembly	Component	Material [1]	Reference Table
Shell Assembly	Cylindrical Shell	SA-240, Type 316	Table 3.3-3
	Bottom Closure Plate	SA-240, Type 316	Table 3.3-3
	Bottom End Plate	SA-240, Type 316	Table 3.3-3
	Bottom Shield Plug	A36	Table 3.3-6
	Top Inner Closure Plate	SA-240, Type 316	Table 3.3-3
	Top Outer Closure Plate	SA-240, Type 316	Table 3.3-3
	Shield Plug Assembly	SA-516, Grade 55 or 60 or SA-36	Table 3.3-9 or Table 3.3-6
	Shield Caps (Top Shield Plug)	A36	Table 3.3-6
	Shield Plate Dowel Plug	SA-516, Grade 55 or 60 or SA-36	Table 3.3-9 or Table 3.3-6
	Shield Plug Support Bars	SA-240, Type 316	Table 3.3-5
Basket Assembly	LTP Spacer Plate	SA-240, Type XM-19	Table 3.3-5
	General Spacer Plate	SA-517, Grade P or F A514, Grade P or F	Table 3.3-7
	Engagement Spacer Plate	SA-240, Type XM-19	Table 3.3-5
	Support Tube	SA-240, Type XM-19	Table 3.3-5
	Support Sleeve	SA-240, Type 304	Table 3.3-3
	Guide Tube	SA-240, Type 316	Table 3.3-3
	Guide Tube Attachment Bracket	SA-240, Type 316	Table 3.3-3
	Neutron Absorber Sheet Retainer	SA-240, Type 316	Table 3.3-3
	Neutron Absorber Sheet	A887, Type 304 B5	Table 3.3-8

Notes:

(1) Permissible welding processes and weld filler metals are specified on the general arrangement drawings in Section 1.5.1.

Table 3.3-2 - FuelSolutions™ W74T Canister Material Summary

Assembly	Component	Material[1]	Reference Table
Shell Assembly	Cylindrical Shell	SA-240, Type 304	Table 3.3-3
	Bottom Closure Plate	SA-240, Type 304	Table 3.3-3
	Bottom End Plate	SA-240, Type 304	Table 3.3-3
	Bottom Shield Plug	A36	Table 3.3-6
	Top Inner Closure Plate	SA-240, Type 304	Table 3.3-3
	Top Outer Closure Plate	SA-240, Type 304	Table 3.3-3
	Shield Plug Assembly	SA-516, Grade 55 or 60 or SA-36	or Table 3.3-6
	Shield Caps (Top Shield Plug)	A36	Table 3.3-6
	Shield Plate Dowel Plug	SA-516, Grade 55 or 60 or SA-36	or Table 3.3-6
	Shield Plug Support Bars	SA-240, Type 304	Table 3.3-3
Basket Assembly	General Spacer Plate	SA-517, Grade P or F A514, Grade P or F	Table 3.3-7
	Engagement Spacer Plate	SA-240, Type XM-19	Table 3.3-5
	Support Tube	SA-240, Type XM-19	Table 3.3-5
	Support Sleeve	SA-240, Type 304	Table 3.3-3
	Guide Tube	SA-240, Type 316	Table 3.3-3
	Neutron Absorber Sheet Retainer	SA-240, Type 316	Table 3.3-3
	Neutron Absorber Sheet	A887, Type 304 B5	Table 3.3-8
	Guide Tube Retainer Clip	SA-240, Type 316	Table 3.3-3

Notes:

(1) Permissible welding processes and weld filler metals are specified on the general arrangement drawings in Section 1.5.1.

Table 3.3-3 - Type 316 and Type 304 Stainless Steel Material Properties

Material Spec.	Temp. (°F)	Yield Strength,(1) S_y (ksi)	Ultimate Strength,(2) S_u (ksi)	Design S.I.,(3) S_m (ksi)	Elastic Modulus,(4) E (ksi ×10^3)	Mean Coefficient of Thermal Expansion,(5,6) (in/in/°F x 10^{-6})
SA-240 Type 316	-40	30.0	75.0	20.0	28.9	8.23
	-20	30.0	75.0	20.0	28.7	8.28
	70	30.0	75.0	20.0	28.3	...
	100	30.0	75.0	20.0	28.1	8.54
	200	25.8	75.0	20.0	27.6	8.76
	300	23.3	73.4	20.0	27.0	8.97
	400	21.4	71.8	19.3	26.5	9.21
	500	19.9	71.8	18.0	25.8	9.42
	600	18.8	71.8	17.0	25.3	9.60
	700	18.1	71.8	16.3	24.8	9.76
	735	17.9	71.5	16.2	---	---
SA-240 Type 304	-40	30.0	75.0	20.0	28.9	8.21
	-20	30.0	75.0	20.0	28.7	8.26
	70	30.0	75.0	20.0	28.3	...
	100	30.0	75.0	20.0	28.1	8.55
	200	25.0	71.0	20.0	27.6	8.79
	300	22.5	66.0	20.0	27.0	9.00
	400	20.7	64.4	18.7	26.5	9.19
	500	19.4	63.5	17.5	25.8	9.37
	600	18.2	63.5	16.4	25.3	9.53
	700	17.7	63.5	16.0	24.8	9.69

Notes:

(1) ASME B&PV Code, Section II, Part D, Table Y-1.

(2) ASME B&PV Code, Section II, Part D, Table U.

(3) ASME B&PV Code, Section II, Part D, Table 2A.

(4) ASME B&PV Code, Section II, Part D, Table TM-1, Material Group G.

(5) ASME B&PV Code, Section II, Part D, Table TE-1, 16Cr-12Ni-2Mo, Coefficient B (mean from 70ºF) for Type 316 stainless steel.

(6) ASME B&PV Code, Section II, Part D, Table TE-1, 18Cr-8Ni, Coefficient B (mean from 70ºF) for Type 304 stainless steel.

Table 3.3-4 - Type 316 Stainless Steel Plastic Material Properties

Strain	0.2%	0.273%(1)	0.3%	0.8%	4.0%	40%
Values(2) at 600°F (ksi)	21.0	21.4	21.5	25.0	37.5	---
Values at 715°F (ksi)	---	18.0	---	21.1	31.6	71.4(3)

Notes:

(1) Strain corresponding to 0.2% offset yield.

(2) From NUREG/CR-0481, SAND77-1872, R-7, *An Assessment of Stress-Strain Data Suitable for Finite-Element Elastic-Plastic Analysis of Shipping Containers*, Figure 8(d), heat 297.

(3) Minimum elongation of Type 316 stainless steel from Part II, Section A, SA-240, Table 2 of the ASME Code.

Table 3.3-5 - Type XM-19 Stainless Steel Material Properties

Material Spec.	Temp. (°F)	Yield Strength,(1) S_y (ksi)	Ultimate Strength,(2) S_u (ksi)	Design S.I.,(3) S_m (ksi)	Elastic Modulus,(4) E (ksi ×10^3)	Mean Coefficient of Thermal Expansion,(5) (in/in/°F x 10^{-6})
SA-240	-40	55.0	100.0	33.3	28.9	8.05
	-20	55.0	100.0	33.3	28.7	8.08
	70	55.0	100.0	33.3	28.3	...
	100	55.0	100.0	33.3	28.1	8.30
	200	47.0	99.5	33.2	27.6	8.48
	300	43.4	94.3	31.4	27.0	8.65
	400	40.8	90.7	30.2	26.5	8.79
	500	38.8	89.1	29.7	25.8	8.92
	600	37.3	87.8	29.2	25.3	9.03
	700	36.3	86.5	28.8	24.8	9.15

Notes:

(1) ASME B&PV Code, Section II, Part D, Table Y-1, for material annealed at 1925ºF-1975ºF.

(2) ASME B&PV Code, Section II, Part D, Table U.

(3) ASME B&PV Code, Section II, Part D, Table 2A.

(4) ASME B&PV Code, Section II, Part D, Table TM-1, Material Group G.

(5) ASME B&PV Code, Section II, Part D, Table TE-1, 22Cr-13Ni, Coefficient B (mean from 70ºF).

Table 3.3-6 - SA-36 or A36 Carbon Steel Material Properties

Material Spec.	Temp. (°F)	Yield Strength,(2) S_y (ksi)	Ultimate Strength,(3) S_u (ksi)	Design S.I.,(4) S_m (ksi)	Elastic Modulus,(5) E (ksi ×10^3)	Mean Coefficient of Thermal Expansion,(6) (in/in/°F x 10^{-6})
SA-36 or A36(1)	-40	36.0	57.9	19.3	30.0	5.03
	-20	36.0	57.9	19.3	29.9	5.10
	70	36.0	57.9	19.3	29.5	...
	100	36.0	57.9	19.3	29.3	5.53
	200	32.8	57.9	19.3	28.8	5.89
	300	31.9	57.9	19.3	28.3	6.26
	400	30.8	57.9	19.3	27.7	6.61
	500	29.1	57.9	19.3	27.3	6.91
	600	26.6	53.1	17.7	26.7	7.17
	700	25.9	51.9	17.3	25.5	7.41

Notes:

(1) Material properties for ASTM A36 carbon steel based on SA-36 properties from Part D of the ASME Code.

(2) ASME B&PV Code, Section II, Part D, Table Y-1.

(3) S_u for SA-36 is not provided in Table U and is conservatively taken as $3S_m$.

(4) ASME B&PV Code, Section II, Part D, Table 2A.

(5) ASME B&PV Code, Section II, Part D, Table TM-1, Carbon Steels with C ≤ 0.30%.

(6) ASME B&PV Code, Section II, Part D, Table TE-1, Material Group C, Coefficient B (mean from 70ºF).

Table 3.3-7 - SA-517, Grades P and F, and A514, Grades P and F Carbon Steel Material Properties

Material Spec.	Temp. (°F)	Yield Strength,(1) S_y (ksi)	Ultimate Strength,(2) S_u (ksi)	Design S.I.,(3) S_m (ksi)	Elastic Modulus,(4) E (ksi ×10^3)	Mean Coefficient of Thermal Expansion,(5) (in/in/°F x 10^{-6})
SA-517 Gr. F and P	-40	100.0	115.0	38.3	30.0	5.89
	-20	100.0	115.0	38.3	29.9	5.95
	70	100.0	115.0	38.3	29.5	...
	100	100.0	115.0	38.3	29.3	6.27
	200	95.8	115.0	38.3	28.8	6.54
	300	93.0	115.0	38.3	28.3	6.78
	400	90.2	115.0	38.3	27.7	6.98
	500	89.5	115.0	38.3	27.3	7.16
	600	87.5	115.0	38.3	26.7	7.32
	700	84.4	112.6	37.5	25.5	7.47
A514 Gr. F and P	-40	100.0	110.0	36.7	30.0	5.89
	-20	100.0	110.0	36.7	29.9	5.95
	70	100.0	110.0	36.7	29.5	...
	100	100.0	110.0	36.7	29.3	6.27
	200	95.5	110.0	36.7	28.8	6.54
	300	92.5	110.0	36.7	28.3	6.78
	400	89.8	110.0	36.7	27.7	6.98
	500	87.6	110.0	36.7	27.3	7.16
	600	85.5	110.0	36.7	26.7	7.32
	700	83.0	107.7	35.9	25.5	7.47

Notes:

(1) ASME B&PV Code, Section II, Part D, Table Y-1, < 2½ in. (SA-517) and Code Case N-71-16, Table 3 (A514).

(2) ASME B&PV Code, Code Case N-71-16, Table 5.

(3) ASME B&PV Code, Section II, Part D, Table 2A, < 2½ in. (SA-517) and Code Case N-71-16, Table 1 (A514).

(4) ASME B&PV Code, Section II, Part D, Table TM-1, Carbon Steels with C ≤ 0.30%.

(5) ASME B&PV Code, Section II, Part D, Table TE-1, Material Group E, Coefficient B (mean from 70ºF).

Table 3.3-8 - Neutron Absorber Material Properties

Material Specification	Temp. (°F)	Yield Strength, S_Y (ksi)	Ultimate Strength, S_u (ksi)	Elastic Modulus, E (ksi ×10^3)	Mean Coefficient of Thermal Expansion[2] (in/in/°F x 10^{-6})
ASTM A887,	70	30.0	75.0	28.3	---
Type 304 B5	500	19.4	63.5	25.8	9.37
Borated Stainless Steel[1]	700	17.7	63.5	24.8	9.69

Notes:

(1) Properties based on SA-240, Type 304 stainless steel.

(2) Mean coefficient of thermal expansion from 70°F.

Table 3.3-9 - SA-516, Grades 55 and 60 Carbon Steel Material Properties

Material Spec.	Temp. (°F)	Yield Strength S_y(1) (ksi)	Ultimate Strength S_u(2) (ksi)	Design S.I. S_m(3) (ksi)	Elastic Modulus E(4) (ksi ×10^3)	Mean Coefficient of Thermal Expansion,(5, 6) (in/in/°F x 10^{-6})
SA-516, Grade 55	70	30.0	55.0	18.3	29.5	---
	100	30.0	55.0	18.3	29.3	5.73
	200	27.3	55.0	18.3	28.8	6.09
	300	26.6	55.0	17.7	28.3	6.43
	400	25.7	55.0	17.2	27.7	6.74
	500	24.5	55.0	16.2	27.3	7.06
SA-516, Grade 60	70	32.0	60.0	20.0	29.5	---
	100	32.0	60.0	20.0	29.3	5.53
	200	29.2	60.0	19.5	28.8	5.89
	300	28.3	60.0	18.9	28.3	6.26
	400	27.4	60.0	18.3	27.7	6.61
	500	25.9	60.0	17.3	27.3	6.91

Notes:

(1) ASME B&PV Code, Section II, Part D, Table Y-1.

(2) ASME B&PV Code, Section II, Part D, Table U.

(3) ASME B&PV Code, Section II, Part D, Table 2A.

(4) ASME B&PV Code, Section II, Part D, Table TM-1, carbon steels with C ≤ 0.30%,

(5) SA-516, Gr. 55 (C-Si): ASME B&PV Code, Section II, Part D, Table TE-1, material group B, coefficient B (mean from 70°F).

(6) SA-516, Gr. 60 (C-Mn-Si): ASME B&PV Code, Section II, Part D, Table TE-1, material group C, coefficient B (mean from 70°F).

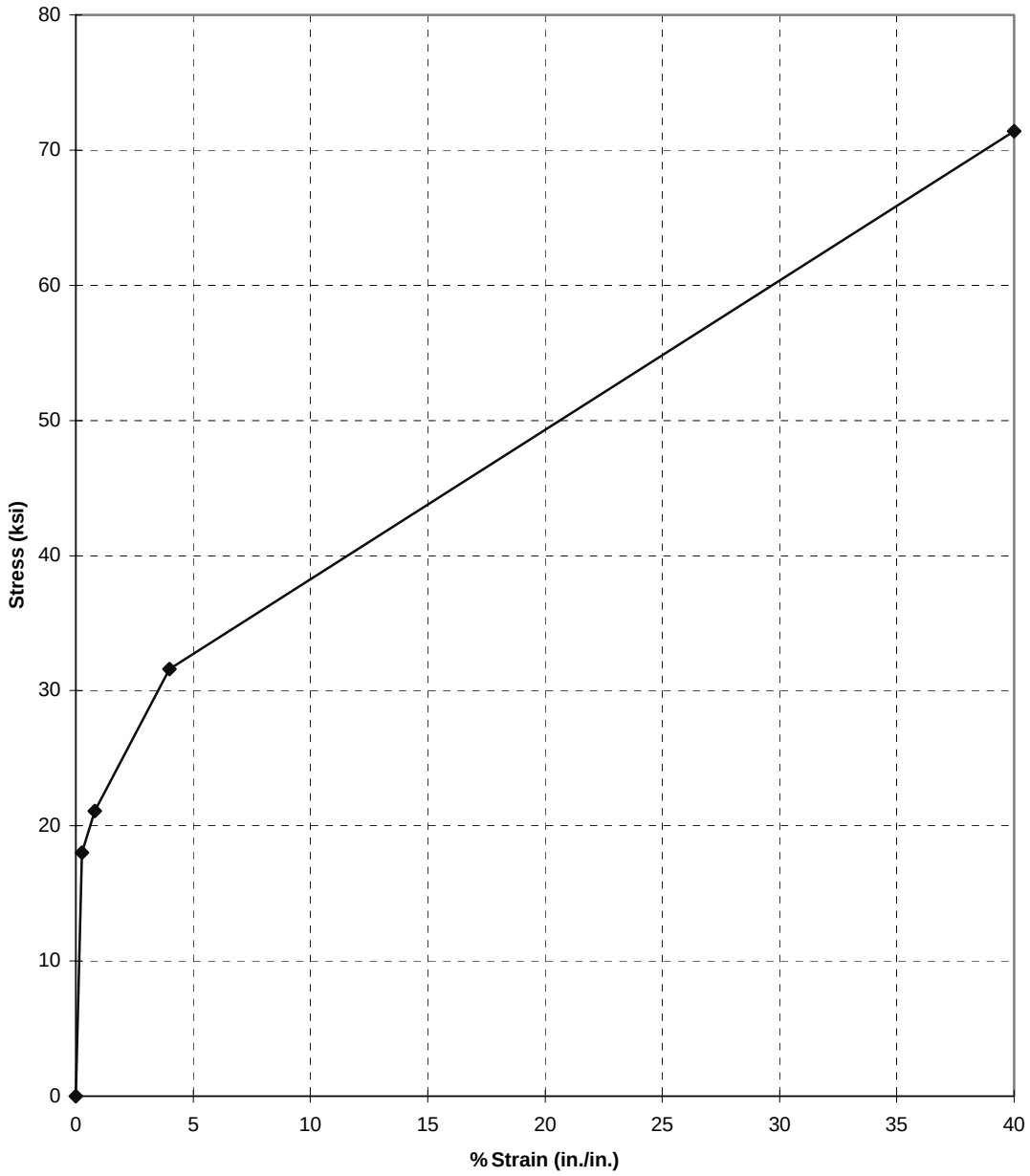

Figure 3.3-1 - Type 316 Stainless Steel Plastic Stress-Strain Curve at 715°F

This page intentionally left blank.

3.4 General Standards for Casks

3.4.1 Chemical and Galvanic Reactions

The service conditions for the W74 canisters include immersion in BWR fuel pools, vacuum drying (hot) conditions, on-site storage conditions (helium backfill), off-site transportation, and potential canister opening (water reflood) conditions. BWR spent fuel pools are generally filled with air saturated, demineralized water having a neutral pH (5.6 to 7.1) and low impurities.

FuelSolutions™ W74M and W74T canisters are constructed from austenitic stainless steel, electroless nickel (EN) coated carbon steel, and borated stainless steel (used for neutron absorber panels). The corrosion of austenitic stainless steels is generally extremely low, as these materials quickly form a protective passive film in the spent fuel pool environments. The EN coating on carbon steel spacer plates is for corrosion protection following canister fabrication, and for the brief immersion period during fuel loading and canister sealing.

Electroless nickel coatings are widely used for corrosion protection and wear resistance in the electronics, petrochemical, automotive, and food industries, most often on steel and alloy steel substrates. During immersion and subsequent canister sealing, hydrogen production is relatively low. When compared to carbo-zinc or aluminum flame spray coating systems in boric acid, the hydrogen generation rate of EN is much lower than that of carbo-zinc and in the same range as aluminum flame spray. Once the canister is drained, dried, sealed, and backfilled with helium, the corrosion mechanism is removed and the EN coating is inert during storage.

The W74M and W74T canisters are evaluated to determine the potential for chemical, galvanic, or other reactions in the intended service conditions, as required by NRC Bulletin 96-04.[14] The hydrogen generation analysis of the W74 canisters considers the effects of radiolytic generation of spent fuel pool water and corrosion of the canister materials under the most limiting service conditions. The results of the hydrogen generation analysis show that the estimated time to reach a concentration limit of 10% of the Lower Explosive Limit (LEL) (0.4% hydrogen by volume) in the canister cavity is approximately 42 hours. Therefore, there will be continuous monitoring for combustible gases prior to and during all welding, cutting, grinding or other spark producing activities until the canister has been drained down (loading), or until the inner closure plate has been removed from the canister (unloading). If necessary, the canister cavity may also be purged with an inert gas after the small volume of water is removed during loading or unloading activities as an additional measure against combustible gas buildup and to provide a means to reduce combustible gas concentration levels below 10% of the LEL. Further discussion of the procedures for monitoring and purging the canister during welding and canister opening are provided in Sections 8.1 and 8.2 of the FuelSolutions™ Storage System SAR.

The FuelSolutions™ W74 damaged fuel can is fabricated from the same materials as the guide tube assemblies. Thus, the presence of the damaged fuel cans has no significant effect on the potential for chemical, galvanic, and other reactions in the intended service conditions.

[14] NRC Bulletin 96-04,*Chemical, Galvanic, or Other Reactions in Spent Fuel Storage and Transportation Casks*, United States Nuclear Regulatory Commission Office of Nuclear Reactor Regulations, OMB No. 3150-0011, July 5, 1996.

3.4.2 Positive Closure

The FuelSolutions™ W74 canister is welded shut, and has no penetrations. The canister is confined within the transfer cask during movement to or from the ISFSI site, and confined within the storage cask during dry storage. Both the transfer cask and the storage cask have bolted closures to secure and retain the canister within the cavity of these casks during normal operations, as described in the FuelSolutions™ Storage System SAR.

3.4.3 Lifting Devices

The lifting and handling features of the FuelSolutions™ W74 canister are designed as special lifting devices in accordance with the requirements of ANSI N14.6[15] for critical lift conditions, including vertical canister transfer, vertical lift of the empty canister prior to fuel loading, and vertical lifts of the canister top shield plug and top closure plates.

During vertical canister transfer operations, the sealed W74 canister is lifted and lowered vertically using the canister vertical lift fixture described in Section 1.2.1.4.3 of the FuelSolutions™ Storage System SAR which engage with a lift adapter which bolts onto the canister top outer closure plate. The canister shell top closure plate and its attachment weld to the canister shell are designed in accordance with ANSI N14.6 stress design factors for non-redundant lifting devices of six against yield and ten against ultimate for this condition. Therefore, the allowable stress for the W74 canister shell, conservatively based on the weaker SA-240, Type 304 material of the W74T canister shell at an upper bound design temperature of 300°F, is 3.75 ksi. The vertical canister transfer design load is based on a bounding canister weight of 82.8 kips plus an additional 15% factor to account for dynamic effects or 95.2 kips.

In accordance with Section 3.2.1.2 of ANSI N14.6, the stress design factors are not intended to apply to situations where high local stresses are relieved by slight yielding of the material, such as the top outer closure plate to shell weld structural discontinuity. Therefore, the structural evaluation of the top outer closure plate for the vertical canister transfer loading is performed assuming no edge bending restraint is provided by the canister shell and closure weld. The maximum bending stress due to the vertical canister transfer load is calculated for a simply supported circular plate subjected to an annular line load at the lifting plate bolt circle (Roark,[16] Table 24, case 9a, r_o = 28.5 inches, a = 32.375 inches, t = 2.0 inches) as follows:

$$\sigma = \frac{6M}{t^2} = \frac{6L_9 wa}{t^2}$$

The uniform annular line load due to the 95.2 kip lifting load distributed around the 57.0 inch diameter bolt circle is 532 pounds per inch, and the value of L_9 for r_o/a equal to 0.8803 (=28.5/32.375) is 0.1076. The bending stress due to the vertical canister transfer load is 2.78 ksi. Thus, the design margin for the ANSI N14.6 requirement is:

$$DM = \frac{3.75}{2.78} - 1 = +0.35$$

[15] ANSI N14.6, *Special Lifting Devices for Shipping Containers Weighing 10,000 Pounds (4,500 kg) or More*, American National Standards Institute, 1993.

[16] Young, W.C., *Roark's Formulas of Stress and Strain*, Sixth Edition, McGraw-Hill Book Company, 1989.

The maximum thread shear stress in the top closure plate for a bounding vertical lift load of 95.2 kips is determined as follows:

$$\tau = \frac{V}{A} = 1.80 \text{ ksi}$$

where:

V = 5.95 kips/bolt, bolt tensile load (= 95.2 kips/16 bolts).

A = $A_I L_e$, thread shear area.

A_I = 2.648 in^2, 1-1/8 - 7 UNC-2B thread shear area per inch of thread engagement per Boucher.[17]

L_e = 1.25 in., minimum thread engagement for 1.50 inch deep bolt hole.

The allowable thread shear stress taken as one sixth of the shear yield strength ($0.6S_y$), or 2.25 ksi. Therefore, the W74 canister top outer closure plate meets the ANSI N14.6 stress requirements for the vertical canister transfer loading.

The average shear stress in the top outer closure weld due to the vertical lift load of 95.2 kips is determined using hand calculations. The total shear area of the top outer closure weld, based on the minimum weld throat of 0.63 inches, is 126.7 in^2. The resulting average shear stress in the top outer closure weld for the vertical lift condition is 0.75 ksi. The allowable shear stress taken as one sixth of the base metal shear yield strength ($0.6S_y$), or 2.25 ksi. Therefore, the W74 canister top outer closure weld meets the ANSI N14.6 stress requirements for the vertical canister transfer loading.

The empty W74 canister, including the shell assembly and the upper and lower basket assemblies, is lifted vertically from the top shield plug support bars with a lifting device similar to that described in Section 1.2.1.4.4 of the FuelSolutions™ Storage System SAR and placed into the transfer cask prior to loading fuel. The maximum weight of the empty W74 canister without the top shield plug and top closure plates is approximately 34.7 kips. A bounding weight of 37 kips is conservatively used. Therefore, the design load for this lift condition, including an additional 15% factor to account for dynamic effects, is 42.6 kips. The canister is lifted using four of the eight shield plug support bars. The governing stress for this lift condition is due to pure shear in the support bar attachment weld. Each support bar is welded to the canister shell by two 5/16-inch by 10.5-inch long partial penetration groove welds. Therefore, the average weld shear stress for the vertical lift of the empty W74 canister is:

$$\tau = \frac{42.6}{8\text{x}0.31\text{x}10.5} = 1.64\text{ksi}$$

The allowable weld shear stress is equal to one-third of the shear yield strength of the base material, where the shear yield is taken as 60% of the tensile yield strength or 18 ksi for Type 304 stainless steel at room temperature. Therefore, the allowable weld shear stress is 6.0 ksi. Thus, the design margin for the ANSI N14.6 requirement is +2.66.

[17] Boucher, R., *Strength of Threads*, Product Engineering, November 27, 1961.

The canister top shield plug, inner closure plate, and outer closure plate are each lifted from four attachment points on the top surface of the plates for placement on the canister inside the spent fuel building. For design purposes, the full weight of the components is assumed to be supported by two lifting attachments. The design load for each attachment includes an additional 15% allowance for crane hoist motion. In accordance with ANSI/ASME B30-9,[18] the standard lifting slings and lifting attachments have a minimum ultimate capacity exceeding 5 times the design load.

As discussed in Section 3.1.1, the loaded FuelSolutions™ W74 damaged fuel can is lifted vertically. The vertical lift evaluation of the damaged fuel can is performed using a bounding BRP fuel assembly weight of 485 pounds plus the damaged fuel can self-weight. In addition, the vertical lift load is increased by 15% to account for possible crane hoist motion.

The structural evaluation of the damaged fuel can for the vertical lift condition is performed using classical hand calculations. Evaluations are performed to determine the maximum shear and bending stresses in the bottom end plate and bottom end plate attachment weld. In addition, the maximum direct tensile stress, bearing stress, and shear tear-out stress at the top end of the damaged fuel can near the slotted holes from which the damaged fuel can is supported during a vertical lift are evaluated. The results of the evaluation demonstrate that the maximum stresses and stress intensities in the damaged fuel can due to the vertical lift condition are all lower than the corresponding Service Level A allowable stresses and stress intensities.

The maximum bending and shear stress in the bottom end plate of the damaged fuel can are conservatively calculated for a simply supported square plate subjected to a uniform pressure load using Roark,[19] Table 26, case 1a. The uniform pressure load on the plate due to the weight of the fuel assembly plus the bottom end plate self-weight, including a 15% increase to account for dynamic effects, is 15 psi. The resulting maximum shear and bending stresses in the bottom end plate are 0.4 ksi and 14.6 ksi, respectively. The corresponding membrane plus bending stress intensity is 14.6 ksi. The allowable Service Level A membrane plus bending stress intensity for SA-240, Type 316 stainless steel at a bounding design temperature of 700°F is 24.5 ksi. Therefore, the minimum design margin in the damaged fuel can bottom end plate for the vertical lift condition is +0.68.

The bottom end plate is connected to the damaged fuel can tube with an all-around 0.09-inch fillet weld. The minimum required weld size is calculated using the maximum edge shear load from the bottom end plate evaluation (R = 0.04 kip/in.) and an allowable Service Level A weld shear stress of 3.4 ksi, equal to the base metal allowable from above with a 35% weld efficiency factor for a fillet weld with surface visual inspection in accordance with Table NG-3352-1 of the ASME Code. The resulting minimum required fillet weld size is 0.02-inches [= 0.04/(0.707 x 3.4)]. Therefore, the 0.09-inch fillet weld size provided is adequate.

The maximum direct tensile stress in the side wall of the damaged fuel can occurs at the top end of the damaged fuel can. The total axial load due to the weight of the fuel assembly plus a bounding weight of 130 pounds for the damaged fuel can, including a 15% increase to account for dynamic effects, is 0.71 kips. The net cross-sectional area of the tube at the location of the

[18] ANSI/ASME-30-9-1984, *Slings.*

[19] Young, W. C., *Roark's Formulas of Stress and Strain*, Sixth Edition, McGraw-Hill Book Company, 1989.

slotted holes for the top lid assembly engagement dogs is 2.34 in^2. The resulting tensile stress in the tube is 0.3 ksi. There is no shear stress. The corresponding membrane stress intensity is 0.3 ksi. The allowable Service Level A primary membrane stress intensity for SA-240, Type 316 stainless steel at a bounding design temperature of 700°F is 16.3 ksi. Therefore, the minimum design margin for general primary membrane stress in the damaged fuel can side wall is +53.3.

The maximum bearing stress in the damaged fuel can side wall at the interface with the top lid assembly engagement dogs is evaluated assuming that the vertical lift load is supported by only two engagement dogs. Therefore, the total load per engagement dog is 0.36 kips. The projected bearing area of the engagement dog is 0.028 in^2 (= 0.09” x 0.31”). Therefore, the average bearing stress in the tube is 12.9 ksi. The allowable Service Level A bearing stress is limited to the material yield strength, or 18.1 ksi for SA-240, Type 316 stainless steel at a bounding design temperature of 700°F. Therefore, the minimum design margin for bearing stress in the tube side wall is +0.40.

Shear tear-out of the tube side wall is also evaluated assuming that the vertical lift load is supported by only two engagement dogs. The total shear area per side, conservatively based on the minimum edge distance between the slotted hole and the top end of the tube, is 0.18 in^2 (= 2 x 0.09” x 1.0”). Therefore, the shear tear-out stress is 2.0 ksi compared to an allowable shear stress of 9.8 ksi. The minimum design margin for shear tear-out stress in the tube side wall is +3.90.

The structural evaluation of the damaged fuel can top lid assembly for the vertical lift condition is performed using a combination of classical hand calculations and finite element analysis. The stresses in the top lid handle and attachment hardware are evaluated using classical hand calculations. The stresses in the top lid base plate are evaluated using finite element analysis. The results of the structural evaluation demonstrate that the maximum stresses in the top lid assembly due to the vertical lift condition are all lower than the corresponding Service Level A allowable stresses and stress intensities.

The shear stress at the small end of the engagement dog which interfaces with the tube are calculated for the 0.36 kip vertical lift design load. The shear area at the small end of the engagement dog is 0.12 in^2 (= 0.31” x 0.38”). The resulting shear stress is 3.0 ksi compared to an allowable shear stress of 9.8 ksi. The minimum design margin for shear stress in the engagement dog is +2.27.

The maximum stresses in the top lid handle due to the vertical lift load are calculated using simple beam theory. The governing tensile, shear, and bending stresses in the handle due to the vertical lift load are 0.7 ksi, 0.4 ksi, and 12.0 ksi, respectively. These results show that the bending stress in the handle controls. The corresponding membrane plus bending stress intensity is 12.7 ksi. The allowable Service Level A primary membrane plus bending stress intensity for SA-240, Type 316 stainless steel at a bounding design temperature of 700°F is 24.5 ksi. Therefore, the minimum design margin in the damaged fuel can top lid handle for the vertical lift condition is +0.90.

The top lid handle is connected to the base plate at each of the four vertical legs with full penetration groove welds. The allowable weld stresses are equal to those of the base metal multiplied by the appropriate weld efficiency factor. Per Table NG-3352-1 of the ASME code, the weld efficiency factor for a full penetration weld with surface PT examination is 0.65. Therefore, the allowable primary membrane plus bending stress intensity for the weld is 15.9 ksi.

The governing tensile, shear, and bending stresses at the weld location are 0.4 ksi, 0.7 ksi, and 12.0 ksi, respectively. The corresponding maximum primary membrane plus bending stress intensity in the handle is 12.5 ksi. Conservatively assuming this stress occurs in the weld, the minimum design margin for the handle attachment weld is +0.27.

The stresses in the damaged fuel can top lid assembly base plate due to the vertical lift condition are evaluated using the ¼-symmetry finite element model shown in Figure 3.4-1. The base plate is modeled using elastic shell elements (SHELL63) with a 3/8-inch uniform thickness. The slotted holes that accommodate the engagement hardware are included in the model. Symmetry boundary conditions are applied at the two planes of symmetry, as shown in Figure 3.4-1. In addition, the nodes at the location of the handle are restrained in the vertical direction (i.e., UZ=0).

The loads applied to the model are determined based on a bounding weight of 720 pounds for the BRP fuel assembly and the damaged fuel can. Each attachment dog supports one fourth of the total design load, or 180 pounds. The loads applied to the finite element model are determined assuming that the attachment dog behaves as a rigid beam.

A free body diagram of the attachment dog for the vertical lift condition is shown in Figure 3.4-2. Based upon the principal of static equilibrium, the reaction loads R_1 and R_2 are determined to be +285 pounds (upward) and –105 pounds (downward), respectively. The reaction load at the outside attachment bolt (i.e., R_1) is applied to the nodes around the perimeter of the slotted hole at the outside end, as shown in Figure 3.4-1. The reaction load at the inner end of the attachment dog (i.e., R_2) is applied to the base plate nodes corresponding to the end of the attachment dog when in the extended position, as shown in Figure 3.4-1.

As shown in Figure 3.4-3, the results of the finite element evaluation show that the maximum stresses in the top lid assembly base plate occur in the region at the corner of the rectangular cutout. The maximum general primary membrane (P_m), primary membrane plus bending (P_L+P_b), and primary plus secondary (P_L+P_b+Q) stress intensities are 10.4 ksi, 17.5 ksi, and 28.8 ksi, respectively. The corresponding Service Level A general primary membrane, primary membrane plus bending, and primary plus secondary stress intensities for SA-240,Type 316 stainless steel at 700°F are 16.3 ksi, 24.5 ksi, and 48.9 ksi, respectively. Therefore, the minimum design margin in the top lid assembly base plate for the vertical lift condition is +0.40, due to primary membrane plus bending.

3.4.4 Canister Service Life

The term of the 10CFR72, Subpart L C of C granted by the NRC is for 20 years. Nonetheless, the FuelSolutions™ W74 canister is designed for 100 years of service while satisfying the conservative design requirements defined in Chapter 2 of this SAR, including the regulatory requirements of 10CFR72. In addition, the canister is designed, fabricated and inspected in accordance with the applicable requirements of the ASME Code as described in Section 2.1.2 under the comprehensive Quality Assurance program discussed in Chapter 13 of the FuelSolutions™ Storage System SAR which assures high design margins, the use of materials with known characteristics, high quality fabrication, and verification of compliance through rigorous inspection and testing as described in Chapter 9 of this SAR. Technical specifications, as defined in Chapter 12 of this SAR and the FuelSolutions™ Storage System SAR, have been

developed and imposed on the canister which assure that the integrity of the canister and the contained SNF assemblies are maintained throughout the 100 year service life of the canister.

The inclusion of BRP MOX, partial, and damaged fuel assemblies in the FuelSolutions™ W74 canister has no significant effect on principal design considerations that bear on the canister service life.

The principal design considerations which bear on the adequacy of the FuelSolutions™ W74 canister for the design basis service life and the means in which they are addressed follows:

Corrosion

All canister materials which are susceptible to corrosion or that come in contact with the SNF assemblies are fabricated from corrosion resistant austenitic stainless steel, as described in Section 3.1.1. In addition the associated weld filler metal (see Table 3.3-1 and Table 3.3-2) utilized for the canister is selected to provide the same level of corrosion protection as the base metal. The corrosion resistant characteristics of such materials for dry SNF storage canister applications, as well as the protection offered by these materials against other material degradation effects such as radiation embrittlement, aging and creep, are discussed in EPRI TR-102462.[20] The canister is vacuum dried to remove all oxidizing liquids and gasses, and back-filled with dry inert helium at the time of closure to maintain a atmosphere in the canister to provide corrosion protection for the canister basket assembly and SNF cladding throughout the dry storage period. The preservation of this non-corrosive atmosphere is assured by the canister confinement boundary integrity as described in Section 7.1 of this SAR.

Structural Fatigue

The passive non-cyclic nature of dry storage conditions do not subject the canister to conditions which might lead to a structural fatigue failure. Ambient temperature and insolation cycling during normal dry storage conditions and the resulting fluctuations in canister thermal gradients and internal pressure is the only mechanism for fatigue. These low stress, high cycle conditions will not lead to a fatigue failure of the canister. All other off-normal or postulated accident conditions are infrequent or one time occurrences which do not lead to fatigue failures. The effects of fatigue on the canister are specifically evaluated for a 100 year service life in Section 3.5.1.4 and is shown to meet the applicable requirements of the ASME Code. In addition, the canister utilizes materials which are not susceptible to brittle fracture or which have sufficient fracture toughness to resist brittle fracture during extreme cold conditions, as discussed in Section 3.1.2.3.

Maintenance of Helium Atmosphere

The inert helium atmosphere in the canister provides a non-oxidizing environment for the SNF cladding to assure its integrity during long term dry storage. The preservation of the helium atmosphere in the canister is assured by the robust design of the canister confinement boundary described in Section 7.1 of this SAR. Maintaining an inert environment in the canister mitigates conditions that might otherwise lead to SNF cladding failures. The required mass quantity of helium which is back-filled into the canister at the time of closure as defined in the *technical specification* contained in Section 12.3 of this SAR, and the associated leak tightness

[20] EPRI TR-102462, *Shipment of Spent Fuel in Storage Canister*, Electric Power Research Institute, June 1993.

requirements for the canister defined in the *technical specification* contained in Section 12.3 of the FuelSolutions™ Storage System SAR, are specifically derived to assure that an inert helium atmosphere is maintained in the canister throughout the 100 year service life. Further discussion on the basis for the amount of helium required and the development of the leak rate acceptance basis is provided in Section 4.4.1.9 of this SAR.

Allowable Fuel Cladding Temperatures

The helium atmosphere in the canister promotes heat removal and thus reduces SNF cladding temperatures during dry storage. In addition, the SNF decay heat will substantially decay over a 100 year dry storage period. Maintaining the fuel cladding temperatures below allowable levels during long term dry storage mitigates the damage mechanisms which might otherwise lead to SNF cladding failures. The allowable long term SNF cladding temperatures utilized for thermal acceptance of the canister design are conservatively based on a 100 year service life, as discussed in Section 4.3.2 of this SAR. This additional conservatism results in lower allowable cladding temperatures than would otherwise result from shorter time periods and increased design margin.

Neutron Absorber Boron Depletion

The effectiveness of the fixed borated neutron absorbing material utilized in the canister basket design requires that sufficient concentrations of boron be present to assure criticality safety during worst case design basis conditions over the 100 year service life of the canister. Information on the characteristics of the borated neutron absorbing material utilized in the canister basket assembly is provided in Section 1.5.2.1 of this SAR. The relatively low neutron flux, which will continue to decay over time, to which this borated material is subjected does not result in significant depletion of the material's available boron to perform its intended safety function. In addition, the boron content of the material used in the criticality safety analysis is conservatively based on the minimum specified boron concentration (rather than the nominal) verified by testing during material manufacture which is further reduced by 25% for analysis purposes, as described in Section 6.3.2 of this SAR. Thus, sufficient levels of boron are present in the basket assembly neutron absorbing material to maintain criticality safety function over the 100 year service life of the canister.

The above findings are consistent with those of the NRC's Waste Confidence Decision Review[21] which concluded that dry storage systems designed, fabricated, inspected and operated in accordance with such requirements are adequate for a 100 year service life while satisfying the requirements of 10CFR72.

[21] Title 10, U.S. Code of Federal Regulations, Part 51 (10CFR51), *Waste Confidence Decision Review*, U.S. Nuclear Regulatory Commission, September 11, 1990.

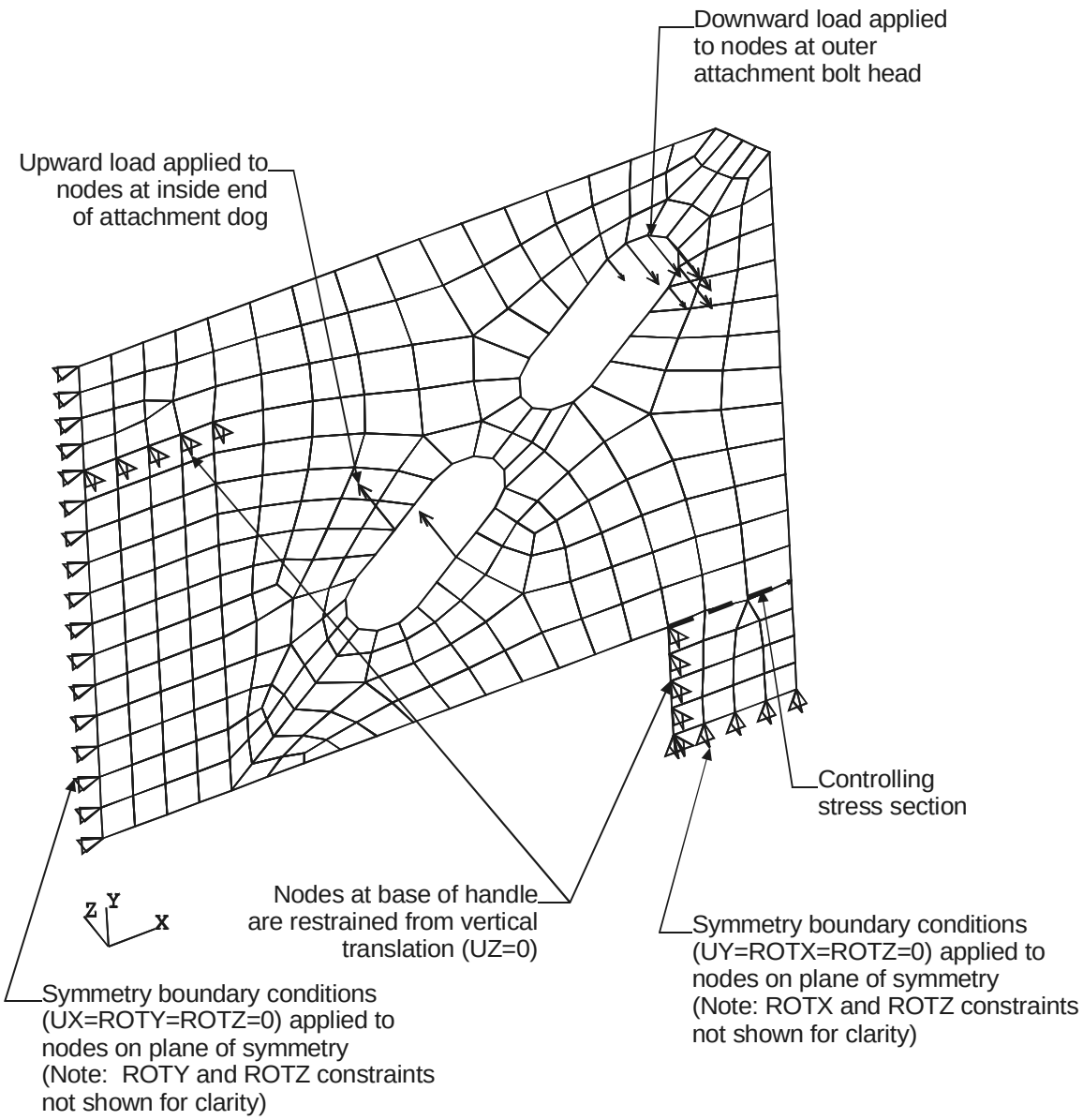

Figure 3.4-1 - W74 Damaged Fuel Can Top Lid Assembly Base Plate ¼-Symmetry Finite Element Model

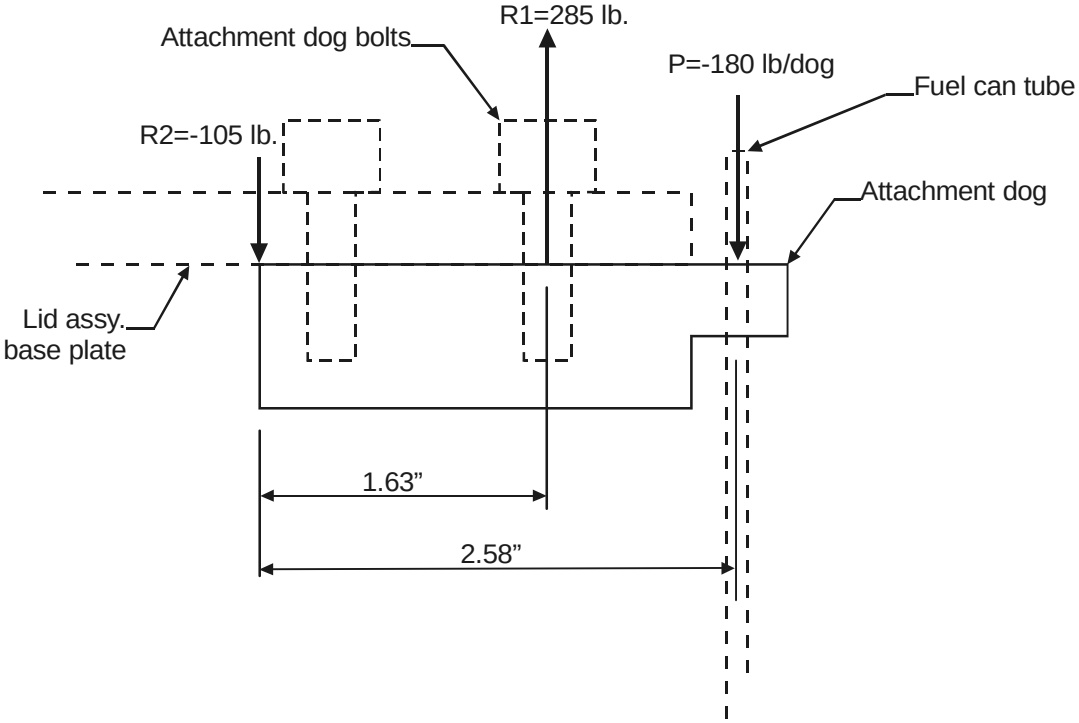

Figure 3.4-2 - Free Body Diagram of Attachment Dog for Vertical Lift

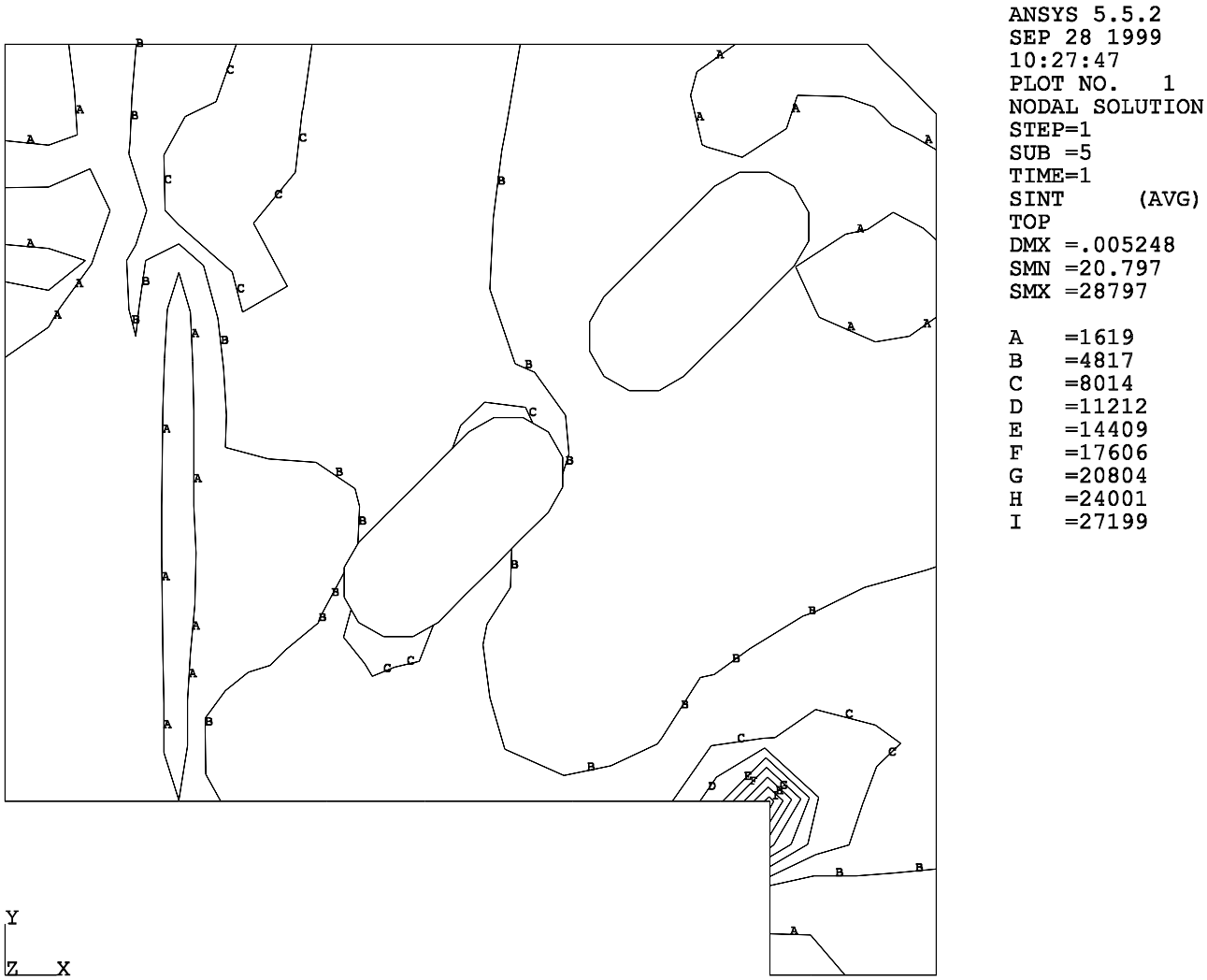

Figure 3.4-3 - W74 Damaged Fuel Can Top Lid Base Plate Vertical Lift Stress Intensity Contour Plot

This page intentionally left blank.

3.5 Evaluation of Normal Conditions

The FuelSolutions™ W74 canister is evaluated for loads occurring during normal or routine operation. Normal conditions are defined in accordance with ANSI/ANS-57.9[22] and include loads which occur regularly during normal operation. As defined in Section 2.4.1 of this SAR, normal loads considered in the structural evaluation of the FuelSolutions™ W74 canister include the following:

- Normal temperature and insolation loading
- Normal internal pressure
- Dead weight
- Normal handling

The results of the structural evaluations performed herein demonstrate that the FuelSolutions™ W74 canisters described in Section 1.2.1.3 can withstand the effects of normal load conditions without affecting structural safety function and remain in compliance with the applicable acceptance criteria. The following sections present the evaluation of the FuelSolutions™ W74 canister for the design basis normal conditions which demonstrate that the requirements of 10 CFR 72.122 are satisfied.

The structural evaluations of the canister shell assembly are performed for the bounding canister design, determined to be the W74T canister as discussed in Section 3.1.1.1. The basket assembly structural evaluations are performed for the bounding components as described in Section 3.1.1.2. The load combinations evaluated for normal conditions are defined in Table 2.3-1. The normal load combination evaluations are provided in Section 3.5.5.

The evaluation of the FuelSolutions™ W74 canister for BRP MOX, partial, and damaged fuel assemblies for normal operating conditions considers the effect these fuel assemblies have on the existing structural evaluation of the W74 canister shell assembly and basket assemblies. The structural evaluation of the FuelSolutions™ W74 damaged fuel can for normal conditions is included in this section.

With the exception of the vertical handling evaluation presented in Section 3.4.3, the structural evaluation of the FuelSolutions™ W74 damaged fuel can is based on the results of the FuelSolutions™ guide tube assembly structural evaluation. As discussed in Section 3.1.1, the design of the FuelSolutions™ W74 damaged fuel can is similar to that of the guide tube assembly. The damaged fuel can is fabricated from the same material and has the same cross-section properties as the guide tube. The total weight of the damaged fuel can is slightly higher than that of the guide tube (121 pounds versus 84 pounds) due to the inclusion of the top lid assembly, bottom end plate, and four neutron absorber panels (versus two per guide tube).

Another significant difference between the damaged fuel cans and the guide tubes is the basket assembly interfaces. The damaged fuel cans are placed within the support tube openings, whereas the guide tubes are positioned inside the spacer plate openings. Thus, when subjected to

[22] ANSI/ANS-57.9, *Design Criteria for an Independent Spent Fuel Storage Installation (Dry Storage Type)*, American National Standards Institute, 1984.

lateral loads, the damaged fuel can receives continuous support from the support tubes and the guide tubes are supported intermittently by the spacer plates.

The evaluation of the effects of normal conditions on the storage cask and transfer cask are provided in the FuelSolutions™ Storage System SAR.

3.5.1 Normal Temperature and Insolation Loadings

The FuelSolutions™ W74 canister is evaluated in the transfer cask and storage cask for steady state thermal gradients resulting from normal ambient conditions and the design basis heat load. As discussed in Chapter 4 of this SAR, a bounding axial heat flux profile is used to calculate the W74 canister temperatures for normal transfer and storage conditions. The FuelSolutions™ W74 canister temperatures are calculated for a range of normal ambient conditions for the design basis fuel decay heat load. The normal thermal conditions are identified as follows:

Normal Average: Steady state thermal gradients resulting from a lifetime average ambient temperature of 77°F, maximum fuel decay heat, and insolation in accordance with 10CFR71.71(c)(1) averaged over a 24 hour period.

Normal Cold: Steady state thermal gradients resulting from an ambient temperature of 0°F, maximum fuel decay heat, and no insolation.

Normal Hot: Steady state thermal gradients resulting from an ambient temperature of 100°F, maximum fuel decay heat, and insolation in accordance with 10CFR71.71(c)(1) averaged over a 24 hour period.

The temperature distribution in the canister for the normal thermal conditions are determined in Chapter 4 of this SAR. The canister stresses due to the governing thermal conditions are combined with those due to other normal operating loads, including dead weight, normal handling, and internal pressure loads. The stresses due to each of the individual normal load conditions are addressed in the following sections and the combined effects are calculated in Section 3.5.5. The results of the canister structural evaluation for normal design loads show that the FuelSolutions™ W74 canister satisfies the applicable design criteria.

As discussed in Chapter 4 of this SAR, the FuelSolutions™ W74 canister thermal design loads for normal conditions bound those for a FuelSolutions™ W74 canister containing any amount of intact BRP MOX fuel and partial fuel assemblies, and up to eight damaged fuel assemblies. Therefore, the FuelSolutions™ W74 canister shell assembly and basket assembly stresses calculated for the design basis normal thermal loads are bounded for a FuelSolutions™ W74 canister containing any amount of intact BRP MOX fuel and partial fuel assemblies, and up to eight damaged fuel assemblies.

3.5.1.1 Summary of Pressures and Temperatures

The canister shell assembly provides primary confinement for on-site transfer and storage conditions. As shown in Chapter 4 of this SAR, the maximum internal pressure for the normal hot thermal conditions is 9.8 psig with no rod failures. Conservatively assuming 1% of the fuel rods fail under normal conditions of storage results in a maximum internal pressure of 10.0 psig. The canister shell assembly is evaluated for a bounding normal condition design internal pressure of 10 psig. The canister basket assembly does not serve any pressure retaining function.

The temperatures in the FuelSolutions™ W74 canister for the normal on-site transfer and storage thermal conditions are calculated in Section 4.4 of this SAR. The maximum W74 canister temperatures for normal thermal conditions within the storage cask and within the transfer cask, and the bounding temperatures upon which the component material properties are based for calculating allowable stresses are summarized in Table 3.5-1.

As discussed in Chapter 4 of this SAR, the temperature differential between the W74 support tube and the damaged fuel can is approximately 12°F. As shown in Table 3.5-1, the maximum temperatures for the W74 support tube and guide tube for normal storage and transfer conditions are 683°F and 716°F, respectively. Accounting for the 12°F temperature differential between the support tube and the damaged fuel can, the maximum temperature of the damaged fuel can for the same condition is approximately 695°F. Therefore, the guide tube temperatures bound the maximum temperature of the damaged fuel can. The guide tube design temperature of 715°F is conservatively used for the structural evaluation of the damaged fuel can.

3.5.1.2 Differential Thermal Expansion

Differential thermal expansion of the W74M canister components and the storage cask or transfer cask is evaluated. The results of this evaluation demonstrate that the canister shell assembly expands freely within the storage cask and transfer cask cavities under all normal, off-normal, and accident thermal conditions. Similarly, the basket assembly components expand freely within the canister shell under all normal, off-normal, and accident conditions. The differential thermal expansion evaluation is discussed in the following subsections.

3.5.1.2.1 Canister Shell Assembly

The FuelSolutions™ W74 canisters are all designed to expand freely inside the storage cask and transfer cask under all normal, off-normal, and accident on-site storage and transfer thermal conditions. Differential thermal expansion between the canister shell and the transfer cask or storage cask is addressed in the FuelSolutions™ Storage System SAR.[23] The canister shell expands freely under the most severe thermal loading.

3.5.1.2.2 Canister Basket Assembly

The FuelSolutions™ W74 basket assembly expands freely within the canister shell assembly as shown by the basket assembly differential thermal expansion evaluation. This evaluation considers the radial and longitudinal growth of the basket assemblies within the canister cavity.

Spacer Plates

The diametral clearance between the shell and the basket is governed by the differential thermal expansion of the spacer plates and the canister shell. This relative expansion is calculated using the temperature differential between the two components at the hottest axial section because the heat flux and, therefore, the temperature gradient are maximized at that section. The worst case temperature differential between the spacer plates and the canister shell is obtained from the thermal analysis (Table 4.5-3) and corresponds to the highest canister heat load and the coldest

[23] WSNF-220, *FuelSolutions™ Storage System Final Safety Analysis Report*, NRC Docket Number 72-1026, BNFL Fuel Solutions Corporation.

ambient air temperature (e.g., the off-normal cold storage condition). The carbon steel general spacer plates are much hotter than the stainless LTP spacer plates and engagement spacer plate and, therefore, govern despite the somewhat lower coefficient of thermal expansion. The diametral thermal expansion (δ_D) of the spacer plates relative to the canister shell is calculated as follows:

$$\delta_D = D\left[\alpha_{sp}(T_{sp} - 70) - \alpha_{sh}(T_{sh} - 70)\right] = 0.11\text{-inch}$$

where:

D = 64.75 inches, inside diameter of the canister shell

T_{sp} = 571°F, maximum temperature of the general spacer plate for off-normal cold storage thermal condition

α_{sp} = 7.32×10^{-6} in/in/°F, mean coefficient of thermal expansion for the general spacer plate material (SA-517 or A514, Grades F or P carbon steel) at an upper bound temperature of 600°F

T_{sh} = 291°F, corresponding temperature of the canister shell at the location of the hottest general spacer plate for the off-normal cold storage thermal condition

α_{sh} = 8.86×10^{-6} in/in/°F, mean coefficient of thermal expansion for the shell material (SA-240, Type 316 stainless steel) at a lower bound temperature of 250°F

This bounding differential expansion is lower than the nominal 0.375-inch diametral clearance provided between the spacer plates and the canister shell. Therefore, the W74 spacer plates expand freely within the canister shell cavity under all normal, off-normal, and accident conditions.

Support Tubes

The support tubes are designed with sufficient axial and transverse clearances to allow free longitudinal and transverse thermal expansion within the canister shell cavity and the spacer plate support tube holes for all normal, off-normal, and accident thermal conditions. The support tube differential thermal expansion evaluation is performed using hand calculations, as described below.

The support tube longitudinal differential thermal expansion evaluation is performed based on the temperature differential at the hottest axial section of the canister. This is conservative because it assumes that the maximum gradient is maintained along the entire cavity length. Similar to the diametral expansion above, the worst case temperature differential between the support tubes and the canister shell results from the off-normal cold storage condition. The axial thermal expansion (δ_L) of the support tubes relative to the canister shell is calculated as follows:

$$\delta_L = L\left[\alpha_t(T_t - 70) - \alpha_{sh}(T_{sh} - 70)\right] = 0.31\text{-inch}$$

where:

L = 173 inches, total length of the canister cavity

T_t = 444°F, maximum temperature of support tube for off-normal cold storage condition (conservatively use an upper bound temperature of 450°F)

α_t = 8.86×10^{-6} in/in/°F, mean coefficient of thermal expansion for the support tube material (SA-240, Type XM-19) at 450°F

T_{sh} = 291°F, corresponding temperature of the canister shell for off-normal cold storage condition (conservatively use a lower bound shell temperature of 250°F)

α_{sh} = 8.90×10^{-6} in/in/°F, mean coefficient of thermal expansion for the canister shell material (SA-240, Type 304) at 250°F.

The calculated axial expansion is smaller than the minimum 0.4-inch nominal longitudinal clearance provided between the support tubes and the canister shell cavity. Therefore, the W74 support tubes expand freely in the longitudinal direction under all normal, off-normal, and accident conditions.

Transverse differential thermal expansion between the support tube and the corresponding holes in the W74 general spacer plates is evaluated to assure that the clearance provided is sufficient to accommodate bowing of the support tubes due to transverse thermal gradients. The maximum transverse thermal gradient across the support tube is 83°F and occurs for the off-normal cold storage condition. Conservatively using the maximum transverse thermal gradient along the entire length of support tube and a maximum temperature of 700°F, the corresponding upper bound lateral deflection of the support tube at its center is calculated using Roark, Case 6e as follows:

$$\delta = (\alpha L^2/8d) \times \Delta T = 0.073 \text{ inch}$$

where:

L = 82.75 in., maximum distance between top and bottom spacer plate supports (weld to weld)

α = 9.15×10^{-6} in/in/°F, mean coefficient of thermal expansion for the support tube material (SA-479, Type XM-19) at 700°F

d = 8.90 in., depth of the support tube section

ΔT = 83°F, lateral (through depth) temperature difference of the support tube.

This is within the 0.075-inch lateral clearance [(9.05 - 8.90)/2] provided between the support tubes and the corresponding holes in the general spacer plates. Therefore, no interference will occur between the support tubes and the general spacer plates under any normal or off-normal thermal condition.

Guide Tubes

The guide tubes are designed with sufficient transverse and axial clearance to allow free longitudinal thermal expansion within the upper and lower basket assemblies for all normal, off-normal, and accident thermal conditions. The W74 guide tube differential thermal expansion evaluation considers both transverse differential thermal expansion between the guide tubes and the spacer plate openings and longitudinal differential thermal expansion between the guide tubes and the support tubes.

The transverse differential thermal expansion between the guide tube and the general spacer plate openings is calculated based upon an upper bound guide tube and spacer plate temperature of 738°F for all normal and off-normal storage and transfer thermal conditions as follows:

$$\delta_T = D(\alpha_{gt} - \alpha_{cp})\,(T-70) = 0.01 \text{ inches}$$

where:

D = 7.40 inches, Spacer plate maximum hole width.

α_{gt} = 9.82×10^{-6} in/in/°F, mean coefficient of thermal expansion for the guide tube (SA-240, Type 316) at 738°F.

α_{cp} = 7.53×10^{-6} in/in/°F, mean coefficient of thermal expansion for the general spacer plate material (SA-517 or A514, Grades F or P) extrapolated at 738°F.

The nominal clearance between the outside of the guide tube assembly and the general spacer plate opening is 0.17 inches. The minimum clearance remaining between the guide tube and the spacer plate openings is 0.16 inches. Therefore, no transverse interference between the W74 guide tube assemblies and the spacer plates could occur.

The longitudinal differential thermal expansion between the guide tubes and the support tubes is evaluated based on the temperature differential at the hottest axial section of the canister. This is conservative because it assumes that the maximum gradient is maintained along the entire cavity length. The worst case temperature differential between the hottest guide tube and support tubes results from the off-normal cold storage condition. The axial thermal expansion (δ_L) of the hottest guide tube relative to the support tubes is calculated as follows:

$$\delta_L = L\left\lfloor \alpha_{gt}(T_{gt} - 70) - \alpha_{st}(T_{st} - 70) \right\rfloor = 0.19 \text{ inches}$$

where:

L = 85.25 inches, length of the support tubes

T_{gt} = 600°F, upper bound guide tube temperature at the hottest axial location for the off-normal cold storage thermal condition

α_{gt} = 9.60×10^{-6} in/in/°F, mean coefficient of thermal expansion for the guide tube material (SA-240, Type 316) at 600°F

T_{st} = 400°F, average support tube temperature at the hottest axial location for the off-normal cold storage thermal condition

α_{st} = 8.79×10^{-6} in/in/°F, mean coefficient of thermal expansion for the support tube material (SA-240, Type XM-19) at a lower bound temperature of 400°F.

The calculated axial expansion is smaller than the minimum 0.38-inch clearance provided between the support tubes and guide tubes in the W74 basket. The guide tubes are captured between the canister cavity ends and the engagement plate which are spaced by the support tubes. Therefore, since the support tubes are shown to maintain their clearance relative to the canister shell cavity and since the guide tubes are shown maintain their clearance relative to the support tubes, no axial interference would occur.

Hence, the canister shell allows free thermal expansion of its internals in both diametral and axial directions for all normal conditions.

3.5.1.3 Thermal Stress Calculations

This section presents the FuelSolutions™ W74 canister stress analyses for the normal thermal loads. A combination of hand calculations and finite element analyses are used to determine the stresses in the affected canister components.

3.5.1.3.1 Canister Shell Assembly

Thermal stresses in the canister shell assembly are caused primarily by thermal gradients between the cylindrical shell and the top inner and outer closure plates, and between the shell and the bottom end closure plate. The highest stresses in the canister shell assembly result from the thermal condition producing the largest thermal gradients. A comparison of the shell assembly thermal gradients for the normal transfer and storage thermal conditions is provided in Table 3.5-2. These results show that the maximum W74 shell assembly thermal gradients result from the normal cold thermal condition in the transfer cask. A bounding design thermal gradient is used for the thermal stress evaluation of the FuelSolutions™ canister shell assemblies. The bounding axial thermal gradient applied to the length of the canister shell is that of a fourth order polynomial equation developed based upon a curve fit of the bounding canister shell temperatures for the off-normal cold transfer thermal condition with the maximum thermal load. A constant offset temperature is applied to the canister shell temperatures calculated using the polynomial equation to obtain a bounding canister shell temperature of 560°F. As shown in **Error! Reference source not found.**, the design thermal gradient used for the canister shell thermal stress evaluation is much larger than that of the W74 canister shell. For the canister shell radial temperature distribution, a bounding 60°F thermal gradient is applied assuming a cubic variation of temperature versus radial distance from the canister centerline. In this manner, the applied thermal gradient bounds the three key characteristics of the canister shell thermal loading: maximum temperature, maximum axial gradient, and maximum radial gradient.

Thermal stresses in the canister shell assembly are calculated for the bounding thermal condition using the axisymmetric finite element model described in Section 3.9.2.1. The model includes the temperature dependent material properties of SA-240, Type 304 stainless steel, corresponding to the weaker canister shell material.

As discussed in Article NB-3213.12 of the ASME Code,[24] thermal stresses are self-limiting in nature. General thermal stress associated with the gross distortion of the structure is classified as secondary stress. General thermal stresses are taken as the linearized membrane plus bending stress at each stress location. Local thermal stresses, which include peak stresses occurring at the structural discontinuities, do not produce any significant distortion in the canister shell assembly.

The canister shell general thermal stress intensities resulting from the bounding normal thermal condition are summarized in Table 3.5-4. The results show that the maximum general thermal stress intensity in the canister shell is less than the corresponding Service Level A allowable primary plus secondary stress intensity.

[24] The American Society of Mechanical Engineers (ASME) Boiler and Pressure Vessel Code, Section III, Division 1, Subsection NB, 1992 Edition with 1994 Addenda.

3.5.1.3.2 General and LTP Spacer Plates

The FuelSolutions™ W74 basket assembly general spacer plates and LTP spacer plates are evaluated for thermal stresses resulting from the range of normal thermal conditions. Spacer plate thermal stresses are primarily due to radial thermal gradients. These stresses are highest for the spacer plates located in the middle of the basket assembly since the radial thermal gradients are largest in this region. In addition, thermal stresses in the top and bottom end spacer plates in each basket assembly can also result from moment reactions at the support tube connections due to support tube curvature resulting from radial thermal gradients through the support tube cross section. The spacer plate stresses due to both of these effects are calculated separately and added together absolutely and irrespective of location to determine the maximum spacer plate thermal stresses.

The spacer plate radial thermal gradients resulting from normal thermal conditions in the storage cask and in the transfer cask are provided in Chapter 4 of this SAR. The spacer plate radial thermal gradients and the resulting thermal stresses are generally highest for the condition with the maximum internal heat generation rate and the lowest ambient air temperature. This is verified by evaluated both the hottest general spacer plate and hottest LTP spacer plate for the radial thermal gradients for all normal storage and transfer thermal conditions. The results show that the maximum thermal stresses in the general spacer plate result from normal cold storage condition. Similarly, the maximum thermal stresses in the LTP spacer plate result from the normal cold transfer thermal condition. The details of the spacer plate thermal stress analysis are discussed in the following paragraphs.

The thermal stresses in the hottest general and LTP spacer plates resulting from the radial thermal gradients due to the normal, normal cold, and normal hot storage and transfer thermal conditions are calculated using the plane stress finite element model described in Section 3.9.2.4.1, with the appropriate material properties and plate thickness. As discussed in Section 3.5.1.2.2, the spacer plates expand freely within the canister shell under all normal thermal conditions. Consequently, the finite element model is pinned to prevent rigid body translation and allow free radial thermal expansion. The temperature dependent material properties of SA-517, Grade P[25] carbon steel and SA-240, Type XM-19 stainless steel are used for the general and LTP spacer plate thermal stress analyses, respectively. The finite element analysis results show that the maximum general thermal stress intensity (i.e., membrane plus bending stress intensity) in the general and LTP spacer plates are 47.5 ksi and 35.4 ksi, respectively.

As discussed above, thermal stresses also occur in the spacer plates at the top and bottom end of each basket assembly due to curvature of the support tubes resulting from radial thermal gradients within the support tubes. For this condition, the unrestrained angle of rotation at the ends of the support tubes, calculated assuming simply supported ends, is 0.00260 radians. The actual end rotation of the support tube is less than the unrestrained rotation since bending of the support tubes is resisted by the top and bottom end spacer plates.

[25] The carbon steel spacer plates are fabricated from either SA-517, Grades F or P or A514, Grades F or P carbon steel. The temperature dependent material properties (i.e., E and α) of all these carbon steels are identical. Therefore, the thermal stress analysis is valid for all material alternatives.

The rotation at the support tube to end spacer plate location is calculated using the principal of static equilibrium based upon the relative stiffness of the support tube and spacer plate. The rotational stiffness of the W74 general and LTP spacer plate is calculated using the spacer plate shell model described in Section 3.9.2.4.3. Unit rotation (i.e., UX=UY=±0.001-radian) are applied to the model nodes at the center of each support tube opening. The bending stiffness of the W74 general and LTP spacer plates, equal to the maximum moment reaction divided by the applied joint rotations, are 410 inch-kips/radian and 7,500 in-kips/radian, respectively. The bending stiffness of the support tube, calculated using simple beam theory for a simply supported beam subjected to equal end moments, is 166,900 in-kips/radian. The support tube end rotations required to satisfy static equilibrium are 0.00259 radians for the W74 general spacer plate and 0.00249 radians for the W74 LTP spacer plate. The corresponding moment reactions at the support tube ends are 1.06 in-kips for the W74T support tubes (i.e., general spacer plates at ends) and 18.68 in-kips for the W74M support tubes (i.e., LTP spacer plates at ends).

The spacer plate stresses resulting from the support tube end rotations calculated above are determined using the W74 LTP and general spacer plate shell model described in Section 3.9.2.4.3 and shown in Figure 3.9-8. A unit rotation (0.001-radian) is applied to the spacer plate nodes located at the center of each support tube hole, resulting in maximum thermal membrane plus bending stress intensities of 1.14 ksi in the general spacer plate and 2.92 ksi in the LTP spacer plate. The maximum stresses due to the calculated support tube end rotations, determined by scaling the stresses due to the unit rotation, are 2.95 ksi for the general spacer plate and 7.27 ksi for the LTP spacer plate. The spacer plate stresses resulting from the curvature of the support tube are conservatively combined with the maximum spacer plate thermal stresses due to the spacer plate radial thermal gradients, as follows.

The maximum general thermal stress intensity in the general spacer plate due to the radial thermal gradient for the governing thermal condition is 47.5 ksi. The maximum thermal bending stress in the general spacer plate due to the curvature of the support tubes is 2.95 ksi. Therefore, the combined thermal stress in the general spacer plate is 50.5 ksi. As discussed above, general thermal stress intensity is classified as secondary. The Service Level A allowable secondary stress intensity for SA-517, Grades F or P and A514, Grades F or P carbon steels at 700°F are 112.5 ksi and 107.7 ksi, respectively. Therefore, the maximum general thermal stress intensity in the general spacer plate is less than the allowable. Therefore, the minimum design margin for thermal stress in the W74 general spacer plate is +1.13.

The maximum general thermal stress intensity in the LTP spacer plate, resulting from the normal cold transfer thermal condition, is 35.4 ksi. This stress is combined with the maximum membrane plus bending stress intensity of 7.27 ksi due to the thermal curvature of the support tube, as discussed above. Therefore, the maximum combined thermal stress intensity in the LTP spacer plate is 42.7 ksi. As discussed above, general thermal stress intensity is classified as secondary. The Service Level A allowable secondary stress intensity for SA-240, Type XM-19 stainless steel at 650°F is 87.0 ksi. Therefore, the minimum design margin for thermal stress in the LTP spacer plate is +1.04.

3.5.1.3.3 Engagement Spacer Plate

Thermal stresses in the W74 engagement spacer plate result from radial thermal gradients. The highest stresses in the engagement spacer plate result from the thermal condition producing the largest radial thermal gradient. A comparison of the engagement spacer plate radial thermal

gradients for the normal transfer and storage thermal conditions is provided in Table 3.5-3. The results show that the thermal gradients do not vary significantly for the range of normal on-site transfer and storage thermal conditions and that the maximum thermal gradients result from the normal cold storage and transfer conditions. The W74 engagement spacer plate normal thermal stress evaluation is performed for both the normal cold storage and normal cold transfer thermal gradients.

Thermal stresses in the engagement spacer plate are calculated for the normal thermal gradients using the plane stress half-symmetry finite element model described in Section 3.9.2.5 and shown in Figure 3.9-16. The model includes the temperature dependent material properties of the W74 engagement spacer plate SA-240, Type XM-19 stainless steel material. The model includes symmetry boundary displacement constraints (UX=0) applied to the nodes lying on the symmetry plane. In addition, the node at the bottom centerline is restrained (UY=0) to prevent rigid body translation. The bounding normal thermal gradient is applied as nodal temperature constraints and a reference temperature of 70°F is specified.

The maximum general thermal stress intensity, resulting from the normal cold storage thermal condition, is 38.3 ksi. The allowable Service Level A primary plus secondary stress intensity for SA-240, Type XM stainless steel material at a bounding design temperature of 600°F is 87.6 ksi. Therefore, the minimum design margin in the W74 engagement spacer plate for general thermal stress due to the bounding normal thermal condition is +1.29.

3.5.1.3.4 Support Tubes and Support Sleeves

The W74M and W74T support tubes and support sleeves are evaluated for thermal stresses due to normal thermal loading. The W74 support tube and support sleeve stresses resulting from longitudinal differential thermal expansion of the basket assembly components and from radial thermal gradients through the cross section of the support tube are evaluated in this section using hand calculations. In addition, the stresses in the W74T support sleeve attachment welds and W74M LTP spacer plate attachment welds resulting from normal thermal loading are evaluated in this section.

Support Tube Stress Evaluation

The longitudinal differential thermal expansion of the W74 support tubes, support sleeves, and spacer plates produces axial compressive stress in the support sleeves and tensile stress in the support tubes. As shown in Chapter 4 of this SAR, the maximum support tube temperatures result from the normal hot thermal condition in the transfer cask. The maximum temperature at the hottest axial section of the support tubes for this condition is 683°F. The stresses in the W74 support tubes and support sleeves due to longitudinal differential thermal expansion are conservatively calculated for a bounding temperature of 700°F.

The largest differential thermal expansion between the support tubes, support sleeves, and spacer plates in the upper and lower basket assemblies for the bounding temperature of 700°F are 0.01354-inch for the W74T (lower basket assembly) and 0.01420-inch for the W74M (lower basket assembly). The axial load in the support tube and support sleeves due to the differential thermal expansion is calculated based upon the principal of static equilibrium. The axial load is equal to the product of the differential thermal expansion and the equivalent axial stiffness of the support tube, support sleeves, and spacer plates. The equivalent axial stiffness of the system is calculated assuming the support sleeves, spacer plates, and attachment sleeves (W74T only) act

as springs in series and together they act in parallel with the support tube stiffness. The resulting maximum axial loads are 23.2 kips for the W74T support tubes and support sleeves and 24.2 kips for the W74M support tube and support sleeves.

The 23.2 kip axial load in the W74T results in a tensile stress of 1.0 ksi in the support tube and a compressive axial stress of 3.1 ksi in the support sleeve. Similarly, the 24.2 kip axial load in the W74M results in a tensile stress of 1.0 ksi in the support tube and a compressive axial stress of 3.2 ksi in the support sleeve.

The results of the thermal evaluation presented in Section 4.4 of this SAR show that under normal thermal conditions the temperature on the sides of the support tube facing inward are higher than the temperature on the outward facing sides. As a result, the support tubes will curve inward slightly, as shown in Figure 3.5-2. For the W74M basket assemblies, the curvature of the support tubes is resisted by the top and bottom end LTP spacer plates which are welded to the support tubes. Similar restraint is conservatively assumed for the W74T basket assemblies. Since the bending stiffness of the support tubes is much larger than the bending stiffness of the basket assembly end spacer plates, the moment reactions at the ends of the support tube resulting from the thermal curvature are small and the associated support tube stresses are negligible. However, the stresses in the welds which connect the support tubes to the LTP spacer plates (W74M) or the attachment sleeves (W74T) are evaluated to assure the structural integrity of the connections. The weld thermal stress evaluations are discussed as follows.

W74T Support Sleeve Attachment Weld Stresses

The top and bottom end support sleeves in both the W74T upper and lower basket assemblies are welded to the support tubes with all-around ¼-inch fillet welds to capture the basket assembly spacer plates and interior support sleeves. The stresses in these welds due to normal thermal loading are evaluated using hand calculations. The weld stress evaluation addresses thermal stresses due to differential thermal expansion of dissimilar materials and thermal gradients within the basket assembly.

As discussed above, differential thermal expansion of the W74T basket assembly due to normal thermal conditions results in an axial load of 23.2 kips. The resulting average shear stress in the support sleeve attachment weld is 4.4 ksi. Additional shear stresses occur in these welds due to the moment reaction resulting from thermal curvature of the support tubes. As discussed in Section 3.5.1.3.2, the maximum moment reaction at the LTP spacer plate attachment weld resulting from thermal curvature of the support tubes is 1.06 in-kips. The moment reaction is carried in shear through the weld, resulting in a maximum weld shear stress of 0.1 ksi. The combined weld shear stress is equal to 4.5 ksi. The corresponding Service Level A allowable average shear stress intensity is 6.9 ksi, based on SA-240, Type XM-19 material properties at 700°F and including a 40% weld efficiency factor for single sided fillet weld with surface PT examination in accordance with Table NG-3352-1 of the ASME Code. Therefore, the minimum design margin for shear stress in the W74T support sleeve attachment weld due to the controlling thermal load condition is +0.53.

W74M Support Tube/LTP Spacer Plate Weld Stresses

The top and bottom end LTP spacer plates in both the W74M upper and lower basket assemblies are welded to the support tubes with all-around ½-inch groove welds with ¼-inch cover fillet welds. The stresses in these welds due to normal thermal loading are evaluated using hand

calculations. The weld stress evaluation addresses thermal stresses due to differential thermal expansion of dissimilar materials and thermal gradients within the basket assembly.

As discussed above, differential thermal expansion of the W74M basket assembly due to normal thermal conditions results in an axial load of 24.2 kips. The resulting average shear stress in the LTP spacer plate attachment weld is 1.5 ksi. Additional shear stresses occur in these welds due to the moment reaction resulting from thermal curvature of the support tubes. As discussed in Section 3.5.1.3.2, the maximum moment reaction at the LTP spacer plate attachment weld resulting from thermal curvature of the support tubes is 18.7 in-kips. The moment reaction is carried in shear through the weld, resulting in a maximum weld shear stress of 0.4 ksi. Therefore, the combined shear stress in the weld is 1.9 ksi. The corresponding Service Level A allowable average shear stress is 6.9 ksi, based on SA-240, Type XM-19 stainless steel material properties at 700°F and including a 40% weld efficiency factor for single groove weld with surface PT examination in accordance with Table NG-3352-1 of the ASME Code. Therefore, the minimum design margin for shear stress in the W74M LTP spacer plate attachment weld due to normal thermal loading is +2.70.

3.5.1.3.5 Guide Tubes

As shown in Section 3.5.1.2.2, the W74 guide tubes expand freely under all normal thermal conditions. Consequently, no significant thermal stresses occur in the W74 guide tubes as a result of normal thermal loading.

3.5.1.4 Fatigue Evaluation

3.5.1.4.1 Shell Assembly

The canister confinement components, consisting of the cylindrical shell, top inner and outer closure plates, and bottom closure plate, are evaluated in accordance with the requirements of NB-3222.4(d). Specifically, the six criteria of NB-3222.4(d) are evaluated to demonstrate that a detailed analysis of the W74 canister shell for cyclical service is not required. These criteria are discussed below.

1. *Atmospheric to Service Pressure Cycle*: The maximum number of pressure cycles associated with startup and shutdown is limited to 30,000 for the W74 canister shell, based on the fatigue curve from Figure I-9.2.1 of the ASME Code for $3S_m$ = 51 ksi, where the lower bound value of S_m is conservatively taken as 17 ksi for the W74T canister shell Type 304 material design temperature of 550°F. The canister normal service includes one vacuum drying operation and one helium fill after closure. All other pressure fluctuations during storage are due to changes in atmospheric conditions. Hence, the canister is never cycled back to the atmospheric pressure during normal service. Therefore, the first criterion is satisfied.
2. *Normal Service Pressure Fluctuation*: The total number of pressure cycles is less than 10^6 because the pressure cycles only occur due to changes in the ambient temperature (assuming one cycle a day, obtain 1×365×100 =36,500 over the lifetime). As specified in this criterion, the value of S is determined for 10^6 cycles and is 28.3 ksi from Figure I-9.2.1 of the ASME Code. The design pressure is 10 psig. Therefore, the cut-off for the significant pressure fluctuation is

$$SPF = \frac{1}{3} \times DP \times \left(\frac{S}{S_m} \right) = \frac{1}{3} \times 10 \times \left(\frac{28.3}{17} \right) = 5.5 psi$$

As shown in Table 4.4-4, the W74 canister shell internal pressure ranges from a minimum of 6 psig to a maximum of 10 psig for normal conditions. Hence, no significant pressure fluctuations are expected during storage. Therefore, the second criterion is satisfied.

3. *Temperature Difference - Startup and Shutdown*: The temperature difference between any two adjacent points on the canister shell during startup and shutdown is limited to:

$$\frac{S_a}{2E\alpha} = 1{,}289\,^{\circ}F$$

where S_a is determined to be 708 ksi from Figure I-9.2.1, conservatively based on 10 startup-shutdown cycles, and the values of E and α are conservatively taken as $28.9(10)^6$ psi and $9.5(10)^{-6}$ in/in/°F, respectively. Since the temperature difference between any two points in the canister never approaches this quantity, the third criterion is clearly satisfied.

4. *Temperature Difference - Normal Service*: As determined in (2) above, the value of S is 28.3 ksi. The significant temperature fluctuation is determined as:

$$STF = \frac{28.3}{2(28{,}900)(9.5 \cdot 10^{-6})} = 51°F$$

The normal service in this criterion does not include startups and shutdowns, hence, the only temperature variations are due to changes in the ambient conditions. As shown in Table 3.5-2, the temperature difference between any two points in the canister shell does not change significantly from normal cold to normal hot condition. Temperatures at all points drop uniformly by approximately 125°F. Therefore, there are no significant variations in the temperature gradient during normal service and the fourth criterion is satisfied.

5. *Temperature Difference- Dissimilar Materials*: The canister shell confinement components are fabricated entirely of Type 304 (W74T) or Type 316 (W74M) stainless steel. Hence, no dissimilar materials are used. Therefore, the fifth criterion is satisfied.

6. *Mechanical Loads*: The only significant mechanical loads during the canister service are those due to lifting and transfers. Conservatively estimating the number of these load fluctuations as 100, the S_a value is found to be 261 ksi (Table I-9.1 of the ASME Code). The mechanical loads do not exceed this value and, therefore, the sixth criterion is satisfied.

Therefore, fatigue is not a concern for the canister pressure boundary components.

3.5.1.4.2 Basket Assembly

The canister basket assembly components, consisting of the guide tubes, support tubes, support sleeves, general spacer plates, LTP spacer plates, and engagement spacer plate are evaluated in accordance with NG-3222.4(d) for fatigue. Per NG-3222.4(d), these components do not need a detailed fatigue evaluation if the four specified criteria are satisfied. These criteria are discussed below.

1. *Temperature Difference - Startup and Shutdown*: The temperature difference between any two adjacent points on the canister basket assembly during startup and shutdown is limited to:

$$S_a / 2E\alpha = 680^\circ F$$

   where S_a is determined to be 400 ksi from Figures I-9.1 and I-9.2.1 of the ASME Code, conservatively based on 10 startup-shutdown cycles, and the values of E and α are conservatively taken as $30(10)^6$ psi and $9.8(10)^{-6}$ in/in/°F, respectively.

   As shown in Chapter 4, the axial temperature difference within any basket component does not exceed 400°F and the radial temperature difference within any basket spacer disk does not exceed 350°F. All of these values are below 680°F. Therefore, the first criterion is satisfied.

2. *Temperature Difference - Normal Service*: The conservative value of S for 10^6 cycles is 12 ksi (Figures I-9.1 and I-9.2.1 of the ASME Code). The significant temperature fluctuation is:

$$STF = 12 / 2(30{,}000)(9.8 \cdot 10^{-6}) = 20°F$$

   As shown in Chapter 4, the temperature difference between any two points in the tubes does not change significantly from normal cold to normal hot condition. Temperatures at all points drop uniformly by approximately 100°F. Therefore, there are no significant variations in the temperature gradient during normal service. The second criterion is satisfied.

3. *Temperature Difference- Dissimilar Materials*: The cut-off value for significant temperature fluctuations is determined as (S =12 ksi per (2) above):

$$STF = \frac{S}{2(E_1\alpha_1 - E_2\alpha_2)} = \frac{12}{2\left(24{,}800 \cdot (9.8 \cdot 10^{-6}) - 25{,}500 \cdot (7.5 \cdot 10^{-6})\right)} = 116°F$$

   The E and α values are taken for SA-240, Type 316 stainless steel and SA-517 or A514, Grades F or P carbon steel at the mean temperature of 700°F. These values provide the minimum STF and bound all other basket materials.

As shown in Table 4.4-3, the temperature fluctuation between normal cold and normal hot conditions is approximately 100°F. Therefore, only a very few significant temperature fluctuations per year are possible. Assuming the number of 10 per year and a canister lifetime of 100 years, there are 1000 significant temperature fluctuations over the life of the canister. The lower bound value of S_a is 78 ksi (Table I-9.1 of the ASME Code). The resulting allowable temperature range is:

$$\frac{S_a}{2\left(E_1\alpha_1 - E_2\alpha_2\right)} = \frac{78}{2\left(24{,}800 \cdot \left(9.8 \cdot 10^{-6}\right) - 25{,}500 \cdot \left(7.5 \cdot 10^{-6}\right)\right)} = 753°F$$

This value is higher than the temperature difference between any two components in the basket during normal service. Therefore, the third criterion is satisfied.

4. *Mechanical Loads*: The only significant mechanical loads during the canister service are those due to transfers. Conservatively estimating the number of these load fluctuations as 100, the Sa value is found to be 175 ksi (Table I-9.1 of the ASME Code). The mechanical loads do not exceed this value and, therefore, the fourth criterion is satisfied.

Therefore, fatigue is not a concern for the fuel basket components.

3.5.2 Internal Pressure

The canister shell assembly is evaluated for internal pressure loads associated with canister loading operations (draining internal pressure) and normal on-site transport and storage conditions. These conditions are described and evaluated in the following sections.

As discussed in Chapter 4 of this SAR, the FuelSolutions™ W74 canister internal pressure design loads for normal conditions bound those for a FuelSolutions™ W74 canister containing any amount of intact BRP MOX fuel and partial fuel assemblies, and up to eight damaged fuel assemblies. Therefore, the FuelSolutions™ W74 canister shell assembly and basket assembly stresses calculated for the design basis normal internal pressure loads are bounded for a FuelSolutions™ W74 canister containing any amount of intact BRP MOX fuel and partial fuel assemblies, and up to eight damaged fuel assemblies.

3.5.2.1 Canister Draining Internal Pressure

After installation of the inner closure plate, a compressed gas pressure of 30 psig is applied to the canister cavity to speed the water draining process during canister closure operations, thus minimizing the personnel dose. The automated canister welder/opener and auxiliary shield plate, described in Section 1.2.1.4.1 of the FuelSolutions™ Storage System SAR, are attached to the inner closure plate and a strongback is installed on the transfer cask top flange, as shown in Figure 1.2-14 of the FuelSolutions™ Storage System SAR. The strongback and auxiliary shield plate provide structural support for the canister top inner closure plate and ensure that no permanent deformation of the inner closure plate results from the drainage pressure loading which could potentially interfere with the proper placement and installation of the outer closure plate.

The structural evaluation of the W74 canister shell assembly for the drainage internal pressure load is performed using a combination of hand calculations and finite element analysis. Hand

calculations are used to determine the bending stiffness of the strongback support beams which are used to support the canister top inner closure plate. The lower bound stiffness of the two 10x5x5/8 structural tubes which support the canister top inner closure plate is calculated assuming the beams are simply supported with a concentrated force applied at the mid-span, as follows:

$$K = 2\left(\frac{P}{\delta}\right) = 2\left(\frac{48EI}{l^3}\right) = 2.16\text{x}10^6 \text{ lb/in.}$$

where:

E = $27\text{x}10^6$ psi, Elastic modulus of structural steel.

I = 183 in^4, Moment of inertia for a 10x5x5/8 tube section per AISC.

l = 60.4 in., Span length of strongback beam.

The canister shell stresses due to the 30 psig canister draining pressure condition are calculated using the axisymmetric canister shell model described in Section 3.9.2.1. The top outer closure plate is not included in the model since it is not installed during the blowdown pressure condition. The auxiliary shield plate is not included in the canister shell finite element model, conservatively neglecting the structural support it provides to the inner closure plate. Instead, the resisting force of the strongback is modeled as a linear spring with the stiffness calculated above. The strongback spring is attached to the canister top inner closure plate at the location of the auxiliary shield plate inner ring (i.e., R=20.2 inches). A uniform pressure load of 30 psig is applied to the inner surface of the inner closure plate and the cylindrical shell. In addition, a 1*g* vertical acceleration is applied to the model to account for the self weight of the canister shell assembly. The weight of the auxiliary shield plate and welding machine are conservatively ignored for this calculation.

The canister shell assembly results for the water draining internal pressure condition are summarized in Table 3.5-4. The analysis results show that the maximum stress intensities in the canister shell assembly due to the water drainage pressure loading are below the Service Level A allowable stress intensities.

3.5.2.2 Normal Transfer and Storage Internal Pressure

The maximum canister internal pressures are calculated in Chapter 4 of this SAR for each fuel assembly class under the most severe normal transfer and storage conditions. The maximum canister internal pressure for the normal hot storage condition is 9.8 psig, assuming no rod failures. With the postulated failure of 1% of the fuel rods, the maximum normal internal pressure increases to 10.0 psig. The normal internal pressure stress evaluation of the canister shell is performed for the maximum 10 psig internal pressure load.

The normal internal pressure stress evaluation of the bounding canister shell assembly is performed using the axisymmetric finite element model described in Section 3.9.2.1. For the normal on-site transfer and storage internal pressure condition, canister shell assembly stresses are determined for internal pressure loads acting on the top inner and outer closure plates independently. The maximum canister shell stresses resulting from a 10 psig normal internal

pressure load are summarized in Table 3.5-4. The results show that the maximum canister shell stress intensities resulting from bounding 10 psig normal internal pressure loading are less than the corresponding Service Level A allowable stresses.

3.5.3 Dead Weight Load

The canister is transferred in the vertical or horizontal orientations and stored in the vertical orientation. This section presents the structural evaluation of the canister structural components for dead weight loads in both the vertical and horizontal orientations.

The structural evaluation of the FuelSolutions™ W74 canister for dead weight and normal handling loads is performed using a bounding BRP intact fuel assembly weight of 485 pounds per assembly plus a bounding damaged fuel can weight of 200 pounds in each of the support tube openings. As discussed in Section 2.2 of this SAR, the weights of all BRP MOX fuel assemblies, partial fuel assemblies, and damaged fuel assemblies are bounded by the weight of the BRP intact fuel assemblies. Therefore, the dead weight and normal handling loads and calculated stresses in the FuelSolutions™ W74 canister shell assembly and basket assemblies bound those for a FuelSolutions™ W74 canister containing any amount of intact BRP MOX fuel and partial fuel assemblies, and up to eight damaged fuel assemblies.

3.5.3.1 Canister Shell Assembly

3.5.3.1.1 Vertical Dead Weight

The FuelSolutions™ canister shell assemblies are evaluated for the vertical dead weight loading associated with normal transfer and storage. For the vertical dead load condition, the bottom end of the canister rests on either the transfer cask bottom cover plate or the storage cask canister support tubes, as described in Section 1.2.1 of the FuelSolutions™ Storage System SAR. For both conditions, the support conditions are nearly uniform over the entire bottom surface of the canister shell assembly. Therefore, a single vertical dead weight analysis is performed for the controlling canister shell assembly configuration assuming uniform support over its bottom end.

The vertical dead weight stress evaluation of the bounding canister shell assembly is performed using the axisymmetric finite element model described in Section 3.9.2.1. The dead weight of the spent fuel assemblies and canister basket assemblies is modeled as a uniform pressure load across the inner surface of the bottom closure plate. As shown in Section 3.2, the maximum combined weight of the canister shell assembly internals (spent fuel and upper and lower basket assemblies) is approximately 51.6 kips for the W74M design with heaviest Big Rock Point fuel and damaged fuel canisters. For conservatism, a bounding weight of 57 kips is used for the combined weight of the spent fuel assemblies and the canister basket assemblies for the bounding canister shell vertical dead weight analysis. A unit vertical acceleration is applied to the analytical model to account for the self weight of the canister shell assembly.

The stress intensities resulting from vertical dead weight in the bounding canister shell assembly are summarized in Table 3.5-4. The results demonstrate that the maximum canister shell stress intensities for vertical dead weight loading are less than the corresponding Service Level A allowable stresses.

The maximum stresses in the W74 top shield plug assembly due to vertical dead weight loading are determined by scaling the maximum stresses calculated for the 50*g* bottom end drop in

Section 3.7.3.1 by 1*g*/50*g*. The resulting maximum primary membrane and primary membrane plus bending stress intensities in the W74 top shield plug are 0.1 ksi (=5.0x1*g*/50*g*) and 0.5 ksi (=27.1x1*g*/50*g*), respectively. The Service Level A allowable primary membrane and primary membrane plus bending stress intensities for the W74 top shield plug, based on A516, Grade 55 carbon steel at 300°F, are 17.7 ksi and 26.6 ksi, respectively. Therefore, the minimum design margins in the W74 top shield plug for vertical dead weight loading are large.

The W74 top shield plug is supported by eight support bars which are welded to the inside of the canister shell. Each support bar is 3/4-inch thick (radial), 2.3-inch wide (circumferential), and 12-inches long (longitudinal). Each support bar is welded to the canister shell with 10.4 inch load by 5/16 effective throat partial penetration groove welds on both sides bar. The average bearing stress at the top end of the support bars and shear stress in the support bar attachment welds due to vertical dead weight loading are determined using hand calculations. The total load supported by all eight support bars is conservatively assumed equal to the combined weight of the top shield plug assembly (i.e., shield plate and shield caps) plus the weight of the top inner and outer closure plates, or 9.6 kips. The average bearing area at the top end of the support bars is calculated as follows:

$$A_b = 8(b)(OR_p - IR_b) = 8.5 \text{ in}^2$$

where:

b = 1.7 in., width of support bar at interface with top shield plug

OR_p = 32.25 in., outside radius of top shield plug

IR_b = 31.625 in. inside radius of support bar

= 33.0 - 0.625 - 0.75

Therefore, the average bearing stress on the top shield plug support bars is 1.1 ksi. The average bearing stress is limited to S_y for Service Level A conditions in accordance with Subsection NF of the ASME Code. Conservatively using the lowest yield strength of the shield plug or support bar materials gives an allowable bearing stress of 26.6 ksi (based on A516, Grade 55 carbon steel at 300°F). Therefore, the minimum design margin for bearing stress in the top shield plug and support bars for vertical dead weight loading is +22.5.

The total shear area of the support bar attachment welds is 52.0 in^2. Therefore, the average shear stress in the support bar attachment welds due to vertical dead weight loading is 0.2 ksi. The allowable shear stress for the W74 top shield plug support bar attachment welds is limited to the lesser of $0.3S_u$ (weld metal) or $0.4S_y$ (base metal) in accordance with Table NF-3324.5(a)-1 of the ASME Code. Therefore, the allowable weld shear stress is 9.0 ksi, based on the weaker shell material (SA-240, Type 304 stainless steel) at 300°F. The minimum design margin in the W74 top shield plug support bar attachment weld due to vertical dead weight loading is +49.0.

3.5.3.1.2 Horizontal Dead Weight

The W74 canister is supported by two rails in the transfer cask or storage cask when in the horizontal orientation. The centerline of the rails in both the transfer cask and storage cask are located at 22.5° on either side of the bottom centerline of the canister. The cask rails provide

continuous support along entire length of the canister. Since the canister support conditions provided by the transfer cask and storage cask rails are identical, only one horizontal dead weight evaluation is performed for the W74 canister shell.

The horizontal dead weight analysis is performed using the half-symmetry three dimensional finite element model described in Section 3.9.2.2. The loading is applied as a 1*g* vertical acceleration, which is reacted at the support rails. The resulting maximum stress intensities in the canister shell assembly due to horizontal dead weight are summarized in Table 3.5-4. The results show that the maximum stress intensities in the canister shell due to horizontal dead weight are less than the corresponding Service Level A allowable stresses.

3.5.3.2 General and LTP Spacer Plates

The FuelSolutions™ W74 canister basket assembly general and LTP spacer plate stresses due to dead weight in the vertical and horizontal orientations meet the stress acceptance criteria of Subsection NG for Service Level A, as defined in Section 3.1.2. The spacer plate dead weight structural evaluations and stress results are discussed in the following sections. Table 3.5-5 summarizes the maximum spacer plate stresses due to vertical and horizontal dead load.

3.5.3.2.1 Vertical Dead Weight

When oriented vertically, the LTP spacer plates and general spacer plates are supported by the four support tube assemblies and loaded only by their own weight. The SNF assemblies and damaged fuel canisters in the upper basket assembly are supported by the engagement spacer plate. The lower basket SNF assemblies and damaged fuel cans bear directly on canister shell bottom closure plate and do not load the LTP spacer plates or general spacer plates. The guide tube assemblies in the W74M upper and lower basket assemblies are secured to the bottom end LTP spacer plate with attachment brackets. Therefore, the bottom end LTP spacer plate in the W74M upper and lower basket assemblies are loaded by their own weight plus the weight of 28 guide tube assemblies. The guide tubes in the W74T upper and lower basket assemblies are not mechanically fastened to the spacer plates. Instead, they are captured between the engagement spacer plate and the ends of the canister shell cavity. Therefore, the W74 general spacer plates support only their own weight under vertical dead weight loading.

The stresses in the W74 general and LTP spacer plates due to vertical dead weight loading are determined using the spacer plate shell finite element model described in Section 3.9.2.4.2. The spacer plate thickness real constant is specified as 0.75-inches (general) and 2.00-inches (LTP) for these analyses. The finite element model material properties and boundary conditions are described in Section 3.9.2.4.2. As discussed above, the W74 general spacer plates and top end LTP spacer plate are loaded only by their own weight for vertical dead weight load condition. Therefore, the only load applied to these models is a 1*g* longitudinal acceleration. The bottom end LTP spacer plates are loaded by the weight of the guide tubes in addition to their own weight. The loads from the guide tubes are applied to the finite element model as concentrated nodal forces at the locations of the guide tube attachment brackets, as described in Section 3.9.2.4.2. The results of the W74 general and LTP spacer plate vertical dead weight stress analyses

General Spacer Plates

The results of the W74 general spacer plate vertical dead weight finite element analysis show that the plate behavior is essentially pure bending, with a maximum membrane plus bending stress intensity of 0.39 ksi and a maximum total stress intensity (i.e., including peak stresses) of 1.23 ksi. The Service Level A allowable primary membrane plus bending and primary plus secondary stress intensities for the general spacer plate material at 700°F are 53.9 ksi and 107.7 ksi, respectively. The corresponding minimum design margins for primary membrane plus bending (P_m+P_b) and primary plus secondary (P_m+P_b+Q) in the W74 general spacer plate for the vertical dead weight condition are large.

LTP Spacer Plates

As discussed above, separate vertical dead weight stress analyses are performed for the LTP spacer plates at the top and bottom end of the W74M basket assembly since the loads differ by the weight of the guide tube assemblies. The maximum primary membrane plus bending and total stress intensities in the top end LTP spacer plate, which supports only its own weight, are 0.15 ksi and 0.47 ksi, respectively. The maximum primary membrane plus bending and total stress intensities in the bottom end LTP spacer plate, which supports the weight of 28 guide tubes in addition to its own weight, are 0.69 ksi and 2.40 ksi, respectively. The Service Level A allowable primary membrane plus bending and primary plus secondary stress intensities for the LTP spacer plate material at 650°F are 43.5 ksi and 87.0 ksi, respectively. Therefore, the minimum design margins in the LTP spacer plates for primary membrane plus bending and primary plus secondary stress intensity are +61.1 and +35.3, respectively.

3.5.3.2.2 Horizontal Dead Weight

When oriented horizontally, the basket assembly spacer plates provide structural support for the SNF assemblies, damaged fuel cans, guide tube assemblies, support tubes, and support sleeves. The spacer plates are supported along their bottom edge by the canister shell. The basket assembly spacer plates are supported by the canister shell and the canister shell is supported by two cask rails. Under relatively low magnitude loads such as horizontal dead weight, the weight of the SNF assemblies is conservatively assumed to load the W74 guide tubes only at the locations of the fuel assembly grid spacers. The worst case loading for each spacer plate results when fuel assembly grid spacer located directly over that spacer plate.

The structural evaluation of the W74 spacer plates for the horizontal dead weight condition is performed using the plane-stress finite element model described in Section 3.9.2.4.1. The W74 spacer plate horizontal dead weight evaluation is performed assuming that the spacer plates are supported radially only at the cask rail locations, conservatively neglecting the support provided by the canister shell between the cask rails.

The horizontal dead weight loads are applied to the plane stress finite element models as described in Section 3.9.2.4.1. The model loads include the self-weight of the W74 spacer plates, the weight of the guide tubes, support tube and support sleeves tributary to the spacer plate, and the fuel assembly grid spacer tributary weights. The self-weight of the spacer plate is included in the model and accounted for by applying a 1*g* vertical (Y-axis) acceleration to the model. The spacer plate loading due to the tributary weights of the guide tubes, support tubes, support sleeves, and the fuel grid spacer loads are applied as pressure loads to the supporting horizontal ligaments of the spacer plate. These loads are calculated as described in Section 3.9.2.4.1. Elastic

stress analyses are performed for the W74 general and LTP spacer plates having the largest tributary lengths. The fuel loading for the general and LTP spacer plates are based on the maximum in-core grid spacer tributary weight of 108.1 pounds and maximum end fitting tributary weight of 54.1 pounds, respectively. The results of the W74 general and LTP spacer plate horizontal dead weight stress analyses are as follows.

General Spacer Plate

The maximum primary membrane (P_m) and primary membrane plus bending (P_m+P_b), stress intensities in the most highly loaded W74 general spacer plate for the horizontal dead weight loading are 1.84 ksi and 3.74 ksi, respectively. The maximum total stress intensity in the most highly loaded W74 general spacer plate, which is conservatively classified as primary plus secondary (P_m+P_b+Q), is 3.89 ksi. The Service Level A allowable primary membrane, primary membrane plus bending, and primary plus secondary stress intensities for the carbon steel spacer plate material at 700°F are 35.9 ksi, 53.9 ksi, and 107.7 ksi, respectively. Therefore, the minimum design margins for primary membrane, membrane plus bending, and primary plus secondary stress intensities in the most highly loaded W74 general spacer plate for horizontal dead weight loading are +18.5, +13.4, and +26.7, respectively.

LTP Spacer Plate

The maximum primary membrane (P_m) and primary membrane plus bending (P_m+P_b), stress intensities in the most highly loaded W74 LTP spacer plate for the horizontal dead weight loading are 0.44 ksi and 0.90 ksi, respectively. The maximum total stress intensity in the most highly loaded W74 LTP spacer plate, which is conservatively classified as primary plus secondary (P_m+P_b+Q), is 0.93 ksi. The Service Level A allowable primary membrane, primary membrane plus bending, and primary plus secondary stress intensities for SA-240, Type XM-19 stainless steel at 650°F are 29.0 ksi, 43.5 ksi, and 87.0 ksi, respectively. Therefore, the minimum design margins for primary membrane, membrane plus bending, and primary plus secondary stress intensities in the most highly loaded W74 LTP spacer plate due to horizontal dead weight loading are +64.9, +47.3, and +92.5, respectively.

3.5.3.3 Engagement Spacer Plate

3.5.3.3.1 Vertical Dead Weight

Under vertical dead weight loading, the engagement spacer plate supports the weight of the upper basket assembly and its SNF assemblies, in addition to its own weight. The engagement spacer plate is supported by the lower basket assembly support tubes. The engagement spacer plate loading due to vertical dead weight is proportional to the end drop loading and the boundary conditions are identical. Therefore, the engagement spacer plate stresses due to vertical dead weight loading are determined by scaling the stresses calculated for the storage cask bottom end drop conditions in Section 3.7.3.2.2 by the ratio of the loads (1*g*/50*g*). The maximum engagement spacer plate stress intensities due to vertical dead weight loading are provided in Table 3.5-5. The results show that the maximum stress intensities in the engagement spacer plate due to vertical dead weight loading are less than the Service Level A allowable stress intensities for SA-240, Type XM-19 stainless steel at a bounding design temperature of 600°F.

3.5.3.3.2 Horizontal Dead Weight

When the W74 canister is in the horizontal orientation, the W74 engagement spacer plate is loaded only by its own self weight. This condition is bounded by the vertical dead weight condition, since the engagement spacer plate vertical dead weight load includes the weight of the SNF assemblies, damaged fuel cans, and guide tube assemblies in the upper basket, in addition to its own weight. Also, vertical dead weight load cause bending about the weak axis of the plate, whereas horizontal dead weight loads act in the plane of the plate.

The maximum stresses in the W74 engagement spacer plate due to horizontal dead weight loading are determined by scaling the maximum stresses resulting from the 2*g* on-site transport load by the factor 1*g*/2*g*. The resulting horizontal dead weight stresses in the W74 engagement spacer plate are reported in Table 3.5-5. The results show that the maximum stresses due to horizontal dead weight loading are less than the corresponding Service Level A allowable stresses for SA-240, Type XM-19 stainless steel at a bounding design temperature of 600°F.

3.5.3.4 Support Tubes

3.5.3.4.1 Vertical Dead Weight

When oriented vertically during on-site transfer or storage operations, the upper basket assembly support tubes provide longitudinal support for the upper basket assembly spacer plates, guide tubes, and support sleeves, and the lower basket assembly support tubes provide longitudinal support for the entire upper basket assembly and its SNF assemblies plus the lower basket assembly spacer plates, guide tubes, and support sleeves. Therefore, the vertical dead weight loading on the lower basket assembly support tubes bounds that of the upper basket assembly. As shown in Section 3.2, the weight of the W74M basket assemblies bound those of the W74T basket assemblies. Therefore, since the W74M and W74T support tube cross sections are identical, the stresses in the W74M lower basket assembly support tubes bound those in the W74T lower basket support tubes. Since both the W74M and W74T support tubes are fabricated from Type XM-19 stainless steel, the minimum design margins for vertical dead weight are those of the W74M lower basket support tubes.

The vertical dead weight stresses in the W74M lower basket assembly support tube and associated welds are determined by scaling the maximum stresses calculated for the 50*g* storage cask end drop in Section 3.7.3.2.3 by the ratio of the loads (i.e., 1*g*/50*g*). The resulting stresses in the W74M and W74T support tubes are summarized in Table 3.5-5. The results show that the maximum stresses in the support tubes due vertical dead weight are less than the Service Level A allowable stresses for Type XM-19 stainless steel at of 700°F.

3.5.3.4.2 Horizontal Dead Weight

When the W74 canister is oriented horizontally, the dead weight loading on the support tubes includes the support tube self weight, the weight of the support sleeves, and the weight of the SNF assembly and damaged fuel canister inside the support tube. Therefore, the horizontal dead weight loadings for the W74M and W74T support tubes are approximately equal. A bounding structural evaluation is performed using conservative boundary condition and loading assumptions as discussed below.

The maximum stresses in the W74 support tubes and the associated welds due to horizontal dead weight loading are determined by scaling the maximum stresses calculated for the 60*g* transfer cask side drop load by the ratio of the loads (i.e., 1*g*/60*g*). The resulting support tube stresses are summarized in Table 3.5-5. The results show that the maximum support tube stresses due to horizontal dead weight loading are less than the corresponding Service Level A allowable stresses for XM-19 stainless steel at 700°F.

3.5.3.5 Support Sleeves

3.5.3.5.1 Vertical Dead Weight

When the W74 canister is oriented vertically, each support sleeve is loaded by its self weight plus the weight of all other support sleeves and general spacer plates above it within the basket assembly. The most highly loaded support sleeves for the vertical dead weight condition are those at the bottom end of the upper and lower basket assemblies since they support the most weight. Since there are twelve (12) general spacer plates above the bottom end support sleeve in each of the W74M and W74T basket assemblies, the vertical dead weight loading on the bottom end support sleeve is approximately equal for all designs. The stresses in the W74 support sleeves and support sleeve attachment welds due to vertical dead weight loading are determined by scaling the maximum stress intensities calculated for the 50*g* storage cask bottom end drop in Section 3.7.3.2.4 by the ratio 1*g*/50*g*. The resulting support sleeve vertical dead weight stresses are summarized in Table 3.5-5. The results show that the maximum stresses in the W74 support sleeves due to vertical dead weight are less than the corresponding Service Level A allowable stress intensities.

3.5.3.5.2 Horizontal Dead Weight

In the horizontal orientation, the support sleeve supports only its own weight. As such, the stresses in the support sleeves due to horizontal dead weight are very small and do not control the design.

3.5.3.6 Guide Tubes

3.5.3.6.1 Vertical Dead Weight

For vertical dead weight loading, the W74 guide tubes are loaded only by their own weight. The W74M guide tubes are secured to the bottom end LTP spacer plate in the upper and lower basket assemblies with welded attachment brackets. The W74T guide tubes are not mechanically fastened to the basket assembly spacer plates and rest directly on the engagement spacer plate (upper basket assembly) or the canister shell bottom closure plate (lower basket assembly).

As discussed in Section 3.1.1.2, the dimensions and top and bottom end details of all W74 guide tube assemblies are identical and all W74 guide tubes are fabricated from the same material. However, there are two different guide tube configurations which differ in the number of neutron absorber sheets which are attached to the guide tube. All of the W74 guide tubes include two neutron absorber sheets on opposing faces in the interior of the basket assemblies, whereas the guide tubes on the perimeter of the basket assembly include only one neutron absorber sheet. Since no structural credit is taken for the support that the neutron absorber sheets provide to the guide tube and their mass is assumed to load the guide tube, bounding structural evaluations of

the W74 guide tube are performed for the interior guide tubes which include two neutron absorber sheets. The stresses in the W74 guide tubes, neutron absorber panel retainers, guide tube attachment brackets, and attachment bracket welds are determined using hand calculations.

Guide Tube Stresses

The limiting guide tube vertical dead weight stress is uniaxial compression at the bottom end of the W74T guide tubes which bear on the supporting engagement spacer plate (upper basket) or canister shell bottom closure plate (lower basket). The maximum axial compressive stress across the guide tube due to vertical dead weight, occurring near the bottom end, is calculated as follows:

$$f_a = \frac{P}{A} = 0.03 \text{ ksi}$$

where:

P = 84.2 lb., maximum W74 guide tube assembly weight

A = W74 guide tube cross-section area
= 4(6.90+0.090)(0.090)
= 2.52 in^2

The corresponding Service Level A allowable primary membrane stress intensity, conservatively based on SA-240, Type 316 stainless steel material properties at 715°F, is 16.2 ksi. Therefore, the minimum design margin for primary membrane stress intensity in the W74 guide tube is large.

Neutron Absorber Panel Retainer Stresses

The stresses in the neutron absorber panels and retainers for the vertical dead weight condition are bounded by those due to horizontal dead weight loading.

Attachment Bracket Stress Evaluation

The W74M guide tube attachment brackets are designed with a ¼-inch wide reduced section. The controlling vertical dead weight bending and shear stresses in the attachment bracket base material occur at this section. The maximum shear and bending stresses in the guide tube attachment bracket due to vertical dead weight loading are determined using hand calculations. For this analysis, the guide tube attachment bracket is treated as a guided cantilever beam with a concentrated load at one end. The maximum shear and bending stresses are calculated in accordance with Roark, Table 3, Case 1b as follows:

$$f_v = \frac{V}{A_v} = 2.54 \text{ ksi}$$

$$f_b = \frac{Vl}{2S} = 14.0 \text{ ksi}$$

where:

V = 43 lb., maximum load per attachment bracket (1/2 guide tube weight)

A_v = 0.0169 in^2, Attachment bracket shear area at reduced section.

= 0.1875 x 0.09

l = 0.17 in., Unsupported span of attachment bracket

S_V = 2.53×10^{-4} in^2, section modulus at bracket reduced section

= $1/6 \times 0.1875 \times (0.09)^2$

The maximum primary membrane stress intensity in the attachment bracket is taken as twice the maximum shear stress, or 5.1 ksi. The maximum primary membrane plus bending stress intensity in the guide tube attachment bracket is calculated based on the shear and bending stresses as follows:

$$P_m + P_b = \sqrt{f_b^{\,2} + 4f_v^{\,2}} = 14.9 \text{ ksi}$$

The Service Level A allowable primary membrane and primary membrane plus bending stress for SA-240, Type 316 stainless steel, based on the LTP design temperature of 650°F, are 16.6 ksi and 25.0 ksi, respectively. Therefore, the minimum design margins in the W74M attachment bracket for vertical dead weight loading are +2.60 for primary membrane stress intensity and +0.53 for primary membrane plus bending stress intensity.

Attachment Bracket Weld Evaluation

The W74M guide tube attachment brackets are welded to the guide tube and bottom end spacer plate with full depth (0.075-inch) fillet welds on each side of the attachment bracket leg. The welds between the attachment bracket and guide tube are loaded in pure shear under vertical dead weight conditions. The shear stress in the guide tube to attachment bracket weld is calculated as follows:

$$f_v = V/A_w = 0.57 \text{ ksi}$$

where:

V = 43 lb., maximum load per attachment bracket (1/2 guide tube weight)

A_w = 0.0751 in^2, weld shear area
= $(2d)(0.707 \times t_w)$

d = 0.59 in., weld length at sides of attachment bracket leg.

t_w = 0.09 in., weld leg size

The welds between the attachment brackets and bottom end spacer plate support both a direct shear and bending moment under vertical dead weight conditions. Therefore, the stresses in the attachment bracket welds at the bottom end spacer plate will bound those in the welds at the

guide tubes. The maximum shear stress in the attachment bracket to bottom end spacer plate welds due to vertical dead weight loading is calculated as follows:

$$f_v = V/A_w + M/_{Sw} = V/A_w + V(e)/S_w = 3.25 \text{ ksi}$$

where V and A_w are defined above, and:

e = 0.46 in., Moment arm to centroid of weld
= 0.80 + 0.09/2 - 0.59/2

S_w = 0.00738 in^3, Weld section modulus
= $0.707\ t_w\ [\ 2\ (1/12)\ (0.59)^3\ ]\ /\ 0.295$

d = 0.59 in., Weld length at sides of attachment bracket leg.

The Service Level A allowable primary shear stress is limited to 0.6Sm, or 10.0 ksi for SA-240, Type 316 stainless steel at 650°F. For the attachment bracket welds, a 40% weld efficiency factor is applied in accordance with Table NG-3352-1 of the ASME Code for a single fillet with surface PT examination. Therefore, the allowable weld shear stress is 4.0 ksi. The minimum design margin in the W74M guide tube attachment bracket weld for shear stress due to vertical dead weight loading is +0.23.

3.5.3.6.2 Horizontal Dead Weight

The guide tube assembly is loaded by its own weight and the weight of the contained fuel assembly for the horizontal dead weight condition. The spacer plate ligaments provide vertical support along the bottom face of the guide tube assembly. The fuel assembly dead weight rests directly on the guide tube bottom face. The maximum bending stresses occur in the bottom face of the guide tube since it supports the entire fuel assembly weight in addition to its own weight. The horizontal dead weight structural evaluation of the W74 guide tubes considers two bounding conditions for the fuel loading on the guide tube: 1) uniform fuel load assumption (i.e., SNF assembly load applied as a uniform pressure load over the supporting face of the guide tube), and 2) concentrated load at SNF assembly grid spacers. These two conditions are evaluated as follows:

Uniform Fuel Loading

The maximum guide tube horizontal dead weight stresses for the uniform fuel loading assumption are calculated by scaling the stresses from the 60*g* side drop load evaluated in Section 3.7.5.2.5 by the ratio of the loads (i.e., 1*g*/60*g*). The resulting guide tube stresses are summarized in Table 3.5-6. The results show that the maximum stresses in the W74 guide tube assembly due to horizontal dead weight loading are less than the corresponding Service Level A allowable stresses at a bounding design temperature of 715°F.

Concentrated Loading at Fuel Grid Spacer Locations

In addition to the uniform fuel loading assumption, the fuel assembly dead weight is assumed to be applied to the guide tube as concentrated loads at the location of the SNF grid spacers. As discussed in Section 3.9.1, the maximum in-core grid spacer tributary weight for Big Rock Point fuel is 108.1 pounds. A conservative horizontal dead weight stress analysis is performed for the W74 guide tubes using a bounding grid spacer tributary weight of 123.6 pounds and the largest

unsupported guide tube span for the W74M and W74T upper and lower basket assemblies (i.e., 6.38 inch unsupported span between adjacent spacer plates).

The horizontal dead weight stress analysis of the W74 guide tube is performed using the ½-symmetry multi-span finite element model described in Section 3.9.2.6.2. The SNF assembly dead weight load is applied as a uniform pressure over the area of the guide tube bottom panel which supports the SNF assembly grid spacer. The width and depth of the Big Rock Point fuel in-core grid spacers are approximately 5.72 inches and 2.06 inches, respectively. Thus, the resulting pressure load due to the fuel grid spacer tributary weight is 10.5 psi.

The maximum stress intensity at the middle fiber of the guide tube shell elements, which is conservatively classified as primary membrane, is 0.93 ksi. The maximum stress intensity at the extreme fibers of the guide tube shell elements (i.e., top and bottom fibers) is 3.75 ksi. This stress intensity is localized at the corner of the area supporting the fuel grid spacer. As such, it is classified as primary plus secondary since local yielding would relieve the stress without resulting in significant distortion. However, the primary membrane plus bending stress intensity is taken conservatively as the same value as the maximum primary plus secondary stress intensity. The Service Level A allowable primary membrane (P_m) and primary membrane plus bending (P_m+P_b) stress intensities for SA-240, Type 316 stainless steel at 715°F are 16.2 ksi and 24.3 ksi, respectively. Therefore, the minimum design margins in the W74 guide tube for the horizontal dead weight condition are +16.4 for primary membrane stress intensity and +5.48 for primary membrane plus bending stress intensity.

The stresses in the W74 guide tube longitudinal seam weld due to the horizontal dead weight load for the concentrated fuel load assumption are also evaluated using the finite element solution. The guide tube longitudinal seam welds subjected to both RT and PT examinations can be placed at any location on the width of the panel that will allow an RT examination. The guide tube longitudinal seam welds that are subjected to a surface PT examination only must be located at the ¼ span of the panel width. In the W74 guide tube longitudinal seam weld that is subjected to a surface PT examination only, the results show that the maximum primary membrane and primary membrane plus bending stress intensities due to horizontal dead weight loading (concentrated fuel load assumption) are 201 psi and 572 psi, respectively. In accordance with Table NG-3352-1 of the ASME Code, a 65% weld efficiency factor is applied to the allowable stresses for a full penetration weld with surface PT examination, and thus, the W74 guide tube seam weld Service Level A allowable primary membrane and primary membrane plus bending stress intensities are 10.5 ksi and 15.8 ksi. Therefore, the minimum design margins for primary membrane and primary membrane plus bending stress intensity in the W74 guide tube longitudinal seam weld for the horizontal dead weight condition are both very large.

3.5.4 Normal Handling

This section provides the structural evaluation of the loaded FuelSolutions™ W74 canister for normal handling loads. The FuelSolutions™ Storage System is designed to transfer the canister both vertically and horizontally between the transfer cask, storage cask, and transportation cask, as described in Chapter 1 of the FuelSolutions™ Storage System SAR. The three following normal handling load conditions are evaluated for the FuelSolutions™ W74 canister:

1. *Vertical Canister Transfer Handling*: This load is equal to the dead weight of the canister plus an additional 15% increase to account for impulsive loading due to crane hoist motion, as discussed in Section 2.3.1.4.
2. *Horizontal Canister Transfer Handling*: This load is equal to a hydraulic ram force of 45 kips applied to the top or bottom end of the canister and opposed by friction forces developed between the canister shell and the cask guide rails when the canister is transferred horizontally between casks, as defined in Section 2.3.1.4.
3. *On-site Transport Vibration*: These are loads encountered while towing the transfer trailer between the plant's fuel building and ISFSI. As discussed in Section 2.3.1.4, a design shock and vibration load of $\pm 0.6g$ vertical, $\pm 0.3g$ longitudinal, and $\pm 0.2g$ transverse are conservatively used to provide a bounding structural evaluation.

The structural evaluation of the canister components for the handling loads is presented in the following sections. The results demonstrate that the W74 canisters satisfy the applicable design criteria for the most severe normal handling loads.

3.5.4.1 Vertical Canister Transfer

In normal or routine handling, the canister is transferred vertically between the transfer cask and storage cask using the canister vertical lift fixture and/or an overhead crane, as described in Section 1.2.1.4.3 of the FuelSolutions™ Storage System SAR. The loaded canister is supported by a lift adapter which is bolted to the canister shell top outer closure plate. The lift adapter distributes the lifting load to the perimeter of the outer closure plate and provides structural support for the outer closure plate. Of primary concern for this lift condition is the structural integrity of the canister shell assembly components in the top end region through which the lifting load is transferred.

3.5.4.1.1 Canister Shell Assembly

The structural analysis of the bounding canister shell assembly for the handling loads is performed using the axisymmetric finite element model described in Section 3.9.2.1. The canister shell axisymmetric finite element model does not include the vertical lift fixture which bolts to the top outer closure plate, conservatively ignoring the additional structural support it provides to the top outer closure plate.

The vertical lifting load is equal to dead weight of the dry loaded canister, plus an additional 15% to account for dynamic loads due to crane hoist motion. A bounding combined weight for the upper and lower basket assembly and fuel of 57 kips is conservatively assumed, which results in 65.6 kips with the additional 15% factor for dynamic effects. The load on the shell assembly due to the weight of the basket assemblies and fuel is modeled as a uniform pressure over the inside of the bottom closure plate. A $1.15g$ vertical acceleration is applied to account for the self weight of the canister shell assembly plus 15% for dynamic effects.

The resulting maximum stresses in the canister shell components are reported in Table 3.5-4. The results show that the maximum stress intensities in the bounding canister shell due to the vertical canister transfer loading are less than the Service Level A allowable stress intensities.

The W74 canister shell top outer closure plate is also evaluated in Section 3.4.3 and shown to provide factors of safety greater than 6 against yield and 10 against ultimate, in accordance with the requirements of ANSI N14.6 for non-redundant lifting devices used for critical lifts.

3.5.4.1.2 Basket Assembly

For vertical canister transfer handling conditions, the canister basket assembly loading and boundary conditions are identical to those for the vertical dead weight condition. The stresses in the W74M and W74T canister basket assembly due to vertical canister transfer handling loads are equal to 15% of those calculated for vertical dead weight to account for dynamic loads due to crane hoist motion. The W74 canister basket assembly stresses due to the 1.15*g* vertical dead weight plus handling load are equal to 1.15 times the maximum basket assembly stresses due to vertical dead weight only. The resulting canister basket assembly stresses due to vertical dead weight plus canister transfer handling loads are presented in Table 3.5-5. The results show that the canister basket assembly stresses due to the combined vertical dead weight plus handling loads are less than the corresponding Service Level A allowable stress intensities.

3.5.4.2 Horizontal Canister Transfer

In normal or routine handling, the canister is transferred horizontally between the transfer cask and storage cask or transfer cask and transportation cask using a hydraulic ram and pintle system. The forces developed in the hydraulic ram result from friction forces between the canister shell and the transfer cask, storage cask, or transportation cask support rails. For normal transfer operations, the coefficient of friction between the canister shell and the rails is assumed to be 0.5. The magnitude of the pulling force in the hydraulic ram due to the sliding friction force between the canister shell and the support rails is conservatively based on a bounding canister weight of 90,000 pounds. The resulting pulling force is 45,000 pounds.

The canister handling loads due to horizontal canister transfer affect only the canister shell assembly. For horizontal canister transfer conditions in which the canister is pushed by the hydraulic ram, as described in the FuelSolutions™ Storage System SAR, the canister top outer closure plate and bottom end plate are backed by the shield plugs and the top inner closure plate and bottom closure plate. The support provided by the top inner closure plate, bottom closure plate, and shield plugs minimizes the stresses in the outer plates and welds. Even if no structural credit is taken for the backing support provided by the shield plugs, the stresses in canister shell assembly due to horizontal push forces will be less than or equal to those due to horizontal pull forces since the pushing loads are opposed by the canister internal pressure. When the canister is pulled, the hydraulic ram forces are transferred to the canister shell assembly through a pintle plate which is bolted to the top outer closure plate or the bottom end plate. The outer closure plate and its weld support the entire load. Therefore, the canister shell assembly stresses are highest for the horizontal canister transfer condition in which the canister is pulled. The canister basket assembly is not affected by the horizontal transfer ram load. Therefore, no structural evaluation of the canister basket assembly is performed for handling loads due to horizontal canister transfer.

As discussed in Section 3.1.1.1, the W74T canister configuration is considered to be the most limiting for the structural analysis. The bounding canister shell stresses due to the normal horizontal canister transfer handling loads are evaluated using the axisymmetric finite element model described in Section 3.9.2.1 and shown in Figure 3.9-1. Two horizontal transfer stress

analyses are performed with each model: a 45 kip pulling force applied to the top outer closure plate, and a 45 kip pulling force applied to the bottom end plate. For both ends, the pull force is applied as an annular line load at the pintle plate bolt circle radius (R=16 inches). In both cases, the canister shell is restrained longitudinally at a single shell node opposite the end of the pull force. The shell assembly stresses due to horizontal dead weight are evaluated separately (Section 3.5.3.1.2) from the horizontal transfer pull force.

The bounding canister shell stresses due to normal horizontal canister transfer loading are reported in Table 3.5-4. The analysis results show that the maximum canister shell stress intensities due to the normal horizontal canister transfer loading are less than the corresponding Service Level A allowable stresses.

3.5.4.3 On-Site Transport

The FuelSolutions™ W74 canister is transported between the plant's fuel building and ISFSI inside the transfer cask which is mounted horizontally on the transfer skid and trailer, as described in the FuelSolutions™ Storage System SAR. The loads associated with shock and vibration loads which occur during on-site transport operations are evaluated and shown to meet the structural design criteria. As described in Section 2.3.1.4 of this SAR, peak accelerations of 1.6*g* vertical (including dead weight), $\pm$0.2*g* lateral, and $\pm$0.3*g* longitudinal are conservatively used for on-site transport of the canister within the transfer cask.

3.5.4.3.1 Canister Shell Assembly

The maximum stresses in the canister shell assembly due to on-site transport shock and vibration loads are insignificant in comparison to the canister shell stresses resulting from the normal vertical and horizontal canister transfer loads. This is based on a comparison of the canister shell stresses due to normal horizontal transfer and scaled stresses from the horizontal and vertical dead weight conditions. For the on-site transport shock and vibration load condition, the canister shell stresses are approximately equal to 0.63 times the horizontal dead weight (i.e., SRSS of 0.6*g* vertical and 0.2*g* lateral) plus 0.3*g* times the vertical dead weight. As shown in Table 3.5-4, the canister shell stresses due to the normal vertical and horizontal transfer load conditions are substantial greater than those due to dead weight loads, even without applying the reduction factors described above. Therefore, the canister shell stresses due to on-site transport shock and vibration loads are clearly lower than the corresponding Service Level A allowable stresses.

3.5.4.3.2 General and LTP Spacer Plates

The most heavily loaded W74 general spacer plate and LTP spacer plate evaluated for the bounding on-site transport shock and vibration loads of +1.6*g* vertical (including dead weight), 0.3*g* longitudinal, and 0.2*g* lateral. The vector sum of the +1.6*g* vertical and 0.2*g* lateral accelerations is 1.61*g* at an angle of 7° from vertical. In order to provide a bounding analysis for the on-site transport loads, a 2*g* vertical load is used to bound the vector sum of the in-plane vibration loads. The stresses in the most highly loaded W74 general and LTP spacer plates due to the 2*g* in-plane load and the 0.3*g* longitudinal load are calculated separately and the maximums are conservatively combined irrespective of sign and location. Therefore, the W74 general and LTP spacer plate stresses for the 2*g* vertical vibration load are equal to twice the maximum spacer plate stresses due to horizontal dead weight. The spacer plate stresses due to the 0.3*g* longitudinal vibration load are calculated by scaling the maximum spacer plate stresses due to

vertical dead weight loading by 30%. The maximum stresses in the W74 general and LTP spacer plates due to on-site transport handling loads are presented in Table 3.5-5. The results show that the W74 general and LTP spacer plate stresses due to the on-site transport handling load are less than the Service Level A allowable stresses.

3.5.4.3.3 Engagement Spacer Plate

The W74 engagement spacer plate is designed for bounding on-site transport shock and vibration loads of +1.6*g* vertical (including dead weight), 0.3*g* longitudinal, and 0.2*g* lateral. The vector sum of the +1.6*g* vertical and 0.2*g* lateral accelerations is 1.61*g* at an angle of 7° from vertical. In order to provide a bounding analysis for the on-site transport loads, a 2*g* vertical load is used to bound the vector sum of the in-plane vibration loads. The stresses in the engagement spacer plate due to the 2*g* in-plane load and the 0.3*g* longitudinal load are calculated separately and the maximums are conservatively combined irrespective of sign and location.

The W74 engagement spacer plate stresses for the 2*g* vertical vibration load are calculated using the ½-symmetry plane stress finite element model described in Section 3.9.2.5 and shown in Figure 3.9-16. Only the geometry of the engagement spacer plate is modeled, neglecting the attachment sleeves which are welded to the engagement spacer plate. Since the total weight of the attachment sleeves is less than 1% of the engagement spacer plate weight, their omission is considered negligible. The edge support provided by the canister shell is modeled using radial gap elements to reflect the non-linear interface. The engagement spacer plate is supported only at the locations of those gap elements which close under on-site transport loading. The angle of support is shown to be small for on-site transport loading (approximately 8°) due to the relatively high in-plane stiffness of the engagement spacer plate low magnitude of the loads. The peak stress intensity in the W74 engagement spacer plate due to the 2*g* in-plane load is 1.0 ksi.

For the 0.3*g* longitudinal load, the engagement spacer plate is assumed to support the entire either the upper or lower basket assembly plus the weight of the fuel assemblies inside the basket assembly. Consequently, the stresses due to the 0.3*g* longitudinal load are equal to 30% of the vertical dead weight stresses. As discussed above, these stresses are conservatively combined with those calculated for the 2*g* in-plane load irrespective of sign and location. The resulting maximum primary membrane, primary membrane plus bending, and primary plus secondary stress intensities in the W74 engagement spacer plate due to on-site transport handling loads are 1.2 ksi, 1.2 ksi, and 1.8 ksi, respectively. The corresponding Service Level A allowable primary membrane, primary membrane plus bending, and primary plus secondary stress intensities for SA-240, Type XM-19 stainless steel at 600°F are 29.2 ksi, 43.8 ksi, and 87.6 ksi, respectively. Therefore, the W74 engagement spacer plate stresses due to the on-site transport handling loads are less than the corresponding Service Level A allowable stress intensities.

3.5.4.3.4 Support Tubes and Support Sleeves

The W74 support tubes and support sleeves are designed for bounding on-site transport shock and vibration loads of +1.6*g* vertical (including dead weight), 0.3*g* longitudinal, and 0.2*g* lateral. The vector sum of the +1.6*g* vertical and 0.2*g* lateral accelerations is 1.61*g* at an angle of 7° from vertical. The stresses in the most highly loaded W74 support tubes and support sleeves due to the bounding on-site transport shock and vibration loads are determined by scaling the maximum stresses calculated for the transfer cask side drop and storage cask end drop by the appropriate factors and combining the maximum stresses irrespective of sign and location. The support tube

and support sleeve stresses due to on-site transport shock and vibration loads are evaluated as follows.

Support Tube Stresses

The stresses in the support tubes due to the 1.61*g* transverse load are determined by scaling the stresses calculated for the postulated side drop load in Section 3.7.5.2.3 by the ratio of the transverse loads (i.e., 1.61*g*/60*g*). The resulting maximum primary membrane and primary membrane plus bending stress intensities in the W74 support tube due to the 1.61*g* transverse load are 0.04 ksi (=1.44 ksi x 1.61*g*/60*g*) and 0.17 ksi (=6.44 ksi x 1.61*g*/60*g*), respectively. The support tube stresses due to the 0.3*g* longitudinal load are calculated by scaling the maximum stresses calculated for the storage cask end drop loads by the ratio of the longitudinal loads. The maximum primary membrane and primary membrane plus bending stress intensities in the most highly loaded support tubes are taken as the larger of the stresses calculated for the 20*g* end drop load multiplied by 0.3*g*/20*g* or those calculated for the 50*g* end drop load multiplied by 0.3*g*/50*g*. The resulting maximum primary membrane and primary membrane plus bending stress intensities in the W74 support tube due to the 0.3*g* longitudinal load are 0.12 ksi (=7.9 ksi x 0.3*g*/20*g*) and 0.14 ksi (=9.2 ksi x 0.3*g*/20*g*), respectively. Therefore, the combined primary membrane and primary membrane plus bending stress intensities in the most highly loaded support tube due to on-site transport shock and vibration loads are 0.16 ksi and 0.31 ksi, respectively. The Service Level A allowable primary membrane and primary membrane plus bending stress intensities for SA-240, Type XM-19 stainless steel at 700°F are 28.8 ksi and 43.2 ksi, respectively. Therefore, the minimum design margins for primary membrane and primary membrane plus bending stress intensity in the most highly loaded W74 support tubes for on-site transport shock and vibration loading are large.

The stresses in the support tube corner seam welds are evaluated in the same manner as the stresses in the support tube base metal, as described above. Since longitudinal loads do not produce any significant stresses in the support tube corner welds, only transverse loads are considered for the weld stress evaluation. As shown in Section 3.7.5.2.3, the maximum shear stress in the support tube corner weld due to the 60*g* side drop load is 1.34 ksi. Therefore, the maximum shear stress in the weld due to the 1.61*g* transverse load is 0.04 ksi (=1.34 ksi x 1.61*g*/60*g*). The corresponding Service Level A allowable shear stress is 6.1 ksi, based on SA-240, Type XM-19 stainless steel at 700°F with a weld quality factor or 35% for single fillet weld with surface visual examination per Table NG-3352-1 of the ASME Code. Therefore, the minimum design margin in the support tube corner weld for the on-site transport shock and vibration loads is large.

Support Sleeve Stresses

As discussed in Section 3.7.5.2.4, the support sleeve stresses due to transverse loads are insignificant since the support sleeves are loaded only by their own weight in this direction. Consequently, only longitudinal loads are considered for the support sleeve on-site transport handling stress evaluation. The maximum stresses in the most highly loaded support sleeve due to the 0.3*g* longitudinal vibration load are calculated by scaling the support sleeve stresses calculated for the 50*g* end drop load by 0.3*g*/50*g*. As discussed in Section 3.7.3.2.4, the 50*g* end drop condition results in a maximum axial compressive stress of 8.1 ksi in the most heavily loaded support sleeve, which is classified as a primary membrane stress intensity. Therefore, the maximum primary membrane stress intensity in the most highly loaded support sleeve due to the

0.3*g* longitudinal load is 0.05 ksi (=8.1 ksi x 0.3*g*/50*g*). The Service Level A allowable primary membrane stress intensities for SA-240, Type 304 stainless steel at 700°F is 16.0 ksi. Therefore, the minimum design margin for primary membrane stress intensity in the most highly loaded W74 support sleeves for on-site transport shock and vibration loading is large.

The shear stress in the support sleeve seam welds are evaluated in the same manner as the stresses in the support tube seam weld, as described above. Since longitudinal loads do not produce any significant stresses in the support sleeve seam welds, only transverse loads are considered for the weld stress evaluation. As shown in Section 3.7.5.2.4, the maximum shear stress in the support sleeve seam weld due to the 60*g* side drop load is 2.36 ksi. Therefore, the maximum shear stress in the weld due to the 1.61*g* transverse load is 0.06 ksi (=2.36 ksi x 1.61*g*/60*g*). The corresponding Service Level A allowable shear stress is 3.4 ksi, based on SA-240, Type 304 stainless steel at 700°F with a weld quality factor or 35% for single fillet weld with surface visual examination per Table NG-3352-1 of the ASME Code. Therefore, the minimum design margin in the support sleeve seam weld for the on-site transport shock and vibration loads is +57.0.

3.5.4.3.5 Support Tube Attachment Welds

Each W74M support tubes are welded to the top and bottom end LTP spacer plates using ½-inch partial penetration groove welds with ¼-inch cover fillets on all four sides of the tube. Similarly, the W74T support tubes are welded to the attachment sleeves at each end using ¼-inch fillet welds on all four sides of the tube. The stresses in these support tube attachment welds due to the on-site transport shock and vibration loads are calculated by scaling the maximum stresses calculated for the storage cask end drop and transfer cask side drop loads in the same manner as done for the support tubes in the previous section. The only significant weld stresses resulting from transverse loads are due to the shear reactions at the end spacer plates. As discussed in Section 3.7.5.2.4, the maximum shear stress in the W74M support tube attachment welds due to the 60*g* side drop load is 0.44 ksi and the shear stress in the W74T support tube attachment welds due to the 60*g* side drop load are insignificant. The resulting maximum shear stress in the W74M support tube attachment weld due to the 1.61*g* transverse load is 0.01 ksi (=0.44 ksi x 1.61*g*/60*g*). The W74M and W74T support tube attachment weld stresses due to the 0.3*g* longitudinal load are calculated by scaling the maximum weld stresses calculated for the storage cask end drop loads by the ratio of the longitudinal loads. The maximum shear stresses in the W74M and W74T support tube attachment welds are taken as the larger of the stresses calculated for the 20*g* end drop load multiplied by 0.3*g*/20*g* or those calculated for the 50*g* end drop load multiplied by 0.3*g*/50*g*. The resulting maximum shear stress in the W74M support tube attachment welds and W74T support tube attachment welds due to the 0.3*g* longitudinal load are 0.05 ksi (=3.2 ksi x 0.3*g*/20*g*) and 0.13 ksi (=8.6 ksi x 0.3*g*/20*g*), respectively. Therefore, the combined shear stress in the W74M and W74T support tube attachment welds due to on-site transport shock and vibration loads are 0.06 ksi and 0.13 ksi, respectively. The Service Level A allowable shear stress for SA-240, Type XM-19 stainless steel at 700°F is 6.9 ksi. Therefore, the minimum design margins for shear stress in the W74M and W74T support tube attachment welds for on-site transport shock and vibration loading are +114 and +52.1, respectively.

3.5.4.3.6 Guide Tubes

As discussed in Section 2.3.1 of this SAR, the W74 guide tubes are designed for bounding shock and vibration loads of +1.6*g* vertical (including dead weight), 0.3*g* longitudinal, and 0.2*g* lateral. The W74 guide tube stresses due to the on-site transport vibration loads are determined by scaling the maximum guide tube stresses due to vertical and horizontal dead weight loads and adding the resulting stresses irrespective of sign and location. The vector sum of the +1.6*g* vertical and 0.2*g* lateral accelerations is 1.61*g* at an angle of 7° from vertical. In order to provide a bounding analysis for the on-site transport loads, a 1.65*g* vertical load is used to bound the vector sum of the in-plane vibration loads. Therefore, the W74 guide tube stresses for the 1.65*g* vertical vibration load are equal to 1.65 times the maximum guide tube stresses due to horizontal dead weight. The guide tube stresses due to the 0.3*g* longitudinal vibration load are calculated by scaling the maximum guide tube stresses due to vertical dead weight loading by 30%. The maximum stresses in the W74 guide tubes due to on-site transport handling loads are presented in Table 3.5-5. The results show that the maximum stresses in the W74 guide tubes and all related components (i.e., guide tube longitudinal seam weld, W74M guide tube attachment brackets and welds, neutron absorber panel, and neutron absorber panel retainer welds) due to the on-site transport handling load are less than the corresponding Service Level A allowable stresses.

3.5.5 Load Combinations and Comparison with Allowable Stresses

The maximum stress intensities in FuelSolutions™ W74 canister components resulting from the individual normal on-site transfer and storage load conditions are evaluated in the previous sections and summarized in Table 3.5-4 and Table 3.5-5 along with the corresponding Service Level A/B allowable stress intensity. The results show that the canister component stresses due to the normal on-site transfer and storage load conditions meet the Service Level A/B stress acceptance criteria.

Load combinations are performed for the FuelSolutions™ W74 canister in accordance with Section 2.3 for normal conditions. The normal load combinations are defined in Table 2.3-1. The structural evaluations of the W74 canister shell assembly and basket assembly for normal load combinations are presented in the following sections.

3.5.5.1 Shell Assembly

The W74 canister normal load combinations defined in Table 2.3-1 are simplified by identifying the bounding load combinations. Load combination A1 (vertical dead weight plus canister drainage internal pressure) is evaluated in Section 3.5.2.1. Load combination A3 is bounded by load combination A5 and need not be evaluated. Therefore, the canister shell normal load combination evaluation presented in this section considers only load combinations A2, A4, and A5.

The canister shell assembly stresses due to load combinations A2, A4, and A5 are evaluated using the axisymmetric and three-dimensional finite element model described in Section 3.9.2.1. Separate evaluations are performed for internal pressure acting on both the top inner and outer closures. Thermal loads are only included for the evaluation of secondary stress intensities.

For load combination A2, vertical dead weight, normal internal pressure, and normal thermal loads are applied simultaneously to the canister shell axisymmetric finite element model. For this

condition, the canister shell is supported at the bottom end. The evaluation for load combination A4 is performed in a similar manner to load combination A2 with the addition of vertical canister transfer loads. For load combination A4, the canister shell is supported vertically at the location of the vertical transfer pintle plate bolt circle on top outer closure plate. The load combination A5 evaluation uses both the axisymmetric and three-dimensional finite element models. The axisymmetric model is used to determine the canister shell stresses due to normal horizontal canister transfer, normal internal pressure, and normal thermal loads. The canister shell stresses due to horizontal dead weight, which are calculated using the three-dimensional half-symmetry finite element model described in Section 3.9.2.2, are conservatively added absolutely to the maximum stresses calculated with the axisymmetric model.

The governing canister shell stresses for load combinations A1, A2, A4, and A5 are summarized in Table 3.5-6. The results show that the canister shell stresses for all normal load combinations are less than the corresponding Service Level A allowable stresses.

3.5.5.2 Basket Assembly

Since the W74 basket assembly is not a pressure retaining component, and therefore need not be evaluated for internal pressure loads, the governing normal load combination for the W74 basket assembly are A4 ($D_v + L_{hv} + T$) and A5 ($D_h + L_{hh} + T$). The W74 basket assembly stresses due to these normal load combinations are conservatively calculated by adding the maximum stresses due to the individual load conditions absolutely and irrespective of location. The governing load combination stress results for each of the W74 basket assembly structural components are summarized in Table 3.5-7. The results show that the maximum stresses due to governing normal load combinations are less than the corresponding Service Level A allowable stresses.

3.5.5.3 Damaged Fuel Can

The higher weight of the damaged fuel can only affects the stresses resulting from the vertical dead weight and vertical canister transfer handling conditions. As shown in Table 3.5-5, the guide tube stresses due to vertical dead weight and vertical handling loads are insignificant. The only significant stresses in the guide tube results from horizontal dead weight and horizontal handling loads. For these load conditions, the loads acting on the damaged fuel can are approximately equal to those acting on the guide tube. However, the damaged fuel can is continuously supported by the basket assembly support tubes, whereas, the guide tubes are supported intermittently by the basket assembly spacer plates. Consequently, the stresses in the damaged fuel can due to horizontal dead weight and horizontal handling loads are bounded by the stresses in the guide tube.

The results of the normal condition evaluation of the damaged fuel can show that the maximum stresses in the damaged fuel can for the controlling normal load conditions are bounded by those calculated for the guide tube. Therefore, since the guide tube satisfies the structural design criteria, the damaged fuel can also satisfies the structural design criteria.

3.5.6 Cold

The normal cold steady state ambient temperature of 0°F with no fuel decay heat and no insolation results in a uniform temperature of 0°F throughout the canister. For this condition, the effects of differential thermal expansion between dissimilar materials within the canister

assembly and the potential for brittle fracture and freezing of liquids are considered. Differential thermal expansion of the W74 canister for cold thermal conditions is bounded by the normal thermal conditions evaluated in Section 3.5.1.2. Brittle fracture of the canister components for a lowest service temperature of 0°F is addressed in Section 3.1.2.3. Since the canister does not include any liquids, there is no potential damage due to freezing of liquids.

Table 3.5-1 - W74 Canister Temperatures for Normal Thermal Conditions

Canister Component	Maximum Temperatures (°F)		Design Temperature[1] (°F)
	In Storage Cask	In Transfer Cask	
Guide Tube	716	714	715
W74M Guide Tube Attachment Brackets	506[2]	661[2]	650[2]
General Spacer Plate	699	700	700
LTP Spacer Plate	506	661	650
Engagement Spacer Plate	445	506	600
Support Tube & Support Sleeve	584	683	700
Canister Shell (center/ends)[3]	445/215	543/302	300[3]

Notes:

(1) Temperature upon which allowable stresses are based.

(2) Based on temperature of hottest LTP spacer plate to which the guide tube attachment brackets are welded.

(3) The maximum canister shell temperature in the central region of the canister cavity and at the end of the canister cavity are reported. The design temperature of 300°F is used for the canister shell assembly since all of the controlling stresses occur in the top and bottom end regions.

Table 3.5-2 - Comparison of W74 Canister Shell Temperatures for Normal Thermal Conditions

Gradient Location	Canister Shell Temperature Gradients (°F)			
	Storage		Transfer	
	Normal Cold	Normal Hot	Normal Cold	Normal Hot
Axial	231	245	342	306
Radial	32	34	49	44
Overall	233	246	345	308

Table 3.5-3 - W74 Engagement Spacer Plate Normal Thermal Temperatures

Location	Engagement Spacer Plate Temperatures (°F)			
	In Storage Cask		In Transfer Cask	
	Normal Cold	Normal Hot	Normal Cold	Normal Hot
1	343	443	459	506
2	337	437	439	487
3	337	437	413	462
4	343	443	376	428
5	222	328	395	443
6	256	360	413	460
7	224	330	395	440
8	256	360	370	418
9	224	328	263	322
Maximum(1)	**343**	**443**	**459**	**506**
Minimum(1)	**222**	**328**	**263**	**322**
Gradient(2)	**121**	**115**	**196**	**184**

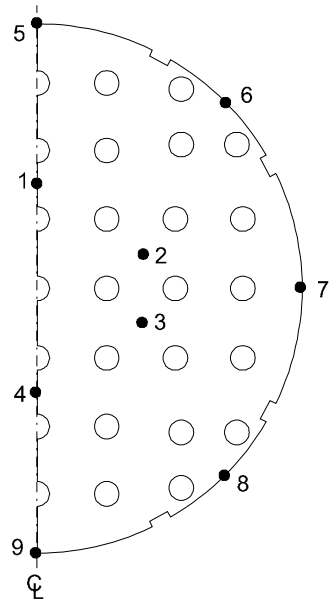

Notes:

(1) Maximum and minimum temperatures at any location on the engagement spacer plate.

(2) Difference between maximum and minimum temperatures.

Table 3.5-4 - W74 Canister Shell Assembly Normal Condition Stress Summary

Shell Component	Stress Type	Maximum Stresses[1] (ksi)							Allowable Stress[2] (ksi)
		Dead Weight		Handling		Internal Pressure		Normal Thermal	
		Vertical	Horizontal	Vertical	Horizontal[3]	Normal[4]	Drainage[5]		
Top End	P_m	0.0	0.4	0.4	0.6	0.2	[7]	N/A	20.0
Outer Closure	P_m+P_b [6]	0.2	0.0	2.8	11.1	3.2	[7]	N/A	30.0
Plate	P_m+P_b+Q	0.2	0.7	2.8	11.1	3.2	[7]	6.9	60.0
Top End	P_m	0.1	0.8	1.8	2.6	1.1	[7]	N/A	16.0[9]
Outer Closure	Shear[8]	0.0	0.0	0.8	0.4	0.3	[7]	N/A	9.6[9]
Weld	P_m+P_b+Q[6]	0.6	3.9	5.2	13.7	5.9	[7]	2.5	48.0[9]
Top End	P_m	0.0	1.6	0.1	0.3	0.2	0.5	N/A	20.0
Inner Closure	P_m+P_b	0.3	3.6	0.8	0.7	1.3	9.4	N/A	30.0
Plate	P_m+P_b+Q	0.3	3.6	0.8	0.7	1.3	9.4	6.7	60.0
Top End	P_m	0.2	8.9	0.8	1.7	1.3	0.8	N/A	18.0[10]
Inner Closure	Shear[8]	0.1	4.5	0.4	0.9	0.6	0.4	N/A	10.8[10]
Weld	P_m+P_b+Q	0.2	8.9	0.8	0.9	1.3	0.8	0.5	54.0[10]
Top Shield Plug[12]	P_m	0.1	[11]	0.1	[11]	---	---	N/A	17.7
	P_m+P_b	0.5	[11]	0.6	[11]	---	---	N/A	26.6
Cylindrical Shell	P_m	0.2	3.3	2.5	5.3	2.3	1.6	N/A	20.0
	P_m+P_b	0.5	7.7	9.7	12.0	5.2	2.1	N/A	30.0
	P_m+P_b+Q	0.5	7.7	9.7	12.0	5.2	2.1	2.8	60.0
Bottom Closure Plate	P_m	0.0	1.6	0.4	0.0	0.2	0.2	N/A	20.0
	P_m+P_b	0.2	3.6	5.5	0.1	2.5	1.0	N/A	30.0
	P_m+P_b+Q	0.2	3.6	5.5	0.1	2.5	1.0	6.9	60.0
Bottom Shell Extension[12]	P_m	0.2	3.3	2.1	4.2	0.8	0.2	N/A	20.0
	P_m+P_b	0.6	7.7	2.8	5.2	1.1	0.5	N/A	30.0
	P_m+P_b+Q	0.6	7.7	2.8	5.2	1.1	0.5	1.8	60.0
Bottom End Plate	P_m	0.1	1.6	0.2	0.8	0.3	0.1	N/A	20.0
	P_m+P_b	0.1	3.6	6.9	15.5	3.4	0.1	N/A	30.0
	P_m+P_b+Q	0.1	3.6	6.9	15.5	3.4	0.1	6.5	60.0
Top Shield Plug Supt. Bar Weld[12]	Shear	0.2	---	0.2	---	0.0	0.2	---	9.0
Shell Extension Top Weld[12]	Shear	0.3	0.3	0.8	0.7	0.3	0.2	0.1	9.0
Shell Extension Bottom Weld[12]	Shear	0.3	0.3	0.4	0.6	0.2	0.2	0.1	9.0

Notes on following page:

Table 3.5-4 Notes:

(1) Stresses from "bounding" canister shell structural evaluations.

(2) The canister shell allowable stress intensities are conservatively based on the properties of the weaker of the W74M and W74T canister shell materials (Type 304 stainless steel) properties at 300°F.

(3) Stresses due to horizontal ram load only, not including horizontal dead weight.

(4) Bounding stresses due to 10 psig normal internal design pressure, considered pressure acting on the top inner and outer closure plates, independently.

(5) Stresses due to 30 psig water drainage pressure plus vertical dead weight. For this condition, the canister shell top outer closure plate is not installed and the auxiliary shield plug and strongback are installed on top of the transfer cask and canister.

(6) The maximum bending stress in the top outer closure plate is determined using hand calculations assuming simply support edge conditions to demonstrate that the bending stress in the top outer closure weld may be classified as secondary.

(7) The top outer closure plate and weld are not attached to the canister shell for this condition.

(8) Pure shear stress in the welds are determined using hand calculations.

(9) The allowable stresses for the top outer closure weld include a 0.8 weld efficiency factor in accordance with ISG-4.

(10) The allowable stresses for the top inner closure weld include a 0.9 weld efficiency factor in accordance with Section 3.1.2.2 of this SAR.

(11) The stresses in the top shield plug for horizontal dead weight and handling loads are bounded by those due to vertical dead weight and handling loads.

(12) Evaluated in accordance with Subsection NF of the ASME Code. Accordingly, secondary stresses need not be considered.

Table 3.5-5 - W74 Canister Basket Assembly Normal Condition Stress Summary (2 Pages)

Basket Component	Stress Type	Maximum Stresses (ksi)					Allowable Stress (ksi)
		Dead Weight		Handling[1]		Normal Thermal[2]	
		Vertical	Horizontal	Vertical	Horizontal		
W74M LTP Spacer Plate	P_m	0.0	0.4	0.0	0.9	N/A	29.0
	P_m+P_b	0.7	0.9	0.8	2.0	N/A	43.5
	P_m+P_b+Q	2.4	0.9	2.8	2.6	42.7	87.0
W74M and W74T General Spacer Plate	P_m	0.0	1.8	0.0	3.7	N/A	35.9
	P_m+P_b	0.4	3.7	0.5	7.6	N/A	53.9
	P_m+P_b+Q	1.2	3.9	1.4	8.2	50.5	107.7
W74M and W74T Engagement Spacer Plate	P_m	0.6	0.5	0.7	1.2	N/A	29.2
	P_m+P_b	0.7	0.5	0.9	1.2	N/A	43.8
	P_m+P_b+Q	2.5	0.5	2.9	1.8	38.3	87.6
W74M Support Tube	P_m	0.4	0.0	0.5	0.2	N/A	28.8
	P_m+P_b	0.5	0.1	0.5	0.3	N/A	43.2
	P_m+P_b+Q	0.5	0.1	0.5	0.3	1.0	86.4
W74M Support Tube Longitudinal Seam Weld	Shear	0.0	0.0	0.0	0.0	---	6.1[3]
W74M Support Tube Attachment Weld	Shear	0.2	0.0	0.2	0.1	1.9	6.9[4]
W74T Support Tube	P_m	0.4	0.0	0.5	0.2	N/A	28.8
	P_m+P_b	0.5	0.1	0.5	0.3	N/A	43.2
	P_m+P_b+Q	0.5	0.1	0.5	0.3	1.0	86.4
W74T Support Tube Longitudinal Seam Weld	Shear	0.0	0.0	0.0	0.0	---	6.1[3]
W74T Support Tube Attachment Weld	Shear	0.4	0.0	0.5	0.1	4.5	6.9[4]
W74M Support Sleeve	P_m	0.2	0.0	0.2	0.1	N/A	16.0
	P_m+P_b	0.2	0.0	0.2	0.1	N/A	24.0
	P_m+P_b+Q	0.2	0.0	0.2	0.1	3.2	48.0
W74M Support Sleeve Seam Weld	Shear	0.0	0.0	0.0	0.1	---	3.4[3]
W74T Support Sleeve	P_m	0.2	0.0	0.2	0.1	N/A	16.0
	P_m+P_b	0.2	0.0	0.2	0.1	N/A	24.0
	P_m+P_b+Q	0.2	0.0	0.2	0.1	3.2	48.0
W74T Support Sleeve Seam Weld	Shear	0.0	0.0	0.0	0.1	---	3.4[3]

Table 3.5-5 - W74 Canister Basket Assembly Normal Condition Stress Summary (2 Pages)

W74M and W74T Guide Tube	P_m	0.0	0.9	0.0	1.4	N/A	16.2
	P_m+P_b	0.0	3.8	0.0	6.2	N/A	24.3
	P_m+P_b+Q	0.0	3.8	0.0	6.2	0.0	48.6
W74M & W74T Guide Tube Seam Weld	P_m	0.0	0.2	0.0	0.3	N/A	10.5(5)
	P_m+P_b	0.0	0.6	0.0	1.0	N/A	15.8(5)
W74M Guide Tube Attachment Bracket	P_m	5.1	(6)	5.9	(6)	N/A	16.6
	P_m+P_b	14.9	(6)	17.1	(6)	N/A	25.0
	Weld Shear	3.3	(6)	3.7	(6)	N/A	4.0(4)
Guide Tube Neutron Absorber Panels	P_m+P_b	(7)	0.1	(7)	0.1	N/A	23.9
Neutron Absorber Panel Retainer Weld	Shear	(7)	0.1	(7)	0.2	N/A	2.9(8)

Notes:

(1) Handling stress results include dead weight.

(2) General thermal stress is classified as secondary stress intensity in accordance with NG-3213.12(a). General thermal stress intensity is taken as the linearized membrane plus bending stress intensity.

(3) Includes a 35% weld quality factor for a single fillet weld with surface visual examination in accordance with Table NG-3352-1 of the ASME Code.

(4) Includes a 40% weld quality factor for a single fillet weld or single bevel groove weld with surface PT examination in accordance with Table NG-3352-1 of the ASME Code.

(5) Includes a 65% weld quality factor for a full penetration weld with surface PT examination in accordance with Table NG-3352-1 of the ASME Code. Full penetration longitudinal seam welds examined with both RT and PT have a weld quality factor of 100%, and are evaluated as guide tube base metal.

(6) Bounded by vertical dead weight and vertical handling stresses.

(7) Bounded by horizontal orientation.

(8) Includes a 30% weld quality factor for a plug weld in accordance with Table NG-3352-1 of the ASME Code.

Table 3.5-6 - W74 Canister Shell Assembly Normal Load Combination Results

Canister Shell Component	Stress Type	Allowable Stress[1] (ksi)	L.C. A1 ($D_{v1}+P_b$) Maximum Stress[2] (ksi)	L.C. A1 ($D_{v1}+P_b$) Design Margin	L.C. A2 (D_v+P+T) Maximum Stress[2] (ksi)	L.C. A2 (D_v+P+T) Design Margin	L.C. A4 ($D_v+L_{hv}+P+T$) Maximum Stress[2] (ksi)	L.C. A4 ($D_v+L_{hv}+P+T$) Design Margin	L.C. A5 ($D_h+L_{hh1}+P+T$) Maximum Stress[2] (ksi)	L.C. A5 ($D_h+L_{hh1}+P+T$) Design Margin
Top End	P_m	20.0	[4]	[4]	0.1	+Large	0.5	+41.8	1.0	+18.6
Outer Closure	P_m+P_b[3]	30.0	[4]	[4]	3.0	+8.87	6.0	+3.99	14.4	+1.09
Plate	P_m+P_b+Q	60.0	[4]	[4]	9.0	+5.65	11.5	+4.22	20.6	+1.91
Top End	P_m	16.0[6]	[4]	[4]	1.0	+14.8	2.7	+4.84	4.5	+2.57
Outer Closure	Shear[5]	9.6[6]	[4]	[4]	0.3	+37.4	1.0	+8.50	0.6	+14.5
Weld	P_m+P_b+Q[3]	48.0[6]	[4]	[4]	5.8	+7.32	12.0	+3.00	24.6	+0.95
Top End	P_m	20.0	0.5	+40.8	0.2	+Large	0.5	+38.7	2.3	+7.55
Inner Closure	P_m+P_b	30.0	9.4	+2.20	1.2	+23.6	2.5	+11.1	10.1	+1.98
Plate	P_m+P_b+Q	60.0	9.4	+5.38	7.9	+6.60	8.5	+6.07	15.4	+2.91
Top End	P_m	18.0[8]	0.8	+21.4	1.2	+14.7	3.2	+4.56	13.6	+0.32
Inner Closure	Shear[7]	10.8[8]	0.4	+25.9	0.6	+17.8	1.6	+5.67	6.8	+0.58
Weld	P_m+P_b+Q	54.0[8]	0.8	+66.5	1.0	+53.7	4.3	+11.5	16.1	+2.35
Top Shield Plug[9]	P_m	17.7	0.1	+Large	0.1	+Large	0.1	+Large	[10]	[10]
	P_m+P_b	26.6	0.5	+52.2	0.5	+52.2	0.6	+43.3	[10]	[10]
Cylindrical	P_m	20.0	1.6	+11.8	2.1	+8.52	4.7	+3.25	11.5	+0.73
Shell	P_m+P_b	30.0	2.1	+13.3	4.7	+5.35	14.0	+1.14	24.9	+0.20
	P_m+P_b+Q	60.0	2.1	+27.6	5.3	+10.3	14.8	+3.05	25.4	+1.36
Bottom	P_m	20.0	0.2	+98.5	0.1	+Large	3.0	+5.76	7.4	+1.70
Shell Extension[8]	P_m+P_b	30.0	0.5	+55.9	0.1	+Large	3.9	+6.80	12.8	+1.34
Bottom	P_m	20.0	0.2	+91.1	0.1	+Large	0.5	+38.6	1.9	+9.41
Closure	P_m+P_b	30.0	1.0	+30.3	0.4	+69.3	8.0	+2.76	10.0	+2.01
Plate	P_m+P_b+Q	60.0	1.0	+59.0	7.9	+6.57	13.4	+3.47	16.4	+2.67
Bottom End	P_m	20.0	0.1	+Large	0.1	+Large	0.3	+61.3	2.4	+7.40
Plate	P_m+P_b	30.0	0.1	+Large	0.1	+Large	9.7	+2.10	19.1	+0.57
	P_m+P_b+Q	60.0	0.1	+Large	6.5	+8.29	15.4	+2.90	25.4	+1.36
Top Shield Plug Supt. Bar Weld[9]	Shear[11]	9.0	0.2	+52.3	0.2	+52.3	0.2	+52.3	0.0	+Large
Shell Extension Top Weld[9]	Shear[11]	9.0	0.2	+42.5	0.0	+Large	1.1	+7.34	1.7	+4.42
Shell Extension Bottom Weld[9]	Shear[11]	9.0	0.2	+36.2	0.0	+Large	0.6	+14.8	1.2	+6.40

Notes on following page

Table 3.5-6 Notes:

(1) The allowable stresses are conservatively based on the properties of the weaker of the W74M and W74T canister shell materials (Type 304 stainless steel) at 300°F.

(2) Stresses from "bounding" canister shell structural evaluations.

(3) The maximum bending stress in the top outer closure plate is determined using hand calculations assuming simply support edge conditions to demonstrate that the bending stress in the top outer closure weld may be classified as secondary.

(4) For this condition, the canister shell top outer closure plate is not installed and the auxiliary shield plug and strongback are installed on top off the transfer cask and canister.

(5) The average shear stresses in the top outer closure weld are determined using hand calculations.

(6) The allowable stresses for the top outer closure weld include a 0.8 weld efficiency factor in accordance with ISG-4.

(7) The shear stress in the top inner closure weld is conservatively assumed equal to half of the maximum primary membrane stress intensity from the finite element solution.

(8) The allowable stresses for the top inner closure weld include a 0.9 weld efficiency factor in accordance with Section 3.1.2.2 of this SAR.

(9) Evaluated in accordance with Subsection NF of the ASME Code. Accordingly, secondary stresses need not be considered.

(10) Stresses due to load combination A5 are not significant.

(11) Shear stress in the shield plug support bar welds and bottom shell extension welds are calculated using the combined nodal forces from the finite element solution.

Table 3.5-7 - W74 Canister Basket Assembly Normal Load Combination Results

Basket Assembly Component	Stress Type	Allowable Stress (ksi)	L.C. A4 ($D_v+L_{hv}+P+T$) Maximum Stress (ksi)	L.C. A4 ($D_v+L_{hv}+P+T$) Minimum Design Margin	L.C. A5 ($D_h+L_{hh2}+P+T$) Maximum Stress (ksi)	L.C. A5 ($D_h+L_{hh2}+P+T$) Minimum Design Margin
LTP Spacer Plate	P_m	29.0	0.0	+Large	0.9	+31.2
	P_m+P_b	43.5	0.8	+53.4	2.0	+20.8
	P_m+P_b+Q	87.0	45.5	+0.91	45.3	+0.92
General Spacer Plate	P_m	35.9	0.0	+Large	3.7	+8.70
	P_m+P_b	53.9	0.5	+Large	7.6	+6.09
	P_m+P_b+Q	107.7	51.9	+1.08	58.7	+0.83
Engagement Spacer Plate	P_m	29.2	0.7	+40.7	1.2	+23.3
	P_m+P_b	43.8	0.9	+47.7	1.2	+33.5
	P_m+P_b+Q	87.6	41.2	+1.13	40.1	+1.19
W74M & W74T Support Tube	P_m	28.8	0.5	+63.0	0.2	+Large
	P_m+P_b	43.2	0.5	+80.5	0.3	+Large
	P_m+P_b+Q	86.4	1.6	+54.0	1.4	+63.0
W74M & W74T Support Tube Seam Weld	Shear	6.1(1)	0.0	+Large	0.0	+Large
W74M Support Tube Attachment Weld	Shear	6.9(2)	2.0	+2.38	1.9	+2.59
W74T Support Tube Attachment Weld	Shear	6.9(2)	5.0	+0.38	4.6	+0.49
W74M & W74T Support Sleeve	P_m	16.0	0.2	+83.2	0.1	+Large
	P_m+P_b	24.0	0.2	+Large	0.1	+Large
	P_m+P_b+Q	48.0	3.4	+13.0	3.3	+13.6
	Buckling	10.1(3)	3.4	+1.95	3.3	+2.08
W74T Support Sleeve Seam Weld	Shear	3.4(1)	0.0	+Large	0.1	+55.0
W74M and W74T Guide Tube	P_m	16.2	0.0	+Large	1.4	+10.6
	P_m+P_b	24.3	0.0	+Large	6.2	+2.92
	P_m+P_b+Q	48.6	0.0	+Large	6.2	+6.84
Guide Tube Longitudinal Seam Weld	P_m	10.5(4)	0.0	+Large	0.3	+34.0
	P_m+P_b	15.8(4)	0.0	+Large	1.0	+14.8
W74M Guide Tube Attachment Bracket	P_m	16.6	5.9	+1.81	5.1	+2.25
	P_m+P_b	25.0	17.1	+0.46	14.9	+0.68
	Weld Shear	4.0(2)	3.7	+0.07	3.3	+0.23
Neutron Absorber Panel	P_m+P_b	23.9	(5)	(5)	0.1	+Large
NAP Retainer Weld	f_w	2.9(6)	(5)	(5)	0.2	+17.1

Notes on following page:

Table 3.5-7 Notes:

(1) Includes a 35% weld quality factor for a single fillet weld with surface visual examination in accordance with Table NG-3352-1 of the ASME Code.

(2) Includes a 40% weld quality factor for single fillet or single bevel groove welds with surface PT examination in accordance with Table NG-3352-1 of the ASME Code.

(3) Allowable stress is equal to ½ of theoretical buckling stress for normal conditions in accordance with NUREG/CR-6322.

(4) Includes a 65% weld quality factor for full penetration welds with surface PT examination in accordance with Table NG-3352-1 of the ASME Code. Full penetration longitudinal seam welds examined with both RT and PT have a weld quality factor of 100%, and are evaluated as guide tube base metal.

(5) Bounded by load combination A5.

(6) Includes a 30% weld quality factor for a plug weld in accordance with Table NG-3352-1 of the ASME Code.

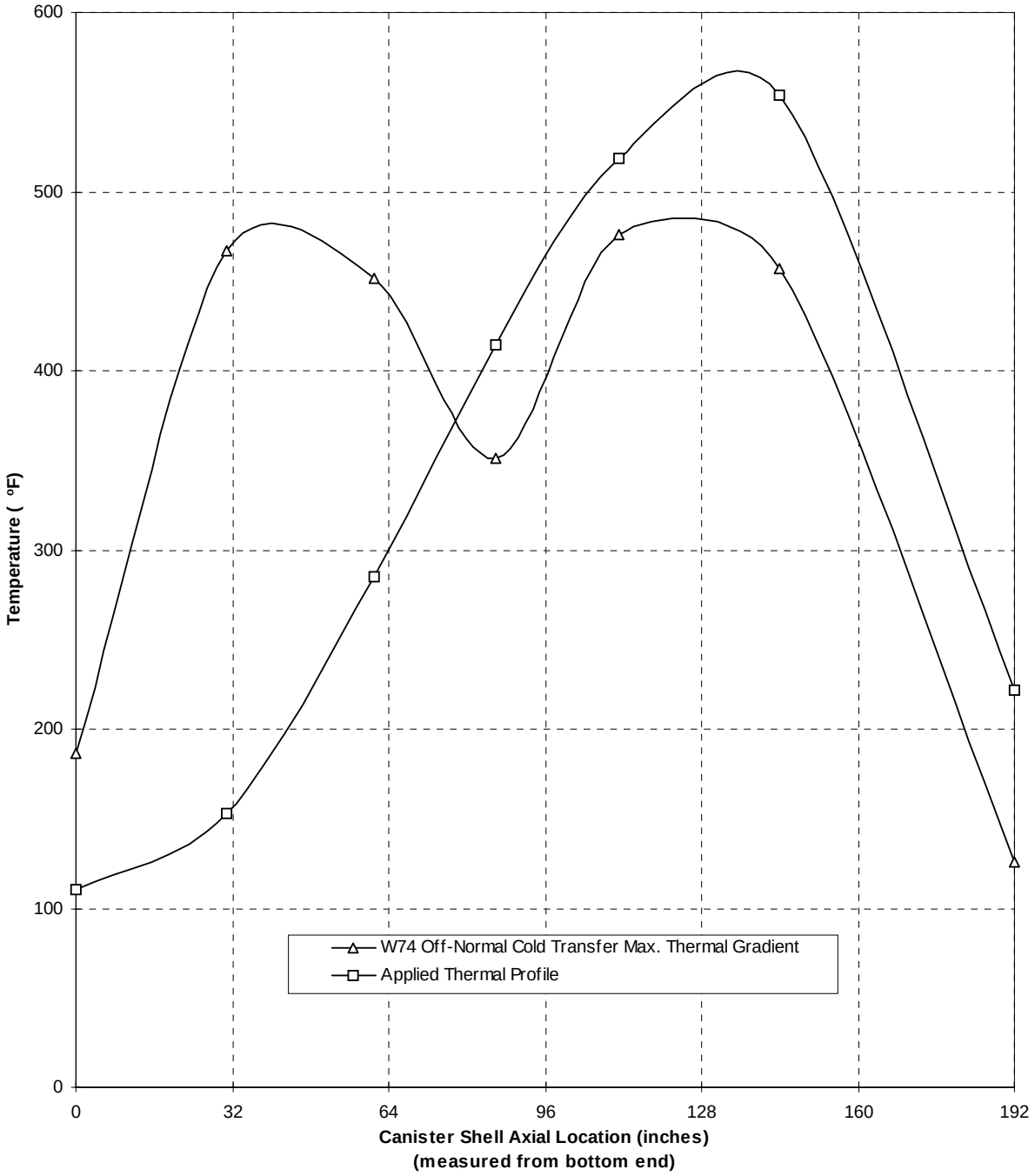

Figure 3.5-1 - Canister Shell Axial Temperature Distribution for the Bounding Normal Thermal Condition

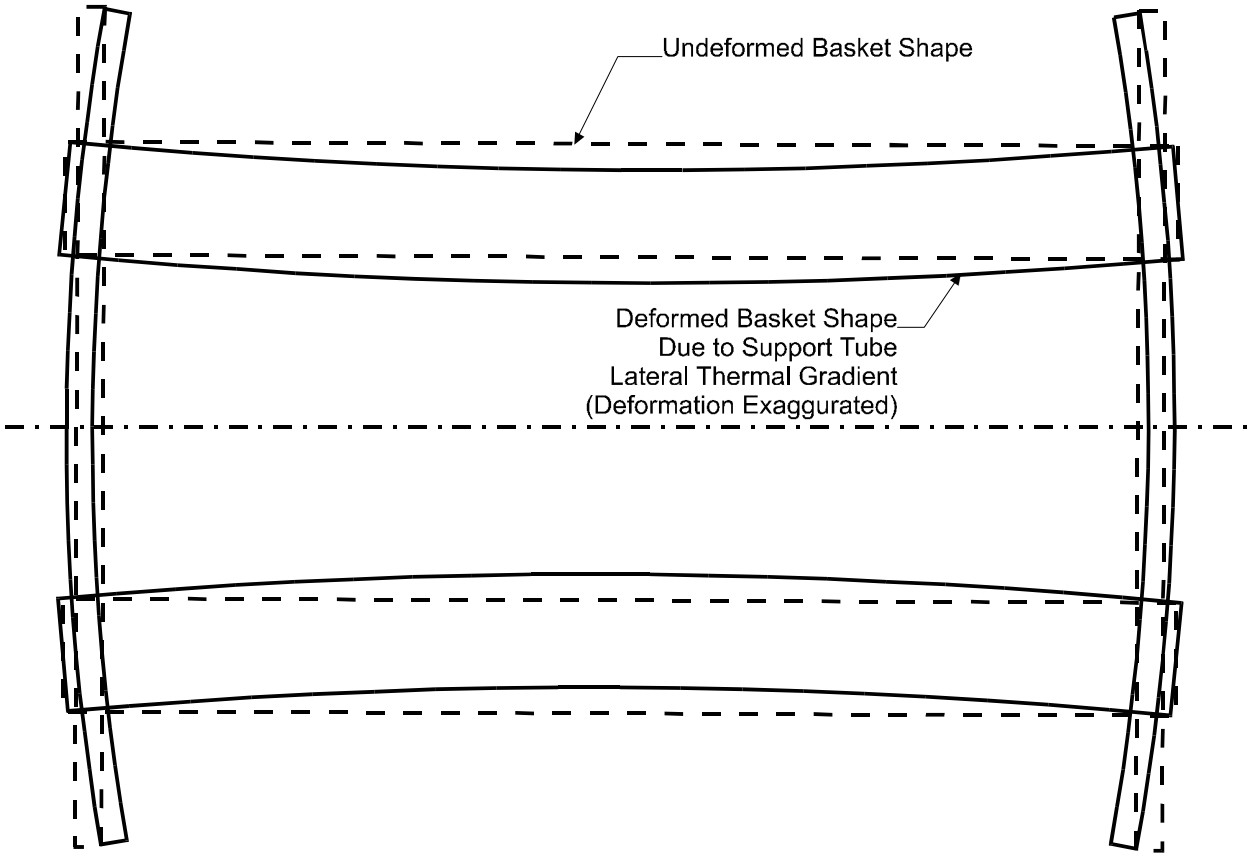

Figure 3.5-2 - W74 Canister Support Tube and End Spacer Plate Curvature due to Lateral Thermal Gradient

This page intentionally left blank.

3.6 Evaluation of Off-Normal Conditions

The FuelSolutions™ W74 canister is evaluated for all credible and significant design basis events resulting from off-normal operation. Off-normal conditions and events are defined in accordance with ANSI/ANS-57.9[26] and include events which, although not occurring regularly, can be expected to occur with moderate frequency on the order of no more than once a year. As defined in Section 2.3.2 of this SAR, off-normal events considered in the structural evaluation of the FuelSolutions™ W74 canister include the following:

- Off-normal temperature and insolation loading
- Off-normal internal pressure
- Potential misalignment of casks during horizontal canister transfer
- Reflood of the canister to facilitate fuel retrieval

The results of the structural evaluations performed herein demonstrate that the FuelSolutions™ W74 canister classes described in Section 1.2.1.3 can withstand the effects of off-normal events without affecting structural safety function and remain in compliance with the applicable acceptance criteria. The following sections present the evaluation of the FuelSolutions™ W74 canister for the design basis off-normal conditions which demonstrate that the requirements of 10 CFR 72.122 are satisfied.

The load combinations evaluated for off-normal conditions are defined in Table 2.3-1. The load combinations include both normal loads which are evaluated in Section 3.5 of this SAR and off-normal loads which are evaluated in this section. The off-normal load combination evaluations are provided in Section 3.6.5.

The structural evaluations of the canister shell assembly are performed for the bounding canister design, determined to be the W74T canister as discussed in Section 3.1.1.1.

The basket assembly structural evaluations are performed for the bounding components as described in Section 3.1.1.2.

The evaluation of the FuelSolutions™ W74 canister for BRP MOX, partial, and damaged fuel assemblies for off-normal conditions considers the effect these fuel assemblies have on the existing structural evaluation of the W74 canister shell assembly and basket assemblies. The structural evaluation of the FuelSolutions™ W74 damaged fuel can for off-normal conditions is included in this section.

The evaluation of the effects of off-normal conditions on the storage cask and transfer cask are provided in the FuelSolutions™ Storage System SAR.

3.6.1 Off-Normal Temperature and Insolation Loadings

Many regions of the United States are subject to maximum summer temperatures in excess of 100ºF, and minimum winter temperatures that are significantly below 0°F. Therefore, to bound

[26] ANSI/ANS-57.9, *Design Criteria for an Independent Spent Fuel Storage Installation (Dry Type)*, American National Standards Institute, 1984.

the expected temperatures of the storage cask during these short term periods of extreme off-normal ambient conditions, conservative analyses are performed to calculate the steady state W74 canister and fuel cladding temperatures for a maximum 125ºF ambient temperature with maximum insolation and for a minimum -40ºF ambient without insolation. The design basis heat load for the W74 canister, as documented in Chapter 4 of this SAR, is used for this analysis.

As discussed in Chapter 4 of this SAR, the FuelSolutions™ W74 canister thermal design loads for off-normal conditions bound those for a FuelSolutions™ W74 canister containing any amount of intact BRP MOX fuel and partial fuel assemblies, and up to eight damaged fuel assemblies. Therefore, the FuelSolutions™ W74 canister shell assembly and basket assembly stresses calculated for the design basis off-normal thermal loads are bounded for a FuelSolutions™ W74 canister containing any amount of intact BRP MOX fuel and partial fuel assemblies, and up to eight damaged fuel assemblies.

3.6.1.1 Summary of Pressures and Temperatures

The canister shell assembly provides primary confinement for on-site transfer and storage conditions. As shown in Table 4.5-2 of this SAR, the maximum internal pressure for the off-normal hot thermal conditions is 12.3 psig. The canister shell assembly is evaluated for an off-normal condition design internal pressure of 16 psig. The canister basket assembly does not serve any pressure retaining function.

The temperatures in the FuelSolutions™ W74 canister for the off-normal storage and on-site transfer are calculated in Section 4.5 and summarized in Tables 4.5-1 and 4.5-3, respectively. With the exception of the reflood condition, thermal stresses resulting from the most severe off-normal thermal conditions are evaluated in Section 3.6.1.3 using Service Level B allowable stress design criteria. The reflood thermal condition is defined as a Service Level C condition. In accordance with the Subsections NB and NG of the ASME Code, general thermal stresses are classified as secondary and need not be evaluated for Service Level C conditions. The short-term elevated temperatures resulting from the storage cask horizontal unloading condition (Table 4.5-1, Case 13b) and canister vacuum drying (Table 4.5-3, Case 6) are not combined with other off-normal or accident load conditions. As discussed in Section 3.3, these short term temperatures have no long-term effect on the mechanical properties of the canister materials.

The design temperatures used for the evaluation of the off-normal internal pressure load and cask misalignment are identical to the normal design temperatures shown in Table 3.5-1. These design temperatures bound the maximum component temperatures due to the off-normal hot storage thermal condition (Table 4.5-1, Case 9) upon which the maximum off-normal internal pressure load is based, and the normal thermal conditions which are combined with the cask misalignment condition.

3.6.1.2 Differential Thermal Expansion

Differential thermal expansion of the W74M canister components are evaluated, as described in Section 3.5.1.2. The results of this evaluation demonstrate that the basket assembly components expand freely within the canister shell under all normal, off-normal, and accident conditions. As documented in the FuelSolutions™ Storage System SAR, the canister shell assembly expands freely within the storage cask and transfer cask cavities under all conditions.

3.6.1.3 Thermal Stress Calculations

3.6.1.3.1 Canister Shell Assembly

The thermal stress evaluation of the canister shell assembly presented in Section 3.5.1.3.1 is performed using a design gradient that bounds the maximum thermal gradients in the canister shell assembly for all normal and off-normal thermal conditions. The canister shell assembly thermal stresses resulting from the bounding thermal load are summarized in Table 3.5-4. The results show that the bounding general thermal stress intensities in the canister shell assembly are less than the corresponding Service Level A allowable stress intensities.

3.6.1.3.2 Canister Basket Assembly

Spacer Plates

Thermal stresses in the W74 general spacer plates, LTP spacer plates, and engagement spacer plate are proportional to the difference between $\alpha E(T-70)$ at the maximum and minimum spacer plate temperatures for any thermal condition, where α and E are the mean coefficient of thermal expansion and elastic modulus of the spacer plate material at the temperature of interest (T). The values of relative thermal stress are calculated for the hottest W74 general spacer plate, LTP spacer plate, and engagement spacer plate using the temperatures for the normal cold and off-normal cold storage conditions.

The cold thermal conditions are evaluated rather than the hot thermal conditions because they produce the highest radial thermal gradients within the spacer plates, and thus, the highest thermal stresses. Only the storage thermal conditions are evaluated since they generally produce higher thermal stresses than the corresponding transfer conditions. Furthermore, the relative increase in thermal stress for transfer conditions will be approximately equal to that for the storage conditions. The results show that the maximum relative thermal stress values ($\Delta\alpha E(T-70)$) for all W74 spacer plates are approximately 3% higher for the off-normal cold storage condition than they are for the normal cold storage condition. Since off-normal conditions are evaluated using Service Level B allowable stress limits which are 10% greater than the Service Level A limits against which the normal thermal stresses are compared, the minimum design margins in the W74 general spacer plate, LTP spacer plate, and engagement spacer plate for off-normal thermal conditions are greater than those for normal thermal conditions.

Support Tubes and Support Sleeves

Thermal stresses in the W74 support tubes and support sleeves due to differential thermal expansion resulting from a bounding normal thermal design temperature of 700°F are calculated in Section 3.5.1.3.4. As shown in Tables 4.5-1 and 4.5-3 of this SAR, the maximum temperature of the W74 support tubes and support sleeves for off-normal thermal conditions is less than 700°F. Since the normal condition design temperature bounds the maximum off-normal thermal condition temperatures, the W74 support tube and support sleeve thermal stresses for off-normal conditions are also bounded.

Guide Tubes

As shown in Tables 4.5-1 and 4.5-3, the maximum temperature of the W74 guide tubes for off-normal thermal conditions is 738°F. As shown in Section 3.5.1.2.2, the W74 guide tubes

expand freely within the W74 canister at the bounding off-normal temperature of 738°F. Therefore, there are no significant thermal stresses in the W74 guide tubes for off-normal thermal conditions.

3.6.2 Off-Normal Internal Pressure

As discussed in Section 4.5.1.4 and summarized in Table 4.5-2, the design basis off-normal condition internal pressure for the FuelSolutions™ W74 canister is based upon the required backfill of helium in accordance with the *technical specification* contained in Section 12.3 of this SAR, elevated to the extreme off-normal condition canister cavity gas temperature. In addition, a concurrent non-mechanistic failure of 10% of the fuel rods with complete release of their fill gas and 30% of their fission gasses into the canister cavity elevated to the extreme off-normal condition canister cavity gas temperature is assumed. As shown in Table 4.5-2, the W74 canister maximum internal pressure for off-normal conditions is 12.3 psig. A bounding internal pressure of 16 psig is conservatively used in the analysis.

The W74 canister shell assembly stresses due to the bounding off-normal internal pressure of 16 psig are calculated using the canister shell axisymmetric finite element model described in Section 3.9.2.1 in the same manner as the normal internal pressure stress evaluation presented in Section 3.5.2.2 of this SAR. The resulting stresses for this loading condition are provided in Table 3.6-1. The results show that the maximum stresses in the W74 canister shell due to the bounding 16 psig off-normal internal pressure load are less than the corresponding Service Level C allowable stresses.

As discussed in Chapter 4 of this SAR, the FuelSolutions™ W74 canister internal pressure design loads for off-normal conditions bound those for a FuelSolutions™ W74 canister containing any amount of intact BRP MOX fuel and partial fuel assemblies, and up to eight damaged fuel assemblies. Therefore, the FuelSolutions™ W74 canister shell assembly and basket assembly stresses calculated for the design basis off-normal internal pressure loads are bounded for a FuelSolutions™ W74 canister containing any amount of intact BRP MOX fuel and partial fuel assemblies, and up to eight damaged fuel assemblies.

3.6.3 Cask Misalignment

The FuelSolutions™ storage system is evaluated for a maximum hydraulic ram load resulting from cask misalignment or interference during horizontal canister transfer. The misalignment ram load is limited to a maximum pushing force of 70 kips or a maximum pulling force of 50 kips on either the top or bottom end of the canister shell assembly. The structural consequences of the hydraulic ram pushing force of 70 kips and pulling force of 50 kips are evaluated for both the top and bottom ends of the canister shell assembly. The canister shell stresses due to the cask misalignment condition are evaluated using Service Level B limits. The canister basket assembly is contained inside the canister shell cavity and protected from the externally applied ram loads. Therefore, the canister basket assembly is not affected by the cask misalignment load condition.

The stresses in the canister shell assembly due to the cask misalignment 50 kip pull force are equal to 110% (i.e., 50/45) of those calculated in Section 3.5.4.2 for the normal horizontal transfer 45 kip pull force. As shown in Table 3.1-4, the Service Level B allowable stresses are also equal to 110% of the Service Level A allowable stresses. Therefore, the minimum design

margins in the canister shell assembly for the cask misalignment 50 kip pull force are equal to those calculated for the normal horizontal transfer 45 kip pull force.

The structural evaluations of the W74 canister shell assembly for the 70 kip pushing force on the top and bottom ends of the canister shell are performed using the same analytical methodology and finite element model used for the normal horizontal canister transfer structural evaluation, as described in Section 3.5.4.2. The 70 kip pushing force is applied to the ends of the canister shell assembly in the same manner as the normal horizontal transfer load. The canister shell maximum primary stress intensities resulting from the 70 kip pushing force applied to either the top or bottom end of the canister are summarized in Table 3.6-1. The results show that the canister shell maximum stress intensities due to the cask misalignment load are less than the corresponding Service Level B allowable stresses.

Since the maximum load is independent of the canister weight and only affects the canister shell, the cask misalignment stresses in the FuelSolutions™ W74 canister shell and basket assemblies bound those for a FuelSolutions™ W74 canister containing any amount of intact BRP MOX fuel and partial fuel assemblies, and up to eight damaged fuel assemblies.

3.6.4 Canister Opening/Reflood

The FuelSolutions™ W74 canister is evaluated for the effects of reflooding the canister after the canister cavity is drained and dried. This could occur prior to or after dry storage. The operating procedures provided in Section 8.2.3 of the FuelSolutions™ Storage System SAR states that the maximum internal pressure for this condition is 100 psig. The structural evaluation provided in this section demonstrates that the FuelSolutions™ W74 canister can accommodate a maximum reflood internal pressure of 100 psig without compromising the integrity of the canister.

The canister shell assembly is designed in accordance with Subsection NB of the ASME Code. The reflood internal pressure load is a condition which can occur in the design life of a canister when it is necessary to retrieve the fuel from the canister shell. Per NCA-2142.4(b), Service Level C allowable stresses "permit large deformations in areas of structural discontinuity which may necessitate the removal of the component from service for inspection or repair of damage to the component or support." Accordingly, the design allowable stresses for Service Level C conditions are applied for the reflood condition. The Service Level C allowable stresses include inherent factors of safety which ensure the safety of the plant personnel performing the reflood operation.

The structural evaluation of the canister shell assembly for the reflood pressure load is performed using a combination of hand calculations and finite element analysis. The evaluation addresses the potential structural failure of the entire canister shell assembly, including the end plate closure welds and vent/drain port closure welds.

The stresses in the canister shell due to reflood internal pressure plus vertical dead weight loading are evaluated on an elastic basis using the axisymmetric finite element model described in Section 3.9.2.1 and shown in Figure 3.9-1. The top outer closure plate remains attached to the canister shell for the reflood condition and small holes are cut into the top outer closure plate to gain access to the vent and drain ports. These holes have no significant effect on the structural capacity of the top outer closure plate and are neglected in the model. The results obtained from this model are applicable to both the FuelSolutions™ W74M and W74T canister shell assemblies since the controlling deformations and stresses due to reflood pressure occur in the canister shell

top closure region, which is the same for both W74 canister designs. Since the top end shield plug does not provide any support for the top end closure plates for the reflood pressure condition, it is only included in the model for the effect of its dead weight.

The dead weight of the canister basket assemblies and SNF are modeled as a uniform pressure load over the inner surface of the canister shell bottom closure plate. A bounding weight of 60 kips is conservatively used for the basket assemblies and fuel. A bounding reflood internal pressure load of 125 psi is applied to the inner surfaces of the canister shell bottom closure plate, cylindrical shell, and top inner closure plate. The maximum canister shell stresses resulting from the 125 psi reflood internal pressure load are summarized in Table 3.6-1. The results show that the maximum stresses in the canister shell assembly due to a bounding reflood internal pressure of 125 psi are less than the allowable stress intensities.

In addition to the main structural components of the canister shell assembly evaluated above, the W74 canister shell vent/drain port closure weld are evaluated for reflood internal pressure to demonstrate its structural adequacy. The evaluation is performed in two parts: 1) A plastic analysis of the canister shell assembly is performed using the axisymmetric shell model described in Section 3.9.2.1 and shown in Figure 3.9-1 to determine the amount of deflection in the inner closure plate at the vent and drain port locations (i.e., R=28.5-inch), and 2) The local deflection of the inner closure plate at the vent and drain port locations which corresponds to the load capacity of the vent and drain port welds is calculated using hand calculations and compared to the deflection from the plastic analysis to determine the reflood internal pressure load at which the vent/drain port weld reaches the Service Level C primary stress allowable. The results of this analysis show that the deflection of the inner closure plate at the vent and drain port weld locations due to a 100 psi internal pressure is 0.049 inches. The local deflection of the inner closure plate corresponding to the Service Level C load capacity of the vent and drain port closure welds is 0.051 inches. Therefore, the stress in the W74 canister shell vent and drain port closure welds due to a 100 psi reflood internal pressure are less than the Service Level C allowable stress.

As discussed above, the design load for the postulated canister reflood condition is an internal pressure load of 100 psig. The magnitude of the reflood internal pressure load is proportional to the temperature of the canister assembly. As discussed in Chapter 4 of this SAR, the FuelSolutions™ W74 canister temperatures for off-normal conditions bound those for a FuelSolutions™ W74 canister containing any amount of intact BRP MOX fuel and partial fuel assemblies, and up to eight damaged fuel assemblies. Therefore, the FuelSolutions™ W74 canister design basis reflood internal pressure load is bounding and no additional evaluation is required for a FuelSolutions™ W74 canister containing any amount of intact BRP MOX fuel and partial fuel assemblies, and up to eight damaged fuel assemblies.

3.6.5 Off-Normal Load Combinations

Load combinations are performed for the FuelSolutions™ W74 canister in accordance with Section 2.3.2 for off-normal conditions. The load combinations include normal loads, which are evaluated in Section 3.5, and off-normal loads, which are evaluated in this section. Load combinations are summarized in Table 2.3-1. The structural evaluation of the W74 canister shell assembly and basket assembly for off-normal load combinations are presented in the following sections.

3.6.5.1 Canister Shell Assembly

The W74 canister off-normal load combinations defined in Table 2.3-1 of this SAR are evaluated using a combination of finite element analysis and hand calculations. Load combinations B1 ($D_v + P_o + T_o$) and B2 ($D_v + L_{hv} + P_o + T_o$) are evaluated using the canister shell assembly axisymmetric finite element model described in Section 3.9.2.1. For these load combinations, the individual loads are applied to the model simultaneously. For load combinations B3 ($D_h + (L_{hh1}$ or $L_{hh2}) + P_o + T_o$) and B4 ($D_v + L_m + P + T$), the canister shell stresses for all combined loads, excluding horizontal dead weight, are determined using the axisymmetric finite element model described in Section 3.9.2.1.

These load combination evaluations are performed for canister horizontal transfer handling loads applied to both the top and bottom ends of the canister shell assembly. The maximum stresses due to horizontal dead weight are then conservatively combined with the maximum stresses from the finite element solution for each canister shell assembly component, irrespective of sign and location.

For load combinations B1 through B4, internal pressure loads are considered separately for both the inner closure plate and outer closure plate . Load combination C5 (vertical dead weight plus reflood internal pressure) is addressed in Section 3.6.4. The W74 canister shell load combination results for off-normal load combinations are reported in Table 3.6-2. The results show that all stresses are less than the corresponding Service Level C allowable stresses.

3.6.5.2 Canister Basket Assembly

The off-normal load combinations for the W74 canister are shown in Table 2.3-1. They include dead weight, normal handling, cask misalignment, off-normal and reflood internal pressure, and off-normal and reflood thermal loads. As discussed in Section 3.6.3, the basket assembly components are not affected by the cask misalignment loading. Since the basket assembly is not a pressure retaining component, it is not evaluated for internal pressure loading. Therefore, the basket assembly off-normal load combinations reduce to dead weight plus normal handling plus off-normal thermal.

The only difference between the basket assembly off-normal load combinations and the corresponding normal load combinations is the difference between normal and off-normal thermal stresses. As discussed in Section 3.6.1.3.2, the basket assembly design margins for off-normal thermal stress are bounded by those due to normal thermal stress. Therefore, the basket assembly design margins for the off-normal load combinations are also bounded by those due to the corresponding normal load condition.

3.6.5.3 Damaged Fuel Can

The structural evaluation of the FuelSolutions™ W74 damaged fuel can is based on the results of the FuelSolutions™ W74 guide tube assembly structural evaluation. As discussed above, off-normal design loads do not produce any significant stresses in FuelSolutions™ W74 canister basket assembly components. Thus, the guide tubes satisfy the applicable structural design criteria for off-normal conditions. Therefore, it is concluded that the damaged fuel can also satisfies the applicable structural design criteria for off-normal conditions.

Table 3.6-1 - W74 Canister Shell Assembly Off-Normal Condition Stress Summary

Shell Component	Stress Type	Maximum Stresses (ksi)			Allowable Stress[3] (ksi)
		Off-Normal Internal Pressure	Reflood Internal Pressure[1]	Misalignment Horizontal Transfer[2]	
Top Outer	P_m	0.3	2.5	0.8	22.0 / 24.0
Closure Plate	P_m+P_b	5.2	35.8	17.3	33.0 / 36.0
Top	P_m	1.7	N/A	2.3	17.6 / 19.2
Outer Closure	Shear	0.4	--	0.6	9.6 / 9.6
Weld	P_m+P_b	N/A	26.3	N/A	26.4 / 28.8
	P_m+P_b+Q	9.4	N/A	16.6	52.8 / N/A
Top Inner	P_m	0.3	1.7	0.8	22.0 / 24.0
Closure Plate	P_m+P_b	2.1	17.9	5.5	33.0 / 36.0
Top	P_m	2.0	N/A	3.9	19.8 / 21.6
Inner Closure	Shear	1.0	--	1.9	10.8/ 10.8
Weld	P_m+P_b	N/A	31.2	N/A	29.7 / 32.4
Cylindrical	P_m	3.7	N/A	6.6	22.0 / 24.0
Shell	P_m+P_b	8.3	20.1	17.8	33.0 / 36.0
Bottom End	P_m	1.3	[4]	3.2	22.0 / 24.0
Shell Extension	P_m+P_b	1.7	[4]	3.3	33.0 / 36.0
Bottom	P_m	0.3	0.8	0.7	22.0 / 24.0
Closure Plate	P_m+P_b	4.0	4.0	10.3	33.0 / 36.0
Bottom End Plate	P_m	0.5	16.2	1.2	22.0 / 24.0
	P_m+P_b	5.4	27.9	16.6	33.0 / 36.0
Top Shield Plug Supt. Bar Weld	Shear	0.0	[4]	0.0	12.0 / 13.5
Shell Extension Top Weld	Shear	0.5	[4]	0.8	12.0 / 13.5
Shell Extension Bottom Weld	Shear	0.2	[4]	0.9	12.0 / 13.5

Notes:

(1) Stresses are for bounding reflood internal pressure of 125 psig.

(2) Stresses due to 70 kip pushing load.

(3) Allowable stress intensities are based on the weaker of the W74M and W74T canister shell assembly materials (SA-240, Type 304 stainless steel) properties at 300°F.

(4) Stresses are insignificant for the reflood internal pressure load condition.

Table 3.6-2 - W74 Canister Shell Assembly Off-Normal Load Combination Results (2 Pages)

Canister Shell Component	Stress Type	Allowable Stress[2] (ksi)	L.C. B1 ($D_v+P_o+T_o$)		L.C. B2 ($D_v+L_{hv}+P_o+T_o$)		L.C. B3 ($D_h+L_{hh}+P_o+T_o$)		L.C. B4[1] (D_h+L_m+P+T)	
			Maximum Stress (ksi)	Design Margin	Maximum Stress (ksi)	Design Margin	Maximum Stress (ksi)	Design Margin	Maximum Stress (ksi)	Design Margin
Top End Outer Closure Plate	P_m	22.0	0.2	+90.7	0.5	+40.5	1.1	+19.0	1.2	+17.0
	P_m+P_b[3]	33.0	5.0	+5.63	8.0	+3.15	16.3	+1.03	17.3	+0.91
	P_m+P_b+Q	66.0	10.8	+5.12	13.3	+3.98	22.4	+1.95	14.8	+3.47
Top End Outer Closure Weld	P_m	17.6[4]	1.7	+9.60	3.4	+4.24	5.1	+2.43	2.5	+6.10
	Shear[5]	9.6[4]	0.4	+22.4	1.2	+7.21	0.8	+11.3	0.6	+16.5
	P_m+P_b+Q	52.8[4]	8.9	+4.93	15.4	+2.42	28.0	+0.89	15.1	+2.49
Top End Inner Closure Plate	P_m	22.0	0.3	+77.6	0.6	+34.5	2.5	+7.91	2.3	+8.65
	P_m+P_b	33.0	2.0	+15.3	3.3	+9.00	10.8	+2.06	8.2	+3.02
	P_m+P_b+Q	66.0	8.5	+6.73	9.1	+6.22	16.3	+3.05	14.7	+3.49
Top End Inner Closure Weld	P_m	19.8[6]	1.9	+9.42	4.0	+3.94	14.4	+0.38	12.0	+0.66
	Shear[5]	10.8[6]	1.0	+10.4	2.0	+4.37	7.2	+0.50	6.0	+0.81
	P_m+P_b+Q	59.4[6]	1.9	+31.1	5.8	9.19	17.7	+2.36	15.8	+2.77
Top Shield Plug	P_m	22.0	0.0	+Large	0.1	+Large	0.9	+23.4	0.2	+Large
	P_m+P_b	33.0	1.0	+32.0	1.2	+26.5	2.3	+13.3	7.3	+3.50
Cylindrical Shell	P_m	22.0	3.5	+5.32	6.1	+2.61	12.9	+0.70	8.2	+1.67
	P_m+P_b	33.0	7.8	+3.23	16.6	+0.99	28.0	+0.18	20.6	+0.60
	P_m+P_b+Q	66.0	8.4	+6.86	17.5	+2.78	28.6	+1.31	19.9	+2.31
Bottom Shell Extension	P_m	22.0	0.1	+Large	3.5	+5.36	7.3	+2.00	5.8	+2.82
	P_m+P_b	33.0	0.4	+83.6	4.5	+6.35	12.8	+1.59	10.3	+2.21
Bottom Closure Plate	P_m	22.0	0.2	+Large	0.6	+35.7	2.1	+9.43	2.1	+9.63
	P_m+P_b	33.0	0.8	+40.3	9.5	+2.49	14.1	+1.35	12.2	+1.71
	P_m+P_b+Q	66.0	8.0	+7.21	14.5	+3.55	20.2	+2.26	17.2	+2.83
Bottom End Plate	P_m	22.0	0.1	+Large	0.4	+56.9	2.4	+8.24	2.8	+6.86
	P_m+P_b	33.0	0.4	+74.0	11.4	+1.90	19.1	+0.73	17.5	+0.89
	P_m+P_b+Q	66.0	6.4	+9.25	17.0	+2.87	25.4	+1.60	24.4	+1.70

Table 3.6-2 - W74 Canister Shell Assembly Off-Normal Load Combination Results (2 Pages)

Canister Shell Component	Stress Type	Allowable Stress[2] (ksi)	L.C. B1 ($D_v+P_o+T_o$)		L.C. B2 ($D_v+L_{hv}+P_o+T_o$)		L.C. B3 ($D_h+L_{hh}+P_o+T_o$)		L.C. B4[1] (D_h+L_m+P+T)	
			Maximum Stress (ksi)	Design Margin	Maximum Stress (ksi)	Design Margin	Maximum Stress (ksi)	Design Margin	Maximum Stress (ksi)	Design Margin
Top Shield Plug Supt. Bar Weld	Shear	12.0	0.1	+Large	0.1	+Large	0.0	+Large	0.0	+Large
Shell Extension Top Weld	Shear	12.0	0.2	+65.7	1.3	+8.52	1.5	+7.05	0.9	+13.1
Shell Extension Bottom Weld	Shear	12.0	0.2	+79.0	0.7	+17.2	1.1	+9.91	1.1	+10.2

Notes:

(1) Load combination B4 stresses are determined using a cask misalignment 70 kip pushing force. The minimum design margins in the canister shell assembly for the 50 kip pulling force are equal to those reported for load combination A5 in Table 3.5-6.

(2) The allowable stresses are conservatively based on the properties of the weaker of the W74M and W74T canister shell materials (SA-240, Type 304 stainless steel) at 300°F.

(3) The maximum bending stress in the top outer closure plate is determined using hand calculations assuming simply support edge conditions to demonstrate that the bending stress in the top outer closure weld may be classified as secondary.

(4) The allowable stresses for the top outer closure weld include a 0.8 weld efficiency factor in accordance with ISG-4.

(5) Shear stress in the welds are determined using hand calculations.

(6) The allowable stresses for the top inner closure weld include a 0.9 weld efficiency factor in accordance with Section 3.1.2.2 of this SAR.

3.7 Evaluation of Accident Conditions

The FuelSolutions™ W74 canister is evaluated for a range of postulated accidents and natural phenomena, as defined in Sections 2.3.3 and 2.3.4.

The design basis postulated accident conditions and natural phenomena considered are in accordance with ANSI/ANS-57.9,[25] and include events which are postulated because their consequences may result in maximum potential impact on the immediate environs. Evaluations are performed for a range of postulated accidents, including those with the potential to result in an annual dose greater than 25 mrem outside the controlled area in accordance with 10CFR72. The design basis postulated accident and natural phenomena events evaluated for the W74 canister include the following:

- Fully blocked storage cask inlet and outlet vents
- Loss of transfer cask neutron shield
- Cask drop and tip-over
- Fire
- Flood
- Earthquake
- Accident Pressurization

As discussed in Sections 2.3.3 and 2.3.4, the canister is not subjected to loads due to explosive overpressure, tornado, wind, burial under debris, lightning, and snow and ice.

The results of the structural evaluations performed herein demonstrate that the FuelSolutions™ W74 canisters described in Section 1.2.1.3 can withstand the effects of all credible accident conditions and natural phenomena without affecting structural safety function and remain in compliance with the applicable acceptance criteria. The load combinations evaluated for postulated accident conditions are defined in Table 2.3-1. The load combinations include normal loads which are evaluated in Section 3.5, off-normal loads which are evaluated in Section 3.6, and accident loads which are evaluated in this section. The accident load combination evaluations are provided in Section 3.7.10.

The structural evaluations of the canister shell are performed for the bounding canister design, determined to be the W74T canister assembly as discussed in Section 3.1.1.1.

The basket assembly structural evaluations are performed for the bounding components as described in Section 3.1.1.2.

The evaluation of the FuelSolutions™ W74 canister for BRP MOX fuel assemblies, partial fuel assemblies, and damaged fuel assemblies for accident conditions considers the effect these fuel assemblies have on the existing structural evaluation of the W74 canister shell assembly and

[25] ANSI/ANS-57.9, *Design Criteria for an Independent Spent Fuel Storage Installation (Dry Type)*, American National Standards Institute, 1984.

basket assemblies. The structural evaluation of the FuelSolutions™ W74 damaged fuel can for accident conditions is included in this section.

The evaluations for the effects of the design basis postulated accident events on the FuelSolutions™ W150 Storage Cask and W100 Transfer Cask are provided in the FuelSolutions™ Storage System FSAR.

3.7.1 Fully Blocked Storage Cask Inlet and Outlet Vents

The FuelSolutions™ W74 canister, loaded with design basis fuel assemblies and dry stored vertically in the storage cask, is evaluated for a postulated accident thermal event in which complete blockage of all storage cask inlet and outlet vents occurs. A steady state ambient temperature of 100°F with insolation, as defined in the FuelSolutions™ Storage System FSAR, are conservatively postulated to occur concurrently.

As shown in Chapter 4 of this FSAR, the maximum temperatures in the W74 canister assembly due to the storage cask blocked vent accident thermal condition are bounded by those resulting from the transfer cask loss of neutron shield accident thermal condition. The maximum internal pressure in the W74 canister due to the accident thermal conditions is 30.0 psig per Section 4.6.1.4 of this FSAR. A design basis accident internal pressure load of 69 psig is conservatively used for the canister shell stress evaluation. Therefore, the canister shell accident pressure analysis discussed in Section 3.7.9 bounds the pressure due to the blocked vent condition.

In general, thermal stresses within the canister result from internal thermal gradients. These gradients are generally highest for the thermal conditions with the highest internal heat generation rate and the lowest ambient temperature. As shown in Figure 4.6-2, the thermal gradient between the maximum spacer plate temperature and the maximum canister shell temperature is reduced during the blocked vent storage accident. In the same manner, the thermal gradients within the canister shell and basket assemblies are also reduced during the postulated blocked vent accident. For this reason, and since the maximum canister temperatures for the storage cask blocked vent condition are bounded by those for the transfer cask loss of neutron shield accident, the canister thermal stresses for the storage cask blocked vent condition are bounded by other conditions.

As discussed in Chapter 4 of this FSAR, the FuelSolutions™ W74 canister thermal design loads for accident conditions bound those for a FuelSolutions™ W74 canister containing any amount of intact BRP MOX fuel and partial fuel assemblies, and up to eight damaged fuel assemblies. Therefore, the FuelSolutions™ W74 canister shell assembly and basket assembly stresses calculated for the design basis accident thermal loads are bounded for a FuelSolutions™ W74 canister containing any amount of intact BRP MOX fuel and partial fuel assemblies, and up to eight damaged fuel assemblies.

3.7.2 Loss of Transfer Cask Neutron Shield

The FuelSolutions™ W74 canister, loaded with design basis fuel assemblies while in the transfer cask, is evaluated for a postulated accident thermal event in which the transfer cask liquid neutron shield is drained. A steady-state ambient temperature of 100°F with insolation, as

defined in the FuelSolutions™ Storage System FSAR, are conservatively postulated to occur concurrently.

As discussed in Section 4.6 of this FSAR, the W74 canister internal pressure resulting from the loss of neutron shield accident is less than the design basis accident pressure of 69 psig. Therefore, the canister shell accident pressure analysis discussed in Section 3.7.9 bounds the pressure due to the loss of neutron shield condition.

In general, thermal stresses within the canister result from internal thermal gradients. These gradients are generally highest for the thermal conditions with the highest internal heat generation rate and the lowest ambient temperature. As shown in Section 4.6.2 of this FSAR, the thermal gradient between the maximum spacer plate temperature and the maximum canister shell temperature is significantly reduced during the loss of neutron shield accident. In the same manner, the thermal gradients within the canister shell and basket assemblies are also reduced during the postulated loss of neutron shield accident. Therefore, the canister thermal stresses for the loss of neutron shield accident are bounded by other conditions, with the exception of the basket assembly support tubes and support sleeves.

As discussed in Section 3.5.1.3.4, thermal stresses in the W74 support tubes and support sleeves result from differential thermal expansion of dissimilar materials at elevated temperatures. These stresses are highest for the maximum support tube temperatures. As shown in Chapter 4 of this FSAR, the loss of neutron shield accident thermal condition results in the highest overall support tube temperature for all normal, off-normal, and accident conditions of 806°F. Therefore, the bounding support tube and support sleeve accident thermal stresses are evaluated for this condition. Since general thermal stress is classified as secondary in accordance with Subsection NG of the ASME Code, the support tube stresses due to loss of neutron shield accident need not be evaluated using the ASME Service Level D allowable stress design criteria. However, a buckling evaluation of the W74 support sleeves, which are loaded in axial compression as a result of the differential thermal expansion, is performed in accordance with NUREG/CR-6322 to assure that the support sleeves remain stable under these conditions. In addition, the support tube attachment weld stresses resulting from the accident thermal load condition are evaluated.

Support Sleeve Buckling Evaluation

The W74 support sleeve stresses are calculated for a bounding temperature of 810°F using the same methodology that is used for the support sleeve normal thermal stress evaluation. The support sleeve thermal stresses are determined using hand calculations, treating the support tubes as axial members which act in parallel with the support sleeves and spacer plates. The maximum axial load in the W74M and W74T upper and lower basket assembly support tubes and support sleeves at the bounding temperature of 810°F are calculated based on the principal of static equilibrium. The maximum axial loads in the W74M and W74T support tubes are 30.5 kips and 29.4 kips, respectively. The resulting maximum axial compressive stress in the support sleeves is 4.1 ksi.

The W74 support sleeve allowable axial compressive stress for accident conditions is calculated in accordance with NUREG/CR-6322 using Equation 33 for carbon steel material. The theoretical buckling stress, calculated in accordance with NUREG/CR-6322, Figure 8, case E, and based on SA-240, Type 304 stainless steel material properties at 810°F, is 19.5 ksi. The

allowable axial compressive stress is limited to 2/3 of the theoretical buckling stress in accordance with NUREG/CR-6322, or 13.0 ksi. Therefore, the minimum design margin for buckling of the W74 support sleeves due to accident thermal conditions is +2.20.

Support Tube Attachment Weld Stress Evaluation

The stresses in the W74 support tube attachment welds are also evaluated for the maximum axial loads resulting from the bounding accident thermal condition. The maximum axial loads of 30.5 kip in the W74M support sleeves and 29.4 kips in the W74T support sleeves are carried in pure shear by the support tube attachment welds. The W74M support tubes are welded to the top and bottom end LTP spacer plates with ½-inch groove welds with ¼-inch cover fillets on all four sides of each tube and have an effective weld shear area of 16.55 in^2. The W74T support tubes are welded to the top and bottom end attachment sleeves with ¼-inch fillet welds on all four sides of each tube and have an effective weld shear area of 5.23 in^2. The resulting shear stresses in the W74M and W74T support tube attachment welds are 1.8 ksi and 5.6 ksi, respectively.

In addition to the weld shear stresses due to the axial loads caused by longitudinal differential thermal expansion, the support tube attachment welds are loaded by the moment reactions resulting from thermal curvature of the support tubes, as discussed in Section 3.5.1.3.4. The weld moment reactions, and thus the resulting weld stresses, are proportional to the lateral thermal gradient across the support tube section. Since these gradients are lower for the accident thermal conditions than for the normal thermal conditions, the associated weld stresses are also bounded by those due to normal thermal loading. As shown in Section 3.5.1.3.4, the maximum shear stresses in the W74M and W74T support tube attachment welds due to the bounding normal thermal support tube transverse gradients are 0.4 ksi and 0.1 ksi, respectively. These shear stresses are combined with the maximum weld shear stresses due to the axial loads. The resulting total shear stress in the W74M and W74T support tube attachment welds are 2.2 ksi and 5.7 ksi, respectively. These shear stresses are conservatively classified as primary since excessive loading of the welds could result in gross failure.

The Service Level D allowable shear stresses for the W74M and W74T attachment welds, based on SA-240, Type XM-19 stainless steel material properties at 810°F and including a 40% weld efficiency factor for single fillet welds and single bevel groove welds with surface PT examination, are both 13.5 ksi. Therefore, the minimum design margin for shear stress in the W74M and W74T attachment welds due to the bounding accident thermal condition are +5.03 and +1.38, respectively.

3.7.3 Storage Cask Drop

The storage cask is evaluated for a non-mechanistic drop as discussed in Section 2.3.3.2 and evaluated in the FuelSolutions™ Storage System FSAR. The accidental storage cask drop scenario is a postulated vertical drop onto the bottom end of the storage cask from a height of 36 inches. The storage cask end drop results in a canister assembly rigid body response, characterized as a half-sine wave pulse with a peak acceleration of 28*g*. The FuelSolutions™ W74 canister is evaluated for the postulated storage cask end drop scenario using equivalent static loads. The equivalent static end drop acceleration is equal to the peak acceleration multiplied by a Dynamic Load Factor (DLF) to account for possible dynamic amplification

within the canister. The maximum DLF for an undamped system subjected to a half-sine wave pulse is 1.75 (Figure 2.15 of NUREG/CR-396626[26]). Therefore, the maximum equivalent static acceleration for the W74 canister shell and basket assemblies due to the postulated storage cask end drop is 49*g*. A bounding storage cask end drop equivalent static acceleration of 50*g* is conservatively used for the structural evaluation of the W74 canister.

The structural evaluation of the FuelSolutions™ W74 canister for the storage cask drop loads is performed using a bounding BRP intact fuel assembly weight of 485 pounds per assembly plus a bounding damaged fuel can weight of 200 pounds in each of the support tube openings. As discussed in Section 2.2 of this FSAR, the weights of all BRP MOX, partial, and damaged fuel assemblies are bounded by the weight of the BRP intact fuel assemblies. Therefore, the cask drop loads and calculated stresses in the FuelSolutions™ W74 canister shell assembly and basket assemblies bound those for a FuelSolutions™ W74 canister containing any amount of intact BRP MOX fuel and partial fuel assemblies, and up to eight damaged fuel assemblies.

3.7.3.1 Canister Shell

Canister Shell Stresses

The W74 canister shell assembly is evaluated for a bounding 50*g* bottom end drop using a combination of finite element analysis and closed form hand calculations. The stresses in all of the canister shell components, except for the top shield plug and the top shield plug support bar attachment welds, are evaluated using the axisymmetric finite element model discussed in Section 3.9.2.1 and shown in Figure 3.9-1. As discussed in Section 3.9.2.1, the top end shield plug assembly and shield plug supports are included in the axisymmetric model to account for the weight of the top shield plug and the loads transferred to the shell.

In the event of a storage cask bottom end drop, the canister is supported by the crush pipes located in the bottom end of the storage cask. The storage cask crush pipes provide uniform support over the outer 14-inch radius of the canister bottom plate. As discussed in Section 3.9.2.1, uniform gap element support is assumed over the entire surface of the bottom end plate, rather than just the outer 14.0 inches of the canister radius. However, this difference has no significant impact on the resulting stresses in the bottom region of the canister shell due to the rigidity of the canister shell bottom end plates.

The load from the W74 canister contents (basket assembly and spent fuel assemblies) is supported on the bottom end of the cavity. The load from the contents is modeled as a uniform pressure on the inner surface of the bottom closure plate, assuming a bounding payload weight of 57 kips. The resulting pressure applied to the bottom closure plate is 866 psi. A vertical acceleration of 50*g* is applied to the model to account for the self weight of the shell assembly. The maximum canister shell stress intensities resulting from the 50*g* bottom end drop load are reported in Table 3.7-1. The results show that all stresses within the canister shell are lower than the Service Level D allowable stresses.

[26] NUREG/CR-3966, *Methods for Impact Analysis of Shipping Containers*, T.A. Nelson, R.C. Chun, U.S. Nuclear Regulatory Commission, November 1987.

Top Shield Plug Assembly Stresses

The W74 top end shield plug assembly is evaluated for the bounding 50*g* storage cask bottom end drop load using the quarter-symmetry model described in Section 3.9.2.3 and shown in Figure 3.9-5. The top shield plug model includes only the shield plate. The weight of the tube shield caps is accounted for in the model by adjusting the density of the elements in the region of the shield caps, as discussed in Section 3.9.2.3. The shield plug is modeled with simply supported boundary conditions at the locations of the shield plug support bars. The maximum primary membrane and primary membrane plus bending stress intensities in the W74 top end shield plug due to the 50*g* bottom end drop load are 5.0 ksi and 27.1 ksi, respectively. The W74 top end shield plug is designed in accordance with Subsection NF of the ASME Code. The Service Level D allowable primary membrane and primary membrane plus bending stress intensities for the shield plug assembly carbon steel material at 300°F are 31.9 ksi and 47.9 ksi, respectively. Therefore, the W74 top shield plug assembly stresses due to a bounding 50*g* bottom end drop are lower than the corresponding Service Level D allowable stress intensities.

Shield Plug Support Bar Stresses

The stresses in the shield plug support bars and their attachment welds to the canister shell are evaluated for the storage cask bottom end drop condition using hand calculations. The only significant stresses in the shield plug support bars due to the bottom end drop loading are bearing stresses at the shield plug support locations and shear stresses attachment welds. In accordance with F-1331.3 of the ASME Code, bearing stress need not be evaluated for Service Level D conditions. Therefore, only the shear stress in the support bar attachment welds need be evaluated. Each shield plug support bar is attached to the canister shell with a 10.5-inch long 5/16-inch double sided partial penetration groove weld. The average shear stress in the weld due to a bounding 60*g* bottom end drop load is 9.2 ksi.

In accordance with article F-1334.2 of the ASME Code, the average shear stress in the weld is limited to the lesser of 0.72Sy and 0.42Su for Service Level D conditions. Therefore, the allowable weld shear stress is equal to 16.2 ksi based on the material properties of the weaker shell base material (i.e., SA-240, Type 304 stainless steel) at 300°F. Therefore, the minimum design margin for shear stress in the shield plug support bar welds resulting from the bounding 50*g* storage cask bottom end drop is +0.76.

Buckling Evaluation

The stability of the W74 canister shell is evaluated for the postulated storage cask end drop to ensure that it has adequate design margin against buckling. The end drop condition results in the highest axial compressive stresses in the canister shell. Internal pressure loads, which result in tensile stresses in the shell, thereby offsetting the impact loads, are conservatively ignored for the buckling evaluation. The canister shell is loaded by its self-weight and the weight of the top end closure components for a bottom end drop. The load from the canister payload does not load the canister shell since it is supported directly by the bottom closure plate. The buckling evaluation of the canister shell is performed in accordance with ASME Code Case N-284.

For a bottom end drop, the canister shell is loaded by its self weight plus the weight of the top shield plug assembly and top inner and outer closure plates. As shown in Table 3.2-1, the total weight of the W74 top shield plug assembly and top inner and outer closure plates is 9.5 kips. The weight of the W74 canister cylindrical shell is 7.1 kips. Therefore, the total weight supported

by the canister shell for the bottom end drop is 16.6 kips. The axial compressive stress in the shell due to a bounding tributary weight of 18 kips is 8.4 ksi. The calculated axial compressive stress is adjusted to account for a factor of safety and capacity reduction factors. A factor of safety of 1.34 is used for accident conditions in accordance with ASME Code Case N-284. Therefore the shell axial stress is multiplied by 1.34. In addition, the capacity reduction factor for axial compression, $\alpha_{\phi L}$ = 0.207, is based on the canister shell geometry and material properties in accordance with Paragraph -1511 of ASME Code Case N-284, resulting in an adjusted shell compressive stress of 44.0 ksi.

The theoretical buckling stress is calculated in accordance with Paragraph -1712 of ASME Code Case N-284 to be 306.5 ksi, based on nominal shell dimensions and material properties at an average shell temperature of 400°F. The resulting canister shell buckling interaction ratio for the bounding 50*g* bottom end drop is:

$$\frac{44.0}{306.5} = 0.14 \leq 1.00$$

Therefore, the W74 canister shell will not buckle due to the bounding 50*g* end drop load.

3.7.3.2 Basket Assembly

3.7.3.2.1 General and LTP Spacer Plates

Spacer Plate Stress Evaluation

For the storage cask bottom end drop load condition, each W74 and LTP spacer plate, with the exception of the bottom end LTP spacer plate in the W74M upper and lower basket assemblies, supports only its own weight. The bottom end LTP spacer plates in the W74M upper and lower basket assemblies support the weight of the guide tube assemblies in addition to their own weight. As discussed in Section 3.1.1.2, the guide tube attachment brackets which secure the guide tubes to the bottom end LTP spacer plate are not designed to withstand the storage cask end drop load, but will fail at an acceleration load less than the 50*g* bottom end drop load. Conservatively neglecting the potential for failure of the attachment bracket weld, the upper bound ultimate load capacity of the guide tube attachment brackets is conservatively based on the ultimate shear capacity of the 3/16-inch wide "necked-down" shear section. The ultimate shear strength of annealed stainless steels is approximately 2/3 of the ultimate tensile strength.[27] Therefore, the ultimate shear strength for the attachment bracket SA-240, Type 316 stainless steel material, conservatively using the strength properties at a lower bound temperature of -40°F is 50 ksi (= 2/3 x 75 ksi). The shear stress in the attachment bracket shear section due to the weight of a W74 guide assembly is calculated as follows:

$$\tau = \frac{V}{A_V} = 2.5 \text{ ksi}$$

[27] U.S. Department of Defense, *Military Standardization Handbook, Metallic Materials and Elements for Aerospace Vehicle Structures*, MIL-HDBK-5B, September 1971.

where:

V = 42.1 lb., maximum load per attachment bracket, equal to ½ the weight of the heaviest W74 guide tube assembly

A_V = 0.0169 in^2, attachment bracket shear area

= (0.090)(0.1875)

Therefore, the ultimate load capacity of the attachment bracket is 20*g*.

The W74 spacer plate bottom end drop stresses are determined by scaling the maximum vertical dead weight stresses from Section 3.5.3.2.1. The maximum stresses in the bottom end LTP spacer plate for the bottom end drop condition are taken as the larger of 20 times the maximum vertical dead weight stresses in bottom end LTP spacer plate (i.e., with guide tubes attached) or 50 times the maximum vertical dead weight stresses in the top end LTP spacer plate (i.e., spacer plate self-weight only). The bottom end drop stresses in the W74 general spacer plates are equal to 50 times the maximum vertical dead weight stresses. The maximum stresses in the W74 general and LTP spacer plates due to the storage cask bottom end drop are presented in Table 3.7-2. The results show that the W74 spacer plate stresses due to the storage cask bottom end drop are less than the corresponding Service Level D allowable stresses.

LTP Spacer Plate Attachment Weld Stresses

The LTP spacer plate attachment welds are evaluated for the storage cask end drop loading using hand calculations. The most heavily loaded attachment welds for the storage cask end drop condition are those at the bottom end top and bottom basket assemblies since these welds must support the entire inertial load from the weight of the LTP spacer plate plus the twelve general spacer plates and all support sleeves within the basket assembly. In addition, the bottom end LTP spacer plate supports the weight of the guide tube assemblies up to the ultimate load capacity of the guide tube attachment brackets (i.e., 20*g*). However, the maximum stresses in the W74M LTP spacer plate attachment welds result from the 50*g* bottom end drop loads without the guide tubes attached.

Each LTP spacer plate is welded to the four support tubes with ½-inch partial penetration welds and ¼-inch cover fillets on all four sides, having an effective weld shear area of 16.5 in^2 per tube. The total shear load on each of the four attachment welds is 50.0 kips. Therefore, the average shear stress in the most heavily loaded LTP spacer plate attachment weld is 3.0 ksi. In addition, the moment reaction from the LTP spacer plate produces shear stresses in the LTP spacer plate attachment weld. As shown in Section 3.7.3.2.3, the maximum moment reaction on the LTP spacer plate attachment weld due to the end drop load is 8.0 in-kips. The weld section modulus is 47.1 in^3. Therefore, the maximum weld shear stress due to the moment reaction is 0.2 ksi. The combined weld shear stress is 3.2 ksi. The allowable weld shear stress, based on the SA-240, Type XM-19 stainless steel base material at a bounding temperature of 700°F and including a 40% weld efficiency factor for a single bevel groove weld with surface PT examination, is 13.8 ksi. Therefore, the minimum design margin for shear stress in the LTP spacer plate attachment weld due to bounding 50*g* bottom end drop load is +3.31.

3.7.3.2.2 Engagement Spacer Plate

The W74 engagement spacer plate is evaluated for a bounding bottom end drop acceleration load of 50*g* using finite element analysis. For this load condition the W74 engagement spacer plate is loaded by the weight of the upper basket assembly, which includes the engagement spacer plate self weight, plus the weight of 32 fuel assemblies and four damaged fuel canisters contained in the upper basket assembly. As shown in Section 3.2, this load is highest for the W74M engagement spacer plate which supports a total weight of 26.6 kips. The engagement spacer plate is supported in the longitudinal direction by the four support tubes of the lower basket assembly.

The stresses in the W74 engagement spacer plate due to the bounding 50*g* bottom end drop acceleration are determined using the quarter-symmetry finite element model described in Section 3.9.2.5 and shown in Figure 3.9-14. The W74 engagement spacer plate is loaded by its self weight, the weight of 32 fuel assemblies, 28 guide tube assemblies, and four damaged fuel canisters. Bounding design weights of 485 pounds per SNF assembly, 85 pounds per guide tube assembly, and 200 pounds per damaged fuel canister are conservatively used. The loading from the upper basket assembly, SNF assemblies, guide tube assemblies, and damaged fuel canisters is modeled as uniform pressure loads applied to the regions of the engagement spacer plate over which the various components are supported, as discussed in Section 3.9.2.5. The self weight of the engagement spacer plate is included by applying a 50*g* acceleration load to the model.

The maximum stresses in the engagement spacer plate due to the bounding 50*g* bottom end drop are reported in Table 3.7-2. The results show that the engagement spacer plate stresses resulting from the 50*g* bottom end drop are lower than the Service Level D allowable stresses for SA-240, Type XM-19 stainless steel at a bounding design temperature of 600°F. Additionally, the maximum primary plus secondary plus peak stress intensity in the W74 engagement spacer plate due to the bounding 50*g* end drop load is 126.3 ksi. Although secondary stresses need not be evaluated for accident conditions, this stress is scaled for the evaluated of normal conditions.

3.7.3.2.3 Support Tube

When subjected to the storage cask bottom end drop loading, the upper basket assembly support tubes provide longitudinal support for the upper basket assembly spacer plates and support sleeves, and the lower basket assembly support tubes provide longitudinal support for the entire upper basket assembly and its SNF assemblies plus the lower basket assembly spacer plates, guide tube assemblies, and support sleeves. Therefore, the bottom end drop loading on the lower basket assembly support tubes bounds that of the upper basket assembly. As shown in Section 3.2, the weight of the W74M basket assemblies bounds that of the W74T basket assemblies. Therefore, since the W74M and W74T support tube cross sections are identical, the stresses in the W74M lower basket assembly support tubes bound those in the W74T lower basket support tubes. Since both the W74M and W74T support tubes are fabricated from Type XM-19 stainless steel, the minimum design margins for the bottom end drop condition are those of the W74M lower basket support tubes.

As discussed in Section 3.7.3, the W74 canister is designed for a bounding 50*g* bottom end drop load. As discussed above, the support tube end drop loads include the weight of the guide tube assemblies. However, the attachment brackets which secure the guide tubes to the basket assembly are not designed to withstand the 50*g* end drop load. Therefore, two separate loading conditions are considered for the support tube end drop evaluation: a 20*g* end drop load

(i.e., corresponding to the upper bound failure load of the guide tube attachment brackets) with the weight of the upper and lower basket guide tubes carried by the lower basket support tubes, and; a 50*g* end drop load without the weight of the lower basket assembly guide tubes loading the lower basket support tubes. For each end drop loading condition, stress and buckling evaluations are performed with hand calculations for the most highly loaded W74 support tubes, as follows.

Stress Evaluation

The stresses in the W74M lower basket assembly support tube due to the storage cask bottom end drop are determined using hand calculations. The support tubes are evaluated using a bounding bottom end drop equivalent static accelerations of 20*g* (with guide tube loads) and 50*g* (without guide tube loads), as discussed above. The total axial load acting at the bottom end of the four support tubes in the lower basket assembly is equal to the inertial load of the upper basket assembly containing 32 fuel assemblies and four damaged fuel cans, plus the weight of the lower basket assembly, not including the weight of the lower basket assembly fuel, or 740 kips for the 20*g* end drop load and 1,750 kips for the 50*g* end drop load. The resulting maximum axial stress in the W74 support tube is 7.9 ksi for the 20*g* end drop load and 18.8 ksi for the 50*g* end drop load. These axial compressive stresses are classified as primary membrane.

In addition to the axial loads, the W74M support tubes are loaded in bending by the moment reactions at the top and bottom end LTP spacer plates which are welded to the support tubes. Also, the bending stresses due to the P-δ effect resulting from thermal curvature of the support tubes is considered. The maximum bending stress in the support tube due to these loads is calculated as follows:

$$f_b = \frac{(M_{SP} + P\delta)c}{I} = 0.91 \text{ ksi (20}g\text{ end drop) or } 0.67 \text{ ksi (50}g\text{ end drop)}$$

where:

M_{SP}	=	support tube moment reaction from LTP spacer plate due to end drop load
	=	42 in-kips (20*g* load = 20x vertical dead weight reaction with guide tube loads)
	=	8.0 in-kips (50*g* load = 50x vertical dead weight reaction without guide tube loads)
c	=	4.45 in., distance from support tube centroid to outer fiber
I	=	273 in^4, support tube moment of inertia
P	=	maximum support tube axial compressive force
	=	185 kips (20*g* load: = 740 kips / 4 support tubes)
	=	438 kips (50*g* load: = 1750 kips / 4 support tubes)
δ	=	0.075 in., maximum lateral deflection of support tube due to thermal loading per Section 3.5.1.3.4.

The bending stress in the W74 support tube are multiplied by 1.414 to account for the combined effects of equal bending stress about both axes of the support tube cross-section. Therefore, the maximum bending stress in the W74 support tube is 1.3 ksi for the 20*g* end drop load and 0.9 ksi for the 50*g* end drop load. The maximum bending stress is conservatively added to the maximum axial compressive stress calculated above, irrespective of sign and location, and classified as primary membrane plus bending. Therefore, the maximum primary membrane and primary membrane plus bending stresses in the W74 support tube due to the 20*g* end drop are 7.9 ksi and 9.2 ksi, respectively. Similarly, the maximum primary membrane and primary membrane plus bending stresses in the W74 support tube due to the 50*g* end drop are 18.8 ksi and 19.7 ksi, respectively. The corresponding Service Level D primary membrane and primary membrane plus bending stress intensities for SA-240, Type XM-19 stainless steel at an upper bound design temperature of 700°F are 60.6 ksi and 90.8 ksi, respectively. Therefore, the minimum design margins for primary membrane and primary membrane plus bending stress intensity in the W74 support tubes for the postulated storage cask end drop condition are +2.22 and +3.61, respectively.

Buckling Evaluation

Buckling of the most heavily loaded W74 support tubes is evaluated for the storage cask end drop using the criteria of NUREG/CR-6322 for linear-type support subjected to combined axial compression and bending. As shown above, the maximum support tube stresses result from the 50*g* end drop load. The maximum axial stress in the most heavily loaded W74 support tube are determined using hand calculations. The maximum support tube axial stress of 18.8 ksi calculated above occurs only in the region of the lower basket assembly support tubes below the bottom end spacer plate. The buckling evaluation is performed using the maximum support tube axial compressive stress occurring in the free span above the bottom end spacer plate. The total axial load in this region, due to the inertial load of the upper basket assembly and 32 SNF assemblies plus the weight of the lower basket assembly support tubes and LTP spacer plate welded to the top end of the lower basket assembly support tubes, is 1,500 kips. The resulting support tube axial compressive stress is 16.1 ksi.

The maximum bending stress in the support tube due to the storage cask bottom end drop is calculated based on the support tube moment reaction from the LTP spacer plate end drop evaluation plus the bending stress due to the eccentricity of the support tube caused by curvature due to the maximum radial support tube thermal gradient (e.g., P-δ effect). The resulting support tube bending stress due to these effects is 0.59 ksi.

Per NUREG/CR-6322, members subjected to combined compression and bending must satisfy the following equations:

$$\frac{f_a}{F_a} + \frac{C_m f_{bx}}{\left(1 - \frac{f_a}{F_{ex}^{'}}\right) F_{bx}} + \frac{C_m f_{by}}{\left(1 - \frac{f_a}{F_{ey}^{'}}\right) F_{by}} \leq 1.0$$

$$\frac{f_a}{2x0.6S_y} + \frac{f_{bx}}{F_{bx}} + \frac{f_{by}}{F_{by}} \leq 1.0$$

The allowable support tube compressive stress, Fa, for accident conditions is calculated in accordance with Section 6.31 of NUREG/CR-6322, accounting for the allowable stress for austenitic stainless steels. The allowable axial compressive stress, based on XM-19 stainless steel material properties at 700°F, is 22.4 ksi. The allowable bending stress, F_b, is taken as $f \cdot S_y$, as the support tube qualifies as a compact section under the criteria of NF-3322.1(d). The plastic shape factor *f* for the support tube is 1.22. Therefore the allowable bending stress is 44.3 ksi.

Conservatively assuming that the equivalent moment factor C_m is equal to 1.0, the highest buckling interaction ratio is 0.75. Therefore the support tubes satisfy the buckling criteria of NUREG/CR-6322 for the combined effects of bending and axial compression due to the 50*g* end drop load.

3.7.3.2.4 Support Sleeve

When subjected to the storage cask bottom end drop loading, each support sleeve is loaded by its own weight plus the weight of all other support sleeves and general spacer plates above it within the basket assembly. The most highly loaded support sleeves for the bottom end drop condition are those at the bottom end of the upper and lower basket assemblies since they support the most weight. Since there are twelve (12) general spacer plates above the bottom end support sleeve in each of the W74M and W74T basket assemblies, the bottom end drop loading on the bottom end support sleeve is approximately equal for all designs.

Stress Evaluation

The most heavily loaded W74 support sleeve is evaluated for the storage cask end drop using hand calculations. A bounding bottom end drop equivalent static acceleration load of 50*g* is conservatively used. The resulting axial load on the bottom end support sleeves is 168.6 kips (i.e., 42.2 kips per support sleeve), based on the W74M lower basket assembly weights. The total area of the four support sleeve in the bottom layer, conservatively based on only the outer 14”x14”x0.19” thick outer angle, is 20.86 square inches. The resulting axial stress in the most heavily loaded support sleeve is 8.1 ksi. The allowable primary membrane stress intensity for Service Level D conditions is 38.4 ksi for Type 304 stainless steel at 700°F. Therefore, the minimum design margin in the most highly loaded W74 support sleeve for the storage cask bottom end drop is +3.74.

Buckling Evaluation

The elastic stability of the support sleeves for the postulated storage cask end drop condition is evaluated in accordance with NUREG/CR-6322. The support sleeve critical buckling stress is conservatively calculated for a thin plate subjected to uniformly distributed edge loads assuming one simply supported edge and one free edge (NUREG/CR-6322, Figure 8, case E). The width of the support sleeve is conservatively taken as 14 inches, neglecting the support provided by the inner angle. The theoretical buckling stress, based on Type 304 stainless steel material properties at 700°F, is shown to be 20.1 ksi. Per NUREG/CR-6322, the design allowable is limited to 2/3 of the theoretical buckling stress, or 13.4 ksi. As shown above, the maximum axial compressive stress in the most highly loaded W74 support sleeve is 8.1 ksi for the bounding 50*g* bottom end drop load. The corresponding minimum design margin for support sleeve buckling is +0.65.

Support Sleeve Attachment Weld Stresses

The top end bottom end support sleeves in both the W74T upper and lower basket assemblies are welded to the support tubes with all-around ¼-inch fillet welds to capture the basket assembly spacer plates and interior support sleeves. The stresses in the W74T support sleeve attachment welds due to storage cask end drop are determined using hand calculations. The total shear load on the most heavily loaded W74T support sleeve attachment welds due to the 50*g* end drop load is equal to the combined inertial load of thirteen general spacer plates and all support sleeves within the basket assembly, or 45.2 kips. The minimum weld shear area for all four support sleeve attachment welds is 5.23 square inches. The resulting weld shear stress is 8.6 ksi. The Service Level D allowable shear stress is 13.8 ksi, based on SA-240, Type XM-19 stainless steel properties at 700°F and including a 40% weld efficiency factor for single sided fillet weld with surface PT examination in accordance with Table NG-3352-1 of the ASME Code. Therefore, the minimum design margin in the W74T support sleeve attachment weld for the bounding 50*g* storage cask end drop load is +0.60.

3.7.3.2.5 Guide Tube

For the postulated storage cask bottom end drop condition, the W74 guide tubes are loaded only by their own weight. As discussed in Section 3.1.1.2, the dimensions and top and bottom end details of all W74 guide tube assemblies are identical and all W74 guide tubes are fabricated from the same material. However, there are two different guide tube configurations which differ in the number of neutron absorber sheets which are attached to the guide tube. All of the W74 guide tubes in the interior of the basket assemblies include two neutron absorber sheets on opposing faces, whereas the guide tubes on the perimeter of the basket assembly include only one neutron absorber sheet. Since no structural credit is taken for the support that the neutron absorber sheets provide to the guide tube and their mass is assumed to load the guide tube, bounding structural evaluation of the W74 guide tube are performed for the interior guide tubes which include two neutron absorber sheets.

Stress Evaluation

The most heavily loaded W74 guide tubes are evaluated for the postulated storage cask bottom end drop condition using hand calculations. A bounding equivalent static acceleration load of 50*g* is conservatively used for the guide tube bottom end drop evaluation. The limiting guide tube vertical deadweight stress is uniaxial compression at the bottom end which bears on the supporting engagement spacer plate (upper basket) or canister shell bottom closure plate (lower basket). The weight of the heaviest guide tube assembly is 84.2 pounds. The guide tube area at the bottom end is reduced due to the cutouts on two opposing faces. The cross section area at the bottom end of the guide tube is 1.74 square inches. Therefore, the average axial compressive stress at the base of the guide tube is 2.4 ksi. The corresponding Service Level D allowable primary membrane stress intensity, conservatively based on Type 316 stainless steel material properties at 715°F, is 38.8 ksi. Therefore, the minimum design margin for primary membrane stress intensity in the W74 guide tubes for the bounding 50*g* storage cask bottom end drop condition is +15.2.

Buckling Evaluation

Buckling of the W74 guide tubes is evaluated in accordance with NUREG/CR-6322. The notched region at the bottom of the guide tubes has the lower factor of safety against buckling

due to the increased stresses in this region and formation of a free edge at the notch. The theoretical elastic buckling stress for the guide tube at the bottom notch region is determined using classical methods. The guide tube panel is evaluated as a rectangular plate under uniform compression of equal magnitude on the top and bottom opposing edges. The top, bottom, and corner of the plate are assumed to be simply supported and the other edge free as shown in Figure 3.7-1. The theoretical buckling stress for these conditions, calculated in accordance with Roark, Table 35, Case 1d, is 129 ksi based on Type 316 stainless steel material properties at 715°F. In accordance with NUREG/CR-6322, the allowable stress for the accident condition is limited to 2/3 of the critical stress, or 86 ksi. As shown above, the maximum axial compressive stress in the bottom end region of the guide tubes is 2.4 ksi. Therefore, the minimum design margin for bucking of the W74 guide tube for the bounding 50*g* end drop load is +34.8.

Neutron Absorber Panel Retainer Weld Stress Evaluation

The neutron absorber panels are attached to the guide tubes using stainless steel retainers. A minimum of seven retainers are used per neutron absorber panel with a maximum center-to-center spacing of 12 inches. Each retainer is welded to the guide tube with a plug weld. Since the total tributary load supported by each retainer for the 50*g* storage cask end drop is bounded by the tributary load due to the 60*g* transfer cask side drop evaluated in Section 3.7.5.2.5, the plug weld stresses due to the storage cask end drop are bounded by those due to the transfer cask side drop. Therefore, no evaluation of the retainer weld stresses for the storage cask end drop is required.

3.7.4 Storage Cask Tip-Over

The storage cask is evaluated for a postulated accidental tip-over event as discussed in Section 2.3.3.3 and evaluated in the FuelSolutions™ Storage System FSAR. The storage cask tip-over event results in a peak rigid body acceleration of 21.9*g* at the top end of the storage cask, with a ramped load having a 15 msec rise time. The structural evaluation of the W74 canister for the postulated tip-over condition is performed using equivalent static loads. The equivalent static acceleration load is equal to the peak rigid-body acceleration multiplied by a DLF to account for possible dynamic amplification within the canister assembly. The transverse natural frequencies of the W74 canister assembly are all greater than 100 Hz. Per Figure 2.1 of NUREG/CR-3966, the maximum DLF for tr/T greater than or equal to 1.5 (e.g., for natural frequencies of 100 Hz and greater) is approximately 1.2. Therefore, the maximum equivalent static acceleration at the top end of the canister for the storage cask tip-over is 26.3*g*. A bounding equivalent static acceleration load of 30*g* is conservatively used for the W74 canister tip-over structural evaluation.

The structural evaluation of the FuelSolutions™ W74 canister for storage cask tip-over is performed using a bounding BRP intact fuel assembly weight of 485 pounds per assembly plus a bounding damaged fuel can weight of 200 pounds in each of the support tube openings. As discussed in Section 2.2 of this FSAR, the weights of all BRP MOX, partial, and damaged fuel assemblies are bounded by the weight of the BRP intact fuel assemblies. Therefore, the cask tip-over loads and calculated stresses in the FuelSolutions™ W74 canister shell assembly and basket assemblies bound those for a FuelSolutions™ W74 canister containing any amount of intact BRP MOX fuel and partial fuel assemblies, and up to eight damaged fuel assemblies.

3.7.4.1 Canister Shell Assembly Tip-Over Analysis

For the postulated storage cask tip-over condition, the W74 canister shell assembly is supported by the two storage cask rails which run the full length of the canister shell and are located at 22.5° on both sides of the canister bottom centerline. The canister shell is loaded by its own weight in addition to the weight of the upper and lower basket assemblies and SNF assemblies contained in the canister shell cavity. The structural evaluation of the W74 canister shell assembly for the postulated storage cask tip-over load condition is performed using the three-dimensional half-symmetry finite element model described in Section 3.9.2.2. This model represents the top end region of the W21M-LS canister shell and basket assembly. As discussed in Section 3.9.2.2, the W21M-LS canister shell assembly stresses due to the storage cask tip-over loads bound those in the W74 canister shell assemblies since the geometry of the canister shell top end regions are similar and the total weight of the W21M-LS basket assembly and fuel bounds that of the W74 canister. Since the tip-over loads at the bottom end of the canister shell assembly are much lower than those at the top end, the stresses in the bottom end of the canister shell are bounded by those in the top end region and, consequently, need not be evaluated.

The top end shield plug and basket assembly spacer plates are included in the finite element model and connected to the canister shell with gap elements in order to accurately capture the non-linear interaction between the these components and the canister shell for the tip-over load condition. In addition, radial gap elements are used to model the non-linear support interface between the outside of the canister shell and the storage cask rail supports. A more detailed description of the canister shell three-dimensional half-symmetry finite element model is provided in Section 3.9.2.2.

For the tip-over condition, the canister shell is loaded by its own weight plus the weight of the basket assembly and fuel. The inertial loads of the canister shell, top outer and inner closure plates, the shield plug, and the self weight of the spacer plates are accounted for by applying an appropriate acceleration in the direction of the loading. The inertial loads of the fuel assembly and the guide tube are applied as uniform pressure loads over the width of the supporting spacer plate ligaments, as shown in Figure 3.9-4. The ligament pressure load are calculated for each spacer plate based upon the guide tube and fuel tributary weights presented in Section 3.9.2.2.

The stresses in the canister shell due to the tip-over load condition are calculated using a linear-elastic static analysis. The maximum stresses in the canister shell due to the tip-over condition are summarized in Table 3.7-1. The maximum stresses in the canister shell due to the bounding 30*g* tip-over load are shown to be lower than the corresponding Service Level D allowable stresses.

3.7.4.2 Canister Basket Assembly Tip-Over Analysis

3.7.4.2.1 General and LTP Spacer Plates

When subjected to tip-over loading, the W74 general and LTP spacer plates are relied upon to support and maintain the positions of the guide tube assemblies and SNF assemblies for criticality control. The W74 general and LTP spacer plates are loaded by their own weight and the weight of the SNF assemblies, guide tube assemblies, support tubes, support sleeves, and damaged fuel canisters. The spacer plates are supported by the canister shell in the region of impact and the canister shell is supported by two storage cask rails.

As discussed in Section 3.7.4, the W74 basket assembly is designed for a bounding 30*g* tip-over load. A linear-elastic stress analysis is performed for the most highly loaded W74 general and LTP spacer plates based on a uniform fuel load assumption. In addition, a plastic stress analysis is performed assuming the fuel load is applied to the W74 general and LTP spacer plates as concentrated loads at the fuel grid spacer locations. The primary purpose of the plastic stress analysis is to determine the maximum spacer plate permanent deformation resulting from the storage cask tip-over for consideration in the criticality evaluation. Lastly, buckling evaluations of the W74 general and LTP spacer plates are performed for the storage cask tip-over, considering both beam-column buckling in accordance with NUREG/CR-6322 and general instability in accordance with Appendix F of the ASME Code.

Tip-Over Elastic Stress Analysis

The W74 general and LTP spacer plate stress evaluation for the bounding 30*g* storage cask tip-over load is performed using an elastic system analysis based on a uniform fuel load assumption (i.e., spacer plate fuel loads proportional to spacer plate longitudinal pitch). For the tip-over evaluation, the W74 spacer plates are assumed to be supported only at the locations of the storage cask rails, conservatively neglecting the support provided by the canister shell. This is conservative since the assumed boundary conditions result in more concentrated reaction loads which produce higher stresses in the spacer plates.

Only the most highly loaded W74 general and LTP spacer plates are evaluated for the 30*g* storage cask tip-over load. For the tip-over condition, the acceleration load varies in magnitude, from approximately zero at the bottom end of the canister to the maximum acceleration at the top end of the canister. The impact load for each spacer plate is equal to the product of the transverse acceleration at its longitudinal location and the spacer plate tributary weight. The W74 general spacer plates having the highest tributary weights are those near the mid-length of the upper and lower basket assemblies since they have the largest longitudinal pitch. The W74 LTP spacer plates with the largest tributary weights are those nearest the mid-length of the canisters. Therefore, in order to provide a bounding analysis for the postulated storage cask tip-over condition, the bounding 30*g* tip-over acceleration, which occurs at the top end of the canister, is applied to the W74 general and LTP spacer plates which support the largest tributary weight.

As discussed in Section 3.9.1, the most highly loaded W74 general and LTP spacer plate have total tributary weights of 2,034 pounds and 2,041 pounds, respectively. Therefore, the most highly loaded W74 general and LTP spacer plates support total in-plane loads for the 30*g* storage cask tip-over of 61.0 kips and 61.2 kips, respectively.

The W74 general and LTP spacer plate tip-over elastic stress analyses are performed using the plane stress finite element model described in Section 3.9.2.4.1. The spacer plate loading from the support tubes, support sleeves, guide tube assemblies, damaged fuel canisters, and fuel assemblies are determined for the 30*g* tip-over load as described in Section 3.9.2.4.1. Linear-elastic static analyses are performed for the most highly loaded W74 general and LTP spacer plates.

The results of the W74 general and LTP spacer plate tip-over elastic system stress analyses show that the total reaction loads from the finite element solutions are greater than or equal to the tip-over impact load calculated above. The maximum primary membrane and primary membrane plus bending stress intensities in the most highly loaded W74 general spacer plate are 26.4 ksi and 53.2 ksi, respectively. The Service Level D allowable primary membrane and primary

membrane plus bending stress intensities for the general spacer plate A514, Grade F or P[28] material at 700°F are 75.4 ksi and 113.1 ksi, respectively. Therefore, the minimum design margins for primary membrane and primary membrane plus bending stress intensities in the most highly loaded W74 general spacer plate due to bounding 30*g* storage cask tip-over loading are +1.86 and +1.13, respectively.

The maximum primary membrane and primary membrane plus bending stress intensities in the most highly loaded W74 LTP spacer plate are 9.8 ksi and 19.7 ksi, respectively. The Service Level D allowable primary membrane and primary membrane plus bending stress intensities for the SA-240, Type XM-19 LTP spacer plate material at 700°F are 61.1 ksi and 91.5 ksi, respectively. Therefore, the minimum design margins for primary membrane and primary membrane plus bending stress intensities in the most highly loaded W74 LTP spacer plate due to bounding 30*g* storage cask tip-over loading are +5.23 and +3.64, respectively.

Tip-Over Permanent Deformation Analysis

The W74 spacer plates are evaluated for the bounding 30*g* storage cask tip-over load using plastic system analysis. The purpose of this plastic analysis is to determine the maximum permanent deformation of the W74 spacer plates due to the storage cask tip-over loading. For this analysis, the loads from the SNF assemblies are conservatively applied to the supporting basket assembly structure as concentrated loads at the fuel grid spacer locations. The worst case loading for each W74 spacer plate results when the fuel assembly grid spacer is located directly over that spacer plate. As discussed in Section 3.9.1, the maximum tributary weights for the Big Rock Point fuel in-core grid spacer and end fittings are 108.1 pounds and 54.1 pounds, respectively. The analysis for the postulated storage cask tip-over condition is performed using a bounding 30*g* tip-over acceleration, occurring at the top end of the canister, which is conservatively applied to the W74 spacer plates with the largest longitudinal center-to-center spacing. This is conservative since these spacer plates are not located at the top end of the canister where the tip-over g-loads are highest.

The W74 general and LTP spacer plates plastic stress analysis for the storage cask tip-over condition is performed using the full plane-stress finite element model described in Section 3.9.2.4.1. The plane stress finite element model includes a single spacer plate only, conservatively taking no credit for the support tubes and guide tubes which provide load sharing with the adjacent spacer plates. The general spacer plate is modeled with a 0.75-inch thickness and a tributary length of 7.125 inches. The LTP spacer plate is modeled with a 2.00-inch thickness and a tributary length of 5.625 inches. The spacer plate loading due to the tributary weight of the guide tubes, support tubes, support sleeves, and damaged fuel canisters plus the fuel assembly grid spacer tributary weights are applied to the model as pressure loads on the supporting spacer plate ligaments. These loads are calculated as described in Section 3.9.2.4.1.

For the W74 spacer plate tip-over plastic analysis, the model loads are ramped up to 30*g* and then reduced to 1*g* in order to determine permanent deformations. The results of the W74 general and LTP spacer plate plastic tip-over analyses show that the spacer plate plastic strain and permanent deformation due to the bounding tip-over loads are small. The maximum peak stress

[28] The general spacer plate allowable stresses are conservatively based on A514, Grade F or P carbon steel material properties (i.e., S_m, S_y, and S_u), which are lower than the alternative SA-517, Grade F or P carbon steel material properties.

intensity in the most highly loaded W74 general spacer plate from the tip-over plastic analysis is 91.3 ksi, compared to the general spacer plate material yield strength of 83.0 ksi at 700°F. The maximum equivalent plastic strain and permanent deformation in the most highly loaded general spacer plate are 0.7% and 0.005 inches, respectively. The maximum peak stress intensity in the most highly loaded W74 LTP spacer plate from the tip-over plastic analysis is 38.1 ksi, compared to the LTP spacer plate material yield strength of 36.8 ksi at 650°F. The LTP spacer plate does not experience any significant plastic strain, and consequently no permanent deformation, as a result of the 30*g* tip-over loading.

Tip-Over Buckling Analysis

The buckling evaluation of the W74 general and LTP spacer plates for the postulated storage cask tip-over condition considers beam-column buckling in accordance with NUREG/CR-6322 and general plastic instability in accordance with Appendix F of the ASME Code.

The W74 spacer plates are evaluated for buckling due to the storage cask tip-over condition as linear type supports subjected to combined axial compression and bending in accordance with NUREG/CR-6322. Buckling evaluations are performed for the most highly stressed ligaments in the most highly loaded W74 general and LTP spacer plate for the bounding 30*g* tip-over loading both with and without the bounding normal thermal loads superimposed. For this buckling evaluation, the spacer plate stresses are calculated using an elastic system analysis.

The maximum stresses in the W74 spacer plates due to the storage cask tip-over are evaluated using interaction equations (26), (27), and (28) of NUREG/CR-6322, defined as follows:

$$\frac{f_a}{F_a} + \frac{C_{mx} f_{bx}}{\left(1 - \frac{f_a}{F'_{ex}}\right) F_{bx}} + \frac{C_{my} f_{by}}{\left(1 - \frac{f_a}{F'_{ey}}\right) F_{by}} \le 1.0 \qquad \text{(Eq. 26)}$$

$$\frac{f_a}{2 \times 0.6 S_y} + \frac{f_{bx}}{F_{bx}} + \frac{f_{by}}{F_{by}} \le 1.0 \qquad \text{(Eq. 27)}$$

If $f_a/F_a \le 0.15$, then equation (28) may be used in lieu of equations (26) and (27):

$$\frac{f_a}{F_a} + \frac{f_{bx}}{F_{bx}} + \frac{f_{by}}{F_{by}} \le 1.0 \quad \text{if } \frac{f_a}{F_a} \le 0.15 \qquad \text{(Eq. 28)}$$

The allowable axial stress, F_a, bending stress, F_b, and Euler buckling stress, F_e', are calculated for all ligament sizes for both the W74 general (carbon steel) and LTP (stainless steel) spacer plate. Per NUREG/CR-6322, the allowable compressive stress for carbon steel is defined as follows:

$$F_a = \frac{P_{33}}{A_g} \text{ (carbon steel - general)}$$

$$F_a = \frac{P_{40}}{A_g} \text{ (stainless steel - LTP)}$$

where, A_g is the gross area of the spacer plate ligament, and the maximum allowable load, P33, is the allowable compressive load determined in accordance with NUREG/CR-6322 as follows:

$$P_{33} = \frac{(1-\lambda^2/4)}{1.11+0.5\lambda+0.17\lambda^2-0.28\lambda^3} S_y A_g \quad (\text{for } 0 \le \lambda \le 1)$$

and,

$$P_{40} = \frac{(P_{45})(P_{33})}{P_{43}}$$

where:

$$\lambda = \left(\frac{KL}{r_x}\right)\left(\frac{1}{\pi}\right)\sqrt{\frac{S_y}{E}}$$

where:

K = 0.65, Effective length factor for fixed-fixed support per Figure 6 of NUREG/CR-6322

L = 7.40 in., Unsupported length of spacer plate ligaments

r_x = $\sqrt{I_x/A_g}$ in., Ligament radius of gyration

I_x = $b^3t/12$, Ligament moment of inertia

A_g = bt, Ligament gross area

b = Ligament width
= 1.125 in., Centermost ligaments (hereafter referred to as Ligament “A”)
= 1.005 in., 1st ligaments from center, excluding those adjacent to the support tube holes (hereafter referred to as Ligament “B”)
= 1.050 in., vertical ligaments adjacent to support tube hole (hereafter referred to as Ligament “Bx”)
= 0.975 in., horizontal ligaments adjacent to support tube hole (hereafter referred to as Ligament “By”)
= 0.875 in., Outermost ligaments (hereafter referred to as Ligament “C”)

t = spacer plate thickness
= 0.75 in., General spacer plate
= 2.00 in., LTP spacer plate

S_y = Spacer plate material yield strength
= 83.0 ksi, general spacer plate at 700°F
= 36.8 ksi, LTP spacer plate at 650°F

E = Spacer plate material elastic modulus
= 25.1×10^6 psi, general spacer plate at 700°F
= 25.5×10^6 psi, LTP spacer plate at 650°F

C_m = 0.85, Coefficient for members in frames where sidesway is permitted per NUREG/CR-6322

The Euler buckling stress, calculated in accordance with Section 6.32 of NUREG/CR-6322, is defined as follows:

$$F_e' = \frac{\pi^2 E}{1.30(KL/r_x)^2} \quad \text{(carbon steel - general)}$$

$$F_e' = \frac{\pi^2 E}{1.46(KL/r)^2} \quad \text{(stainless steel - LTP)}$$

The allowable bending stress for compact sections, F_b, is defined in NUREG/CR-6322 as:

$$F_b = fS_y$$

where the plastic shape factor is f=1.5 for a solid rectangular section per Roark, Table 1, Case 2.

The allowable stresses are calculated for each of the W74 general and LTP spacer plate ligament types and summarized in Table 3.7-3 and Table 3.7-4, respectively.

As discussed previously, the W74 general and LTP spacer plate stresses used for the buckling evaluation are calculated using an elastic system analysis. The spacer plate stresses are determined for the bounding 30*g* tip-over load, both with and without thermal loading superimposed. The 30*g* tip-over loads for the spacer plates are calculated and applied to the W74 general and LTP spacer plate plane stress finite element models as described in Section 3.9.2.4.1. The thermal gradient which is applied to the model is based on the temperature distribution in the hottest W74 general spacer plate for normal cold storage conditions. As discussed in Section 3.5.1.3.2, the normal cold storage thermal condition results in the highest general spacer plate thermal stresses, and therefore, the worst case initial condition for general spacer plate buckling. In order to facilitate application of the thermal gradient to the model, the general spacer plate gradient is approximated using the following third order polynomial equation, which provides the temperature (T) as a function of the radial distance from the spacer plate centerline:

$$T(r) = 0.0073r^3 - 0.7257r^2 + 9.6784r + 577.09$$

Figure 3.7-2 shows the design thermal gradient versus the actual W74 general spacer plate temperatures for the normal cold storage thermal condition. A comparison of the thermal stresses calculated using the polynomial function and those from the actual thermal gradient shows that the design thermal gradient produces thermal stresses in the W74 general spacer plate which bound those calculated for the normal cold storage thermal gradient. Therefore, the design thermal gradient is bounding. This design thermal gradient is also conservatively used for the W74 LTP spacer plate buckling evaluation.

The maximum axial compressive stress and bending stress in the most highly loaded W74 general and LTP spacer plate ligaments for the tip-over loading, both with and without thermal

loading superimposed, are summarized in Table 3.7-5 along with the resulting interaction ratios. The results show that the highest interaction ratio in the W74 general spacer plate is 0.44 in Ligament Bx for combined tip-over plus thermal loading. Similarly, the highest interaction ratio in the W74 LTP spacer plate is 0.60 in Ligament Bx for the combined tip-over plus thermal loading. Therefore, the minimum design margins for local buckling of the most highly loaded W74 general and LTP spacer plate for the bounding 30*g* tip-over load are +1.27 and +0.67, respectively.

In addition to the NUREG/CR-6322 elastic beam-column buckling analysis, general plastic instability of the W74 spacer plates is evaluated for the bounding 30*g* storage cask tip-over load, both with and without the bounding normal thermal loading, using plastic large deflection analyses. General instability of the W74 spacer plates occurs when the spacer plate experiences a global longitudinal plate buckling mode. Since the longitudinal bending stiffness of the W74 general spacer plates is proportional to the plate thickness cubed, the bending stiffness of the 2.00-inch thick W74 LTP spacer plates is approximately 19 times greater than that of the ¾-inch thick W74 general spacer plates. Therefore, general instability will be controlled by the general spacer plates and the LTP spacer plates need not be evaluated.

For this analysis, the loads from the SNF assemblies are conservatively applied to the supporting basket assembly structure as concentrated loads at the fuel grid spacer locations. The worst case loading for each W74 spacer plate results from the SNF fuel with the highest grid spacer tributary weight for the fuel assembly grid spacer located directly over that spacer plate. As discussed in Section 3.9.1, the maximum tributary weights for the Big Rock Point fuel in-core grid spacer and end fittings are 108.1 pounds and 54.1 pounds, respectively. The analysis for the postulated storage cask tip-over condition is performed using a bounding 30*g* tip-over acceleration, occurring at the top end of the canister, which is conservatively applied to the W74 spacer plates with the largest longitudinal center-to-center spacing. This is conservative since these spacer plates are not located at the top end of the canister where the tip-over g-loads are highest.

The W74 general spacer plate plastic large deflection buckling analysis for the storage cask tip-over condition is performed using the half-symmetry multi-span shell finite element model described in Section 3.9.2.4.4. The finite element model includes three general spacer plates; the center spacer plate over which the fuel grid spacers are assumed to be positioned, and the adjacent spacer plates on either side. All spacer plates are modeled with at uniform pitch of 7.125 inches. The spacer plates are modeled using plastic shell elements which have both membrane and bending stiffness. The guide tubes and support tubes are also modeled using plastic shell elements. The spacer plates are supported longitudinally by the support sleeves, which are modeled discretely using brick elements.

The bi-linear kinematic hardening material model with a 0.1% tangent modulus is conservatively used for the W74 general spacer plate, guide tube, support tube, and support sleeve materials. For the tip-over loads without thermal, the material properties at 700°F are assumed. For the combined tip-over plus thermal loading, the temperature dependent material properties from Section 3.3 are used for the general spacer plates, guide tubes, support tubes, and support sleeves.

The fuel load is applied to the bottom panel of the guide tubes and support tubes directly above the center spacer plate. The spacer plate self-weight and the weight of the guide tubes, support

tubes, and support sleeves are accounted for by applying an in-plane acceleration load. In addition to the in-plane model loading, a constant 10*g* longitudinal acceleration load is applied to the finite element model to introduce an initial eccentricity to the spacer plates.

The thermal gradient which is applied to the model is based on the temperature distribution in the hottest W74 general spacer plate for normal cold storage conditions. The bounding design thermal gradient discussed previously is conservatively used for this analysis. Further discussion of the finite element model construction, material properties, boundary conditions, and loading are described in detail in Section 3.9.2.4.4.

For the W74 general spacer plate tip-over plastic large deflection buckling analysis, the loads are applied such that the variable "time" is equal to the load factor (i.e., time = 1.5 corresponds to 150% of the tip-over load). The 10*g* longitudinal acceleration and thermal gradient are applied as initial conditions (i.e., time = 0.01 seconds). All model in-plane loads are ramped up to 1.5 times the tip-over load (i.e., 45*g* at time = 1.5 seconds). Spacer plate plastic instability is indicated by numerical instability in the finite element solution (i.e., unconverged solution). The results show that the most highly loaded W74 general spacer plate remains stable up to 150% of the bounding tip-over load, both with and without thermal loading superimposed. The deformed shape of the most highly loaded W74 general spacer plate at 150% of the bounding 30*g* tip-over load (i.e., 45*g*) plus the bounding thermal load is shown in Figure 3.7-3.

3.7.4.2.2 Engagement Spacer Plate

The engagement spacer plate loads due to the postulated storage cask tip-over condition are approximately equal to half of those due to the transfer cask side drop. Therefore, the engagement spacer plate stresses due to the postulated storage cask tip-over condition are bounded by those due to the transfer cask side drop and need not be evaluated.

3.7.4.2.3 Support Tubes and Support Sleeves

The support tube and support sleeve loads due to the postulated storage cask tip-over condition are bounded by those due to the transfer cask side drop. Furthermore, the support tube and support sleeve boundary conditions for the storage cask tip-over are similar to those for the transfer cask side drop. Therefore, the support tube and support sleeve stresses need not be evaluated for the postulated storage cask tip-over condition.

3.7.4.2.4 Guide Tubes

The guide tube loads due to the postulated storage cask tip-over condition are bounded by those due to the transfer cask side drop. Furthermore, the guide tube boundary conditions for the storage cask tip-over are similar to those for the transfer cask side drop. Therefore, the guide tube stresses need not be evaluated for the postulated storage cask tip-over condition.

3.7.5 Transfer Cask Drop

The transfer cask is evaluated for a postulated accidental side drop event as discussed in Section 2.3.3.2.2 and evaluated in Section 3.7.5 of the FuelSolutions™ Storage System FSAR. The accidental transfer cask drop scenario is a postulated side drop from a height of 72 inches. The transfer cask side drop results in a rigid body response, characterized as a half-sine wave pulse with a duration of t_1 = 0.0225 seconds and a peak acceleration of 46*g*. The FuelSolutions™

W74 canister is evaluated for the postulated transfer cask side drop scenario using equivalent static loads. The equivalent static side drop acceleration is equal to the peak acceleration multiplied by a DLF to account for possible dynamic amplification within the canister. The maximum DLF for the W74 canister assembly is based on the natural frequencies of the W74 canister structural components. The lowest natural frequency of the W74 canister assembly is 101 Hz for the guide tubes. From Figure 2.15 of NUREG/CR-3966, the maximum DLF for a half-sine pulse load where $t_1/T = 2.3$ (= 0.0225 x 101) or higher is 1.15. Therefore, the maximum equivalent static acceleration for the transfer cask side drop is 53*g*. The FuelSolutions™ W74 canister is evaluated for a bounding 60*g* side drop deceleration load resulting from the postulated transfer cask side drop scenario in the following sections.

3.7.5.1 Canister Shell Assembly Side Drop Analysis

For the postulated transfer cask side drop condition, the W74 canister shell assembly is supported by the transfer cask inner shell and loaded by its own weight in addition to the weight of the basket assembly and SNF assemblies contained in the canister shell cavity. The W74 canister shell assembly is evaluated for the postulated transfer cask side drop analysis using a bounding equivalent static deceleration load of 60*g*. The side drop load condition is evaluated using the three dimensional half-symmetry finite element model described in Section 3.9.2.2 and shown in Figure 3.9-2. This model represents the top end region of the W21M-LS canister shell and basket assembly. As discussed in Section 3.9.2.2, the W21M-LS canister is selected as the bounding design over the W74 canister shells since it has the largest overall combined weight for the basket assembly and fuel and the heaviest top end shield plug. In addition, the W21M-LS canister shell top end geometry is identical to that of the W74 canisters, but uses a solid carbon steel shield plug versus a segmented shield plug. The top end shield plug and basket assembly spacer plates are included in the finite element model and connected to the canister shell with gap elements in order to accurately capture the non-linear interaction between the these components and the canister shell for the tip-over load condition. In addition, radial gap elements are used to model the non-linear support interface between the outside of the canister shell and inside shell of the transfer cask. A more detailed description of the canister shell three-dimensional half-symmetry finite element model is provided in Section 3.9.2.2.

For the transfer cask side drop condition, the canister shell is loaded by its own weight plus the weight of the basket assembly and fuel. The inertial loads of the canister shell, top outer and inner closure plates, the shield plug, and the self weight of the spacer plates are accounted for by applying an appropriate acceleration in the direction of the loading. The inertial loads of the fuel assembly and the guide tube are applied as uniform pressure loads over the width of the supporting spacer plate ligaments, as shown in Figure 3.9-4. The ligament pressure load are calculated for each spacer plate based upon the guide tube and fuel tributary weights.

The stresses in the canister shell due to the 60*g* side drop load condition are calculated using a linear-elastic static analysis. The maximum primary membrane and primary membrane plus bending stress intensities in the canister shell due to the 60*g* side drop are reported in Table 3.7-1. The results of the canister shell side drop analysis show that the maximum stresses are less than the corresponding Service Level D allowable stresses.

3.7.5.2 Canister Basket Assembly Side Drop Analysis

3.7.5.2.1 General and LTP Spacer Plates

When subjected to the postulated transfer cask side drop loading, the basket assembly spacer plates provide structural support for the SNF assemblies, damaged fuel cans, guide tube assemblies, support tubes, and support sleeves. The structural stability of the spacer plates is of primary importance for the side drop condition since the spacer plates are relied upon to maintain the relative spacing of the poisoned guide tube assemblies and SNF assemblies and ensure subcriticality. A rigorous structural evaluation of the W74 general spacer plates and LTP spacer plates is performed for the bounding 60*g* side drop load.

Structural evaluations of the most highly loaded W74 general and LTP spacer plates are performed for the postulated transfer cask side drop condition using two bounding fuel loading assumptions: 1) Uniform fuel loading assumption (i.e., fuel weight distributed uniformly to basket assembly spacer plates), and 2) Concentrated fuel loading at the fuel assembly grid spacers. The uniform fuel loading assumption is used for elastic system stress analyses in accordance with Appendix F of the ASME Code. The concentrated fuel loading assumption is used for plastic stress analyses to determine the maximum spacer plate permanent deformation in the most highly loaded W74 general and LTP spacer plates resulting from the 60*g* side drop load for consideration in the criticality evaluation. Finally, a buckling evaluation of the W74 spacer plates is performed which considers beam-column buckling in accordance with NUREG/CR-6322 (uniform fuel load), and general instability in accordance with Appendix F of the ASME Code (concentrated fuel load).

Elastic Stress Analysis - Uniform Fuel Loading

The W74 spacer plate side drop elastic stress analysis is performed using the plane stress finite element model described in Section 3.9.2.4.1. Only the most highly loaded W74 general and LTP spacer plates are evaluated for the 60*g* side drop. Since the side drop acceleration load does not vary in magnitude over the length of the basket assembly, the most heavily loaded W74 spacer plates are those which support the largest tributary weight. The spacer plate in-plane tributary weights are defined as the portion of the SNF assembly (and damaged fuel canister, if required), guide tube, support tube, and support sleeve weights that are supported by each spacer plate in the transverse direction, combined with the spacer plate self-weight

The maximum tributary weights of the W74 general and LTP spacer plates are 2,034 pounds and 2,041 pounds, respectively. Therefore, the most highly loaded W74 general and LTP spacer plates support total loads for the 60*g* side drop of 122.0 kips and 122.5 kips, respectively.

The spacer plate side drop analysis is performed for seven separate impact orientations, as shown in Figure 3.7-4. These include impacts along the 0°, 15°, 30°, 45°, 60°, 75°, and 90° azimuths. Since the spacer plate geometry is symmetric about both the horizontal and vertical centerlines, these seven impact orientations adequately envelope all possible side drop impact orientations. The spacer plate loading from the support tubes, support sleeves, guide tube assemblies, damaged fuel canisters, and fuel assemblies are applied to the supporting spacer plate ligaments as pressure loads. These loads are calculated as described in Section 3.9.2.4.1.

For each side drop orientation, a linear-elastic static analysis is performed. The primary stress intensities in the spacer plates are evaluated as discussed in Section 3.9.3.3. The maximum

primary membrane (P_m) and primary membrane plus bending (P_m+P_b) stress intensities in the most highly loaded W74 general and LTP spacer plates are summarized in Table 3.7-6 for each side drop orientation.

The stress results show that the highest primary membrane and primary membrane plus bending stress intensities the most heavily loaded W74 general spacer plate due to the HAC side drop load result from the 15° and 45° impact orientations, respectively. The maximum primary membrane and primary membrane plus bending stress intensities are 35.3 ksi and 78.9 ksi, respectively. The Service Level D allowable primary membrane and primary membrane plus bending stress intensities for the weakest general spacer plate material at 700°F are 75.4 ksi and 113.1 ksi, respectively. Therefore, the minimum design margins for primary membrane and primary membrane plus bending stress intensities in the most highly loaded W74 general spacer plate due to bounding 60*g* side drop loading are +1.14 and +0.43, respectively.

The maximum primary membrane and primary membrane plus bending stress intensities in the most highly loaded W74 LTP spacer plate due to the HAC side drop load result from the 0° and 30° impact orientations, respectively. The maximum primary membrane and primary membrane plus bending stress intensities are 17.4 ksi and 51.3 ksi, respectively. The Service Level D allowable primary membrane and primary membrane plus bending stress intensities for SA-240, Type XM-19 stainless steel at 650°F are 61.1 ksi and 91.5 ksi, respectively. Therefore, the minimum design margins for primary membrane and primary membrane plus bending stress intensities in the most highly loaded W74 LTP spacer plate due to the bounding 60*g* side drop loading are +2.51 and +0.78, respectively.

Permanent Deformation Analysis - Concentrated Fuel Loading at Fuel Grid Spacers

In addition to the uniform fuel load case, the loads from the SNF assemblies are conservatively applied to the supporting basket assembly structure as concentrated loads at the fuel grid spacer locations. The worst case loading for each W74 spacer plate results from the SNF fuel with the highest grid spacer tributary weight for the fuel assembly grid spacer located directly over that spacer plate. As discussed in Section 3.9.1, the maximum tributary weights for the Big Rock Point fuel in-core grid spacer and end fittings are 108.1 pounds and 54.1 pounds, respectively. The analysis for the postulated transfer cask side drop condition is performed using a bounding 60*g* equivalent static acceleration, which is conservatively applied to the W74 spacer plates with the largest longitudinal center-to-center spacing. For this analysis, as with the uniform loading condition, impact orientations of 0°, 45°, and 90° are considered.

The W74 spacer plates plastic stress analyses for the transfer cask side drop condition are performed using the full plane-stress finite element model described in Section 3.9.2.4.1. The plane stress finite element model includes a single spacer plate only, conservatively taking no credit for the support tubes and guide tubes which provide load sharing with the adjacent spacer plates. The general spacer plate is modeled with a 0.75-inch thickness and a tributary length of 7.125 inches. The LTP spacer plate is modeled with a 2.00-inch thickness and a tributary length of 5.625 inches. The spacer plate loading due to the tributary weight of the guide tubes, support tubes, support sleeves, and damaged fuel canisters plus the fuel assembly grid spacer tributary weights are applied to the model as pressure loads on the supporting spacer plate ligaments. These loads are calculated as described in Section 3.9.2.4.1. The finite element model loads for the 60*g* side drop conditions are ramped up to 60*g* and then reduced to 1*g* in order to determine the spacer plate permanent deformations.

The results of the W74 general and LTP spacer plate 60*g* side drop plastic analyses shows that the plastic strain in the most highly loaded W74 general and LTP spacer plates for the bounding 60*g* side drop load are small and occur only in localized regions. The maximum equivalent plastic strain in the most highly loaded W74 general spacer plate is 0.5% and occurs for the 0° impact orientation. The minimum elongation of the W74 general spacer plate SA-517 or A514, Grade F or P carbon steel is 16% per the ASME Code. Therefore, the plastic strain in the most highly loaded W74 general spacer plate is much less than that corresponding to ultimate tensile failure. The maximum permanent deformation in the most highly loaded W74 general spacer plate results from the 45° impact orientation and is calculated to be 0.04 inches.

The maximum equivalent plastic strain in the most highly loaded W74 LTP spacer plate due to the bounding 60*g* side drop load is 0.2% and occurs for the 45° impact orientation. The minimum elongation of SA-240, Type XM-19 stainless steel is 35% per the ASME code. Thus, the plastic strain in the W74 LTP spacer plates is much less than that corresponding to ultimate tensile failure. The maximum permanent deformation in the most highly loaded W74 LTP spacer plate also occurs for the 45° impact orientation and is calculated to be 0.014 inches.

Spacer Plate Buckling

The buckling evaluation of the spacer plates for the postulated transfer cask side drop condition considers both beam-column buckling in accordance with NUREG/CR-6322 and general plastic instability in accordance with Appendix F of the ASME Code.

For the beam-buckling condition, the W74 spacer plates are evaluated for buckling due to the postulated transfer cask side drop condition using the criteria of NUREG/CR-6322 for linear type supports subjected to combined axial compression and bending. Buckling evaluations are performed for the most highly loaded ligaments in both the W74 general and LTP spacer plates for the bounding 60*g* side drop loading, both with and without the bounding normal thermal loads superimposed.

The maximum stresses in the W74 spacer plates due to the postulated transfer cask side drop are evaluated using interaction equations (26), (27), and (28) of NUREG/CR-6322, as defined in Section 3.7.4.2.1. The allowable stresses are calculated for each of the W74 spacer plate ligament types and summarized in Table 3.7-6.

As discussed previously, the spacer plate stresses used for the NUREG/CR-6322 buckling evaluation are calculated on an linear-elastic basis using the W74 spacer plate plane stress finite element model described in Section 3.9.2.4.1. The spacer plate stresses are determined for the bounding 60*g* side drop load, both with and without thermal loading superimposed. The 60*g* side drop loads for the spacer plates are calculated and applied to the finite element models as described in Section 3.9.2.4.1. The thermal gradient which is applied to the model is based on the temperature distribution in the hottest W74 carbon steel spacer plate for normal cold storage conditions. The bounding design thermal gradient discussed in Section 3.7.4.2.1 is conservatively used for this analysis.

The maximum axial compressive stress and bending stress in the W74 general and LTP spacer plate ligaments for the 60*g* side drop loading, both with and without the bounding normal thermal loading superimposed, are summarized in Table 3.7-7 through Table 3.7-10 along with the resulting interaction ratios. The results of the analysis show that the highest interaction ratios resulting from the bounding 60*g* side drop load are 0.52 for the W74 general spacer plate and

0.96 for the W74 LTP spacer plate. Therefore, the minimum design margins for ligament buckling of the most highly loaded W74 general and LTP spacer plates for the bounding 60*g* side drop load are +0.52 and +0.04, respectively.

In addition to the elastic beam-column buckling analysis, general plastic instability of the W74 spacer plates is evaluated for the bounding 60*g* transfer cask side drop load, both with and without thermal loading, using plastic large deflection analyses. General instability of the W74 spacer plates occurs when the spacer plate experiences a global longitudinal plate buckling mode. Since the longitudinal bending stiffness of the W74 general spacer plates is proportional to the plate thickness cubed, the bending stiffness of the 2.00-inch thick W74 LTP spacer plates is much greater than that of the 3/4-inch thick W74 general spacer plates. In addition, the results of the W74 spacer plate elastic stress analysis for the side drop load show that the spacer plate stress levels relative to the material yield strengths are comparable. Therefore, general instability will be controlled by the W74 general spacer plates and the LTP spacer plates need not be evaluated.

The W74 general spacer plate plastic large deflection buckling analysis for the transfer cask side drop condition is performed using the full multi-span shell finite element model described in Section 3.9.2.4.5. The finite element model includes three ¾-inch thick carbon steel spacer plates: the center spacer plate, over which the fuel grid spacers are assumed to be positioned, and the adjacent spacer plates on either side. All spacer plates are modeled with at uniform pitch of 7.125 inches. The spacer plates are modeled using plastic shell elements which have both membrane and bending stiffness. The guide tubes and support tubes are also modeled using plastic shell elements. The spacer plates are supported longitudinally by the support sleeves, which are modeled discretely using brick elements.

For this analysis, the loads from the SNF assemblies are conservatively applied to the supporting basket assembly structure as concentrated loads at the fuel grid spacer locations. The worst case loading for each W74 spacer plate results from the SNF fuel with the highest grid spacer tributary weight for the fuel assembly grid spacer located directly over that spacer plate. As discussed in Section 3.9.1, the maximum tributary weights for the Big Rock Point fuel in-core grid spacer and end fittings are 108.1 pounds and 54.1 pounds, respectively.

The bi-linear kinematic hardening material model with a 0.1% tangent modulus is conservatively used for the spacer plate, support tube, support sleeve, and guide tube materials. For the side drop loads without thermal, the material properties at 700°F are assumed. For the combined side drop plus thermal loading, temperature dependent material properties are used for the spacer plates, support tubes, support sleeves, and guide tubes. The thermal gradient which is applied to the model is based on the temperature distribution in the hottest W74 general spacer plate for normal cold storage conditions

For the W74 general spacer plate side drop plastic large deflection buckling analysis, all in-plane loads are ramped up to 1.5 times the side drop load (i.e., 90*g*). Spacer plate plastic instability is indicated by numerical instability in the finite element solution (i.e., unconverged solution). The results show that the most highly loaded W74 general spacer plate remains stable up to 1.5 times the bounding side drop load, both with and without thermal loading superimposed. The spacer plate deflections are slightly higher for the case which includes thermal loading than for side drop loading alone.

3.7.5.2.2 Engagement Spacer Plate

Stress Evaluation

The W74 engagement spacer plate is evaluated for a 60*g* side drop load using the plane stress finite element models described in Section 3.9.2.5. The side drop orientations include impacts at the 0°, 28°, 36°, and 45° azimuths, as shown in Figure 3.7-7. Since the W74 engagement spacer plate is symmetric with respect to the horizontal and vertical centerlines, these impact orientations encompass all of the orientations expected to cause the most severe spacer plate stresses. The 0° impact side drop evaluation is performed using the half-symmetry plane stress finite element model shown in Figure 3.9-16. The 28°, 36°, and 45° impact side drop evaluations are performed using the full engagement plate plane stress finite element model shown in Figure 3.9-17.

The engagement spacer plate side drop stress analysis shows that the maximum primary plus secondary plus peak stress intensity of 16.4 ksi results from the 36° azimuth impact orientation. This stress intensity is conservatively compared with the allowable Service Level D primary membrane stress intensity. The allowable Service Level D primary membrane stress intensity for the engagement spacer plate SA-240, Type XM-19 stainless steel material at the design temperature of 600°F is 61.4 ksi. Therefore, the minimum design margin in the W74 engagement spacer plate for the postulated transfer cask side drop condition is +2.74.

Buckling Evaluation

The elastic stability of the W74 engagement spacer plate is evaluated for the effects of a bounding free drop impact loads (i.e., 60*g* in-plane and 45*g* out-of-plane) combined with the bounding thermal gradient shown in Table 3.5-3. The evaluations demonstrate that the engagement spacer plate does not fail due to elastic buckling and provides the required factor of safety against buckling for the bounding drop loads.

The stability of the 2-inch thick W74 stainless steel engagement spacer plate is evaluated for the bounding free drop impact loads using the half-symmetry finite element model described in Section 3.9.2.5. Both eigenvalue and large deflection buckling analyses are performed. Eigenvalue buckling analyses are performed for the bounding impact loads with and without thermal loading to determine the controlling load combination for buckling. For this controlling load combination, a large deflection buckling analysis is performed in which gap elements are used to model the non-linear edge support condition provided by the canister shell assembly. The engagement spacer plate is modeled using elastic shell elements to account for both in-plane and out-of-plane response. The elastic stability is evaluated for the 0° impact orientation only since the bending stiffness of the engagement spacer plate does not vary significantly with respect to the in-plane impact orientation.

Two eigenvalue buckling analyses are performed for the side drop condition: 1) bounding free drop impact loads only (i.e., no thermal loads), and 2) combined bounding free drop impact and thermal loading. Since eigenvalue buckling analyses is limited to linear behavior, the non-linear gap elements used to model the interface contact between the spacer plate and the canister shell for the stress analysis are replaced with equivalent radial displacement constraints in the region where the spacer plate and shell come in contact, as shown by the 0° side drop stress analysis results. Symmetry boundary constraints (e.g., UX=ROTY=ROTZ=0) are applied to the nodes which lie on the symmetry plane (X=0). Longitudinal constraints are applied to a single node in

the region of each support tube, conservatively assuming simple support conditions. For drop loading without thermal, perimeter buckling is expected to control. Therefore, for this condition longitudinal constraints are applied to the nodes located at the corners of the support tubes closest to the center of the engagement spacer plate to maximize the unsupported length at the perimeter of the plate. For combined side drop and thermal loading, center buckling of the engagement spacer plate is expected to control. Therefore, for this condition, longitudinal constraints are applied to the nodes located at the corners of the support tubes furthest to the center of the engagement spacer plate to maximize the unsupported length in the center of the plate.

The engagement spacer plate eigenvalue buckling evaluations are performed using bounding longitudinal and transverse equivalent static accelerations of 45*g* and 60*g*, respectively. For the 45*g* longitudinal load, the engagement spacer plate is loaded by its own weight in addition to the weight of the fuel and basket assembly opposite the side of impact. The loads from the fuel assemblies, guide tubes, damaged fuel canisters, and basket assembly are applied as uniform pressures of the respective regions of the model. The magnitudes of the pressure loads are determined by scaling those calculated for the 50*g* end drop in Section 3.9.2.5 by the ratio of the longitudinal g-loads (45*g*/50*g*).

The material properties used in the finite element model are described in Section 3.9.2.5. The temperature dependent properties (E and α) of SA-240, Type 316 stainless steel are conservatively used for the buckling evaluation in which thermal loading is superimposed. The use of SA-240, Type 316 stainless steel properties is conservative since it has higher coefficients of thermal expansion than SA-240, Type XM-19 stainless steel, which results in higher thermal stresses and a lower factor of safety against buckling.

The results of the engagement spacer plate eigenvalue buckling analysis show that the factors of safety for the 0° side drop impact with and without thermal loading superimposed are 5.9 and 22.4, respectively. These results show that the lowest factor of safety against buckling results from side drop impact load plus thermal.

In order to address the effects of the non-linear edge support conditions provided by the canister shell, a large deflection buckling evaluation is performed for the combined side drop and thermal loads. This evaluation is performed using the half-symmetry finite element model described in Section 3.9.2.5, with shell elements to allow out-of-plane displacements. The bounding engagement spacer plate thermal gradient shown in Table 3.5-3 is applied to the model as a preload. The spacer plate impact loads corresponding to a 60*g* in-plane acceleration and a 45*g* longitudinal acceleration, as described above, are applied to the model and gradually increased until the solution does not converge or a load factor (i.e., factor of safety) of 6.0 is reached. The results of the large deflection buckling evaluation show that the W74 engagement spacer plate remains stable at a load factor of 6.0. Therefore, the minimum factor of safety against buckling of the W74 engagement spacer plate is conservatively taken as 6.0 for the bounding side drop load condition. The required factor of safety against buckling is 1.5. Therefore, the W74 engagement spacer plate meets the Service Level D buckling design criteria for the side drop.

3.7.5.2.3 Support Tube

The support tube stresses resulting from the 60*g* side drop load are evaluated using simple beam theory. For the side drop load conditions, the horizontally oriented support tubes are loaded in

the vertical direction by their own weight plus the weight of the support sleeves and the SNF assembly inside the support tube. Since the support tube is designed to contain either intact or damaged SNF assembly, the weight of the damaged fuel can is also included. The support tube stresses are calculated for the 60*g* side drop load by evaluating the following cases:

1. Case 1 - The support tube is evaluated as a uniformly loaded beam, simply supported at each spacer plate. The maximum bending stress, shear stress, primary membrane and primary membrane plus bending stress intensities are calculated for the largest spacer plate span (7.125 inches) using standard beam theory.
2. Case 2 - The width (lateral direction) of the bottom face of the support tube is evaluated as a simply supported beam with a 1-inch unit width in the tube's longitudinal direction. The bending stress, shear stress, primary membrane and primary membrane plus bending stress intensities due to the weight of the fuel inside the support tube are calculated using standard beam theory.
3. Combination of Cases 1 & 2 - The maximum primary membrane plus bending stress in the support tube is calculated by combining the stresses from Cases 1 & 2.

Case 1 (Beam Bending)

The longitudinal beam bending stress in the W74 support tubes is calculated for the largest spacer plate center-to-center span length (7.125 inches), assuming fixed end conditions due to symmetry. The fuel, support tube and sleeve weights are treated as uniformly distributed loads and the total distributed load is calculated as follows:

$$w = G(A_{st}\rho + A_{ss}\rho + w_{fuel}) = 1{,}021 \text{ lb/in.}$$

where:

G = 60*g*, equivalent static side drop load

A_{st} = 23.33 in^2, area of support tube

= $[(8.90)^2-(7.40)^2] - 4(0.75)^2/2$

A_{ss} = 7.51 in^2, area of the support sleeve

= $2[(14.0-0.188/2)(0.188) + (9.1+0.125/2)(0.125)]$

ρ = 0.290 lb/in^3, weight density of stainless steel

w_{fuel} = 8.08 lb/in., SNF assembly + damaged fuel can line load

= (485 lb. + 200 lb)/84.8 in.

The maximum bending moment on the support tube is calculated as follows:

$$M_{max} = \frac{wL^2}{12} = 4.32 \text{ in-kips}$$

where:

w = 1.021 kips/in., weight per unit length of the support tube calculated above.

L = 7.125 in., the free span of the support tube.

The maximum bending stress in the support tube is calculated as follows:

$$\sigma = \frac{Mc}{I} = 0.07 \text{ ksi}$$

where:

c = 4.45 in., distance to the neutral axis of the support tube.

I = 273 in^4, area moment of inertia of the support tube

= $(8.90^4 - 7.40^4)/12$

The maximum shear force at each support is calculated as follows:

$$V = \frac{wL}{2} = 3.64 \text{ kips}$$

The shear stress at the ends of the support tube is calculated as follows:

$$\tau = \frac{V}{A} = 0.33 \text{ ksi}$$

where:

V = 3.64 kips, shear force calculated above .

A = 11.1 in^2, area of support tube webs

= 2(0.75)(7.40)

Since the maximum bending stress and maximum shear stress occur at different locations their effects do not add. The maximum primary membrane (P_m) is conservatively taken as the larger of twice the maximum shear stress (0.66 ksi) or the maximum bending stress (0.07 ksi). Therefore, the maximum primary membrane stress intensity is 0.66 ksi.

Case 2 (Panel Bending)

For this case, the fuel and support tube weights are treated as uniformly distributed loads on a 1-inch wide segment on the inside bottom panel of the support tube, as shown in Figure 3.7-8. The total distributed load is calculated as follows:

$$w = G(A_{st}\rho + w_f) = 78.5 \text{ lb/in.}$$

where:

G = 60*g*, equivalent static side drop acceleration

A_{st} = area of a 1 inch deep segment of the support tube

= (0.75 in.)(1 in.) = 0.75 in^2

ρ = 0.290 lb/in^3, density of stainless steel support tube.

w_f = SNF fuel assembly + damaged fuel can weight line load (485 + 200 = 685 lb. spread over 84.8”) spread across a one inch deep segment across the inside width (7.40”) of the support tube.

= 1.09 lb/in.

The maximum bending moment on the support tube is calculated as follows:

$$M_{max} = \frac{wL^2}{8} = 0.537 \text{ in-kips}$$

The maximum bending stress in the support tube bottom panel is calculated as follows:

$$\sigma = \frac{6M}{t^2} = 5.73 \text{ ksi}$$

The maximum shear force on the support tube is calculated as follows:

$$V = \frac{wL}{2} = 0.29 \text{ kips}$$

The corresponding shear stress is calculated as follows:

$$\tau = \frac{V}{A} = 0.39 \text{ ksi}$$

The maximum primary membrane (P_m) and the primary membrane plus bending (P_m+P_b) stress intensities are calculated as follows:

$$P_m = 2\tau = 0.78 \text{ ksi}$$

$$P_m + P_b = 2\sqrt{\left(\frac{\sigma}{2}\right)^2 + \tau^2} = 5.78 \text{ ksi}$$

Combined Support Tube Stresses

The total primary membrane and bending stress intensities for the support tube are calculated by adding the bending of the support tube calculated for case 1 to the bottom panel bending stresses from case 2 as follows:

$$P_m = 0.66 + 0.78 = 1.44 \text{ ksi}$$

$$P_m + P_b = 0.66 + 5.78 = 6.44 \text{ ksi}$$

The Service Level D allowable primary membrane and primary membrane plus bending stress intensities for SA-240 Type XM-19 stainless steel at 700oF are 60.6 ksi and 90.8 ksi, respectively. The minimum design margins for primary membrane and primary membrane plus bending stress intensity due to the bounding 60*g* side drop load are +41.1 and +13.1, respectively.

Support Tube Longitudinal Seam Weld Stress Evaluation

When subjected to the 60*g* side drop loading, the support tube longitudinal seam welds are designed to support the internal longitudinal shear forces resulting from beam bending (see case 1 above) plus the vertical shear reactions at the edges of the bottom panel which supports the weight of the SNF assembly (see case 2 above).

The maximum weld shear stress due to the internal longitudinal shear forces resulting from beam bending behavior occur at the ends of the support tubes where the maximum shear load occurs.

As shown above, the maximum shear load due to the 60*g* side drop load is 3.64 kips. The resulting weld shear stress is calculated as follows:

$$\tau_1 = \frac{VQ(y)}{It(y)} = 0.51 \text{ ksi}$$

where:

V = 3.64, maximum shear load

Q(y) = (8.90 x 0.75)(4.45 - 0.75/2) = 27.2 in^3

I = 273 in^4, support tube area moment of inertia

t(y) = 0.71 in., thickness of two seam welds

= 2(0.5 x 0.707)

The direct shear stress in the support tube longitudinal seam weld resulting from the shear reaction force calculated for case 2 is calculated as follows:

$$\tau_2 = \frac{V}{A} = 0.83 \text{ ksi}$$

where:

V = 0.29 kips, shear force per unit length of weld

A = 0.35 in^2, weld shear stress area per unit length of weld

= (0.50 x 0.707)(1)

The combined weld shear is conservatively taken as the absolute sum of the two shear stresses calculated above, or 1.34 ksi. The Service Level D allowable shear stress for the support tube longitudinal seam weld, conservatively based on the support tube Type XM-19 material properties at an upper bound temperature of 700oF and including a 35% weld efficiency factor for a single fillet weld with surface visual inspection in accordance with Table NG-3352-1 of the ASME Code, is 12.1 ksi (= 34.6 x 0.35). Therefore, the minimum design margin in the support tube longitudinal seam weld for the bounding 60*g* side drop loading is +8.03.

3.7.5.2.4 Support Sleeve

In the horizontal orientation, the support sleeve supports only its own weight. As such, the stresses in the support sleeves due to postulated transfer cask side drop are very small and do not control the design. The governing stress in the support sleeve is the shear stress in the 2-inch long by 1/8-inch single fillet weld between the sleeve retainer (i.e., small inner angle) and sleeve wall (i.e., large outer angle). The evaluation of the shear stress in this weld is performed using hand calculations. Since all the sleeves carry the same load per unit area for NCT vibration, the sleeve retainer weld shear stress is calculated on a per unit length basis. It is conservatively assumed that the 1/8-inch fillet weld on one leg of the retainer angle carries all the weight of the retainer and sleeve in shear as follows:

$$\tau = \frac{V}{A} = 2.36 \text{ ksi}$$

where:

A = 0.353 in^2, shear stress area of the weld

$$= \frac{2(0.125)(2.0)}{\sqrt{2}}$$

V = WG, weld shear force

= 0.833 kips

W = 13.9 lb., weight of heaviest support sleeve

= (7.51)(6.375)(0.29)

G = 60*g*, equivalent static side drop acceleration load.

The Service Level D allowable weld shear stress, calculated based on SA-240, Type 304 stainless steel properties at 700°F with a 35% weld efficiency factor for a single fillet weld with surface visual examination, is 6.7 ksi (=19.2 ksi x 0.35). Therefore, the minimum design margin in the W74 support sleeve longitudinal seam weld for the bounding 60*g* side drop load is +1.85.

3.7.5.2.5 Guide Tube

For the postulated transfer cask side drop condition, the W74 guide tube assemblies are loaded by the inertial load due to their own weight plus the weight of the fuel assembly within each guide tube. The stress evaluation of the W74 guide tube is performed for a bounding 60*g* side drop load using an elastic system analysis. Since the stresses in the guide tube resulting from the 60*g* side drop load are higher than the yield strength of the guide tube SA-240, Type 316 stainless steel material, some permanent deformation of the guide tube is expected to occur. In order to quantify the amount of permanent deformation experienced by the guide tube, plastic analyses of the guide tube are performed for the side drop condition. The side drop plastic analysis of the W74 guide tube considers two bounding conditions for the fuel loading on the guide tube: 1) uniform fuel loads along the entire length of the fuel assembly, and 2) concentrated loading at SNF assembly grid spacers. The maximum permanent deformations resulting from both of these side drop loading conditions are considered in the accident condition criticality evaluation in Chapter 6 of this FSAR. In addition, buckling of the W74 guide tubes due to the side drop is evaluated in accordance with NUREG/CR-6322. Stress evaluations are also performed for the W74 guide tube neutron absorber panels and the retainers which secure them to the guide tubes. The W74 guide tube side drop evaluations are described as follows:

Stress Evaluation

The stresses in the largest span of the W74 guide tube due to the 60*g* transfer cask side drop load are evaluated using the half-symmetry periodic finite element model described in Section 3.9.2.6. The model represents a segment of the W74 guide tube spanning from the centerline of a spacer plate to the mid-span between the adjacent spacer plate support, taking advantage of longitudinal symmetry. The guide tube is modeled using shell elements. The material density used for the guide tube elements is adjusted to account for the mass of the neutron absorber panels, conservatively taking no credit for structural support of the guide tube provided by the neutron absorber panels. As shown in Section 2.10.4.3, the adjusted density of the guide tube is 0.51 lb/in^3. An equivalent static side drop load of 66*g* is applied to the model. The load from the

fuel assembly is applied as a uniform pressure load on the supporting guide tube panel. The fuel assembly pressure load due to the 60*g* side drop load is 49.1 psi.

The guide tube stresses are determined using a linear-elastic static analysis. The maximum primary membrane and primary membrane plus bending stress intensities in the guide tube due to the bounding 60*g* side drop load are 15.4 ksi and 54.6 ksi, respectively. The Service Level D allowable primary membrane and primary membrane plus bending stress intensities for SA-240, Type 316 stainless steel at the guide tube design temperature of 715°F are 38.8 ksi and 58.3 ksi, respectively. Therefore, the minimum design margins in the W74 guide tube for the bounding 60*g* side drop load are +1.52 for primary membrane stress intensity and +0.07 for primary membrane plus bending stress intensity.

The stresses in the guide tube longitudinal seam welds are also evaluated using the maximum nodal forces and moment from the finite element solution. The guide tube longitudinal seam welds subjected to both RT and PT examinations can be placed at any location on the width of the panel that will allow an RT examination. For full penetration welds subjected to both RT and PT examinations, a weld efficiency factor of 100% is applicable in accordance with Table 3352-1 of the ASME Code; therefore, these welds are evaluated (modeled) as guide tube base metal.

The guide tube longitudinal seam welds subjected to surface PT examination only are located at the ¼ span of the panel width. In these welds, the maximum primary membrane and primary membrane plus bending stress intensities due to the 60*g* side drop load are 5.5 ksi and 28.6 ksi, respectively.

In accordance with Table NG-3352-1 of the ASME Code, a 65% weld efficiency factor is applied to the allowable stresses for a full penetration weld with surface PT examination. Therefore, the W74 guide tube seam weld Service Level D allowable primary membrane and primary membrane plus bending stress intensities, based on SA-240, Type 316 stainless steel properties at a design temperature of 715°F, are 25.2 ksi (=38.8 x 0.65) and 37.9 ksi (=58.3 x 0.65), respectively. Therefore, the minimum design margins for primary membrane and primary membrane plus bending stress intensities in the W74 guide tube seam weld are +3.56 and +0.33, respectively.

Permanent Deformation - Uniform Fuel Loading

In addition to the linear-elastic stress analysis performed above, the W74 guide tubes are evaluated for the bounding 60*g* side drop load on a plastic basis to determine the maximum guide tube permanent deformation. The finite element model used for the guide tube plastic analysis has the same geometry, loading, and boundary conditions as that used for the linear-elastic stress analysis. The plastic material properties of SA-240, Type 316 stainless steel at a bounding temperature of 715°F, as described in Section 2.3 of this FSAR, are conservatively used for the guide tube plastic analysis. The guide tube permanent deformation is determined by applying the loads corresponding to the 60*g* transverse load and subsequently removing the loads.

The maximum permanent deformation at the center of the guide tube panel that supports the load from the fuel assembly is 0.066 inch. The maximum permanent strain in the guide tube is 0.44%, which is less than the 40% minimum elongation of SA-240, Type 316 stainless steel per the ASME Code. Therefore, the guide tube meets the plastic acceptance criteria for a bounding 60*g* side drop load.

Permanent Deformation - Concentrated Loading at Fuel Grid Spacers

The W74 guide tubes are evaluated for the 60*g* side drop load assuming the fuel assembly loads are applied to the guide tube as concentrated loads at the fuel grid spacer locations. The purpose of this evaluation is to determine the maximum guide tube permanent displacements which could result from the postulated side drop condition.

The 60*g* side drop evaluation of the W74 guide tube with a concentrated load at the fuel grid spacer is performed using the half-symmetry multi-span finite element model described in Section 3.9.2.6.2. As discussed in Section 3.9.1, the maximum in-core grid spacer tributary weight for Big Rock Point fuel is 108.1 pounds. The maximum center-to-center spacer plate spacing for the W74 spacer plates is 7.125 inches. The W74 guide tube permanent deformation analysis for concentrated fuel grid spacer loading is performed using a bounding fuel grid spacer tributary weight of 123.6 pounds and the maximum span between spacer plates.

The fuel load is applied to the model at the mid-span of the largest guide tube span (i.e., midway between spacer plate supports) since this will result in the largest guide tube deformations for a given load. The applied loads are shown in Figure 3.7-9 and include: 1) a 60*g* side drop acceleration applied to account for the guide tube self-weight, 2) a grid spacer protrusion displacement imposed on the guide tube bottom panel nodes in the region of the grid spacer, and 3) a uniform pressure load applied to those spans which do not have the imposed displacement loading to account for the balance of the fuel weight not accounted for by the imposed displacement.

The magnitude of the imposed displacement is based upon the maximum protrusion of the Big Rock Point fuel grid spacer beyond the fuel rod envelope (i.e., distance from edge of grid spacer to outermost fuel rod), recognizing that the displacement of the guide tube is limited by this fuel parameter. The maximum grid spacer protrusion is 0.148 inches. A bounding 0.15-inch displacement is imposed onto the guide tube bottom panel in the area of the grid spacer support. In addition, a uniform pressure load of 50 psig is applied to the guide tube span without the imposed displacement load.

The plastic material properties of SA-240, Type 316 stainless steel at a bounding temperature of 715°F, as described in Section 2.3 of this FSAR, are conservatively used for the guide tube plastic analysis. The guide tube permanent deformation is determined by applying the loads corresponding to the 60*g* transverse load and subsequently removing the loads. The total reaction load from the finite element solution is slightly larger than the calculated load.

The analysis results show that the maximum stress intensity and maximum equivalent plastic strain at the middle fiber of the guide tube shell elements are 17.7 ksi and 1.7%, respectively. The maximum stress intensity and equivalent plastic strain at the extreme fibers (i.e., top and bottom) of the guide tube shell elements are 24.2 ksi and 6.6%, respectively. As shown in Figure 3.7-10, the plastic strain in the guide tube only exceeds 1% in a very small region near the edge of the grid spacer support area. The minimum elongation of SA-240, Type 316 stainless steel is 40%. The maximum permanent deformation of the guide tube, occurring at the location of the concentrated grid spacer loading, is 0.128 inches. Figure 3.7-11 shows the deformed shape of the W74 guide tube assembly due to the bounding 60*g* side drop load.

Guide Tube Buckling Evaluation

Buckling of the W74 guide tube is evaluated for the 60*g* side drop load using the criteria of NUREG/CR-6322 for linear-type members subjected to combined axial compressive an bending loads. The axial compressive stress and bending stress in the side panels of the W74 guide tube are determined using classical solutions. The side panel is evaluated as a fixed-fixed span, assuming half of the panel weight is applied at the end (top panel contribution) and the self-weight of the side panel is distributed along its length. As a result, the axial compression is not constant but varies along the side panel length. Since the theoretical buckling stress for linearly varying axial compressive stress in a column is higher than that of a column subjected to a uniform axial compressive stress on which the NUREG/CR-6322 acceptance criteria are based, an equivalent value of axial stress is calculated for use in the interaction equations. The equivalent axial load corresponding to the theoretical buckling stress of the guide tube side panel is determined using Roark, Table 34, Case 3a, assuming *a/l* = 1 and *P/pl* = 0.5. The critical load *pa* is calculated to be $3.94(\pi^2 EI/L^2)$ for the total of $5.94(\pi^2 EI/L^2)$ at the base of the panel (i.e., 1.5 *pa*). This compares to a critical axial compressive load $4\pi^2 EI/L^2$ for a linear member with a uniform axial compressive stress distribution. Therefore, the equivalent axial stress in the side panel is calculated as follows:

$$f_a = \frac{4}{5.9}\left(L + \frac{L}{2}\right)\rho G = 176\,\text{psi}$$

where:

G = 60*g*, bounding equivalent static side drop load

L = 6.99 in., width of the guide tube panel

ρ = 0.51 lb/in^3, effective guide tube density accounting for the weight of neutron absorber panel, as calculated above.

The maximum bending stress in the guide tube side panel due to moment reactions from the top and bottom panels is calculated based on the maximum bending stress at the ends of the guide tube side panels due to the side drop loading. Since buckling is a global effect, the bending stress is averaged over the span between the spacer plates. The average stress intensity along the bottom edge of the side panel due to a 60*g* side drop load is 15.7 ksi based on the results of the side drop linear elastic stress analysis discussed above.

The allowable axial and bending stresses for the guide tube are calculated in accordance with NUREG/CR-6322 for linear members subjected to combined axial compressive and bending loads. The allowable axial compressive stress for the guide tube, calculated in accordance with Equation 40 of NUREG/CR-6322 for a bounding guide tube design temperature of 715°F, is 4.32 ksi. The allowable bending stress per NUREG/CR-6322 is Fb = fSy or 27.2 ksi for Type 316 stainless steel at 715°F, where f =1.5 is the plastic shape factor for rectangular cross-section. Therefore, the interaction ratio for equation (28) of NUREG/CR-6322 is calculated as follows:

$$\frac{f_a}{F_a} + \frac{f_b}{F_b} = \frac{0.175}{4.09} + \frac{15.7}{27.2} = 0.62 < 1.0$$

No thermal stresses exist in the guide tube because sufficient clearances are provided. Therefore, the guide tube is adequate to withstand the 60*g* side drop load without buckling.

Neutron Absorber Panel Stress Evaluation

The maximum bending stress and average bearing stress in the neutron absorber panel resulting from the 60*g* side drop load are evaluated using hand calculations. The W74 guide tube neutron absorber panels are designed to support their own weight over the span between each spacer plate in the event of a side drop. The maximum bending stress in the largest unsupported span of the neutron absorber panel due to the 60*g* side drop load is calculated for a fixed-fixed beam to be 4.42 ksi. The Service Level D allowable primary membrane plus bending stress intensity for the neutron absorber sheet, based on SA-240, Type 304 stainless steel properties at 715°F is 57.4 ksi. Therefore, the maximum bending stress in the neutron absorber panel is less than the corresponding Service Level D allowable stress intensity.

Neutron Absorber Panel Retainer Weld Stress Evaluation

The neutron absorber panels are attached to the guide tubes using stainless steel retainers. A minimum of seven retainers are used per neutron absorber panel with a maximum center-to-center spacing of 15 inches. Each retainer is welded to the guide tube with a 3/16-inch plug weld. Shear plug welds are relied upon to support the maximum neutron absorber sheet retainer shear load due to the tributary weight of the neutron absorber sheet on the vertical side of the guide tube. The maximum weld shear stress resulting from a 60*g* side drop load is 4.5 ksi. This stress is lower than the allowable weld shear stress of 5.7 ksi, based on SA-240, Type 316 stainless steel at 715°F and including a 30% weld efficiency factor for a plug weld in accordance with Table NG-3352-1 of the ASME Code. Therefore, the plug weld between the neutron absorber panel retainers and the guide tubes are sufficient to withstand the bounding 60*g* side drop load.

3.7.6 Fire

The FuelSolutions™ W74 canister in the storage cask is evaluated for a postulated accidental fire event. The storage cask evaluation for this postulated fire accident is discussed in Section 11.2.5 of the FuelSolutions™ Storage System FSAR.

The postulated fire accident is defined in Section 2.3.3.4 of the FuelSolutions™ Storage System FSAR.

As documented in Section 4.6.1.4, the maximum canister pressure as a result of the postulated fire accident is less than 38.6 psig. The fire condition pressure is much less than the design basis accident pressure of 69 psig. Further, the external heating acts to reduce the thermal gradients on the canister, resulting in lower thermal gradients and therefore lower stresses than for the normal ambient conditions. Therefore the structural effects of this postulated accident on the canister are bounded by the accident pressure condition evaluated in Section 3.7.9 and the bounding thermal gradients evaluated in Section 3.5.1.3.

3.7.7 Flood

The FuelSolutions™ W74 canister is evaluated for the effects of an enveloping design basis flood, postulated to result from natural phenomena such as a tsunami and seiches, as specified by 10 CFR 72.122(b). For the purpose of this evaluation, a 50 foot flood height is used as defined in

Section 2.3.4.1. The W74 canister is protected from the lateral forces due to the flood current by the storage cask. The only flood load affecting the canister is the 21.7 psi hydrostatic pressure due to the 50 foot flood head.

The effects of the flood hydrostatic pressure on the W74 canister are much less severe than those of the design basis 69 psig accident internal pressure load evaluated in Section 3.7.9. This is due to the relative magnitude of the flood pressure load compared that of the design basis accident internal pressure and the nature of the pressure loads. Internal pressure loading produces higher stresses in the end regions of the shell assembly than does external pressure loading since the canister closure plates are supported by the shield plugs under external pressure loading only. Therefore, the canister shell stresses due to flood loading are bounded by those due to accident internal pressure.

Shell buckling due to an external pressure of 21.7 psi is governed by hoop compression. The hoop stress due to an external pressure of 21.7 psi is 1.14 ksi. Using Paragraph -1712 of ASME Code Case N-284, the theoretical hoop buckling stress is 10.64 ksi, based on nominal shell dimensions and material properties at a bounding temperature of 600°F. Applying a factor of safety of 2.0 and a capacity reduction factor of 0.8 in accordance with Paragraphs -1400 and -1511 of ASME Code Case N-284, respectively, the allowable hoop buckling stress is 4.26 ksi. Using the interaction equations of Paragraph -1713.1.1 of ASME Code Case N-284, the maximum interaction equation due to an external pressure of 21.7 psi is:

$$1.14/4.26 = 0.27 < 1.0$$

Therefore, the canister shell does not buckle due to the 50-foot head external flood pressure.

The design basis flood loads are not affected by any amount of intact BRP MOX fuel and partial fuel assemblies, and up to eight damaged fuel assemblies stored within the FuelSolutions™ W74 canister.

3.7.8 Earthquake

As discussed in the FuelSolutions™ Storage System FSAR, the design basis seismic accelerations for the FuelSolutions™ storage system are 0.25*g* horizontally (in each of two orthogonal directions, or a 0.35*g* resultant horizontal acceleration) and 0.25*g* vertically. Since the lowest fundamental frequency of the W74 canister is much greater than 33 Hz, no amplification of the seismic loading occurs within the W74 canister assembly. Bounding seismic accelerations of 1.1*g* along the canister longitudinal axis and 1.3*g* transverse to the canister longitudinal axis are conservatively used for the structural evaluation of the W74 canister basket assembly.

The structural evaluation of the FuelSolutions™ W74 canister for earthquake loads is performed using a bounding BRP intact fuel assembly weight of 485 pounds per assembly plus a bounding damaged fuel can weight of 200 pounds in each of the support tube openings. As discussed in Section 2.2 of this FSAR, the weights of all BRP MOX, partial, and damaged fuel assemblies are bounded by the weight of the BRP intact fuel assemblies. Therefore, the earthquake loads and calculated stresses in the FuelSolutions™ W74 canister shell assembly and basket assemblies bound those for a FuelSolutions™ W74 canister containing any amount of intact BRP MOX fuel and partial fuel assemblies, and up to eight damaged fuel assemblies.

3.7.8.1 Canister Shell Assembly

The canister shell assembly stresses due to the design basis seismic loads are considered to be bounded by those due to the postulated cask drop conditions. This is due to the relative magnitudes of the seismic and drop loads (i.e., 0.25*g* versus a *50g* end drop, and 0.35*g* versus a 60*g* side drop). Therefore, the canister shell stresses are not calculated for the seismic load condition.

3.7.8.2 Canister Basket Assembly

The W74 basket assembly components are evaluated for bounding seismic loads of 1.1*g* in the longitudinal direction and 1.3*g* normal to the canister longitudinal axis. These seismic loads envelope the maximum seismic canister acceleration for both the vertical storage orientation and the horizontal transfer orientation. The structural evaluation of the W74 basket assembly components for the bounding seismic loads is described in the following sections.

3.7.8.2.1 General and LTP Spacer Plates

The stresses in the most heavily loaded W74 general spacer plate and LTP spacer plate due to the bounding basket assembly seismic loads are determined by scaling the maximum stresses due to other load conditions. The stresses due to the 1.1*g* longitudinal seismic acceleration are scaled from the vertical dead weight stress results from Section 3.5.3.2.1. The spacer plate stresses due to the 1.3*g* transverse seismic acceleration are scaled from the horizontal dead weight stress results from Section 3.5.3.2.2. The maximum stresses due to the longitudinal and transverse seismic loads are conservatively combined irrespective of sign and location. The resulting seismic stresses in the most heavily loaded general spacer plate and LTP spacer plate are reported in Table 3.7-2. The results show that the maximum stresses in the W74 general and LTP spacer plates due to the bounding seismic loads are less than corresponding Service Level D allowable stresses.

3.7.8.2.2 Engagement Spacer Plate

The engagement spacer plate stresses due to the bounding basket assembly seismic loads are determined by scaling the maximum stresses due to other load conditions. The stresses due to the 1.1*g* longitudinal seismic acceleration are scaled from the 50*g* storage cask end drop stress results from Section 3.7.3.2.2. The spacer plate stresses due to the 1.3*g* transverse seismic acceleration are scaled from the 2*g* in-plane on-site transport handling stress results from Section 3.5.4.3.3. The maximum stresses due to the longitudinal and transverse seismic loads are conservatively combined irrespective of sign and location. The resulting W74 engagement spacer plate stresses due to seismic loading are reported in Table 3.7-2. The results show that the maximum stresses are less than corresponding Service Level D allowable stresses for SA-240, Type XM-19 stainless steel at a bounding design temperature of 600°F.

3.7.8.2.3 Support Tubes

The support tube stresses due to the bounding basket assembly seismic loads are determined by scaling the maximum stresses calculated for other loading conditions. The stresses due to the 1.1*g* longitudinal seismic load are determined by scaling the maximum stresses calculated for the 50*g* end drop load (Section 3.7.3.2.3) by the ratio 1.1*g*/50*g*. The stresses due to the 1.3*g* lateral

load are determined by scaling the maximum stresses calculated for the 60g transfer cask side drop load (Section 3.7.5.2.3) by the ratio 1.3*g*/60*g*. The stresses due to the 1.1*g* longitudinal and 1.3*g* lateral seismic loads are conservatively added irrespective of sign and location. The resulting W74 support tube seismic stresses are reported in Table 3.7-2. The results show that the maximum support tube seismic stresses are less than corresponding Service Level D allowable stresses for XM-19 stainless steel at 700°F.

3.7.8.2.4 Support Sleeves

As discussed in Section 3.5.3.5.2, the support sleeve stresses due to lateral loading are insignificant. Therefore, only the longitudinal seismic loads produce any significant stresses in the support sleeves. Since the longitudinal seismic load is much lower than the storage cask end drop load, the support sleeve stresses due to seismic loading are bounded by those due to the storage cask end drop. Therefore, no further evaluation of the support sleeve seismic stresses is required.

3.7.8.2.5 Guide Tubes

The guide tube stresses due to the bounding basket assembly seismic loads are determined by scaling the maximum stresses calculated for other loading conditions. The stresses due to the 1.1*g* longitudinal seismic load are determined by scaling the maximum stresses calculated for the vertical dead weight load (Section 3.5.3.6.1) by the ratio 1.1*g*/1*g*. The stresses due to the 1.3*g* lateral load are determined by scaling the maximum stresses calculated for the horizontal dead weight load (Section 3.5.3.6.2) by the ratio 1.3*g*/1*g*. The stresses due to the 1.1*g* longitudinal and 1.3*g* lateral seismic loads are conservatively added irrespective of sign and location. The resulting W74 guide tube seismic stresses are reported in Table 3.7-2. The results show that the maximum guide tube seismic stresses are less than corresponding Service Level D allowable stresses for SA-240, Type 316 stainless steel at 715°F.

3.7.9 Accident Internal Pressure

As discussed in Section 4.6.1.4 and summarized in Table 4.6-2, the maximum postulated accident condition internal pressure for the FuelSolutions™ W74 canister is 30.0 psig, based upon the required backfill of helium and a concurrent non-mechanistic failure of 100% of the fuel rods with complete release of their fill gas and 30% of their fission gasses into the canister cavity. All gas is assumed to be at the extreme off-normal condition canister cavity gas temperature. The W74 canister is conservatively designed for a bounding accident internal pressure of 69 psig.

The structural evaluation of the W74 canister for the accident internal pressure condition is performed using the axisymmetric finite element model described in Section 3.9.2.1 and shown in Figure 3.9-1 of this FSAR. The analysis methodology, including the methodology for application of the pressure loads and calculation of stresses, is described in Section 3.5.2 of this FSAR. The resulting canister shell stresses due to a 69 psig accident internal pressure applied to either the canister inner or outer pressure boundary are provided in Table 3.7-1. All canister shell stresses due to accident internal pressure are within the corresponding Service Level D allowable stresses.

As discussed in Chapter 4 of this FSAR, the FuelSolutions™ W74 canister internal pressure design loads for accident conditions bound those for a FuelSolutions™ W74 canister containing any amount of intact BRP MOX fuel and partial fuel assemblies, and up to eight damaged fuel assemblies. Therefore, the FuelSolutions™ W74 canister shell assembly and basket assembly stresses calculated for the design basis accident internal pressure loads are bounded for a FuelSolutions™ W74 canister containing any amount of intact BRP MOX fuel and partial fuel assemblies, and up to eight damaged fuel assemblies.

3.7.10 Accident Condition Load Combinations

Load combinations are performed for the FuelSolutions™ W74 canister in accordance with Section 2.3.5 for accident conditions. The load combinations include normal loads evaluated in Section 3.5, off-normal loads evaluated in Section 3.6, and accident loads evaluated in this FSAR section. Load combinations are summarized in Table 2.3-1. The structural evaluation of the W74 canister shell assembly and basket assembly for accident load combinations are presented in the following sections.

3.7.10.1 Canister Shell Assembly

The W74 canister accident load combinations defined in Table 2.3-1 are simplified by identifying the bounding load combinations. For service level D conditions, general thermal stresses are classified as secondary and consequently need not be considered. Therefore, load combination D7 reduces to vertical dead weight plus off-normal internal pressure, which is identical to load combination C1 evaluated in Section 3.6.5.1. Since the allowable stresses for Service Level D conditions are greater than those for Service Level C conditions, load combination D7 need not be evaluated. In addition, load combination D6 includes seismic loads, which are insignificant when compared to the postulated cask drop and tip-over loads. Therefore, load combination D6 is also insignificant in comparison to those load combinations which include the postulated cask drop and tip-over loads. Consequently load combination D6 is not evaluated for the canister shell assembly. The canister shell load combination evaluations for the remaining accident load combinations (i.e., D1 through D5) are performed as described below.

The canister shell assembly stresses due to load combinations D1 through D5 are evaluated using the axisymmetric and three-dimensional finite element models described in Sections 3.5.2.1 and 3.5.2.2, respectively. Load combination evaluations are performed for both the “bounding” canister shell model, which bounds all W74 canister shell assemblies. Separate evaluations are performed for internal pressure acting on both the top inner and outer closures. Thermal loads are considered since thermal stresses are classified as secondary, and as such need not be evaluated for Service Level D conditions.

For load combination D1, vertical dead weight, vertical transfer, and accident internal pressure loads are applied simultaneously to the canister shell axisymmetric finite element model. For this condition, the canister shell is supported vertically at the location of the vertical transfer pintle plate bolt circle on top outer closure plate. The evaluation for load combination D3 is performed in a similar manner to load combination D1, but includes the storage cask end drop and off-normal internal pressure loads. For load combination D3, the canister shell is supported at the bottom end. For load combinations D2, both the axisymmetric and three-dimensional finite element models are used. The axisymmetric model is used to determine the canister shell stresses due to normal horizontal canister transfer and accident internal pressure loads. The canister shell

stresses due to horizontal dead weight, which are calculated using the three-dimensional half-symmetry finite element model described in Section 3.9.2.2, are conservatively added absolutely to the maximum stresses calculated with the axisymmetric model. Load combinations D4 and D5 are evaluated using only the three-dimensional finite element model. The load combination D4 (side drop plus off-normal internal pressure) evaluation is performed in the same manner as the side drop stress evaluation described in Section 3.7.5.1, but includes the off-normal internal pressure load on the inside of the canister shell. Similarly, the load combination D5 (tip-over plus off-normal internal pressure) evaluation is performed in the same manner as the tip-over stress evaluation described in Section 3.7.4.1, but includes the off-normal internal pressure load on the inside of the canister shell.

The maximum stresses in the canister shell due to load combinations D1 through D5 are summarized in Table 3.7-11 through Table 3.7-15, respectively. The results show that the maximum stresses in the canister shell for all accident load combinations are less than the corresponding Service Level D allowable stresses.

3.7.10.2 Canister Basket Assembly

The accident load combinations for the W74 canister include dead weight, normal handling, off-normal and accident internal pressure, normal and accident thermal loads, seismic, and postulated cask drop loads. Since the basket assembly is not a pressure retaining component, it is not subjected to internal pressure loading. In addition, stresses due to thermal loading are classified as secondary stresses, which need not be evaluated for Service Level D conditions. However, thermal loads are considered in combination with drop loads for the basket assembly buckling analyses where the combined loads result in lower factors of safety against buckling.

Load combinations D1 and D2 reduce to dead weight plus normal handling, and are bounded by load combinations A4 and A5 evaluated in Section 3.5.5.2. Load combinations D3 through D5 consist of accidental cask drop and tip-over loads only, which are evaluated in Sections 3.3.3 through 3.3.5. Load combination D6 reduces to dead weight plus seismic. Load combination D7 reduces to horizontal dead weight only and is bounded by load combination A3. The W74 canister basket assembly accident load combination results are reported in Table 3.7-16. The results show that all stresses are less than the corresponding Service Level D allowable stresses.

3.7.10.3 Damaged Fuel Can

The structural evaluation of the FuelSolutions™ W74 damaged fuel can for accident conditions is based on the results of the FuelSolutions™ W74 guide tube assembly structural evaluation. As discussed in Section 3.5, the total weight of the damaged fuel can is slightly higher than that of the guide tube (121 pounds versus 84 pounds) due to the inclusion of the top lid assembly, bottom end plate, and four neutron absorber panels (versus two per guide tube). Consequently, the stresses in the damaged fuel can due to longitudinal loads, such as the bottom end drop, will be proportionally higher than those in the guide tube. However, the stresses in the damaged fuel can due to transverse loads, such as those resulting from the postulated storage cask tip-over and transfer cask side drop, are bounded by those in the guide tube. As discussed in Section 3.5, this is true since the guide tube and damaged fuel can loads are equal and the damaged fuel can is continuously supported while the guide tube is intermittently supported.

As shown in Table 3.7-2 and Table 3.7-16, the controlling load condition for the guide tubes is the transfer cask side drop. As discussed above, the stresses in the damaged fuel can due to the transfer cask side drop are bounded by the stresses in the guide tube.

The results of the normal condition evaluation of the damaged fuel can show that the maximum stresses for the controlling accident load conditions are bounded by those calculated for the guide tube. Therefore, since the guide tube satisfies the structural design criteria for accident conditions, the damaged fuel can also satisfies the structural design criteria for accident conditions.

Table 3.7-1 - W74 Canister Shell Assembly Accident Condition Stress Summary

Shell Component	Stress Type	Maximum Stresses (ksi)				Allowable Stress[1] (ksi)
		Accident Internal Pressure	Storage Cask End Drop	Storage Cask Tip-Over	Transfer Cask Side Drop	
Top Outer Closure Plate	P_m	1.1	0.9	5.4	14.7	46.2
	P_m+P_b[2]	22.3	9.4	9.1	24.3	69.3
Top Outer Closure Weld	P_m	7.4	4.4	7.6	11.4	37.0[3]
	Shear[4]	1.8	0.8	[6]	[6]	22.1[3]
Top Inner Closure Plate	P_m	1.3	1.6	12.4	21.4	46.2
	P_m+P_b	9.2	16.5	26.6	42.9	69.3
Top Inner Closure Weld	P_m	8.7	10.0	34.6	32.4	41.6[5]
	Shear[4]	4.3	5.0	17.3	16.2	24.9[5]
Top Shield Plug	P_m	0.0	1.9	[6]	[6]	46.2
	P_m+P_b	0.3	48.4	[6]	[6]	69.3
Cylindrical Shell	P_m	15.8	11.8	12.4	23.3	46.2
	P_m+P_b	35.9	25.7	31.0	31.0	69.3
Bottom Shell Extension	P_m	5.8	8.0	[7]	[7]	46.2
	P_m+P_b	7.4	29.8	[7]	[7]	69.3
Bottom Closure Plate	P_m	1.1	2.0	[7]	[7]	46.2
	P_m+P_b	17.1	8.8	[7]	[7]	69.3
Bottom End Plate	P_m	2.3	3.1	[7]	[7]	46.2
	P_m+P_b	23.1	5.1	[7]	[7]	69.3
Top Shield Plug Supt. Bar Weld	Shear	0.1	5.3	[6]	[6]	16.2
Shell Extension Top Weld	Shear	2.0	12.4	[7]	[7]	16.2
Shell Extension Bottom Weld	Shear	1.1	13.7	[7]	[7]	16.2

Notes:

(1) Allowable stress intensities are based on the weaker of the W74M and W74T canister shell materials (SA-240, Type 304 stainless steel) properties at 300°F.

(2) The maximum bending stress in the top outer closure plate is determined using hand calculations assuming simply support edge conditions to demonstrate that the bending stress in the top outer closure weld may be classified as secondary.

(3) The allowable stresses for the top outer closure weld include a 0.8 weld efficiency factor in accordance with ISG-4.

(4) Shear stress in the welds are determined using hand calculations.

(5) The allowable stresses for the top inner closure weld include a 0.9 weld efficiency factor in accordance with Section 3.1.2.2 of this FSAR.

(6) Bounded by stresses due to storage cask end drop.

(7) Bounded by stresses in canister shell top end region.

Table 3.7-2 - W74 Canister Basket Assembly Accident Condition Stress Summary

Basket Component	Stress Type	Maximum Stresses (ksi)				Allowable Stress[1] (ksi)
		Earth-quake	Storage Cask End Drop	Storage Cask Tip-Over	Transfer Cask Side Drop	
W74M LTP Spacer Plate	P_m	0.6	0.0	9.8	17.4	61.1
	P_m+P_b	1.9	13.8	19.7	51.3	91.5
	Buckling I.R.[3]	N/A	N/A	0.60	0.96	1.0[3]
W74M and W74T General Spacer Plate	P_m	2.4	0.0	26.4	35.3	75.4
	P_m+P_b	5.3	19.5	53.2	78.9	113.1
	Buckling I.R.[3]	N/A	N/A	0.44	0.66	1.0[3]
W74M and W74T Engagement Spacer Plate	P_m	1.3	30.2	[4]	16.4	61.4
	P_m+P_b	1.5	37.0	[4]	16.4	92.2
	Buckling F.S.[7]	N/A	N/A	[4]	6.0	1.5[7]
W74M and W74T Support Tubes	P_m	0.5	18.8	[4]	1.4	60.6
	P_m+P_b	0.7	19.7	[4]	6.4	90.8
	Buckling I.R.[3]	0.02	0.75	[4]	N/A	1.0[3]
Support Tube Longitudinal Seam Weld	Shear	0.0	0.0	[4]	1.3	12.1
W74M Support Tube Attachment Welds	Shear	0.2	3.2	[4]	0.4	13.8
W74T Support Tube Attachment Welds	Shear	0.5	8.6	[4]	0.0	13.8
W74M and W74T Support Sleeve	P_m	0.2	8.1	[4]	[5]	38.4
	P_m+P_b	0.2	8.1	[4]	[5]	57.6
	Buckling	0.2	8.1	[4]	N/A	13.4
Support Sleeve Longitudinal Seam Weld	Shear	0.1	0.0	[4]	2.4	6.7
W74M and W74T Guide Tube	P_m	1.2	2.4	[4]	15.4	38.8
	P_m+P_b	4.9	2.4	[4]	54.6	58.3
	Buckling	[5]	2.4	[4]	$0.62 \leq 1.0$[3]	86.0
Guide Tube Seam Weld	P_m	[4]	[4]	[4]	5.5	25.2[9]
	P_m+P_b	[4]	[4]	[4]	28.6	37.9[9]
Neutron Absorber Panels	P_m+P_b	[4]	[4]	[4]	4.7	57.4
NAP Retainer Welds	Shear	[4]	[4]	[4]	4.5	5.9[10]

Notes:

(1) Allowable stresses are based on design temperatures presented in Table 3.5-1, unless otherwise noted.
(2) Bounded by general spacer plate buckling design margin for side drop.
(3) Buckling interaction ratio in accordance with NUREG/CR-6322.
(4) Bounded by transfer cask side drop.
(5) Bounded by storage cask end drop.
(6) Includes a quality factor of 40% for a single bevel weld with surface PT examination in accordance with Table NG-3352-1 of the ASME Code.
(7) Minimum factor of safety against buckling required per Appendix F of the ASME Code.
(8) Includes a quality factor of 35% for a fillet weld with surface visual examination in accordance with Table NG-3352-1 of the ASME Code.
(9) Includes a quality factor of 65% for a full penetration weld with surface PT examination in accordance with Table NG-3352-1 of the ASME Code. Full penetration longitudinal seam welds examined with both RT and PT have a weld quality faction of 100%, and are evaluated as guide tube base metal.
(10) Includes a quality factor of 30% for a plug weld in accordance with Table NG-3352-1 of the ASME Code.

Table 3.7-3 - W74 General Spacer Plate Allowable Buckling Stresses

Spacer Plate Buckling Characteristics	Ligament Type				
	A (1)	Bx(2)	By(3)	B(4)	C(5)
Width, b (in.)	1.125	1.050	0.975	1.005	0.875
Thickness, t (in.)	0.75	0.75	0.75	0.75	0.75
Height, L (in.)	7.325	7.40	7.25	7.325	7.325
Gross Area, A_g (in^2)	0.84	0.79	0.73	0.75	0.66
Ixx (in^4)	0.089	0.072	0.058	0.063	0.042
r_x (in.)	0.325	0.303	0.281	0.290	0.253
Effective Length Factor, K	0.65	0.65	0.65	0.65	0.65
Kl/r_x	14.66	15.87	16.74	16.41	18.85
S_y @ 700°F (ksi)	83.0	83.0	83.0	83.0	83.0
E @ 700°F (ksi)	$25.5x10^3$	$25.5x10^3$	$25.5x10^3$	$25.5x10^3$	$25.5x10^3$
Lambda	0.266	0.288	0.304	0.298	0.342
P_{33} (kips)	55.0	50.7	46.7	48.3	41.0
P_{43} (kips)	N/A	N/A	N/A	N/A	N/A
P_{45} (kips)	N/A	N/A	N/A	N/A	N/A
P_{40} (kips)	N/A	N/A	N/A	N/A	N/A
F_a (ksi)	65.2	64.4	63.9	64.1	62.5
F_b (ksi)	124.5	124.5	124.5	124.5	124.5
F_e' (ksi)	900.7	768.8	690.6	718.8	544.9

Notes:

(1) Ligament A properties apply to the two centermost rows/columns of ligaments

(2) Ligament B properties apply to the 2nd row/column of ligaments from the center, excluding the ligament adjacent to the support tube holes.

(3) Ligament B_x properties apply to the vertical ligaments adjacent to the support tube holes.

(4) Ligament B_y properties apply to the horizontal ligaments adjacent to the support tube holes.

(5) Ligament C properties apply to the outermost row/column of ligaments.

Table 3.7-4 - W74 LTP Spacer Plate Allowable Buckling Stresses

Spacer Plate Buckling Characteristics	Ligament Type				
	A(1)	Bx(2)	By(3)	B(4)	C(5)
Width, b (in.)	1.125	1.050	0.975	1.005	0.875
Thickness, t (in.)	2.00	2.00	2.00	2.00	2.00
Height, L (in.)	7.325	7.40	7.25	7.325	7.325
Gross Area, A_g (in^2)	2.25	2.10	1.95	2.01	1.75
Ixx (in^4)	0.237	0.193	0.154	0.169	0.112
r_x (in.)	0.325	0.303	0.281	0.290	0.253
Effective Length Factor, K	0.65	0.65	0.65	0.65	0.65
Kl/r_x	14.66	15.87	16.74	16.41	18.85
S_y @ 650°F (ksi)	36.8	36.8	36.8	36.8	36.8
E @ 650°F (ksi)	$25.1x10^3$	$25.1x10^3$	$25.1x10^3$	$25.1x10^3$	$25.1x10^3$
Lambda	0.179	0.194	0.204	0.200	0.230
P_{33} (kips)	68.3	63.2	58.4	60.3	51.6
P_{43} (kips)	47.9	44.6	41.3	42.6	36.8
P_{45} (kips)	36.1	33.5	30.9	31.9	27.4
P_{40} (kips)	51.4	47.5	43.7	45.2	38.5
F_a (ksi)	22.8	22.6	22.4	22.5	22.0
F_b (ksi)	55.2	55.2	55.2	55.2	55.2
F_e' (ksi)	787.8	672.5	604.1	628.7	476.6

Notes:

(1) Ligament A properties apply to the two centermost rows/columns of ligaments

(2) Ligament B properties apply to the 2nd row/column of ligaments from the center, excluding the ligament adjacent to the support tube holes.

(3) Ligament B_x properties apply to the vertical ligaments adjacent to the support tube holes.

(4) Ligament B_y properties apply to the horizontal ligaments adjacent to the support tube holes.

(5) Ligament C properties apply to the outermost row/column of ligaments.

Table 3.7-5 - W74 General Spacer Plate Tip-Over Stresses and Buckling Interaction Ratios

Drop Condition	Stresses and Interaction Ratios	Ligament Type				
		A	B_x	B_y	B	C
General Spacer Plate (30*g* Tip-Over)	Axial Stress (ksi)	6.63	18.27	0.30	14.76	0.30
	Bending Stress (ksi)	16.35	9.24	26.71	7.76	10.70
	Interaction Ratio (Eq. 26)	0.21	0.35	0.19	0.28	0.08
	Axial Stress (ksi)	6.63	18.27	0.30	14.76	0.30
	Bending Stress (ksi)	16.35	9.24	26.71	7.76	10.70
	Interaction Ratio (Eq. 27)	0.20	0.26	0.22	0.21	0.09
General Spacer Plate (30*g* Tip-Over + Thermal)	Axial Stress (ksi)	10.35	25.51	10.05	21.92	7.83
	Bending Stress (ksi)	23.67	6.00	23.92	4.99	23.45
	Interaction Ratio (Eq. 26)	0.32	0.44	0.32	0.38	0.29
	Axial Stress (ksi)	10.35	25.51	7.85	21.92	3.25
	Bending Stress (ksi)	23.67	6.00	27.42	4.99	31.58
	Interaction Ratio (Eq. 27)	0.29	0.30	0.30	0.26	0.29
LTP Spacer Plate (30*g* Tip-Over)	Axial Stress (ksi)	2.55	6.87	0.10	5.61	0.43
	Bending Stress (ksi)	6.26	3.38	9.70	2.74	3.33
	Interaction Ratio (Eq. 26)	0.21	0.36	0.15	0.29	0.07
	Axial Stress (ksi)	2.55	6.87	0.10	5.61	0.11
	Bending Stress (ksi)	6.26	3.38	9.70	2.74	4.05
	Interaction Ratio (Eq. 27)	0.17	0.22	0.18	0.18	0.08
LTP Spacer Plate (30*g* Tip-Over + Thermal)	Axial Stress (ksi)	5.58	12.83	6.81	11.59	7.75
	Bending Stress (ksi)	11.10	2.14	9.71	1.11	14.38
	Interaction Ratio (Eq. 26)	0.42	0.60	0.45	0.53	0.58
	Axial Stress (ksi)	5.58	12.83	6.81	5.45	4.94
	Bending Stress (ksi)	11.10	2.14	9.71	10.46	19.41
	Interaction Ratio (Eq. 27)	0.33	0.33	0.33	0.31	0.46

Table 3.7-6 - W74 Spacer Plate 60*g* Side Drop Elastic Stress Analysis Results

Impact Angle[1]	Maximum Stress Intensities (ksi)			
	General Spacer Plate		LTP Spacer Plate	
	P_m	P_m+P_b	P_m	P_m+P_b
0°	33.3	59.2	17.4	32.3
15°	35.3	74.1	12.7	40.8
30°	31.7	77.0	11.7	51.3
45°	25.5	78.9	10.5	51.2
60°	23.1	78.7	12.3	47.0
75°	26.5	77.6	13.7	42.1
90°	28.0	59.0	14.2	31.7

Note:
(1) Impact orientations are shown in Figure 3.7-4.

Table 3.7-7 - W74 General Spacer Plate 60*g* Side Drop (No Thermal) Stresses and Buckling Interaction Ratios

Impact Angle	Stresses and Interaction Ratios	General Spacer Plate Ligament Type				
		A	B_x	B_y	B	C
0°	Axial Stress (ksi)	23.10	21.49	4.96	17.43	8.65
	Bending Stress (ksi)	6.59	11.63	30.77	23.64	27.44
	Interaction Ratio (Eq. 26)	0.40	0.42	0.29	0.44	0.33
	Axial Stress (ksi)	23.10	21.49	2.15	17.43	8.65
	Bending Stress (ksi)	6.59	11.63	35.97	23.64	27.44
	Interaction Ratio (Eq. 27)	0.28	0.31	0.31	0.36	0.31
15°	Axial Stress (ksi)	16.51	21.38	0.44	14.78	11.05
	Bending Stress (ksi)	49.45	28.96	61.28	56.10	50.24
	Interaction Ratio (Eq. 26)	0.60	0.54	0.43	0.62	0.53
	Axial Stress (ksi)	11.04	21.38	0.44	14.78	11.05
	Bending Stress (ksi)	56.65	28.96	61.28	56.10	50.24
	Interaction Ratio (Eq. 27)	0.57	0.45	0.50	0.60	0.51
30°	Axial Stress (ksi)	10.32	18.32	0.17	12.19	7.53
	Bending Stress (ksi)	64.77	24.32	64.20	56.53	44.13
	Interaction Ratio (Eq. 26)	0.61	0.45	0.44	0.58	0.43
	Axial Stress (ksi)	10.32	18.32	0.17	6.78	0.83
	Bending Stress (ksi)	64.77	24.32	64.20	69.04	59.37
	Interaction Ratio (Eq. 27)	0.62	0.38	0.52	0.62	0.49
45°	Axial Stress (ksi)	8.29	2.29	0.74	4.81	0.76
	Bending Stress (ksi)	69.83	48.21	60.71	69.68	59.71
	Interaction Ratio (Eq. 26)	0.61	0.37	0.43	0.55	0.42
	Axial Stress (ksi)	8.29	2.29	0.74	4.81	0.76
	Bending Stress (ksi)	69.83	48.21	60.71	69.68	59.71
	Interaction Ratio (Eq. 27)	0.64	0.41	0.50	0.61	0.49
60°	Axial Stress (ksi)	10.25	3.34	19.78	8.43	9.00
	Bending Stress (ksi)	66.95	50.56	17.66	69.42	44.36
	Interaction Ratio (Eq. 26)	0.62	0.40	0.43	0.61	0.45
	Axial Stress (ksi)	10.25	3.34	1.18	8.43	1.53
	Bending Stress (ksi)	66.95	50.56	53.48	69.42	56.35
	Interaction Ratio (Eq. 27)	0.64	0.44	0.44	0.64	0.47
75°	Axial Stress (ksi)	15.42	3.81	23.31	10.53	12.60
	Bending Stress (ksi)	52.43	47.58	20.47	66.39	50.96
	Interaction Ratio (Eq. 26)	0.60	0.39	0.51	0.62	0.56
	Axial Stress (ksi)	15.42	3.81	23.31	10.53	12.60
	Bending Stress (ksi)	52.43	47.58	20.47	66.39	50.96
	Interaction Ratio (Eq. 27)	0.58	0.42	0.40	0.64	0.54
90°	Axial Stress (ksi)	22.40	4.68	22.87	17.00	6.90
	Bending Stress (ksi)	4.53	25.77	11.19	23.31	28.05
	Interaction Ratio (Eq. 26)	0.38	0.25	0.44	0.43	0.30
	Axial Stress (ksi)	18.40	0.84	22.87	17.00	6.90
	Bending Stress (ksi)	10.03	32.23	11.19	23.31	28.05
	Interaction Ratio (Eq. 27)	0.27	0.27	0.32	0.36	0.29

Table 3.7-8 - W74 General Spacer Plate 60*g* Side Drop + Thermal Stresses and Buckling Interaction Ratios

Impact Angle	Stresses and Interaction Ratios	General Spacer Plate Ligament Type				
		A	B_x	B_y	B	C
0°	Axial Stress (ksi)	27.96	26.78	11.86	23.19	15.78
	Bending Stress (ksi)	5.04	9.38	33.49	19.68	37.49
	Interaction Ratio (Eq. 26)	0.46	0.48	0.42	0.50	0.52
	Axial Stress (ksi)	27.96	26.78	8.84	23.19	15.78
	Bending Stress (ksi)	5.04	9.38	38.32	19.68	37.49
	Interaction Ratio (Eq. 27)	0.32	0.34	0.40	0.39	0.46
15°	Axial Stress (ksi)	18.57	25.65	7.58	23.00	15.48
	Bending Stress (ksi)	38.97	11.09	59.37	39.78	46.26
	Interaction Ratio (Eq. 26)	0.56	0.48	0.53	0.64	0.57
	Axial Stress (ksi)	18.57	25.65	7.58	15.79	15.48
	Bending Stress (ksi)	38.97	11.09	59.37	52.00	46.26
	Interaction Ratio (Eq. 27)	0.50	0.35	0.55	0.58	0.53
30°	Axial Stress (ksi)	17.68	22.84	8.06	14.82	15.01
	Bending Stress (ksi)	46.77	9.28	62.47	59.01	47.80
	Interaction Ratio (Eq. 26)	0.60	0.42	0.56	0.64	0.58
	Axial Stress (ksi)	13.35	7.13	8.06	14.82	15.01
	Bending Stress (ksi)	53.16	38.53	62.47	59.01	47.80
	Interaction Ratio (Eq. 27)	0.56	0.38	0.58	0.62	0.53
45°	Axial Stress (ksi)	15.81	6.38	8.85	12.90	14.18
	Bending Stress (ksi)	53.77	44.39	59.55	59.61	47.68
	Interaction Ratio (Eq. 26)	0.62	0.40	0.55	0.62	0.56
	Axial Stress (ksi)	15.81	6.38	8.85	12.90	14.18
	Bending Stress (ksi)	53.77	44.39	59.55	59.61	47.68
	Interaction Ratio (Eq. 27)	0.59	0.42	0.57	0.61	0.53
60°	Axial Stress (ksi)	17.51	5.47	9.29	17.27	12.99
	Bending Stress (ksi)	51.67	46.41	51.63	53.57	45.05
	Interaction Ratio (Eq. 26)	0.63	0.40	0.50	0.64	0.52
	Axial Stress (ksi)	17.51	5.47	9.29	17.27	11.62
	Bending Stress (ksi)	51.67	46.41	51.63	53.57	47.81
	Interaction Ratio (Eq. 27)	0.59	0.43	0.51	0.60	0.50
75°	Axial Stress (ksi)	21.69	5.09	26.72	19.01	14.98
	Bending Stress (ksi)	36.33	43.59	13.10	51.15	43.65
	Interaction Ratio (Eq. 26)	0.59	0.38	0.51	0.66	0.55
	Axial Stress (ksi)	18.42	5.09	9.29	19.01	14.98
	Bending Stress (ksi)	43.58	43.59	40.71	51.15	43.65
	Interaction Ratio (Eq. 27)	0.53	0.40	0.42	0.60	0.50
90°	Axial Stress (ksi)	27.98	10.89	28.72	22.71	14.02
	Bending Stress (ksi)	6.08	26.23	5.89	20.13	34.34
	Interaction Ratio (Eq. 26)	0.47	0.35	0.49	0.50	0.47
	Axial Stress (ksi)	27.98	10.89	28.72	22.71	14.02
	Bending Stress (ksi)	6.08	26.23	5.89	20.13	34.34
	Interaction Ratio (Eq. 27)	0.33	0.32	0.34	0.39	0.42

Table 3.7-9 - W74 LTP Spacer Plate 60*g* Side Drop (No Thermal) Stresses and Buckling Interaction Ratios

Impact Angle	Stresses and Interaction Ratios	LTP Spacer Plate Ligament Type				
		A	B_x	B_y	B	C
0°	Axial Stress (ksi)	11.75	6.67	2.05	5.53	4.49
	Bending Stress (ksi)	5.08	6.34	10.97	11.51	13.23
	Interaction Ratio (Eq. 26)	0.59	0.39	0.26	0.42	0.41
	Axial Stress (ksi)	11.75	6.67	1.06	5.53	4.49
	Bending Stress (ksi)	5.08	6.34	12.75	11.51	13.23
	Interaction Ratio (Eq. 27)	0.36	0.27	0.26	0.33	0.34
15°	Axial Stress (ksi)	6.95	10.40	0.37	1.37	6.19
	Bending Stress (ksi)	31.96	19.12	20.57	39.48	23.54
	Interaction Ratio (Eq. 26)	0.80	0.76	0.34	0.67	0.65
	Axial Stress (ksi)	6.95	10.40	0.37	1.37	0.96
	Bending Stress (ksi)	31.96	19.12	20.57	39.48	35.38
	Interaction Ratio (Eq. 27)	0.74	0.58	0.38	0.75	0.66
30°	Axial Stress (ksi)	6.61	9.14	5.49	5.50	4.94
	Bending Stress (ksi)	34.20	17.80	13.19	35.40	32.90
	Interaction Ratio (Eq. 26)	0.82	0.68	0.45	0.79	0.74
	Axial Stress (ksi)	2.31	9.14	0.00	1.50	4.94
	Bending Stress (ksi)	43.53	17.80	25.34	42.22	32.90
	Interaction Ratio (Eq. 27)	0.84	0.53	0.46	0.80	0.71
45°	Axial Stress (ksi)	6.09	7.63	7.48	4.40	4.33
	Bending Stress (ksi)	38.27	15.33	14.78	40.76	30.04
	Interaction Ratio (Eq. 26)	0.86	0.58	0.56	0.83	0.66
	Axial Stress (ksi)	2.15	7.63	0.00	4.40	4.33
	Bending Stress (ksi)	44.35	15.33	26.47	40.76	30.04
	Interaction Ratio (Eq. 27)	0.85	0.45	0.48	0.84	0.64
60°	Axial Stress (ksi)	7.24	5.77	9.12	9.08	6.01
	Bending Stress (ksi)	34.68	12.00	15.76	26.38	33.22
	Interaction Ratio (Eq. 26)	0.86	0.44	0.65	0.82	0.79
	Axial Stress (ksi)	5.41	1.76	9.12	3.08	6.01
	Bending Stress (ksi)	38.87	20.42	15.76	42.04	33.22
	Interaction Ratio (Eq. 27)	0.83	0.41	0.49	0.83	0.74
75°	Axial Stress (ksi)	9.09	1.42	10.56	9.00	6.95
	Bending Stress (ksi)	24.94	16.23	16.19	15.83	24.02
	Interaction Ratio (Eq. 26)	0.79	0.31	0.72	0.65	0.69
	Axial Stress (ksi)	6.30	1.42	10.56	0.78	0.10
	Bending Stress (ksi)	29.28	16.23	16.19	36.24	39.04
	Interaction Ratio (Eq. 27)	0.67	0.33	0.53	0.67	0.71
90°	Axial Stress (ksi)	11.17	1.93	6.99	5.29	4.06
	Bending Stress (ksi)	4.49	9.14	6.61	11.28	12.39
	Interaction Ratio (Eq. 26)	0.56	0.23	0.41	0.41	0.38
	Axial Stress (ksi)	11.17	1.93	6.99	5.29	0.74
	Bending Stress (ksi)	4.49	9.14	6.61	11.28	19.34
	Interaction Ratio (Eq. 27)	0.33	0.21	0.28	0.32	0.37

Table 3.7-10 - W74 LTP Spacer Plate 60*g* Side Drop + Thermal Stresses and Buckling Interaction Ratios

Impact Angle	Stresses and Interaction Ratios	LTP Spacer Plate Ligament Type				
		A	B_x	B_y	B	C
0°	Axial Stress (ksi)	15.13	11.69	7.76	10.83	10.25
	Bending Stress (ksi)	3.19	5.68	13.71	10.38	20.22
	Interaction Ratio (Eq. 26)	0.71	0.61	0.56	0.64	0.78
	Axial Stress (ksi)	13.67	11.69	6.54	10.83	10.25
	Bending Stress (ksi)	5.61	5.68	15.30	10.38	20.22
	Interaction Ratio (Eq. 27)	0.41	0.37	0.43	0.43	0.60
15°	Axial Stress (ksi)	12.29	13.95	5.92	12.33	9.97
	Bending Stress (ksi)	23.88	11.13	23.23	14.74	30.21
	Interaction Ratio (Eq. 26)	0.91	0.79	0.63	0.78	0.93
	Axial Stress (ksi)	9.20	13.95	5.92	5.29	9.97
	Bending Stress (ksi)	28.39	11.13	23.23	32.51	30.21
	Interaction Ratio (Eq. 27)	0.72	0.52	0.56	0.71	0.77
30°	Axial Stress (ksi)	8.09	12.77	5.48	9.93	9.31
	Bending Stress (ksi)	34.87	9.68	26.00	24.66	30.24
	Interaction Ratio (Eq. 26)	0.90	0.72	0.65	0.83	0.90
	Axial Stress (ksi)	6.22	12.77	5.48	6.54	9.31
	Bending Stress (ksi)	37.50	9.68	26.00	33.62	30.24
	Interaction Ratio (Eq. 27)	0.82	0.46	0.60	0.76	0.76
45°	Axial Stress (ksi)	7.82	11.29	11.47	7.93	8.46
	Bending Stress (ksi)	38.18	7.45	9.32	31.69	28.64
	Interaction Ratio (Eq. 26)	0.94	0.62	0.66	0.85	0.83
	Axial Stress (ksi)	7.82	4.03	5.27	6.15	8.46
	Bending Stress (ksi)	38.18	19.56	26.32	36.33	28.64
	Interaction Ratio (Eq. 27)	0.87	0.45	0.60	0.80	0.71
60°	Axial Stress (ksi)	10.63	9.62	13.07	8.19	8.48
	Bending Stress (ksi)	30.52	4.61	10.17	29.30	29.82
	Interaction Ratio (Eq. 26)	0.94	0.50	0.74	0.82	0.85
	Axial Stress (ksi)	8.88	4.24	5.27	5.94	8.48
	Bending Stress (ksi)	34.19	19.11	24.79	34.89	29.82
	Interaction Ratio (Eq. 27)	0.82	0.44	0.57	0.77	0.73
75°	Axial Stress (ksi)	12.79	4.76	14.39	13.15	10.09
	Bending Stress (ksi)	24.45	16.61	10.55	14.41	31.91
	Interaction Ratio (Eq. 26)	0.94	0.47	0.81	0.81	0.96
	Axial Stress (ksi)	12.79	4.76	14.39	7.24	10.09
	Bending Stress (ksi)	24.45	16.61	10.55	29.11	31.91
	Interaction Ratio (Eq. 27)	0.73	0.41	0.52	0.69	0.81
90°	Axial Stress (ksi)	14.95	7.08	12.55	10.57	9.06
	Bending Stress (ksi)	2.35	10.16	3.78	10.53	17.95
	Interaction Ratio (Eq. 26)	0.69	0.47	0.62	0.63	0.69
	Axial Stress (ksi)	13.58	7.08	12.55	10.57	8.35
	Bending Stress (ksi)	5.82	10.16	3.78	10.53	19.51
	Interaction Ratio (Eq. 27)	0.41	0.34	0.35	0.43	0.54

Table 3.7-11 - W74 Canister Shell Assembly Accident Load Combination D1 Results

Shell Component	Stress Type	Allowable Stress[1] (ksi)	Maximum Stress (ksi)	Minimum Design Margin
Top Outer Closure Plate	P_m	46.2	1.2	+36.4
	P_m+P_b[2]	69.3	25.1	+1.76
Top Outer Closure Weld	P_m	37.0[3]	8.9	+3.13
	Shear[4]	22.1[3]	2.5	+7.70
Top Inner Closure Plate	P_m	46.2	1.6	+27.5
	P_m+P_b	69.3	10.4	+5.66
Top Inner Closure Weld	P_m	41.6[5]	10.7	+2.89
	Shear[4]	24.9[5]	5.3	+3.66
Top Shield Plug	P_m	46.2	0.1	+Large
	P_m+P_b	69.3	1.4	+47.3
Cylindrical Shell	P_m	46.2	18.3	+1.52
	P_m+P_b	69.3	42.8	+0.62
Bottom Shell Extension	P_m	46.2	7.9	+4.84
	P_m+P_b	69.3	10.2	+5.79
Bottom Closure Plate	P_m	46.2	1.5	+30.9
	P_m+P_b	69.3	22.6	+2.07
Bottom End Plate	P_m	46.2	0.9	+51.3
	P_m+P_b	69.3	26.2	+1.65
Top Shield Plug Supt. Bar Weld	Shear	16.2	0.2	+79.2
Shell Extension Top Weld	Shear	16.2	2.8	+4.76
Shell Extension Bottom Weld	Shear	16.2	1.5	+10.1

Notes:

(1) Allowable stress intensities are based on the weaker of the W74M and W74T canister shell materials (SA-240, Type 304 stainless steel) properties at 300°F.

(2) The maximum bending stress in the top outer closure plate is determined using hand calculations assuming simply support edge conditions to demonstrate that the bending stress in the top outer closure weld may be classified as secondary.

(3) The allowable stresses for the top outer closure weld include a 0.8 weld efficiency factor in accordance with ISG-4.

(4) Shear stress in the welds are determined using hand calculations.

(5) The allowable stresses for the top inner closure weld include a 0.9 weld efficiency factor in accordance with Section 3.1.2.2 of this FSAR.

Table 3.7-12 - W74 Canister Shell Assembly Accident Load Combination D2 Results

Shell Component	Stress Type	Allowable Stress[1] (ksi)	Maximum Stress (ksi)	Minimum Design Margin
Top Outer Closure Plate	P_m	46.2	1.8	+24.1
	P_m+P_b[2]	69.3	33.4	+1.07
Top Outer Closure Weld	P_m	37.0[3]	10.8	+2.42
	Shear[4]	22.1[3]	2.2	+9.28
Top Inner Closure Plate	P_m	46.2	3.5	+12.3
	P_m+P_b	69.3	17.8	+2.90
Top Inner Closure Weld	P_m	41.6[5]	21.0	+0.98
	Shear[4]	24.9[5]	10.5	+1.37
Top Shield Plug	P_m	46.2	0.9	+48.2
	P_m+P_b	69.3	2.6	+25.9
Cylindrical Shell	P_m	46.2	25.1	+0.84
	P_m+P_b	69.3	55.6	+0.25
Bottom Shell Extension	P_m	46.2	11.6	+2.99
	P_m+P_b	69.3	18.2	+2.82
Bottom Closure Plate	P_m	46.2	2.9	+15.1
	P_m+P_b	69.3	26.2	+1.65
Bottom End Plate	P_m	46.2	2.7	+16.4
	P_m+P_b	69.3	34.0	+1.04
Top Shield Plug Supt. Bar Weld	Shear	16.2	0.1	+Large
Shell Extension Top Weld	Shear	16.2	2.7	+4.97
Shell Extension Bottom Weld	Shear	16.2	1.6	+9.23

Notes:

(1) Allowable stress intensities are based on the weaker of the W74M and W74T canister shell materials (SA-240, Type 304 stainless steel) properties at 300°F.

(2) The maximum bending stress in the top outer closure plate is determined using hand calculations assuming simply support edge conditions to demonstrate that the bending stress in the top outer closure weld may be classified as secondary.

(3) The allowable stresses for the top outer closure weld include a 0.8 weld efficiency factor in accordance with ISG-4.

(4) Shear stress in the welds are determined using hand calculations.

(5) The allowable stresses for the top inner closure weld include a 0.9 weld efficiency factor in accordance with Section 3.1.2.2 of this FSAR.

Table 3.7-13 - W74 Canister Shell Assembly Accident Load Combination D3 Results

Shell Component	Stress Type	Allowable Stress[1] (ksi)	Maximum Stress (ksi)	Minimum Design Margin
Top Outer Closure Plate	P_m	46.2	0.7	+63.4
	P_m+P_b[2]	69.3	6.9	+9.01
Top Outer Closure Weld	P_m	37.0[3]	2.8	+12.3
	Shear[4]	22.1[3]	0.5	+44.1
Top Inner Closure Plate	P_m	46.2	1.5	+30.3
	P_m+P_b	69.3	16.6	+3.18
Top Inner Closure Weld	P_m	41.6[5]	9.4	+3.44
	Shear[4]	24.9[5]	4.7	+4.32
Top Shield Plug	P_m	46.2	1.9	+22.9
	P_m+P_b	69.3	48.4	+0.43
Cylindrical Shell	P_m	46.2	8.6	+4.36
	P_m+P_b	69.3	26.2	+1.64
Bottom Shell Extension	P_m	46.2	7.7	+5.01
	P_m+P_b	69.3	28.8	+1.40
Bottom Closure Plate	P_m	46.2	2.1	+20.7
	P_m+P_b	69.3	9.0	+6.69
Bottom End Plate	P_m	46.2	3.0	+14.7
	P_m+P_b	69.3	5.0	+13.0
Top Shield Plug Supt. Bar Weld	Shear	16.2	5.3	+2.04
Shell Extension Top Weld	Shear	16.2	11.9	+0.36
Shell Extension Bottom Weld	Shear	16.2	13.3	+0.22

Notes:

(1) Allowable stress intensities are based on the weaker of the W74M and W74T canister shell materials (SA-240, Type 304 stainless steel) properties at 300°F.

(2) The maximum bending stress in the top outer closure plate is determined using hand calculations assuming simply support edge conditions to demonstrate that the bending stress in the top outer closure weld may be classified as secondary.

(3) The allowable stresses for the top outer closure weld include a 0.8 weld efficiency factor in accordance with ISG-4.

(4) Shear stress in the welds are determined using hand calculations.

(5) The allowable stresses for the top inner closure weld include a 0.9 weld efficiency factor in accordance with Section 3.1.2.2 of this FSAR.

Table 3.7-14 - W74 Canister Shell Assembly Accident Load Combination D4 Results

Shell Component	Stress Type	Allowable Stress[1] (ksi)	Maximum Stress (ksi)	Minimum Design Margin
Top Outer Closure Plate	P_m	46.2	14.8	+2.12
	P_m+P_b[2]	69.3	25.0	+1.77
Top Outer Closure Weld	P_m	37.0[3]	13.7	+1.70
	Shear[4]	22.1[3]	0.3	+84.0
Top Inner Closure Plate	P_m	46.2	20.6	+1.24
	P_m+P_b	69.3	44.6	+0.55
Top Inner Closure Weld	P_m	41.6[5]	31.8	+0.31
	Shear[4]	24.9[5]	15.9	+0.57
Top Shield Plug	P_m	46.2	[6]	[6]
	P_m+P_b	69.3	[6]	[6]
Cylindrical Shell	P_m	46.2	24.5	+0.89
	P_m+P_b	69.3	36.6	+0.89
Bottom Shell Extension	P_m	46.2	24.5	+0.89
	P_m+P_b	69.3	36.6	+0.89
Bottom Closure Plate	P_m	46.2	20.6	+1.24
	P_m+P_b	69.3	44.6	+0.55
Bottom End Plate	P_m	46.2	20.6	+1.24
	P_m+P_b	69.3	44.6	+0.55
Top Shield Plug Supt. Bar Weld	Shear	16.2	[6]	[6]
Shell Extension Top Weld	Shear	16.2	[6]	[6]
Shell Extension Bottom Weld	Shear	16.2	[6]	[6]

Notes:

(1) Allowable stress intensities are based on the weaker of the W74M and W74T canister shell materials (SA-240, Type 304 stainless steel) properties at 300°F.

(2) The maximum bending stress in the top outer closure plate is determined using hand calculations assuming simply support edge conditions to demonstrate that the bending stress in the top outer closure weld may be classified as secondary.

(3) The allowable stresses for the top outer closure weld include a 0.8 weld efficiency factor in accordance with ISG-4.

(4) Shear stress in the welds are determined using hand calculations.

(5) The allowable stresses for the top inner closure weld include a 0.9 weld efficiency factor in accordance with Section 3.1.2.2 of this FSAR.

(6) Stresses are insignificant.

Table 3.7-15 - W74 Canister Shell Assembly Accident Load Combination D5 Results

Shell Component	Stress Type	Allowable Stress[1] (ksi)	Maximum Stress (ksi)	Minimum Design Margin
Top Outer Closure Plate	P_m	46.2	5.6	+7.25
	P_m+P_b[2]	69.3	10.9	+5.36
Top Outer Closure Weld	P_m	37.0[3]	8.0	+3.62
	Shear[4]	22.1[3]	0.3	+84.0
Top Inner Closure Plate	P_m	46.2	12.1	+2.82
	P_m+P_b	69.3	26.6	+1.61
Top Inner Closure Weld	P_m	41.6[5]	32.8	+0.27
	Shear[4]	24.9[5]	16.4	+0.52
Top Shield Plug	P_m	46.2	[6]	[6]
	P_m+P_b	69.3	[6]	[6]
Cylindrical Shell	P_m	46.2	18.6	+1.48
	P_m+P_b	69.3	32.2	+1.15
Bottom Shell Extension	P_m	46.2	18.6	+1.48
	P_m+P_b	69.3	32.2	+1.15
Bottom Closure Plate	P_m	46.2	12.1	+2.82
	P_m+P_b	69.3	26.6	+1.61
Bottom End Plate	P_m	46.2	12.1	+2.81
	P_m+P_b	69.3	26.6	+1.61
Top Shield Plug Supt. Bar Weld	Shear	16.2	[6]	[6]
Shell Extension Top Weld	Shear	16.2	9.8	+0.65
Shell Extension Bottom Weld	Shear	16.2	9.8	+0.65

Notes:

(1) Allowable stress intensities are based on the weaker of the W74M and W74T canister shell materials (SA-240, Type 304 stainless steel) properties at 300°F.

(2) The maximum bending stress in the top outer closure plate is determined using hand calculations assuming simply support edge conditions to demonstrate that the bending stress in the top outer closure weld may be classified as secondary.

(3) The allowable stresses for the top outer closure weld include a 0.8 weld efficiency factor in accordance with ISG-4.

(4) Shear stress in the welds are determined using hand calculations.

(5) The allowable stresses for the top inner closure weld include a 0.9 weld efficiency factor in accordance with Section 3.1.2.2 of this FSAR.

(6) Stresses are insignificant.

Table 3.7-16 - W74 Canister Basket Assembly Accident Load Combination Results

Basket Component	Stress Type	Allowable Stress (ksi)	L.C. D3 ($T+A_s$)		L.C. D4 ($T+A_t$)		L.C. D5 ($T+A_{s1}$)		L.C. D6 ($D^{(1)}+T+E$)	
			Maximum Stress (ksi)	Minimum Design Margin	Maximum Stress (ksi)	Minimum Design Margin	Maximum Stress (ksi)	Minimum Design Margin	Maximum Stress (ksi)	Minimum Design Margin
LTP Spacer Plate	P_m	61.1	0.0	+Large	17.4	+2.51	9.8	+5.23	1.0	+60.1
	P_m+P_b	91.5	13.8	+5.63	51.3	+0.78	19.7	+3.64	2.8	+31.7
	Buckling I.R.(2)	1.0	(5)	(5)	0.96	+0.04	0.60	+0.67	(5)	(5)
General Spacer Plate	P_m	75.4	0.0	+Large	35.3	+1.14	26.4	+1.86	4.2	+17.0
	P_m+P_b	113.1	19.5	+4.80	78.9	+0.43	53.2	+1.13	9.0	+11.6
	Buckling I.R.(2)	1.0	(5)	(5)	0.66	+0.52	0.44	+1.27	(5)	(5)
Engagement Spacer Plate	P_m	61.4	30.2	+1.03	16.4	+2.74	(5)	(5)	1.9	+31.3
	P_m+P_b	92.2	37.0	+1.49	16.4	+4.62	(5)	(5)	2.2	+40.9
	Buckling F.S.(7)	1.5	(5)	(5)	4.4	+2.93	(5)	(5)	(5)	(5)
W74M and W74T Support Tubes	P_m	60.6	18.8	+2.22	1.4	+41.1	(5)	(5)	0.9	+68.7
	P_m+P_b	90.8	19.7	+3.61	6.4	+13.1	(5)	(5)	1.1	+80.8
	Buckling I.R.(2)	1.0	0.75	+0.33	(3)	(3)	(3)	(3)	0.04	+24.0
Support Tube Longitudinal Seam Weld	Shear	12.1	(5)	(5)	1.3	+8.03	(5)	(5)	0.1	+Large
W74M Support Tube Attachment Welds	Shear	13.8	5.1	+1.71	2.3	+5.00	(5)	(5)	2.2	+5.24
W74T Support Tube Attachment Welds	Shear	13.8	8.7	+0.59	4.5	+2.07	(5)	(5)	5.4	+1.56
W74M and W74T Support Sleeves	P_m	38.4	8.1	+3.74	(3)	(3)	(3)	(3)	0.3	+Large
	P_m+P_b	57.6	11.3	+6.11	(3)	(3)	(3)	(3)	0.3	+Large
	Buckling	13.4(8)	8.1	+0.19	3.2	+3.15	(5)	(5)	3.6	+2.75
Supt. Sleeve Seam Weld	Shear	6.7	(5)	(5)	2.4	+1.85	(5)	(5)	0.1	+73.7
Guide Tube	P_m	38.8	2.4	+15.2	15.4	+1.52	(5)	(5)	1.2	+31.3
	P_m+P_b	58.3	2.4	+23.3	54.6	+0.07	(5)	(5)	4.9	+10.9
	Buckling	1.0(2)/86.0(4)	2.4(4)	+34.8	0.62(2)	+0.61	(5)	(5)	(5)	(5)
Guide Tube Longitudinal Seam Weld	P_m	25.2(6)	(5)	(5)	5.5	+3.56	(5)	(5)	(5)	(5)
	P_m+P_b	37.9(6)	(5)	(5)	28.6	+0.33	(5)	(5)	(5)	(5)

Notes on following page:

Table 3.7-16 Notes:

(1) Either vertical or horizontal dead weight.

(2) Buckling interaction ratio calculated in accordance with NUREG/CR-6322.

(3) Bounded by storage cask end drop condition.

(4) The allowable guide tube axial compressive stress for the storage cask end drop condition is limited to 2/3 of the theoretical buckling stress as discussed in Section 3.7.3.2.5.

(5) Bounded by transfer cask side drop condition.

(6) Allowable stresses include a 65% weld efficiency factor for full penetration weld with surface PT examination. Full penetration longitudinal seam welds examined with both RT and PT have a weld quality factor of 100%, and are evaluated as guide tube base metal.

(7) A minimum factor of safety against buckling of 1.5 is required per Appendix F of the ASME Code.

(8) The allowable buckling stress for the support sleeves is limited to 2/3 of the theoretical buckling stress.

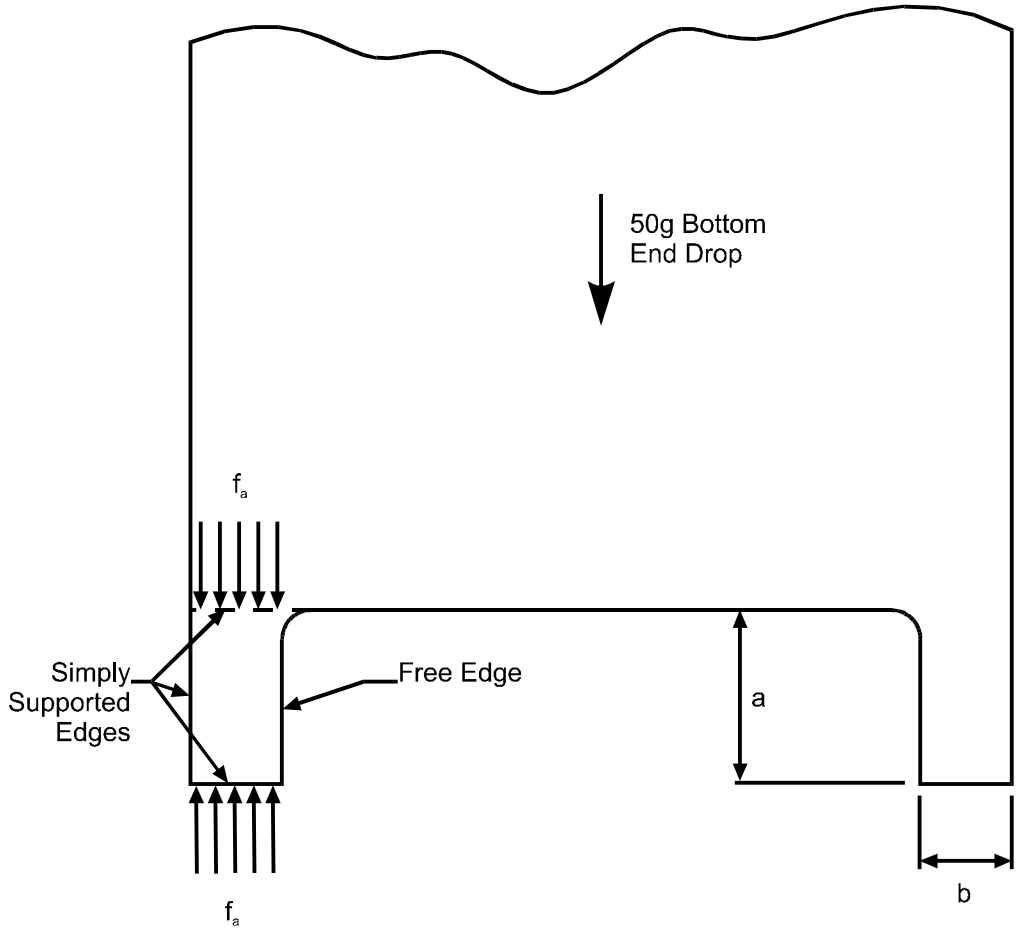

Figure 3.7-1 - Guide Tube End Drop Buckling Boundary Conditions

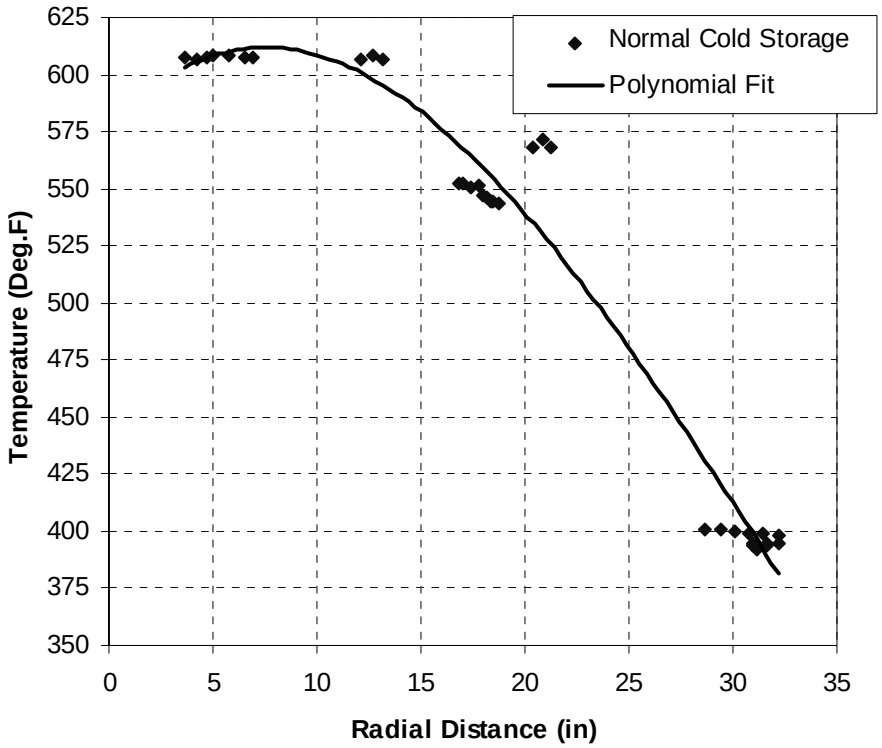

Figure 3.7-2 - W74 Spacer Plate Design Thermal Gradient

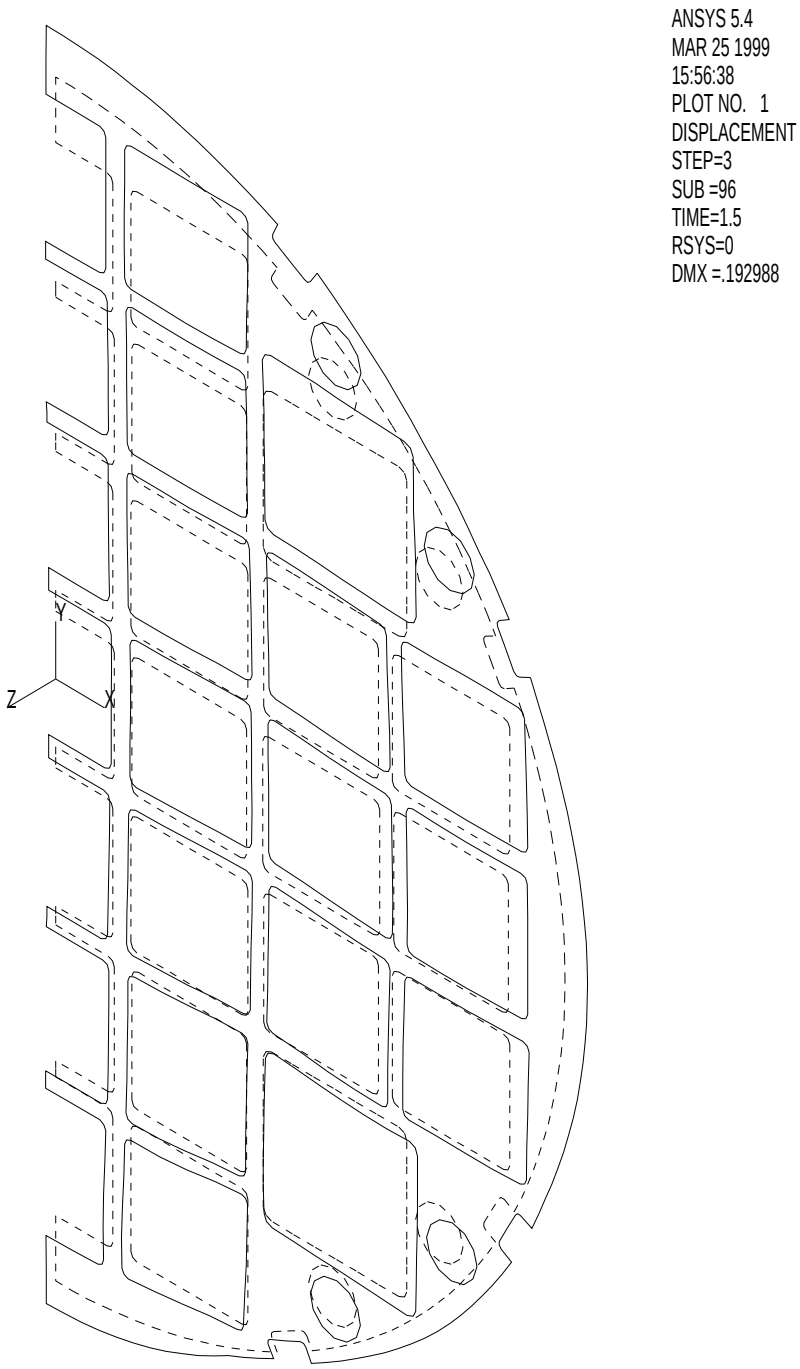

Figure 3.7-3 - W74 General Spacer Plate Longitudinal Displacement For Tip-Over (45*g*) plus Thermal Plastic Instability Analysis

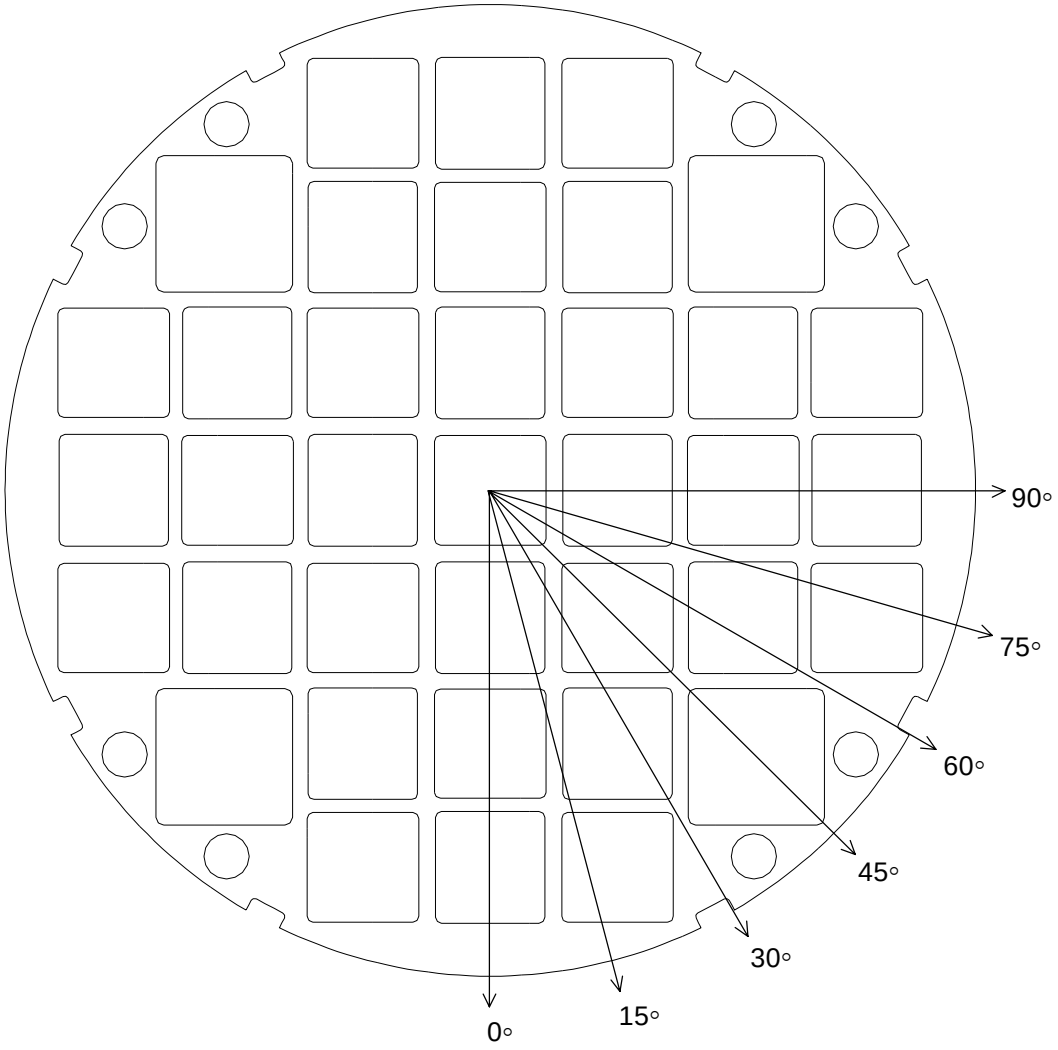

Figure 3.7-4 - W74 General Spacer Plate and LTP Spacer Plate Side Drop Impact Orientations

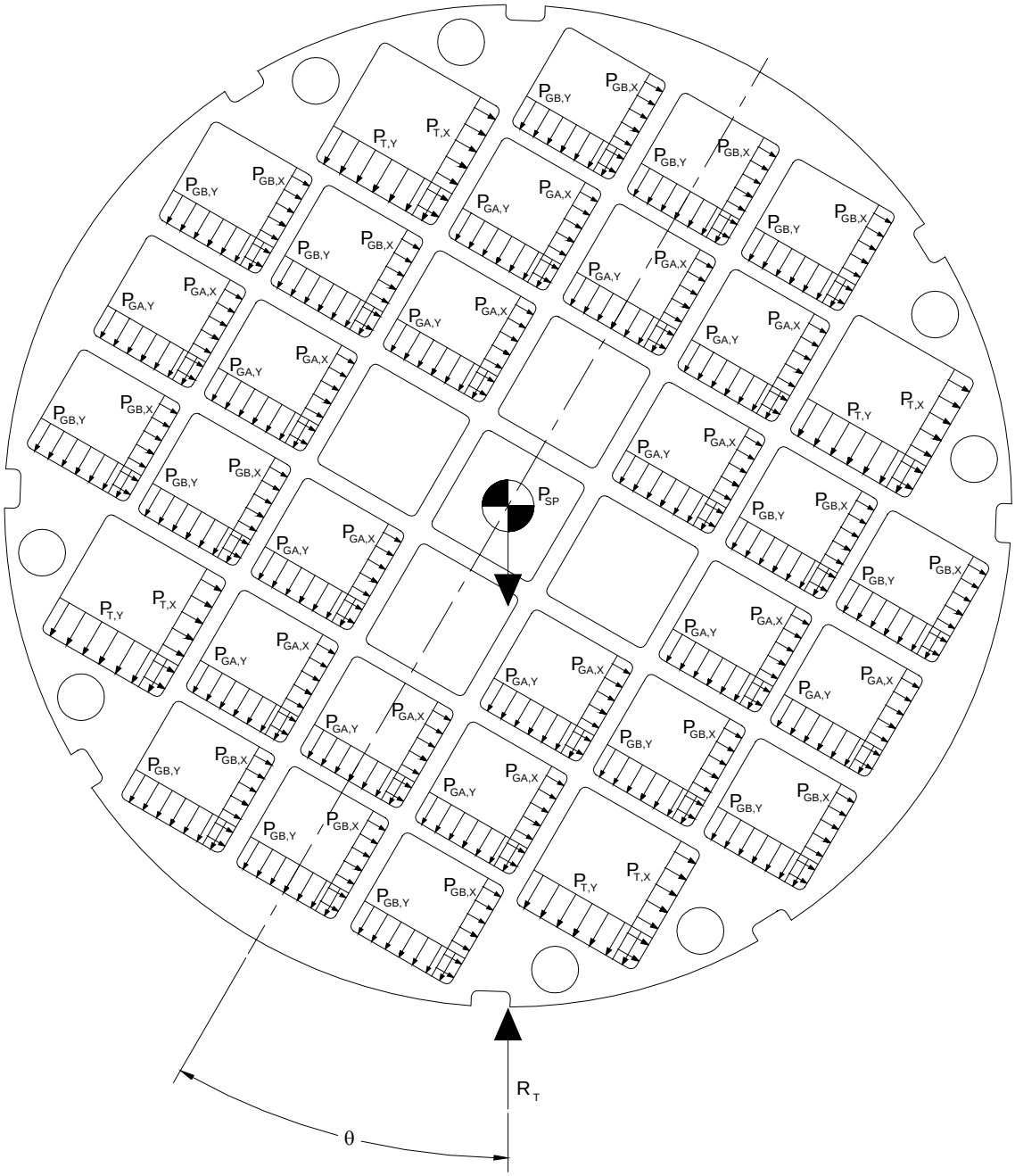

Figure 3.7-5 - W74 General and LTP Spacer Plate Side Drop Loading Diagram

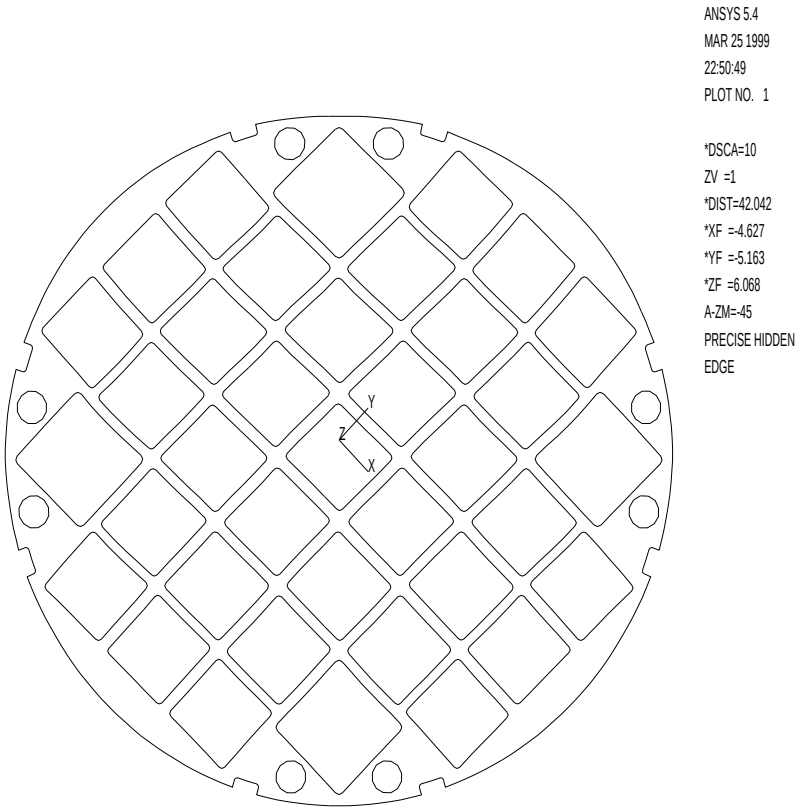

Note: Deformed Plot Scaled by a Factor of 10

Figure 3.7-6 - W74 General Spacer Plate Longitudinal Displacement For 45° Side Drop (90*g*) plus Thermal Plastic Instability Analysis

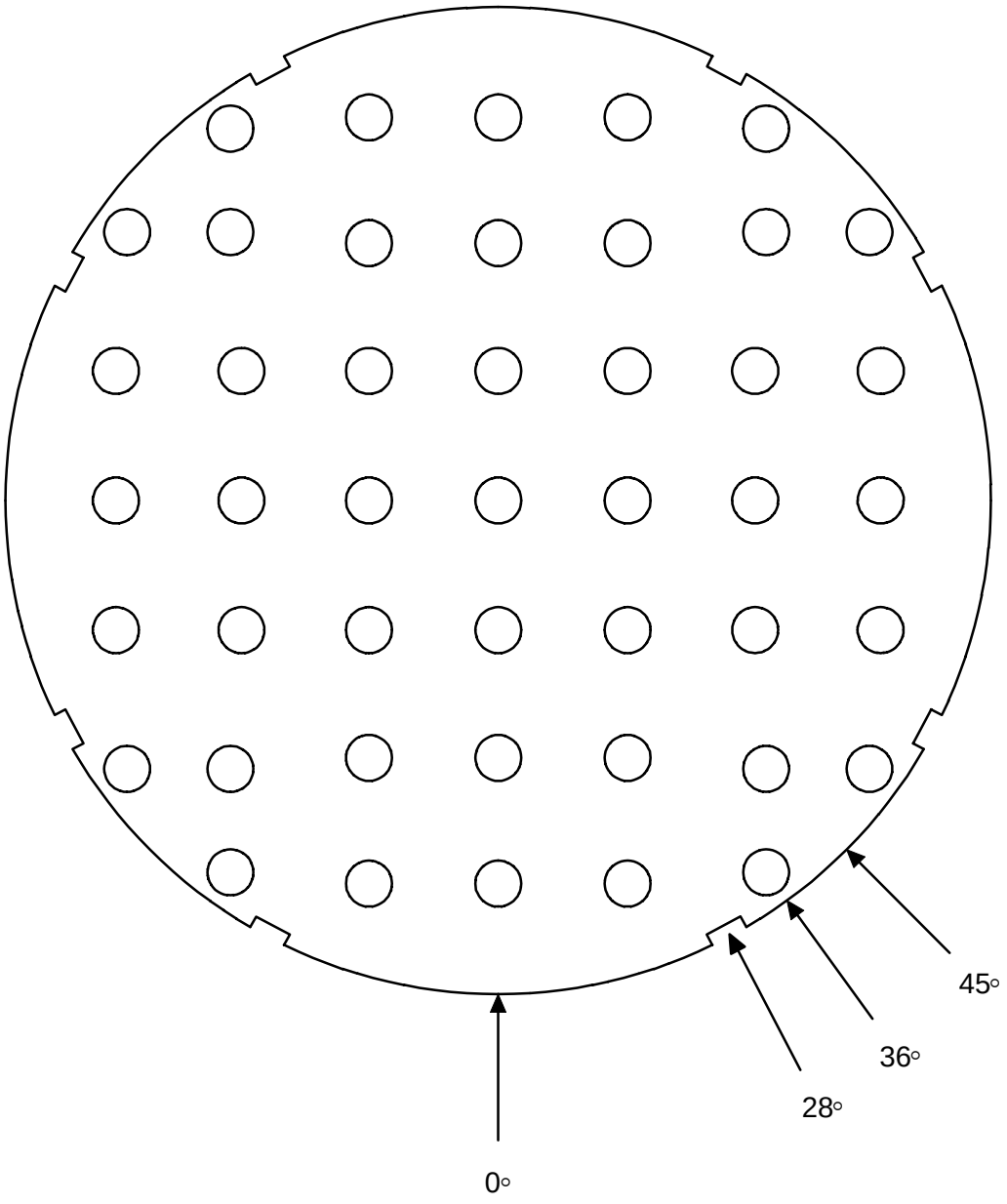

Figure 3.7-7 - W74 Engagement Spacer Plate Side Drop Impact Orientations

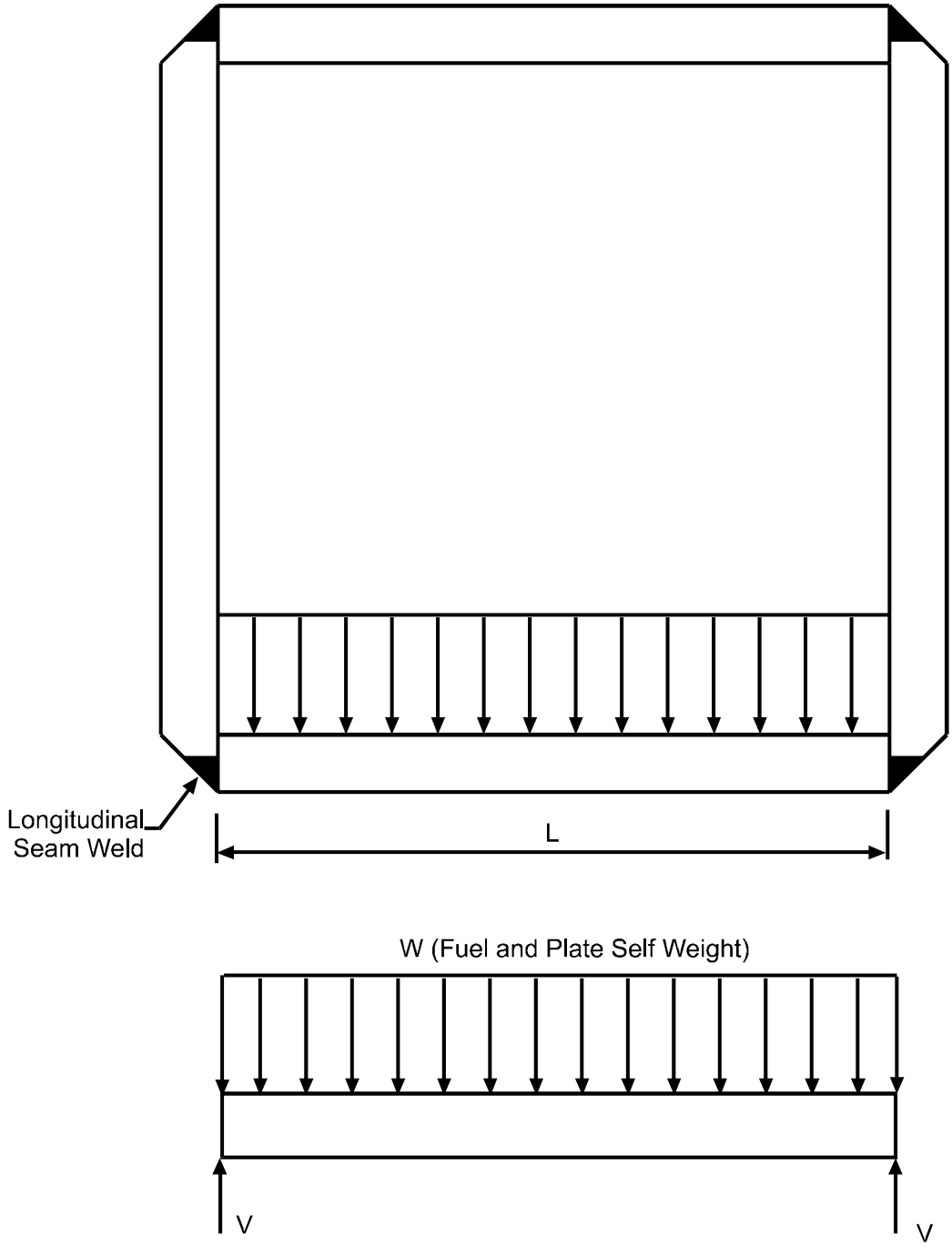

Figure 3.7-8 - W74 Canister Support Tube On-Site Transport Loading Diagram

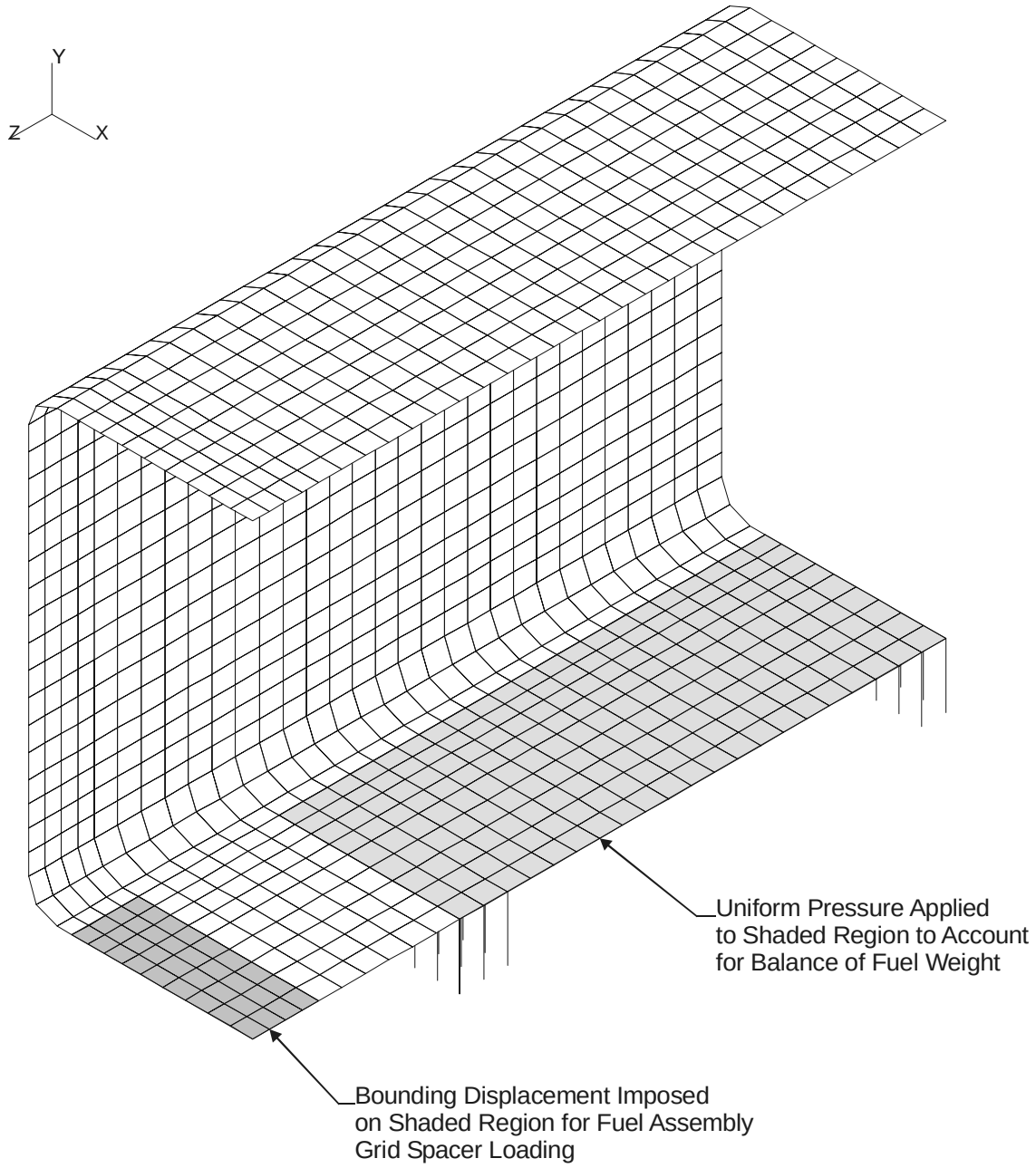

Figure 3.7-9 - W74 Guide Tube 60*g* Side Drop Loads for Concentrated Fuel Grid Spacer Loading Evaluation

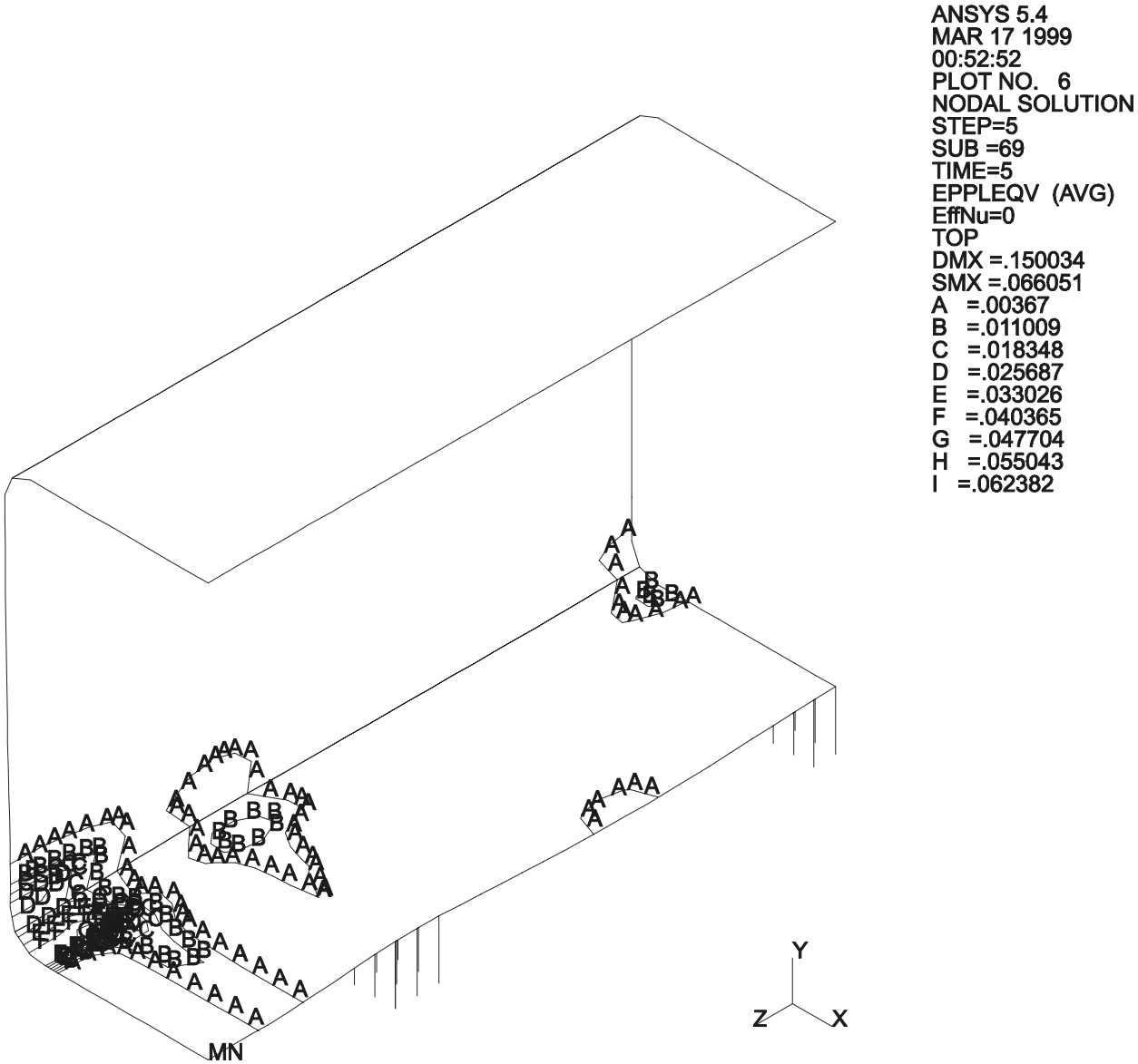

Figure 3.7-10 - W74 Guide Tube 60*g* Side Drop Plastic Strain for Concentrated Load at Fuel Assembly Grid Spacer

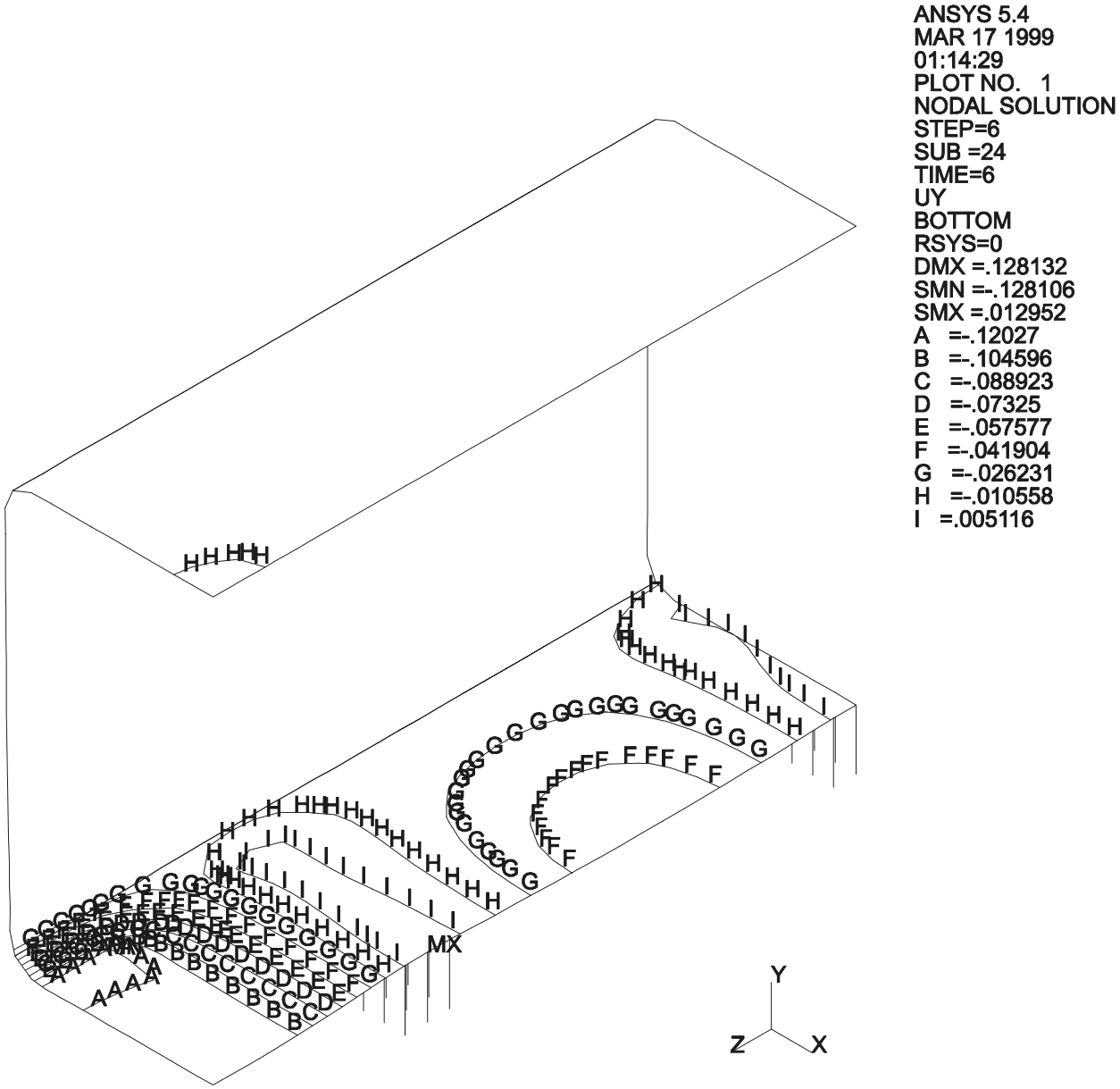

Figure 3.7-11 - W74 Guide Tube 60*g* Side Drop Permanent Deformation for Concentrated Load at Fuel Assembly Grid Spacer

3.8 Fuel Rods

Confinement provided by the SNF cladding is considered in the design criteria for the FuelSolutions™ W74 canisters. As such, the structural integrity of the fuel rod cladding is maintained throughout the canister storage life in accordance with 10CFR72 regulations. The structural evaluation of the fuel cladding considers thermally induced failures and structural failure (i.e., buckling) due to the postulated storage cask end drop.

The risk of gross cladding failure in zircaloy clad fuels is effectively eliminated by maintaining peak cladding temperatures are sufficiently low to limit creep in dry storage. As shown in Chapter 4 of this FSAR, the peak fuel cladding temperatures for all SNF accommodated in the FuelSolutions™ W74 canisters do not exceed the allowable cladding temperatures. Therefore, the potential for thermally induced gross cladding failure is effectively eliminated.

In addition to thermally induced cladding failure, structural failure of the fuel cladding in the event of a storage cask tip-over , transfer cask side drop, or storage cask bottom end drop is evaluated. The FuelSolutions™ W74 canister is designed to withstand a bounding storage cask end drop load of 50*g* and bounding tip-over and transfer cask side drop loads of 30*g* and 60*g*, respectively.

The fuel rod structural analysis, which is based on BRP intact UO_2 fuel assemblies, is bounding for all BRP partial and MOX fuel assemblies. The fuel rod clad dimensions and unsupported lengths used for the structural analysis of the BRP intact UO_2 fuel assemblies are bounding for all BRP partial and MOX fuel assemblies. Furthermore, the total weight per fuel rod used for the BRP fuel rod structural evaluation bounds that of all BRP partial and MOX fuel assemblies. Finally, since no structural credit is taken for the fuel pellet material or lateral support from adjacent fuel rods, the differences in fuel pellet composition and number of fuel assembly rods does not effect the fuel rod buckling analysis results.

For transverse impact loads resulting from the storage cask tip-over or transfer cask side drop, studies indicate that damage to SNF rods will not occur for loads less than 63*g*.[29] Therefore, the structural integrity of the fuel cladding will be maintained in the event of a postulated storage cask tip-over or transfer cask side drop.

Structural failure of the BRP SNF cladding for a postulated storage cask end drop is evaluated using classical hand calculations. The Euler buckling load is calculated for each BRP fuel type conservatively assuming that the entire weight of the fuel assembly, including the weight of the fuel pellets, is supported by the cladding tubes. The longest unsupported span of the fuel rod is taken as the maximum distance between the fuel assembly grid spacers. The Euler buckling evaluation of the fuel cladding tube is conservatively performed assuming pinned end conditions. The results of this evaluation show that the lower bound buckling load for all BRP SNF types is 86*g*. Since this is greater than the 50*g* bottom end drop design load, the BRP fuel cladding structural integrity will be maintained in the event of a storage cask bottom end drop.

Therefore, fuel cladding integrity is maintained throughout the 100 year design life of the FuelSolutions™ W74 canister.

[29] UCID-21246, *Dynamic Impact Effects on Spent Fuel Assemblies*, Chun, Witte, and Schwartz, Lawrence Livermore National Laboratory, September 1987.

As discussed in Chapter 4 of this FSAR, the allowable cladding temperatures for all BRP MOX, partial, and damaged fuel assemblies is greater than or equal to the allowable cladding temperature of intact UO_2 fuel. In addition, the maximum cladding temperature for BRP MOX, partial, and damaged fuel assemblies is bounded by the maximum cladding temperature of intact UO_2 fuel. Therefore, the risk of gross cladding failure in all BRP MOX, partial, and damaged fuel assemblies is effectively eliminated. During postulated accident drop conditions, no credit is taken for the structural integrity of the damaged BRP fuel inside the damaged fuel can.

3.9 Supplemental Data

3.9.1 Spacer Plate In-Plane Tributary Weights

The spacer plate in-plane tributary weights for each of the FuelSolutions™ W74M and W74T canister basket assemblies are calculated to identify the most heavily loaded spacer plate for the elastic stress analyses performed for the postulated storage cask tip-over and transfer cask side drop conditions. The spacer plate tributary weight includes the spacer plate self-weight plus the tributary weight of the support tubes, support sleeves, guide tube assemblies, SNF assemblies, and damaged fuel cans. The tributary width of each spacer plate is taken as the distance from the middle of the span on one side of the spacer plate to the middle of the span on the opposite side. The top and bottom end spacer plate tributary widths are equal to the distance from the end of the basket assembly to the middle of the span interior to the spacer plate.

The weights of the SNF assemblies, damaged fuel cans, and guide tube assemblies are assumed to be evenly distributed over their lengths. The maximum design weight and irradiated length of Big Rock Point fuel without channels are 485 pounds and 84.8 inches, respectively. The resulting SNF assembly maximum weight per unit length is 5.72 pounds per inch. The tributary weight of the damaged fuel cans is based on a bounding weight of 200 pounds per can distributed evenly over the length of the fuel, or 2.36 pounds per inch.

The tributary weights of each spacer plate in the W74M lower and upper basket assemblies are shown in Table 3.9-1 and Table 3.9-2, respectively. Since the largest tributary lengths of the W74T general spacer plates are equal to those of the W74M general spacer plates, the maximum W74T general spacer plate tributary weight is equal to that calculated for the W74M general spacer plate. Consequently, only the W74M spacer plate tributary weights are reported. The W74 spacer plates with the largest tributary weights are those spacer plates that have the greatest spacing. The highest tributary weights for the W74 general and LTP spacer plates are 1868 pounds and 1,865 pounds, respectively.

In order to evaluate the most conservative loading for various horizontal loading conditions, such as dead weight or transfer cask side drop, the fuel assembly loads are applied to the supporting basket assembly structure as concentrated loads at the fuel grid spacers. The grid spacer tributary weight is equal to the fuel line load times the grid spacer pitch. The largest longitudinal spacing of the in-core grid spacers for Big Rock Point fuel is 18.9 inches. Therefore, the largest tributary weight for the in-core grid spacers is 108.1 pounds. For the top and bottom end fittings, the tributary length is conservatively taken as half of the in-core grid spacer tributary length, or 9.45 inches. Therefore, the maximum tributary weight for the top and bottom end fittings is 54.1 pounds.

3.9.2 Finite Element Model Descriptions

3.9.2.1 Canister Shell Axisymmetric Finite Element Model

The two-dimensional axisymmetric finite element model described in this section and shown in Figure 3.9-1 is used for analyzing the axisymmetric load conditions for the W74 canister shell assembly, with the exception of the top end shield plug. The load conditions evaluated using the axisymmetric model include normal thermal, internal pressure, vertical deadweight, vertical

canister transfer, horizontal canister transfer (excluding horizontal dead weight), storage cask bottom end drop, and all associated load combinations.

As discussed in Section 3.1.1.1, a bounding canister shell axisymmetric model is used for the W74 canister shell assembly structural evaluation. The basic geometry of the W74 canister shell assemblies are similar to all other FuelSolutions™ canister shell assemblies with carbon steel shield plugs, with the exception of the top end shield plug assembly and its supports. The bounding canister shell assembly axisymmetric model is based on a canister shell assembly design that includes lead top and bottom shield plugs with bounding weights. The canister shell stresses calculated using this bounding canister shell model bound those in the W74 canister shell since the lead shield plugs included in the bounding model have a bounding weights and lower stiffness (i.e., lower elastic modulus).

The shell assembly axisymmetric model is comprised primarily of 2-D structural solid (PLANE42) elements. These elements are used to model the bottom end plate, bottom shield plug, bottom closure plate, bottom end shell extension, cylindrical shell, top end shield plug assembly and supports, top inner closure plate, and top outer closure plate. Each PLANE42 element is defined by four nodes, with two translational degrees of freedom (UX and UY) per node. The partial penetration groove weld which attaches the top outer closure plate to the canister shell is modeled discretely using PLANE42 elements. All other canister shell partial penetration welds are modeled by coupling the degrees of freedom (radial and axial) at the coincident nodes of the connected parts. The resulting nodal forces at the coupled locations are used to compute the weld shear stresses and stress intensities for the weld stress evaluation. The canister shell welds are all modeled with the minimum acceptable weld throats.

Non-linear 2-D point to point contact (CONTAC12) elements are used to model the interface between adjacent surfaces which may maintain or break physical contact, including the top closure plates and closure shield plug, and the bottom end plate, bottom closure plate, and bottom shield plug. In addition, contact elements are used to model the non-linear interface conditions between the outer surface of the bottom end plate and the supporting storage cask or transfer cask surface which is represented by ground nodes. The contact elements transfer only compressive loads normal to the contact surface and have no stiffness in tension. The contact surfaces between the cover plates and shield plugs are modeled using CONTAC12 elements with a contact stiffness of $1.0(10)^7$ lb/in. The contact surfaces between the outer end plate and the supporting structure is modeled using CONTAC12 with a contact stiffness of $1.0(10)^8$ lb/in. The initial gap size and orientation angle are defined by real constants. All gaps are assumed to be initially closed and not sliding. Gap friction is conservatively ignored.

Material Properties

The temperature dependent material properties of the shell assembly Type 304 stainless steel material provided in Section 3.3 are used for all thermal load conditions and load combinations including thermal. These properties are used since the Type 304 stainless steel material has lower allowable stresses than the Type 316 stainless steel and, therefore, is the limiting design despite the slightly lower coefficient of thermal expansion values. For all other load conditions, material properties corresponding to a temperature of 300°F are used.

Adjusted weight densities of 0.424 lb/in^3 and 0.570 lb/in^3 are conservatively used for the top end bottom shield plug lead materials, respectively, such that the total modeled weight of the top and bottom shield plug assemblies bound the weights of the W74 canister shield plugs.

Boundary Conditions and Loading

The specific model boundary conditions and loading used for each structural evaluation are described in the respective sections of this FSAR.

3.9.2.2 Canister Shell Half-Symmetry Finite Element Model

The W74 canister shell assembly stresses due to loads which act transverse to the canister longitudinal axis, such as horizontal deadweight, storage cask tip-over, and transfer cask side drop loads, are evaluated using the three dimensional half-symmetry finite element model shown in Figure 3.9-2 through Figure 3.9-4. This model, which represents to the top end region of the W21M-LS canister assembly, is used to provide a bounding stress analysis for the W74 canister shell assembly. The W21M-LS canister assembly stresses are bounding since the total weight of the basket assembly and SNF assemblies are significantly higher than that of the W74 canisters (i.e., 56.1 kips versus 51.6 kips).

The top end of the canister shell assembly is modeled because the stresses in the top end region are expected to bound those in the bottom end region since the top shield plug is heavier than the bottom shield plug. Also, the bottom shield plug is sandwiched between the two closure plates, and the upper shield plug is captured between the top inner closure plate and the shield plug support ring. The top eleven spacer plates of the W21M-LS basket assembly are included in the model, with the two top end 3/4-inch thick plates modeled as a single 1.5-inch thick plate, as shown in Figure 3.9-2.

The W21M-LS canister shell three-dimensional half-symmetry model includes the canister shell, top inner and outer closure plates and welds, top end shield plug, and the basket assembly spacer plates. The canister shell assembly top inner and outer closure plates, top shield plug, and cylindrical shell are modeled using brick shell elements (SOLID45), as shown in Figure 3.9-3. The top outer closure weld is modeled discretely. The top inner closure partial penetration weld is modeled as a pinned connection, since this weld is not designed as a moment connection. The stresses in the top inner and outer closure welds are evaluated in the same manner as described for the canister shell axisymmetric finite element model.

The assembly spacer plates are modeled using elastic shell elements (SHELL63). Since the spacer plates are included in this model only for the purpose of accurately modeling their loads on the canister shell, a coarse mesh is used for the spacer plates, as shown in Figure 3.9-4. The spacer plate mesh in the bottom region is adjusted to align the nodes radially with the corresponding nodes on the canister shell.

Radial gap elements are placed between the basket assembly spacer plates and inside of the canister shell and between the top shield plug and the inside of the canister shell to model the non-linear interface between these components. The shield plug and spacer plate gap elements are modeled with an initial radial gap sizes of 0.1875 inches and 0.175 inches, respectively. The gap element radial orientation is maintained throughout the analyses. The element status (open or closed) and the gap size for each gap element are continuously updated through an iterative solution. For each increment of loading applied to the model, the solution iterates until the convergence criteria has been satisfied (i.e., forces are balanced). At the end of each substep, each gap element size and status is updated based upon the locations of the gap element end nodes. For gap elements which are open, there is no associated stiffness. The gap element contact stiffness is modeled as $1x10^7$ lb/inch. Friction at the gap interfaces is conservatively ignored.

For the evaluation of horizontal dead weight and storage cask tip-over loads, the outside of the canister shell is supported by two 4-inch wide cask rails, which run the entire length of the canister and are located at 22.5° on both sides of the canister bottom centerline. Radial gap elements are used to model the interface between the outside of the canister shell and the rail supports. These gap elements are modeled without friction, initially closed, with a contact stiffness of $1x10^7$ lb/inch.

For the transfer cask side drop evaluation, the canister assembly is supported by the transfer cask inner shell (i.e., cylinder within a cylinder). For this condition, radial gap elements are used to model the non-linear interface between the outside of the canister shell and the inside of the transfer cask inner shell. These gap elements are similar to those used between the spacer plates and canister shell, but have an initial radial gap size of 0.5 inches and a contact stiffness of $1x10^8$ lb/inch.

Boundary Conditions

The global Z coordinate system goes from the bottom end to the top end. The half model is represented from the top (0° azimuth) to the bottom (180° azimuth). Along the half-symmetry plane, the nodes are restrained from translating along the X-axis, and rotating about Y-axis and Z-axis. Another plane of symmetry is located on the bottom end of the model, near the last spacer plate. The canister shell nodes at this location are restrained from translating along the Z-axis and rotating about X-axis (radial) and Y-axis (circumferential).

For the horizontal dead weight and storage cask tip-over analysis, the cask support rail gap element ground nodes are restrained in all degrees of freedom. Similarly, for the transfer cask side drop analysis, the gap element ground nodes are fixed.

To maintain model stability for the spacer plate, the top and bottom nodes of the spacer plates are restrained from translation in the Z direction.

Material Properties

The canister shell, top outer closure plate and weld, the inner closure plate, and the spacer plates are modeled with an elastic modulus of $27.0x10^6$ lb/in^2, a density of 0.29 lb/in^3, and a Poisson's ratio of 0.29. The carbon steel plug is modeled with an elastic modulus of $27.0x10^6$ lb/in^2, a density of 0.284b/in^3, and a Poisson's ratio of 0.29.

Applied Loading

The inertial loads of the canister shell, top outer and inner closure plates, the shield plug, and the self weight of the spacer plates are accounted for by applying an appropriate acceleration in the direction of the loading. The inertial loads of the fuel assembly and the guide tube are applied as uniform pressure loads over the width of the supporting spacer plate ligaments, as shown in Figure 3.9-4. The ligament pressure loads are scaled using the appropriate acceleration applicable in the selected loading condition.

For the canister shell load combination evaluation, the transverse canister loads are applied in combination with the canister off-normal internal pressure load of 16 psig is applied as a uniform pressure load on surfaces of interest: 1) For inner boundary pressure, the uniform pressure is applied on the inside surface of the canister shell (up to the top inner closure weld), and on the inside faces of the inner closure plate. 2) For outer boundary pressure, the uniform pressure is

applied on the inside surface of the canister shell (up to the top outer closure weld), and on the inside surfaces of the outer closure plate.

3.9.2.3 Top Shield Plug Model

The W74 top shield plug assembly is evaluated for the 50*g* bottom end drop load using the quarter-symmetry finite element model shown in Figure 3.9-5. The model is of the shield plate only, including the guide tube and support tube shield cap cutouts and the support bar recess cutouts, but does not include the vent/drain port. The guide tube shield caps and support tube shield caps are not included in the model. However, the weight of the shield caps is included in the model through the use of an adjusted density for the elements in the ligament region, as shown in Figure 3.9-6. In addition, the density of the shield plate elements are adjusted to include the weight of the top inner and outer closure plates.

Symmetry boundary conditions are applied to the shield plug quarter-symmetry finite element model (i.e., UX=0 for all nodes at X=0 and UY=0 for all nodes at Y=0). Longitudinal displacement constraints (UZ=0) are applied to a single line of nodes at the top of each support bar access cutout, assuming the shield plate pivots about the inner edge of each support bar. Since the model densities are adjusted to include the weight of the shield caps and closure plates, the only loading applied to the model is a 50*g* longitudinal acceleration load.

3.9.2.4 General and LTP Spacer Plate Models

3.9.2.4.1 Spacer Plate Plane-Stress Models

The most heavily loaded W74 general spacer plate and LTP spacer plate are evaluated for loads which act normal to the canister longitudinal axis (i.e., in-plane) using the two-dimensional plane stress model shown in Figure 3.9-7. The spacer plate geometry is constructed using PLANE42 plane stress elements (4 node quadrilateral) with the spacer plate thickness input as a real constant. CONTAC52 gap elements (3D node to node) are modeled along the perimeter of the model to capture the non-linear support conditions provided by the canister shell. The contact elements are modeled with a 0.1875-inch gap equal to the nominal radial clearance between the spacer plates and the canister shell. The gap element radial orientation is maintained throughout the analyses. The element status (open or closed) and the gap size for each gap element are continuously updated through an iterative solution. For each increment of loading applied to the model, the solution iterates until the convergence criteria has been satisfied (i.e., forces are balanced). At the end of each substep, each gap element size and status is updated based upon the locations of the gap element end nodes. For gap elements which are open, there is no associated stiffness. The gap element contact stiffness is modeled as $9(10)^5$ lbs/in, based on the compliance of the canister shell. Friction between the spacer plate and canister shell is conservatively ignored.

Boundary Conditions

Because the contact elements do not provide any initial constraint to the model, three COMBIN14 longitudinal spring elements were constructed in a radial orientation at the 0°, +45°, and +90° positions at the model edges. These elements provide a very small amount of restraint to the model thereby allowing the solution to converge. A spring constant of 100 lb/in is specified for each element. The “ground” node of each gap and spring element was restrained in

all degrees of freedom. Additionally, to prevent rigid body rotation of the model, the node on the model edge at the impact location for the corresponding impact angle was restrained from translating in the circumferential direction.

Material Properties

The W74 general and LTP spacer plates are modeled with the material properties of A514, Grade P[30] carbon steel and SA-240, Type XM-19 stainless steel, respectively. The material properties at the design temperatures of 700°F and 650°F are used for the general spacer plate and LTP spacer plate, respectively. Elastic analyses are performed using linear-elastic material properties per Section 3.3. For the storage cask tip-over and transfer cask side drop plastic stress analyses, bilinear kinematic hardening with a 0.1% tangent modulus is assumed for all materials. The weight density and Poisson's ratio are taken as 0.283 lb/in^3 and 0.3 for carbon steel and 0.290 lb/in^3 and 0.30 for stainless steel.

Loading

The spacer plate model is loaded with an acceleration and a pressure loading. The weight of the spacer plate is represented by the volume of the spacer plate model times the spacer plate weight density. The inertial load of the SNF assemblies, damaged fuel cans, guide tube assemblies, support tubes, and support sleeves are modeled as uniform pressure loads over the width of the supporting spacer plate ligaments. The pressure load on each of the supporting support tube hole or guide tube hole ligaments in the global X and Y directions due to an applied acceleration G is determined as follows:

Support Tube Holes: $q_{T,X} = (W_F + W_C + W_{SS} + W_{FF})(G)(sin(\theta))/A_{lig}$

$q_{T,Y} = (W_F + W_C + W_{SS} + W_{FF})(G)(cos(\theta))/ A_{lig}$

Guide Tube Holes: $q_{G,X} = (W_F + W_G)(G)(sin(\theta))/A_{lig}$

$q_{G,Y} = (W_F + W_G)(G)(cos(\theta))/ A_{lig}$

where:

W_F = tributary weight of the SNF assembly (pounds)

W_C = tributary weight of the support tube assembly (pounds)

W_{SS} = tributary weight of the support sleeves (pounds)

W_{FF} = tributary weight of the damaged fuel can (pounds)

W_G = tributary weight of the guide tube assembly (pounds)

A_{lig} = ligament surface area over which the pressure is applied (in^2)

[30] The general spacer plates are fabricated from either SA-517, Grades F or P, or A514, Grades F or P carbon steel. Except for the yield strength, the material properties used in the finite element model (i.e., E, ν, and density) are identical for all of these carbon steels. The yield strength of the bounding A514 material is used in the plastic analyses. Therefore, the results of the finite element analysis are valid for all W74 general spacer plate material alternatives.

G = resultant in-plane equivalent static load (*g's*)

θ = angle of resultant load vector G measure CCW relative to 0° azimuth (degrees)

The appropriate pressure loading is automatically calculated in the analysis run using pre-defined constants and the ANSYS parametric design language (APDL). The pre-defined constants are essentially those constants that allow the "line loads" of the fuel assembly, support tubes/sleeves, and guide tubes to be determined. The line loads are calculated and then used in conjunction with the orientation angle, acceleration loading, and tributary length to determine the appropriate pressure loading to be applied. The orientation angle, acceleration loading, and tributary length are variable user specified inputs to the ANSYS analysis input file. This allows the input file to be used generically in the analysis of all in plane loading conditions. Some conservative simplifications were made in the calculation of the tributary weight line loads used in the analysis input file. These conservative simplifications cause the tributary weight to be somewhat higher in the analysis compared to the more accurate tributary weights listed in Table 3.9-1and Table 3.9-2.

3.9.2.4.2 Spacer Plate Shell Models

The W74 general spacer plate and LTP spacer plate are evaluated for the storage cask end drop using a shell model. The spacer plate shell model geometry was constructed using SHELL93 elements (8 node structural shell) with the spacer plate thickness input as a real constant. The model is similar to the 2D plane stress model described above. Essentially, the shell model is created by re-defining the 2D plane stress elements as shell elements. This keeps the mesh and the entity numbering consistent between the models. It is noted that the contact elements from the original plane stress model are not removed, but essentially inactive for the longitudinal loading conditions. The spring elements from the original model are also left intact in order to prevent rigid body motion in the transverse direction. Similarly, a node on the edge of the model is left restrained in the "theta direction" in order to prevent rigid body rotation.

An additional restraint (pinned boundary condition) was imposed on the W74 general spacer plate model to represent the longitudinal support provided by the support sleeves in the longitudinal direction. For the W74 LTP spacer plate model, additional fixed restraints (fixed boundary conditions) are imposed to represent the support provided by the support tube to spacer plate weld.

For loading in the longitudinal direction, the spacer plates support only their self-weight. The rest of the tributary weight is carried directly by the support tube or canister end-shell. Therefore, the only required loading for the spacer plate model is an acceleration loading in the longitudinal direction. The acceleration loading is input in units of g's and is applied to the self-weight of the spacer plate. The self-weight of the spacer plate is represented by the volume of the spacer plate model times the spacer plate weight density.

3.9.2.4.3 Spacer Plate Shell Models for Thermal Bending Stress Analysis

The W74 general and LTP spacer plates are evaluated for bending reaction loads from the support tubes caused by curvature of the support tubes due to lateral thermal gradients (see Section 3.5.1.3.2) using the finite element model shown in Figure 3.9-8. This finite element model is similar to the shell model used for the end drop stress analysis, with the addition of 3-D beam elements (BEAM4) between the centerline of the support tube openings and the perimeter

of the spacer plate support tube holes. The beam elements are defined with the following rigid properties in order to maintain a plane section at the support tube hole:

AREA = 100 in^2
IZZ = IYY = 1,000 in^4
TKZ = TKY = 10 in.

The elastic modulus used in the model is conservatively based on lower bound temperatures of 400°F for the W74 general spacer plate and 300°F for the LTP spacer plate.

The spacer plate loading resulting from the curvature of the support tubes is defined by imposing unit rotational displacement constraints (ROTX = ROTY = $\pm$0.001 radian) to the nodes located at the centerlines of the support tube holes.

3.9.2.4.4 Spacer Plate Half-Symmetry Multi-Span Shell Model

The half-symmetry multi-span shell model shown in Figure 3.9-9 and described in this section is used for the W74 general spacer plate plastic instability analyses for the postulated storage cask tip-over and transfer cask side drop (0° orientation) conditions. The W74 general spacer plate half-symmetry multi-span shell finite element model includes three general spacer plates; the center spacer plate over which the fuel grid spacers are assumed to be positioned, and the adjacent spacer plates on either side. The W74 general spacer plates are modeled with a uniform pitch of 7.125 inches. The W74 guide tubes and support tubes extend 3.5625 inches beyond the centerlines of the outer spacer plates on each side.

The spacer plates are modeled using plastic shell elements (SHELL 43), which permit treatment of longitudinal deflections. The spacer plate model mesh density is coarser than that of the spacer plate finite element models discussed in previous sections in order to maintain reasonable computer run times and the required hard disk space. Since the model is used only for buckling analyses, in which displacements are of interest rather than stresses, the mesh density is sufficient to accurately predict the overall response of the spacer plates for tip-over and side drop conditions.

The W74 guide tubes and support tubes are also modeled using plastic shell elements (SHELL43). The guide tubes are modeled with a 0.090-inch thickness, conservatively neglecting the structural capacity of the guide tube neutron absorber sheets. However, an adjusted weight density is used for the guide tube material to account for the weight of the neutron absorber sheets, conservatively addressing two neutron absorber sheets per guide tube. The adjusted weight density of the guide tube is calculated as follows:

$$\rho = \frac{\rho_{ss}\left(A_{GT}+A_N\right)}{A_{GT}} = 0.40 \text{ lbs/in}^3$$

where:

ρ_{ss} = 0.290 lbs/in^3, weight density of stainless steel

A_{GT} = 2.52 in^2, guide tube cross-sectional area

= 4(6.90 + 0.090) (0.090)

A_N = 0.96 in^2, cross-sectional area of 2 neutron absorber panels

= 2 (6.4) (0.075)

Two dimensional node-to-node gap elements (CONTAC12) are included between the bottom of the guide and support tubes and the supporting spacer plate ligaments, in order to provide the proper guide tube and support tube to spacer plate interface for the storage cask tip-over and 0° transfer side drop events. The normal contact stiffness of $1x10^6$ lbs/inch is used for these gap elements.

The W74 support sleeves are modeled using three dimensional structural solid elements (SOLID45). Nonlinear spring elements (COMBIN39), having a stiffness in compression of $1x10^7$ lbs/in and a stiffness in tension of 10 lbs/in, are included between the nodes of the support sleeves at their interface with the spacer plate and the corresponding spacer plate nodes. Three dimensional point-to-surface contact elements (CONTAC49), having a normal contact stiffness of $1x10^6$ lbs/in, are included between the extended portions of the sleeves at their interface with the spacer plate and the associated spacer plate nodes.

Three dimensional node-to-node gap elements (CONTAC52) are included around the perimeter of each spacer plate for the transfer cask side drop condition to model the non-linear support provided by the canister shell. These gap elements are modeled with a uniform 3/16-inch nominal gap size and a normal contact stiffness of $9.0x10^5$ lbs/in. The gap contact stiffness is based on a compliance analysis of the canister shell. When the spacer plate loading is initially applied, the spacer plates are moved into contact with the ground nodes at the initial point of contact with the canister shell. The gap element sizes are updated based upon the new node locations.

Soft spring elements (COMBIN14) are placed on the perimeter of each spacer plate at locations of 0°, -45°, and -90° in the global cylindrical coordinate system (CSYS=1) for added numerical stability. The stiffness of the soft springs is specified as 100 lbs/in., such that their presence has no significant effect on the accuracy of the solution. These springs are also used to maintain stability of the guide tubes and support tubes during solution convergence.

Material Properties

The W74 general spacer plates are modeled using the material properties of A514, Grade F or P[31] carbon steel. The W74 guide tubes are modeled using SA-240, Type 316 stainless steel material properties. The W74 support tubes are modeled using SA-240, XM-19 stainless steel material properties. The W74 support sleeves are modeled using SA-240, Type 304 stainless steel material properties. Bi-linear kinematic hardening with a 0.1% tangent modulus is assumed for all materials. For the tip-over and side drop conditions without thermal loading, uniform material properties at a bounding design temperature of 700°F are used. For the combined tip-over or side drop plus thermal loading, temperature dependent material properties are used, as

[31] The general spacer plates are fabricated from either SA-517, Grades F or P, or A514, Grades F or P, carbon steel. Except for the yield strength, the material properties used in the finite element model (i.e., E, ν, and density) are identical for all of these carbon steels. The yield strength of the bounding A514 material is used in the plastic analyses. Therefore, the results of the finite element analysis are valid for all W74 carbon steel spacer plate material alternatives.

specified in Section 3.3. The weight density and Poisson's ratio are taken as 0.283 lbs/in^3 and 0.3 for carbon steel and 0.290 lbs/in^3 and 0.3 for stainless steel.

Boundary Conditions

For the storage cask tip-over conditions, the spacer plates are supported along their bottom edge by the canister shell which is supported by the storage cask or transfer cask rails. Both the storage cask and transfer cask use two full length rails to support the canister. The cask rails are 4.0 inches wide and separated by 45° (i.e. 22.5° on both sides of the spacer plate bottom center). The support provided by the canister shell is conservatively neglected and the spacer plates are restrained radially (UX in the cylindrical coordinate system) at locations of the cask rails.

For the transfer cask side drop conditions, the “ground” nodes of each spacer plate perimeter gap element are restrained in all directions. Additionally, to prevent rigid body rotation of the model, the node on the model edge at the impact location is restrained in the “theta” direction.

Symmetry boundary constraints are applied to the model nodes located on the half-symmetry plane (i.e. UX = ROTY = ROTZ = 0) for spacer plate and guide tube elements. Symmetry boundary conditions (i.e. UZ=ROTX=ROTY = 0) are also applied to the nodes on the end planes of the guide tubes and support tubes. The spacer plate boundary conditions are illustrated in Figure 3.9-10.

Loading

The model loading includes the self-weight of the spacer plates, guide tubes, support tubes and support sleeves, in addition to the loads from the weight of the fuel assemblies (including damaged fuel cans). Since the spacer plates, guide tubes, support tubes and support sleeves are discretely modeled, an acceleration load is applied to the model to account for their load due to their self-weight. The loads due to the weight of the fuel assemblies are modeled as concentrated nodal forces as discussed below.

The fuel grid spacer load per unit acceleration (G) is applied as nodal forces to the guide tube bottom panel directly above the center spacer plate in the finite element model. As discussed in Section 3.9.1, the maximum fuel grid spacer tributary load is 108 pounds for intact fuel assemblies. Each guide tube includes 4 equally sized elements over the width of the fuel grid spacer. Therefore, one fourth of the grid tributary load (27 x G pounds) is distributed to each of the guide tube interior nodes over the width of the fuel grid spacer and one eighth of the grid spacer tributary load (13.5 x G) pounds is applied to the guide tube nodes at the edge of the grid spacer and those located on the half-symmetry plane, as shown in Figure 3.9-11. The maximum fuel grid spacer tributary load is 108 + 44.6 (tributary weight of damaged fuel canister) = 152.6 pounds for the fuel assemblies and damaged fuel canister stored within the support tubes. A similar approach to that described above is applied in distributing the grid tributary load to the support tube interior and edge nodes.

Buckling evaluations are performed for the tip-over and 0° side drop loads both with and without the bounding normal thermal gradients superimposed. For those conditions including thermal, the thermal gradient is applied to the model as an initial condition and held constant for the remainder of the analysis. Further discussion of the bounding thermal gradient used for these analyses is provided in Section 3.7.4.2.1. A constant 10*g* longitudinal acceleration is also applied to the models as an initial condition for the buckling evaluations to introduce an initial eccentricity in the spacer plates. For the buckling evaluations, the model in-plane impact loads

are continually ramped up until the solution no longer converges or the loads are at least 1.5 times the design loads.

3.9.2.4.5 Spacer Plate Full Multi-Span Shell Model

The full spacer plate multi-span shell model shown in Figure 3.9-12 and described in this section is used for the 45° transfer cask side drop plastic instability analysis of the W74 general spacer plates. The basic geometry of the multi-span shell model shown in Figure 3.9-12 is similar to that of the half-symmetry spacer plate multi-span shell model described in the previous section.

Material Properties

The material properties used in the multi-span shell model are identical to those described in Section 3.9.2.4.4.

Boundary Conditions

In general, the model boundary conditions for the 45° transfer cask side drop plastic large deflection buckling analyses are the same as those used for the 0° transfer cask side drop plastic large deflection buckling analysis, as described in Section 3.9.2.4.4. Because a full model is used for the 45° drop, the half-symmetry boundary constraints shown in the half-symmetry spacer plate multi-span shell model, are not applicable.

Loading

The finite element in-plane side drop loads are applied in the same manner as described in Section 3.9.2.4.4, with some clarification. The calculated loads for the fuel assemblies are multiplied by the sine and cosine of the angle to obtain the loads acting along the X-axis and Y-axis, respectively. The X-direction loads are applied to the guide tube and support tube side panels which are supported by the spacer plate vertical ligaments and the Y-direction loads are applied to the guide tube and support tube bottom panels which are supported by the spacer plate horizontal ligaments. The spacer plate loads for the 45° impact angle is shown in Figure 3.9-13.

3.9.2.5 Engagement Spacer Plate Models

Three separate finite element models are used for the structural evaluation of the W74 engagement spacer plate. These include: 1) A half-symmetry plane stress finite element model which is used for the thermal stress evaluation, and 2) A full plane stress finite element model which is used for the transfer cask side drop evaluation, and 3) A quarter-symmetry solid model which is used for the bottom end drop evaluation. Each of these models are described in this section. The material properties used in each of the engagement spacer plate finite element models are those of XM-19 stainless steel at a design temperature of 600°F from Section 3.3. Poisson's ratio and the density of stainless steel are modeled as 0.29 and 0.290 lb/in^3, respectively.

3.9.2.5.1 Half-Symmetry Plane Stress Model

The W74 engagement spacer plate half-symmetry plane stress finite element model, shown in Figure 3.9-16, is used for the evaluation of on-site transport handling, thermal stress, and the 0° side drop. The finite element model includes two-dimensional isoparametric plane stress elements (PLANE42), representing the geometry of the engagement spacer plate. A total of

5,132 nodes and 4,678 plane-stress elements are used to model the engagement spacer plate. Each plane stress element has four nodes, each node having two degrees of freedom (UX and UY). The spacer plate thickness is input as a real constant.

The non-linear contact support provided by the canister shell is modeled using 3-D point-to-point contact (gap) elements (CONTAC52). The gap elements are modeled with the nominal radial gap size based on the engagement spacer plate and shell element ground nodes being initially concentric. The engagement spacer plate is then moved to close the gap in the region of initial contact and the gap element sizes are updated based on the new node locations. This effectively models the variation in the size of the gap between around the perimeter of the engagement spacer plate. The gap element contact stiffness is modeled as $9(10)^5$ pounds per inch. Friction between the spacer plate and the canister shell is conservatively ignored in the gap elements.

3.9.2.5.2 Full Plane Stress Model

The full engagement plate plane stress finite element model, shown in Figure 3.9-17, is used for the evaluation of side drop angles of 28°, 36°, and 45°. The model geometry is developed by reflecting the engagement spacer plate finite element mesh of the half-symmetry plane stress finite element model about the vertical centerline (i.e., YZ plane). The gap elements used to model the non-linear contact between the engagement spacer plate and the canister shell are modeled using the same approach used for the half-symmetry model. Gap elements are generated for all nodes along the perimeter of the plate in the lower right hand quadrant (e.g., 270° to 360°). The full engagement spacer plate finite element model includes 10,065 nodes and 9,257 elements. The material properties used in the model are identical to those used for the half-symmetry model.

3.9.2.5.3 Quarter-Symmetry Solid Model

The engagement spacer plate quarter-symmetry finite element model, shown in Figure 3.9-14, is used for the evaluation of the bottom end drop loads. As discussed in Section 3.7.5.2.2, a bounding equivalent static end drop acceleration of 52*g* is used for the end drop stress analysis. The engagement spacer plate is modeled using nominal dimensions. The end drop stress analysis model, which includes the engagement spacer plate and the attachment sleeve, consists entirely of 8-node solid brick elements. Each node of the brick elements includes three translational degrees of freedom (UX, UY, and UZ). A total of 13,659 nodes and 12,579 elements are used in the model. The model does not include the engagement sleeve since these components are not relied upon for structural support in the end drop.

The end drop loads are applied as follows. An acceleration of 52*g* is applied to the model to account for the self weight of the engagement spacer plate. The loading of components supported by the engagement spacer plate is modeled as uniform pressure applied to the respective model regions, corresponding to the regions shown in Figure 3.9-15. The applied pressure loading for each region is calculated as follows:

> *Region I: Interior Fuel Cells*: A single intact spent fuel assembly and guide tube assembly is supported by the engagement spacer plate in the region of each fuel cell. The uniform end drop pressure load (q1) applied over these regions is calculated as follows:

$$q_1 = \frac{50g\,x\,(W_{fa} + W_{gt})}{A_{fc}} = 703.0\,psi$$

where:

W_{fa} = 485 lb., maximum weight of fuel assembly

W_{fa} = 85 lb., bounding weight of guide tube assembly

A_{fc} = Area in fuel cell region, assumed equal to area within guide tube I.D.

= $6.90^2 - \pi(1.50)^2 = 40.54\ in^2$

Region II: Support Tube Fuel Cells: A SNF assembly and damaged fuel can are supported by the engagement spacer plate in the region of each support tube cell. The applied end drop pressure load (q2) used for this regions is calculated as follows:

$$q_2 = \frac{50g\,x\,W_p}{A_{st}} = 718.2\,psi$$

where:

W_p = 685 lb., maximum combined weight of SNF assembly and damaged fuel can

A_{st} = Area of support tube cell region, assumed equal to area within support tube I.D.

= $[7.40^2 - \pi(1.50)^2] = 47.69\ in^3$

Region III: Support Tube Bearing (Basket Weight): One quarter of the basket assembly weight is applied to the region in which the support tube bears on the engagement spacer plate. The pressure load (q3) used for this region is calculated as follows:

$$q_3 = \frac{50g\,x\,W_b}{A_{stb}} = 5{,}161\,psi$$

where:

W_b = 2,250 lb., ¼ of bounding upper basket assembly weight (9,000 pounds, less engagement spacer plate)

A_{stb} = Area in support tube bearing region, modeled as area between attachment sleeve i.d. and support tube i.d.

= $8.75^2 - 7.40^2 = 21.80\ in^3$

Symmetry displacement constraints are applied to the nodes lying on the engagement spacer plate symmetry boundaries (UX=0 for all nodes at X=0 and UY=0 for all nodes at Y=0). Longitudinal restraint of the engagement spacer plate is provided by the support tubes upon which the engagement spacer plate bears. Only those nodes in the region of the support tube which are loaded in compression are restrained such that the engagement spacer plate is not prevented from uplifting. Based upon preliminary analyses, the engagement spacer plate was shown to pivot about the two exterior edges of the support tube which face toward the center of

the basket assembly. No other contact is developed between the engagement spacer plate and the supporting tube. This is verified by examining the end drop stress analysis results, which show that the reaction forces at all constrained nodes are compressive and that the plate lifts off the tube in all other regions.

3.9.2.6 Guide Tube Models

3.9.2.6.1 Guide Tube Half-Symmetry Single Span Model

The FuelSolutions™ W74 guide tube assembly is evaluated for transverse loads resulting from the normal and accident conditions using the half-symmetry single span finite element model shown in Figure 3.9-18. This model is used for the evaluation of uniform fuel loading assumptions (i.e., fuel weight evenly distributed over its full length), such as those which could result from the accident side drop condition. The model represents the segment of the guide tube in which the highest stresses are shown to occur. The model spans from the centerline of a spacer plate ligament support to the mid-span between the adjacent spacer plate ligament support, taking advantage of longitudinal symmetry.

The guide tube is modeled with plastic shell elements (SHELL43) having three translational (UX, UY, UZ) and three rotational degrees of freedom (ROTX, ROTY, ROTZ) at each node. The shell elements include both membrane and bending stiffness and have both stress stiffening and large deflection capabilities. The guide tube assembly model includes only the guide tube for structural support, conservatively neglecting the structural contributions of the neutron absorber panels. The load on the guide tube due to the neutron absorber panels is accounted for by adjusting the weight density of the guide tube as discussed below.

Material Properties

For the linear-elastic stress analyses, the guide tube is modeled with the elastic modulus of SA-240, Type 316 stainless steel material properties at 700°F, which is slightly conservative. The guide tube plastic analyses are performed using the elastic-plastic stress-strain curve for Type 316 stainless steel at 715°F. The material properties of SA-240, Type 316 stainless steel are summarized in Section 3.3. For both analyses, Poisson's ratio for the guide tube material is taken as 0.29. As discussed above, the guide tube density is adjusted to account for the load on the guide tube due to the weight of the neutron absorber panels. The adjusted weight density is calculated as follows:

$$\rho_{ss}(A_{GT} + A_N)/A_{GT} = 0.51 \text{ lb/in}^3$$

where:

ρ_{ss} = 0.290 lb./in^3, weight density of stainless steel

A_{GT} = 2.52 in^2, guide tube cross-sectional area
= 4(6.90+0.090)(0.090)

A_N = 1.92 in^2, cross-sectional area of four neutron absorber panels
= 2(6.40)(0.075)

Boundary Conditions

The model includes symmetry boundary constraints along the half-symmetry plane and along the vertical plane passing through the nodes located at the spacer plate support. Vertical displacement constraints are applied to the guide tube nodes at the location of the spacer plate ligament support.

Loading

The guide tube loading for the accident side drop evaluation is described in Section 3.7.5.2.5.

3.9.2.6.2 Guide Tube Half-Symmetry Multi-Span Model

The FuelSolutions™ W74 guide tube assembly is evaluated for transverse loads resulting from the normal and accident conditions using the half-symmetry multi-span finite element model shown in Figure 3.9-19. This model is used for the evaluation of non-uniform fuel loading assumptions (i.e., fuel weight applied at the fuel assembly grid spacer locations). The model includes 1½ guide tube spans, taking advantage of longitudinal symmetry. The guide tube is modeled with plastic shell elements (SHELL43) having three translational (UX, UY, UZ) and three rotational degrees of freedom (ROTX, ROTY, ROTZ) at each node. A total of 1240 plastic shell elements are included in the model. The shell elements include both membrane and bending stiffness and have both stress stiffening and large deflection capabilities. The plastic capabilities of these shell elements are not used for the guide tube normal condition linear-elastic stress analysis, but only for the evaluation of the guide tube permanent deformations resulting from the postulated accident side drop condition. The guide tube assembly model includes only the guide tube for structural support, conservatively neglecting the structural contribution of the neutron absorber panels. The load on the guide tube due to the neutron absorber panels is accounted for by adjusting the weight density of the guide tube as discussed below.

Gap elements (CONTAC52) elements are included in the model at the locations of the spacer plate ligament supports. A total of 55 gap elements are used. Each 3-D point-to-point gap element is connected on one end to a single guide tube node and on the other end to ground (i.e., node restrained in all DOF). The gap elements are modeled with a normal stiffness of $1x10^5$ pounds/inch and zero sliding stiffness. The specified gap normal stiffness is much higher than the stiffness of the guide tube panel, thereby avoiding errors in the solution caused by excessive gap interference. The initial gap status is specified as closed and not sliding. In addition, a single soft spring element (COMBIN14) is used to maintain stability during the unloading in the final load step, which is used to determine the post-drop, permanent deformation.

Material Properties

For the linear-elastic stress analysis, the guide tube is modeled with the elastic modulus of SA-240, Type 316 stainless steel material properties at 700°F, which is slightly conservative. The guide tube plastic analysis is performed using the elastic-plastic stress-strain curve for Type 316 stainless steel at 715°F, per Table 3.3-4. For both analyses, Poisson's ratio for the guide tube material is taken as 0.29. As discussed in Section 3.9.2.6.1, an adjusted guide tube density of 0.51 lb/in^3 is used to account for the load on the guide tube due to the weight of the neutron absorber panels.

Boundary Conditions

The model includes symmetry boundary constraints along the half-symmetry plane and along the vertical planes passing through the nodes located at the ends of the guide tube model. In addition, the gap element ground nodes are restrained in all DOF.

Loading

The guide tube loading for the horizontal dead weight and accident side drop evaluations are described in Sections 3.1.1.6.2 and 3.3.5.2.5, respectively.

3.9.3 Stress Evaluation Criteria

3.9.3.1 Canister Shell Stress Evaluation Locations

The W74 canister shell structural evaluation is performed using the axisymmetric and three-dimensional finite element models described in Sections 3.5.2.1 and 3.5.2.2, respectively. Linearized section stresses are used to determine the average membrane, linearized membrane plus bending, and total (primary plus secondary plus peak) stress distribution at the critical sections of the canister shell for comparison with the stress limits defined in the ASME Code. Section stresses are determined using the stress linearization routine described in the ANSYS User's Theory Manual. For each section, the linearized stresses are determined at the innermost radial position of the section (“I”), the center of the section (“C”), and the outermost radial position of the section (“O”). For consistency, the “I” and “O” nodes are defined on the inside and outside surfaces of the canister shell.

For the canister shell assembly structural evaluations performed using the axisymmetric finite element model described in Section 3.9.2.1, a total of 36 locations are evaluated. The canister shell stress evaluation locations in the top and bottom regions and the cavity region of the axisymmetric model are shown in Figure 3.9-21 and Figure 3.9-22. The stress evaluation locations selected include all of the regions of the canister shell in which the highest stresses occur. Stress evaluation sections are provided at the center and edge of each end plate, as well as at intermediate locations. Stress evaluation sections are also provided in the shell cavity region and in the shell end regions at the junction of the end plates. The stresses in all canister shell partial penetration welds are also evaluated using the finite element analysis results. The top outer closure weld, which is discretely modeled, is evaluated using section stresses as described above. All other canister shell partial penetration weld connections are modeled by coupling the nodes of the connected components at the location of the weld. For these welds, the weld shear stress and membrane stress intensity are calculated based on the nodal forces from the finite elements solution. The weld shear stress is calculated as the resultant nodal force divided by the minimum effective weld throat and the primary membrane stress intensity is equal to twice the shear stress.

For the canister shell structural evaluation performed using the three-dimensional half-symmetry model described in Section 3.9.2.2, the linearized stresses are evaluated at all locations on the lower half of the shell. The shear stress and membrane stress intensity in the inner closure weld, which is modeled as a pinned connection between the inner closure plate and cylindrical shell, are calculated using the nodal forces, as described above.

3.9.3.2 Canister Shell Stress Classifications

The stresses in the canister shell confinement components are classified in accordance with Article NB-3217 and Table NB-3217-1 of Subsection NB of the ASME Code. In general, the linearized membrane stress intensity at each section of the canister shell due to internal pressure and mechanical loads is classified as primary membrane (P_m). The linearized membrane plus bending stress intensity at each canister shell section due to internal pressure and mechanical loads is either classified as primary membrane plus bending (P_m+P_b) or primary plus secondary (P_m+P_b+Q), depending on the location of the stress. The canister shell general thermal stresses due to thermal loading are classified as secondary since these stresses are self-limiting. General thermal stress intensity is taken as the linearized membrane plus bending stress intensity at each section, neglecting peak stress intensity.

As discussed above, the membrane plus bending stress intensity due to internal pressure and mechanical loads is classified as primary plus secondary for certain locations within the canister shell assembly. Specifically, the bending stress at the junction of the shell and head (i.e., end plates) is classified as secondary if the moment restraint provided at the edge of the end plate is not required to maintain the bending stresses in the middle of the plate to acceptable limits (i.e., allowable P_m+P_b stress intensity). This criteria is used for classification of the bending stresses in the top outer closure welds. In order to demonstrate that these stresses can be classified as secondary, the top outer closure plate is evaluated as a simply supported circular plate using hand calculations for all internal pressure and mechanical loads and associated load combinations which produce significant bending stress in the top outer closure plate. The bending stresses in the top outer closure plate is either calculated assuming a uniform pressure load or an annular line load, or both, using the formulas from Table 24 of Roark[32] (cases 9a and 10a). Table 3.9-3 provides a summary of the applied loads, calculated bending stresses, allowable primary plus bending stress intensities, and the associated design margins for each applicable load condition and load combination. The results demonstrate that the moment restraint provided by the top outer closure weld is not required to maintain the bending stresses in the top outer closure plate within primary limits. Therefore, the bending stress in the top outer closure weld is classified as secondary.

3.9.3.3 General and LTP Spacer Plate Stress Evaluation Points

The W74 general and LTP spacer plates are evaluated using the finite element models described in Section 3.9.2.4. The section stresses at all critical spacer plate locations are evaluated for each loading condition. A total of 160 stress sections are considered, as shown in Figure 3.9-20. In general, the section stresses are evaluated at each end of the spacer plate ligaments and at the thinnest ligaments located along the outside edge of the spacer plate.

Section stresses are used to determine the average membrane, linearized membrane plus bending, and total (primary plus secondary plus peak) stress distribution across each section for comparison with the stress limits defined in the ASME Code. Section stresses are determined using the stress linearization routine described in Section 19.4 of the ANSYS User's Theory Manual. For each section, the linearized stresses are determined at the innermost radial position of the section (“I”), the center of the section (“C”), and the outermost radial position of the

[32] Young, W.C., *Roark’s Formulas of Stress and Strain*, Sixth Edition, McGraw-Hill Book Company, 1989.

section ("O"). For analyses which utilize shell elements, linearizations are determined at three additional section locations; the top ("T"), middle ("M"), and bottom ("B") surfaces of the elements.

3.9.4 Canister Closure Weld Critical Flaw Size Determination

The FuelSolutions™ W74 canister closure is described in Section 1.2.1.3 and shown in Figure 1.2-3 of this FSAR. The shell assembly (the canister shell, bottom closure plate, and the top inner and outer closure plates) is designed and fabricated as a Class 1 component pressure vessel in accordance with ASME B&PVC Section III, Subsection NB, to the maximum extent practicable as discussed in Section 2.1.2 of this FSAR. The principal exception is the top end inner and outer closure plate welds to the canister shell which do not meet the provisions of Subsection NB for volumetric examination but do provide redundant sealing of the canister's confinement boundary. As an alternative to the weld examination requirements of Subsection NB, guidance is taken from USNRC ISG-4.[33] In accordance with this criteria, the canister top end closure welds are partial penetration welds that are structurally qualified by analysis using the appropriate weld joint efficiency factor as described in this FSAR chapter, and are progressively ("multi-level") PT examined during canister closure operations in accordance with NB-5350 as defined on the drawings provided in Section 1.5.1 of this FSAR.

In order to assure that the canister closure weld examination requirements specified are adequate to detect a critical flaw, an elastic-plastic fracture mechanics (EPFM) analysis is performed in accordance with the requirements of ASME B&PVC Section XI to determine the critical flaw size for varying magnitudes of weld stress. As a result, the number/distribution of PT examination layers required to assure the absence of an unacceptable flaw size in this weld is determined.

Because not every weld layer is PT examined, there is a small potential that a flaw could extend around the entire circumference of the weld for the depth of the weld between PT examination layers. Though this scenario is highly unlikely, a conservative fracture mechanics model is used to bound any indication. The model selected is an infinitely long part through-wall surface flaw at the inside (root) or outside (top surface) of the weld. This model is conservative in application to the problem at hand because any flaw between the PT examination layers is a subsurface flaw which can be larger than a surface flaw and still meet the requirements of ASME B&PVC Section XI. For completeness, a second model is used to address through-wall flaws in the unlikely event that they are encountered. The EPFM unstable tearing formulation for these two crack models are widely used in the industry[34] and are based on the Ramberg-Osgood stress-strain law.

The material properties for stainless steel welds used in the EPFM unstable tearing analysis including the J-R curves and stress-strain data are taken from the literature.[35] Representative and

---

[33] ISG-4, *Cask Closure Weld Inspections*, Spent Fuel Project Office Interim Staff Guidance-4, United States Nuclear Regulatory Commission, Revision 1, May 21, 1999.

[34] Shih, C.F., et al., *An Engineering Approach for Elastic-Plastic Fracture Analysis*, Electric Power Research Institute (EPRI) Topical Report No. NP-1931, July 1981.

[35] Westinghouse Electric Corporation, *Toughness of Austenitic Stainless Steel Pipe Welds*, EPRI Report No. NP-4768, October 1986.

consistent properties for SMAW and GTAW (TIG) welds are used. Based on the analysis documented in Chapter 4 of this FSAR, the temperature of the canister top end outer closure weld is expected to be a maximum of 250°F and a minimum of -40°F. The stress-strain and J-R curve parameters for the GTAW and SMAW weld are determined for these two temperatures and conservatively used in this analysis.

For a linear indication along the circumference of the canister closure weld, the stress component that causes flaw/crack extension is the radial stress. The allowable flaw sizes are determined for a range of radial stress levels for both normal operating and accident conditions. Consistent with ASME B&PVC Section XI methodology, a safety factor of 3 is used for normal operating conditions and 2 is used for accident conditions to determine the allowable flaw size. In the EPFM unstable tearing analysis, the J-Integral/Tearing Modulus approach is used to determine the allowable flaw size. In doing so, the material J-R curve is translated into a material J-T curve with plots increasing load (at a given flaw size) or increasing flaw size (at a given load). The resulting applied load J-T curve vs. material J-T curve are then used to determine the predicted flaw size at instability. This value is then used to calculate the critical flaw size ratio. Since the stresses used in the analyses include the prescribed ASME BPVC Section XI safety factor, the resulting crack size is thus the acceptable flaw size for the weld.

The results of the EPFM unstable tearing analyses establish the following FuelSolutions™ top end outer closure weld allowable flaw sizes for upper-end radial stress conditions per ASME B&PVC Section XI requirements:

1. 360° long inner or outer surface flaws could have acceptable depths ranging from 0.19” to 0.49” and 0.10” to 0.47” in welds applied using either the GTAW or SMAW processes, respectively, for varying magnitudes of normal operating condition stress.
2. 360° long inner or outer surface flaws could have acceptable depths ranging from 0.27” to 0.56” and 0.19” to 0.47” in welds applied using either the GTAW or SMAW processes, respectively, for varying magnitudes of accident condition stress.
3. 100% through-wall flaws would have to be over 100” to 180” and over 40” to 180” in acceptable circumferential length in welds applied using either the GTAW or SMAW processes, respectively, for varying magnitudes of normal operating condition stress.
4. 100% through-wall flaws would have to be over 120” to 180” and over 78” to 180” in acceptable circumferential length in welds applied using either the GTAW or SMAW processes, respectively, for varying magnitudes of accident condition stress.

The following conservatisms are inherent to the acceptable flaw depths presented above:

1. Even though the PT examination of the root and cover layers assures that there are no surface flaws in the weld, the analytical models used to calculate the acceptable flaw depths assume the flaws are indeed surface flaws. As recognized by ASME BPVC Section XI, depending on the location of a subsurface flaw relative to the thickness of the weld, the acceptable flaw size for a subsurface flaw can increase by as much as a factor of 2.
2. Even though PT examination of the root and cover layers assures that there are no 100% through-wall flaws, the analytical models used demonstrate the ability of the weld to

sustain 100% through-wall flaws with significant lengths (> 90° of the circumferential weld length).

Based on the critical flaw size evaluation described above, it can also be concluded that:

1. For welds applied using the GTAW process, root, intermediate, and cover PT examinations adequately assure that there are no flaws that are unacceptable per ASME B&PVC Section XI requirements for nominal normal operating stress magnitudes of up to approximately 10 ksi and nominal accident condition stress magnitudes of up to approximately 22 ksi.
2. For welds applied using the SMAW process, root, intermediate, and cover PT examinations adequately assure that there are no flaws that are unacceptable per ASME BPVC Section XI requirements for nominal normal operating stress magnitudes of up to approximately 7 ksi and nominal accident condition stress magnitudes of up to approximately 14 ksi.
3. The location of the proposed intermediate level PT examination is established as the middle layer between the root and cover PT examination layers of their associated 3/4" nominal (5/8" minimum) thickness depositions. This approach is consistent with ASME BPVC Section III, Paragraph NB-5200 which only requires progressive surface examinations to be performed at the "lesser of one-half of the maximum welded joint dimension measured parallel to the center line of the connection or ½ in." for some partial penetration joint configurations.

Based on the top end outer closure weld primary stresses for normal conditions presented in Table 3.5-6 for axisymmetric load cases and for all accident conditions presented in Table 3.7-11 through Table 3.7-15, the above conditions for root, intermediate and cover PT examination are met. Therefore, the guidance provided in ISG-4 is met for the FuelSolutions™ W74 canister outer closure plate weld to the canister shell with the weld examination requirements specified on the drawings in Section 1.5.1 of this FSAR.

Table 3.9-1 - W74M Lower Basket Assembly Spacer Plate In-Plane Tributary Weights

Spacer Plate No.	Longitudinal Position(1) (inches)	Spacer Plate Thickness (inches)	Tributary Length (inches)	Tributary Weight (lb.)					Total Tributary Weight (lb.)
				Spacer Plate	Fuel Ass'y(1)	Guide Tube	Support Tube(1)	Damaged Fuel (2)	
1	2.00	2.00	3.63	629	581	94	112	117	1,533
2	4.63	0.75	3.63	230	581	94	123	117	1,145
3	9.88	0.75	5.50	230	881	143	189	178	1,621
4	15.63	0.75	5.88	230	941	153	203	190	1,716
5	21.63	0.75	6.00	230	961	156	207	194	1,748
6	27.63	0.75	6.56	230	1,051	171	227	212	1,891
7	34.75	0.75	7.13	230	1,141	186	247	230	2,034
8	41.88	0.75	7.13	230	1,141	186	247	230	2,034
9	49.00	0.75	7.13	230	1,141	186	247	230	2,034
10	56.13	0.75	7.13	230	1,141	186	247	230	2,034
11	63.25	0.75	7.13	230	1,141	186	247	230	2,034
12	70.38	0.75	7.13	230	1,141	186	247	230	2,034
13	77.50	0.75	5.88	230	941	153	203	190	1,716
14	82.75	2.00	5.49	629	879	143	178	177	2,006

Notes:

(1) Longitudinal distance from bottom end of lower basket assembly support tubes to the spacer plate centerline.

(2) The support tube assembly weights include the support tubes and support sleeves.

(3) Weight of damaged fuel plus SNF fuel in support tubes.

Table 3.9-2 - W74M Upper Basket Assembly Spacer Plate In-Plane Tributary Weights

Spacer Plate No.	Longitudinal Position[1] (inches)	Spacer Plate Thickness (inches)	Tributary Length (inches)	Tributary Weight (lb.)					Total Tributary Weight (lb.)
				Spacer Plate	Fuel Ass'y[1]	Guide Tube	Support Tube[1]	Damaged Fuel [2]	
1	4.75	2.00	5.63	629	901	146	183	182	2,041
2	9.88	0.75	5.81	230	931	151	200	188	1,701
3	17.00	0.75	7.13	230	1,141	186	247	230	2,034
4	24.13	0.75	7.13	230	1,141	186	247	230	2,034
5	31.25	0.75	7.13	230	1,141	186	247	230	2,034
6	38.38	0.75	7.13	230	1,141	186	247	230	2,034
7	45.50	0.75	7.13	230	1,141	186	247	230	2,034
8	52.63	0.75	6.94	230	1,111	181	240	224	1,986
9	59.38	0.75	6.50	230	1,041	169	225	210	1,875
10	65.63	0.75	6.13	230	981	159	212	198	1,780
11	71.63	0.75	5.88	230	941	153	203	190	1,716
12	77.38	0.75	5.63	230	901	146	194	182	1,653
13	82.88	0.75	3.50	230	561	91	118	113	1,113
14	85.00	2.00	3.68	629	589	96	113	119	1,545

Notes:

(1) Longitudinal distance from bottom end of upper basket assembly support tubes to the spacer plate centerline.

(2) The support tube assembly weights include the support tubes and support sleeves.

(3) Weight of damaged fuel plus SNF fuel in support tubes.

Table 3.9-3 - Canister Shell Top Outer Closure Plate Bending Stresses with No Edge Moment Restraint

Load Condition or Load Combination	Uniform Pressure Load (psi)	Annular Line Load (lb/in.)	Maximum Bending Stress (ksi)	Allowable Bending S.I. (ksi)	Design Margin
Vertical Dead Weight (D_v)	0.6	0	0.2	30.0	+Large
Normal Internal Pressure (P)	10	0	3.2	30.0	+8.28
Vertical Transfer (L_{hv})	0	532	2.8	30.0	+9.79
Normal Horizontal Transfer ($L_{hh1)}$	0	895	11.1	30.0	+1.70
Off-Normal Internal Pressure (P_o)	16	0	5.2	36.0	+5.96
Misalignment Horiz. Transfer (L_m)	0	1,392	17.3	36.0	+1.08
Accident Internal Pressure (P_a)	69	0	22.3	69.3	+2.11
Storage Cask End Drop (A_s)	29	0	9.4	69.3	+6.37
L.C. A2 (D_v + P + T)	9.4	0	3.0	30.0	+8.87
L.C. A4 (D_v + L_{hv} + P + T)	10	532	6.0	30.0	+3.99
L.C. A5 (D_h + L_{hh1} + P + T)	10	895	14.3	30.0	+1.09
L.C. C1 (D_v + P_o + T_o)	15.4	0	5.0	36.0	+6.23
L.C. C2 (D_v + L_{hv} + P_o + T_o)	16	532	8.0	36.0	+3.53
L.C. C3 (D_h + L_{hh1} + P_o + T_o)	16	895	16.3	36.0	+1.21
L.C. C4 (D_h + L_m + P + T)	10	1,392	20.5	36.0	+0.75
L.C. D1 (D_v + L_{hv} + P_a + T_o)	69	532	25.1	69.3	+1.76
L.C. D2 (D_h + L_{hh1} + P_a + T_o)	69	895	33.4	69.3	+1.07
L.C. D3 (P_o + T + A_s)	13	0	6.2	69.3	+10.2

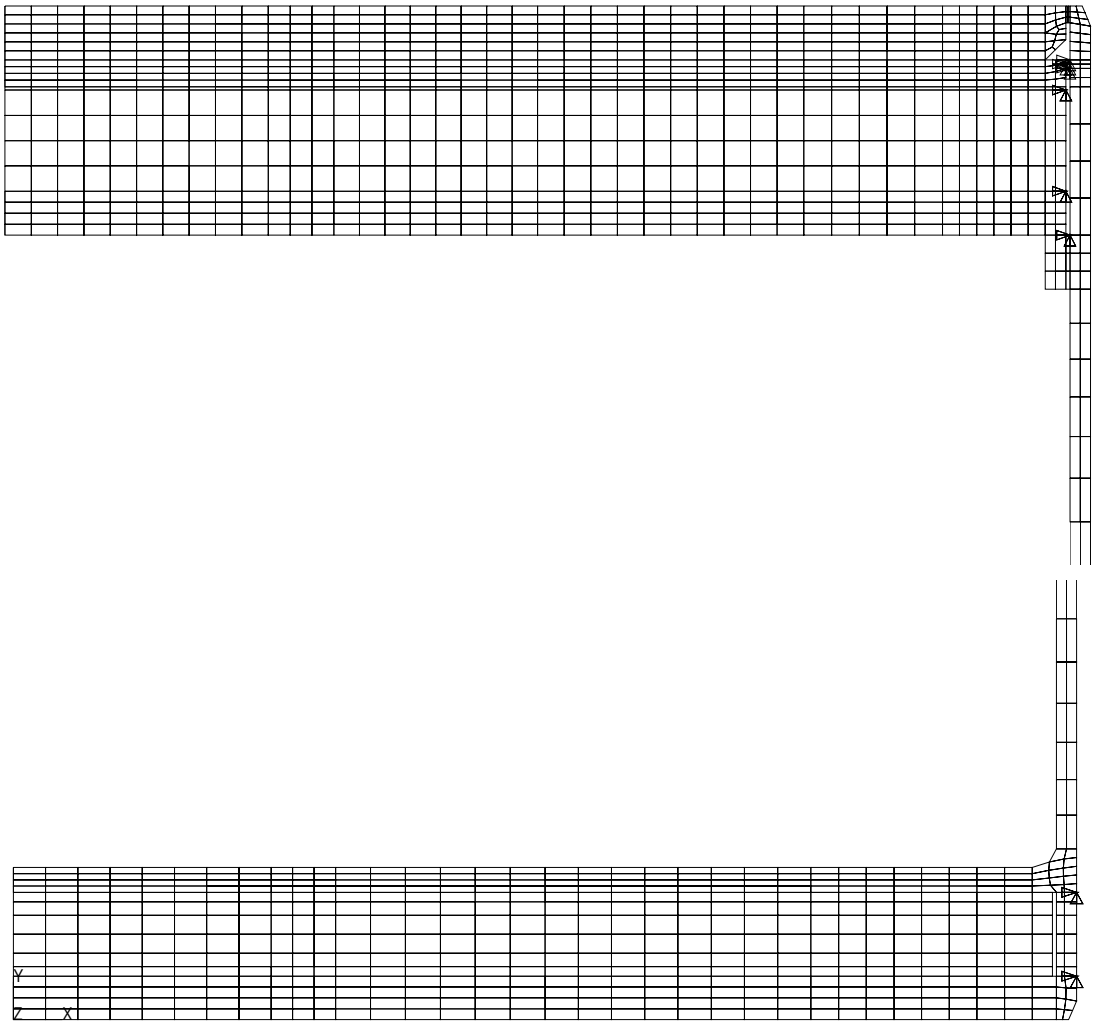

Figure 3.9-1 - Bounding Canister Shell Assembly Axisymmetric Finite Element Model

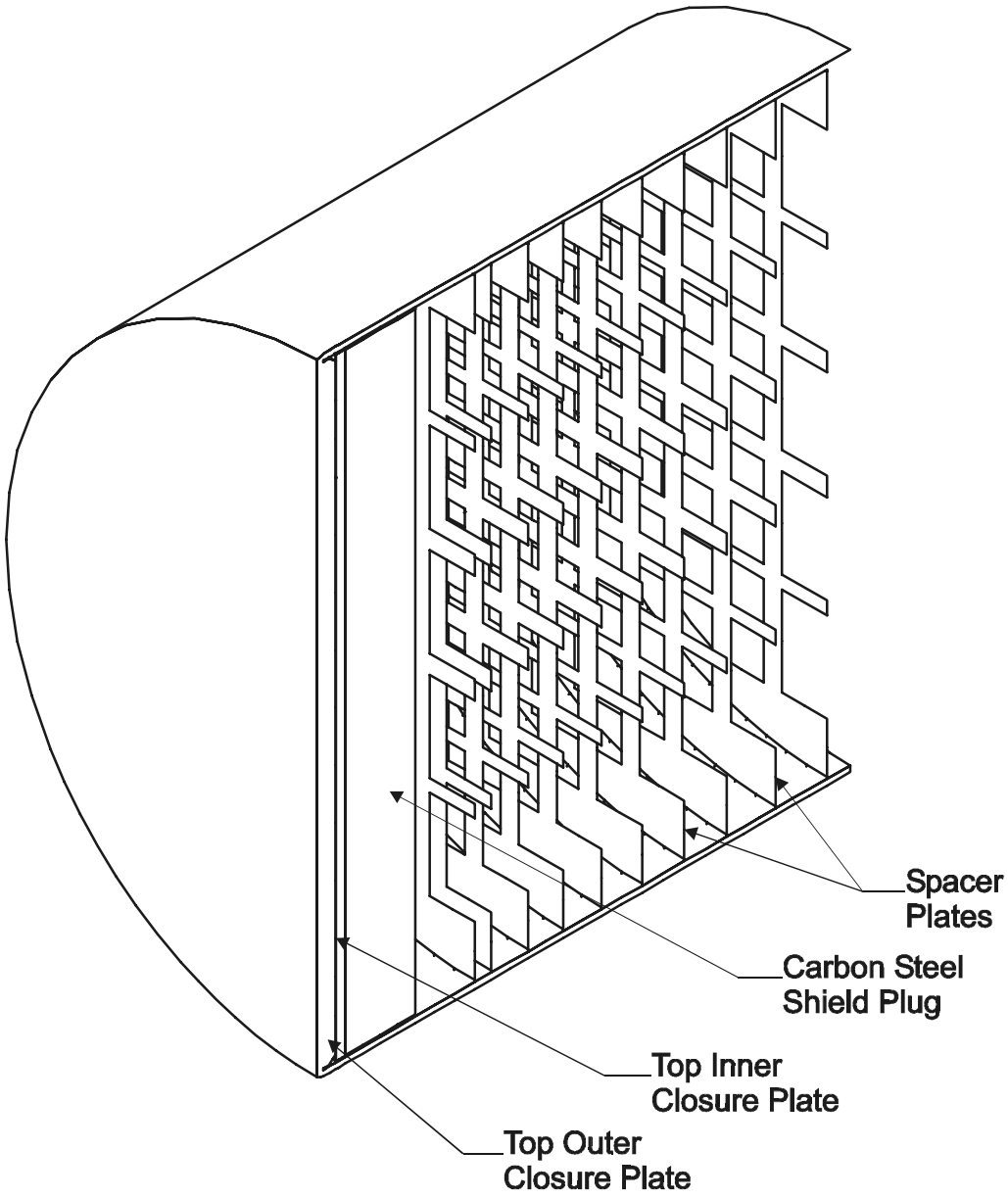

Figure 3.9-2 - Canister Shell Half-Symmetry Finite Element Model

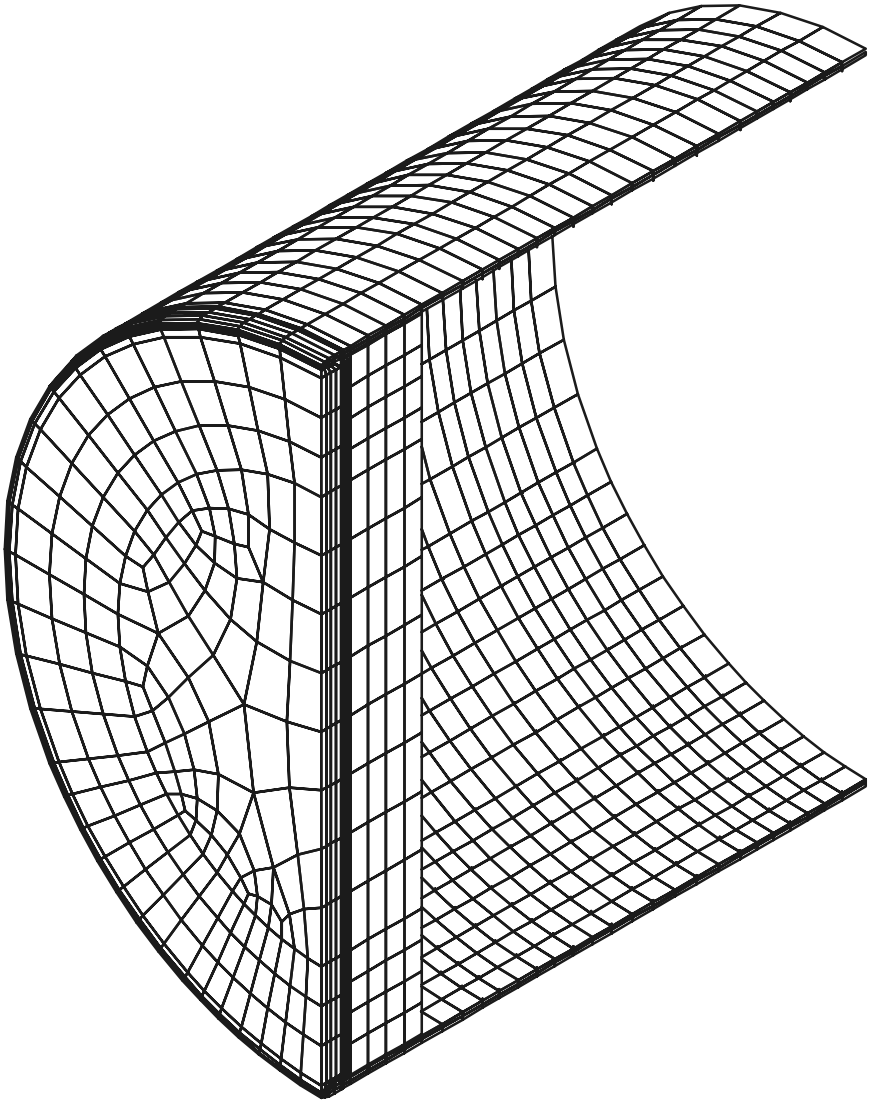

Figure 3.9-3 - Canister Shell Assembly Half-Symmetry Finite Element Model, Shell Assembly Mesh

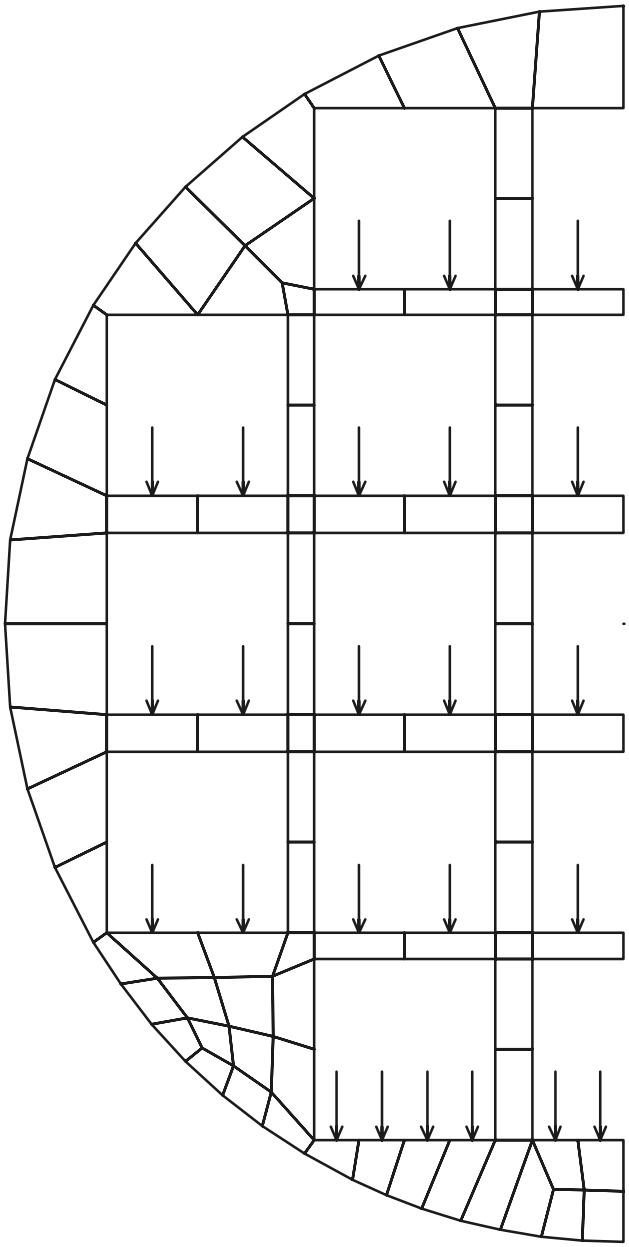

Figure 3.9-4 - Canister Shell Assembly Half-Symmetry Finite Element Model - Spacer Plate Mesh and Loading

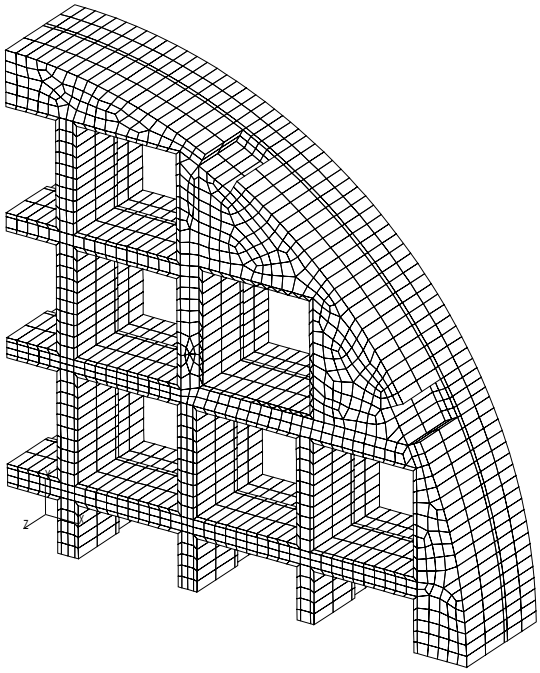

View from Bottom

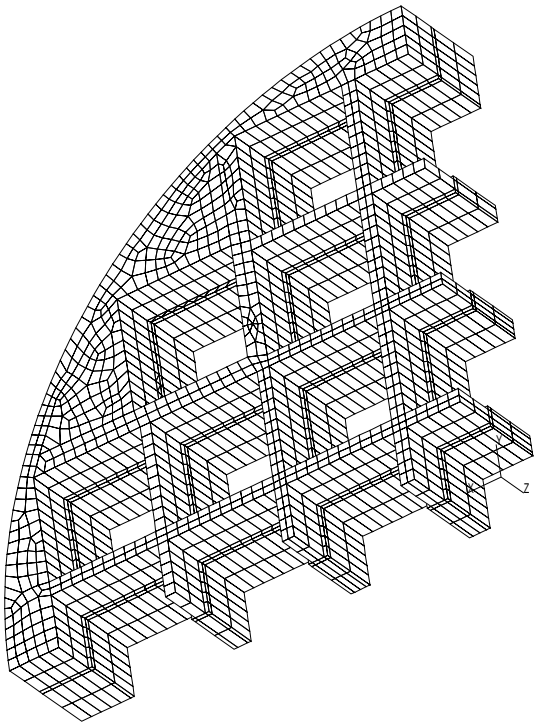

View from Top

Figure 3.9-5 - W74 Top Shield Plug Assembly Quarter-Symmetry Vertical Deadweight Finite Element Model

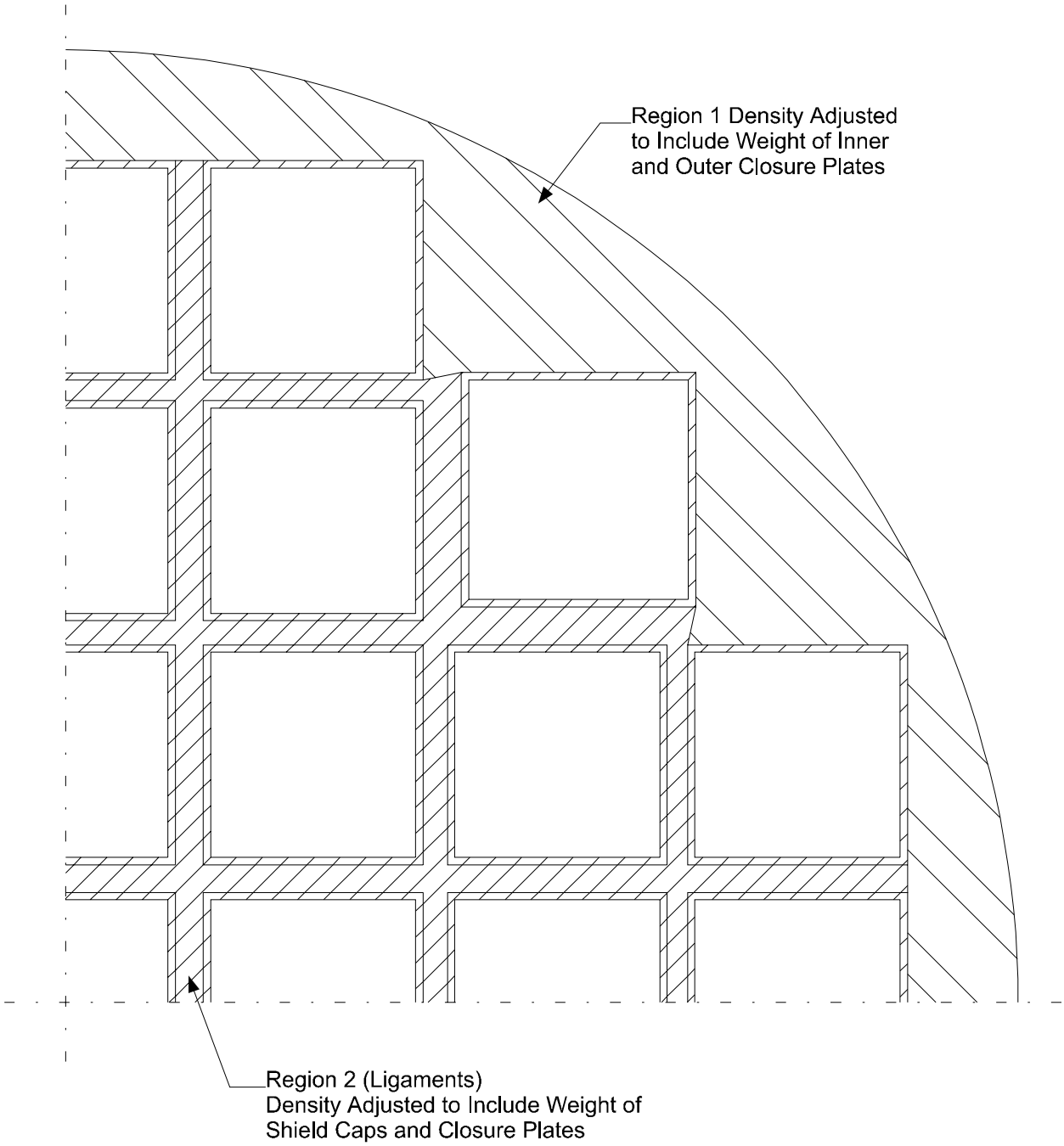

Figure 3.9-6 - W74 Top Shield Plug Quarter-Symmetry Model Adjusted Density Regions

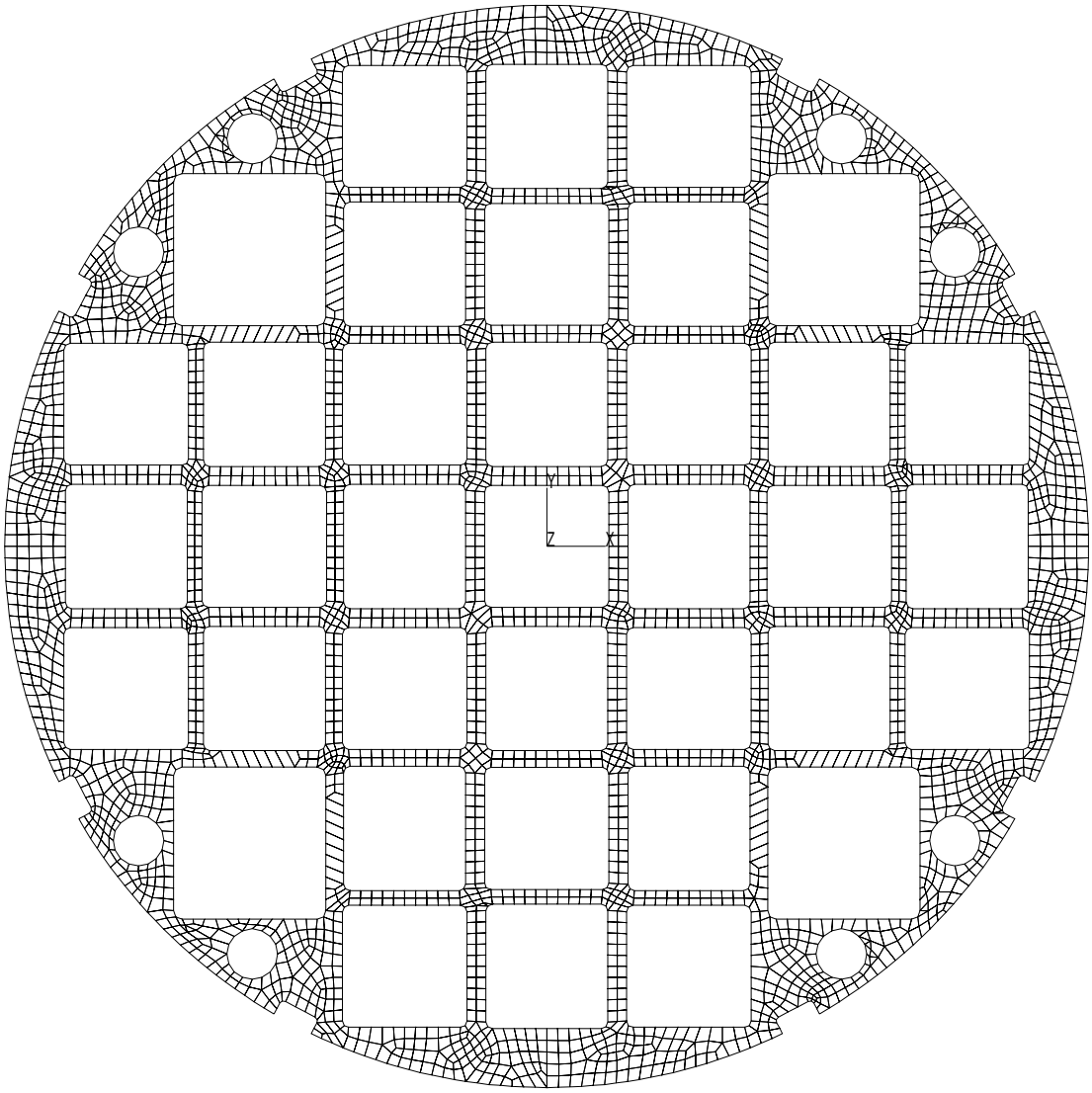

Figure 3.9-7 - W74 Canister General and LTP Spacer Plate Plane Stress Finite Element Model

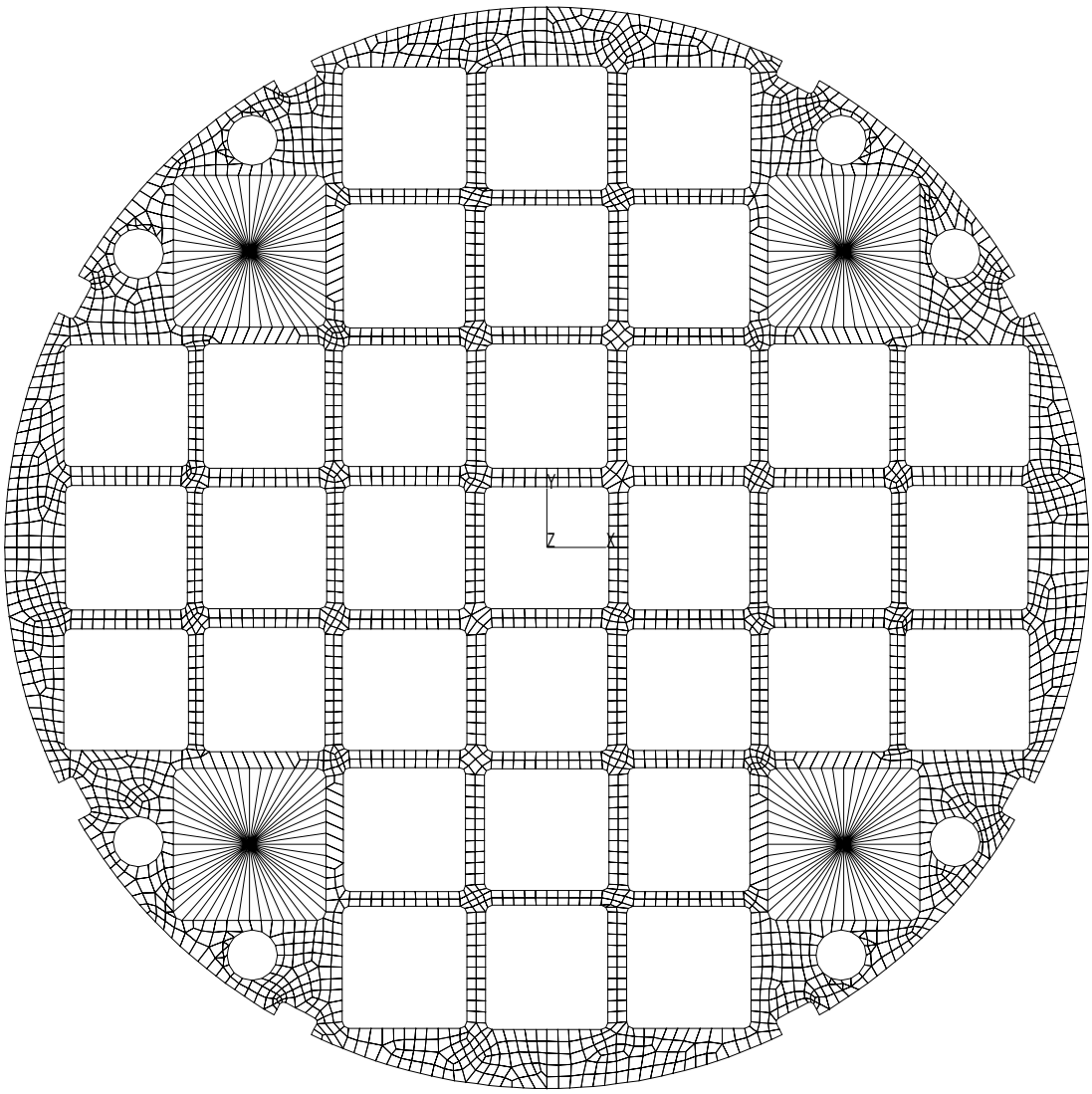

Figure 3.9-8 - W74 Canister General and LTP Spacer Plate Shell Model for Thermal Bending Stress Analysis

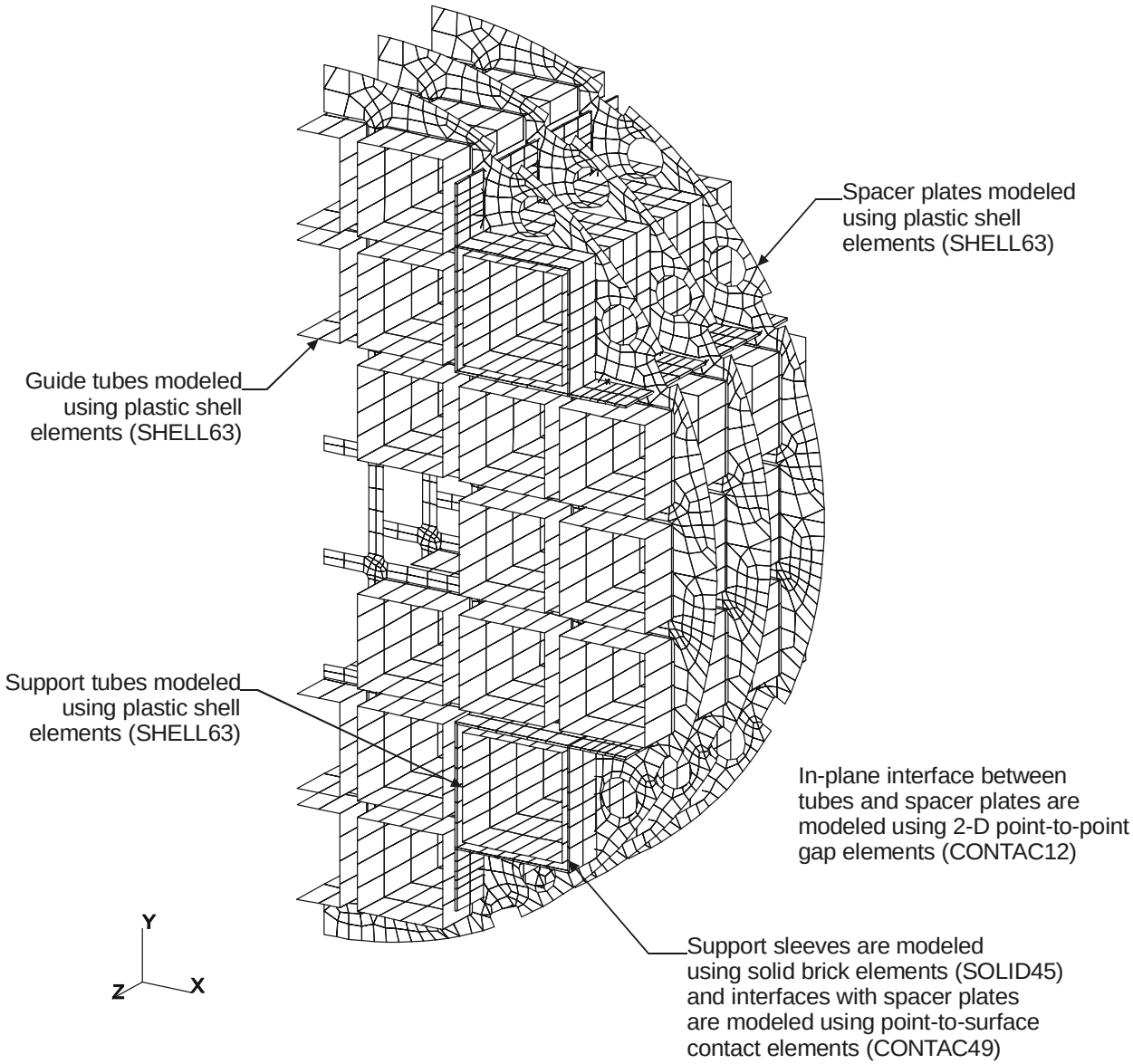

Figure 3.9-9 - W74 Canister General Spacer Plate Half-Symmetry Multi-Span Shell Model for Tip-Over and 0° Side Drop Plastic Instability Analyses

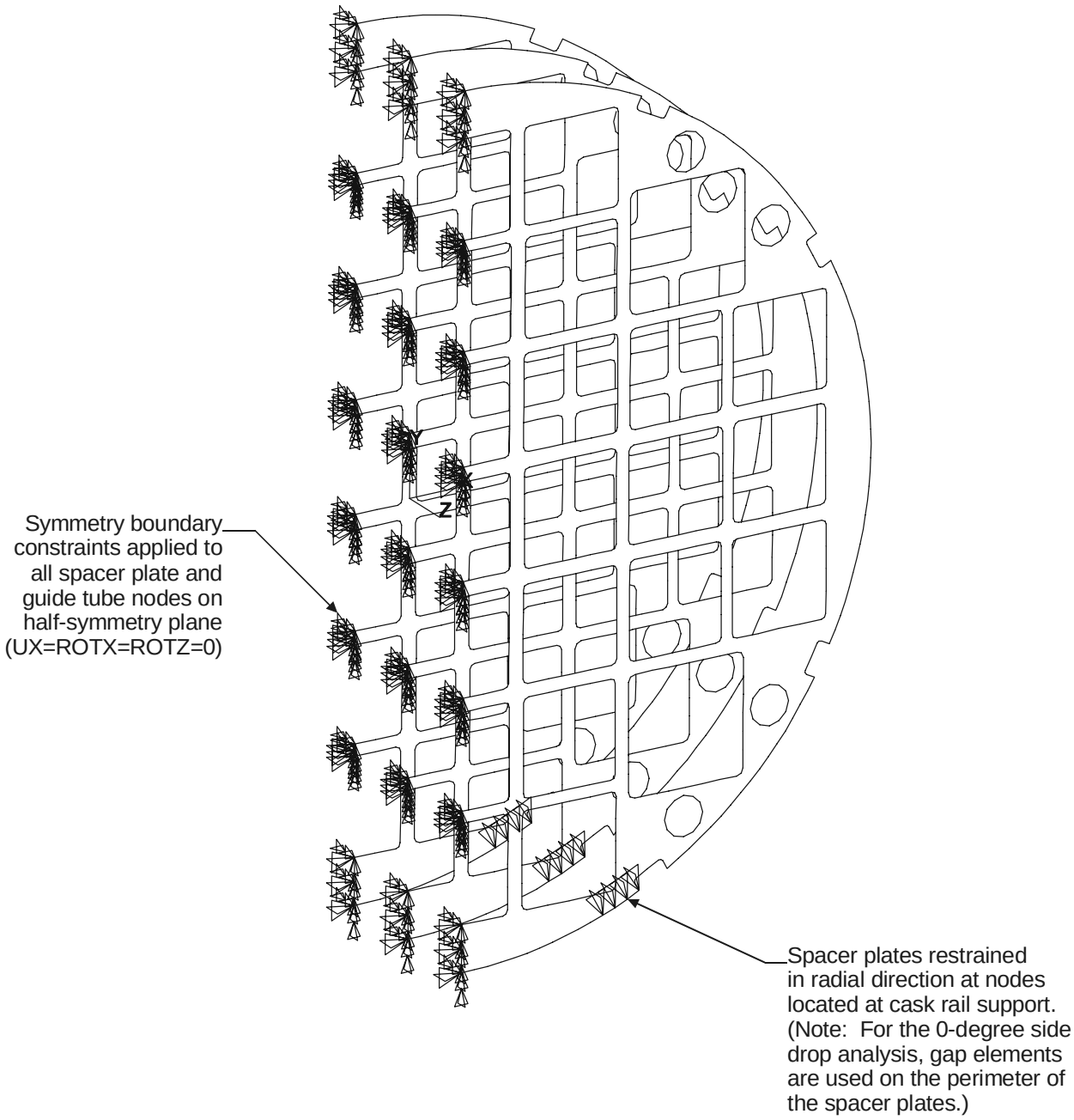

Note: For clarity, guide tubes not shown

Figure 3.9-10 - W74 General Spacer Plate Half-Symmetry Multi-Span Shell Finite Element Model Boundary Conditions

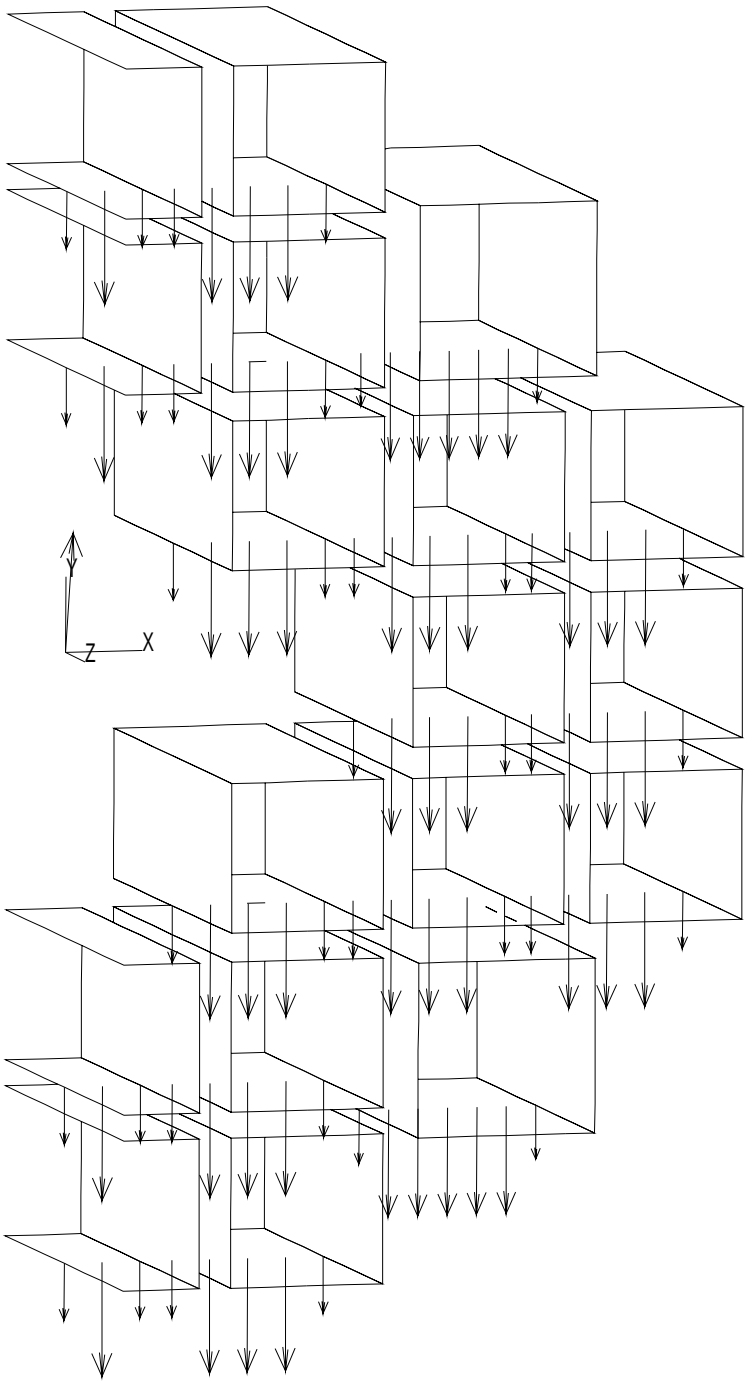

Note: For clarity, spacer plates not shown

Figure 3.9-11 - W74 General Spacer Plate Half-Symmetry Multi-Span Shell Finite Element Model Applied Loads

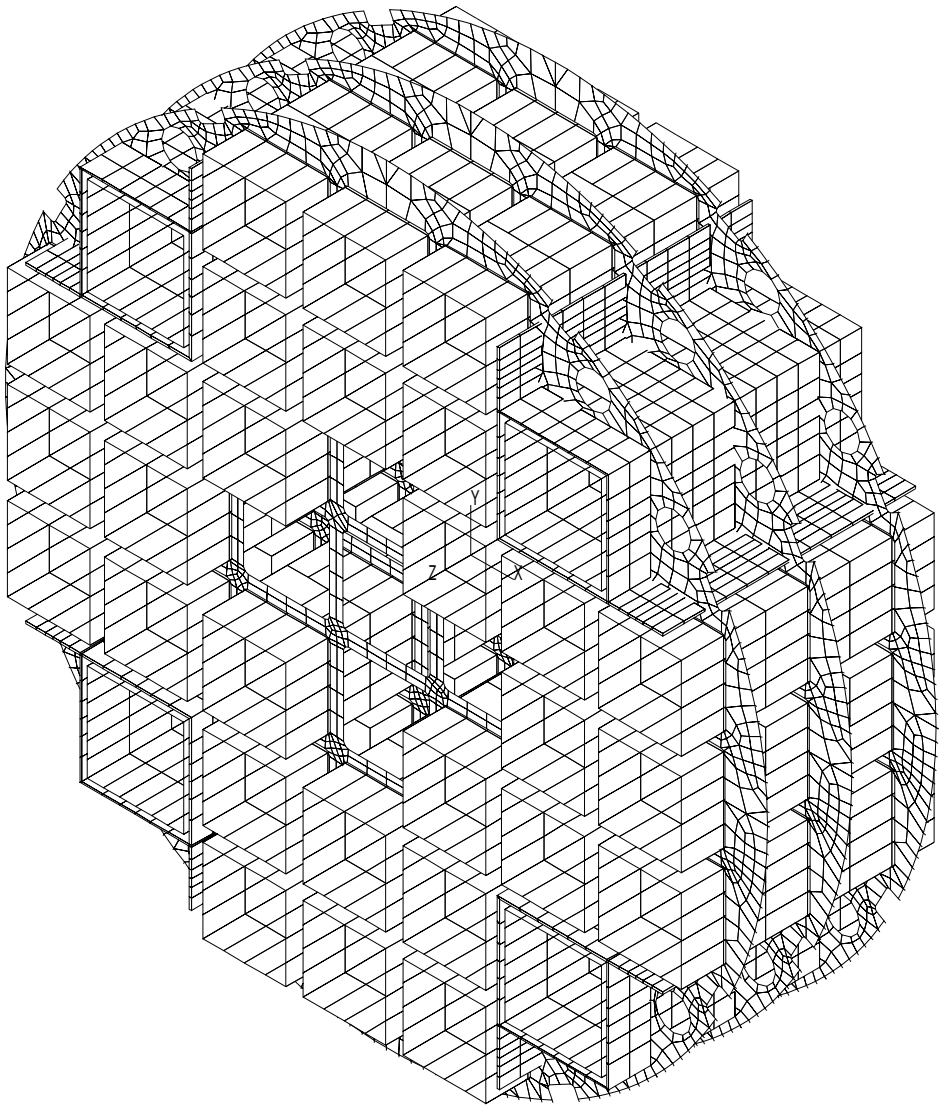

Figure 3.9-12 - W74 General Spacer Plate Full Multi-Span Shell Finite Element Model for 45° Side Drop Plastic Instability Analysis

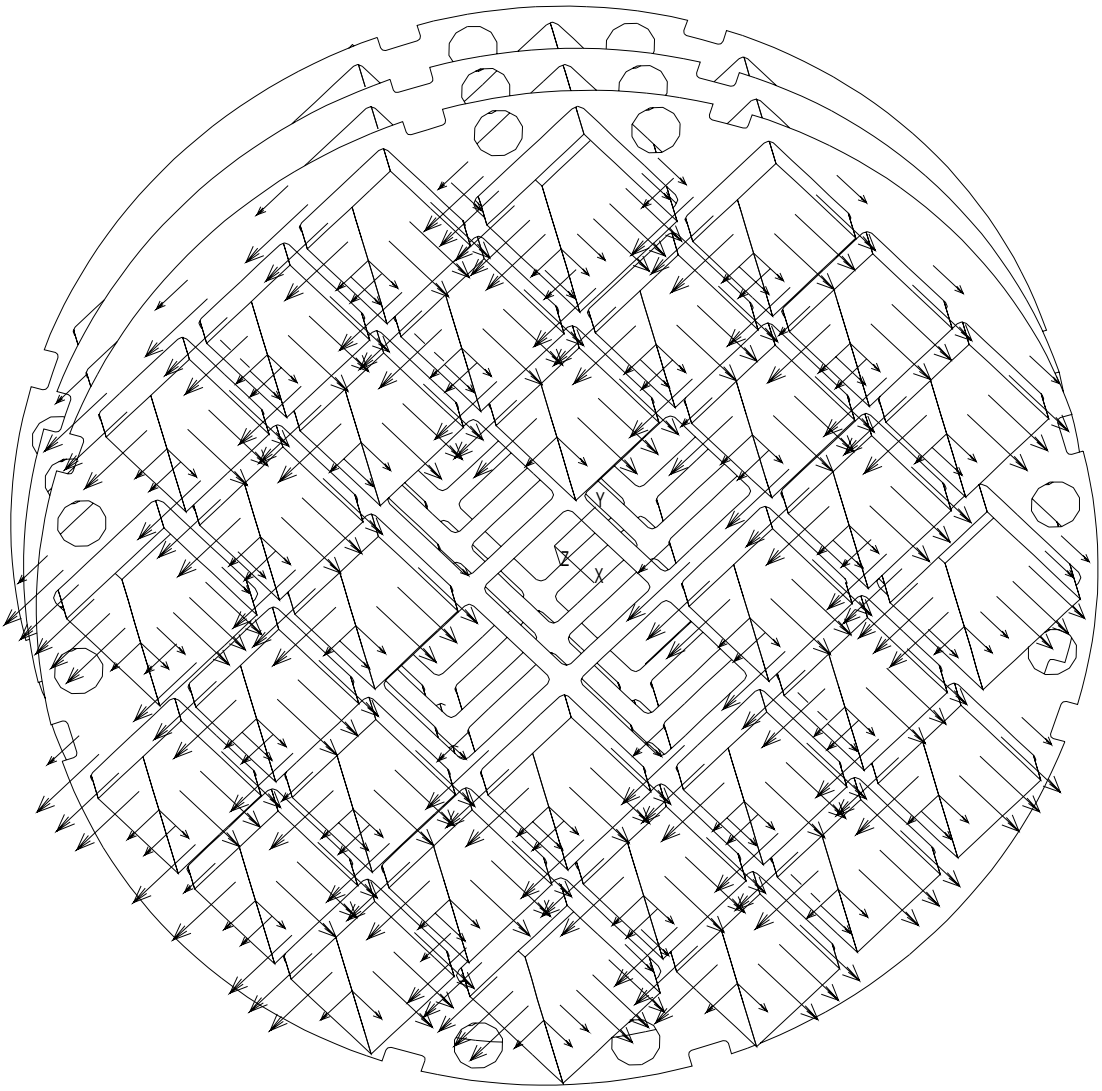

Figure 3.9-13 - W74 General Spacer Plate Full Multi-Span Shell Finite Element Model Applied Loads for 45° Side Drop

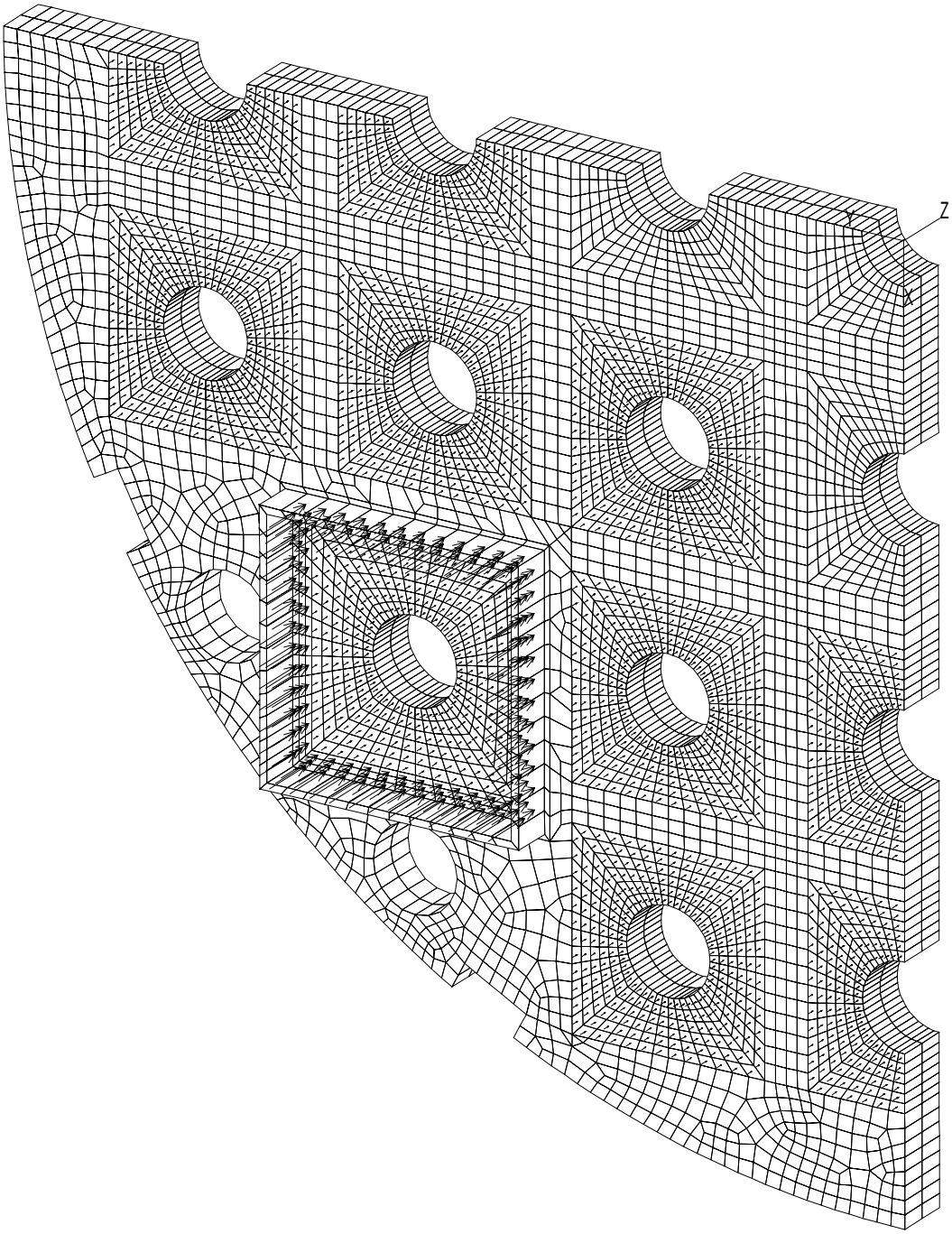

Figure 3.9-14 - W74 Engagement Spacer Plate Bottom End Drop Quarter-Symmetry Finite Element Model

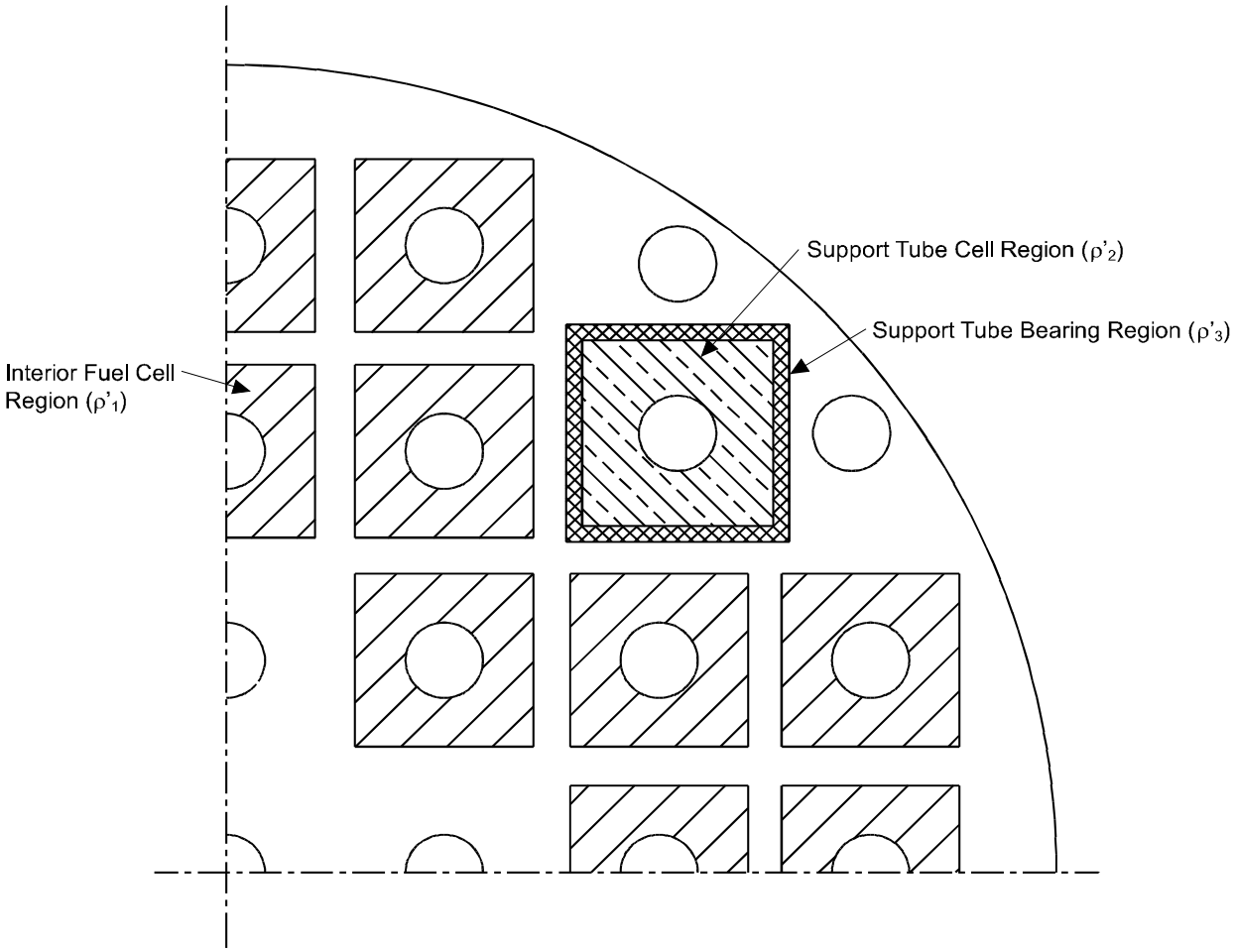

Figure 3.9-15 - W74 Engagement Spacer Plate End Drop Loading Regions

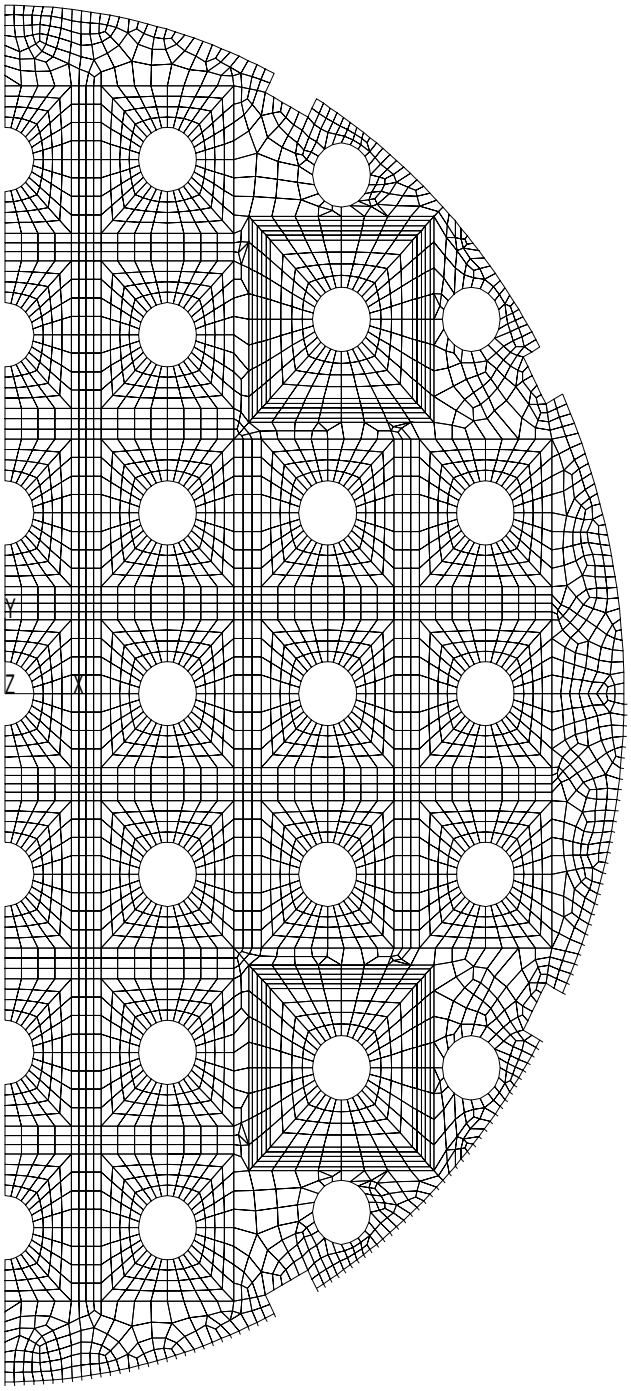

Figure 3.9-16 - W74 Engagement Spacer Plate Half-Symmetry Plane Stress Finite Element Model

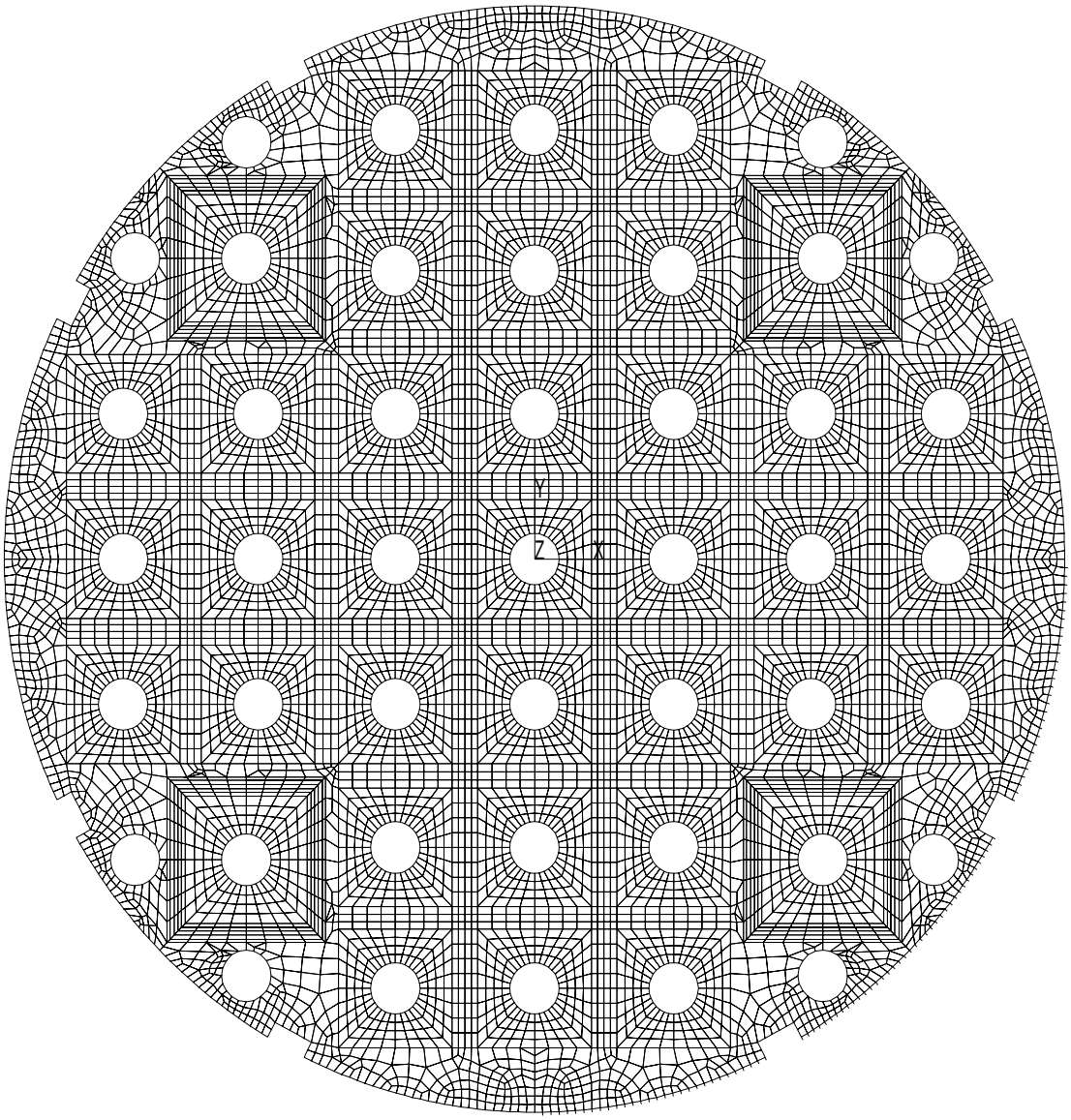

Figure 3.9-17 - W74 Engagement Spacer Plate Full Plane Stress Finite Element Model

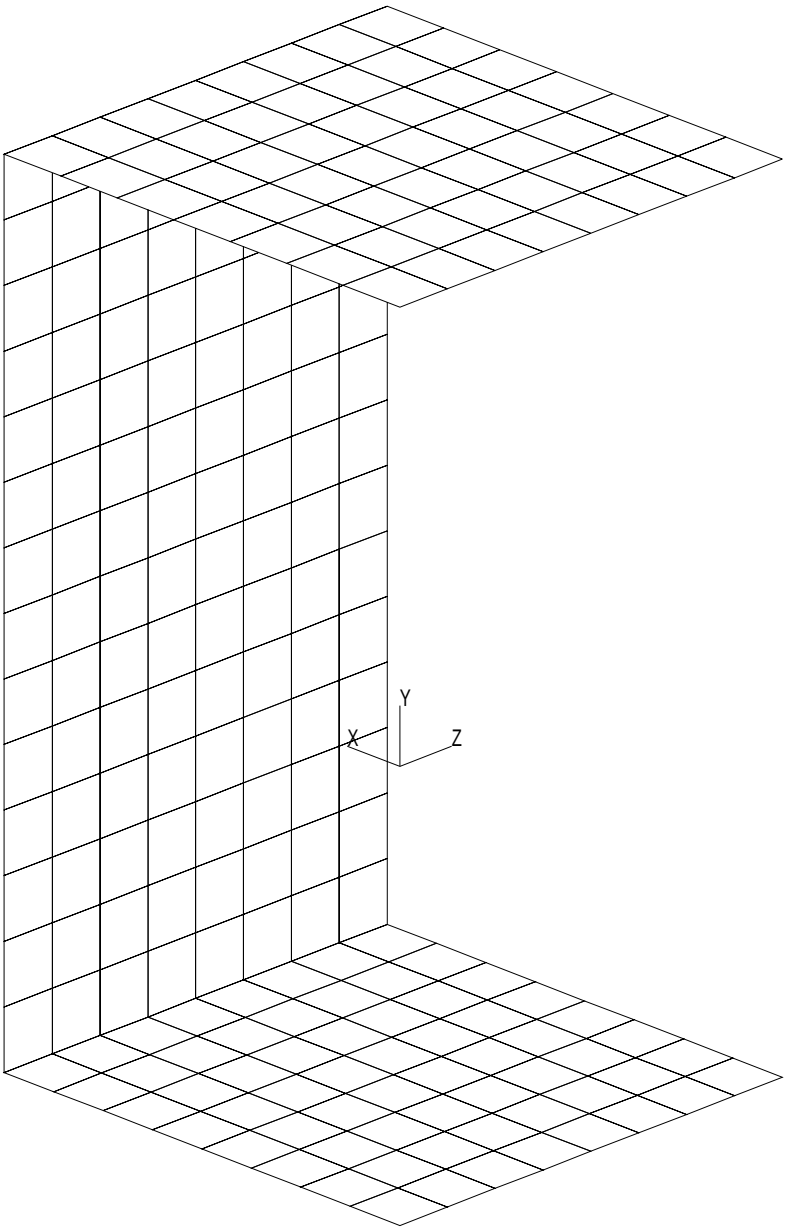

Figure 3.9-18 - W74 Guide Tube Half-Symmetry Single Span Finite Element Model

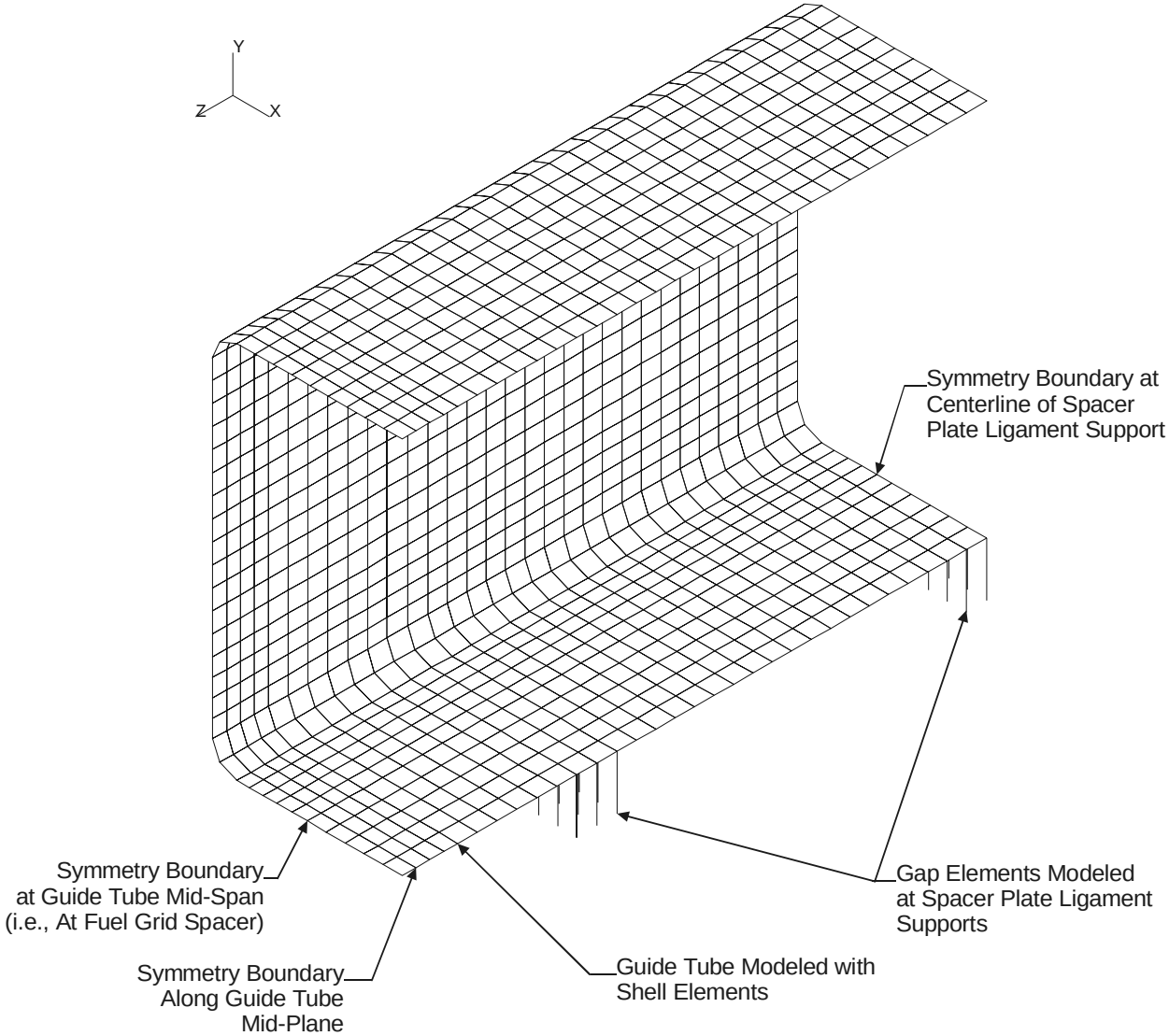

Figure 3.9-19 - W74 Guide Tube Half-Symmetry Multi-Span Finite Element Model

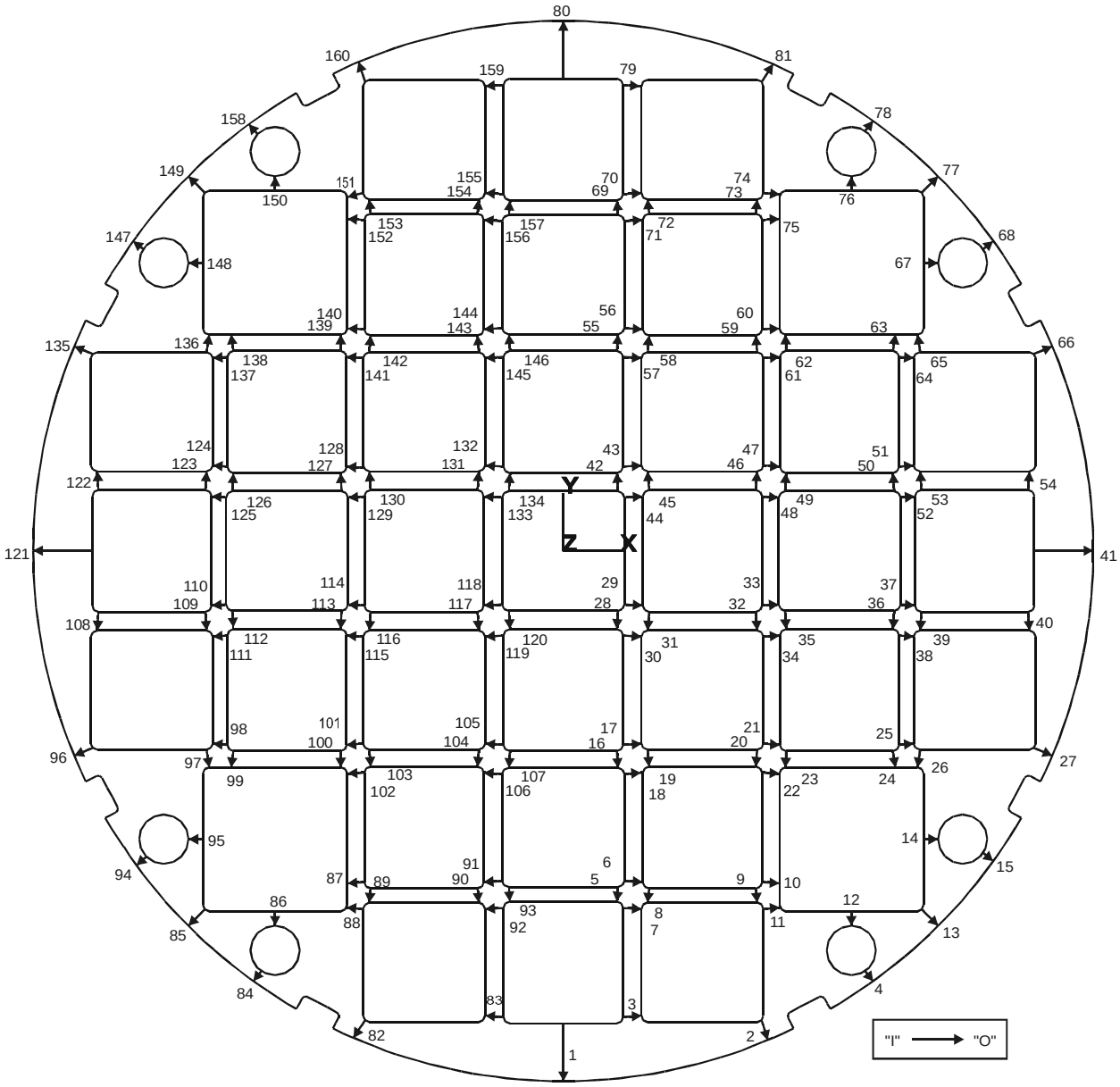

Figure 3.9-20 - W74 General and LTP Spacer Plate Stress Evaluation Sections

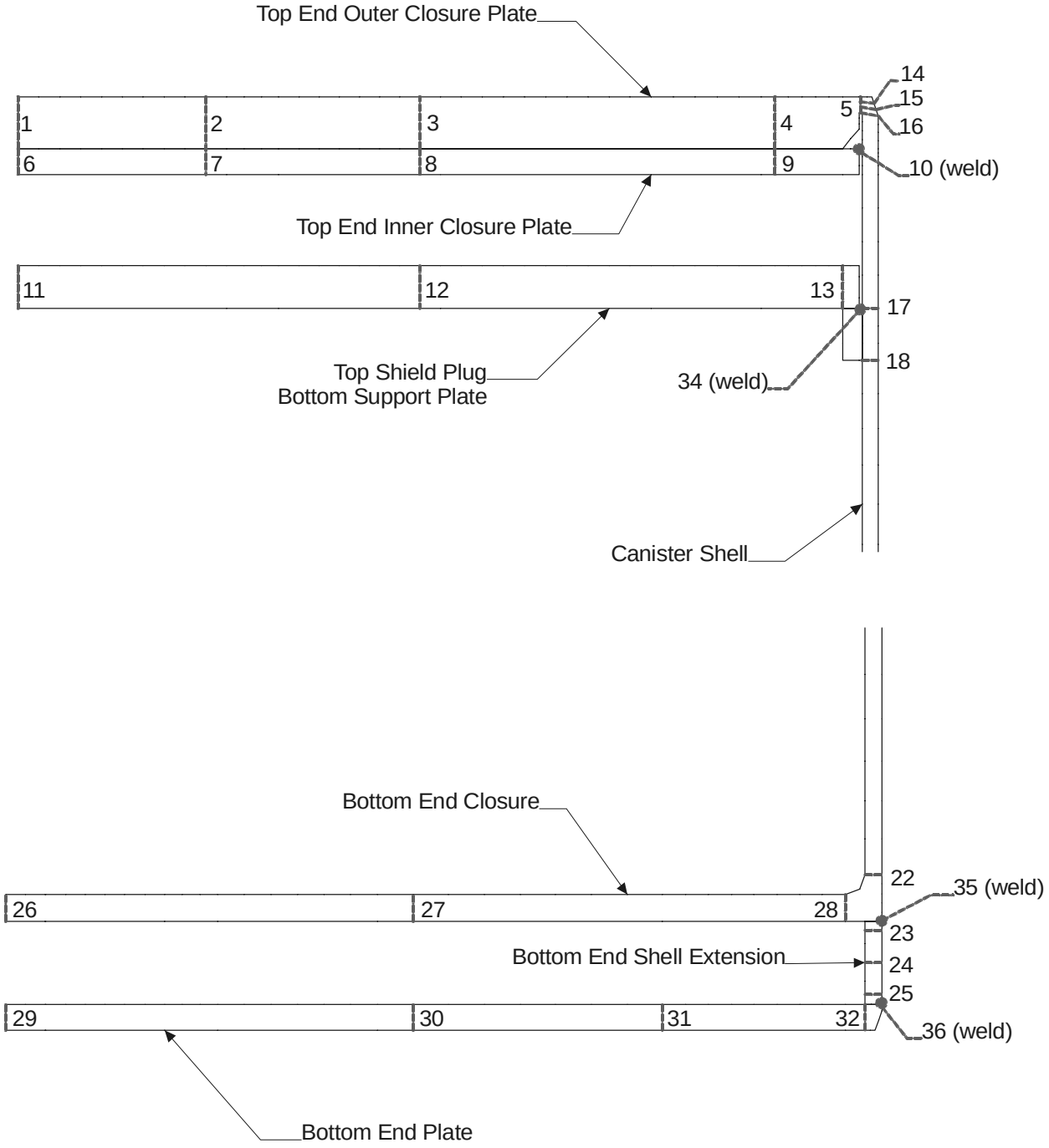

Figure 3.9-21 - Canister Shell Stress Evaluation Locations, Top and Bottom End Region

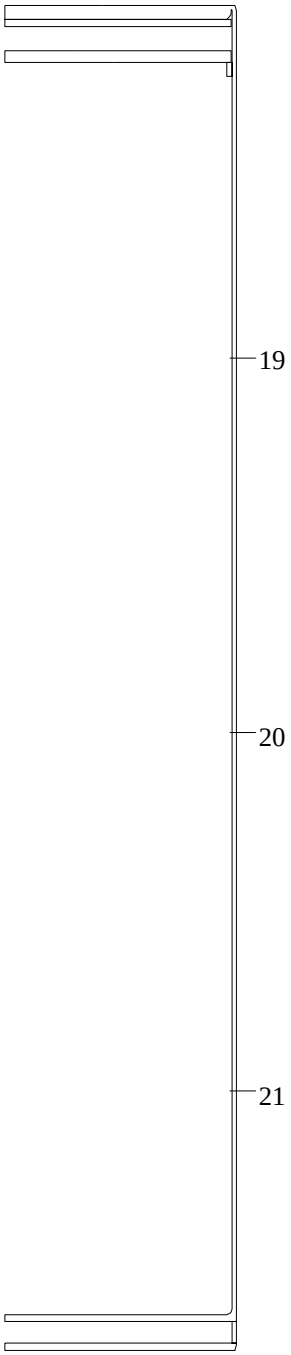

Figure 3.9-22 - Canister Shell Stress Evaluation Locations, Cavity Region

This page intentionally left blank.

4. THERMAL EVALUATION

This chapter presents the thermal evaluations which demonstrate that the FuelSolutions™ W74 canister meets the thermal requirements of 10CFR72,[1] as defined in Section 2.3 of this FSAR, for dry storage of SNF when used as an integral part of the FuelSolutions™ Storage System. The FuelSolutions™ W74 canister is designed to provide confinement of SNF assemblies during transfer and storage within the FuelSolutions™ W100 Transfer Cask and the W150 Storage Cask. The thermal design and safety evaluation for the FuelSolutions™ transfer and storage casks are provided in Chapter 4 of the FuelSolutions™ Storage System FSAR. The thermal evaluation of the FuelSolutions™ W74 canister is compared with the results presented in the FuelSolutions™ Storage System FSAR to assure that the thermal interface criteria for the transfer and storage casks in Section 2.2 and Chapter 4 of that FSAR are met.

As presented in this chapter, the FuelSolutions™ W74 canister is evaluated to assure that the thermal performance of the combined canister and cask system complies with the regulatory safety requirements during all credible normal, off-normal, and postulated accident conditions. The maximum thermal ratings for the FuelSolutions™ W74 canister are established based on the applicable allowable temperatures for the materials of fabrication for the canister, casks, and for the SNF assembly cladding. This assures that the canister/cask component temperatures are maintained below their respective allowable temperatures throughout transfer and dry storage operations and that the fuel cladding is protected against degradation and gross ruptures. The maximum thermal ratings for the FuelSolutions™ storage and transfer casks envelope those determined for the FuelSolutions™ W74 canister herein. A W74 canister may not be loaded in the storage cask or transfer cask unless the total canister heat load is bounded by the thermal ratings of both the storage and transfer casks. In this manner, the thermal safety of both the canister and the casks is assured.

It should be noted that the heat load generated by the SNF assemblies within the canister on either the storage cask or the transfer cask is represented by a bounding axial heat flux distribution that envelopes the heat load arising from any SNF assembly class and type that can be accommodated by any of the FuelSolutions™ canister subsystems described in Section 4.1.3 of the FuelSolutions™ Storage System FSAR. The heat load for the W74 canister is represented by a bounding axial heat flux for the Big Rock Point fuel assemblies. This bounding heat flux simulates both the axial variation in decay heat from each of the loaded fuel assemblies and the presence of upper and lower basket assemblies. In this manner, the thermal qualification of the W74 canister is decoupled from the qualification and licensing of the W150 storage cask, W100 transfer cask, and other FuelSolutions™ canisters.

The thermal evaluations presented herein for the W74 canister within the transfer and storage casks for the design basis thermal load conditions are accomplished using both steady-state and transient analyses. These thermal load conditions, defined in Section 2.3 of this FSAR, envelope the thermal conditions expected during all normal and off-normal operations and postulated accident conditions within the transfer and storage casks. The W74 canister thermal rating

[1] Title 10, Code of Federal Regulations, Part 72 (10CFR72), *Licensing Requirements for the Independent Storage of Spent Nuclear Fuel and High-Level Radioactive Waste*, U.S. Nuclear Regulatory Commission, 1995.

defined within this chapter is also used to predict temperatures within the canister and cask systems. The applicable allowable temperatures are presented and comparisons are made with calculated temperatures as a basis for acceptance.

As discussed in Chapter 7 of this FSAR, confinement of all radioactive materials is provided by the FuelSolutions™ W74 canister. Although the thermal design of the storage cask and transfer cask provide assurance that the fuel assemblies remain sufficiently protected against degradation during dry storage that might otherwise lead to gross cladding ruptures, both casks are vented to atmosphere and cannot become pressurized. Evaluation of the W74 canister maximum internal pressure resulting from normal, off-normal, and postulated accident conditions is presented in this chapter.

This chapter presents FuelSolutions™ W74 canister thermal evaluation results for the design basis normal, off-normal, and postulated accident conditions. Section 4.2 provides the thermal properties for the W74 canister materials, and Section 4.3 provides the corresponding material specifications. Storage cask and transfer cask material properties and specifications are presented in the FuelSolutions™ Storage System FSAR.

W74 canister analytical model descriptions and thermal results are given in Sections 4.4, 4.4, and 4.6, for normal, off-normal, and postulated accident conditions, respectively. The storage cask and transfer cask analytical models, which interface with the W74 canister model, are described in the FuelSolutions™ Storage System FSAR.

Supplemental data are given in Section 4.7. Descriptions of the computer codes used in the analysis are described in Section 4.7.3. Sections 4.7.4, 4.7.5, and 4.7.6 give the thermal evaluations for any amount of Big Rock Point (BRP) mixed-oxide (MOX) and partial fuel assemblies, and up to eight damaged fuel assemblies, respectively. The evaluation for damaged fuel assemblies includes an assessment of the thermal effects imposed by the presence of the damaged fuel can.

4.1 Discussion

The thermal loads imposed on the FuelSolutions™ W74 canister arise from the decay heat of the SNF assemblies and from the external environment, including insolation. During storage system operations, the loaded W74 canister is always surrounded by either the storage cask or transfer cask and is, therefore, not directly subjected to ambient conditions such as insolation. The W74 canister is designed to passively dissipate the decay heat from the SNF to the transfer cask or storage cask while maintaining component material temperatures and fuel assembly cladding temperatures within their allowable values. The effects of ambient conditions on the W74 canister, including insolation acting on the surrounding cask, are addressed under the normal and off-normal conditions discussed in Sections 4.4 and 4.4, respectively. The thermal response of the W74 canister under postulated accident conditions, including a postulated storage cask fire event and a loss of transfer cask liquid neutron shielding, is discussed in Section 4.6.

The thermal analysis of the FuelSolutions™ W74 canister is performed for normal, off-normal, and accident conditions using the SINDA/FLUINT[2] computer program. An overview of the SINDA/FLUINT computer program is presented in Section 4.7.3.1.

This section provides a description of the thermal design features for the FuelSolutions™ W74 canister, the interface conditions with the storage cask and transfer cask, the design basis ambient conditions used, the design basis SNF heat flux profiles, the thermal modes of operation, the canister thermal ratings and the canister internal pressure.

These descriptions, bases of analysis, and canister thermal ratings remain valid for the storage of BRP MOX, partial, and damaged fuel assemblies within the FuelSolutions™ W74 canister. The specific assumptions, modeling approach, and predicted thermal performance relating to MOX, partial, and damaged fuel assemblies are respectively given in Sections 4.7.4, 4.7.5, and 4.7.6.

4.1.1 Design Features

FuelSolutions™ W74 canister design features are described in Section 1.2.1 of this FSAR. Storage cask and transfer cask design features are described in Section 1.2.1 of the FuelSolutions™ Storage System FSAR. The configuration of the W74 canister is shown in Figure 1.2-2. Drawings of the W74 canister are provided in Section 1.5 of this FSAR. This section summarizes the W74 canister design features that affect thermal performance. Since the W74 canister is always placed in the cavity of either the storage cask or transfer cask, a brief description of the cask design features that affect thermal performance is also included.

4.1.1.1 W74 Canister

The FuelSolutions™ W74 canister subsystem includes two classes of FuelSolutions™ canister assembly configurations (i.e., the W74M and W74T). A full discussion of the canister types and the differences between them is presented in Section 1.2.1 of this FSAR. While the canister basket configurations may vary somewhat in the number, placement, and material used for the

[2] SINDA/FLUINT, *Systems Improved Numerical Differencing Analyzer and Fluid Integrator*, Version 4.0, Prepared for NASA, Johnson Spacecraft Center, Contract NAS9-19365, by Cullimore and Ring Technologies, Inc., Littleton, CO, 1998.

spacer plates, both configurations share the same basic heat transfer characteristics in that each canister configuration uses a spacer plate and guide tube type of basket assembly to position and support the fuel assemblies within the canister. The W74 canister is unique to other FuelSolutions™ canisters since the W74 canister contains an upper and a lower basket assembly designed specifically for shorter length Big Rock Point BWR fuel. Since the basket assemblies are not mechanically attached to the canister wall, the principal means of heat transfer between the fuel assemblies and the canister shell is via radiation and convection. The following paragraphs provide a brief overview of the thermal similarities and differences between the W74M and W74T class canister configurations.

The following general design features are used to enhance the thermal performance of both canister assembly configurations:

- Carbon steel spacer plates for increased thermal conductance.
- Basket assembly layouts configured to maximize convective flow areas for the horizontal transfer configuration.
- The use of a helium gas back-fill for a canister internal pressure of 24 psia at the normal hot storage condition to enhance both conduction and convection heat transfer across void spaces in the basket.

Although the W74 canister can physically accommodate a total of seventy-four Big Rock Point BWR fuel assemblies, fuel assemblies will not be loaded within the five cell locations in the center of each basket. As such, the W74 canister fuel loading is limited to a maximum of thirty-two (32) fuel assemblies in each of the upper and lower baskets for a total of up to sixty-four (64) fuel assemblies for each FuelSolutions™ W74 canister configuration. The basket design includes hardware barriers installed at the time of basket fabrication to physically prevent the loading of fuel assemblies in the center five cell locations.

The fuel assemblies are zircaloy clad fuel, as described in Section 2.2 of this FSAR. Fuel assembly acceptance specifications which satisfy the thermal requirements presented in this chapter are given in the *technical specifications* contained in Section 12.3 and in the fuel cooling tables in Section 5.2 of this FSAR.

Both classes of FuelSolutions™ W74 canisters consist of the same major components: a right cylindrical shell, top end inner closure plate, top end outer closure plate, bottom end plate, bottom closure plate, top and bottom end shield plugs, and vent and drain ports. The W74T canister shells are fabricated of Type 304 stainless steel versus the Type 316 stainless steel used in the W74M canister shell. Both the W74M and W74T canister designs include only the long (192”) canister shell configuration. Additionally, both canister classes use only carbon steel material for the top and bottom end shield plugs.

The W74T upper and lower basket assemblies use carbon steel spacer plates to position and support the fuel assemblies. In addition, the W74T upper basket includes a stainless steel engagement plate at its lower end to provide a structural interface with the lower basket assembly. The W74M canister design uses a similar number of spacer plates, but substitutes a stainless steel spacer plate in lieu of the carbon steel plates at the top and bottom ends of both the upper and lower baskets. The W74M upper basket also includes a stainless steel engagement plate for interface between the baskets.

Both the W74T and W74M basket assemblies use stainless steel support tubes and sleeves to align and separate the spacer plates. Both canister types use stainless steel guide tubes in the upper and lower baskets.

4.1.1.2 Storage Cask

The thermal design features of the FuelSolutions™ W150 Storage Cask are discussed in Section 4.1.1 of the FuelSolutions™ Storage System FSAR. As summary of the primary thermal design features of the storage cask as they relate to the FuelSolutions™ W74 canister subsystem include:

- The long storage cask configuration accommodates both W74 canister classes.
- Passive heat removal by natural convection is enhanced through the use of the "chimney effect" to induce the flow of ambient air through the cask and across the canister.
- An inner annulus between the canister shell and the inner surface of storage cask's thermal shield and an outer annulus between the thermal shield outer surface and the interior surface of the storage cask's steel liner provide dual air paths for natural convection cooling.
- The thermal shield protects the storage cask concrete from elevated temperatures by blocking the direct transfer, via radiation, of heat from the surface of the canister shell and by providing a physical barrier to separate the hotter airflow near the canister from the airflow near the concrete.
- The canister is supported vertically above the bottom of the storage cask cavity by support tubes which permit radial air flow distribution under the canister and into the annulus with a minimum of air flow resistance.
- A centering guide rail system is used to provide a minimum positive separation distance between the canister and the storage cask inner wall.
- Two thermocouples are provided for storage cask temperature monitoring. One thermocouple is provided at mid-height and mid-thickness of the storage cask concrete wall and a second thermocouple is located at mid-height on the liner/concrete interface. These thermocouples provide the means for periodic temperature monitoring of the storage cask thermal performance and indirect monitoring of the canister temperatures.

4.1.1.3 Transfer Cask

The thermal design features of the FuelSolutions™ W100 Transfer Cask are discussed in Section 4.1.1 of the FuelSolutions™ Storage System FSAR. A summary of the primary thermal design features of the transfer cask as they relate to the FuelSolutions™ W74 canister subsystem include:

- The FuelSolutions™ W74 canister transfers the decay heat from the fuel assemblies to the transfer cask through a combination of conduction, radiation, and convection.
- Since the inside diameter of the transfer cask cavity is larger than the canister outside diameter, an annulus exists between the canister and the cask.

- During fuel loading operations the canister/cask annulus is filled with water and sealed to prevent radiological contamination of the canister outer shell and transfer cask cavity. The water in the annulus also serves to provide additional radiation shielding and enhances conductive heat transfer.
- Following canister vacuum drying and closure operations, the annulus is drained and vented.
- The transfer cask/canister annulus is provided with vent and drain connections on opposite sides of the cask to allow the circulation of cooling water through the annulus prior to canister draining or re-flooding operations.
- A thermocouple is provided at mid-height on the surface of the transfer cask structural shell to provide a means of periodic temperature monitoring of the transfer cask thermal performance and indirect monitoring of the canister temperatures.

4.1.2 Design Basis Ambient Conditions

In accordance with 10CFR72,[1] a range of long and short-term natural ambient conditions are considered in the thermal evaluation of the FuelSolutions™ W74 canister in the storage cask and transfer cask as defined in Section 2.3 of the FuelSolutions™ Storage System FSAR. These ambient conditions are assumed to occur concurrently with the design basis normal, off-normal, and postulated accident events (e.g., all vents blocked, loss of neutron shield, etc.) and form the design basis thermal loading conditions for the W74 canister within the storage and transfer casks.

The design basis off-normal and postulated accident design conditions for the W74 canister are as defined in Section 2.3 of this FSAR. Off-normal events are defined as those that are expected to occur on the order of once per calendar year. Accident events are defined as those that might occur only once during the use of the canister within the storage cask or transfer cask.

The thermal analyses of the W74 canister presented herein are based on conservative assumptions and methodologies. Because of this conservative approach, the actual thermal response of the canister to the design basis events is expected to produce larger positive design margins than reported herein (i.e., lower temperatures and thermal stresses).

As defined in Section 2.3 of the FuelSolutions™ Storage System FSAR, a normal long-term annual average design temperature of 77°F is selected for indoor and outdoor FuelSolutions™ Storage System operations which bounds all site locations in the contiguous United States. To facilitate a bounding thermal stress analysis of the W74 canister provided in Chapter 3 of this FSAR, steady-state thermal evaluations are performed with variations from the average ambient temperature value in the range of 0°F (normal cold) to 100°F (normal hot). The effects of extreme off-normal ambient temperatures in the range of -40°F to 125°F are evaluated for the design basis W74M canister within the storage and transfer casks. Since these ambient conditions do not exist for extended periods of time, short-term allowable temperatures apply for the fuel assembly cladding and the canister materials of construction. For the W74 canister off-normal and postulated accident thermal conditions involving storage cask or transfer cask configuration changes (i.e., all vents blocked, loss of liquid neutron shielding), the steady-state normal hot ambient temperature of 100°F is conservatively assumed.

The 10CFR71[3] recommended values for insolation are used. These insolation values are applied to the storage cask and transfer cask as discussed in Section 4.1.2 of the FuelSolutions™ Storage System FSAR and their effects are included in the W74 canister thermal evaluations provided herein.

4.1.3 Bounding Axial Heat Flux Profile

The FuelSolutions™ W74 canister is designed to accommodate only Big Rock Point BWR fuel. In order to ensure that the W74 canister design configurations presented in Section 1.2.1 of this FSAR are qualified to accommodate the worst case thermal loads, a bounding axial heat flux profile is used in the thermal analysis. The axial heat flux profile and, hence, the temperature profile within the FuelSolutions™ W74 canister are dependent upon the variation in the heat load and axial location of the fuel assembly loaded within each basket. The distribution of the heat load within the canister is a function of: 1) the fuel assembly class (i.e., Big Rock Point BWR); 2) the corresponding heavy metal content, burnup and cooling time; 3) the number of fuel assemblies in the canister; 4) the active length of the fuel assemblies; and 5) the axial position of the active fuel length within the canister. The above variables are set by the canister type and the characteristics of the specific Big Rock Point fuel to be loaded. Sections 4.1.3.1 and 4.1.3.2 describe how the bounding heat flux profile is determined and applied.

In order to address the axial heat profile variations with fuel assembly class and burnup, two thermal acceptance criteria are used for the W74 canister thermal rating qualification. These thermal acceptance criteria are: 1) a maximum heat load rating (Q_{max}), and 2) the maximum linear heat generation rate ($LHGR_{max}$) on a per unit length basis. Both thermal criteria are needed to define the allowable W74 canister thermal loading. Although the total heat load is the major determining factor in the overall temperature levels within the W74 canister, the temperature levels at any specific location are more directly affected by the linear heat generation rate. This is especially true where the cask and/or canister design and the material thermal conductivity combine to limit the axial spreading of localized heat effects.

4.1.3.1 Development of Bounding Axial Heat Flux Profiles

Development of PWR and BWR axial heat flux profiles is addressed in detail in Section 4.1.3 of the FuelSolutions™ Storage System FSAR. The variation in linear heat generation rate within the W74 canister is a function of the axial location of the active fuel within the canister. To create a bounding canister axial heat flux profile for use in analyzing the W74 canister, the design basis peaking factor curve for the generic BWR fuel type (Figure 4.1-2 of the FuelSolutions™ Storage System FSAR) is adjusted for the location and length of the active fuel region of the Big Rock Point fuel assemblies within the upper and lower baskets in the W74 canister. Using this profile, a W74 canister specific axial heat profile is developed. This bounding W74 canister profile, termed the “Big Rock Point” profile (see Figure 4.1-1), envelopes the worst case axial heat profile expected from the fuel to be stored within the W74 canister.

[3] Title 10, Code of Federal Regulations, Part 71 (10CFR71), *Packaging and Transportation of Radioactive Materials*, U.S. Nuclear Regulatory Commission, 1997.

A total active fuel length of 140” is assumed for the “Big Rock Point” profile. This active fuel length represents twice the active fuel length of an individual Big Rock Point fuel assembly (70”). The composite heat loads in the upper and lower baskets each represent half of the total W74 canister heat load. Since the W74 canister is designed specifically to accommodate only Big Rock Point fuel and since shorter BWR fuels do not exist, there is no need for a shorter “Max. Thermal Gradient” profile, as used in the thermal analysis of other FuelSolutions™ canisters. Therefore, only the “Big Rock Point” profile is needed to bound all possible W74 canister fuel loadings.

Table 4.1-1 presents in tabular form the bounding “Big Rock Point” canister axial heat profile illustrated in Figure 4.1-1.

4.1.3.2 Application of Axial Heat Profiles for Canister Analysis

The FuelSolutions™ W74 canister analytical model used for the thermal evaluation includes the fuel assembly axial heat flux as a boundary condition. Using the Big Rock Point axial profile in Figure 4.1-1, the maximum heat load (Q_{local}) at a specific axial location within the fuel assemblies in the analytical model is determined as follows:

$$Q_{Local} = \left(\frac{Q_{Assy}}{AFL} \right) \cdot PF \cdot L$$

where:

Q_{Local}	=	Local fuel assembly heat load at the nodal location
Q_{Assy}	=	Total fuel assembly heat load for the given axial profile
AFL	=	Active fuel length in inches for the associated axial profile (i.e., 70”)
PF	=	Local peaking factor at the center of the region being modeled (from Figure 4.1-1 or Table 4.1-1)
L	=	Length in inches of the region being modeled

For determination of the allowable W74 canister thermal rating within the storage cask or transfer cask, the value of Q_{Assy} is increased until one or more of the canister or cask allowable material temperatures or the allowable fuel cladding temperature are reached. The maximum value of Q_{Assy} that meets all canister/cask allowable temperatures is multiplied by the total number of assemblies (64) to determine the maximum heat load rating (Q_{max}) for the canister.

The maximum linear heat generation rate is determined as follows:

$$LHGR_{max} = \frac{Q_{max} \cdot PF}{AFL}$$

where:

$LHGR_{max}$	=	Maximum canister linear heat generation rate for the given profile
Q_{max}	=	Maximum heat load rating for canister
1.22	=	BWR fuel maximum peaking factor
AFL	=	Active fuel length for the profile analyzed. Equals 140” for Big Rock Point fuel (two baskets/canister, 70” each)

The calculated maximum heat load rating (Q_{max}) and maximum linear heat generation rate ($LHGR_{max}$) become the thermal ratings for the W74 canister.

These W74 canister thermal ratings are then used to generate the cooling tables presented in Section 5.2 of this FSAR. With the use of this methodology, any change in the fuel cooling time which increases the heat load above the qualified Q_{max} for the canister restricts loading of that candidate fuel assembly until sufficient additional cooling time has occurred to reduce the total canister heat load to within the qualified Q_{max} for the canister. Likewise, any change in heat load or active fuel length which yields a linear heat generation rate above the qualified $LHGR_{max}$ for the canister restricts fuel loading until sufficient additional cooling time has occurred.

The fuel cooling tables developed in Section 5.2 of this FSAR account for the variation in axial heat profile peaking factor with burnup. This variation is presented for BWR fuel in Figure 4.1-4 of the FuelSolutions™ Storage System FSAR. As burnup level increases, the maximum peaking factor decreases and the axial profile because more uniform. Because the bounding BWR axial heat profile used for determination of the W74 canister thermal rating is compiled assuming 29 GWd/MTU burned fuel, lower burnup levels are penalized to account for the higher peaking factors associated with lower burnup fuels. Burnup dependent penalty factors are applied by derating the maximum canister thermal ratings (Q_{max} and $LHGR_{max}$) during development of the cooling tables.

4.1.4 Thermal Operating Modes

The W74 canister is analyzed within a set of design basis thermal conditions in order to bound canister thermal performance for all normal, off-normal, and accident conditions expected during handling within the transfer cask and long-term storage within the storage cask. The thermal design of the canister is governed by the requirement to maintain the temperatures and/or thermal gradient within the fuel assemblies and structural components during a combination of normal and off-normal events below allowable values. The thermal acceptance criteria is selected to prevent thermally induced failures and the loss of structural properties within the fuel cladding, critical basket components, and the containment boundary components due to elevated temperatures and/or thermal gradients.

4.1.4.1 W74 Canister within Storage Cask

As discussed in Chapters 1 and 8, and the FuelSolutions™ Storage System FSAR, the versatility of the FuelSolutions™ W150 Storage Cask creates numerous operating modes that subject the W74 canister to varying thermal parameters. The primary operating parameters that influence W74 canister thermal performance within the storage cask include location (inside, outside); orientation (vertical, horizontal); top cover installation (on, off); inlet and outlet vent condition

(open, blocked); ambient temperature (-40°F, 0°F, 77°F, 100°F, 125°F); and solar radiation (24 hour averaged or none). Various combinations of these parameters define the bounding W74 canister normal, off-normal, and accident thermal conditions for storage. The range of possible W74 canister thermal operating modes within the storage cask is presented in Table 4.1-1 of the FuelSolutions™ Storage System FSAR.

Of the fifteen operating modes listed in Table 4.1-1 of the FuelSolutions™ Storage System FSAR, many are similar enough to other operating modes that the associated thermal performance can be characterized by another, bounding operating mode. Table 4.1-2 summarizes the specific W74 canister thermal load cases selected to bound the range of normal, off-normal, and accident operating modes. The eight limiting cases considered in the thermal evaluation of the W74 canister within the storage cask include: normal storage (case 5), normal cold storage (case 6), normal hot storage (case 7), off-normal cold storage (case 8), off-normal hot storage (case 9), all vents blocked accident (case 11), canister transfer (case 13), and fire accident (case 15).

Canister temperatures during the other seven operating conditions listed in Table 4.1-1 of the FuelSolutions™ Storage System FSAR are bounded by one of these eight cases. Canister temperatures during vertical loading (cases 1 through 3) and during air pallet transfer (case 4) are bounded by the all vents blocked accident (case 11) when the vents are blocked and by the normal storage conditions (case 5) when the vents are open. The outlet vents blocked (case 10) is bounded by the transient analysis for all vents blocked (case 11), while the horizontal modes (cases 12 and 14) are bounded by the transient analysis for canister transfer (case 13).

For the determination of the maximum W74 canister thermal rating, only the normal hot storage condition (case 7) is evaluated. In those cases where some short-term operating modes may result in steady-state temperatures at the thermal ratings which exceed allowable material temperatures, transient analyses of these short-term operating modes (i.e., all vents blocked, horizontal transfer) are performed to determine the system temperatures as a function of time and relation between key component temperatures and the predicted reading of the thermocouple used to monitor the system performance. The results of these analyses are used to establish the operational *technical specification* limits contained in Section 12.3 of this FSAR. These *technical specification* limits are based on measured values of key cask response temperatures for these operating conditions. The W74 canister thermal ratings are applied concurrently with the thermal load cases in Table 4.1-2 to determine the temperature distribution within the W74 canister for each case.

4.1.4.2 W74 Canister within Transfer Cask

Similar to the storage cask, the various operating modes of the FuelSolutions™ W100 Transfer Cask also create numerous combinations of thermal parameters for the W74 canister. The primary operating parameters influencing W74 canister thermal performance within the transfer cask include location (inside, outside), orientation (vertical, horizontal), ambient temperature (-40°F, 0°F, 77°F, 100°F, 120°F, and 125°F), annulus fluid (stagnant water, flowing water, air), top cover installation, bottom cover installation, liquid neutron shield fluid (water, air), W74 canister cavity (water, vacuum, helium, air), and solar radiation. The bounding W74 canister

normal, off-normal, and accident thermal conditions within the transfer cask are summarized in Table 4.1-2 of the FuelSolutions™ Storage System FSAR.

Many of the twenty operating modes listed in Table 4.1-2 of the FuelSolutions™ Storage System FSAR are similar enough to other operating modes such that the associated thermal performance can be characterized by another bounding operating mode. Table 4.1-3 summarizes the ten design basis thermal load cases selected to bound the range of normal, off-normal, and accident operating modes for the W74 canister within the transfer cask. The design basis cases considered include: vacuum drying (case 6), cask handling (case 10), normal transfer (case 13), normal cold transfer (case 14), normal hot transfer (case 15), off-normal cold transfer (case 16), off-normal hot transfer (case 17), loss of neutron shield (case 18), canister reflood (case 19), and postulated fire accident (case 20).

For determination of thermal performance within the transfer cask, the system temperatures during loading and canister closure operations (cases 1 through 4) are bounded by the analyzed cask handling conditions (case 10). Canister draindown (case 5) is bounded by the vacuum drying condition (case 6). The annulus draining condition (case 7) is an accident scenario that will not be allowed under the operating procedures for periods sufficient to reach steady-state conditions. As such, the transient temperatures under case 7 are also bounded by the case 6 design conditions. Conditions during canister inerting, vertical handling, and transfer (cases 8 through 11) are bounded by the analyzed handling condition (case 10). The thermal performance for the case 12 conditions for inside normal transfer is bounded by the analyzed normal transfer for outside conditions, case 13. A transient analysis (case 19) is performed at the W74 canister thermal rating to establish the boundary conditions for the canister reflood analysis, presented in Section 4.4.2 of this FSAR.

The maximum W74 canister thermal rating within the transfer cask is determined based only on the steady-state normal hot condition. Although short-term temperature limits for fuel cladding i.e., 1058 °F(570 °C) apply for operations in the transfer cask, the basket and canister structural materials do not have short-term temperature limits if material properties are relied upon for a structural load combination (such as postulated transfer cask drop accidents). As a result, long-term limits for canister steel components apply for all normal conditions of transfer. The off-normal and accident thermal conditions (i.e., vacuum drying, off-normal hot transfer, loss of neutron shield) are short duration conditions which do not need to be combined with an off-normal structural load condition. Higher material limits are established for off-normal and accident thermal conditions, as discussed later in Section 4.3.1. Only the normal hot transfer condition (case 15) is evaluated for determining the canister rating during transfer.

4.1.5 Thermal Rating Summary

The W74 canister thermal rating in the storage and transfer casks is determined by applying the bounding canister axial heat flux profile (Section 4.1.3) to the W74 canister within the storage cask and transfer cask steady-state thermal models under design basis ambient conditions (Section 4.1.2), for the design basis cask operating modes (Section 4.1.4). The canister maximum heat load rating (Q_{max}) and maximum linear heat generation rate ($LHGR_{max}$) are established when a canister allowable material temperature is reached as described in Sections 4.4.1 and 4.4.2 of this FSAR. The W74 canister thermal ratings for storage are presented in Table 4.1-4.

The maximum allowable material temperatures for the W74 canister are presented in Section 4.3.1, while spent fuel cladding allowable temperatures are presented in Section 4.3.2. The spent fuel cladding is the limiting material for long-term storage. Long-term fuel cladding allowable temperatures do not apply in the transfer cask. Fuel cladding allowable temperature is largely dependent upon the fuel burnup level (as discussed in Section 4.3.2). Since Big Rock Point fuel does not exist at burnup levels greater than 40 GWd/MTU, this bounding burnup level is established for all Big Rock Point fuel to be loaded within the W74 canister. Since internal rod pressure and resultant stress levels decrease with decreasing burnup level, the allowable cladding temperature determined for 40 GWd/MTU burned BRP fuel bounds fuel with lower burnups.

The associated storage and transfer cask thermal ratings are also presented to illustrate that the canister is the limiting component. In addition, a W74 canister thermal rating which is based solely on the canister's structural material temperature limits is presented to demonstrate that the allowable fuel cladding temperature controls the thermal rating of the canister.

Cask thermal ratings are discussed further in Section 4.4.1 and 4.4.2 of the FuelSolutions™ Storage System FSAR. The canister system temperatures under the various bounding cask operating modes are presented in Sections 4.4, 4.4, and 4.6 for normal, off-normal, and accident conditions, respectively.

4.1.6 Canister Internal Pressure Summary

The W74 canister is pressurized due to fuel rod fill gas, fuel rod fission gas, and canister cavity back-fill gas. As discussed in Chapter 8 of this FSAR, the W74 canister is back-filled with helium during closure operations. The quantity of inert gas in moles needed for canister cavity back-fill are determined in order to achieve 10 psig (1.68 atm) in the canister cavity under normal hot storage conditions (100°F ambient, Section 4.1.2) with 1% rod failures. The maximum W74 canister internal pressure is determined assuming rupture of 1%, 10%, and 100% of the fuel rods under normal, off-normal, and accident conditions, respectively. As discussed within the internal pressure evaluations presented in Sections 4.4, 4.4, and 4.6, pressure calculations conservatively assume the release of 100% of the rod fill gas and 30% of the rod fission gas for each postulated failed fuel rod.

Table 4.1-1 - Bounding W74 Canister Axial Heat Profile

Canister Axial Location (inches)	Big Rock Fuel Profile (dimensionless)
0	0
10	0 (13”) / 0.21
20	0.99
30	1.19
40	1.21
50	1.19
60	1.13
70	0.99
80	0.4889
90	0. (83”)
100	0 (98”) / 0.21
110	1.14
120	1.20
130	1.20
140	1.17
150	1.08
160	0.81
170	0.210 (168”)
172	0 (170”)
182	0
192	0

Table 4.1-2 - Design Basis Thermal Cases for W74 Canister within Storage Cask

Case	Mode	FSAR Section	Ambient Temp. (°F)	W74 Cavity	Insolation by Surface Type & Orientation (BTU/hr-ft^2 (W/m^2))			Type of Analysis
					top (cask vert)	sides (cask vert./horiz)	top (cask horiz)	
5	Normal Storage	4.4	77	He	123 (388)	62 (194)	n/a	Steady-State
6	Normal Cold Storage	4.4	0	He	0	0	n/a	Steady-State
7	Normal Hot Storage	4.4	100	He	123 (388)	62 (194)	n/a	Steady-State
8	Off-normal Cold Storage	4.5	-40	He	0	0	n/a	Steady-State
9	Off-normal Hot Storage	4.5	125	He	123 (388)	62 (194)	n/a	Steady-State
11	All Vents Blocked Accident	4.6	pre-event, 77	He	123 (388)	62 (194)	n/a	Steady-State
			during event, 100		123 (388)	62 (194)	n/a	Transient
13a	Canister Horizontal Transfer (Loading)	4.5	pre-event, (empty cask) 100	He	123 (388)	62 (194)	n/a	Steady-State
			during event, 100		n/a	62 (194)	31 (97)	Transient
13b	Canister Horizontal Transfer (Unloading)	4.5	pre-event, 77	He	123 (388)	62 (194)	n/a	Steady-State
			during event, 100		n/a	62 (194)	31 (97)	Transient
15	Fire Accident	4.6	pre-event, 100	He	123 (388)	62 (194)	n/a	Steady-State
			during event, 1475		0	0	n/a	Transient
			postevent 100		123 (388)	62 (194)	n/a	Transient

Table 4.1-3 - Design Basis Thermal Cases for W74 Canister within Transfer Cask

Case	Mode	FSAR Section	Ambient Temp. (°F)	W74 Cavity	Insolation by Surface Type & Orientation (BTU/hr-ft^2 (W/m^2))			Type of Analysis
					Top (Cask Vert)	Sides (Cask Vert./Horiz)	Top (Cask Horiz)	
6	Vacuum Drying	4.4	77	Vacuum	n/a	n/a	n/a	Steady-State
10	Cask Handling	4.4	77	He	n/a	n/a	n/a	Steady-State
13	Normal Transfer	4.4	77	He	n/a	62 (194)	31 (97)	Steady-State
14	Normal Cold Transfer	4.4	0	He	n/a	0	0	Steady-State
15	Normal Hot Transfer	4.4	100	He	n/a	62 (194)	31 (97)	Steady-State
16	Off-normal Cold Transfer	4.5	-40	He	n/a	0	0	Steady-State
17	Off-normal Hot Transfer	4.5	125	He	n/a	62 (194)	31 (97)	Steady-State
18	Loss of Neutron Shield	4.6	100	He	n/a	62 (194)	31 (97)	Steady-State
19	Canister Reflood	4.4	77	Air	n/a	n/a	n/a	Transient
20	Fire Accident	4.6	pre-event, 100	He	n/a	62 (194)	31 (97)	Steady-State
			during event, 1475		n/a	0	0	Transient
			postevent 100		n/a	62 (194)	31 (97)	Transient

Table 4.1-4 - W74 Canister Thermal Rating for Storage[(1)]

Cooling Table	Axial Heat Profile	Q_{max} (kW)	$LHGR_{max}$ (kW/in)
0 to 40 GWd/MTU	Max Thermal	24.8	0.216
	Max Thermal Gradient	N/A	N/A
	Thermal Rating	**24.8**	**0.216**
W74 Basket Structure Thermal Rating		26.4	0.230
Storage and Transfer Cask Thermal Rating		28.0	0.253

Note:

(1) The W74 canister thermal rating is set by the minimum heat load qualification in the storage and transfer casks. The W74 canister thermal rating is limited by the maximum allowable fuel cladding temperature. As shown above, the W74 canister structure can accommodate a higher thermal rating.

Table 4.1-5 - FuelSolutions™ W74 Canister Design Internal Pressures

Condition	W74 Canister Pressure (40 GWd/MTU BRP Fuel) (psig)
Normal	10.0
Off-Normal (max)	12.3
Accident (max)	30.0

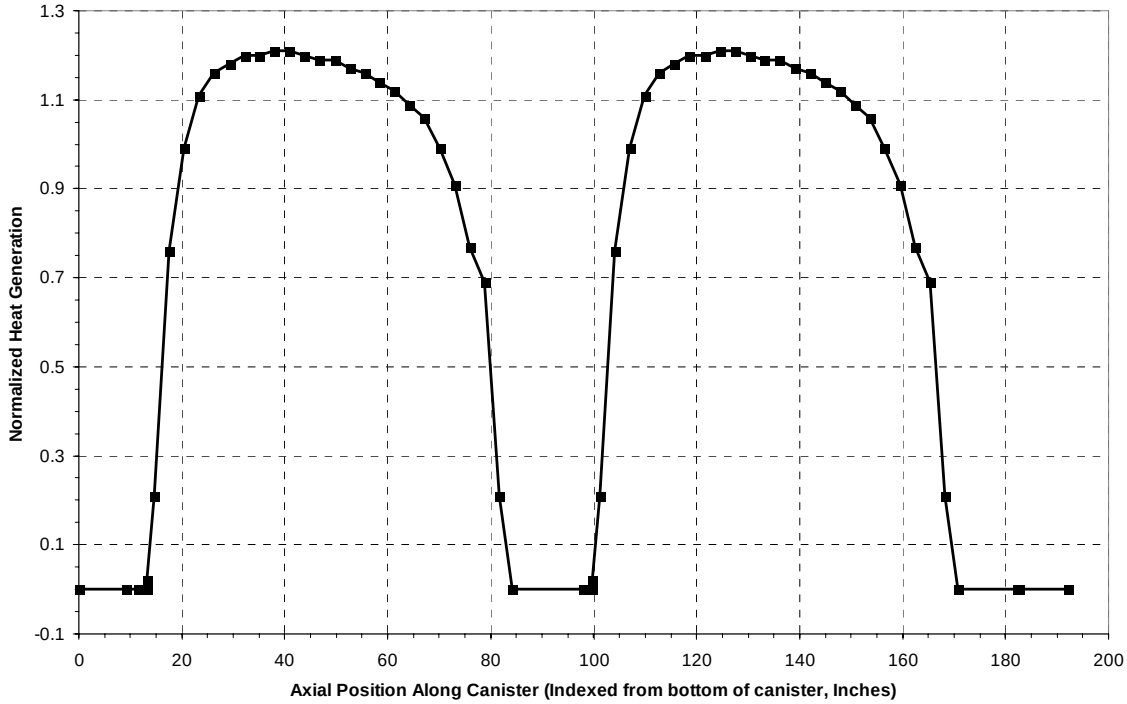

Figure 4.1-1 - Design Basis Axial Heat Profiles for W74 and Generic BWR Canister Analysis

This page intentionally left blank.

4.2 Summary of Thermal Properties of Materials

The analysis of the W74 canister heat transfer within the storage cask and transfer casks requires that thermal properties be defined for the materials used in their fabrication. Table 4.2-1 tabulates the relevant thermal properties for the materials used in the fabrication of the FuelSolutions™ W74 canister. The materials used in the fabrication of the storage cask and transfer cask are presented in the FuelSolutions™ Storage System FSAR.

Table 4.2-2 summarizes the W74 canister material emissivity values used for radiation heat transfer analyses. Table 4.2-3 summarizes the fluid material properties used for thermal analysis.

The impact on heat transfer rates as a result of possible fission gas release from failed fuel rods was evaluated. While the evaluation shows that the thermal conductivity of the resulting gas mixture could be reduced by approximately 60% for the worst case fission gas release, the other thermal properties of the gas mixture which affect convection within the canister will act to improve the heat transfer ability of the gas mixture. This beneficial impact of fission gas release on thermal performance has been conservatively ignored for the thermal analyses.

Sections 4.7.4.3, 4.7.5.2, and 4.7.6.3 present the modeling approach for determining the effective thermal conductivity for BRP MOX, partial, and damaged fuel assemblies. Given that the fuel pellets are conservatively ignored when computing the effective thermal conductivity of the fuel assemblies, the thermal properties for UO_2 and MOX fuel are not required for this analysis.

4.2.1 W74 Canister

The FuelSolutions™ W74 canister shell assemblies are fabricated from stainless steel and have carbon steel shield plugs at the ends. The W74M and W74T basket assemblies each contain spacer plates fabricated from carbon steel. The W74M basket also contains stainless steel spacer plates. The basket guide tube assembly is fabricated with a stainless steel inner sleeve and with borated stainless steel neutron absorbing material attached on one side or two sides, depending on the guide sleeve location within the baskets. Both the W74M and W74T basket support tubes and support sleeves are fabricated of stainless steel. The damaged fuel can is fabricated from Type 304 and Type 316 stainless steel.

4.2.2 Big Rock Point Fuel

The individual components of the BWR fuel assemblies are not discretely modeled; rather, the fuel assemblies are included as composite thermal masses with an effective radial thermal conductance based on the work of Manteufel and Todreas.[4] Specifically, the non-linear form of the lumped k_{eff}/h_{edge} model for a typical BWR assembly as presented in Equations (31) and (32) and Table II of Manteufel and Todreas is used. These equations relate the maximum temperature within the fuel assembly (T_M) to the temperature at the edge of the assembly (T_E) via the equation:

$$Q = 17.38(T_M - T_E) = 3.60E-8(T_M^4 - T_E^4)$$

[4] Manteufel, R. D., and Todreas, N. E., *Effective Thermal Conductivity and Edge Conductance Model For A Spent-Fuel Assembly*, Nuclear Technology, Vol. 105, pp. 421-440, March 1994.

and from the edge of the assembly (T_E) to the temperature at the guide tube surface (T_W) via the equation:

$$Q = 36.54(T_E - T_W) + 2.49E-8(T_E^4 - T_W^4)$$

where Q is in terms of watts and T_M, T_E, and T_W are in degrees Kelvin.

Before their use in the thermal model, the equation coefficients are modified to remove the assumed 1.2 peaking factor correction, since the effects of peaking factor are computed directly within the SINDA/FLUINT model, and to replace the assumed helium gas thermal conductivity of 0.2 W/m-K with a temperature dependent value. Incorporation of these changes results in the above equations becoming:

$$Q/meter = 7.122951 \bullet k_{Helium} \bullet (T_M - T_E) + 2.95082E-9(T_M^4 - T_E^4)$$

and

$$Q/meter = 14.97541 \bullet k_{Helium} \bullet (T_E - T_W) + 2.039904E-9(T_E^4 - T_W^4)$$

where “Q/meter” represents the net heat transfer between the fuel assembly and a meter length of each guide tube wall. Axial conductance within the fuel assemblies is limited to that which will occur within the thickness of the zircaloy cladding.

The same correlation is assumed for either horizontal or vertical orientation of the fuel basket. No credit is taken for direct contact between the fuel assemblies and the guide tubes for either basket orientation. These equations are valid for the case where helium is used as the backfill gas.

The thermal mass of the fuel assembly used in the thermal analysis is based on a typical Big Rock Point fuel assembly which has a total assembly weight of 457 pounds, an active fuel length of 70 inches, and an effective specific heat of 0.03 BTU/lb-°F.

Table 4.2-1 - W74 Canister Homogenous Material Properties (3 Pages)

Material	Temperature (°F)	Thermal Conductivity (BTU/hr-ft-°F)	Density[1] (lb/ft^3)	Specific Heat (BTU/lb-°F)
Type 304 Stainless Steel [2]	-40	8.2[6]	503	0.111[6]
	70	8.6		0.113
	100	8.7		0.114
	200	9.3		0.119
	300	9.8		0.122
	400	10.4		0.125
	500	10.9		0.127
	600	11.3		0.129
	700	11.8		0.131
	800	12.2		0.132
	900	12.7		0.134
	1000	13.2		0.135
Type 316 Stainless Steel[2]	-40	6.9[6]	502	0.110[6]
	70	7.7		0.114
	100	7.9		0.116
	200	8.4		0.119
	300	9.0		0.124
	400	9.5		0.125
	500	10.0		0.128
	600	10.5		0.129
	700	11.0		0.131
	800	11.5		0.132
	900	12.0		0.134
	1000	12.4		0.134
Type XM-19 Stainless Steel[2]	-40	5.7[6]	494	0.103[6]
	70	6.4		0.113
	100	6.6		0.115
	250	7.4		0.121
	400	8.2		0.126
	600	9.3		0.132
	700	9.9		0.135
	800	10.4		0.136
	900	10.9		0.137
	1000	11.4		0.138

Table 4.2-1 - W74 Canister Homogenous Material Properties (3 Pages)

Material	Temperature (°F)	Thermal Conductivity (BTU/hr-ft-°F)	Density[1] (lb/ft^3)	Specific Heat (BTU/lb-°F)
A-514/SA-517	-40	21.1[4]	501	0.096[4]
Grade F	70	21.8		0.103
Carbon	150	22.3		0.109
Steel[2]	250	22.4		0.115
	350	22.4		0.120
	400	22.3		0.122
	500	22.0		0.127
	600	21.5		0.132
	800	20.4		0.143
	1000	19.2		0.157
A-514/SA-517	-40	19.8[4]	501	0.097[4]
Grade P	70	21.3		0.105
Carbon	150	22.2		0.111
Steel[2]	250	22.9		0.117
	350	23.3		0.123
	400	23.3		0.125
	500	23.1		0.130
	600	22.7		0.135
	800	21.6		0.149
	1000	20.2		0.167
A36/A516	-40	22.9[4]	489	0.096[4]
Carbon	70	23.6		0.106
Steel[2]	200	24.4		0.118
	300	24.4		0.123
	400	24.2		0.128
	500	23.7		0.133
	600	23.1		0.136
	700	22.4		0.143
	800	21.7		0.149
	900	20.9		0.156
	1000	20.0		0.165

Table 4.2-1 - W74 Canister Homogenous Material Properties (3 Pages)

Material	Temperature (°F)	Thermal Conductivity (BTU/hr-ft-°F)	Density[1] (lb/ft^3)	Specific Heat (BTU/lb-°F)
1.25% Borated Stainless Steel[3]	77	8.6	487	0.118
	212	9.2		0.124
	302	9.6		0.127
	392	10.0		0.128
	482	10.4		0.129
	752	11.5		0.132
	932	12.2		0.133

Notes:

(1) Single values are shown for homogeneous material Density, since this material property does not vary significantly with temperature.

(2) Material properties have been obtained from ASME Boiler and Pressure Vessel Code, Section II, Part D, 1995 Edition.

(3) Micro-Melt® NeutroSorb PLUS®, *Alloy Data for Modified Type 304 Stainless with Boron ASTM A887-89 Grade "A" Alloys*, Document #1-94/5M, Carpenter Technology Corporation, 1994.

(4) Extrapolated value.

Table 4.2-2 - W74 Canister Surface Emissivities

Material	Conditions	Emissivity (ε)
304, 316, XM-19 and Borated Stainless Steel[1,2]	slightly oxidized, <250°F slightly oxidized, 250-500°F oxidized, >500°F	0.30[1] 0.40 0.45[3]
A36/A516 and A-514/SA-517 Grades F and P Carbon Steel[1,4]	Electroless nickel plated	0.11

Notes:

(1) Gubareff, G. G., Janssen, J. E., and Torborg, R. H., *Thermal Radiation Properties Survey*, 2nd Edition, Honeywell Research Center, 1960.

(2) Frank, R. C., and Plagemann, W. L., *Emissivity Testing of Metal Specimens*, Boeing Analytical Engineering coordination sheet No. 2-3623-2-RF-C86-349, August 21, 1986.

(3) Components such as the neutron absorber sheet attachment buttons and retainer clips could have an emissivity range of 0.15 to 0.45.

(4) Siegel, R., and Howell, J. R., *Thermal Radiation Heat Transfer*, 3rd Edition, Hemisphere Publishing Corporation, Washington, D. C., 1992.

Table 4.2-3 - W74 Canister Material Properties, Fluids

Material	Temp. (ºF)	Thermal Conductivity (BTU/hr-ft-°F)	Specific Heat (BTU/lb-°F)	Density (lb/ft)[1]	Prandtl No.	Expansion Coefficient (1/K)	Viscosity (Centipoise)
Air[1,2,3]	-99	0.010	0.239	Use ideal gas law			0.01336
	81	0.015	0.240				0.01853
	261	0.019	0.242				0.02294
	441	0.023	0.246				0.02682
	621	0.026	0.251				0.03030
	801	0.030	0.257				0.03349
	981	0.033	0.262				0.03643
	1161		0.267				0.03918
Helium[4,5,6]	-99	0.067	1.239	Use ideal gas law			0.0150
	81	0.087					0.0199
	261	0.104					0.0243
	441	0.122					0.0283
	621	0.143					0.0320
	801	0.161					0.0355
	981	0.177					0.0388
	1161	0.194					0.0420
Liquid Water[7]	32	0.329	1.007	62.44	12.99	-68.05e-6	1.750
	81	0.354	0.998	62.25	5.83	276.1e-6	0.855
	126	0.373	0.999	61.63	3.42	471.2e-6	0.528
	171	0.386	1.002	60.75	2.29	624.2e-6	0.365
	212	0.393	1.007	59.82	1.76	750.1e-6	0.279

Notes:

(1) Eckert, E. R.G. and Drake, Jr., R. M., *Analysis of Heat and Mass Transfer*, McGraw-Hill Book Company, New York, 1972.

(2) Rohsenow, Hartnett, and Ganic, *Handbook of Heat Transfer Fundamentals*, 2nd edition, McGraw-Hill Publishers.

(3) Kreith, F., *Principles of Heat Transfer*, 3rd Edition, Harper & Row Publishers.

(4) Touloukian, Y.S., *Specific Heat - Nonmetallic Liquids and Gases*, Thermophysical Properties of Matter, the TPRC Data Series, Vol. 6, 1970.

(5) Touloukian, Y.S., *Thermal Conductivity - Nonmetallic Liquids and Gases*, Thermophysical Properties of Matter, the TPRC Data Series, Vol. 3, 1970.

(6) Touloukian, Y.S., *Viscosity - Nonmetallic Liquids and Gases*, Thermophysical Properties of Matter, the TPRC Data Series, Vol. 11, 1970.

(7) Incropera, F. P. and Dewitt, D. P., *Fundamentals of Heat and Mass Transfer*, 3rd Edition, John Wiley & Sons, New York, 1990.

This page intentionally left blank.

4.3 Specifications for Components

4.3.1 W74 Canister

The materials used in the FuelSolutions™ W74 canister that are considered temperature sensitive are the zircaloy cladding on the SNF assembly rods, borated stainless steel, and the canister structural components.

Since the borated stainless steel is not used for structural purposes, its maximum temperature is maintained less than 1000ºF for continuous operation in order to prevent material changes due to annealing, etc. The actual melting point is approximately 2550ºF. No allowable temperature is needed for the minimum cold conditions.

In accordance with Section III of the ASME B&PV Code,[5] the maximum allowable temperatures of the canister materials are limited to 800°F for austenitic stainless steel (e.g., Type 304, 316, and XM-19) and 700°F for carbon steel (A36, SA-517 Grades F and P, and A-514 Grades F and P). These allowable temperatures are applied to the canister materials for all normal design conditions.

Short-term elevated temperatures in excess of these allowable values may occur during fabrication, loading operations, off-normal transfer, or accident storage conditions in which a postulated cask drop accident is not credible or need not be combined with another accident condition. Both carbon and stainless steel have a melting point well above 2500°F (1371°C).[6] As shown in ASME Code Case N-47-33,[7] the strength properties of steels do not change due to short-term exposure up to 1000°F. Therefore, short-term exposure to the temperatures of this magnitude does not have any significant effect on mechanical properties of the basket assembly materials.

Additionally, United States Steel brochure "*Steels for Elevated Temperature Service*"[8] provides tested material properties for the A-514/SA-517, Grades F and P material up to 1900°F without significant effect on mechanical properties. Therefore, a maximum allowable short-term temperature of 1000°F is applied for canister structural stainless steel and carbon steel materials.

These component specifications remain valid and bounding for the analysis of the BRP MOX, partial, and damaged fuel assemblies within the FuelSolutions™ W74 canister.

4.3.2 Fuel Cladding Allowable Temperatures

This section presents the methodology for long-term allowable cladding temperature determination for 40 GWd/MTU burned BRP fuel assemblies. This method is designed to

---

[5] ASME Boiler and Pressure Vessel Code, Section III, Division 1 - Subsections NB and NG, 1995 Edition.

[6] ASME Boiler and Pressure Vessel Code, Section II, Part D, 1995 Edition.

[7] Case N-47-33, *Class 1 Components in Elevated Temperature Service*, American Society of Mechanical Engineers (ASME) Boiler and Pressure Vessel Code, 1995 Code Cases, Nuclear Components, 1995 Edition.

[8] "Steels for Elevated Temperature Service", United States Steel Corporation, 600 Grant Street, Pittsburgh, PA 15230.

determine allowable long-term cladding temperature, which is the primary means used to assure integrity of fuel assembly cladding during dry storage.

The calculation method is based on cladding degradation due to material creep behavior which is a result of more recent testing for spent fuel with burnups to 60 GWd/MTU (herein referred to as the "creep methodology").

The allowable cladding temperatures determined using the creep methodology presented in this section apply only to zircaloy clad commercial LWR fuel. It should also be noted that the applicability of the creep methodology to stainless steel clad fuel has not been established. Qualification of stainless steel clad fuel in the FuelSolutions™ W74 canister is not currently being sought.

The creep methodology is in accordance with 10CFR72.72(h)[1] and NUREG-1536,[9] wherein the FuelSolutions™ Storage System is designed to prevent degradation of fuel cladding that results in gross cladding failure throughout the entire storage life. Gross cladding failure can be characterized as a type of cladding breach, such as axial splits or ductile fracture, where irradiated UO_2 particles may be released as described in Section 2.2 of this FSAR. The design intent is to avoid cladding rupture and maintain sufficient cladding structural integrity to allow handling at the end of storage life.

Both UCID-21181[10] and EPRI Report TR-103949[11] agree that SNF cladding allowable temperatures for dry storage should be determined primarily by the creep properties of the cladding.

Extensive cladding creep testing of moderate and high burnup spent fuel assemblies has been performed at simulated dry storage temperature and stress conditions and documented in various reports published internationally within the nuclear industry. Westinghouse has developed mathematical correlations based on this test data which are used for development of a creep-based methodology for the determination of allowable peak cladding temperature during dry storage.[12]

The MOX fuel rods used at Big Rock Point have design operating parameters that are equal to or bounded by those for conventional UO_2 fuel rods. As such, the bounding operational temperature (e.g., in-reactor) experience of the two fuel rod configurations is similar. Further, since the 35 GWd/MTU burnup value of the BRP MOX fuel is below the design basis 40 GWd/MTU burnup for the conventional BRP fuel, the MOX fuel internal rod pressures and operating temperature effects will be bounded by those for the conventional BRP fuel. Although the BRP MOX fuel assemblies have lower internal rod pressures and, therefore, lower cladding stress levels than the design basis BRP fuel assemblies, the same long-term allowable cladding

---

[9] NUREG-1536, *Standard Review Plan for Dry Cask Storage Systems*, U.S. Nuclear Regulatory Commission, January 1997.

[10] UCID-21181, *Spent Fuel Cladding Integrity during Dry Storage*, Lawrence Livermore National Laboratory, September 1987.

[11] EPRI TR-103949, *Temperature Limit Determination for the Inert Dry Storage of Spent Nuclear Fuel*, Electric Power Research Institute, May 1994.

[12] WCAP-15168, *Dry Storage of High Burnup Spent Nuclear Fuel*, Westinghouse Electric Company, March 1999.

temperature limit is used for both fuel types as a bounding value. Section 4.7.4.4 presents the basis for this assumption.

4.3.2.1 Cladding Temperature Decay

Peak cladding temperature will decrease over the storage period due to reductions in the heat load caused by radioactive decay of fission products. SNF with higher burnup levels has a proportionally higher percentage of long lived radionuclides, which decay slower than short lived radionuclides. As a result, the canister heat load and corresponding peak cladding temperature will decrease more slowly over the storage period for higher burned fuel. Since cladding creep depends upon time at temperature, higher burned fuel has a lower allowable initial cladding temperature. Big Rock Point fuel does not have burnups greater than 40 GWd/MTU, therefore this burnup level is established to bound all Big Rock Point BWR fuel to be loaded within the W74 canister.

The peak cladding and peak rod average gas temperature decay curves depend upon the canister's specific temperature versus heat load curve and the decay heat reduction over the storage period. The W74 canister heat load versus temperature curves are shown in Figure 4.3-1. The curves illustrated in Figure 4.3-1 are developed by exercising the combined W74 canister-storage cask thermal model described in Section 4.4.1.1 under the normal hot storage conditions for a variety of canister heat loads.

The canister heat load decay over the storage life depends on the type of fuel (PWR or BWR) to be stored and the burnup level. The decay heat curve for 40 GWd/MTU Big Rock Point (BWR) fuel assemblies is presented in Figure 4.3-2.

The heat load decay curve (Figure 4.3-2) is entered graphically with the calculated assembly specific heat load (kW/MTU) to determine the post-irradiation time (years) necessary to achieve the heat load for the specified burnup level. The post-irradiation time and rod temperatures corresponding to the heat load from Figure 4.3-1 are then plotted to determine the temperature decay curves at each burnup level. Figure 4.3-3 presents the peak cladding and peak rod average gas temperature decay curves for 40 GWd/MTU Big Rock Point fuel. These temperature decay curves are used as input to the creep methodology equations presented later. A 100-year storage life is assumed for the creep methodology.

4.3.2.2 Fuel Rod Pressure and Hoop Stress

Determination of the long-term allowable cladding temperature using the creep correlation is largely dependent on the cladding stress. Under dry storage conditions, the primary concern is development of cladding hoop stress due to the rod internal pressure. Fuel rod internal pressure is influenced by the initial inert gas backfill, generation of fission gas, rod internal free volume, and average gas temperature. As presented later in Section 4.4.1.7, the generation of fission gas is dependent upon burnup. As the fuel burnup increases, the internal rod free volume decreases due to fuel pellet swelling and cladding diametrical creepdown, which is caused by the differential pressure between fuel rod internal pressure and the reactor operating pressure. Fission gas generation and void volume reduction contribute to increasing internal rod pressures with increasing burnup level.

The rod pressures for moderate burnup (up to 40 GWd/MTU) BRP fuel assemblies are determined by assuming the release of 30% of the generated fission gas into the rod. Consistent

with EPRI Report TR-103949,[11] the fuel rod pressure varies with average fuel rod gas temperature by the ideal gas law. The average fuel rod gas temperature is determined using the W74 canister thermal model presented in Section 4.4.1.1 for normal hot storage conditions. The peak rod average gas temperature is calculated as a weighted average of the fuel cladding temperature over the active fuel length and gas plenum region.

Once in dry storage, the fuel rod internal pressure varies only with peak rod average gas temperature. As shown in Figure 4.3-3, the peak rod average gas temperature decays significantly over the storage lifetime.

From PNL-6189,[13] the cladding stress can be determined from the fuel assembly parameters as follows:

$$\sigma_{\infty} = \frac{\Delta P D_{mid}}{2t}$$

where:

σ_{∞}	=	Cladding mid-wall hoop stress
ΔP	=	Differential pressure across fuel cladding
D_{mid}	=	Cladding mid-wall diameter (fuel assembly specific)
t	=	Cladding wall thickness (fuel assembly specific)

Fuel rod cladding thickness is reduced due to waterside cladding oxidation. From PNL-4835, BWR cladding oxide layer thickness ranges from 1 to 125 μm. For conservatism, an oxide layer of 125 μm is assumed for all BWR rod stress calculations.

Cladding baseline hoop stress and peak rod average gas temperature for moderate burnup BRP fuel are 69.9 MPa and 257.4°C (for the creep correlation) and 311°C (for the CSFM method, which does not account for the effect of the peak rod average gas temperature), respectively. These baseline stress and temperatures are used for determination of allowable cladding temperature.

4.3.2.3 Long-Term Allowable Cladding Temperatures

Creep Methodology Correlation

The cladding creep correlation presented in WCAP-15168 is used with one conservative exception. The creep methodology cladding strain formulas are based on the behavior of unirradiated zircaloy cladding. The calculated unirradiated strain values are then adjusted downward by a Spilker correction factor to determine strain values for irradiated cladding. This adjustment factor is based on a comparison of measured strain rates for irradiated and unirradiated zircaloy cladding. A cladding strain (Spilker) reduction factor of “2” is used for these calculations in lieu of the factor used in WCAP-15168.

[13] PNL-6189, *Recommended Temperature Limits for Dry Storage of Spent Light Water Reactor Zircaloy-Clad Fuel Rods in Inert Gas*, Pacific Northwest Laboratory, May 1987.

As such, the modified WCAP-15168 method is used to determine the allowable cladding temperature for the BWR fuel classes which may be accommodated by the W74 canister. Both moderate and high burnup levels are considered. The creep methodology includes the following equation:

$$\varepsilon = At^m$$

where:

ε	=	strain
A	=	initial strain
t	=	storage time

The term m is defined as:

$$m = c_1 + c_2 T_f + c_3 T_f^{\,2} + \ldots + c_{11} T_f^{\,10}$$

where:

c_1 to c_{11} = correlation constants (WCAP-15168, Table 4-2)

$$T_f = T(°C) + (\sigma - 80)\left(45/70\right)$$

and:

σ = Hoop stress. Determined by a ratio of the baseline stress and temperature to the peak rod average gas temperature (Figure 4.3-3).

T = Peak cladding temperature, from Figure 4.3-3.

The peak cladding temperature which corresponds to a calculated cladding strain of 1% at the end of the 100-year dry storage period is the maximum allowable cladding temperature for the given burnup level and fuel assembly type. The maximum allowable cladding temperature determined using the creep correlation for moderate burnup BRP fuel is 385.5°C.

Bounding Long-term Allowable Cladding Temperature

The allowable cladding temperature of 385.5°C bounds all BRP fuel assembly types and burnup levels to be accommodated in the W74 canister, as reported in Table 4.3-1.

4.3.2.4 Short-Term Allowable Cladding Temperature

The short-term allowable cladding temperature is established as 570°C.[14] In order to confirm that the 570°C short-term allowable cladding temperature is valid for burnups above 28 GWd/MTU (as specified in NUREG-1536), the worst case rod stress is calculated using a Big Rock Point assembly under 40 GWd/MTU burnup conditions for peak internal pressure and cladding oxidation. This calculated maximum cladding stress is compared with the tabulation of failure mode observations presented in EPRI Report TR-103949.

[14] PNL-4835, *Technical Basis for Storage of Zircaloy-Clad Spent Fuel in Inert Gases*, Pacific Northwest Laboratory, September, 1983.

$$\sigma_{\infty} = \frac{PD_{mid}}{2t} = \frac{(11.9MPa)(0.5295in)}{2(0.033in)} = 95.5MPa$$

where:

$$P = (1200\,psi)\frac{(570^{\circ}C + 273K)}{(311^{\circ}C + 273K)}\left(\frac{6894.75Pa}{psi}\right)\left(\frac{MPa}{10^{6}Pa}\right) = 11.9MPa$$

D_{mid} = 0.5625 in -0.033 in = 0.5295 in

t = (0.034 in-.000984 in) = 0.033 in

The maximum short-term cladding stress calculated above (95.5 MPa) is conservative due to the conservatism of the 40 GWd/MTU rod pressure and the use of peak rod temperature for the rod pressure calculation, instead of the average rod temperature.

Regardless, the calculated maximum short-term cladding stress is much lower than the average rod stress (395 MPa) reported in EPRI Report TR-103949,[11] Table A-1, for stress-rupture observations of irradiated zircaloys. The calculated maximum stress is also much less than the lowest rod stress reported for Zr-2 clad BWR fuel (337 MPa). Additionally, no rod failures were reported by PNL-4835 for rods tested up to 570°C, and only pinhole defects (no gross failures) were observed for unirradiated rods tested up to 800°C. This provides additional assurance that the 570°C short-term allowable temperature is conservative, and that no gross cladding failures will occur if short-term temperatures are maintained below this value.

This short-term cladding allowable temperature applies during all W74 canister thermal accident conditions within the transfer cask (i.e., loss of neutron shield, fire) and the storage cask (i.e., all vents blocked, fire).

It is not feasible to uniquely define the effects on creep associated with changes in hydriding and annealing characteristics of Zircaloy-2 and Zircaloy-4 fuel assembly cladding during dry storage if the necessary loading cycle operations prior to initiating dry storage entail lengthy periods with temperatures above 400°C (752°F). Therefore, the maximum allowable short-term fuel cladding temperature is limited to 400°C during fuel loading and storage operations for normal and off-normal conditions to assure that the total cladding creep is less than 1%.

Table 4.3-1 - W74 Canister Component Allowable Temperatures

Component	Max. Temperature (°F)	Max. Short-Term[1] Temperature (°F)
Fuel Cladding	726 (385.5°C)	752 (400°C)[2] 1058 (570°C)
Load Bearing Carbon Steel	700	1000
Load Bearing Stainless Steel	800	1000
Borated Stainless Steel	1000	1000

Note:

(1) Short-term allowable temperatures apply under conditions when storage cask or transfer cask drop accidents are not postulated.

(2) The 400°C limit applies to normal and off-normal conditions; the 570°C limit applies to accident conditions.

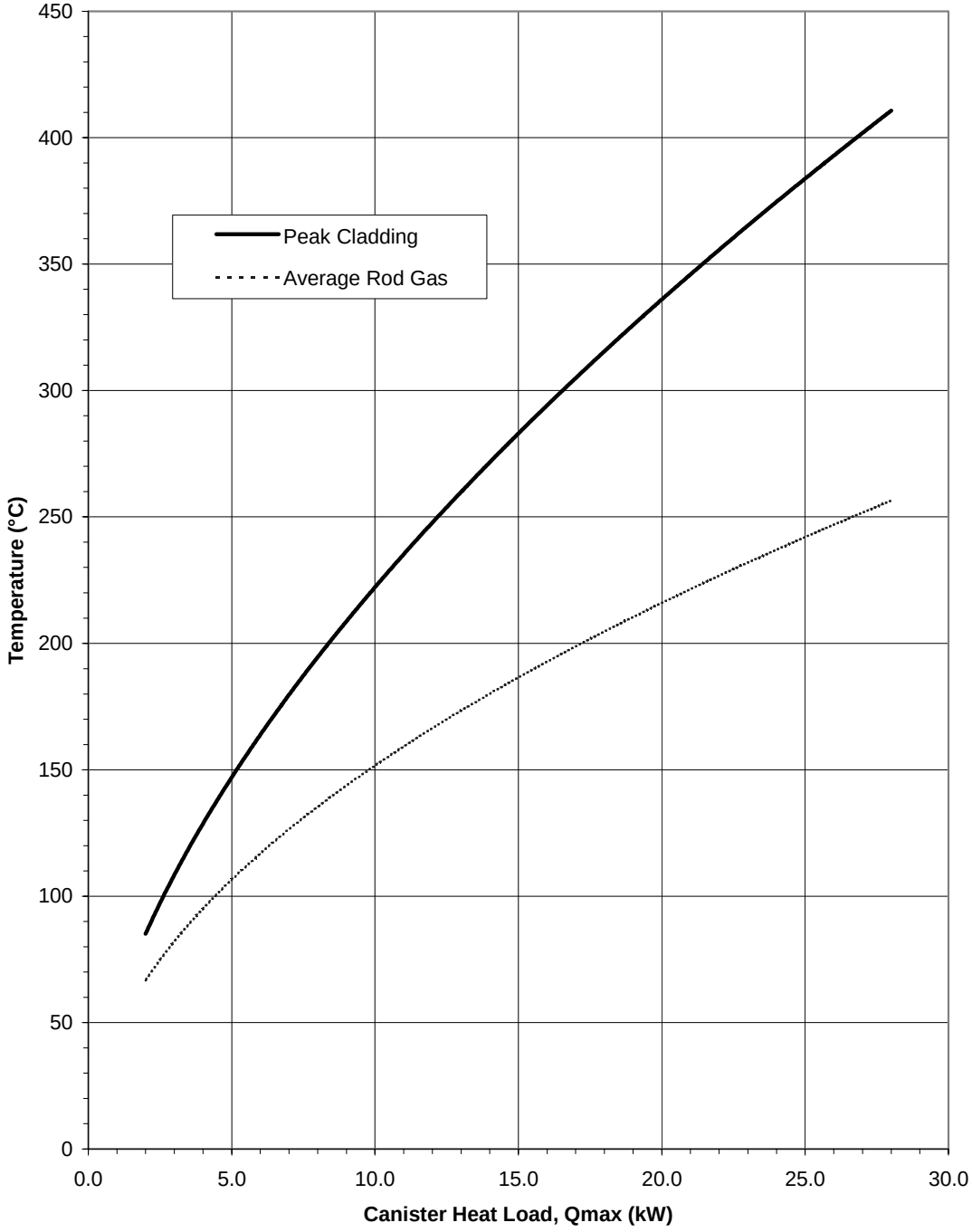

Figure 4.3-1 - W74 Canister Heat Load (Q_{max}) vs. Temperature

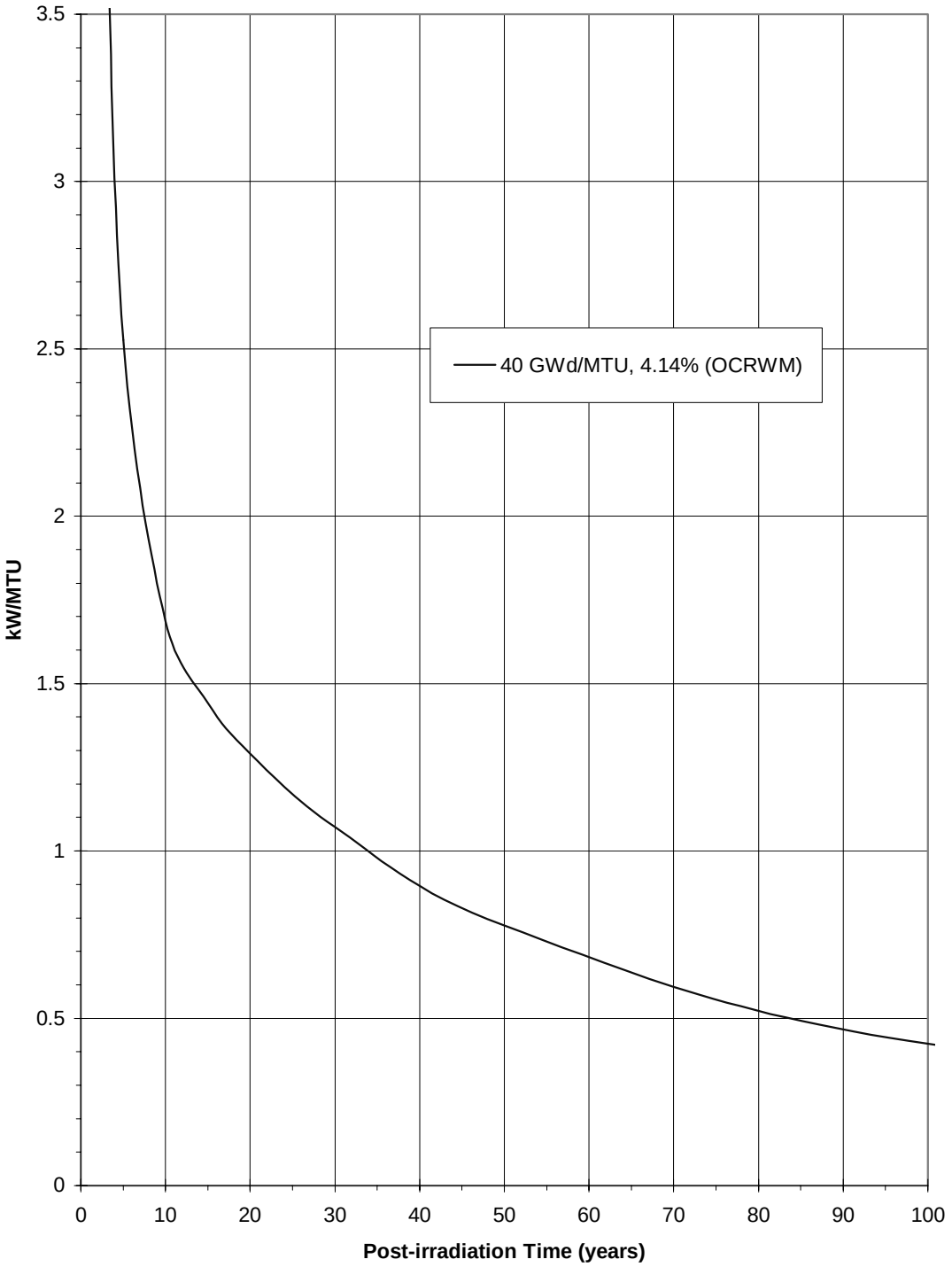

Figure 4.3-2 - Big Rock Point BWR Fuel Decay Heat Curve

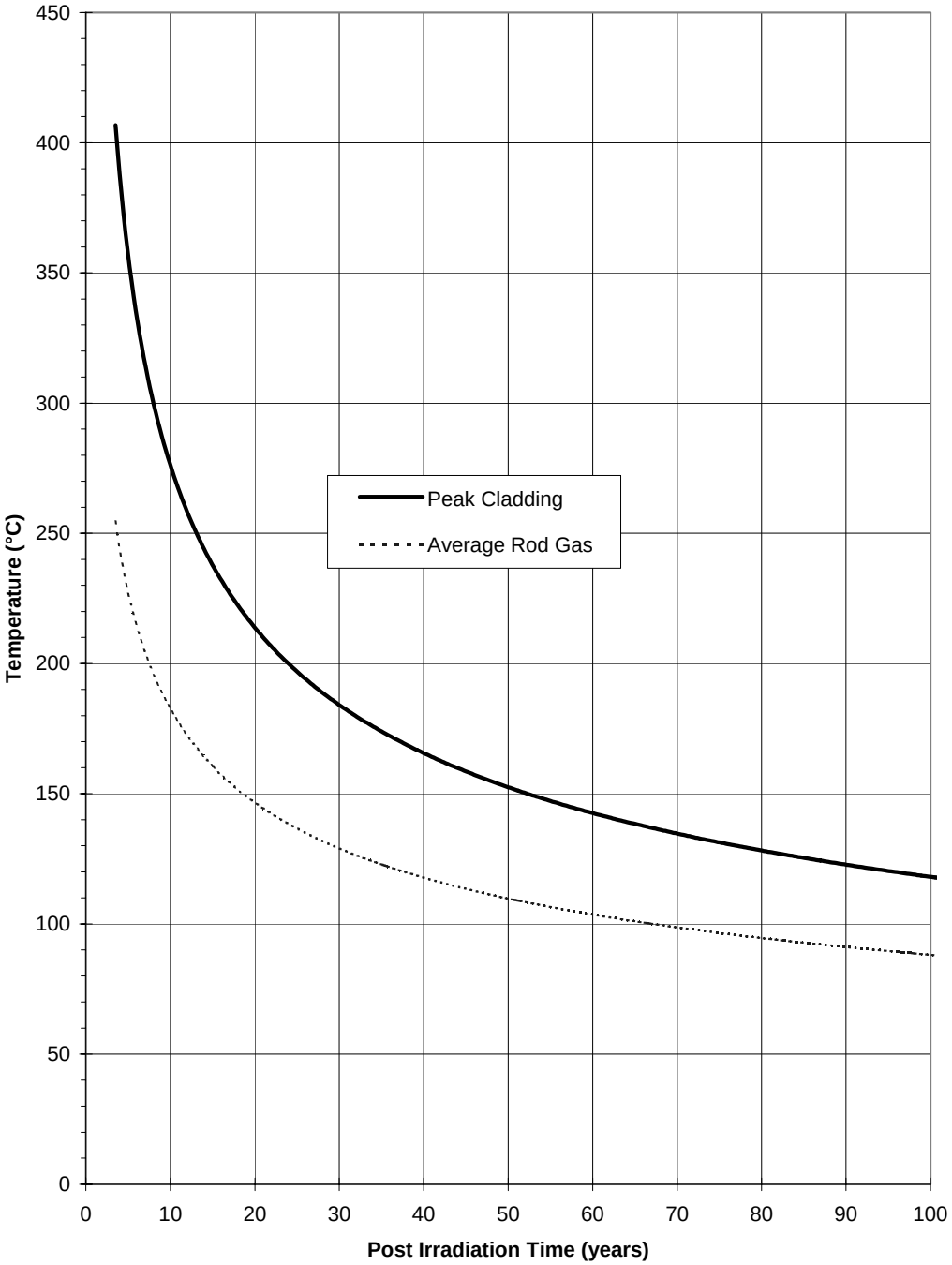

Figure 4.3-3 - Big Rock Point Temperature Decay Curves

4.4 Thermal Evaluation for Normal Conditions of Storage

This section provides a discussion of the thermal analysis methodology and results for the FuelSolutions™ W74 canister when used in conjunction with the FuelSolutions™ W150 Storage Cask and the FuelSolutions™ W100 Transfer Cask. The applicable canister assembly thermal ratings, temperature distributions, and thermal performance are evaluated to verify that the canister and cask thermal design features adequately perform their intended functions under normal, off-normal, and accident conditions. Off-normal and accident conditions are further summarized in Chapter 11 of this FSAR.

The thermal evaluations of the W74 canister in the storage and transfer casks are performed using conservative analytical techniques. Canister and cask thermal values are established to ensure that all materials are maintained within their applicable minimum and maximum allowable temperature during all modes of operation.

Transient thermal analyses of some off-normal and accident scenarios are performed to support establishment of any necessary operational *technical specifications* included in Section 12.3 of this FSAR.

The thermal analysis methodology and results for the FuelSolutions™ W74 canister with BRP MOX, partial, and damaged fuel assemblies are presented in Sections 4.7.4, 4.7.5, and 4.7.6, respectively.

4.4.1 W74 Canister within Storage Cask

To validate the performance of the FuelSolutions™ W74 canister within the W150 Storage Cask under normal conditions of storage, the combined thermal model for the W74 canister and the storage cask is evaluated for the design basis normal climatic conditions presented in Table 4.1-2 using the enveloping W74 canister heat flux profile. The analysis presented herein is designed to establish a thermal rating and to demonstrate that the W74 canister and storage cask allowable material temperatures are not exceeded for the established canister thermal rating at any site within the contiguous United States.

This section presents the thermal analysis of the canister within the storage cask. The thermal model of the W74 is described in this section along with a discussion how the canister thermal model is interfaced with that for the storage cask. The specifics of the thermal model for the FuelSolutions™ W150 Storage Cask is presented in Section 4.4.1 of the FuelSolutions™ Storage System FSAR and is not repeated here.

4.4.1.1 W74 Thermal Model In Storage Cask

The analytical thermal model of the W74 canister assembly is developed for use with the SINDA/FLUINT computer program.[2] Section 4.7.3.1 presents an overview of the SINDA/FLUINT program and its past use for the analysis of nuclear systems. The thermal modeling of the W74 canister assembly is presented in the following paragraphs.

Canister Modeling Approach

The basic thermal modeling approach used for the W74 canister is to divide the basket assembly into common geometry segments, such as a spacer plate and the sections of guide tubes and the

canister shell extending from that spacer plate to the next spacer plate. By defining the basic thermal model in this manner, the thermal mass and conductance for all other sections of the basket is modeled by applying a set of scaling factors as a function of the spacer plate thickness and the distance between the spacer plates. This approach not only simplifies the thermal modeling, but eases the verification process by minimizing the amount of original coding required to provide a complete thermal representation of the system. Precisely how this feature is used for this analysis is explained below.

The FuelSolutions™ W74 canister includes the shell and basket assembly components. The canister shell assembly components include the right cylindrical shell, top end inner closure plate, top end outer closure plate, bottom end plate, bottom closure plate, top and bottom end shield plugs, and vent and drain ports.

From a thermal point of view, the differences between the W74M and W74T versions of the FuelSolutions™ W74 canister are slight. The use of four additional carbon steel spacer plates in the W74T version over that used in the W74M version has essentially no impact on the thermal performance. This is due to the facts that the thicker stainless steel spacer plates and the lower emissivity associated with the electroless nickel plated carbon steel plates combine to effectively cancel the higher thermal conductivity of SA-517/A-514 Grades F and P carbon steel over 316 stainless steel.

Taken together, the design differences between the W74M and W74T versions of the basket assemblies will result in no significant impact on the thermal performance of the baskets. Therefore, the thermal model documented herein is for the W74M version of the FuelSolutions™ W74 Canister design, but is applicable to the W74T version of the canisters as well.

Three general categories of analytical thermal submodels are used to analyze the performance of W74 canister assembly within the storage and transfer casks. These submodels are:

1. A thermal submodel of a typical spacer plate or group of spacer plates, including the associated sections of the spent fuel assemblies and guide tubes, within the W74 basket assembly.
2. A submodel of the bottom end of the canister assembly, together with the bottom end shield plug and the associated basket assembly spacer plate sections.
3. A submodel of the top end of the canister assembly, together with the closure end shield plug and the associated basket assembly spacer plate sections.

Program features within SINDA/FLUINT[2] are used to combine the thermal modeling of these common elements to complete the thermal modeling for every other section within the basket. The individual thermal sections, or submodels, are thermally connected to complete a full length representation of the W74 canister configuration. A total of eight submodels are used in the thermal model of the W74 canister assembly.

Figure 4.4-1 illustrates the placement and extent of the model submodels used in the thermal model of the W74M canister. Each thermal submodel represents a 90° section of the basket assembly and canister shell. Symmetry conditions are assumed at the boundaries of the model for the geometry and thermal conditions within the storage cask.

The thermal model of each canister configuration consists of submodels “SA”, “SB”, “SC”, “SD”, “SE”, and “SF” through the mid-section of the canister and basket assembly, and model sections “END” at the bottom end and “LID” at the top end of the canister. Figure 4.4-2 through Figure 4.4-8 present the layout of the thermal sections and nodes used within each of the model submodels.

Taken together, the model submodels and their associated thermal sections provide a quasi-three-dimensional thermal model of the entire FuelSolutions™ W74M canister. The model is referred to as “quasi- three-dimensional” because it uses a combination of two-dimensional and three-dimensional modeling to represent different segments of the canister. Those portions of the assemblies (i.e., the interior of the basket assemblies and the canister side wall) that have significant variation in heat transfer in all three dimensions (“r”, “θ“, and “z”) are represented with a three-dimensional model. The bottom end and closure lid shield plugs are represented with axisymmetric modeling (i.e., “r”, and “z” dimensions only) since the temperature variation in the “θ“ direction (e.g., around the circumference) is small for the thermal boundary conditions imposed by the casks.

Modeling of the entire length of the canister permits simulation of the axial variation in decay heat within the fuel assemblies, the ability to model differences in axial placement of the fuel assemblies within the canister, and an accurate determination of the thermal end effects introduced by the canister shield plugs and the variation in decay heat with axial position.

The approach used to model the canister assembly is further illustrated by examining the makeup of the thermal modeling for the “END” submodel. The “END” submodel encompasses the canister bottom, the shield plug, and the first three spacer plate sections of the basket assembly. Figure 4.4-2 illustrates the section of the canister assembly covered by the “END” submodel and the thermal node layout in the canister bottom and shield plug. Thermal nodes at six radial locations are used to provide temperature resolution within the bottom end plate, the shielding material, and the bottom closure plate. In addition to the nodes shown, an additional five thermal nodes are used on the inner surface of the bottom closure plate to represent surface temperatures. The thermal modeling in the shield plug represents an axisymmetric model of these components which is appropriate for the expected temperature variation within the components.

Canister Modeling Basis

A 1.0 inch space is assumed to separate the bottom closure plate and the bottom of the first spacer plate. This dimension represents the 1 inch distance which support tubes extend below the spacer plate. Heat transfer between the inside surface of the shield plug and the first spacer plate is via radiation and conduction/convection through the helium gas. No direct contact is assumed between the basket and the shield plug.

Temperature dependent properties for specific heat and thermal conductivity are used for all components of the shield plug. No direct contact is assumed between the bottom end plate and the shield material, or between the shield material and the bottom closure plate. Instead, an air gap of 0.060 inches (1.5 mm) is assumed between each pair of materials. This modeling approach provides a conservative estimate of the internal canister temperatures and the axial thermal gradient within the shield plug.

Figure 4.4-3 to Figure 4.4-5 illustrate the thermal modeling used for the fuel assemblies, the guide tubes, and the spacer plates within this section of the canister assembly. Figure 4.4-3 presents the thermal node layout used for the typical modeling of the fuel assemblies and the basket assembly in the region between spacer plates. A 90º segment is represented with symmetry conditions used at the boundaries for the vertical orientation. An additional 90º segment is added to simulate the lower half of the basket for case when the canister is in the horizontal orientation. The temperature within each fuel assembly is simulated by one thermal node representing the peak fuel rod cladding temperature and a node at each face of the fuel assembly to provide the edge temperatures. This node layout complies with the lumped k_{eff}/h_{edge} model described in Manteufel and Todreas[4] (see Section 4.2). The same k_{eff}/h_{edge} model correlation is assumed for either horizontal or vertical orientation of the basket assembly. Helium gas is assumed as the medium within the canister.

A single node is used to represent each wall of the guide tube despite the fact that the guide tube wall is actually composed of 2 separate layers (e.g., the guide tube wall and the borated steel neutron absorber sheet) on one or two faces of the guide tube. This level of modeling is appropriate since the thickness of the materials used and the direct contact between the materials limits the temperature difference between the layers to a few degrees Centigrade. Each guide tube is conservatively assumed to be centered in its respective spacer plate cutout (i.e., no credit is taken for direct contact between the guide tube and spacer plate surfaces) and each fuel assembly is conservatively assumed to be centered within the guide tubes. This assumption is used for the horizontal as well as the vertical orientation to account for possible imperfect contact, high centering between a series of spacer plates, etc.

The dimension of the gap between the guide tube and the spacer plate is set based on the nominal gap that exists at the time of basket assembly. This assumption is conservative given the higher temperature of the guide tube material and its higher coefficient of thermal expansion. As such, both the higher temperature and greater thermal expansion will cause the guide tubes to expand more than the surrounding hole in either the carbon or stainless steel plates.

The thermal modeling provides temperature resolution for the peak cladding temperature in the fuel assembly (i.e., nodes 10, 20, 30, … 340), the edge of the fuel assemblies (i.e., nodes 12, 13, 21, 22, … 344), the walls of the guide tubes (i.e., nodes 16, 17, 25, 26, … 348), the support sleeves (i.e., nodes 355 to 358), and the canister shell (i.e., nodes 502 to 522) at each spacer plate section in the basket assembly. To differentiate between the various sections of the basket assembly being modeled within the SINDA/FLUINT program,[2] the node numbers are incremented in steps of 1000 for each spacer plate section within the submodel (i.e., node 1502 is a section of canister side wall between the first two spacer plates, 2502 is between the second and third spacer plates, etc.).

Figure 4.4-4 illustrates the modification to the typical thermal modeling of the fuel assemblies and guide tubes to simulate the short loading of the W74 canisters to achieve a total of 64 SNF assemblies per canister. As seen in the figure, not only are the center five fuel assemblies not present, but the associated guide tubes are also absent from the basket assembly. This basket configuration results in a void region in the center of the basket assembly.

Figure 4.4-5 illustrates the thermal node layout used at each spacer plate. Again, the modeling represents a 90º segment of the spacer plate over either the 0.75 inch thickness of the SA-517 carbon steel spacer plate or the 2.0 inch thickness of the Type 316 stainless steel spacer plate.

Symmetry conditions are used at the boundaries for the vertical orientation, or an additional 90º segment is used for the horizontal orientation forty-eight nodes (i.e., nodes 202 to 283) are used to simulate portions of the spacer plate within each 90º segment. The modeling level chosen is aimed at providing thermal resolution within the spacer plate, while limiting the overall complexity of the model. As indicated in the figure, the same thermal nodes used to represent the fuel assemblies and guide tubes between the spacer plates are used to simulate these components at the spacer plates. While the presence of the spacer plate will result in a local decrease in the temperature of these components, the amount of the decrease is small because of the thickness of the plates in comparison with their separation distances. As such, the added complexity required to capture this effect was deemed unnecessary.

Heat transfer from the guide tubes to the spacer plates is assumed to be via conduction and radiation across a gap. For conservatism, direct contact between the guide tube and spacer plate is not assumed. Heat transfer within the spacer plates is calculated using temperature dependent properties. The basket assembly is assumed to be centered in the canister for all vertical orientation analysis. As such, the heat transfer between the circumference of the spacer plates and the canister side wall is via conduction and radiation across a gap. A view factor of 1.0 is assumed, together with a thermal emissivity of 0.40 for the edge of the stainless steel plates, 0.11 for the electroless nickel plated carbon steel plates, and 0.40 for the canister shell. Calculations for the horizontal orientation assume contact between the bottom of the spacer plates and the canister shell. The contact thermal resistance is increased by 40% to account for potential imperfect contact.

Canister Model Presentation

Figure 4.4-6 presents an isometric view of the node layout as it would appear between the first and second spacer plate in each thermal submodel. Axial conductors are used to complete the three dimensional modeling of the basket assembly by providing thermal communication between the thermal nodes at one spacer plate section and the those at the next. A similar modeling approach to that depicted in Figure 4.4-3 and Figure 4.4-5 is used to represent the basket components in the other thermal submodels.

Figure 4.4-7 illustrates the thermal submodel used for the typical mid-body section (i.e., submodels SA, SB, SC, SD, SE, and SF) in the canister assembly. The length of each thermal submodel is selected to encompass three to four spacer plate sections within the W74M basket assembly. The modeling of the fuel and basket assembly region between the spacer plates is similar to that shown in Figure 4.4-3, except that the length is adjusted as required to match the separation distance between spacer plates. The thermal model at the individual spacer plates is the same as shown in Figure 4.4-5. Axial conductors within the canister shell, the guide tubes, and the fuel assemblies are used to tie the various submodels together.

As illustrated in Figure 4.4-8, the thermal submodel at the top end of the canister is similar to that used at the bottom end. The differences include the added layers of steel used in the closure and the differences in the basket layout. The thermal node layout for the spacer plates and the basket assembly between plates is similar to that shown in Figure 4.4-3 and Figure 4.4-5. Again, axial conductors within the canister shell, the guide tubes, and the fuel assemblies are used to provide thermal communication between the various submodels. Although the W74 top shield

plug assembly includes a shield plate with 37 individual plugs, it is modeled as a solid plate. This approach is appropriate for a combination of reasons. First, the tight fit-up between the individual plugs and the shield plate in which they fit means that the thermal resistance between the plugs and the shield plate are relatively low. Second, the relatively low thermal heat flux at this location results in associated low thermal gradients in the radial direction. Taking these facts together, treating the top shield plug assembly as a solid plate yields a temperature distribution that is sufficient for the purposes of this calculation. The heat transfer in the axial direction through the shield plug is largely unaffected by the presence of the individual plugs in the shield plate.

The modeling of the heat transfer within the basket assembly consists of a series of heat exchanges between the fuel assemblies, guide tubes, spacer plates, support tubes, and the canister side wall. The heat transfer modeling used to simulate the heat transfer modes for each set of spacer plates and the sections of guide tubes between them forms another layer of thermal submodeling within the SINDA/FLUINT program.[2] This thermal submodel is repeated and scaled as appropriate to represent other spacer plate sections of the basket assembly. The following paragraphs describe the approach used to simulate the combined heat transfer mechanisms from the fuel assemblies to the canister side wall for a single spacer plate section.

Radiation Heat Transfer

The radiation view factor program RadCAD[15] is used to compute the radiation exchange factors from the guide tubes to adjacent guide tubes, the spacer plates, and the canister shell. Likewise, radiation heat transfer is modeled from the spacer plates to the adjacent spacer plates and to the canister shell. The emissivity values for the surfaces are taken from material properties listed in Section 4.2. The number of thermal nodes used to simulate the various surfaces of the guide tubes, spacer plates, and canister side wall results in approximately 500 radiation conductors interconnecting the various surfaces between the typical spacer plate section of the basket assembly, or somewhere between 14,000 and 15,000 radiation conductors for the entire basket assembly.

Convection Heat Transfer

Beyond conduction and radiation heat transfer, the principal heat transfer mode within the basket assembly is convection. This is true for both the vertical and the horizontal orientations of the basket assembly. The fundamental approach and equations used to compute the convection heat transfer within the basket assembly is presented in Section 4.7.1. The convection heat transfer that occurs between the fuel assemblies and the guide tubes is included as part of the of Manteufel and Todreas[4] non-linear form of the lumped k_{eff}/h_{edge} model for a typical BWR fuel assembly (see Section 4.2.2). Global convection heat transfer between the gas within the fuel guide tubes and the canister shell (i.e., the potential flow upward through the guide tube and downward along the canister shell) is conservatively ignored for this evaluation.

Figure 4.4-9 and Figure 4.4-10 present the modeled flow pattern within the vertical orientation of the canister.

---

[15] RadCAD™, *CAD Based Thermal Radiation Analyzer,* Version 2.0, Prepared for NASA, Johnson Spacecraft Center, Contract NAS8-40560, Prepared by Cullimore and Ring Technologies, Inc., Littleton, CO, 1997.

Canister to Storage Cask Model

The modeling of the W74 canister in the storage cask is accomplished by combining the thermal model of the W74M canister assembly as defined above with the thermal model of the storage cask as defined in Section 4.4.1 of the FuelSolutions™ Storage System FSAR. The thermal modeling used in the storage cask portion of the model to connect a generic canister to the storage cask is deleted and a new set of thermal connections specific to the geometry of the W74M canister is substituted in its place. These W74M specific thermal connections consist of a series of convection and radiation conductors that reflect the thermal submodeling used for the W74M canister thermal model. The original coding within the storage cask model for convection between the canister and the inner air stream is retained and the values computed are scaled to match the specific lengths of the canister shell represented by each thermal node on the W74 canister shell. This approach is used for the normal, off-normal, and accident conditions of storage. Radiation connections from the W74 canister to the storage cask thermal nodes are also redefined for the specific thermal modeling used in the combined W74 canister and storage cask thermal model.

The twenty-two variable length sections used to provide temperature resolution in the side wall section of the cask model are re-defined to thermally match up with the thermal submodeling used for the W74 canister. Figure 4.4-11 presents a visual depiction of the alignment between the side wall sections of the storage cask and the thermal submodels of the W74 canister.

4.4.1.2 Canister Thermal Rating

The FuelSolutions™ W74 design basis thermal load cases are summarized in Table 4.1-2. For the determination of the W74 canister thermal rating, only steady-state normal hot conditions are considered. The combined W74 canister and storage cask thermal model is exercised using the normal hot storage conditions (case 7, 100°F ambient) for determination of the W74 canister thermal rating. The long-term allowable material temperatures are assumed for the analysis. The W74 canister thermal rating is established based on the most limiting normal hot conditions in the storage and transfer casks. Since the fuel cladding is the most limiting material, and long-term cladding allowable temperature applies only in the storage cask, the W74 canister thermal rating is based on normal hot storage conditions.

The W74 canister thermal rating in the storage cask is based on the normal air flow path in the vertical orientation. Off-normal flow conditions such as all vents blocked or horizontal orientation are not considered as the basis for establishing the canister thermal rating. Since steady-state temperatures at the thermal rating for these operating modes may exceed the allowable material temperatures, transient analyses of these operating modes are performed to establish an operational *technical specification* limit. These transient cases are addressed in Sections 4.5 and 4.6 for off-normal and accident conditions, respectively.

The methodology discussed in Section 4.1.3.2 was implemented for the thermal rating case. The bounding canister axial heat profile for Big Rock Point fuel in Figure 4.1-1 is applied as a boundary condition for the normal hot storage condition. The allowable long-term material temperatures in Table 4.3-1 are assumed and the total canister heat load (Q_{Total}) gradually increased until an allowable material temperature is reached. The results for the W74 canister

maximum heat load rating (Q_{max}) and maximum linear heat generation rate ($LHGR_{max}$) are presented in Table 4.4-1.

Given that the resulting W74 thermal rating yields substantial thermal margins for the canister structural materials, the above process was repeated to establish the maximum canister thermal rating based on structural material thermal limits only. This higher canister structure heat load rating (and associated linear heat generation rate) are also shown in Table 4.4-1. A comparison of the resulting canister and cask component temperatures with the allowable component temperatures for operations at the qualified W74 canister thermal rating are presented in Table 4.4-2. Temperature data is presented for both the actual rated heat load of the W74 canister (i.e., based upon the maximum allowable fuel cladding temperature) and the higher canister heat load limit that can be accommodated by the W74 basket structure.

As seen from Table 4.4-2, the peak fuel clad temperature is just under its allowable value at the canister heat load rating of 24.8 kW. At this heat load, all of the canister structural materials are well below their maximum allowable values. At the higher heat load of 26.4 kW (the maximum W74 canister structure heat load), the carbon steel spacer plate temperature is just under its allowable value, whereas all other canister components have greater thermal margins. These results demonstrate that the maximum allowable fuel clad temperature limit is met at the rated canister heat load of 24.8 kW, whereas the thermal margins for the canister's structural components are sufficient to support a higher heat load of 26.4 kW.

The majority of the thermal calculations presented in this FSAR are conservatively based on the higher canister structure maximum heat load of 26.4 kW. The results of these calculations will be bounding (conservative) for the peak temperatures and thermal gradients associated with canister payloads rated for a maximum heat load of 24.8 kW. The thermal results with the lower canister heat load of 24.8 kW are presented for the normal and normal hot conditions of storage to verify that the maximum long-term fuel clad temperature is met at the 24.8 kW heat load.

In addition to the normal and normal hot conditions of storage, two other off-normal condition cases are addressed at the maximum heat load of 24.8 kW (as discussed in Section 4.1) to demonstrate that the peak fuel cladding temperature does not exceed the short-term 400°C limit during canister loading or storage. For all other thermal calculations, including those for basket component temperature, gas pressure analyses, accident analyses, and transient analyses are conservatively based on the higher canister heat load limit of 26.4 kW. As such, operations at the canister heat load rating of 24.8 kW will yield higher thermal margins, available operation time, etc. than indicated by the results presented.

4.4.1.3 Maximum Temperatures

The W74 canister design basis thermal load cases for normal conditions within the storage cask are presented in Table 4.1-2, specifically cases 5, 6, and 7. For normal conditions, only steady-state analysis with the normal air flow path, vertical orientation, and normal ambient conditions (0°F, 77°F, and 100°F) apply. The system temperatures resulting from operation under normal conditions are presented in Table 4.4-3. All W74 canister component temperatures are within their material allowable temperatures for each load case. Note that the maximum temperatures presented in the table are based on operations at the thermal rating of the W74 canister for the normal and normal hot conditions of storage. The temperatures at the normal cold conditions of storage are based on a conservative (i.e., higher thermal gradients) heat load of 26.4 kW.

Selected storage cask temperatures at the storage cask thermal rating are presented for comparison purposes. The full presentation of the storage cask temperatures are presented in the FuelSolutions™ Storage System FSAR. Since the storage cask thermal ratings are higher than the W74 canister thermal rating, the storage cask material temperatures resulting from operations with the W74 canister are bounded by the analyses presented in the FuelSolutions™ Storage System FSAR. This verifies that the results and conclusions drawn for the storage cask only evaluation are not invalidated by this analysis.

Figure 4.4-12 and Figure 4.4-13 present axial temperature distributions within the components of the W74 canister and the storage cask for the normal hot and normal cold conditions of storage, respectively. These temperature distributions are conservatively based on the maximum canister structure heat load of 26.4 kW. The variation in the heat load profile in the double stack of Big Rock Point fuel is clearly visible in the plots. The temperatures in the upper basket are slightly higher than those seen in the lower basket due to a combination of temperature stratification in the canister and heating of the air stream within the storage cask as it rises in the cask. This latter effect and the direction of movement in the cooling air through the cask is also visible in the plots via the steady rise in the storage cask component temperatures from the bottom to the top of the cask.

Figure 4.4-14 and Figure 4.4-15 present the temperature distribution within the hottest spacer plates for the same normal hot and normal cold conditions of storage, respectively, and at the maximum canister structure heat load of 26.4 kW. The temperature results in the plots illustrate the expected symmetry conditions when the canister is in the vertical orientation.

4.4.1.4 Minimum Temperatures

The temperatures in the canister and storage cask components under normal cold conditions are listed in Table 4.4-3. Note that the temperatures shown are for a design basis canister at the canister structure thermal rating and, therefore, do not represent the lowest expected component temperatures.

The low temperature compatibility of the storage cask components is also evaluated for the bounding load case of 0°F (-18°C) ambient temperature, zero decay heat load, and no insolation. The steady-state temperatures of the W74 canister and storage cask components for this analytically trivial case are 0°F (-18°C). This temperature level is within the allowable minimum temperatures for all components.

4.4.1.5 Internal Pressures

The W74 canister internal pressure depends upon the quantity of rod fill gas, rod fission gas, and canister back-fill gas present under normal conditions within the canister cavity.

Fission gas generation depends primarily upon the fuel assembly MTU loading and burnup level. For the purpose of rod pressure determination, the only significant fission gas contributors are Krypton (Kr) and Xenon (Xe). All isotopes of Kr and Xe are considered for fission gas generation. Other fission products are neglected because they either exist in insignificant quantities or do not exist in the gaseous form at dry storage temperatures.

Consistent with NUREG-1536,[9] 30% of the fission gas yield within a fuel pellet is assumed to be available for release within the fuel rod. As a result, 30% of the fission gas yield and 100% of the rod fill gas are assumed to be released into the canister cavity for each postulated rod failure.

For normal conditions of storage, 1% of the fuel rods are postulated to fail. For off-normal conditions of storage, 10% of the fuel rods are postulated to fail. For accident conditions of storage, 100% of the fuel rods are postulated to fail. Off-normal and postulated accident internal pressure analyses are discussed in Sections 4.4 and 4.6, respectively.

The smallest loaded W74 canister free volume, based on worst case geometry tolerances, is conservatively used. Both W74 canister configurations and fuel loading options are evaluated to determine the limiting free volumes for each fuel class and type.

The W74 canister cavity average gas temperature for normal hot storage conditions (100°F ambient, Section 4.1.4) is conservatively assumed for the normal pressure analysis.

4.4.1.6 Fuel Rod Fill Gas

The total moles of helium fill gas within each fuel assembly depends on the assembly specific fuel rod total free volume and the fill gas pressure. Since the rods are back-filled during fabrication and prior to irradiation or exposure to elevated temperatures, the nominal rod dimensions are used. The ideal gas law applies for determination of fuel rod fill gas moles:

$$N_{Fill} = \frac{P_{Fill} V_{rod}}{RT}$$

where:

P_{Fill} = Rod fill gas pressure (atm)

V_{rod} = Fuel assembly rod internal free volume (liters)

R = Ideal Gas Constant (0.0821 atm-liter/gmole-°K)

T = Temperature at rod back-fill (293°K)

Moles of rod fill gas within the Big Rock Point fuel assemblies is summarized in Table 4.4-5.

4.4.1.7 Fuel Rod Fission Gas Generation

Fission gas generation is primarily dependent upon the fuel MTU loading and burnup level. For Big Rock Point Fuel, only 40 GWd/MTU burnup is evaluated.

Two independent methods are used to determine the fission gas generation. The first method uses the RADDB[16] to obtain the quantity of Krypton (Kr) and Xenon (Xe) gases generated for the given burnup levels assuming standard enrichment and a representative 5 year decay. The second method is a direct calculation of the moles of Kr and Xe fission gas using standard industry constants and fuel specific burnup and MTU loading. The method which results in the largest quantity of fission gas generation is conservatively used in the pressure calculations. Basic methodologies are described below:

[16] *LWR Radiological Data Base (RADDB)* v 1.1, U.S. Department of Energy, Office of Civilian Radioactive Waste Management, Prepared by Oak Ridge National Laboratory, July 1992.

Fission Gas Yield from RADDB

$$N_{Kr} = (m_{Kr}\frac{grams}{MTIHM})(\frac{mole}{83.8 grams Kr})(\frac{MTU}{assy})(\frac{64 assy}{canister})$$

$$N_{Xe} = (m_{Xe}\frac{grams}{MTIHM})(\frac{mole}{131.3 grams Xe})(\frac{MTU}{assy})(\frac{64 assy}{canister})$$

$$N_{Fission} = N_{Kr} + N_{Xe}$$

where:

N_{Kr}	=	gmoles of Kr/canister
N_{Xe}	=	gmoles of Xe/canister
m_{Kr}	=	Grams Kr/MTIHM (from RADDB)
m_{Xe}	=	Grams Xe/MTIHM (from RADDB)
MTU/assy	=	Fuel assembly class specific

Calculation of Fission Gas Yield

$$N_{Fission} = (\frac{GWd}{MTU})(1.0\cdot 10^{9}\frac{W}{GW})(86{,}400\frac{sec}{day})(\frac{MeV}{1.602\cdot 10^{-13} Joules})(\frac{1 fission}{207 MeV})(0.303\frac{atoms Kr + Xe}{fission})$$
$$\cdot(\frac{mole}{6.02\cdot 10^{23} atoms})(\frac{MTU}{assy})(\frac{64 assy}{canister})$$

where:

$N_{Fission}$	=	gmoles of Kr and Xe fission gas/canister
MTU/assy	=	Fuel assembly class specific

Industry constants:

207 MeV/fission[17]

0.303 moles Kr and Xe/fission[18]

Moles of rod fission gas for the 40 GWd/MTU burned Big Rock Point fuel are summarized in Table 4.4-5.

4.4.1.8 Normal Canister Pressure

The quantity of inert gas in terms of moles needed for canister cavity back-fill are determined in order to achieve 10 psig (1.68 atm) in the canister cavity under normal hot storage conditions

[17] Lamarsh, John R., *Introduction to Nuclear Engineering*, Addison-Wesley Publishing Company, 1977.

[18] Olander, Donald R., *Fundamental Aspects of Nuclear Reactor Fuel Elements*, Energy Research and Development Administration, 1976.

(100°F ambient, Section 4.1.4) with 1% rod failures. The ideal gas law is again used to calculate the moles of canister back-fill gas as follows:

$$N_{Total\ \ Normal} = \frac{P_{Normal} V_{canister}}{RT_{Normal}}$$

$$N_{Normal} = 0.01 \cdot N_{Rods}$$

$$N_{Canister} = N_{Total\ \ Normal} - N_{Normal}$$

where:

$N_{Total\ Normal}$ = Total moles of gas in canister cavity under normal conditions.

N_{normal} = Total moles of rod gas released into the canister cavity, assuming 1% rod failures

N_{Rods} = Total moles of fuel rod fill gas and fission gas available for release

$N_{Canister}$ = Total moles of canister back-fill gas (Table 4.4-5)

P_{Normal} = Canister pressure for normal hot storage (10 psig, 1.68 atm)

$V_{Canister}$ = Worst case canister cavity free volume(Table 4.4-5)

T_{Normal} = Canister gas temperature for normal hot storage (°K)

Since the assumption of 1% rod failures may not be conservative for some canister thermal analyses, the canister pressure under normal hot storage conditions is also calculated considering only the canister back-fill gas:

$$P_{Canister} = \frac{N_{Canister} RT_{Normal}}{V_{Canister}}$$

where:

$P_{Canister}$ = Canister pressure for normal hot storage, no rod failures

The W74 canister normal pressure at the thermal rating under normal hot storage conditions with 1% rod failures is 10 psig. The canister normal pressure under the same conditions with no rod failures for 40 GWd/MTU Big Rock Point fuel is 9.8 psig, as summarized in Table 4.4-4.

The canister cavity helium pressure of 9.3 psig (24 psia) is conservatively assumed for heat transfer analyses under normal hot storage conditions. As discussed above, during canister closure operations, the canister is back-filled with helium in order to achieve 10 psig under normal hot storage conditions with 1% rod failures. The canister shell design, fabrication, inspection, and closure processes ensure that the canister does not leak as discussed in Section 7.1 of this FSAR. A helium loss at the allowable canister leak rate over the entire 100-year storage life does not significantly reduce the canister cavity pressure or adversely impact heat transfer.

4.4.1.9 Maximum Thermal Stresses

FuelSolutions™ W74 canister maximum thermal stresses developed within the storage cask under normal conditions are addressed in Chapter 3. Calculation of these thermal stresses is

based on the maximum canister structure heat load of 26.4 kW, and is conservative (bounding) for the actual canister heat rating of 24.8 kW.

4.4.1.10 Evaluation of Canister Performance for Normal Conditions

The results of the steady-state analyses demonstrate that the storage cask allowable material temperatures under normal conditions are met for the maximum canister thermal rating, as presented in Table 4.4-1. Over the long-term storage period the spent fuel decay heat decreases, thus increasing the margins relative to the allowable temperatures. Therefore, the W74 canister is suitable for the dry storage of Big Rock Point BWR fuel within the FuelSolutions™ W150 Storage Cask.

Table 4.4-4 presents the summary of canister pressures for normal conditions of storage. As seen from the table, the canister pressurization for normal conditions of storage are within the design allowables.

The W74 canister heat balance under normal hot storage conditions and the maximum heat load rating (Q_{max}) is presented schematically in Figure 4.4-16. As can be seen, heat input to the storage cask is from spent fuel decay heat (26.4 kW, based on the canister structural heat load rating) and solar (3.03 kW on top, 2.86 kW on sides). Most of the heat is lost to natural convection air flow (24.46 kW) with the remaining heat lost through the storage cask to ambient through natural convection (1.45 kW for top, 2.16 kW from sides) and radiation (1.86 kW from top, 2.35 kW from sides).

The storage cask liner thermocouple reading (163°F) under normal hot storage conditions with the design basis W74 canister loaded is used as the basis for establishing the *technical specification* for normal daily temperature monitoring, contained in Section 12.3 of this FSAR.

Table 4.4-1 - W74 Canister Thermal Rating in Storage Cask

Applicable Fuel Group	Axial Heat Profile	Q_{max} (kW)	$LHGR_{max}$ (kW/in)
Big Rock Point BWR Fuel	Max Thermal	24.8	0.216
	Max Thermal Gradient	N/A	N/A
	Thermal Rating	**24.8**	**0.216**
W74 Canister Structure Thermal Rating		26.4	0.230
Storage Cask Thermal Rating		28.0	0.253

Table 4.4-2 - W74 Canister System Temperature at Q_{max} in Storage Cask

Component	Component Maximum Temperature (24.8 kW)	Component Maximum Temperature (26.4 kW)	Max. Allowable Temperature
Peak Fuel Rod Cladding	384.6°C	399.8°C	385.5°C
Guide Tube	690°F	716°F	800°F
Spacer Plates:			
Stainless Steel	488°F	506°F	800°F
Carbon Steel	673°F	699°F	700°F
Engagement Plate	431°F	445°F	800°F
Support Tube	563°F	584°F	800°F
Helium Bulk	495°F	513°F	N/A
Canister Shell	431°F	445°F	800°F
Max. Concrete	175°F	176°F	200°F
Liner Thermocouple(1)	163°F	166°F	N/A

Note:
(1) Estimated thermocouple reading for analyzed condition.

Table 4.4-3 - Maximum W74 Canister System Temperature at Q_{max} for Storage[1]

Component	Case 5 Normal Storage[1]	Case 6 Normal Cold Storage[2]	Case 7 Normal Hot Storage[1]	Allowable Temperature
Peak Fuel Rod Cladding	373.7°C	353.2°C	384.6°C	385.5°C
Guide Tube	668°F	627°F	690°F	800°F
Spacer Plates:				
Stainless Steel	466°F	408°F	488°F	800°F
Carbon Steel	652°F	608°F	673°F	700°F
Engagement Plate	408°F	346°F	431°F	800°F
Support Tube	540°F	485°F	563°F	800°F
Helium Bulk	473°F	415°F	495°F	n/a
Canister Shell	407°F	337°F	431°F	800°F
Max. Concrete	150°F	49°F	175°F	200°F
Liner Thermocouple[3]	136°F	41°F	163°F	n/a
Reference Results From Table 4.4-7 of the FuelSolutions™ Storage System FSAR				
Canister Shell[4]	*423 °F*	*337 °F*	*447 °F*	
Max. Concrete[4]	*169 °F*	*61 °F*	*197 °F*	
Liner Thermocouple[3,4]	*150 °F*	*48 °F*	*179 °F*	

Notes:

(1) Except as noted, temperatures are based on a heat load of 24.8 kW.
(2) Temperatures based on a heat load of 26.4 kW.
(3) Estimated thermocouple reading for analyzed condition.
(4) Temperatures based on heat load of 28 kW.

Table 4.4-4 - W74 Canister Normal Conditions Pressure Summary

Condition	W74 Canister Pressure (psig)
Normal Hot (no rod failures, min)	9.8
Normal (1% rod failures)	10.0

Table 4.4-5 - Big Rock Point Fuel Normal Pressure Nominal Parameters

Parameter	Minimum	Maximum
Rod Fill Gas/canister (moles)	7.4	34.9
Rod Fission Gas /canister (moles)	137.8	153.1
Peak Rod Press(1) (psig)	449	1075
Min. Canister Free Volume (liters)	5981	-
Canister Back-Fill Gas(2) (moles)	224.8	225.1
Canister Normal Press (no rod Failures) (psig)	9.8	9.8
Fuel Rod Fill Pressure (psig)	0	30
Fuel Rod Free Volume/Assembly (in^3)	100	263
Canister Helium Backfill (grams)	899	901
Canister Helium Backfill (gmoles/liter)	0.0376	0.0376

Notes:

(1) Peak rod pressures based on reactor operating temperature (311°C for BWR).

(2) Canister backfill moles calculated to achieve canister cavity pressure of 10 psig at normal hot storage conditions with 1% rod failures.

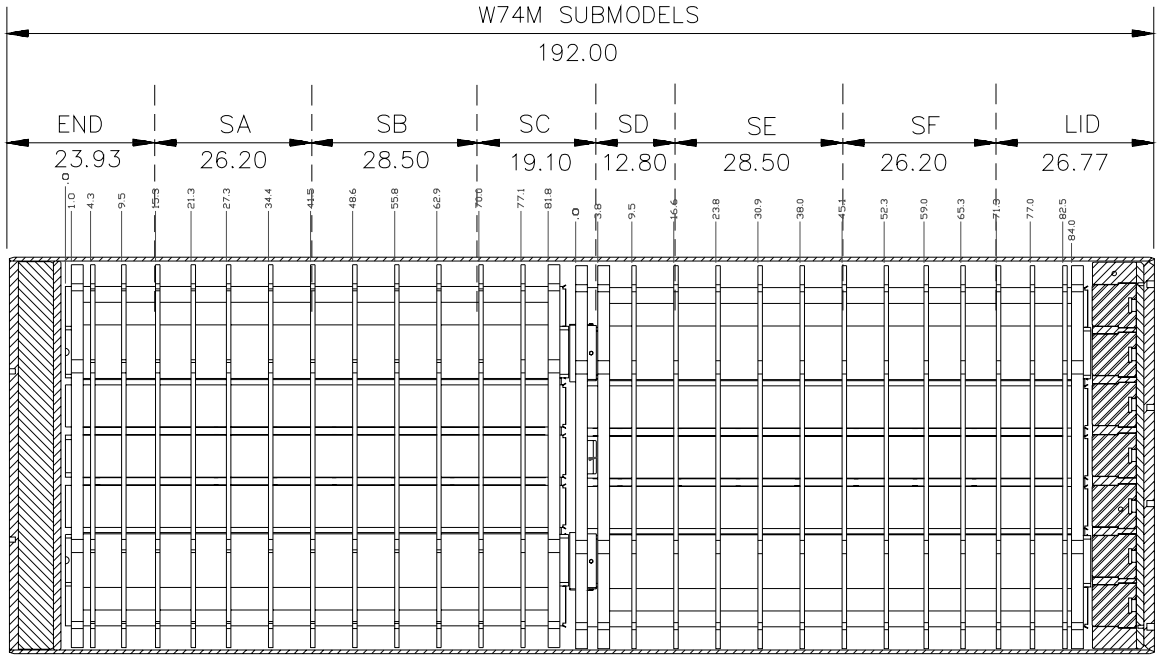

Figure 4.4-1 - FuelSolutions™ W74M Canister Thermal Submodel Layout

FIGURE WITHHELD UNDER 2.390

Figure 4.4-2 - Node Layout for W74 Canister Bottom End

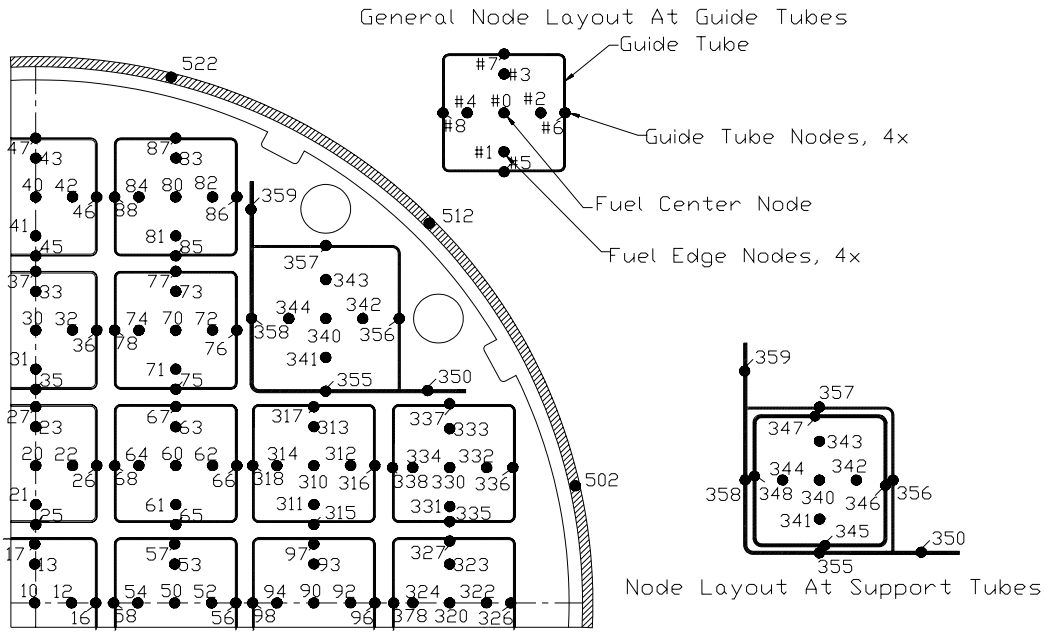

Figure 4.4-3 - Typical Node Layout Between W74 Spacer Plates

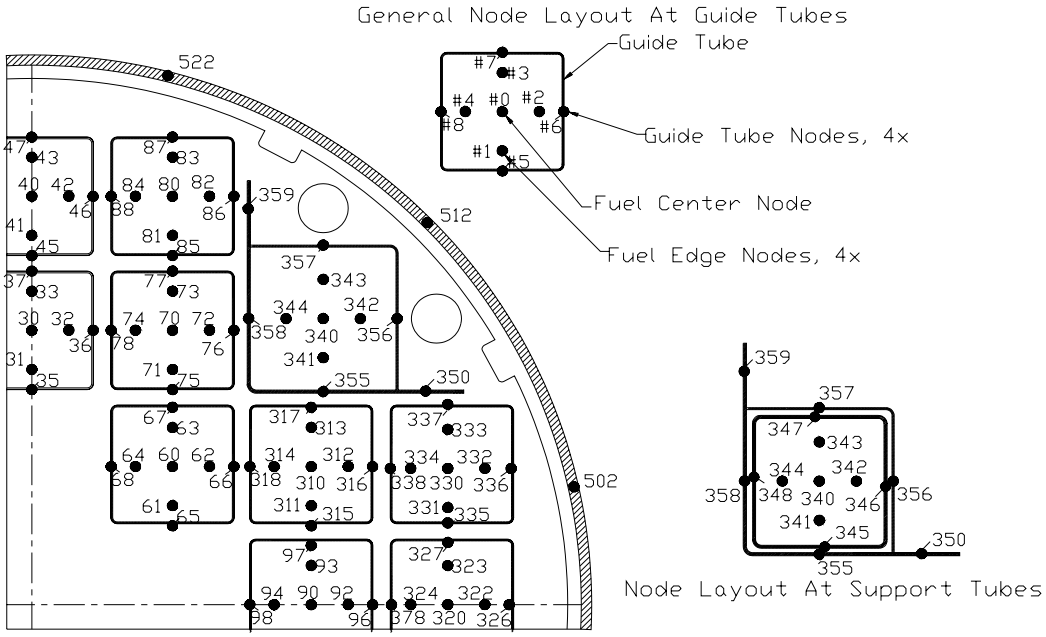

Figure 4.4-4 - Node Layout for W74 Canister Fuel Load Configuration

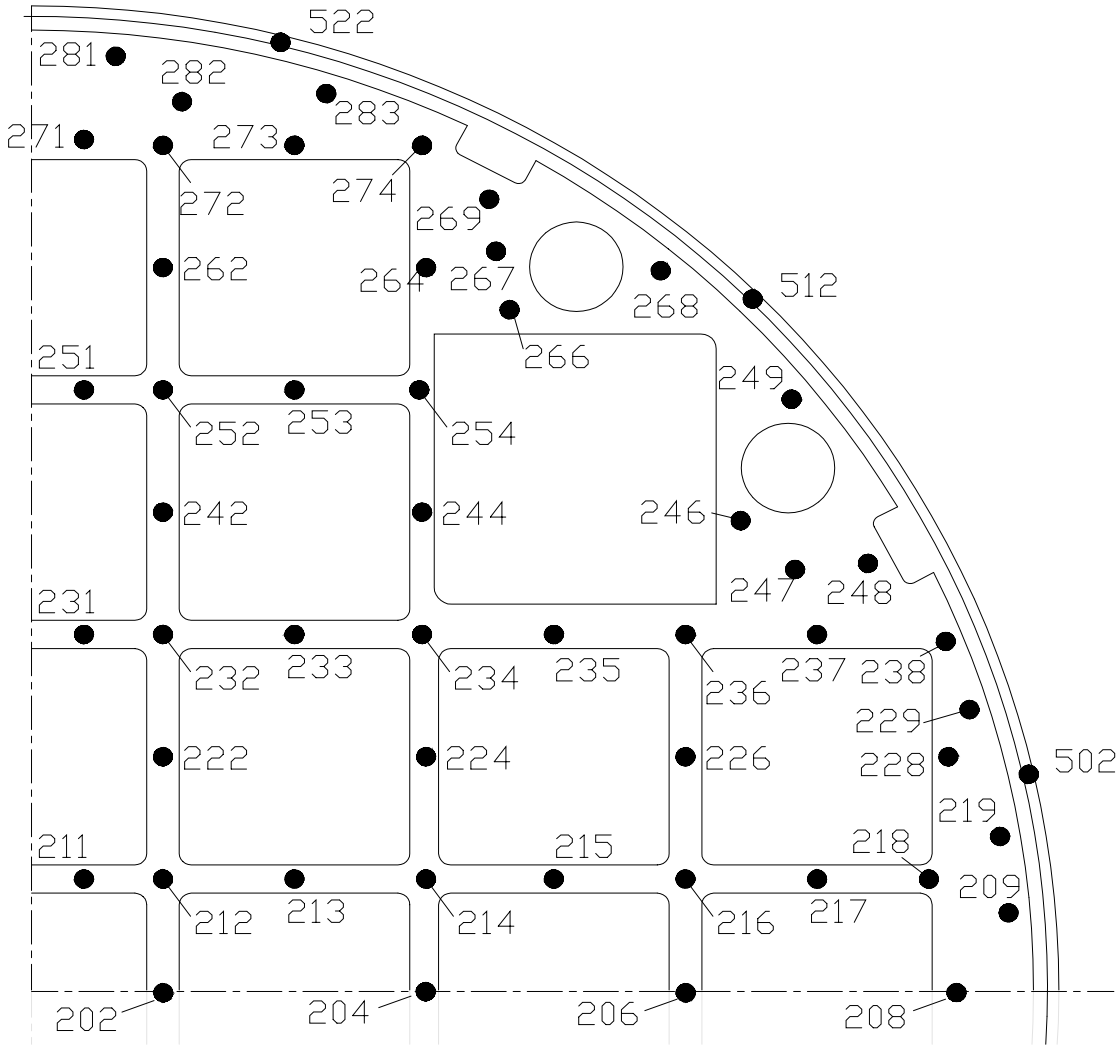

Figure 4.4-5 - Typical Node Layout for W74 Spacer Plate

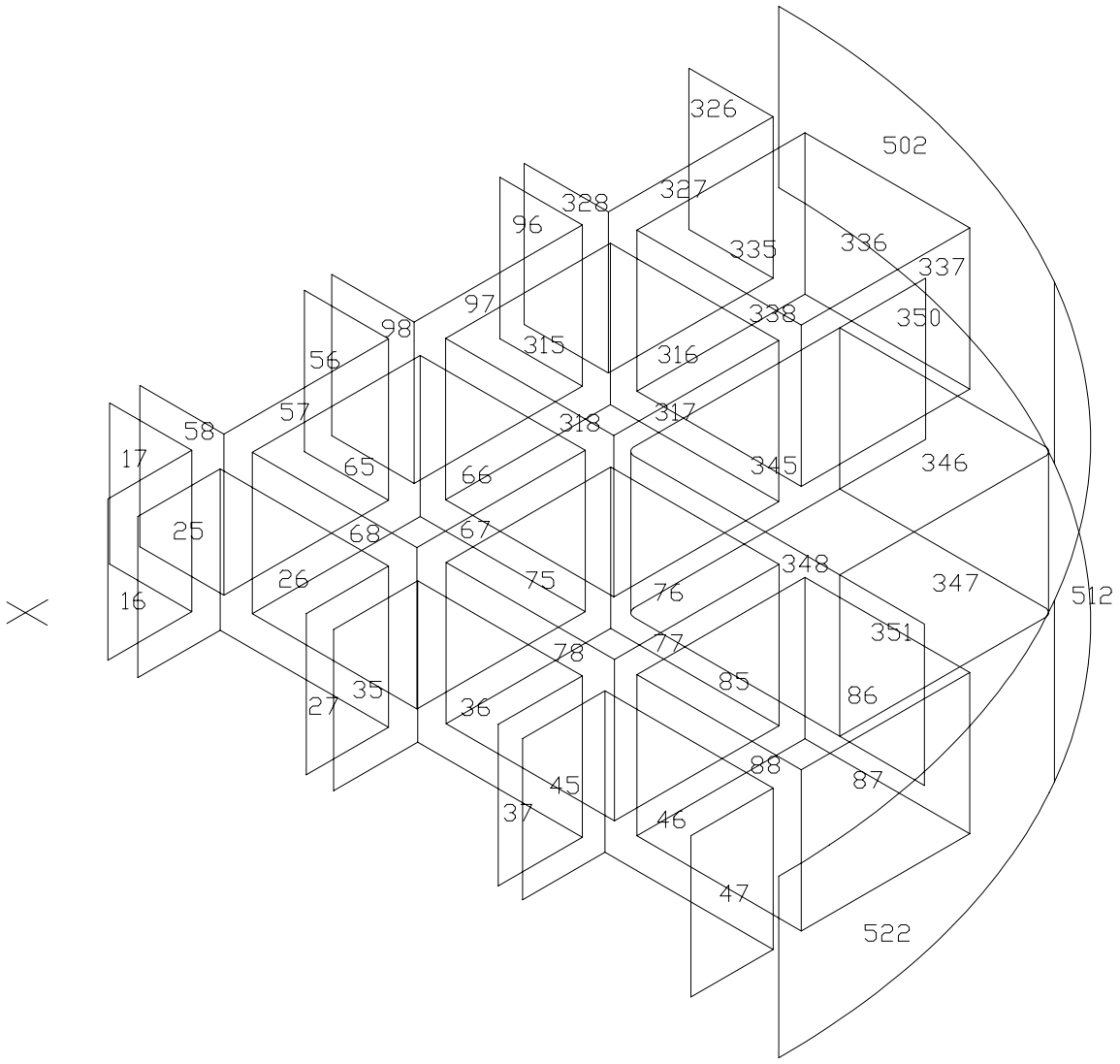

Figure 4.4-6 - Isometric View of Node Layout Between Typical Set of W74 Spacer Plates

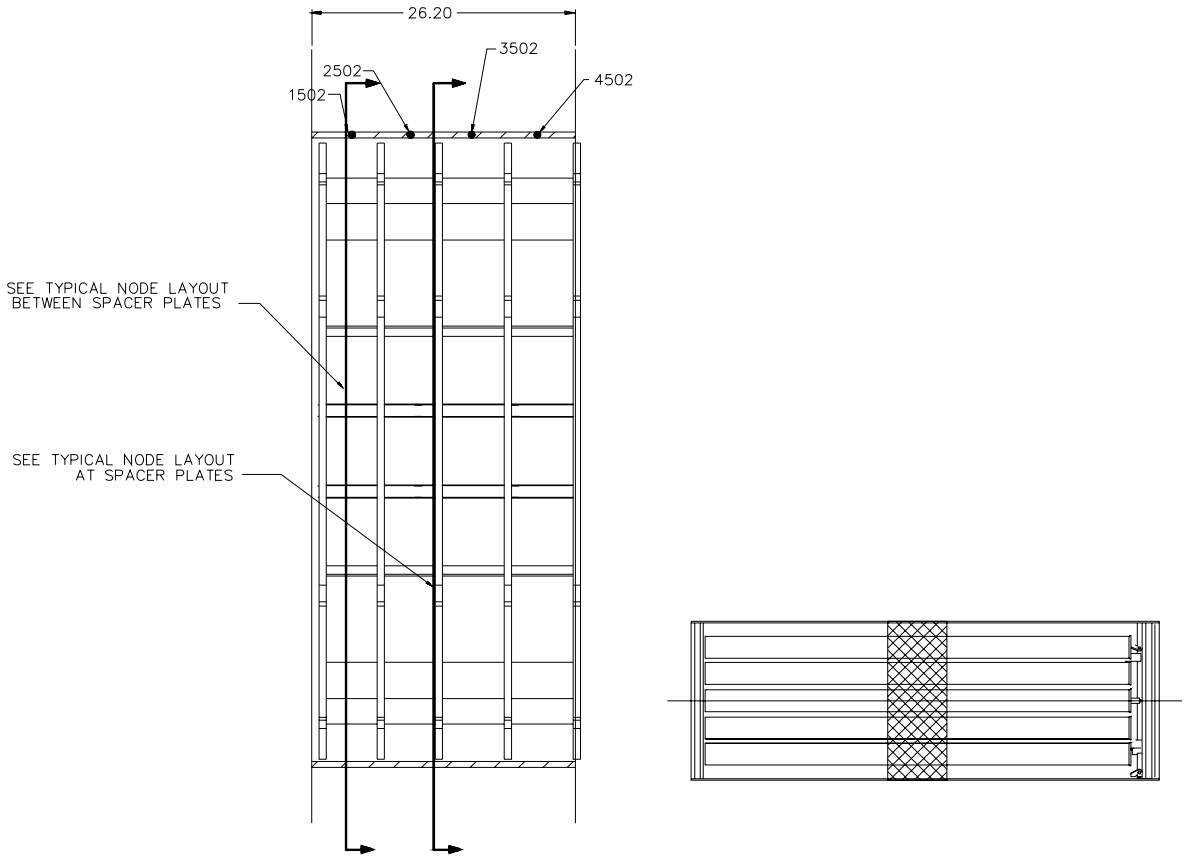

Figure 4.4-7 - Node Layout for W74 Canister Mid-Body Section

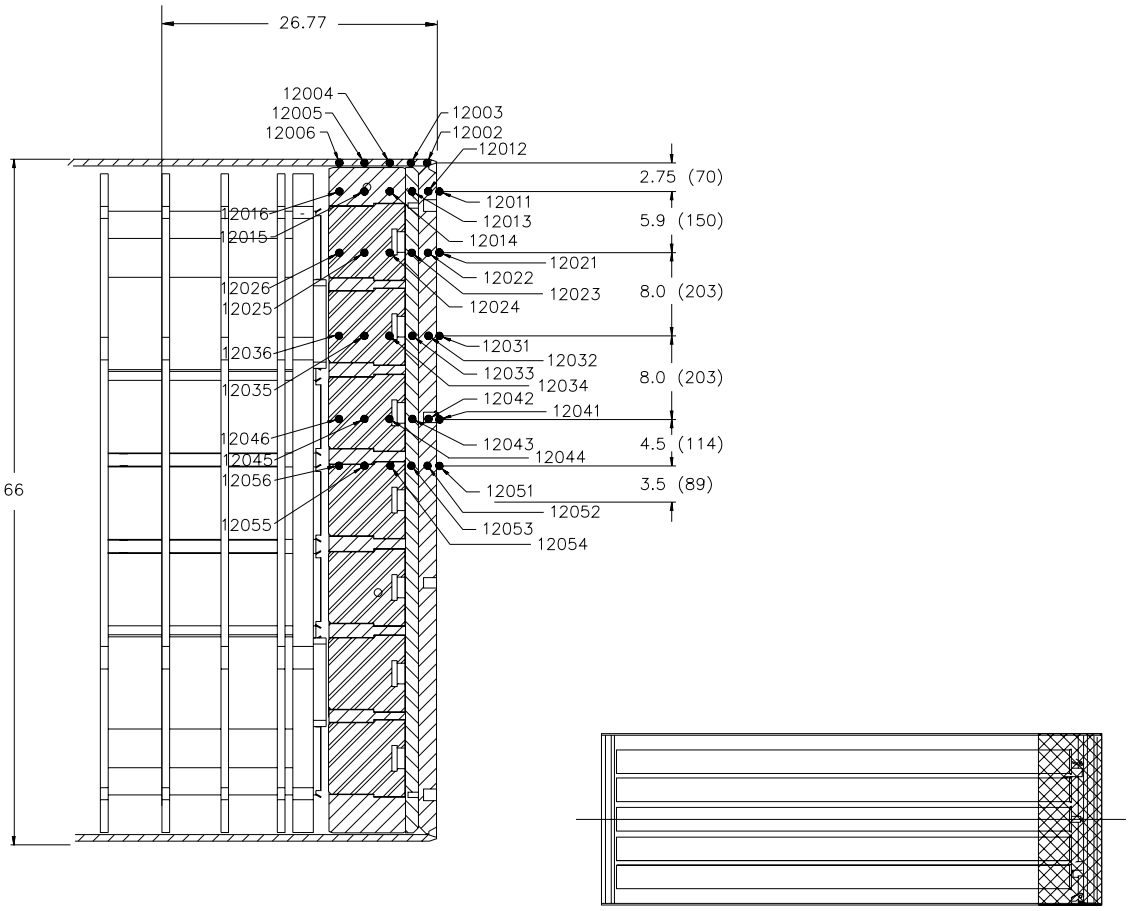

Figure 4.4-8 - Node Layout for W74 Top End

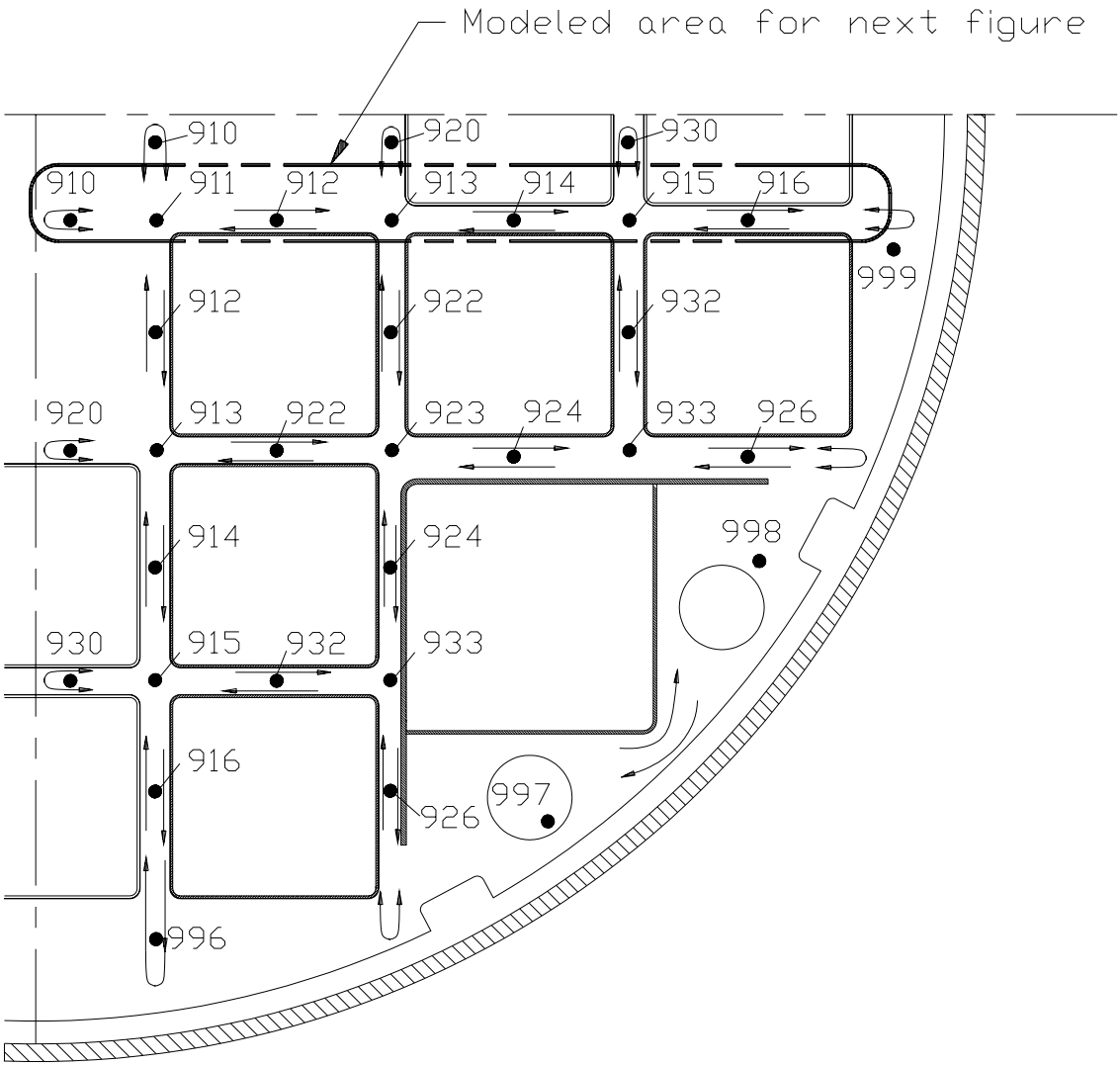

Figure 4.4-9 - Gas Node Layout for Vertical W74 Canister

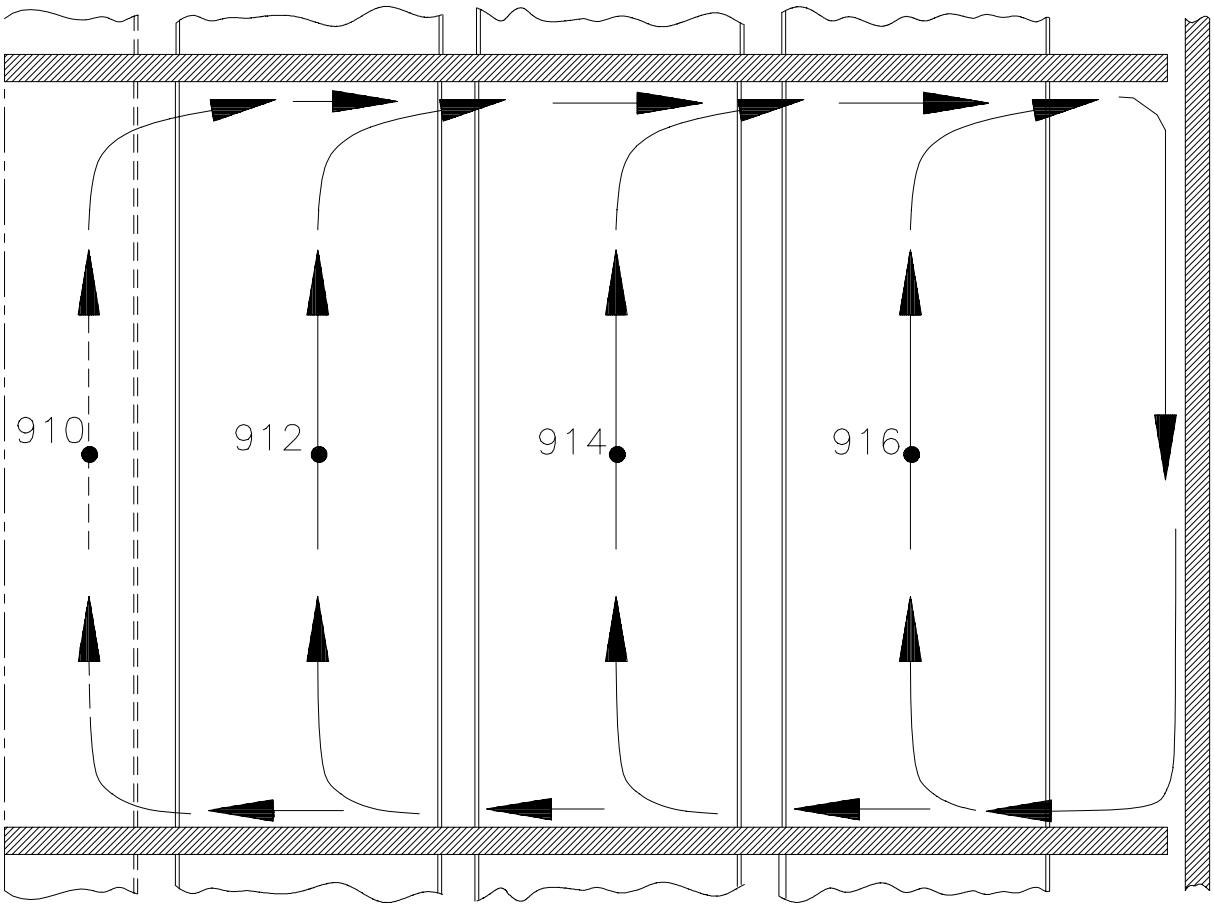

Figure 4.4-10 - Modeled Flow Pattern within Vertical W74 Canister

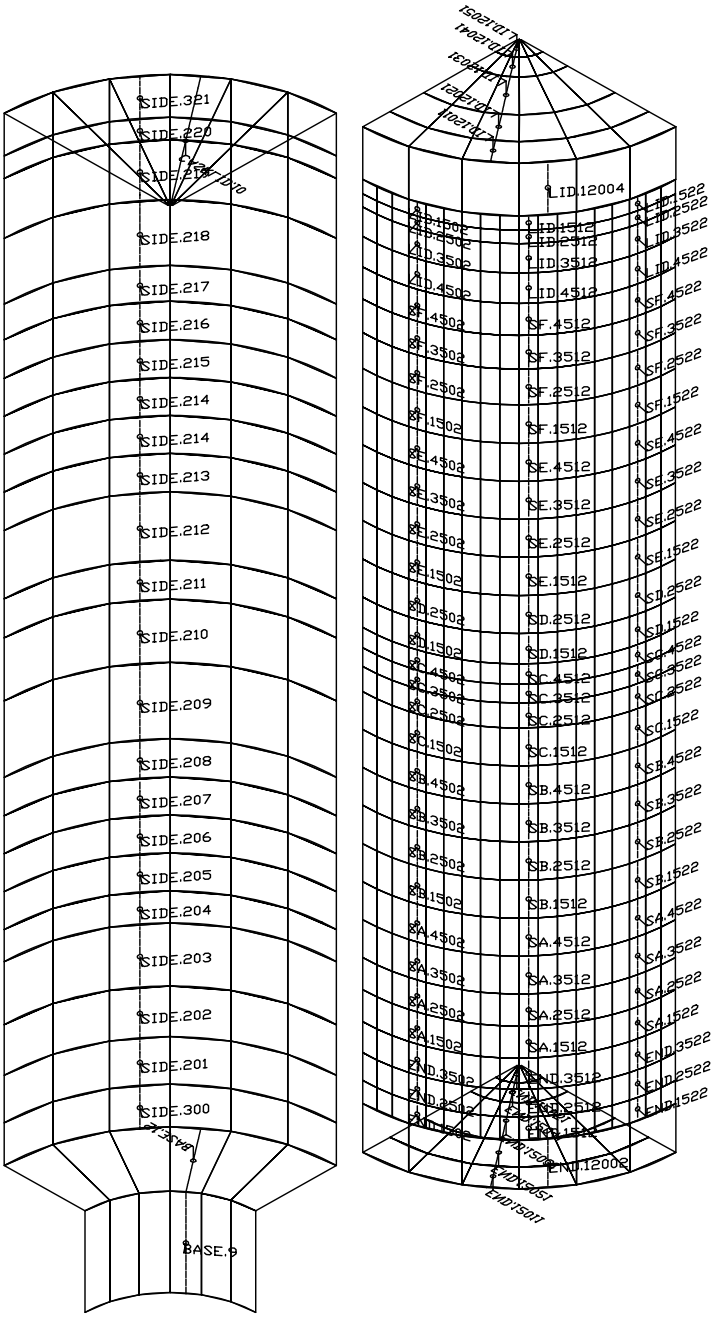

Figure 4.4-11 - Thermal Submodel Alignment for Storage Cask and W74 Canister

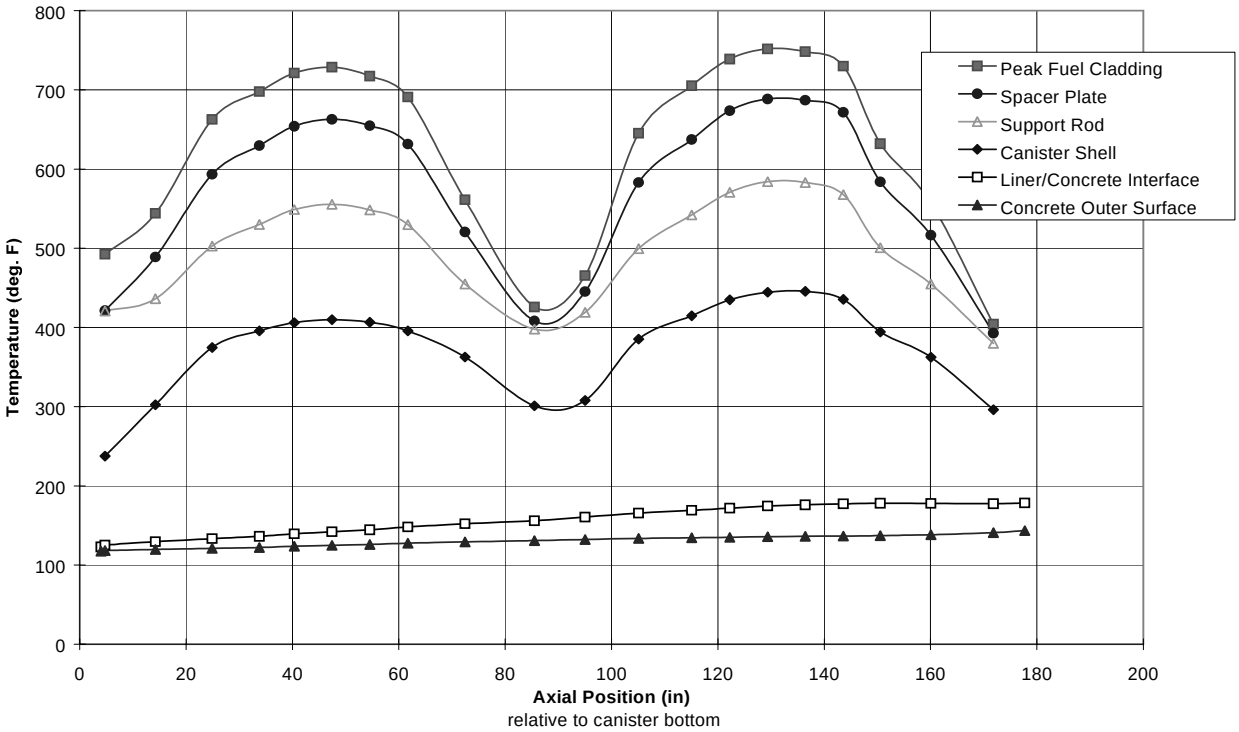

Figure 4.4-12 - W74 Canister Axial Temperature Distribution for Normal Hot Condition in Storage Cask at Q_{max}

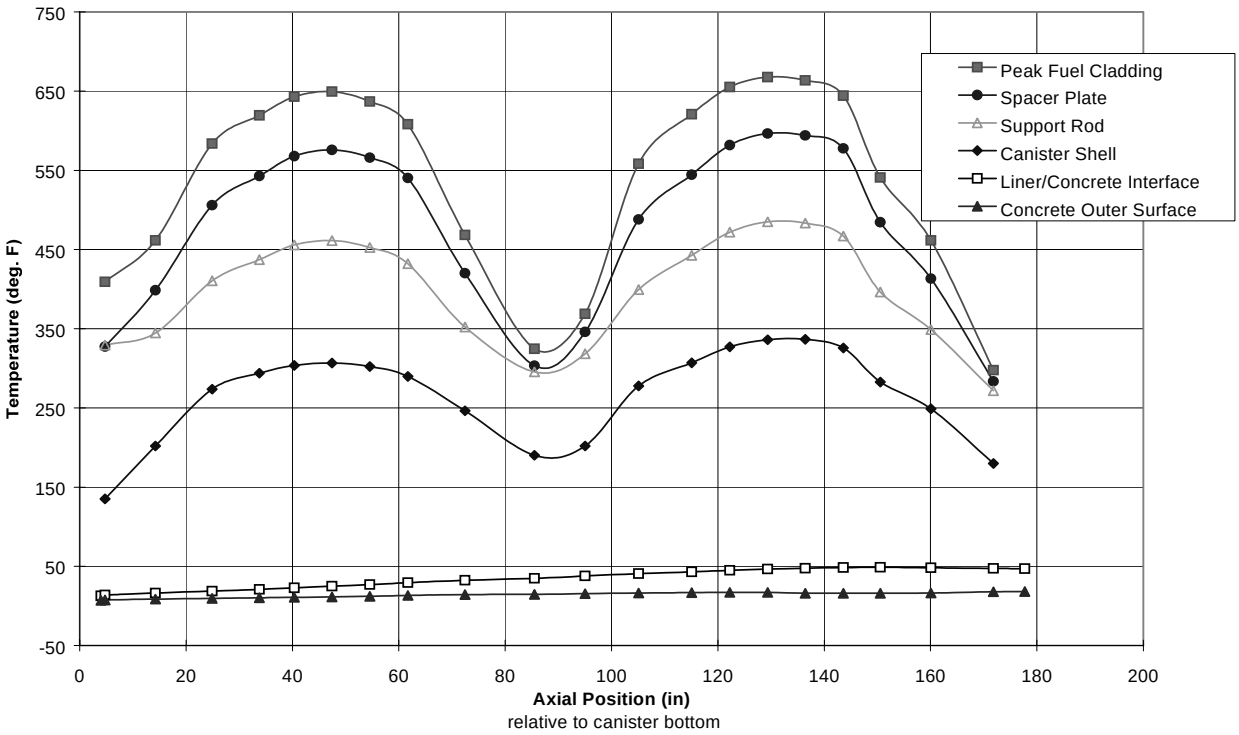

Figure 4.4-13 - W74 Canister Axial Temperature Distribution for Normal Cold Condition in Storage Cask at Q_{max}

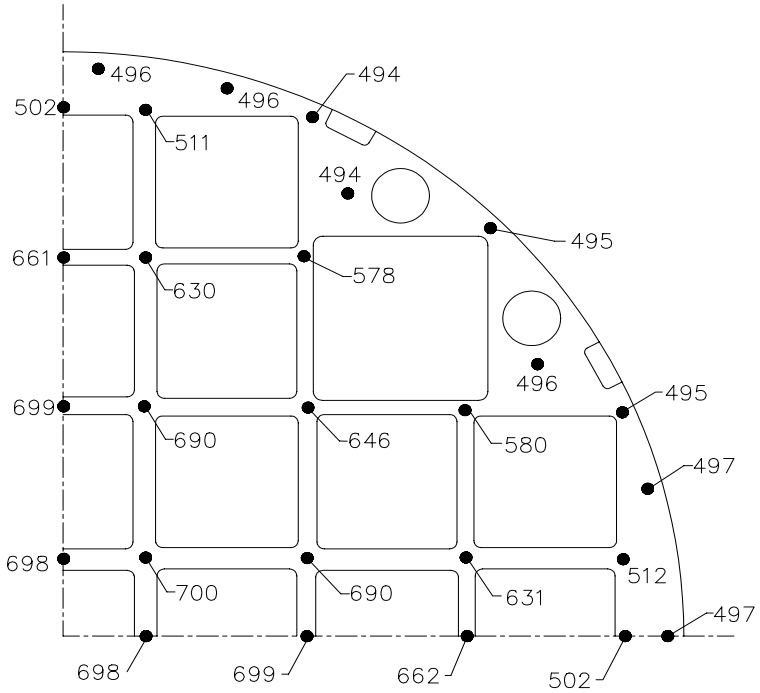

Figure 4.4-14 - W74 Spacer Plate Temperature Distribution for Normal Hot Condition in Storage Cask at Q_{max}

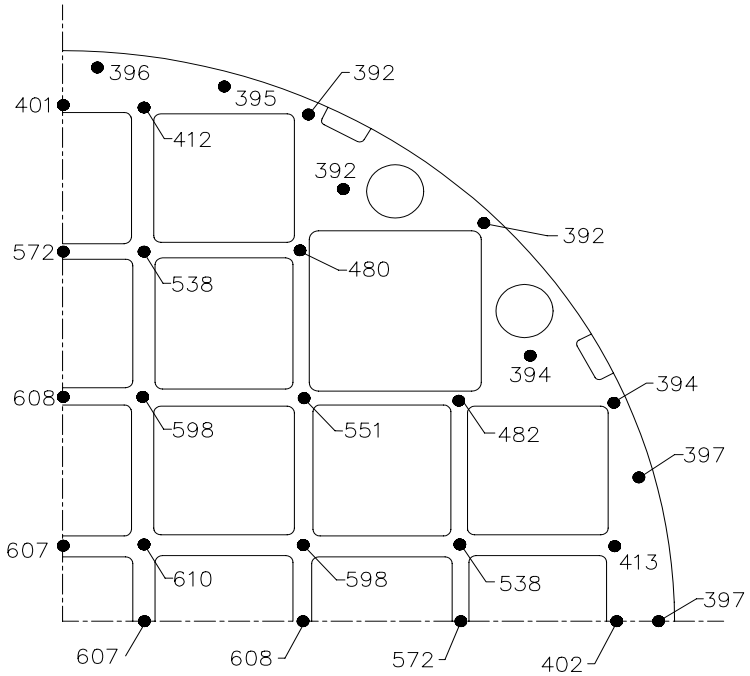

Figure 4.4-15 - W74 Spacer Plate Temperature Distribution for Normal Cold Condition in Storage Cask at Q_{max}

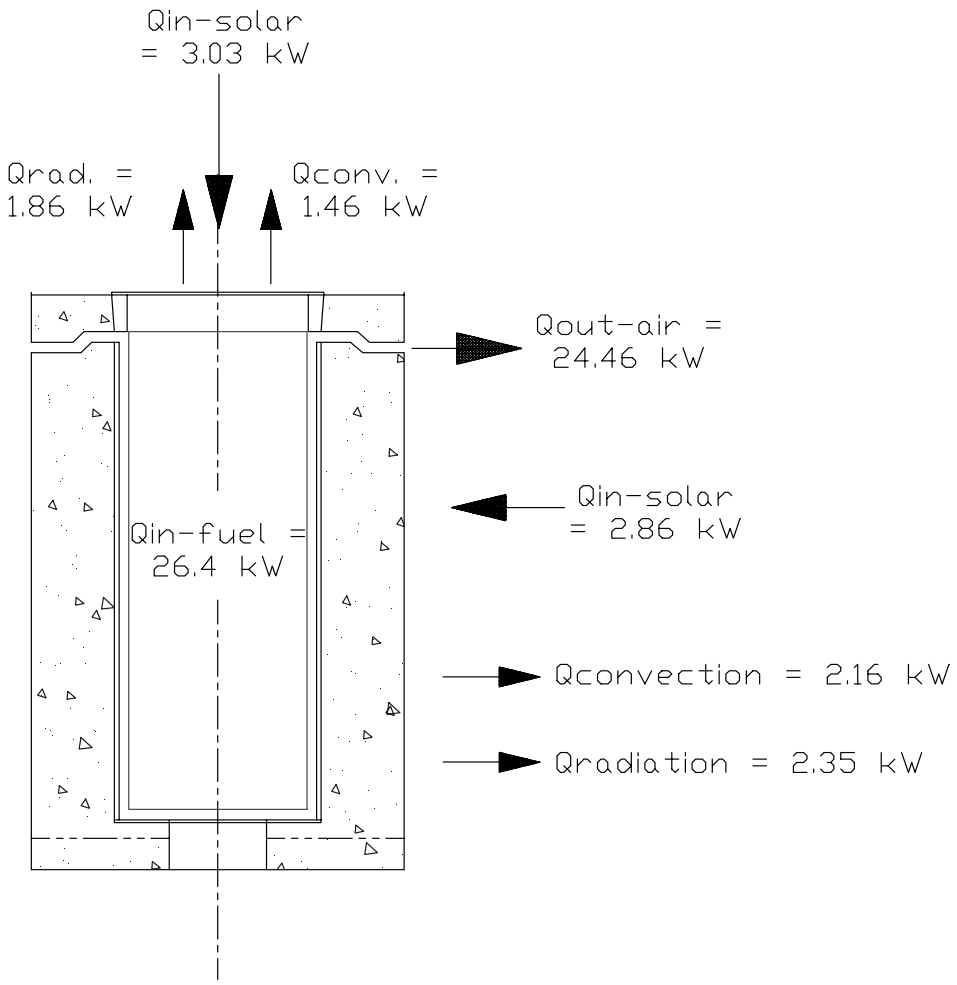

Figure 4.4-16 - W74 Canister Heat Balance for Normal Hot Storage Conditions at Q_{max}

4.4.2 W74 Canister within Transfer Cask

To validate the performance of the FuelSolutions™ W74 canister within the W100 Transfer Cask under normal conditions of transfer, the combined thermal model for the W74 canister and the transfer cask is evaluated for the design basis normal climatic conditions presented in Table 4.1-3 using the enveloping W74 canister heat flux profile. The analysis presented herein is designed to establish a thermal rating and to demonstrate that the W74 canister and W100 Transfer Cask allowable material temperatures are not be exceeded for the established canister thermal rating at any site within the contiguous United States.

This section presents the thermal analysis of the canister within the transfer cask. The thermal model of the W74 is described along with a discussion how the canister thermal model is interfaced with that for the transfer cask. The specifics of the thermal model for the FuelSolutions™ W100 Transfer Cask is presented in Section 4.4.2 of the FuelSolutions™ Storage System FSAR and is not repeated here.

The analysis presented herein demonstrates that the acceptance criteria in Section 4.3 is met with the FuelSolutions™ W74 canister in the transfer cask for the enveloping canister decay heat dissipation and at any site within the contiguous United States. Insolation is specified in 10CFR71[3] for a twelve hour on, twelve hour off loading. In order to represent the insolation in the steady-state, the insolation specified is averaged over a twenty-four hour day.

4.4.2.1 W74 Thermal Model in Transfer Cask

The analytical thermal model of the W74 canister is essentially the same as that used for the analysis in the storage cask (see Section 4.4.1.1). As stated previously, the model is developed for use with the SINDA/FLUINT computer program.[2] Section 4.7.3.1 presents an overview of the SINDA/FLUINT program and its past use for the analysis of nuclear systems. The following paragraphs describe the differences in the thermal modeling of the W74 canister between that used for analysis in the storage cask and that used for analysis in the transfer cask. The thermal model of the FuelSolutions™ W100 Transfer Cask is presented in Section 4.4.2 of the FuelSolutions™ Storage System FSAR.

The W74 canister thermal model used for the analysis in the transfer cask includes additional modeling for simulating the canister in the horizontal orientation and the modeling within the transfer cask. Modifications to the W74 canister thermal model for simulating the canister in the horizontal orientation consisted of adding model sections “ENDBOT”, “SABOT”, “SBBOT”, “SCBOT”, “SDBOT”, “SEBOT”, “SFBOT”, and “LIDBOT” to complete a 180° representation of the basket assembly. These additional submodels are identical to their upper half counterparts. Thermal connections are provide between the upper and lower halves of the basket assembly for conduction within the spacer plates and for the convection heat transfer loop. Figure 4.4-17 illustrates the gas flow pattern for convection heat transfer within a horizontal canister.

The modeling of the W74 canister in the transfer cask is accomplished in a similar fashion to that used for the storage cask. Again, the thermal model of the W74M canister assembly is combined with the thermal model of the transfer cask as defined in Section 4.4.2 of the FuelSolutions™ Storage System FSAR. The canister and cask thermal models are brought into the combined thermal model as separate thermal submodels.

The canister does not sit symmetrically within the transfer cask, but rests on two 0.125 inch thick guide rails positioned 45° apart. This eccentric positioning results in a set of non-axisymmetric boundary conditions between the canister and the transfer cask for those load cases that involve the canister in the horizontal position. Simulation of this condition is accomplished using the 180° thermal model of the canister and the cask to permit simulation of the variation in gap between the canister shell and the cask inner liner.

4.4.2.2 Conditions During Canister Loading

This section presents evaluations for W74 canister certain operating modes within the W100 Transfer Cask during canister loading. These evaluations demonstrate that the W74 canister vent port is adequate to prevent canister overpressurization during closure operations. As discussed in Chapter 8 of this FSAR, the transfer cask/canister annulus and the canister cavity may remain filled with water until canister closure operations are completed. If the canister cavity and annulus remain filled with water during extended closure operations, steady-state temperatures may be achieved which result in boiling of the annulus water. Boiling is not desirable from an industrial safety consideration. Boiling may be prevented by transfer cask/canister annulus water recirculation.

Although the canister cavity water properties (i.e., density, boric acid concentration) are not relied upon for shielding or criticality control, it is prudent to prevent boiling. Additionally, since the canister venting evaluation demonstrates that the canister shell is not overpressurized beyond the 30 psig blowdown pressure limit defined in the operating procedures contained in Section 8.1.8 of the FuelSolutions™ Storage System FSAR, no time limit is necessary for canister cavity draindown operations.

4.4.2.2.1 Canister Venting Evaluation

The steam to be vented is conservatively assumed to be generated by the canister maximum heat load rating above the ambient losses to the transfer cask when the peak canister shell temperature is at 212°F. Steam is generated at saturation conditions for the maximum assumed canister pressure (30 psig). The 30 psig blowdown pressure limit is based on canister ASME level A allowable stresses for the canister with the top end inner closure plate welded in place and the AW/OS and strong-back installed. These saturation conditions define the maximum rate of vaporization, the highest mass flow rate, and the lowest steam density. All of these factors are conservative for calculating the vent flow rate.

In order demonstrate the adequacy of the W74 canister vent capacity, a pressure drop analysis is performed for the vent path using conservative assumptions for the steam generation rate and the canister vent line configuration. A maximum vent flow capacity of 0.0234 lb_m/s is determined based on achieving choked flow conditions for a canister pressure of 30 psig, and considering the pressure drops through each section of the canister vent line. This resulting maximum vent flow capacity corresponds to a maximum 23.0 kW of steam generation, assuming all heat goes to latent heat of vaporization.

A total heat loss of 11.9 kW (determined in Section 4.4.2.2.2) results from heat losses to the transfer cask with the canister shell outer surface at 212°F. Since the W74 canister maximum heat load rating is 24.8 kW (Table 4.1-4), the total heat load available for steam generation is

12.9 kW (24.8 kW-11.9 kW). The total heat load available for steam generation (12.9 kW) is less than the vent line maximum heat load for steam generation (23.0 kW). This demonstrates that a considerable margin exists between the W74 canister maximum heat generation rate and the limiting vent flow rate.

4.4.2.2.2 Annulus Boiling Evaluation

The transient and steady-state temperature responses of the canister shell are determined from a simplified, one-dimensional analysis. The steady-state model calculates the temperature drop across each successive transfer cask wall material layer for an assumed heat flux from the canister shell. This simplified, one-dimensional model employs a closed-form thermal analysis instead of the SINDA models described above. The temperature distribution is determined from the solution of a thermal network representing the heat transfer through the transfer cask. Heat transfer from the canister top end outer closure plate to ambient by radiation and convection is included along with the radial heat transfer through the transfer cask wall. Heat is transferred to ambient from the liquid neutron shield shell outer surface by radiation and convection. For the annulus boiling analysis, the canister shell outer surface is assumed to be at 212°F with the ambient air at 77°F. The resulting steady-state heat transfer rate from the canister surface is 11.9 kW.

Since the W74 canister maximum heat load rating (24.8 kW) is greater than the heat load necessary to cause boiling in the annulus, makeup water may have to be added to the annulus periodically to replace water lost due to boiling and to maintain the water level. Based on the steady-state analysis summarized above, an effective heat transfer coefficient is determined from the canister shell through the transfer cask to ambient.

4.4.2.2.3 Canister Cavity Boiling Evaluation

Section 4.4.2.2.2 stated that canister heat loads in excess of 11.9 kW results in canister shell outer surface temperatures greater than 212°F, and the canister cavity is also above the boiling point. Since the W74 maximum heat load rating is greater than 11.9 kW, the canister cavity water boils at the canister thermal rating. The closed form thermal analysis described above is again used to determine the time to cavity boiling.

The W74 canister and transfer cask are assumed to start at an initial uniform temperature of 120°F, which is the typical spent fuel pool maximum operating temperature. A representative canister thermal mass is assumed. Canister cavity water is assumed to boil when the guide tube/fuel surface temperature reaches the saturation temperature at 1 atm. Boiling analysis conservatively assumed a canister heat load of 28.0 kW, which is higher than the W74 canister maximum thermal rating (24.8 kW). Under these conservative assumptions, the W74 canister cavity water boils after 18 hours.

Annulus cooling may be used to recirculate the water within the transfer cask/canister annulus to remove canister heat in order to keep the cavity water below the boiling point. Similar to the flow rate evaluation to prevent annulus boiling presented in 4.4.2.2.2, canister cavity boiling is prevented by maintaining the canister internals below the saturation temperature at 1 atm. A minimum flow rate of 1.89 gpm within the transfer cask/canister annulus is necessary to prevent canister cavity boiling.

4.4.2.3 Conditions During Canister Reflooding

In the unlikely event that a W74 canister must be unloaded after an extended period in dry storage, the fuel and canister is flooded with water to allow canister opening and fuel unloading. During canister reflooding, contact with the hot canister internals and fuel rods causes steam generation which pressurizes the canister shell. The resulting steam generation is evaluated to show that the peak pressure transients experienced during the canister reflood operations do not exceed the canister shell pressure limit (100 psig) in accordance with the procedures contained in Section 8.2.3 of the FuelSolutions™ Storage System FSAR.

As discussed in Chapter 8 of this FSAR, transfer cask annulus water recirculation is performed for canister temperature control before and during the reflooding. During canister reflooding operations, quench water is introduced into the cavity through the canister drain line at a maximum flow rate of 10 gpm. The quench water impinges on the hot bottom end plate and flashes to steam. The saturated steam rises through the canister cavity to the open vent port at the top of the canister. During this process, the saturated steam becomes superheated as it contacts the hot fuel and canister internals. The superheated steam exits through the open canister vent and exhausts to a heat sink, typically the plant's spent fuel pool. As the water level in the canister cavity steadily rises, localized boiling at the top surface of the water (quench front) is expected to occur due to the large amount of heat stored in the canister internals.

Following reflooding, the canister may be further cooled by continuing transfer cask annulus cooling. A specific canister's SNF decay heat, the prevailing ambient conditions, available annulus cooling water parameters, site specific temperature limitations, as well as the lead time needed to initiate annulus cooling operations to prevent canister water boiling determine the temperature below which a canister's water should be maintained. Post reflood cooldown should be evaluated by the license on a site specific basis.

In addition to the analysis presented herein, the effects of canister reflooding and unloading operations should also be evaluated by the license on a site specific basis to include the following:

- The potential structural loads on the canister vent line.
- Possible siphon effect and resultant canister vacuum which may result from the site specific vent line configuration.
- Heat load necessary to condense the discharge steam including potential effects on stored fuel if the spent fuel pool is used as a heat sink.
- The potential for steam chugging, water hammer and steam condensation oscillation in the vent line.

The analysis presented in this section conservatively demonstrates that the canister pressure limit of 100 psig is not exceeded during canister reflooding operations. The analysis is based on a typical FuelSolutions™ canister at the W74 canister structure maximum heat load rating (Q_{max} = 26.4 kW). This analysis bounds the W74 canister specific model since the typical basket design is similar, the spacer plates have a higher thermal mass than the W74 spacer plates, the peak spacer plate temperatures are nearly identical between the two canisters, and the minimum free volume is smaller than the W74 canister.

4.4.2.3.1 Spacer Plate Temperature Distribution Prior to Reflood

A transient analysis is performed using the thermal model discussed in Section 4.4.1.1 for canister reflood conditions (case 19, Table 4.1-3). The initial conditions for the transient analysis are steady-state conditions with the transfer cask and canister in the vertical orientation, air in the canister cavity, and air in the annulus. Since reflooding is performed inside the plant fuel building, ambient conditions of 77°F with no insolation are assumed. The assumption of air in the canister bounds temperatures seen with a full or partial helium environment. Additionally, a breached canister, which may result in the loss of helium back-fill gas, is a postulated accident scenario which may require canister reflooding and unloading.

Annulus water recirculation is initiated at the minimum flow rate of 5 gpm and an inlet temperature of 100°F after the loaded transfer cask is positioned in the unloading area. The typical spacer plate axial temperature distribution after four hours is shown in Figure 4.4-18. This axial temperature distribution corresponds to start of canister reflooding operations with the introduction of water. The corresponding cavity gas temperature as measured through the canister vent port is 487°F.

For analysis purposes, the spacer plate axial temperature distribution shown in Figure 4.4-18 is conservatively assumed to remain constant throughout the reflood transient. No credit is taken for fog cooling of canister internals by vented superheated steam, continuation of annulus cooling during the reflood, or the increased conduction and cooling effects of filling the canister cavity with water.

4.4.2.3.2 Cladding Thermal Stress During Reflooding

In accordance with NUREG-1536,[9] fuel rod cladding total stresses are limited so that the fuel rod's total stress is less than the material's yield stress. The total stress includes thermal stress combined with cladding hoop stress. This approach is considered conservative since thermal stresses are typically classified as peak stresses and only considered for fatigue evaluation. Additionally, thermal stresses are self limiting. Since canister reflooding is an infrequent activity, high cyclic fatigue is not a concern. Rod cladding total stress is compared to test results from EPRI Report TR-103949.[11]

Thermal stresses imposed on fuel rods have been extensively evaluated by LWR fuel vendors, including Westinghouse, during postulated loss-of-coolant (LOCA) accident conditions. In Westinghouse report NFD-E-813,[19] the peak thermal stress reported for an unoxidized zircaloy tube under reactor reflood conditions is 5800 psi (40 MPa). The cladding thermal stresses from the Westinghouse analysis are presented in Figure 4.4-19.

The Westinghouse thermal stress analysis considered the thermal and mechanical effects of the zirconium oxide layer and used surface heat transfer coefficients appropriate for the mode of heat transfer during rod quenching. The presence of an oxide layer on the fuel rod during quenching results in a significant reduction in the cladding surface effective heat transfer coefficient and the corresponding thermal stress. This is evident on the oxidized cladding curve

[19] NFD-E-813, *Consideration of Thermal Shock on Fuel Rods During the Reflood Phase of a LOCA*, Westinghouse Electric Corporation, April 1973.

in Figure 4.4-19. Since SNF to be stored typically has an oxide layer on the cladding, the thermal stresses within actual fuel assemblies are bounded by the maximum reported by NFD-E-813[19].

The results presented in NFD-E-813[19] are applicable to canister reflood conditions following dry storage. The thermal stress results presented in NFD-E-813[19] are based on a heat sink (quench water) temperature of 300°F. The saturation temperature corresponding to the maximum W74 canister pressure during reflood (100 psig) is 338°F. Due to the geometry of fuel end fittings and axial spacers and the introduction of quench water through the drain tube, the fuel rods are not directly exposed to the cold quench water (70°F minimum) until the water level rises within the canister cavity. Even if canister saturation conditions for maximum allowable pressure are not achieved before the water level reaches the fuel rods, quench water is pre-heated within the drain tube and by the thermal mass of the canister shell and basket components. Additionally, as discussed in NFD-E-813[19], if fuel rods are quenched with room temperature water at atmospheric pressure, the initial mode of cooling would be transition boiling instead of nucleate boiling, which tends to reduce the thermal stresses imposed across the cladding.

The fuel assembly temperature at the bottom of the canister is much cooler than the peak fuel rod temperature. As a result, the initial fuel cladding stresses are much less than the maximum reported by NFD-E-813[19]. Additionally, canister and fuel cooling continues during the reflooding operations due to cask/canister annulus cooling, steam venting to the spent fuel pool, and rising water level in the cavity. The peak fuel rod cladding temperature is significantly reduced before the quench water level reaches the peak axial location.

The maximum thermal stress level for reflood 5800 psi (40 MPa) is only a fraction of the maximum rod stress of 95.5 MPa calculated in Section 4.3.2.4 corresponding to the short-term allowable cladding temperature of 570°C. Even if the thermal stress is conservatively added to the maximum rod stress, the total rod stress (135.5 MPa) is still less than the average rod stress reported in EPRI Report TR-103949,[11] Table A-1, (395 MPa) for stress-rupture observations of irradiated zircaloys. In summary, thermal stresses induced within the fuel cladding during canister reflooding operations following dry storage are not significant.

Since PWR and BWR fuel assemblies from other fuel vendors (including Big Rock Point fuel) are similar in design and materials to Westinghouse PWR fuel, the maximum cladding stresses reported in NFD-E-813[19] are representative of all LWR assemblies which can be accommodated by the W74 canister.

4.4.2.3.3 Canister Pressure During Reflooding

The reflood water is assumed to enter the canister at a maximum temperature of 100°F. The minimum quench water temperature is 70°F based on the fuel cladding stress discussion presented above. The use of the higher quench temperature (100°F) is conservative for analysis purposes since the higher temperature water boils faster and result in a higher canister pressure .

The canister reflood transient is analyzed through the use of a canister mass balance. The mass balance considers the steam generation, caused by contact between the quench water and the hot canister internals, and the vented steam. Any mass imbalance between the steam generation rate and venting rate results in a pressure increase within the canister cavity, which is predicted using the ideal gas equation.

The steam generation rate is determined by performing a heat transfer analysis on the limiting canister internal components, which are the bottom end plate and the spacer plates. Conservative assumptions are used to maximize the heat transfer and therefore overestimate the amount of steam generated. The HEATING 7.2f[20] computer code is used to determine the transient steam generation rate for the bottom end plate. HEATING 7.2f[20] is capable of solving three-dimensional steady-state and transient heat conduction problems and is therefore appropriate for this application.

The steam venting rate is determined using the RELAP5[21] computer code, which is a thermal hydraulic finite difference computer program. Conservative assumptions are used to minimize the mass flow rate through the vent system and maximize the canister backpressure.

The first phase of the reflood transient is the initial quench water impingement on the canister cavity bottom end plate. For steam generation analysis, a stagnant pool of saturated water is assumed to be present above the bottom end plate at the start of the transient. This is conservative since sensible heat input to the water is neglected. Additionally, the subcooling effect of inlet water at 10 gpm is sufficient to overcome the heat flux from the bottom end plate ensuring no interruption of quench flow. Heat input from the canister internals directly above the bottom end plate is considered. The entire bottom end plate transient is conservatively evaluated at the lowest possible saturation temperature (212°F), and the heat flux reduction for temperatures in the transition boiling regime is ignored.

Since the quick-connect normally installed in the canister vent port has a small throat area which creates a flow restriction, the quick-connect is assumed to be removed prior to reflooding. The vent system configuration assumed for the analysis includes 100 feet of 2-inch corrugated steel hose which discharges steam at the bottom of the spent fuel pool. Typical hose turns, fittings, and exit losses are incorporated into the hose loss coefficient. For the vent capacity evaluation, the steam exit temperature is conservatively assumed to be 800°F.

Once the bottom plate pressure transient in completed, the reflood water continues to accumulate within the canister cavity and the water level slowly rises due to the 10 gpm injection flow rate. As the water level rises, canister internals and fuel are cooled. The limiting basket components considered within the analysis are the large spacer plates located throughout the axial length of the canister. The relatively small linear mass of the fuel, guide tubes, support rods, and shell do not produce significant steam generation compared to the spacer plates. The carbon steel spacer plates, although thinner than the stainless spacer plates, are the bounding components for steam generation during the remaining canister reflood transient. The carbon steel spacer plates have a higher conductivity and higher ratio of surface area to mass than the stainless steel plates and will therefore release heat at a much faster rate. Additionally, the W74 upper and lower baskets contain stainless steel spacer plates only at the ends of the baskets, which are much cooler than carbon steel plates located within the active fuel region.

The large initial temperature difference between the quench water and the spacer plates produces film boiling, thus limiting the heat flux. As the spacer plate surface temperature drops to the

[20] ORNL/TM-12262, HEATING 7.2f Computer Code, Multi-Dimensional Finite-Difference Heat Conduction Analysis, Oak Ridge National Laboratory, February 1993.

[21] RELAP5 Computer Code, Version MOD 3.1.

nucleate boiling range, the heat flux increases significantly resulting in a high rate of steam generation. The mass balance between the steam generation rate and the vent capacity, results in a canister pressure spike.

The mass balance between the steam generation rate and the vent capacity during the bottom end plate quench transient results in a maximum canister pressure of 12 psig, which is well below the 100 psig maximum reflood pressure. The reflood process yields a series of transient pressure spikes. The mass balance for the limiting spacer plate quench transient results in a peak canister pressure of 70 psig, which is also well below the 100 psig maximum reflood pressure. The limiting spacer plate pressure transient is presented graphically in Figure 4.4-20.

The 10 gpm maximum quench flow rate ensures that only one spacer plate is generating steam at a given time. As can be seen in Figure 4.4-20, the spacer plate quench transient duration is much faster than the time required for the quench water level to progress between spacer plates.

4.4.2.4 Maximum Temperatures

The W74 canister design basis thermal load cases for normal conditions within the transfer cask are presented in Table 4.1-3, specifically cases 13, 14, and 15. For the normal condition evaluations, a steady-state analysis of the W74 canister in a horizontal transfer cask is conducted with normal ambient conditions (0°F, 77°F, and 100 °F). The system temperatures are presented in Table 4.4-6. The W74 canister component temperatures are within their material allowable temperatures in all cases.

The limiting component in each case is typically the peak carbon steel spacer plate since it has no short-term allowable temperature, whereas the fuel cladding allowable temperature under transfer conditions is 570°C.

Note that the maximum temperatures, including the fuel cladding temperatures, are conservatively based on the maximum W74 canister structure thermal rating of 26.4 kW. As such, greater thermal margins than indicated in the table will exist for operations under the W74 heat load rating of 24.8 kW. The table results demonstrate that the short-term fuel cladding temperature limit of 400°C is met for the normal transfer cases, even if the higher canister structure heat load of 26.4 kW (as opposed to 24.8 kW) is assumed.

Representative axial profiles through the canister and storage cask are presented in Figure 4.4-21 and Figure 4.4-22 for the normal hot and normal cold conditions of transfer, respectively, and at the higher canister structural heat load rating of 26.4 kW. The variation in the heat load profile in the stacked W74 canister baskets is clearly visible in the plots. Figure 4.4-23 and Figure 4.4-24 present the temperature distribution within the hottest spacer plates for the same normal hot and normal cold conditions of transfer, respectively. The temperature results in the plots illustrate the expected variation across the plate when the canister is in the horizontal orientation.

As shown in Table 4.4-7, the results for cask handling (case 10) show that the allowable temperatures are exceeded under steady-state conditions for the peak fuel cladding and for selected areas on the carbon steel spacer plates when the canister-cask annulus is filled with air. However, allowable temperatures are not exceeded if the annulus is filled with 120°F water. Evaluation of the transient temperature response (Figure 4.4-25) shows that approximately 15 hours is available once the canister-cask annulus is drained before the long-term allowable

temperature for the carbon steel spacer plates is exceeded. At the time when the spacer plate temperatures reach their limit, the fuel clad temperature will be just under its limit of 400°C.

Figure 4.4-25 presents the transient response of the peak fuel rod cladding, peak spacer plate, canister shell, and the transfer cask inner shell and lead shield following the draining of the canister-cask annulus. The water in the canister-cask annulus is assumed to be completely drained at time = 0. As seen from the transient plot, steady-state conditions are essentially established after about 50 hours following the canister-cask annulus draining. However, after about 15 hours the peak carbon steel spacer plate temperatures exceed their long-term allowable temperature of 700°F, and the fuel cladding exceeds its short-term allowable limit of 400°C. The 15 hour time period forms the basis for a *technical specification* presented in Section 12.3 of this FSAR. Given that the transient analysis is based on a canister heat load of 26.4 kW, the use of the 15 hour limit will conservatively bound the actual time available under the rated canister heat load of 24.8 kW.

4.4.2.5 Minimum Temperatures

The temperatures for the W74 canister components under normal cold conditions are listed in Table 4.4-6. The temperatures shown are for operation at the W74 canister structure thermal rating (26.4 kW) and, therefore, do not represent the lowest expected component temperatures. The results bound the thermal gradients that will occur with the rated canister heat load of 24.8 kW.

The low temperature compatibility of the W74 canister and transfer cask are evaluated for the bounding case of 0°F ambient temperature, zero decay heat load, and no insolation. The steady-state temperatures of the W74 canister and transfer cask for this analytically trivial case are 0°F. The component temperatures are within minimum allowable material temperatures for all materials.

Transient analysis is presented in Section 4.5.2.3 of the FuelSolutions™ Storage System FSAR to illustrate the time frame available when operating in freezing weather. An associated *technical specification* is established, as presented in Section 12.3 of the FuelSolutions™ Storage System FSAR, based on a bounding transient analysis which assumes no decay heat load.

4.4.2.6 Internal Pressures

W74 canister normal internal pressures for transfer are a function of the maximum canister pressurization established for normal hot conditions of storage (i.e., 24 psia) and the ideal gas law variation for the W74 canister temperatures within the transfer cask. Table 4.4-8 presents the W74 canister pressures for the normal conditions of transfer.

Since the canister thermal rating is lower than the transfer cask thermal rating, the liquid neutron shield internal pressure is bounded by that presented in Section 4.4.2 of the FuelSolutions™ Storage System FSAR.

Peak canister internal pressure during reflooding operations is discussed in Section 4.4.2.3.3.

4.4.2.7 Maximum Thermal Stresses

W74 canister maximum thermal stresses developed within the transfer cask under normal transfer conditions are addressed in Chapter 3 of this FSAR. Calculation of these thermal

stresses is based on the maximum canister structure heat load of 26.4 kW, and is conservative (bounding) for the actual canister heat rating of 24.8 kW.

4.4.2.8 Evaluation of Canister Performance for Normal Conditions

The results of the steady-state analyses demonstrate that the W74 and transfer cask allowable material temperatures under normal conditions are met for the maximum W74 canister structure thermal rating of 26.4 kW. As such, the demonstrated thermal margins will be even greater for operations under the actual canister heat load rating of 24.8 kW, as presented in Table 4.4-1. Therefore, the W74 canister is suitable for loading, closure, and transfer of Big Rock Point BWR fuel within the FuelSolutions™ W100 Transfer Cask. The W74 canister is qualified for 26.4 kW for operations within the transfer cask.

Figure 4.4-26 presents the W74 canister heat balance for normal hot transfer conditions at the maximum heat load rating (Q_{max}) and for steady-state at the normal hot conditions of transfer. Heat into the transfer cask is from the spent fuel (26.4 kW) and insolation (1.9 kW). All heat (28.3 kW) is lost through the cask to ambient by natural convection and radiation.

The canister pressurization for normal conditions of transfer are within the design allowables for the canister. Additionally, conservative analysis demonstrates that the peak canister pressure during reflooding operations will remain below the design basis reflood pressure for the canister (100 psig).

Table 4.4-6 - W74 System Temperatures for Normal Transfer[1]

Component	Case 13 Normal Transfer	Case 14 Normal Cold Transfer	Case 15 Normal Hot Transfer	Material Allowable[4]
Peak Fuel Rod Cladding[6]	379.0°C	362.2°C	383.6°C	400°C
Guide Tube	705°F	673°F	714°F	800°F
Spacer Plates:				
Stainless Steel	652°F	617°F	661°F	800°F
Carbon Steel	693°F	658°F	700°F	700°F
Engagement Plate	496°F	459°F	506°F	800°F
Support Tube	674°F	641°F	683°F	800°F
Helium Bulk Temp.	581°F	544°F	591°F	n/a
Canister Shell	533°F	497°F	543°F	800°F
Cask Inner Shell	323°F	277°F	336°F	800°F
Cask Lead Shield	319°F	273°F	332°F	620°F
Cask Outer Shell	233°F	172°F	249°F	800°F
Liquid Neutron Shield	216°F	154°F	233°F	293°F
Neutron Shield Pressure	16.1 psia	14.6 psia	22.1 psia	60 psia[5]
Cask Thermocouple[2]	225°F	165°F	242°F	n/a
Reference Results From Table 4.4-11 of the FuelSolutions™ Storage System FSAR				
Cask Lead Shell[3]	*332 °F*	*281 °F*	*345 °F*	
Cask Thermocouple[2,3]	*240 °F*	*180 °F*	*257 °F*	

Notes:

(1) Except as noted, temperatures are based on a heat load of 26.4 kW.
(2) Estimated thermocouple reading for analyzed condition.
(3) Temperatures based on heat load of 28 kW.
(4) Canister allowable temperatures are from Table 4.3-1 of this FSAR. Transfer cask material allowable temperatures are from Table 4.3-2 of the FuelSolutions™ Storage System FSAR.
(5) Neutron shield allowable pressure is from Table 2.0-1 of the FuelSolutions™ Storage System FSAR.
(6) Temperatures based on heat load of 24.8 kW.

Table 4.4-7 - W74 Canister System Temperatures During Handling[1]

Component	Case 10, Cask Handling		Material Allowable[4]
	w/ Air In Annulus[2]	w/ Water In Annulus[3]	
Peak Fuel Rod Cladding	468.6°C[5]	299.0°C	400°C
Guide Tube	847°F	517°F	800°F
Spacer Plates:			
Stainless Steel	655°F	335°F	800°F
Carbon Steel	832°F[5]	498°F	700°F
Engagement Plate	597°F	255°F	800°F
Support Tube	723°F	373°F	800°F
Helium Bulk Temp.	653°F	328°F	n/a
Canister Shell	591°F	177°F	800°F
Cask Inner Shell	301°F	143°F	800°F
Cask Lead Shield	298°F	143°F	620°F
Cask Outer Shell	229°F	121°F	800°F
Liquid Neutron Shield	214°F	113°F	293°F
Neutron Shield Pressure	15.4 psia	14.7 psia	60 psia[6]
Cask Thermocouple[7]	219°F	114°F	n/a

Notes:

(1) Temperatures are based on a heat load of 26.4 kW.

(2) Results for steady-state operation.

(3) Assumes water in the canister to cask annulus and water or air in the liquid neutron shield.

(4) Canister allowable temperatures are from Table 4.3-1 of this FSAR. Transfer cask material allowable temperatures are from Table 4.3-2 of the FuelSolutions™ Storage System FSAR.

(5) Fuel cladding and spacer plate temperatures reach their limits (of 400°C and 700°F, respectively) roughly 15 hours after drainage of the annulus (see Figure 4.4-25). Operational time in this mode limited by *technical specifications* in Section 12.3.

(6) Neutron shield allowable pressure is from Table 2.0-1 of the FuelSolutions™ Storage System FSAR.

(7) Estimated thermocouple reading for analyzed condition.

Table 4.4-8 - W74 Canister Pressures for Normal Transfer[1]

Component	Case 13 Normal Transfer	Case 14 Normal Cold Transfer	Case 15 Normal Hot Transfer
Helium Bulk	581°F	544°F	591°F
Helium Pressure[2]	25.7 psia	24.8 psia	25.9 psia

Notes:

(1) Temperatures/pressures are based on a heat load of 26.4 kW.

(2) Estimated canister pressure based on a pressure of 24 psia at "Normal Hot Storage" condition and ideal gas law. Pressurization due to fuel rod failure is not included.

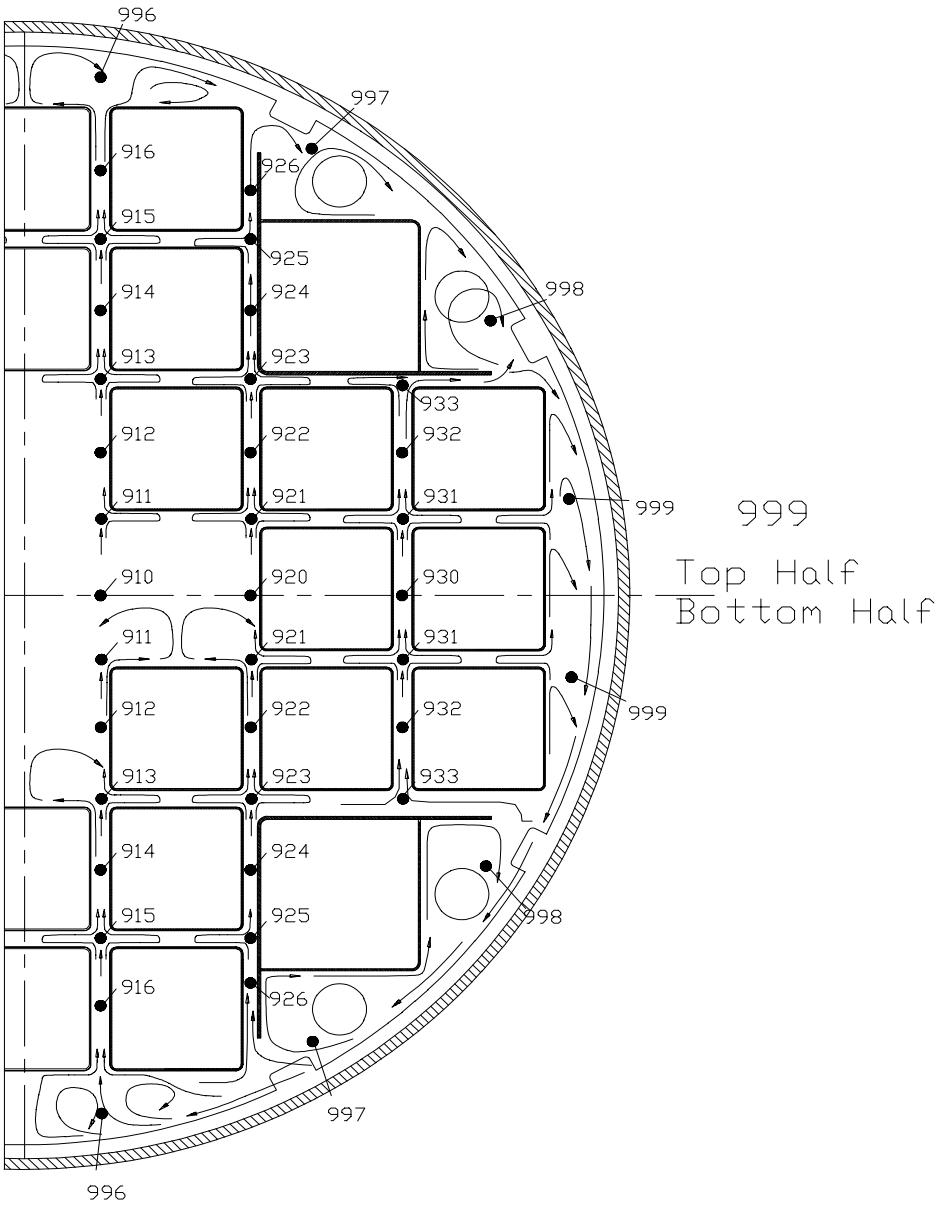

Figure 4.4-17 - Assumed Flow Pattern within Horizontal Canister

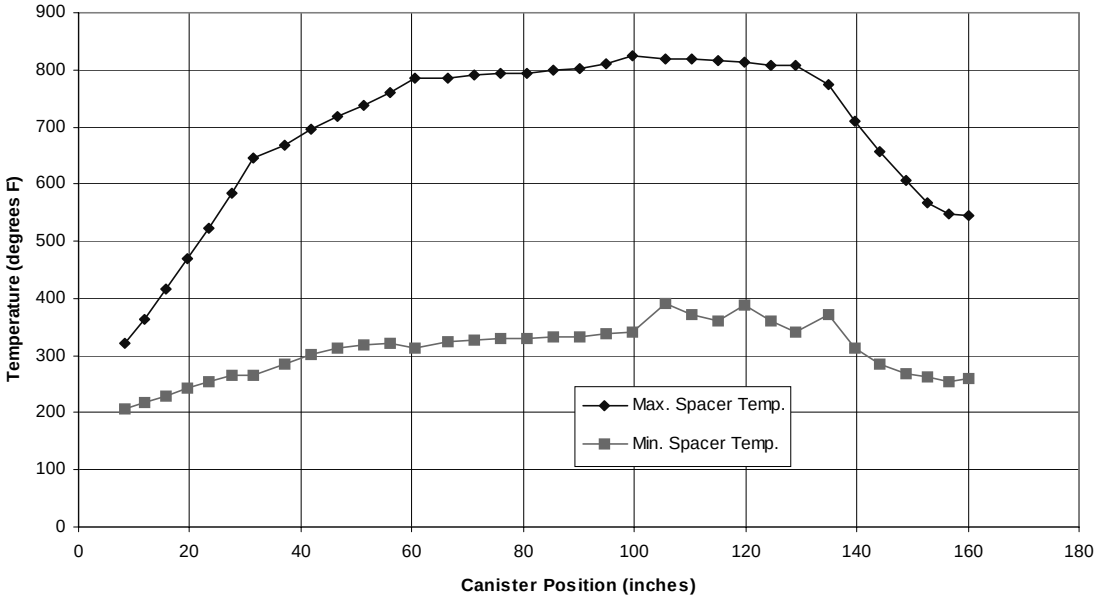

Figure 4.4-18 - Typical Spacer Plate Axial Temperature Distribution Prior to Reflood (with 4 hours of cooling)

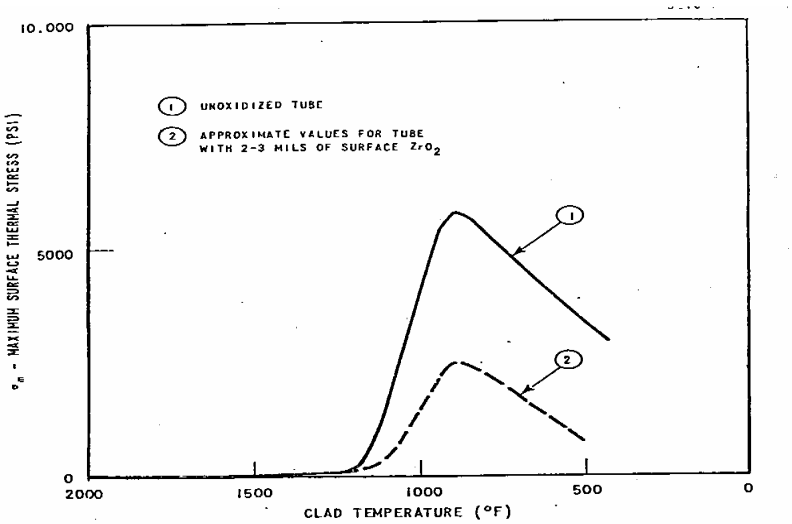

Figure 4.4-19 - Clad Thermal Stress During Core Reflooding

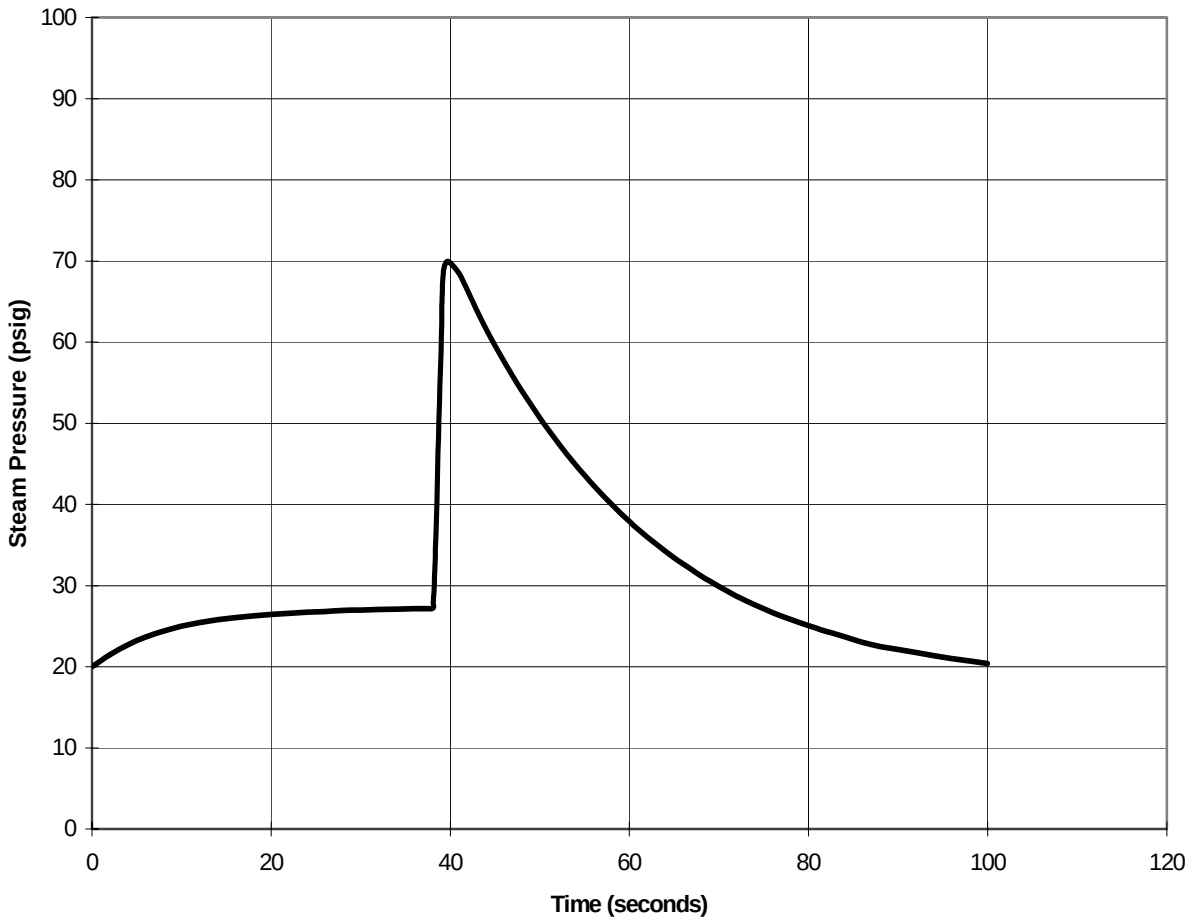

Figure 4.4-20 - Canister Pressure During Limiting Spacer Plate Quenching

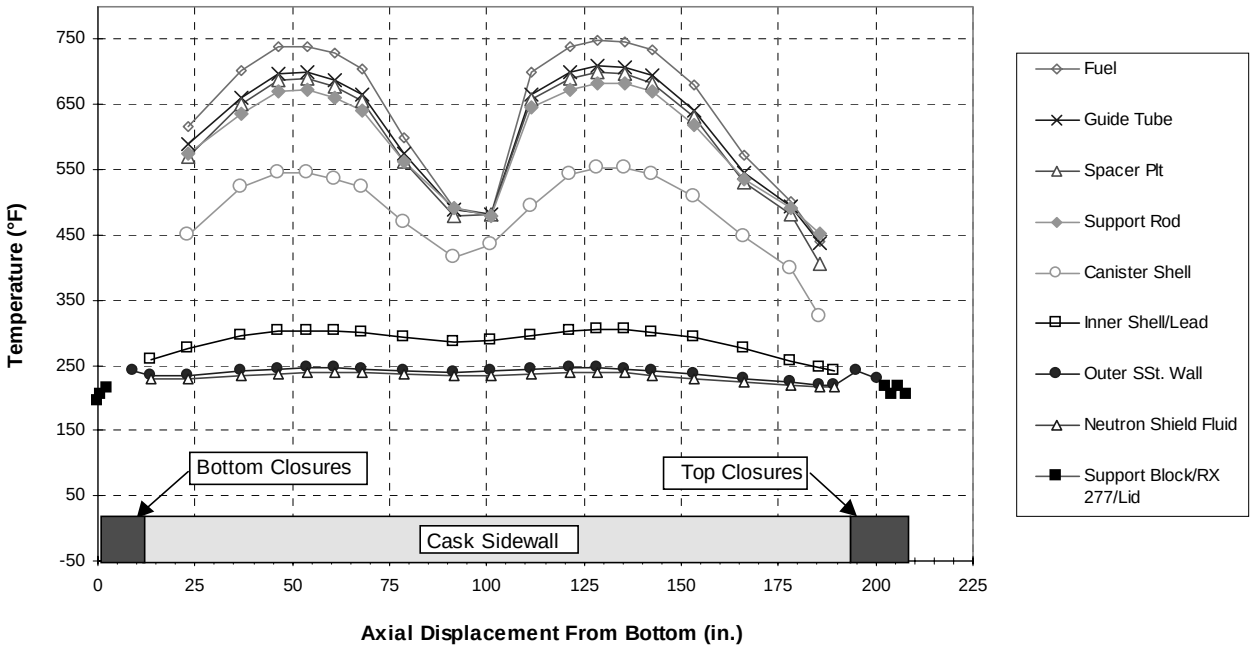

Figure 4.4-21 - W74 Canister Axial Temperature Distribution for Normal Hot Transfer Condition at Q_{max}

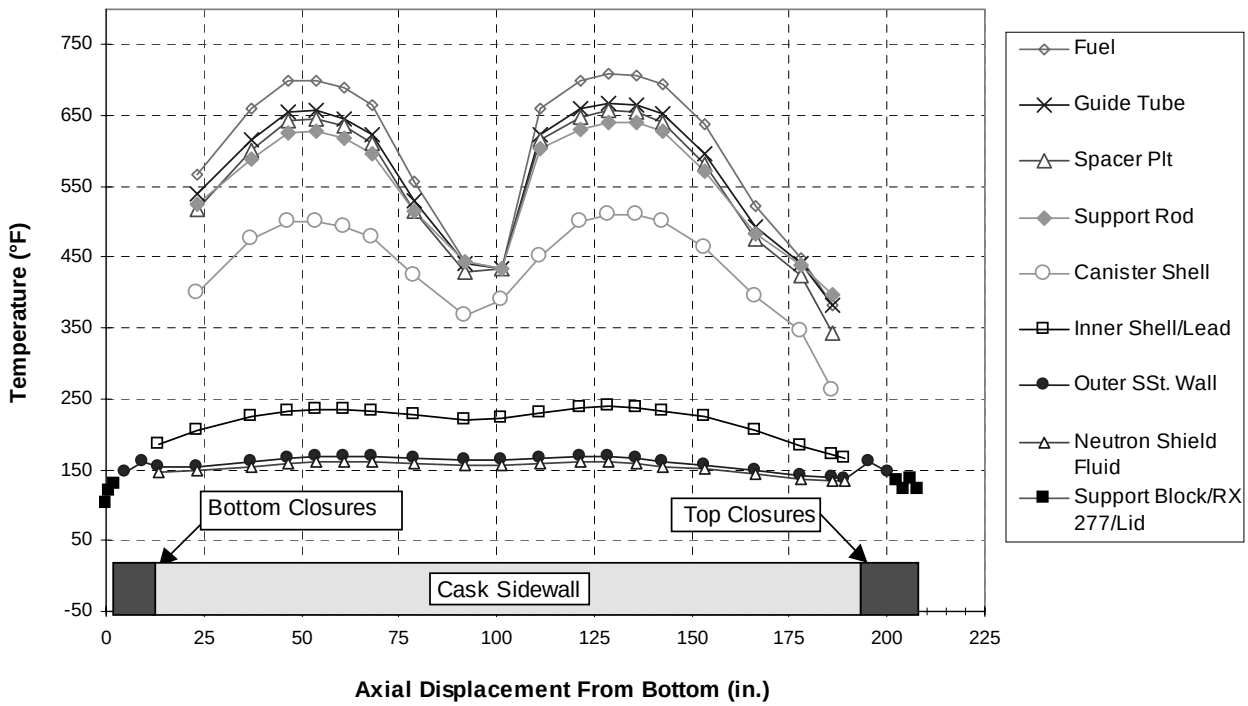

Figure 4.4-22 - W74 Canister Axial Temperature Distribution for Normal Cold Transfer Condition at Q_{max}

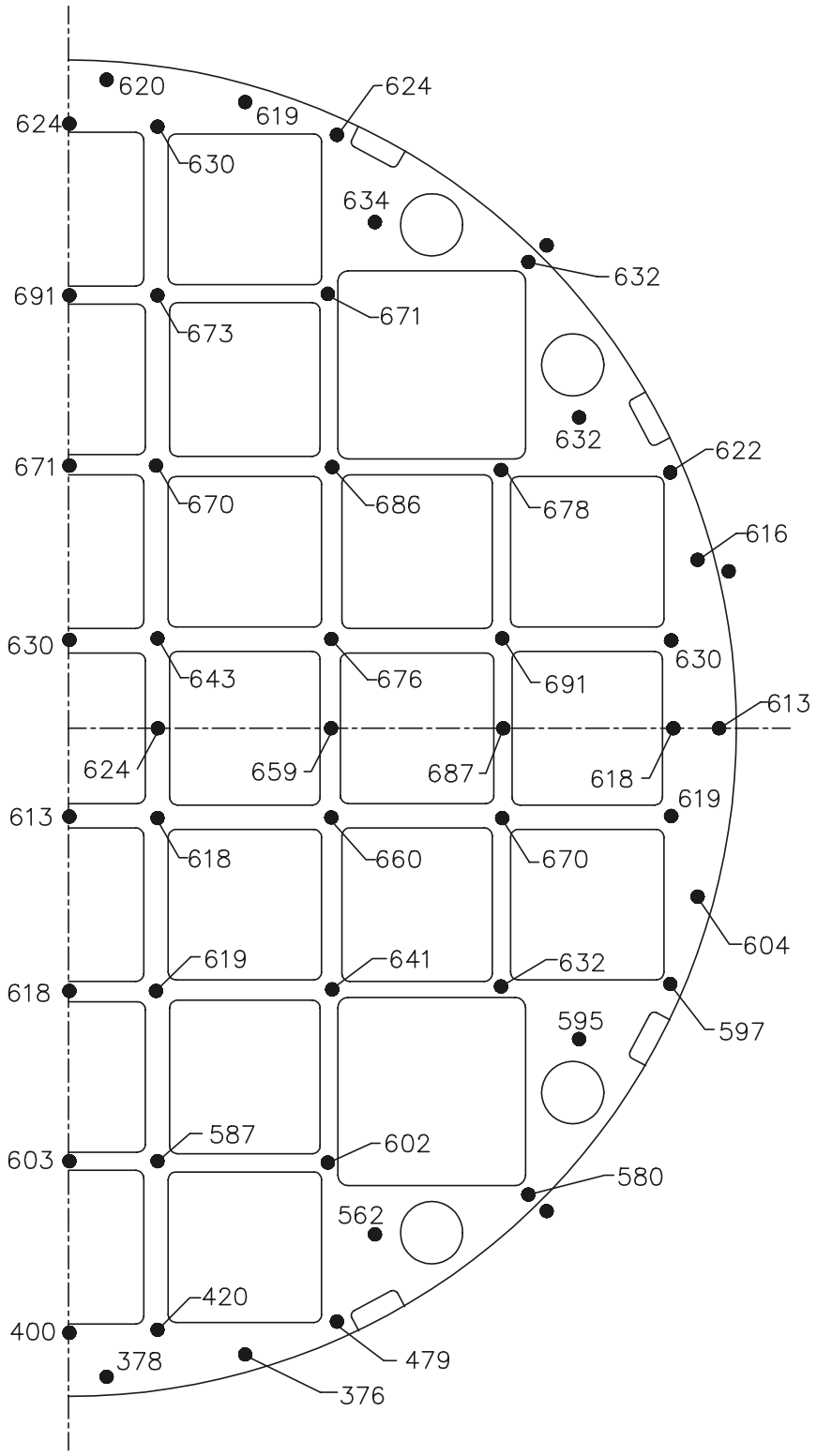

Figure 4.4-23 - W74 Spacer Plate Temperature Distribution for Normal Hot Transfer Condition at Q_{max}

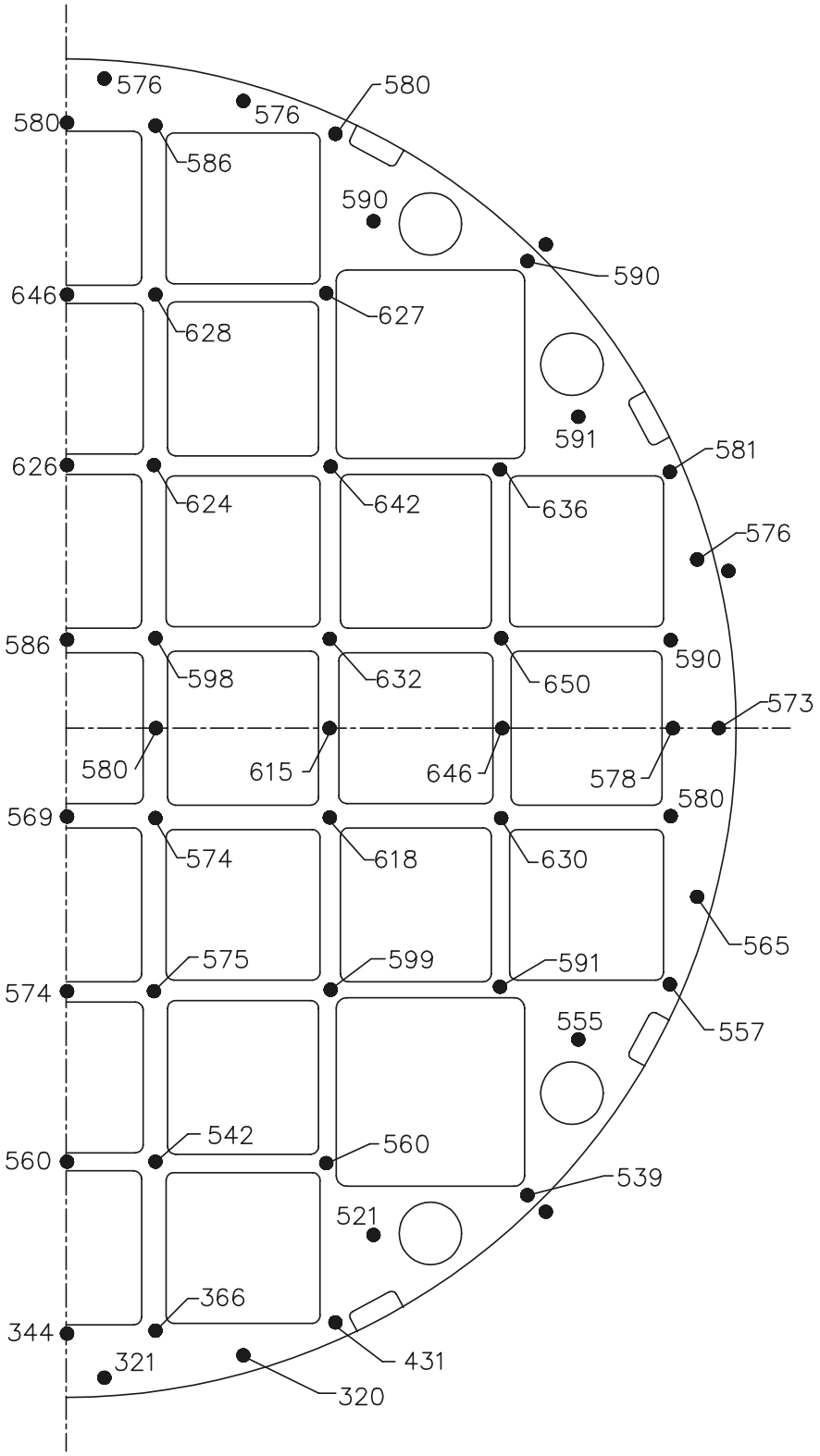

Figure 4.4-24 - W74 Spacer Plate Temperature Distribution for Normal Cold Transfer Condition at Q_{max}

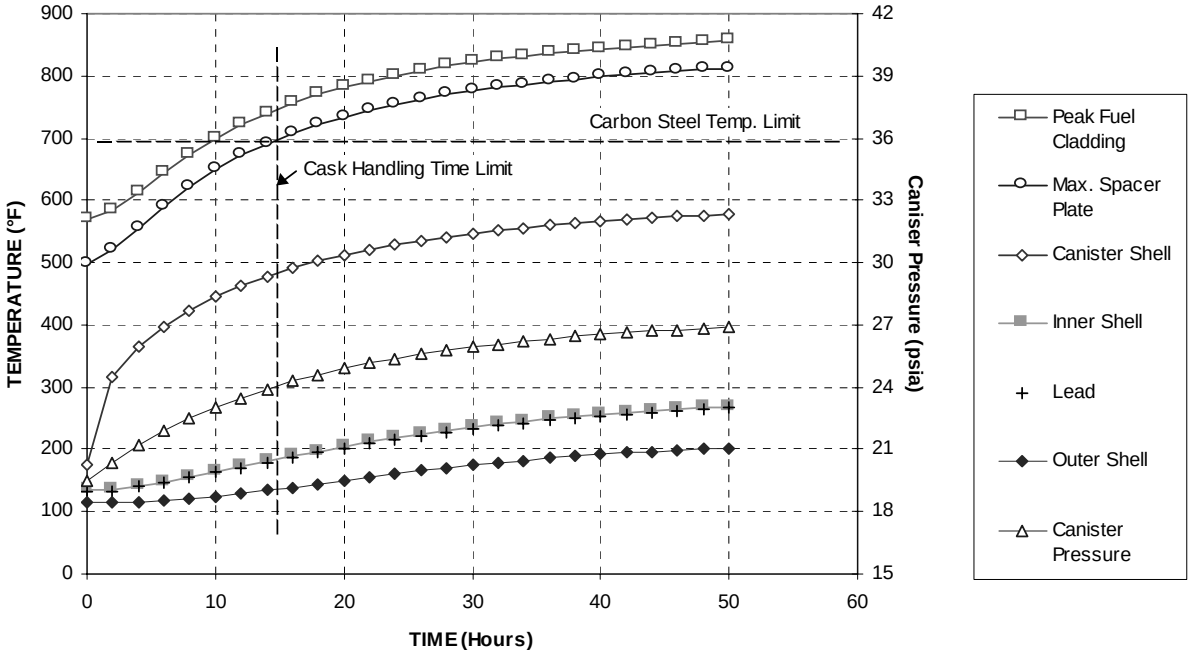

Figure 4.4-25 - Transfer Cask Handling (Case 10) Transient at Q_{max}

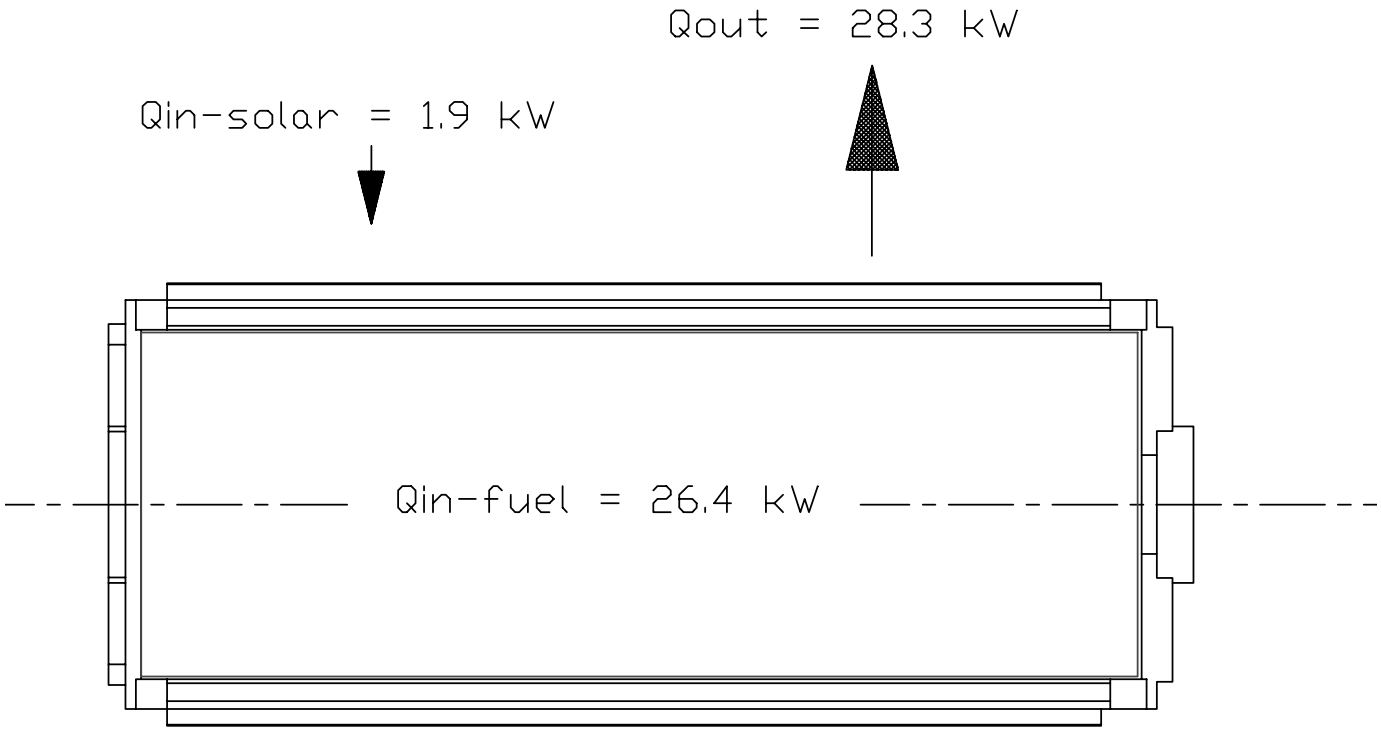

Figure 4.4-26 - W74 Canister Heat Balance within the Transfer Cask for Normal Hot Transfer Conditions at Q_{max}

This page intentionally left blank.

4.5 Thermal Evaluation for Off-Normal Conditions of Storage

This section provides a discussion of the thermal analysis methodology and results for the FuelSolutions™ W74 canister when used in conjunction with the FuelSolutions™ W150 Storage Cask and the FuelSolutions™ W100 Transfer Cask under off-normal conditions. The applicable canister assembly thermal ratings, temperature distributions, and thermal performance are evaluated to verify that the canister and cask thermal design features adequately perform their intended functions.

The conclusions presented in Sections 4.7.4, 4.7.5, and 4.7.6 demonstrate that the following results for off-normal conditions with intact BRP UO_2 fuel assemblies are bounding for the FuelSolutions™ W74 canister with BRP MOX, partial, and damaged fuel assemblies.

4.5.1 W74 Canister within Storage Cask

The storage cask off-normal conditions considered in this section include off-normal cold storage (case 8), off-normal hot storage (case 9), and canister horizontal transfer (case 13). The applicable storage cask operating conditions for these cases are summarized in Table 4.1-2 and Table 4.1-4.

4.5.1.1 Thermal Model

The thermal model used for evaluation of the W74 canister within the vertical storage cask under off-normal ambient conditions is identical to that described above in Section 4.4.1.1. The thermal model for evaluation of the W74 canister within the storage cask during horizontal transfer differs slightly from the vertical model. The major modeling difference is internal convection, which is discussed in Section 4.7.1.

The thermal model used in the evaluation of the storage cask under normal flow conditions (all vents open) in the vertical orientation for off-normal ambient conditions is the same as that used for the normal conditions (see Section 4.4.1.1). Discussion of the all vents blocked case in the vertical orientation is included in the accident conditions discussion (Section 4.6). Storage cask horizontal modeling is discussed in Section 4.5.1 of the FuelSolutions™ Storage System FSAR.

4.5.1.2 Maximum Temperatures

Maximum storage cask system temperatures are presented below for off-normal ambient conditions and horizontal canister transfer conditions.

4.5.1.2.1 Off-Normal Ambient Conditions

As discussed in Section 4.4.1.2, the maximum thermal rating for the W74 canister within the storage cask is established based on the normal hot operating conditions. This same canister thermal rating is applied for the off-normal thermal analysis. The off-normal cold storage (-40°F ambient, case 8) and off-normal hot storage (125°F ambient, case 9) conditions are summarized in Table 4.1-2 and Table 4.1-4.

The steady-state canister and storage cask off-normal system temperatures are presented in Table 4.5-1. All material temperatures are within their associated allowable values. Since off-normal thermal events do not have a concurrent structural drop condition, short-term

allowable temperatures apply to all canister components. A maximum allowable temperature of 400°C applies for the fuel cladding. Representative temperatures from the W150 Storage Cask system temperature evaluations (Section 4.5.1 of the FuelSolutions™ Storage System FSAR) are also presented in the table for comparison purposes. As expected, the results for the W74 canister are bounded by those for the storage cask evaluation.

4.5.1.2.2 Horizontal Canister Transfer Conditions

The W74 canister operating conditions for canister horizontal transfer are summarized in Table 4.1-2 and Table 4.1-4 for case 13. Two horizontal cases, loading and unloading, are considered. For the loading conditions the W74 canister and storage cask are assumed to start at steady-state temperature for the empty cask (100°F ambient). For the unloading case, the W74 canister and storage cask initial temperatures for the horizontal transient analysis are taken as the steady-state temperatures at the W74 canister structural thermal rating (26.4 kW) for the normal storage condition (77°F ambient). These unloading initial conditions are conservative since the cask decay heat generation decreases with storage time, and unloading operations will most likely be performed following long-term storage. Of the two unloading conditions, canister unloading (case 13b) with the maximum W74 canister thermal rating is the most limiting of the two conditions since the thermal mass of the storage cask is already heated.

The W74 canister off-normal transient temperatures in the horizontal storage cask are presented in Table 4.5-1 for initial (i.e., normal storage, case 5) and at the 66 hour time point after the start of the horizontal unloading process where the maximum allowable carbon steel spacer plate temperature (700°F) is reached. For the W74 canister structural heat load rating of 26.4 kW, this occurs at 9.5 hours. Note that, at this time value, all temperatures are below their applicable allowable material temperatures. This transient time period forms the basis for the *technical specification* limit contained in Section 12.3 of this FSAR.

Application of the *technical specifications* by the licensee is based on measured temperatures from the cask liner thermocouple installed at mid-height and at the liner/concrete interface of the storage cask, as described in Section 1.2.1 of the FuelSolutions™ Storage System FSAR. Figure 4.5-1 illustrates the W74 canister carbon steel spacer plate temperature as a function of time for the horizontal unloading transient. The corresponding storage cask thermocouple temperature is also displayed over the transient time period. From the figure, a concrete thermocouple temperature of 185°F corresponds to a maximum carbon steel spacer plate allowable temperature of 700°F. The W74 canister materials are more thermally limiting than the storage cask materials during horizontal unloading, and the *technical specification* based on canister material allowables also provides protection for the cask materials.

Should equipment mechanical difficulties occur during horizontal canister transfer operations which result in an extended period with the loaded storage cask in the horizontal orientation, mitigating actions are required prior to exceeding the W74 canister carbon steel spacer plate allowable material temperature, as correlated to the monitored liner thermocouple temperature. Mitigating actions include uprighting the cask and returning the canister to the transfer cask as defined in the *technical specifications* in Section 12.3 of this FSAR.

4.5.1.3 Minimum Temperatures

The temperatures in the storage cask components under off-normal cold conditions are listed in Table 4.5-1. The temperatures shown are for the W74 canister at its maximum structural thermal rating of 26.4 kW and, therefore, do not represent the lowest expected component temperatures.

The low temperature compatibility of the W74 canister components are also evaluated for the bounding load case of -40°F (-40°C) ambient temperature, zero decay heat load, and no insolation. The steady-state temperatures of the canister and storage cask system for this analytically trivial case are -40°F (-40°C). The component temperatures are within their minimum allowable temperatures in all cases.

4.5.1.4 Internal Pressures

For determination of the off-normal canister pressure, 10% rod failures are assumed. Additionally, the canister gas cavity temperature for off-normal hot storage conditions (125°F ambient, Section 4.1.4) is conservatively assumed. As discussed in Section 4.5.1.2.2, W74 canister horizontal transfer operations within the storage cask must be terminated if the storage cask thermocouple temperature limit is reached. The W74 canister average gas temperature under off-normal storage conditions (125°F ambient) bounds the horizontal transfer case.

W74 canister off-normal pressure is determined as follows:

$$P_{Off-Normal} = \frac{N_{Off-Normal} R T_{Off-Normal}}{V_{Canister}}$$

$$N_{Off-Normal} = N_{Canister} + 0.10 \cdot N_{Rods}$$

Where:

N_{Rods} = Total moles of fuel rod fill gas and fission gas available for release

$N_{Off\text{-}Normal}$ = Total moles of gas in the canister cavity, assuming 10% rod failures

$P_{Off\text{-}Normal}$ = Canister off-normal pressure

$V_{Canister}$ = Worst case canister cavity free volume (liters), (Table 4.4-5)

$T_{Off\text{-}Normal}$ = Canister gas temperature for off-normal hot storage (°K)

The canister pressure for off-normal cold storage conditions, with no rod failures, is also calculated to support structural analyses. The same methodology described above is used to calculate the off-normal pressure, using the canister back-fill quantity in moles ($N_{Canister}$) and the canister gas temperature ($T_{Off\text{-}Normal}$) for off normal cold storage conditions (-40°F ambient, Section 4.1.4).

W74 canister off-normal pressures for 40 GWd/MTU Big Rock Point fuel are summarized in Table 4.5-2.

4.5.1.5 Maximum Thermal Stresses

W74 canister maximum thermal stresses within the storage cask during off-normal conditions are addressed in Chapter 3 of this FSAR. Calculation of these thermal stresses is based on the

maximum canister structure heat load of 26.4 kW, and is conservative (bounding) for the actual canister heat rating of 24.8 kW.

4.5.1.6 Evaluation of Canister Performance for Off-Normal Conditions

Results of the steady-state analyses demonstrate that the W74 canister allowable material temperatures under off-normal conditions within the storage cask are not exceeded for the enveloping canister decay heat dissipation at all sites within the contiguous United States. Therefore, the W74 canister is suitable for the dry storage of all Big Rock Point fuel loadings with decay thermal ratings that are bounded by the storage cask thermal rating summarized in Table 4.1-4. Over the long-term storage period the spent fuel decay heat will decrease, thus increasing the margins relative to the allowable temperatures.

Table 4.5-1 - Maximum W74 Canister System Temperature at Q_{max} for Storage[1]

Component	Case 8 Off-Normal Cold Storage	Case 9 Off-Normal Hot Storage	Case 13b[2] Horizontal Unloading, Initial/Peak[3]	Material Allowable[4]
Peak Fuel Rod Cladding	334.2°C	395.8°C[5]	389.5°C / 391.5°C	400°C
Guide Tube	589°F	738°F	697°F / 707°F	800/1000°F
Spacer Plates:				
Stainless Steel	367°F	529°F	484°F / 623°F	800/1000°F
Carbon Steel	571°F	721°F	679°F / 698°F	700/1000°F
Engagement Plate	305°F	469°F	423°F / 422°F	800/1000°F
Support Tube	444°F	608°F	562°F / 670°F	800/1000°F
Helium Bulk	375°F	536°F	491°F / 563°F	n/a
Canister Shell	291°F	471°F	422°F / 550°F	800/1000°F
Max. Concrete	3°F	208°F	153°F / 200°F	350°F
Liner Thermocouple[6]	-5°F	192°F	139°F / 185°F	n/a
Reference Results From Tables 4.4-7 and 4.5-2 of FuelSolutions™ Storage System FSAR				
Canister Shell[7]	*290 °F*	*473 °F*	*423 °F / 662 °F*	
Max. Concrete[7]	*12 °F*	*228 °F*	*169 °F / 348 °F*	
Liner Thermocouple[6,7]	*0 °F*	*210 °F*	*150 °F / 312 °F*	

Notes:

(1) Except as noted, temperatures are based on a heat load of 26.4 kW.

(2) *Technical specification* will prevent steady-state canister temperatures from occurring for case 13b (horizontal storage cask unloading).

(3) Peak temperatures taken from 9.5 hour point in the transient analysis.

(4) Short-term steel allowable temperatures apply for cases 8 and 9. Mitigating actions are required prior to exceeding long-term allowable temperatures for case 13b (see Section 12.3 of this FSAR). Canister allowable temperatures are from Table 4.3-1 of this FSAR. Storage cask material allowable temperatures are from Table 4.3-1 of the FuelSolutions™ Storage System FSAR

(5) Peak fuel cladding temperature and liner thermocouple temperature for Case 9 are based on a canister heat load of 24.8 kW; all other canister component temperatures assume a heat load of 26.4 kW.

(6) Estimated thermocouple reading for analyzed condition.

(7) Temperatures based on heat load of 28 kW.

Table 4.5-2 - W74 Canister Off-Normal Pressures

Parameter	W74 Canister Pressure (psig)
Off-Normal Pressure (min., no rod failures)	6.3
Off-Normal Pressure (max., 10% rod failures)	12.3

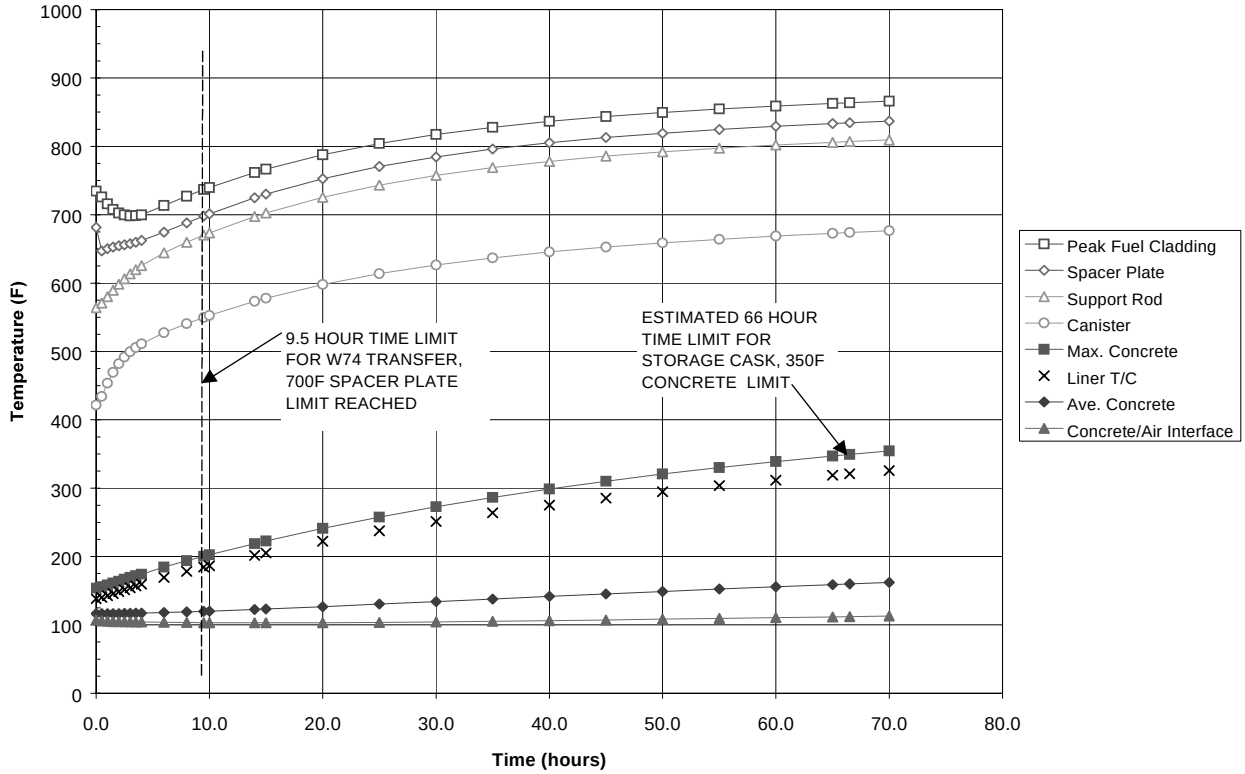

Figure 4.5-1 - W74 Canister/Storage Cask Temperatures During Horizontal Unload Transient (26.4 kW)

4.5.2 W74 Canister within Transfer Cask

4.5.2.1 Thermal Model

The W74 canister thermal model used in the evaluation of the off-normal conditions within the transfer cask is the same as that used for the normal conditions (see Section 4.4.2.1).

4.5.2.2 Maximum Temperatures

Table 4.5-3 presents the W74 canister system temperatures for the off-normal transfer cases for vacuum drying (case 6), off-normal cold (case 16), and off-normal hot (case 17) conditions of transfer. The evaluations are made for the maximum thermal rating for the W74 canister structure (26.4 kW). The system configurations associated with these off-normal cases are summarized in Table 4.1-3 and Table 4.1-5.

All canister component temperatures are within their associated short-term allowable temperatures, with the exception of the peak fuel cladding temperature at the steady-state vacuum drying condition. Since off-normal thermal events do not have a concurrent structural drop condition, short-term allowable temperatures apply to all canister components. Representative temperatures from the W100 Transfer Cask system temperature evaluations (Section 4.5.2 of the FuelSolutions™ Storage System FSAR) are also presented in the table for comparison purposes. As expected, the results for the W74 canister are bounded by those for the transfer cask evaluation.

The peak fuel cladding temperature is shown to be below its maximum allowable short-term temperature of 400°C during off-normal hot and cold transfer (steady-state). However, for vacuum drying, the peak fuel cladding could reach its short-term allowable temperature (400°C) if near vacuum conditions are maintained for approximately 7 hours. To avoid this, the licensee will apply the *technical specification* to manage the vacuum drying process. Figure 4.5-2 illustrates the predicted thermal response of this managed vacuum drying process for a generic canister with a heat load of 26.4 kW.

As seen from the figure, the typical canister loading cycle is divided into the multiple phases that a canister will typically undergo prior to placement in the storage cask. Phases 1 and 2 cover removal from the pool, decon, and welding of the canister lids; Phase 3 is the canister drain down; Phase 4 is the vacuum drying of the canister; Phases 5 and 6 involve canister inspections and possible re-evacuation of the canister; Phase 7 involves outer closure plate welding, PT and NDE evaluations, rigging, etc.; Phase 8 is vertical transfer handling operations; and Phase 9 is interim storage of the canister in the storage cask.

The Figure 4.5-2 transient demonstrates that if the vacuum drying time is limited to an initial maximum period of 7 hours, the short-term fuel cladding limit of 400°C will not be exceeded. If additional vacuum drying time is required, the controlled vacuum drying process will require at least 4 hours of cooling under helium gas backfill prior to initiating another 4 hour period of vacuum drying. This cycle of cooling under helium backfill and re-evacuation may be repeated as often as necessary to achieve the desired level of dryness within the canister. This approach will prevent annealing and hydride readsorption and reorientation that could occur in the

Zircaloy-2 or Zircaloy-4 cladding at temperatures greater than 400°C (752°F), and will assure that the total cladding creep during fuel loading and storage operations is less than 1%.

The remainder of the Figure 4.5-2 transient demonstrates that the short-term fuel cladding limit of 400°C will not be exceeded under the other canister handling operations and time frames that precede placement in interim storage.

4.5.2.3 Minimum Temperatures

The temperatures in the transfer cask components under off-normal cold conditions are listed in Table 4.5-3. The temperatures shown are for the W74 canister at its structural thermal rating of 26.4 kW and, therefore, do not represent the lowest expected component temperatures.

The low temperature compatibility of the W74 canister components are also evaluated for the bounding load case of -40°F (-40°C) ambient temperature, zero decay heat load, and no insolation. The steady-state temperatures of the canister and transfer cask system for this analytically trivial case are -40°F (-40°C). The component temperatures are within their minimum allowable temperatures in all cases.

Transient analysis is presented in Section 4.5.2.3 of the FuelSolutions™ Storage System FSAR to illustrate the time frame available when operating in freezing weather. An associated *technical specification* is established, as presented in Section 12.3 of the FuelSolutions™ Storage System FSAR, based on a bounding transient analysis which assumes no decay heat load.

4.5.2.4 Internal Pressures

Table 4.5-4 presents the W74 canister pressures for off-normal transfer cases.

Since the canister thermal rating is lower than the transfer cask thermal rating, the liquid neutron shield internal pressure is bounded by the that in the FuelSolutions™ Storage System FSAR.

4.5.2.5 Maximum Thermal Stresses

W74 canister maximum thermal stresses within the transfer cask during off-normal conditions are addressed in Chapter 3 of this FSAR.

4.5.2.6 Evaluation of Canister Performance for Off-Normal Conditions

The results of the steady-state analyses demonstrate that the W74 and transfer cask allowable material temperatures under off-normal conditions are met for the maximum canister thermal rating of 24.8 kW (as presented in Table 4.4-1). The analyses also show that the peak fuel cladding temperature reached under these conditions complies with the short-term temperature limit for off-normal transfer conditions. Therefore, the W74 canister is suitable for the transfer of Big Rock Point BWR fuel within the FuelSolutions™ W100 Transfer Cask for canister heat loads of 24.8 kW or less.

The canister pressurization for off-normal conditions of transfer are within the design basis pressures for the canister.

Table 4.5-3 - W74 System Temperatures for Off-Normal Transfer[1]

Component	Case 6 Vacuum Drying	Case 16 Off-Normal Cold Transfer	Case 17 Off-Normal Hot Transfer	Material Allowables[2]
Peak Fuel Rod Cladding	535.5°C[3]	368.9°C	388.7°C[4]	400°C
Guide Tube	975°F	657°F	724°F	1000°F
Spacer Plates: Stainless Steel Carbon Steel	 669°F 947°F	 600°F 642°F	 672°F 713°F	 1000°F 1000°F
Engagement Plate	517°F	441°F	517°F	1000°F
Support Tube	662°F	625°F	693°F	1000°F
Helium Bulk Temp.	n/a	527°F	602°F	n/a
Canister Shell	169°F	481°F	554°F	1000°F
Cask Inner Shell	143°F	255°F	350°F	1000°F
Cask Lead Shield	143°F	251°F	346°F	620°F
Cask Outer Shell	120°F	143°F	268°F	1000°F
Liquid Neutron Shield	113°F	123°F	251°F	293°F
Neutron Shield Pressure	14.7 psia	14.7 psia	30.6 psia	60 psia[5]
Cask Thermocouple[6]	114°F	135°F	260°F	n/a
Reference Results From Table 4.5-6 of the FuelSolutions™ Storage System FSAR				
Cask Lead[7]	*not analyzed*	*258 °F*	*360 °F*	
Cask Thermocouple[6,7]	*not analyzed*	*151 °F*	*274 °F*	

Notes:
(1) Except as noted, temperatures are based on a heat load of 26.4 kW.
(2) Canister allowable temperatures are from Table 4.3-1 of this FSAR. Transfer cask material allowable temperatures are from Table 4.3-2 of the FuelSolutions™ Storage System FSAR.
(3) Steady-state values shown for information only. Vacuum drying process will limit the fuel clad temperature to its maximum short-term value of 400°C. A heat load of 17.5 kW or less will result in a maximum steady-state cladding temperature of 400°C or less. See discussion in Section 4.5.2.2.
(4) Peak fuel cladding temperature based on a heat load of 24.8 kW, all other canister temperatures based on a canister heat load of 26.4 kW.
(5) Neutron shield allowable pressure is from Table 2.0-1 of the FuelSolutions™ Storage System FSAR.
(6) Estimated thermocouple reading for analyzed condition.
(7) Temperatures based on heat load of 28 kW.

Table 4.5-4 - W74 Canister Pressures for Off-Normal Transfer at Q_{max}[(1)]

Component	Case 6 Vacuum Drying	Case 16 Off-Normal Cold Transfer	Case 17 Off-Normal Hot Transfer
Helium Bulk	n/a	527°F	602°F
Helium Pressure[(2)]	0.0 psia	24.4 psia	26.2 psia

Notes:

(1) Temperatures/pressures in this table are based on a heat load of 26.4 kW

(2) Estimated canister pressure based on a design pressure of 24 psia at 'Normal Hot Storage' condition and ideal gas law. Pressurization due to fuel rod failure is not included.

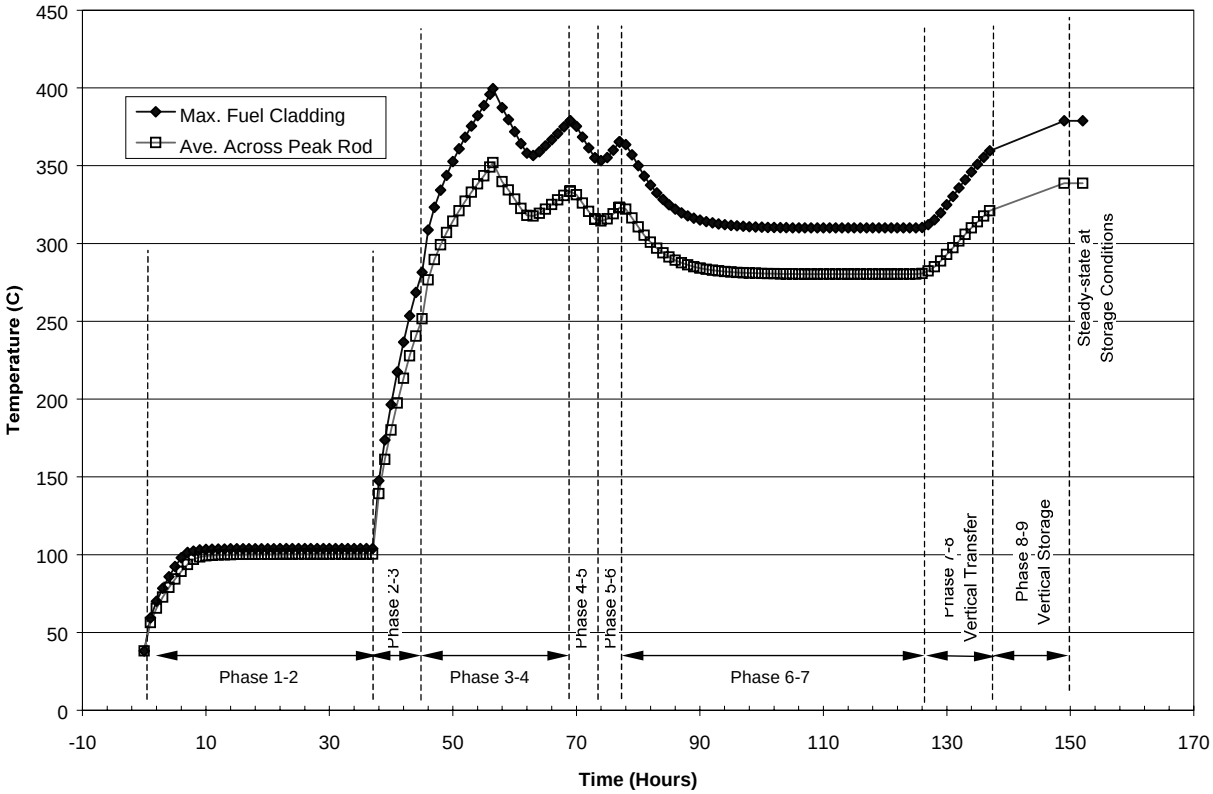

Figure 4.5-2 - Generic Canister Loading Cycle Temperature Histogram For Vertical Transfer

4.6 Thermal Evaluation for Accident Conditions of Storage

This section provides a discussion of the thermal analysis methodology and results for the FuelSolutions™ W74 canister when used in conjunction with the FuelSolutions™ W150 Storage Cask and the FuelSolutions™ W100 Transfer Cask under accident conditions. The applicable canister assembly thermal ratings, temperature distributions, and thermal performance are evaluated to verify that the canister and cask thermal design features adequately perform their intended functions.

The conclusions presented in Sections 4.7.4, 4.7.5, and 4.7.6 demonstrate that the following results for postulated accident conditions with intact BRP UO_2 fuel assemblies are bounding for the FuelSolutions™ W74 canister with BRP MOX, partial, and damaged fuel assemblies.

4.6.1 W74 Canister within Storage Cask

The two storage cask postulated accident conditions considered are the all vents blocked accident (case 11) and a postulated fire accident (case 15). The applicable storage cask operating conditions for these cases are summarized in Table 4.1-2 and Table 4.1-4. All accident storage condition thermal analyses are conservatively based on a 26.4 kW canister heat load, the maximum heat load that can be accommodated by the W74 canister structure. The analyses are bounding (conservative) for the actual W74 canister heat load rating of 24.8 kW (which is based on the temperature limits of the canister payload).

4.6.1.1 Thermal Model

4.6.1.1.1 All Vents Blocked

The W74 canister thermal model used in the evaluation of the storage cask for the all vents blocked accident condition is identical to that used for the normal conditions (see Section 4.4.1.1). The storage cask thermal model differences for the all vents blocked accident condition are fully described in Section 4.6.1 of the FuelSolutions™ Storage System FSAR. Briefly, the storage cask model assumes that at time t = 0, the inlet and outlet vents become fully blocked. An internal flow loop is set up by this blockage, wherein the air flow circulates between the canister, the thermal shield, and the steel liner of the storage cask. The strength of this internal flow loop is computed within the storage cask thermal model as a function of the density differences between the inner and outer air columns. All other aspects of the storage cask model remain the same as that used to compute the normal conditions of storage discussed in Section 4.4.1 of this FSAR.

4.6.1.1.2 Storage Cask Fire

As presented in Section 4.6.1 of the FuelSolutions™ Storage System FSAR, the loaded storage cask is analyzed for a postulated fire accident during long-term storage. The transient response of the storage cask under postulated fire accident conditions is simulated using the lumped parameter heat transfer code SINDA with thermal modeling similar to that described for normal conditions. Two postulated fire events are simulated: 1) a 5-minute engulfing fire, and 2) a 5-minute fire within the storage cask inlet vents. The thermal models for the two postulated storage

cask fire events are nearly identical to the normal model with minor modifications for the ambient conditions and natural convection.

Both fire transient analyses assume an initial steady-state temperature distribution for normal hot storage conditions. Immediately following the 5-minute fire event, ambient conditions are returned to normal hot storage conditions for evaluation of the post-event transient response.

Engulfing Fire

The normal vertical storage cask model presented in Section 4.4.1.1 of the FuelSolutions™ Storage System FSAR, simulates the natural convection flow upward through the annulus induced the buoyancy driven forces resulting from heavier (cooler) ambient air. During a fire event, the ambient (flame) temperature is much higher than that of the canister surface, the heat shield, and the cask liner. As a result, the gas in the storage cask annulus is heavier than the ambient gas creating reversed natural circulation flow. Hot combustion gas flows into the annulus gap from the top vents, flow downward along the annulus gap, and exit the cask through the bottom channels. While the gas flows downward along the annulus gaps, heat is transferred to the canister shell and the cask liner. Minor modifications to the normal air flow model are performed to account for the reverse convection. The air flow in the storage cask annulus reverses direction back to the normal vertical storage conditions immediately after the fire ceases.

In order to conservatively bound the canister shell temperature during the transient, no heat transfer is assumed between the shell and the canister internals. The normal vertical storage cask model used for transient analysis assumes that the entire thermal mass of the canister is concentrated at the canister shell. In order to allow conservative determination of the canister shell temperature response during the fire event, the canister shell is modeled with only its thermal mass, not the total canister thermal mass.

Consistent with NUREG-1536,[9] the flame and surface emissivities specified in 10CFR71.73(c)(4)[3] are assumed to bound any credible storage cask fire because of the high heat and the proximity of the flames. The storage cask is conservatively assumed to become engulfed in a hydrocarbon fuel/air fire of sufficient extent, and in sufficiently quiescent ambient conditions, to provide an average emissivity coefficient of 0.9, with an average flame temperature of 1475°F for a period of 5 minutes. The flame source is conservatively assumed to extend 10 feet beyond any external surface of the cask.

The mechanisms and models for coupling the fire energy to the cask surface include forced convection in relation to the flame velocity as well as thermal radiation. In order to conservatively maximize radiation and convection heat transfer, the flame is assumed to surround the cask with a flame temperature of 1475°F and a maximum velocity of 15 m/s (49.2 ft/sec), which gives the highest convection coefficient. A convection coefficient value of 3.8 Btu/hr-ft^2-°F was conservatively utilized for all exterior surfaces of the storage cask.

Inlet Vent Fire

There is no significant modeling change required to simulate the postulated 5- minute inlet vent fire. The basic flow pattern is the same as that for the normal vertical operation. However, it is assumed that the liquid fuel burns within the cask inlet vents and the base section bottom hole, thus the temperatures for the air nodes of the base sub-model are set to the fire temperature

1475°F (801.7°C). The hot combustion gases rise along the vertical annulus gaps, giving up heat to the canister shell, the heat shield, and the cask liner along the way. The exhaust gas exits the cask from the outlet vents.

Similar to the 5-minute engulfing fire, the canister shell is modeled with only its thermal mass, not the total canister thermal mass in order to conservatively bound the canister shell temperature during the transient.

4.6.1.2 Maximum Temperatures

Transient analyses are performed for both the all vents blocked and fire accident conditions to assure that the W74 canister allowable material temperatures are not exceeded. For the all vents blocked accident condition, vent clearance requirements are established within the *technical specification* presented in Section 12.3 of the FuelSolutions Storage System FSAR.

For the fire accident, there is no corresponding *technical specification* which correlates surface concrete temperature to the thermocouple reading. This is due to the fact that the cask outer surface concrete temperatures exceed 350°F nearly instantaneously during the fire accident, and the storage cask thermocouples cannot be expected to remain functional following the fire accident. However, the operating procedures presented in Section 8.1.10 of the FuelSolutions™ Storage System FSAR will limit the quantity of combustible fuel at the ISFSI.

4.6.1.2.1 All Vents Blocked

Figure 4.6-1 presents the transient temperature plot for storage design basis case 11 (i.e., all vents blocked). The transient starts at the steady-state conditions for normal conditions of storage (i.e., case 5). At time 0, the inlet and outlet vents are assumed to be fully blocked and to remain that way for the duration of the 70 hour transient. The temperature rise in the canister and cask components is primarily a function of the thermal mass of the component since heat loss to the ambient is greatly reduced for this condition. Like the storage cask only analysis, the results for the W74 canister in the storage cask demonstrate that the maximum cask concrete temperature is the controlling component for the analysis. The trend in the data indicates that steady-state conditions could be reached without exceeding the maximum fuel cladding temperatures or any canister component allowable temperature. Further, the results of this analysis show that the storage cask temperatures remain below their maximum allowable temperature well past the 41 hour time period determined under the design basis storage cask thermal evaluation. The primary reasons for the difference in the results between the two analyses are:

1. The storage cask analysis assumed 28 kW versus the 26.4 kW used in the W74 canister analyses,
2. The W74 canister analysis provides a more accurate modeling of the thermal mass and heat distribution within the canister than is possible with the storage cask model,
3. The stacked basket assemblies in the W74 canister acts to spread out the peak heat flux across a longer section of the cask side wall than assumed in the storage cask only analysis, and

4. The W74 canister analysis assumes a conservatively low emissivity (in terms of the canister temperatures) on the back side of the heat side (i.e., the side facing the cask liner) of 0.15 for a new shield.

The storage cask analysis indicates that a maximum liner thermocouple reading of 334°F corresponds to a maximum allowable concrete temperature of 350 °F. Applying this same logic to the results for the W74 canister analysis indicates an available recovery time of approximately 58 hours. The maximum concrete temperature predicted to occur at this time point is 345 °F.

Table 4.6-1 presents the maximum component temperatures for the canister and cask prior to the start of the all vents blocked transient and at the point where the maximum allowable concrete temperature is reached (i.e., 58 hours). The results from the storage cask only analysis are also provided for comparison purposes.

4.6.1.2.2 Fire Accident

Figure 4.6-2 and Figure 4.6-3 present the temperature response for the storage cask and generic canister to a 5 minute engulfing fire event and 5 minute inlet fire event, respectively. As seen from the figures, the canister shell shows a steady increase in temperature during the fire durations due to the hot air which is induced through the canister/cask annulus. The peak canister shell temperature prior to the fire event is 447°F (Table 4.4-7 of the FuelSolutions™ Storage System FSAR), and the peak canister temperatures for the engulfing and inlet vent fires are 475°F and 478°F, respectively (Table 4.6-2 of the FuelSolutions™ Storage System FSAR). This corresponds to a maximum rise of 31°F in the canister shell during the 5 minute fire transient. Due to the large thermal capacitance of the canister, the temperature rise within the canister during the 5 minute fire is much lower than the shell. At the end of the fire event, ambient air is cooler than the air within the storage cask annulus, resulting in resumption of normal vertical ventilation flow. Since the canister shell temperature begins to drop after the fire, the resultant maximum possible rise in canister internals and peak fuel cladding is limited to 31°F (17°C). By comparison with system temperatures at the beginning of the fire transient (case 7, Section 4.4.1.3), peak fuel cladding is well under the short-term allowable temperature of 570°C and all steel material are well under the 1000°F short-term allowable temperature.

4.6.1.3 Minimum Temperatures

There are no accident conditions applicable to minimum allowable material temperatures.

4.6.1.4 Internal Pressures

For determination of the accident canister pressure, 100% rod failures are postulated while conservatively assuming the W74 canister average gas temperature for off-normal hot storage conditions (125°F ambient, Section 4.1.4). Although the W74 canister average gas temperature under the postulated all vents blocked and fire accident conditions may exceed the corresponding gas temperature for off-normal hot storage conditions, failure of 100% of the rods does not need to be postulated concurrently with the other postulated accident conditions. Since the short-term fuel cladding allowable temperature presented in Section 4.3.2.4 (570°C) is not exceeded during W74 canister design basis accident conditions, gross cladding failures do not occur.

The W74 canister accident internal pressure is calculated as follows:

$$P_{Accident} = \frac{N_{Accident} R T_{Off-Normal}}{V_{Canister}}$$

$$N_{Accident} = N_{Canister} + N_{Rods}$$

where:

N_{Rods} = Total moles of fuel rod fill gas and fission gas available for release.

$N_{Accident}$ = Total moles of gas in the canister cavity, assuming 100% rod failures

$P_{Accident}$ = Canister pressure for off-normal hot storage conditions (125°F ambient)

$V_{Canister}$ = Worst case canister cavity free volume (liters), from Table 4.4-5.

$T_{Off-Normal}$ = Canister gas temperature for off-normal hot storage (°K)

W74 canister accident pressure for 40 GWd/MTU Big Rock Point fuel is 30.0 psig as presented in Table 4.6-2. Significant margin exists between this calculated accident pressure and the W74 canister accident design pressure of 69.0 psig.

Even if off-normal rod failures (10%) are conservatively assumed under the postulated all vents blocked conditions (728°F bulk helium temperature), the resultant canister internal pressure is still bound by the assumed condition of 100% rod failures at the off-normal hot storage temperature (536°F bulk helium temperature). This can be illustrated by comparing the relative quantities (maximums) of rod gas and canister back-fill gas presented in Table 4.4-5 for Big Rock Point fuel. Assuming 100% rod failures, the maximum total moles of rod gas (fill gas + fission gas) shown in Table 4.4-5 for Big Rock Point fuel is 188.0 moles (34.9 + 153.1). The maximum quantity of canister fill gas shown in Table 4.4-5 is 225.1 moles, for a total canister 413.1 moles. Assuming 10% rod failures, the maximum total quantity a gas in the canister would be 243.9 moles (18.8 + 225.1). The reduction in the number of moles would result in a proportional 59.0% reduction in canister pressure (243.9 moles / 413.1 moles), while the increased absolute accident temperature would result in only a 19.3% proportional pressure increase (1188°R / 996°R). The net effect is a pressure which is 70% of the accident pressure with 100% rod failures under off-normal hot storage conditions.

4.6.1.5 Maximum Thermal Stresses

W74 canister maximum thermal stresses within the storage cask during accident conditions are addressed in Chapter 3 of this FSAR.

4.6.1.6 Evaluation of Canister Performance for Accident Conditions

4.6.1.6.1 All Vents Blocked

A transient analysis of the all vents blocked accident case demonstrates that the short-term allowable material temperatures for the W74 canister and the W150 storage cask are not exceeded for the enveloping canister thermal rating for any site within the contiguous United States, provided the all vents blocked conditions do not exist for longer than a 58 hour period. Therefore, the W74 canister in the FuelSolutions™ W150 Storage Cask provide adequate

protection of the fuel cladding and canister components during a credible blocked vent event for the storage cask. The operational *technical specification* contained in Section 12.3 of the FuelSolutions™ Storage System FSAR provides for daily monitoring and corrective actions to mitigate any vent blockage conditions.

4.6.1.6.2 Fire Accident

A transient analysis of the fire accident for the W74 canister in the storage cask demonstrates that the W74 canister short-term allowable material temperatures are not exceeded for a fire accident consistent with the requirements of 10CFR71.73(c)(4).[3] Therefore, the W74 canister and storage cask are suitable for the dry storage of fuel with thermal ratings which are bounded by the W74 canister thermal rating summarized in Table 4.1-4.

Table 4.6-1 - W74 Canister System Temperature for All Vents Blocked[1]

Component	Case 11 All Vents Blocked, Initial/Peak[2]	Material Allowable Temperature[5]
Peak Fuel Rod Cladding	389.5°C / 506.3°C	570°C
Guide Tube	697°F / 919°F	1000°F
Spacer Plates:		
Stainless Steel	484°F / 724°F	1000°F
Carbon Steel	679°F / 903°F	1000°F
Engagement Plate	423°F / 665°F	1000°F
Support Tube	562°F / 804°F	1000°F
Helium Bulk	491°F / 728°F	n/a
Canister Shell	422°F / 685°F	1000°F
Max. Concrete	153°F / 350°F	350°F
Liner Thermocouple[3]	139°F / 340°F	n/a
Reference Results From Table 4.4-7 and 4.6-2 of the FuelSolutions™ Storage System FSAR		
Canister Shell[4]	*423 °F /644 °F*	
Max. Concrete[4]	*169 °F/349 °F*	
Liner Thermocouple[3,4]	*150 °F/334 °F*	

Notes:

(1) Except as noted, temperatures are based on a heat load of 26.4 kW.

(2) Peak temperature taken from the 58 hour point in the transient analysis.

(3) Estimated thermocouple reading for analyzed condition.

(4) Temperatures based on heat load of 28 kW.

(5) Canister allowable temperatures are from Table 4.3-1 of this FSAR. Storage cask material allowable temperatures are from Table 4.3-1 of the FuelSolutions™ Storage System FSAR.

Table 4.6-2 - W74 Canister Accident Pressures

Parameter	W74 Canister Pressure (psig)
Accident Pressure	30.0

Note:

(1) Pressure presented for the limiting fuel assembly type within each class which results in the highest canister accident pressure. Pressure based on 100% postulated rod failures.

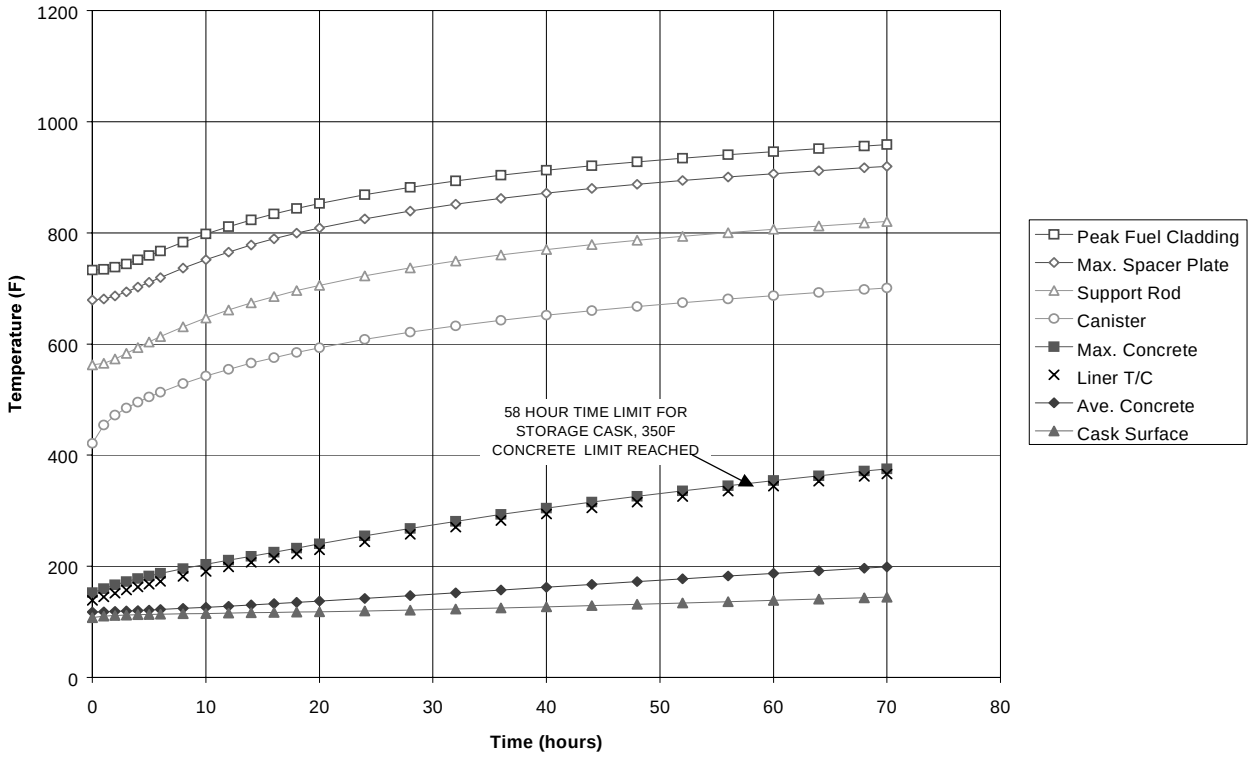

Figure 4.6-1 - Storage Cask all Vents Blocked Transient with W74 Canister

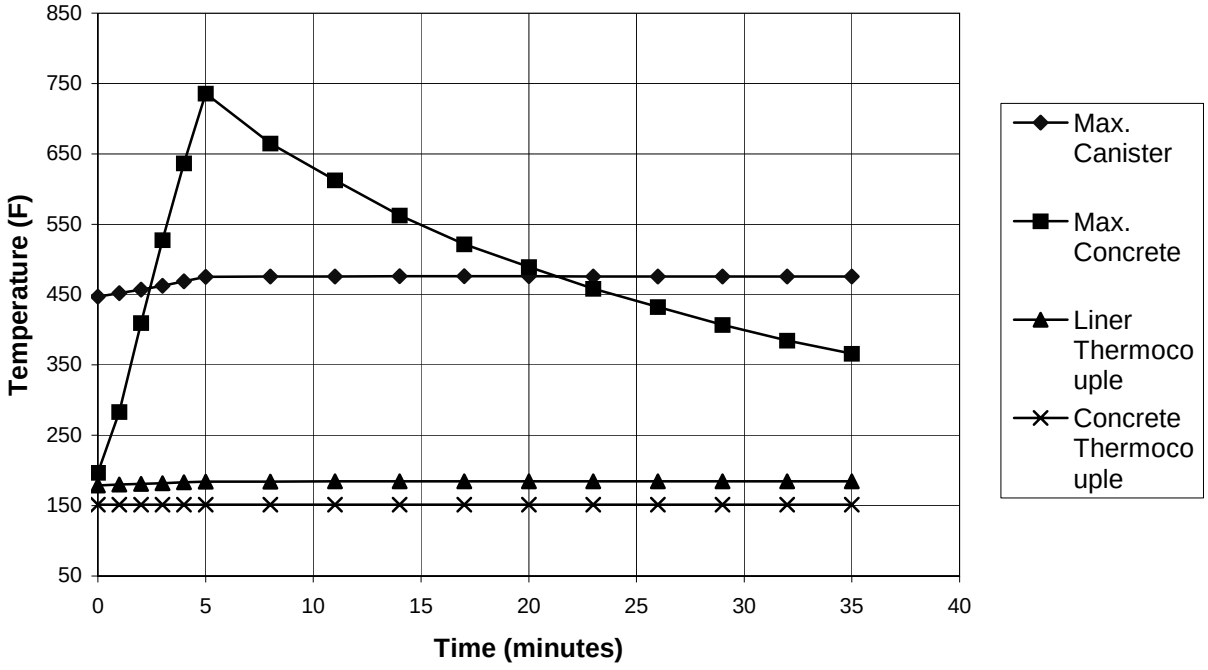

Figure 4.6-2 - Storage Cask and Canister Response To 5 Minute Engulfing Fire

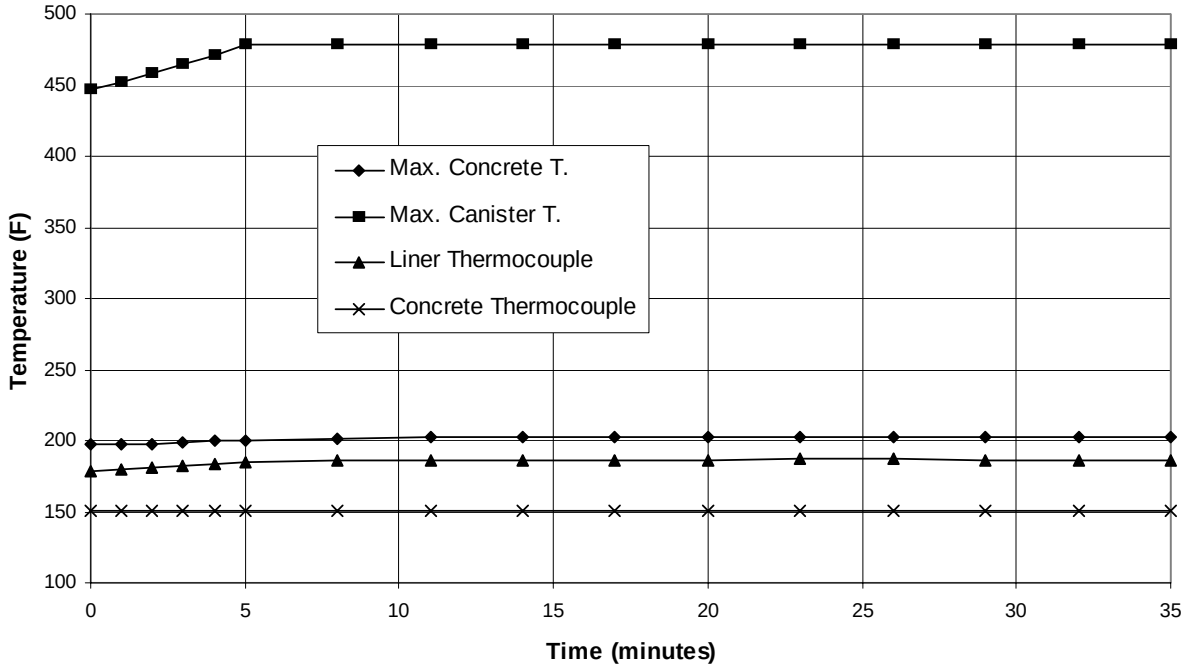

Figure 4.6-3 - Storage Cask and Canister Response To 5 Minute Inlet Vent Fire

4.6.2 W74 Canister within Transfer Cask

The two transfer cask postulated accident conditions considered are a postulated loss of neutron shield (case 18) and a fire accident (case 20). The applicable transfer cask operating conditions for these cases are summarized in Table 4.1-3 and Table 4.1-5. All accident condition transfer cask thermal analyses are conservatively based on a 26.4 kW canister heat load, the maximum heat load that can be accommodated by the W74 canister structure. The analyses are bounding (conservative) for the actual W74 canister heat load rating of 24.8 kW (which is based on the temperature limits of the canister payload).

4.6.2.1 Thermal Model

4.6.2.1.1 Drained Liquid Neutron Shield

The combined W74 canister and transfer cask thermal model used to analyze the drained liquid neutron shield condition is the same as that described in Section 4.4.2 with the exception that the conduction and convection across a water filled annulus is replace with conductors representing convection and radiation across an air filled annulus. All other aspects of the thermal model remain the same. The analysis is conducted using a steady-state evaluation.

4.6.2.1.2 Fire Accident

The canister thermal model used in the evaluation of the accident conditions within the transfer cask is similar to the model presented for normal conditions (see Section 4.4.2.1). Modifications to the transfer cask model for the fire analysis are discussed in Section 4.6.2 of the FuelSolutions™ Storage System FSAR. The fire accident scenario is assumed to start with the cask and canister system at the case 15 steady-state conditions (i.e., normal hot transfer). A maximum flame temperature of 1475°F, with an effective emissivity of 0.9, is assumed for the fire. The fire duration simulated is 5 minutes.

4.6.2.2 Maximum Temperatures

The peak temperatures noted in the W74 canister and transfer cask for the postulated loss of neutron shield accident are presented in Table 4.6-3. The temperatures for all components are within their respective allowable temperatures. The results from the transfer cask design basis analysis (see Section 4.6.2 of the FuelSolutions™ Storage System FSAR) are presented for comparison purposes and are seen as encompassing those for the W74 canister in the transfer cask.

Peak canister and cask temperatures for the postulated 5-minute transfer cask fire accident are presented in Table 4.6-4. Figure 4.6-4 and Figure 4.6-5 illustrate the temperature response of the canister and the transfer cask to the postulated 5 minute fire. With the exception of the neutron shield shell, all canister and cask components remain below the short-term allowable temperatures for the component. The large thermal mass of the canister assembly and cask, plus the thermal radiation shielding provided by the neutron shield shell, combined to largely mitigate the heat pulse from the fire. As a result, with the exception of the cask components at the edges of the cask, little temperature impact is seen from the presence of the fire. In fact, the bulk of the

temperature increase exhibited between the initiation of the fire and the post-fire steady-state conditions is due to the assumption that the liquid neutron shield is lost.

Over 200 gallons of combustible fuel are required to create the engulfing fire conditions simulated by the analysis. The duration of the fire is limited to less than 5-minutes by limiting the fuel quantity as indicated in the operating procedures in Section 8.1.10 of the FuelSolutions™ Storage System FSAR.

4.6.2.3 Minimum Temperatures

The minimum temperatures during a fire accident event are bounded by the normal cold and off-normal cold transfer conditions (cases 14 and 16).

4.6.2.4 Maximum Internal Pressures

W74 canister accident internal pressures are presented in Section 4.6.1.4. For determination of the accident canister pressure, 100% rod failures are postulated while conservatively assuming the W74 canister average gas temperature for off-normal hot storage conditions (125°F ambient, Section 4.1.4). Although the W74 canister average gas temperature under the postulated loss of neutron shield accident conditions within the transfer cask exceeds the corresponding gas temperature for off-normal hot storage conditions, failure of 100% of the rods does not need to be postulated concurrently with the other postulated transfer cask accident conditions. Since the short-term allowable cladding temperature presented in Section 4.3.2.4 (570°C) is not exceeded during W74 canister design basis accident conditions within the transfer cask, gross cladding failures do not occur. Similar to the discussion presented in Section 4.6.1.4, the canister accident internal pressure determined under the assumed condition of 100% rod failures at the off-normal hot storage temperature bounds even the conservative assumption of off-normal rod failures (10%) under the loss of neutron shield accident conditions.

As discussed in the FuelSolutions™ Storage System FSAR, the loss of neutron shield accident is caused by a breach of the liquid neutron shield pressure boundary, resulting in atmospheric pressure within the neutron shield.

4.6.2.5 Maximum Thermal Stresses

W74 canister thermal stresses within the transfer cask during accident conditions are addressed in Chapter 3 of this FSAR.

4.6.2.6 Evaluation of Canister Performance for Accident Conditions

4.6.2.6.1 Drained Liquid Neutron Shield

A steady-state analysis of the drained liquid neutron shield case demonstrates that the short-term allowable material temperatures for the W74 canister and the W100 transfer cask are not exceeded for the enveloping canister thermal rating for any site within the contiguous United States.

4.6.2.6.2 Fire Accident

A transient analysis of the fire accident for the W74 canister in the transfer cask demonstrates that the W74 canister short-term allowable material temperatures are not exceeded for a fire accident consistent with the requirements of 10CFR71.73(c)(4).[3] Therefore, the W74 canister and transfer cask are suitable for the transfer of fuel with thermal ratings which are bounded by the W74 canister thermal rating summarized in Table 4.1-4.

Table 4.6-3 - W74 System Temperatures for Postulated Transfer Cask Loss of Neutron Shield Accident[1]

Component	Case 18 Loss of Neutron Shield	Material Allowable[4]
Peak Fuel Rod Cladding	465.3°C	570°C
Guide Tube	844°F	1000°F
Spacer Plates: Stainless Steel Carbon Steel	 802°F 838°F	 1000°F 1000°F
Engagement Plate	651°F	1000°F
Support Tube	806°F	1000°F
Helium Bulk Temp.	718°F	n/a
Canister Shell	680°F	1000°F
Cask Inner Liner	526°F	1000°F
Cask Lead Shield	522°F	620°F
Cask Structural Shell	494°F	1000°F
Liquid Neutron Shield	n/a	n/a
Neutron Shield Pressure	n/a	n/a
Cask Thermocouple[2]	459°F	n/a
Reference Results From Table 4.6-4 of the FuelSolutions™ Storage System FSAR		
Cask Lead Shell[2]	*568°F*	
Cask Thermocouple[2,3]	*514°F*	

Notes:

(1) Except as noted, temperatures are based on a heat load of 26.4 kW.

(2) Estimated thermocouple reading for analyzed condition.

(3) Temperatures based on heat load of 28 kW.

(4) Canister allowable temperatures are from Table 4.3-1 of this FSAR. Transfer cask material allowable temperatures are from Table 4.3-2 of the FuelSolutions™ Storage System FSAR.

Table 4.6-4 - W74 Canister Peak Temperatures During Transfer Cask Fire Accident[1]

Component	Pre-Fire Steady-State	Fire Transient ($0 \leq t \leq 30$ min.)	Post-Fire[2] Cool-Down / Steady-State	Short-Term Limit[4]
Peak Fuel Rod Cladding	406°C	406°C	454°C	570°C
Spacer Plate	710°F	710°F	812°F	1000°F
Canister Shell	556°F	559°F	671°F	1000°F
Cask Inner Shell	338°F	338°F	522°F	1000°F
Cask Lead Shield	334°F	334°F	519°F	620°F
Cask Outer Shell	255°F	273°F	491°F	1000°F
Liquid Neutron Shield Skin	240°F	1116°F[3]	236°F	1000°F

Notes:

(1) Analysis performed for a conservative Q_{max} of 28 kW.

(2) Based on steady-state temperature.

(3) Peak stainless steel temperature at the liquid neutron shield outer shell exceeds the short-term allowable temperature, but remains lower than the stainless steel melting point temperature (2600°F).

(4) Short-term allowable temperatures apply. Canister allowable temperatures are from Table 4.3-1 of this FSAR. Transfer cask material allowable temperatures are from Table 4.3-2 of the FuelSolutions™ Storage System FSAR.

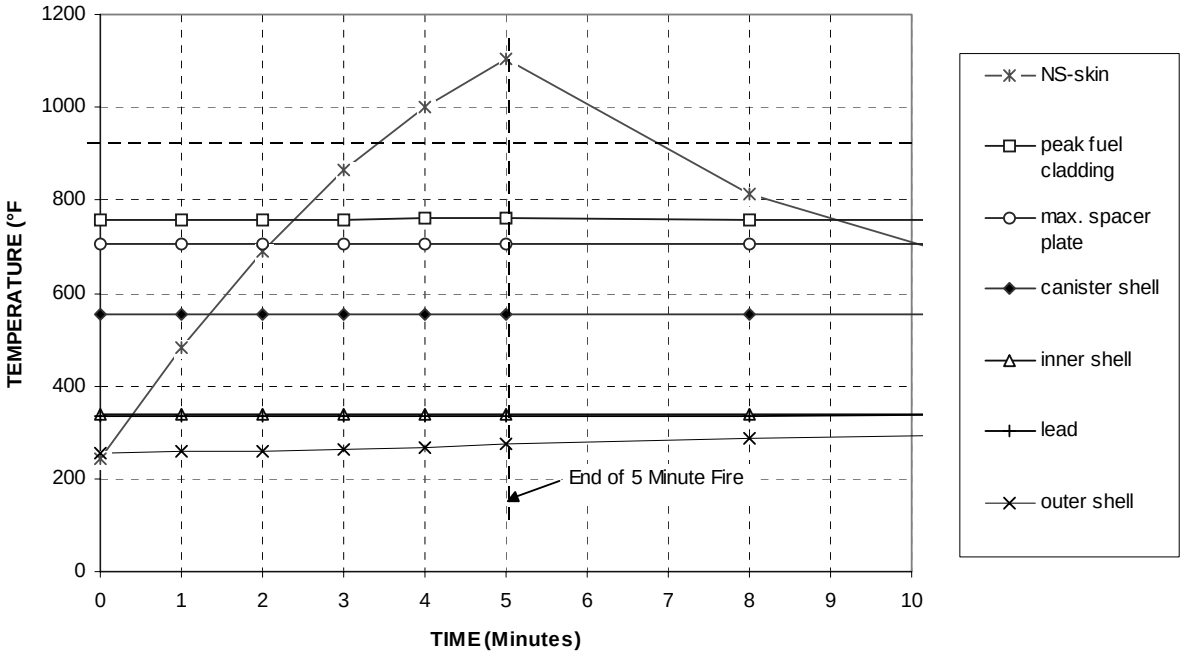

Figure 4.6-4 - Canister and Transfer Cask Fire Accident Temperature Response (0-10 minutes)

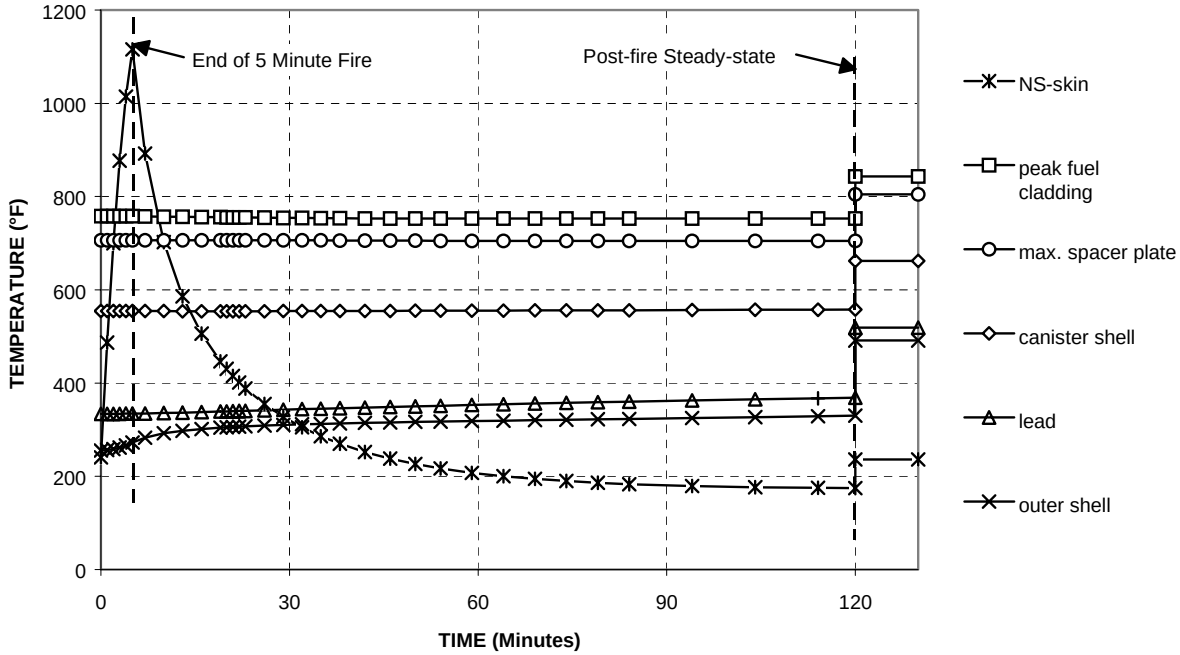

Figure 4.6-5 - Canister and Transfer Cask Fire Accident Temperature Response (0-2 hours)

4.7 Supplemental Data

4.7.1 Canister Internal Convection

Beyond conduction and radiation heat transfer, the principal heat transfer mode within the basket assembly is convection. This is true for both the vertical and the horizontal orientations of the basket assembly. The following paragraphs provide a description of the approach and equations used for the W74 basket assembly.

To account for the natural convection heat transfer interaction within the W74 basket assembly, the internal flow environment is divided into a series of related flow regions and the results from each region superimposed on the global solution to arrive at a unified result. Convection heat transfer coefficients are determined for each flow region based on its particular physical and behavioral characteristics. The analytical algorithms used to determine these coefficients are computed as a function of the local environment (i.e., geometry, temperatures, and pressures) and are incorporated into the SINDA/FLUINT[2] iterative solution. The following paragraphs describe the approach for each orientation.

Horizontal Orientation

The fact that the basket assemblies are keyed within the canister and the transfer and transportation casks ensures that the global orientation of the fuel assemblies remains essentially constant for each transport cycle. As such, the analysis of the fluid flow due to convection within a horizontally oriented basket is approached as an analysis of a series of vertically oriented channels. The general flow pattern is one where the helium blanket gas is transported upward under buoyancy forces through the basket and then downward along the inside circumference of the canister. Superimposed on this predominant flow pattern is a series of sub-flow paths at each of the double open-ended cavities created between the upper and lower edges of adjacent guide tubes.

A representation of the assumed flow pattern is presented in Figure 4.7-1 for the W74 basket assembly. The two main underlying assumptions for this type of buoyancy driven re-circulating flow field are that it is incompressible and that the flow is nominally two-dimensional. Although discontinuities occur at the upper and lower edges of each guide tube, the vertical channels formed between pairs of guide tubes can be analytically treated as smooth wall channels for the purposes of determining the governing convection heat transfer rates. This results since the guide tubes are relatively closely spaced and the estimated flow velocities yield Reynolds numbers on the order of 100. The assumed flow pattern and the smooth wall channel assumption are confirmed by the measured flow velocities from the testing on a similar basket layout conducted by Kawasaki Heavy Industries.[22] The results of this testing is summarized by Figure 4.7-2 and Figure 4.7-3.

[22] Nishimura, M., et al., *Natural Convection Heat Transfer in the Horizontal Dry Storage System for the LWR Spent Fuel Assemblies*, Journal of Nuclear Science and Technology, Vol. 33, No. 11, pp. 821-828, November 1996.

Based on these assumptions, the natural convection in vertical channels with symmetric and uniform wall heat flux is estimated using equations 3.65 and 3.66 of Bar-Cohen[23] where the characteristic length is the height of the channel. These equations are applicable over the range of $3 \cdot 10^{-1} < Ra^* < 3 \cdot 10^4$ and are as follows:

$$Nu_{\frac{L}{2}} = \frac{h_c L}{k} = \left\{ \left(\frac{12}{Ra^*} \right) + \frac{17}{70} \right\}^{-1} \qquad 3 \cdot 10^{-1} < Ra^* < 3 \cdot 10^4$$

for the mean value on each wall and

$$Nu_L = \frac{h_c L}{k} = \left\{ \left(\frac{48}{Ra^*} \right) + \frac{17}{70} \right\}^{-1} \qquad 3 \cdot 10^{-1} < Ra^* < 3 \cdot 10^4$$

for the exit region value on each wall. Ra* is defined as:

$$Ra^* = Gr \cdot Pr = \frac{g \beta q b^5 \mu C_P}{L \nu^2 \kappa^2}$$

where:

g	=	Gravitational acceleration
β	=	Coefficient of thermal expansion
q	=	Heat flux density
b	=	Channel gap width
μ	=	Dynamic viscosity
C_P	=	Specific heat
L	=	Height of the channel
ν	=	Kinematic viscosity
κ	=	Thermal conductance

The wall heat flux, q, used in the equations is computed using the surface area of the guide tube over the active length of the fuel and then adjusted at each specific basket location to account for the placement of the fuel within the basket and the fuel peaking factor along the length of the fuel assembly. The computed heat flux is further adjusted to account for the fact that any heat dissipated out the horizontal surfaces of the guide tubes ultimately ends up in the vertical channel and is available to feed the buoyancy driven flow.

[23] Bar-Cohen, A. and Kraus, A. D., *Advances In Thermal Modeling of Electronic Components and Systems*, Volume 1, Hemisphere Publishing Corporation, 1988.

Radiation and conduction from the guide tubes into the spacer plates results in the spacer plate temperatures being significantly above the local gas temperature. As such, the characteristic heat transfer coefficients determined for the guide tube walls are also applied to the adjacent spacer plate surfaces. Although this assumption of two-dimensional flow behavior is not necessarily conservative, it is offset by the assumption that the flow within the vertical channels is fully developed and by the fact that the channel flow correlation includes the flow that is within an enclosure. In reality, based on a Reynolds analogy, the approximate flow development length within the largest vertical channel for the W74 basket assembly is approximately half of the channel height. This means that higher than predicted convection heat transfer rates actually exist within the channels.

The convection heat transfer rates from the upper and lower surfaces of each guide tube pair is addressed using a correlation for the average Nusselt number within horizontal cavities. The correlation is developed using the findings presented in several papers pertaining to buoyant driven flow from open-ended cavities.

The correlation includes the effects of the cavity configuration, the Rayleigh number (Ra), and aspect ratio (A), defined as:

$$A = \frac{H}{L},$$

where H is the separation distance between the guide tubes and L is one-half the width of the guide tubes.

The cavity Rayleigh number is defined as:

$$Ra = Gr \cdot Pr,$$

where:

$$Gr = \frac{g\beta(T_W - T_\infty)H^3}{\nu^2},$$

and

$$Pr = \frac{\mu C_p}{\kappa} = \frac{\nu}{\alpha}.$$

The cavity configuration depicted in Figure 4.7-4 is the most similar to the horizontally oriented double open-ended cavities occurring in the W74 basket geometry. The correlation selected for the double open-ended cavities within the W74 basket assembly is:

$$\overline{Nu_c} = \frac{h_c L}{k} = 0.110 \cdot ((A)^{\frac{3}{2}} \cdot Ra)^{0.345} \qquad 60 \le Ra \le 2(10)^3$$

where the characteristic length is the one-half of the width of the guide tube. This correlation is evaluated within the SINDA/FLUINT thermal model based on the local thermal properties and cavity aspect ratio for each horizontal cavity formed by the upper and lower surfaces of the guide tubes. The resulting Nusselt number is used to compute a convective heat transfer rate from the horizontal surfaces of the guide tubes and the local gas temperature within the vertical channels.

The convection heat transfer from the guide tube and spacer plate surfaces which lie outside of the basket interior are computed using the isolated surface correlations for flat plates in the horizontal and vertical orientation. The same correlations are used for the canister shell surfaces.

Vertical Orientation

Convection heat transfer within a vertically oriented canister is assumed to be symmetrical about a 1/8 segment of the basket. However, since the basic thermal model encompasses a 90° segment, it is used for the computation of the temperature distribution in the vertical orientation. Figure 4.7-6 illustrates the layout of the gas nodes used in the SINDA/FLUINT model.

The principal flow pattern between each pair of spacer plates is as depicted in Figure 4.7-7. The flow pattern consists of a series of overlapping convection loops starting at the canister wall and extending into the center of the basket. As the convection flow passes along the topside of the lower spacer plate the flow bifurcates. A portion of the flow separates and is carried upward due to the convection flow at each guide tube surface. The balance of the flow continues inward toward the center of the basket. The outward flow pattern consists of a flow along the underside of the upper spacer plate, with the flow at each pair of guide tubes joining in and adding strength to the outward bound flow. Upon reaching the canister wall, the flow is cooled, drop to the lower plate and begin the loop over again.

By idealizing the channels formed between the guide tubes as horizontal channels with heated and cooled ends and perfecting conducting horizontal surfaces, an estimate can be made of the strength of the convection flow between the inside surface of the canister (i.e., the cold wall) and the interior of the basket (i.e., the hot wall). The fact that guide tube surfaces between the center of the basket and the canister wall are not adiabatic, but actively participate in adding heat energy to the flow acts to offset any negative impact due to the proximity of the side walls (i.e., the guide tubes) on the convection flow.

It should be noted that axial convective heat transfer in the region within the guide tubes is conservatively ignored. The only mechanisms for heat transfer within this fuel region are conduction and radiation (refer to Section 4.2.2). This is particularly conservative for the vertical orientation, wherein the “chimney effect” would produce additional convective cooling in the hottest active fuel regions.

The spacing between spacer plates is 6 inches or less, while the inner radius of the canister is 32.375 inches. These dimensions lead to enclosure aspect ratios of less than 0.2. Equations 18 and 20 from Churchill[24] recommend the Nusselt number be computed via the following:

[24]Churchill, S. W., *Free Convection in Layers and Enclosures*, Heat Exchanger Design Handbook, Section 2.5.8, Hemisphere, Washington, 1983.

$$Nu_d = 1 + \frac{(Ra_h \alpha)^2}{362{,}880}$$, Eqn. 18 for the laminar asymptotic region

$$Nu_d = \alpha^{-1}\left[\frac{Ra_h f(Pr)}{10.66}\right]^{0.2}$$, Eqn. 20 for the laminar boundary-layer regime

where:

$Nu_d = h_c\ d/k$

α = aspect ratio, height of cavity/depth of cavity, h/d < 0.6

Ra_h = Rayleigh number based on cavity height, h < 10^8

$f(Pr)$ = function of Prandtl number, = $\left[1+\left(\frac{0.5}{Pr}\right)^{\frac{9}{16}}\right]^{\frac{-16}{9}}$

Equation 20 from Churchill demonstrates the fact that the heat transfer coefficient in the channel is increasingly independent of the depth of the channel (d) as the Rayleigh number increases into the boundary layer regime (i.e., Ra > 10^5).

In practice, the distance between the spacer plates is taken as “h” and the distance between each pair of guide tubes and the canister shell wall is taken as “d”. In this manner, the strength of each convection loop shown in Figure 4.7-7 is estimated via the following steps:

1. Assume “d” equals the distance from the gas node to the canister shell (i.e., one-half of the ID of the canister shell for the inner gas node),

2. Evaluate Equations 18 and 20 from Churchill and select the minimum of the two values,

3. The estimated Nusselt number is converted to an effective thermal conductance between the gas node at inner guide tube pair and the gas node at the next guide tube pair via the equation: $G = (h\ w\ Nu_d\ k_{helium}/d) \cdot d/L$, where h = spacing between spacer plates, w = gap between the guide tube pair, d = distance to the canister shell wall, and L = distance to next gas node.

4. Repeat steps 1 to 3 for the next gas node and add the computed effective thermal conductance for the previous gas node pair. In this manner, the strength of the convection loop will increase as thermal energy from each guide tube pair is added.

5. Repeat the entire sequence for the other channels formed by the space between guide tubes.

The convection heat transfer from the guide tube and spacer plate surfaces which lie outside of the basket interior are computed using the isolated surface correlations for flat plates in the horizontal and vertical orientation. The same correlations are used for the canister shell surfaces.

4.7.2 Other Modes of Heat Transfer

Natural convection from a discrete vertical surface is computed using Equations 6-39 to 6-42 of Rohsenow,[25] where the characteristic length is the height of the surface. These equations are applicable over the range $1 < Ra < 10^{12}$ as follows:

$$Nu^T = \overline{C}_L Ra^{1/4}$$

$$\overline{C}_L = 0.75\left[\frac{0.503}{\left(1+\left(0.492/Pr\right)^{9/16}\right)^{4/9}}\right]$$

$$Nu_L = \frac{2.8}{\ln\left(1+2.8/Nu^T\right)}$$

$$Nu_t = C_t^V Ra^{1/3}$$

$$C_t^V = \frac{0.13\,Pr^{0.22}}{\left(1+0.61\,Pr^{0.81}\right)^{0.42}}$$

$$Nu = \frac{h_c L}{k} = \left[(Nu_L)^6 + (Nu_t)^6\right]^{1/6}$$

Natural convection from horizontal surfaces facing upwards is computed from Equations 7-21 and 7-22 of Kreith,[26] where the characteristic dimension (L) is typically the width of the surface, or for non-square shapes, the characteristic length may be calculated from L = 0.9 diameter for disk shapes and L = mean of the length and the width for rectangles. These equations are applicable over the range $10^5 < Ra < 3x10^{10}$ as follows:

$$Nu = \frac{h_c L}{k} = 0.54 Ra^{1/3} \qquad 10^5 < Ra < 2\cdot 10^7$$

$$Nu = \frac{h_c L}{k} = 0.14 Ra^{1/3} \qquad 2\cdot 10^7 < Ra < 3\cdot 10^{10}$$

[25] Rohsenow, Harnett, and Ganic, *Handbook of Heat Transfer Fundamentals*, 2nd Edition, McGraw-Hill, Inc., 1989.

[26] Kreith, F., *Principles of Heat Transfer*, 3rd Edition, Intext Press, Inc., 1973.

Natural convection from horizontal surfaces facing downwards is computed from Equation 7-23a of Kreith[26]. The characteristic length is the length of the surface. This equation is applicable over the range $3x10^5 < Ra < 3x10^{10}$ as follows:

$$Nu = \frac{h_c L}{k} = 0.27 Ra^{1/4} \qquad 3 \cdot 10^5 < Ra < 3 \cdot 10^{10}$$

Natural convection from cylindrical surfaces is computed from Equation 3-43 of Chapter 1 from Guyer.[27] The characteristic length is the diameter of the cylinder. This equation is applicable over the range $10^{-5} < Ra < 10^{12}$ and is as follows:

$$Nu = \frac{h_c d}{k} = \left\{ 0.60 + \frac{0.387 Ra^{1/6}}{\left[1 + \left(0.559/Pr\right)^{9/16}\right]^{8/27}} \right\}^2 \qquad 10^{-5} < Ra < 10^{12}$$

The modes of heat transfer discussed in detail within this section are used within the W74 canister thermal analysis discussed in Section 4.4, 4.1, and 4.6 for normal, off-normal, and postulated accident conditions, respectively.

4.7.3 Computer Code Descriptions

4.7.3.1 SINDA/FLUINT Computer Code

The analytical thermal models for the W74 Canister, the W150 Storage and W100 Transfer Casks are developed using the SINDA/FLUINT[2] heat transfer code. This generalized, finite difference, lumped parameter code was developed under the sponsorship of the NASA Johnson Space Center and has been evaluated and validated for simulating the thermal response of transportation packages.[28] The program is available as either a public domain code from the government software libraries, or in one of several forms from private vendors. In addition, the code has been used for the analysis and subsequent regulatory licensing of several other transportation packages for nuclear material, including the RTG transportation package[29] and the TRUPACT-II transportation package.[30]

The SINDA/FLUINT code[2] provides the capability to simulate steady-state and transient temperatures using temperature dependent material properties and heat transfer via conduction,

---

[27] Guyer, E. C., *Handbook of Applied Thermal Design*, McGraw-Hill, Inc., 1989.

[28] Glass, R. E., et. al., *Standard Thermal Problem Set for the Evaluation of Heat Transfer Codes Used in the Assessment of Transportation Packages*, Sandia Report SAND88-0380, August 1988.

[29] DOE Docket No. 94-6-9904, *Radioisotope Thermoelectric Generator Transportation System Safety Analysis Report for Packaging*, WHC-SD-RTG-SARP-001, prepared for the U.S. Department of Energy Office of Nuclear Energy under Contract No. DE-AC06-87RL10930 by Westinghouse Hanford Company, Richland, WA.

[30] NRC Certificate of Compliance Number 9218 for TRUPACT-II Package, application docket number 71-9218 prepared for the U.S. Nuclear Regulatory Commission by Nuclear Packaging Inc., Federal Way, WA, March 3, 1989.

convection, and radiation. Heat transfer solutions for one, two, or three-dimensional problems may be programmed. Complex algorithms may be programmed into the solution process for the purposes of computing the various heat transfer coefficients as a function of geometry, fluid, and temperatures or, for example, to estimate the effects of buoyancy driven heat transfer. Standard algorithms are used for computing the convection heat transfer from common surfaces (i.e., vertical and horizontal plates, cylinders, etc.) as a function of the surface geometry, the fluid properties, and the temperatures.

A major feature of the SINDA/FLUINT code[2] used for this modeling is the ability to use thermal submodels to represent common geometry sections of the canister shell, guide tubes, spacer plates, etc. A thermal submodel is defined as a thermal model which contains the necessary information to be independently solved for the temperatures of the components which it simulates, but which depends on one or more other thermal submodels for some or all of its boundary conditions. Thermal interconnections are provided to allow the various thermal submodels to "communicate" with each other. This thermal modeling approach simplifies the modeling and verification process by minimizing the amount of original coding required to provide a complete thermal representation of the system.

4.7.3.2 RadCAD Computer Code

The radiation exchange thermal conductors for the W74 Canister are developed using the RadCAD® computer code.[15] RadCAD, developed under the sponsorship of the NASA Johnson Space Center, is a software system designed to calculate radiation exchange factors from complex geometries for use with the SINDA/FLUINT thermal analyzer. It uses the AutoCAD™ computer program as the 3-D visualization and mesh generation engine. Options are available for specifying the radiation properties of each surface, specifying whether a surface is active or inactive, etc.

4.7.4 Big Rock Point Mixed-Oxide (MOX) Fuel

The thermal evaluations provided in this chapter address UO_2 9x9 and 11x11 BRP fuel assemblies. The analysis for UO_2 fuel bounds the condition of a FuelSolutions™ W74 canister loaded with any number of MOX fuel assemblies. The BRP MOX fuel assemblies are similar to the UO_2 assemblies with respect to all assembly physical characteristics (including fuel mass, fuel density, fuel rod cladding dimensions, cladding material, rod fill pressures, and active fuel height) except initial fuel material composition. In addition, as discussed in Section 4.7.4.4, the design operating parameters of MOX fuel is equal to or bounded by those for conventional UO_2 fuel assemblies. All existing BRP MOX fuel has a burnup level under 35 GWd/MTIHM and an assembly cooling time of at least 15 years.

4.7.4.1 Heat Generation of BRP MOX Fuel

Assembly heat generation levels are explicitly calculated for BRP MOX fuel using the ORIGEN 2.1 point-depletion code (see Section 5.5.2 of the FuelSolutions™ Storage System FSAR). Based on this analysis, the maximum heat generation level for any existing BRP MOX fuel assembly is less than 150 watts/assembly. This is 61% less than the design basis maximum assembly heat generation level of 387.5 watts/assembly that forms the basis of the canister thermal

rating given in Table 4.1-4, and the minimum required assembly cooling times shown in Table 5.2-1 of this FSAR.

4.7.4.2 Axial Heat Flux Profile of BRP MOX Fuel

The bounding axial heat flux distribution discussed in Section 4.1.3 of this FSAR is applicable to both MOX and UO_2 BRP fuel assemblies. The physical dimensions (such as active fuel height) of the MOX assemblies are the same as those of the corresponding UO_2 assemblies. Furthermore, the MOX and UO_2 fueled BRP assemblies are irradiated in the same reactor core, often in close proximity to each other, and they have similar linear heat ratings, maximum clad operating temperatures, etc. The BRP MOX fuel assemblies also contain a large number of UO_2 fuel rods around their periphery. For these reasons, the axial heat flux profile is expected to be very similar for BRP UO_2 and MOX assemblies.

4.7.4.3 Effective Thermal Conductivity of BRP MOX Fuel

As discussed in Section 4.2.2 of this FSAR, the intact UO_2 fuel assembly is modeled as a homogenous mass that has an effective radial and axial conductivity. Given that the cladding dimensions (i.e., diameter and thickness), the number of fuel rods, and the fuel rod pitch are essentially identical for UO_2 and MOX fuel assemblies, the only significant difference between the UO_2 and MOX assembly types is the fuel material within the fuel rods. However, the fuel material does not contribute significantly to the overall axial or radial assembly conductivity[31] because the fuel material conductivity is lower than that of the fuel rod cladding. Additionally, there are potential gaps between the individual fuel pellets and between the fuel pellets and the cladding. With respect to the effective radial assembly conductivity, the majority of the thermal resistance occurs between the fuel rods, as opposed to within or across the fuel rods.

The temperature difference across the individual fuel rods is very small, even if only conduction through the cladding is considered. Therefore, the fuel material's thermal properties are conservatively neglected in the methodology used to compute the fuel assembly's axial and effective radial thermal conductivity (see Section 4.2.2). As such, the calculated axial and radial conductivities for UO_2 and MOX BRP fuel are the same.

4.7.4.4 Allowable Cladding Temperature for BRP MOX Fuel

Based on proprietary data in Jersey Nuclear and Exxon Nuclear design reports, the design operating parameters of MOX fuel assemblies used at Big Rock Point are equal to or bounded by those for conventional UO_2 fuel assemblies. As such, the bounding operational temperature (e.g., in-reactor) experience of the two fuel rod configurations are similar. Further, since the 35 GWd/MTU burnup value of the BRP MOX fuel is below the design basis 40 GWd/MTU burnup for the conventional BRP fuel, the MOX fuel internal rod pressures and operating temperature effects will be bounded by those for the conventional BRP fuel.

The peak BRP fuel rod pressure given in Table 4.4-5 (1075 psig) is based on a generated fission gas quantity of about 8 moles per fuel assembly. The data presented in Table 4.4-5 assume a 30% release fraction; therefore, the total fission gas quantity available for release is about

[31] Manteufel, R. D. and Todreas, N. E., *Effective Thermal Conductivity and Edge Conductance Model for a Spent-Fuel Assembly*, Nuclear Technology, Vol. 105, March 1994.

2.4 moles per assembly. This molar fission gas quantity calculation (using the methodologies given in Section 4.4.1.7) is based on a UO_2 fueled BRP assembly with a design basis burnup level of 40 GWd/MTU and a cooling time of 5 years.

The generated fission gas inventory, which is calculated using ORIGEN 2.1 (see Section 5.5.2), is less than 6 moles per assembly for all BRP MOX fuel due to its lower burnup value (under 35 GWd/MTU versus a design basis UO_2 fuel burnup of 40 GWd/MTU). Assuming a 30% release fraction, the quantity of fission gas available for release would be less than 1.8 moles per assembly. Therefore, the MOX fission gas available for release is bounded. It is also noted that the longer assembly cooling time (a minimum of 15 years versus a design basis UO_2 assembly cooling time of 5 years) yields lower rod temperatures and, thus, rod pressures.

Given that other parameters such as cladding dimensions, gas plenum volume, and fill gas pressure are similar for the MOX and UO_2 assemblies, and given the lower MOX fuel internal rod pressure, the cladding stress levels determined for design basis BRP UO_2 fuel at any given temperature are bounding for BRP MOX fuel.

Because the cladding stress levels are lower for MOX fuel, the allowable cladding temperature based on the creep methodology given in Table 4.3-1 of this FSAR, is bounding for all BRP MOX fuel. For cooling time based methodologies for determining the allowable cladding temperature, the ORIGEN 2.1 calculations show that the maximum heat generation for the MOX fuel is bounded at all cooling time values by the design basis heat generation levels shown in Figure 4.3-2. This is partly due to the fact that the maximum burnup level for the MOX fuel is under 35 GWd/MTU, as compared to the design basis fuel burnup level of 40 GWd/MTU.

4.7.4.5 Canister Internal Pressure for BRP MOX Fuel

Since the BRP MOX fuel assemblies have lower fission gas quantities and, therefore, lower internal rod pressures than the design basis BRP assemblies, the canister internal pressures calculated in Sections 4.4, 4.1, and 4.6 of this FSAR are bounding for a canister containing any amount of MOX fuel.

4.7.4.6 Thermal Summary for BRP MOX Fuel

BRP MOX fuel assemblies have an axial heat generation profile, an effective assembly thermal conductivity (axial and radial), and an assembly heat generation decay curve that are similar to those of BRP design basis (UO_2 fueled) assemblies. Furthermore, the BRP MOX fuel assemblies have lower internal rod pressures, 61% lower heat generation levels due to lower burnup level, and much longer cooling times than the BRP design basis assemblies. For these reasons, BRP MOX fuel assemblies will produce lower peak fuel cladding temperatures (when loaded into the canister), while having fuel rod cladding temperature limits that are at least as high as those of BRP design basis fuel assemblies.

As such, the thermal evaluations for normal conditions of storage presented in Section 4.4 of this FSAR are valid and bounding for canisters containing BRP MOX fuel assemblies. Similarly, the lower canister heat loads and initial temperatures that occur with canisters containing MOX fuel assemblies means that the thermal evaluations for off-normal and accident conditions of storage, as presented in Sections 4.1 and 4.6, are bounding for canisters containing MOX fuel assemblies.

Therefore, it is concluded that all existing BRP MOX fuel assemblies are thermally qualified for loading into the FuelSolutions™ W74 canister and no further thermal or assembly heat generation calculations need to be performed.

4.7.5 Big Rock Point Partial Fuel Assemblies

Partial assemblies have fuel rods missing from the design basis assembly array. The thermal evaluations previously provided in this chapter assume intact fuel assemblies. However, the analysis bounds the assumption of a canister loaded with any number of partial fuel assemblies.

4.7.5.1 Required Cooling Time for BRP Partial Fuel Assemblies

Table 5.2-1 in this FSAR specifies the required cooling time for BRP assemblies as a function of assembly burnup and initial enrichment. The cooling times shown in Table 5.2-1 apply for both intact and partial BRP assemblies.

For a given assembly burnup, initial enrichment, and cooling time, a lower number of fuel rods results in a lower assembly fuel loading, and therefore a lower level of assembly heat generation. The required cooling times shown in Table 5.2-1 are based on a heat load of no more than 24.8 kW for a FuelSolutions™ W74 canister completely loaded with intact BRP assemblies. For a canister loaded with one or more partial BRP assemblies, the required cooling times given in Table 5.2-1 will always yield a canister heat load lower than the allowable value of 24.8 kW.

4.7.5.2 Effective Thermal Conductivity of BRP Partial Fuel Assemblies

The effective thermal conductivities for BRP partial assemblies are similar to and bounded by those of intact BRP fuel assemblies. In fact, missing fuel rods will increase the effective radiative conductivity of the assembly due to higher values of radiation heat exchange within the assembly.

Radiative heat transfer between fuel rods is a primary mode of heat transfer across the assembly fuel rod array.[31] Each row of rods effectively forms a radiation barrier; that is, it adds to the overall thermal resistance of the assembly. For a given rate of heat flow across the assembly, there is a given temperature drop (required to move the heat via radiation and conduction) between each row of fuel rods. The lower the number of “jumps” the heat has to make while crossing the assembly, the higher the effective assembly thermal conductivity. Thus, the removal of fuel rods allows heat transfer via radiation to pass directly through those fuel rod locations to the rods on the other side. This reduction in the need for absorption and re-radiation will enhance the overall radiative heat transfer across the assembly.

It is also true that removing rods opens up larger void spaces between rods that will allow for greater convective heat transfer across the assembly. While the conductivity within an individual fuel rod is greater than the conductivity of the helium that would occupy that location if the rod were removed, the enhanced radiative and convective heat transfer that results from the removal of a fuel rod offsets the increased local value of thermal conductivity due to the rod’s presence.

For these reasons, the removal of fuel rods will enhance the effective conductivity of a fuel assembly, as well as reduce the assembly heat generation level.

4.7.5.3 Thermal Summary for BRP Partial Fuel Assemblies

For the above reasons, it is concluded that BRP intact assemblies bound partial assemblies with respect to thermal considerations. Therefore, the required cooling times given in Table 5.2-1 of this FSAR apply for both intact and partial BRP fuel assemblies. The thermal evaluations for normal, off-normal, and accident conditions of storage respectively presented in Sections 4.4, 4.1, and 4.6, of this FSAR are valid and bounding for canisters containing partial fuel assemblies.

4.7.6 Big Rock Point Damaged Fuel

The thermal evaluations provided in this chapter assume intact fuel assemblies. However, the analysis bounds the assumption of a canister loaded with up to eight damaged fuel assemblies. Damaged includes fuel rod damage in excess of hairline cracks or pinhole leaks. Fuel assemblies with damaged grid spacers (defined as damaged to a degree where fuel rod structural integrity cannot be assured, or where grid spacers have shifted vertically from their design position) will also be stored in damaged fuel cans. The relatively minor nature of the fuel assembly damage contained within this definition supports the basic assumption that the fuel assemblies to be placed in the damaged fuel cans have the basic geometric configuration of an undamaged fuel assembly and are expected to retain this geometry throughout normal and off-normal storage and handling events.

The evaluation for damaged fuel assemblies includes an assessment of the thermal effects imposed by the presence of the damaged fuel can. The effect of the damaged fuel can on the overall (smeared) heat transfer coefficient of the damaged fuel assemblies is deemed negligible. Because the damaged fuel has the same design heat generation rate as intact fuel, the steady-state effect would be a slight increase in the damaged fuel cladding temperatures, and would not result in a change in the spacer plate temperature distribution (see Section 4.7.6.5).

Since it is not possible to definitively know the full extent of damage to each fuel assembly, the evaluation for damaged fuel also includes an assessment of the predicted temperatures within the damaged fuel can and within the W74 canister in response to a potential reconfigured fuel assembly within the damaged fuel can(s).

4.7.6.1 Heat Generation of BRP Damaged Fuel

Assembly heat generation levels are calculated for BRP damaged UO_2 and damaged MOX fuel assemblies using the ORIGEN 2.1 point-depletion code (see Section 5.5.2 of this FSAR). The maximum heat generation level permitted for any BRP damaged fuel assembly to be loaded into the FuelSolutions™ W74 canister is equal to the design basis maximum assembly heat generation level of 387.5 watts/assembly. Per Section 4.7.4.1, damaged MOX fuel assemblies have heat loads that are 61% less than those of the design basis assembly. The design basis heat generation rate forms the basis of the canister thermal rating given in Table 4.1-4 and the minimum required assembly cooling times shown in Table 5.2-1 of this FSAR.

4.7.6.2 Axial Heat Flux Profile of BRP Damaged Fuel

The bounding axial heat flux distribution discussed in Section 4.1.3 is applicable for damaged and intact UO_2 and MOX BRP fuel assemblies. The physical dimensions (such as active fuel height) of the damaged fuel assemblies are the same as those of the corresponding intact

assemblies. The damaged fuel assemblies are also irradiated in the same reactor core as the intact fuel assemblies. Therefore, for given burnup and cooling time, the BRP damaged fuel axial heat flux profile is the same as that for the BRP intact fuel assemblies.

The axial heat flux profile associated with a potential reconfigured damaged fuel assembly is addressed in the following section.

4.7.6.3 Effective Thermal Conductivity of BRP Damaged Fuel

Given the level of damage expected for BRP damaged fuel, the thermal resistance between the damaged fuel can and the damaged fuel assembly is expected to be encompassed by that used for the evaluation of the intact fuel assemblies. As discussed in Section 4.2.2, the fuel assembly is modeled as a homogenous mass that has an effective radial and axial conductivity. The effective radial and axial conductivities are assumed to be the same for both the UO_2 and MOX damaged fuel assemblies (see Section 4.7.4.3). A mis-positioned grid spacer, or damage in the excess of a pinhole leak or hairline crack in a few rods will not affect the overall pin-to-pin heat transfer via radiation or conduction/convection that characterizes an intact fuel assembly. Also, the loss of a rod's internal gas pressure due to a defect will not affect the computed effective conductivity for the assembly because the presence of both the fill gas and the fuel material is conservatively ignored by the methodology used (see Section 4.2.2).

Since damaged rods will have released their gas prior to placement within the canister, there will be no introduction of fission gas from the damaged fuel into the canister atmosphere. Further, analysis has shown that the presence of fill gas constituents within the canister environment will not adversely affect the overall heat transfer rates.

Therefore, damaged BRP fuel will not have an effect on the overall (smeared) fuel assembly effective thermal conductivity. For these reasons, the effective thermal conductivity of the BRP damaged fuel is predicted to be bounded by the UO_2 and MOX intact fuel assemblies (refer also to the discussion on the effective thermal conductivity of MOX fuel in Section 4.7.4.3). However, since it is not possible to definitively know the full extent of damage to each fuel assembly, the evaluation for damaged fuel also includes an assessment of the predicted temperatures within the damaged fuel can and within the W74 canister in response to a potential reconfigured fuel assembly within the damaged fuel can(s).

A reconfigured fuel assembly is expected only as the result of an accident condition. The two credible accident scenarios that could yield significant failure to the damaged fuel assemblies are a side drop or an end drop. A side drop accident could result in damage levels ranging from nothing, to a bounding scenario involving the fracture and collapse of the fuel assembly against the wall of the damaged fuel can. Given that only a nominal 0.35 inches of space exists between the edges of the fuel assembly and the walls of the damaged fuel can and that the effective radial thermal conductivity for the intact fuel assembly (see Section 4.2.2) takes no credit for convection within the fuel assembly or contact between the assembly and the damaged fuel can walls, a partial collapse of the fuel assembly will not significantly affect the heat transfer within the damaged fuel can.

The bounding side drop damage scenario, which involves the fracture and collapse of the fuel assembly against the wall of the damaged fuel can, will yield a situation where the fuel rod sections are in direct contact with one another and/or the wall of the damaged fuel can. The heat

transfer within this reconfigured fuel assembly would actually improve due to the direct contact between the individual fuel rods and the increase in surface area as the debris spreads across the width of the fuel can. Combined with the direct contact between the fuel assembly and the wall of the damaged fuel can, this would yield an overall improvement in the heat transfer and temperature distribution within the damaged fuel can and the W74 canister. This conclusion is confirmed by the end drop scenario analysis results discussed in Section 4.7.6.6.

A key assumption in the above side drop damage scenario is that the axial distribution of heat within the reconfigured fuel assembly will be consistent with the undamaged fuel assembly. The antithesis to this assumption is that the fuel debris collects in a concentrated rubble pile. The most credible event leading to this situation will occur if the canister is upended subsequent to the side drop induced damage and the broken sections of fuel are concentrated at the bottom of the damaged fuel can. A bounding scenario for the concentrated rubble pile is addressed below as part of the end drop scenario.

The second credible accident scenario that could yield significant failure to the damaged fuel assemblies is an end drop. An end drop could ultimately result in a damaged fuel assembly fracturing and ending up in a pile at the bottom of the damaged fuel can. A similar geometry would result if a canister containing a fuel assembly damaged from a side drop is upended. Based on the bounding minimum solid volume presented by the range of BRP fuel, the fuel assembly could ultimately collapse to occupy the lower 38.7 inches of the damaged fuel can. This volume is based on the absence of flow channels (removed prior to loading) and a porosity of 0.45 (based on the minimum value typical for granular material). A shorter height is not feasible based on the use of the minimum solid volume and porosity. Contrarily, a larger height dimension would yield a lower decay heat density within the rubble and a larger surface area to transfer the heat. Conservatively, the decay heat within this shortened rubble pile is distributed using the same peaking factor curve used for the undamaged fuel assemblies.

Heat transfer within the rubble pile is evaluated three ways: as a tightly packed group of rods, as a loosely packed group of rods,[32] or as a porous media.[33] Table 4.7-1 shows the effective thermal conductivity as a function of temperature for these three means of representing the rubble pile. The lowest effective heat transfer coefficient among these three options (i.e., a loosely packed group of rods) is used to compute the temperatures within the rubble pile. The void space above the rubble pile is treated as a combination of convection and radiation between the walls of the damaged fuel can.

4.7.6.4 Allowable Cladding Temperature for BRP Damaged Fuel

The appropriate allowable temperature limit for BRP damaged fuel is the same as that for the intact fuel assemblies since, despite the presence of the damaged fuel can, the design goal is to avoid any additional failures. Sections 4.3.2 and 4.7.4.4 address the allowable cladding temperatures for intact UO_2 and MOX fuel assemblies. The cladding temperature for the BRP damaged fuel is estimated in Section 4.7.6.5.

---

[32] *License Application Design Selection Feature Report: Rod Consolidation*, OCRWM Report #BOOOOOOOO-0717-2.200-0210, Rev. 0, June 1999.

[33] Kaviany, M, *Principles of Heat Transfer in Porous Media*, 2nd Edition, 1995, Springer-Verlag, New York, New York.

4.7.6.5 Estimated Cladding Temperature for BRP Damaged Fuel

It is concluded that the damaged fuel assemblies will not exceed the cladding temperature limits for the reasons summarized below. As noted in Table 4.4-3 of this FSAR, the normal hot storage case temperature difference between the peak intact fuel rod and the hottest guide tube wall is approximately 34°F (i.e., 724°F - 690°F). This temperature difference increases to approximately 54°F (i.e., 584°F - 530°F) at the support tube location where a damaged fuel can would be contained. The higher temperature difference is due primarily to the additional heat flow passing through this location from the fuel assemblies located from the interior guide tubes. The added thermal resistance created by the presence of the damaged fuel can walls will act to slightly increase this required delta temperature.

Given the same assembly decay heat load, a similar temperature difference (34°) will exist between the damaged fuel assemblies and the walls of the damaged fuel can. This assumption is justified because, with the exception of its vented top and bottom covers, the cross-section of the damaged fuel can has a similar geometry and surface finish properties as a guide tube and because the heat transfer mechanisms from the damaged fuel assembly and the damaged fuel can are the same as for the intact fuel assembly and the basket support tube walls. Although this assumption is based on a damaged fuel assembly that maintains a similar geometry as an intact fuel assembly, considerable latitude exists. For example, a missing or bowed fuel rod will increase the radiation and convection exchange between the interior of the fuel assembly and the walls of the can.

The presence of the damaged fuel can within the support tube will introduce an added thermal resistance due to the additional need to transfer heat from the damaged assembly to the support tube walls. This thermal resistance can be conservatively estimated assuming conduction across the gap between the walls of the damaged fuel can and the basket support tube. This gap is a nominal 0.085 inches [i.e., (7.4” – 7.23”)/2]. Given a width of 7.23 inches and a conservatively high peak heat generation rate of 24.8 kw/64 assemblies/70 inch active fuel length*1.21 peaking factor = 6.70 watts/inch. The delta T required to pass this heat generation rate across the gap between the damaged fuel can wall and the support tube wall via conduction alone is:

$\Delta T = QL/(kA)$ * ratio of interior to local heat generation

where:

ΔT = temperature difference
Q = heat generation rate (6.70 watts/inch)
L = gap width (0.085 inches)
K = thermal conductivity for helium (~0.122 BTU/hr-ft-F)
A = area (7.23 inches)
interior to local heat generation ratio = 54°F/34°F
ΔT = 6.70 watts/inch*3.413 BTU/hr/watt * 0.085 inches* (54°F/34°F)/
[0.122 BTU/hr-ft-F*4*7.23 inches/12)
= 10.5ºF
= 5.8ºC

This estimated temperature increase would be less if the contribution of radiation heat transfer had been included. Based on this analysis, the peak rod temperature within the damaged fuel

assembly is conservatively estimated to be 5.8ºC higher than an intact fuel assembly at the same location, or 313ºC at the normal hot storage condition (i.e., 307ºC + 5.8ºC). This is well within the allowable cladding temperature limit established for BRP fuel.

The presence of damaged fuel cans in the support tubes will not significantly affect the peak fuel rod temperatures for the limiting assemblies near the center of the basket. Only a small fraction of the heat from the other assemblies in the basket flows through the support tube interior (i.e., approximately 60% of the heat flow from one assembly, as evidenced by the 54°F/34°F ratio of interior to local heat generation). Most of the heat travels around the support tubes via convection or through the thick (0.75”) steel support tube walls. Thus, the temperature increase at the basket center will be much smaller than the increase seen for the fuel inside the support tube, which is 5.8 °C. It is therefore concluded that the basket center temperature increase will be insignificant (~ 1°C or less).

Similar arguments apply to all other FuelSolutions™ W74 canister storage cases. For the normal and off-normal transfer cases, the short-term cladding limit for intact fuel assemblies increases to 400°C. Given that a minimum margin of 11.3°C exists between the hottest fuel cladding location and the 400°C limit, (e.g., per the ‘Off-Normal Hot’ condition in Table 4.5-3 of this FSAR), a sufficient margin exists to accommodate the added 5.8°C due to the presence of the damaged fuel can. In reality, since the support tube is not the location of the hottest fuel cladding, an even greater thermal margin will exist. Therefore, it can be concluded that a canister loaded with damaged fuel assemblies would not approach the fuel cladding temperature limit for any case.

Finally, a similar argument applies to all intact fuel accident cases analyzed (e.g., per Table 4.6-4, a 116°C margin exists for the post-fire cool-down/steady-state case). Once again, it is predicted the damaged fuel cladding temperatures for all accident cases would not approach the cladding temperature limit.

4.7.6.6 Estimated Cladding Temperature for BRP Fuel Rubble

An alternative analysis examines the temperatures within the damaged fuel can and W74 canister assuming the BRP damaged fuel is reconfigured due to an accident scenario. The damaged fuel can serves to confine the resulting sections of fuel assembly within the can, with the material occupying the lower 38.7 inches of the damaged fuel can. This rubble volume is based on the dimensions of the damaged fuel can, the minimum feasible solid volume for the intact fuel assembly, and the minimum porosity for granular material. Larger rubble volumes will act to decrease temperatures due to a reduction in the decay heat density and an increase in the surface area available for heat transfer.

The thermal models described in Sections 4.4.1.1 and 4.4.2.1 of this FSAR were modified to simulate the presence of the damaged fuel can and the fuel rubble at the four basket locations where damaged fuel cans may be placed. The modifications consisted of replacing the thermal conductivity for intact fuel assemblies with that for the fuel rubble discussed in Section 4.7.6.3, and with the damaged fuel can discussed in Section 4.7.6.5 over the lower 38.7 inches of each damaged fuel can location. Heat transfer above this height was treated as convection and radiation across an empty damaged fuel can.

Using this thermal modeling, thermal evaluations for the ‘Normal Hot’ conditions of storage and the ‘Off-Normal Hot’ conditions of transfer were conducted and compared to those reported in

Sections 4.4.1.3 and 4.4.2.4. Figure 4.7-8 illustrates the temperature comparison for the 'Normal Hot' conditions of storage between a canister full of intact fuel assemblies and a canister with reconfigured, damaged fuel assemblies. The parameters chosen for comparison are the intact fuel cladding temperatures at the peak location (near the basket center), the maximum temperature around the support tube, and the temperature of the cladding/failed fuel at the support tube location. As seen from the figure, the presence of the reconfigured fuel within the failed fuel can is clearly seen by the downward shift and shortening of the temperature distribution at this location. While the peak temperature at this location increased by 18°F due to the higher decay heat density of the reconfigured fuel, it is over 100°F below the peak fuel cladding temperature within the canister.

While support tube temperature distribution also exhibit a downward shift as a result of the reconfigured fuel, there is essentially no increase in the temperature. Likewise, the peak cladding temperatures within the W74 canister are seen to be nearly identical between the two simulations. Although a slight downward shift is noted at the peak fuel cladding temperature location, the results indicate that the presence of the damaged fuel can and its contents have only a negligible effect (only 1°F) on the peak temperatures within the canister.

Similar results are seen in Figure 4.7-9 for the 'Off-Normal Hot' conditions of transfer. Again, a downward shift in the location of the peak temperatures within the canister is evident. The peak fuel cladding temperature within the canister increases by 10°F due to the presence of the damaged fuel can and the reconfigured fuel, while the peak cladding/failed fuel temperature at the support tube location increases by 30°F. The larger temperature increases over those seen under storage conditions is directly related to the orientation of the basket and the change in the convection heat flow for the horizontal orientation. Nevertheless, the peak canister temperatures are seen as remaining within their allowable limits.

Thus, it is concluded that the presence of the damaged fuel can will not cause the W74 canister temperatures to exceed their allowables, whether the damaged fuel remains intact or under the conservative assumption that the fuel reconfigures into a pile as a result of an accident scenario. The limited effect for these results seen for the end drop scenario also serve as justification for the conclusions drawn for the bounding side drop scenario discussed in Section 4.7.6.3.

4.7.6.7 Canister Internal Pressure for BRP Damaged Fuel

The intact fuel rods within the BRP damaged fuel assemblies are assumed to have the same internal rod pressures as the design basis BRP assemblies. As such, the canister interior pressures calculated in Sections 4.4, 4.1, and 4.6 of this FSAR are bounding for any canister containing damaged fuel assemblies because the gas released from the damaged fuel rods prior to loading will not contribute to canister pressurization.

4.7.6.8 Thermal Summary for BRP Damaged Fuel Assemblies

For the above reasons, it is concluded that the thermal analyses for BRP intact assemblies presented in Sections 4.4, 4.1, and 4.6 of this FSAR, bound the damaged fuel assemblies with respect to thermal considerations. Therefore, the required cooling times given in Table 5.2-1 of this FSAR apply for both intact and damaged BRP fuel assemblies.

Table 4.7-1 - W74 Damaged Fuel Effective Conductivity

Material	Temperature (°F)	Effective Thermal Conductivity (BTU/hr-ft-°F)	Density[1] (lb/ft^3)	Specific Heat (BTU/lb-°F)
Loosely Packed Consolidated Fuel Rods	77	0.324[1]	Not needed	Not needed
	122	0.347		
	212	0.393		
	302	0.451		
	392	0.509		
	482	0.572		
	572	0.636		
	662	0.711		
	752	0.786		
Tightly Packed Consolidated Fuel Rods	77	0.416[1]	Not needed	Not needed
	122	0.480		
	212	0.624		
	302	0.780		
	392	0.954		
	482	1.133		
	572	1.306		
	662	1.474		
	752	1.630		
Porous Media	392	2.040[2]	Not needed	Not needed
	572	1.699		
	752	1.560		

Notes:

(1) Table 5-1, *License Application Design Selection Feature Report: Rod Consolidation*, OCRWM Report #BOOOOOOOO-0717-2.200-0210, Rev. 0, June 1999.

(2) Based on the thermal conductivity of helium and uranium oxide and the methodology presented in *Principles of Heat Transfer in Porous Media*, 2nd Edition, M. Kaviany, 1995, Springer-Verlag, New York, New York.

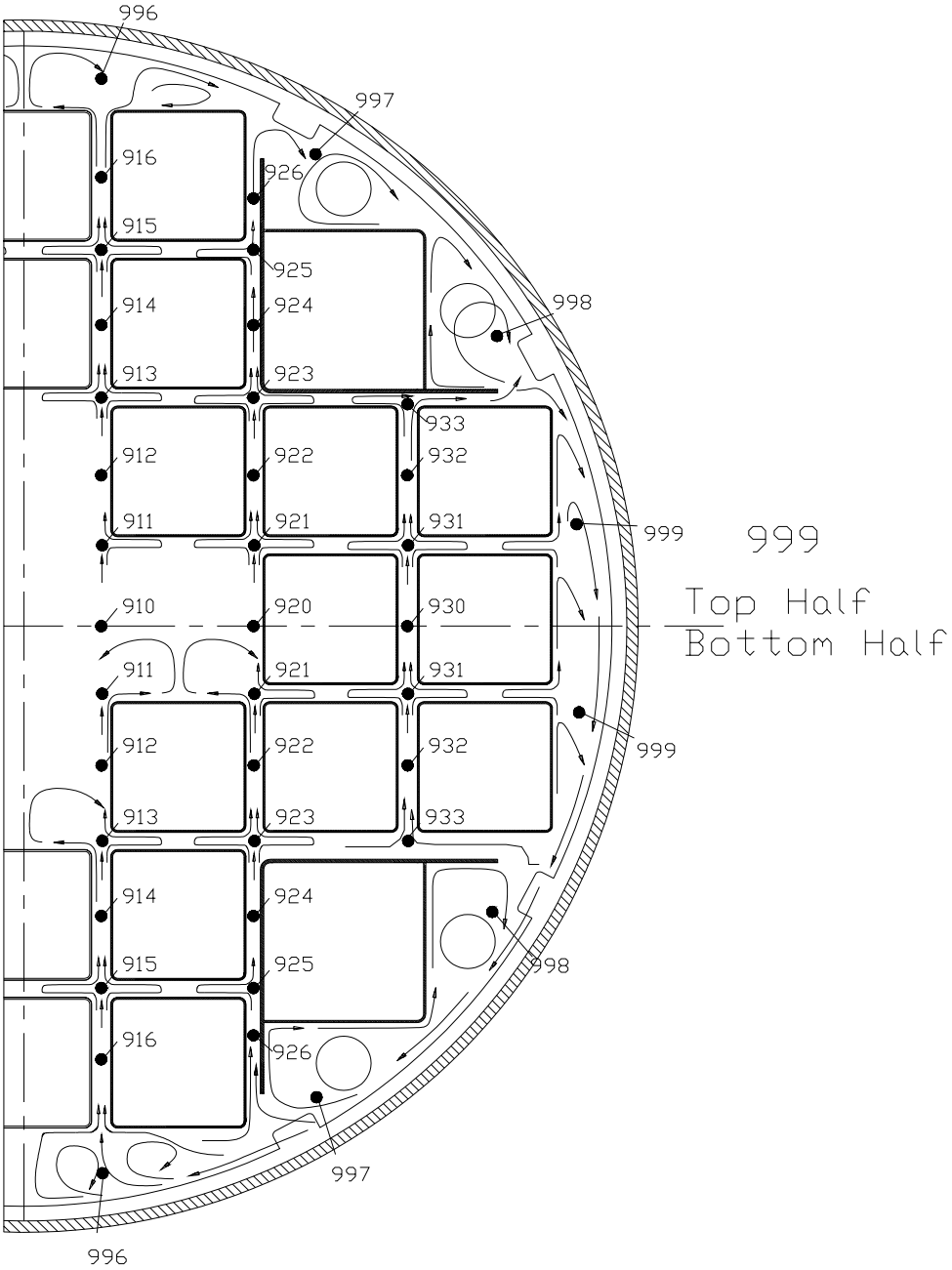

Figure 4.7-1 - Gas Node and Flow Pattern in Horizontal Canister

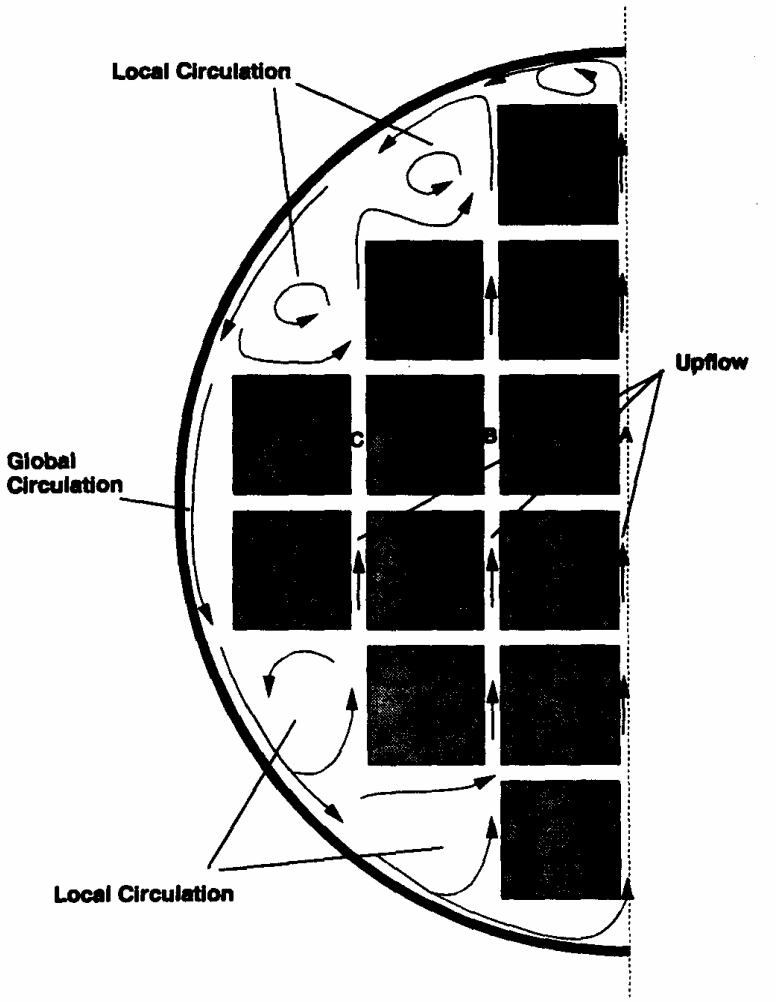

(a) Ra=9.3×10^6, Fluid: Air

Figure 4.7-2 - Circulation Pattern within NUHOMS® 24 Unit DSC

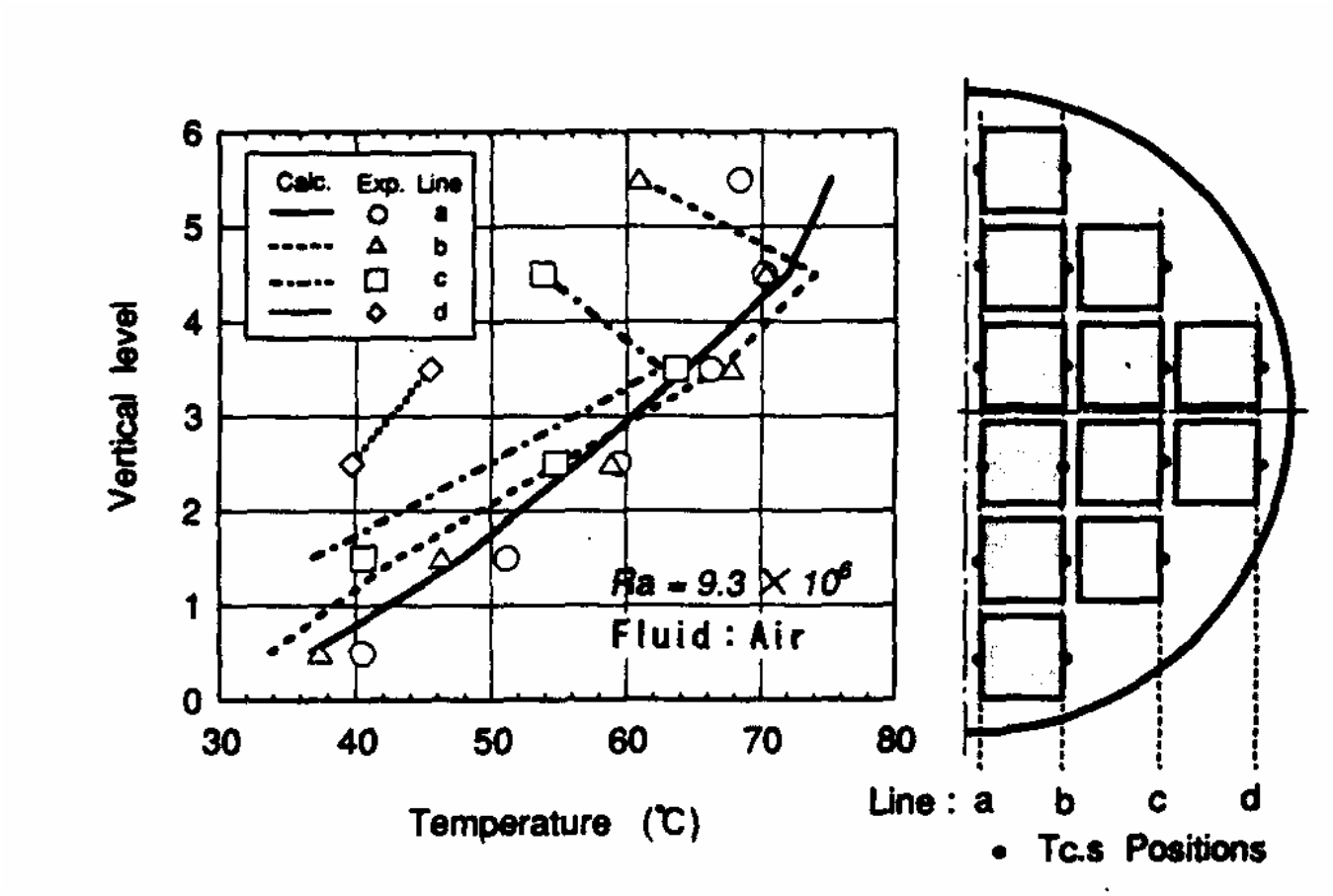

Figure 4.7-3 - Temperature Distribution in NUHOMS® 24 Unit Basket

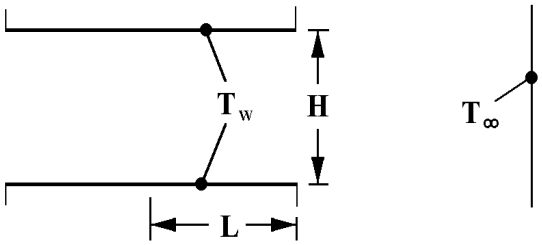

Figure 4.7-4 - Double Open-ended Cavity with Two Heated Walls

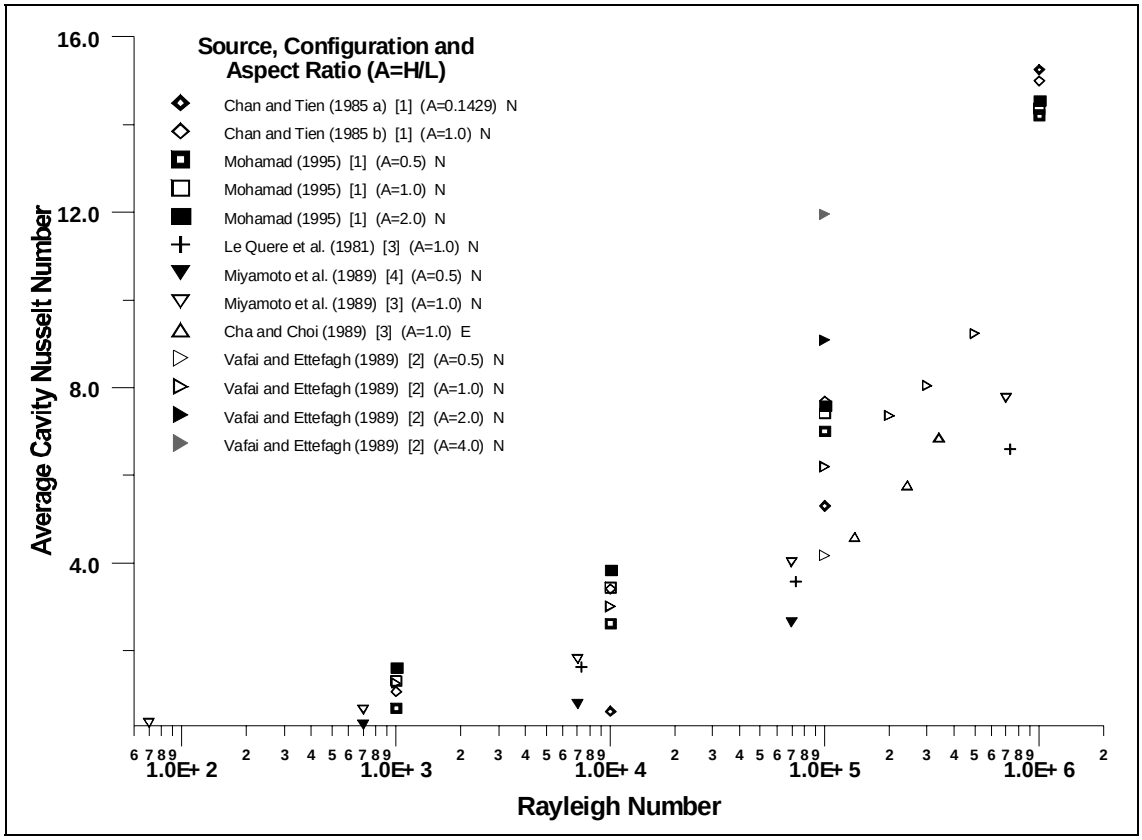

Figure 4.7-5 - Average Cavity Nusselt Number as a Function of Rayleigh Number and Aspect Ratio

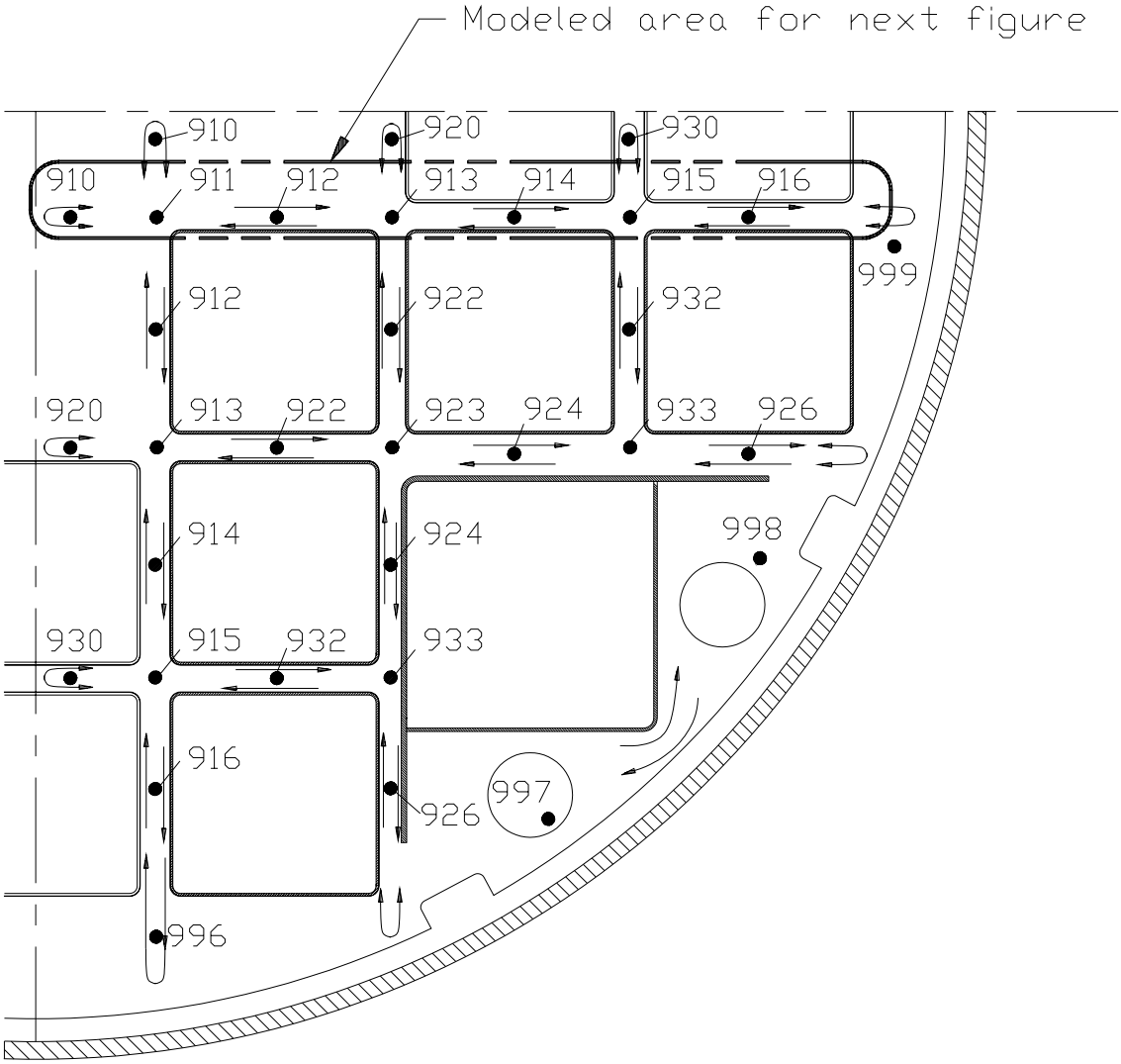

Figure 4.7-6 - Gas Node Layout for Vertical Canister

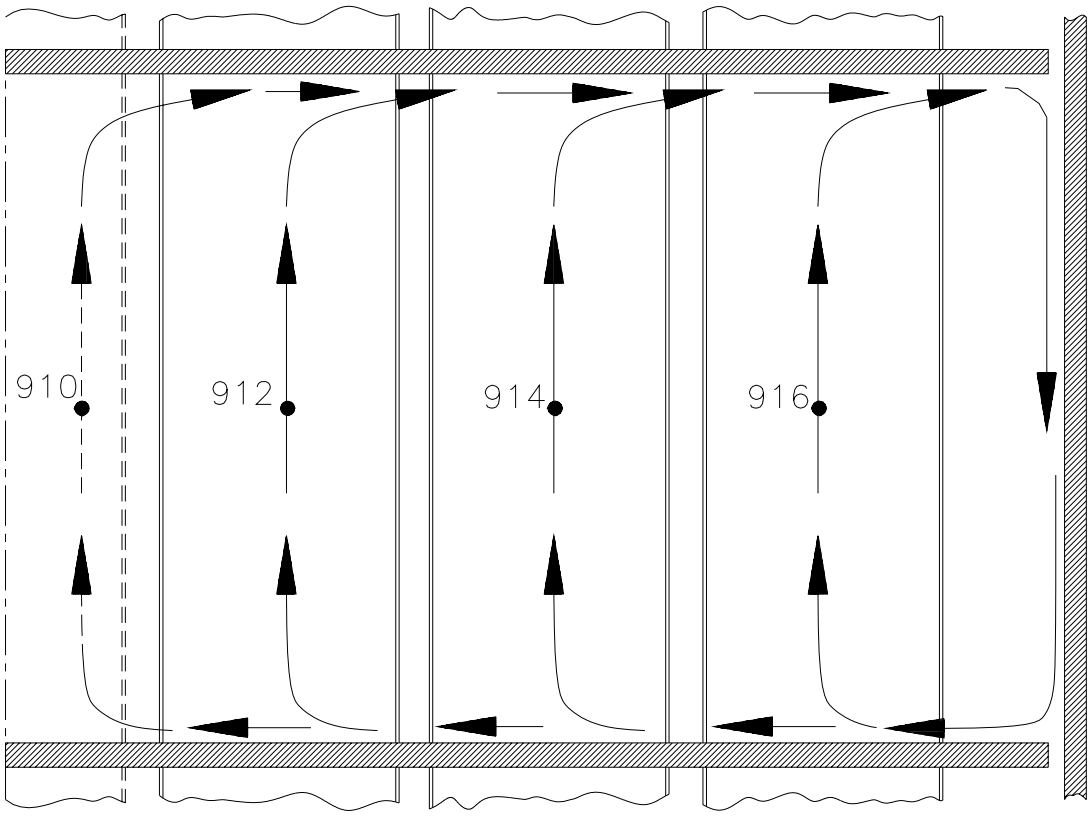

Figure 4.7-7 - Flow Pattern for Vertical Canister

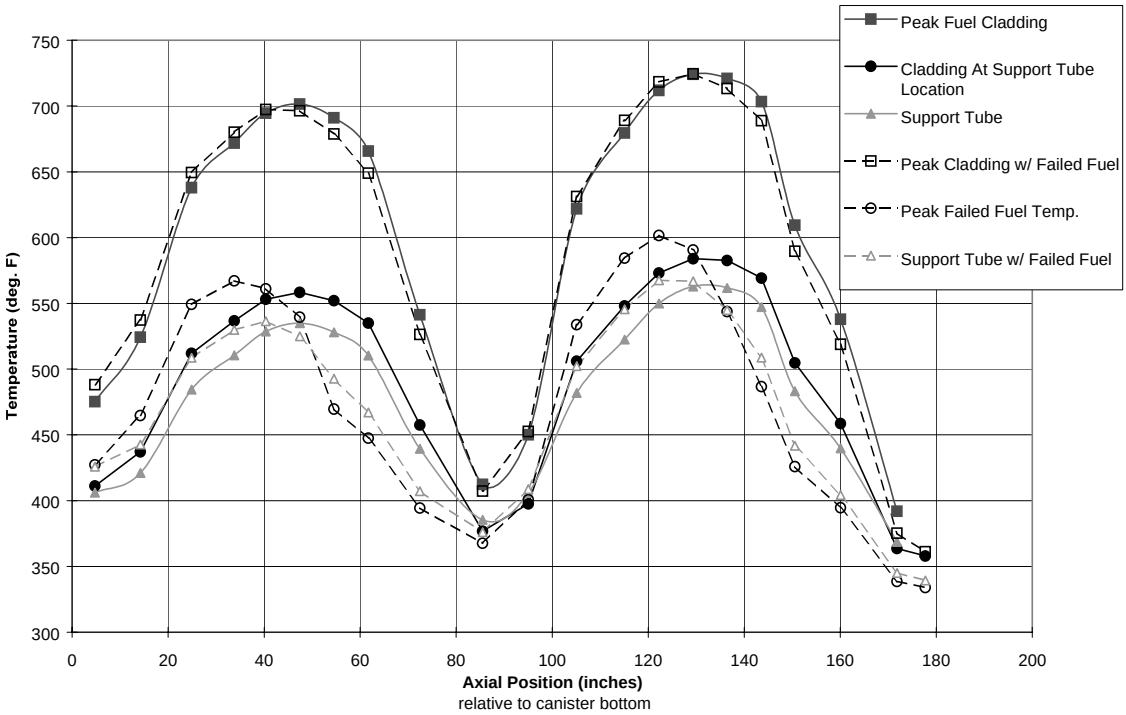

Figure 4.7-8 - Effect of Reconfigured Damaged Fuel On W74 Canister Temperatures, Storage Conditions

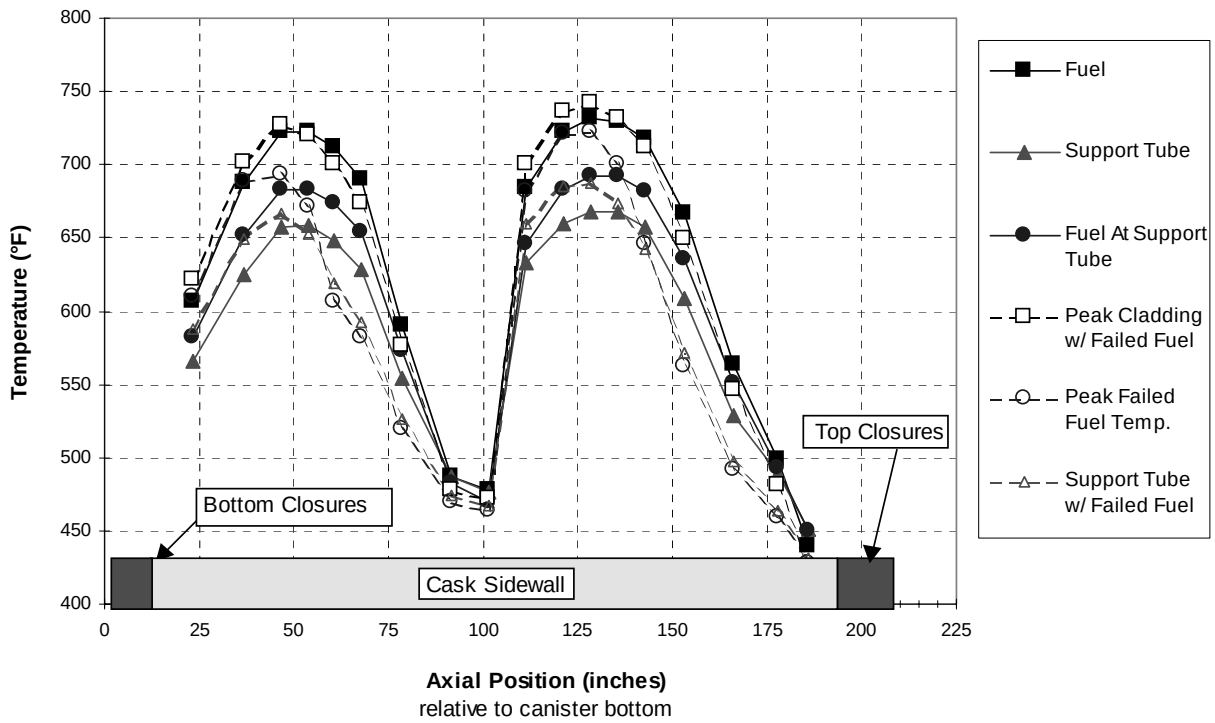

Figure 4.7-9 - Effect of Reconfigured Damaged Fuel On W74 Canister Temperatures, Transfer Conditions

5. SHIELDING EVALUATION

This chapter presents the shielding evaluation for the FuelSolutions™ W74 canister. It describes the canister's major shielding design features, presents the W74 fuel cooling tables (the primary method of controlling radiological and thermal source terms for SNF to be stored in the FuelSolutions™ W74 canister), and presents the W74 canister-unique shielding calculations.

This chapter of the FuelSolutions™ W74 canister storage FSAR describes the:

- Shielding design features for the FuelSolutions™ W74 canister.
- Fuel cooling tables for the FuelSolutions™ W74 canister.
- Canister-specific shielding calculations.
- Differences from the generic methodology described in Chapter 5 of the FuelSolutions™ Storage System FSAR.
- BRP fuel source term and shielding calculations performed to qualify mixed-oxide (MOX) fuel for loading into the W74 canister.
- Effect of BRP partial fuel assemblies on the shielding analyses.

Chapter 5 of the FuelSolutions™ Storage System FSAR describes:

- Shielding design features for the FuelSolutions™ Storage System components.
- Shielding analysis results for the FuelSolutions™ Storage System components.
- Radiological source terms and the fuel cooling tables and how they are derived.
- Shielding methodologies and assumptions used.

Chapter 10 (Radiation Protection) of this FSAR discusses:

- Any differences between the estimated occupational and public exposures for the FuelSolutions™ Storage System given in Chapter 10 of the FuelSolutions™ Storage System FSAR, and for the FuelSolutions™ W74 canister.
- Estimated radiological consequences of postulated accident conditions for the FuelSolutions™ W74 canister.

This page intentionally left blank.

5.1 Discussion and Results

5.1.1 FuelSolutions™ W74 Canister Shielding Design Features

The FuelSolutions™ W74 canister provides containment for radionuclides via the welded stainless steel shell assembly, and radiation shielding in the axial directions via thick metal shield plugs located at both ends of the canister. This axial shielding maintains radiation exposures ALARA during canister sealing operations, canister transfer operations, and dry storage. The canister cylindrical shell provides a relatively small amount of shielding in the radial direction in addition to its confinement function.

The FuelSolutions™ W74 canister differs from other FuelSolutions™ canister designs because of its stacked upper and lower basket arrangement and segmented top shield plug. Although operationally dissimilar from other FuelSolutions™ canisters, the shielding design features of the W74 canister are the same because the axial shielding and canister shell are similar.

The W74 canister is available in two classes: the W74M and W74T, as described in Section 1.2.1.3. Drawings for the FuelSolutions™ W74 Canister are provided in Section 1.5.1 of this FSAR. Both classes of canisters and the canister types within a canister class are similar from a shielding safety standpoint since they have the same cylindrical shells, closure plates, and similar internal basket components. The W74 canister is available only with a long canister shell and steel shield plugs. Table 5.1-1 summarizes the FuelSolutions™ W74 shielding materials.

5.1.2 FuelSolutions™ W74 Canister Fuel Cooling Tables

The primary shielding evaluation results in this chapter are in the FuelSolutions™ W74 canister fuel cooling tables. The fuel cooling tables define the required cooling times based on the SNF initial enrichment and burnup, and hence control the source terms for SNF to be stored in the FuelSolutions™ W74 canister. Section 5.2 presents the fuel cooling tables, describes their use, and discusses the criteria used for their construction.

Analyses presented in Section 5.5.2 show that all existing BRP MOX fuel assemblies are qualified for storage in the FuelSolutions™ W74 canister. Thus, the cooling tables are not used with respect to the BRP MOX fuel assemblies.

As discussed in Sections 5.5.3 and 5.5.4, the fuel cooling tables in this FSAR are applicable for partial and damaged fuel assemblies.

Section 5.1 of the FuelSolutions™ Storage System FSAR gives a general description of the fuel cooling tables and their construction.

5.1.3 FuelSolutions™ W74 Canister Adjoint Shielding Models

Key parameters used in constructing the FuelSolutions™ W74 fuel cooling tables are the adjoint importance functions. The importance functions relate the primary gamma, secondary gamma, and neutron dose rates for a W74 canister when stored in the W150 Storage Cask.

The W74 adjoint shielding model and results (importance functions) are presented in Sections 5.3 and 5.4, respectively. Chapter 5 of the FuelSolutions™ Storage System FSAR provides a general description of the adjoint shielding models.

Table 5.1-1 - FuelSolutions™ W74 Canister Shielding Design Features Summary

	Canister Class and Type							
***Class*[1]→**	**W74M**				**W74T**			
***Type*[2] →**	**-LD**	**-LS**	**-SD**	**-SS**	**-LL**	**-LS**	**-SL**	**-SS**
Shell	0.63” Stainless Steel (all types)							
Top Closure								
Outer Closure Plate	2.00” Stainless Steel (all types)							
Inner Closure Plate	1.00” Stainless Steel (all types)							
Shield Plug (Top Plate)	--	N/A	--	--	--	N/A	--	--
Shield Plug (Material)	--	7.25” Steel	--	--	--	7.25” Steel	--	--
Shield Plug (Bottom Plate)	--	N/A	--	--	--	N/A	--	--
Bottom Closure								
Closure Plate	--	1.0” Steel	--	--	--	1.0” Steel	--	--
Shield Plug (Material)	--	5.8” Steel	--	--	--	5.8” Steel	--	--
End Plate	--	1.8” Steel	--	--	--	1.8” Steel	--	--

Notes:
(1) M = MPC, T = Transport/Storage
(2) The W74 canister is only available with a long canister shell/steel axial shields.

This page intentionally left blank.

5.2 Source Specification

5.2.1 Fuel Cooling Tables

The FuelSolutions™ W74 canister fuel cooling tables define the minimum required cooling times for UO_2 fueled SNF to meet the FuelSolutions™ system safety and design requirements defined in Chapter 2 of this FSAR. The cooling times are a function of the SNF initial enrichment and burnup. Section 5.2 of the FuelSolutions™ Storage System FSAR generically describes how FuelSolutions™ fuel cooling tables are constructed and their bases.

Because gamma dose rates vary depending on the fuel assembly cobalt content, two W74 canister fuel cooling tables are presented. There is a standard table for assemblies with relatively low cobalt content, and a high-cobalt table for assemblies with higher cobalt content. The fuel cooling tables are shown in Table 5.2-1 and Table 5.2-2. Each table includes an applicability statement and a summary of the design basis used to construct the table.

5.2.2 Design Bases for the Fuel Cooling Tables

The design bases for the W74 canister fuel cooling tables include maximum allowable canister heat loads and the allowable dose rate at the side wall of the FuelSolutions™ W150 Storage Cask.

The allowable heat loads are based on thermal calculations to determine the controlling bulk heat load for casks and canister independently (i.e., the storage cask/transfer cask, and canister). In order to address the effects of active fuel length and peaking factors, there is also a corresponding allowable on the maximum linear heat load for each component. The allowable heat load for a specific component may be due to temperature dependent allowable stresses for materials of construction or allowable cladding temperatures (for canisters). The most limiting of these heat loads are used as the thermal criteria for generating the W74 canister fuel cooling tables, as summarized in Table 5.2-3. Refer to Chapter 4 of the FuelSolutions™ Storage System FSAR for the storage cask and transfer cask maximum heat load discussions. Chapter 4 of this FSAR presents the maximum heat load discussion for the W74 canister.

The radiological criterion for generating the W74 canister fuel cooling tables is a calculated allowable dose rate of 50 mrem/hr at the storage cask side wall. This basis is chosen to control the storage cask side wall dose rate, which is the most important contributor to off-site doses to the public because of the orientation and relatively small size of the storage cask penetrations.

Any SNF assembly meeting the requirements of the *technical specification* provided in Section 12.3 of this FSAR and the fuel cooling tables may be stored in the FuelSolutions™ W74 canister. The cooling tables are valid for either W74 canister class because the differences in W74 canister designs do not significantly change the adjoint importance functions used to construct the fuel cooling tables. Since each statepoint (i.e., burnup, enrichment pair) represents a cooling time for which all thermal and radiological constraints are met for a full canister load of similar SNF assemblies (assuming an upper bound loading of 0.1421 MTU/assy over 70 inches of active fuel), canisters may be loaded with fuel assemblies meeting the cooling requirements of any cell in the fuel cooling tables. In all cases, the fuel assembly initial enrichment must not exceed the limit specified by Table 2.2-1 of this FSAR.

The fuel cooling tables are based on adjoint shielding models for a canister filled with 64 SNF assemblies. Short loading (i.e., some storage cell locations contain no SNF assemblies) of a canister to less than 64 assemblies is acceptable from a shielding safety standpoint because short loading reduces the amount of source term material and, hence, the occupational and off-site dose rates.

5.2.3 Special Considerations for the W74 Fuel Cooling Tables

Section 5.2.1 of the FuelSolutions™ Storage System FSAR describes the four areas where factors are included in the methodology to account for special considerations. These factors are included in the W74 ADSORB runs as described below.

A. *Burnup-specific thermal peaking factor*
Thermal calculations to determine maximum allowable heat loads are performed using peaking profiles at a design burnup of 29,000 MWd/MT for BWR fuels. SNF assemblies with lower burnup have more pronounced axial peaks. Maximum canister heat loads are specified in units of bulk watts/canister. In order to assure that allowable system temperatures are not exceeded because of specifying bulk heats, an adjustment factor is assigned in ADSORB to reduce the allowable heat load in any burnup group less than these values. Any burnup greater than these values is acceptable because its axial peaking factor is bounded by the one assumed in the heat transfer calculations. An additional burnup-specific factor is included to account for non-UO_2 heat generation in SNF assemblies. The burnup-specific penalty factors used to generate the W74 canister cooling tables are summarized in Table 5.2-4.

B. *Burnup-specific radiological axial peaking factors*
Factors are applied in ADSORB to the calculated storage cask surface dose rates to account for axial burnup peaking in the SNF. Based on a review of peaking factors for BWR burnup profiles,[1] burnup-dependent peaking factors are applied to gamma and neutron dose rates in ADSORB. The increase in primary gamma ray dose rate is assumed to be equal to the burnup peaking factors (see Table 5.2-4). Neutron and secondary gamma dose rates are assumed to vary as the fourth power of the burnup (see Table 5.2-6). The way these effects are accounted for is to artificially increase the gamma and neutron dose rates ADSORB calculates prior to comparing the total calculated dose rate to the dose rate criterion ADSORB uses to determine acceptable cooling times.

C. *Activated SNF hardware*
The generic gamma source term library does not account for activation of cladding and other non-fuel material. When calculating gamma dose rates for comparison against allowable values, ADSORB multiplies the primary gamma dose rate by a factor to account for activation, and then adds the product to BUGLE energy group 57 (1.0-1.5 MeV) before summing the dose contribution from all gamma groups. The factor varies as a function of burnup, enrichment, and cooling time as shown in Table 5.2-5. Calculation of the assembly hardware gamma source strength factor, for each cooling table statepoint, is described in detail in Section 5.5.3 of the FuelSolutions™ Storage System FSAR. This FSAR section

[1] Commonwealth Edison BWR Fuel Data, Letter from A. S. Pallotta of BWR Nuclear Design, Nuclear Fuel Services to A. G. Panagos, NFS:BND:95-083, July 10, 1995.

explicitly describes functions (i.e., data strings) that are to be entered into the ADSORB code to perform the assembly hardware gamma source strength calculation for each statepoint.

D. *Subcritical neutron multiplication*
The generic neutron source term library does not account for subcritical neutron multiplication. When calculating neutron and secondary gamma dose rates, ADSORB multiplies these dose rates by a factor to account for subcritical multiplication. The subcritical neutron multiplication factor and related parameters used to construct the W74 canister cooling tables are summarized in Table 5.2-6.

5.2.4 Use of the Fuel Cooling Tables

In order to determine the minimum cooling time for a candidate SNF assembly:

1. Determine the fuel assembly's burnup (MWd/MT), and initial enrichment (w/o ^{235}U) from plant records.
2. Burnups greater than 40,000 MWd/MT are not qualified for dry storage.
3. Enrichments less than the minimum shown on the fuel cooling tables, or greater than the criticality maximum allowable enrichment in Table 2.2-1 of this FSAR, are not qualified for dry storage.
4. Determine which cooling table (Table 5.2-1 or Table 5.2-2) to use based upon the assembly's core zone initial cobalt content. As discussed in Table 2.2-1, assemblies with more than 2.9 grams of initial core zone cobalt must use Table 5.2-2.
5. Look up the minimum required cooling time by rounding up in burnup, and down in enrichment. This is for conservatism because higher burnups produce higher thermal and radiological sources, and (for a given burnup) lower enriched fuel has higher actinide concentrations which results in higher neutron sources and heat generation.

The criteria listed above are also applicable for partial and damaged UO_2 fueled BRP assemblies, as discussed in Sections 5.5.3 and 5.5.4. Section 5.5.2 shows that all existing BRP MOX fuel assemblies meet the established criteria and are qualified for storage in the FuelSolutions™ W74 canister.

Table 5.2-1 - Fuel Cooling Table W74-1-A

APPLICABILITY:

Canister:	FuelSolutions™ W74-M and W74-T Canisters
Loading Specification:	W74-1, W74-3, and W74-5
Description:	Up to 64 fuel assemblies
SNF Assemblies:	Valid for all BRP assemblies as indicated in Table 2.2-1
Cobalt Range:	≤ 2.9 g in active fuel region (low-cobalt)

QUALIFICATION BASES:

Storage Cask Dose Rate	≤ 50 mrem/hr
Canister Heat Load	≤ 24.8 kW/Canister, and ≤ 0.216 kW/inch-Canister

Maximum Burnup (MWd/MTU)(1)	**Required Minimum Cooling Time (yr.)**					
	Minimum Average Initial Enrichment (w/o ^{235}U)(1,2)					
	1.5	2.0	2.5	3.0	3.5	4.0
15,000	3.2	3.1	3.1	3.0	3.0	3.0
20,000	3.4	3.3	3.2	3.2	3.1	3.1
25,000	3.6	3.5	3.4	3.4	3.3	3.3
30,000	3.9	3.8	3.6	3.6	3.5	3.4
32,000	3.9	3.8	3.7	3.6	3.5	3.5
34,000	4.2	3.9	3.8	3.7	3.6	3.6
36,000	4.8	4.4	4.1	3.9	3.8	3.7
38,000	5.2	4.8	4.5	4.2	4.0	3.9
40,000	5.6	5.3	4.9	4.6	4.3	4.1

Notes:
(1) Rounding: round up to next highest burnup, round down to next lowest enrichment.
(2) Enrichments less than 1.5% or greater than the criticality limit presented in Chapter 6 of this FSAR are not qualified.

Table 5.2-2 - Fuel Cooling Table W74-1-B

APPLICABILITY:

Canister:	FuelSolutions™ W74-M and W74-T Canisters
Loading Specification:	W74-1, W74-3, and W74-5
Description:	Up to 64 fuel assemblies
SNF Assemblies:	Valid for all BRP assemblies as indicated in Table 2.2-1
Cobalt Range:	≤ 15.0 g in active fuel region (high-cobalt)

QUALIFICATION BASES:

Storage Cask Dose Rate	≤ 50 mrem/hr
Canister Heat Load	≤ 24.8 kW/Canister, and ≤ 0.216 kW/inch-Canister

Maximum Burnup (MWd/MTU)[1]	Required Minimum Cooling Time (yr.)					
	Minimum Average Initial Enrichment (w/o ^{235}U)[1,2]					
	1.5	2.0	2.5	3.0	3.5	4.0
15,000	4.2	4.0	3.9	3.8	3.8	3.7
20,000	4.7	4.3	4.2	4.1	4.0	3.9
25,000	5.2	4.9	4.8	4.6	4.5	4.4
30,000	5.8	5.6	5.1	4.9	4.8	4.7
32,000	6.0	5.8	5.3	5.1	5.0	4.9
34,000	6.4	6.2	5.5	5.4	5.2	5.1
36,000	6.5	6.2	6.0	5.5	5.4	5.3
38,000	6.8	6.6	6.4	5.8	5.6	5.5
40,000	7.0	6.8	6.6	5.8	5.6	5.5

Notes:
(1) Rounding: round up to next highest burnup, round down to next lowest enrichment.
(2) Enrichments less than 1.5% or greater than the criticality limit presented in Chapter 6 of this FSAR are not qualified.

Table 5.2-3 - Heat Load Criteria for Constructing the W74 Fuel Cooling Tables

	Bulk Heat Load (kW/canister)(1)	Linear Heat Load (kW/canister-inch)(1)
W100 Transfer Cask	28.0	0.274
W150 Storage Cask	28.0	0.253
W74 Canister	24.8	0.216
Criterion for W74 Fuel Cooling Tables(2)	**24.8**	**0.216**

Notes:

(1) Maximum heat loads for the W100 Transfer Cask and W150 Storage Cask are discussed in Chapter 4 of the FuelSolutions™ Storage System FSAR.

(2) The most limiting of the transfer cask/storage cask, and canister maximum heat loads is used as the thermal criterion for constructing the fuel cooling tables.

Table 5.2-4 - Burnup-Specific Heat Load Factors

Cooling Table Burnup Interval (GWd/MT)	Maximum Peaking Factor(1)	Axial Derating Factor(2)	Assembly Hardware Factor(3)	Assembly Lattice Geometry Factor(3)	ADSORB Derating Factor(2)
0-15	1.459	0.836	5.4 %	1.5%	0.779
15-20	1.305	0.935	5.4 %	1.5%	0.871
20-25	1.263	0.966	5.4 %	1.5%	0.900
25-30	1.231	0.991	5.4 %	1.5%	0.924
30-32	1.211	1.000	5.4 %	1.5%	0.932
32-34	1.202	1.000	4.2 %	1.5%	0.944
34-36	1.192	1.000	4.2 %	1.5%	0.944
36-38	1.184	1.000	4.2 %	1.5%	0.944
38-40	1.176	1.000	3.7 %	1.5%	0.949

Notes:

(1) Maximum peaking factors for worst-case burnup profiles (reference 1) were fit to $PF=1.8983\cdot(BU)^{-0.1308}$ where BU is the average burnup in MWd/MT.

(2) The axial derating factor is equal to 1.22/PF, where 1.22 is the peaking factor used for the maximum heat load calculations.

(3) Heat load contribution for non-UO_2 hardware vs. burnup expressed in percent of the total UO_2 heat load.

(4) Factor to account for possible underprediction of BRP UO_2 heat sources (ORIGEN2.1 vs. SAS2H) due to fuel assembly lattice geometry effects.

(5) Derating factor is applied to bulk and linear maximum allowable heat loads for specific burnups in ADSORB. This effectively reduces the allowable heat load, thus increasing required cooling times, for the specific burnup range. Calculated per the following example for the 0-15 GWd/MT row: 0.836 * (1-0.054) * (1-0.015) = 0.779.

Table 5.2-5 - Burnup-Specific Gamma Factors

Cooling Table Burnup Interval (GWd/MT)	Maximum Peaking Factor(1)	ADSORB Gamma Factor(2,3)
0-15	1.459	1.459
15-20	1.305	1.305
20-25	1.263	1.263
25-30	1.231	1.231
30-32	1.211	1.211
32-34	1.202	1.202
34-36	1.192	1.192
36-38	1.184	1.184
38-40	1.176	1.176

Notes:

(1) Maximum axial peaking factors for worst case burnup profiles (reference 1) were fit to $PF=1.8983\cdot(BU)^{-0.1308}$ where BU is the average burnup in MWd/MT.

(2) The gamma peaking factor is equal to the maximum axial peaking factor. The overall gamma factor is applied to the gamma source term in ADSORB for each burnup group. This increases the gamma dose rate, thus increasing required cooling times for the specific burnup range.

(3) The gamma source strengths are increased further to account for irradiated non-UO_2 hardware (including control components). BUGLE energy group 57 (1.0-1.5 MeV) is increased by an additional gamma source strength equal to 0%-6.2% of the total gamma source strength. The percentage varies with assembly burnup, enrichment, cooling time, and core zone cobalt content. The calculation of the hardware source strength percentage is discussed in Section 5.5.3 of the FuelSolutions™ Storage System FSAR. The data that is entered into ADSORB to calculate these percentages is described in that FSAR section.

Table 5.2-6 - Burnup-Specific Neutron Factors

Cooling Table Burnup Interval (GWd/MT)	Maximum Peaking Factor(1)	Subcritical Neutron Mult. Factor(2)	ADSORB Neutron Factor(3)
0-15	1.459	1.5	6.797
15-20	1.305	1.5	4.350
20-25	1.263	1.5	3.817
25-30	1.231	1.5	3.444
30-32	1.211	1.5	3.226
32-34	1.202	1.5	3.131
34-36	1.192	1.5	3.028
36-38	1.184	1.5	2.948
38-40	1.176	1.5	2.869

Notes:

(1) Maximum axial peaking factors for worst-case burnup profiles (reference 1) were fit to $PF=1.8983\cdot(BU)^{-0.1308}$ where BU is the average burnup in MWd/MT.

(2) All subcritical multiplication factors are based on a dry, fresh fuel assumption which yields $k_{eff}=0.33$. No credit is taken for burnup. The subcritical multiplication factor for all burnup groups is therefore 1/(1-0.33) = 1.5.

(3) The neutron peaking factor is equal to the maximum axial peaking factor to the fourth power times the subcritical multiplication factor. The overall neutron factor is applied to the neutron source term in ADSORB for each burnup group. This increases the neutron dose rate, thus increasing required cooling times for the specific burnup range.

This page intentionally left blank.

5.3 Model Specification

5.3.1 Description of the Shielding Configuration

The storage cask adjoint models are intended to derive a set of importance functions by energy group which relate the radiological source term inside the canister to a dose rate on the outside of the storage cask. This is accomplished using an R-θ slice through the storage cask at the midplane of the active fuel (or location of source peak). This way, the azimuthal peak can be determined (i.e., the point along the circumference of the "slice" with the highest dose rate). Figure 5.3-1 shows a sketch of the radial shielding configuration, along with the dose point location and significant shield dimensions used for the analysis.

The stacked upper and lower basket design of the W74 canister is properly accounted for in the analysis because the gamma and neutron source terms are multiplied by peaking factors. The R-θ model therefore represents a slice of an infinitely tall storage cask, which bounds the physical combination of a real W74 canister in the W150 Storage Cask.

The major modeling choices that relate to the shielding configuration are summarized in Table 5.3-1. The model includes a W74 canister with SNF assemblies. The assemblies are modeled as a homogenized volume (shaped like the perimeter of the fuel storage cells), which includes the fuel assembly with the canister guide sleeves (borated stainless steel, tubes, and wrappers) and canister air. A cylindrical region is modeled with no fuel present because the innermost storage cells are not loaded with fuel. The radius for the unfueled region is based on equivalent areas. All assembly hardware mass is conservatively neglected in the material mixture. The W74 canister spacer plates are conservatively neglected in the shielding models.

The canister shell is modeled as shown in Figure 5.3-1, but the storage cask thermal shield and guide rails are conservatively ignored. The storage cask steel liner and concrete are modeled as shown in Figure 5.3-1. Small voids in the W150 Storage Cask such as the liner joint, thermocouple wells, and segment joints are neglected in the model because they have a small area and are designed with dogleg paths to reduce radiation streaming.

The mesh point selected for adjoint response functions is selected on the basis of scoping "forward" runs. It is located on the surface of the storage cask directly off the corner assembly. The circumferential dose rate variation was noted to be about 25%; thus selecting the maximum dose point for adjoint fluxes introduces a small amount of conservatism in terms of the average storage cask dose rate.

For simplicity, the canister is modeled as being filled with air, as it is during canister closure. This has a negligible effect since the macroscopic cross-sections for air and helium (the canister fill gas) are both extremely small.

These models are used only for generating adjoint importance functions used to create the fuel cooling tables. There are no accident conditions modeled using the storage cask adjoint cases.

5.3.2 Shield Regional Densities

Section 5.3 of the FuelSolutions™ Storage System FSAR describes several mixtures used throughout the FuelSolutions™ shielding analyses. The densities for these standard materials, such as concrete, stainless steel, carbon steel, etc., are used in the W74 canister adjoint model.

Three canister-unique mixtures were created for the W74 canister adjoint model: the W74 SNF cells, the W74 support tube SNF cells (which have thicker tubes surrounding them and a slightly larger size), and the canister interstitial area outside those SNF cells. The assumptions for these mixtures are described above and in Table 5.3-1, and the regional densities are listed in Table 5.3-2.

Table 5.3-1 - FuelSolutions™ W74 Canister Adjoint Model Parameters

Parameter	Model	Comments
Model configuration	R-θ slice of W74 canister in a W150 storage cask	Suitable for desired adjoint response functions - corresponds to highest cask wall dose rate
Canister type	Conservative representation of W74M and W74T classes	See interstitial gaps below. Shield plug design variations not important to R-θ model
Fuel cells	Homogenized Big Rock Point SNF assembly (0.1421 MTIHM over 70 inches), stainless steel guide tube, neutron poison	Selected high-MTIHM fuel design for conservatism
Interstitial gaps	No shielding credit taken for spacer plates	Conservative modeling assumption

Table 5.3-2 - FuelSolutions™ W74 Canister-Specific Regional Densities

Component(1)	Standard Material(2)	Volume Fraction
Homogenized SNF Cell	UO_2	0.1925
	Zr-4/Zr-2	0.0772
	SS-316	0.0365
	Borated Stainless Steel	0.0102
	Air	0.6938

Notes:
(1) Canister-unique mixture. See Chapter 5 of the FuelSolutions™ Storage System FSAR for standard FuelSolutions™ materials.
(2) See Chapter 5 of the FuelSolutions™ Storage System FSAR for standard FuelSolutions™ materials.

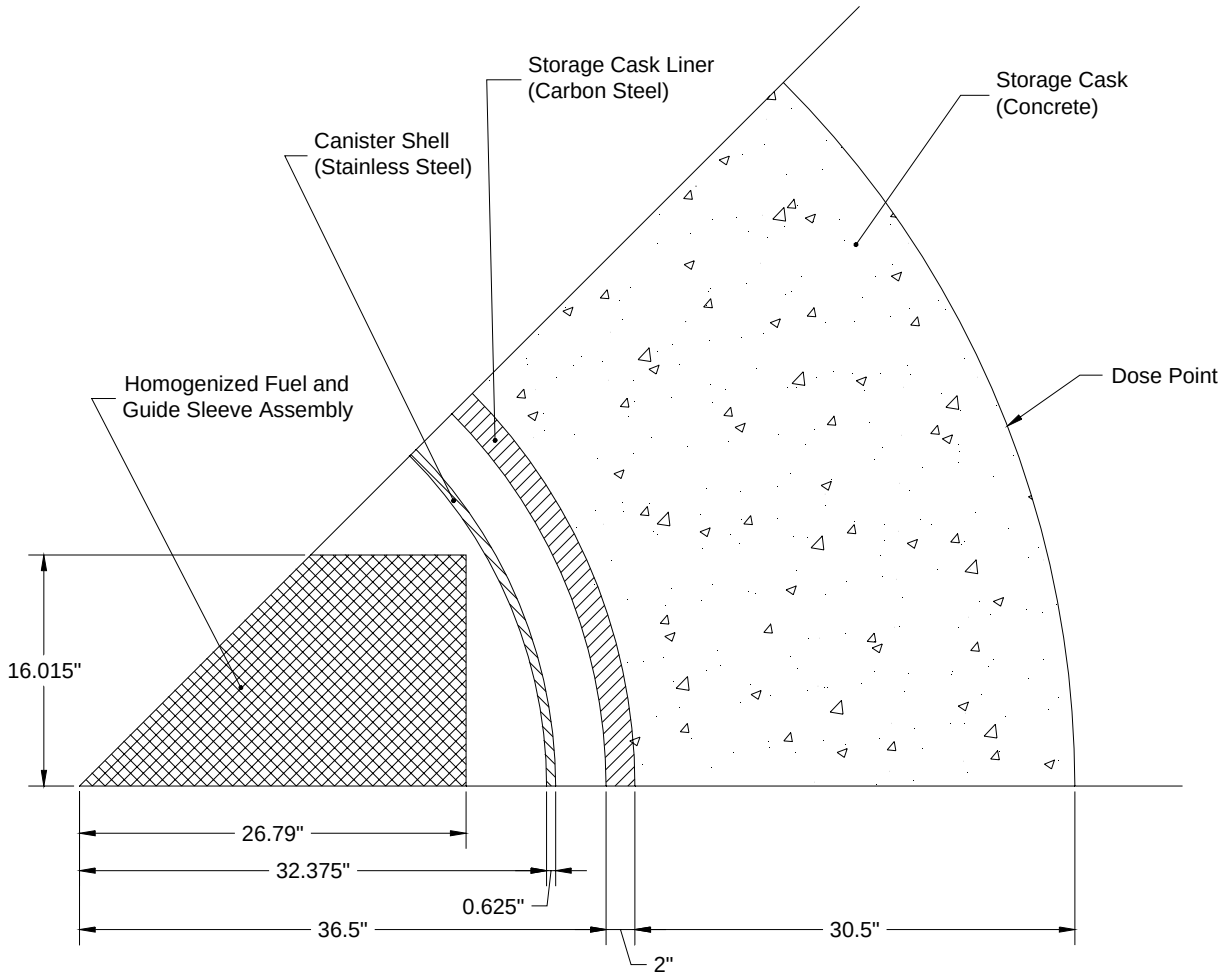

Figure 5.3-1 - FuelSolutions™ W74 Canister Adjoint Model

5.4 Shielding Evaluation

The information in this section is applicable to intact BRP UO_2 fuel as well as to partial and damaged UO_2 assemblies, as discussed in Sections 5.5.3 and 5.5.4 of this FSAR.

The shielding evaluation for MOX fuel is provided in Section 5.5.2.

5.4.1 W74 Canister Adjoint Calculation Methodology

An adjoint shielding model is used to obtain the importance functions for the FuelSolutions™ W74 canister. Chapter 5 of the FuelSolutions™ Storage System FSAR has a general description of the adjoint method and how the resulting response functions are used in constructing the fuel cooling tables.

The key parameters for the W74 adjoint model are presented in Table 5.4-1.

There is no spatial source distribution, since this model is an adjoint calculation. The active fuel region was assumed to be uniform, with all fuel cells homogenized as shown in Figure 5.3-1. Because this is an R-θ slice through the canister and storage cask, there is no axial source distribution and the end fitting regions are not modeled.

5.4.2 W74 Canister Adjoint Calculation Results

Three tables summarize the results of the W74 canister adjoint calculations, which are used to generate the fuel cooling tables and forward calculation representative dose rates for the W74 canister.

Table 5.4-2 shows the primary gamma adjoint importance function. These values represent the primary gamma ray dose rate, in mrem/hr at the side of the storage cask, which results from a one primary gamma ray per second per axial cm source term. To obtain the primary gamma dose rate at the storage cask surface, multiply each value in the Table 5.4-2 by the appropriate primary gamma group source term, then sum.

Table 5.4-3 shows the secondary gamma adjoint importance function. These values represent the secondary gamma ray dose rate, in mrem/hr at the side of the storage cask, which results from a one neutron per second per axial cm source term. To obtain the secondary gamma dose rate at the storage cask surface, multiply each value in the Table 5.4-3 by the appropriate neutron group source term, then sum.

Table 5.4-4 shows the neutron adjoint importance function. These values represent the neutron dose rate, in mrem/hr at the side of the storage cask, which results from a one neutron per second per axial cm source term. To obtain the neutron dose rate at the storage cask surface, multiply each value in the Table 5.4-4 by the appropriate neutron group source term, then sum.

These importance functions are used as input to ADSORB to generate the W74 canister cooling tables.

Table 5.4-1 - Key W74 Canister Adjoint Model Parameters

Parameter	Value
Computer Code	DORT[1]
Method of Solution	Adjoint
Mesh	204 (radial) x 90 (azimuthal) Octant R-θ Model
Cross-section Library	BUGLE-93[1] (20g,47n coupled)
Order of Expansion	P_3
Quadrature	Fully symmetric S_{16}
Source Term	ANSI-ANS-6.1.1-1977 response factors
Flux-to-Dose Factors	N/A for adjoint run

Notes:

(1) See Section 5.5 of the FuelSolutions™ Storage System FSAR for descriptions of the computer codes and cross-section libraries.

Table 5.4-2 - W74 Canister Primary Gamma Adjoint Importance Functions

BUGLE Group	Upper Energy (MeV)	mrem/hr per source particle/s-cm[(1)]
48	12.000	2.300E-09
49	9.000	1.847E-09
50	7.500	1.504E-09
51	6.500	1.119E-09
52	5.500	8.185E-10
53	4.500	4.940E-10
54	3.500	2.253E-10
55	2.500	5.407E-11
56	1.750	9.839E-12
57	1.250	1.376E-12
58	0.900	1.081E-13
59	0.750	2.320E-14
60	0.650	7.498E-15
61	0.500	1.345E-15
62	0.300	1.453E-17
63	0.150	1.477E-20
64	0.080	6.555E-21
65	0.045	1.845E-21
66	0.025	8.678E-22
67	0.015	1.474E-21

Note:

(1) Importance function units are mrem/hr primary gamma at the surface of the W150 Storage Cask per gamma/s-cm, where cm refers to the active fuel length.

Table 5.4-3 - W74 Canister Secondary Gamma Adjoint Importance Functions

BUGLE Group	Energy (MeV)	mrem/hr per Source Particle/s-cm[1]	BUGLE Group	Energy (MeV)	mrem/hr per Source Particle/s-cm[1]
1	1.576E+01	2.684E-08	25	2.402E-01	1.181E-08
2	1.320E+01	2.382E-08	26	1.471E-01	1.053E-08
3	1.111E+01	2.138E-08	27	8.924E-02	8.978E-09
4	9.304E+00	2.020E-08	28	5.412E-02	7.752E-09
5	8.008E+00	1.917E-08	29	3.635E-02	6.818E-09
6	6.737E+00	1.806E-08	30	2.894E-02	6.377E-09
7	5.516E+00	1.788E-08	31	2.512E-02	6.422E-09
8	4.322E+00	1.691E-08	32	2.303E-02	5.966E-09
9	3.345E+00	1.675E-08	33	1.845E-02	5.156E-09
10	2.869E+00	1.716E-08	34	1.107E-02	4.113E-09
11	2.596E+00	1.679E-08	35	5.228E-03	3.414E-09
12	2.416E+00	1.696E-08	36	2.470E-03	3.017E-09
13	2.356E+00	1.732E-08	37	1.019E-03	2.546E-09
14	2.289E+00	1.637E-08	38	3.342E-04	2.047E-09
15	2.076E+00	1.567E-08	39	1.579E-04	1.891E-09
16	1.787E+00	1.540E-08	40	6.928E-05	1.717E-09
17	1.503E+00	1.525E-08	41	2.397E-05	1.271E-09
18	1.178E+00	1.533E-08	42	7.860E-06	9.364E-10
19	9.117E-01	1.556E-08	43	3.450E-06	2.179E-09
20	7.818E-01	1.543E-08	44	1.366E-06	1.921E-09
21	6.754E-01	1.511E-08	45	6.452E-07	1.597E-09
22	5.530E-01	1.398E-08	46	2.570E-07	1.231E-09
23	4.334E-01	1.289E-08	47	5.001E-08	7.344E-10
24	3.330E-01	1.252E-08			

Note:

(1) Response function units are mrem/hr secondary gamma at the surface of the W150 Storage Cask per neutron/s-cm, where cm refers to the active fuel length.

Table 5.4-4 - W74 Canister Neutron Adjoint Importance Functions

BUGLE Group	Energy (MeV)	mrem/hr per Source Particle/s-cm[1]	BUGLE Group	Energy (MeV)	mrem/hr per Source Particle/s-cm[1]
1	1.576E+01	8.244E-08	25	2.402E-01	1.792E-11
2	1.320E+01	5.847E-08	26	1.471E-01	1.294E-11
3	1.111E+01	4.916E-08	27	8.924E-02	7.971E-12
4	9.304E+00	4.529E-08	28	5.412E-02	5.438E-12
5	8.008E+00	4.427E-08	29	3.635E-02	4.014E-12
6	6.737E+00	4.291E-08	30	2.894E-02	3.599E-12
7	5.516E+00	3.132E-08	31	2.512E-02	3.577E-12
8	4.322E+00	1.522E-08	32	2.303E-02	3.127E-12
9	3.345E+00	1.218E-08	33	1.845E-02	2.355E-12
10	2.869E+00	1.024E-08	34	1.107E-02	1.481E-12
11	2.596E+00	9.612E-09	35	5.228E-03	9.532E-13
12	2.416E+00	9.069E-09	36	2.470E-03	6.505E-13
13	2.356E+00	7.966E-09	37	1.019E-03	4.164E-13
14	2.289E+00	4.552E-09	38	3.342E-04	1.908E-13
15	2.076E+00	1.081E-09	39	1.579E-04	1.314E-13
16	1.787E+00	4.029E-10	40	6.928E-05	8.451E-14
17	1.503E+00	1.906E-10	41	2.397E-05	3.721E-14
18	1.178E+00	9.517E-11	42	7.860E-06	1.646E-14
19	9.117E-01	7.870E-11	43	3.450E-06	1.136E-14
20	7.818E-01	6.923E-11	44	1.366E-06	6.756E-15
21	6.754E-01	5.971E-11	45	6.452E-07	2.350E-15
22	5.530E-01	3.550E-11	46	2.570E-07	7.443E-16
23	4.334E-01	2.398E-11	47	5.001E-08	1.188E-17
24	3.330E-01	2.166E-11			

Note:

(1) Response function units are mrem/hr neutron at the surface of the W150 Storage Cask per neutron/s-cm, where cm refers to the active fuel length.

This page intentionally left blank.

5.5 Supplemental Data

Supplemental data used for the FuelSolutions™ W74 canister shielding evaluation, such as flux-to-dose conversion factors and descriptions of computer codes, are described in Chapter 5 of the FuelSolutions™ Storage System FSAR.

5.5.1 Fuel Cooling Table Domains

Table 5.5-4 and Table 5.5-5 provide general information regarding the cooling tables. They indicate whether heat ("Q") or radiological dose ("D") controls the required cooling time for each statepoint in the cooling tables.

5.5.2 BRP Mixed-Oxide (MOX) Fuel Assembly Qualification

The BRP fuel assembly inventory contains a number of MOX fuel assemblies. To qualify these fuel assemblies for the FuelSolutions™ W74 canister, calculations are performed to determine bounding gamma and neutron source strengths. These source strengths are compared to the set of UO_2 fuel assembly gamma and neutron source strengths that correspond to one of the locations (i.e., burnup-enrichment pairs) in the base cooling table (Table 5.2-1).

All BRP UO_2 fuel assemblies with the combinations of burnup, cooling time, and initial enrichment given in Table 5.2-1 are shown to meet all radiological and thermal requirements for storage in the FuelSolutions™ W74 canister. Thus, the gamma and neutron source strengths that occur for any of the points in the cooling table are shown to be acceptable. If it is shown that the maximum gamma and neutron source strengths for all BRP MOX fuel are bounded by the gamma and neutron source strengths that occur for BRP UO_2 fuel at any one of the locations in the cooling table, then all BRP MOX fuel is radiologically qualified for storage in the FuelSolutions™ W74 canister.

The cooling table statepoint (i.e., combination of burnup and enrichment) that is chosen for comparison with BRP MOX fuel is the point at the lower left corner of Table 5.2-1. This statepoint has a burnup of 40 GWd/MTU, an initial enrichment of 1.5 w/o ^{235}U, and a cooling time of 5.6 years. This cooling table statepoint was chosen because it has the highest neutron source strength of all cooling table statepoints. Thus, this case is most likely to bound the relatively high neutron source strength of the MOX fuel. This statepoint has the lowest gamma source strength, but it still bounds the gamma source strengths of all BRP MOX fuel, which have a minimum cooling time of 15 years for G-Pu and 22 years for DA/J2 type fuels.

For these MOX fuel comparison analyses, the cooling time of 5.6 years is rounded up to six years. Thus, the MOX fuel source terms are compared to source terms for 40 GWd/MTU, 1.5 w/o ^{235}U, six year cooled, UO_2 fueled BRP assemblies. This is conservative since the six year UO_2 fuel source terms are lower than the actual cooling table statepoint (5.1 year cooled) source terms.

The first step in the process is to calculate bounding gamma and neutron source strengths for the inventory of BRP MOX fuel assemblies.

There are three BRP MOX fuel assembly designs, the J2 (9x9) assembly, the DA (11x11) assembly, and the G-Pu (11x11) assembly. These assemblies are described in detail in

Section 6.6.1 of this FSAR. The BRP MOX assembly arrays contain a mixture of one or more types of MOX fuel rods and UO_2 fuel rods of multiple ^{235}U enrichment levels. Figures 6.6-1 through 6.6-3 of this FSAR illustrate the fuel rod array for the three MOX fuel assembly types. The locations of the different rod types are shown, along with their ^{235}U enrichment levels and their fuel material plutonium weight fractions.

Point-depletion calculations are performed with the ORIGEN 2.1 code[2] to determine bounding fuel gamma and neutron source strengths for each of the three MOX fuel assembly designs. The ORIGEN 2.1 calculations are performed using the BWRPUU.LIB cross-section library. This ORIGEN 2.1 cross-section library is tailored to model a mixture of plutonium and uranium fuels within a BWR reactor. This best characterizes BRP MOX fuel, which contains a mixture of MOX and UO_2 fuel pins.

As input, ORIGEN 2.1 requires the burnup level of the fuel material along with the mass of each uranium and plutonium isotope within the fuel assembly. An assembly thermal power level (during reactor operation) is also required in units of MW/assembly. The user must also enter the length of the irradiation period, which is simply determined by dividing the assembly's final burnup level (in MWd/MTIHM) by the assembly thermal power (in MW/assembly), and multiplying the result by the assembly heavy metal loading (in MTIHM/assembly). The BWRPUU.LIB cross-section library includes the effects of assembly geometry, based on a typical BWR assembly.

The ORIGEN 2.1 code can model outage periods of reactor operation. These analyses conservatively exclude any such outage periods. This maximizes source strengths since radionuclide decay during reactor outage periods is neglected.

Table 5.5-1 shows the maximum assembly burnup level, the assembly power level (during reactor operation), the total assembly heavy metal loading, and the total (per assembly) mass of each significant plutonium and uranium isotope for each of the three BRP MOX fuel assembly designs. Table 5.5-1 contains all of the data required to perform the ORIGEN 2.1 runs for the three BRP MOX fuel assembly types. The irradiation period can be determined by multiplying the burnup level by the assembly heavy metal quantity and dividing by the assembly power level.

Based on the parameters given in Table 5.5-1, the ORIGEN 2.1 code calculates fuel gamma and neutron source strengths on a per assembly basis, as a function of assembly cooling time, for each of the three BRP MOX fuel assembly designs. As specified in the *technical specifications* in Section 12.3 of this FSAR, the minimum cooling time for all BRP J2 and DA assemblies is 22 years. The minimum cooling time for G-Pu assemblies is 15 years. Based on these minimum cooling times, gamma and neutron source strengths are determined for each of the three assembly types.

Table 5.5-2 shows the bounding total fuel gamma source strengths of each of the three BRP MOX fuel assembly types on a gammas/sec-assembly basis. The gamma source strengths are presented in the ORIGEN energy group structure. The fuel gamma source strength that

[2] BWRPUU.LIB, *ORIGEN 2.1 - Isotope Generation and Depletion Code, Matrix Exponential Method*, RSICC Computer Code Collection CCC-371, OakRidge National Laboratory, February 1996.

corresponds to 40 GWd/MTU, 1.5 w/o enriched, six year cooled, UO_2 fueled assemblies is also presented in Table 5.5-2 for comparison.

The Table 5.5-2 data show that the BRP UO_2 fuel gamma source strength (from the selected statepoint in Table 5.2-1) bounds that of all BRP MOX fuel assemblies for every gamma energy line. The G-Pu MOX fuel assembly, which produces the highest MOX fuel gamma source strengths, has an assembly heavy metal loading of 0.127 MTIHM, as opposed to the uranium loading of 0.138 MTIHM used for the design basis UO_2 assembly source strengths shown in Table 5.5-2. Note that Table 5.2-1 is based on cask external dose rates that have been conservatively adjusted upwards by 3% to cover fuel with uranium loadings up to 0.1421 MTIHM.

Thus, on a gammas/sec-MTIHM basis, the G-Pu assembly gamma source strengths are slightly higher relative to those of the UO_2 fueled assembly than they are on a per assembly basis. However, even on a gammas/sec-MTIHM basis, the BRP UO_2 fueled assembly gamma source strengths still completely bound the highest BRP MOX fuel gamma source strengths for every gamma energy line.

The MOX assembly source term analyses are based on representative isotope masses and total heavy metal loadings. Some G-Pu assemblies have slightly higher overall metal masses. Other G-Pu assemblies have had UO_2 fuel rods added to one or more array corner locations (the design basis assembly array has empty corner locations). For these reasons, some G-Pu assemblies have a total heavy metal loading of up to 0.131 MTIHM. This corresponds to a ~3% increase over the heavy metal mass modeled in the G-Pu source term analyses. However, as shown in this section, the G-Pu MOX fuel source terms are bounded by the design basis (UO_2) values by margins of much more than 3%. Furthermore, as discussed above, the BRP MOX fuel source terms per MTIHM of fuel are shown to be less than that of design basis UO_2 BRP fuel. Therefore, the per assembly MOX fuel source terms are bounded by the design basis values for MOX assembly heavy metal loadings up to 0.1421 MTIHM/assembly.

Thus, the fuel gamma source strength for 40 GWd/MTU, 1.5 w/o enriched, six year cooled, BRP UO_2 fuel bounds the fuel gamma source strengths of all BRP MOX fuel assemblies by a significant margin. The primary reason the fuel gamma source strengths of the BRP MOX fuel assemblies are significantly lower than those of design basis UO_2 fuel assemblies is that they have longer cooling times (at least 15 years) than the cooling times shown in Table 5.2-1.

It is assumed that the assembly hardware activation gamma sources for the BRP UO_2 fueled assemblies bound those of all BRP MOX fuel assemblies. ORIGEN 2.1 calculates fuel gamma source strengths for MOX fuel that are not significantly different from those of UO_2 fuel with a similar burnup and cooling time. Therefore, the level of hardware activation is not expected to be significantly different either. Since BRP MOX fuel assemblies have cooling times that are at least nine years longer than those for BRP UO_2 fuel, and since the assembly hardware gamma sources (which are almost entirely due to ^{60}Co) decay with a half-life of approximately five years, the MOX fuel assembly hardware gamma sources will be bounded by those of BRP UO_2 fueled assemblies.

Table 5.5-3 shows the maximum total neutron source strengths (per assembly) for each of the three BRP MOX fuel assembly types. The neutron source strength for 40 GWd/MTU, 1.5 w/o enriched, six year cooled, UO_2 fueled BRP assemblies is shown for comparison. The per

assembly neutron source strengths are also converted into per MTIHM neutron source strengths, based on the assembly heavy metal loading data given in Table 5.5-1, and on a BRP assembly loading of 0.138 MTIHM/assembly. These per MTIHM neutron source strengths are also presented in Table 5.5-3.

The neutron energy spectrum given in Section 5.2 is assumed to apply for MOX fuel assemblies as well as UO_2 assemblies. Spontaneous fission of ^{244}Cm is the primary source of neutrons for both MOX and UO_2 fuel, so a similar neutron source spectrum is expected. The axial burnup profile is also assumed not to be significantly different for MOX fuel, versus UO_2 fuel. A similar burnup profile is expected because the MOX and UO_2 BRP fuel assemblies have the same physical dimensions and they are irradiated in the same reactor core. Given a similar energy spectrum and axial source strength profile, cask exterior neutron dose rates are directly proportional to the total neutron source strengths presented in Table 5.5-3.

The total neutron source strengths shown and compared in Table 5.5-3 do not include the effects of the axial burnup profile or sub-critical neutron multiplication. These effects significantly increase the total assembly neutron source strength. These effects are included in the neutron source strengths used in the W74 canister shielding calculations. For the purposes of comparing MOX and UO_2 fuel neutron source strengths, however, the unadjusted neutron source strengths (taken directly from the ORIGEN 2.1 code) are used.

Table 5.5-3 shows that the per assembly neutron source strength for 40 GWd/MTU, 1.5 w/o enriched, six year cooled, UO_2 fueled BRP fuel bounds that of all BRP MOX fuel assembly types. The neutron source strengths for BRP MOX fuel are also bounded on a per MTIHM basis.

Thus, the gamma and neutron source strengths for 40 GWd/MTU, 1.5 w/o enriched, six year cooled, BRP UO_2 fuel completely bound the gamma and neutron source strengths of all existing BRP MOX fuel assemblies. As discussed in Section 5.2, the W74 shielding calculations show that all radiological requirements are met for all statepoints (i.e., all combinations of burnup, enrichment, and cooling time) in the W74 cooling tables.

Since BRP UO_2 fuel at the cooling table statepoint described above is known to meet all radiological requirements, and since the gamma and neutron source strengths of all BRP MOX fuel assemblies are completely bounded by those of such UO_2 fuel assemblies, then all BRP MOX fuel assemblies are known to meet all radiological requirements. Therefore, all existing BRP MOX fuel assemblies are radiologically qualified for storage in the FuelSolutions™ W74 canister.

Two UO_2 BRP assemblies contain two inserted MOX fuel rods, as illustrated in Figure 6.6-4 of this FSAR. The source terms for these assemblies are assumed to be bounded by the design basis UO_2 BRP fuel source terms (for 40 GWd/MTU, 1.5% enriched, 5.6 year cooled fuel) for the following reasons:

- Out of a total of 77 rods, the assemblies each have only two MOX fuel rods.
- By the analyses presented herein, BRP MOX fuel rods have been shown to have lower source terms than design basis BRP UO_2 fuel rods.
- The two assemblies will have a cooling time of over 25 years at the time of loading.
- The two assemblies have a low burnup level (under 20 GWd/MTU).

5.5.3 BRP Partial Fuel Assembly Qualification

Partial fuel assemblies have one or more fuel rods missing from the design basis assembly array. A number of partial BRP assemblies are known to exist.

The gamma and neutron source strengths per MTU of BRP fuel are a function of the burnup, cooling time, and initial enrichment of the fuel. The W74 canister shielding calculations are based on these per MTU source strengths and an upper bound BRP assembly uranium loading of 0.1421 MTU/assembly. A larger assembly uranium loading yields a proportionally larger gamma and neutron source strength on a per assembly basis. Shielding sensitivity calculations show that the increase in gamma and neutron source strengths causes an increase in cask surface gamma and neutron dose rates, despite the increase in assembly self-shielding due to the increased uranium mass. Thus, assuming a maximum assembly uranium loading is conservative.

Removing fuel rods from the assembly array reduces the assembly uranium loading. The gamma and neutron source strengths for each fuel rod remain the same for a given assembly burnup, cooling time, and initial enrichment. Thus, partial fuel assemblies are equivalent to assemblies with a lower uranium loading. Their uranium mass is lower and their gamma and neutron source strengths are proportionally lower. For a given set of fuel parameters, for both partial assemblies and low uranium loading assemblies, the gamma and neutron source strengths per MTU of fuel are the same as those of the (maximum loading) design basis BRP fuel assembly. As discussed above, lower uranium loading assemblies are shown by calculation to produce lower cask external dose rates, for a given burnup, enrichment, and cooling time. Therefore, partial BRP assemblies produce lower cask external dose rates than intact BRP fuel assemblies.

For the above reasons, the W74 shielding analyses, which are based on intact BRP fuel assemblies with an upper bound uranium loading, are bounding for all partial BRP fuel assemblies. Therefore, the required cooling times given in the W74 canister cooling table (Table 5.2-1) apply for both intact and partial BRP fuel assemblies.

5.5.4 BRP Damaged Fuel Assembly Qualification

Damaged assemblies are assemblies with damage in excess of pinhole leaks or hairline cracks.[3] Fuel assemblies with damaged grid spacers (defined as damaged to a degree where fuel rod structural integrity cannot be assured, or where grid spacers have shifted vertically from their design position) will also be stored in damaged fuel cans.

All BRP assemblies classified as damaged must be placed inside a damaged fuel can, which is then loaded into one of the eight support tube locations of the W74 basket. The damaged fuel can is similar to a W74 canister guide tube, with 0.09 inch thick stainless steel walls and 0.075 inch thick borated stainless steel poison sheets attached to each of the four walls.

With respect to all assembly parameters that affect shielding, damaged fuel assemblies must meet all of the same limitations as intact assemblies. The required cooling times presented in the W74 canister cooling tables apply for both damaged and undamaged (i.e., intact or partial) BRP fuel assemblies.

[3] ISG-1, *Damaged Fuel*, Spent Fuel Project Office Interim Staff Guidance, United States Nuclear Regulatory Commission, November 1998.

Assembly damage does not affect the quantity of fuel or assembly hardware materials, or the radiation source strengths of a given quantity of fuel or hardware materials. Thus, assembly damage does not affect the radiation source strengths. Bent fuel rods would not significantly affect the source strength distribution. Therefore, the shielding analyses for intact BRP assemblies are applicable for damaged BRP assemblies.

If some fuel rods in a damaged assembly have missing pellets or sections that have broken off, they effectively have a missing rod over some section of the axial length. As discussed in Section 5.5.3, assemblies with missing rods have lower source terms than design basis assemblies and are, therefore, bounded by the intact assembly shielding analyses.

Furthermore, damaged fuel assemblies must be placed in the damaged fuel cans which have stainless steel walls and borated stainless steel poison sheets. These damaged fuel can materials provide additional shielding within the canister interior that is not present for canisters loaded with intact fuel. Due to this additional shielding, the dose rates for canisters containing damaged fuel are bounded by those calculated for the intact fuel case.

Rod fragments and/or loose pellets (i.e., fuel debris) are not qualified for loading into the damaged fuel cans in the W74 canister.

To be placed inside the damaged fuel cans, fuel assemblies designated as damaged must be "handleable." The assemblies must have sufficient structural integrity to support their own weight so they will not collapse into rubble while they are stored in the canister.

There are no known credible normal or off-normal condition events, such as cask drops, that produce significant loads on the assembly. Since these fuel assemblies are expected to maintain their overall configuration during normal and off-normal conditions of storage, the fuel assembly material and associated radiation source strengths will remain evenly distributed throughout the damaged fuel can interior volume. Given that this is the case, and given that fuel debris is not qualified for storage, the design basis shielding analyses will remain bounding for all allowable damaged fuel can contents.

Unlike intact fuel assemblies, fuel assemblies designated as damaged have the potential to collapse into rubble after a cask drop event (i.e., under accident conditions). Therefore, under accident conditions, the effects of a solid pile of rubble inside the damaged fuel can must be considered.

The shielding requirements for accident conditions are that the total dose at the controlled area boundary not exceed 5000 mrem over the duration of the accident event. Assuming a period of one week to mitigate the cask drop event (i.e., unload the cask, put temporary shielding in place, etc.), this corresponds to a dose rate of 30 mrem/hr at the controlled area boundary. Under normal conditions, the entire ISFSI must produce only 25 mrem/year at the controlled area boundary, with a single cask yielding significantly less than that. Assuming a 2000 hour/year occupancy factor at the boundary, this corresponds to a dose rate of 0.0125 mrem/hr (a higher occupancy factor would correspond to an even lower dose rate). Thus, the dose rate from the dropped cask would have to increase by over a factor of 1000 from its design basis normal condition value before the accident condition dose rate limit is exceeded.

An assembly collapsing into a pile of rubble will not cause the cask exterior dose rates to increase by a factor of 1000 for the following reasons. Dose rates at a distance from the cask

(such as at the controlled area boundary) are governed by the total source strength inside the cask, as opposed to its distribution within the cask. Since the total radiation source of the collapsed assembly is the same as that of the uncollapsed assembly, the dose rates at a distance from the cask will not change.

Table 5.5-1 - ORIGEN 2.1 Data for BRP MOX Fuel Assemblies

Assembly Parameter	J2 Assembly Value	DA Assembly Value	G-Pu Assembly Value
Maximum Burnup (GWd/MTIHM)	22.82	21.85	34.22
Assembly Thermal Power (MW/assy.)	2.86	2.86	2.86
Total Heavy Metal Loading (MT/assy.)(1)	0.124	0.126	0.127
^{235}U Quantity (gram/assembly)(1)	3193	2714	3926
^{238}U Quantity (gram/assembly)(1)	119,409	121,205	122,041
^{239}Pu Quantity (gram/assembly)(1)	1072	1354	1074
^{240}Pu Quantity (gram/assembly)(1)	280	328	249
^{241}Pu Quantity (gram/assembly)(1)	81	122	108
^{242}Pu Quantity (gram/assembly)(1)	16	30	23

Note:

(1) Representative value for assemblies of that type. Small variations in these masses (on the order of one percent) may occur between individual BRP MOX assemblies. The analyses are still applicable for all assemblies of each type, as discussed in Section 5.5.2.

Table 5.5-2 - BRP MOX Fuel Gamma Source Strengths

ORIGEN Group	Upper Energy (MeV)	Lower Energy (MeV)	Average Energy (MeV)	22 Year Old J2 MOX Fuel Source (g/s-assy.)	22 Year Old DA MOX Fuel Source (g/s-assy.)	15 Year Old G-Pu MOX Fuel Source (g/s-assy.)	Design Basis BRP Assy. Fuel Source (g/s-assy.)
1	0.0	0.02	0.01	1.12E+14	1.04E+14	2.01E+14	3.66E+14
2	0.02	0.03	0.025	2.19E+13	2.01E+13	4.01E+13	8.40E+13
3	0.03	0.045	0.0375	2.73E+13	2.57E+13	5.18E+13	1.04E+14
4	0.045	0.07	0.0575	2.78E+13	2.75E+13	4.30E+13	7.13E+13
5	0.07	0.1	0.085	1.18E+13	1.09E+13	2.25E+13	4.75E+13
6	0.1	0.15	0.125	9.35E+12	8.65E+12	2.08E+13	5.41E+13
7	0.15	0.3	0.225	9.84E+12	8.66E+12	1.87E+13	3.75E+13
8	0.3	0.45	0.375	4.11E+12	3.71E+12	7.91E+12	2.25E+13
9	0.45	0.7	0.575	1.97E+14	1.91E+14	3.56E+14	8.03E+14
10	0.7	1.0	0.85	2.95E+12	2.82E+12	1.27E+13	1.88E+14
11	1.0	1.5	1.25	2.58E+12	2.50E+12	9.21E+12	8.76E+13
12	1.5	2.0	1.75	8.68E+10	8.35E+10	2.87E+11	1.23E+12
13	2.0	2.5	2.25	7.44E+06	8.59E+06	1.78E+08	2.28E+11
14	2.5	3.0	2.75	1.01E+07	1.11E+07	4.95E+07	1.27E+10
15	3.0	4.0	3.5	2.51E+06	3.17E+06	1.21E+07	1.67E+09
16	4.0	6.0	5.0	1.06E+06	1.35E+06	4.26E+06	1.56E+07
17	6.0	8.0	7.0	1.23E+05	1.55E+05	4.91E+05	1.79E+06
18	8.0	11.0	9.5	1.41E+04	1.78E+04	5.64E+04	2.07E+05
Total Gamma Source				4.26E+14	4.06E+14	7.84E+14	1.87E+15

Table 5.5-3 - BRP MOX Assembly Total Neutron Source Strengths

Assembly Type	Max Burnup (GWd/MTU)	Cooling Time (years)	Neutron Source Strength	
			(n/sec-assembly)	(n/sec-MTIHM)
J2 MOX Assembly	22.82	22	2.512E+07	2.025E+08
DA MOX Assembly	21.85	22	3.169E+07	2.519E+08
G-Pu MOX Assembly	34.22	15	9.861E+07	7.738E+08
Limiting UO_2 Assembly	40.00	6	3.594E+08	2.604E+08

Table 5.5-4 - Fuel Cooling Table W74-1-A Domains

Maximum Burnup (MWd/MTU)	Required Minimum Cooling Time (yr.)					
	Minimum Average Initial Enrichment (w/o ^{235}U)					
	1.5	2.0	2.5	3.0	3.5	4.0
15,000	D	D	D	D	D	D
20,000	D	D	D	D	D	D
25,000	D	D	D	D	D	D
30,000	D	D	D	D	D	D
32,000	D	D	D	D	D	D
34,000	Q	D	D	D	D	D
36,000	Q	Q	Q	Q	Q	Q
38,000	Q	Q	Q	Q	Q	Q
40,000	Q	Q	Q	Q	Q	Q

Notes:

(1) "Q" indicates that the statepoint is controlled by heat generation. "D" indicates that the statepoint is controlled by radiological dose.

Table 5.5-5 - Fuel Cooling Table W74-1-B Domains

Maximum Burnup (MWd/MTU)	Required Minimum Cooling Time (yr.) Minimum Average Initial Enrichment (w/o ^{235}U)					
	1.5	2.0	2.5	3.0	3.5	4.0
15,000	D	D	D	D	D	D
20,000	D	D	D	D	D	D
25,000	D	D	D	D	D	D
30,000	D	D	D	D	D	D
32,000	D	D	D	D	D	D
34,000	D	D	D	D	D	D
36,000	D	D	D	D	D	D
38,000	D	D	D	D	D	D
40,000	D	D	D	D	D	D

Notes:

(2) "Q" indicates that the statepoint is controlled by heat generation. "D" indicates that the statepoint is controlled by radiological dose.

This page intentionally left blank.

6. CRITICALITY EVALUATION

This chapter presents an evaluation that demonstrates that the FuelSolutions™ W74 canister meets the criticality safety requirements of 10CFR72[1] and is acceptable for use as an integral part of the FuelSolutions™ SFMS. The FuelSolutions™ W74 canister satisfies the criticality safety acceptance criteria stated in Chapter 6 of the FuelSolutions™ Storage System FSAR.[2] The criticality safety evaluation for the FuelSolutions™ W74 canister presented in this chapter further demonstrates the following:

- The effective neutron multiplication factor (k_{eff}), including all biases and uncertainties at a 95% confidence level, does not exceed 0.95 under all credible normal, off-normal, and accident conditions.
- No credible event or sequence of events could cause criticality in the FuelSolutions™ W74 canister, because the maximum allowable enrichment specified for the W74 bounds the maximum planar-averaged enrichment for all fuel assemblies in the Big Rock Point (BRP) spent fuel inventory.

In addition to presenting the evaluations necessary to demonstrate that the criticality safety criteria are satisfied, this chapter describes FuelSolutions™ W74 canister criticality control design features, specifies the limiting characteristics for fuel assembly acceptance, and documents the criticality analysis method verification. The general approach used to perform the criticality safety evaluation for the FuelSolutions™ W74 canister is described in Chapter 6 of the FuelSolutions™ Storage System FSAR.

[1] Title 10, U.S. Code of Federal Regulations, Part 72 (10CFR72), *Licensing Requirements for the Independent Storage of Spent Nuclear Fuel and High Level Radioactive Waste*, 1995.

[2] WSNF-220, *FuelSolutions™ Storage System Final Safety Analysis Report*, NRC Docket No. 72-1026, BNFL Fuel Solutions Corporation.

This page intentionally left blank.

6.1 Discussion and Results

The FuelSolutions™ W74 canister design is based on both favorable geometry and fixed borated neutron absorber materials (poison). The criticality safety evaluation credits only 75% of the manufacturer's minimum assured boron content and the continued efficacy of fixed neutron absorber materials is demonstrated.

To qualify for storage in the FuelSolutions™ W74 canister, BRP fuel assemblies must meet the fuel acceptance criteria listed in Table 6.1-1. The maximum allowable assembly average enrichment is 4.1 weight percent (w/o) ^{235}U. The ^{235}U enrichment limit is derived from calculations that demonstrate the highest calculated k_{eff}, less than or equal to 0.95, that might occur under any design condition involving loading, closure, on-site transfer, and dry storage. This maximum allowable enrichment value applies for all intact UO_2 fueled BRP assemblies. The assembly average enrichment is defined as the average enrichment of the existing fuel rods in the assembly array. If this average enrichment varies with axial position, the highest value that occurs for any axial position is used.

Since the BRP fuel assemblies contain multiple pin enrichments, a maximum pin-weighted average enrichment is calculated considering all radial cross-sections along the axis of the assembly. The maximum pin-weighted enrichment is then compared to the enrichment limit specified in Table 6.1-1 to verify fuel acceptance. As shown in Figure 6.3-1, loading of up to 64 fuel assemblies is permitted in the FuelSolutions™ W74 basket guide tube locations.

The BRP criticality evaluation includes analyses for the Siemens 11x11 and General Electric/Siemens 9x9 fuel assembly designs. Based on case studies (see Section 6.4) involving all BRP fuel configurations, the Siemens 11x11 fuel assembly design is established to be the most reactive in the FuelSolutions™ W74 canister. Therefore, the Siemens 11x11 fuel assembly design is used to establish the maximum allowable ^{235}U enrichment for the storage of BRP fuel in the W74 canister.

The only difference between the three analyzed 11x11 BRP assembly configurations is the number of solid zircaloy pins in the fuel rod array (1, 2, or 4). The three analyzed 9x9 BRP assembly configurations are: a case with no water holes in the array, a case with one water hole in the array center, and a case with one water hole with a pellet diameter of 0.4715 inches (as opposed to 0.471 inches). The 9x9 and 11x11 assembly arrays are otherwise identical to each other.

The analyses show that all of the configurations meet the criticality requirements, and that replacing fuel rods with solid zircaloy rods always causes k_{eff} to decrease. For this reason, the specifications simply state that 11x11 assemblies with any number of solid zircaloy rods are qualified for storage.

The analyses assume a uniform rod enrichment assembly array with fuel rods in all four corners. As discussed in Section 6.6.2, this assumption is bounding for assemblies with any number of fuel rods missing from the four array corner locations. Thus, the intact assembly analyses are applicable for assemblies with any number of array corner fuel rods. The number of non-corner water holes specified in Table 6.1-1 is the number of non-corner water holes that determines whether an assembly is classified as intact or partial (as discussed below).

Specific criticality analyses are performed for all existing intact and partial BRP mixed-oxide (MOX) assemblies. The MOX fuel criticality analyses described in Section 6.6.1 show that all existing BRP MOX fuel assemblies are significantly less reactive than the design basis 4.1 w/o enriched UO_2 assemblies. Thus, all existing BRP MOX fuel assemblies are qualified for loading into the W74 canister.

Section 6.6.2 determines a separate enrichment criterion for partial BRP assemblies that have fuel rods missing from the design basis assembly configuration. Since BRP assemblies are under-moderated, partial assemblies may be significantly more reactive than intact assemblies. The maximum allowable assembly average enrichment values for BRP partial assemblies are 3.55 w/o (GE 9x9) and 3.6 w/o (Siemens 11x11), versus the 4.1 w/o value established for all intact BRP assemblies. As discussed in Section 6.6.2, the lower enrichment limits only apply for BRP assemblies with fuel rods missing from locations other than the four corner locations of the rod array. Also, the 4.1 w/o enrichment limit still applies for 9x9 BRP assemblies that have up to one fuel rod missing from non-corner locations.

Criticality analyses for damaged BRP fuel assemblies are described in Section 6.6.3. These analyses model damaged fuel cans inside each of the eight W74 canister support tubes. The damaged fuel cans have stainless steel walls, each of which has an attached borated stainless steel poison sheet. Each damaged fuel can contains a damaged BRP fuel assembly. The analyses model optimum configurations of fissile material inside each damaged fuel can. The analyses establish a maximum allowable fuel material enrichment (for any given fuel pellet within the assembly) of 4.61 w/o for the W74 damaged fuel can contents. As discussed in Section 6.6.3, the analyses also qualify all combinations of enriched uranium and plutonium that exist for the fuel material in BRP MOX fuel assemblies. Thus, both damaged MOX and damaged UO_2 BRP assemblies are qualified for loading into the damaged fuel cans.

Since the damaged fuel analyses model (and establish) the most reactive possible configuration of fissile material within the damaged fuel cans, undamaged assemblies, including assemblies that do not meet the dimensional parameter specifications for BRP fuel, may be loaded into the W74 canister damaged fuel cans. The maximum fuel pellet enrichment value of 4.61 w/o applies for all such assemblies. Such assemblies would have to physically fit inside the damaged fuel can. They would also have to meet the overall assembly weight and uranium loading specifications for BRP fuel in order to satisfy structural, thermal, and shielding requirements.

Table 6.1-1 - W74 Canister Fuel Specification for Big Rock Point

Fuel Assembly Array	GE 9x9	Siemens 9x9	Siemens 11x11	Siemens 11x11
Clad Material	Zr	Zr	Zr	Zr
Initial ^{235}U Enrichment(1)	≤ 4.10	≤ 4.10	≤ 4.10	≤ 4.10
Pellet Stack UO_2 Density	≤ 96.5%	≤ 96.5%	≤ 96.5%	≤ 96.5%
Number of Fuel Rods	≤ 81	≤ 81	≤ 121	≤ 121
Clad O.D. (in)	0.5625	0.5625	0.449	0.449
Clad Thickness (in)	0.040	0.040	0.034	0.034
Pellet Diameter (in)	0.471	0.4715	0.3715	0.3735
Fuel Rod Pitch (in)	0.707	0.707	0.577	0.577
Active Fuel Length (in)	≤ 70	≤ 70	≤ 70	≤ 70
Number of Non-Corner Water Holes(2)	≤ 1	0	0	0
Number of Inert Rods(3)	≥ 0	≥ 0	≥ 0	≥ 0
Bottom Tie Plate Height (in)	≥ 1.25	≥ 1.25	≥ 1.25	≥ 1.25

Notes:

(1) To qualify BRP fuel assemblies that have multiple pin enrichments, a maximum pin-weighted average enrichment is calculated considering all radial cross-sections along the axis of the assembly. The maximum pin-weighted enrichment is compared to the specified enrichment limit to verify fuel acceptance. No individual pin enrichment shall exceed 4.62 w/o ^{235}U.

(2) A water hole is defined as an empty array location, a hollow (water) rod, a smaller fuel rod, or any other object that displaces less water than a standard fuel rod.

(3) Inert rods are defined as solid steel or Zircaloy rods that have a diameter that is equal to or greater than that of a fuel rod.

This page intentionally left blank.

6.2 Spent Fuel Loading

The criticality safety evaluation for the FuelSolutions™ W74 canister includes analysis of the BRP fuel assembly designs listed in Table 6.2-1. Based on the analysis for fuel assembly types described in Table 6.2-1, the Siemens 11x11 fuel assembly design is established to be the most reactive in the FuelSolutions™ W74 basket array as described in Section 6.4. A maximum initial enrichment of 4.1 w/o ^{235}U is established to satisfy the $k_{eff} \leq 0.95$ criticality acceptance criterion for a full loading of up to 64 BRP fuel assemblies.

The criticality analysis assumes that fuel pins in BRP fuel assemblies contain a uniform enrichment, even though all BRP fuel assembly designs incorporate multiple fuel pin enrichments. Section 6.4 shows that modeling the BRP fuel assembly configurations in this manner is conservative.

In the criticality analysis, the maximum enrichment listed in Table 6.1-1 is applied over the entire length of each fuel stack, and the fuel is assumed to be undamaged. No credits are taken for fuel pellet dishing, fuel burnup, or fuel-related burnable neutron absorbers. The maximum uranium loading is not used directly in the criticality analysis, which instead assumes BRP fuel assemblies have pellets with an average nominal density that is 96.5% of UO_2 theoretical density. The UO_2 density is bounding for all BRP fuel assemblies and is listed in Table 6.1-1 as one of the fuel acceptance criteria.

The BRP MOX fuel assemblies contain combinations of MOX fuel rods and UO_2 fuel rods with several different enrichment levels. The specific MOX fuel criticality analyses, described in Section 6.6.1, explicitly model the fuel material mixtures present in each of the fuel rods in the assembly. Thus, no assembly averaging of fuel rod enrichments is performed. No maximum allowable assembly average enrichment is determined by the MOX fuel analyses. Instead, it is explicitly shown that all existing BRP MOX fuel assemblies are qualified for loading into the W74 canister.

The maximum uranium loading is not used directly in any of the MOX fuel criticality analyses. Instead the pellet geometry and percent theoretical densities shown in Table 6.1-1 are used. No credits are taken for fuel burnup or fuel-related burnable neutron absorbers.

The partial assembly criticality analyses described in Section 6.6.2 assume assembly average enrichments. In the case of partial assemblies, the assembly average enrichment is defined as the average enrichment of the remaining fuel rods. The partial assembly criticality analyses establish a maximum allowable assembly average enrichment for any given axial section of the fuel assembly. The maximum allowable assembly average enrichments for partial BRP fuel assemblies are given in Sections 6.1 and 6.6.2.

The damaged assembly criticality analyses described in Section 6.6.3 model arrays of fissile material inside the damaged fuel cans, including pure UO_2 fuel material, and several different MOX fuel material mixtures. In all cases, a uniform material composition is modeled over the entire fissile material configuration. The damaged fuel analyses model either partial or intact BRP assembly configurations inside the other (guide tube) fuel locations of the canister. These partial or intact assemblies have pure UO_2 fuel. The enrichment of the fissile material configuration inside the damaged fuel cans (for the UO_2 fuel case) is 4.61%, as discussed in

Section 6.1. The MOX fuel compositions that are analyzed for the fissile material configuration are described in Section 6.6.3.

Table 6.2-1 - Specific Fuel Assembly Parameters

Parameter	GE 9x9	GE 9x9	Siemens 9x9	Siemens 11x11	Siemens 11x11	Siemens 11x11	Siemens 11x11
Number of Fuel Rods per Assembly	80	81	81	121	120	117	121
Assembly Pin Pitch (in.)	0.707	0.707	0.707	0.577	0.577	0.577	0.577
Fuel Rod Clad Outer Diameter (in)	0.5625	0.5625	0.5625	0.449	0.449	0.449	0.449
Fuel Rod Clad Inner Diameter (in)	0.4825	0.4825	0.4825	0.381	0.381	0.381	0.381
Fuel Pellet Outer Diameter (in)	0.471	0.471	0.4715	0.3715	0.3715	0.3715	0.3735
Fuel Pellet Density (% Theo. UO_2)	96.5	96.5	96.5	96.5	96.5	96.5	96.5
Fuel Pellet Dishing Factor (%)	0	0	0	0	0	0	0
Number of Inert (Zr) Rods / Assembly	0	0	0	0	1	4	0
Solid Zr Rod Outer Diameter (in)	N/A	N/A	N/A	N/A	0.449	0.449	N/A
Number of Water Holes / Assembly	1	0	0	0	0	0	0
Active Fuel Length (in)	70	70	70	70	70	70	70
Bottom Tie Plate Height (in)	1.25	1.25	1.25	1.25	1.25	1.25	1.25

This page intentionally left blank.

6.3 Model Specification

The primary model geometry differences between the MOX, partial, and damaged BRP assembly criticality analyses and the intact BRP assembly criticality analyses described in this section pertain to the fuel assemblies (i.e., there are few differences in the cask or canister model geometry). The modeled MOX, partial, and damaged BRP assembly configurations are described in Sections 6.6.1, 6.6.2, and 6.6.3, respectively.

There are also some minor differences in the W74 basket geometry modeled in the intact, MOX, partial, and damaged BRP assembly criticality analyses. The basket geometry modeled in the MOX and damaged BRP assembly criticality analyses is illustrated in Figure 6.3-2. The basket geometry modeled in the partial BRP assembly analyses is shown in Figure 6.3-3. The basket geometry modeled in the intact BRP assembly analyses is shown in Figure 6.3-1. The specific differences are described below.

The basket geometry modeled in the MOX and damaged assembly analyses, shown in Figure 6.3-2, is the actual W74 basket geometry. The differences between the partial assembly analysis basket geometry model and the actual basket geometry can be seen by comparing Figure 6.3-3 to Figure 6.3-2. The support tube centerline has been moved out from a distance (from the basket center) of 44.45 cm (17.5 in.) to a distance of 44.831 cm (17.65 in.). The modeled boron concentrations within the borated stainless steel poison sheets is only 1.0 w/o in the partial assembly analyses, versus the actual value of 1.25 w/o. The partial assembly analyses conservatively neglect four poison sheets that lie adjacent to the support tubes. These four locations can be seen by comparing Figure 6.3-2 and Figure 6.3-3. Finally, the actual support tube wall thickness of 0.75 inches is modeled in the MOX and damaged assembly analyses, while the partial assembly analyses model a wall thickness of only 0.625 inches. (The wall thickness is not illustrated in the figures.)

As shown in Figure 6.3-1, the intact BRP assembly criticality analyses model a support tube centerline location of 44.831 cm and a poison sheet boron concentration of 1.0 w/o. They conservatively neglect the four poison sheets (adjacent to the support tubes) shown in Figure 6.3-2. The intact assembly analyses also model a support tube wall thickness of 0.75 inches.

The modeling of the four basket features which differ between the analyses are summarized in Table 6.3-1.

It should be noted that the poison sheet boron concentration referred to in Figure 6.3-2 and Figure 6.3-3, and in Table 6.3-1, is the actual boron concentration in the poison sheet. These concentrations are then reduced by a factor of 0.75 in the criticality analyses, in accordance with the analysis methodology recommended in NUREG-1536.[3] Thus, the partial assembly criticality analyses actually model a boron concentration of 0.75%, and the MOX and damaged assembly analyses actually model a boron concentration of 0.9375%.

[3] NUREG-1536, *Standard Review Plan for Dry Storage Cask Systems*, U.S. Nuclear Regulatory Commission, January 1997.

All of the criticality analyses are based on either accurate or conservative values for these four basket geometry features. Reducing the support tube wall thickness, moving the support tube in toward the basket center, reducing the poison sheet boron concentration, and neglecting the presence of four poison sheets all cause reactivity (k_{eff}) to increase. For this reason, the partial and intact assembly analyses are based on a conservative (i.e., more reactive) basket geometry model, whereas the MOX and damaged assembly analyses are based on an accurate basket geometry model.

The damaged assembly criticality analyses have one additional W74 basket model geometry difference (in addition to the differences in the modeled assembly geometries). The damaged fuel can is also modeled inside each of the eight support tubes of the W74 canister. The damaged fuel can geometry is shown in Figure 6.3-4. The damaged fuel can is identical to a W74 canister guide tube, with four 0.09 inch thick stainless steel walls, and an inner cavity width of 6.9 inches. A 0.075 inch thick borated stainless steel poison sheet is attached to each of the four walls of the damaged fuel can. The poison sheets contain 1.25 w/o boron. These poison sheets have the same dimensions and material composition (i.e., boron concentration) as the poison sheets attached to the other guide tubes in the W74 basket. The damaged fuel can walls shown in Figure 6.3-4 are modeled over the entire axial length of the support tube, and the poison sheets are modeled over most of the axial length. No other damaged fuel can structures, including the can top and bottom lids, are modeled in the criticality analyses.

The damaged BRP assembly analyses model several fissile material configurations inside the damaged fuel can interior. The analyses establish the most reactive possible fissile material configuration. These fissile material configurations are described in more detail in Section 6.6.3. In the other fuel locations of the canister, the analyses model either the optimum partial assembly configuration (described in Section 6.6.1), or an intact 11x11 BRP assembly configuration.

6.3.1 Configuration

The analytical models used in the criticality analysis include cases for normal and postulated accident conditions applicable to the FuelSolutions™ SFMS. The normal condition models are applicable for off-normal conditions of storage. The FuelSolutions™ W74 canister includes a stackable upper and lower basket assembly and a shell assembly, as described in Section 1.2.1 of this FSAR. Drawings for the FuelSolutions™ W74 canister are provided in Section 1.5.1 of this FSAR. Separate overpack casks are used for on-site transfer, and dry storage, as described in Chapter 1 of the FuelSolutions™ Storage System FSAR.

The FuelSolutions™ W74 canister basket consists of an array of guide tube assemblies, support tubes, and spacer plates arranged in a manner to provide structural integrity and to prevent criticality of the stored fuel assemblies. The FuelSolutions™ W74 basket cross-section is depicted in Figure 6.3-1 with nominal dimensions provided. Figure 6.3-1 is a top view of the basket that is sliced horizontally through an axial point to include one of the spacer plates. The spacer plates provide a minimum separation for the guide tube assemblies. As shown in Figure 6.3-1, there are two types of guide tube assemblies used in the FuelSolutions™ W74 basket. Figure 6.3-5 shows the Type A guide tube assembly, which has two borated stainless steel panels, located on two opposing sides of the guide tube. Figure 6.3-6 shows the Type B guide tube assembly which has only one borated stainless steel panel located on one side of the guide tube. In Figure 6.3-1, the borated stainless steel panel orientations within the

FuelSolutions™ W74 basket are denoted by arrows except for the center non-fuel positions which are modeled as water holes. Additional product information for borated stainless steel is provided in Section 1.5.2 of this FSAR.

The actual W74 canister has four additional poison sheets that are not shown in Figure 6.3-1. The four additional poison sheets are conservatively neglected in the W74 intact and partial BRP assembly criticality analyses. Thus, the configuration shown in Figure 6.3-1 is that which is modeled in the intact and partial assembly criticality analyses. The MOX and damaged BRP assembly criticality analyses (described in Sections 6.6.1 and 6.6.3, respectively) model the actual W74 basket configuration, which is shown in Figure 6.3-2.

The four additional poison sheets mentioned above are mounted on the four guide tube walls that face the upper or lower walls of the (larger) support tubes. As shown in Figure 6.3-1, there are no poison sheets attached to the adjacent guide tube walls directly below the upper two support tubes and directly above the lower two support tubes (the adjacent guide tubes have single arrows pointing away from the support tubes). Thus, these adjacent guide tubes are shown as being Type B guide tubes, when they are actually Type A guide tubes.

The geometric arrangement of the guide tube assemblies within the FuelSolutions™ W74 basket is shown in Figure 6.3-1. In basket regions between the guide tubes, a water gap is formed. The water gap is bounded in the axial direction by spacer plates, on one side by a borated stainless steel poison sheet, and on the other side by the outer wall of the adjacent guide tube.

The FuelSolutions™ W74 canister criticality calculations show that moving the spacer plates closer together axially, or increasing the spacer plate thickness in the FuelSolutions™ W74 basket leads to a decrease in system reactivity.

Both FuelSolutions™ W74M and W74T canister basket and shell assembly types are considered in the criticality analysis. The two designs differ with respect to the materials used for the alignment bars, vent/drain port covers, outer closure plates, inner closure plates, canister shells, and engagement spacer plates. In the W74M, SS-316 is used for these components, while in the W74T, the material is SS-304. In addition to the material differences in the FuelSolutions™ W74M and W74T, the number, separation distances, and thickness of the spacer plates in each canister basket are also different. The spacer plate thickness and axial location have a significant influence on the reactivity of the basket since they affect the neutron physics in the water gaps between adjacent guide tubes. The effects of the material and spacer plate differences between the two FuelSolutions™ W74 versions on criticality control effectiveness are evaluated in Section 6.4. Based on the evaluation in Section 6.4, the FuelSolutions™ W74T configuration is modeled in subsequent design basis criticality calculations.

The analyses presented in Section 6.4 are based on cask models which include an infinite array of FuelSolutions™ W74T basket and shell assemblies inside a representative transportation cask configuration. The FuelSolutions™ W74 canister shell assembly and transportation cask body cross-section is shown in Figure 6.3-7. The transportation cask configuration represents a worst-case configuration for any mode of canister use. The worst-case nature of the transportation configuration relative to storage and transfer configurations is discussed further in Section 6.6 of the FuelSolutions™ Storage System FSAR.

Criticality of fuel assemblies in the FuelSolutions™ W74 canister is prevented by the mechanical design of the canister. Neutronic interaction between fuel assemblies is limited by favorable geometry (fixing the minimum separation between fuel assemblies) and the use of borated neutron absorber panels. The design basis for criticality prevention is to demonstrate that the effective neutron multiplication factor of the fuel assemblies within the FuelSolutions™ canister is less than the Upper Subcritical Limit (USL)[4] established using the analysis methodology presented in NUREG/CR-5661[5] and a diverse set of critical experiments (see Section 6.5).

Both normal and hypothetical accident conditions are considered in the criticality analysis for the FuelSolutions™ W74 canister. The normal conditions for the FuelSolutions™ W74 canister conservatively includes: complete flooding with water at a density that results in optimum moderation, worst case asymmetric assembly placement within the guide tubes, and application of worst case material and fabrication tolerances. The hypothetical accident condition for the FuelSolutions™ W74 canister includes all the normal conditions, plus a bounding 0.08 inch permanent deformation of the guide tubes resulting from a hypothetical cask drop accident, axial detachment of the guide tubes from the basket structure, and removal of the transportation cask neutron shield assembly. The deformation and detachment of the guide tubes, and the loss of the transportation cask neutron shield are consistent with the physical conditions of the package after being subjected to the worst case hypothetical accident conditions defined in 10CFR71.[6] Although the hypothetical accident condition deformation assumptions are not applicable to FuelSolutions™ SFMS storage and on-site transfer configurations, they represent bounding assumptions for the canister which is also designed for transportation conditions under 10CFR71.

The structural calculations show that, as a result of the 9 meter drop specified in 10CFR71, the only significant permanent changes (relative to criticality) to the W74 canister and cask geometry are the deformation of the basket assembly guide tubes and their detachment from the basket internals. In the FuelSolutions™ W74 models, a 0.08 inch deformation is assumed to occur throughout the entire length of the basket guide tubes, reducing the center-to-center spacing between assemblies. The 0.08 inch maximum deformation is based upon a uniform axial assembly loading of the guide tubes. A localized loading of the guide tube from the fuel assembly grid spacers results in an increase in the maximum localized guide tube deformation to ~0.125 inch. However, this deformation occurs only in every third span between spacer plates, and the maximum deformation in other spans is negligible. In Section 6.4, modeling the deformation at 0.08 inch over the entire length of the guide tube is demonstrated to be more conservative than modeling a 0.125 inch maximum deflection within axial spans that contain fuel assembly mid-grids.

---

[4] ORNL///TM-13211 NUREG/CR-6361, *Criticality Benchmark Guide for Light-Water-Reactor Fuel in Transportation and Storage Packages,* Lichtenwalter, J. J., et al., March 1997.

[5] NUREG/CR-5661, ORNL, *Recommendations for Preparing the Criticality Safety Evaluation of Transportation Packages*, Dyer, H. R., and Parks, C. V., April 1997.

[6] Title 10, U.S. Code of Federal Regulations, Part 71 (10CFR71), *Packaging and Transportation of Radioactive Materials*, 1995.

The MCNP 4a code package[7] is used for the criticality analysis of the FuelSolutions™ W74 canister to demonstrate that the storage of the fuel assembly types identified in Table 6.2-1 satisfies the USL acceptance criterion. MCNP models are developed for the FuelSolutions™ W74 canister under normal and hypothetical accident conditions. The FuelSolutions™ W74 canister analytical models used include single-package models, and a worst-case multiple package array model. The worst-case multiple package array model is conservatively used to establish the maximum acceptable enrichment and the corresponding design basis k_{eff} value for each fuel assembly design described in Table 6.2-1. As discussed in Section 6.6 of the FuelSolutions™ Storage System FSAR, the transportation cask array analysis, which is performed considering internal and interspersed optimum moderation, bounds all credible storage array configurations.

The following assumptions are used to develop the analytical models for the criticality safety evaluation of the FuelSolutions™ W74 canister:

- FuelSolutions™ W74 canister models are analyzed for the BRP fuel types identified in Table 6.2-1 in the unchanneled configuration. All fuel assemblies modeled contain UO_2 with a uniform pin enrichment of 4.1 weight percent ^{235}U. The enrichments are applied over the entire length of each fuel stack, and the fuel is assumed to be undamaged.
- The fuel pellets are conservatively modeled assuming a 96.5% theoretical density of UO_2 and no dishing fraction. This assumption is conservative since actual pellets are chamfered and manufactured to a UO_2 theoretical density of 95% or less.
- Unirradiated fuel conditions are assumed (fresh fuel isotopic concentrations). No credit is taken for any ^{234}U or ^{236}U in the fuel, nor is any credit taken for the buildup of fission product poison material.
- No credit is taken for any spacer grids, spacer sleeves, or top and bottom tie plates. In addition, the top and bottom tie plates displace moderator from an array and are manufactured from stainless steel 304, which removes neutrons by radiative capture.
- No credit is taken for any burnable absorber in the fuel rods.
- Fully flooded conditions are assumed, including water present in the fuel rod-cladding gap. The fully flooded conditions are the most conservative since the FuelSolutions™ W74 canister is an under-moderated system. The moderator is assumed to be pure water at a density of 1.0 g/cm^3, which is shown to produce the most reactive conditions (see the Section 6.4.1 case studies for further discussion).
- In the intact and partial BRP assembly criticality analyses, a nominal loading of 1.0 weight percent of natural boron is used as the analysis basis for the borated stainless steel, versus the manufacturer's minimum specified boron concentration of 1.25 w/o that is verified during material manufacture. This 1.25 w/o loading corresponds to a minimum ^{10}B areal density of 3.1 mg/cm^2, including consideration of thickness, density, and poison content. The MOX and damaged BRP assembly criticality analyses (described in Sections 6.6.1 and 6.6.3,

[7] Briesmeister, J., *MCNP-4A General Monte Carlo Code N-Particle Transport Code*, Version 4A, LA-12625-M, November 1993.

respectively) model the actual 1.25 w/o boron concentration. In all analyses, credit is taken for only 75% of the nominal boron concentrations specified above (i.e., 75% of 1.0 w/o or 1.25 w/o).

- Worst case material and fabrication tolerance dimensions are applied to the nominal dimensions for the FuelSolutions™ W74 canister model. The tolerances are summarized in Table 6.3-2.
- A full 64-assembly loading configuration for the FuelSolutions™ W74 canister is analyzed. As shown in Figure 6.3-1, the design basis loading configuration requires the 5 central guide tube positions of both the upper and lower baskets to remain empty. These locations are modeled as water filled holes and no assemblies or other materials are assumed to be loaded into these locations. The W74 canister configuration employs a mechanical block-out structure over the openings of the five central guide tube positions to prevent the inadvertent loading of fuel assemblies into these locations.
- The radial boundary is defined as either the intact cask body (normal conditions) or the cask body with the neutron shield assembly removed (hypothetical accident conditions). The single package model is surrounded by twelve inches of water for reflection. The multiple package array model consists of an infinite number of FuelSolutions™ W74 canisters in a closely packed arrangement (triangular pitch array) with the adjacent casks in contact with one another.
- The FuelSolutions™ W74 canister is modeled axially from the middle of the bottom end shield plug to a point just below the top shield plug assembly. Reflected planes are conservatively inserted at these points to prohibit neutron leakage thus maximizing k_{eff}.
- The engagement spacer plate is modeled using SS-304. The actual material specified for the engagement spacer plate is XM-19. The substitution of SS-304 for XM-19 as the engagement spacer plate material is suitable since SS-304 and XM-19 interact similarly with neutrons.
- Fuel assembly positions within guide tubes are assumed to be shifted radially in such a manner as to maximize system reactivity. The worst case fuel position configuration is demonstrated by analysis (see the Section 6.4 case studies for further discussion).
- Both normal conditions and hypothetical accident conditions are evaluated. The normal condition models of the FuelSolutions™ W74 canister system include consideration of: a) complete flooding with water at a density sufficient for optimum moderation, b) worst case asymmetric assembly placement within the guide tubes, and c) application of worst case material and fabrication tolerances. The hypothetical accident condition models for the FuelSolutions™ W74 canister system include all the normal conditions as well as the addition of a 0.08 inch permanent deformation of the guide tubes between spacer plates and the axial detachment of the guide tubes from the basket structure. The loss of the transportation cask neutron shield structure is also assumed. The 0.08 inch guide tube deformation, which occurs as a result of a cask side drop, is the only significant change in the basket structure that occurs for any postulated storage accident events or event sequences. The 0.08 inch value is a bounding value which is based on lateral *g*-loads that are bounding for all storage drop events.

6.3.1.1 Hypothetical Accident Conditions

The hypothetical accident conditions modeled for the FuelSolutions™ W74 canister system includes the following worst case assumptions:

- Complete flooding with water at a density which produces optimum moderation
- Worst case asymmetric fuel assembly placement within the guide tubes
- Application of worst case material and fabrication tolerances
- Consideration of a bounding 0.08 inch permanent deformation of guide tubes between spacer plates and the axial detachment of the guide tubes from the basket structure
- Loss of the transportation cask body neutron shield

The deformation and detachment of the guide tubes and the removal of the outer cask neutron shield are consistent with the physical condition of the FuelSolutions™ W74 canister after being subjected to the hypothetical accident conditions specified in 10CFR71.

The hypothetical accident conditions model is an accurate representation of the FuelSolutions™W74 lower and upper baskets. The canister is modeled axially from the middle of the bottom end shield plug to a point just below the top shield plug assembly. Reflected planes are inserted at these points preventing axial leakage of neutrons from the canister. Figure 6.3-8 shows a horizontal cross-section of MCNP model. Figure 6.3-9, Figure 6.3-10, and Figure 6.3-11 show vertical cross-section views of the accident condition model that has been sliced with vertical planes to expose the lower, middle, and upper portions of the canister. As shown in Figure 6.3-9, the lower portion of the model begins at the middle of the bottom end shield plug. Next, the bottom closure plate is modeled followed by the water gap between the bottom closure plate and the bottom of the fuel stack.

The bottom of the fuel in the lower basket begins at an elevation of 1.895 inches above the bottom closure plate. The bottom of the lower basket guide tubes and the borated stainless steel poison sheets are conservatively positioned at an elevation of 2.5 inches above the bottom closure plate. The position of the bottom of the borated stainless steel panels relative to the bottom of the fuel leaves about 0.61 inch of fuel in a non-poisoned region of the lower basket which maximizes system reactivity. The lower basket guide tubes are modeled axially to the top of the borated stainless steel sheets as shown in Figure 6.3-10. Water is placed between the top of the lower basket guide tubes and the bottom of the engagement spacer plate which separates the lower and upper baskets in the FuelSolutions™ W74 canister. The axial placement of the guide tubes within the basket is consistent with the damage expected to occur from a nine meter drop in a representative transportation cask (as specified for the hypothetical accident in 10CFR71.

The axial placement of the guide tubes within the upper basket is also consistent with the damage incurred from a nine meter drop specified for the hypothetical accident in 10CFR71. The bottoms of the upper basket guide tubes and the borated stainless steel poison sheets are positioned at an elevation of 3.525 inches above the top of the engagement spacer plate as shown in Figure 6.3-10.

The position for the bottom of the fuel stack in the upper basket is 1.895 inches above the top of the engagement spacer plate. The position of the bottom of the borated stainless steel sheets

relative to the bottom of the fuel leaves about 1.63 inches of fuel in a non-poisoned region of the upper basket which maximizes system reactivity. The upper basket guide tubes are modeled axially to the top of the borated stainless steel sheets as shown in Figure 6.3-11. The top of the guide tubes in the upper basket extend through the top spacer plate. Water is placed between the top of the upper basket guide tubes and the bottom of the top shield plug assembly.

As a result of a nine meter drop, the guide tubes separate from the basket internals and are free to move in the axial plane within the boundaries of the spacer plate holes. To maximize the effect of the guide tube relocation on system reactivity, the tops of the lower basket guide tubes are modeled resting against the bottom of the engagement spacer plate, and the tops of the upper basket guide tubes are modeled resting against the bottom of the top shield plug assembly. This results in a vertical guide tube shift of approximately 0.5 inch for the lower basket and 1.4 inches for the upper basket. The guide tube shift is maximized in the upper basket since it results in more fuel exposure in the middle of the canister. If the shift has been maximized in the lower basket, the fuel exposure results in a high probability for the loss of neutrons from the system by leakage.

To further maximize reactivity by exposing more fuel below the borated stainless steel sheets, the flared ends at the top of the guide tubes are also assumed to flatten during the accident resulting in an additional upward shift of 0.5 inch. Figure 6.3-11 shows the position of the top of the borated stainless steel sheets when the tops of the upper basket guide tubes rest against the top shield plug assembly. The final positions for the bottom of the borated stainless steel sheets after the accident is 2.5 inches above the bottom closure plate for the lower basket guide tubes and 3.525 inches above the engagement spacer plate for the upper basket guide tubes.

The active fuel stack for all BRP fuel is conservatively modeled beginning at a height of 1.895 inches and ending at a height of 71.895 inches. This represents an active fuel length of 70 inches which is equivalent to the active fuel length of the fuel assembly types considered for storage in the FuelSolutions™ W74 canister. The position of the fuel stack bottom assumes a bottom tie plate height of 1.25 inches and a bottom end plug height of 0.645 inch. The fuel stack in the lower basket could have been shifted upward to decrease the distance between the fuel in the upper and lower baskets of the FuelSolutions™ W74 canister, however, the length of the top tie plate and the plenum region of the fuel results in more than 12 inches of separation between the two systems. Therefore, the decision is made to maximize the amount of fuel exposed below the borated stainless steel in both the upper and lower baskets.

The nominal dimensions for the guide tubes, neutron absorber panels, spacer plates, spacer plate openings, support tubes, and support sleeves as well as material and fabrication tolerances are summarized in Table 6.3-2. The factors that primarily affect the reactivity of the FuelSolutions™ system are neutron absorption and fuel assembly separation. Two parameters that affect neutron absorption are the neutron absorber panel thickness and the spacer plate thickness. The parameters that affect fuel assembly separation include fuel assembly position, spacer plate opening size and location; guide tube wall thickness; guide tube inside width; and neutron absorber panel thickness. Tolerances are applied to the FuelSolutions™ W74 canister components in such a manner to maximize system reactivity as follows:

- The neutron absorption within the FuelSolutions™ W74 canister system is influenced by the thickness of both the neutron absorber panel and the spacer plates. The application of the material and fabrication tolerances that decrease the neutron absorber and spacer plate

thickness result in a decrease in the neutron absorption of the system. The decrease in the neutron absorption within the system results in an increase in the neutrons available for fission that correspondingly increases system reactivity.

- As fuel assemblies are brought closer together in the FuelSolutions™ W74 canister, the neutron interaction between assemblies increases, resulting in a higher system reactivity. In conjunction with assuming worst case asymmetric assembly placement within the guide tubes, fuel assembly interaction is maximized in the FuelSolutions™ W74 canister models by shifting guide tube assemblies within the spacer plate openings and applying worst case component material and fabrication tolerances. Three separate fuel/guide tube assembly shift configurations are analyzed to determine a worst case configuration for use in the FuelSolutions™ W74 canister model. The three configurations considered are shown in Figure 6.3-12 through Figure 6.3-14. The worst case configuration determined through analysis is the configuration depicted by Figure 6.3-14 (see the Section 6.4 case studies for further discussion). As shown in Figure 6.3-14, the fuel assemblies are moved into the corner of each guide tube as indicated and the guide tubes are correspondingly relocated within the spacer plate opening in the same direction. The tolerances that further minimize separation of the fuel assemblies are then applied as follows: a) the spacer plate opening size is increased, b) the spacer plate opening locations are moved within allowed fabrication tolerances in the indicated directions, c) the thickness of the neutron absorber panel is decreased, d) the thickness of the guide tube wall is decreased, and e) the inside width of the guide tube is increased.
- Another adjustment is made to the guide tube walls to incorporate the bounding 0.08 inch permanent deformation that occurs for the basket *g*-loads expected under a hypothetical nine-meter transportation cask drop. These assumed *g*-loads are bounding for all storage conditions and drop events. The lower face on each guide tube wall is deflected downward along the full length of the guide tube. This is a conservative representation of the permanent guide tube deformation, since the actual deformation does not occur over the full length of the guide tube (i.e., deformation is limited to regions between basket spacer plates). The effect of the guide tube deflection in the hypothetical accident conditions model is to further decrease the center-to-center spacing of the fuel assemblies in the FuelSolutions™ W74 model.

The neutron shield assembly for the canister overpack (i.e., the solid neutron shielding material, support ribs, and outer jacket), shown in Figure 6.3-7, is expected to experience damage during a hypothetical nine-meter cask drop. For this reason, it is completely removed in the hypothetical accident conditions model.

6.3.1.2 Normal Operating Condition

The normal operating conditions model for the FuelSolutions™ W74 canister includes the following: complete flooding with water with a density that results in optimum moderation, worst case asymmetric assembly placement within the guide tubes, and application of worst case material and fabrication tolerances.

The normal operating conditions model is an accurate representation of the FuelSolutions™W74 lower and upper baskets. The canister is modeled axially from the middle of the bottom end

shield plug to a point just below the top shield plug assembly. Reflected planes are inserted at these points preventing axial leakage of neutrons from the canister. Figure 6.3-15, Figure 6.3-16, and Figure 6.3-17 show side views of the FuelSolutions™W74 normal operating conditions model that has been sliced with vertical planes to expose the lower, middle, and upper portions of the canister.

As shown in Figure 6.3-15, the lower portion of the model begins at the middle of the bottom end shield plug. Next, the bottom closure plate is modeled followed by the water gap between the bottom closure plate and the bottom of the active fuel. The bottom of the active fuel is modeled just below the bottom spacer plate at an elevation of 1.895 inches above the bottom spacer plate. The bottom of the borated stainless steel panel is conservatively located at an elevation of 1.5 inches above the bottom closure plate. The actual elevation of the borated stainless steel panel bottom is only 0.375 inch off the bottom closure plate. The bottoms of the lower basket guide tubes are modeled at a height of 1.5 inches above the bottom closure plate, which is a conservative placement since the guide tube faces with borated stainless steel sheets attached begin at the surface of the bottom closure plate. The lower basket guide tubes are modeled axially to the top of the borated stainless steel panels as shown in Figure 6.3-16. Water is placed between the tops of the lower basket guide tubes and the bottom of the engagement spacer plate which separates the lower and upper baskets in the FuelSolutions™W74 canister.

The bottom of the active fuel in the upper basket is located at an elevation of 1.895 inches above the top of the engagement spacer plate. The bottoms of the upper basket guide tubes and the borated stainless steel panels are both conservatively positioned at an elevation of 1.5 inches above the top of the engagement spacer plate. The upper basket guide tubes are modeled axially to the top of the borated stainless steel panels as shown in Figure 6.3-17. Water completely fills the region between the tops of the upper basket guide tubes and the bottom of the top shield plug assembly with the exception of the volume containing the top spacer plate.

The active fuel stack for all BRP fuel is modeled beginning at a height of 1.895 inches and ending at a height of 71.895 inches. This represents an active fuel length of 70 inches which is equivalent to the actual active fuel length of the fuel assembly types considered for storage in the FuelSolutions™ W74 canister. The position of the fuel stack bottom assumes a bottom tie plate height of 1.25 inches and a bottom end plug height of 0.645 inch.

The nominal dimensions for the guide tubes, neutron absorption panels, spacer plates, spacer plate openings, support tubes, and support sleeves are shown in Figure 6.3-1 through Figure 6.3-6 as well as on the drawings provided in Section 1.5.1 of this FSAR. Material and fabrication tolerances are specifically evaluated for effects on system reactivity in case studies presented in Section 6.4. Worst case material and fabrication tolerances are summarized in Table 6.3-2. The factors that primarily affect the reactivity of the FuelSolutions™ W74 canister system are neutron absorption and fuel assembly separation. Two parameters that affect neutron absorption are the neutron absorber panel thickness and the spacer plate thickness. The parameters that affect fuel assembly separation include fuel assembly position; spacer plate opening size and location; guide tube wall thickness; guide tube inside width; and neutron absorber panel thickness. With the exception of the accident induced guide tube deformation and axial detachment, fuel assemblies are positioned and tolerances are applied in the normal conditions model consistent with the description provided in Section 6.3.1.1 for accident conditions.

6.3.2 Material Properties

The number densities used to model moderator materials and the FuelSolutions™ W74 canister basket, shell, and reflector materials are presented in Table 6.3-3 through Table 6.3-12. These material properties are used in all FuelSolutions™ W74 canister single package and multiple package array models.

The FuelSolutions™ W74 canister basket incorporates panels of borated stainless steel neutron-absorbing material. The borated stainless steel alloy incorporates a minimum of 1.25 weight percent (w/o) natural boron. As discussed at the beginning of Section 6.3, the MOX and damaged BRP assembly criticality analyses model the above boron concentration of 1.25 w/o. The intact and partial BRP assembly analyses, however, conservatively model a lower boron concentration of 1.0 w/o. The borated stainless steel material descriptions given in Table 6.3-7 and Table 6.3-13 correspond to boron concentrations of 1.0 w/o and 1.25 w/o, respectively. Stainless steel alloys are ideally suited for use in fuel pools containing demineralized or borated water, as well as long-term dry storage cask radiation and thermal environments. The borated stainless steel is manufactured and verified under the control and surveillance of the QA program described in Chapter 13 of the FuelSolutions™ Storage System FSAR. Product literature for this type of material is provided in Section 1.5.2 of this FSAR.

The continued efficacy of borated stainless steel is demonstrated by the process controls under which the material is manufactured and verified which assure a homogeneous dispersion of boron throughout the alloy. In addition, the effects of long-term exposure to neutron flux from irradiated fuel is negligible because the thermal neutron flux during dry storage is low. This fact, coupled with the use of the minimum boron concentration specified by the material manufacturer (rather than the nominal) further reduced by 25%, more than accounts for any boron depletion which may occur over the 100 year design life of the FuelSolutions™ W74 canister.

Table 6.3-1 - W74 Basket Model Differences Between Intact, Partial, MOX, and Damaged BRP Assembly Criticality Analyses

W74 Basket Feature	Intact Assembly Analyses	Partial Assembly Analyses	MOX Assembly Analyses	Damaged Assembly Analyses
Poison Sheet Boron Concentration (w/o)	1.0(1)	1.0(1)	1.25(2)	1.25(2)
Poison Sheets Adjacent to Support Tubes?	No(1)	No(1)	Yes(2)	Yes(2)
Support Tube Center Location (cm)(3)	44.831(2)	44.45(1)	44.831(2)	44.831(2)
Support Tube Wall Thickness (inch)	0.75(2)	0.625(1)	0.75(2)	0.75(2)
Basket Geometry Model Illustration	Figure 6.3-5	Figure 6.3-3	Figure 6.3-2	Figure 6.3-2

Notes:

(1) Conservative value. Yields higher reactivity than actual basket design value.

(2) Actual W74 basket design value.

(3) Defined as the distance, in both the X and Y directions, between the support tube centerline and the basket centerline.

Table 6.3-2 - Worst Case Material and Fabrication Tolerances for the FuelSolutions™ W74 Canister

Parameter	Tolerance (inches)
Borated Stainless Steel Thickness	- 0.007
Borated Stainless Steel Width	- 0.05
Spacer Plate Thickness	- 0.03
Spacer Plate Opening Width	+ 0.015
Spacer Plate Opening Location(1)	± 0.015
Guide Tube Thickness	- 0.008
Guide Tube Inner Dimension	+ 0.05
Support Tube Thickness (in)	- 0.055
Support Tube Inner Dimension	+ 0.05

Note:

(1) The arrows in Figure 6.3-12 through Figure 6.3-14 indicate the direction of application for the spacer plate opening location tolerance.

Table 6.3-3 - UO_2 Number Densities as a Function of Enrichment

^{235}U Enrichment (w/o)	Number Density (atoms/b-cm)				UO_2 Material Density (atoms/b-cm)
	UO_2	^{235}U	^{238}U	O	
4.0	0.0235956	0.0009554	0.0226402	0.0471912	0.0707867
4.1	0.0235958	0.0009793	0.0226166	0.0471917	0.0707875
4.2	0.0235961	0.0010032	0.0225929	0.0471922	0.0707883
4.3	0.0235964	0.0010271	0.0225693	0.0471928	0.0707891
4.4	0.0235966	0.0010509	0.0225457	0.0471933	0.0707899
4.5	0.0235969	0.0010748	0.0225221	0.0471938	0.0707907
4.6	0.0235972	0.0010987	0.0224985	0.0471943	0.0707915
4.7	0.0235974	0.0011226	0.0224748	0.0471949	0.0707923
4.8	0.0235977	0.0011465	0.0224512	0.0471954	0.0707931
4.9	0.023598	0.0011704	0.0224276	0.0471959	0.0707939
5.0	0.0235982	0.0011942	0.022404	0.0471965	0.0707947

Table 6.3-4 - Water Number Densities as a Function of Density

H_2O Density (g/cm^3)	H_2O Molecular Weight (g/mole)	H Number Density (atoms/b-cm)	O Number Density (atoms/b-cm)	H_2O Material Density (atoms/b-cm)
1.0	18.01528	0.066863	0.033432	0.1002949
0.9	18.01528	0.060177	0.030088	0.0902654
0.8	18.01528	0.053491	0.026745	0.0802359
0.7	18.01528	0.046804	0.023402	0.0702064
0.6	18.01528	0.040118	0.020059	0.0601769
0.5	18.01528	0.033432	0.016716	0.0501474
0.4	18.01528	0.026745	0.013373	0.0401179
0.3	18.01528	0.020059	0.010029	0.0300885
0.2	18.01528	0.013373	0.006686	0.020059
0.1	18.01528	0.006686	0.003343	0.0100295
0.08	18.01528	0.005349	0.002675	0.0080236
0.06	18.01528	0.004012	0.002006	0.0060177
0.04	18.01528	0.002675	0.001337	0.0040118
0.02	18.01528	0.001337	0.000669	0.0020059

Table 6.3-5 - Zircaloy-4 Number Densities

Element	Zirc-4 Density (g/cm^3)	Element Molecular Weight (g/mole)	Weight Percent	Number Density (atoms/b-cm)
Sn	6.56	118.71	1.45	0.000483
Fe	6.56	55.847	0.21	0.000149
Cr	6.56	51.9961	0.10	7.6×10^{-05}
Zr	6.56	91.224	98.0975	0.042487
0	6.56	15.9994	0.12	0.000296
C	6.56	12.011	0.014	4.61×10^{-05}
Si	6.56	28.0855	0.0085	1.2×10^{-05}
Zirc-4 Material Density (atoms/b-cm)				0.043548

Table 6.3-6 - 304 Stainless Steel Number Densities

Element	304 SS Density (g/cm^3)	Element Molecular Weight (g/mole)	Weight Percent	Number Density (atoms/b-cm)
Fe	8.027	55.847	69.75	0.06038
Mn	8.027	54.93805	2.0	0.00176
Cr	8.027	51.9961	19.0	0.017666
Ni	8.027	58.69	9.25	0.00762
304 SS Material Density (atoms/b-cm)				0.087426

Table 6.3-7 - Borated Stainless Steel Number Densities (1.0 w/o natural boron)[1]

Element or Isotope	Borated Stainless Steel Density (g/cm^3)	Element or Isotope Weight Percent	Element or Isotope Number Density (atoms/b·cm)	^{10}B & ^{11}B 75% Adjusted Number Densities (atoms/b·cm)
^{10}B	7.76	0.184311	0.000860	0.000645
^{11}B	7.76	0.815692	0.003463	0.002597
Fe	7.76	64.1025	0.053646	
Mn	7.76	1.98	0.001684	
Si	7.76	0.7425	0.001236	
Cr	7.76	18.81	0.016907	
Ni	7.76	13.365	0.010643	
Borated Stainless Steel Material Density (atoms/b·cm)				0.087359

Note:

(1) The 1.0 w/o borated stainless steel described in this table is modeled in the intact and partial BRP assembly criticality analyses.

Table 6.3-8 - 316 Stainless Steel Number Densities

Element	SS-316 Density (g/cm^3)	Element Molecular Weight (g/mole)	Element Weight Percent	Number Density (atoms/b-cm)
Fe	8.027	55.847	65.75	0.056918
Mn	8.027	54.93805	2.0	0.00176
Si	8.027	28.0855	0.75	0.001291
Cr	8.027	51.9961	17.0	0.015806
Ni	8.027	58.69	12.0	0.009885
Mo	8.027	95.94	2.5	0.00126
316 SS Material Density (atoms/b-cm)				0.086920

Table 6.3-9 - 517 P Carbon Steel Number Densities

Element	Carbon Steel Density (g/cm^3)	Element Weight Percent	Element Molecular Weight (g/mole)	Element Number Density (atoms/b-cm)
Fe	7.86	96.51	55.847	0.0818076
Mn	7.86	0.59	54.93805	0.0005084
Cr	7.86	1.025	51.9961	0.0009332
Mo	7.86	0.525	95.94	0.0002590
Ni	7.86	1.35	58.69	0.0010889
517 P CS Material Density (atoms/b-cm)				0.0845971

Table 6.3-10 - XM-19 Stainless Steel Number Densities

Element	XM-19 Density (g/cm^3)	Element Weight Percent	Element Molecular Weight (g/mole)	Element Number Density (atoms/b-cm)
Fe	8.027	57.5	55.847	0.049776
Mn	8.027	5.0	54.93805	0.004400
Si	8.027	0.75	28.0855	0.001291
Cr	8.027	22.0	51.9961	0.020455
Ni	8.027	12.5	58.69	0.010297
Mo	8.027	2.25	95.94	0.001134
XM-19 SS Material Density (atoms/b-cm)				0.087353

Table 6.3-11 - Depleted Uranium Number Densities

Isotope	Depleted Uranium Density (g/cm^3)	Isotope Weight Percent	Isotope Molecular Weight (g/mole)	Isotope Number Density (atoms/b-cm)
^{235}U	18.9	0.22	235.043924	0.000106545
^{238}U	18.9	99.78	238.050785	0.047712715
Depleted Uranium Material Density (atoms/b-cm)				0.04781926

Table 6.3-12 - Solid Neutron Shield Number Densities

Material Type	Element or Isotope	Heterogeneous Material Number Densities (atoms/b·cm)	Heterogeneous Material Volume Fractions (w/o)	Neutron Shield Region Mixture Number Densities (atoms/b·cm)
NS-4	C	0.0224074	0.942	0.0211078
	O	0.0255763	0.942	0.0240929
	H	0.0569188	0.942	0.0536176
	N	0.0013653	0.942	0.0012861
	Al	0.0076192	0.942	0.0071773
	^{10}B	0.0002109	0.942	0.0001987
	^{11}B	0.0008491	0.942	0.0007998
SS-304 Bars	Fe	0.0603800	0.026	0.0015699
	Mn	0.0017600	0.026	0.0000458
	Cr	0.0176660	0.026	0.0004593
	Ni	0.0076200	0.026	0.0001981
Copper Ribs	Cu	0.0847400	0.032	0.0027117
Total Number Density (atoms/b·cm)				0.1132650

Table 6.3-13 - Borated Stainless Steel Number Densities (1.25 w/o natural boron)[1]

Element or Isotope	Borated Stainless Steel Density (g/cm^3)	Element or Isotope Weight Percent	Element or Isotope Number Density (atoms/b·cm)	^{10}B & ^{11}B 75% Adjusted Number Densities (atoms/b·cm)
^{10}B	7.76	0.230389	0.001075	0.0008065
^{11}B	7.76	1.019615	0.004328	0.003246
Fe	7.76	63.9406	0.053510	
Mn	7.76	1.975	0.001680	
Si	7.76	0.7406	0.001232	
Cr	7.76	18.7625	0.016865	
Ni	7.76	13.3313	0.010616	
Borated Stainless Steel Material Density (atoms/b·cm)				0.087957

Note:

(1) The 1.25 w/o borated stainless steel described in this table is modeled in the MOX and damaged BRP assembly criticality analyses.

FIGURE WITHHELD UNDER 2.390

Figure 6.3-1 - FuelSolutions™ W74 Basket Model for Intact Assembly Analyses (Nominal Dimensions)

FIGURE WITHHELD UNDER 2.390

Figure 6.3-2 - FuelSolutions™ W74 Basket Model for MOX and Damaged Assembly Analyses (Nominal Dimensions)

FIGURE WITHHELD UNDER 2.390

Figure 6.3-3 - FuelSolutionsTM W74 Basket Model for Partial Assembly Analyses (Nominal Dimensions)

FIGURE WITHHELD UNDER 2.390

Figure 6.3-4 - W74 Damaged Fuel Can Configuration

FIGURE WITHHELD UNDER 2.390

Figure 6.3-5 - FuelSolutions™ W74 Type A Guide Tube Assembly (Nominal Dimensions)

FIGURE WITHHELD UNDER 2.390

Figure 6.3-6 - FuelSolutions™ W74 Type B Guide Tube Assembly (Nominal Dimensions)

FIGURE WITHHELD UNDER 2.390

Figure 6.3-7 - FuelSolutions™ W74 Shell Assembly and Transport Cask

(For Clarity, Basket Not Shown)

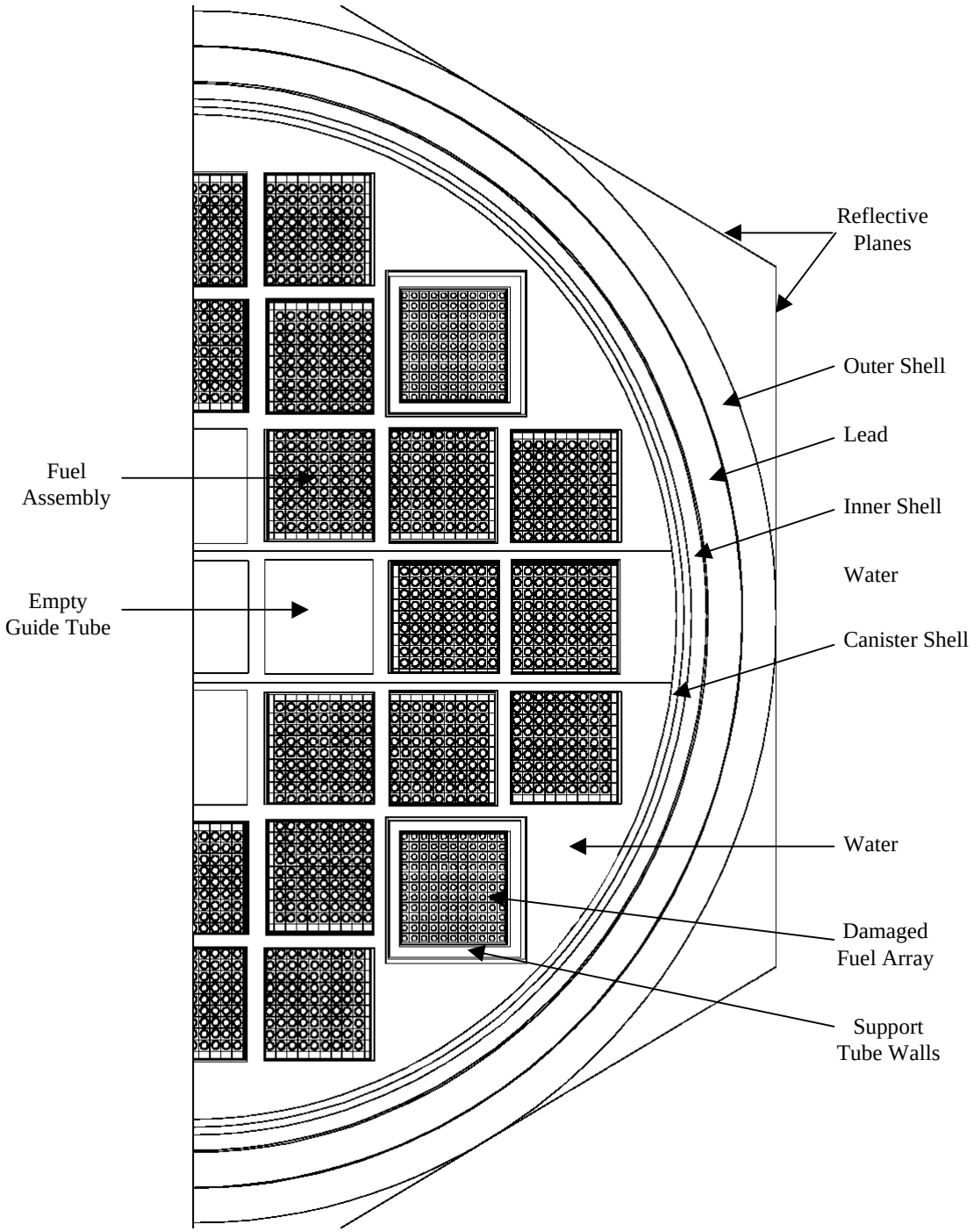

Figure 6.3-8 - Horizontal Cross-Section of MCNP Model

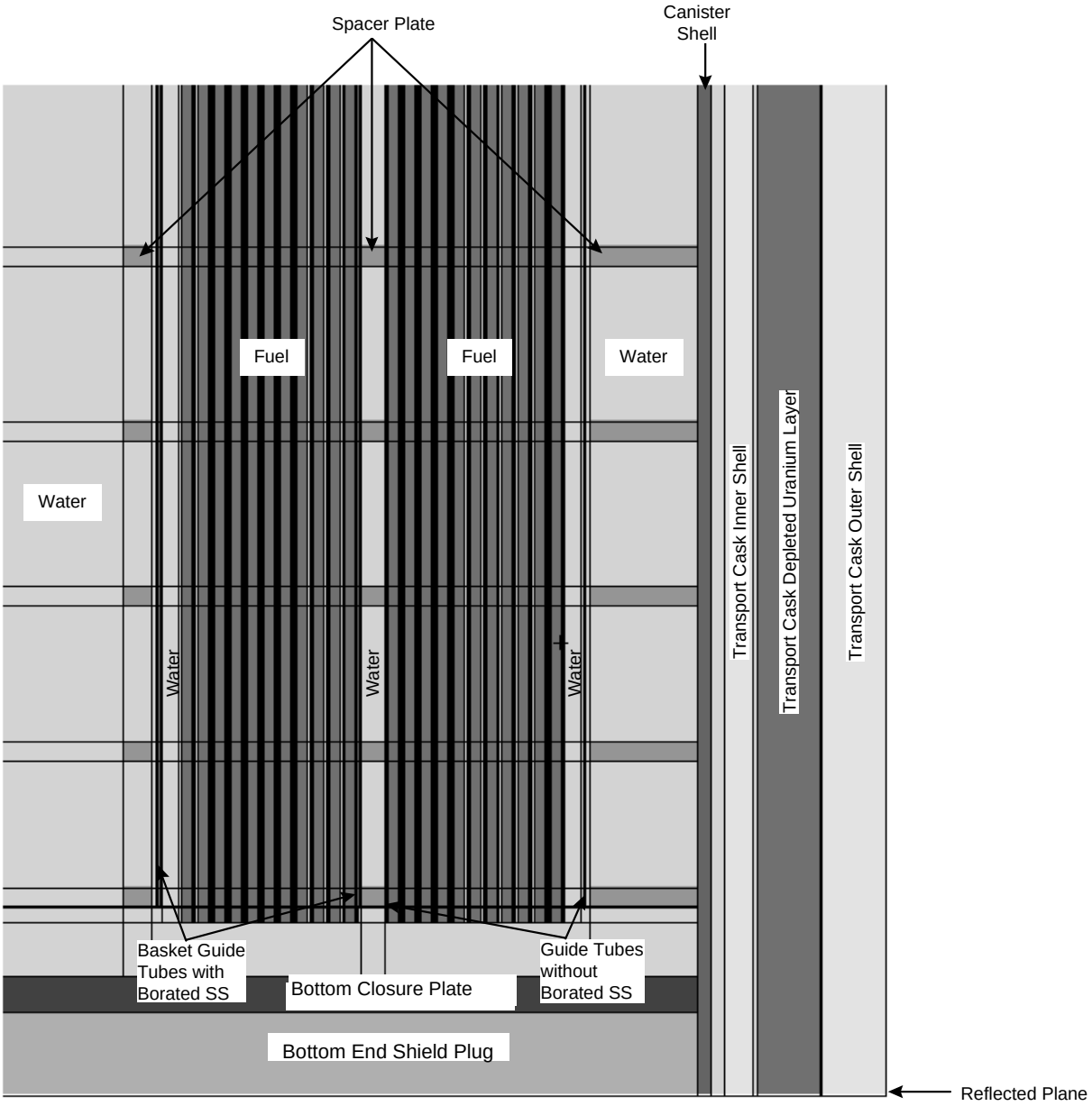

Figure 6.3-9 - Side View of Lower Portion of FuelSolutions™ W74 Hypothetical Accident Conditions Model (cut-away)

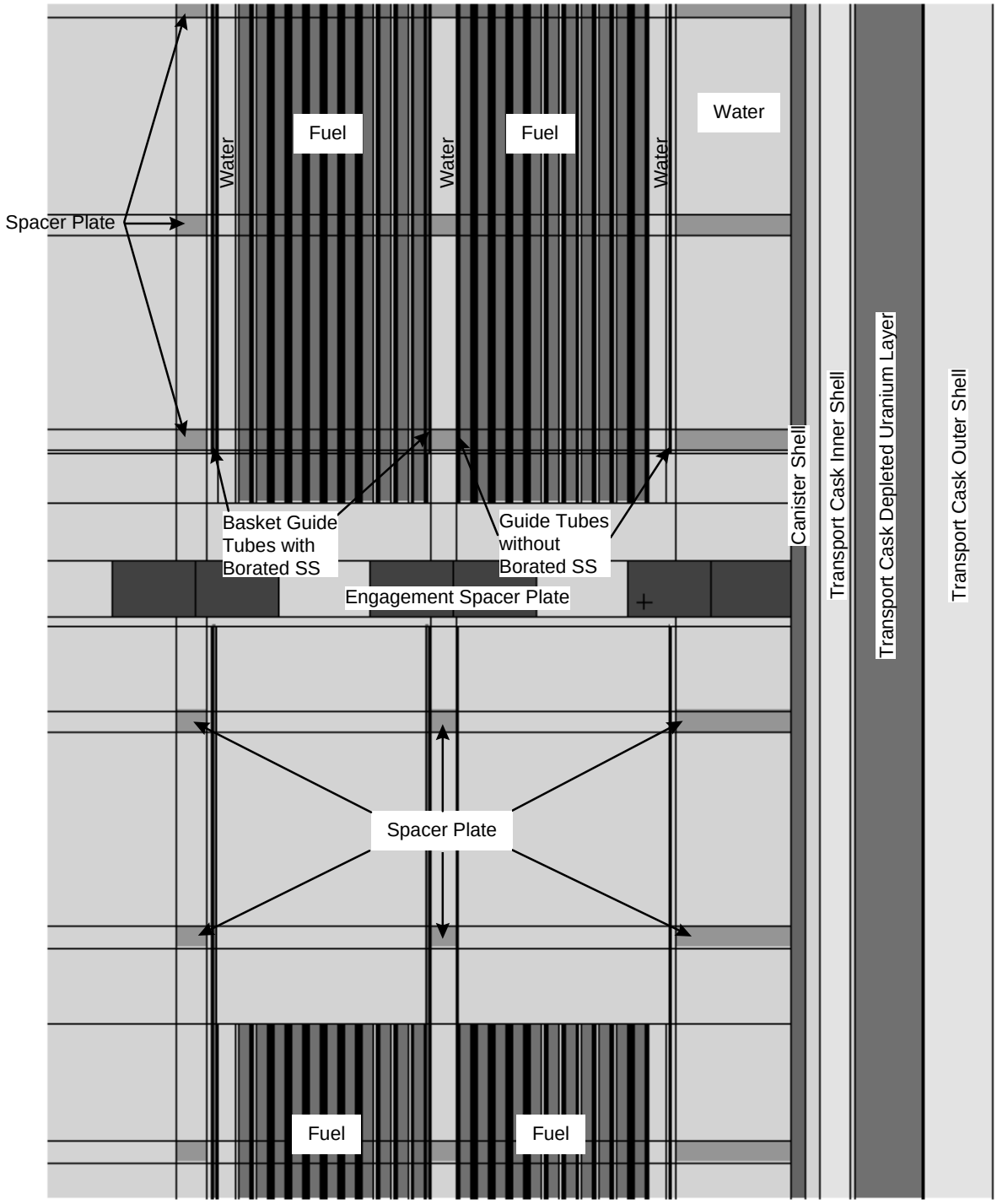

Figure 6.3-10 - Side View of Middle Portion of the FuelSolutions™ W74 Hypothetical Accident Conditions Model (cut-away)

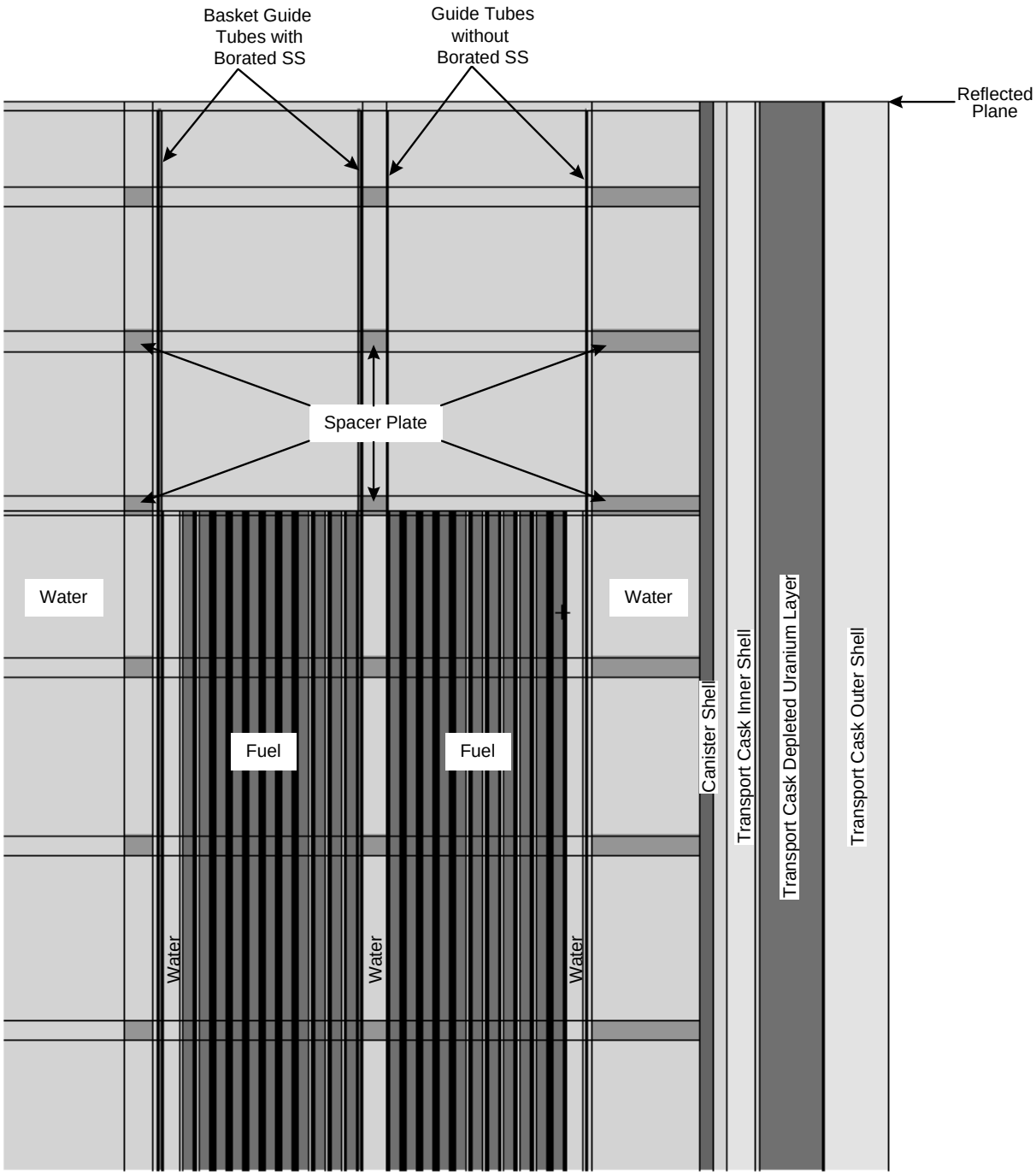

Figure 6.3-11 - Side View of Upper Portion of the FuelSolutions™ W74 Hypothetical Accident Conditions Model (cut-away)

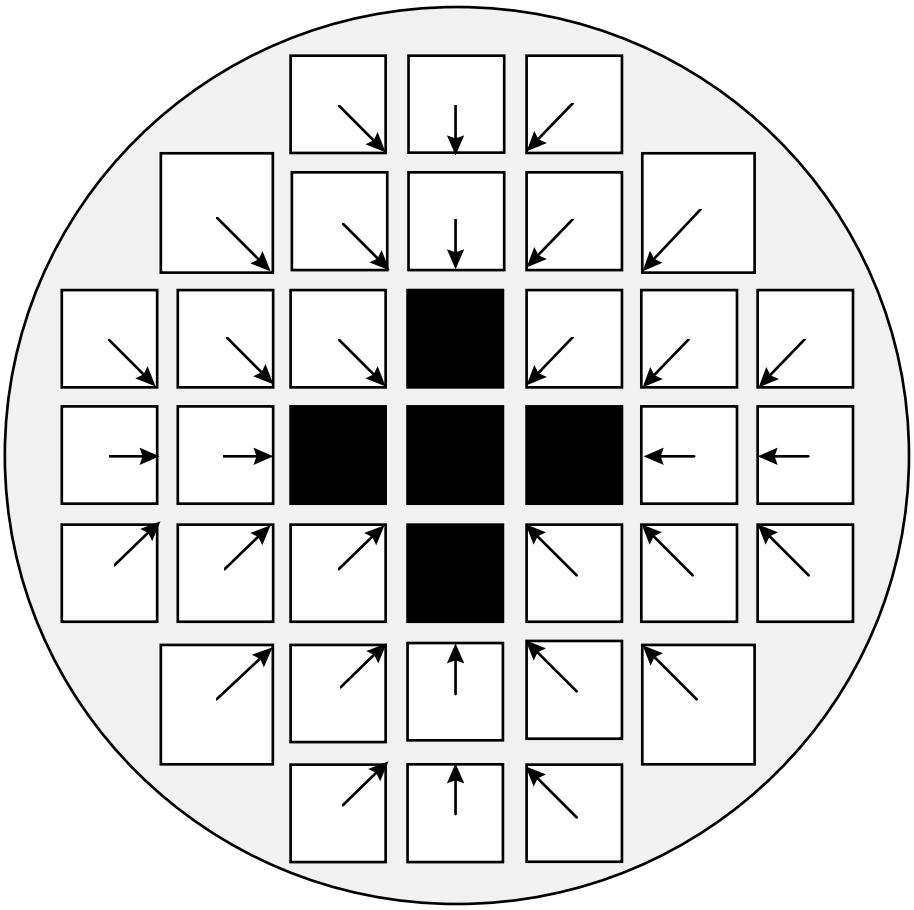

Figure 6.3-12 - FuelSolutions™ W74 Fuel Pattern No. 1 Basket Configuration

Note: The arrows indicate the direction of application for the spacer plate opening location tolerance.

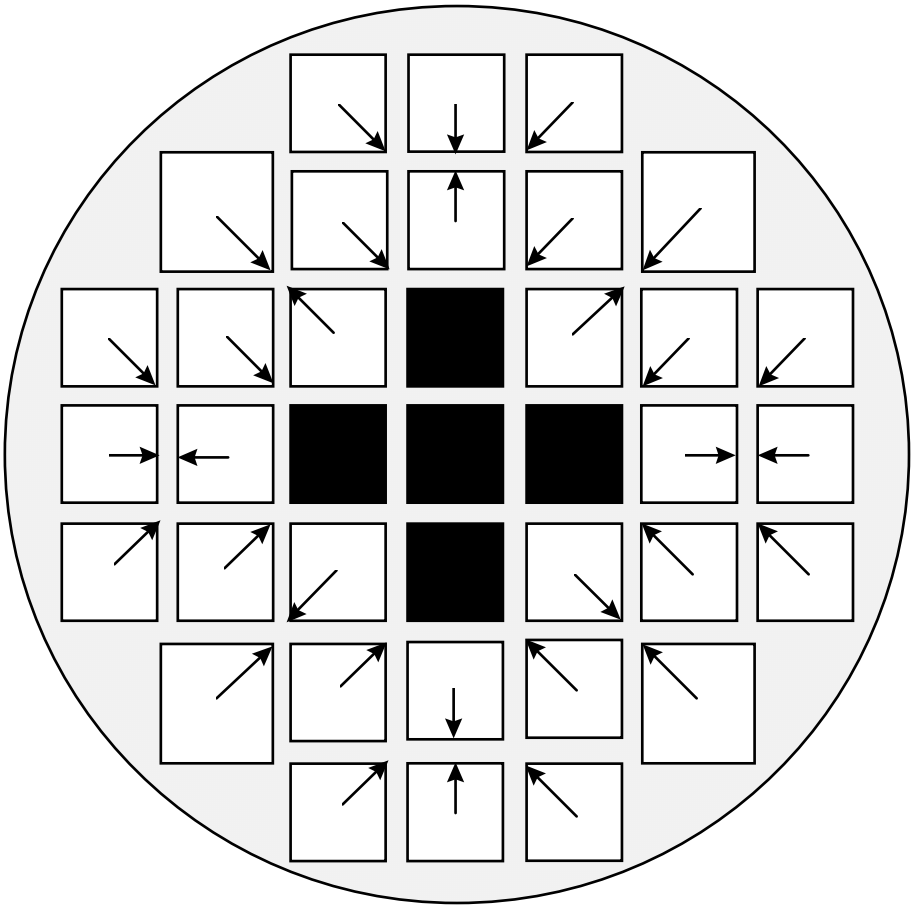

Figure 6.3-13 - FuelSolutions™ W74 Pattern No. 2 Basket Configuration

Note: The arrows indicate the direction of application for the spacer plate opening location tolerance.

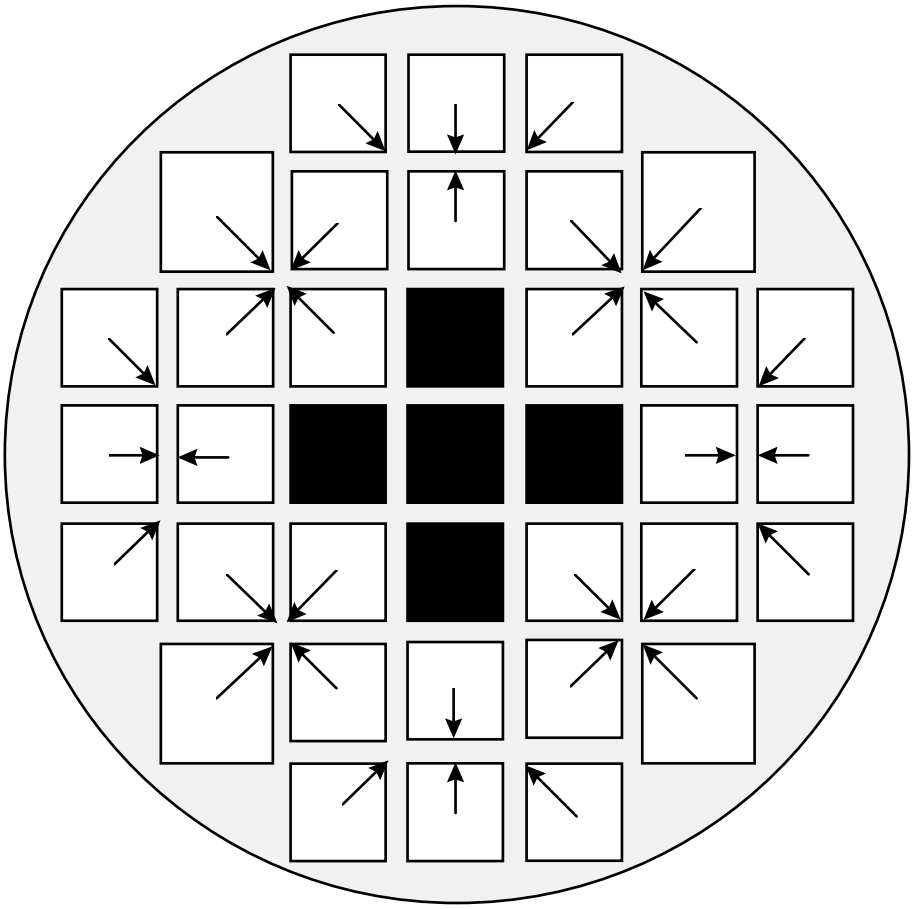

Figure 6.3-14 - FuelSolutions™ W74 Pattern No. 3 Basket Configuration

Note: The arrows indicate the direction of application for the spacer plate opening location tolerance.

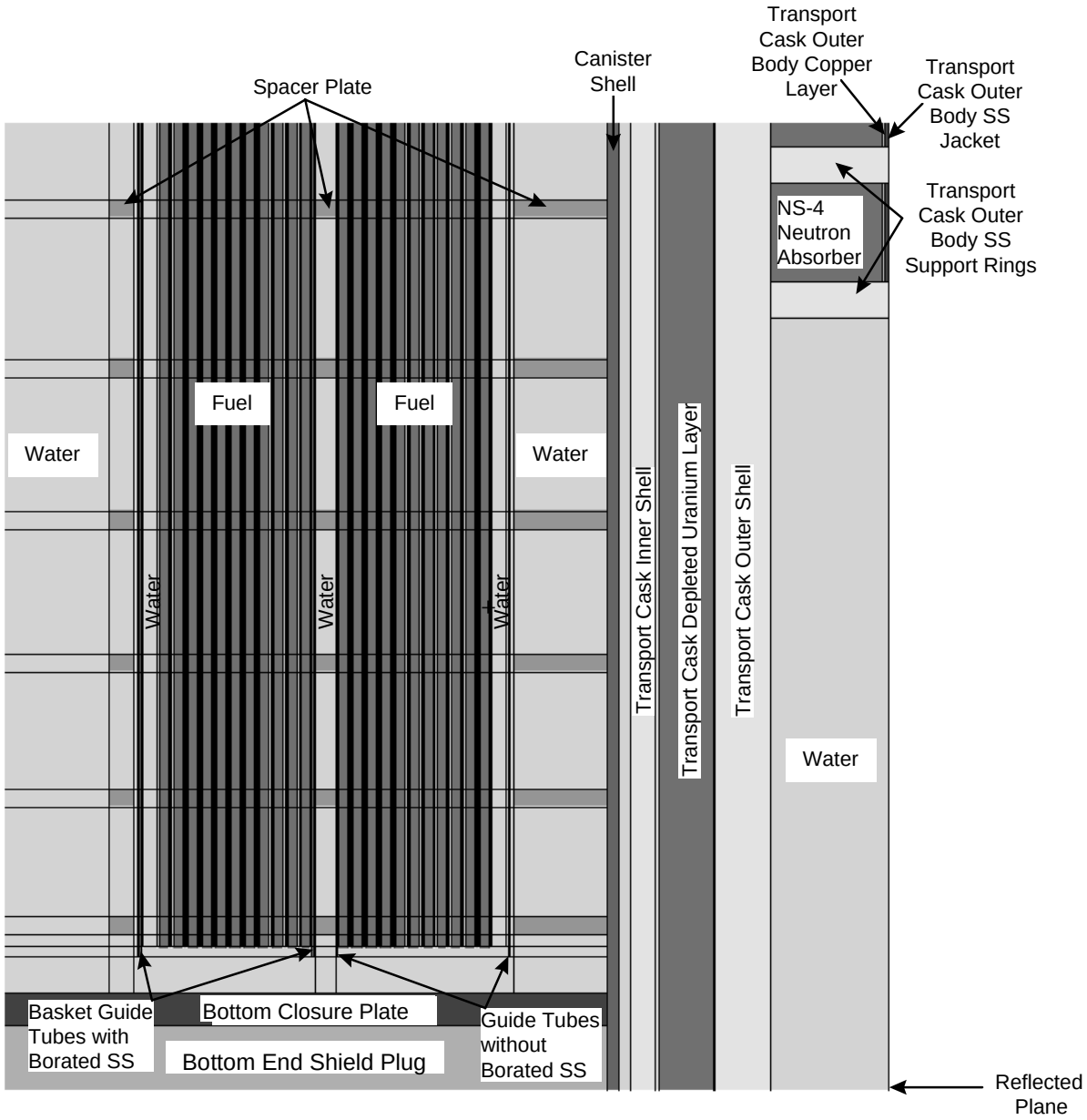

Figure 6.3-15 - Side View of Lower Portion of FuelSolutions™ W74 Normal Conditions Model (cut-away)

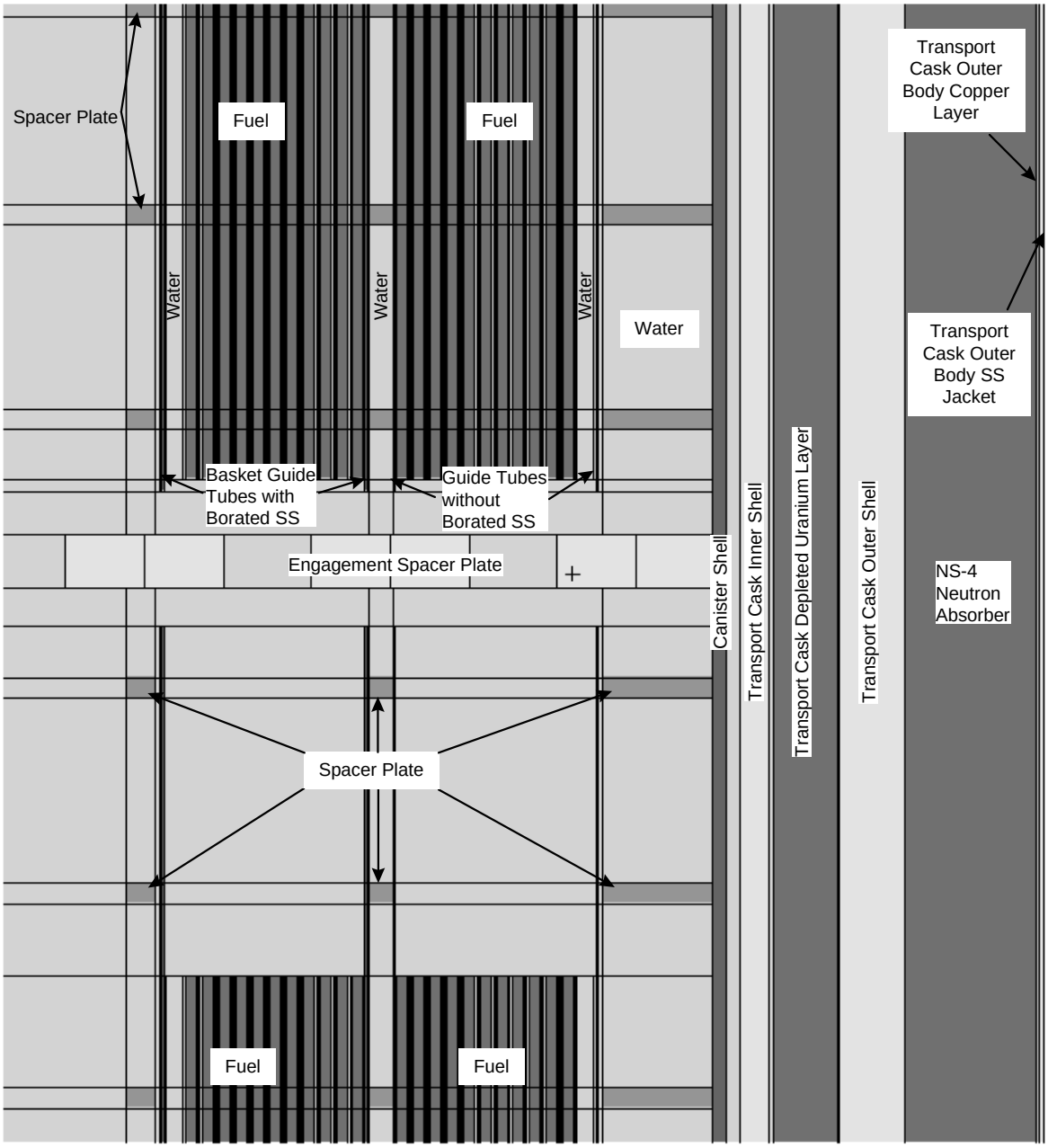

Figure 6.3-16 - Side View of Middle Portion of FuelSolutions™ W74 Normal Conditions Model (cut-away)

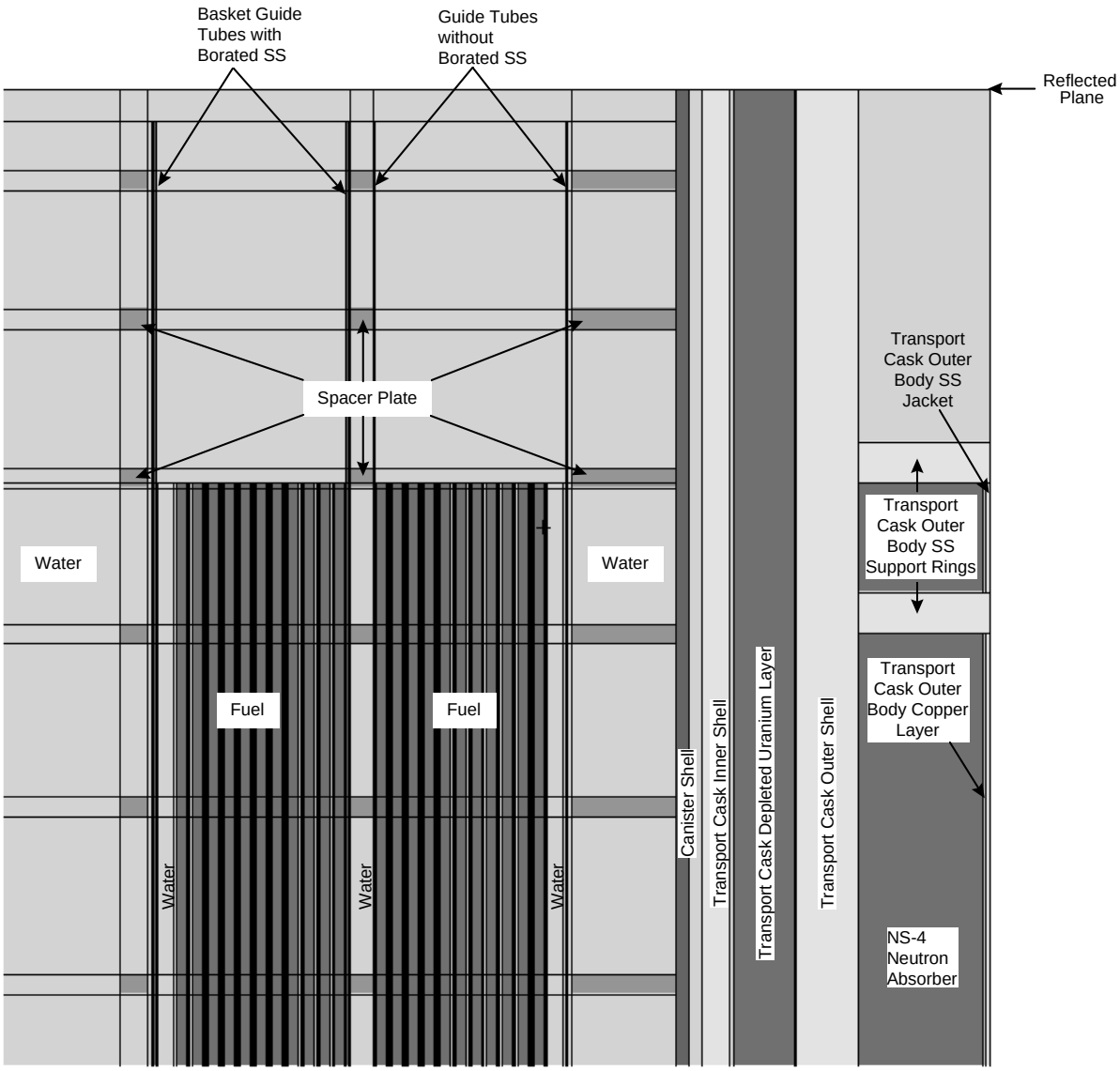

Figure 6.3-17 - Side View of Upper Portion of the FuelSolutions™ W74 Normal Conditions Model (cut-away)

6.4 Criticality Evaluation

6.4.1 Computer Programs

The design method for the FuelSolutions™ W74 canister system analysis uses the MCNP 4a[8] code package for reactivity determination to assure the criticality safety of stored fuel assemblies. MCNP is a general purpose Monte Carlo code that can be used for neutron, photon, electron, or coupled neutron/photon/electron transport. It is suitable for criticality analysis since it has the capability to calculate eigenvalues for critical systems. MCNP treats an arbitrary three dimensional configuration of materials in geometric cells bounded by first and second degree surfaces.

To calculate the effective multiplication factor, MCNP uses three separate estimators: collision, absorption, and track length. The three estimators are statistically combined to provide the best estimate confidence interval for k_{eff}. The primary sources of nuclear data for MCNP are evaluations from the Evaluated Nuclear Data File (ENDF) system, the Evaluated Nuclear Data Library (ENDL), the Activation Library (ACTL) compilations from Lawrence Livermore Laboratory, and evaluations from the Applied Nuclear Science (T-2) Group at Los Alamos. The information from these various sources is incorporated into continuous energy nuclear and atomic data libraries that MCNP uses during a calculation. The primary cross section data file used for the FuelSolutions™ criticality analysis is the ENDF/B-V.

All of the W74 MCNP criticality analyses are performed using 2000 particles per generation, and 400 cycles (or generations). Fifty generations are skipped before tallying the k_{eff} results. This ensures adequate source convergence, particularly in zones of interest, such as the small axial zone at the bottom of the W74 canister where the fuel is not covered by the poison sheets.

6.4.2 Multiplication Factor

6.4.2.1 Package Array

The FuelSolutions™ criticality analyses model infinite arrays of canisters inside a representative transportation cask geometry. Since FuelSolutions™ W74 canisters are stored in the dry condition, the transportation cask array configuration is selected for evaluation as the bounding array condition. The applicability of transportation cask array models to storage conditions is discussed further in Section 6.6 of the FuelSolutions™ Storage System FSAR. The modeled transportation cask geometry does not correspond to any specific transportation cask design for which a 10CFR71 license is being sought.

The array model consists of an infinite number of FuelSolutions™ W74 canisters/casks with adjacent casks in contact with one another in a close packed (triangular pitch) arrangement with interspersed moderator. Case studies are first presented to establish:

[8] Briesmeister, J., *MCNP-4A General Monte Carlo Code N-Particle Transport Code Version 4A*, LA-12625-M, November 1993.

- The worst case canister configuration
- The optimum pure water moderator density condition
- The limiting case between the W100 transfer cask and the modeled transportation cask array
- The limiting case between the uniform enrichment and the multiple pin enrichment configurations
- The limiting BRP fuel assembly design configuration

The hypothetical accident and the normal conditions of operation models, which provide the analytical basis for the initial enrichment fuel acceptance criterion, are analyzed for the design basis fuel loading case of up to 64 Siemens 11x11 fuel assemblies.

6.4.2.1.1 Case Studies

6.4.2.1.1.1 Canister Configuration

Two canister designs, designated FuelSolutions™ W74M and FuelSolutions™ W74T, are considered for the FuelSolutions™ W74 models. The two designs differ with respect to the materials used for the support tubes, alignment bars, vent/drain port covers, bottom end plates, bottom closure plates, canister shell assemblies, and engagement spacer plates. In the W74M, SS-316 is used for these components, while in the W74T, the material is SS-304. Since SS-316 and SS-304 undergo similar interaction with neutrons, the material differences between the two canister designs are not expected to produce appreciable reactivity differences.

In addition to the material differences in the FuelSolutions™ W74M and W74T, the number, separation distances, and thickness of the spacer plates in each canister basket are also different. The spacer plate thickness and axial location have a significant influence on the reactivity of the basket. The FuelSolutions™ W74 basket is not a true “flux trap” design, as it does not have poison sheets on both sides of its water gaps.

The spacer plate thickness and axial locations influence the size and the physics of the water gaps in the FuelSolutions™ W74 basket and, therefore, have an impact on the reactivity of the system. Since there is no borated stainless steel sheet on one side of the water gap in the FuelSolutions™ W74 basket, the replacement of water in that region with spacer plate material is a reactivity benefit. The relatively high thermal neutron flux in the FuelSolutions™ W74 water gap results in a higher probability of resonance absorption by the iron and manganese present in the spacer plates, providing a negative reactivity impact.

To validate the discussion of spacer plate impact on system reactivity, three cases are run using the package array, hypothetical accident case model for the FuelSolutions™ W74 canister. Each model contains the Siemens 11x11 fuel assembly at a uniform pin enrichment of 4.10 w/o ^{235}U. The first case is an infinite axial model with 3.0 inches of water separating each spacer plate; the second case involves the same infinite axial model with 5.0 inches of water separating each spacer plate; the final case includes the infinite axial model with 7.0 inches of water separating each spacer plate.

The results of the spacer plate study are shown in Table 6.4-1. As evident from the results in Table 6.4-1, the spacer plates reduce the reactivity of the system by their presence in the water gaps of the FuelSolutions™ W74.

Since the spacer plate study shows that maximum spacer plate spacing increases system reactivity, the FuelSolutions™ W74M and W74T basket configurations are compared to determine which one contains spacer plates with maximum axial separation. From the comparison, it is evident that the W74T basket has slightly larger axial spacing for its spacer plates in some regions, however, the difference is so small that it is considered to have a negligible impact on reactivity. Because the spacer plate spacing in the FuelSolutions™ W74M and W74T canister designs are so similar for the two basket configurations, neither design configuration is expected to dominate the other with respect to reactivity. If any discernible differences in reactivity exist, the FuelSolutions™ W74T design is expected to be slightly more reactive than the W74M design since it has fewer spacer plates and contains Type A spacer plates which are 0.75 inch thick and provide less absorption of neutrons than the two inch thick Type A spacer plates in the W74M design. Therefore, the FuelSolutions™ W74T design is chosen for the remaining criticality calculations.

Three fuel assembly placement patterns are investigated to determine the worst case asymmetric placement of assemblies and the worst case applications of the spacer plate hole location tolerances. The three patterns are shown in Figure 6.3-12 through Figure 6.3-14. Figure 6.3-12 presents the Pattern 1 basket configuration in which the assemblies and spacer plate holes are shifted toward the center of the basket. Figure 6.3-13 depicts the Pattern 2 basket configuration in which the assemblies and spacer plate holes immediately adjacent to the flat surfaces of the non-fuel positions are shifted away from the center of the basket, while all other assemblies and spacer plate holes are shifted toward the center of the basket. Figure 6.3-14 shows the Pattern 3 basket configuration in which assemblies and spacer plate holes on the periphery are shifted toward the center of the basket while those in the center are shifted toward the periphery of the basket. MCNP models are developed for the three assembly placement patterns and runs are performed to determine the most reactive configuration. The MCNP models are constructed using the Siemens 11x11 fuel assembly in the package array under hypothetical accident conditions.

The results of the assembly placement calculations are shown in Table 6.4-1. Based on the results in Table 6.4-1, the Pattern 3 assembly placement is demonstrated to yield the highest reactivity. Therefore, the Pattern 3 assembly placement configuration is used in subsequent criticality calculations.

The Pattern 3 asymmetric assembly placement is used to determine a bounding configuration for the damage incurred by the FuelSolutions™ W74 basket from a 9 meter transportation cask drop (which is bounding for all storage conditions or drop events). Structural calculations indicate that the damage consists of a maximum guide tube deflection of ~0.125 inch within the basket spans containing fuel assembly mid-grids. There are no guide tube deformations within any of the other axial spans between basket spacer plates. To simplify the MCNP models for subsequent calculations, two MCNP runs are made to demonstrate that modeling the deformation at 0.08 inch over the entire length of the guide tube is more conservative than modeling a 0.125 inch maximum deflection within axial spans that contain fuel assembly mid-grids. The first model contains four spacer plates with reflected boundary conditions for the top and bottom spacer plates resulting in an infinite axial model. The bounding radial configuration from the asymmetric assembly placement is used for the first model. This configuration incorporates a 0.08 inch deflection over the entire length of the guide tube. The second model is identical to the

first except that a 0.125 inch maximum guide tube deflection is incorporated in every third span between spacer plates.

The results from the two MCNP runs are shown in Table 6.4-1 and are compared to determine the bounding representation of guide tube damage incurred from the nine meter drop. As shown in Table 6.4-1, the case with a 0.08 inch deflection over the entire length of the guide tube bounds the case with a maximum guide tube deflection of 0.125 inch in every third span between spacer plates. Therefore, it is conservative in subsequent models to use the 0.08 inch deflection over the entire length of the guide tube to represent the damage incurred by the W74 basket in a nine meter drop.

6.4.2.1.1.2 Material and Manufacturing Tolerance Scoping Analyses for the FuelSolutions™ W74T Canister Design

The material and manufacturing tolerances applied to the MCNP models for the FuelSolutions™ W74 criticality analysis are listed in Table 6.3-2. To demonstrate that these variations from the canister nominal dimensions result in worst case reactivity conditions, the Siemens 11x11 fuel assembly is placed into the infinite array, hypothetical accident case model, and an MCNP run is initiated. The results from this run, which is designated the base case, are compared to six other tolerance cases.

The six other tolerance cases are created from the base case model by successively incorporating the opposing tolerance limit for the guide tube inside and outside dimensions, the borated stainless steel width and thickness, and the support tube inside and outside dimensions. The spacer plate thickness, hole width, and hole location tolerances are not studied in the Material and Manufacturing Tolerance Scoping Analysis. The impact of spacer plate thickness on system reactivity is inferred from the results of the spacer plate scoping calculations. The spacer plate hole location tolerances are investigated during the asymmetric assembly placement study. The spacer plate hole width is chosen to decrease the fuel assembly center-to-center spacing, thus increasing fuel assembly interaction and overall reactivity. The final results for the tolerance scoping analysis are shown in Table 6.4-2. Based on the results in Table 6.4-2, the tolerances listed in Table 6.3-2 are demonstrated to be worst case.

6.4.2.1.1.3 Optimum Moderator Density Scoping Analyses for the FuelSolutions™ W74T Canister Design

The hypothetical accident and normal operating conditions models for the FuelSolutions™ W74 canister are completely flooded with water at a density sufficient for optimum moderation. Optimum moderation is the condition that produces the highest k_{eff} value over the range of moderation conditions. In the FuelSolutions™ W74 multiple package array models, water is present inside the containment boundary of the canisters as well as in between casks. Therefore, two cases are considered for the optimum moderation calculations: the interspersed moderator case in which the moderator density is varied outside the containment boundary, and the interior moderator case in which the moderator density is varied inside the containment boundary.

For the interspersed moderator case, the Siemens 11x11 bounding fuel assembly is placed into the hypothetical accident condition, multiple package array model; and the moderator density outside the containment boundary is varied between 0.0 and 1.0 g/cc. The assumptions listed in

Section 6.3.1 are used for the model, and the fuel is modeled with uranium dioxide at a uniform pin enrichment of 4.10 w/o ^{235}U over the entire length of each fuel stack.

MCNP calculations are performed for each interspersed moderator density case and the results are shown in Table 6.4-3. As shown in Table 6.4-3, optimum interspersed moderation occurs at a water density of 1.0 g/cc. Based on these results, all multiple package array calculations are made using an interspersed water density of 1.0 g/cc.

For the interior moderator case, the Siemens 11x11 bounding fuel assembly is placed into the hypothetical accident condition, multiple package array model; and the moderator density inside the containment boundary is varied between 0.0 and 1.0 g/cc. The assumptions listed in Section 6.3.1 are used for the model, and the fuel is modeled with uranium dioxide at a uniform pin enrichment of 4.10 w/o ^{235}U over the entire length of each fuel stack.

MCNP calculations are performed for each interior moderator density case and the results are shown in Table 6.4-4. As shown in Table 6.4-4, optimum interior moderation occurs at a water density of 1.0 g/cc. Based on these results, all calculations for the FuelSolutions™ W74 canisters are made with an interior water density of 1.0 g/cc.

6.4.2.1.1.4 Scoping Analysis for the W74 Canister Inside the W100 Transfer Cask

For the FuelSolutions™ Spent Fuel Management System, the fuel storage criticality calculations are performed using a model of an infinite array of transportation cask configurations. Analyses for the storage mode of operation are not specifically performed. Instead, it is assumed that calculations for the modeled transportation cask configuration is bounding because:

- The severity of the hypothetical accident conditions assumed for transportation bound all conditions (canister *g*-loads, etc.) of storage. This results in a limiting system configuration to be analyzed because of limiting canister basket deformations and damage to the cask body.
- The modeled transportation cask configuration has a depleted uranium (DU) shield design in contrast to the W100 cask which is lead shielded. The W100 cask is shown to be no more reactive than the modeled transportation cask under similar basket configurations.

MCNP runs are made to confirm the W100 transfer cask is no more limiting than the representative transportation cask configuration. A single transportation package under hypothetical accident conditions, surrounded by 12 inches of water for reflection is modeled. The transfer cask model includes a single basket and cask configuration under normal operating conditions, since the transfer cask is not subjected to the hypothetical accident. The single transfer cask is surrounded by 12 inches of water for reflection, similar to the transport cask model. The results of the MCNP runs for the transportation and transfer casks are shown in Table 6.4-5. As demonstrated in Table 6.4-5, the transportation cask is more limiting than the transfer cask under these assumed conditions. In addition to these two calculations, an MCNP run is performed for a transfer cask that contains a basket assembly subjected to the same hypothetical accident conditions as the transport cask. This calculation is performed to demonstrate that, even under similar basket configurations, the transfer cask is not more limiting than the transport cask. The results of this run are also shown in Table 6.4-5, and indicate no statistically significant difference between the transportation and transfer casks. Therefore, the

calculations performed using a representative transportation cask configuration are bounding and applicable for all conditions of storage with the FuelSolutions™ dry storage system.

6.4.2.1.1.5 Uniform Pin Enrichment Analysis

The fuel assembly designs that are considered for storage in the FuelSolutions™ W74 canister have multiple pin enrichments rather than a single enrichment for the entire fuel assembly. For fuel qualification, it is desirable to specify a single enrichment limit for a fuel assembly type of interest without including fuel rod enrichment patterns. A uniform enrichment may be determined for a fuel assembly that contains multiple fuel rod enrichments by calculating a pin weighted average enrichment for any radial cross-section along the axis of the fuel assembly. In order to use the pin weighted average enrichment to qualify fuel with multiple pin enrichments, it must be demonstrated that the average enrichment applied uniformly throughout the assembly is an adequate or conservative representation of the multiple pin enrichments present in that fuel assembly.

Among the BRP fuel assemblies that contain uranium (no mixed oxide fuel), eight multiple fuel rod enrichment patterns are identified. Four of the multiple enrichment patterns are associated with General Electric 9x9/Siemens fuel assemblies and are shown in Figure 6.4-1 through Figure 6.4-4. The remaining four patterns are affiliated with the Siemens 11x11 fuel assembly type and are shown in Figure 6.4-5 through Figure 6.4-8. The uniform enrichment used to represent these fuel assemblies is calculated in the following manner:

- The number of fuel rods at a particular enrichment is multiplied by that enrichment, and the result is divided by the total number of fuel rods in the assembly.
- The sum of the results for all enrichments within an assembly gives the desired uniform enrichment.
- The burnable absorber present in certain fuel rods within the assemblies is neglected for the purposes of establishing the uniform enrichment. The fuel rods with burnable absorbers are treated as though they contain only UO_2.
- The cobalt rod locations in the corners of some fuel assemblies are filled with UO_2 rods at the highest enrichment present in the assembly. As a result, these locations, which are currently empty, can be filled with fuel rods prior to loading the assembly in the FuelSolutions™ W74 canister as long as the assembly meets the specified uniform enrichment limit with the fuel rods in place.

Once the uniform enrichments for the eight BRP fuel assembly patterns are established, two sets of MCNP calculations are made using the infinite array, hypothetical accident case model. The first set of MCNP calculations consist of eight separate models in which the FuelSolutions™W74 is filled with each fuel assembly type depicted in Figure 6.4-1 through Figure 6.4-8. The second set of MCNP calculations consist of eight models in which the FuelSolutions™W74 is filled with each fuel assembly type at the calculated uniform enrichment for the patterns shown in Figure 6.4-1 through Figure 6.4-8. The results of the first set of calculations is shown in Table 6.4-6 and is compared to the results of the second set of calculations shown in Table 6.4-7. Based on a comparison of the results in Table 6.4-6 and Table 6.4-7, the uniform pin enrichment cases bound the appropriate multiple pin enrichment cases. Therefore, a single enrichment may be specified as an acceptance criterion for BRP fuel

assemblies with multiple pin enrichments. To be qualified for storage in the FuelSolutions™ W74 canister, BRP fuel assemblies must have a maximum lattice enrichment less than or equal to the specified limit, where lattice enrichment means the highest pin-weighted enrichment average along the axial length of the fuel.

6.4.2.1.2 Hypothetical Accident Conditions Analyses for the FuelSolutions™ W74 Canister

Using the assumptions listed in Section 6.3.1, a multiple package array hypothetical accident condition model is developed for each BRP fuel assembly design listed in Table 6.2-1. MCNP calculations are performed to determine the bounding fuel assembly design, which will be used to calculate the maximum allowable ^{235}U enrichment for BRP fuel in the FuelSolutions™ W74 canister. The results of the MCNP runs are shown in Table 6.4-8. Table 6.4-8 shows the calculated final k_{eff} results for the hypothetical accident condition calculations, along with the limiting (lowest) USL value and the margin between the final k_{eff} and the limiting USL value, for each specific assembly configuration listed in Table 6.2-1.

The analyses results show that the maximum final calculated k_{eff} value, as well as the lowest margin versus the limiting USL value, occurs for the Siemens 11x11 fuel assembly with all 121 lattice locations filled with fuel rods. The results presented in Table 6.4-8 also show that the final calculated k_{eff} values remain under the limiting USL value for each of the specific assembly designs. Thus the analyses verify that, at the maximum allowable enrichment defined in Table 6.1-1, the criticality requirements are met for all BRP fuel assemblies.

For all BRP fuel assemblies, either the water/fuel or pin pitch USL is the limiting USL value. The water/fuel USL is the limiting value for the General Electric and Siemens 9x9 fuel assembly designs, while the pin pitch USL is limiting for the Siemens 11x11 fuel assembly designs. Thus, either the water/fuel or pin pitch USL value is presented in Table 6.4-8 and is used to determine the criticality margins shown in that table. Simple formulas shown in Section 6.5 give the USL values as a function of assembly pin pitch, enrichment, water-to-fuel volume ratio, and H-to-^{235}U ratio. For each of these four USL parameters, the ranges covered by the specific fuel assembly types described in Table 6.2-1 are presented in Table 6.4-9. Table 6.4-9 also presents the corresponding USL value range for each of the four parameters.

6.4.2.1.3 Normal Operating Conditions Analyses for FuelSolutions™ W74 Canister Design

Using the assumptions listed in Section 6.3.1, a multiple package array normal operating condition model is developed for the Siemens 11x11 BRP fuel assembly design. MCNP calculations are performed to demonstrate that the maximum allowable ^{235}U enrichments calculated in Section 6.4.2.1.2 for a FuelSolutions W74 canister loading of 64 Siemens 11x11 BRP fuel assemblies is acceptable under normal operating conditions. The result of the normal operating condition calculation is shown in Table 6.4-10. Comparison of the final calculated k_{eff} value for normal operating conditions calculation to the accident condition k_{eff} value shown in Table 6.4-8 shows that the accident condition is more reactive (i.e., bounding). The USL values do not change between accident and normal operating conditions, so the calculated k_{eff} values may be compared directly to determine which case is more limiting with respect to criticality.

6.4.2.2 Single Package

The single package models demonstrate that a FuelSolutions™ W74 canister remains adequately subcritical. The assumptions listed in Section 6.3.1 are used to develop the hypothetical accident and the normal conditions model for a single FuelSolutions™ W74 canister. The Siemens 11x11 BRP fuel assembly design is selected as a representative fuel type for the single package model.

6.4.2.2.1 Hypothetical Accident Conditions Analyses for FuelSolutions™ W74 Canister Design

Using the assumptions listed in Section 6.3.1, a single package hypothetical accident condition model is developed assuming a FuelSolutions™ W74 canister loading of 64 assemblies using the Siemens 11x11 BRP fuel assembly design. MCNP calculations are performed using the single package, hypothetical accident condition model and the results are compared to those from the package array hypothetical accident condition calculations. The results from the single package hypothetical accident condition calculation are shown in Table 6.4-11. Based on a comparison of the results in Table 6.4-8 and Table 6.4-11 for loadings under accident conditions, there is no statistically significant difference between the results for the multiple package array case and the single package case under hypothetical accident conditions. This finding indicates that the fuel assemblies within a canister are effectively isolated from the fuel assemblies in an adjacent container.

6.4.2.2.2 Normal Operating Conditions Analyses for FuelSolutions™ W74 Canister Design

Using the assumptions listed in Section 6.3.1, a single package normal operating condition model is developed assuming a FuelSolutions™ W74 canister loading of 64 assemblies using the Siemens 11x11 BRP fuel assembly for the FuelSolutions™ W74 canister. MCNP calculations are performed using the single package normal operating condition model and the results are compared to the results from the package array normal operating condition calculation. The results from the single package normal operating condition calculation are shown in Table 6.4-11. Based on the comparison of results presented in Table 6.4-10 and Table 6.4-11, there is no statistically significant difference between the results for the package array case and the single package case under normal operating conditions. Therefore, as demonstrated previously, the fuel assemblies within a given canister are effectively isolated from the fuel assemblies in neighboring canisters.

Table 6.4-1 - MCNP Results for the Canister Design Case Studies

Case	Description	^{235}U Enrichment (w/o)	k_{eff}	Uncertainty	$k_{eff} + 2\sigma$
1	W74T - HAC - Spacer Plate Spacing 3.0”	4.10	0.94220	0.00083	0.94386
2	W74T - HAC - Spacer Plate Spacing 5.0”	4.10	0.94467	0.00092	0.94651
3	W74T - HAC - Spacer Plate Spacing 7.0”	4.10	0.94638	0.00087	0.94812
4	W74T-HAC Asymmetric Assembly Pattern 1	4.10	0.91986	0.00087	0.92160
5	W74T-HAC Asymmetric Assembly Pattern 2	4.10	0.93622	0.00089	0.93800
6	W74T-HAC Asymmetric Assembly Pattern 3	4.10	0.93831	0.00088	0.94007
7	W74T-HAC Asymmetric Assembly Pattern 3, 0.08” Guide Tube Deformation	4.10	0.94758	0.00087	0.94932
8	W74T-HAC Asymmetric Assembly Pattern 3, 0.125” Guide Tube Deformation	4.10	0.94450	0.00084	0.94618

Table 6.4-2 - Material and Fabrication Tolerance Results for the FuelSolutions™ W74 Canister

Case	Description	^{235}U Enrichment	k_{eff}	Uncertainty	$k_{eff}+2\sigma$
1	Siemens 11x11, Pattern 3 Base Case	4.10	0.93831	0.00088	0.94007
2	11x11 Array, Borated SS Thickness tolerance + 0.007”	4.10	0.93129	0.00092	0.93313
3	11x11 Array, Borated SS Width tolerance + 0.05”	4.10	0.93536	0.00092	0.93720
4	11x11 Array, Guide Tube Inner Dimension tolerance - 0.05”	4.10	0.93436	0.00085	0.93606
5	11x11 Array, Guide Tube Outer Dimension tolerance + 0.008”	4.10	0.93280	0.00091	0.93462
6[(1)]	11x11 Array, Support Tube Inner Dimension tolerance - 0.05”	4.10	0.93697	0.00090	0.93877
7	11x11 Array, Support Tube Outer Dimension tolerance + 0.055”	4.10	0.93430	0.00091	0.93612

Note:

(1) The difference between the results for this case and the base case is statistically insignificant.

Table 6.4-3 - Optimum Interspersed Moderator Case Results for the FuelSolutions™ W74 Canister

Case	Moderator Density (g/cm^3)	^{235}U Enrichment (w/o)	k_{eff}	Uncertainty	$k_{eff} + 2\sigma$
1	1.0	4.10	0.93831	0.00088	0.94007
2	0.8	4.10	0.93754	0.00087	0.93928
3	0.6	4.10	0.93686	0.00093	0.93872
4	0.4	4.10	0.93618	0.00096	0.93810
5	0.2	4.10	0.93717	0.00090	0.93897
6	0.1	4.10	0.93572	0.00087	0.93746
7	0.08	4.10	0.93610	0.00090	0.93790
8	0.06	4.10	0.93687	0.00088	0.93863
9	0.04	4.10	0.93520	0.00093	0.93706
10	0.02	4.10	0.93676	0.00094	0.93864
11	0.00	4.10	0.93704	0.00091	0.93886

Table 6.4-4 - Optimum Interior Moderator Case Results for the FuelSolutions™ W74 Canister

Case	Moderator Density (g/cm^3)	^{235}U Enrichment (w/o)	k_{eff}	Uncertainty	$k_{eff} + 2\sigma$
1	1.0	4.10	0.93831	0.00088	0.94007
2	0.8	4.10	0.89845	0.00092	0.90029
3	0.6	4.10	0.84791	0.00087	0.84965
4	0.4	4.10	0.77633	0.00088	0.77809
5	0.2	4.10	0.67329	0.00077	0.67483
6	0.1	4.10	0.59582	0.00063	0.59708
7	0.08	4.10	0.57204	0.00060	0.57324
8	0.06	4.10	0.54017	0.00059	0.54135
9	0.04	4.10	0.49778	0.00053	0.49884
10	0.02	4.10	0.44076	0.00049	0.44174
11	0.00	4.10	0.42738	0.00046	0.42830

Table 6.4-5 - MCNP Results for the Single Package Transportation Cask and the Single Package Transfer Cask

Case	Description	^{235}U Enrichment (w/o)	k_{eff}	Uncertainty	$k_{eff} + 2s$
1	Siemens 11x11 Single Package Transportation Cask (HAC)	4.10	0.93716	0.00085	0.93886
2	Siemens 11x11 Single Package Transfer Cask (Normal Basket Conditions)	4.10	0.93382	0.00088	0.93558
3	Siemens 11x11 Single Package Transfer Cask (HA Basket Conditions)	4.10	0.93707	0.00089	0.93885

Table 6.4-6 - MCNP Results for the FuelSolutions™ W74 Canister and Big Rock Point Fuel Assemblies with Multiple Fuel Rod Enrichments

Case	Fuel Pattern	^{235}U Enrichment (w/o)	k_{eff}	Uncertainty	k_{eff} + 2s
1	GE 9x9/ Figure 6.4-1	2.50, 3.40, 4.50	0.89783	0.00087	0.89957
2	GE 9x9/ Figure 6.4-2	2.50, 3.299, 4.50	0.89839	0.00087	0.90013
3	GE 9x9/ Figure 6.4-3	2.50, 3.299, 4.50	0.90114	0.00086	0.90286
4	Siemens 9x9/ Figure 6.4-4	2.55, 3.30, 4.50	0.89946	0.00089	0.90124
5	Siemens 11x11/ Figure 6.4-5	2.30, 3.20, 4.60	0.91266	0.00090	0.91446
6	Siemens 11x11/ Figure 6.4-6	1.50, 2.52, 3.82	0.86146	0.00089	0.86324
7	Siemens 11x11/ Figure 6.4-7	1.66, 2.79, 4.24	0.88098	0.00087	0.88272
8	Siemens 11x11/ Figure 6.4-8	1.80, 2.80, 4.18	0.88099	0.00091	0.88281

Table 6.4-7 - MCNP Results for the FuelSolutions™ W74 Canister and Big Rock Point Fuel Assemblies with Multiple Fuel Rod Enrichments

Case	Fuel Pattern	^{235}U Enrichment (w/o)	k_{eff}	Uncertainty	k_{eff} + 2s
1	GE 9x9/ Figure 6.4-1	3.58	0.90743	0.00087	0.90917
2	GE 9x9/ Figure 6.4-2	3.57	0.90662	0.00086	0.90834
3	GE 9x9/ Figure 6.4-3	3.56	0.90718	0.00092	0.90902
4	Siemens 9x9/ Figure 6.4-4	3.58	0.90647	0.00092	0.90831
5	Siemens 11x11/ Figure 6.4-5	3.90	0.92325	0.00081	0.92487
6	Siemens 11x11/ Figure 6.4-6	3.14	0.87741	0.00083	0.87907
7	Siemens 11x11/ Figure 6.4-7, Figure 6.4-8	3.43	0.89664	0.00091	0.89846

Table 6.4-8 - Multiple Package Array, Hypothetical Accident Condition Results to Determine the Bounding Fuel Assembly Configuration

Fuel Assembly Type	Final k_{eff} (k_{eff} + 2σ)	Minimum USL	Δ
GE-9x9, 81 Fuel Rods	0.93646	0.94358	0.00712
GE-9x9, 1 Water Pin	0.93739	0.94358	0.00619
Siemens 9x9, 81 Fuel Rods	0.93494	0.94358	0.00864
Siemens 11x11, 121 Fuel Rods	0.94007	0.94286	0.00279
Siemens 11x11, 4 Zirc Rods	0.93419	0.94286	0.00867
Siemens 11x11, 1 Zirc Rod	0.93826	0.94286	0.00460
Siemens 11x11, 0.3735” Pellet	0.93721	0.94286	0.00565

Table 6.4-9 - Big Rock Point Fuel Assembly USL Value Ranges

USL Parameter	Parameter Range	USL Value Range
Pin Pitch (cm)	1.47 - 1.80	0.94286 - 0.94382
Enrichment (w/o ^{235}U)	4.10	0.94470
Water-to-Fuel Volume Ratio	1.49 - 1.66	0.94358 - 0.94368
H-to-^{235}U Ratio	101.507 - 113.510	0.94417 - 0.94421

Table 6.4-10 - Multiple Package Array, Normal Operating Condition Results

Fuel Assembly	^{235}U Enrichment (w/o)	k_{eff}	Uncertainty	Final k_{eff} ($k_{eff} + 2\sigma$)
Siemens 11x11, 121 Fuel Rods	4.10	0.93599	0.00091	0.93781

Table 6.4-11 - MCNP Results for the Single Package Models

Case	Description	^{235}U Enrichment (w/o)	k_{eff}	Uncertainty	$k_{eff} + 2\sigma$
1	Single Package Hypothetical Accident Condition	4.10	0.93716	0.00085	0.93886
2	Single Package Normal Operating Condition	4.10	0.93422	0.00089	0.93600

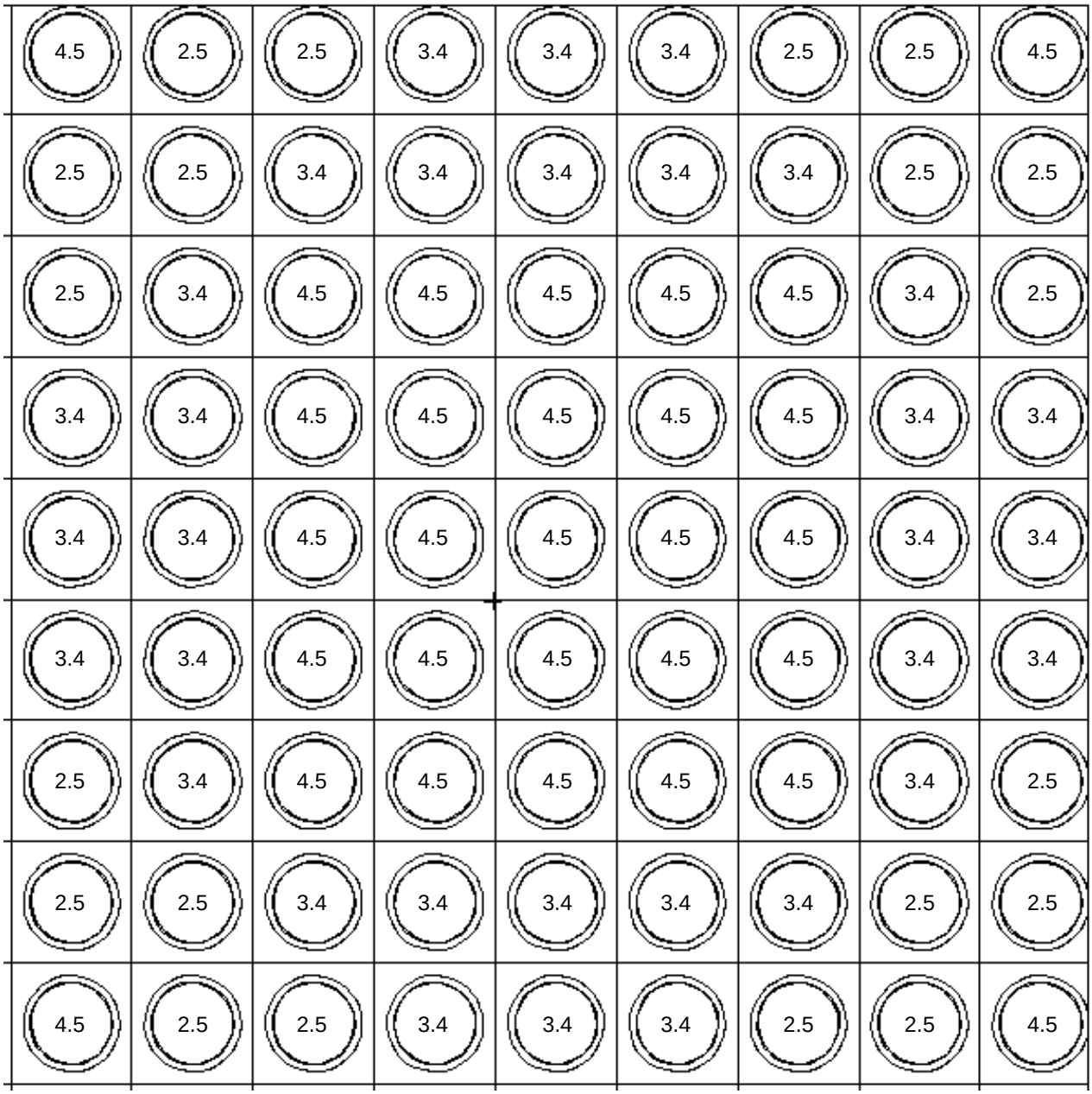

Figure 6.4-1 - Multiple Pin Enrichment Pattern 1 for the Big Rock Point GE 9x9 Fuel

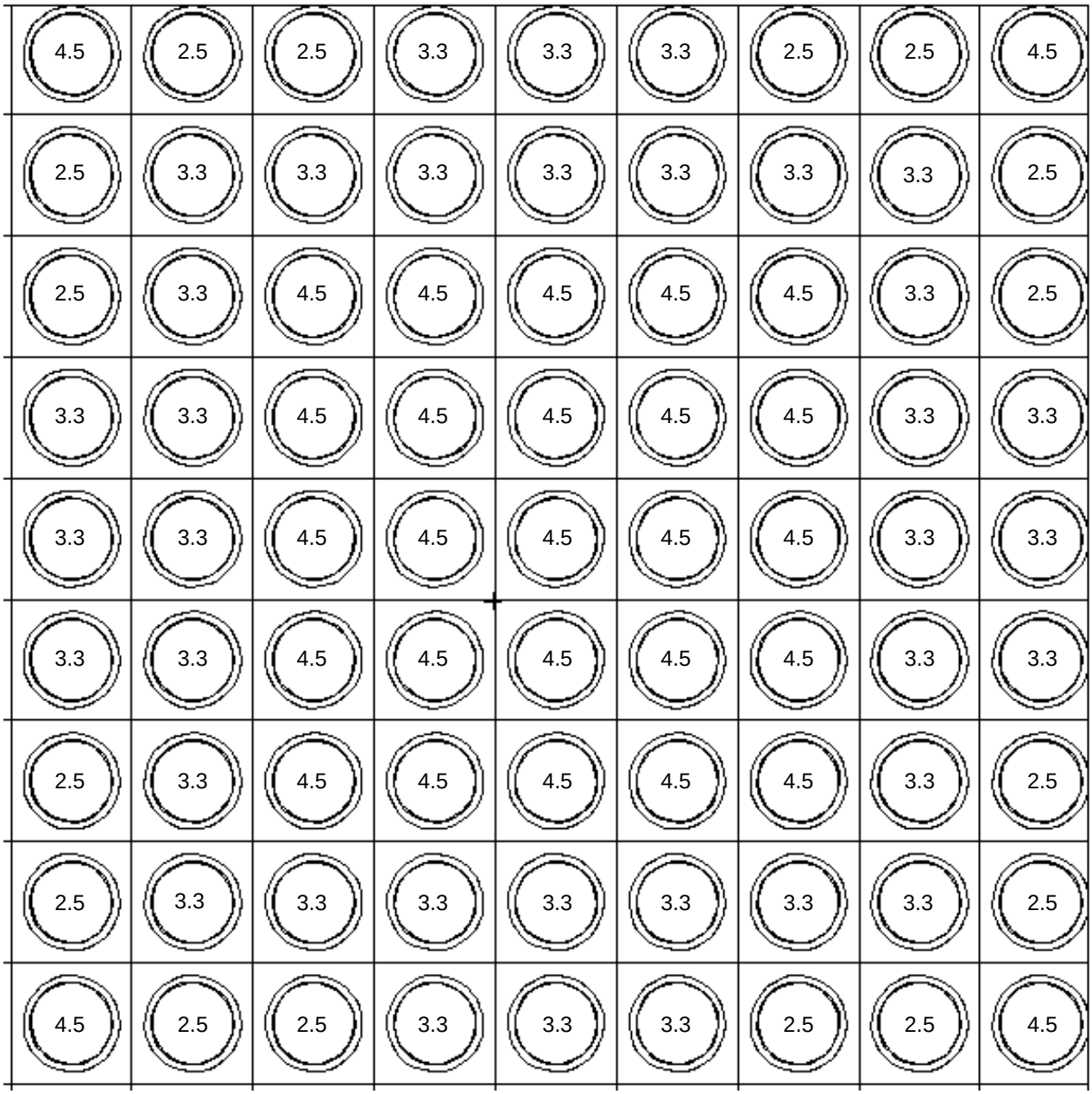

Figure 6.4-2 - Multiple Pin Enrichment Pattern 2 for the Big Rock Point GE 9x9 Fuel Assembly.

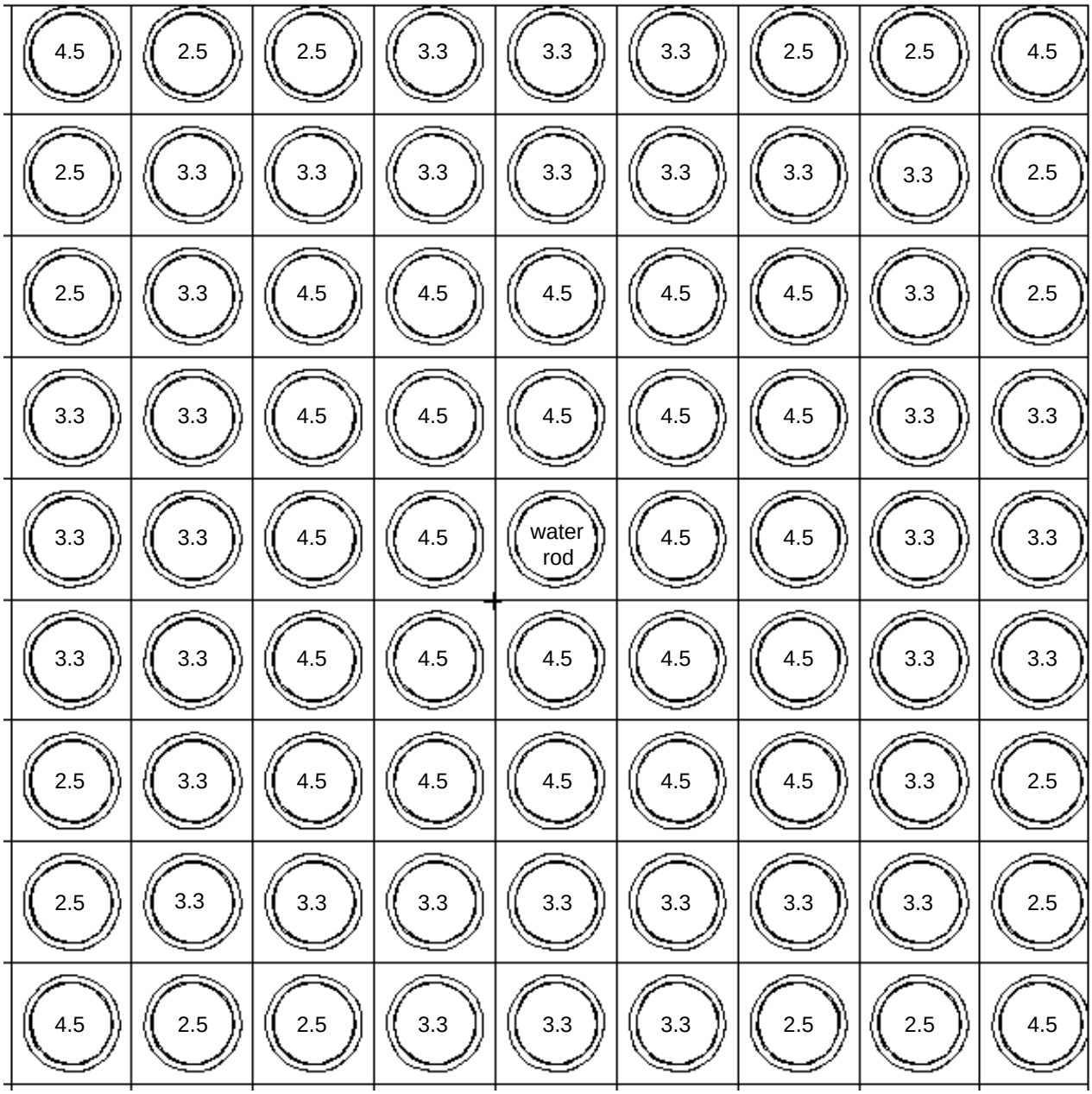

Figure 6.4-3 - Multiple Pin Enrichment Pattern 3 for the Big Rock Point GE 9x9 Fuel Assembly

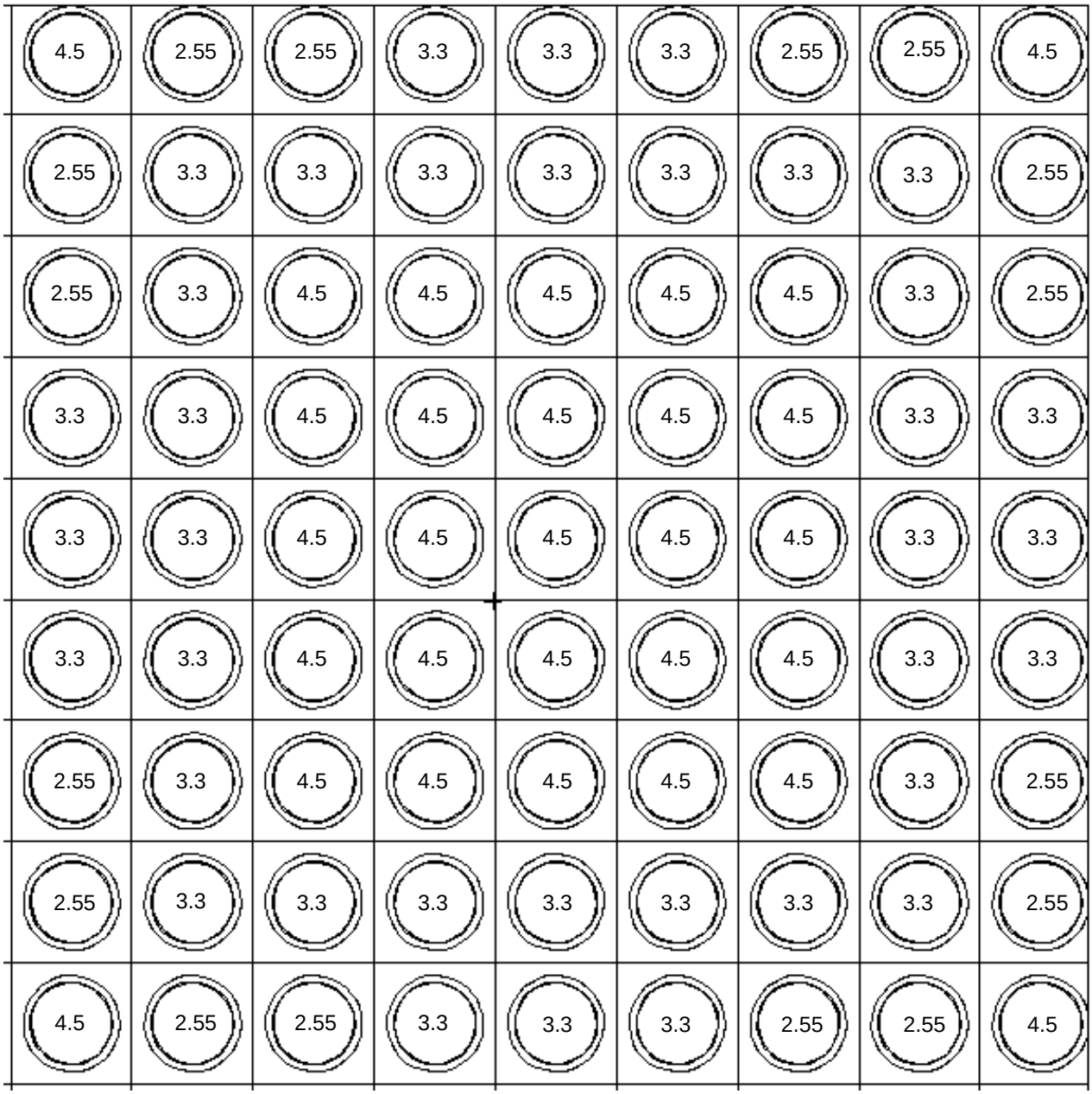

Figure 6.4-4 - Multiple Pin Enrichment Pattern 4 for the Big Rock Point Siemens 9x9 Fuel Assembly

4.6	2.3	2.3	3.2	3.2	3.2	3.2	3.2	2.3	2.3	4.6
2.3	3.2	3.2	4.6	4.6	4.6	4.6	4.6	3.2	3.2	2.3
2.3	3.2	4.6	4.6	4.6	4.6	4.6	4.6	4.6	3.2	2.3
3.2	4.6	4.6	4.6	4.6	4.6	4.6	4.6	4.6	4.6	3.2
3.2	4.6	4.6	4.6	Zirc Rod	4.6	Zirc Rod	4.6	4.6	4.6	3.2
3.2	4.6	4.6	4.6	4.6	4.6	4.6	4.6	4.6	4.6	3.2
3.2	4.6	4.6	4.6	Zirc Rod	4.6	Zirc Rod	4.6	4.6	4.6	3.2
3.2	4.6	4.6	4.6	4.6	4.6	4.6	4.6	4.6	4.6	3.2
2.3	3.2	4.6	4.6	4.6	4.6	4.6	4.6	4.6	3.2	2.3
2.3	3.2	3.2	4.6	4.6	4.6	4.6	4.6	3.2	3.2	2.3
4.6	2.3	2.3	3.2	3.2	3.2	3.2	3.2	2.3	2.3	4.6

Figure 6.4-5 - Multiple Pin Enrichment Pattern 1 for the Big Rock Point Siemens 11x11 Fuel Assembly

1.5	1.5	2.52	2.52	2.52	2.52	2.52	2.52	2.52	1.5	1.5
1.5	2.52	2.52	3.82	3.82	3.82	3.82	3.82	2.52	2.52	1.5
2.52	2.52	3.82	3.82	3.82	3.82	3.82	3.82	3.82	2.52	2.52
2.52	3.82	3.82	3.82	3.82	3.82	3.82	3.82	3.82	3.82	2.52
2.52	3.82	3.82	3.82	Zirc Rod	3.82	Zirc Rod	3.82	3.82	3.82	2.52
2.52	3.82	3.82	3.82	3.82	3.82	3.82	3.82	3.82	3.82	2.52
2.52	3.82	3.82	3.82	Zirc Rod	3.82	Zirc Rod	3.82	3.82	3.82	2.52
2.52	3.82	3.82	3.82	3.82	3.82	3.82	3.82	3.82	3.82	2.52
2.52	2.52	3.82	3.82	3.82	3.82	3.82	3.82	3.82	2.52	2.52
1.5	2.52	2.52	3.82	3.82	3.82	3.82	3.82	2.52	2.52	1.5
1.5	1.5	2.52	2.52	2.52	2.52	2.52	2.52	2.52	1.5	1.5

Figure 6.4-6 - Multiple Pin Enrichment Pattern 2 for the Big Rock Point Siemens 11x11 Fuel Assembly

1.66	1.66	2.79	2.79	2.79	2.79	2.79	2.79	2.79	1.66	1.66
1.66	2.79	2.79	4.24	4.24	4.24	4.24	4.24	2.79	2.79	1.66
2.79	2.79	2.79	4.24	4.24	4.24	4.24	4.24	2.79	2.79	2.79
2.79	4.24	4.24	4.24	4.24	4.24	4.24	4.24	4.24	4.24	2.79
2.79	4.24	4.24	4.24	Zirc Rod	4.24	Zirc Rod	4.24	4.24	4.24	2.79
2.79	4.24	4.24	4.24	4.24	4.24	4.24	4.24	4.24	4.24	2.79
2.79	4.24	4.24	4.24	Zirc Rod	4.24	Zirc Rod	4.24	4.24	4.24	2.79
2.79	4.24	4.24	4.24	4.24	4.24	4.24	4.24	4.24	4.24	2.79
2.79	2.79	2.79	4.24	4.24	4.24	4.24	4.24	2.79	2.79	2.79
1.66	2.79	2.79	4.24	4.24	4.24	4.24	4.24	2.79	2.79	1.66
1.66	1.66	2.79	2.79	2.79	2.79	2.79	2.79	2.79	1.66	1.66

Figure 6.4-7 - Multiple Pin Enrichment Pattern 3 for the Big Rock Point Siemens 11x11 Fuel Assembly

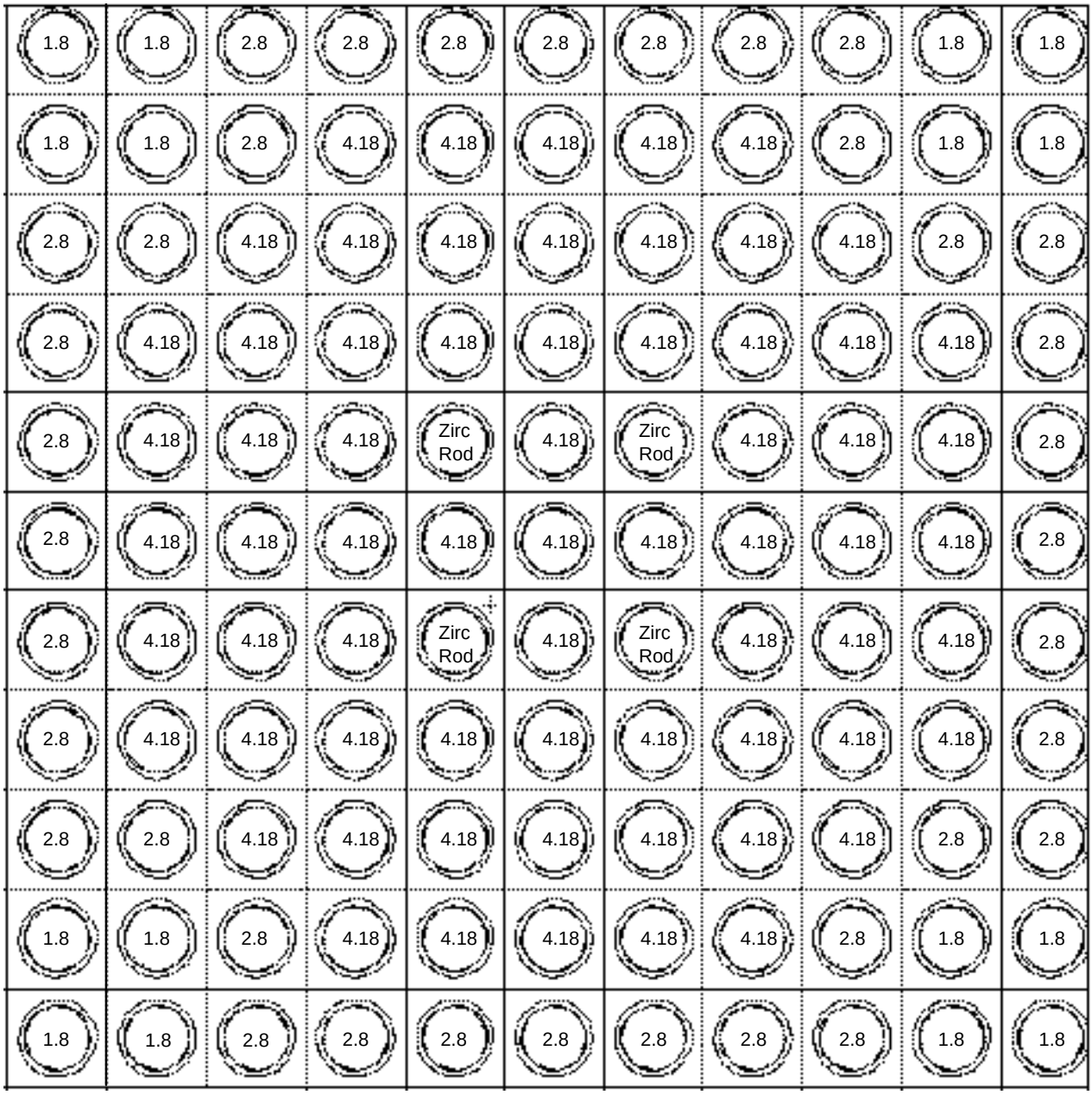

Figure 6.4-8 - Multiple Pin Enrichment Pattern 4 for the Big Rock Point Siemens 11x11 Fuel Assembly

6.5 Criticality Benchmark Experiments

The criticality calculation method is verified by comparison with critical experiment data that is sufficiently diverse to establish that the method bias and uncertainty are applicable to canister conditions considered in the criticality analysis of the FuelSolutions™SFMS. A set of 49 critical experiments is analyzed using MCNP to demonstrate its applicability to criticality analysis and to establish a set of Upper Subcritical Limits (USLs) that define acceptance criteria. Benchmark experiments are selected with compositions, configurations, and nuclear characteristics that are comparable to those encountered in a FuelSolutions™ W74 canister loaded with fuel as described in Table 6.1-1. The experiments analyzed are summarized in Table 6.5-1. The critical experiments are described in detail in NUREG/CR-6361.

Forty-nine critical benchmark cases are selected for their similarity to the FuelSolutions™ system casks and canisters. The cases include different combinations of fixed neutron absorber materials and reflector wall materials. Sixteen of the benchmark experiments have BORAL®, borated stainless steel, or unborated stainless steel absorbing plates with no reflecting walls. Twenty-five of the cases have steel or depleted uranium reflecting walls with no neutron absorbing panels. Five of the cases have both neutron absorbing panels and reflecting walls. Three of the cases are simple lattices without neutron absorbing panels or reflectors. The fuel pins in the experiments have enrichments of 2.35, 4.31, or 4.74 w/o ^{235}U. A comparison of FuelSolutions™ system attributes with these experiments demonstrates the wide range of applicability of the criticality calculation method.

A set of Upper Subcritical Limits is determined using the results from the 49 critical experiments and USL Method 1, Confidence Band with Administrative Margin, described in Section 4 of NUREG/CR-6361. The USL Method 1 applies a statistical calculation of the method bias and its uncertainty plus an administrative margin (0.05 Δk) to a linear fit of the critical experiment benchmark data. The USLs are determined as a function of the critical experiment system parameters; enrichment, water-to-fuel ratio, hydrogen-to-^{235}U ratio, and pin pitch.

- The following equation is determined for the USL as a function of enrichment:
  $USL = 0.94082 + (9.4676 \times 10^{-4})x$ for all x
  The applicable range for enrichment is $2.35 \leq x \leq 5.00$.

- The following equation is determined for the USL as a function of water-to-fuel ratio:
  $USL = 0.94272 + (5.8009 \times 10^{-4})x$ for all x
  The applicable range for water-to-fuel ratio is $1.44 \leq x \leq 3.88$.

- The following equation is determined for the USL as a function of hydrogen-to-^{235}U:
  $USL = 0.94458 - (3.6041 \times 10^{-6})x$ for all x
  The applicable range for hydrogen-to-^{235}U ratio is $80.895 \leq x \leq 398.7$.

- The following equation is determined for the USL as a function of pin pitch:
  $USL = 0.93854 + (2.9355 \times 10^{-3})x$ for $x < 2.412$
  $USL = 0.94562$ for $x \geq 2.412$
  The applicable range for pin pitch is $1.24 \leq x \leq 2.54$.

The preceding equations are used to determine a minimum USL for each fuel assembly type considered for use with the FuelSolutions™ W74 canister (see Table 6.2-1). USL values are calculated as a function of the various parameters presented above for each candidate fuel design. The k_{eff} for a canister containing each specific fuel assembly type is compared to the minimum USL established for that fuel assembly to assure subcriticality. The following equation is used to develop the k_{eff} for the storage of fuel in the FuelSolutions™ canister:

$$k_{eff} = k_{case} + 2\sigma_{k_{eff}}$$

where:

k_{case} = MCNP k_{eff} for a particular case of interest

$\sigma_{k_{eff}}$ = uncertainty in calculated MCNP k_{eff} for a particular case of interest

Table 6.5-1 - Benchmark Critical Experiments (2 Pages)

Name	K_{eff}	Sigma	Enrich	Pitch	H_2O/Fuel	H/X	Plate	B (w/o)	Plate thick	Wall	Wall thick
nse71sq	0.99903	0.00110	4.74	1.26	1.823	110	-	-	-	-	-
nse71w1	0.99632	0.00115	4.74	1.26	1.823	110	-	-	-	-	-
nse71w2	0.99554	0.00108	4.74	1.26	1.823	110	-	-	-	-	-
p2438ba	1.00049	0.00096	2.35	2.032	2.918	398.7	B	28.7	0.713	-	-
p2438ss	0.99822	0.00092	2.35	2.032	2.918	398.7	SS	-	0.485	-	-
p2615ba	1.00007	0.00096	4.31	2.54	3.883	256.1	B	28.7	0.713	-	-
p2615ss	0.99893	0.00105	4.31	2.54	3.883	256.1	SS	-	0.485	-	-
p3314ba	0.99853	0.0011	4.31	1.892	1.6	105.4	B	28.7	0.713	-	-
p3314bc	1.00053	0.00112	4.31	1.892	1.6	105.4	B	31.9	0.231	-	-
p3314bs1	0.9967	0.001	2.35	1.684	1.6	218.6	SS	1.1	0.298	-	-
p3314bs2	0.9936	0.001	2.35	1.684	1.6	218.6	SS	1.6	0.298	-	-
p3314bs3	0.99733	0.00107	4.31	1.892	1.6	105.4	SS	1.1	0.298	-	-
p3314bs4	1.00069	0.00109	4.31	1.892	1.6	105.4	SS	1.6	0.298	-	-
p3314ss1	0.99508	0.00104	4.31	1.892	1.6	105.4	SS	-	0.302	-	-
p3314ss2	1.00132	0.00111	4.31	1.892	1.6	105.4	SS	-	0.302	-	-
p3314ss3	0.99387	0.00105	4.31	1.892	1.6	105.4	SS	-	0.485	-	-
p3314ss4	0.99837	0.00103	4.31	1.892	1.6	105.4	SS	-	0.485	-	-
p3314ss5	0.99454	0.00097	2.35	1.684	1.6	218.6	SS	-	0.302	-	-
p3314ss6	0.99928	0.00116	4.31	1.892	1.6	105.4	SS	-	0.302	-	-
p3602bb	0.99809	0.0011	4.31	1.892	1.6	105.4	B	30.4	0.292	SS	1.96
p3602bs1	1.00125	0.00096	2.35	1.684	1.6	218.6	SS	1.1	0.298	SS	1.32
p3602bs2	1.00064	0.00111	4.31	1.892	1.6	105.4	SS	1.1	0.298	SS	1.96
p3602n11	0.99677	0.00094	2.35	1.684	1.6	218.6	-	-	-	SS	-
p3602n12	0.99822	0.00094	2.35	1.684	1.6	218.6	-	-	-	SS	0.66
p3602n13	0.99767	0.00096	2.35	1.684	1.6	218.6	-	-	-	SS	1.68
p3602n14	0.99563	0.00098	2.35	1.684	1.6	218.6	-	-	-	SS	3.91
p3602n21	0.99907	0.00091	2.35	2.032	2.918	398.7	-	-	-	SS	2.62
p3602n22	0.99895	0.00091	2.35	2.032	2.918	398.7	-	-	-	SS	0.66
p3602n31	1.00072	0.00106	4.31	1.892	1.6	105.4	-	-	-	SS	0
p3602n32	1.00028	0.00112	4.31	1.892	1.6	105.4	-	-	-	SS	0.66
p3602n33	1.00361	0.00117	4.31	1.892	1.6	105.4	-	-	-	SS	1.32
p3602n34	1.00233	0.00113	4.31	1.892	1.6	105.4	-	-	-	SS	1.96
p3602n35	1.00068	0.0011	4.31	1.892	1.6	105.4	-	-	-	SS	2.62
p3602n36	0.99925	0.00102	4.31	1.892	1.6	105.4	-	-	-	SS	5.41

Table 6.5-1 - Benchmark Critical Experiments (2 Pages)

Name	K_{eff}	Sigma	Enrich	Pitch	H_2O/Fuel	H/X	Plate	B (w/o)	Plate thick	Wall	Wall thick
p3602n41	1.00211	0.00103	4.31	2.54	3.883	256.1	-	-	-	SS	-
p3602n42	1.0016	0.00104	4.31	2.54	3.883	256.1	-	-	-	SS	1.32
p3602n43	1.00014	0.00107	4.31	2.54	3.883	256.1	-	-	-	SS	2.62
p3602ss1	1.00077	0.00101	2.35	1.684	1.6	218.6	SS	-	0.302	SS	1.32
p3602ss2	0.99815	0.0011	4.31	1.892	1.6	105.4	SS	-	0.302	SS	1.96
p2827u1	0.9955	0.00086	2.35	2.032	2.918	398.7	-	-	-	U	-
p2827u2	0.99426	0.00091	2.35	2.032	2.918	398.7	-	-	-	U	1.96
p2827u3	0.99946	0.00099	4.31	2.54	3.883	256.1	-	-	-	U	-
p2827u4	0.99939	0.00101	4.31	2.54	3.883	256.1	-	-	-	U	1.96
p3926u1	0.99408	0.00091	2.35	1.684	1.6	218.6	-	-	-	U	-
p3926u2	0.99664	0.00094	2.35	1.684	1.6	218.6	-	-	-	U	1.32
p3926u3	0.99786	0.00086	2.35	1.684	1.6	218.6	-	-	-	U	3.91
p3926u4	0.99799	0.00104	4.31	1.892	1.6	105.4	-	-	-	U	-
p3926u5	0.9994	0.00102	4.31	1.892	1.6	105.4	-	-	-	U	1.96
p3926u6	0.99896	0.0011	4.31	1.892	1.6	105.4	-	-	-	U	3.28

6.6 Big Rock Point MOX, Partial, and Damaged Fuel Assemblies

6.6.1 Big Rock Point Mixed-Oxide Fuel Assembly Criticality Evaluation

Criticality analyses are performed to show that all existing BRP mixed-oxide (MOX) fuel assemblies are qualified for loading into the FuelSolutions™ W74 canister. Specific analyses are performed for each existing MOX fuel assembly configuration. The analyses show that every existing MOX assembly is much less reactive than the design basis 4.1% enriched UO_2 fueled assembly, and that a W74 canister loaded with any of these assembly types meets all 10CFR72 criticality requirements by a wide margin.

6.6.1.1 MOX Fuel Criticality Analyses

There are three existing types of BRP MOX assemblies: the J2 (9x9) assembly, the DA (11x11) assembly, and the G-Pu (11x11) assembly. These three BRP MOX fuel assembly designs are illustrated in Figure 6.6-1 through Figure 6.6-3. The three figures illustrate the different types of rods, describe their fuel material composition, and give the locations of each assembly type within the assembly array. The locations of any dummy rods or water rods are specifically indicated.

In addition to the three MOX fuel assembly designs, two UO_2 fueled assemblies have had two of their fuel rods replaced by MOX fuel rods (E65 and E72). Both of these assemblies are shown in Figure 6.6-4.

The geometric dimensions of the 9x9 and 11x11 MOX fuel assemblies are almost identical to those presented in Table 6.1-1for the design basis UO_2 9x9 and 11x11 assemblies. The only exception is that the J2 9x9 MOX assembly has a fuel pellet diameter of 0.4715 inches, as opposed to 0.471 inches (the diameter shown for 9x9 fuel in Table 6.1-1). It is noted that some J2 assemblies have a pellet diameter of 0.4515 inches and a clad inner diameter of 0.4626 inches, as opposed to the J2 assembly values of 0.4715 and 0.4825, respectively. Thus, 0.02 inches of cladding replaces 0.02 inches of fuel. Replacing fuel with cladding causes reactivity to decrease, so these assemblies are bounded by the J2 assembly configuration modeled in the criticality analyses.

The two MOX fuel rods inserted into the E65 and E72 assemblies have a fuel pellet diameter of 0.471 inches, and a fuel stack height of 68.62 inches (although the criticality analyses conservatively model a fuel height of 70.0 inches). The fuel pellets in these MOX fuel rods may be solid, or they may be annular, with interior void region diameters of 0.1 or 0.2 inches. All three fuel pellet configurations are considered in the criticality evaluation.

The primary difference between the MOX assemblies and the design basis UO_2 assemblies is the fuel material compositions within the rods. Each of the three MOX fuel assembly types has several different types of fuel rods in the assembly array, and each contains a different fuel material composition. All three MOX fuel types contain a number of MOX fuel rods in the center of the assembly array, and UO_2 fuel rods of two to three different enrichment levels around the edge of the assembly array, with the lower enriched UO_2 rods closest to the assembly edge. Each of the three MOX assembly types has a different set of plutonium and uranium

isotope concentrations in its MOX fuel rods. The DA assemblies have two different types of MOX fuel rod, each with its own set of heavy metal isotope concentrations.

The three MOX fuel assembly types also contain dummy (solid zircaloy) fuel pins in locations different from those of the design basis UO_2 assemblies. The diameter of these dummy rods is the same as the fuel rod diameter. Also, the DA 11x11 MOX fuel assembly has four "water rods" near the center of the assembly array. These rods are modeled as hollow, water-filled zircaloy rods with the same clad O.D. and I.D. as the fuel rods.

The UO_2 fuel material description for each of the enrichment levels that occur for UO_2 rods within the MOX fuel assemblies is given in Table 6.6-1. The material description for each of the four MOX fuel rod types shown in Figures 6.6-1 through Table 6.6-3 is given in Table 6.6-2. The partial densities (in a/b-cm) are given for each uranium and plutonium isotope. BRP MOX fuel assembly data give the plutonium isotope distribution (i.e., the percentage of the total Pu in the form of each Pu isotope) for each of the MOX fuel rod types. The isotope partial densities shown in Table 6.6-2 are calculated based on this data, the fuel rod plutonium weight percentages given in Figure 6.6-1 through Figure 6.6-3, and a conservative assumed fuel material density of 10.586 g/cc (96.5% of UO_2 theoretical density). The uranium isotope densities given for the UO_2 fuel rods in Table 6.6-1 are calculated based on this same fuel material density, and the applicable UO_2 fuel rod enrichment level.

Figure 6.6-4 shows total plutonium mass per rod, as opposed to a plutonium weight percentage. This overall plutonium mass applies for all three fuel pellet types that occur in the E65 and E72 assembly MOX rods, even though the fuel material volume varies between the cases. The plutonium concentration is increased for the annular pellet cases, so that the overall plutonium mass is retained. An upper bound metal-oxide density of 95% (of UO_2 theoretical) is modeled for the E65/E72 MOX rods. The material composition for each of the E65/E72 assembly MOX fuel pellet types is shown in the right three columns of Table 6.6-2. A bounding (i.e., most reactive) plutonium isotope distribution of 100% ^{241}Pu is assumed for these MOX fuel rods.

The fuel material descriptions given for the MOX fuel assemblies in Table 6.6-1 and Table 6.6-2 correspond to fresh MOX fuel. No credit is taken for MOX fuel burnup. However, credit is taken in the MOX fuel criticality analyses for ^{241}Pu decay into ^{241}Am. Therefore, an ^{241}Am density is included in the MOX fuel material description, as shown in Table 6.6-2. It is assumed that exactly half of the ^{241}Pu has decayed into ^{241}Am. Since the half-life of ^{241}Pu is approximately 15 years, this assumption corresponds to an assumed MOX fuel assembly cooling time of approximately 15 years. All MOX fuel assemblies are at least 15 years old (as specified in Chapter 12), so the above ^{241}Pu decay assumption is valid and conservative. Table 6.6-2 therefore shows equal densities for ^{241}Pu and ^{241}Am. Each of these densities is half of the initial ^{241}Pu density. The plutonium in the two inserted MOX fuel rods shown in Figure 6.6-4 is conservatively assumed to contain 100% ^{241}Pu, and credit is not taken for ^{241}Pu decay for that assembly configuration. Thus, the full, initial concentration of ^{241}Pu is modeled, with no ^{241}Am present.

The assembly geometry data given in Table 6.1-1, the fuel material data given in Table 6.6-1 and Table 6.6-2, and the fuel rod array descriptions given in Figure 6.6-1 through Figure 6.6-4 are sufficient to completely describe the BRP MOX fuel assemblies with respect to the criticality models. (The zircaloy material description given in Section 6.3 of this FSAR is assumed for BRP MOX fuel.)

The actual design basis G-Pu MOX assembly does not have fuel rods in any of the four array corner positions. However, there are several modified G-Pu MOX assemblies that do contain additional UO_2 fuel rods in some or all of the corner locations. As shown in Section 6.6.2.1 (for UO_2 fueled assemblies), adding fuel rods to the corners increases assembly reactivity. Thus, these modified assemblies are more reactive than the design basis G-Pu assembly. The criticality model of the G-Pu MOX fuel assembly includes four 4.6% enriched UO_2 fuel rods in each of the four corners of the assembly array. As shown in Figure 6.6-1 through Figure 6.6-4, this is the maximum UO_2 fuel rod enrichment for all MOX fuel. With four maximum enrichment UO_2 fuel rods in the corners of the assembly array, the criticality model of the G-Pu MOX assembly bounds all of the modified G-Pu assemblies. Figure 6.6-3 includes these four corner fuel rods (i.e., the figure corresponds to the assembly modeled in the criticality analyses, as opposed to the actual design basis assembly).

Some of the fuel rods in the J2 and G-Pu MOX fuel assembly arrays contain a gadolinium burnable poison. These poisoned fuel rods are illustrated and described in Figure 6.6-1 through Figure 6.6-4. However, as with the UO_2 assembly criticality analyses (see Section 6.3.1), no credit is taken for this absorber material in the MOX fuel criticality analyses. In the analyses, these rods are modeled as pure UO_2 fuel rods at the ^{235}U enrichment level shown for the poisoned rods in Figure 6.6-1 through Figure 6.6-4.

There are also four “partial” BRP MOX fuel assemblies that have one or more fuel rods missing from locations other than the four corners of the assembly array (two J2 assemblies and two G-Pu assemblies). Fuel rods missing from non-corner locations may cause the assembly reactivity to increase, as discussed in Section 6.6.2.2. Thus, these four partial MOX fuel assemblies are potentially more reactive than their design basis assemblies. For this reason, separate, specific criticality analyses are performed on these four partial MOX fuel assembly configurations.

The two partial J2 MOX fuel assembly configurations (D72 and D73) are illustrated in Figure 6.6-5 and Figure 6.6-6. The two partial G-Pu MOX fuel assembly configurations (G01 and G02) are illustrated in Table 6.6-7 and Table 6.6-8. These partial MOX fuel assembly configurations are identical to their corresponding design basis MOX fuel assembly configurations, except that fuel rods are removed from certain locations in the rod array. The only other difference is that zircaloy dummy rods are placed in some additional locations within the G-Pu assembly array, as illustrated in Table 6.6-8. Thus, very minor changes to the criticality models are required for the partial MOX assembly analyses.

Specific criticality analyses are performed for each of the three design basis MOX fuel assembly types and for each of the four partial MOX fuel assembly configurations. Three criticality analyses are performed for the UO_2 assembly configuration with two inserted MOX fuel rods (i.e., the E65 and E72 assembly configuration), and one for each of the three MOX fuel pellet configurations discussed earlier. All existing Big Pock Point MOX fuel assemblies are identical to one of these ten MOX assembly configurations that are specifically analyzed. The only exceptions to this are G-Pu assemblies that have either no fuel rod or a lower enriched UO_2 fuel rod in one or more of the corner locations where the G-Pu assembly criticality model has maximum enrichment UO_2 fuel rods. In this case, the modeled G-Pu assembly configuration is clearly bounding. Other specific G-Pu assemblies have zircaloy dummy pins in place of fuel rods at some array locations. Replacing fuel rods with dummy pins, however, always reduces

assembly reactivity. Finally, some specific J2 and G-Pu assemblies (including the "D72 and "D73" assemblies) have UO_2 fuel rods in certain non-corner array locations that have a lower enrichment level than that which exists (for that array location) in the analyzed (design basis) configurations (as shown in Figure 6.6-1, Figure 6.6-3, Figure 6.6-5, and Figure 6.6-6). Since lowering the enrichment of a given fuel rod in the assembly array will clearly reduce assembly reactivity, these assemblies are also clearly bounded by the analyzed G-Pu assembly configuration. Therefore, analyzing the ten assembly configurations described above is sufficient to qualify all existing BRP MOX fuel for loading into the W74 canister.

The MCNP-4a[9] code is used for the MOX fuel assembly criticality analyses, with the bounding criticality model described in Sections 6.3 and 6.4. The W74 canister geometry models described in Sections 6.3 and 6.4 are used for the MOX fuel analyses presented here. In each of the analyses, a W74 canister is modeled that is completely filled with the MOX fuel assembly configuration being analyzed. An infinite cask array under hypothetical accident conditions is modeled. The worst case set of assembly and guide sleeve positions is modeled along with the worst case set of dimensions and material thicknesses (i.e., worst case tolerances). Full water density (1.0 g/cc) is assumed for the canister interior. This canister and cask configuration is shown by analysis to be bounding for all possible storage conditions. The 11x11 and 9x9 assembly models are used to perform the DA, the G-Pu, and the J2 MOX fuel assembly analyses, respectively. The only change made to the UO_2 fuel assembly models is in the fuel material descriptions. All geometric features of the model are left unchanged, except the fuel pellet diameter of the J2 9x9 MOX assembly, which is increased from 0.471 inches to 0.4715 inches. The material descriptions in Section 6.3.2 are used in the MOX fuel criticality models. The fuel material descriptions for MOX fuel are given in Table 6.6-1 and Table 6.6-2.

Almost all modeling assumptions for the UO_2 BRP assembly criticality analyses in Section 6.3.1 are made for the MOX fuel analyses as well. The only exception is the assumption for the assembly average enrichment in the UO_2 fuel analyses. The UO_2 fuel analyses assume a single average enrichment for all of the fuel rods in the assembly array. The MOX fuel criticality analyses, however, explicitly model the fuel material properties of each individual fuel rod within the assembly array (as described in Figure 6.6-1 through Figure 6.6-3). The MOX fuel rods, as well as the different types of UO_2 fuel rods (each with a different uranium enrichment level), are explicitly modeled.

The results of the specific criticality analyses for the three MOX fuel designs and the four partial MOX assembly configurations, as well as for the assemblies with two inserted MOX rods (which include three MOX fuel pellet configurations), are presented in Table 6.6-3. Criticality analysis results for W74 canisters filled with 4.1% enriched intact 9x9 and 11x11 UO_2 BRP fuel assemblies are also given for comparison. The MOX fuel USL value is discussed in Section 6.6.1.2. The UO_2 assembly USLs are taken from Table 6.4-8.

The UO_2 assembly configurations modeled in the 9x9 and 11x11 UO_2 assembly cases shown in Table 6.6-3 are identical to the intact UO_2 BRP assembly configurations described in Section 6.2. The UO_2 assembly cases are given in Table 6.6-3 because the UO_2 assembly analyses model a slightly different W74 basket geometry, as discussed in Section 6.3. The UO_2 assembly cases

[9] Briesmeister, J., *MCNP-4A General Monte Carlo Code N-Particle Transport Code Version 4A*, LA-12625-M, November 1993.

presented in Table 6.6-3 are based on the exact same W74 basket configuration as the MOX fuel assembly cases to allow for a direct comparison of reactivity between the MOX and UO_2 assemblies.

The results show that the BRP MOX fuel assembly configurations are much less reactive than design basis 4.1% UO_2 fueled BRP assemblies. The most reactive MOX fuel assembly configuration is the design basis G-Pu assembly, which has a final calculated k_{eff} value of ~0.875. This value is much lower than the final k_{eff} value of ~0.923 given for design basis (4.1% enriched) UO_2 fuel. Thus, the most reactive MOX fuel assembly is clearly much less reactive than the design basis UO_2 fueled BRP assembly. In addition, since the maximum calculated k_{eff} value for MOX fuel is more than 6% less than the minimum USL value for MOX fuel, all existing MOX fuel is shown to meet the 10CFR72 criticality requirements by a wide margin.

The two specific UO_2 fueled BRP assemblies that have two inserted MOX rods are much less reactive than design basis UO_2 BRP fuel because their assembly average enrichment level is much lower than the design basis value of 4.1%. The two inserted MOX fuel rods do not significantly affect the reactivity of those two assemblies.

An additional set of criticality analyses is performed to verify that a maximum canister interior moderator density produces the maximum reactivity level for MOX fuel, as it does for UO_2 fuel. The G-Pu MOX assembly criticality model was run at several canister interior water density levels. The 11x11 G-Pu assembly was selected for this analysis because it has a higher water-to-fuel volume ratio than the 9x9 MOX fuel assembly. The 11x11 assembly is therefore less under-moderated, and is more likely to become more reactive at lower moderator densities. The results of the canister interior moderator density analyses are shown in Table 6.6-4. The results show that, as with BRP UO_2 fuel, maximum reactivity occurs at maximum water density. Although it has a higher water-to-fuel volume ratio than the 9x9 assembly, the 11x11 MOX assembly is still somewhat under-moderated at full water density, so maximum reactivity occurs at maximum water density.

The criticality analysis results verify that a W74 canister loaded with BRP UO_2 or MOX fuel meets the criticality requirements. Additional analyses also verify that canisters filled with mixtures of UO_2 and MOX fuel meet the criticality requirements. These additional analyses confirm that the MOX and UO_2 assemblies do not neutronically affect each other in a way that would increase canister reactivity.

Criticality analyses are performed for four mixed loading patterns of BRP MOX and UO_2 assemblies within the W74 canister. These patterns include checkerboard loading patterns, which maximize neutronic interaction between the MOX and UO_2 assemblies. The analyses show that combinations of MOX and UO_2 fuel within the W74 canister also meet the criticality requirements. As expected, the calculated k_{eff} values for mixtures of UO_2 and MOX fuel are ~0.90, which lies roughly halfway between the calculated k_{eff} value for UO_2 fuel (~0.923) and the calculated k_{eff} value for MOX fuel (~0.875). Thus, the results indicate that the UO_2 and MOX assemblies are not significantly affecting each other's reactivity.

Also of note is the fact that the maximum final k_{eff} value for the FuelSolutions ™ W74 canister loaded with design basis BRP UO_2 fuel (0.92290) is below the MOX fuel USL value of 0.94141, as well as the minimum UO_2 fuel USL value of 0.94286. Section 6.6.1.2 states that the lower of the two USL values, MOX or UO_2, is conservatively used if any MOX at all is present within the

W74 canister. If a tiny amount of MOX were present, the calculated k_{eff} value for the canister would be very near the UO_2 fuel value of 0.9229. However, this calculated k_{eff} value would still be under the USL value even if the lower MOX fuel USL value of 0.94141 were applied. As more MOX is added to the system, the calculated k_{eff} value would decrease. Thus, even when the lowest USL value is used, any mixture of MOX and UO_2 fuel in the W74 canister meets the criticality requirements.

In conclusion, specific criticality analyses are performed on all existing BRP MOX fuel assembly configurations. These analyses explicitly show that all existing MOX fuel assemblies are significantly less reactive than the design basis UO_2 fueled assembly modeled in the criticality analyses described in Sections 6.3 and 6.4. The analyses also explicitly show that all MOX fuel assembly configurations meet 10CFR72 criticality requirements by a wide margin. Furthermore, the analyses show that any combination of MOX and UO_2 assemblies loaded into the W74 canister will meet the criticality requirements. Thus, all existing MOX assemblies and MOX/UO_2 combination assemblies are qualified for loading into the FuelSolutions™ W74 canister. With respect to criticality requirements, there are no restrictions on canister loading location for MOX fuel, or on the quantities of MOX and/or UO_2 BRP assemblies loaded into the canister.

6.6.1.2 MOX Fuel Criticality Benchmarks

A set of 24 MOX fuel critical experiments is analyzed with the MCNP code to verify the accuracy and applicability of the code for MOX fuel criticality analyses. Based on the MCNP calculated k_{eff} values for the 24 MOX fuel critical experiments, USL values are determined using the same NUREG/CR-6361[10] methodology that is used for UO_2 fuel as described in Section 6.5.

As with the UO_2 fuel benchmark calculations, USLs are calculated as a function of assembly pin pitch, water-to-fuel volume ratio, enrichment, and hydrogen-to-^{235}U ratio. For MOX fuel, the "enrichment" is more generally defined as the fissile material percentage, which is the percentage of the overall heavy metal mass in the form of fissile material. Based on this definition, the fissile material percentage is simply the ^{235}U enrichment for pure UO_2 fuel. For MOX fuel, the fissile material percentage includes the masses of the fissile plutonium nuclides, ^{239}Pu and ^{241}Pu. Thus, for MOX fuel, the USL is calculated as a function of fissile material percentage, as opposed to ^{235}U enrichment. Similarly, for MOX fuel, the hydrogen-to-^{235}U ratio is generalized as the hydrogen-to-fissile nuclide ratio.

The set of MOX fuel experiments consists of regular square arrays of MOX fuel rods with full water reflection. The experiments cover a wide range of pin pitch values. Due to the range of pin pitches, the experiments also cover a wide range of water-to-fuel ratio and hydrogen-to-fissile nuclide ratio values. In addition, the experiments cover a very wide range of fissile material percentages (from roughly 2.5% to over 20%). The fissile material is mostly plutonium for all of the experiments.

The 24 MOX fuel critical experiments are described in Table 6.6-5. For each experiment, the value for each of the four physical parameters described above is listed along with the MCNP

[10] NUREG/CR-6361, *Criticality Benchmark Guide for Light-Water-Reactor Fuel in Transportation and Storage Packages*, ORNL///TM-13211, March 1997.

calculated k_{eff} value for that experiment. The statistical error level (1σ) is also listed for each experiment. Table 6.6-5 contains all the data necessary to perform the NUREG/CR-6361 USL calculations for each of the four system parameters. Table 6.6-5 also lists a fifth physical parameter, the percentage of fissile material that is plutonium (as opposed to uranium), for each MOX fuel experiment. The use of this parameter is discussed below.

USLs are calculated as a function of each of the four physical parameters described above, based upon the 24 MOX fuel critical experiments. USLs are also calculated for the combined set of MOX and UO_2 critical experiments. The set of 24 MOX fuel critical experiments described in Table 6.6-5 and the 49 UO_2 fuel critical experiments described in Table 6.5-1 are combined to form a mixed set of 73 critical experiments. As a function of each of the four system parameters, USLs are calculated for this combined set of 73 critical experiments. The USLs for the MOX fuel experiment case, the combined experiment case, and the UO_2 fuel experiment case are compared for each of the four parameters, and the lowest of the three USLs is selected.

This approach is used for several reasons. First, this approach increases the number of critical experiments that form the statistical basis of the calculated USLs. Second, this assures that the final MOX fuel USL values are based on a set of experiments that feature a wider range of physical features, reflector materials, and absorber materials. The set of UO_2 experiments covers a wider range of these features than do the MOX fuel experiments. Using this approach, the USL based on the combined set of experiments (which includes all the UO_2 experiments) would be used if it is lower than the MOX fuel only USL.

The MOX fuel USLs are to be applied to criticality analyses on systems that contain mixtures of MOX fuel and UO_2 fuel. The BRP MOX fuel assemblies contain mixtures of MOX and UO_2 fuel rods. As discussed in Section 6.6.1.1, loading the W74 canister with a mixture of MOX and UO_2 BRP assemblies is to be allowed. Therefore, if the USLs calculated for the set of UO_2 experiments or the combined set of MOX and UO_2 fuel experiments are lower than those calculated for the MOX fuel experiments only, then the UO_2 or combined set USL values clearly must be used if mixed loading is to be allowed. Otherwise, a situation would exist where the applied USL would suddenly increase just because a small amount of MOX fuel material was added to the system. If the MOX fuel only USL values are lower, however, then they are to be applied if any amount of MOX material is present in the system. Thus, the applied USL values would suddenly drop if even a small amount of MOX fuel were added to the system. This is clearly a conservative approach.

Finally, analyzing the combined set of MOX and UO_2 experiments allows one to evaluate whether or not there is any shift in the MCNP code bias between uranium and plutonium fuels. A fifth physical system parameter, the percentage of fissile material that is plutonium (as opposed to uranium) is defined. A fifth USL is calculated as a function of this parameter for the combined set of MOX and UO_2 fuel experiments. For all the UO_2 experiments, the value of this parameter is zero. For all of the MOX fuel experiments, the fissile material is primarily plutonium. The value of the plutonium percentage parameter varies from 73% to just over 97% in the MOX experiments (as shown in Table 6.6-5). Thus, this parameter does not vary over a wide range in either the set of UO_2 fuel experiments or the set of MOX fuel experiments. However, when the two sets of experiments are contrasted to each other, this parameter varies over a very wide range (from 0% to almost 100%). By calculating a USL function for this fifth parameter for the

combined set of MOX and UO_2 fuel experiments, the variance in MCNP code bias between uranium and plutonium fuels will be adequately evaluated and treated.

The USL value functions calculated for each of the five system physical parameters are listed in Table 6.6-6. For each parameter, the USL function (which gives the USL value as a function of the parameter value) is listed. For each parameter, the USL function for the set of MOX experiments, and for the combined set of MOX and UO_2 experiments are shown. In addition, the USL function for the set of 49 UO_2 experiments (taken directly from Section 6.5) is also shown. For the fifth parameter, the percentage of fissile material that is plutonium, a USL function is only calculated for the combined set of UO_2 and MOX fuel experiments, for the reasons discussed above.

Final USL functions are determined for each parameter by selecting the case (UO_2 only, MOX only, or combined UO_2 plus MOX) which yields the lowest USL values. If different cases are lower over different sections of the parameter range, then the parameter range is divided into those sections and the USL formula that yields the lowest USL values is applied over each section.

Using the above approach, five final USL equations could be determined, one for each of the studied physical parameters. In some cases, these equations would be sub-divided into several sections of the parameter range, with different linear formulas applying over each section. However, examination of the set of USL functions shown in Table 6.6-6 shows that a simpler final result can be obtained. In fact, a single final USL formula, which bounds all of the USL formulas shown in Table 6.6-6 can be determined. Fortunately, the nature of the USL formulas is such that a single bounding formula can be applied without a significant amount of unnecessary conservatism.

The MOX only case USLs for fissile material percentage and hydrogen-to-fissile nuclide ratio are approximately 0.942 over the entire parameter range. The MOX only case water-to-fuel volume ratio USL is 0.94141 at the minimum water-to-fuel volume ratio value of 1.195. The first simplifying step in this process is to establish a USL upper bound of 0.94141. This assumption does not result in a large amount of conservatism because the MOX only USLs for fissile material percentage and hydrogen-to-fissile nuclide ratio would never allow a USL value over 0.942 anyway (for any set of system parameter values). Examination of the Table 6.6-6 USL formulas show that the USLs for all parameters other than pin pitch are over 0.94141 over their entire parameter ranges for all three cases (MOX only, UO_2 only, and combined UO_2 plus MOX).

Examination of the pin pitch USL formulas show that the MOX only and MOX plus UO_2 USLs both reach a value of 0.94141 at a pin pitch of 1.32 cm. The USL values are under 0.94141 for pin pitch values under 1.32 cm. The pin pitch USL for the UO_2 only case is higher than the MOX only or combined case USLs for all pin pitch values of 1.32 or less (and it is higher than 0.94141 at a pin pitch of 1.32 cm). For pin pitch values under 1.32 cm, the MOX only pin pitch USL formula yields lower USL values than the mixed case pin pitch USL formula. Thus, the MOX only pin pitch formula applies (i.e., is lowest) for all pin pitch values under 1.32 cm. For pin pitch values over 1.32 cm, the upper bound USL value of 0.94141 applies.

The final result of this analysis is a single USL formula, shown below, that gives the USL value solely as a function of pin pitch. The pin pitch of the analyzed system is determined and entered

into the formula to calculate a final, lower bound USL value to be used for the criticality calculation. USL values determined using any of the formulas shown in Table 6.6-6 are bounded by this single USL formula, regardless of the physical parameter values of the system, given that the system's physical parameters are within the ranges covered by the set of critical experiments.

$$USL = 0.93372 + (5.8336 \times 10^{-3})x \quad \text{for } x < 1.32$$
$$USL = 0.94141 \quad \text{for } x \geq 1.32$$

where "x" is the pin pitch of the fuel assemblies, in cm.

As shown in Table 6.1-1, the minimum pin pitch for BRP fuel assemblies is 0.577 inches, or 1.466 cm. Since this is higher than 1.32 cm, the upper bound USL value of 0.94141 is to be applied for all BRP MOX fuel criticality analyses.

In order for the above USL value to be applicable, however, it must be verified that the physical parameters of the FuelSolutions™ W74 canister containing BRP MOX fuel lie within the ranges covered by the combined set of MOX and UO_2 fuel critical experiments. Table 6.6-7 lists the minimum and maximum values that occur in the MOX and UO_2 critical experiments for each of the five analyzed physical system parameters. The table then lists the minimum and maximum values that occur for those parameters in the entire inventory of BRP MOX fuel assemblies. For the BRP MOX fuel assembly inventory, the minimum and maximum values calculated for the fissile material percentage, the hydrogen-to-fissile nuclide ratio, and the fissile plutonium percentage, are conservatively based on individual fuel rods, as opposed to assembly averages. Since the BRP MOX fuel assemblies contain different types of fuel rods with material properties that vary over wide ranges, the rod by rod approach yields a much wider range of parameter values than would an assembly average approach.

The Table 6.6-7 results show that, with respect to pin pitch, water-to-fuel volume ratio, and hydrogen-to-fissile atom ratio, the ranges covered by the BRP MOX fuel inventory are bounded by the ranges covered by both the set of UO_2 critical experiments and the set of MOX fuel critical experiments. The fraction of fissile material that is plutonium ranges from approximately 33% to 86% in the BRP MOX fuel rods. These values are bounded by those of the combined set of UO_2 and MOX fuel critical experiments (from which the plutonium percentage USL was calculated), which range from 0% to 97.3%.

The pairs of MOX fuel rods in the E65 and E72 assemblies have a fissile material percentage of 2.0%. The G-Pu MOX assemblies also contain a small number of 2.3% enriched UO_2 fuel rods near the corners of the assembly array. The DA assemblies contain a larger number of MOX fuel rods with a fissile material percentage of 2.33%. These enrichment / fissile percentage values are slightly less than the minimum value that occurs in either the MOX or the UO_2 critical experiments.

This is not an issue for the following reasons. NUREG/CR-6361 allows for USL formulas to be extrapolated for parameter values that lie "slightly" outside the range covered by the set of critical experiments. If a fissile percentage value of 2.0% is entered into any of the three fissile percentage USL formulas (MOX only, UO_2 only, or combined), the resulting USL values are all above the upper bound USL value of 0.94141. Thus, if such an extrapolation were applied, it would have no effect on the final applied USL value. Furthermore, these minimum fissile material percentages of 2.00%, 2.30%, and 2.33% are based on worst-case individual fuel rods. The assembly average fissile material percentage is over 3.0% for all BRP MOX fuel, which is

well within the range covered by either set of critical experiments (UO_2 or MOX). The MCNP code bias is more likely to be governed by the assembly average fissile material percentage. It should be noted that the USL formulas show a very weak dependence of code bias (i.e., USL value) on the fissile material percentage. Finally, the criticality analysis results presented in Table 6.6-3 show that the most reactive BRP MOX fuel assembly produces a final k_{eff} value that is under the USL value by over 6%. Thus, the criticality requirements are met by a very wide margin. A low fissile material percentage occurring in a few individual fuel rods within the assembly arrays will not cause the MCNP code bias or USL values to shift by more than 6% in k_{eff}.

In conclusion, the MCNP code is accurate and applicable for BRP MOX fuel criticality analyses. A single USL value of 0.94141 is applicable and bounding for all such analyses.

6.6.2 Big Rock Point Partial Fuel Assembly Criticality Evaluation

The primary criticality analyses described in Sections 6.3 and 6.4 model BRP 9x9 and 11x11 assemblies that have fuel rods in all four corners of the assembly array. Partial assemblies have fuel rods missing from the design basis assembly array. Most BRP partial assemblies have fuel rods missing from one or more of the four corner locations, with the rest of the assembly array being intact. A smaller number of BRP assemblies have fuel rods missing from locations other than the four corners.

Two sets of criticality analyses are performed for the two different types of BRP partial assemblies. The two sets of analyses use different approaches as described below in Sections 6.6.2.1 and 6.6.2.2.

As discussed in Section 6.3, the partial assembly analyses conservatively model a poison sheet boron concentration of 1.0 w/o (as opposed to the actual value of 1.25 w/o), and conservatively neglect the four guide tube poison sheets that face the support tubes, as shown in Figure 6.3-2. Thus, the partial assembly analyses use the same basket geometry model that is used for the intact BRP assembly analyses. As these conservative analysis assumptions cause canister reactivity to increase, the results of the partial assembly analyses are bounding and applicable for the actual W74 basket configuration.

As with the intact BRP assembly analyses, the models are based on accident conditions, an infinite array of transportation casks, the worst case set of canister interior dimensions, tolerances, and assembly positions (as described in Section 6.3), and a maximum canister internal moderator density of 1.0 g/cc. These conditions are modeled because they yield the maximum reactivity for the W74 canister. Furthermore, analyses show that this configuration bounds all possible configurations that may occur during storage of the W74 canister.

6.6.2.1 Partial Assemblies with Missing Corner Rods

The first set of analyses shows that BRP 9x9 and 11x11 assemblies with one or more fuel rods missing from the four corner locations are less reactive than the design basis BRP assemblies analyzed in the primary criticality analyses. Thus, the assembly average enrichment limit of 4.1% that applies for intact BRP assemblies will also apply for all BRP assemblies with fuel rods missing from any of the four corner locations.

Two criticality analyses are performed to verify that BRP assemblies with array corner rods missing are less reactive than design basis BRP assemblies: one for the 9x9 assembly, and one for the 11x11 assembly. In each analysis, a W74 canister completely loaded with the analyzed partial BRP assembly is modeled. In each case, all four corner fuel rods are removed from the assembly array. Other than the removed corner rods, these two models are identical to the bounding primary BRP 9x9 and 11x11 criticality models presented in Sections 6.3 and 6.4. As with the primary criticality analyses, the partial BRP assemblies in these analyses are modeled with a uniform UO_2 fuel enrichment of 4.1%. Calculations show that a uniform enrichment assumption is conservative for all BRP fuel (i.e., for all fuel rod enrichment patterns that occur for BRP fuel).

The results of the missing corner rod criticality analyses are presented in Table 6.6-8. K_{eff} values are determined for BRP 9x9 and 11x11 assemblies with all four corner rods missing. Sections 6.4 and 6.1 give calculated k_{eff} values of 0.93739 and 0.94007 for the design basis 9x9 and 11x11 assemblies, respectively. The calculated k_{eff} values for the assemblies with all four corner rods missing are significantly lower than the design basis assembly values.

It is assumed that since assemblies with all four corner rods removed are significantly less reactive than design basis assemblies with all four corner rods present, then assemblies with any number of the corner rods removed are also bounded by the design basis assembly. It is therefore concluded that the design basis BRP assemblies bound any BRP assemblies with any number of fuel rods missing from the corners of the rod array. The design basis assembly average enrichment limit of 4.1% applies for all such assemblies. Note that for partial assemblies, the assembly average enrichment is defined as the enrichment averaged over the rods that remain in the assembly.

Since the calculated k_{eff} values for the BRP assemblies with missing corner rods are lower than those of the design basis BRP assemblies, the assemblies with missing corner rods will meet all 10CFR72 criticality requirements as long as the USL values applied to the analysis results do not change. This is the case, as discussed below.

The set of USL values (as discussed in Section 6.1) that apply to the design basis BRP assemblies also apply to the assemblies with corner rods missing. The assemblies with missing corner rods were analyzed at the same design basis enrichment level of 4.1%, so the enrichment USL value does not change. The assembly pin pitch does not change with the removal of corner rods, so the pin pitch USL value does not change. Also, since the rods are removed from the corners of the fuel rod array, the effective water-to-fuel ratio and H-to-^{235}U ratio do not change. The effective H-to-^{235}U ratio for the assembly is not affected unless rods are removed from internal array locations. Therefore, the USL values shown in Section 6.5 are applicable to the missing corner rod assemblies.

In conclusion, BRP 9x9 and 11x11 assemblies that have any number of rods missing from the four corner positions of the assembly array are less reactive than the design basis 9x9 and 11x11 assemblies analyzed in the primary criticality analyses. Thus, the maximum allowable BRP assembly enrichment level of 4.1% that was determined in the primary criticality analyses also applies for all BRP fuel with missing corner rods.

For the above reasons, BRP assemblies that have fuel rods missing from any number of the array corner locations are classified as “intact,” as opposed to “partial,” in the fuel specifications given

in Chapter 12 of this FSAR. The assembly average enrichment limit of 4.1% applies for all assemblies classified as “intact”.

BRP assemblies that have fuel rods missing from non-corner locations of the rod array are classified as “partial” and are treated by the analyses described below in Section 6.6.2.2.

It should be noted that one of the design basis BRP 9x9 assembly configurations analyzed in the intact assembly criticality analyses presented in this FSAR has a water hole (i.e., a missing fuel rod) in the center of the rod array. This is the array location where a single water hole will cause the maximum increase in assembly reactivity. The intact assembly analyses qualified this assembly configuration at the maximum intact assembly enrichment level of 4.1%. For this reason, a BRP 9x9 assembly may have up to one water hole, in any array location, and still be classified as “intact”. BRP 9x9 assemblies with two or more non-corner water holes, or BRP 11x11 assemblies with any non-corner water holes, are classified as “partial” assemblies.

6.6.2.2 Partial Assemblies with Missing Array-Interior or Array-Edge Rods

As shown in Section 6.6.2.1, removing fuel rods from the corners of the BRP 9x9 and 11x11 assembly arrays reduces their reactivity level. A different situation exists when rods are removed from the interior or sides of the assembly arrays. Removal of rods from non-corner array locations effectively increases the H-to-^{235}U ratio of the assembly. Since the BRP assemblies are under-moderated, this causes the reactivity of the assembly to increase. Thus, partial BRP assemblies with fuel rods missing from non-corner array locations tend to be more reactive than the design basis BRP assemblies.

Due to the large number of fuel rod locations in the BRP assembly arrays, an extremely large number of partial array configurations is possible, each with a different overall reactivity level. For simplicity, a bounding (optimum) assembly array is found for each of the two BRP assembly types (9x9 and 11x11). These bounding arrays are the most reactive possible geometry (or arrangement) for any number of 9x9 or 11x11 fuel rods.

To determine the bounding fuel rod arrays for the BRP 9x9 and 11x11 assemblies, the fuel rods are arranged into a regular square-pitched array. Criticality calculations are performed that determine k_{eff} values for rod arrays with various rod pitch values. The pitch of this array is varied until maximum reactivity is achieved. In other words, the pitch is varied until the optimum H-to-^{235}U ratio is reached.

These optimum rod pitch calculations are performed for rod arrays surrounded by full water reflection. The fuel rods contain 4.1% enriched UO_2 fuel. The rod arrays are limited in size to the envelope volumes of the corresponding BRP assembly. The assembly envelope volume has a square cross-section with a width that is equal to the assembly’s nominal pitch times the number of rods on each side of the array. Thus, the fuel rod arrays for the BRP 9x9 assembly are confined to a square area with a width of 6.363 inches (9 rods times a nominal rod pitch of 0.707). The rod array for the BRP 11x11 assembly is limited to a square area with a width of 6.347 inches (11 rods times a nominal rod pitch of 0.577 inches).

Since the BRP assemblies are under-moderated, the optimum pitches for the bounding fuel rod arrays are larger than the assembly nominal pitches. The bounding array criticality analyses start with the nominal assembly pitch and increase the pitch from there. As the fuel rod pitch is increased, a smaller number of rods fit into the fixed assembly envelope area. Thus, as the pitch

is increased, the number of fuel rods in the assembly array is reduced. Despite this, however, the fuel rod array reactivity increases as the rod pitch is increased over the assembly nominal value.

For each assembly case, several rod pitch values are studied, starting with the nominal assembly pitch value. The pitch values in the tables are expressed relative to the nominal assembly pitch value (e.g., "1.09 times the nominal pitch"), as well as in inches. For all cases, the fuel rod dimensions are those shown for the 9x9 and 11x11 assemblies in Table 6.1-1. A pellet diameter of 0.3715 is assumed for the 11x11 assembly analyses. Some BRP 11x11 assemblies have a fuel pellet diameter of 0.3735 inches, 0.5% larger than the standard diameter. This very small change in fuel pellet diameter will not significantly affect the reactivity of the optimum partial array configuration, so the results of the partial assembly analyses are considered applicable for these assemblies. For each analyzed case, the tables also present the water-to-fuel volume ratio and the H-to-^{235}U ratio. These parameters are calculated based on the analyzed pitch, the fuel rod dimensions from Table 6.1-1, a fuel material density of 96.5% UO_2 theoretical density, and a UO_2 fuel enrichment level of 4.1%.

The set of rod pitch values analyzed do not correspond to an integral number of fuel rod rows fitting exactly into the defined fuel assembly envelope. As the rod pitch is increased, and a row of fuel rods partially intersects the edge of the defined assembly envelope, the rod row is not completely removed. Instead, a row of partial volume rods is modeled at the envelope edge. In all cases, only water exists outside the envelope edge. Thus, the optimum array pitch results do not correspond to any integral rod array size (10x10, etc.).

The results of the optimum fuel rod pitch analyses for the 9x9 and 11x11 assemblies are presented in Table 6.6-9 and Table 6.6-10, respectively. The optimum pitch analysis results are also presented graphically in Figure 6.6-9 and Figure 6.6-10. The figures show a curve fit to the data points given in Table 6.6-9 and Table 6.6-10 that gives k_{eff} versus H-to-^{235}U ratio.

The results show that, for an array of 9x9 assembly fuel rods, the optimum H-to-^{235}U ratio (determined from the formula given in Figure 6.6-9) is 139.6. The corresponding fuel rod pitch is approximately 1.09 times that of the 9x9 assembly nominal pitch of 0.707 inches. The optimum H-to-^{235}U ratio for an array of 11x11 assembly fuel rods (taken from the formula in Figure 6.6-10) is 146.3. The corresponding optimum rod pitch is approximately 1.08 times the 11x11 assembly nominal pitch of 0.577 inches.

These optimum pitch arrays represent the most reactive possible configuration of fuel rods within the assembly envelope. The optimum arrays also contain the optimum number of fuel rods that may occur within the given assembly envelope area. The most reactive number of rods is less than the number of rods present in the intact BRP assembly, because the assemblies are under-moderated and the optimum pitch is greater than the nominal assembly pitch. Partial BRP assemblies, however, may actually have this optimum lower number of rods, so the optimum pitch arrays must be modeled in order to bound all possible partial assembly configurations.

Analyses are performed to verify that the regular, square, optimum pitch arrays of fuel rods described in this section are bounding for all actual partial BRP assembly configurations. A series of calculations is performed where a single fuel rod is removed from various locations of the BRP assembly array. These calculations determine which rods have the greatest reactivity worth (i.e., which rods increase assembly reactivity by the greatest amount when they are removed). Then a set of analyses is performed to determine assembly reactivity as a function of

the number of fuel rods removed. Rods are removed from the highest reactivity worth locations first. Then the rods with the next highest worth are removed, and so on. Rods are removed until the assembly H-to-^{235}U ratio is the same as that of the optimum pitch fuel rod array determined by the analyses presented earlier in this section.

These analyses show two things. First, the reactivity level of the actual assembly arrays with removed rods remains significantly below that of the optimum pitch fuel rod array for any number of removed rods. Second, the actual assembly arrays reach maximum reactivity at a lower H-to-^{235}U ratio (i.e., at a lower number of removed rods) than that which occurs for the optimum pitch fuel rod array. When a sufficient number of rods was removed so that the H-to-^{235}U ratio equaled that of the optimum pitch rod array, the k_{eff} values were already sloping downwards. For this reason, assembly configurations with greater numbers of removed rods did not have to be studied. Thus, this set of analyses confirms that the optimum pitch rod arrays are a bounding model for any actual partial BRP assembly configuration. In fact, the analyses show that the optimum pitch rod arrays are a very conservative model for any BRP partial assembly, with a reactivity level on the order of 2% (in k_{eff}) higher than that of any actual partial BRP assembly that could possibly exist. The optimum pitch rod arrays are more reactive than actual partial assembly arrays with a similar H-to-^{235}U ratio because the water is more evenly distributed around the fuel rods.

Once the optimum pitch arrays are determined for each of the two assembly types, criticality analyses are performed to determine the maximum allowable enrichment for BRP partial 9x9 and 11x11 assemblies. These criticality models are identical to the primary criticality models described in Sections 6.3 and 6.4, except that the intact BRP assemblies contained in each of the 64 loaded fuel sleeves are replaced with the optimum pitch fuel rod arrays described in this section. Thus, the models effectively consider a W74 canister that is fully loaded with worst case (i.e., as reactive as possible) BRP partial assemblies.

Due to the more reactive assembly geometry, the maximum allowable enrichment level for BRP partial assemblies is lower than that of intact assemblies. The results of the maximum allowable enrichment calculations are presented in Table 6.6-11. The maximum allowable enrichment for 9x9 partial assemblies is 3.55%. The maximum allowable enrichment for 11x11 partial assemblies is 3.6%. Table 6.6-11 also lists the optimum fuel rod array pitch, water-to-fuel volume ratio and H-to-^{235}U ratio for each assembly case.

The optimum fuel rod array pitch analyses determine an optimum fuel rod pitch and an optimum H-to-^{235}U ratio for arrays of 4.1% enriched UO_2 fuel rods. If the enrichment of the fuel rods is lowered to 3.55% or 3.6%, the H-to-^{235}U ratio for an array of a given rod pitch will increase. It is assumed (and verified as discussed later) that maximum reactivity occurs at the optimum H-to-^{235}U ratio determined in the optimum array analyses, as opposed to the optimum fuel rod pitch (i.e., the H-to-^{235}U ratio is the more important parameter, which must be kept at its optimum value). For the criticality analyses that are run with fuel rod enrichment levels of 3.55% and 3.6%, the fuel rod pitches in the optimum rod arrays are reduced in order to keep the H-to-^{235}U ratios constant. As shown in Table 6.6-11, the H-to-^{235}U ratios for the 9x9 assembly (3.55%) case and the 11x11 assembly (3.6%) case are the same as the optimum ratios determined for those assemblies in the optimum rod pitch analysis (presented in Table 6.6-9 and Table 6.6-10). The fuel rod pitch and water-to-fuel volume ratios, however, are lower than those shown in Table 6.6-9 and Table 6.6-10.

The final calculated k_{eff} values shown in Table 6.6-11 are compared to all applicable USL values using the methodology discussed in Section 6.1. In the final criticality analyses of the partial assemblies, all of the physical parameters of the analyzed assemblies (or rod arrays) are different from those of the design basis BRP assemblies. The analyzed enrichment levels are lower, the pin pitch values of the optimum pitch fuel rod arrays are higher. Due to the higher pin pitch values, the water-to-fuel and H-to-^{235}U ratios are also higher for the optimum pitch rod arrays. The applicable USL values will change for the partial assembly analysis for all four physical assembly parameters treated in Section 6.1. The USL values that apply for the partial BRP assembly analyses are given in Table 6.6-12. For each of the two BRP assembly types, and for each of the four studied physical assembly parameters, Table 6.6-12 lists the value of the physical parameter along with the corresponding USL value.

The bounding final calculated k_{eff} values for partial 9x9 and 11x11 BRP fuel shown in Table 6.6-11 are lower than all of the corresponding partial assembly USL values shown in Table 6.6-12. Section 6.1 also lists the range of USL formula applicability for each of the four parameters. The parameter values for the optimum pitch fuel rod arrays (for both 9x9 and 11x11 fuel) shown in Table 6.6-12 lie within these ranges of applicability. Therefore, it is concluded that 3.55% enriched partial 9x9 BRP assemblies and 3.6% enriched partial 11x11 assemblies meet all 10CFR72 criticality requirements. Note that since the optimum pitch fuel rod arrays modeled in the partial assembly criticality analyses are significantly more reactive than any actual partial BRP assembly, the enrichment limits specified above actually meet the 10CFR72 criticality requirements by a wide margin for all BRP partial fuel assemblies.

Additional criticality analyses are performed to confirm that the optimum H-to-^{235}U ratio determined for 4.1% enriched BRP assembly fuel rods also applies for 3.55% and 3.6% enriched fuel rods. These analyses also confirm that the optimum H-to-^{235}U ratio based on a single assembly array surrounded by full water reflection is also the optimum H-to^{235}U ratio for arrays of rods within the guide sleeves of the W74 canister. The models that produce the Table 6.6-11 results (which have arrays of 3.55% enriched 9x9 assembly fuel rods and 3.6% enriched 11x11 assembly fuel rods in each guide sleeve of the W74 canister) are re-run with different fuel rod array pitch values and therefore, different H-to-^{235}U ratios. These analyses show that if the rod pitch and/or H-to^{235}U ratio values are either reduced or increased from the optimum values shown in Table 6.6-11, the W74 canister k_{eff} value decreases. Thus, the results indicate that the optimum H-to-^{235}U ratios determined by the single, water reflected assembly analysis (with 4.1% enriched fuel) is also applicable for lower enrichment fuel inside the W74 canister.

In conclusion, criticality analyses are performed on a W74 canister containing optimum pitch fuel rod arrays in place of intact design basis BRP fuel assemblies. These optimum pitch rod arrays are shown to be more reactive than any possible partial assembly configuration. These analyses show that the maximum allowable fuel rod enrichment level for a W74 canister loaded with optimum pitch arrays of 9x9 assembly fuel rods is 3.55%. For a canister loaded with optimum 11x11 assembly fuel rod arrays, the maximum allowable enrichment level is 3.6%. Therefore, a maximum allowable assembly average fuel enrichment level of 3.55% is established for all partial 9x9 BRP assemblies. A maximum allowable assembly average enrichment level of 3.6% is established for all partial 11x11 BRP assemblies. The assembly average enrichment is defined as the enrichment level averaged over the remaining fuel rods in the partial assembly array.

6.6.3 Big Rock Point Damaged Fuel Assembly Criticality Evaluation

Damaged BRP assemblies are defined as assemblies with fuel rod damage in excess of pinhole leaks or hairline cracks. The fuel rod damage criterion is based on NRC guidance.[11] Fuel assemblies with damaged grid spacers (defined as damaged to a degree where fuel rod structural integrity cannot be assured, or where grid spacers have shifted vertically from their design position) will also be stored in damaged fuel cans.

All damaged BRP assemblies must be placed into damaged fuel cans that are then loaded into one of the eight support tube locations in the W74 canister. These damaged fuel cans (discussed in Section 6.3 and illustrated in Figure 6.3-4) are similar to a standard W74 canister guide tube, with standard W74 canister poison sheets attached to all four walls of the guide tube.

Fuel debris or fuel rod fragments are not qualified for storage in the W74 damaged fuel cans. These are pellets or fuel rod segments that are no longer attached to (or confined within) the fuel assembly.

With respect to criticality, it is conservatively assumed that damaged fuel assemblies do not maintain their geometry during storage in the W74 canister. Thus, the W74 canister, when fully loaded with fresh water, is required to remain sub-critical for any assembly geometry configuration within the damaged fuel cans. The canister must remain sub-critical with damaged fuel cans in all eight support tube locations.

6.6.3.1 W74 Canister Model for the Damaged Assembly Analyses

Therefore, criticality analyses are performed to determine the most reactive possible configuration of fissile material within the damaged fuel can interior volume. These analyses are performed using a full model of the W74 canister. The same canister and cask configuration (and assumptions) used in the intact BRP assembly criticality analyses (described in Sections 6.3 and 6.4) are used for these analyses. This configuration is shown in the intact assembly analyses to be bounding for all conditions of storage for the W74 canister.

These analyses model various fissile material configurations, inside damaged fuel cans, in all eight support tube locations. The other (guide tube) locations in the W74 canister are filled with the most reactive partial BRP assembly configuration, which is determined as discussed in Section 6.6.2.2. This configuration is a regular square array of 3.55% enriched 11x11 BRP assembly fuel rods with and $H/^{235}U$ ratio of 139.64. This partial assembly configuration is more reactive than the design basis (4.1% enriched) intact BRP assembly configuration.

Since a full canister model is used to determine the most reactive fissile material configuration for the damaged fuel can interiors, the same analyses can be used to verify that the most reactive fissile material configuration remains sub-critical (i.e., meets all 10CFR72 criticality requirements) when loaded into the damaged fuel cans that are placed within the W74 canister. As these analyses are also used to verify compliance with the criticality requirements, the most reactive possible contents of the other (guide tube) fuel locations must also be modeled. The

[11] ISG-1, *Damaged Fuel*, Spent Nuclear Fuel Project Office Interim Staff Guidance, United States Regulatory Commission, November 1998.

bounding partial BRP assembly configuration described above is modeled in the other canister fuel locations for that reason.

After the most reactive fissile material configuration is determined, additional analyses which model the bounding intact BRP assembly configuration (a 4.1% enriched 11x11 BRP assembly) in the other (guide tube) fuel locations are performed. These analyses verify that the case with partial assemblies in the other fuel locations is the bounding case, and that all 10CFR72 criticality requirements are met whether bounding intact BRP fuel assemblies or bounding partial BRP fuel assemblies are loaded into the other fuel locations.

6.6.3.2 Damaged Fuel Can Contents Model Description

It is conservatively assumed that, during drop events, damaged fuel rods break into segments and/or break open and release their fuel pellets into the damaged fuel can interior. Screens at the bottom end of the cans will prevent any fissile material from leaving the damaged fuel can interior volume. Grid spacers are also assumed to fail, allowing any spacing between rods to occur. In theory, it would be remotely possible for all fuel rods to fail and release all of their pellets. Then, the fuel rods, and all other assembly hardware, would break apart and fall into a pile at one end of the damaged fuel can interior. This would leave an array of fuel pellets occupying the rest of the damaged fuel can interior. To cover this extremely unlikely scenario, an extremely conservative assumption is made for the damaged assembly criticality analyses. The damaged fuel can interior is assumed to be occupied by a mixture of pure (unburned) fuel material and full density water. Thus, all assembly hardware materials, including the fuel rod cladding, are conservatively neglected. As these materials absorb neutrons and displace a large amount of water, this assumption greatly increases the reactivity of the modeled fissile material configuration.

The bulk of the damaged assembly analyses are performed to determine the most reactive possible configuration of fuel material and water that may occupy the interior of the damaged fuel cans. The analyses consider several different arrays of fuel pellets and water. In all cases these fuel pellet arrays are assumed to fill the entire damaged fuel can interior. The damaged fuel can steel walls and interior volume shown in Figure 6.3-4 is modeled over the entire axial length of the support tube in the criticality models (with the poison sheets being modeled over most of the axial length). Thus, the fissile material configuration is also assumed to extend over the entire axial length. The end geometry of the damaged fuel cans is not modeled in the analyses, as the full length geometry assumption is bounding.

The analyses model pure 4.61% enriched UO_2 fuel, with a density that is 96.5% of UO_2 theoretical density, over the entire fuel material configuration in the damaged fuel can interior. Three types of array configurations are analyzed, a hexagonal array of fuel spheres, a hexagonal array of fuel cylinders, and a square array of fuel cylinders. The fuel cylinders in the arrays are oriented along the Z-axis of the canister, and extend over the full axial length of the support tube. The cylinders are arranged in a square or hexagonal array in the horizontal direction. The array of fuel spheres is arranged in a hexagonal array in the horizontal direction. The spheres are then evenly spaced (in columns) in the axial direction, at a spacing equal to the pitch value of the horizontal array. Thus, the spacing between the spheres is the same in all directions.

The fuel sphere array analysis is performed assuming a fuel sphere diameter of 0.9 cm. The fuel cylinder array analyses are performed for two cylinder diameters, 0.471 inches and 0.3715

inches. These diameters correspond to the pellet diameters of the BRP 9x9 and 11x11 assemblies, respectively. As noted earlier in this section, fuel debris is not qualified for loading in the damaged fuel cans. Thus, virtually all fuel material that may exist within the damaged fuel can interior (after a possible drop event) will be in the form of loose BRP assembly fuel pellets. For this reason, analyses are performed for the two BRP assembly pellet diameters. The fuel cylinders modeled in the analysis correspond to an axial stack of fuel pellets, with the fuel rod cladding conservatively removed.

Since two diameters are analyzed for each of the two fuel cylinder arrays (hexagonal and square), there are a total of five array types that are analyzed. For each analyzed array type, the spacing between the fuel cylinders (or spheres) is varied over a wide range. The array pitch value that yields the maximum canister k_{eff} value is then determined. This corresponds to the optimum $H/^{235}U$ ratio for the array. After the optimum pitch value is determined for each of the five array types, the calculated k_{eff} value (at the optimum array pitch) is compared for the five array types. The array type which yields the highest calculated k_{eff} value is selected as the most reactive possible configuration of fuel material inside the damaged fuel can interior.

As discussed earlier, the arrays are assumed to completely fill the damaged fuel can interior, so the volume of the fissile material array is fixed. Thus, as the array pitch is increased, the number of fuel cylinders (or spheres) in the array decreases. Since the diameter of the fuel cylinders (or spheres) is constant, the quantity of fuel material within the damaged fuel can interior also varies with the pitch value. Since the pitch value that yields maximum reactivity (considering these effects) is determined, the optimum fissile material configuration (at the optimum pitch value) is bounding for any quantity of fuel material inside the damaged fuel can interior.

It is assumed that an array with a regular spacing of fuel particles that fills the damaged fuel can interior volume, with no other assembly materials present, is the most reactive possible configuration. Materials other than fuel or water clearly reduce reactivity. There are an infinite number of irregular configurations of fuel material that could occur within the damaged fuel can. A regular array at an optimum spacing, or pitch (i.e., an optimum $H/^{235}U$ ratio) should bound all such irregular configurations, however. Whereas an optimum regular array would have the optimum $H/^{235}U$ ratio at all locations within the array, an irregular geometry would have sections with ratios that are too high and sections with ratios that are too low (i.e., over-moderated and under-moderated sections). Thus, all such configurations will have reactivity levels that are similar to or lower than those of the analyzed regular arrays. Any small differences in reactivity levels that could occur between the infinite number of possible configurations that have an optimum $H/^{235}U$ ratio are much smaller than the increase in reactivity created in these analyses by the (ultra-conservative) removal of all other assembly materials. It is therefore concluded that analyzing both types of regular arrays (hexagonal and square), using both basic types of fuel particle geometry (sphere and cylinder), is sufficient to establish the most reactive possible fuel material configuration.

6.6.3.3 Damaged Assembly Criticality Analysis Results

The results of the optimum fissile material array calculations are presented in Table 6.6-13 through Table 6.6-18. For each of the five array types (described in Section 6.6.3.2), calculated k_{eff} values are presented for several analyzed array pitch values. For each array pitch value, the corresponding $H/^{235}U$ ratio for the array is presented. For each case, the k_{eff} value calculated by

MCNP, the statistical error level in the MCNP result (1σ), and the final k_{eff} value (calculated as k_{eff} + 2σ) are presented. The analyses results are also presented graphically in Figure 6.6-11 through Figure 6.6-15. The graphs show curve fits to the k_{eff} data from Table 6.6-13 through Table 6.6-18. Thus the plots show function curves given k_{eff} as a function of H/^{235}U ratio for each of the five analyzed array types.

The results presented in Table 6.6-13 through Table 6.6-18 show that a square array of 0.3715 inch diameter fuel cylinders (corresponding to 11x11 BRP assembly fuel pellets), at a pitch value of 0.655 inches, and an H/^{235}U ratio of 180, is the most reactive possible configuration of fuel material inside the damaged fuel can. The analyses also show that hexagonal arrays are somewhat less reactive than square arrays, and that there is virtually no dependence of maximum reactivity on pellet diameter. The maximum final k_{eff} values for the square arrays of 0.3715 inch fuel cylinders and 0.471 inch fuel cylinders are virtually the same (the difference between them being one fifth of the statistical error level of the criticality code).

An additional set of analyses, which model the square array of 0.3715 inch fuel cylinders in the damaged fuel can interior, are performed assuming design basis intact BRP assemblies (i.e., 4.1% enriched 11x11 BRP assemblies) in the other fuel locations in the W74 canister (as discussed in Section 6.6.3.1). These analyses are performed for the same set of array pitches shown in Table 6.6-14. The results of these analyses are presented in Table 6.6-18. These analyses show a maximum k_{eff} value at the same array pitch (0.655 inches) and H/^{235}U ratio (180) shown for the partial assembly configuration case in Table 6.6-14. The analyses also show that the maximum k_{eff} value for the 4.1% enriched intact 11x11 assembly case is lower than that of the 3.55% enriched partial 9x9 assembly case. This is expected since the intact, 4.1% enriched assembly configuration is somewhat less reactive than the optimum partial, 3.55% enriched assembly configuration (as shown by comparing the k_{eff} results shown for the intact assembly in Table 6.4-8 with the results shown for the partial 9x9 assembly in Table 6.6-11).

The maximum calculated k_{eff} values for the damaged BRP assembly analyses are compared to their corresponding USL values in Table 6.6-19. The cases shown correspond to the most reactive fuel material configuration in the damaged fuel can interior, i.e., a square array of 0.3715 inch diameter fuel cylinders with a pitch of 0.655 inches, and a fuel enrichment of 4.61%. Damaged fuel cans containing this configuration are modeled in all eight W74 support tube locations. Two cases are shown in Table 6.6-19. One corresponds to an optimum, 3.55% enriched, partial 9x9 BRP assembly configuration modeled in the other fuel locations, and the other corresponds to a design basis, intact, 4.1% enriched, 11x11 BRP assembly configuration modeled in the other fuel locations.

The overall reactivity of the canister is governed by the contents of the other 56 fuel locations in the W74 canister, as opposed to the contents of the damaged fuel cans loaded in the eight support tube locations that lie at the edge of the W74 canister. This is true even though the analyses show that the presence of the damaged fuel cans increases the overall reactivity of the W74 canister somewhat. For this reason, the USL values that apply for the W74 canister are governed by the parameters of the configurations modeled in the other fuel locations, as opposed to the damaged fuel can interiors. Therefore, the limiting USL values shown in Table 6.6-18 correspond to the optimum partial 9x9 BRP assembly configuration and the intact 11x11 BRP assembly configuration. The intact assembly minimum USL value is taken from Table 6.4-8. The minimum USL value for the partial assembly configuration is taken from Table 6.6-12.

The data in Table 6.6-19 shows that the final k_{eff} values are below the corresponding minimum USL values for both the partial and intact assembly cases. Thus, the results show that all 10CFR72 criticality requirements are met for a W74 canister loaded with up to eight damaged fuel cans containing the most reactive possible assembly configuration inside each damaged fuel can. This conclusion applies even if all of the other fuel locations in the canister are loaded with the most reactive allowable contents, including the most reactive allowable intact BRP assembly configuration (a 4.1% enriched 11x11 assembly), and/or the most reactive partial BRP assembly configuration (a 3.55% enriched 9x9 assembly).

As discussed in Section 6.6.3.2, the analyses model a uniform fuel enrichment of 4.61% over the entire fuel material array inside the damaged fuel can. Thus, these analyses qualify a maximum fuel enrichment level of 4.61% for the contents of the damaged fuel can. Although extremely unlikely, it is theoretically possible for a group of maximum enrichment pellets to escape their fuel rods and congregate in one section of the damaged fuel can interior. For this reason, the analyses conservatively assume that the fuel enrichment modeled for the damaged fuel can interior array corresponds to the maximum enrichment of any individual fuel pellet within the assembly. Thus, the maximum enrichment limit of 4.61% applies for each individual fuel pellet in any candidate assembly. Therefore, in conclusion, any fuel assembly that has no fuel pellets with enrichment levels over 4.61% may be loaded into a damaged fuel can which may then be loaded into one of the support tube locations of the W74 canister.

6.6.3.4 Damaged Fuel Can Preferential Flooding Analysis

The preceding calculations verify that any arrangement of fuel pellets with a pellet enrichment of 4.6% or less within the damaged fuel can does not cause the criticality requirements to be exceeded. These analyses are based upon full moderator (water) density within the damaged can interior and within the rest of the W74 canister interior. In general, for cask systems containing unpoisoned water, this is the most reactive case. Calculations verify that the most reactive uniform water density for the canister interior is 1.0 g/cc (full density).

However, since screens are employed by the damaged fuel cans, it may be possible for preferential flooding to occur. That is to say that a situation may arise where the water density within the damaged fuel can is not the same as the water density outside the damaged fuel can (i.e., in the rest of the W74 canister interior). For this reason, additional analyses are performed which consider various combinations of damaged fuel can interior and exterior water densities. These criticality models are identical to the those presented in the preceding sections, other than the water densities present in the canister and the damaged fuel can.

Two sets of analyses are performed. In the first set of analyses, the canister interior water density is maintained at 1.0 g/cc while the damaged can interior water density is varied from 1.0 g/cc down to 0.0 g/cc. In the second set of analyses, the damaged can interior water density is maintained at 1.0 g/cc while the canister interior water density is varied from 1.0 g/cc down to 0.0 g/cc.

The results of the preferential flooding analyses are presented in Figure 6.6-16. The results show that full water density inside the damaged fuel can and in the rest of the canister interior is indeed the most reactive case. If the water density is reduced in either region, k_{eff} decreases. As expected, the k_{eff} dependence was stronger for the canister interior (damaged fuel can exterior) water, since it occupies a much larger fraction of the overall canister interior volume.

Thus, the damaged fuel criticality results and enrichment limits remain valid after considering preferential flooding effects.

6.6.3.5 Damaged BRP MOX Assembly Analyses

There exists some damaged BRP MOX fuel that may require storage in the W74 canister. Therefore, damaged fuel analyses, similar to those described earlier in this section, are performed for several MOX fuel compositions.

Other than the isotopic composition of the fuel material inside the damaged fuel cans, these analyses are identical to the damaged UO_2 fuel analyses presented earlier in this section. The MOX fuel analyses model the most reactive fuel configuration determined in Section 6.6.3.3 inside all of the (8) damaged fuel cans (i.e., a square array of 0.3715 inch diameter fuel cylinders with a pitch of 0.655 inches). The optimum partial 9x9 BRP assembly configuration is modeled for all other fuel locations in the canister.

The MOX fuel material is a mixture of enriched uranium (^{235}U and ^{238}U) and plutonium. All plutonium metal is conservatively modeled with an isotope distribution of 85% ^{239}Pu and 15% ^{240}Pu.

Analyses are performed for several combinations of uranium enrichment and plutonium concentration (assuming the plutonium isotope distribution given above). The analyzed MOX fuel compositions are presented in Table 6.6-20. Table 6.6-20 also presents the calculated atom densities within the fuel (in atoms/barn-cm) for each of the analyzed cases. The uranium enrichment shown in the table is defined as the ^{235}U mass in the fuel material divided by the total uranium mass. The plutonium weight percentage is defined as the total plutonium mass (over all Pu isotopes) divided by the total heavy metal mass (U + Pu).

The set of MOX fuel composition cases presented in Table 6.6-20 follows the formula shown below:

$$E_{U\text{-}235} + 0.7 \times P_{Pu} = 4.61\%$$

where $E_{U\text{-}235}$ is the ^{235}U enrichment of the uranium in the fuel, and P_{Pu} is the overall weight percentage of plutonium metal. The Pu weight percentage is defined as the mass of Pu metal divided by the total heavy metal (U + Pu) mass. The ^{235}U enrichment of the uranium is defined as the ^{235}U mass divided by the total uranium mass in the fuel.

This is an arbitrary formula, which defines an allowable MOX fuel parameter envelope for the W74 damaged fuel can contents. The formula was selected to bound all MOX fuel material that exists at Big Rock Point. Criticality analyses are performed for a large number of points (i.e., specific MOX fuel compositions) that lie along that defined line (as shown in Table 6.6-20).

The results of the damaged MOX fuel analyses are presented in Table 6.6-21. For each analyzed case, Table 6.6-21 presents the uranium enrichment, the plutonium concentration, the k_{eff} value calculated by MCNP, the statistical error level (1σ) in the calculated k_{eff} result, and the final k_{eff} value (calculated as $k_{eff} + 2\sigma$). The Table 6.6-21 results show that the most reactive MOX fuel case is a mixture of natural uranium plus 5.57 w/o plutonium. The final k_{eff} value for this case is 0.94107. This is under the minimum USL value of 0.94375 which corresponds to the optimum

partial 9x9 BRP assembly, the assembly configuration that is modeled in the other fuel locations of the canister in all of the damaged MOX assembly analyses. As discussed in Section 6.6.3.3, this USL is therefore the governing USL for all of the damaged MOX fuel analyses. It is also true that the final k_{eff} value is also under the minimum USL for all MOX fuel analyses of 0.94141 (see Section 6.6.1.2). Thus, the criticality analyses verify compliance with all 10CFR72 criticality requirements for all of the analyzed MOX fuel compositions presented in Table 6.6-20.

All of the analyzed compositions presented in Table 6.6-20 follow the uranium enrichment versus plutonium concentration formula shown above. Given that a large number of points along the line defined by the formula are analyzed and shown (in Table 6.6-21) to meet the criticality requirements, it is concluded that all assemblies whose MOX fuel composition is bounded by the formula also meet the criticality requirements.

Thus, it is concluded that all MOX assemblies that meet the formula below are qualified for loading into the damaged fuel cans of the W74 canister:

$$E_{U\text{-}235} + 0.7 \text{ x } P_{Pu} \leq 4.61\%$$

where $E_{U\text{-}235}$ is the ^{235}U enrichment of the uranium in the fuel, and P_{Pu} is the overall weight percentage of plutonium metal. The Pu weight percentage is defined as the mass of Pu metal divided by the total heavy metal (U + Pu) mass. The ^{235}U enrichment of the uranium is defined as the ^{235}U mass divided by the total uranium mass in the fuel.

Note that only two parameters, the uranium enrichment and the overall plutonium metal weight percentage are specified. There is no specification on the fissile plutonium quantity or the quantity of any given plutonium isotope. This is because a bounding plutonium isotope distribution is already assumed in the criticality analyses. The criticality analyses therefore conservatively overestimate the fissile plutonium concentrations for any given plutonium metal concentration.

6.6.3.6 Other Allowable Damaged Fuel Can Contents

As discussed in Section 6.6.3.3, a maximum allowable enrichment of 4.61% is established for all assemblies to be loaded into the W74 canister damaged fuel cans. This enrichment limit applies for each individual fuel pellet within the assembly. This criterion is intended to apply for all damaged BRP assemblies that are to loaded into the damaged fuel cans of the W74 canister.

However, the damaged assembly criticality analyses presented in this section may also be used to qualify a very broad range of possible contents for the damaged fuel cans. As discussed in Section 6.6.3.3, it is concluded that the analyses presented determine the most reactive possible configuration of fissile material inside the damaged fuel cans, given a maximum fuel enrichment of 4.61% and a maximum fuel density of 96.5% UO_2 theoretical. The calculations do not merely determine the most reactive possible configuration for a damaged BRP assembly. The conclusions of the analysis are much broader.

Other than the enrichment and fuel density limits discussed above, all assembly parameters that may affect criticality in a standard (intact assembly) criticality analysis are clearly bounded, over all possible values, by these analyses. These analyses determine the optimum pitch (and

optimum H/U ratio) for the fissile material array, so all possible assembly pitch values are covered. All possible fuel rod array layouts (number and location of water holes, etc.) are also covered for the same reason. Since these analyses very conservatively neglect all assembly cladding and hardware materials, all values of cladding thickness, clad material, and clad diameter are clearly bounded by these analyses. Since these analyses model the fissile material array as completely filling the damaged fuel can interior volume, all values for assembly array size and active fuel length are clearly bounded by these analyses (given that the assembly can physically fit inside the damaged fuel can). The only parameter for which specific values are assumed in these analyses is the pellet diameter. The effects of pellet diameter on fissile material configuration reactivity are discussed below.

Analyses were performed for two fuel cylinder (i.e., fuel pellet) diameters, 0.471 inches and 0.3715 inches, which correspond to the typical pellet diameters of 9x9 and 11x11 BRP fuel assemblies, respectively. Examination of the k_{eff} results shown for square arrays of fuel cylinders in Table 6.6-13 and Table 6.6-14 shows that the maximum k_{eff} value does not vary significantly with cylinder (i.e., pellet) diameter. A k_{eff} value of 0.9364 is shown for the 0.471 inch diameter case, versus a k_{eff} value of 0.9366 for the 0.3715 inch diameter case. These results are virtually identical, with the difference being only one fifth the level of statistical error in the code results (0.0002 vs. an error level of ~0.001).

It is therefore concluded that the maximum fuel material configuration reactivity does not vary significantly with fuel pellet diameter. Any differences in reactivity are much smaller than the increase in k_{eff} due to the extremely conservative assumptions made in these analyses (such as removing all cladding material and assuming all fuel is at the maximum fuel pellet enrichment level). Thus, it is concluded that these analyses are applicable for a very wide range of possible fuel assembly pellet diameter values.

Some BRP 11x11 assemblies have a fuel pellet diameter of 0.3735 inches, as opposed to the more typical value of 0.3715 inches. The 0.3735 inch value is only ~0.5% larger than the 0.3715 value studied in the damaged assembly analyses. Since no measurable difference in reactivity is seen between pellet diameters of 0.3715 inches and 0.471 inches, the is clearly no significant difference between diameters of 0.3715 inches and 0.3735 inches.

It should also be noted that, as stated in Section 6.6.3.3, these analyses do not apply for fuel debris. Broken or crumbled fuel pellets would fall into that category. Therefore, fissile material particle diameters that differ dramatically from the two values considered in these analyses will not occur for any of the potential damaged fuel can contents.

For the above reasons, these analyses show that virtually any assembly geometry may be loaded into the damaged fuel cans of the W74 canister while meeting all 10CFR72 criticality requirements. Therefore, the only assembly parameters that will be specified (for loading into the damaged fuel cans) are the maximum fuel pellet enrichment level and the maximum fuel material density. The maximum allowable pellet enrichment is 4.61% and the maximum allowable fuel density is 96.5% of theoretical UO_2 density. These are the only two parameters that need to be specified to ensure compliance with the criticality requirements. Other parameters such as assembly weight, assembly width, uranium loading, uranium loading per inch of fuel height, burnup, cooling time, etc. would have to be specified in order to meet the structural, thermal, and shielding requirements. However, none of the assembly array dimensions (which are generally specified to meet the criticality requirements) will have to be specified. The

specifications shown in Chapter 12 of this FSAR for assemblies loaded into the damaged fuel can therefore do not restrict any of these assembly array geometry parameters.

Thus, the damaged fuel cans placed in the W74 canister support tubes may perform a second function. As well as accommodating all damaged BRP fuel, these cans may accommodate any assembly configuration, discovered at BRP, that does not meet the assembly geometry specifications for intact or partial BRP fuel assemblies. Any assembly geometry (damaged or undamaged) may be loaded into the damaged fuel cans as long as the maximum enrichment is under 4.61% and the fuel density is under 96.5% theoretical (given that the assembly physically fits inside the cans). For MOX fuel, any assembly that meets the fuel density requirement and meets the MOX fuel composition criteria given in Section 6.6.3.5 can be loaded into the damaged fuel cans.

Table 6.6-1 - Uranium Isotope Atom Densities for UO_2 Fuel Rods in BRP MOX Assemblies

UO_2 Rod Enrichment (w/o ^{235}U)(1)	BRP MOX Assembly Type	^{235}U Atom Density (atom/barn-cm)	^{238}U Atom Density (atom/barn-cm)
2.3	G-Pu	5.504 E-04	2.309 E-02
2.4	DA	5.743 E-04	2.306 E-02
2.5	E65/E72(2)	5.983 E-04	2.304 E-02
2.55	J2	6.102 E-04	2.303 E-02
3.2	G-Pu	7.658 E-04	2.287 E-02
3.3	J2	7.897 E-04	2.285 E-02
3.4	E65/E72(2)	8.136 E-04	2.283 E-02
4.5	J2	1.077 E-03	2.257 E-02
4.6	G-Pu	1.101 E-03	2.254 E-02

Notes:

(1) UO_2 rod enrichments are shown for each BRP MOX assembly type in Figure 6.6-1 through

(2) Figure 6.6-8.

(3) Two UO_2 assemblies that each have two inserted MOX fuel rods.

Table 6.6-2 - BRP Assembly MOX Fuel Pin Isotope Densities (atom/barn-cm)

Isotope	J2 Assembly MOX Fuel Pin 0.711% ^{235}U 3.65% PuO_2	DA Assembly MOX Fuel Pin #1 1.56% ^{235}U 1.03% PuO_2	DA Assembly MOX Fuel Pin #2 2.4% ^{235}U 2.45% PuO_2	G-Pu Assembly MOX Fuel Pin 0.711% ^{235}U 5.45% PuO_2	E65/E72 Assembly MOX Fuel Pins 0.711% ^{235}U + 25.4 g/rod Pu		
					Solid Pellet (cylindrical)	Annular Pellet (0.1" hole)	Annular Pellet (0.2" hole)
^{235}U	1.639 E-04	3.695 E-04	5.603 E-04	1.609 E-04	1.651 E-04	1.650 E-04	1.645 E-04
^{238}U	2.260 E-02	2.302 E-02	2.250 E-02	2.218 E-02	2.276 E-02	2.275 E-02	2.269 E-02
^{238}Pu	3.665 E-06	1.314 E-06	3.126 E-06	8.242 E-06	-	-	-
^{239}Pu	6.548 E-04	1.777 E-04	4.227 E-04	9.255 E-04	-	-	-
^{240}Pu	1.397 E-04	4.313 E-05	1.026 E-04	2.314 E-04	-	-	-
^{241}Pu	2.478 E-05	7.979 E-06	1.898 E-05	4.635 E-05	3.318 E-04	3.471 E-04	4.058 E-04
^{242}Pu	1.000 E-05	3.901 E-06	9.280 E-06	2.254 E-05	-	-	-
^{241}Am	2.478 E-05	7.979 E-06	1.898 E-05	4.635 E-05	-	-	-

Table 6.6-3 - MCNP Calculated Keff Values for W74 Baskets Fully Loaded with BRP MOX Fuel (Full Water Density)

Computer Run ID	BRP Assembly	Calculated k_{eff}	Relative Error	Final k_{eff}	Limiting USL	Criticality Margin
W74_J2	J2 (9x9)	0.83289	0.00091	0.83471	0.94141	0.10670
W74_DA	DA (11x11)	0.81525	0.00086	0.81697	0.94141	0.12444
W74_G-Pu	G-Pu (11x11)	0.87361	0.00089	0.87539	0.94141	0.06602
W74_D72	D72 (partial J2)	0.84606	0.00090	0.84786	0.94141	0.09355
W74_D73	D73 (partial J2)	0.84632	0.00081	0.84794	0.94141	0.09347
W74_G01	G01 (partial G-Pu)	0.84101	0.00094	0.84289	0.94141	0.09852
W74_G02	G02 (partial G-Pu)	0.84674	0.00090	0.84854	0.94141	0.09287
W74_EG0	E65 / E72 (1)	0.85684	0.00088	0.85860	0.94141	0.08281
W74_EG1	E65 / E72 (1)	0.85699	0.00093	0.85885	0.94141	0.08256
W74_EG2	E65 / E72 (1)	0.85808	0.00090	0.85988	0.94141	0.08153
W74_U09	UO_2 (9x9)	0.92106	0.00092	0.92290	0.94358(2)	0.02068
W74_U11	UO_2 (11x11)	0.92130	0.00089	0.92308	0.94286(2)	0.01978

Notes:

(1) Two UO_2 assemblies that each have two inserted MOX fuel rods. The "EG0," "EG1," and "EG2" cases refer to MOX fuel pellets with inner void region diameters of 0.0, 0.1, and 0.2 inches, respectively.

(2) UO_2 assembly USLs are taken from

(3) Table 6.4-8.

Table 6.6-4 - MCNP Calculated K_{eff} for MOX Fuel vs. W74 Interior Water Density (G-Pu Fuel Assemblies)

Moderator Density (% of FD)	Calculated k_{eff}	Relative 1σ Error	Final k_{eff}
0	0.37460	0.00035	0.37530
10	0.58551	0.00063	0.58677
20	0.64152	0.00073	0.64298
40	0.72203	0.00079	0.72361
60	0.78502	0.00081	0.78664
70	0.81303	0.00089	0.81481
80	0.83485	0.00087	0.83659
90	0.85673	0.00092	0.85857
95	0.86496	0.00088	0.86672
100	0.87361	0.00089	0.87539

Table 6.6-5 - MOX Fuel Benchmark Critical Experiments

Name	K_{eff}	Sigma	Fissile %(1)	Pitch	H_2O/Fuel	H/Fissile(2)	Pu %(3)
M1-1	0.99649	0.00092	20.354	0.9525	3.335	50.4	97.3
M1-2	0.99818	0.00091	20.354	1.2588	6.868	103.9	97.3
M1-3	1.00177	0.00096	20.354	1.5342	10.881	164.6	97.3
M1-4	1.00598	0.00090	20.354	1.905	17.534	265.2	97.3
M2-30	0.99771	0.00085	2.571	1.778	1.195	146.2	73.0
M2-31	0.99893	0.00086	2.571	1.778	1.195	146.2	73.0
M2-32	1.00393	0.00083	2.571	2.2091	2.525	309.0	73.0
M2-33	1.00988	0.00084	2.571	2.2091	2.525	308.8	73.0
M2-34	1.00588	0.00080	2.571	2.5145	3.641	445.6	73.0
M2-35	1.00903	0.00079	2.571	2.5145	3.641	445.4	73.0
M3-1	0.99633	0.00091	6.698	1.3208	1.681	73.9	90.1
M3-2	0.99827	0.00094	6.698	1.4224	2.164	95.3	90.1
M3-3	0.99848	0.00095	6.698	1.4224	2.164	95.2	90.1
M3-4	1.00465	0.00089	6.698	1.8679	4.706	206.8	90.1
M3-5	1.00315	0.00089	6.698	2.0116	5.672	249.7	90.1
M3-6	1.00679	0.00085	6.698	2.6416	10.754	473.1	90.1
M4-1	0.99692	0.00089	2.962	1.825	2.42	407.1	76.7
M4-5	0.99897	0.00084	2.962	1.825	2.42	409.6	76.7
M4-6	0.99719	0.00090	2.962	1.956	2.976	500.6	76.7
M4-10	0.99933	0.00086	2.962	1.956	2.976	505.3	76.7
M4-11	0.99897	0.00081	2.962	2.225	4.239	712.6	76.7
M4-15	0.99994	0.00074	2.962	2.225	4.239	717.6	76.7
M4-16	1.00214	0.00077	2.962	2.474	5.552	933.6	76.7
M4-18	1.00055	0.00074	2.962	2.474	5.552	936.9	76.7

Notes:

(1) Defined as the mass of fissile nuclides (^{235}U, ^{239}Pu and ^{241}Pu) over the total heavy metal mass.

(2) Defined as the ratio of the number of hydrogen atoms over the total number of fissile nuclide atoms within the fuel assembly array

(3) Defined as the percentage of fissile material within the assembly that is plutonium as opposed to uranium.

Table 6.6-6 - Upper Sub-Critical Limit Formulas for the MOX Only, UO_2 Only, and MOX + UO_2 Sets of Critical Experiments

System Physical Parameter	Critical Experiment Set	Min. Value	Max. Value	USL Equation ("x" = parameter value)
Pin Pitch (cm)	MOX Only	0.9525	2.6416	$0.93372 + (5.8336 \times 10^{-3} * x)$; for $(x < 1.72)$ 0.94375 ; for $(x \geq 1.72)$
Pin Pitch (cm)	UO_2 Only	1.24	2.54	$0.93854 + (2.9355 \times 10^{-3} * x)$; for $(x < 2.412)$ 0.94562 ; for $(x \geq 2.412)$
Pin Pitch (cm)	MOX + UO_2	0.9525	2.6416	$0.93555 + (4.4440 \times 10^{-3} * x)$; for $(x < 2.05)$ 0.94466 ; for $(x \geq 2.05)$
Water-to-Fuel Volume Ratio	MOX Only	1.195	17.534	$0.94093 + (4.2845 \times 10^{-4} * x)$; for $(x < 1.75)$ 0.94168 ; for $(x \geq 1.75)$
Water-to-Fuel Volume Ratio	UO_2 Only	1.44	3.88	$0.94272 + (5.8009 \times 10^{-4} * x)$; for all x values
Water-to-Fuel Volume Ratio	MOX + UO_2	1.195	17.534	$0.94143 + (5.8269 \times 10^{-4} * x)$; for $(x < 3.93)$ 0.94372 ; for $(x \geq 3.93)$
Fissile Material %	MOX Only	2.57	20.354	0.94197 ; for all x values
Fissile Material %	UO_2 Only	2.35	5.00	$0.94082 + (9.4676 \times 10^{-4} * x)$; for all x values
Fissile Material %	MOX + UO_2	2.35	20.354	$0.94260 + (1.1082 \times 10^{-4} * x)$; for $(x < 9.926)$ 0.94370 ; for $(x \geq 9.926)$
H-to-Fissile Ratio	MOX Only	50.4	936.9	0.94199 ; for all x values
H-to-Fissile Ratio	UO_2 Only	80.9	398.7	$0.94458 - (3.6041 \times 10^{-6} * x)$; for all x values
H-to-Fissile Ratio	MOX + UO_2	50.4	936.9	$0.94230 + (3.8900 \times 10^{-6} * x)$; for $(x < 398.5)$ 0.94385 ; for $(x \geq 398.5)$
Fissile Pu Percentage	MOX + UO_2	0.0	97.3	$0.94304 + (3.1082 \times 10^{-5} * x)$; for $(x < 46)$ 0.94449 ; for $(x \geq 46)$

Table 6.6-7 - Parameter Ranges Covered by Critical Experiments and BRP MOX Fuel Assemblies

Physical Parameter	MOX Fuel Experiments		UO_2 Fuel Experiments		BRP MOX Fuel Assemblies[1]	
	Min. Value	Max. Value	Min. Value	Max. Value	Min. Value	Max. Value
Pin Pitch (cm)	0.9525	2.6416	1.24	2.54	1.46	1.8
Water-to-Fuel Ratio	1.195	17.534	1.44	3.88	1.44	1.61
Fissile Material %	2.57	20.354	2.35	5.00	2.0[2]	4.8
H-to-Fissile Ratio	50.4	936.9	80.9	398.7	89.5	196
Fissile Pu %	73.0	97.3	0.0	0.0	0.0	86.0

Notes:

(1) Limiting BRP assembly fissile material %, H-to-fissile, and fissile Pu % parameters are calculated based on individual fuel rods, as opposed to assembly average values.

(2) Based on the two MOX fuel rods in the E65 and E72 assemblies. A small number of individual 2.3% UO_2 fuel rods also occur in the G-Pu MOX assembly. The DA assembly also contains a larger number of 2.33% UO_2 fuel rods. The assembly average fissile material % for the G-Pu assembly is over 3.9%. The lowest assembly average fissile material % for BRP MOX fuel is 3.02%, which occurs for the DA assembly.

Table 6.6-8 - Calculated K_{eff} Values for BRP Assemblies with Missing Array Corner Rods

BRP Assembly Type	Enrichment (w/o ^{235}U)	Calculated k_{eff}	Relative Error Level	Final k_{eff}
GE 9x9	4.1%	0.90893	0.00086	0.91065
Siemens 11x11	4.1%	0.92090	0.00097	0.92284

Table 6.6-9 - Calculated K_{eff} vs. Fuel Rod Pitch for 4.1% Enriched GE 9x9 BRP Assembly Fuel Rods (Single Assembly with Full Water Reflection)

Fuel Rod Pitch (vs. Nominal Value)	Rod Pitch (inches)	Water-to-Fuel Volume Ratio	H-to-^{235}U Ratio	Calculated k_{eff}	Relative Error	Final k_{eff}
1.00 x Nominal	0.707	1.492	101.9	0.74223	0.00084	0.74391
1.05 x Nominal	0.742	1.786	121.9	0.77288	0.00089	0.77466
1.09 x Nominal	0.771	2.043	139.5	0.78395	0.00093	0.78581
1.10 x Nominal	0.778	2.094	143.0	0.78234	0.00080	0.78394
1.125 x Nominal	0.795	2.254	153.9	0.77764	0.00084	0.77932
1.25 x Nominal	0.884	3.118	212.9	0.74595	0.00085	0.74765

Table 6.6-10 - Calculated K_{eff} vs. Fuel Rod Pitch for 4.1% Enriched Siemens 11x11 BRP Assembly Fuel Rods (Single Assembly with Full Water Reflection)

Fuel Rod Pitch (vs. Nominal Value)	Rod Pitch (inches)	Water-to-Fuel Volume Ratio	H-to-^{235}U Ratio	Calculated k_{eff}	Relative Error	Final k_{eff}
1.00 x Nominal	0.577	1.663	113.5	0.74679	0.00094	0.74867
1.05 x Nominal	0.606	1.977	135.0	0.77607	0.00089	0.77785
1.08 x Nominal	0.623	2.144	146.4	0.77934	0.00083	0.78100
1.09 x Nominal	0.629	2.240	153.0	0.77673	0.00088	0.77849
1.10 x Nominal	0.635	2.308	157.5	0.77413	0.00091	0.77595
1.125 x Nominal	0.649	2.478	169.2	0.76248	0.00083	0.76414
1.14 x Nominal	0.658	2.583	176.3	0.75376	0.00083	0.75542

Table 6.6-11 - Calculated K_{eff} for BRP Partial Assemblies at Maximum Allowable Enrichment (Optimum Pitch Fuel Rod Arrays Inside the W74 Canister)

BRP Assembly Type	Rod Pitch (inches)	Water-to-Fuel Volume Ratio	H-to-^{235}U Ratio	Calculated k_{eff}	Relative Error	Final k_{eff}
GE 9x9	0.741	1.771	139.6	0.94113	0.00099	0.94311
Siemens 11x11	0.597	1.882	146.3	0.93797	0.00082	0.93961

Table 6.6-12 - Physical Parameters and USL Values for the Optimum BRP Fuel Rod Arrays

Rod Array Physical Parameter	GE 9x9 Fuel Rod Array		Siemens 11x11 Fuel Rod Array	
	Parameter Value	USL Value	Parameter Value	USL Value
Pin Pitch (in.)	0.741	0.94406	0.597	0.94300
Water-to-Fuel Ratio	1.771	0.94375	1.882	0.94381
H-to-^{235}U Ratio	139.6	0.94408	146.3	0.94405
Fuel Rod Enrichment	3.55%	0.94418	3.6%	0.94423

Table 6.6-13 - Calculated K_{eff} Values for a W74 Canister w/ 8 Damaged Fuel Cans Containing a Square Array of 0.471" Diameter Fuel Cylinders

(Guide Tubes Contain Partial 9x9 BRP Assembly Configurations)

Array Pitch (in.)	H / ^{235}U Ratio	MCNP Calculated K_{eff}	Statistical Error (1σ)	Final K_{eff} ($k_{eff} + 2\sigma$)
0.679	100	0.92862	0.00087	0.93036
0.777	150	0.93436	0.00086	0.93608
0.795	160	0.93455	0.00091	0.93637
0.830	180	0.93390	0.00083	0.93556
0.864	200	0.93061	0.00091	0.93243

Table 6.6-14 - Calculated K_{eff} Values for a W74 Canister w/ 8 Damaged Fuel Cans Containing a Square Array of 0.3715" Diameter Fuel Cylinders

(Guide Tubes Contain Partial 9x9 BRP Assembly Configurations)

Array Pitch (in.)	H / ^{235}U Ratio	MCNP Calculated K_{eff}	Statistical Error (1σ)	Final K_{eff} (k_{eff} + 2σ)
0.535	100	0.92592	0.00091	0.92774
0.613	150	0.93385	0.00088	0.93561
0.655	180	0.93487	0.00087	0.93661
0.682	200	0.93449	0.00093	0.93635
0.720	230	0.93217	0.00091	0.93399

Table 6.6-15 - Calculated K_{eff} Values for a W74 Canister w/ 8 Damaged Fuel Cans Containing a Hexagonal Array of 0.471" Diameter Fuel Cylinders

(Guide Tubes Contain Partial 9x9 BRP Assembly Configurations)

Array Pitch (in.)	H / ^{235}U Ratio	MCNP Calculated K_{eff}	Statistical Error (1σ)	Final K_{eff} (k_{eff} + 2σ)
0.729	100	0.92779	0.00086	0.92951
0.794	130	0.93091	0.00086	0.93263
0.892	180	0.93103	0.00091	0.93285
0.929	200	0.92947	0.00084	0.93115

Table 6.6-16 - Calculated K_{eff} Values for a W74 Canister w/ 8 Damaged Fuel Cans Containing a Hexagonal Array of 0.3715" Diameter Fuel Cylinders
(Guide Tubes Contain Partial 9x9 BRP Assembly Configurations)

Array Pitch (in.)	H / ^{235}U Ratio	MCNP Calculated K_{eff}	Statistical Error (1σ)	Final K_{eff} (k_{eff} + 2σ)
0.575	100	0.92557	0.00088	0.92733
0.627	130	0.92911	0.00084	0.93079
0.704	180	0.93218	0.00093	0.93404
0.732	200	0.92992	0.00091	0.93174
0.812	260	0.92901	0.00089	0.93079

Table 6.6-17 - Calculated K_{eff} Values for a W74 Canister w/ 8 Damaged Fuel Cans Containing a Hexagonal Array of 0.9 cm Diameter Fuel Spheres
(Guide Tubes Contain Partial 9x9 BRP Assembly Configurations)

Array Pitch (in.)	H / ^{235}U Ratio	MCNP Calculated K_{eff}	Statistical Error (1σ)	Final K_{eff} (k_{eff} + 2σ)
1.134	140	0.92973	0.00090	0.93153
1.170	160	0.93269	0.00091	0.93451
1.204	180	0.93363	0.00089	0.93541
1.237	200	0.93381	0.00091	0.93563
1.311	250	0.92957	0.00085	0.93127

Table 6.6-18 - Calculated K_{eff} Values for a W74 Canister w/ 8 Damaged Fuel Cans Containing a Square Array of 0.3715" Diameter Fuel Cylinders (Guide Tubes Contain Intact 11x11 BRP Assembly Configurations)

Array Pitch (in.)	H / ^{235}U Ratio	MCNP Calculated K_{eff}	Statistical Error (1σ)	Final K_{eff} (k_{eff} + 2σ)
0.535	100	0.92246	0.00091	0.92428
0.655	150	0.92742	0.00091	0.92924
0.682	180	0.92927	0.00088	0.93103
0.720	230	0.92719	0.00092	0.92903

Table 6.6-19 - W74 Damaged Assembly 10CFR72 Criticality Margin Calculation (0.655" Pitch Square Array of 0.3715" Diameter Fuel Cylinders in All Damaged Fuel Cans)

Contents of Other (guide tube) Fuel Locations	MCNP Calculated K_{eff}	Statistical Error (1σ)	Final K_{eff} (k_{eff} + 2σ)	Limiting USL(1)	Criticality Margin
Optimum Partial (9x9) BRP Assembly	0.93487	0.00087	0.93661	0.94375	0.00714
Most Reactive Intact (11x11) BRP Assembly	0.92927	0.00088	0.93103	0.94286	0.01183

Note:

(1) Limiting USL for optimum partial assembly case is taken from Table 6.6-12. The intact assembly USL is taken from

(2) Table 6.4-8.

Table 6.6-20 - MOX Fuel Isotope Densities (atom/barn-cm)

Isotope	3.5% U-235 1.5857% Pu	2.5% U-235 3.0143% Pu	1.5% U-235 4.4429% Pu	0.711% U-235 5.5700% Pu	0.0% U-235 6.5857% Pu
U-235	8.243 E-04	5.802 E-04	3.430 E-04	1.607 E-04	-
U-238	2.244 E-02	2.234 E-02	2.224 E-02	2.215 E-02	2.207 E-02
Pu-239	3.171 E-04	6.029E-04	8.886 E-04	1.114 E-03	1.317 E-03
Pu-240	5.573 E-05	1.059 E-04	1.562 E-04	1.958 E-04	2.315 E-04
Oxygen	7.091 E-02	7.090 E-02	7.088 E-02	7.087 E-02	7.082 E-02

Table 6.6-21 - Calculated K_{eff} Values for a W74 Canister w/ 8 Damaged Fuel Cans Containing a Square Array of 0.3715" Diameter MOX Fuel Cylinders

(Guide Tubes Contain Partial 9x9 BRP Assembly Configurations)

Uranium Enrichment (w/o U-235)	Pu Fraction (w/o)	MCNP Calculated K_{eff}	Statistical Error (1σ)	Final K_{eff} ($k_{eff} + 2\sigma$)
4.61	0.0	0.93487	0.00087	0.93661
3.5	1.5857	0.93525	0.00088	0.93701
2.5	3.0143	0.93709	0.00085	0.93879
1.5	4.4429	0.93665	0.00084	0.93833
0.711	5.5700	0.93929	0.00089	0.94107
0.0	6.5857	0.93655	0.00081	0.93817

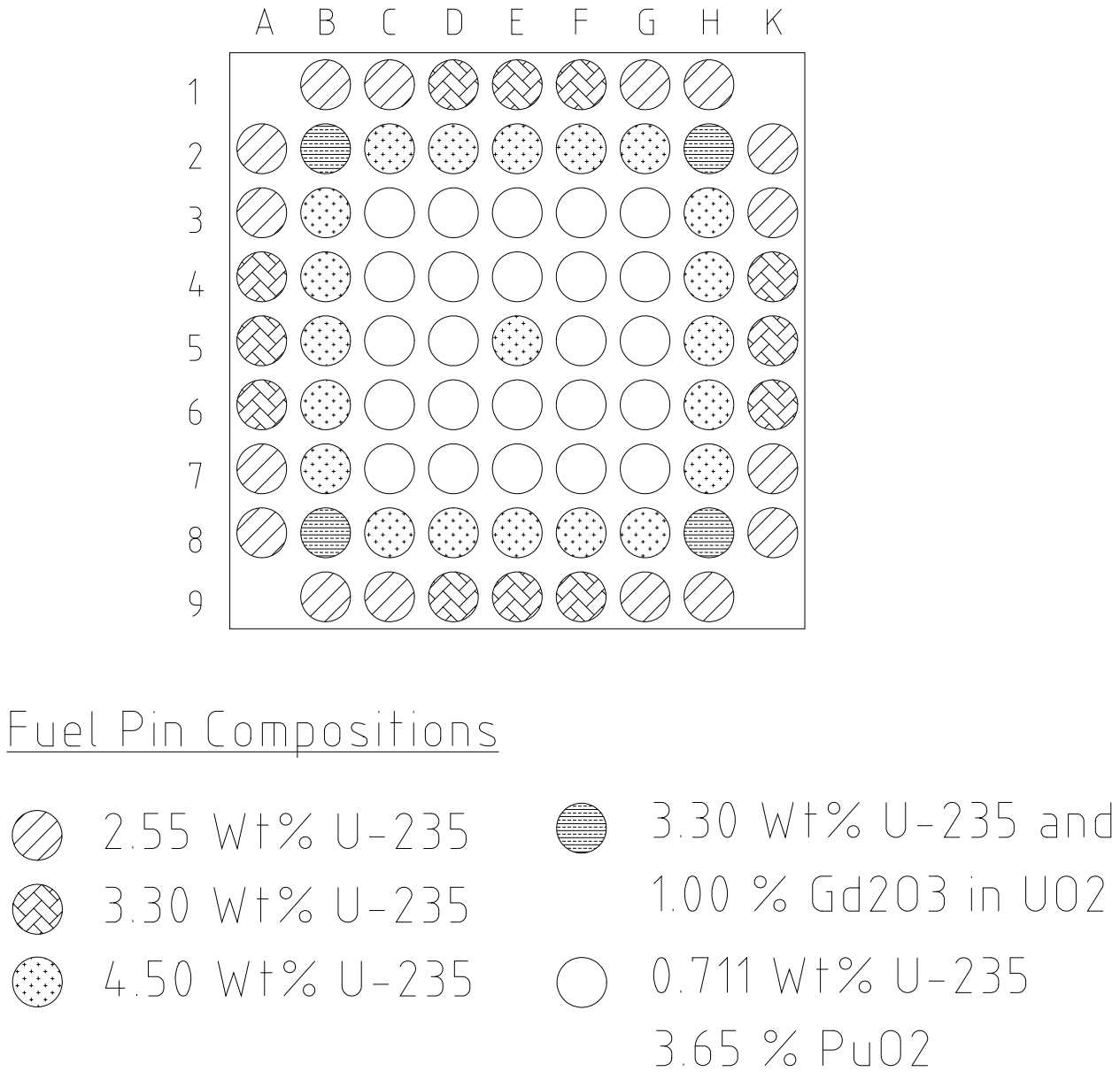

Figure 6.6-1 - J2 (9x9) BRP MOX Assembly Array

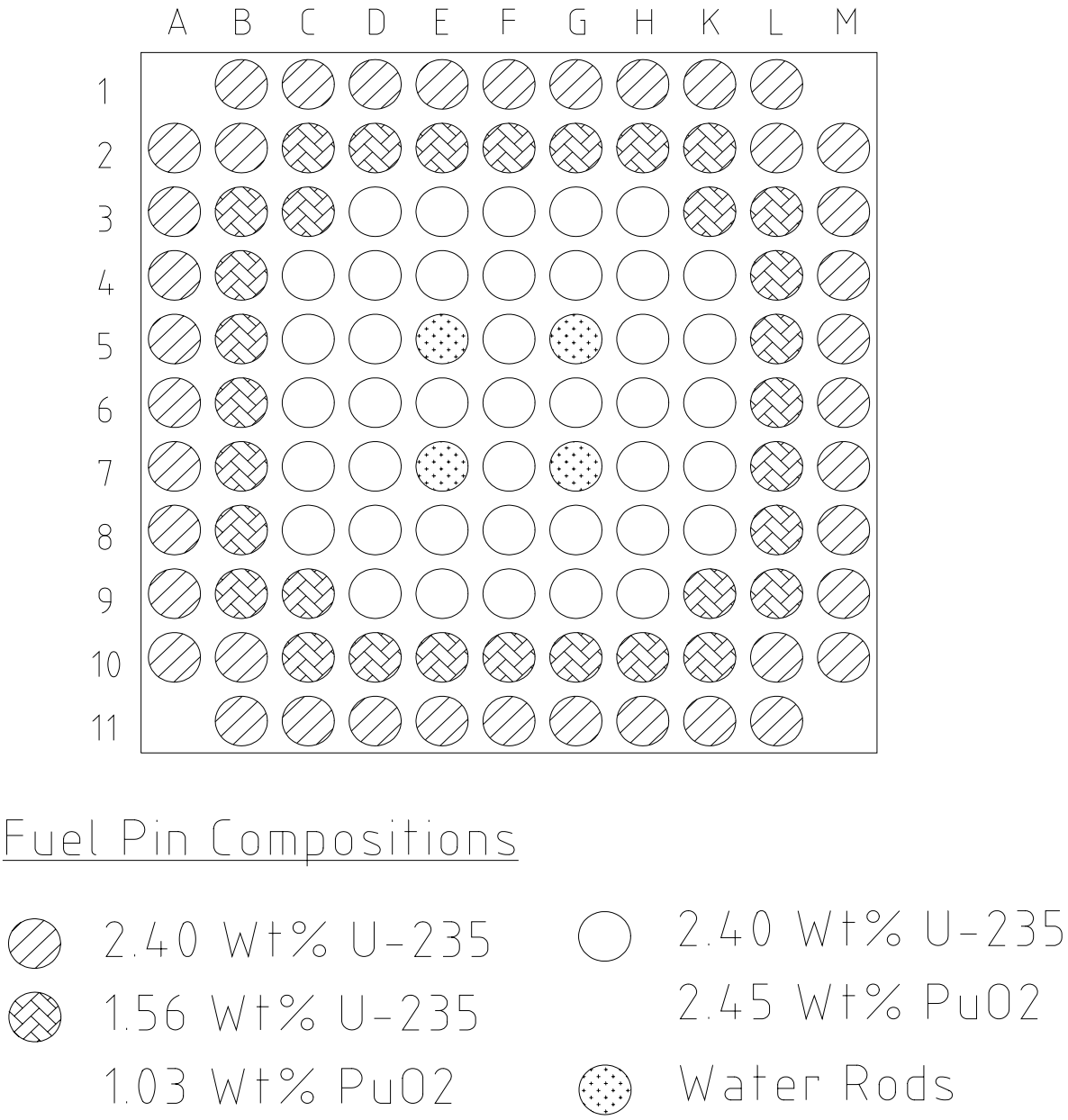

Figure 6.6-2 - DA (11x11) BRP MOX Assembly Array

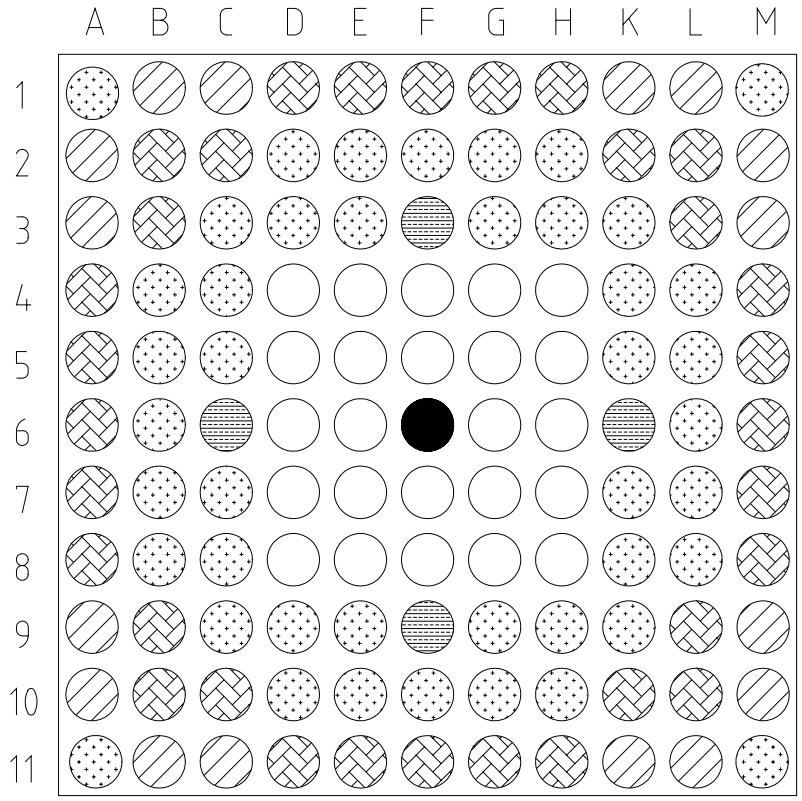

Fuel Pin Compositions

- 2.30 Wt% U-235
- 3.20 Wt% U-235
- 4.60 Wt% U-235
- Solid Zirc Rod
- 4.60 Wt% U-235 1.20 Wt% Gd2O3
- 0.711 Wt% U-235 5.45 Wt% PuO2

Figure 6.6-3 - G-Pu (11x11) BRP MOX Assembly Array

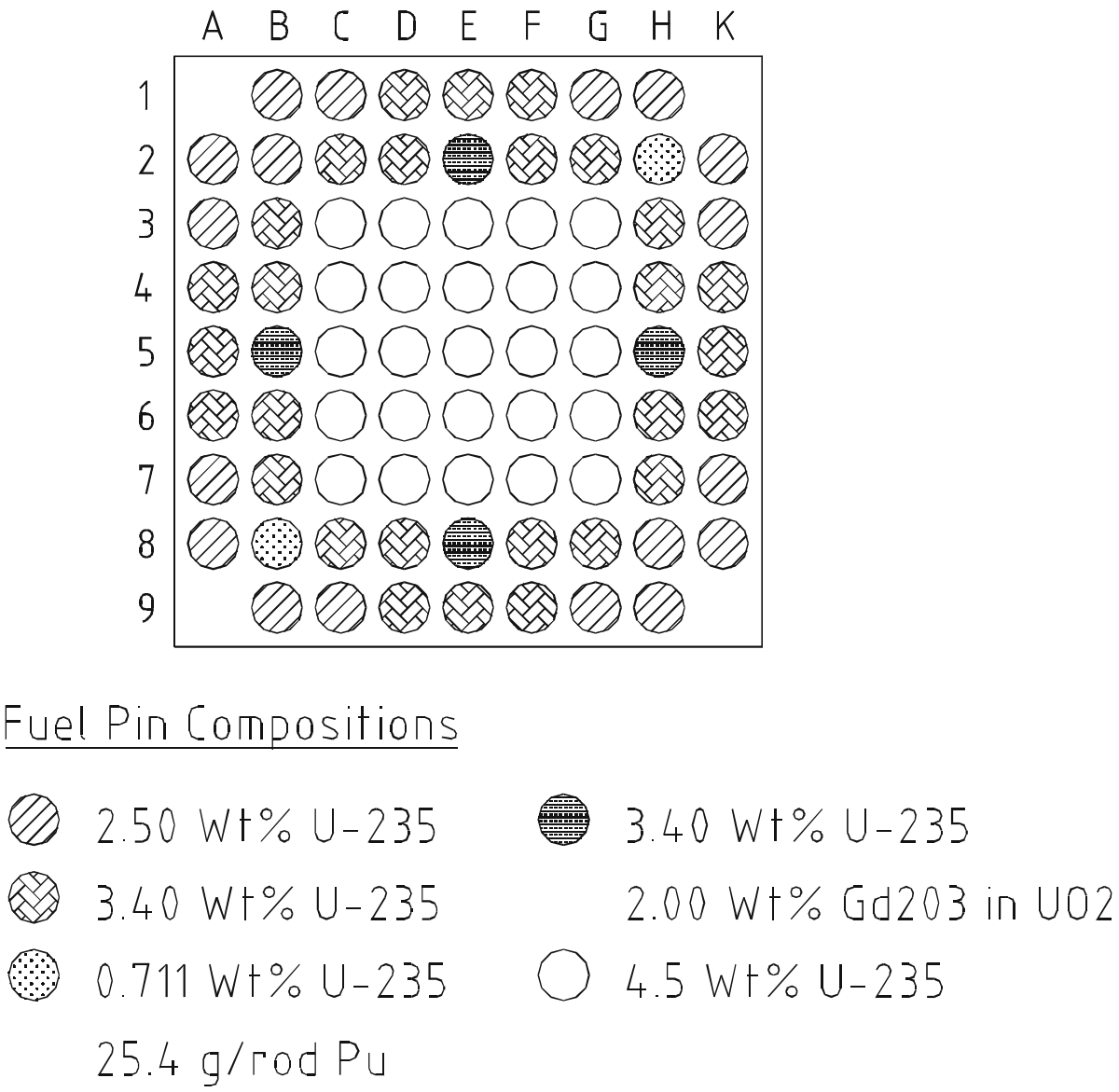

Figure 6.6-4 - UO_2 9x9 BRP Assembly with Two Inserted MOX Rods

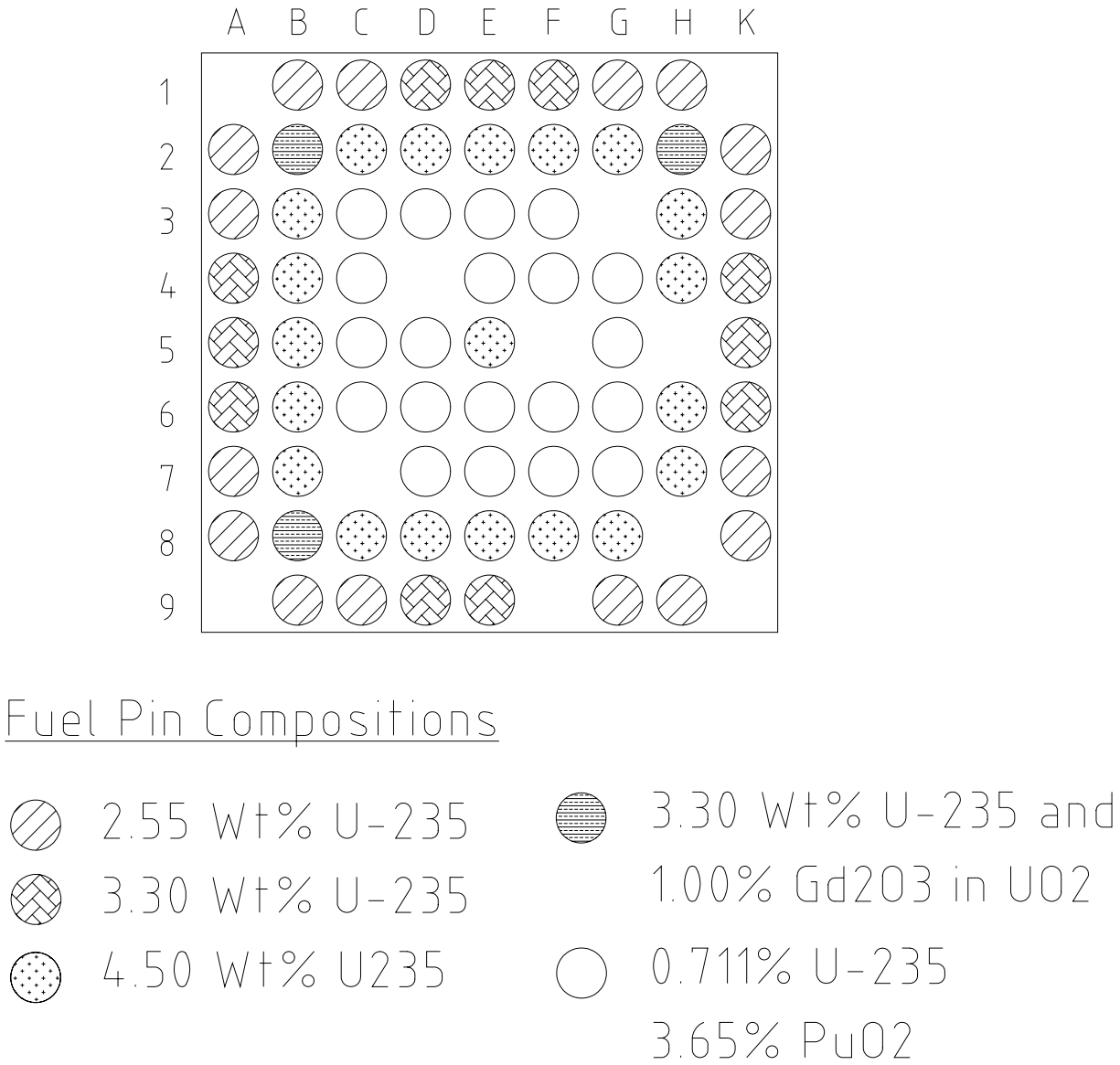

Figure 6.6-5 - D72 Partial Assembly Array - J2 Assembly Type

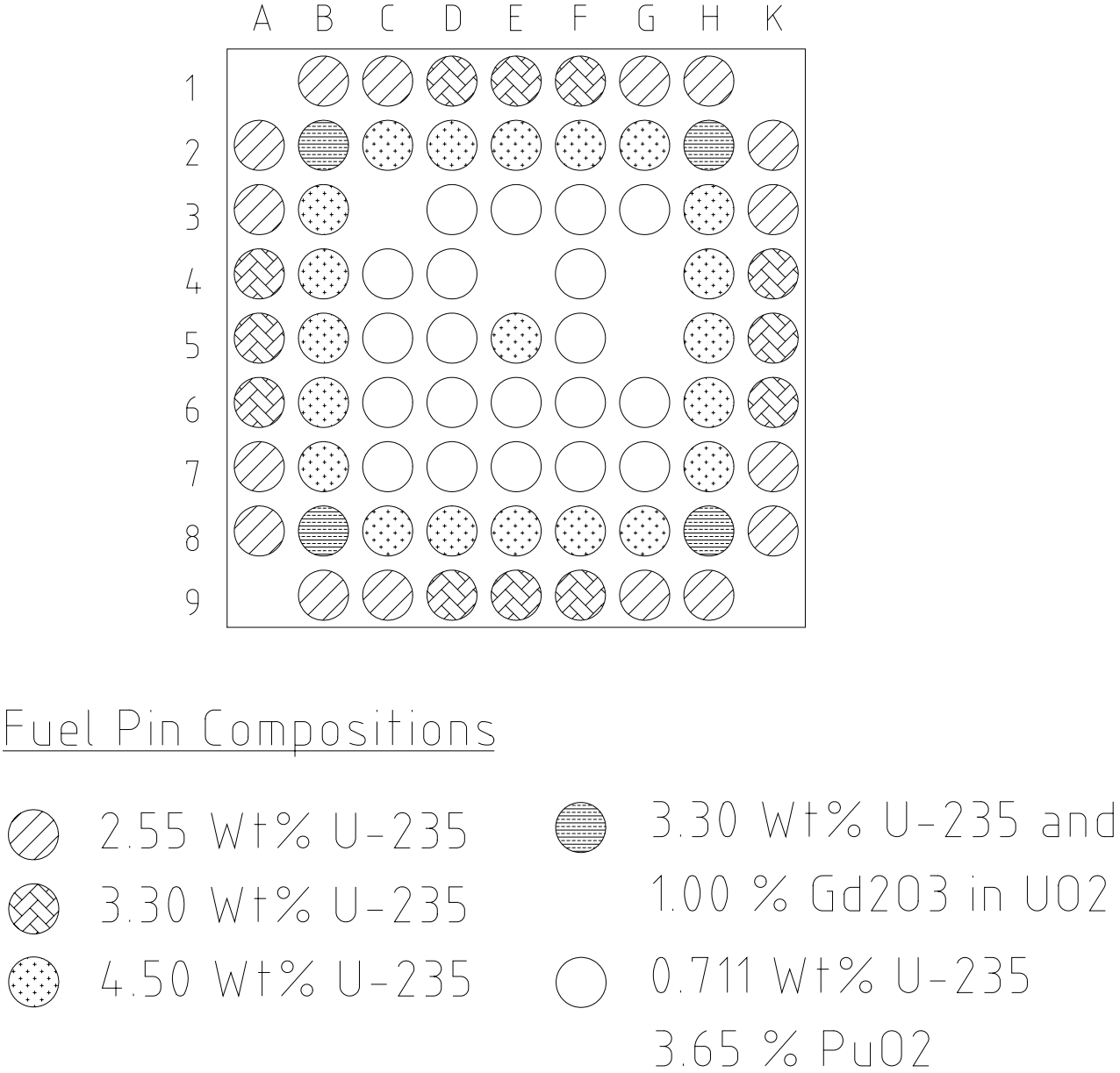

Figure 6.6-6 - D73 Partial Assembly Array - J2 Assembly Type

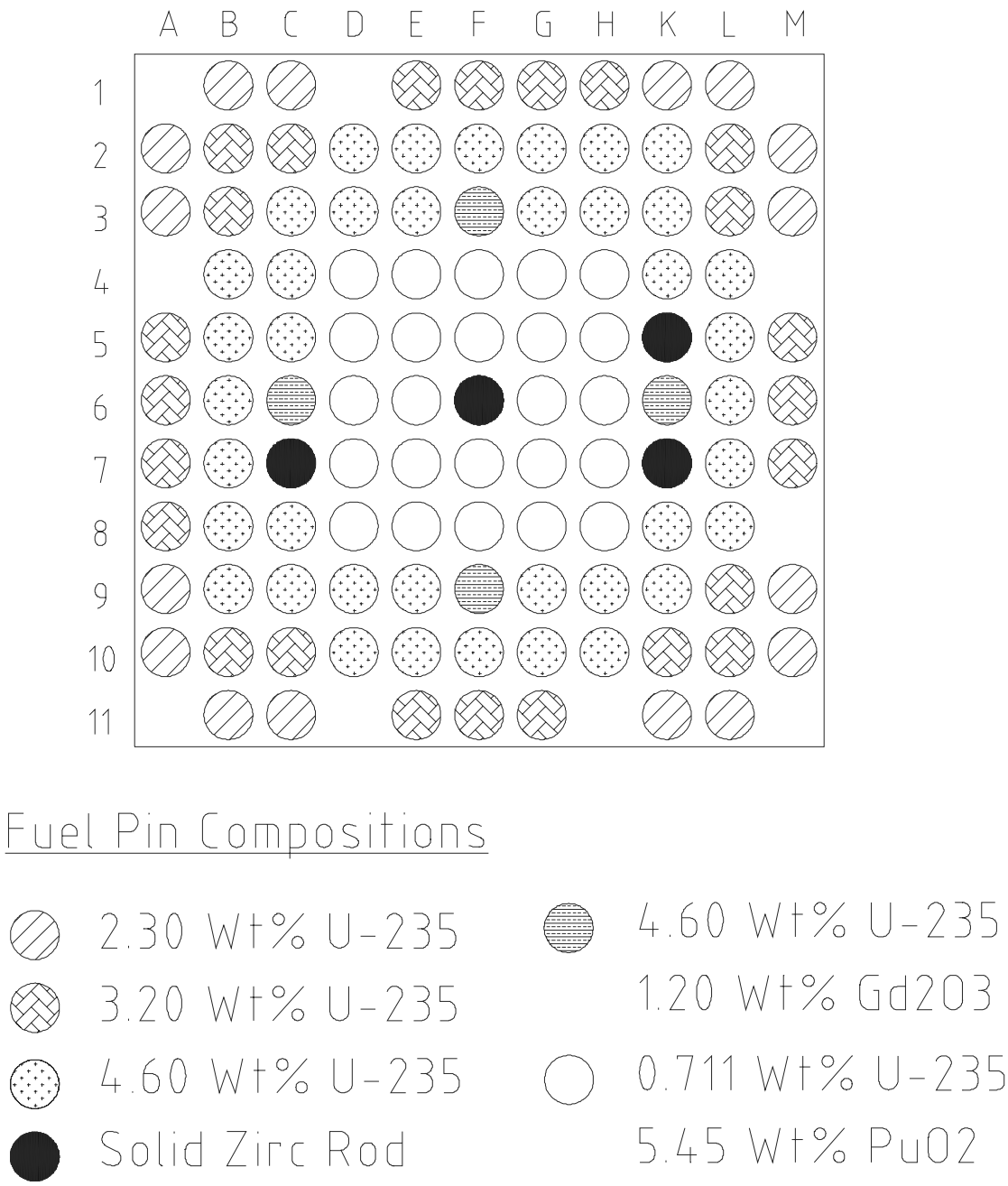

Figure 6.6-7 - G01 Partial Assembly Array - G-Pu Assembly Type

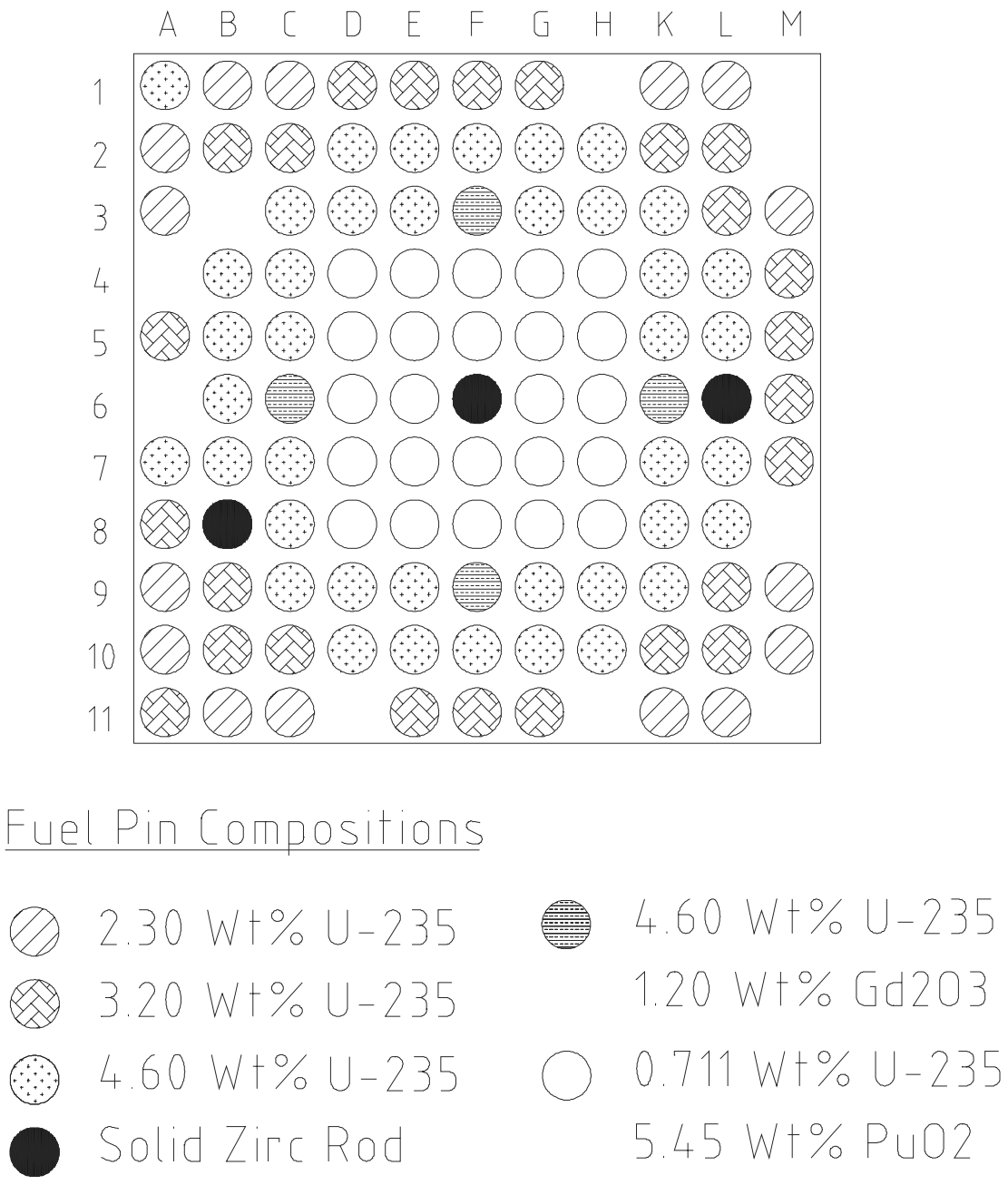

Figure 6.6-8 - G02 Partial Assembly Array - G-Pu Assembly Type

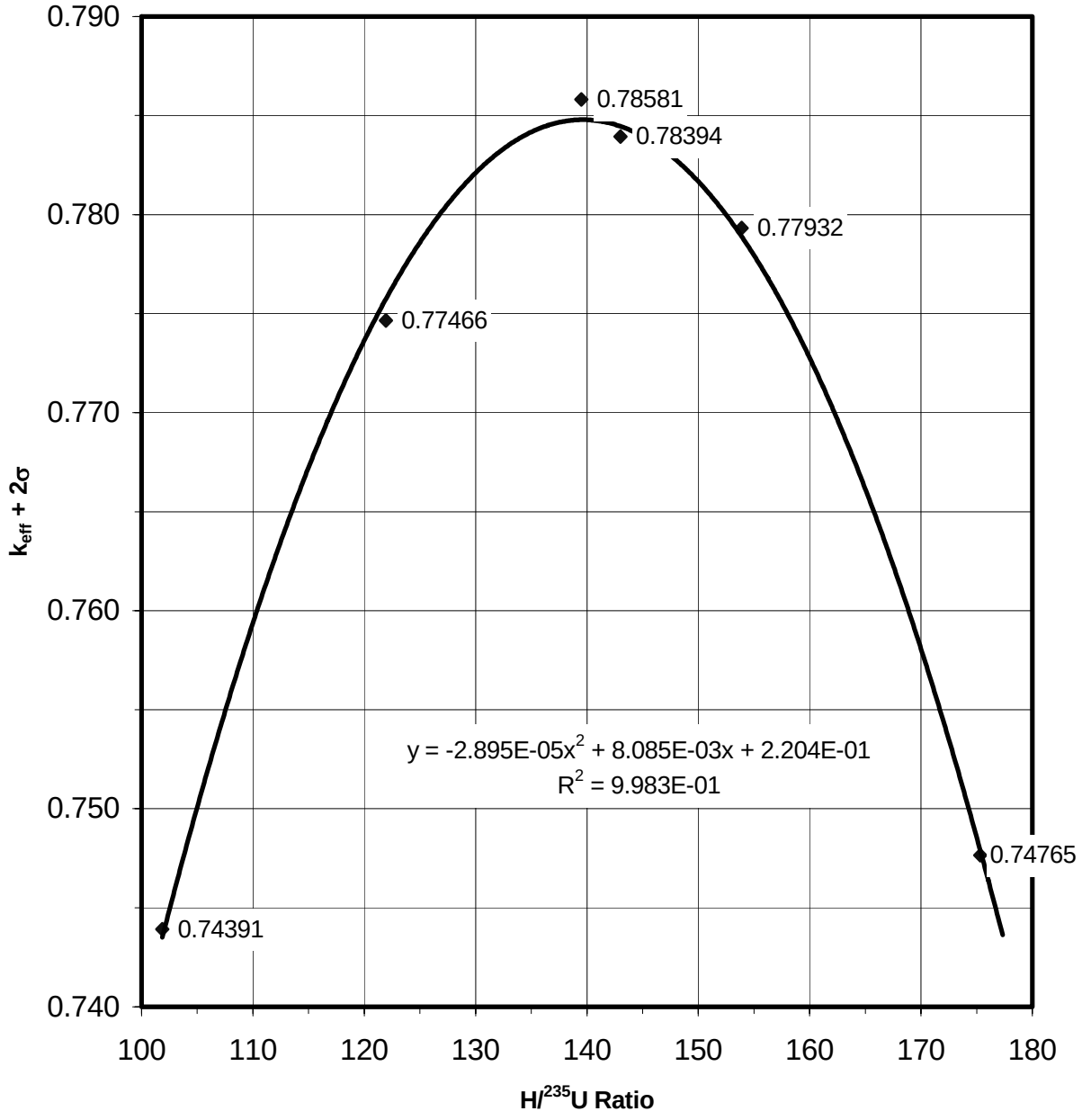

Figure 6.6-9 - K_{eff} vs. H-to-^{235}U Ratio for GE 9x9 BRP Fuel Rod Arrays (Single Assembly Sized Fuel Rod Array with Full Water Reflection)

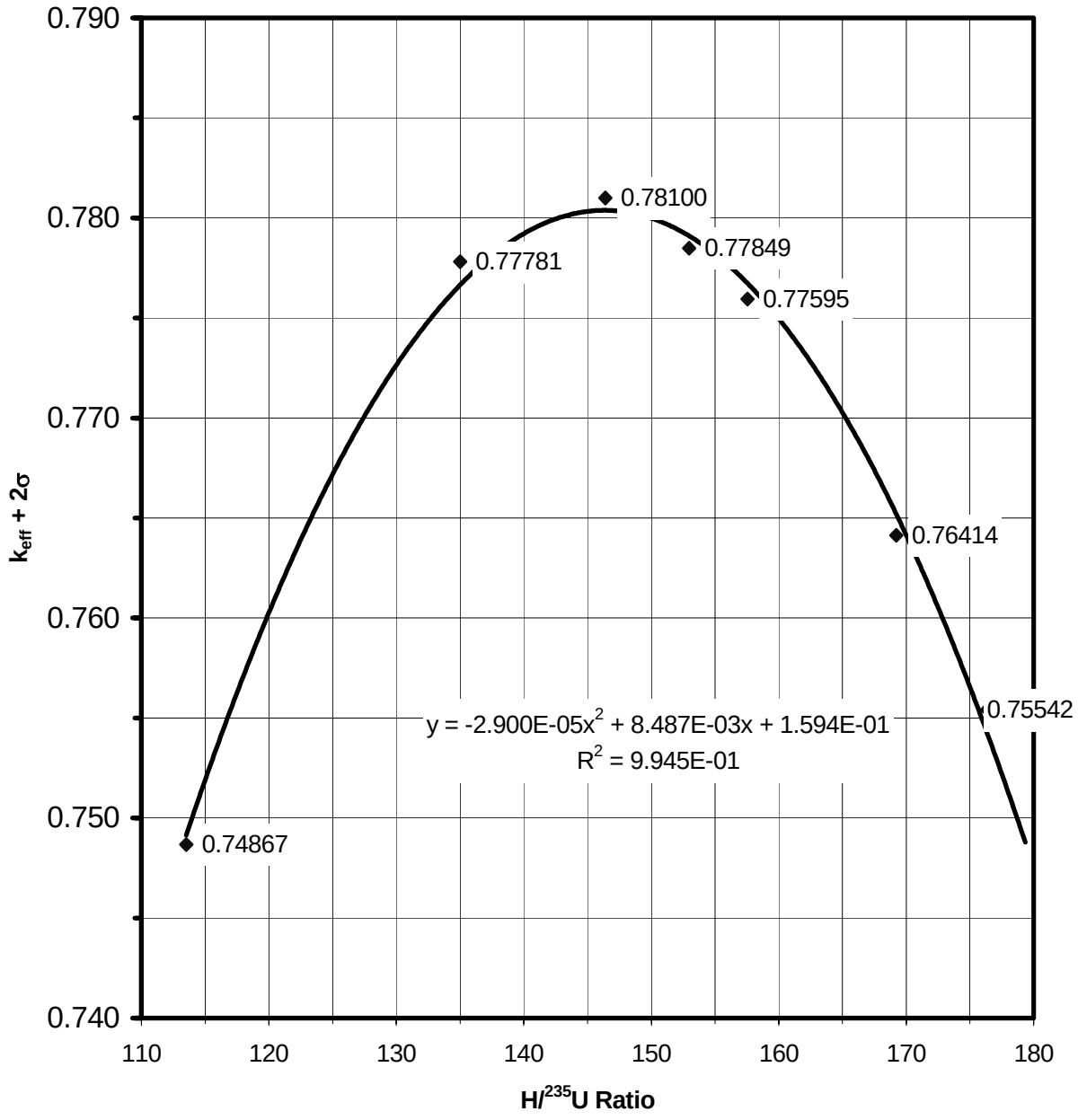

Figure 6.6-10 - K_{eff} vs. H-to-^{235}U Ratio for Siemens 11x11 BRP Fuel Rod Arrays (Single Assembly Sized Fuel Rod Array with Full Water Reflection)

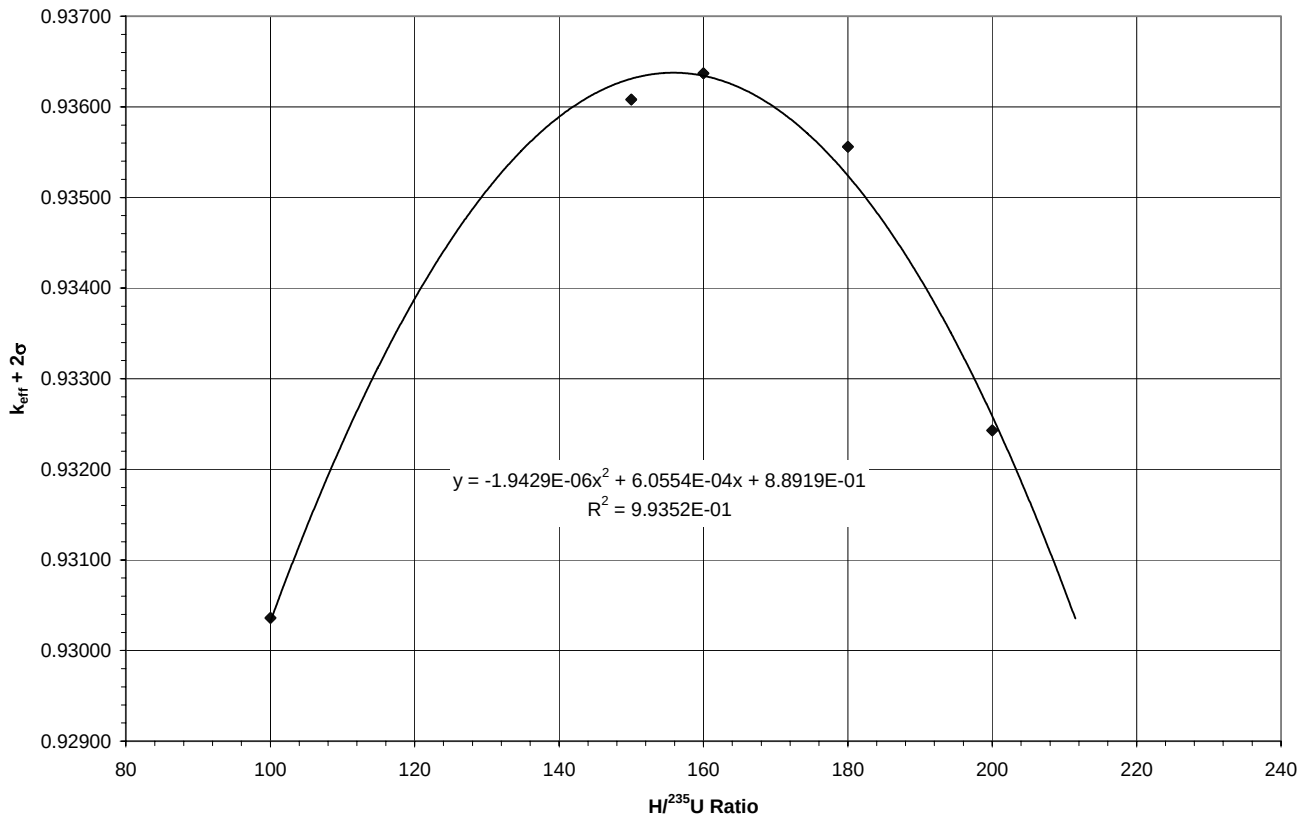

Figure 6.6-11 - K_{eff} vs. H / ^{235}U Ratio for a Square Array of 0.471" Diameter Fuel Cylinders

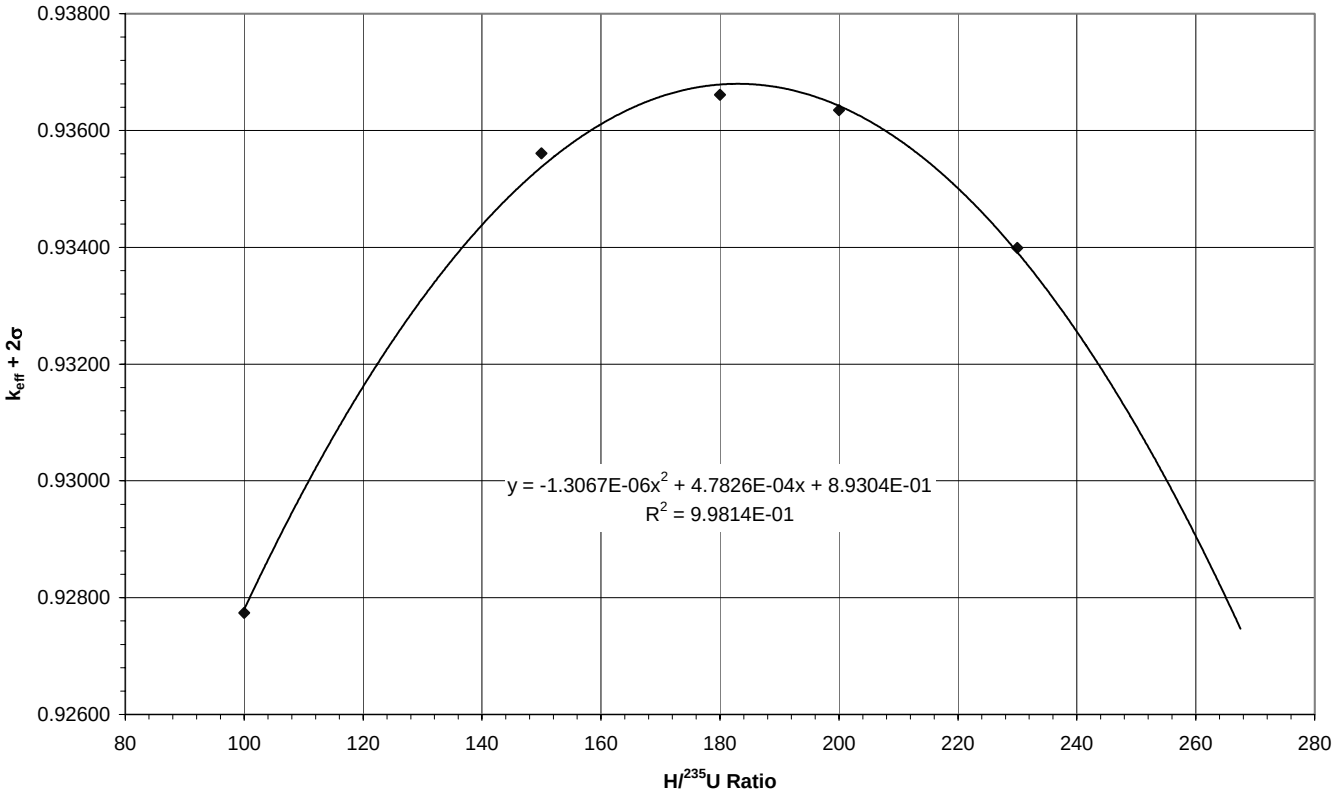

Figure 6.6-12 - K_{eff} vs. H / ^{235}U Ratio for a Square Array of 0.3715" Diameter Fuel Cylinders

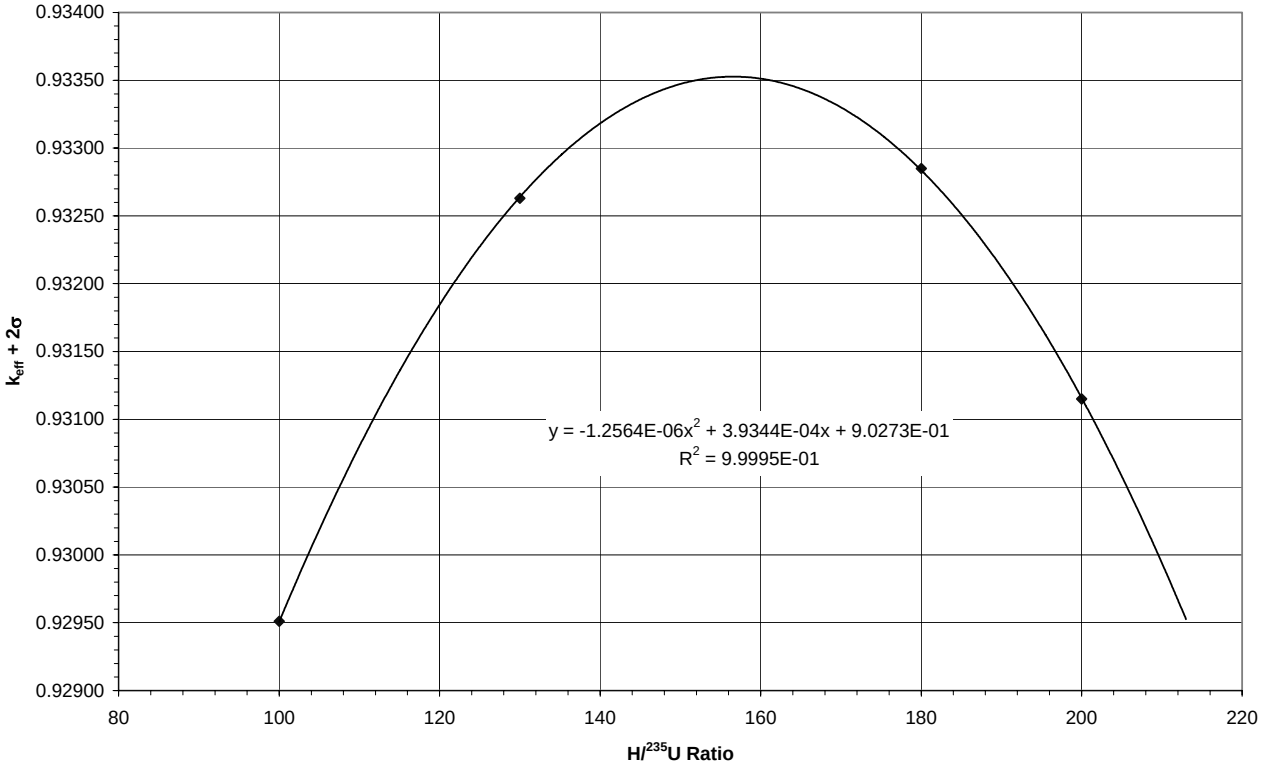

Figure 6.6-13 - K_{eff} vs. H / ^{235}U Ratio for a Hexagonal Array of 0.471" Diameter Fuel Cylinders

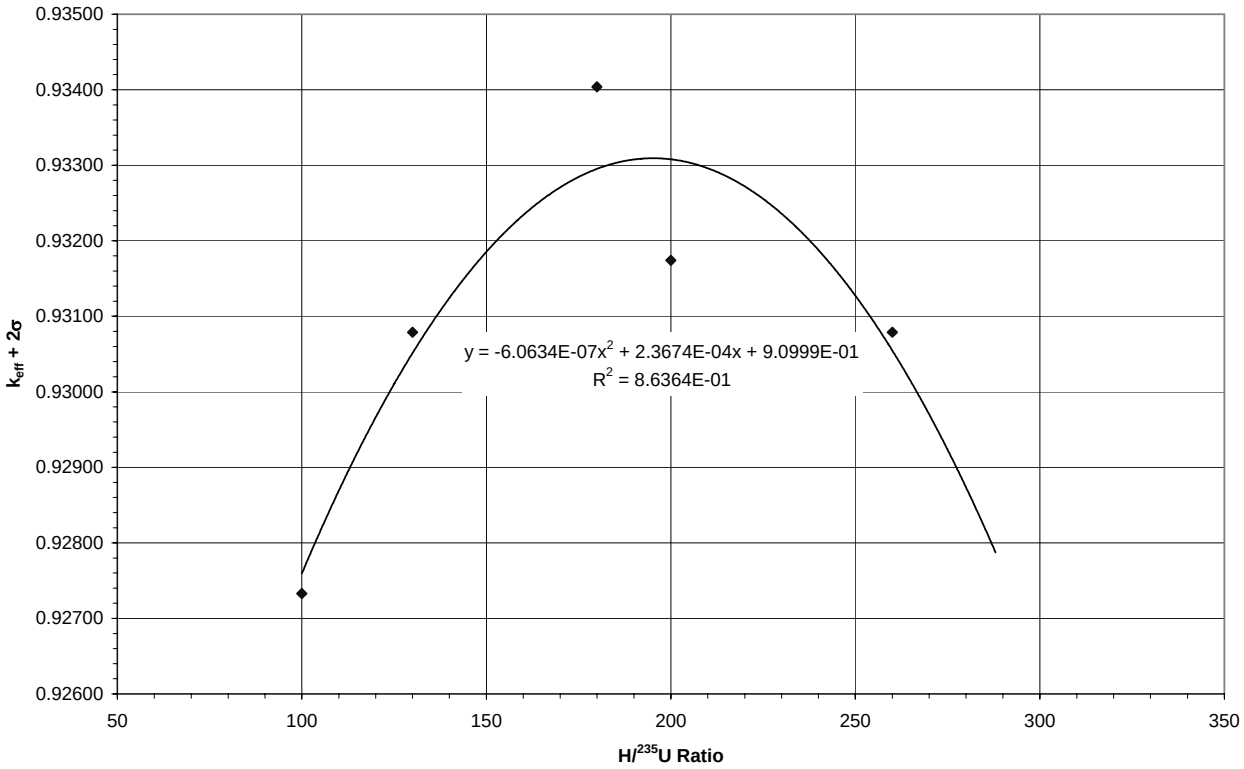

Figure 6.6-14 - K_{eff} vs. H / ^{235}U Ratio for a Hexagonal Array of 0.3715" Diameter Fuel Cylinders

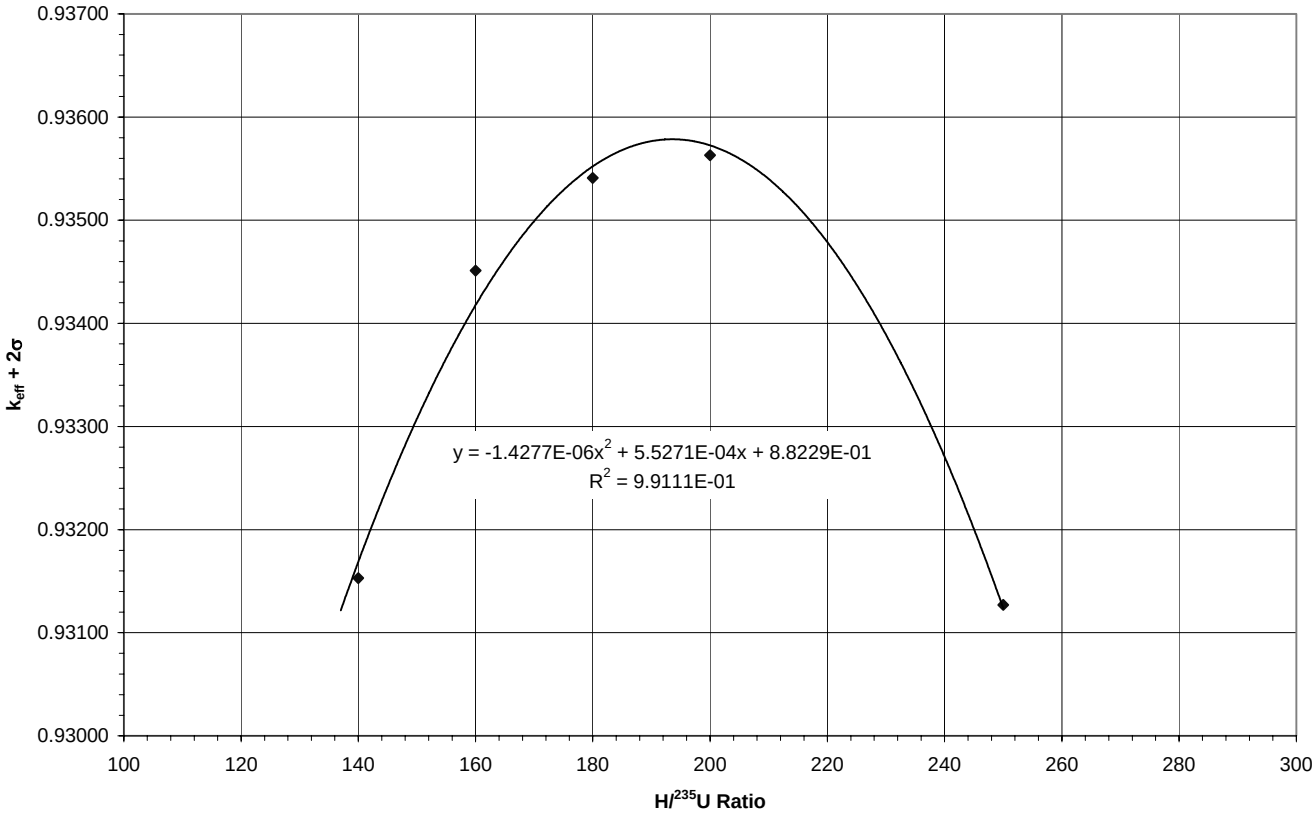

Figure 6.6-15 - K_{eff} vs. H / ^{235}U Ratio for a Hexagonal Array of 0.9 cm Diameter Fuel Spheres

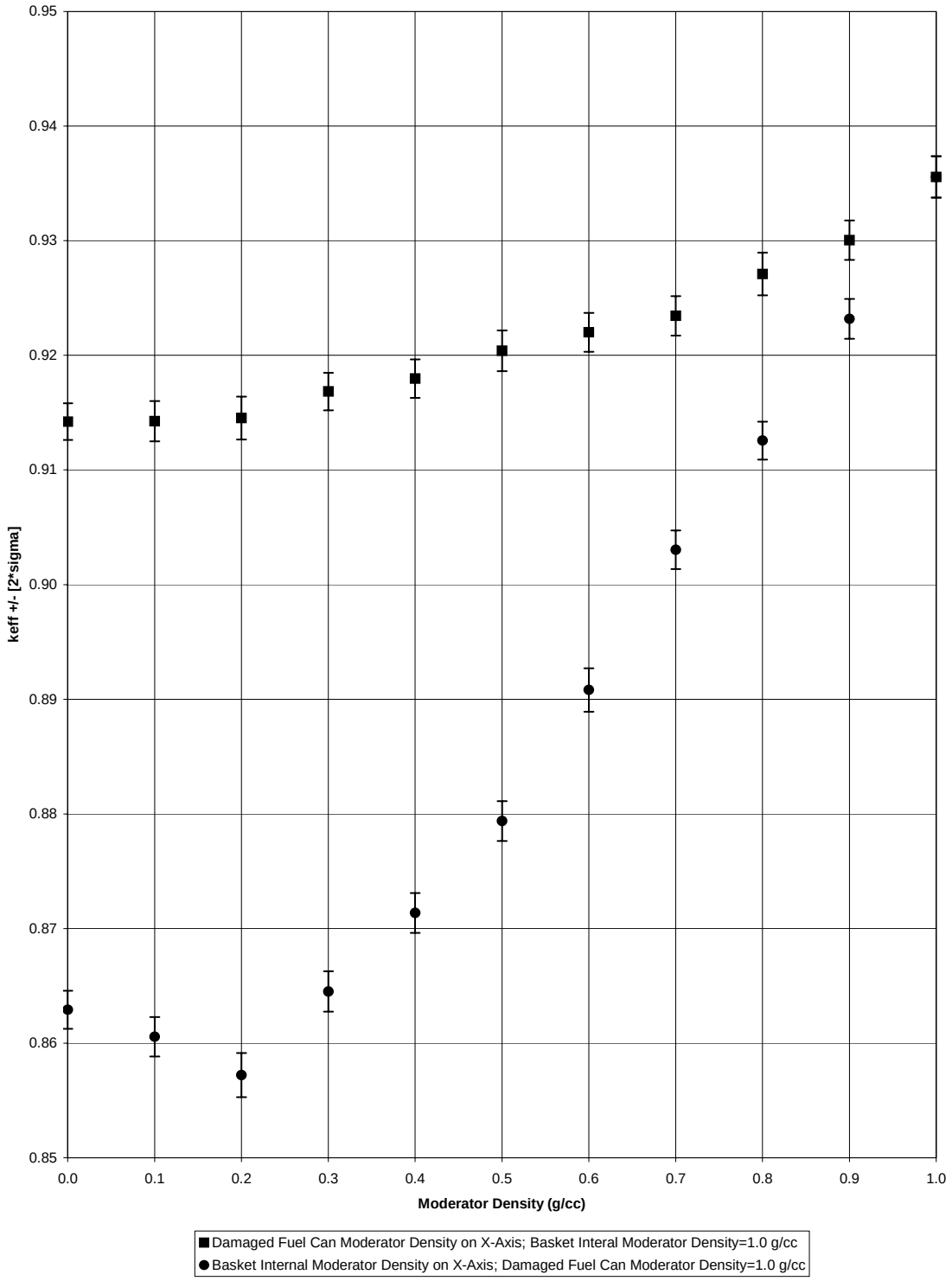

Figure 6.6-16 - W74 Canister k_{eff} vs. Damaged Fuel Can Interior and Canister Interior Moderator Densities

7. CONFINEMENT

Confinement of all radioactive materials in the FuelSolutions™ Storage System is provided by a FuelSolutions™ canister. The design of the FuelSolutions™ W74 canister confinement boundary assures that there is no credible design basis events that would result in a radiological release to the environment. To assure that the integrity of the canister confinement boundary is maintained, the FuelSolutions™ W150 Storage Cask and W100 Transfer Cask are designed to provide physical protection for a FuelSolutions™ W74 canister during normal, off-normal, and postulated accident conditions. The inert atmosphere in a FuelSolutions™ canister and the passive heat removal capabilities of the FuelSolutions™ storage cask also assure that the SNF assemblies remain protected from degradation, which might otherwise lead to gross cladding ruptures during dry storage.

The structural adequacy of the canister is demonstrated by the analyses documented in Chapter 3 of this FSAR. The heat removal capabilities of the FuelSolutions™ W74 canister are demonstrated by the thermal analyses documented in Chapter 4 of this FSAR. The physical protection of a FuelSolutions™ canister provided by a FuelSolutions™ W150 Storage Cask and a W100 Transfer Cask is demonstrated by the structural analyses documented in Chapter 3 of the FuelSolutions™ Storage System FSAR.[1] Likewise, the heat removal capabilities of a FuelSolutions™ W150 Storage Cask and a W100 Transfer Cask are demonstrated by the thermal analyses documented in Chapter 4 of the FuelSolutions™ Storage System FSAR.

This chapter describes the FuelSolutions™ W74 canister confinement boundary design and describes how the design satisfies the confinement requirements of 10CFR72.[2] It also provides an evaluation of the consequences of releases from the FuelSolutions™ W74 canister for the design basis leakage rate in accordance with NUREG-1536[3] and ISG-5.[4]

Storage of BRP mixed-oxide (MOX) and partial fuel assemblies has no effect on the integrity of the FuelSolutions™ W74 canister confinement boundary. With the addition of the damaged fuel can, damaged fuel assemblies also do not affect the integrity of the confinement boundary.

The normal, off-normal, and accident atmospheric release doses presented as a function of distance from the canister in Sections 7.2 and 7.3 are shown in Section 7.4.2 to be bounding for all BRP MOX, partial, and damaged fuel assemblies.

---

[1] WSNF-220, *FuelSolutions™ Storage System Final Safety Analysis Report*, NRC Docket No. 72-1026, BNFL Fuel Solutions Corporation.

[2] Title 10, U.S. Code of Federal Regulations, Part 72 (10CFR72), *Licensing Requirements for the Independent Storage of Spent Nuclear Fuel and High-Level Radioactive Waste*, 1995.

[3] NUREG-1536, *Standard Review Plan for Dry Cask Storage Systems*, U.S. Nuclear Regulatory Commission, January 1997.

[4] ISG-5, *Normal, Off-Normal, and Hypothetical Accident Dose Estimate Calculations for the Whole Body, Thyroid, and Skin*, Revision 1, Spent Fuel Project Office Interim Staff Guidance, United States Nuclear Regulatory Commission, May 1999.

This page intentionally left blank.

7.1 Confinement Boundary

The confinement boundaries for the fission products that are contained within the SNF assemblies include the fuel rod cladding itself, the FuelSolutions™ canister cylindrical shell, the bottom end closure, and the redundant top end closure. In addition, the FuelSolutions™ canister shell assembly provides for confinement of fixed and loose contamination, or CRUD (Chalk River Unidentified Deposits [debris/residue]), on the external surface of the fuel assemblies. The confinement boundary for the FuelSolutions™ canister is designed for the maximum allowable leak rate requirements defined in the *technical specification* contained in Section 12.3 of the FuelSolutions™ Storage System FSAR. The configuration of the FuelSolutions™ canister confinement boundary, which is the same for all FuelSolutions™ canister designs, is shown in Figure 7.1-1.

The FuelSolutions™ canister confinement boundary is comprised of the following:

- Cylindrical shell
- Bottom end closure plate (shop installed)
- Top end inner and outer closure plates (field installed)
- Instrument port cover (shop installed)
- Vent and drain port bodies (shop installed)
- Vent and drain port covers (field installed)
- Outer closure plate leak test port cover (shop installed)
- Associated welds

The canister shell longitudinal and circumferential seam welds are full penetration welds. The bottom end closure plate is welded to the shell with a full penetration groove weld, which also forms part of the confinement boundary. The vent and drain port bodies are attached to the top end of the canister shell, although these attachment welds do not form part of the confinement boundary. The top end closure of the canister confinement boundary is installed following canister fuel loading.

After loading the FuelSolutions™ W74 canister with SNF, the inner closure plate is welded to the canister shell and to the vent and drain port bodies at the two openings in the inner closure plate. Following completion of FuelSolutions™ canister draining, vacuum drying, pressure and leak testing, and inerting operations; vent and drain port covers are welded over the vent and drain ports to seal the FuelSolutions™ canister cavity. This completes the formation of the inner confinement boundary. The outer closure plate, including the shop welded leak test port cover, is welded to the canister shell using a partial penetration groove weld. This completes the formation of the outer (redundant) confinement boundary at the top end of the canister. The redundant closure of the FuelSolutions™ canister satisfies the requirements of 10CFR72.236(e).

7.1.1 Confinement Vessel

The FuelSolutions™ W74 canister cylindrical shell, the bottom end closure plate, the top end inner and outer closure plates, and the vent, drain, instrument, and leak test ports with their associated covers comprise the confinement vessel. They are designed, fabricated, and tested in accordance with the applicable requirements of ASME Section III, Subsection NB,[5] using ASME Section II, Part D,[6] austenitic stainless steel, as discussed in Sections 2.1.2 and 2.5.1 of this FSAR.

The FuelSolutions™ canister cylindrical shell circumferential and longitudinal seam butt welds and bottom closure plate to shell weld are full penetration, 100% radiographically examined welds. These welds are pneumatic pressure tested to 125% of canister design pressure, in accordance with the applicable requirements of ASME Section III, Subsection NB.

The bottom shield plug enclosure, consisting of the shell extension and the bottom end plate, provides structural support for the bottom shield plug. This assembly provides biological shielding but has no confinement function.

The canister confinement vessel is sealed at the top end by inner and outer closure plates that are installed after canister SNF loading is complete. The top shield plug, installed above the SNF and below the inner closure plate, provides biological shielding but has no confinement function.

The multiple-pass inner closure plate root pass and final surface and the multiple-pass outer closure plate root, intermediate, and final surface welds are dye penetrant inspected in accordance with the applicable requirements of ASME Section III, Subsection NB. A pneumatic pressure test of the inner closure plate welds is also performed. The inner closure plate welds are also helium leak tested to a sensitivity of 8.52×10^{-6} ref-cc/sec, using a calibrated detection system capable of detecting a leak rate less than or equal to one-half of the allowable test leakage rate. Canister leak testing is performed in accordance with the leak testing requirements described in the *technical specification* contained in Section 12.3 of the FuelSolutions™ Storage System FSAR. Using helium as the test medium instead of water or air provides an additional degree of conservatism because of its relatively small molecular size.

Three port covers close the penetrations through the top end inner closure plate and one port cover closes the penetration through the outer closure plate, as described in Section 7.1.2. These port cover closure final surface welds are dye penetrant inspected in accordance with the applicable requirements of ASME Section III, Subsection NB.

After final vacuum drying, the FuelSolutions™ canister cavity is backfilled with helium in accordance with the *technical specification* contained in Section 12.3 of this FSAR. The helium backfill provides an inert atmosphere within the FuelSolutions™ canister cavity that precludes oxidation and hydride attack of the SNF cladding. Use of a helium atmosphere within the FuelSolutions™ canister contributes to the long-term integrity of the fuel cladding, reducing the potential for release of fission gas or other products to the FuelSolutions™ canister cavity.

---

[5] American Society of Mechanical Engineers (ASME) Boiler and Pressure Vessel Code, Section III, Division 1, Subsection NB, *Class 1 Components*, 1995 Edition.

[6] American Society of Mechanical Engineers (ASME), Boiler and Pressure Vessel Code, Section II, *Materials*, Part D, *Properties*, 1995 Edition.

Helium also aids in heat transfer within the FuelSolutions™ canister and reduces the fuel cladding maximum temperatures. Canister inerting, in conjunction with the thermal design features of the canister and storage cask, assures that the fuel assemblies are sufficiently protected against degradation, which might otherwise lead to gross cladding ruptures during long-term storage.

7.1.2 Confinement Penetrations

The top end inner closure plate has two through-holes to accommodate the vent and drain ports. Partial penetration groove welds join the inner closure plate with the vent and drain port adapters. The individual vent and drain ports, which penetrate the shield plug, are provided to pressurize, drain, dry, and backfill the FuelSolutions™ canister confinement vessel after installation of the inner closure plate. To minimize plant personnel occupational exposure, quick-connect fittings are used in the ports for connections made to the vacuum drying system.

The quick-connect fittings provide operator protection from airborne contamination that may be present within the canister cavity. The self-sealing feature of these fittings temporarily closes the confinement boundary when they are disconnected from their mating fitting. The quick-connect fittings are for operational convenience and ALARA, and are not relied on as part of the FuelSolutions™ canister confinement boundary.

After canister draining, vacuum drying, and inerting, the vent and drain ports are sealed by covers that are welded to the vent and drain port bodies. The port cover seal welds are dye penetrant inspected (final surface). An identical cover is welded by the fabricator into the inner closure plate over the instrument port. The instrument port weld is dye penetrant shop-inspected (final surface) and pressure tested. This instrumentation port is normally used during canister reflood operations only. These covers form a part of the canister inner confinement boundary.

The top end outer closure plate has one penetration to accommodate potential leak testing of the outer closure plate, should it ever become necessary. This leak test port cover is welded to the outer closure plate in the shop during canister fabrication and is dye penetrant inspected (final surface). This cover forms part of the outer canister confinement boundary.

The FuelSolutions™ W74 canister has no bolted closures or mechanical seals. There are no external penetrations for pressure monitoring or overpressure protection. Such penetrations would increase the probability of a potential leakage path.

7.1.3 Seals and Welds

As previously noted, the FuelSolutions™ W74 canister shell seam welds, bottom closure weld, leak test port cover weld, and instrument port cover weld are made during shop fabrication, with the remaining top end closure welds made in the field following loading of the SNF into a FuelSolutions™ W74 canister.

Section 7.1.1 describes the design of the confinement vessel seals and welds. Confinement boundary welds performed by the fabricator include canister shell seam welds, the bottom end closure plate-to-shell weld, the leak test port cover to top end outer closure plate weld, and the instrument port cover to top end inner closure plate weld. Welds performed during field closure operations include the top end inner closure plate-to-shell weld, the vent and drain port body to

inner closure plate welds, the vent and drain port cover welds, and the outer closure plate-to-shell weld.

Confinement boundary welds are performed, inspected, and tested in accordance with the applicable requirements of ASME Section III, Subsection NB. The use of multi-pass welds and dye penetrant inspection essentially eliminates the chance of a pinhole leak through the weld. The shop welds and inner closure plate welds are also helium leak tested, providing added assurance of weld integrity. Shop fit-up of all field-welded components results in a uniform root opening of minimum size and eliminates the need for shims or backing that could restrain the weld joint and induce residual weld stresses. The ductile stainless steel material used for the canister confinement boundary is not susceptible to lamilar tearing or hydrogen-induced cracking. The closure weld redundancy assures that failure of any single FuelSolutions™ W74 canister confinement boundary closure weld does not result in release of radioactive material to the environment.

7.1.4 Closure

As discussed above, closure of the FuelSolutions™ W74 canister is provided by the inner and outer closure plates and the drain, vent, instrument, and leak test port covers. These canister closures are designed to maintain a positive seal during normal conditions of storage, off-normal conditions, and postulated accident conditions. There are no unique or special closure devices.

Since the FuelSolutions™ W74 canister uses an entirely welded redundant closure system, no direct monitoring of the closure is required, as discussed in Section 7.2 of the FuelSolutions™ Storage System FSAR.

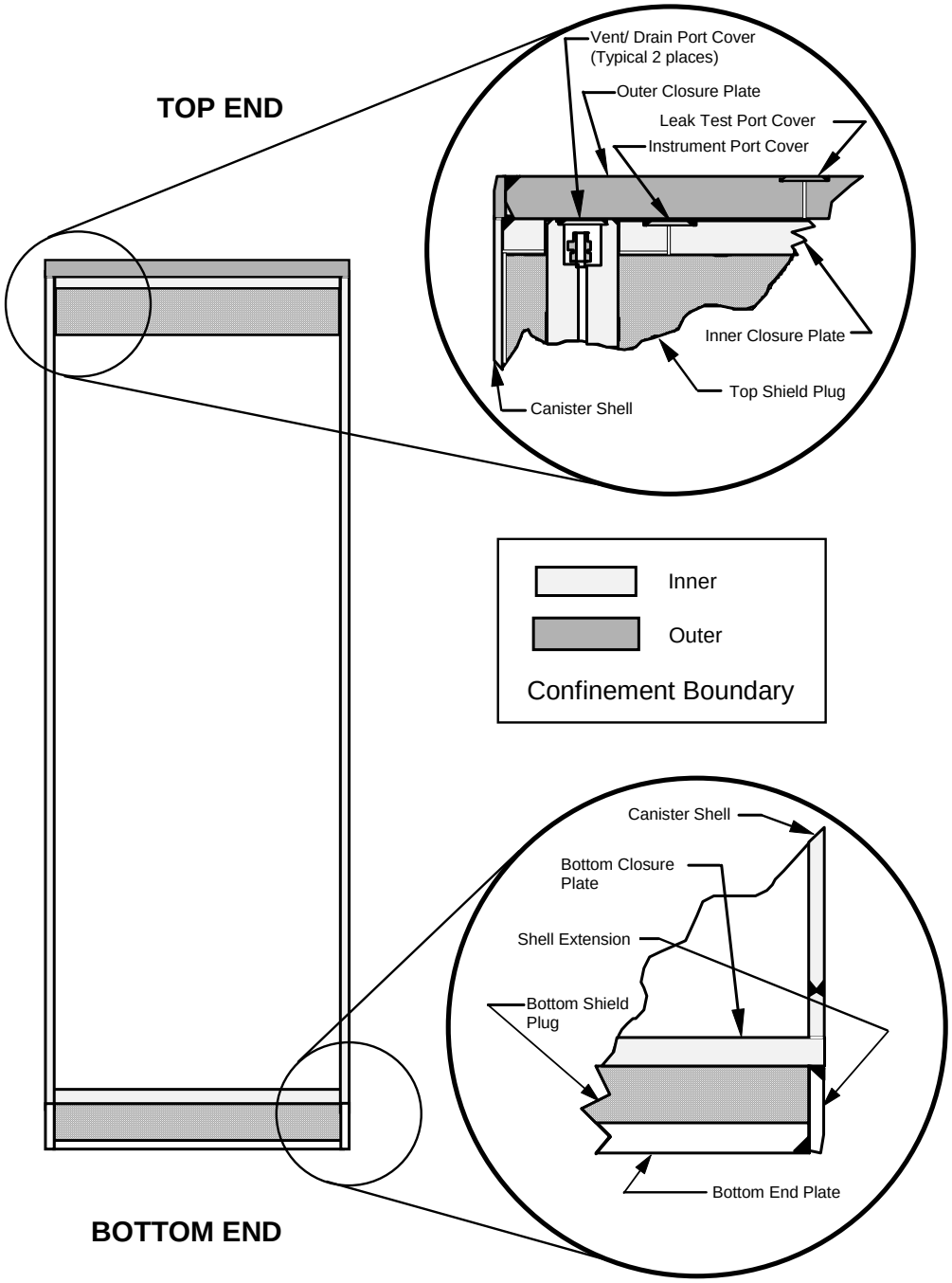

Figure 7.1-1 - FuelSolutions™ Canister Confinement Boundaries

This page intentionally left blank.

7.2 Requirements for Normal and Off-Normal Conditions of Storage

The FuelSolutions™ W74 canister uses multiple confinement barriers provided by the fuel cladding and the canister shell assembly to assure that there is no release of radioactive material to the environment. This includes no release of fuel fission gases, volatiles, fines, or fuel CRUD for all normal, off-normal, and postulated accident storage conditions. Nonetheless, it is assumed that the canister leaks at the design leakage rate per the *technical specification* contained in Section 12.3 of the FuelSolutions™ Storage System FSAR. The performance of the FuelSolutions™ W74 canister confinement boundary for normal and off-normal conditions is discussed in this section.

7.2.1 Release of Radioactive Material for Normal and Off-Normal Conditions

7.2.1.1 Confinement Integrity During Dry Storage

Vacuum drying and helium backfilling provide a non-oxidizing atmosphere to protect the fuel assemblies against cladding degradation. The analyses presented in Sections 3.5 and 3.6 of this FSAR demonstrate that the canister confinement boundary remains intact during all normal and off-normal storage and transfer conditions. The confinement boundary design, fabrication, inspection, and testing are performed under a Quality Assurance program, which is described in Chapter 13 of the FuelSolutions™ Storage System FSAR. Therefore, there is no credible mechanism or event that results in a release of radioactive material from the FuelSolutions™ W74 canister under normal or off-normal conditions.

The consequences of leakage of the FuelSolutions™ W74 canister under normal conditions of storage are evaluated. The normal pressure of 10.0 psig that is defined in Section 2.3.1 of this FSAR is assumed as an initial condition for this evaluation. This pressure is based on the conservative assumption that 1% of the design basis fuel rods fail, and that 30% of the fission gas and 100% of the fill gas is released from each failed rod under the worst case temperature and backfill pressure conditions. The resulting Total Effective Dose Equivalent (TEDE), thyroid, and other critical organ doses at downstream distances of 100 to 1000 meters are evaluated.

The confinement evaluations consider the effects of failed fuel rods in the (up to) eight damaged fuel cans in each W74 canister. An upper bound estimate of the number of failed fuel rods in any given assembly classified as damaged is 10%. (Note that, based on an evaluation of the BRP SNF inventory, the actual number of failed fuel rods in any BRP fuel assembly is only ~3% of the total number of rods.) These rods would add to the overall failed rod percentage (which would otherwise be 1%) with respect to the fuel fine atmospheric release dose contributions. Since these rods were failed prior to assembly loading into the W74 canister, they do not affect the overall fission gas, volatile, and CRUD dose contributions (i.e., they are the same as intact rods with respect to these contributions). Examination of the confinement analysis results shows that the increase in the fuel fine dose contributions does not significantly affect the overall atmospheric release doses. This is due to the fact that the number of failed rods in the damaged fuel cans is a small fraction of the total number inside the W74 canister ($\leq$ 1.25%), and the fact that the fuel fine dose contributions are a very small fraction (< 0.3%) of the overall normal

condition atmospheric release dose. Thus, the effect of storing damaged fuel in the W74 canister on the atmospheric release dose is insignificant.

The consequences of leakage of the FuelSolutions™ W74 canister under off-normal conditions of storage is also evaluated. The off-normal pressure of 20.0 psig that is defined in Section 2.3.2 of this FSAR is assumed as an initial condition for this evaluation. This pressure is based on the conservative assumption that 10% of the design basis fuel rods fail, and that 30% of the fission gas and 100% of the fill gas is released from each failed rod under the worst case temperature and backfill pressure conditions. The resulting Total Effective Dose Equivalent (TEDE), thyroid, and other critical organ doses at downstream distances of 100 to 1000 meters are evaluated.

The fission products that are available for release are discussed in Section 7.3.1 of this FSAR. The release of contents is described in Section 7.3.2, except that for normal conditions failure of 1% of the fuel rods is assumed, and for off-normal conditions failure of 10% of the fuel rods is assumed. As with normal conditions, the effects of failed rods within the BRP assemblies inside the W74 damaged fuel cans have been considered. For the same reasons discussed above for the normal condition case, the effect of the additional fuel pin dose contributions from these failed rods is insignificant.

The resulting dose rates for normal and off-normal conditions are discussed in Section 7.2.3.

7.2.1.2 Control of Radioactive Material During Fuel Loading Operations

The procedures for closure of the FuelSolutions™ W74 canister, described in Section 8.1 of the FuelSolutions™ Storage System FSAR, are intended to assure that there is no unintended release of gas, liquid, or solid materials from the canister during dry storage. During canister closure operations, the hoses used for venting or draining are routed to the plant's spent fuel pool or radwaste processing systems. Canister closure operations are performed inside the plant's fuel building in a controlled and monitored environment. Radioactive effluent handling during fuel loading and canister draining, drying, backfilling, and sealing operations is in accordance with the plant's 10CFR50[7] license and radwaste management system.

7.2.1.3 External Contamination Control

The external surface of the FuelSolutions™ W74 canister is protected from contamination by preventing it from coming in contact with the spent fuel pool water. Prior to fuel loading, an inflatable seal is installed at the top of the annulus formed between the canister shell and the transfer or transportation cask cavity. This annulus is filled with clean demineralized water and the seal is inflated. The inflated seal, backed by the demineralized water, is sufficient to preclude the entry of contaminated water into the annulus. It is recommended that a small reservoir of water be connected to the transfer cask annulus port to maintain a slight overpressure in the canister/cask annulus. These steps assure that the canister surface is free of contamination that could become airborne during storage.

Additionally, following fuel loading operations and removal from the spent fuel pool, the upper end of the FuelSolutions™ W74 canister shell is surveyed for loose surface contamination in

[7] Title 10, Code of Federal Regulations, Part 50 (10CFR50), *Domestic Licensing of Production and Utilization Facilities*, 1995.

accordance with the *technical specification* contained in Section 12.3 of the FuelSolutions™ Storage System FSAR.

7.2.2 Pressurization of Confinement Vessel for Normal and Off-Normal Conditions

The FuelSolutions™ W74 canister normal condition pressure conservatively assumes that 1% of the design basis fuel rods fail, and that 30% of the fission gas and 100% of the fill gas escape into the canister cavity free volume from each failed rod under the worst case normal temperature, pressure, and volume conditions. The maximum operating pressure in the canister under normal conditions is 10.0 psig per Section 2.3.1 of this FSAR, which considers the helium backfill pressure as well as the assumed rod failures. The normal condition pressure is also taken as the design pressure for determination of the pressure used for pressure and helium leak testing of the canister confinement boundary as follows:

$$P_{test} = P_{norm} \times 1.25 = 12.5 \text{ psig}$$

The off-normal condition pressure assumes that 10% of the design basis fuel rods fail. The resulting off-normal canister pressure is within the design basis off-normal pressure of 20 psig, as defined in Section 2.3.2 of this FSAR.

7.2.3 Normal and Off-Normal Doses

The method used to calculate the dose rates resulting from the assumed normal and off-normal atmospheric release conditions is provided in Section 7.4.1 of the FuelSolutions™ Storage System FSAR.

The method for determination of the radionuclide release fraction is described in Section 7.4.1.7 of the FuelSolutions™ Storage System FSAR. For the FuelSolutions™ W74 canister, the minimum canister volume is 5.981×10^{6} cc as reported in Table 4.4-5 of this FSAR. The leak rate is 9.494×10^{-6} cc/s for normal conditions and 1.790×10^{-5} cc/s for off-normal conditions, and the duration is one year. The resultant canister release fraction is 5.01×10^{-5} for normal conditions and 9.44×10^{-5} for off-normal conditions.

Table 7.2-1 lists the calculated doses for the normal condition leakage of the FuelSolutions™ W74 canister loaded with 64 SNF assemblies. The TEDE, thyroid, and other critical organ doses for distances from 100m to 1000m are also presented graphically in Figure 7.2-1. Similarly, the results for the off-normal condition are presented in Table 7.2-2 and Figure 7.2-2. The presented critical organ results correspond to the organ that yields the highest doses for normal and off-normal conditions, respectively. For each set of conditions (normal or off-normal) the same organ is limiting for all distances.

The results are reported for a single canister. Evaluation of off-site dose consequences for an ISFSI is provided in Section 10.4 of this FSAR.

Table 7.2-1 - Normal Condition Atmospheric Release Doses for FuelSolutions™ W74 Canister[(1)]

Distance, m	Dose (mrem)		
	TEDE	Thyroid	Other Organ[(2)]
100	3.9750	1.0790	22.8900
110	3.0090	0.8170	17.3300
120	2.4530	0.6660	14.1200
130	2.1030	0.5711	12.1100
150	1.6720	0.4539	9.6260
200	1.1110	0.3018	6.3990
300	0.5234	0.1421	3.0140
400	0.3155	0.0857	1.8160
500	0.2059	0.0559	1.1860
600	0.1656	0.0450	0.9534
700	0.1334	0.0362	0.7681
800	0.0966	0.0262	0.5562
900	0.0802	0.0218	0.4620
1000	0.0701	0.0190	0.4037

Notes:

(1) Doses are reported for a single canister for a duration of one year.

(2) The presented "Other Organ" results correspond to the lung, which is the critical organ that yields the highest doses at all distances for normal conditions.

Table 7.2-2 - Off-Normal Condition Atmospheric Release Doses for FuelSolutions™ W74 Canister[1]

Distance, m	Dose (mrem)		
	TEDE	Thyroid	Other Organ[2]
100	9.5890	2.1280	52.0500
110	7.2580	1.6110	39.4000
120	5.9170	1.3130	32.1200
130	5.0730	1.1260	27.5400
150	4.0330	0.8949	21.8900
200	2.6810	0.5949	14.5500
300	1.2630	0.2802	6.8540
400	0.7610	0.1689	4.1310
500	0.4967	0.1102	2.6960
600	0.3994	0.0886	2.1680
700	0.3218	0.0714	1.7470
800	0.2330	0.0517	1.2650
900	0.1935	0.0430	1.0510
1000	0.1691	0.0375	0.9180

Notes:

(1) Doses are reported for a single canister for a duration of one year.

(2) The presented "Other Organ" results correspond to the lung, which is the critical organ that yields the highest doses at all distances for off-normal conditions.

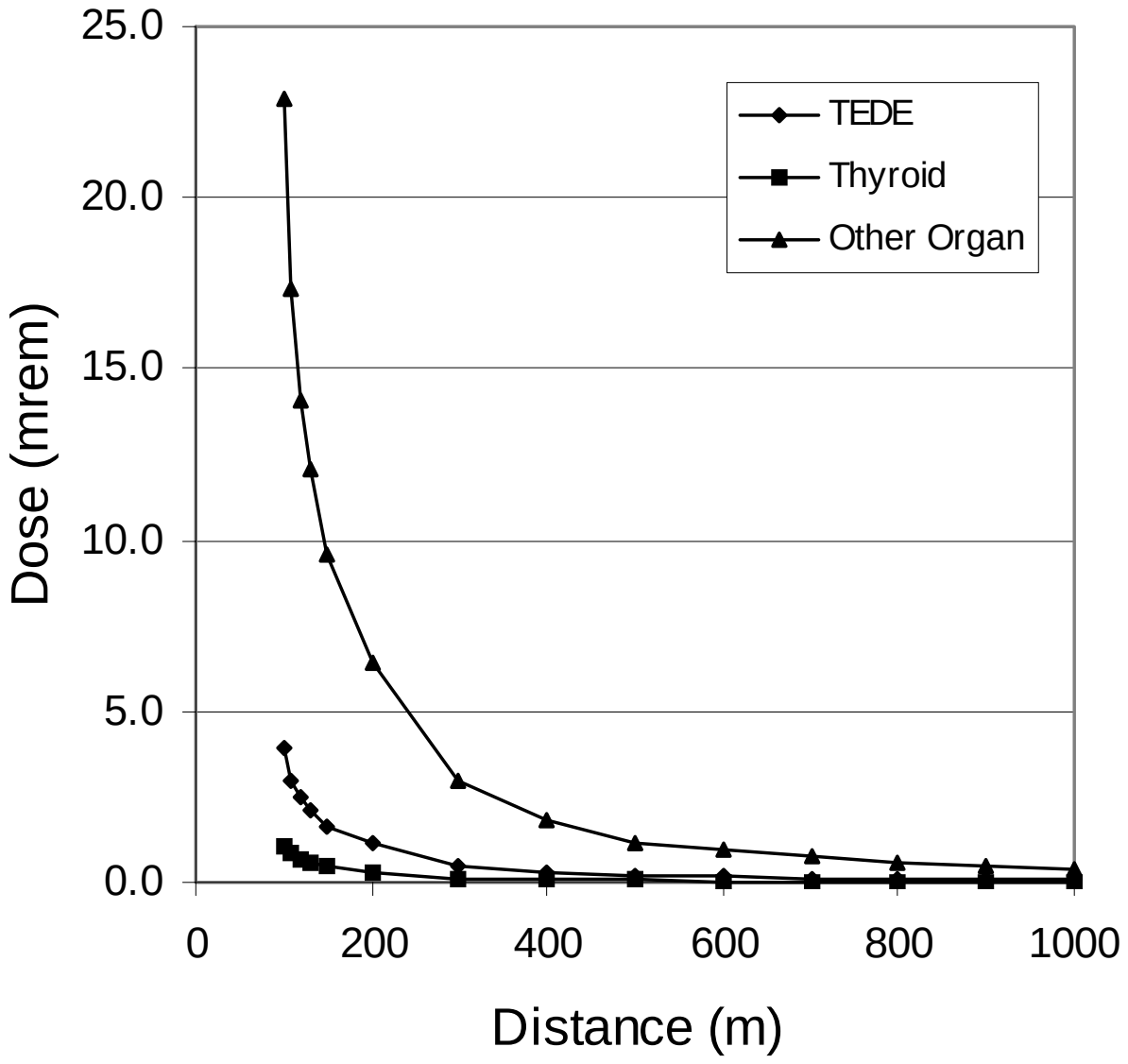

Figure 7.2-1 - Normal Condition Atmospheric Release Dose vs. Distance for FuelSolutions™ W74 Canister

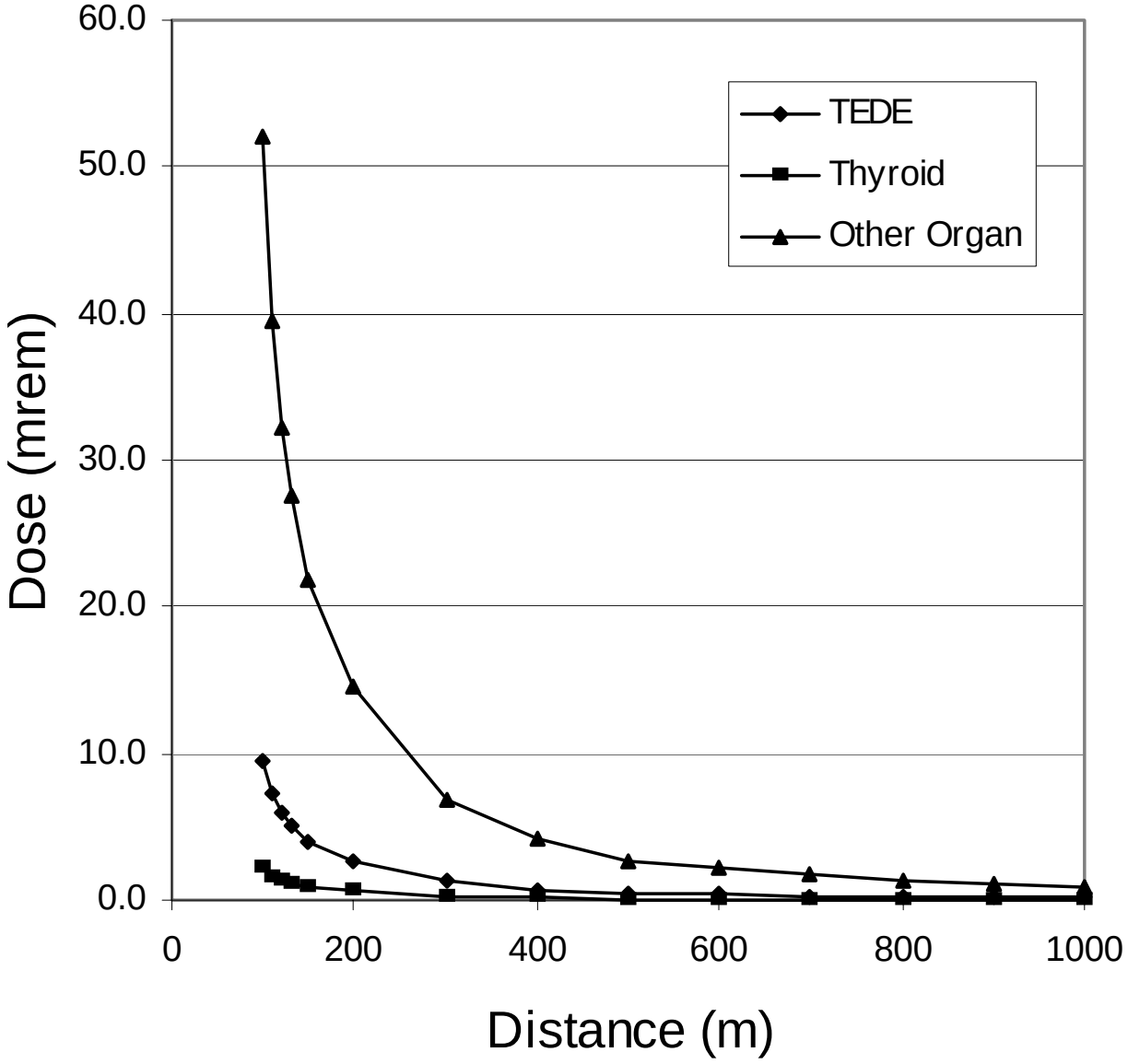

Figure 7.2-2 - Off-Normal Condition Atmospheric Release Dose vs. Distance for FuelSolutions™ W74 Canister

This page intentionally left blank.

7.3 Confinement Requirements for Hypothetical Accident Conditions

The FuelSolutions™ W74 canister shell assembly uses redundant confinement closures to assure that there is no release of radioactive materials, including fission gases or CRUD, for all postulated storage accident conditions. The analyses presented in Section 3.7 of this FSAR demonstrate that the canister confinement boundary remains intact during all postulated accident conditions, including the associated increased internal pressure. Canister confinement boundary design, fabrication, inspection, and testing are performed under a Quality Assurance program, as described in Chapter 13 of the FuelSolutions™ Storage System FSAR. In summary, there is no credible mechanism or event that results in failure of the FuelSolutions™ W74 canister confinement boundary under accident conditions.

The consequences of leakage of the FuelSolutions™ W74 canister under accident conditions are evaluated for an atmospheric release from a single canister. The accident pressure of 70.0 psig that is defined in Section 2.3.3 of this FSAR is assumed as an initial condition for this evaluation. This accident pressure is based on the conservative assumption that 100% of the design basis fuel rods fail, and that 30% of the fission gas and 100% of the fill gas is released from each failed rod under the worst case temperature and backfill pressure conditions. The resulting Total Effective Dose Equivalent (TEDE) and thyroid doses at downstream distances of 100 to 1000 meters are evaluated. The ISFSI controlled area boundary must be at least 100 meters from the nearest loaded FuelSolutions™ W150 Storage Cask, in accordance with 10CFR72.106(b). The doses at these various distances are compared to the regulatory limit of 5 rem TEDE or 50 rem for the sum of the deep-dose equivalent and committed dose equivalent to any organ, per 10CFR72.106(b).

7.3.1 Fission Products

As described in Section 5.2.2 of the FuelSolutions™ Storage System FSAR, the ORIGEN2 program is used to calculate the fission products in the SNF assemblies. The FuelSolutions™ W74 canister is capable of accommodating up to 64 SNF assemblies of the classes/types defined in Section 2.2 of this FSAR. The evaluation provided herein uses a bounding analysis for fission products, as described in the following sections.

7.3.1.1 Fuel Fission Gases, Volatiles, and Particulates

The principal radionuclides available in the SNF are discussed in Section 7.4.1.1 and listed in Table 7.4-1 of the FuelSolutions™ Storage System FSAR.

The total fission product inventory for the radionuclides listed above is based on an assembly initial heavy metal content that conservatively bounds all fuel assembly types qualified for storage in the FuelSolutions™ W74 canister. The highest initial heavy metal loading for all BRP fuel assemblies is 0.1421 MTU[8]. All burnup/enrichment combinations from the fuel cooling table in Section 5.2 of this FSAR are evaluated to determine the worst case contents of the

[8]Rich, J.M., *Big Rock Point Fuel Assembly Database and Comparison with FuelSolutions Criteria*, August 21, 1999.

important radionuclides. In fact, radionuclides for this evaluation are conservatively developed for a 46 GWd/MTU burnup, even though the maximum burnup for all Big Rock Point SNF is less than 40 GWd/MTU. The worst case radionuclides occur for the case of 46 GWd/MTU and 1.5 w/o initial enrichment, with a lower bound cooling time of three years. This evaluation is performed assuming 64 Big Rock Point SNF assemblies.

7.3.1.2 CRUD Radionuclides

As discussed in Section 7.4.1.1 of the FuelSolutions™ Storage System FSAR, the major radionuclide particulate present in the CRUD layer and available for aerosol entrainment and release is Co-60, with an activity at discharge of 1254 μci/cm^2. This activity is decayed to account for three years post-irradiation cooling time, consistent with the worst case fuel assembly discussed above. The resulting curie content is 845 μci/cm^2. Using BWR fuel assembly information from the DOE OCRWM database, the worst case fuel assembly surface area is calculated (see Table 7.4-1 in Section 7.4.1) and applied to the curie loading, to determine the bounding Co-60 inventory for the SNF assembly classes to be stored in the FuelSolutions™ W74 canister. The maximum fuel assembly surface area is 104,950 cm^2 for the BRP 11x11 fuel assembly, for a total activity of about 89 curies per assembly. This evaluation is conservatively performed assuming 74 Big Rock Point SNF assemblies

7.3.2 Release of Contents

7.3.2.1 Fraction Available for Release

The fraction of radionuclides available for release from the fuel is provided in Section 7.4.1.2 and summarized in Table 7.4-1 of the FuelSolutions™ Storage System FSAR.

7.3.2.2 Fraction of Fuel Rods Breached

As discussed in Section 7.4.1.3 of the FuelSolutions™ Storage System FSAR, the fraction of fuel rods assumed to be breached is 1% for normal conditions and 10% for off-normal conditions.

7.3.2.3 Atmospheric Dispersion

The atmospheric dispersion factors (χ/Q) for various downwind distances are discussed in Section 7.4.1.4 and presented in Table 7.4-2 of the FuelSolutions™ Storage System FSAR.

7.3.2.4 Dose Conversion Factors

The exposure to dose conversion factors for the radionuclides considered in this evaluation are discussed in Section 7.4.1.5 and summarized in Table 7.4-3 of the FuelSolutions™ Storage System FSAR.

7.3.2.5 Event Duration and Occupancy Factor

As discussed in Section 7.4.1.6 of the FuelSolutions™ Storage System FSAR, the evaluation for the accident condition is performed for a duration of 30 days, with an assumed occupancy of 100%.

7.3.2.6 Canister Release Fraction

The method for determination of the radionuclide release fraction is described in Section 7.4.1.7 of the FuelSolutions™ Storage System FSAR. For the FuelSolutions™ W74 canister, the minimum canister volume is 5.981×10^{6} cc as reported in Table 4.4-5 of this FSAR. The leak rate for accident conditions is 5.463×10^{-5} cc/s, and the duration is 30 days. The resultant canister release fraction is 2.37×10^{-5}.

7.3.3 Postulated Accident Doses

The methodology used to calculate the postulated accident doses are provided in Section 7.4.1.8 of the FuelSolutions™ Storage System FSAR.

Table 7.3-1 lists the calculated doses for a single FuelSolutions™ W74 canister loaded with 74 SNF assemblies. The TEDE, thyroid, and critical organ doses from 100 to 1000 meters are also presented graphically in Figure 7.3-1.

7.3.4 Site Boundary

As can be seen from Figure 7.3-1, the TEDE dose rates for this postulated accident at the regulatory minimum site boundary distance of 100 meters is ~2% of the accident limit of 5 rem specified in 10CFR72.106(b), and the dose to any organ is insignificant compared to the 10CFR72.106(b) limit of 50 rem.

As the total annual contribution at the site boundary for normal conditions is limited to 0.025 rem (evaluated in Section 10.4.1 of the FuelSolutions™ Storage System FSAR), the effect on the postulated accident dose at the site boundary is negligible (<1%).

Table 7.3-1 - Accident Condition Atmospheric Release Doses for FuelSolutions™ W74 Canister[1]

Distance, m	Dose (mrem)		
	TEDE	Thyroid	Other Organ[2]
100	125.00	25.34	662.80
110	95.84	19.43	508.10
120	80.44	16.30	426.40
130	63.90	12.95	338.70
150	46.95	9.52	248.90
200	35.95	7.29	190.60
300	16.81	3.41	89.11
400	9.53	1.93	50.52
500	7.01	1.42	37.18
600	5.32	1.08	28.20
700	3.74	0.76	19.80
800	3.49	0.71	18.47
900	2.82	0.57	14.94
1000	2.33	0.47	12.34

Notes:

(1) Doses are reported for a single canister for a duration of one month.

(2) The presented "Other Organ" results correspond to the lung, which is the critical organ that yields the highest doses at all distances for accident conditions.

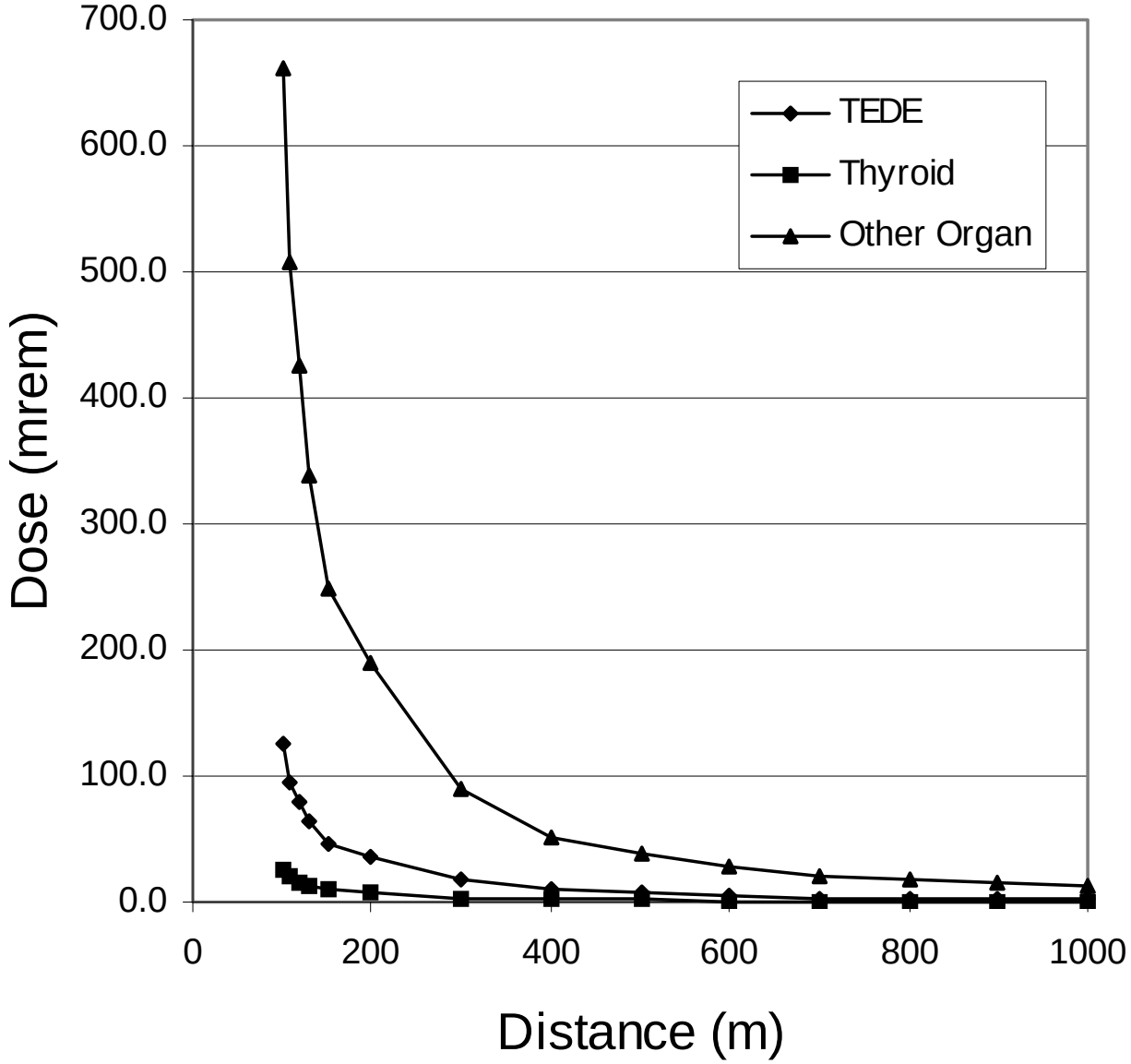

Figure 7.3-1 - Accident Condition Atmospheric Release Dose vs. Distance for FuelSolutions™ W74 Canister

This page intentionally left blank.

7.4 Supplemental Data

7.4.1 Calculation of Bounding Fuel Assembly Surface Area for Co-60 CRUD Contribution Evaluation

The radionuclide content of fuel CRUD contributes to the content of radionuclides available for release from the canister, as discussed in Section 7.3. The quantity available is a function of the activity of the CRUD in curies per unit area, as discussed in Section 7.3.1.2. Therefore, it is necessary to determine the total surface area of the fuel assembly on which it is expected CRUD will form, in order to determine the total radionuclide inventory.

The OCRWM database is used to obtain the fuel assembly characteristics to calculate the surface area for the fuels listed in Table 1.2-3 of this FSAR. Specifically, the OCRWM database contains information on the fuel rod length and outside diameter, as well as the number of rods in the assembly. This information is used to calculate the total surface area of the fuel rods. As information on the non-fuel hardware is not provided, the calculated fuel rod surface area is factored by 1.2 to conservatively account for the surface area of the non-fuel hardware. The area calculations are summarized in Table 7.4-1.

As discussed in EPRI NP-3789,[9] the formation of CRUD deposits is associated with heated surfaces. Since the fuel rod surface is heated to a much greater extent than much of the non-fuel hardware, anticipated CRUD buildup on the hardware would be expected to be less than on the fuel rods. Nonetheless, it is conservatively assumed that the CRUD activity on the non-fuel hardware is equal to that on the fuel rods.

7.4.2 MOX, Partial, and Damaged BRP Fuel

As discussed in the following sections, the atmospheric release doses calculated for design basis (intact UO_2) BRP fuel in Sections 7.2 and 7.3 are bounding for all MOX, partial, and damaged BRP fuel.

7.4.2.1 MOX BRP Fuel

The atmospheric release doses are calculated based on BRP UO_2 fuel with a burnup level of 46 GWd/MTU and a cooling time of only two years. By contrast, BRP MOX fuel has a maximum burnup level of 34.2 GWd/MTIHM and a minimum cooling time of 15 years. Most of the dose to an individual is from the release of relatively short-lived radionuclides (primarily ^{60}Co). For these reasons, the design basis doses shown in Sections 7.2 and 7.3 will bound the doses from a W74 canister loaded with BRP MOX fuel assemblies.

A comparison of BRP MOX and design basis UO_2 assembly isotope activities is presented in Table 7.4-2. The activity level of each isotope considered in the atmospheric release calculations, in Ci/assembly, is presented for each of the three BRP MOX fuel assembly types. For each MOX assembly type, the isotope activity levels are based on the maximum burnup and minimum cooling time that occurs for that assembly type. For comparison, the design basis UO_2 assembly

[9] EPRI NP-3789, *Corrosion Product Buildup on LWR Fuel Rods*, Electric Power Research Institute, April 1985.

isotope activities assumed in the design basis atmospheric release calculations are also presented. The design basis activity levels are based on a burnup level of 46 GWd/MTU and a cooling time of 2 years. The activity levels that correspond to a lower bound (1.5%) and upper bound (5.0%) initial enrichment are presented in Table 7.4-2. The atmospheric release calculations assume either the lower or upper bound enrichment case, whichever gives the highest dose for the organ in question.

The comparison shows that for all isotopes except ^{241}Am, the design basis isotope activity levels bound those of all BRP MOX fuel by a very wide margin. (It is also true that the ^{244}Cm activity for G-Pu MOX fuel is slightly higher than that of the 5.0% enriched UO_2 fuel case.) However, ^{241}Am and ^{244}Cm contribute a very small fraction of the overall atmospheric release dose for normal, off-normal, and accident conditions. The effect of the increase in the activity of these isotopes is much smaller than the effect of the large decreases seen for the other isotopes. The reduction in ^{60}Co (CRUD) activity is the dominant effect. The ^{60}Co activity of the MOX fuel is at most ~20% that of the design basis case, where the ^{60}Co contributes most of the total dose for normal and off-normal conditions.

For the reasons discussed above, the atmospheric release doses calculated and presented in the FuelSolutions™ Storage System FSAR are bounding for all BRP MOX fuel.

7.4.2.2 Partial BRP Fuel

The doses presented in Sections 7.2 and 7.3 are based on intact BRP fuel with a maximum assembly uranium loading of 0.1421 MTU/assembly. For a given burnup level, enrichment, and cooling time, the quantities of each radionuclide within a given fuel assembly are directly proportional to the assembly uranium loading.

Partial BRP fuel assemblies have a lower uranium loading than intact BRP assemblies. Therefore, for a given burnup, enrichment, and cooling time, the radionuclide inventory of partial BRP fuel assemblies is bounded by the inventory of the design basis intact BRP assemblies modeled in the off-site dose calculations. Since the doses are proportional to the quantities of the radionuclides within the canister, partial assemblies would produce lower accident case doses. Therefore, the doses presented in Sections 7.2 and 7.3 are bounding for W74 canisters containing partial BRP assemblies.

7.4.2.3 Damaged BRP Fuel

The doses presented in Sections 7.2 and 7.3 are also bounding for damaged BRP assemblies. Fuel assembly damage does not affect the radionuclide inventory within the fuel rods. Damage of assembly hardware does not affect the fraction of fuel isotopes into the canister interior. The only form of fuel assembly damage that could affect the confinement calculations is a flaw or breach in the fuel rod cladding.

If the fuel rod cladding is breached, gaseous and volatile isotopes will have passed through the breach before the assembly is loaded into the W74 canister. Thus, the gaseous isotopes would no longer be available for release when the assembly is placed into the FuelSolutions™ W74 canister. A fuel rod breach would not affect the amount of ^{60}Co released into the canister from the fuel assembly CRUD, since the CRUD is on the fuel rod exterior. Fuel rod breaches may permit release of solid fuel isotopes from the rod interior.

The FuelSolutions™ W74 canister confinement calculations for normal conditions show that over 95% of the off-site dose is due to CRUD (^{60}Co) release, which is not affected by fuel rod damage. Also, the confinement calculations already assume a 1% fraction of failed fuel rods for normal cask conditions, without taking any credit for release of isotopes through the breach before the assembly is placed into the canister. Damaged fuel is placed in a maximum of eight out of the 64 fuel positions in the FuelSolutions™ W74 canister. Furthermore, the number of breached fuel rods in the BRP damaged fuel assemblies is a small fraction of the total number of rods. Finally, the damaged BRP assemblies are placed in a damaged fuel can, which provides an additional layer of confinement for fuel particles. For these reasons, the contribution of failed rods in damaged fuel assemblies to the off-site doses is covered by the 1% rod failure assumption made in the confinement calculations.

Table 7.4-1 - Fuel Assembly Surface Area Summary

Fuel	Rod Diameter (in)	Rod Length (in)	No. of Rods	Total Assembly Area (in^2)	Total Assembly Area (cm^2)
BRP 11x11	0.449	79.43	121	16,268	104,955
BRP 9x9	0.5625	79.40	81	13,638	87,987

Table 7.4-2 - Comparison of BRP MOX and Design Basis UO_2 Isotope Activity Levels (Ci/assembly)

Isotope	J2 Assembly (22 year)	DA Assembly (22 year)	G-Pu Assembly (15 year)	Design UO_2 Assembly (1.5% Enr.)	Design UO_2 Assembly (5.0% Enr.)
CRUD					
Co-60	7.292E+00	7.292E+00	1.831E+01	8.870E+01	8.870E+01
ACTINIDES					
Pu-238	1.656E+02	1.881E+02	3.940E+02	1.018E+03	9.043E+02
Pu-239	4.528E+01	4.816E+01	4.615E+01	5.725E+01	5.433E+01
Pu-240	7.144E+01	7.977E+01	8.087E+01	1.040E+02	8.529E+01
Pu-241	8.756E+03	1.040E+04	1.205E+04	2.428E+04	1.789E+04
Am-241	5.857E+02	6.966E+02	4.753E+02	1.674E+02	1.288E+02
Cm-242	2.118E+00	2.573E+00	2.685E+00	1.480E+02	8.235E+01
Cm-244	1.709E+02	2.166E+02	6.940E+02	4.369E+03	5.833E+02
FISSION PRODUCTS					
H-3	1.418E+01	1.416E+01	3.089E+01	9.932E+01	8.316E+01
Kr-85	1.729E+02	1.575E+02	4.043E+02	1.052E+03	1.469E+03
Sr-90	3.250E+03	2.917E+03	5.886E+03	8.994E+03	1.370E+04
Y-90	3.251E+03	2.917E+03	5.887E+03	8.997E+03	1.371E+04
Rh-106	1.449E-02	1.576E-02	2.026E+00	1.336E+04	7.871E+03
Ru-106	1.449E-02	1.576E-02	2.026E+00	1.336E+04	7.871E+03
Sb-125	4.739E+00	4.823E+00	3.588E+01	1.392E+03	9.518E+02
Te-125m	1.156E+00	1.177E+00	8.754E+00	3.397E+02	2.322E+02
I-129	2.898E-03	2.917E-03	4.312E-03	7.100E-03	5.911E-03
Cs-134	5.546E+00	5.153E+00	1.164E+02	1.645E+04	1.248E+04
Cs-137	5.379E+03	5.230E+03	9.552E+03	1.868E+04	1.860E+04
Ba-137m	5.089E+03	4.947E+03	9.036E+03	1.767E+04	1.759E+04
Ce-144	2.988E-04	2.887E-04	1.617E-01	7.523E+03	8.732E+03
Pr-144	2.989E-04	2.887E-04	1.617E-01	7.523E+03	8.732E+03
Pm-147	4.474E+01	4.450E+01	2.979E+02	5.870E+03	8.193E+03
Eu-154	1.207E+02	1.179E+02	4.396E+02	2.365E+03	1.604E+03
Eu-155	2.265E+01	2.282E+01	1.129E+02	1.441E+03	9.231E+02

This page intentionally left blank.

8. OPERATING PROCEDURES

The generic operating procedures for the FuelSolutions™ Storage System are presented in Chapter 8 of the FuelSolutions™ Storage System FSAR.[1] The procedures include canister loading, storage cask loading, transfer cask and canister preparation, storage cask preparation, loaded canister retrieval, canister opening and fuel unloading, canister transfer from a storage cask to a transportation cask, and canister transfer from the transfer cask to a transportation cask. The procedures address both horizontal and vertical canister transfer operations. The FuelSolutions™ support equipment and the existing plant systems and equipment are used to accomplish these operations.

The generic operating procedures provided in the FuelSolutions™ Storage System FSAR are applicable to the FuelSolutions™ W74 canister, with some specific exceptions. The following sections outline the operating procedures for the FuelSolutions™ Storage System using the FuelSolutions™ W74 canister, referring to the generic procedures when applicable. These procedures have been developed to assure that all operations required for canister loading, unloading, and transfer are performed safely, minimize personnel exposure, and optimize the sequence of steps required to complete the subject operations. In preparing plant-specific procedures, the licensee may determine that acceptable alternate means may be available to accomplish the same operational objective.

Storage of BRP MOX, partial, and damaged fuel assemblies has no effect on the general FuelSolutions™ W74 canister operating procedures or the BRP site-specific W74 canister operating procedures. However, rather than inserting damaged fuel assemblies directly into selected canister guide tubes as discussed in Section 8.1.4 of the FuelSolutions™ Storage System FSAR, BRP damaged fuel assemblies must first be inserted into the damaged fuel cans described in Section 1.5 of this FSAR.

In addition to outlining specific differences in the operation of the FuelSolutions™ W74 canister not addressed in the FuelSolutions™ Storage System FSAR, this chapter also outlines the operation of the FuelSolutions™ W74 canister at sites with limited cask handling crane capacities. The general flow of these latter operations is provided in Figures 8.0-1 through 8.0-3.

[1] WSNF-220, *FuelSolutions™ Storage System Final Safety Analysis Report*, NRC Docket No. 72-1026, BNFL Fuel Solutions Corporation.

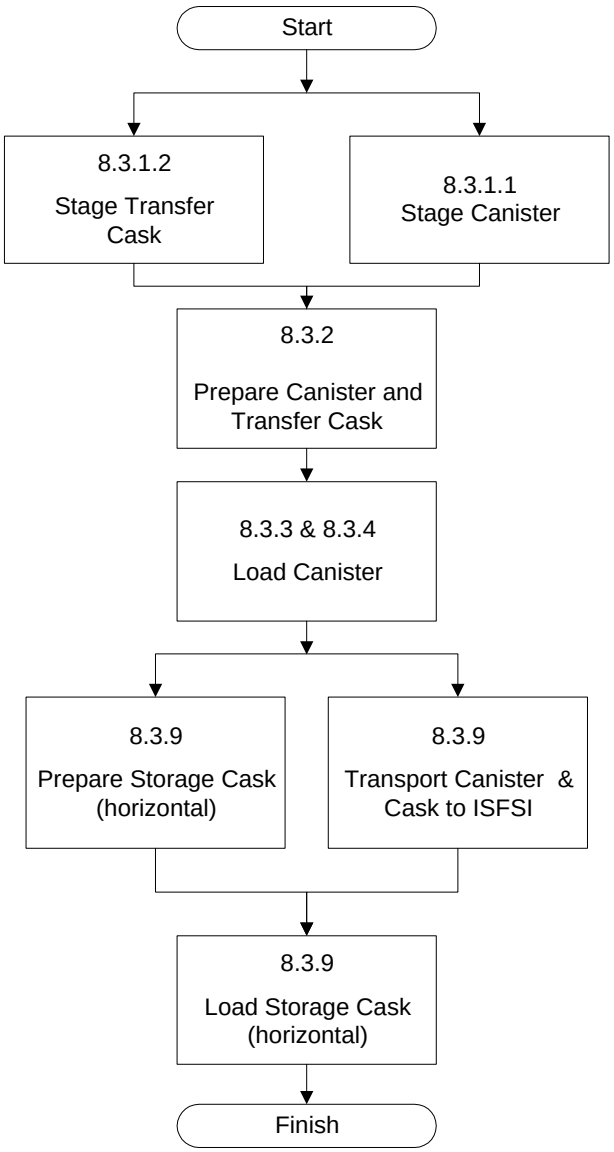

Figure 8.0-1 - Operations Flow Diagram to Place Fuel into Dry Storage in a FuelSolutions™ W74 Canister at Sites with Limited Cask Handling Crane Capacities

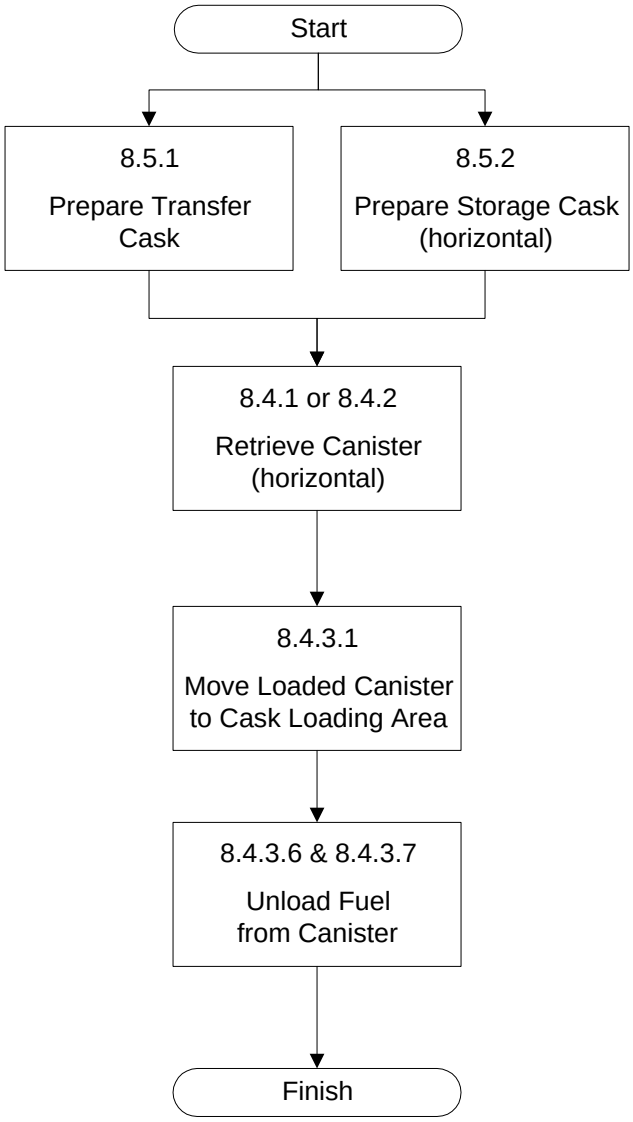

Figure 8.0-2 - Operations Flow Diagram to Retrieve Fuel from Dry Storage and Remove from a FuelSolutions™ W74 Canister at Sites with Limited Cask Handling Crane Capacities

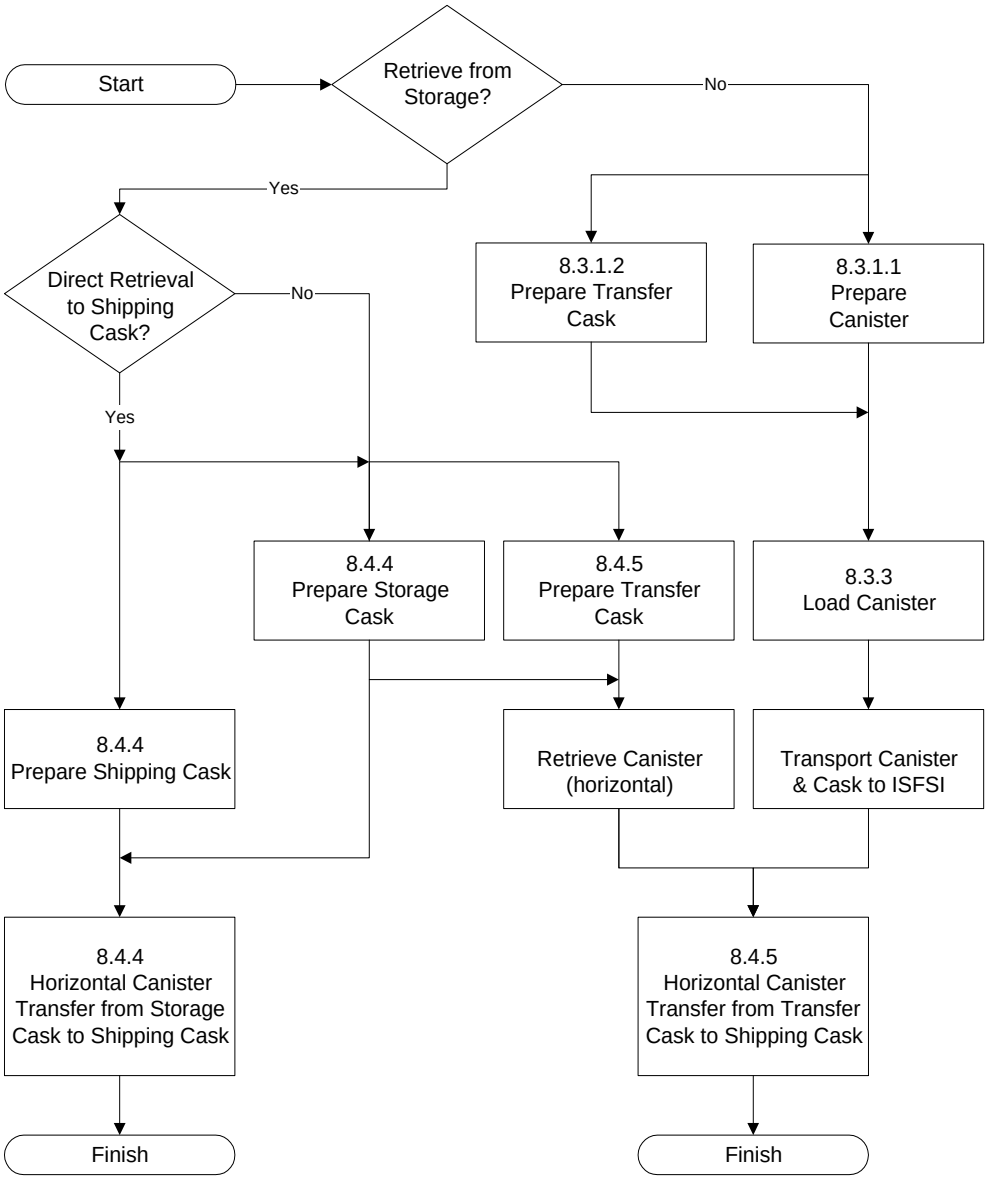

Figure 8.0-3 - Operations Flow Diagram to Place a Loaded FuelSolutions™ W74 Canister in a Transportation Cask at Sites with Limited Cask Handling Crane Capacities

8.1 Procedures for Loading the Cask in the Spent Fuel Pool

The major procedural steps for loading SNF assemblies into a FuelSolutions™ canister housed in a FuelSolutions™ W100 Transfer Cask in a spent fuel pool are outlined in Section 8.1 of the FuelSolutions™ Storage System FSAR. This section outlines specific differences in the operation of the FuelSolutions™ W74 canister during fuel loading in a spent fuel pool. Steps for loading a FuelSolutions™ W74 canister outside the spent fuel pool are provided in Section 8.3.

8.1.1 Stage Canister and Transfer Cask

8.1.1.1 Prepare a FuelSolutions™ W74 Canister for Fuel Loading

These procedures are provided in Section 8.1.1.1 of the FuelSolutions™ Storage System FSAR.

8.1.1.2 Stage a Transfer Cask

These procedures are provided in Section 8.1.1.2 of the FuelSolutions™ Storage System FSAR.

8.1.2 Insert Canister into Transfer Cask

These procedures are provided in Section 8.1.2 of the FuelSolutions™ Storage System FSAR. However, the upper basket of the FuelSolutions™ W74 canister is not placed into the canister at this time.

8.1.3 Place Canister and Transfer Cask into Fuel Pool

These procedures are provided in Section 8.1.3 of the FuelSolutions™ Storage System FSAR. However, the upper basket is removed from the FuelSolutions™ W74 canister after the top shield plug fit check (Section 8.1.3, Step 2) and before the canister is filled with water from the spent fuel pool (Section 8.1.3, Step 4).

8.1.4 Load Fuel into Canister

These procedures are provided in Section 8.1.4 of the FuelSolutions™ Storage System FSAR. However, Steps 1 through 10 of Section 8.1.4 are augmented as follows for loading of the FuelSolutions™ W74 canister upper basket:

11. After completion of loading SNF into the lower basket, install the upper basket into the canister.

    CAUTION: Rigging and handling operations must comply with the plant's NUREG-0612/ANSI N14.6 commitments.

12. Repeat Steps 6 through 10 for each SNF assembly to be loaded into the upper basket.

8.1.4.1 Load Damaged Fuel into Damaged Fuel Can

Storage of BRP damaged fuel assemblies has no effect on the general FuelSolutions™ canister operating procedures or the BRP site-specific W74 canister operating procedures. However,

rather than inserting damaged fuel assemblies directly into selected canister guide tubes as discussed in Section 8.1.4 of the FuelSolutions™ Storage System FSAR, BRP damaged fuel assemblies must be inserted into the damaged fuel can. The damaged fuel cans have been previously inserted into one of the four support tubes of either the lower or upper W74 canister basket assemblies.

The following outline describes the major procedural steps for loading a damaged fuel can with a damaged fuel assembly and the loading of this damaged fuel can into a W74 canister:

1. Examine the empty damaged fuel can and its lid for any physical damage that might have occurred since its on-site receipt inspection was performed. The can and its lid should be clean, and any packaging material or loose debris removed.
2. Test fit the lid inside its associated can and assure that its engagement finger locking devices operate correctly and freely under remote grapple conditions.
3. Place a damaged fuel can in each of the selected support tubes of a W74 canister lower basket assembly prior to insertion of the canister into the transfer cask (Section 8.1.2 of the FuelSolutions™ Storage System FSAR).
4. Place the canister and transfer cask into the fuel pool per Section 8.1.3 of the FuelSolutions™ Storage System FSAR.
5. Load fuel into the canister lower basket per Steps 1 through 10 of Section 8.1.4 of the FuelSolutions™ Storage System FSAR.
6. After loading fuel into a damaged fuel can, use a manual grapple to lower the can's lid into place. The assistance of an underwater video camera or other device may be required.
7. Using a manual grapple with a fixed hex-head ball driver, manipulate the damaged fuel can lid engagement fingers to lock the lid into place.
8. Prior to installation of the W74 upper basket into the canister, place a damaged fuel can in each of the selected support tubes of the W74 canister upper basket assembly.
9. Install the upper basket into the canister and load fuel per Section 8.1.4.
10. Repeat Steps 6 and 7 above for the installation of each damaged fuel can lid.

Complete the handling and transfer of the W74 canister per Sections 8.1.5 through 8.1.11.

8.1.5 Remove Loaded Cask/Canister from Fuel Pool

These procedures are provided in Section 8.1.5 of the FuelSolutions™ Storage System FSAR.

8.1.6 Decontaminate Cask Exterior

These procedures are provided in Section 8.1.6 of the FuelSolutions™ Storage System FSAR.

8.1.7 Install Canister Inner Closure Plate

These procedures are provided in Section 8.1.7 of the FuelSolutions™ Storage System FSAR.

8.1.8 Drain and Backfill Canister with Helium

These procedures are provided in Section 8.1.8 of the FuelSolutions™ Storage System FSAR. The required helium backfill quantity for the FuelSolutions™W74 canister is provided in Table 8.1-1.

8.1.9 Install Canister Outer Closure Plate

These procedures are provided in Section 8.1.9 of the FuelSolutions™ Storage System FSAR.

8.1.10 Transfer Canister from Transfer Cask to Storage Cask (Horizontally)

These procedures are provided in Section 8.1.10 of the FuelSolutions™ Storage System FSAR.

8.1.11 Transfer Canister from Transfer Cask to Storage Cask (Vertically)

These procedures are provided in Section 8.1.11 of the FuelSolutions™ Storage System FSAR.

Table 8.1-1 - Helium Backfill Gas Quantities for the FuelSolutions™ W74 Canister

Fuel Assembly Class	Average Payload Free Volume, $V_{PAYLOAD}$ (liters/assembly)(1)	Canister Free Volume, V_{FREE} (liters) (1)	Quantity of Canister Backfill Helium, m_{He} (grams)(1, 2)
BRP 9x9	32.6	5981	900
BRP 11x11	32.6	5981	900

Note:

(1) Payload free volume and canister free volume are based on intact fuel assemblies. Placement of partial fuel assemblies, dummy fuel assemblies, or fuel assemblies in damaged fuel cans requires adjustment of the free volume and corresponding adjustment of the canister backfill quantity to meet the helium backfill density *technical specification* in Section 12.3.

(2) Tolerance: +/- 25 grams.

8.2 Procedures for Unloading the Cask in the Spent Fuel Pool

The major procedural steps for unloading SNF assemblies from a FuelSolutions™ canister housed in a FuelSolutions™ W100 Transfer Cask in a spent fuel pool are outlined in Section 8.2 of the FuelSolutions™ Storage System FSAR. This section outlines specific differences in the operation of the FuelSolutions™ W74 canister during fuel unloading in a spent fuel pool. Steps for unloading a FuelSolutions™ W74 canister outside the spent fuel pool are provided in Section 8.4.

8.2.1 Retrieve Canister Using Horizontal Canister Transfer

These procedures are provided in Section 8.2.1 of the FuelSolutions™ Storage System FSAR.

8.2.2 Retrieve Canister Using Vertical Canister Transfer

These procedures are provided in Section 8.2.2 of the FuelSolutions™ Storage System FSAR.

8.2.3 Open Canister and Unload Fuel

These procedures are provided in Section 8.2.3 of the FuelSolutions™ Storage System FSAR. However, Steps 1 through 5 of Section 8.2.3.5 are augmented as follows for unloading of the FuelSolutions™ W74 lower basket:

6. Remove the upper basket from the canister and stage in fuel pool until removal of empty canister from the fuel pool (Section 8.2.3.6).

   CAUTION: Rigging and handling operations must comply with the plant's NUREG-0612/ANSI N14.6 commitments.

7. Repeat Steps 1 through 4 for each SNF assembly to be unloaded from the lower basket.

In addition, Steps 1 through 10 of Section 8.2.3.6 are preceded by the following for unloading the FuelSolutions™ W74 canister:

1. Install the upper basket staged in the fuel pool in Section 8.2.3.5 into the canister.

8.2.4 Horizontal Canister Transfer from a Storage Cask to a Transportation Cask

These procedures are provided in Section 8.2.4 of the FuelSolutions™ Storage System FSAR.

8.2.5 Horizontal Canister Transfer from a Transfer Cask to a Transportation Cask

These procedures are provided in Section 8.2.5 of the FuelSolutions™ Storage System FSAR.

8.2.6 Vertical Canister Transfer from a Transfer Cask to a Transportation Cask

These procedures are provided in Section 8.2.6 of the FuelSolutions™ Storage System FSAR.

8.3 Procedures for Loading the Canister Outside of the Spent Fuel Pool

The following outline describes the major procedural steps for loading fuel into a FuelSolutions™ W74 canister that has been placed in a FuelSolutions™ W100 Transfer Cask. With the cask/canister in a suitable staging area, the fuel is loaded into the canister using a fuel assembly shuttle cask to transfer a fuel assembly from the spent fuel pool to the cask. The cask/canister is fitted with a shielded loading collar to facilitate fuel transfer into the canister. Following fuel loading, the canister inner closure plate is installed, and the canister is drained, dried, and backfilled with helium. The canister outer closure plate is then installed and the canister is moved to the cask handling area. The loaded canister is then ready to be moved to storage at the ISFSI or to a transportation cask for shipment off-site. A flowchart of the sequence for loading the canister is provided in Figure 8.3-1.

The following outline briefly describes the major procedural steps for loading fuel into a FuelSolutions™ W74 canister in a transfer cask.

8.3.1 Stage Canister and Transfer Cask

8.3.1.1 Prepare a FuelSolutions™ W74 Canister for Fuel Loading

These procedures are provided in Section 8.1.1.1 of this FSAR.

8.3.1.2 Stage a Transfer Cask

NOTE: Prior to performing the following operations, the transfer cask is to be prepared as described in Sections 8.3.1 of the FuelSolutions™ Storage System FSAR.

1. Place the transfer cask in the vertical position in the designated cask loading area in the containment building. Set the transfer cask on the prestaged transfer cask support pad.

   NOTE: This operation may be performed in the cask decontamination area, the plant's cask receiving bay or a suitable staging area depending on site-specific conditions.

   CAUTION: Horizontal movement of the cask should always be in a direction perpendicular to the plane of the trunnions. In this way, an inadvertent impact with an object will cause the cask to remain engaged with the lifting yoke and rotate on the trunnions.

2. Assure the transfer cask neutron shield is filled with liquid and connected to an overflow bottle.

8.3.2 Prepare Canister and Transfer Cask for Fuel Loading

1. Remove the cask top cover.
2. Using a crane and suitable sling, lower the empty FuelSolutions™ W74 canister containing the lower basket assembly into the transfer cask cavity. Position the canister

circumferentially, to match the cask and canister alignment marks, and radially to provide an approximately even canister/cask annular gap all around.

3. Fill the cask/canister annulus with clean demineralized water. Place the inflatable seal into the upper cask liner recess, and seal the cask/canister annulus by pressurizing the seal with compressed air to the manufacturer's recommendation.
4. Completely fill the canister cavity with water from the fuel pool or an equivalent source to maintain pool chemistry control.
5. Install the shielded loading collar on the top end of the transfer cask. Attach the water management collection tray overflow hose and route the hose to the fuel pool or an overflow tank/reservoir.

   CAUTION: Rigging and handling operations must comply with the plant's NUREG-0612/ANSI N14.6 commitments.

8.3.3 Load Fuel into the Lower Basket

1. Index the shielded loading collar over the fuel position cell in the canister lower basket to be loaded.
2. Grapple a fuel assembly that meets the *technical specification* requirements contained in Section 12.3 of this FSAR from the fuel storage rack position using the fuel assembly shuttle cask, in accordance with the plant's 10CFR50[2] fuel handling procedures.
3. Prior to retrieval of a SNF assembly into the fuel assembly shuttle cask, the identity of the assembly is to be verified by two individuals using an underwater video camera or other means. Read and record the SNF assembly identification number from the fuel assembly. Check this identification number against the canister loading plan. Also check the *technical specification* requirements contained in Section 12.3 of this FSAR, which indicate the fuel assemblies that are acceptable for dry storage.
4. Retrieve the fuel assembly into the fuel assembly shuttle cask using the fuel assembly grapple. Remove the fuel assembly shuttle cask from the spent fuel pool using the plant's cask-handling crane.
5. Position the fuel assembly shuttle cask on the shielded loading collar and open the fuel assembly shuttle cask door.

   CAUTION: Rigging and handling operations must comply with the plant's NUREG-0612/ANSI N14.6 commitments.

6. Load the fuel assembly into the canister lower basket.
7. Release the grapple and retract it into the fuel assembly shuttle cask, verifying that the grapple has been successfully released from the fuel assembly. Then remove the fuel assembly shuttle cask.

[2] Title 10, U.S. Code of Federal Regulations, Part 50 (10CFR50), *Domestic Licensing of Production and Utilization Facilities*, 1995.

8. Record the location of the fuel assembly in the canister and verify its location against the loading plan.
9. Repeat Steps 1 through 8 for each SNF assembly loaded into the canister lower basket.
10. Check the radiation levels near the mid-plane (mid-point) of the lower fuel basket on the outside of the transfer cask to assure that dose rates are below maximum expected values in accordance with site-specific procedures and ALARA requirements (discussed in Section 10.3 of this FSAR). If the radiation levels exceed these requirements, notify the cognizant management representative. Await further instructions before proceeding. If radiation levels are acceptable, proceed.

    NOTE: Temporary shielding may be used to lower personnel radiation exposures. Such shielding should be installed in accordance with site-specific procedures.

8.3.4 Load Fuel into the Upper Basket

1. After completion of fuel loading in the lower basket, fill the canister cavity with water and remove the shielded loading collar. Install the upper basket into the canister. Install the upper basket top shield plug plate with plugs into the canister.

   NOTE: The installation of the upper basket and upper basket top shield plug may require the removal of some water from the canister. The removal of this water should be performed in parallel with the installation of these components.

   CAUTION: Rigging and handling operations must comply with the plant's NUREG-0612/ANSI N14.6 commitments.
2. Visually verify that the top shield plug plate is properly seated in the canister.
3. Reinstall the shielded loading collar on the top end of the transfer cask.
4. Index the shielded loading collar over the fuel position cell in the canister upper basket to be loaded.
5. Grapple a fuel assembly that meets the *technical specification* requirements contained in Section 12.3 of this FSAR from the fuel storage rack position using the fuel assembly shuttle cask, in accordance with the plant's 10CFR50 fuel handling procedures.
6. Prior to retrieval of a SNF assembly into the fuel assembly shuttle cask, the identity of the assembly is to be verified using an underwater video camera or other means. Read and record the fuel assembly identification number from the fuel assembly. Check this identification number against the canister loading plan. Also check the *technical specification* requirements contained in Section 12.3 of this FSAR, which indicate the fuel assemblies that are acceptable for dry storage.
7. Retrieve the fuel assembly into the fuel assembly shuttle cask using the fuel assembly grapple. Remove the fuel assembly shuttle cask from the spent fuel pool using the plant's cask-handling crane.
8. Remove the shield plug corresponding to the fuel position cell in the upper basket to be loaded from the shield plug plate. This is done by positioning the shield plug installation fixture with a crane over the loading collar gate in the shielding loading collar, opening the

loading collar gate, grasping the plug and lifting it into the shield plug installation fixture, closing the loading collar gate, installing a contamination control catch basin or water absorbent material, and removing the shield plug installation fixture to a temporary storage location.

9. Position the fuel assembly shuttle cask on the shielded loading collar and open the fuel assembly shuttle cask door.
10. Load the fuel assembly into the canister upper basket.

    NOTE: The installation of individual SNF assemblies may require the removal of some water from the canister. The removal of this water should be performed in parallel with the installation of these assemblies.

11. Once it is assured that the fuel assembly is fully inserted, release the grapple and retract it into the fuel assembly shuttle cask, verifying that the grapple has been successfully released from the fuel assembly. Close the fuel assembly shuttle cask door. Then remove the fuel assembly shuttle cask.
12. Replace the shield plug into the shield plug plate by reversing the steps given in Step 8.
13. Record the location of the fuel assembly in the canister and verify its location against the fuel loading plan.
14. Repeat Steps 4 through 13 for each SNF assembly loaded into the canister upper basket until the upper basket is loaded as planned.
15. Remove the shielded loading collar from the transfer cask. Assure that water is filled to the top of the canister.
16. Check the radiation levels near the mid-plane (mid-point) of the transfer cask to assure that dose rates are below maximum expected values in accordance with site-specific procedures and ALARA requirements (discussed in Section 10.1.3.2 of the FuelSolutions™ Storage System FSAR). If the radiation levels exceed these requirements, notify the cognizant management representative. Await further instructions before proceeding. If radiation levels are acceptable, proceed.

    NOTE: Temporary shielding may be used to lower personnel radiation exposures. Such shielding should be installed in accordance with site-specific procedures.

17. Deflate and remove the inflatable cask/canister annulus seal.
18. Decontaminate the exposed surfaces of the canister shell perimeter adjacent to the shield plug and the top interior surface of the cask and top exterior surface of the canister above and adjacent to the annulus seal location.

8.3.5 Decontaminate Cask Exterior

These procedures (provided in Section 8.1.6 of the FuelSolutions™ Storage System FSAR) are not applicable, since the transfer cask was not placed into a spent fuel pool.

8.3.6 Install Canister Inner Closure Plate

These procedures are provided in Section 8.1.7 of the FuelSolutions™ Storage System FSAR.

8.3.7 Drain and Backfill Canister with Helium

These procedures are provided in Section 8.1.8 of the FuelSolutions™ Storage System FSAR. The required helium backfill quantity for the FuelSolutions™W74 canister is provided in Table 8.1-1.

8.3.8 Install Canister Outer Closure Plate

These procedures are provided in Section 8.1.9 of the FuelSolutions™ Storage System FSAR.

8.3.9 Transfer Canister from Transfer Cask to Storage Cask (Horizontal Transfer)

These procedures are provided in Section 8.1.10 of the FuelSolutions™ Storage System FSAR.

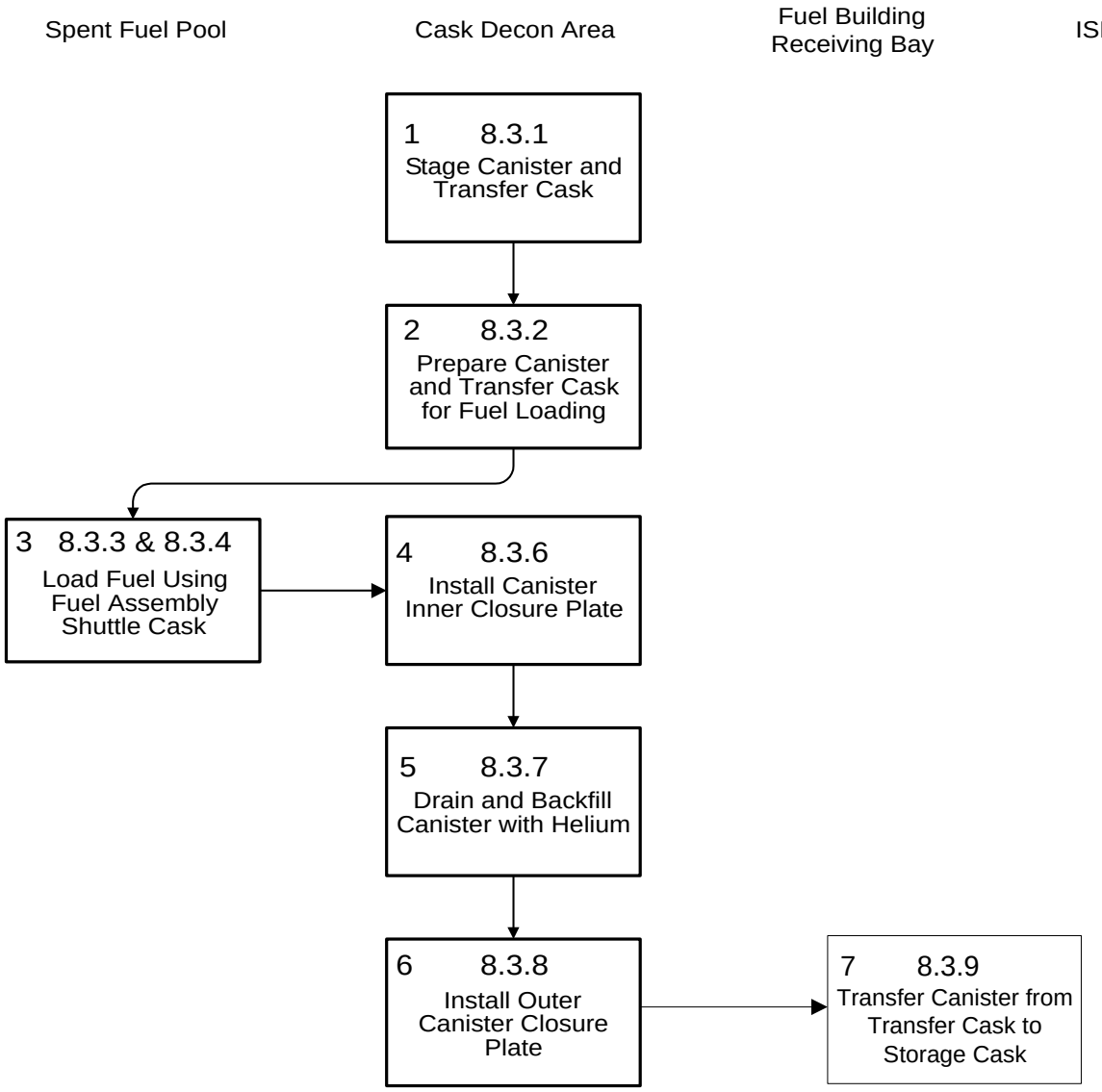

Figure 8.3-1 - Sequence for Loading a FuelSolutions™ W74 Canister Outside of the Spent Fuel Pool

8.4 Procedures for Unloading the Cask Outside of the Spent Fuel Pool

8.4.1 Retrieve Canister Using Horizontal Transfer

These procedures are provided in Section 8.2.1 of the FuelSolutions™ Storage System FSAR.

8.4.2 Retrieve Canister Using Vertical Transfer

These procedures, provided in Section 8.2.2 of the FuelSolutions™ Storage System FSAR, are not applicable for the Big Rock Point site due to plant interface restrictions.

8.4.3 Unload Fuel

The following outline describes the major procedural steps for opening a loaded FuelSolutions™ W74 canister and transferring the fuel back to the fuel pool. The transfer cask/canister is moved to the designated cask loading area in the containment building. The canister is vented and filled with water. The inner and outer closure plates are removed, and the shielded loading collar is installed onto the top end of the transfer cask. Each fuel assembly is retrieved into the fuel assembly shuttle cask, and then the fuel is moved to its designated storage location. A flowchart of the sequence for unloading fuel is provided in Figure 8.4-1.

8.4.3.1 Move Loaded Canister to Cask Loading Area

NOTE: Prior to performing the following operations, the canister shall be retrieved horizontally from the storage cask to the transfer cask, as described in Section 8.2.1 of the FuelSolutions™ Storage System FSAR.

1. Move the transfer cask into the containment building, in accordance with plant procedures.
2. After moving the transfer cask into the designated cask loading area in the containment building, rotate the transfer cask into the vertical position using the plant's cask-handling crane and lifting yoke.

8.4.3.2 Prepare Canister for Vent and Fill

These procedures are provided in Section 8.2.3.1 of the FuelSolutions™ Storage System FSAR.

8.4.3.3 Vent and Fill Canister with Water

These procedures are provided in Section 8.2.3.2 of the FuelSolutions™ Storage System FSAR.

8.4.3.4 Remove the Canister Inner and Outer Closure Plates

These procedures are provided in Section 8.2.3.3 of the FuelSolutions™ Storage System FSAR.

8.4.3.5 Prepare Canister and Transfer Cask for Fuel Unloading

Install the shielded loading collar on the top end of the transfer cask. Attach the water management collection tray overflow hose and route to the fuel pool or overflow tank/container. Fill the space above the shield plug with water from the fuel pool or an equivalent overflow tank/reservoir.

8.4.3.6 Remove Fuel from the Upper Basket

1. Index the shielded loading collar over the fuel position cell in the cask upper basket to be unloaded.
2. Remove the shield plug corresponding to the fuel position cell in the upper basket to be unloaded from the shield plug plate. This is done by positioning the shield plug installation fixture over the loading collar gate in the shielded loading collar, opening the loading collar gate, grasping the plug and lifting it into the shield plug installation fixture, closing the loading collar gate, and removing the shield plug installation fixture to a temporary storage location.
3. Position the fuel assembly shuttle cask on the loading collar and open the fuel assembly shuttle cask door.
4. Lower and engage the grapple on the fuel assembly and retrieve the fuel assembly into the fuel assembly shuttle cask. Close the fuel assembly shuttle cask door and remove the fuel assembly shuttle cask.
5. Replace the shield plug into the shield plug plate by reversing the process described in Step 2.
6. Add water to the canister/shielded loading collar to maintain the water level near the top of the canister, or as required to keep the dose rate ALARA.
7. Move the fuel assembly shuttle cask to the spent fuel pool and place the fuel assembly in a designated fuel storage rack position, in accordance with the plant's 10CFR50 fuel handling procedures.

   NOTE: If fuel damage is observed, follow the appropriate actions in the plant's 10CFR50 procedures for handling of damaged fuel.
8. Read and record the fuel assembly identification number from the fuel assembly. Repeat Steps 1 through 7 for each SNF assembly removed from the canister upper basket.

8.4.3.7 Remove Fuel from the Lower Basket

1. After fuel is unloaded from the upper basket, add water to the canister/shielded loading collar to maintain the water level near the top of the canister. Remove the shielded loading collar and the top shield plug from the canister.
2. Remove the upper basket assembly from the canister being mindful of contamination spread and increased dose rate from the basket.
3. Add water to bring the level to near the canister top, and reinstall the shielded loading collar on the top end of the transfer cask.

4. Index the shielded loading collar over the fuel position cell in the canister lower basket to be unloaded.
5. Position the fuel assembly shuttle cask on the loading collar and open the fuel assembly shuttle cask door.
6. Lower and engage the grapple on the fuel assembly and retrieve into the fuel assembly shuttle cask. Close the fuel assembly shuttle cask door and remove the fuel assembly shuttle cask.
7. Move the fuel assembly shuttle cask to the spent fuel pool and place the fuel assembly in a designated fuel storage rack position, in accordance with the plant's 10CFR50 fuel handling procedures.

   NOTE: If fuel damage is observed, follow the appropriate actions in the plant's 10CFR50 procedures for handling of damaged fuel.
8. Read and record the fuel assembly identification number from the fuel assembly.
9. Add water to bring the level near to the canister top.
10. Repeat Steps 4 through 9 for each SNF assembly removed from the canister lower basket, until all required fuel has been removed from the canister.

8.4.4 Horizontal Canister Transfer from a Storage Cask to a Transportation Cask

These procedures are provided in Section 8.2.4 of the FuelSolutions™ Storage System FSAR.

8.4.5 Horizontal Canister Transfer from a Transfer Cask to a Transportation Cask

These procedures are provided in Section 8.2.5 of the FuelSolutions™ Storage System FSAR.

8.4.6 Vertical Canister Transfer from a Transfer Cask to a Transportation Cask

These procedures, provided in Section 8.2.6 of the FuelSolutions™ Storage System FSAR, are not applicable.

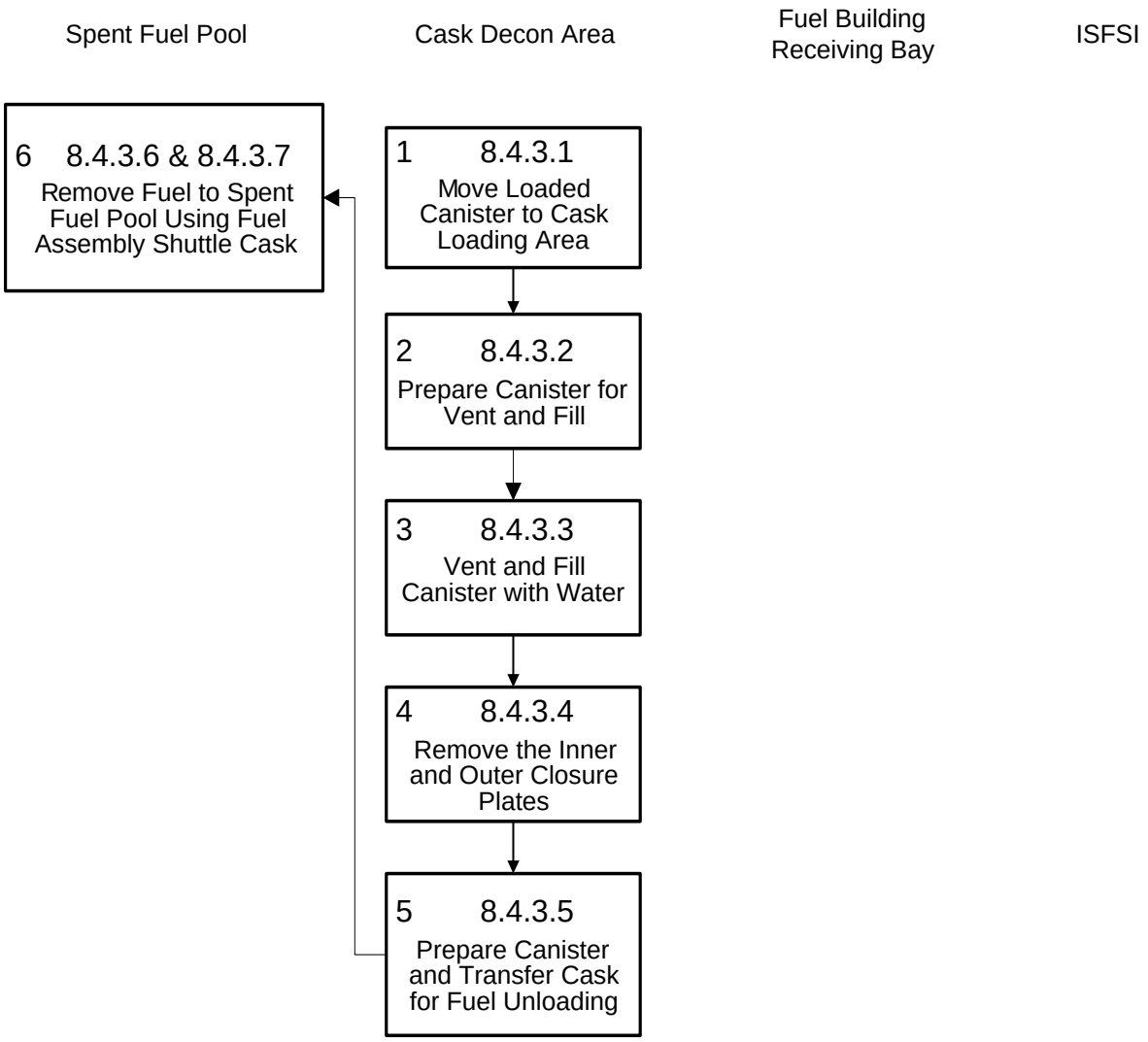

Figure 8.4-1 - Sequence for Unloading Fuel Outside of the Spent Fuel Pool

8.5 Preparation of the Cask

8.5.1 Prepare Transfer Cask for Canister Loading

These procedures are provided in Section 8.3.1 of the FuelSolutions™ Storage System FSAR.

8.5.2 Prepare Storage Cask for Canister Loading

These procedures are provided in Section 8.3.2 of the FuelSolutions™ Storage System FSAR.

This page intentionally left blank.

9. ACCEPTANCE CRITERIA AND MAINTENANCE PROGRAM

This chapter summarizes the acceptance tests and maintenance program to be performed on the FuelSolutions™ W74 canister, which is classified as important to safety. These criteria for the FuelSolutions™ W150 Storage Cask and W100 Transfer Cask are described in Chapter 9 of the FuelSolutions™ Storage System FSAR.[1]

The following sections present the inspections and acceptance testing needed to demonstrate that a fabricated FuelSolutions™ W74 canister meets the design and code of construction requirements set forth in this FSAR. In addition, the periodic maintenance program describes the activities to be carried out to assure that the FuelSolutions™ W74 canister is maintained in proper working condition, so that it continues to perform its intended functions.

Storage of BRP MOX, partial, and damaged fuel assemblies has no effect on the FuelSolutions™ W74 canister acceptance criteria and maintenance program. This chapter summarizes the acceptance tests and maintenance program to be performed on a FuelSolutions™ W74 canister damaged fuel can, which is classified as important to safety. The following sections present the inspections and acceptance testing needed to demonstrate that a fabricated damaged fuel can meets the design and code of construction requirements set forth in this FSAR.

As used in the sections that follow, the term “preoperation” refers to that period of time from the receipt inspection of a FuelSolutions™ canister and associated damaged fuel can until they are actually loaded into a transfer cask for SNF assembly loading.

[1] WSNF-220, *FuelSolutions™ Storage System Final Safety Analysis Report*, NRC Docket No. 72-1026, BNFL Fuel Solutions Corporation.

This page intentionally left blank.

9.1 Acceptance Criteria

9.1.1 FuelSolutions™ W74 Canister

This section discusses the inspections and acceptance tests that are to be performed prior to use of each FuelSolutions™ W74 canister with the associated FuelSolutions™ Storage System components. These inspections and tests provide assurance that the FuelSolutions™ W74 canister is fabricated and initially operated in accordance with the requirements set forth in this FSAR. The inspections and acceptance testing to be performed are intended to demonstrate that the FuelSolutions™ W74 canister, together with the interfacing FuelSolutions™ Storage System components, have been fabricated in accordance with the design and code of construction requirements contained in Section 2.1.2 of this FSAR.

These inspections and tests are also intended to demonstrate that the initial operation of the FuelSolutions™ Storage System using the FuelSolutions™ W74 canister complies with the applicable regulatory requirements and the *technical specifications* contained in Chapter 12 of this FSAR and the FuelSolutions™ Storage System FSAR. Noncompliances encountered during the required inspections and tests performed for the FuelSolutions™ W74 canister will be corrected or dispositioned to bring the item into compliance with this FSAR. This is done in accordance with the BNFL Fuel Solutions (BFS) Quality Assurance program, discussed in Chapter 13 of the FuelSolutions™ Storage System FSAR, or the licensee's NRC-approved Quality Assurance program.

The FuelSolutions™ W74 canister is classified as important to safety. Individual canister components, assemblies, and piece parts are required to be designed, fabricated, and tested to the quality standards commensurate with the item's graded quality category. The quality categories for the FuelSolutions™ W74 canister components which are based on NUREG/CR-6407[2] are identified on the applicable drawings in Section 1.5 of this FSAR. The quality category assessments and the associated critical characteristics to be verified during procurement and fabrication will be developed in accordance with the BFS Quality Assurance program identified in Chapter 13 of the FuelSolutions™ Storage System FSAR.

The testing and inspection acceptance criteria applicable to each FuelSolutions™ W74 canister are listed in Table 9.1-1 and discussed in more detail in the paragraphs that follow. These inspections and tests are intended to demonstrate that a canister has been fabricated and examined in accordance with the criteria contained in Section 2.1.2 of this FSAR.

9.1.2 Damaged Fuel Can

This section discusses the inspections and acceptance tests that are to be performed prior to use of each FuelSolutions™ W74 canister damaged fuel can with the associated FuelSolutions™ W74 Canister and Storage System components. These inspections and tests provide assurance that a damaged fuel can is fabricated and initially operated in accordance with the requirements set forth in this FSAR. The inspections and acceptance testing to be performed are intended to

[2] NUREG/CR-6407, *Classification of Transportation Packaging and Dry Spent Fuel Storage System Components According to Importance to Safety*, U.S. Nuclear Regulatory Commission, February 1996.

demonstrate that the damaged fuel can, together with the interfacing FuelSolutions™ W74 Canister and Storage System components, have been fabricated in accordance with the design and code of construction requirements contained in Section 2.1.2 of this FSAR.

These inspections and tests are also intended to demonstrate that the initial operation of the FuelSolutions™ Storage System using the FuelSolutions™ W74 canister and damaged fuel cans complies with the applicable regulatory requirements and the *technical specifications* contained in Chapter 12 of this FSAR and the FuelSolutions™ Storage System FSAR. Noncompliances encountered during the required inspections and tests performed for a damaged fuel can will be corrected or dispositioned to bring the item into compliance with this FSAR. This is done in accordance with the BNFL Fuel Solutions (BFS) Quality Assurance program, discussed in Chapter 13 of the FuelSolutions™ Storage System FSAR, or the licensee's NRC-approved Quality Assurance program.

The damaged fuel can is classified as important to safety. Individual damaged fuel can components, assemblies, and piece parts are required to be designed, fabricated, and tested to the quality standards commensurate with the item's graded quality category. The quality categories for the damaged fuel can components, which are based on NUREG/CR-6407, are identified on the applicable drawings in Section 1.5 of this FSAR. The quality category assessments and the associated critical characteristics to be verified during procurement and fabrication will be developed in accordance with the BFS Quality Assurance program identified in Chapter 13 of the FuelSolutions™ Storage System FSAR.

The testing and inspection acceptance criteria applicable to each FuelSolutions™ W74 canister damaged fuel can are listed in Table 9.1-2 and discussed in more detail in the paragraphs that follow. These inspections and tests are intended to demonstrate that a damaged fuel can has been fabricated and examined in accordance with the criteria contained in Section 2.1.2 of this FSAR.

Table 9.1-1 - FuelSolutions™ W74 Canister Inspection and Test Acceptance Criteria (3 Pages)

Function	Method of Verification		
	Fabrication	Preoperation	Maintenance
Visual Inspection and Nondestructive Examination (NDE)	a) Assembly and examination of canister components per ASME Code, Section III, Subsections NB[3] and NG.[4] b) A dimensional inspection of the internal basket assemblies (upper and lower) will be performed prior to insertion into the canister shell to verify compliance with design requirements. c) A dimensional inspection of the top end shield plug and inner and outer closure plates and the bottom end shield plug and closure and end plates will be performed prior to inserting into the canister shell to verify compliance with design requirements. d) NDE of weldments will be defined on the drawings using standard American Welding Society[5] NDE symbols and/or notations. e) Cleanliness of the canister will be verified upon completion of fabrication per NQA-1. f) The protection of the canister at the completion of fabrication will be verified per NQA-1.	a) The canister will be visually inspected prior to placement in service at the licensee's facility. b) Canister protection at the licensee's facility will be verified. c) Canister cleanliness and exclusion of foreign material will be verified prior to placing in the spent fuel pool.	None.

[3] American Society of Mechanical Engineers (ASME) Boiler and Pressure Vessel Code, Section III, Division 1, Subsection NB, *Class 1 Components*, 1995 Edition.

[4] American Society of Mechanical Engineers (ASME) Boiler and Pressure Vessel Code, Section III, Division 1, Subsection NG, *Core Support Structures*, 1995 Edition.

[5] American Welding Society (AWS) D1.1-96, *Structural Welding Code - Steel*.

Table 9.1-1 - FuelSolutions™ W74 Canister Inspection and Test Acceptance Criteria (3 Pages)

Function	Method of Verification		
	Fabrication	Preoperation	Maintenance
Structural	a) Assembly and welding of canister components will be performed per ASME Code, Subsections NB and NG. b) Materials analysis (steel, lead, etc.) will be performed and records will be kept in a manner commensurate with "important to safety" classifications. c) ASME Code NB-6000 pressure tests of all canister pressure boundary shop welds will be performed.	None.	a) ASME Code NB-6000 pressure tests of inner closure plate to canister shell and vent and drain port field welds will be performed after closure welding.
Leak Tests	a) Helium leak rate testing will be performed on all canister pressure boundary shop welds. b) Soap bubble leak test of installed vent/drain port quick connect fittings.	None.	a) Helium leak rate testing will be performed on inner closure plate to canister shell and vent and drain port field welds after closure welding.
Criticality Safety	a) The boron content will be verified at the time of neutron absorber material manufacture. b) The correct orientation of the guide tubes and the associated neutron absorber material shall be verified prior to the placement of the basket into the shell.	None.	None.
Shielding Integrity	a) Material compliance will be verified through CMTRs. b) Dimensional verification of top and bottom shield plug thickness will be performed.	None.	None.
Thermal Acceptance	None.	None.	a) Periodic temperature monitoring will be performed during operation.

Table 9.1-1 - FuelSolutions™ W74 Canister Inspection and Test Acceptance Criteria (3 Pages)

Function	Method of Verification		
	Fabrication	Preoperation	Maintenance
Functional Performance Tests	a) Fit-up of the following components is to be tested during fabrication: – Upper basket – Top shield plug with drain tube – Inner top closure plate and vent/drain port covers – Outer top closure plate. b) A functional leak test of the quick connect fittings installed in the vent and drain port openings. c) A gauge test of all basket guide tubes.	a) Fit-up of the following components is to be verified during preoperation: – Upper basket – Top shield plug – Inner top closure plate – Outer top closure plate.	None.
Canister Identification Inspections	a) Verification of identification marking applied at completion of fabrication.	a) Identification marking will be checked for legibility during preoperation.	None.

Table 9.1-2 - FuelSolutions™ W74 Canister Damaged Fuel Can Inspection and Test Acceptance Criteria (2 Pages)

Function	Method of Verification		
	Fabrication	Preoperation	Maintenance
Visual Inspection and Nondestructive Examination (NDE)	a) Assembly and examination of damaged fuel can components per ASME Code, Section III, Subsection NG.[6] b) A dimensional inspection of a damaged fuel can will be performed to verify compliance with design requirements. c) NDE of weldments will be defined on the drawings using standard American Welding Society[7] NDE symbols and/or notations. d) Cleanliness of a damaged fuel can will be verified upon completion of fabrication per NQA-1. e) The protection of a damaged fuel can at the completion of fabrication will be verified per NQA-1.	a) The damaged fuel can will be visually inspected prior to placement in service at the licensee's facility. b) Damaged fuel can protection at the licensee's facility will be verified. c) Damaged fuel can cleanliness and exclusion of foreign material will be verified prior to placing in the canister or spent fuel pool.	None.
Structural	a) Assembly and welding of damaged fuel can components will be performed per ASME Code, Subsection NG. b) Materials analysis (steel, fasteners, etc.) will be performed and records will be kept in a manner commensurate with "important to safety" classifications.	None.	None.
Leak Tests	None.	None.	None.
Criticality Safety	The boron content will be verified at the time of neutron absorber material manufacture.	None.	None.
Shielding Integrity	None.	None.	None.

[6] American Society of Mechanical Engineers (ASME) Boiler and Pressure Vessel Code, Section III, Division 1, Subsection NG, *Core Support Structures*, 1995 Edition.

[7] American Welding Society (AWS) A2.4-98, *Standard Symbols for Welding, Brazing and Nondestructive Testing*, 1998.

Table 9.1-2 - FuelSolutions™ W74 Canister Damaged Fuel Can Inspection and Test Acceptance Criteria (2 Pages)

Function	Method of Verification		
	Fabrication	Preoperation	Maintenance
Thermal Acceptance	None.	None.	Periodic temperature monitoring of the W74 storage cask will be performed during operation.
Functional Performance Tests	A gauge test (both inside and outside) of each damaged fuel can.	None.	None.
Canister Identification Inspections	Verification of unique shop assembly identification number.	Shop assembly identification number will be checked for legibility during preoperation.	None.

9.1.3 Visual Inspection and Nondestructive Examination

9.1.3.1 FuelSolutions™ W74 Canister

The structural, thermal, shielding, criticality safety, and functional performance of the FuelSolutions™ W74 canister is assured by the verification of material properties, fabrication processes, and dimensions. Documentation prepared during canister fabrication is to provide evidence that materials and fabrication comply with the design requirements. The required inspections to be performed to assure canister performance include the following:

1. The FuelSolutions™ W74 canister assemblies and piece parts are to be fabricated and examined in accordance with the codes and standards used for design and construction, as described in Section 2.1.2 of this FSAR. Non-destructive examinations (NDE) of welds specified on the approved design drawings are to be performed in accordance with approved procedures, detailed on a weld inspection plan, and performed by inspection personnel who are certified, in accordance with the code of construction requirements.
2. A documentation package is to be prepared and maintained during fabrication to include detailed records and evidence that the required inspections and tests have been performed under an NRC-approved quality assurance program. Prior to shipment of the canister, the document package is to be reviewed to verify that the FuelSolutions™ W74 canister shell assembly and the canister basket assemblies have been properly fabricated and inspected in accordance with the design and code of construction requirements. The documentation package is to include:
   - Completed Shop Travelers and Referenced Procedures
   - Inspection Records
   - Inspector/Welder Certification Records
   - Nonconformance Reports
   - Material Test Reports
   - NDE Reports
   - Procurement Records
   - As-Built Report
3. A dimensional inspection of the canister shell is to be performed to verify compliance with the design requirements. The canister overall length, diameter, and cylindricity are to be verified to provide assurance that the canister will properly interface with other FuelSolutions™ Storage System components.
4. A dimensional inspection of the internal basket assemblies (upper and lower) is to be performed prior to insertion into the canister shell, to verify compliance with the design requirements. The size and position of the basket assembly structural members are to be verified to provide assurance that the SNF assemblies are properly supported.

5. After assembly of the canister is complete, the top shield plug, inner closure plate, and outer closure plate are to be inserted to verify their proper fit. Proper fit-up of the shield plug and individual closure plates is verified to assure adequate shielding and interface with the handling equipment. Proper fit-up of the canister drain tube is verified to assure the canister can be effectively dewatered.
6. Proper location of the canister alignment marks and vent, drain, and instrument port labels on the outer closure plate is to be verified in accordance with design requirements to assure proper handling during operations.
7. An inspection is to be performed to verify that the canister nameplate is properly attached and contains the required information. Specifically, the nameplate information is to include the canister model number, serial number, and empty weight.
8. Canister cleanliness will be verified as meeting the criteria specified in ASME NQA-1, Subpart 2.1, Class B, upon completion of fabrication.
9. Canister protection at the completion of fabrication will be verified to be in accordance with the requirements of ASME NQA-1,[8] Subpart 2.2, Level C.
10. Canister protection at the licensee's facility will be verified to be commensurate to the requirements specified for fabrication.
11. Canister interior and exterior surfaces will be inspected to verify cleanliness and assure foreign material exclusion prior to placing in the spent fuel pool.
12. Following canister fuel loading and closure, the canister nameplate is to be verified to assure it is properly completed with the loading date.

9.1.3.2 Damaged Fuel Can

The structural, criticality safety, and functional performance of a damaged fuel can is assured by the verification of material properties, fabrication processes, and dimensions. Documentation prepared during damaged fuel can fabrication is to provide evidence that materials and fabrication comply with the design requirements. The required inspections to be performed to assure damaged fuel can performance include the following:

1. The damaged fuel can assemblies and piece parts are to be fabricated and examined in accordance with the codes and standards used for design and construction, as described in Section 2.1.2 of this FSAR. Non-destructive examinations (NDE) of welds specified on the approved design drawings are to be performed in accordance with approved procedures, detailed on a weld inspection plan, and performed by inspection personnel who are certified, in accordance with the code of construction requirements.
2. A documentation package is to be prepared and maintained during fabrication to include detailed records and evidence that the required inspections and tests have been performed under an NRC-approved quality assurance program. Prior to shipment of a damaged fuel can,

[8] ASME NQA-1, *Quality Assurance Program Requirements for Nuclear Facility Applications*, American Society of Mechanical Engineers, 1994.

the document package is to be reviewed to verify that the damaged fuel can assemblies have been properly fabricated and inspected in accordance with the design and code of construction requirements. The documentation package is to include:

- Completed Shop Travelers and Referenced Procedures
- Inspection Records
- Inspector/Welder Certification Records
- Nonconformance Reports
- Material Test Reports
- NDE Reports
- Procurement Records
- As-Built Report

3. A dimensional inspection of a damaged fuel can is to be performed to verify compliance with the design requirements. The damaged fuel can's overall length is to be verified to provide assurance that the damaged fuel can will properly interface with the FuelSolutions™ W74 canister and associated fuel assemblies.
4. Damaged fuel can cleanliness will be verified as meeting the criteria specified in ASME NQA-1, Subpart 2.1, Class B, upon completion of fabrication.
5. Damaged fuel can protection at the completion of fabrication will be verified to be in accordance with the requirements of ASME NQA-1, Subpart 2.2, Level C.
6. Damaged fuel can protection at the licensee's facility will be verified to be commensurate to the requirements specified for fabrication.

Damaged fuel can interior and exterior surfaces will be inspected to verify cleanliness and assure foreign material exclusion prior to placing in the spent fuel pool.

9.1.4 Structural

The structural performance of the FuelSolutions™ W74 canister is assured by the verification of the material properties, assembly dimensions, and weld integrity. The inspections to be performed to assure canister structural performance include the following:

1. Material compliance is to be demonstrated through receipt inspections to assure that it meets the specified design, code of construction, and procurement requirements.
2. Prior to internal basket insertion, all canister shell radiographs are to be reviewed to assure that they meet the design and code of construction requirements. Radiography is required for the canister shell longitudinal and circumferential seam and shell-to-bottom closure plate welds only. The inner and outer top end closure plate welds do not require radiography since the canister shell top end uses redundant closure welds with liquid penetrant examination, and helium leak testing of the inner closure plate welds.
3. Following attachment of the bottom closure plate to the canister shell during shop fabrication, the cavity formed by this plate, the shell, and a temporary closure is filled with

helium to 12.5 psig, using a port through the temporary closure used. All circumferential and longitudinal full-penetration butt welds in the canister shell and the bottom closure plate-to-canister shell welds are then pressure tested in accordance with Subarticle NB-6300 of the ASME Code. This may be done in conjunction with the leak testing as described in Section 9.1.5.

4. Following the placement of the inner top closure plate and evacuation and vacuum drying of the canister following fuel loading, the canister cavity is backfilled with helium to 12.5 psig. The inner top closure plate weld to the canister shell and the welds to the drain and vent port bodies are then pressure tested, as described in Section 8.1.8 of this FSAR.
5. Following the successful pressure and leak rate tests of the inner closure plate welds and a second vacuum drying cycle of the canister cavity, the canister cavity is backfilled with helium in accordance with the *technical specification* contained in Section 12.3 and the canister vent and drain port covers are seal-welded in place. This is followed by placement of the outer top closure plate.

The structural performance of a FuelSolutions™ W74 canister damaged fuel can is assured by the verification of the material properties, assembly dimensions, and weld integrity. Material compliance is to be demonstrated through receipt inspections to assure that it meets the specified design, code of construction, and procurement requirements.

9.1.5 Leak Tests

1. Following the pressurization with helium of the cavity formed by the bottom closure plate, the canister shell, and a temporary closure, as described in Section 9.1.4, the canister shell circumferential and longitudinal full-penetration butt welds and the bottom closure plate-to-shell weld are helium leak rate tested to verify a maximum leak rate of 8.52×10^{-6} ref-cc/sec.
2. Following installation of the vent and drain block assemblies, the installed vent/drain port quick connect fittings will be soap bubble leak tested.
3. Following the pressurization with helium of the cavity formed by the inner top closure plate and the canister shell, as described in Section 9.1.4, the inner top closure plate welds are helium leak rate tested in accordance with the *technical specification* requirements contained in Section 12.3 of the FuelSolutions™ Storage System FSAR.

The damaged fuel can is not a pressure vessel, therefore, leak testing of this component is not required.

9.1.6 Criticality Safety

Criticality safety of the FuelSolutions™ W74 canister is assured by verification of the borated neutron absorber material properties and the basket assembly dimensions. The neutron absorber areal density is an important characteristic that assures subcriticality during all FuelSolutions™ canister operating modes. The tests and inspections to be performed to assure canister criticality safety performance include the following:

1. To assure that the minimum specified boron loading is provided, the FuelSolutions™ W74 canister borated neutron absorber material is to be tested as described in the material manufacturer's product literature provided in Section 1.5.2.1 (i.e. JEN3 testing) or other

neutron attenuation testing. Such testing must be calibrated against a known standard which is to be verified by a chemical assay (e.g. wet chemistry) to verify boron content. Alternatively, areal density can be determined by chemical analysis (e.g., wet chemistry testing) of samples taken from production material, with a minimum of ten samples tested for each heat or lot. Areal density shall meet the minimum value stated in Section 6.3.1.

2. The dimensions of the canister basket assembly are to be verified, as described in Section 9.1.3.

Criticality safety of a damaged fuel can is assured by verification of the properties of the borated neutron absorber material properties. The neutron absorber areal density is an important characteristic that assures subcriticality during all FuelSolutions™ canister/damaged fuel can operating modes. The damaged fuel can borated neutron absorber material is to be tested to assure that the minimum specified boron loading is provided, as discussed under bullet 1 above.

9.1.7 Shielding Integrity

The shielding performance of the FuelSolutions™ W74 canister is assured by the verification of canister material densities and assembly dimensions. The inspections to be performed to assure shielding performance include the following:

1. Material compliance is to be demonstrated through receipt inspections to assure that it meets the specified design, code of construction, and procurement requirements.
2. A dimensional inspection of the top and bottom shield plug thickness is to be performed to verify compliance with the design requirements.

Due to bounding damaged fuel can assumptions in the FuelSolutions™ W74 canister shielding analyses, the shielding performance of the FuelSolutions™ W74 canister is unaffected by the damaged fuel can materials or assembly dimensions.

9.1.8 Thermal Acceptance

Thermal performance of the FuelSolutions™ W74 canister is demonstrated through analysis, helium backfilling during canister sealing, and periodic storage cask temperature monitoring during storage, as described in the FuelSolutions™ Storage System FSAR. The inspections to be performed to assure canister thermal performance include the following:

1. Material compliance is to be demonstrated through receipt inspections to assure that it meets the specified design, code of construction, and procurement requirements.
2. Canister dimensions are to be verified against the design requirements.
3. Canister leak tightness is to be verified by volumetric examination of the canister shell seam welds, liquid penetrant examination of the redundant closure welds, and helium leak testing performed during fabrication and following canister loading. This provides assurance that the inert helium atmosphere needed to promote heat transfer and prevent fuel cladding degradation during storage is maintained.

Due to bounding damaged fuel can assumptions in the FuelSolutions™ W74 canister thermal analyses, the thermal performance of the FuelSolutions™ W74 canister is unaffected by the damaged fuel can materials or assembly dimensions.

9.1.9 Components

9.1.9.1 Functional Performance Tests

The functional performance of each canister is assured by the dimensional inspections of Section 9.1.1 and the following inspections and tests:

1. A fit-up test of the upper basket in the canister/lower basket assembly.
2. A fit-up test of the top shield plug/drain tube assembly in the canister/baskets assembly.
3. A functional leak test of the quick connect fittings installed in the vent and drain port openings.
4. A fit-up test of the individual shield plugs into the top shield plug.
5. A fit-up test of the inner top closure plate and its vent and drain port covers in the canister/baskets/top shield plug assembly.
6. A fit-up test of the outer top closure plate in the canister/baskets/top shield plug/inner top closure plate assembly.
7. After the lower basket is inserted into the canister shell, a gauge test of each of the lower basket guide tubes is to be performed to verify that a fuel assembly size gauge properly fits within each guide tube. The gauge test is to be repeated for the upper basket.

The functional performance of each damaged fuel can is assured by the dimensional inspections of Section 9.1.2 and a gauge test to verify that a fuel assembly size gauge properly fits within each damaged fuel can. A gauge test will also be performed to verify that the damaged fuel can will fit within a canister basket support tube.

9.1.9.2 Identification Inspections

Each canister will be identified by permanent marking that contains the following information:

- Name of Designer – BNFL Fuel Solutions
- Canister Serial Number – RST-LS-XXX-Y

  where, RST is the canister designation (74M or 74T)

  L is the canister length designation (L = long)

  S is the shield plug material designation (S = steel)

  XXX is a sequential number assigned by the license holder

  Y is the fabricator designator
- Empty Weight
- C of C number

Each canister identification mark is to be inspected during fabrication and preoperation for accuracy and legibility.

Because a FuelSolutions™ W74 canister damaged fuel can may be used in any W74 canister, each damaged fuel can will only be identified by a unique, permanently marked shop assembly

identification number. Each damaged fuel can identification mark will be inspected during fabrication and preoperation for accuracy and legibility

9.2 Maintenance Program

This section discusses the maintenance program for the FuelSolutions™ W74 canister and damaged fuel can, which are both classified as important to safety. Noncompliances encountered during the required maintenance activities will be dispositioned in accordance with the BFS Quality Assurance program, discussed in Chapter 13 of the FuelSolutions™ Storage System FSAR, or the licensee's NRC-approved Quality Assurance program. The maintenance program is intended to demonstrate that the FuelSolutions™ W74 canister and any associated damaged fuel cans continue to perform properly and comply with regulatory requirements and the *technical specifications* contained in Chapter 12 of this FSAR and the FuelSolutions™ Storage System FSAR.

The FuelSolutions™ W74 canister and damaged fuel cans rely on no mechanical components or moving parts once in their storage configuration. Exposed materials (damaged fuel cans are completely housed inside W74 canisters and have no exposed materials) are corrosion-resistant stainless steel. No inspection of a loaded canister during storage is required due to the integrity of the canister, as verified during fabrication, acceptance testing, and canister closure. Periodic temperature monitoring of the FuelSolutions™ storage cask, in accordance with the *technical specification* contained in Section 12.3 of this FSAR, provides added assurance that fuel cladding degradation does not occur. Thus, no prescribed maintenance program is necessary during the 100-year design life of the FuelSolutions™ W74 canister or any associated damaged fuel cans.

This page intentionally left blank.

9.3 First Cask In Use Requirements

Section 9.3 of the FuelSolutions™ Storage System FSAR presents requirements for the first FuelSolutions™ storage cask loaded with a FuelSolutions™ W74 canister design to measure its heat removal performance and to establish baseline data.

This page intentionally left blank.

10. RADIATION PROTECTION

This chapter, along with Chapter 10 of the FuelSolutions™ Storage System FSAR,[1] describes the radiation design protection criteria and features; occupational exposures; public exposures, both for normal and postulated accident conditions; and ALARA considerations for the FuelSolutions™ Storage System using a FuelSolutions™ W74 canister.

Section 10.2 of the FuelSolutions™ Storage System FSAR describes radiation protection features for the FuelSolutions™ W100 Transfer Cask, the FuelSolutions™ W150 Storage Cask, and a generic FuelSolutions™ canister. This chapter identifies the canister specific design and operational differences between the FuelSolutions™ W74 canister and the more general canister described in the FuelSolutions™ Storage System FSAR.

Storage of BRP MOX, partial, and damaged fuel assemblies has no effect on the FuelSolutions™ W74 canister radiation protection. As discussed in Chapter 5 of this FSAR, the dose rates for BRP MOX, partial, and damaged fuel assemblies are bounded by those for intact BRP UO_2 assemblies. There are no operational differences (of dose significance) for loading or storing MOX or partial fuel assemblies, as noted in Chapter 8 of this FSAR. As discussed in Chapter 7 of this FSAR, off-site doses due to atmospheric release of radionuclides for W74 canisters containing MOX, partial, and damaged BRP assemblies are bounded by the doses calculated for design basis intact UO_2 BRP fuel.

Therefore, the occupational exposures for the W74 canister provided in this chapter, are conservative for operations associated with loading BRP MOX, partial, or damaged fuel assemblies.

The radiation protection features of the FuelSolutions™ Storage System, including the operational features that minimize occupational and off-site radiation exposures, are discussed in Section 10.3 of the FuelSolutions™ Storage System FSAR. Application of ALARA principles and evaluation of off-site doses are also provided in Chapter 10 of the FuelSolutions™ Storage System FSAR.

[1] WSNF-220, *FuelSolutions™ Storage System Final Safety Analysis Report*, NRC Docket 72-1026, BNFL Fuel Solutions Corporation.

This page intentionally left blank.

10.1 Ensuring that Occupational Radiation Exposures Are As Low As Is Reasonably Achievable (ALARA)

The policy, design, and operational considerations described in Section 10.1 of the FuelSolutions™ Storage System FSAR are applicable to the FuelSolutions™ W74 canister.

This page intentionally left blank.

10.2 Radiation Protection Design Features

The radiological protection design features described in Section 10.2 of the FuelSolutions™ Storage System FSAR are applicable to the FuelSolutions™ W74 canister. In addition, the W74 canister has a segmented top shield plug assembly to facilitate fuel loading outside the spent fuel pool as described in Sections 1.2.1.3 and 1.2.2 of this FSAR.

This page intentionally left blank.

10.3 Estimated On-Site Collective Dose Assessment

The estimated on-site collective dose assessment performed in Chapter 10 of the FuelSolutions™ Storage System FSAR for a typical FuelSolutions™ canister applies to the FuelSolutions™ W74 canister. The following sections describe the key design and operational differences and discuss how they affect the estimates.

10.3.1 FuelSolutions™ W74 Canister-Unique Considerations

The W74 canister is designed exclusively for Big Rock Point SNF and high level waste. Currently, this material exists in two locations: at the Big Rock Point (BRP) plant and at the DOE's West Valley facility. The Big Rock Point plant was shut down in late 1997, therefore the characteristics of the SNF population is known and static.

10.3.1.1 Canister Design Differences that Affect Occupational Exposures

The W74 canister is a full height FuelSolutions™ canister with stackable upper and lower basket assemblies as described in Section 1.2.1.3 of this FSAR. The lower basket assembly is non-removable and must be loaded first or unloaded last. The upper basket assembly is removable in order to load or unload the lower basket. Because of the extra step necessary to handle and load the top basket assembly, this design difference may increase occupational exposure by a small amount for fuel movements to/from the canister using a fuel assembly shuttle cask.

The W74 canister shell assembly is similar to other FuelSolutions™ canisters, except that the top shield plug assembly is segmented such that one of 37 individual shield plugs may be removed to load each SNF assembly. This allows fuel loading to be performed in a spent fuel pool using standard practices, or outside the spent fuel pool as described in Section 1.2.2.1 of this FSAR. This design difference may increase occupational exposure if extra time and steps are necessary to transfer each fuel assembly from the fuel pool to the canister and to handle the individual shield plugs.

10.3.1.2 Canister Operations Differences that Affect Occupational Exposures

The W74 canister may be loaded using typical FuelSolutions™ in-pool loading procedures modified for the W74-unique design features, or it may be loaded using a fuel assembly shuttle cask outside the spent fuel pool if required by plant crane capacity or dimensional constraints. In-pool loading occupational exposures are not expected to differ greatly from the dose estimates for typical FuelSolutions™ canisters provided in Chapter 10 of the FuelSolutions™ Storage System FSAR because the highest exposure operations would be performed underwater. Therefore, the subject of this section is the fuel loading option outside the spent fuel pool.

Loading a W74 canister outside the spent fuel pool using a fuel assembly shuttle cask is performed with the empty canister and transfer cask positioned in the plant's cask receiving area. During fuel loading operations, the canister is flooded with water to minimize occupational exposure. The most significant differences for estimating occupational exposure are the operations necessary to dock and align the shuttle cask, and the operations necessary to pick or place the upper basket assembly. Procedures require the whole canister cavity to be filled with water during this operation to provide the maximum amount of shielding possible.

The shielding provided by the water column above the loaded lower basket for this condition is greater than that offered by the shield plug alone. Therefore, the shielding analysis presented in Chapter 5 of the FuelSolutions™ Storage System FSAR is also conservatively applicable to the FuelSolutions™ W74 canister. Because water is such an effective neutron shield, all significant neutron flux in the half-loaded configuration is attenuated in the first few feet of water. The gamma attenuation through a FuelSolutions™ top shield plug is about 10,000[2], which is equivalent to about 74" of water[2]. Since the water column above the top of the fuel in the lower W74 basket is about 94", using the typical FuelSolutions™ canister top end dose rates is conservative for FuelSolutions™ W74 canister fuel loading operations. The dose rates for the remaining W74 canister closure, transfer, and dry storage operation are the same as the typical FuelSolutions™ canister.

If a shuttle cask is used to move single assemblies from the pool to the canister (inside the transfer cask), the dose rate on the shuttle cask surface must be considered. If this dose rate is significantly higher than the transfer cask surface dose rate, it may affect the occupational exposure estimates for the canister loading process. However, if the shuttle cask surface dose rate is lower than that of the transfer cask, the transfer cask dose rates will govern the canister loading occupational exposure.

10.3.2 On-Site Exposure Estimate

The estimates for W74 canister loading and unloading, based on dose rate estimates from Chapter 5 of the FuelSolutions™ Storage System FSAR and the operating procedures provided in Chapter 8 of this FSAR, are shown in Table 10.3-1 and Table 10.3-2, respectively.

Exposures during on-site storage of FuelSolutions™ W74 canisters are expected to be similar to estimates made in Chapter 10 of the FuelSolutions™ Storage System FSAR because storage cask dose rates for the W74 canister are expected to be less than the "typical" SNF sources used in the FuelSolutions™ Storage System FSAR shielding analysis. There is additional conservatism because a FuelSolutions™ W74 canister ISFSI has fewer casks than the sample 8x8 array assumed for the FuelSolutions™ Storage System FSAR analysis. The occupational exposure estimates given in Table 10.3-1 for the canister loading process are based on the transfer cask side surface dose rate. Thus, the calculations assume that the shuttle cask surface dose rate is not significantly higher than that of the transfer cask.

[2] ANS/SD-76/14, *A Handbook of Radiation Shielding Data*, J. Courtney, ed., Nuclear Science Center, Louisiana State University, July 1976.

Table 10.3-1 - Estimated Cumulative Occupational Exposure for Placing Fuel into Dry Storage

Ch. 8 Sequence Number	Description	Primary Source	W100 Configuration									Effective				"Typical" Person-mrem	"Bounding" Person-mrem
			Wet?			Installed?											
			Canister Cavity	Annulus	Cask Neutron Shield	Inner Closure Plate	Outer Closure Plate	Welder	Cask Top Cover	Ram Access Cover	Cask Bottom Cover	Time in Field (hours)	Number of Personnel	"Typical" Dose Rate (mrem/hr)	"Bounding" Dose Rate (mrem/hr)		
Prepare for Fuel Loading																	
various	Prepare/Stage Transfer Cask and Canister	ambient										8	4	0.1	0.1	3	3
Load Canister																	
8.3.1	Stage Canister and Transfer Cask	ambient										4	6	0.1	0.1	2	2
8.3.2	Prepare Canister and Transfer Cask for Fuel Loading	ambient										2	4	0.1	0.1	1	1
8.3.3	Load Fuel into Lower Basket	W100	3	3	3							8	2	25.7	98.6	411	1578
8.3.4	Load Fuel into Upper Basket	W100	3	3	3							8	2	57.2	219	915	3504
8.3.5	Decontaminate Cask Exterior	W100	3	3	3							2	2	57.2	219	229	876
8.3.6	Install Canister Inner Closure Plate	W100	3	3	3	3		3				1	1	24.9	101	25	101
8.3.7	Drain and Backfill Canister with Helium	W100		3	3	3		3				0.25	1	67.5	289	17	72
8.3.8	Install Canister Outer Closure Plate	W100		3	3	3	3	3				1	1	26.2	161	26	161
Horizontal Canister Transfer																	
8.3.2.1	Prepare for Horizontal Canister Transfer	ambient										4	6	1	1	24	24
8.1.10.1	Install Transfer Cask Top Cover	W100			3	3	3		3	3	3	0.5	2	9.2	63.4	9	63
8.1.10.2	Downend Transfer Cask on Transfer Trailer	ambient										1	4	5	25	20	100
8.1.10.3	Tow Transfer Cask to ISFSI	W100			3	3	3		3	3	3	0.25	2	5	25	3	13
8.1.10.4	Stage Loaded Storage Cask	W100			3	3	3		3	3	3	4	6	1	1	24	24
8.1.10.5	Align/Dock Transfer Cask with Storage Cask	W100			3	3	3		3	3	3	0.25	2	40.6	212	20	106
8.1.10.6	Transfer the Canister to the Storage Cask	ambient			3	3	3		3	3	3	0.25	2	5	25	3	13
8.1.10.7	Upend and Position Storage Cask on ISFSI Pad	W150			3	3	3		3	3	3	2	4	10	50	80	400
Total																**1812**	**7041**

Note:
The steps for loading the canister are from Chapter 8 of this FSAR. The steps for horizontal canister transfer are from Section 8.2 of the FuelSolutions™ Storage System FSAR.

Table 10.3-2 - Estimated Cumulative Occupational Exposure for Retrieval of Fuel from Dry Storage

Ch. 8 Sequence Number	Description	Primary Source	W100 Configuration									Effective				"Typical" Person-mrem	"Bounding" Person-mrem
			Wet?			Installed?											
			Canister Cavity	Annulus	Cask Neutron Shield	Inner Closure Plate	Outer Closure Plate	Welder	Cask Top Cover	Ram Access Cover	Cask Bottom Cover	Time in Field (hours)	Number of Personnel	"Typical" Dose Rate (mrem/hr)	"Bounding" Dose Rate (mrem/hr)		
Prepare for Canister Retrieval																	
8.3.1	Stage Canister and Transfer Cask	none												0.1	0.1	0	0
Retrieve Canister																	
8.2.1.1	Prepare Loaded Storage Cask	W150										8	2	8.2	28.7	131	459
8.2.1.2	Align and Dock Transfer Cask with Storage Cask	W150										0.25	2	5.8	18.9	3	9
8.2.1.3	Transfer Canister to the Transfer Cask	W100		3	3	3	3				3	0.25	2	5	25	3	13
8.2.1.4	Prepare Transfer cask for Onsite Transport	W100		3	3	3	3				3	1	4	40.6	212	162	848
8.2.1.5	Move Canister and Transfer Cask to Decon Area	W100		3	3	3	3		3	3	3	0.25	2	5	25	3	13
Unload Fuel																	
8.4.3.2	Prepare Canister for Vent and Fill	W100		3	3	3	3				3	1	1	19.8	101	20	101
8.4.3.3	Vent and Fill Canister with Water	W100		3	3	3	3				3	1	1	26.2	161	26	161
8.4.3.4	Remove the Canister Inner and Outer Closure Plates	W100	3	3	3	3		3			3	4	1	24.9	101	100	404
8.4.3.5	Prepare Canister and Transfer Cask for Unloading	W100	3	3	3						3	2	4	24.9	101	199	808
8.4.3.6	Remove Fuel from Upper Basket	W100	3	3	3						3	8	2	57.2	219	915	3504
8.4.3.7	Remove Fuel from Lower Basket	W100	3	3	3						3	8	2	25.7	98.6	411	1578
Total																**1973**	**7897**

Note:

The steps for unloading the canister are from Chapter 8 of this FSAR. The steps for horizontal canister retrieval are from Section 8.2 of the FuelSolutions™ Storage System FSAR.

10.4 Estimated Off-Site Collective Dose Assessment

10.4.1 Off-Site Dose for Normal Operations

The information provided in Section 10.4 of the FuelSolutions™ Storage System FSAR is conservatively applicable to the FuelSolutions™ W74 canister. The off-site doses provided in Section 10.4 of the Storage System FSAR is bounding for an ISFSI with W74 canisters/storage casks because of the relatively low source terms for BRP SNF and the fact that there are not enough BRP SNF assemblies to fill the 8x8 ISFSI array assumed for the FuelSolutions™ Storage System off-site dose analysis (the largest population of BRP fuel is at the Big Rock Point plant, where about seven canister's worth of SNF will be dry stored). Site-specific off-site dose analyses should consider these two factors.

10.4.2 Off-Site Dose for Off-Normal Conditions

The off-site dose for off-normal operations is also calculated in Section 10.4 of the Storage System FSAR. The same conservatisms apply as described above.

10.4.3 Off-Site Dose for Accident Conditions

Section 7.3 of this FSAR discusses the accident condition atmospheric release from a single canister and demonstrates compliance with 10CFR72.106(b). Assuming one W74 canister is leaking under accident internal pressure with 100% of the fuel rod cladding failed, and worst case meteorological conditions, the total effective equivalent dose vs. distance are presented for several distances in Table 7.3-1 and Figure 7.3-1. The results show that the 5 rem dose limit of 10CFR72.106(b) is met at the minimum controlled area boundary distance of 100 meters or greater.

This page intentionally left blank.

11. ACCIDENT ANALYSES

This chapter presents the evaluation of the FuelSolutions™ W74 canister for the effects of off-normal and postulated accident conditions. The design basis off-normal and postulated accident events, including those resulting from mechanistic and non-mechanistic causes as well as those caused by natural phenomena, are identified in Sections 2.3.2, 2.3.3, and 2.3.4 of this FSAR. For each postulated event, the event cause, means of detection, consequences, and corrective action are discussed and evaluated. As applicable, the evaluation of consequences include structural, thermal, shielding, criticality, confinement, and radiation protection evaluations for the effects of each design basis event on the FuelSolutions™ W74 canister.

The FuelSolutions™ W74 canister design is described in Section 1.2.1.3, and shown in Figure 1.2-2 of this FSAR. The structural, thermal, shielding, criticality, and confinement features and performance of the canister are discussed in Chapters 3, 4, 5, 6, and 7 of this FSAR. The evaluations provided in this chapter are based on the canister design features and evaluations described therein.

Storage of BRP mixed-oxide (MOX), partial, and damaged fuel assemblies introduces no new postulated accidents and has no effect on the accident analyses for the FuelSolutions™ W74 canister.

The evaluation of the design basis off-normal and postulated accident events on the FuelSolutions™ W150 Storage Cask and the W100 Transfer Cask are contained in Chapter 11 of the FuelSolutions™ Storage System FSAR.[1]

[1] WSNF-220, *FuelSolutions™ Storage System Final Safety Analysis Report*, NRC Docket 72-1026, BNFL Fuel Solutions Corporation.

This page intentionally left blank.

11.1 Off-Normal Operations

The FuelSolutions™ W74 canister is evaluated for all credible and significant design basis events resulting from off-normal operation. Off-normal conditions and events are defined in accordance with ANSI/ANS-57.9,[2] and include events which, although not occurring regularly, can be expected to occur with moderate frequency on the order of no more than once a year. As defined in Section 2.3.2 of this FSAR, off-normal events considered in the evaluation of the FuelSolutions™ W74 canister include the following:

- Extreme ambient conditions
- Off-normal internal pressure
- Potential misalignment of casks during horizontal canister transfer
- Potential failure of the hydraulic ram during horizontal transfer
- Reflood of the canister to facilitate fuel retrieval
- Off-normal fuel rod rupture (evaluated in conjunction with off-normal internal pressure)

The results of the evaluations performed herein demonstrate that the FuelSolutions™ W74 canister classes described in Section 1.2.1.3 can withstand the effects of off-normal events without affecting safety function, and are in compliance with the applicable acceptance criteria. The following sections present the evaluation of the FuelSolutions™ W74 canister for the design basis off-normal conditions which demonstrate that the requirements of 10CFR72.122[3] are satisfied, and that the corresponding radiation doses satisfy the requirements of 10CFR72.106(b) and 10CFR20.[4]

The load combinations evaluated for off-normal conditions are defined in Table 2.3-1. The load combinations include both normal loads which are evaluated in Section 3.5 of this FSAR and off-normal loads which are evaluated in Section 3.6. The off-normal load combination evaluations are discussed in Section 11.1.6.

The evaluation of the effects of off-normal conditions on the storage cask and transfer cask are provided in the FuelSolutions™ Storage System FSAR.

11.1.1 Off-Normal Temperature and Insolation Loadings

Many regions of the United States are subject to maximum summer temperatures in excess of 100ºF, and minimum winter temperatures that are significantly below 0°F. Therefore, to bound the expected temperatures of the storage cask during these short-term periods of extreme off-normal ambient conditions, conservative analyses are performed to calculate the steady-state W74 canister and fuel cladding temperatures for a maximum 125ºF ambient temperature with

---

[2] ANSI/ANS-57.9, *Design Criteria for an Independent Spent Fuel Storage Installation (Dry Storage Type)*, American National Standards Institute, 1984.

[3] Title 10, Code of Federal Regulations, Part 72 (10CFR72), *Licensing Requirements for the Independent Storage of Spent Nuclear Fuel and High-Level Radioactive Waste*, 1995.

[4] Title 10, Code of Federal Regulations, Part 20 (10CFR20), *Standards for Protection Against Radiation*, 1995.

maximum insolation, and for a minimum -40ºF ambient without insolation. The design basis heat loads for the W74 canister, as documented in Chapter 4 of this FSAR, are used for this analysis.

11.1.1.1 Postulated Cause of the Event

While off-normal fluctuations in ambient conditions vary with geographical location and seasons, the selected off-normal ambient conditions bound all historical records for extreme temperatures and insolation over the contiguous United States. Therefore, the probability of extreme temperatures exceeding the off-normal thermal design conditions is negligible.

11.1.1.2 Detection of the Event

No monitoring of the ambient conditions is required at the ISFSI since the assumed off-normal steady-state ambient conditions bound those expected throughout the contiguous United States.

11.1.1.3 Summary of Event Consequences and Regulatory Compliance

Structural

The structural evaluation of the canister for off-normal thermal conditions is discussed in Section 3.6.1 of this FSAR.

Thermal

The thermal analysis of the canister for off-normal thermal conditions is performed using the methodology, material properties, thermal models, and design basis heat loads described in Section 4.5 of this FSAR. The resulting off-normal canister and fuel assembly cladding temperatures for the hot and cold conditions are provided in Tables 4.5-1 and 4.5-3. As can be seen from these tables, all temperatures for off-normal conditions are within the allowable values described in Table 4.3-1 of this FSAR.

Shielding

There is no effect on the shielding performance of the canister as a result of this off-normal event.

Criticality

There is no effect on the criticality control features of the canister as a result of this off-normal event.

Confinement

There is no effect on the confinement function of the canister as a result of this off-normal event.

Radiation Protection

Since there is no degradation in shielding or confinement capabilities as discussed above, there is no effect on occupational or public exposures as a result of this off-normal event.

11.1.1.4 Corrective Actions

The FuelSolutions™ W74 canister is conservatively designed to safely accommodate steady-state extreme off-normal ambient conditions. Therefore, no corrective actions are required.

11.1.2 Off-Normal Internal Pressure

As discussed in Section 2.3.2.2 and summarized in Table 2.0-1 of this FSAR, the design basis off-normal condition internal pressure for the FuelSolutions™ W74 canister is 16 psig. The maximum internal pressure for this condition, as calculated in Section 4.5 of this FSAR, is based upon the required helium backfill in accordance with the *technical specification* provided in Section 12.3, elevated to the extreme off-normal condition canister cavity gas temperature. In addition, a concurrent non-mechanistic failure of 10% of the fuel rods with complete release of their fill gas and 30% of their fission gasses into the canister cavity elevated to the extreme off-normal condition canister cavity gas temperature is assumed. The resulting calculated internal pressure is shown in Table 4.1-5.

11.1.2.1 Postulated Cause of the Event

After fuel assembly loading, the canister is drained, dried, and backfilled with an inert cover gas (helium) to assure long-term cladding integrity during dry storage. Therefore, the probability of failure of intact rods in dry storage is low. Nonetheless, such an event is postulated and evaluated.

11.1.2.2 Detection of the Event

No monitoring of the canister internal pressure is required since the canister design is adequate to withstand the design basis off-normal internal pressure.

11.1.2.3 Summary of Event Consequences and Regulatory Compliance

Structural

The structural evaluation of the canister for off-normal internal pressure conditions is described in Section 3.6 of this FSAR. The resulting stresses for this loading condition are provided in Table 3.6-1. As discussed in Section 3.6.2, all stresses are within the allowable values.

Thermal

The canister internal pressure for off-normal conditions is performed using the methodology, material properties, thermal models, and design basis heat loads described in Section 4.5 of this FSAR. The temperatures resulting from the off-normal thermal analysis are used to determine the corresponding internal pressure provided in Table 4.5-2. As can be seen from these tables, the 16 psig design basis internal pressure used in the structural evaluation described above bounds these calculated values.

Shielding

There is no effect on the shielding performance of the canister as a result of this off-normal event.

Criticality

There is no effect on the criticality control features of the canister as a result of this off-normal event.

Confinement

As discussed in the structural evaluation above, all stresses remain within allowable values, assuring canister integrity. The effects of this event on the release for the design basis canister leak rate is evaluated in Section 7.2 of this FSAR.

Radiation Protection

The postulated release will result in an increase in dose to the public. The analysis of this event is provided in Section 7.2 of this FSAR, and the resulting occupational exposures and off-site doses are addressed in Sections 10.3 and 10.4 of this FSAR, respectively.

11.1.2.4 Corrective Actions

The FuelSolutions™ W74 canister is conservatively designed to safely accommodate the internal pressure resulting from this off-normal condition. Therefore, no corrective actions are required.

11.1.3 Cask Misalignment During Horizontal Canister Transfer

The FuelSolutions storage system is evaluated for a maximum hydraulic ram load of 70 kips pushing or 50 kips pulling resulting from cask misalignment or interference during horizontal canister transfer as defined in Section 2.3.2.3 of this FSAR. The ram load is applied on either the top or bottom end of the canister shell assembly; however the limiting case is the pulling condition because the outer closure plate is required to carry the entire transfer load. For the pushing case the shield plug and inner closure plate also assist in carrying the load, resulting in significantly less strain in the outer closure plate and therefore, lower stresses. The structural consequences of this event are evaluated for all horizontal canister transfer scenarios.

11.1.3.1 Postulated Cause of the Event

As described in Section 1.2.2.3 of the FuelSolutions™ Storage System FSAR, a hydraulic ram is used during horizontal transfer of the canister to the casks. The ram slides the canister from cask to cask by pushing or pulling it between the storage cask and the transfer cask; the transfer cask and the transportation cask; or the storage cask and the transportation cask. Under normal conditions, the hydraulic ram loads are equal to the force required to overcome friction forces between the canister shell and the cask guide rails. Prior to performing horizontal canister transfer operations, the casks are docked, closely aligned, and secured together to prevent shifting or separation. In addition, beveled lead-ins are provided on the ends of the canister shell, cask openings and the cask guide rails to minimize the possibility of interference during horizontal transfer. However, it is postulated that in the unlikely event that the storage cask and the transfer cask, the transfer cask and the transportation cask, or the storage cask and the transportation cask are not properly aligned during transfer, the hydraulic ram load could exceed the normal design loads.

11.1.3.2 Detection of the Event

During horizontal transfer operations, the hydraulic ram pressure (load) is monitored. In addition, the hydraulic ram loads are limited by the hydraulic system using automatic shut-off switches so that normal condition ram loads are not exceeded. If the hydraulic system shuts down, indicating the possibility of a misalignment or interference, the operator may use override

controls to increase the hydraulic ram loads up to the maximum design load of 70 kips pushing or 50 kips pulling after rechecking the cask for proper alignment. The override controls do not allow hydraulic ram loads to be increased above the maximum design load.

11.1.3.3 Summary of Event Consequences and Regulatory Compliance

Structural

The stress evaluation of the canister for increased ram force postulated to occur due to misalignment is discussed in Section 3.6.3 of this FSAR. The resulting stresses for this condition are provided in Table 3.6-1. All stresses are within the allowable values.

Thermal

There is no effect on the thermal performance of the canister as a result of this off-normal event.

Shielding

There is no effect on the shielding performance of the canister as a result of this off-normal event.

Criticality

There is no effect on the criticality performance of the canister as a result of this off-normal event.

Confinement

There is no effect on the confinement performance of the canister as a result of this off-normal event.

Radiation Protection

As there is no degradation in shielding or confinement capabilities, there is no effect on public exposures as a result of this off-normal event.

Recovery from this event, as discussed in Section 11.1.3.4, results in slight increases in occupational exposure due to the additional recovery operations. The estimated occupational exposure for recovery operations is discussed in Section 11.1.2.3.1 of the FuelSolutions™ Storage System FSAR.

11.1.3.4 Corrective Actions

The corrective action for a canister misalignment or interference is discussed in Section 11.1.2.4 of the FuelSolutions™ Storage System FSAR.

11.1.4 Hydraulic Ram Failure During Horizontal Transfer

The FuelSolutions™ storage system is evaluated for the effects of failure of the hydraulic ram during horizontal canister transfer operations, as defined in Section 2.3.2.5 of this FSAR.

11.1.4.1 Postulated Cause of the Event

The postulated cause of this event is discussed in Section 11.1.3.1 of the FuelSolutions™ Storage System FSAR.

11.1.4.2 Detection of the Event

The detection of this event is discussed in Section 11.1.3.2 of the FuelSolutions™ Storage System FSAR.

11.1.4.3 Summary of Event Consequences and Regulatory Compliance

Structural

There are no structural consequences as a result of this postulated event.

Thermal

In Section 4.5.2 of this FSAR, a thermal analysis of the canisters is performed for the transfer cask in the horizontal position for off-normal conditions. This analysis, as described in Section 4.5.2, shows that under steady-state conditions, no canister components exceed the allowable temperatures in the transfer cask.

For the storage cask, the cask liner thermocouple temperature is monitored in accordance with the *technical specification* in Section 12.3 of this FSAR, and corrective actions completed as necessary. The canister temperatures while in the horizontal storage cask is discussed in Section 4.5.1 and reported in Table 4.5-1 of this FSAR.

Shielding

There are no effects on the shielding performance of the canisters as a result of this off-normal event.

Criticality

The are no effects on the criticality performance of the canisters as a result of this off-normal event.

Confinement

There are no effects on the confinement function of the canisters as a result of this off-normal event.

Radiation Protection

As there is no degradation in shielding or confinement, there is no effect on public exposures as a result of this off-normal event. Effects of recovery from this event are discussed in Section 11.1.3.3 of the FuelSolutions™ Storage System FSAR.

11.1.4.4 Corrective Action

The corrective action for this event is discussed in Section 11.1.3.4 of the FuelSolutions™ Storage System FSAR.

11.1.5 Canister Reopening/Reflood

The FuelSolutions™ W74 canister is evaluated for the effects of reflooding the canister after the canister cavity is drained and dried. This could occur prior to or after dry storage. The limiting internal pressure for this condition is 100 psig as defined in Section 2.3.2.4 of this FSAR. The

evaluation provided in this section demonstrates that the FuelSolutions™ W74 canister can accommodate the reflood condition without compromising the integrity of the canister.

11.1.5.1 Postulated Cause of the Event

Under normal conditions, reopening and/or reflooding of the FuelSolutions™ W74 canister is not anticipated to occur. However, it may be required to reflood the canister to remove the fuel for an undetermined reason, possibly for transfer of title of the SNF to DOE. Therefore, the event is postulated and evaluated.

11.1.5.2 Detection of the Event

Reflooding of the canister is a planned activity.

11.1.5.3 Analysis of Effects and Consequences

Structural

The stress evaluation of the canister for internal pressure resulting from the reflood is provided in Section 3.6.4 of this FSAR. All stresses are within the allowable values. The resulting canister pressure stresses are summarized in Table 3.6-1. The fuel cladding thermal stress effects due to reflood are discussed in Section 4.4.2.3 of this FSAR and shown to remain within allowable values.

Thermal

The thermal evaluation of the canister during reflood conditions is provided in Section 4.4.2.3 of this FSAR. All material temperatures remain within the off-normal allowable temperatures for this condition as defined in Table 4.3-1.

Shielding

There is no effect on the shielding performance of the canister as a result of this activity.

Criticality

There is no effect on the criticality performance of the canister as a result of this activity. The canister is evaluated for a full range of pure water moderator densities, as described in Chapter 6 of this FSAR, and evaluated for the most reactive moderator density. No soluble boron credit is taken in the criticality analysis. Therefore, the criticality evaluation bounds the conditions expected during reflood.

Confinement

Since this operation is predicated upon opening the canister, there is no confinement function provided by the canister during this activity.

Radiation Protection

As there is no degradation in shielding or confinement capabilities, there is no effect on public exposures as a result of this off-normal operation. Performing this operation results in occupational exposure which is estimated to be equivalent to the occupational exposure incurred for canister draining, drying, and closure operations. Sampling of the canister internal atmosphere prior to reflood is performed, as discussed in Section 8.2.3.2 of the FuelSolutions™

Storage System FSAR, to preclude unanticipated release of radionuclides. The occupational exposures for these operations is discussed in Section 10.3 of the FuelSolutions™ Storage System FSAR.

11.1.5.4 Corrective Action

There is no corrective action for this off-normal operation.

11.1.6 Off-Normal Load Combinations

Load combinations for off-normal conditions are performed for the FuelSolutions™ W74 canister in accordance with Section 2.3.5 of this FSAR. The load combinations include normal loads, which are evaluated in Section 3.5, and off-normal loads, which are evaluated in Section 3.6. The load combination results for the canister are reported in Table 3.6-2. As shown in the table, all stresses are within allowable values.

11.2 Accidents

The FuelSolutions™ W74 canister is evaluated for a range of postulated accidents and natural phenomena, as defined in Sections 2.3.3 and 2.3.4 of this FSAR. The design basis postulated accident conditions and natural phenomena considered are in accordance with ANSI/ANS-57.9, and include events which are postulated because their consequences may result in maximum potential impact on the immediate environs. Evaluations are performed for a range of postulated accidents, including those with the potential to result in an annual dose greater than 25 mrem outside the controlled area in accordance with 10CFR72. The design basis postulated accident and natural phenomena events evaluated for the W74 canister include the following:

- Fully blocked storage cask inlet and outlet vents
- Cask drop and tip over
- Fire
- Flood
- Earthquake
- Accident internal pressure
- Accident fuel rod rupture (evaluated in conjunction with accident internal pressure)

As discussed in Sections 2.3.3 and 2.3.4, the canister is not subjected to loads due to explosive overpressure; tornado; wind; burial under debris; lightning; and snow and ice.

The results of the evaluations performed herein demonstrate that the FuelSolutions™ W74 canister classes and types described in Section 1.2.1.3 can withstand the effects of all credible accident conditions and natural phenomena without affecting safety function, and are in compliance with the applicable acceptance criteria. The following sections present the evaluation of the FuelSolutions™ W74 canister for the design basis postulated accident conditions and natural phenomena which demonstrate that the requirements of 10CFR72.122 are satisfied, and that the corresponding radiation doses satisfy the requirements of 10CFR72.106(b) and 10CFR20.

The load combinations evaluated for postulated accident conditions are defined in Table 2.3-1. The load combinations include normal loads which are evaluated in Section 3.5, off-normal loads which are evaluated in Section 3.6, and accident loads which are evaluated in Section 3.7. The accident load combination evaluations are provided in Section 3.7.

The evaluation for the effects of the design basis postulated accident events on the FuelSolutions™ W150 Storage Cask and W100 Transfer Cask is provided in the FuelSolutions™ Storage System FSAR.

11.2.1 Fully Blocked Storage Cask Inlet and Outlet Vents

The FuelSolutions™ W74 canister, loaded with design basis fuel assemblies and dry stored vertically in the storage cask, is evaluated for a postulated accident thermal event in which complete blockage of all storage cask inlet and outlet vents occurs.

A steady-state ambient temperature of 100°F with insolation, as defined in Section 2.3 and listed in Table 2.3-2 of the FuelSolutions™ Storage System FSAR, are conservatively postulated to occur concurrently.

11.2.1.1 Postulated Cause of the Event

The postulated cause of this event is discussed in Section 11.2.1.1 of the FuelSolutions™ Storage System FSAR.

11.2.1.2 Detection of the Event

The detection of this event is discussed in Section 11.2.1.2 of the FuelSolutions™ Storage System FSAR.

11.2.1.3 Summary of Event Consequences and Regulatory Compliance

Structural

The maximum canister internal pressure due to the postulated blocked vent accident is less than 30.0 psig as discussed in Section 4.6 of this FSAR.

The blocked vent condition pressure is much less than the design basis accident pressure of 69 psig. Therefore, the accident pressure analysis discussed in Section 11.2.8 bounds the pressure due to the blocked vent condition. Canister thermal stresses for this condition are bounded by other conditions, as discussed in Section 3.7.1 of this FSAR.

Thermal

As described in Section 4.6.1.2.1 of this FSAR, the concrete reaches its allowable temperature as a result of this event. As determined in Section 4.6.1 of this FSAR, the FuelSolutions™ W74 canister cladding temperature is 402ºC at the time the peak temperature is reached, which is well below the short-term allowable cladding temperature of 570ºC. Also as shown in Section 4.6.1, the basket material temperatures remain within the short-term allowable material temperatures defined in Table 4.3-1.

Shielding

There is no effect on the shielding performance of the canister as a result of this postulated event.

Criticality

There is no effect on the criticality control features of the canister as a result of this postulated event.

Confinement

There is no effect on the confinement function of the canister as a result of this postulated event.

Radiation Protection

Since there is no degradation in shielding or confinement, there is no effect on public exposures as a result of this postulated event. Occupational exposure resulting from recovery from this event is discussed in Section 11.2.1.3 of the FuelSolutions™ Storage System FSAR.

11.2.1.4 Corrective Action

The corrective action for this event is discussed in Section 11.2.1.4 of the FuelSolutions™ Storage System FSAR.

11.2.2 Storage Cask Drop

The storage cask is evaluated for a drop as discussed in Section 2.3.3.2.1 and evaluated in Section 3.7 of the FuelSolutions™ Storage System FSAR. The accidental storage cask drop scenario is a postulated vertical end drop onto the bottom end of the storage cask. The FuelSolutions™ W74 canister is evaluated for the deceleration loads resulting from this postulated drop scenario.

11.2.2.1 Postulated Cause of the Event

The postulated cause of this event is discussed in Section 11.2.2.1 of the FuelSolutions™ Storage System FSAR.

11.2.2.2 Detection of the Event

The detection of this event is discussed in Section 11.2.2.2 of the FuelSolutions™ Storage System FSAR.

11.2.2.3 Summary of Event Consequences and Regulatory Compliance

Structural

The canister shell assembly stress evaluation is provided in Section 3.7.3 of this FSAR. The resulting stresses due to the postulated storage cask end drop accident for the canister shell assembly components are summarized in Table 3.7-1. Similarly, the canister basket stress results are provided in Table 3.7-2. All stresses are within allowable values.

Thermal

The temperatures of the storage cask, canister, and fuel cladding may be affected by a postulated accidental drop of the storage cask as a result of damage to the storage cask vents and/or heat shield. The thermal effects of the end drop condition with the storage cask in the vertical orientation are enveloped by the fully blocked vent condition which is evaluated in Section 11.2.1.

Shielding

There is no effect on the shielding performance of the canister as a result of this event. The effects on shielding performance of the storage cask as a result of this postulated accident are addressed in Section 11.2.2 of the FuelSolutions™ Storage System FSAR.

Criticality

There is no effect on the criticality performance of the basket as a result of this postulated accident, as the canister basket components remain within their allowable stress values and the guide tubes remain elastic. Therefore there is no change in basket geometry.

Confinement

There is no effect on the confinement performance of the canister as a result of this postulated accident, as the canister shell components remain within their allowable stress values. Therefore, the canister shell will remain intact.

Radiation Protection

As there is no effect in the shielding or confinement performance of the canister, the canister has no effect on public exposures as a result of this event.

The discussion of public exposure resulting from the effects of this postulated accident on the storage cask is provided in Section 11.2.2.3 of the FuelSolutions™ Storage System FSAR.

Occupational exposure resulting from recovery from this event is also discussed in Section 11.2.2.3 of the FuelSolutions™ Storage System FSAR.

11.2.2.4 Corrective Action

The corrective action for this event is discussed in Section 11.2.2.4 of the FuelSolutions™ Storage System FSAR.

11.2.3 Storage Cask Tip Over on J-Skid

The storage cask is evaluated for a postulated accidental tip over event while on the J-skid as discussed in Section 2.3.3.3 and evaluated in Section 11.2.3 of the FuelSolutions™ Storage System FSAR. The FuelSolutions™ W74 canister is evaluated for the deceleration loads resulting from this tip over scenario.

11.2.3.1 Postulated Cause of the Event

The postulated cause of this event is discussed in Section 11.2.3.1 of the FuelSolutions™ Storage System FSAR.

11.2.3.2 Detection of the Event

The detection of this event is discussed in Section 11.2.3.2 of the FuelSolutions™ Storage System FSAR.

11.2.3.3 Summary of Event Consequences and Regulatory Compliance

Structural

The canister shell assembly and basket spacer plate stress evaluation is provided in Section 3.7.4 of this FSAR.

The structural effects of this event on the basket guide tubes are bounded by the postulated transfer cask side drop event, as discussed in Section 3.7.4 of this FSAR.

The resulting stresses due to the postulated transfer cask side drop accident for the canister shell assembly components are summarized in Table 3.7-1. Similarly, the canister basket stress results are provided in Table 3.7-2. All stresses are within allowable values.

Thermal

The temperatures of the storage cask, canister, and fuel cladding may be affected by a postulated accidental tip over of the storage cask as a result of damage to the storage cask vents and/or heat shield. This condition will be less severe than the accident thermal full vent blockage condition which is evaluated in Section 11.2.1. The results of the postulated vent blockage show that the canister temperatures remain within the short-term allowable temperatures.

The thermal effects of the tip over event with the storage cask in the horizontal orientation are enveloped by the corresponding normal conditions for horizontal canister transfer which is evaluated in Section 4.4.1 of the FuelSolutions™ Storage System FSAR.

A thermal analysis of the canister in the storage cask in the horizontal position under normal conditions is performed in Section 4.5.2 of this FSAR. The *technical specification* in Section 12.3 of this FSAR provides the limits and corrective actions should the allowable concrete temperature be exceeded. The *technical specification* provides corrective actions which assure that the canister allowable temperatures are not exceeded.

Shielding

There is no effect on the shielding performance of the canister as a result of this event. The effects on shielding performance of the storage cask as a result of this postulated accident are addressed in Section 11.2.3.3 of the FuelSolutions™ Storage System FSAR.

Criticality

As discussed in the structural evaluation above, the permanent deformation of the guide tube for the storage cask tip over is bounded by that for the transfer cask side drop. The effects on criticality for the side drop are discussed in Section 11.2.4.3.

Confinement

There is no effect on the confinement performance of the canister as a result of this postulated accident, as the canister shell components remain within their allowable stress values. Therefore the canister shell will remain intact.

Radiation Protection

As there is no effect in shielding or confinement performance of the canister, the canister has no effect on public exposures as a result of this event.

The discussion of public exposure resulting from the effects of this postulated accident on the storage cask is provided in Section 11.2.3.3 of the FuelSolutions™ Storage System FSAR.

Occupational exposure resulting from recovery from this event is also discussed in Section 11.2.3.3 of the FuelSolutions™ Storage System FSAR.

11.2.3.4 Corrective Action

The corrective action for this event is discussed in Section 11.2.3.4 of the FuelSolutions™ Storage System FSAR.

11.2.4 Transfer Cask Drop

The transfer cask is evaluated for a postulated accidental side drop event as discussed in Section 2.3.3.2.2 and evaluated in Section 3.7 of the FuelSolutions™ Storage System FSAR.

The FuelSolutions™ W74 canister is evaluated for the deceleration loads resulting from this non-mechanistic drop scenario.

11.2.4.1 Postulated Cause of the Event

The postulated cause of this event is non-mechanistic and is discussed in Section 11.2.4.1 of the FuelSolutions™ Storage System FSAR.

11.2.4.2 Detection of the Event

The detection of this event is discussed in Section 11.2.4.2 of the FuelSolutions™ Storage System FSAR.

11.2.4.3 Summary of Event Consequences and Regulatory Compliance

Structural

The canister shell assembly stress evaluation is provided in Section 3.7.5 of this FSAR.

The resulting stresses due to the postulated transfer cask side drop accident for the canister shell assembly components are summarized in Table 3.7-1. Similarly, the canister basket stress results are provided in Table 3.7-2. All stresses are within allowable values.

Also as discussed in Section 3.7.5 of this FSAR, the guide tube experiences a small permanent deformation as a result of this accident. The effects of this on the criticality evaluation are discussed in the criticality evaluation below.

Thermal

As discussed in Section 11.2.4.3 of the FuelSolutions™ Storage System FSAR, the transfer cask liquid neutron shield is assumed to be lost as a result of the side drop impact. This results in a reduction of the thermal conductivity through the cask wall, as the drained neutron shield cavity is assumed to be filled with air. The thermal effects of the transfer cask side drop event (i.e., loss of neutron shield) is discussed in Section 4.6.2 of this FSAR. The resulting maximum fuel cladding and canister material temperatures are well below the short-term allowable cladding temperature and the canister structural material allowable temperatures applicable for this postulated accident.

Shielding

There is no effect on the shielding performance of the canister as a result of this event. The effects on the shielding performance of the transfer cask, with the loss of neutron shielding, is evaluated in Section 11.2.4 of the FuelSolutions™ Storage System FSAR.

Criticality

As discussed in the structural evaluation above, the guide tube experiences permanent deformation as a result of this postulated accident. The criticality analysis for the accident condition is provided in Section 6.4.2 of this FSAR. As shown therein, the canister remains

subcritical for optimum moderator conditions, including all biases and uncertainties, for the postulated accident configuration.

Confinement

There is no effect on the confinement performance of the canister as a result of this postulated accident, as the canister shell components remain within their allowable stress values. Therefore, the canister shell will remain intact.

Radiation Protection

As there is no effect on shielding or confinement performance of the canister, the canister has no effect on public exposures as a result of this event.

The discussion of public exposure resulting from the effects of this postulated accident on the transfer cask is provided in Section 11.2.4.3 of the FuelSolutions™ Storage System FSAR.

Occupational exposure resulting from recovery from this event is also discussed in Section 11.2.4.3 of the FuelSolutions™ Storage System FSAR.

11.2.4.4 Corrective Action

The corrective action for this event is discussed in Section 11.2.4.4 of the FuelSolutions™ Storage System FSAR.

11.2.5 Fire

The FuelSolutions™ W74 canister in the storage cask is evaluated for a postulated accidental fire event. Evaluation of the storage cask and the transfer cask for this hypothetical fire accident is discussed in Section 11.2.5 of the FuelSolutions™ Storage System FSAR. The postulated fire accident is defined in Section 2.3.3.4 of the FuelSolutions™ Storage System FSAR.

11.2.5.1 Postulated Cause of the Event

The postulated cause of this event is discussed in Section 11.2.5.1 of the FuelSolutions™ Storage System FSAR.

11.2.5.2 Detection of the Event

The detection of this event is discussed in Section 11.2.5.2 of the FuelSolutions™ Storage System FSAR.

11.2.5.3 Summary of Event Consequences and Regulatory Compliance

Structural

As documented in Section 4.6, the maximum canister pressure as a result of the postulated fire accident is less than 30.0 psig.

The fire condition pressure is much less than the design basis accident pressure of 69 psig. Further, the external heating will act to reduce the thermal gradients on the canister, resulting in lower thermal gradients and therefore, lower stresses than for the normal ambient conditions, as discussed in Section 3.7.6.

Thermal

As discussed in Section 4.6, the fuel cladding and basket structural component temperatures for the postulated fire event result in temperatures which are less than the fuel cladding and material allowable temperatures.

Shielding

There is no effect on the shielding performance of the canister as a result of this event.

Criticality

There is no effect on the criticality control performance of the canister as a result of this event.

Confinement

There is no effect on the confinement performance of the canister as a result of this event.

Radiation Protection

As there is no degradation in shielding or confinement, there is no effect on public exposures as a result of this event. Occupational exposure resulting from recovery from this event is discussed in Section 11.2.5.3 of the FuelSolutions™ Storage System FSAR.

11.2.5.4 Corrective Action

The corrective action for this event is discussed in Section 11.2.5.4 of the FuelSolutions™ Storage System FSAR.

11.2.6 Flood

The FuelSolutions™ W74 canister is evaluated for the effects of an enveloping design basis flood, postulated to result from natural phenomena such as a tsunami and seiches, as specified by 10CFR72.122(b). For the purpose of this evaluation, a 50 foot flood height is used as defined in Section 2.3.4.1.

11.2.6.1 Postulated Cause of the Event

The postulated cause of this event is discussed in Section 11.2.7.1 of the FuelSolutions™ Storage System FSAR.

11.2.6.2 Detection of the Event

The detection of this event is discussed in Section 11.2.7.2 of the FuelSolutions™ Storage System FSAR.

11.2.6.3 Summary of Event Consequences and Regulatory Compliance

Structural

The storage cask has been shown not to tip over during flooding, and therefore, the canister is only subjected to the pressure effects of this postulated event. The 50 foot head of water results in an external pressure of 21.7 psig on the canister, as discussed in Section 2.3.4.1. As discussed in Section 3.7.7, the effects of this loading are bounded by the accident internal pressure effects evaluated in Section 11.2.8.

Thermal

Under postulated flood conditions, the storage cask vents and annular space are filled with water. While this precludes the natural convective air flow relied upon for heat removal during normal storage conditions, the water provides superior heat transfer, and the large thermal mass of the flood water results in lower temperatures than those associated with normal storage conditions as discussed in Section 4.6.1 of the FuelSolutions™ Storage System FSAR. For the case of only the inlet vents blocked, either by flood waters or by debris left as a result of flooding, this condition is bounded by the blocked vent case discussed in Section 11.2.1.

Shielding

There is no reduction in shielding performance as a result of this postulated accident.

Criticality

There is no reduction in criticality control performance of the canister as a result of this postulated accident. Since the canister shell assembly remains intact, there is no water inside the canister as a result of this event. The presence of water outside the canister and cask is bounded by the reflector conditions assumed in the criticality analysis as discussed in Chapter 6.

Confinement

There is no reduction in confinement capability of the canister as a result of this postulated accident.

Radiation Protection

Since there is no effect on shielding and confinement performance of the canister, there is no effect on radiation protection.

11.2.6.4 Corrective Action

The corrective action for this event is discussed in Section 11.2.7.4 of the FuelSolutions™ Storage System FSAR.

11.2.7 Earthquake

The FuelSolutions™ W74 canister is evaluated for the effects of seismic loads during dry storage in the storage cask and during on-site transport in the transfer cask.

11.2.7.1 Postulated Cause of the Event

The postulated cause of this event is discussed in Section 11.2.9.1 of the FuelSolutions™ Storage System FSAR.

11.2.7.2 Detection of the Event

The detection of this event is discussed in Section 11.2.9.2 of the FuelSolutions™ Storage System FSAR.

11.2.7.3 Summary of Event Consequences and Regulatory Compliance

Structural

Design basis seismic accelerations for the canister are evaluated in Section 3.7.8 of this FSAR. The resulting basket stresses are summarized in Table 3.7-2. All stresses are within the allowable stress values.

As discussed in Section 3.7.8.1, the canister shell assembly stresses due to the design basis seismic loads are bounded by those due to postulated drop conditions.

Thermal

There is no effect on the thermal performance of the canister as a result of this postulated accident.

Shielding

There is no effect on the shielding performance of the canister as a result of this postulated accident.

Criticality

There is no effect on the criticality control performance of the canister as a result of this postulated accident.

Confinement

There is no effect on the confinement performance of the canister as a result of this postulated accident.

Radiation Protection

Since there is no effect on shielding and confinement, there is no effect on radiation protection.

11.2.7.4 Corrective Action

Since the canister is not compromised by this postulated accident, and since the storage cask and transfer cask are not compromised as documented in the FuelSolutions™ Storage System FSAR, no corrective actions are required.

11.2.8 Accident Internal Pressure

As discussed in Section 4.6 and summarized in Table 4.6-2, the accident condition internal pressure for the FuelSolutions™ W74 canister is 30.0 psig, which is less than the design basis pressure of 69 psig. The accident pressure is based upon the required helium backfill in accordance with the *technical specification* provided in Section 12.3, elevated to the extreme off-normal condition canister cavity gas temperature. In addition, a concurrent non-mechanistic failure of 100% of the fuel rods with complete release of their fill gas and 30% of their fission gasses into the canister cavity elevated to the extreme off-normal condition canister cavity gas temperature is assumed, as defined in Section 2.3.3.4.

11.2.8.1 Postulated Cause of the Event

After fuel assembly loading the canister is drained, dried, and backfilled with an inert cover gas (helium) to assure long-term cladding integrity during dry storage. Therefore, the probability of failure of intact rods in dry storage is low. Nonetheless, such an event is postulated and analyzed.

11.2.8.2 Detection of the Event

No monitoring of the canister internal pressure is required since the canister is adequate to withstand this postulated event.

11.2.8.3 Summary of Event Consequences and Regulatory Compliance

Structural

The stress evaluation of the canister for accident internal pressure condition is discussed in Section 3.7.9 of this FSAR. The resulting stresses for this condition are provided in Table 3.7-1. All stresses are within allowable values. The accident pressure load has no effect on the basket assembly.

Thermal

The canister internal pressure for accident conditions is performed using the methodology, material properties, thermal models, and design basis heat load described in Section 4.6 of this FSAR. The pressure results of the accident thermal analysis are provided in Table 4.6-2. The design basis internal pressure, which bounds this internal pressure, is used in the structural evaluation described above.

Shielding

There is no effect on the shielding performance of the canister as a result of this postulated event.

Criticality

There is no effect on the criticality control features of the canister as a result of this postulated event.

Confinement

As discussed in the structural evaluation above, all stresses remain within allowable values, assuring canister integrity. The effects of this event on the release for the design basis canister leak rate is evaluated in Section 7.3 of this FSAR.

Radiation Protection

The postulated release will result in a minimal increase in dose to the public. The analysis of this event is provided in Section 7.3 of this FSAR. As shown therein, this event results in dose rates to the public less than the limit established by 10CFR72.106(b).

11.2.8.4 Corrective Actions

The FuelSolutions™ W74 canister is designed to safely accommodate the internal pressure resulting from this postulated event. No corrective actions are required.

11.2.9 Accident Condition Load Combinations

Load combinations are performed for the FuelSolutions™ W74 canister as discussed in Section 3.7.10. The load combinations include normal loads, which are evaluated in Section 3.5; off-normal loads, which are evaluated in Section 3.6; and accident loads, which are evaluated in Section 3.7. The load combination results for the canister shell assembly are provided in Table 3.7-11 through Table 3.7-15. The load combination results for the canister basket assembly are provided in Table 3.7-16. As shown in the tables, all stresses are within allowable values.

12. OPERATING CONTROLS AND LIMITS

This chapter includes operational controls and limits *(technical specifications)* specific to the FuelSolutions™ W74 canister, including canister loading with qualified fuel assemblies. The FuelSolutions™ W74 canister payload specification includes Big Rock Point (BRP) mixed-oxide (MOX), partial, and damaged fuel assemblies.

The remaining controls and limits for the loading, closure, transfer, and dry storage of sealed FuelSolutions™ W74 canisters using the FuelSolutions™ W100 Transfer Cask and the FuelSolutions™ W150 Storage Cask in an ISFSI or CISF, as well as for canister retrieval and unloading, are presented in Chapter 12 of the FuelSolutions™ Storage System FSAR.[1]

[1] WSNF-220, *FuelSolutions™ Storage System Final Safety Analysis Report*, NRC Docket No. 72-1026, BNFL Fuel Solutions Corporation.

This page intentionally left blank.

12.1 Proposed Operating Controls and Limits

The areas where controls and limits specific to the FuelSolutions™ W74 canister are necessary to assure safe operation are shown in Table 12.1-1. The conditions and other characteristics noted in the table are selected based on the safety analyses for design basis normal, off-normal, and postulated accident conditions documented in previous chapters of this FSAR and in the FuelSolutions™ Storage System FSAR. The *technical specifications* are provided in Section 12.3.

Table 12.1-1 - Summary of FuelSolutions™ W74 Canister Operating Controls and Limits

Condition to be Controlled	Applicable Technical Specifications		FSAR Location	
			Storage System	Canister
Criticality Control	2.1.1	Fuel to be Stored		3
Confinement Boundary Integrity	3.1.3	Canister Leak Rate	3	
	3.1.4	Hydraulic Ram Force During Horizontal Canister Transfer	3	
Fuel Integrity	3.1.1	Canister Helium Backfill Density	3	
	3.1.3	Canister Leak Rate	3	
	3.3.2	Storage Cask Temperatures During Storage		3
Radiological Protection	3.2.1	Canister Surface Contamination	3	
	3.4.1	Storage Cask Dose Rates	3	
	3.6.1	Transfer Cask Surface Contamination	3	
Heat Removal Capability	3.1.1	Canister Helium Backfill Density		3
	3.3.1	Storage Cask Air Inlet and Outlet Openings	3	
Structural Integrity	3.1.5	Canister Vertical Time Limit in Transfer Cask		3
	3.3.2	Storage Cask Temperatures During Storage		3
	3.3.3	Storage Cask Temperatures During Horizontal Transfer		3
	3.5.1	Transfer Cask Structural Shell Temperature	3	

12.2 Development of Operating Controls and Limits

The FuelSolutions™ W74 canister operating controls and limits, and their bases, are provided in Section 12.3 of this FSAR. The FuelSolutions™W74 canister payload specification includes BRP mixed-oxide (MOX), partial, and damaged fuel assemblies.

The required dry run activities are discussed in Section 12.2 of the FuelSolutions™ Storage System FSAR.

This page intentionally left blank.

12.3 Supplemental Data

12.3.1 Technical Specifications and Bases for the FuelSolutions™ W74 Canister

The *technical specifications* and bases, in the Improved Technical Specification (ITS) format, are provided in this section. The specifications include BRP mixed-oxide (MOX), partial, and damaged fuel assemblies in addition to intact UO_2 assemblies.

This page intentionally left blank.

TECHNICAL SPECIFICATION AND BASES

FOR THE FuelSolutions™ W74 CANISTER

Amendment 2

Page

1.0 USE AND APPLICATION 1.1-1
1.1 Definitions 1.1-1
1.2 Logical Connectors 1.2-1
1.3 Completion Times 1.3-1
1.4 Frequency 1.4-1

2.0 FUNCTIONAL AND OPERATING LIMITS 2.0-1
2.1 Functional and Operating Limits 2.0-1
2.2 Functional and Operating Limits Violations 2.0-1

3.0 LIMITING CONDITION FOR OPERATION (LCO) APPLICABILITY 3.0-1

3.0 SURVEILLANCE REQUIREMENT (SR) APPLICABILITY 3.0-2

3.1 CANISTER INTEGRITY 3.1-1
3.1.1 W74 Canister Helium Backfill Density 3.1-1
3.1.2 Canister Vacuum Drying Pressure 3.1-2
3.1.3 Canister Leak Rate 3.1-3
3.1.4 Hydraulic Ram Force During Horizontal Canister Transfer 3.1-4
3.1.5 W74 Canister Vertical Time Limit in Transfer Cask 3.1-5

3.2 CANISTER RADIATION PROTECTION 3.2-1
3.2.1 Canister Surface Contamination 3.2-1

3.3 STORAGE CASK INTEGRITY 3.3-1
3.3.1 Storage Cask Air Inlet and Outlet Openings 3.3-1
3.3.2 Storage Cask Temperatures During Storage 3.3-2
3.3.3 Storage Cask Temperatures During Horizontal Transfer 3.3-5

3.4 TRANSFER CASK INTEGRITY 3.4-1
3.4.1 Transfer Cask Structural Shell Temperature 3.4-1

3.5 TRANSFER CASK RADIATION PROTECTION 3.5-1
3.5.1 Transfer Cask Surface Contamination 3.5-1

4.0 DESIGN FEATURES 4.0-1
4.1 Storage System 4.0-1
4.2 Storage Pad 4.0-2
4.3 Site Specific Parameters and Analyses 4.0-2

Page

5.0 ADMINISTRATIVE CONTROLS 5.0-1
5.1 Training Modules 5.0-1
5.2 Preoperational Testing and Training Exercises 5.0-1
5.3 Programs 5.0-1
5.4 Special Requirements for First System in Place 5.0-1

LIST OF TABLES

Table 2.1-1 FuelSolutions™ W74 Loading Specification W74-1 . . . . . 2.0-2
Table 2.1-2 FuelSolutions™ W74 Loading Specification W74-2 . . . . . 2.0-4
Table 2.1-3 FuelSolutions™ W74 Loading Specification W74-3 . . . . . 2.0-5
Table 2.1-4 FuelSolutions™ W74 Loading Specification W74-4 . . . . . 2.0-6
Table 2.1-5 FuelSolutions™ W74 Loading Specification W74-5 . . . . . 2.0-7
Table 2.1-6 FuelSolutions™ W74 Loading Specification W74-6 . . . . . 2.0-8
Table 2.1-7 UO_2 Fuel Assemblies Acceptable for Storage in the FuelSolutions™ W74 Canister 2.0-9
Table 2.1-8 MOX Fuel Assemblies Acceptable for Storage in the FuelSolutions™ W74 Canister 2.0-10
Table 2.1-9 Fuel Cooling Table W74-1-A 2.0-11
Table 2.1-10 Fuel Cooling Table W74-1-B 2.0-12
Table 4.1-1 FuelSolutions™ W74 Canister ASME Code Requirements Compliance Summary 4.0-3

1.0 USE AND APPLICATION

1.1 Definitions

NOTE

The defined terms of this section appear in capitalized type and are applicable throughout these Technical Specifications and Bases.

Term	Definition
ACTIONS	ACTIONS shall be that part of a Specification that prescribes Required Actions to be taken under designated Conditions within specified Completion Times.
CANISTER	The CANISTER is the storage container for SFAs approved for use at the ISFSI.
INDEPENDENT SPENT FUEL STORAGE INSTALLATION (ISFSI)	The facility within the perimeter fence licensed for storage of spent fuel within CANISTERs.
INTACT FUEL	Fuel assemblies with no known or suspected cladding defects greater than hairline cracks or pinhole leaks.
LOADING OPERATIONS	LOADING OPERATIONS include all licensed activities on a CANISTER while it is being loaded with fuel assemblies. LOADING OPERATIONS begin when the first fuel assembly is placed in the CANISTER and end when the CANISTER outer closure plate to shell weld examination is complete.
SPENT FUEL ASSEMBLIES (SFAs)	Irradiated nuclear fuel assemblies that are to be placed in a CANISTER for dry storage.
SPENT FUEL STORAGE SYSTEM (SFSS)	The storage components including the CANISTER, STORAGE CASK, and TRANSFER CASK.
STORAGE CASK	The cask that provides a shielded, ventilated storage environment for the loaded CANISTER. This cask is used for TRANSFER OPERATIONS.
STORAGE OPERATIONS	STORAGE OPERATIONS include all licensed activities that are performed at the ISFSI while a CANISTER containing spent fuel is sitting inside a STORAGE CASK on a storage pad within the ISFSI.

1.1 Definitions

Term	Definition
TRANSFER CASK	The cask that is used for SFA LOADING OPERATIONS and UNLOADING OPERATIONS, and for TRANSFER OPERATIONS.
TRANSFER OPERATIONS	TRANSFER OPERATIONS include all licensed activities that are performed on a CANISTER loaded with one or more fuel assemblies when it is being moved to and from the ISFSI. For movement to the ISFSI, TRANSFER OPERATIONS begin when the CANISTER outer closure plate to shell weld inspection is complete and end when the CANISTER is in the STORAGE CASK in its storage position on the storage pad within the ISFSI. For movement from the ISFSI, TRANSFER OPERATIONS begin when the STORAGE CASK is moved and end when the CANISTER is moved into a transportation cask or the spent fuel building.
UNLOADING OPERATIONS	UNLOADING OPERATIONS include all licensed activities on a CANISTER to be unloaded of the contained fuel assemblies. UNLOADING OPERATIONS begin when the CANISTER is ready to initiate removal of the CANISTER outer closure plate and end when the last fuel assembly is removed from the CANISTER.

1.0 USE AND APPLICATION

1.2 Logical Connectors

PURPOSE	The purpose of this section is to explain the meaning of logical connectors. Logical connectors are used in Technical Specifications (TS) to discriminate between, and yet connect, discrete Conditions, Required Actions, Completion Times, Surveillances, and Frequencies. The only logical connectors that appear in TS are AND and OR. The physical arrangement of these connectors constitutes logical conventions with specific meanings.
BACKGROUND	Several levels of logic may be used to state Required Actions. These levels are identified by the placement (or nesting) of the logical connectors and by the number assigned to each Required Action. The first level of logic is identified by the first digit of the number assigned to a Require Action and the placement of the logical connector in the first level of nesting (i.e., left justified with the number of the Required Action). The successive levels of logic are identified by additional digits of the Required Action number and by successive indentations of the logical connectors. When logical connectors are used to state a Condition, Completion Time, Surveillance, or Frequency, only the first level of logic is used, and the logical connector is left justified with the statement of the Condition, Completion Time, Surveillance, or Frequency.
EXAMPLES	The following examples illustrate the use of logical connectors. EXAMPLE 1.2-1 ACTIONS

CONDITION	REQUIRED ACTION	COMPLETION TIME
A. LCO not met	A.1 Verify... AND A.2 Restore...	

In this example the logical connector AND is used to indicate that when in Condition A, both Required Actions A.1 and A.2 must be completed.

EXAMPLES
(continued)

EXAMPLE 1.2-2

ACTIONS

CONDITION	REQUIRED ACTION	COMPLETION TIME
A. LCO not met	A.1 Stop... OR A.2.1 Verify... AND A.2.2.1 Reduce... OR A.2.2.2 Perform... OR A.3 Remove...	

This example represents a more complicated use of logical connectors. Required Actions A.1, A.2, and A.3 are alternative choices, only one of which must be performed as indicated by the use of the logical connector OR and the left justified placement. Any one of these three Actions may be chosen. If A.2 is chosen, then both A.2.1 and A.2.2 must be performed as indicated by the logical connector AND. Required Action A.2.2 is met by performing A.2.2.1 or A.2.2.2. The indented position of the logical connector OR indicates that A.2.2.1 and A.2.2.2 are alternative choices, only one of which must be performed.

1.0 USE AND APPLICATION

1.3 Completion Times

PURPOSE	The purpose of this section is to establish the Completion Time convention and to provide guidance for its use.
BACKGROUND	Limiting Conditions for Operation (LCOs) specify the lowest functional capability or performance levels of equipment required for safe operation of the facility. The ACTIONS associated with an LCO state Conditions that typically describe the ways in which the requirements of the LCO can fail to be met. Specified with each stated Condition are Required Action(s) and Completion Time(s).
DESCRIPTION	The Completion Time is the amount of time allowed for completing a Required Action. It is referenced to the time of discovery of a situation (e.g., equipment or variable not within limits) that requires entering an ACTIONS Condition unless otherwise specified, providing the facility is in a specified condition stated in the Applicability of the LCO. Required Actions must be completed prior to the expiration of the specified Completion Time. An ACTIONS Condition remains in effect and the Required Actions apply until the Condition no longer exists or the facility is not within the LCO Applicability. Once a Condition has been entered, subsequent subsystems, components, or variables expressed in the Condition, discovered to be not within limits, will <u>not</u> result in separate entry into the Condition unless specifically stated. The Required Actions of the Condition continue to apply to each additional failure, with Completion Times based on initial entry into the Condition.

1.3 Completion Times

EXAMPLES

The following examples illustrate the use of Completion Times with different types of Conditions and changing Conditions.

EXAMPLE 1.3-1

ACTIONS

CONDITION	REQUIRED ACTION	COMPLETION TIME
B. Required Action and associated Completion Time not met.	B.1 Perform Action B.1. AND B.2 Perform Action B.2.	12 hours 36 hours

Condition B has two Required Actions. Each Required Action has its own separate Completion Time. Each Completion Time is referenced to the time that Condition B is entered.

The Required Actions of Condition B are to complete action B.1 within 12 hours AND complete action B.2 within 36 hours. A total of 12 hours is allowed for completing action B.1 and a total of 36 hours (not 48 hours) is allowed for completing action B.2 from the time that condition B was entered. If action B.1 is completed within 6 hours, the time allowed for completing action B.2 is the next 30 hours because the total time allowed for completing action B.2 is 36 hours.

EXAMPLES
(continued)

EXAMPLE 1.3-2

ACTIONS

CONDITION	REQUIRED ACTION	COMPLETION TIME
A. One system not within limit.	A.1 Restore system to within limit.	7 days
B. Required Action and associated Completion Time not met.	B.1 Perform Action B.1. AND B.2 Perform Action B.2.	12 hours 36 hours

When it is determined that a system does not meet the LCO, Condition A is entered. If the system is not restored within 7 days, Condition B is also entered and the Completion Time clocks for Required Actions B.1 and B.2 start. If the system is restored after Condition B is entered, Condition A and B are exited, and therefore, the Required Actions of Condition B may be terminated.

EXAMPLES (continued)

EXAMPLE 1.3-3

ACTIONS

NOTE

Separate Condition entry is allowed for each component.

CONDITION	REQUIRED ACTION	COMPLETION TIME
A. LCO not met.	A.1 Restore compliance with LCO.	4 hours
B. Required Action and associated Completion Time not met.	B.1 Perform Action B.1. AND B.2 Perform Action B.2.	12 hours 36 hours

The Note above the ACTIONS Table is a method of modifying the Completion Time tracking. If this method of modifying the Completion Time tracking were only applicable to a specific Condition, the Note would appear in that Condition rather than at the top of the ACTIONS Table.

The Note allows Condition A to be entered separately for each component, and Completion Times tracked on a per component basis. When a component does not meet the LCO, Condition A is entered and its Completion Time starts. If it is determined that subsequent components do not meet the LCO, Condition A is entered for each component and separate Completion Times start and are tracked for each component.

IMMEDIATE

When “Immediately” is used as a Completion Time, the COMPLETION TIME Required Action should be pursued without delay and in a controlled manner.

1.0 USE AND APPLICATION

1.4 Frequency

PURPOSE	The purpose of this section is to define the proper use and application of Frequency requirements.
DESCRIPTION	Each Surveillance Requirement (SR) has a specified Frequency in which the surveillance must be met in order to meet the associated Limiting Condition for Operation (LCO). An understanding of the correct application of the specified Frequency is necessary for compliance with the SR. The "specified Frequency" is referred to throughout this section and each of the Specifications of Section 3.0, Surveillance Requirement (SR) Applicability. The "specified Frequency" consists of the requirements of the Frequency column of each SR, as well as certain Notes in the Surveillance column that modify performance requirements. Situations where a Surveillance could be required (i.e., its Frequency could expire), but where it is not possible or not desired that it be performed until sometime after the associated LCO is within its Applicability, represent potential SR 3.0.4 conflicts. To avoid these conflicts, the SR (i.e., the Surveillance or the Frequency) is stated such that it is only "required" when it can be and should be performed. With an SR satisfied, SR 3.0.4 imposes no restriction. The use of "met" or "performed" in these instances conveys specific meaning. A Surveillance is "met" only when the acceptance criteria are satisfied. Known failure of the requirements of a Surveillance, even without a Surveillance specifically being "performed," constitutes a Surveillance not "met".

EXAMPLES

The following examples illustrate the various ways that Frequencies are specified:

EXAMPLE 1.4-1

SURVEILLANCE REQUIREMENTS

SURVEILLANCE	FREQUENCY
Verify pressure within limit.	12 hours

Example 1.4-1 contains the type of SR most often encountered in the Technical Specifications (TS). The Frequency specifies an interval (12 hours) during which the associated Surveillance must be performed at least one time. Performance of the Surveillance initiates the subsequent interval. Although the Frequency is stated as 12 hours, an extension of the time interval to 1.25 times the interval specified in the Frequency is allowed by SR 3.0.2 for operational flexibility. The measurement of this interval continues at all times, even when the SR is not required to be met per SR 3.0.1 (such as when it is determined the equipment does not meet the LCO, a variable is outside specified limits, or the unit is outside the Applicability of the LCO). If the interval specified by SR 3.0.2 is exceeded while the cask is in a condition specified in the Applicability of the LCO, the LCO is not met in accordance with SR 3.0.1.

If the interval as specified by SR 3.0.2 is exceeded while the unit is not in a condition specified in the Applicability of the LCO for which performance of the SR is required, the Surveillance must be performed within the Frequency requirements of SR 3.0.2 prior to entry into the specified condition. Failure to do so would result in a violation of SR 3.0.4.

EXAMPLES (continued)

EXAMPLE 1.4-2

SURVEILLANCE REQUIREMENTS

SURVEILLANCE	FREQUENCY
Verify flow is within limits.	Once within 12 hours prior to starting activity AND 24 hours thereafter

Example 1.4-2 has two Frequencies. The first is a one-time performance Frequency, and the second is of the type shown in Example 1.4-1. The logical connector "AND" indicates that both Frequency requirements must be met. Each time the example activity is to be performed, the Surveillance must be performed prior to starting the activity.

The use of "once" indicates a single performance will satisfy the specified Frequency (assuming no other Frequencies are connected by "AND"). This type of Frequency does not qualify for the 25% extension allowed by SR 3.0.2.

"Thereafter" indicates future performances must be established per SR 3.0.2, but only after a specified condition is first met (i.e., the "once" performance in this example). If the specified activity is canceled or not performed, the measurement of both intervals stops. New intervals start upon preparing to restart the specified activity.

2.0 FUNCTIONAL AND OPERATING LIMITS

2.1 Functional and Operating Limits

2.1.1 Fuel to be Stored in the FuelSolutions™ W74 CANISTER.

SFAs meeting the limits specified in Tables 2.1-1 through 2.1-6 may be stored in a W74 CANISTER.

2.2 Functional and Operating Limits Violations

If any Functional and Operating Limits are violated, the following actions shall be completed. These actions are not a substitute for the reporting requirements contained in 10CFR72.75.

2.2.1 The affected fuel assemblies shall be placed in a safe condition without delay and in a controlled manner.

2.2.2 The NRC Operations Center shall be notified within 24 hours.

2.2.3 A special report will be provided to NRC within 30 days that describes the cause of the violation, the actions to restore compliance, and the actions to prevent recurrence.

Table 2.1-1
FuelSolutions™ W74 Loading Specification W74-1

W74-1 Payload Configuration Parameter	Intact UO_2 Fuel Assemblies Limit/Specification
Payload Description:	≤ 64 Big Rock Point BWR intact[1, 2] UO_2 fuel assemblies, as defined in Table 2.1-7. Any remaining empty canister basket guide tubes and/or support tubes may be loaded with fuel assemblies meeting any of the acceptable loading specifications W74-2 through W74-6, subject to the limitations of those specifications. If less than 64 total fuel assemblies are loaded, a dummy fuel assembly shall be placed into each empty CANISTER basket guide tube. Each dummy fuel assembly shall be the approximate weight and size of the actual fuel being loaded.
Cladding Material/Condition:	Zircaloy cladding with no known or suspected cladding defects greater than hairline cracks or pinhole leaks.
Initial Enrichment[3]:	≤ 4.10 w/o ^{235}U. The maximum acceptable enrichments shall not exceed the enrichments defined in Table 2.1-7.
Burnup:	≤ 40,000 MWd/MTU.
Cooling Time:	≥ 3.0 years. The minimum acceptable cooling time varies by fuel assembly class and enrichment, as a function of burnup; and is also dependent on the total cobalt content of the fuel and control components. The effects of the maximum acceptable decay heat, initial uranium content, and gamma and neutron sources are incorporated into the minimum cooling time determination. Fuel assemblies shall not be stored with less than the minimum acceptable cooling time indicated in Table 2.1-9.

Table 2.1-1 Notes:

(1) Intact fuel assemblies include those BRP fuel assemblies with 1 to 4 corner rods missing, and BRP 9x9 fuel assemblies with 1 rod missing from a non-corner location. This includes assemblies with partial length rods, or rod fragments inside stainless tubes, in any of the array corner locations. It also includes 9x9 assemblies with 11x11 assembly rods in corner locations.

(2) Intact assemblies may have any number of fuel rods replaced with solid zircaloy or stainless steel rods, or with poison rods. They may also have any object other than fuel rods placed in the empty array or guide tube locations, including all forms of inserts or control components.

(3) Defined as the maximum array-average enrichment, which is the peak planar average initial enrichment considering all elevations along the assembly axis.

Table 2.1-2
FuelSolutions™ W74 Loading Specification W74-2

W74-2 Payload Configuration Parameter	Intact MOX Fuel Assemblies Limit/Specification
Payload Description:	≤ 64 Big Rock Point BWR intact MOX fuel assemblies, as defined in Table 2.1-8. Any remaining empty canister basket guide tubes and/or support tubes may be loaded with fuel assemblies meeting any of the acceptable loading specifications W74-1 and W74-3 through W74-6, subject to the limitations of those specifications. If less than 64 total fuel assemblies are loaded, a dummy fuel assembly shall be placed into each empty CANISTER basket guide tube. Each dummy fuel assembly shall be the approximate weight and size of the actual fuel being loaded.
Cladding Material/Condition:	Zircaloy cladding with no known or suspected cladding defects greater than hairline cracks or pinhole leaks.
Initial Enrichment:	See Table 2.1-8
Burnup:	See Table 2.1-8
Cooling Time:	See Table 2.1-8

Table 2.1-3
FuelSolutions™ W74 Loading Specification W74-3 (2 pages)

W74-3 Payload Configuration Parameter	Partial UO_2 Fuel Assemblies Limit/Specification
Payload Description:	≤ 64 Big Rock Point BWR partial UO_2 fuel assemblies, as defined in Table 2.1-7. Partial fuel assemblies are defined as those assemblies having one or more rods missing from the design basis assembly array. The empty array locations may contain nothing, partial length rods, hollow zircaloy or stainless steel rods, neutron source rods, or any similar non-fissile fuel assembly component that displaces less water than a design fuel rod. Any remaining empty canister basket guide tubes and/or support tubes may be loaded with fuel assemblies meeting any of the acceptable loading specifications W74-1, W74-2, and W74-4 through W74-6, subject to the limitations of those specifications. If less than 64 total fuel assemblies are loaded, a dummy fuel assembly shall be placed into each empty CANISTER basket guide tube. Each dummy fuel assembly shall be the approximate weight and size of the actual fuel being loaded.
Cladding Material/Condition:	Zircaloy cladding with no known or suspected cladding defects greater than hairline cracks or pinhole leaks.
Initial Enrichment(1):	≤ 3.55 w/o ^{235}U (missing array interior or edge rods - 9x9) ≤ 3.6 w/o ^{235}U (missing array interior or edge rods - 11x11)
Burnup:	≤ 40,000 MWd/MTU.

Table 2.1-3
FuelSolutions™ W74 Loading Specification W74-3 (2 pages)

Cooling Time:	≥ 3.0 years. The minimum acceptable cooling time varies by fuel assembly class and enrichment, as a function of burnup; and is also dependent on the total cobalt content of the fuel and control components. The effects of the maximum acceptable decay heat, initial uranium content, and gamma and neutron sources are incorporated into the minimum cooling time determination. Fuel assemblies shall not be stored with less than the minimum acceptable cooling time indicated in Table 2.1-9.

Note: (1) Defined as the maximum array average initial enrichment, which is the peak planar average initial enrichment considering all elevations along the assembly axis. The averaging is applied only to those fuel pins that are present in the partial array.

Table 2.1-4
FuelSolutions™ W74 Loading Specification W74-4

W74-4 Payload Configuration Parameter	Partial MOX Fuel Assemblies Limit/Specification
Payload Description:	≤ 64 Big Rock Point BWR partial MOX fuel assemblies, as defined in Table 2.1-8. Partial fuel assemblies are defined as those assemblies having one or more rods missing from the design basis assembly array. The empty array locations may contain nothing, partial length rods, hollow zircaloy or stainless steel rods, neutron source rods, or any similar non-fissile fuel assembly component that displaces less water than a design fuel rod. Any remaining empty canister basket guide tubes and/or support tubes may be loaded with fuel assemblies meeting any of the acceptable loading specifications W74-1 through W74-3, W74-5, and W74-6, subject to the limitations of those specifications. If less than 64 fuel assemblies are loaded, a dummy fuel assembly shall be placed into each empty CANISTER basket guide tube. Each dummy fuel assembly shall be the approximate weight and size of the actual fuel being loaded.
Cladding Material/Condition:	Zircaloy cladding with no known or suspected cladding defects greater than hairline cracks or pinhole leaks.
Initial Enrichment:	See Table 2.1-8
Burnup:	See Table 2.1-8
Cooling Time:	See Table 2.1-8

Table 2.1-5
FuelSolutions™ W74 Loading Specification W74-5 (2 Pages)

W74-5 Payload Configuration	Damaged UO_2 Fuel Assemblies
Parameter	Limit/Specification
Payload Description:	≤8 Big Rock Point BWR damaged UO_2 fuel assemblies. Damaged fuel assemblies are defined as those with fuel rod damage in excess of hairline cracks or pinhole leaks. Fuel assemblies with damaged grid spacers (defined as damaged to a degree where fuel rod structural integrity cannot be assured, or where grid spacers have shifted vertically from their design position) will also be stored in damaged fuel cans. Each assembly designated as damaged is placed within a damaged fuel can and loaded into one of the four corner basket support tube locations in the upper and lower basket of the CANISTER. The remaining empty CANISTER basket guide tubes and damaged fuel cans may be loaded with fuel assemblies meeting any of the acceptable loading specifications W74-1 through W74-4 and W74-6, subject to the limitations of those specifications, for a total of ≤64 Big Rock Point BWR fuel assemblies. If less than 64 fuel assemblies are loaded, a dummy fuel assembly shall be placed into each empty CANISTER basket guide tube. Each dummy fuel assembly shall be the approximate weight and size of the actual fuel being loaded.
Cladding Material/Condition:	Zircaloy cladding with fuel rod damage in excess of hairline cracks or pinhole leaks.
Initial Enrichment(1):	≤4.61 w/o ^{235}U
Burnup:	≤40,000 MWd/MTU

Table 2.1-5
FuelSolutions™ W74 Loading Specification W74-5 (2 Pages)

W74-5 Payload Configuration Parameter	Damaged UO_2 Fuel Assemblies Limit/Specification
Cooling Time:	≥ 3.0 years. The minimum acceptable cooling time varies by fuel assembly class and enrichment, as a function of burnup; and is also dependent on the total cobalt content of the fuel and control components. The effects of the maximum acceptable decay heat, initial uranium content, and gamma and neutron sources are incorporated into the minimum cooling time determination. Fuel assemblies shall not be stored with less than the minimum acceptable cooling time indicated in Table 2.1-9.

Note: (1) Defined as peak pellet enrichment.

Table 2.1-6
FuelSolutions™ W74 Loading Specification W74-6

W74-6 Payload Configuration	Damaged MOX Fuel Assemblies
Parameter	Limit/Specification
Payload Description:	≤8 Big Rock Point BWR damaged MOX fuel assemblies. Damaged fuel assemblies are defined as those with fuel rod damage in excess of hairline cracks or pinhole leaks. Fuel assemblies with damaged grid spacers (defined as damaged to a degree where fuel rod structural integrity cannot be assured, or where grid spacers have shifted vertically from their design position) will also be stored in damaged fuel cans. Each assembly designated as damaged is placed within a damaged fuel can and loaded into one of the four corner basket support tube locations in the upper and lower basket of the CANISTER. The remaining empty CANISTER basket guide tubes and damaged fuel cans may be loaded with fuel assemblies meeting any of the acceptable loading specifications W74-1 through W74-5, subject to the limitations of those specifications, for a total of ≤64 Big Rock Point BWR fuel assemblies. If less than 64 fuel assemblies are loaded, a dummy fuel assembly shall be placed into each empty CANISTER basket guide tube. Each dummy fuel assembly shall be the approximate weight and size of the actual fuel being loaded.
Cladding Material/Condition:	Zircaloy cladding with fuel rod damage in excess of hairline cracks or pinhole leaks.
Initial Enrichment(1):	≤4.61% based on the formula $E_{U\text{-}235} + 0.7 \times P_{PU}$, where $E_{U\text{-}235}$ is the ^{235}U enrichment of the uranium in the fuel, and P_{PU} is the overall weight percentage of plutonium metal.
Burnup:	See Table 2.1-8
Cooling Time:	See Table 2.1-8

Note:

(1) Defined as peak pellet enrichment.

Table 2.1-7
UO_2 Fuel Assemblies Acceptable for Storage in the FuelSolutions™ W74 Canister(1)

Assembly Class(2)	Assembly Type	Maximum Uranium Loading (kg)	Linear Uranium Loading (kg/in)	Max. Array Average Initial Enrichment (w/o ^{235}U)	Applicable Cooling Table(3)
Big Rock Point	9x9 GE	143	2.04	≤4.1	W74-1-A W74-1-B
	9x9 ANF	143	2.04	≤4.1	W74-1-A W74-1-B
	11x11 ANF	143	2.04	≤4.1	W74-1-A W74-1-B
	Other(4)				

Notes

(1) Applicable to fuel specifications W74-1, W74-3, and W74-5.

(2) Assembly Class is defined per EIA Spent Fuel Discharge Report.[1]

(3) For any versions of these assembly types that contain up to 2.9 grams cobalt in the non-fuel hardware in the core zone, the Applicable Cooling Table is 74-1-A. For any versions of these assembly types that contain more than 2.9 grams cobalt, up to 15 grams cobalt, in the non-fuel hardware in the core zone, the Applicable Cooling Table is 74-1-B. Assemblies with over 15 grams cobalt in the non-fuel hardware in the core zone are not qualified for storage in the W74 canister.

(4) Other fuel assemblies that meet the defined parameters are qualified for storage.

[1]Energy Information Administration, *Spent Nuclear Fuel Discharges from U.S. Reactors 1993*, U.S. Department of Energy, 1995.

Table 2.1-8
MOX Fuel Assemblies Acceptable for Storage in the FuelSolutions™ W74 Canister[1]

Assembly Class[2]	Assembly Type	Maximum Heavy Metal Loading (kg)	Maximum Burnup (MWd/MTIHM)	Maximum Pin Initial Enrichment (w/o)	Minimum Cooling Time (years)
Big Rock Point	J2 (9x9)[3]	124	22,820	^{235}U - 4.50 PuO_2 - 3.65	22
	DA (11x11)[3]	126	21,850	^{235}U - 2.40 PuO_2 - 2.45	22
	G-Pu (11x11)[3]	131	34,200	^{235}U - 4.60 PuO_2 - 5.45	15
	UO_2 (9x9) w/2 MOX rods[4]	(see Table 2.1-7)			

Notes:

(1) Applicable to fuel specifications W74-2, W74-4, and W74-6.

(2) Assembly Class is defined per EIA Spent Fuel Discharge Report.

(3) Cobalt content shall be ≤ 2.9 g in the active fuel region.

(4) This qualification specifically applies to BRP assemblies E65 and E72.

Table 2.1-9
Fuel Cooling Table W74-1-A

APPLICABILITY:

Canister:	FuelSolutions™ W74-M and W74-T Canisters
Loading Specification:	W74-1, W74-3, and W74-5
Description:	Up to 64 fuel assemblies
SNF Assemblies:	Valid for all BRP assemblies as indicated in Table 2.1-7.
Cobalt Content:	≤ 2.9 g in active fuel region (low-cobalt)

QUALIFICATION BASES:

Storage Cask Dose Rate	≤ 50 mrem/hr
Canister Heat Load	≤ 24.8 kW/Canister, and ≤ 0.216 kW/inch-Canister

Maximum Burnup (MWd/MTU)[1]	Required Minimum Cooling Time (yr.)[1,2]					
	Minimum Initial Enrichment (w/o ^{235}U)					
	1.5	2.0	2.5	3.0	3.5	4.0
15,000	3.2	3.1	3.1	3.0	3.0	3.0
20,000	3.4	3.3	3.2	3.2	3.1	3.1
25,000	3.6	3.5	3.4	3.4	3.3	3.3
30,000	3.9	3.8	3.6	3.6	3.5	3.4
32,000	3.9	3.8	3.7	3.6	3.5	3.5
34,000	4.2	3.9	3.8	3.7	3.6	3.6
36,000	4.8	4.4	4.1	3.9	3.8	3.7
38,000	5.2	4.8	4.5	4.2	4.0	3.9
40,000	5.6	5.3	4.9	4.6	4.3	4.1

Notes:

(1) Rounding: round up to next highest burnup, round down to next lowest enrichment.

(2) Enrichments less than 1.5% or greater than the criticality limit presented in Section 6.1 of the FuelSolutions™ W74 Canister Storage SAR are not qualified.

Table 2.1-10
Fuel Cooling Table W74-1-B

APPLICABILITY:

Canister:	FuelSolutions™ W74-M and W74-T Canisters
Loading Specification:	W74-1, W74-3, and W74-5
Description:	Up to 64 fuel assemblies
SNF Assemblies:	Valid for all BRP assemblies as indicated in Table 2.1-7.
Cobalt Content:	≤ 15.0 g in active fuel region (high-cobalt)

QUALIFICATION BASES:

Storage Cask Dose Rate	≤ 50 mrem/hr
Canister Heat Load	≤ 24.8 kW/Canister, and ≤ 0.216 kW/inch-Canister

Maximum Burnup (MWd/MTU)[1]	Required Minimum Cooling Time (yr.)					
	Minimum Initial Enrichment (w/o ^{235}U)[1,2]					
	1.5	2.0	2.5	3.0	3.5	4.0
15,000	4.2	4.0	3.9	3.8	3.8	3.7
20,000	4.7	4.3	4.2	4.1	4.0	3.9
25,000	5.2	4.9	4.8	4.6	4.5	4.4
30,000	5.8	5.6	5.1	4.9	4.8	4.7
32,000	6.0	5.8	5.3	5.1	5.0	4.9
34,000	6.4	6.2	5.5	5.4	5.2	5.1
36,000	6.5	6.2	6.0	5.5	5.4	5.3
38,000	6.8	6.6	6.4	5.8	5.6	5.5
40,000	7.0	6.8	6.6	5.8	5.6	5.5

Notes:

(1) Rounding: round up to next highest burnup, round down to next lowest enrichment.

(2) Enrichments less than 1.5% or greater than the criticality limit presented in Section 6.1 of the FuelSolutions™ W74 Canister Storage SAR are not qualified.

3.0 LIMITING CONDITION FOR OPERATION (LCO) APPLICABILITY

LCO 3.0.1	LCOs shall be met during specified conditions in the Applicability, except as provided in LCO 3.0.2.
LCO 3.0.2	Upon discovery of a failure to meet an LCO, the Required Actions of the associated Conditions shall be met, except as provided in LCO 3.0.5. If the LCO is met or is no longer applicable prior to expiration of the specified Completion Time(s), completion of the Required Action(s) is not required, unless otherwise stated.
LCO 3.0.3	Not applicable to an SFSS.
LCO 3.0.4	When an LCO is not met, entry into a specified condition in the Applicability shall not be made except when the associated ACTIONS to be entered permit continued operation in the specified condition in the Applicability for an unlimited period of time. This Specification shall not prevent changes in specified conditions in the Applicability that are required to comply with ACTIONS or that are related to the unloading of a CANISTER.
LCO 3.0.5	Equipment removed from service or not in service in compliance with ACTIONS may be returned to service under administrative control solely to perform testing required to demonstrate it meets the LCO or that other equipment meets the LCO. This is an exception to LCO 3.0.2 for the system returned to service under administrative control to perform the testing.
LCO 3.0.6	Not applicable to an SFSS.
LCO 3.0.7	Not applicable to an SFSS.

3.0 SURVEILLANCE REQUIREMENT (SR) APPLICABILITY

SR 3.0.1	SRs shall be met during the specified conditions in the Applicability for individual LCOs, unless otherwise stated in the SR. Failure to meet a Surveillance, whether such failure is experienced during the performance of the Surveillance or between performances of the Surveillance, shall be failure to meet the LCO. Failure to perform a Surveillance within the specified Frequency shall be failure to meet the LCO except as provided in SR 3.0.3. Surveillances do not have to be performed on equipment or variables outside specified limits.
SR 3.0.2	The specified Frequency for each SR is met if the Surveillance is performed within 1.25 times the interval specified in the Frequency, as measured from the previous performance or a measured from the time a specified condition of the Frequency is met. For Frequencies specified as “once”, the above interval extension does not apply. If a Completion Time requires periodic performance on a “once per…” basis, the above Frequency extension applies to each performance after the initial performance. Exceptions to this Specification are stated in the individual Specifications.
SR 3.0.3	If it is discovered that a Surveillance was not performed within its specified Frequency, then compliance with the requirement to declare the LCO not met may be delayed, from the time of discovery, up to 24 hours or up to the limit of the specified Frequency, whichever is less. This delay period is permitted to allow performance of the Surveillance. If the Surveillance is not performed within the delay period, the LCO must immediately be declared not met, and the applicable Condition(s) must be entered. When the Surveillance is performed within the delay period and the Surveillance is not met, the LCO must immediately be declared not met, and the applicable Condition(s) must be entered.
SR 3.0.4	Entry into a specified condition in the Applicability of an LCO shall not be made unless the LCO’s Surveillances have been met within their specified Frequency. This provision shall not prevent entry into specified conditions in the Applicability that are required to comply with ACTIONS or that are related to the unloading of a CANISTER.

3.1 CANISTER INTEGRITY

3.1.1 W74 Canister Helium Backfill Density

LCO 3.1.1 The CANISTER helium backfill density shall be in the range of 0.0376 ± 0.0010 g-moles/liter.

APPLICABILITY: During LOADING OPERATIONS.

ACTIONS

NOTE

Separate Condition entry is allowed for each CANISTER.

CONDITION	REQUIRED ACTION	COMPLETION TIME
A. CANISTER helium backfill quantity limit is not met.	A.1 Establish CANISTER helium backfill quantity within limit.	48 hours
B. Required Action and associated Completion Time are not met.	B.1 Remove all fuel assemblies from CANISTER.	30 days

SURVEILLANCE REQUIREMENTS

NOTE

The helium used for backfill shall have a minimum purity of 99.995%.

SURVEILLANCE		FREQUENCY
SR 3.1.1.1	Verify CANISTER helium backfill quantity is within limit.	Within 24 hours after verifying CANISTER cavity vacuum drying pressure is within limit.

3.1 CANISTER INTEGRITY

3.1.2 Canister Vacuum Drying Pressure

See the Storage System Technical Specification for the applicable LCO.

3.1 CANISTER INTEGRITY

3.1.3 Canister Leak Rate

See the Storage System Technical Specification for the applicable LCO.

3.1 CANISTER INTEGRITY

3.1.4 Hydraulic Ram Force During Horizontal Canister Transfer

See the Storage System Technical Specification for the applicable LCO.

3.1 CANISTER INTEGRITY

3.1.5 W74 Canister Vertical Time Limit in Transfer Cask

LCO 3.1.5 For vertical TRANSFER OPERATIONS, the CANISTER transfer out of the TRANSFER CASK shall be completed within 8 hours after draining the annulus water from the TRANSFER CASK. For horizontal TRANSFER OPERATIONS, the movement of the TRANSFER CASK to the horizontal position on the transfer trailer shall be completed within 8 hours after draining the annulus water from the TRANSFER CASK.

APPLICABILITY: During TRANSFER OPERATIONS.

ACTIONS

NOTE

Separate Condition entry is allowed for each CANISTER.

CONDITION	REQUIRED ACTION	COMPLETION TIME
A. CANISTER time limit in drained annulus TRANSFER CASK is not met.	A.1 Fill annulus with water. AND A.2 Maintain filled annulus.	7 hours. 24 hours.

SURVEILLANCE REQUIREMENTS

SURVEILLANCE		FREQUENCY
SR 3.1.5.1	Verify TRANSFER CASK operations with CANISTER in vertical orientation and annulus drained are completed within time limit.	Within 8 hours after completion of TRANSFER CASK/ CANISTER annulus draining.

3.2 CANISTER RADIATION PROTECTION

3.2.1 Canister Surface Contamination

See the Storage System Technical Specification for the applicable LCO.

3.3 STORAGE CASK INTEGRITY

3.3.1 Storage Cask Air Inlet and Outlet Openings

See the Storage System Technical Specification for the applicable LCO.

3.3 STORAGE CASK INTEGRITY

3.3.2 Storage Cask Temperatures During Storage

LCO 3.3.2 The temperature of a STORAGE CASK with a W74 CANISTER containing fuel assemblies, as indicated by the liner thermocouple, shall meet the following limits:

a. The measured temperature shall not exceed 163°F (73°C) under normal ambient conditions (average ambient temperature up to 100°F (38°C)).

b. The measured temperature shall not exceed 192°F (89°C) under off-normal ambient conditions (average ambient temperature up to 125°F (52°C)).

c. The differential temperature between two successive daily measurements shall not exceed the corresponding differential ambient temperature plus 83°F (46°C).

APPLICABILITY: During STORAGE OPERATIONS.

ACTIONS

NOTE

Separate Condition entry is allowed for each STORAGE CASK.

CONDITION	REQUIRED ACTION	COMPLETION TIME
A. STORAGE CASK concrete temperature exceeds the specified limit.	A.1 Administratively verify correct fuel loading.	24 hours
	AND	
	A.2 Visually check all STORAGE CASK inlet and outlet screens for debris blockage in accordance with LCO 3.3.1.	24 hours
	AND	
	A.3 Check the thermocouple and related instrumentation to assure they are functioning properly.	24 hours
	AND (continued)	

3.3.2 Storage Cask Temperatures During Storage

CONDITION	REQUIRED ACTION	COMPLETION TIME
	A.4 Repair or replace thermocouple and related instrumentation as necessary.	48 hours
	AND	
	A.5 Perform visual inspection of the STORAGE CASK vent channels by removing the debris screens and using visual aids as necessary. If no obstruction is found, the interior of the STORAGE CASK, including the guide rails and heat shield, is to be visually inspected for ventilation obstructions using remote inspection tools or by temporarily removing the STORAGE CASK top cover.	48 hours
	AND	
	A.6 Verify STORAGE CASK temperature returns to within limit.	48 hours
B. Required Actions and associated Completion Times are not met.	B.1 Initiate actions to cool the cask to within the limit.	96 hours
	AND	
	B.2 Return CANISTER to TRANSFER CASK.	30 days
	AND	
	B.3 Return CANISTER to repaired or replacement STORAGE CASK.	270 days

3.3.2 Storage Cask Temperatures During Storage

SURVEILLANCE REQUIREMENTS

SURVEILLANCE		FREQUENCY
SR 3.3.2.1	Verify that the STORAGE CASK temperatures are within limit. NOTE Daily cask temperatures can be expected to vary slightly due to changes in the ambient temperature. This is acceptable as long as the temperatures remain within the specified limit.	24 hours

3.3 STORAGE CASK INTEGRITY

3.3.3 Storage Cask Temperatures During Horizontal Transfer

LCO 3.3.3 The measured temperature of a STORAGE CASK with a W74 CANISTER containing fuel assemblies, as indicated by the liner thermocouple, shall not exceed 185°F (85°C).

APPLICABILITY: During TRANSFER OPERATIONS.

ACTIONS

NOTE

Separate Condition entry is allowed for each STORAGE CASK.

CONDITION	REQUIRED ACTION	COMPLETION TIME
A. STORAGE CASK concrete temperature limit is not met.	A.1 Transfer the CANISTER into the TRANSFER CASK.	24 hours
B. Required Action A.1 and associated Completion Times are not met.	B.1 Inspect the STORAGE CASK for damage.	5 days
	AND	
	B.2.1 If no damage, transfer CANISTER to STORAGE CASK.	7 days
	OR	
	B.2.2 If damaged, transfer CANISTER to new STORAGE CASK.	21 days
C. Required Actions B.1 and B.2-1 or B.1 and B.2.2 and associated Completion Times are not met.	C.1 Return CANISTER to TRANSFER CASK.	30 days
	AND	
	C.2 Return CANISTER to repaired or replacement STORAGE CASK.	270 days

SURVEILLANCE REQUIREMENTS

	SURVEILLANCE	FREQUENCY
SR 3.3.3.1	After the STORAGE CASK is downended to the horizontal orientation, monitor and record STORAGE CASK concrete temperature as indicated by the STORAGE CASK liner thermocouple.	30 minutes

3.4 TRANSFER CASK INTEGRITY

3.4.1 Transfer Cask Structural Shell Temperature

See the Storage System Technical Specification for the applicable LCO.

3.5 TRANSFER CASK RADIATION PROTECTION

3.5.1 Transfer Cask Surface Contamination

See the Storage System Technical Specification for the applicable LCO.

4.0 DESIGN FEATURES

The specifications in this section include the design characteristics of special importance to each of the physical barriers and the maintenance of safety margins in the storage system component design. The principal objective of this category is to describe the design envelope which might constrain any physical changes to essential equipment. Included in this category are the site environmental parameters which provide the bases for design, but are not inherently suited for description as LCOs.

4.1 Storage System

4.1.1 Storage Cask

4.1.1.1 Structural Performance

See the Storage System Technical Specification Section 4.1.1.1 for discussion of STORAGE CASK structural performance features.

4.1.1.2 Codes and Standards

See the Storage System Technical Specification Section 4.1.1.2 for discussion of codes and standards applicable to the STORAGE CASK.

4.1.1.3 Fabrication Exceptions to Codes, Standards, and Criteria

See the Storage System Technical Specification Section 4.1.1.3 for discussion of exceptions to codes, standards, and criteria.

4.1.2 Transfer Cask

4.1.2.1 Structural Performance

See the Storage System Technical Specification Section 4.1.2.1 for discussion of TRANSFER CASK structural performance features.

4.1.2.2 Codes and Standards

See the Storage System Technical Specification Section 4.1.2.2 for discussion of codes and standards applicable to the TRANSFER CASK.

4.1.2.3 Fabrication Exceptions to Codes, Standards, and Criteria

See the Storage System Technical Specification Section 4.1.2.3 for discussion of exceptions to codes, standards, and criteria.

4.1.3 Canister

4.1.3.1 Criticality

The design of the W74 CANISTER, including spatial constraints on adjacent assemblies (minimum basket cell opening of 6.85 inches square) and the boron content of the basket neutron absorber material (minimum 3.1 mg/cm^2 B-10) shall ensure that fuel assemblies are maintained in a subcritical condition with a k_{eff} less than 0.95 under all conditions of operation.

4.1.3.2 Structural Performance

The CANISTER has been evaluated for a side drop resulting in a lateral gravitational (*g*) loading of 60 *g* and an end drop resulting in an axial gravitational loading of 50 *g*.

The maximum weight of a loaded, dried, and sealed W74 CANISTER is 85,000 pounds. The maximum CANISTER weight includes 32 SFAs in each basket, plus four damaged fuel cans at the support tube locations in each basket.

The W74 CANISTER thermal rating of 26.4 kW is determined by the minimum heat load qualification in the STORAGE and TRANSFER CASKS.

4.1.3.3 Codes and Standards

The FuelSolutions™ W74 CANISTER shell structural components are designed in accordance with Subsection NB of the ASME Code, and the basket structural components are designed in accordance with Subsection NG of the ASME Code. Exceptions to the code are listed in Table 4.1-1.

4.1.3.4 Fabrication Exceptions to Codes, Standards, and Criteria

Proposed alternatives to Subsections NB and NG of the ASME Code, including exceptions allowed by Section 4.1.3.3, may be used when authorized by the Director of the Office of Nuclear Material Safety and Safeguards or Designee. The applicant should demonstrate that:

1. The proposed alternatives would provide an acceptable level of quality and safety, or
2. Compliance with the specified requirements of ASME Code, Section III, would result in hardship or unusual difficulty without a compensating increase in the level of quality and safety.

Requests for exception in accordance with this section should be submitted in accordance with 10CFR72.4.

4.2 Storage Pad

Constraints on the storage pad are discussed in Section 4.2 of the Storage System Technical Specification.

4.3 Site Specific Parameters and Analyses

See the Storage System Technical Specification Section 4.3 for discussion of site specific parameters and analyses.

Table 4.1-1
FuelSolutions™ W74 Canister ASME Code Requirements Compliance Summary (15 Pages)

Item	ASME Code Requirement	Issue	Alternative Compliance Basis
Section III, Subsection NCA (applicable to both Canister and Basket):			
1	**General for Subsection NCA**	1. The terms "Certificate Holder" and "Owner" used throughout this subsection are not applicable for a 10CFR72 system. 2. The Division 2 (concrete) requirement provided throughout this subsection are not applicable for a 10CFR72 system.	1. BNFL Fuel Solutions (BFS) bears the responsibilities associated with a "Certificate Holder" or "Owner" relative to the FuelSolutions™ SFMS. 2. This compliance summary table only addresses FuelSolutions™ canisters, which do not contain any concrete.
2	**NCA-1140, "Use of Code Editions, Addenda, and Cases:"** "(a)(1) Under the rules of this Section, the Owner or his designees shall establish the Code Edition and Addenda to be included in the Design Specifications…"	The FuelSolutions™ SFMS documentation does not include an ASME Code Design Specification.	The requirements and criteria typically contained in an ASME Code Design Specification are contained in this SAR.

Table 4.1-1
FuelSolutions™ W74 Canister ASME Code Requirements Compliance Summary (15 Pages)

Item	ASME Code Requirement	Issue	Alternative Compliance Basis
3	**NCA-1210, "Components:"** "Each component of a nuclear power plant shall require a Design Specification (NCA-3250), Design Report (NCA-3350, NCA-3550), and other design documents specified in NCA-3800. Data Reports and stamping shall be as required in NCA-8000."	The FuelSolutions™ SFMS documentation does not contain the following ASME Code documents: 1. Design Specification 2. Design Report 3. Owner's Certificate of Authorization 4. Authorized Inspection Agency Written Agreement 5. Owner's Data Report 6. Overpressure Protection Report.	1. See Item 2. 2. The information typically reported in an ASME Code Design Report is contained in this SAR. 3. An Owner's Certificate of Authorization, a written agreement with an Authorized Inspection Agency, an Owner's Data Report, and an Overpressure Protection Report are not typically provided for components licensed under 10CFR72.
4	**NCA-1220, "Materials"**	Not all non-pressure retaining materials specified in this FuelSolutions™ Canister Storage SAR are listed as ASME Section III materials.	FuelSolutions™ canisters are purchased, identified, controlled, and manufactured using a graded quality approach in accordance with the NRC-approved BFS Quality Assurance Program based on NQA-1, NRC Regulatory Guide 7.10, and NUREG/CR-6407 criteria.

Table 4.1-1
FuelSolutions™ W74 Canister ASME Code Requirements Compliance Summary (15 Pages)

Item	ASME Code Requirement	Issue	Alternative Compliance Basis
5	**NCA-1281, "Activities and Requirements:"** "… Data Reports and stamping shall be as required in NCA-8000."	See Item 19.	See Item 19.
6	**NCA-2000, "Classification of Components"**	The classification of components is usually provided in a Design Specification.	See Item 2.
7	**NCA-2142, "Establishment of Design, Service, and Test Loadings and Limits:"** "In the Design Specification, the Owner or his designee shall identify the loadings and combinations of loadings and establish the appropriate Design, Service, and Test Limits for each component or support…"	See Item 2.	See Item 2.
8	**NCA-3100, "General"**	ASME Code accreditation does not apply.	See Item 1.

Table 4.1-1
FuelSolutions™ W74 Canister ASME Code Requirements Compliance Summary (15 Pages)

Item	ASME Code Requirement	Issue	Alternative Compliance Basis
9	**NCA-3200, "Owner's Responsibilities"**	An Owner's responsibilities under the ASME Code do not apply.	An Owner's Certificate of Authorization, a Design Specification, a Design Report, an Overpressure Protection Report, and an Owner's Data Report are not typically provided for components licensed under 10CFR72.
10	**NCA-3300, "Responsibilities of a Designer - Division 2"**	See Item 1.	See Item 1.
11	**NCA-3400, "Responsibilities of an N Certificate Holder - Division 2"**	See Item 1.	See Item 1.
12	**NCA-3500, "Responsibilities of an N Certificate Holder - Division 1"**	See Item 1.	See Item 1. Design and fabrication requirements are provided in this SAR and related procurement/fabrication drawings and specifications.
13	**NCA-3600, "Responsibilities of an NPT Certificate Holder"**	See Item 1.	See Item 12.
14	**NCA-3700, "Responsibilities of an NA Certificate Holder"**	See Item 1.	See Item 12.

Table 4.1-1
FuelSolutions™ W74 Canister ASME Code Requirements Compliance Summary (15 Pages)

Item	ASME Code Requirement	Issue	Alternative Compliance Basis
15	**NCA-3800, "Metallic Material Organization's Quality System Program"**	Materials for a FuelSolutions™ canister may be purchased from suppliers that are not certified per the requirements of NCA-3800.	Material suppliers are qualified per NCA-3800 or the NRC-approved BFS Quality Assurance Program based on the requirements of NQA-1, NRC Regulatory Guide 7.10, and NUREG/CR-6407 criteria.
16	**NCA-3900, "Nonmetallic Material Manufacturer's and Constituent Suppliers Quality System Programs"**	See Item 1.	See Item 1.
17	**NCA-4000, "Quality Assurance"**	These quality assurance requirements do not apply.	See Item 4.
18	**NCA-5000, "Authorized Inspection"**	The manufacturing or operation of the FuelSolutions™ SFMS does not use an Authorized Inspection Agency.	An Authorized Inspection Agency is not typically used in the manufacturing or operation of components licensed under 10CFR72.
19	**NCA-8000, "Certificates of Authorization, Nameplates, Code Symbol Stamping, and Data Reports"**	The FuelSolutions™ SFMS does not use an ASME Code Certificate of Authorization, Code Symbol Stamping, or a Data Report.	An ASME Code Certificate of Authorization, Code Symbol Stamping, or a Data Report are not typically required for components licensed under 10CFR72. Nameplate information is provided on each FuelSolutions™ canister.

Table 4.1-1
FuelSolutions™ W74 Canister ASME Code Requirements Compliance Summary (15 Pages)

Item	ASME Code Requirement	Issue	Alternative Compliance Basis
Section III, Subsection NB (applicable to Canister):			
20	**NB-1130, "Boundary of Components:"** "The Design Specification shall define the boundary of a component to which piping or another component is attached."	See Item 6.	See Item 6.
21	**NB-1132.2, "Jurisdictional Boundary:"** "The jurisdictional boundary between a pressure-retaining component and an attachment defined in the Design Specification shall not be any closer to the pressure-retaining portion of the component than as defined in (a) through (g) below…"	See Item 6.	See Item 6.

Table 4.1-1
FuelSolutions™ W74 Canister ASME Code Requirements Compliance Summary (15 Pages)

Item	ASME Code Requirement	Issue	Alternative Compliance Basis
22	**NB-2160, "Deterioration of Material In Service:"** "It is the responsibility of the Owner to select material suitable for the conditions stated in the Design Specifications (NCA-3250), with specific attention being given to the effects of service conditions upon the properties of the material. …Any special requirement shall be specified in the Design Specifications (NCA-3252 and NB-3124)…"	See Item 2.	See Item 2.
23	**NB-2610, "Documentation and Maintenance of Quality System Programs:"** "(a) Except as provided in (b) below, Material Manufacturers and Material Suppliers shall have a Quality System Program or an Identification and Verification Program, as applicable, which meets the requirements of NCA-3800…"	See Item 15.	See Item 15.

Table 4.1-1
FuelSolutions™ W74 Canister ASME Code Requirements Compliance Summary (15 Pages)

Item	ASME Code Requirement	Issue	Alternative Compliance Basis
24	**NB-3113, "Service Conditions:"** "Each service condition to which the components may be subjected shall be classified in accordance with NCA-2142 and Service Limits (NCA-2142.4(b)) designated in the Design Specifications in such detail as will provide a complete basis for design, construction, and inspection in accordance with this Article…"	See Item 2.	See Item 2.
25	**NB-3134, "Leak Tightness:"** "Where a system leak tightness greater than that required or demonstrated by a hydrostatic test is required, the leak tightness requirements for each component shall be set forth in the Design Specifications."	See Item 2.	See Item 2.
26	**NB-3220, "Stress Limits for Other Than Bolts"**	This section makes a number of references to an ASME Code Design Specification. See Item 2.	See Item 2.

Table 4.1-1
FuelSolutions™ W74 Canister ASME Code Requirements Compliance Summary (15 Pages)

Item	ASME Code Requirement	Issue	Alternative Compliance Basis
27	**NB-4121, "Means of Certification:"** "The Certificate Holder for an item shall certify, by application of the appropriate Code Symbol and completion of the appropriate Data Report in accordance with NCA-8000, that materials used comply with the requirements of NB-2000 and that the fabrication or installation complies with the requirements of this Article."	The FuelSolutions™ SFMS does not use an ASME Code Symbol Stamp or a Data Report.	An ASME Code Symbol Stamp or Data Report are not typically required for components licensed under 10CFR72. Also see Item 15.

Table 4.1-1
FuelSolutions™ W74 Canister ASME Code Requirements Compliance Summary (15 Pages)

Item	ASME Code Requirement	Issue	Alternative Compliance Basis
28	**NB-4243, "Category C Weld Joints in Vessels and Similar Weld Joints in Other Components:"** "Category C weld joints in vessels and similar weld joints in other components shall be full penetration joints …Either a butt welded joint or a full penetration corner joint as shown in Fig. NB-4243-1 shall be used."	The FuelSolutions™ canister top end closure employs the following cover-to-shell weld types: 1. Top inner cover - a single-sided partial penetration weld. 2. Top outer cover - a single-sided partial penetration weld.	The FuelSolutions™ canister top end closure employs multi-pass, redundant welds subjected to multi-level liquid penetrant examinations and a combined pneumatic pressure and helium leak rate test at a hydrostatic test pressure to assure structural integrity and leak tightness. The design of the inner closure weld incorporates a stress-reduction factor of 0.9 to account for use of multi-pass PT examination and helium leak testing. The design of the outer closure weld complies with ISG-4. The examination of the inner and outer closure plate welds complies with ISG-4.
29	**NB-5231, "General Requirements:"** "(a) Category C full penetration butt welded joints in vessels and similar welded joints in other components shall be examined by the radiographic and either liquid penetrant or magnetic particle method."	The FuelSolutions™ canister top end closures are not radiographically examined.	See Item 28.

Table 4.1-1
FuelSolutions™ W74 Canister ASME Code Requirements Compliance Summary (15 Pages)

Item	ASME Code Requirement	Issue	Alternative Compliance Basis
30	**NB-6112, "Pneumatic Testing:"** "A pneumatic test in accordance with NB-6300 may be substituted for the hydrostatic test when permitted by NB-6112.1(a)." **NB-6112.1, "Pneumatic Test Limitations:"** "(a) A pneumatic test may be used in lieu of a hydrostatic test only when any of the following conditions exists: 1. when components, appurtenances, or systems are so designed or supported that they cannot safely be filled with liquid; 2. when components, appurtenances, or systems which are not readily dried are to be used in services where traces of the testing medium cannot be tolerated. (b) A pneumatic test at a pressure not to exceed 25% of the Design Pressure may be applied, prior to either a hydrostatic or a pneumatic test, as a means of locating	The FuelSolutions™ canisters employ a combined pneumatic pressure and helium leak rate test at a hydrostatic test pressure to assure structural integrity and leak tightness.	Because a dry SNF assembly storage canister is a 10CFR72 licensed component requiring a helium leak rate test, the combination of this leak rate test with a pneumatic pressure test at a hydrostatic test pressure is operationally efficient and consistent with ALARA principles, while still being very conservative due to the molecular size of the testing medium and the use of helium leak rate vs. visual examination acceptance criteria.

Table 4.1-1
FuelSolutions™ W74 Canister ASME Code Requirements Compliance Summary (15 Pages)

Item	ASME Code Requirement	Issue	Alternative Compliance Basis
31	**NB-6200, "Hydrostatic Tests"**	See Item 30.	See Item 30.
32	**NB-7000, "Overpressure Protection"**	A FuelSolutions™ canister is not designed to include an overpressure protection device.	By their very nature, canisters and casks designed to dry store SNF assemblies are licensed without any type of overpressure protection device or vent path of any kind.
33	**NB-8000, "Nameplates, Stamping, and Reports"**	The FuelSolutions™ SFMS does not use an ASME Code Symbol Stamp or a Data Report.	An ASME Code Symbol Stamp or a Data Report are not typically required for components licensed under 10CFR72. Nameplate information is provided on each FuelSolutions™ canister.

Table 4.1-1
FuelSolutions™ W74 Canister ASME Code Requirements Compliance Summary (15 Pages)

Item	ASME Code Requirement	Issue	Alternative Compliance Basis
Section III, Subsection NG (applicable to Basket):			
34	**NG-2160, "Deterioration of Material In Service:"** "It is the responsibility of the Owner to select material suitable for the conditions stated in the Design Specifications (NCA-3250), with specific attention being given to the effects of service conditions upon the properties of the material."	See Item 2.	See Item 2.
35	**NG-2330, "Test Requirements and Acceptance Standards"**	FuelSolutions™ canister basket material is not impact tested to the requirements of NG-2330.	The canister basket is licensed for storage and transportation, and therefore materials are impact tested in accordance with NRC criteria provided in Regulatory Guide 7.11 and NUREG/CR-1815 for Category II materials.

Table 4.1-1
FuelSolutions™ W74 Canister ASME Code Requirements Compliance Summary (15 Pages)

Item	ASME Code Requirement	Issue	Alternative Compliance Basis
36	**NG-2610, "Documentation and Maintenance of Quality System Programs:"** "(a) Except as provided in (b) below, Material Manufacturers and Material Suppliers shall have a Quality System Program or an Identification and Verification Program, as applicable, which meets the requirements of NCA-3800…"	See Item 15.	See Item 15.
37	**NG-3113, "Service Loadings:"** "Each loading to which the structure may be subjected shall be classified in accordance with NCA-2142 and Service Limits (NCA-2142.4(b)) designated in the Design Specifications in such detail as will provide a complete basis for design, construction, and inspection in accordance with this Article…"	See Item 2.	See Item 2.
38	**NG-3220, "Stress Limits for Other Than Threaded Structural Fasteners"**	This section makes a number of references to an ASME Code Design Specification. See Item 2.	See Item 2.

Table 4.1-1
FuelSolutions™ W74 Canister ASME Code Requirements Compliance Summary (15 Pages)

Item	ASME Code Requirement	Issue	Alternative Compliance Basis
39	**NG-4121, "Means of Certification:"** "The Certificate Holder for an item shall certify, by application of the appropriate Code Symbol and completion of the appropriate Data Report in accordance with NCA-8000, that materials used comply with the requirements of NG-2000 and that the fabrication or installation complies with the requirements of this Article."	The FuelSolutions™ SFMS does not use an ASME Code Symbol Stamp or a Data Report.	An ASME Code Symbol Stamp or Data Report are not typically required for components licensed under 10CFR72. Also see Item 15.
40	**NG-8000, "Nameplates, Stamping, and Reports"**	The FuelSolutions™ SFMS does not use an ASME Code Symbol Stamp or a Data Report.	An ASME Code Symbol Stamp or a Data Report are not typically required for components licensed under 10CFR72. Nameplate information is provided on each FuelSolutions™ canister.

5.0 ADMINISTRATIVE CONTROLS

5.1 Training Modules

See the Storage System Technical Specification for the applicable information.

5.2 Preoperational Testing and Training Exercises

See the Storage System Technical Specification for the applicable information.

5.3 Programs

5.3.1-5.3.5

See the Storage System Technical Specification for the applicable information.

5.3.6 Vacuum Drying Program

The FuelSolutions™ W74 CANISTER has been evaluated for allowable fuel cladding temperature during LOADING and STORAGE OPERATIONS. During LOADING OPERATIONS, the fuel cladding temperature is limited to 400°C to assure cladding integrity.

This program shall establish administrative controls and procedures to assure that the spent fuel cladding does not exceed the temperature limit during LOADING OPERATIONS. For a CANISTER loaded with fuel with a total heat load of 24.8 kW, the initial vacuum drying cycle shall be limited to 7 hours. If the vacuum drying LCO 3.1.2 has not been satisfied, the CANISTER shall be backfilled with helium for 4 hours, vacuum dried for 4 hours, backfilled for 4 hours, etc., until the LCO is met.

For a heat load of 12.2 kW or lower, there is no time limit on the initial vacuum drying cycle. For heat loads greater than 12.2 kW but less than 24.8 kW, the program shall either use the 24.8 kW requirements, or establish suitable time limits to maintain the cladding temperature to less than or equal to 400°C for the specific CANISTER heat load.

5.3.7 Cladding Oxide Thickness Measurement Program

Not applicable for the W74 CANISTER.

5.4 Special Requirements for First System in Place

The heat transfer characteristics of the cask system will be recorded by temperature measurements of the first STORAGE CASK placed in service with a heat load equal to or greater than 10kW. In accordance with 10CFR72.4, a letter report summarizing the results of the measurements shall be submitted to the NRC.

For each cask subsequently loaded with a higher heat load (up to the 24.8 kW limit), the calculation and measured temperature data shall be reported to the NRC at every 2 kW increase. The calculation and comparison need not be reported to the NRC for STORAGE CASKS that are subsequently loaded with lesser loads then the latest reported case.

Cask users may satisfy these requirements by referencing validation test reports submitted to the NRC by other users.

TECHNICAL SPECIFICATIONS BASES
FOR THE FuelSolutions™ W74 CANISTER

Revision 4

Page

B 2.0 FUNCTIONAL AND OPERATING LIMITS . . . . . B 2.0-1
B 2.1.1 Fuel to be Stored in the FuelSolutions™ W74 Canister . . . . . B 2.0-1

B 3.0 LIMITING CONDITION FOR OPERATION (LCO) APPLICABILITY . . . . . B 3.0-1

B 3.0 SURVEILLANCE REQUIREMENT (SR) APPLICABILITY . . . . . B 3.0-4

B 3.1 CANISTER INTEGRITY . . . . . B 3.1-1
B 3.1.1 W74 Canister Helium Backfill Density . . . . . B 3.1-1
B 3.1.2 Canister Vacuum Drying Pressure . . . . . B 3.1-4
B 3.1.3 Canister Leak Rate . . . . . B 3.1-5
B 3.1.4 Hydraulic Ram Force During Horizontal Canister Transfer . . . . . B 3.1-6
B 3.1.5 W74 Canister Vertical Time Limit in Transfer Cask . . . . . B 3.1-7

B 3.2 CANISTER RADIATION PROTECTION . . . . . B 3.2-1
B 3.2.1 Canister Surface Contamination . . . . . B 3.2-1

B 3.3 STORAGE CASK INTEGRITY . . . . . B 3.3-1
B 3.3.1 Storage Cask Air Inlet and Outlet Openings . . . . . B 3.3-1
B 3.3.2 Storage Cask Temperatures During Storage . . . . . B 3.3-2
B 3.3.3 Storage Cask Temperatures During Horizontal Transfer . . . . . B 3.3-6

B 3.4 TRANSFER CASK INTEGRITY . . . . . B 3.4-1
B 3.4.1 Transfer Cask Structural Shell Temperature . . . . . B 3.4-1

B 3.5 TRANSFER CASK RADIATION PROTECTION . . . . . B 3.5-1
B 3.5.1 Transfer Cask Surface Contamination . . . . . B 3.5-1

BASES

B 2.0 FUNCTIONAL AND OPERATING LIMITS

B 2.1.1 Fuel to be Stored in the FuelSolutions™ W74 Canister

BASES

BACKGROUND	The CANISTER design requires specifications for the spent fuel to be stored, such as class and type of spent fuel, maximum allowable initial enrichment, maximum burnup, post-irradiation cooling time prior to storage in the CANISTER, and cladding material and condition. Other important limitations are dimensions and weight of the fuel assemblies. These limitations are included in the thermal, structural, radiological, and criticality evaluations performed for the CANISTER and are specified in Section 2.0 (References 1 through 6).
APPLICABLE SAFETY ANALYSIS	To assure that the closure plate is not placed on the CANISTER containing an unauthorized fuel assembly, procedures require verification of the loaded fuel assemblies to assure that the correct fuel assemblies have been loaded in the CANISTER.
FUNCTIONAL AND OPERATING LIMITS VIOLATIONS	The following Functional and Operating Limits Violations are applicable: <u>2.2.1</u> If Functional and Operating Limit 2.1.1 is violated, the limitations on the fuel assemblies in the CANISTER have not been met. Actions must be taken to place the affected fuel assemblies in a safe condition. This safe condition may be established by returning the affected fuel assemblies to the spent fuel pool. However, it is acceptable for the affected fuel assemblies to remain in the CANISTER if that is determined to be a safe condition. <u>2.2.2 & 2.2.3</u> Notification of the violation of a Functional and Operating Limit to the NRC is required within 24 hours. Written reporting of the violation must be accomplished within 30 days. This notification and written report are independent of any reports and notification that may be required by 10CFR72.216.

REFERENCES

1. FuelSolutions™ W74 Canister Storage SAR, Section 2.2
2. FuelSolutions™ W74 Canister Storage SAR, Section 5.2
3. FuelSolutions™ W74 Canister Storage SAR, Section 6.1
4. FuelSolutions™ W74 Canister Storage FSAR, Section 5.5
5. FuelSolutions™ W74 Canister Storage FSAR, Section 6.6

B 3.0 LIMITING CONDITION FOR OPERATION (LCO) APPLICABILITY

BASES

LCOs		LCO 3.0.1, 3.0.2, 3.0.4, and 3.0.5 establish the general requirements applicable to all Specifications and apply at all times, unless otherwise stated.
LCO	3.0.1	LCO 3.0.1 establishes the Applicability statement within each individual Specification as the requirement for when the LCO is required to be met (i.e., when the unit is in the specified conditions of the Applicability statement of each Specification).
LCO	3.0.2	LCO 3.0.2 establishes that upon discovery of a failure to meet an LCO, the associated ACTIONS shall be met. The Completion Time of each Required action for an ACTIONS Condition is applicable from the point in time that an ACTIONS Condition is entered. The Required Actions establish those remedial measures that must be taken within specified Completion Times when the requirements of an LCO are not met. This specification establishes that: f. Completion of the Required Actions within the specified Completion Times constitutes compliance with a Specification; and g. Completion of the Required Actions is not required when an LCO is met within the specified Completion Time, unless otherwise specified. There are two basic types of Required Actions. The first type of Required Action specifies a time limit in which the LCO must be met. This time limit is the Completion Time to restore a system or component or to restore variables to within specified limits. Whether stated as a Required Action or not, correction of the entered Condition is an action that may always be considered upon entering ACTIONS. The second type of Required Action specifies the remedial measures that permit continued operation that is not further restricted by the Completion Time. In this case, compliance with the Required Actions provides an acceptable level of safety for continued operation. Completing the Required Actions is not required when an LCO is met or is no longer applicable, unless otherwise stated in the individual Specifications.

(continued)

LCO 3.0.2 (continued)	The Completion Times of the Required Actions are also applicable when a system or component is removed from service intentionally. The reasons for intentionally relying on the ACTIONS include, but are not limited to, performance of Surveillances, preventive maintenance, corrective maintenance, or investigation of operational problems. Entering ACTIONS for these reasons must be done in a manner that does not compromise safety. Intentional entry into ACTIONS should not be made for operational convenience.
LCO 3.0.3	Not Applicable.
LCO 3.0.4	LCO 3.0.4 establishes limitations on changes in specified conditions in the Applicability when an LCO is not met. It precludes placing the facility in a specified condition stated in that Applicability (e.g., Applicability desired to be entered) when the following exist: a. ISFSI conditions are such that the requirements of the LCO would not be met in the Applicability desired to be entered; and b. Continued noncompliance with the LCO requirements, if the Applicability were entered, would result in ISFSI activities being required to exit the Applicability desired to be entered to comply with the Required Actions. Compliance with Required Actions that permit continued operation for an unlimited period of time in a specified condition provides an acceptable level of safety for continued operation. This is without regard to the status of the ISFSI. Therefore, in such cases, entry into a specified condition in the Applicability may be made in accordance with the provisions of the Required Actions. The provisions of this Specification should not be interpreted as endorsing the failure to exercise the good practice of restoring systems or components before entering an associated specified condition in the Applicability. The provisions of LCO 3.0.4 shall not prevent changes in specified conditions in the Applicability that are required to comply with ACTIONS. In addition, the provisions of LCO 3.0.4 shall not prevent changes in specified conditions in the Applicability that are related to the unloading of a CANISTER. Exceptions to LCO 3.0.4 are stated in the individual Specifications. Exceptions may apply to all the ACTIONS or to a specific Required Action of a Specification.

LCO 3.0.5	LCO 3.0.5 establishes the allowance for restoring equipment to service under administrative controls when it has been removed from service or determined to not meet the LCO to comply with ACTIONS. The sole purpose of this Specification is to provide an exception to LCO 3.0.2 (e.g., to not comply with the applicable Required Actions(s)) to allow the performance of SRS to demonstrate: a. The equipment being returned to service meets the LCO; or b. Other equipment meets the applicable LCOs. The administrative controls assure the time the equipment is returned to service in conflict with the requirements of the ACTIONS is limited to the time absolutely necessary to perform the allowed testing. This Specification does not provide time to perform any other preventive or corrective maintenance.
LCO 3.0.6	Not Applicable.
LCO 3.0.7	Not Applicable.

B 3.0 SURVEILLANCE REQUIREMENT (SR) APPLICABILITY

BASES

SRs	SR 3.0.1 through SR 3.0.4 establish the general requirements applicable to all Specifications and apply at all times, unless otherwise stated.
SR 3.0.1	SR 3.0.1 establishes the requirement that SRs must be met during the specified conditions in the Applicability for which the requirements of the LCO apply, unless otherwise specified in the individual SRs. This Specification is to assure that Surveillances are performed to verify the systems, components, and that variables are within specified limits. Failure to meet a surveillance within the specified Frequency, in accordance with SR 3.0.2, constitutes a failure to meet an LCO. Systems and components are assumed to meet the LCO when the associated SRS have been met. Nothing in this Specification, however, is to be construed as implying that systems or components meet the associated LCO when: a. The systems or components are known to not meet the LCO, although still meeting the SRS; or b. The requirements of the Surveillance(s) are known not to be met between required Surveillance performances. Surveillances do not have to be performed when the facility is in a specified condition for which the requirements of the associated LCO are not applicable, unless otherwise specified. Surveillances, including Surveillances invoked by Required Actions, do not have to be performed on equipment that has been determined to not meet the LCO because the ACTIONS define the remedial measures that apply. Surveillances have been met and performed in accordance with SR 3.0.2, prior to returning equipment to service. Upon completion of maintenance, appropriate post maintenance testing is required. This includes ensuring applicable Surveillances are not failed and their most recent performance is in accordance with SR 3.0.2. Post maintenance testing may not be possible in the current specified conditions in the Applicability due to the necessary facility (continued)

SR 3.0.1 (continued)	parameters not having been established. In these situations, the equipment may be considered to meet the LCO provided testing has been satisfactorily completed to the extent possible and the equipment is not otherwise believed to be incapable of performing its function. This will allow operation to proceed to a specified condition where other necessary post maintenance tests can be completed.
SR 3.0.2	SR 3.0.2 establishes the requirements for meeting the specified Frequency for Surveillances and any Required Action with a Completion Time that requires the periodic performance of the Required Action on a “once per...” interval. SR 3.0.2 permits a 25% extension of the interval specified in the Frequency. This extension facilitates Surveillance scheduling and considers plant operating conditions that may not be suitable for conducting the Surveillance (e.g., transient conditions or other ongoing Surveillance or maintenance activities). The 25% extension does not significantly degrade the reliability that results from performing the Surveillance at its specified Frequency. This is based on the recognition that the most probable result of any particular surveillance being performed is the verification of conformance with the SRs. The exceptions to SR 3.0.2 are those Surveillances for which the 25% extension of the interval specified in the Frequency does not apply. These exceptions are stated in the individual Specifications as a Note in the Frequency stating, “SR 3.0.2 is not applicable.” As stated in SR 3.0.2, the 25% extension also does not apply to the initial portion of a periodic Completion Time that requires performance on a “once per...” basis. The 25% extension applies to each performance after the initial performance. The initial performance of the Required Action, whether it is a particular Surveillance or some other remedial action, is considered a single action with a single Completion Time. One reason for not allowing the 25% extension to this Completion Time is that such an action usually verifies that no loss of function has occurred by checking the status of redundant or diverse components or accomplishes the function of the affected equipment in an alternative manner. The provisions of SR 3.0.2 are not intended to be used repeatedly merely as an operational convenience to extend Surveillance intervals or periodic Completion Time intervals beyond those specified.

SR 3.0.3

SR 3.0.3 establishes the flexibility to defer declaring affected equipment as not meeting the LCO or an affected variable outside the specified limits when a Surveillance has not been completed within the specified Frequency. A delay period of up to 24 hours or up to the limit of the specified Frequency, whichever is less, applies from the point in time that it is discovered that the Surveillance has not been performed in accordance with SR 3.0.2, and not at the time that the specified Frequency was not met.

This delay period provides adequate time to complete Surveillances that have been missed. This delay period permits the completion of a surveillance before complying with Required Actions or other remedial measures that might preclude completion of the Surveillance.

The basis for this delay period includes consideration of facility conditions, adequate planning, availability of personnel, the time required to perform the Surveillance, the safety significance of the delay in completing the required Surveillance, and the recognition that the most probable result of any particular Surveillance being performed is the verification of conformance with the requirements. When a Surveillance with a Frequency based not on time intervals, but upon specified facility conditions or operational situations, is discovered not to have been performed when specified, SR 3.0.3 allows the full delay period of 24 hours to perform the Surveillance.

SR 3.0.3 also provides a time limit for completion of Surveillances that become applicable as a consequence of changes in the specified conditions in the Applicability imposed by Required Actions.

Failure to comply with specified Frequencies for SRS is expected to be an infrequent occurrence. Use of the delay period established by SR 3.0.3 is a flexibility which is not intended to be used as an operational convenience to extend Surveillance intervals.

If a Surveillance is not completed within the allowed delay period, then the equipment is considered to not meet the LCO or the variable is considered outside the specified limits and the Completion times of the Required Actions for the applicable LCO Conditions begin immediately upon expiration of the delay period.

(continued)

SR 3.0.3 (continued)	If a Surveillance is failed within the delay period, then the equipment does not meet the LCO, or the variable is outside the specified limits and the Completion Times of the Required Actions for the applicable LCO Conditions begin immediately upon the failure of the Surveillance. Completion of the Surveillance within the delay period allowed by this Specification, or within the Completion Time of the ACTIONS, restores compliance with SR 3.0.1.
SR 3.0.4	SR 3.0.4 establishes the requirement that all applicable SRS must be met before entry into a specified condition in the Applicability. This Specification assures that system and component requirements and variable limits are met before entry into specified conditions in the Applicability for which these systems and component assure safe operation of the facility. The provisions of this Specification should not be interpreted as endorsing the failure to exercise the good practice of restoring systems or components before entering an associated specified condition in the Applicability. However, in certain circumstances, failing to meet an SR will not result in SR 3.0.4 restricting a change in specified condition. When a system, subsystem, component, device, or variable is outside its specified limits, the associated SR(s) are not required to be performed, per SR 3.0.1, which states that Surveillances do not have to be performed on such equipment. When equipment does not meet the LCO, SR 3.0.4 does not apply to the associated SR(s) since the requirement for the SR(s) to be performed is removed. Therefore, failing to perform the Surveillance(s) within the specified Frequency does not result in an SR 3.0.4 restriction to changing specified conditions of the Applicability. However, since the LCO is not met in this instance, LCO 3.0.4 will govern any restrictions that may (or may not) apply to specified condition changes. The provisions of SR 3.0.4 shall not prevent changes in specified conditions in the Applicability that are required to comply with ACTIONS. In addition, the provisions of LCO 3.0.4 shall not prevent changes in specified conditions in the Applicability that are related to the unloading of a CANISTER. (continued)

SR 3.0.4 (continued)

The precise requirements for performance of SRs are specified such that exceptions to SR 3.0.4 are not necessary. The specific time frames and conditions necessary for meeting the SRs are specified in the Frequency, in the surveillance, or both. This allows performance of Surveillances when the prerequisite condition(s) specified in a surveillance procedure require entry into the specified condition in the Applicability of the associated LCO prior to the performance or completion of a Surveillance. A Surveillance that could not be performed until after entering the LCO Applicability would have its Frequency specified such that it is not "due" until the specific conditions needed are met.

B 3.1 CANISTER INTEGRITY

B 3.1.1 W74 Canister Helium Backfill Density

BASES

BACKGROUND	A TRANSFER CASK with an empty CANISTER is placed in the spent fuel pool and loaded with fuel assemblies meeting the requirements of the Functional and Operating Limits. A shield plug is then placed in the CANISTER, and the TRANSFER CASK is raised to the spent fuel pool surface. The dose rates are measured near the center of the top shield plug. The TRANSFER CASK and CANISTER are then moved to the cask preparation area where the inner closure plate is welded to the CANISTER shell and a pressure test performed. The CANISTER is drained, vacuum-dried, and backfilled with helium. The CANISTER outer top closure plate is then welded to the CANISTER shell. Contamination measurements are completed prior to moving the TRANSFER CASK and CANISTER to the ISFSI. A W74 CANISTER containing fuel assemblies shall be backfilled with helium to maintain an inert atmosphere to prevent cladding degradation and promote heat transfer during storage. The density of helium is specified to maintain the CANISTER internal pressure under normal, off-normal, and postulated accident conditions within the design basis values. In addition, it assures that an adequate mass of helium is present in the CANISTER for heat transfer over the 100-year design life.
APPLICABLE SAFETY ANALYSIS	The confinement of radioactivity during the storage of spent fuel in the CANISTER within the STORAGE CASK is assured by the use of multiple confinement boundaries and systems. The barriers are the fuel pellet matrix, the metallic fuel cladding tubes in which the fuel pellets are contained, and the CANISTER in which the fuel assemblies are stored. Long-term integrity of the fuel and cladding depend on storage in a dry inert atmosphere. This is accomplished by removing water from the CANISTER and backfilling the cavity with an inert gas (Reference 1).
LCO	The backfill density is selected to assure that the CANISTER internal pressure remains within the design basis values used for normal, off-normal, and postulated accident storage conditions. The specified helium backfill density was selected based on a minimum helium purity of 99.995%.

APPLICABILITY	CANISTER helium backfilling is performed during LOADING OPERATIONS prior to transporting the CANISTER to the ISFSI (Reference 1).
ACTIONS	A note has been added to the Actions stating that a separate Condition entry is allowed for each CANISTER. This is acceptable since the Required Actions for each Condition provide appropriate compensatory measures for each CANISTER not meeting the LCO. Subsequent CANISTERs that do not meet the LCO are governed by subsequent Condition entry and application of associated Required Actions. <u>A.1</u> If the required helium backfill cannot be met, actions must be taken to meet the LCO. Re-evacuate the CANISTER and backfill the CANISTER to comply with the LCO limit. See LCO 3.1.4 of the Storage System Technical Specification if the leak rate exceeds 8.52×10^{-6} ref-cc/sec. The Completion Time is sufficient to determine and correct most failures which would prevent backfilling the CANISTER cavity with helium. <u>B.1</u> If the CANISTER cavity cannot be successfully backfilled with helium, the fuel must be removed and placed in a safe condition in the spent fuel pool. The Completion Time is reasonable based on the time required to return the fuel to the spent fuel pool in an orderly manner without challenging personnel.

SURVEILLANCE REQUIREMENTS	SR 3.1.1.1 The long-term integrity of the stored fuel is dependent on storage in a dry, inert environment. Filling the CANISTER cavity with the specified helium density will assure that there will be no air inleakage, which could potentially damage the fuel, and that the CANISTER cavity internal pressure will remain within limits for the 100-year design life of the CANISTER. Backfilling with helium must be performed successfully on each CANISTER before placing it in storage. The surveillance must be performed within 24 hours after verifying the CANISTER cavity vacuum drying pressure is within the limit. This allows sufficient time to backfill the CANISTER cavity with helium while minimizing the time the fuel is in the CANISTER without the assumed inert atmosphere.
REFERENCES	1. FuelSolutions™ Storage System SAR, Section 8.1.8.

B 3.1 CANISTER INTEGRITY

B 3.1.2 Canister Vacuum Drying Pressure

BASES

See the Storage System Technical Specification for the applicable Bases.

B 3.1 CANISTER INTEGRITY

B 3.1.3 Canister Leak Rate

BASES

See the Storage System Technical Specification for the applicable Bases.

B 3.1 CANISTER INTEGRITY

B 3.1.4 Hydraulic Ram Force During Horizontal Canister Transfer

BASES

See the Storage System Technical Specification for the applicable Bases.

B 3.1 CANISTER INTEGRITY

B 3.1.5 W74 Canister Vertical Time Limit in Transfer Cask

BASES

BACKGROUND	During CANISTER draining, vacuum drying, backfill, and closure operations, the TRANSFER CASK annulus is filled with water. Water flow is provided as necessary to minimize TRANSFER CASK and CANISTER temperatures. Upon completion of the final CANISTER closure weld and non-destructive examination, the TRANSFER CASK annulus is drained as a predecessor to TRANSFER OPERATIONS. The TRANSFER OPERATIONS must be initiated within the specified time so the CANISTER basket spacer plate temperatures remain within the design basis temperatures.
APPLICABLE SAFETY ANALYSIS	The thermal analyses of the CANISTER in the TRANSFER CASK (Reference 1) show the CANISTER basket temperatures that correspond to design basis conditions and configuration. Completing the subsequent TRANSFER OPERATIONS within the specified time limit assures that spacer plate strength will be adequate to accommodate a postulated handling accident.
LCO	For vertical TRANSFER OPERATIONS, completion of the CANISTER transfer out of the TRANSFER CASK within the specified time after draining of the annulus water from the TRANSFER CASK assures that the CANISTER remains within design basis limits for all postulated normal, off-normal, and accident conditions. For horizontal TRANSFER OPERATIONS, completion of the movement of the TRANSFER CASK to the horizontal position on the transfer trailer within the specified time after draining of the annulus water from the TRANSFER CASK assures that the CANISTER remains within design basis limits for all postulated normal, off-normal, and accident conditions.
APPLICABILITY	The specified time limit applies during TRANSFER OPERATIONS.
ACTIONS	A note has been added to the Actions stating that a separate Condition entry is allowed for each CANISTER. This is acceptable since the Required Actions for each Condition provide appropriate compensatory measures for each CANISTER not meeting the LCO. Subsequent CANISTERs that do not meet the LCO are governed by subsequent Condition entry and application of associated Required Actions. (continued)

ACTIONS (continued)	A.1 If the indicated time limit is exceeded, then it is required to return the CANISTER to a cooler conditions by providing the heat removal capability provided by the annulus water. The first step in this recovery process is to flood the annulus with water. The Completion Time is sufficient to complete this action. A.2 The use of annulus cooling, if required, aids in the removal of decay heat from the CANISTER. The Completion Time is sufficient to complete the application of cooling. Upon reestablishment of the steady-state condition which existed before the initial draining of the annulus, the annulus may be drained and the time limit measurement restarted for completion of subsequent TRANSFER OPERATIONS.
SURVEILLANCE REQUIREMENTS	SR 3.1.5.1 Verification that the TRANSFER CASK operations with the CANISTER in vertical orientation and annulus drained are completed within the time limit assures that the CANISTER basket temperatures remain within their limits.
REFERENCES	1. FuelSolutions™ W74 Canister Storage SAR, Section 4.4.

B 3.2 CANISTER RADIATION PROTECTION

B 3.2.1 Canister Surface Contamination

BASES

See the Storage System Technical Specification for the applicable Bases.

B 3.3 STORAGE CASK INTEGRITY

B 3.3.1 Storage Cask Air Inlet and Outlet Openings

BASES

See the Storage System Technical Specification for the applicable Bases.

B 3.3 STORAGE CASK INTEGRITY

B 3.3.2 Storage Cask Temperatures During Storage

BASES

BACKGROUND	After placement on the ISFSI pad, the heat from the fuel assemblies within the CANISTER is removed by air flowing past the CANISTER, entering in the inlet vents and exiting through the outlet vents in the STORAGE CASK. Monitoring of the STORAGE CASK concrete temperatures assures that the heat removal capability of the STORAGE CASK is not compromised.
APPLICABLE SAFETY ANALYSIS	The thermal analyses of the STORAGE CASK (Reference 1) and CANISTERs (Reference 2) result in STORAGE CASK concrete temperatures that correspond to the design basis conditions and configuration. Monitoring of the STORAGE CASK concrete temperature assures that the long-term concrete and fuel assembly cladding temperatures remain within allowable values. Temperatures not satisfying the limits may indicate a problem with the conditions or configuration which need to be corrected to maintain temperatures with acceptable values.
LCO	The specified temperature limits assure that the long-term storage cask concrete and fuel assembly cladding temperatures remain within allowable values. This assures long-term integrity of the STORAGE CASK concrete and the fuel assembly cladding.
APPLICABILITY	STORAGE CASK temperature monitoring is performed during STORAGE OPERATIONS.
ACTIONS	A note has been added to the Actions stating that a separate Condition entry is allowed for each STORAGE CASK. This is acceptable since the Required Actions for each Condition provide appropriate compensatory measures for each STORAGE CASK not meeting the LCO. Subsequent STORAGE CASKs that do not meet the LCO are governed by subsequent Condition entry and application of associated Required Actions.

(continued)

ACTIONS (continued)

A.1

If the indicated concrete temperature is greater than any of the specified limits, or if the concrete temperature rise exceeds the specified limits, then it is required to confirm that the CANISTER has been loaded with SNF assemblies that comply with the Functional and Operating limits of Section 2.0 of the W74 CANISTER Technical Specification.

Administrative verification of the fuel loading, by means such as video recordings and records of the loaded fuel assembly serial numbers, can establish whether a misloaded fuel assembly is the cause of the out-of-limit condition.

The Completion Time is sufficient to determine and correct most failure mechanisms.

A.2

All STORAGE CASK inlet and outlet vents and screens should be checked for debris blockage in accordance with LCO 3.3.2 of the FuelSolutions™ Storage System Technical Specification.

The Completion Time is sufficient to determine and correct most failure mechanisms.

A.3 - A.4

Another possible cause of exceeding the temperature limits is equipment malfunction. The thermocouple and related instrumentation should be checked to assure they are functioning properly, and repaired or replaced as necessary.

The Completion Time is sufficient to determine and correct most failure mechanisms.

(continued)

ACTIONS (continued)

A.5

Another possible cause of temperatures exceeding the limits is obstruction inside the vents or the cask. Visual inspection of the STORAGE CASK vent channels is performed by removing the debris screens and using visual aids as necessary. If no obstruction is found, the interior of the STORAGE CASK, including the guide rails and heat shield, should be visually inspected for ventilation obstructions using remote inspection tools or by temporarily removing the STORAGE CASK top cover.

The Completion Time is sufficient to determine and correct most failure mechanisms.

B.1 - B.3

If the temperature cannot be successfully reduced to within the specified limits by the above actions, then mitigating actions must be taken to cool the STORAGE CASK within the limits until other measures can be employed. The CANISTER can be retrieved to the TRANSFER CASK (which has been evaluated to maintain acceptable temperatures under steady state conditions). The licensee will temporarily store the CANISTER in the TRANSFER CASK in a horizontal configuration bounded by that analyzed in the FSAR, and any supplemental shielding that is determined necessary to maintain dose rates within the limits of 10 CFR 72.104 on a site-specific basis will be evaluated in accordance with 10 CFR 72.48. The Completion Times are reasonable based on the time required to establish cooling actions and place the CANISTER into the TRANSFER CASK, and to return CANISTER to a repaired or replacement STORAGE CASK, in an orderly manner without challenging personnel.

The potential for freezing of the transfer cask liquid neutron shield during temporary storage will be evaluated on a cask- and site-specific basis, and measures will be implemented, if necessary, to prevent freezing.

SURVEILLANCE REQUIREMENTS	SR 3.1.2.1 The STORAGE CASK concrete temperatures are to be checked daily to provide adequate frequency to assure that temperatures remain within the specified limits and provide adequate time to initiate corrective actions.
REFERENCES	1. FuelSolutions™ Storage System SAR, Section 4.4. 2. FuelSolutions™ W74 Canister Storage SAR, Section 4.4.

BASES

B 3.3 STORAGE CASK INTEGRITY

B 3.3.3 Storage Cask Temperatures During Horizontal Transfer

BASES

BACKGROUND	When a STORAGE CASK with a CANISTER containing fuel assemblies is in the horizontal orientation, the natural convective air flow that cools the CANISTER is altered. The STORAGE CASK thermocouple temperature is correlated through analysis to the maximum concrete temperature near the liner/concrete interface. Assuring that the storage cask thermocouple temperature limit is not exceeded assures that the short-term allowable concrete temperature is not exceeded.
APPLICABLE SAFETY ANALYSIS	The basis for maintaining this STORAGE CASK temperature limit is the thermal analysis contained in Chapter 4 of the Storage System SAR (Reference 1). The specified temperature limit is correlated to the short-term allowable concrete temperature.
LCO	Limiting the concrete temperature during horizontal CANISTER TRANSFER OPERATIONS maintains the STORAGE CASK concrete temperatures within the design basis.
APPLICABILITY	Temperature monitoring is performed during horizontal TRANSFER OPERATIONS.
ACTIONS	A note has been added to the Actions stating that a separate Condition entry is allowed for each STORAGE CASK. This is acceptable since the Required Actions for each Condition provide appropriate compensatory measures for each STORAGE CASK not meeting the LCO. Subsequent STORAGE CASKs that do not meet the LCO are governed by subsequent Condition entry and application of associated Required Actions. <u>A.1</u> If the STORAGE CASK concrete temperature limit is not met, then it is required to take action to reduce the STORAGE CASK concrete temperature. This may be accomplished by removing the CANISTER from the STORAGE CASK into the TRANSFER CASK. The Completion Time is adequate to perform this task.

(continued)

ACTIONS (continued)

B.1

The STORAGE CASK should be inspected for signs of damage to the concrete. The Completion time is adequate to perform the inspection and assessment.

B.2.1

If the STORAGE CASK is undamaged, it may be reused. The Completion Time is reasonable based on the time to complete the TRANSFER OPERATIONS.

B.2.2

If the STORAGE CASK is damaged, then it may not be used. A new STORAGE CASK will be required to store the CANISTER. The Completion Time is reasonable based on the time to complete the TRANSFER OPERATIONS.

C.1 - C.2

If the CANISTER cannot be placed into storage or retrieved from storage within the specified time, mitigating actions must be initiated. The CANISTER can be retrieved to the TRANSFER CASK (which has been evaluated to maintain acceptable temperatures under steady state conditions). The licensee will temporarily store the CANISTER in the TRANSFER CASK in a horizontal configuration bounded by that analyzed in the FSAR, and any supplemental shielding that is determined necessary to maintain dose rates within the limits of 10 CFR 72.104 on a site-specific basis will be evaluated in accordance with 10 CFR 72.48. The CANISTER will be returned to a repaired or replacement STORAGE CASK for continued long term storage. The Completion Times are reasonable based on the time required to place the CANISTER into the TRANSFER CASK, and to return CANISTER to a repaired or replacement STORAGE CASK, in an orderly manner without challenging personnel.

The potential for freezing of the transfer cask liquid neutron shield during temporary storage will be evaluated on a cask- and site-specific basis, and measures will be implemented, if necessary, to prevent freezing.

BASES

SURVEILLANCE REQUIREMENTS	The STORAGE CASK concrete temperature is to be checked every 30 minutes when the STORAGE CASK is in a horizontal orientation with a CANISTER containing fuel assemblies. The frequency of inspection assumes that temperatures remain within limits and provide adequate time to initiate corrective actions.
REFERENCES	1. FuelSolutions™ Storage System SAR, Section 4.5.

B 3.4 TRANSFER CASK INTEGRITY

B 3.4.1 Transfer Cask Structural Shell Temperature

BASES

See the Storage System Technical Specification for the applicable Bases.

B 3.5 TRANSFER CASK RADIATION PROTECTION

B 3.5.1 Transfer Cask Surface Contamination

BASES

See the Storage System Technical Specification for the applicable Bases.

13. QUALITY ASSURANCE

Quality Assurance of the FuelSolutions™ W74 canister is addressed in the quality assurance discussion provided in Chapter 13 of the FuelSolutions™ Storage System FSAR.[1]

[1] WSNF-220, *FuelSolutions™ Storage System Final Safety Analysis Report*, NRC Docket No. 72-1026, BNFL Fuel Solutions Corporation.

This page intentionally left blank.

14. DECOMMISSIONING

Decommissioning of the FuelSolutions™ W74 canister is addressed in the canister decommissioning discussion provided in Chapter 14 of the FuelSolutions™ Storage System FSAR.[1]

[1] WSNF-220, *FuelSolutions™ Storage System Final Safety Analysis Report*, NRC Docket No. 72-1026, BNFL Fuel Solutions Corporation.

This page intentionally left blank.